

# CHEMICAL & PHARMACEUTICAL BULLETIN

Vol. 35, No. 1

January 1987

---

## Regular Articles

---

[Chem. Pharm. Bull.]  
35(1) 1-8 (1987)

### Reactive Intermediates Produced in the Decomposition of 2-Diazoketone: Mechanism of the Wolff Rearrangement

MINORU TSUDA,\* SETSUKO OIKAWA and KIYOSHI NAGAYAMA

*Laboratory of Bio-physical Chemistry, Faculty of Pharmaceutical  
Sciences, Chiba University, Chiba 260, Japan*

(Received July 2, 1986)

Potential energy hypersurfaces of the nitrogen elimination and the Wolff rearrangement were investigated for both cyclic and open-chain 2-diazoketones by means of semi-empirical MINDO/3 molecular orbital calculations with configuration interaction. In the case of 2-diazobenzene-1-one, the nitrogen elimination takes place simultaneously with the Wolff rearrangement in a concerted fashion and neither ketocarbene nor oxirene is produced. In contrast to the cyclic 2-diazoketone, 2-diazoethan-1-one produces oxirene through nitrogen elimination in a concerted fashion. The oxirene isomerizes to ketene *via* the Wolff rearrangement, passing over a second saddle point of low energy. No ketocarbene intermediate is produced in either case.

**Keywords**—Wolff rearrangement; reaction mechanism; molecular orbital method; MINDO/3; potential energy hypersurface; lowest energy path; 2-diazoethan-1-one; 2-diazobenzene-1-one; oxirene; ketene

### Introduction

4-(2-Aminoethyl)-2-diazobenzene-1-one is a mutagen recently found by Nagao *et al.* to be formed from 4-(2-aminoethyl)phenol-1, a component of soy sauce, after nitrite treatment.<sup>1,2)</sup> Experiments on the carcinogenicity of the mutagen are in progress,<sup>3)</sup> because a benzenediazonium derivative, 4-(hydroxymethyl)benzenediazonium cation, which is a component of mushrooms, was found to induce glandular stomach tumors in mice.<sup>3,4)</sup> Many carcinogenic alkylating agents are believed to owe their activity to conversion to a highly reactive diazonium ion.<sup>5)</sup> Theoretical chemistry confirmed that the benzenediazonium cation produces a reactive intermediate, phenyl cation, by loss of nitrogen in the first step of its decomposition.<sup>6)</sup> In the decomposition of 2-diazoketone, ketocarbene is postulated to be the first product, formed by loss of nitrogen, and then migration of the group next to the carbonyl group takes place to give the corresponding ketene (the Wolff rearrangement),<sup>7-20)</sup> as shown in Fig. 1(a). The ketene formation has been established experimentally. Theoretical studies of the Wolff rearrangement have been carried out starting from the ketocarbene.<sup>7-10)</sup> However, the ketocarbene has not been isolated, and no theoretical research has been done on the step of nitrogen elimination from 2-diazoketone: *i.e.*, ketocarbene formation has not yet been confirmed. Cyclic 2-diazoketones, for example, 2-diazobenzene-1-ones and 2-diazo-

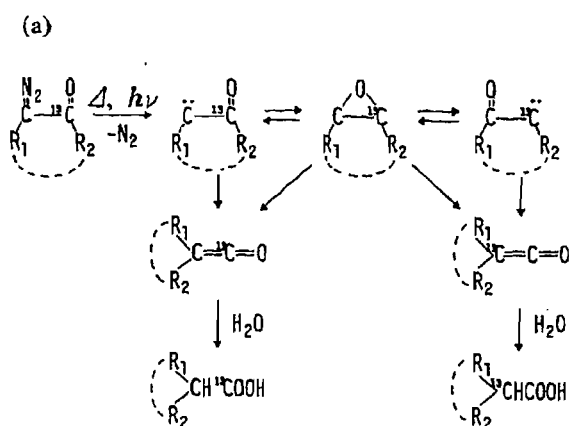


Fig. 1(a). Old Mechanism of the Wolff Rearrangement<sup>1,3,19)</sup>

Because ketocarbene intermediate plays an important role in the mechanism, oxirene is naturally produced and the scrambling of <sup>13</sup>C must be observed in every case. ----- refers to both cyclic and open-chain compounds.

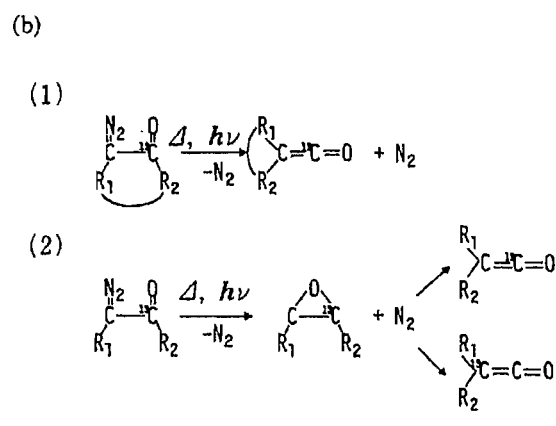


Fig. 1(b). New Mechanism of the Wolff Rearrangement

No ketocarbene intermediate is produced. (1) Ketene is the one-step reaction product. Therefore, no scrambling is observed in the cyclic 2-diazoketone. (2) Oxirene intermediate is produced only in the case of the open-chain 2-diazoketone, where scrambling is observed.

naphthalen-1-ones are widely used in the semiconductor industry in the microfabrication of VLSI (very large scale integrated circuits). One problem with the ketocarbene mechanism is why the ketocarbene produced in the first step does not react with atmospheric oxygen during the microfabrication process, although a nitrene produced from azide by loss of nitrogen reacts strongly with atmospheric oxygen under the same conditions.<sup>18)</sup>

Another question concerns the participation of the oxirene intermediate in the Wolff rearrangement mechanism. Strausz showed the importance of the oxirene pathway in the cases of 3-diazobutan-2-one, 3-diazopropan-2-one and 1,2-diphenyl-2-diazoethan-1-one.<sup>14)</sup> However, the experiments on cyclic compounds, 5-diazohomoadamantan-4-one<sup>19)</sup> and 2-diazonaphthalen-1-one,<sup>20)</sup> excluded the formation of the oxirene intermediate. If 2-ketocarbene were produced, oxirene would be the subsequent product for both cyclic and open-chain 2-diazoketones. What is the origin of this difference?

If no ketocarbene is formed in the reaction of 2-diazoketone, the mechanism of carcinogenesis may be different from that in the case of benzenediazonium. This paper reports the lowest potential energy path of the Wolff rearrangement starting from 2-diazoketone to the final product, ketene, for both cyclic and open-chain 2-diazoketones. The results clearly explain the experimental findings and resolve the above problems.

#### Method

**Determination of the Lowest Energy Path**—The intrinsic reaction co-ordinate (IRC) is the lowest energy path connecting a reactant and a product through the saddle point (the transition state) on the  $3N-6$  dimensional potential energy hypersurface.<sup>21)</sup> For simplicity, the IRC calculations were done on the mass-weighted  $3N$  dimensional hypersurface. Then, the results were revised in such a manner that the center of mass and the three kinds of principal axes of inertia in the structure of the reaction system were always fixed throughout the IRC path. Starting from the saddle point, the IRC path was determined point by point following the procedure proposed by Ishida *et al.*<sup>22)</sup>

**Geometry Optimization**—A systematic method was applied which overcomes the difficulty of finding the stable and the transition state (TS) structures of the reaction system on the multidimensional hypersurface. The details of the method were reported elsewhere.<sup>23)</sup> By this method, we can easily obtain the minima (the stable structures) and the saddle points (the transition state structures) by using the first and second derivatives of the potential energy with respect to the structure change for the determinations of the former and the latter, respectively.

For the potential energy evaluation in the geometry optimization and IRC calculations, the spin-restricted Hartree Fock (RHF) molecular orbital method was adapted with the semi-empirical MINDO/3<sup>24)</sup> parametrization, since *ab initio* calculations are still prohibitive because of the economical and computational limits. The potential energy surfaces were elaborated with configuration interaction (CI) calculations,<sup>25)</sup> which consider the singly and doubly excited electronic configurations less than 14 eV from the ground state (SDCI). In the present cases, however, the potential energy surfaces with or without CI have the same profile, as shown later. This means that the state function of the ground state is essentially expressed by a single RHF configuration function in these cases. The potential energy change obtained here on the reaction path from oxirene to ketene in the case of 2-diazoethan-1-one is very similar to the results obtained by an *ab initio* method with configuration interaction.<sup>9)</sup> Thus, the results obtained in the present calculations should be reliable, at least qualitatively.

## Results

### Potential Energy Change Following the Lowest Energy Path of the Reaction of 2-Diazobenzene-1-one

Potential energy change following the lowest energy path of the nitrogen loss reaction is shown in Fig. 2 in the case of 2-diazobenzene-1-one. This result will be astonishing to the chemist who has accepted the ketocarbene mechanism (Fig. 1(a)). The Wolff rearrangement to ketene occurs simultaneously with the nitrogen molecule liberation. The reaction takes place in one step and there is only one saddle point throughout the reaction path. Neither ketocarbene nor oxirene is formed in the reaction path. Therefore, the experiments which found no influence of atmospheric oxygen on the ketene formation and no oxirene

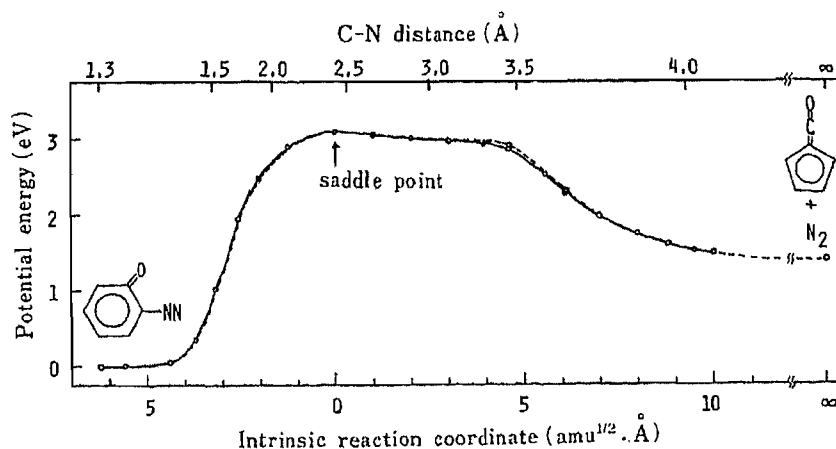


Fig. 2. Potential Energy Change Following the Lowest Energy Path of the Nitrogen Loss Reaction in the Case of 2-Diazobenzene-1-one

—, by MINDO/3; ----, including SDCI.

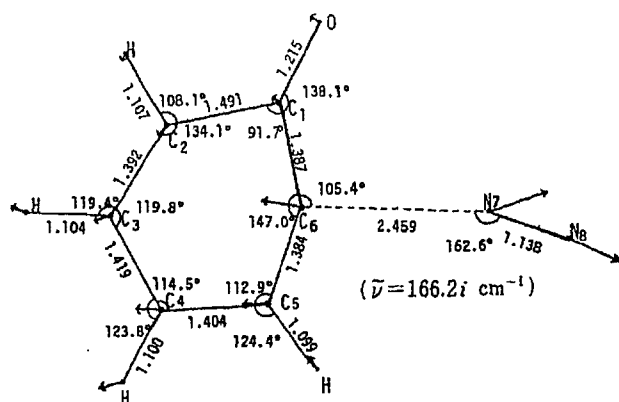


Fig. 3. The Structure at the Saddle Point in the Reaction Path of 2-Diazobenzene-1-one

participation are quite reasonable from the theoretical point of view.

### Molecular Structure Change Following the Lowest Energy Path of the Reaction of 2-Diazobenzen-1-one

The structure at the saddle point is shown in Fig. 3, and is planar. The unique normal mode of vibration of imaginary frequency ( $166.2 i \text{ cm}^{-1}$ ) is shown by an arrow at each of the atoms. The forward progress of the reaction following the arrows leads to loss of nitrogen and the backward reaction recovers the reactant, 2-diazoketone.

Molecular structure changes following the lowest energy path are shown in Fig. 4 from the reactant, 2-diazoketone, to the product, ketene, based on six points on the path of Fig. 2. With the separation of the diazo group from C6 of the aromatic ring, C6 approaches C2 at the *meta* position. Over the saddle point, the bond formation between C2 and C6 proceeds together with the bond fission between C2 and C1, and finally, ketene is produced. The reaction takes place in a concerted fashion throughout the process.

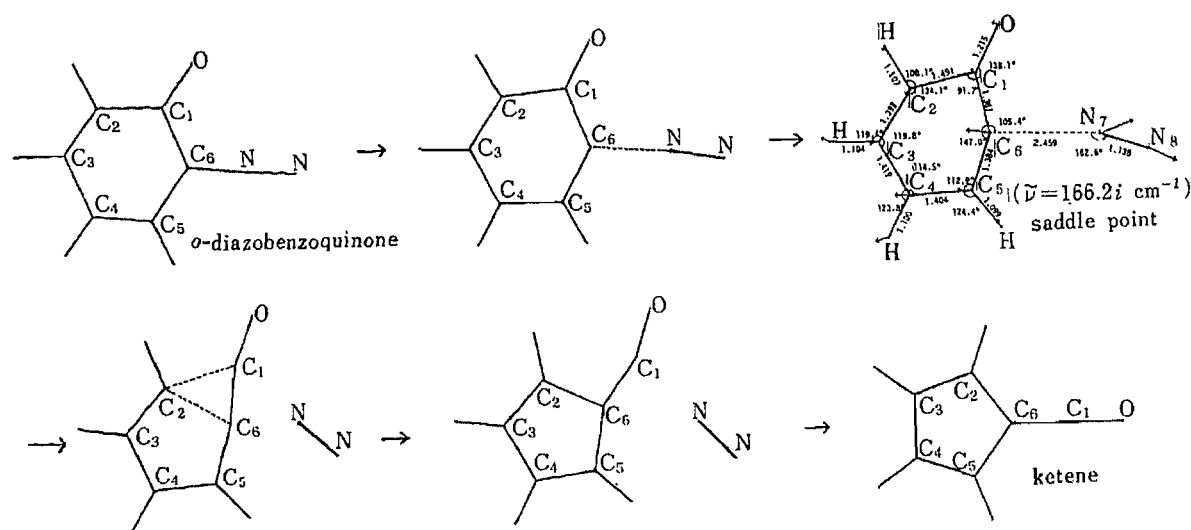


Fig. 4. Molecular Structure Change Following the Lowest Energy Path from the Reactant, 2-Diazobenzen-1-one, to the Product, a Ketene

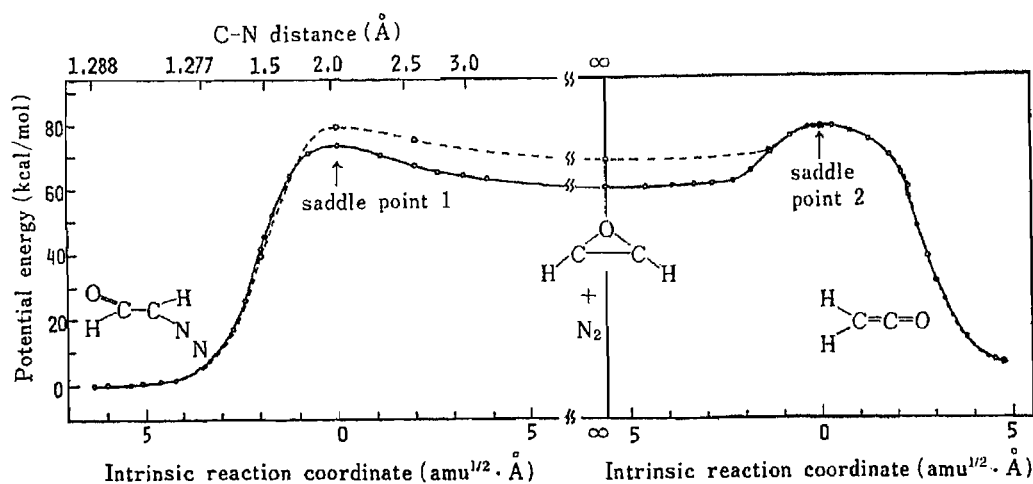


Fig. 5. Potential Energy Change Following the Lowest Energy Path of the Nitrogen Loss Reaction in the Case of 2-Diazoethan-1-one

—, by MINDO/3; ----, including SD-CI.



### Potential Energy Change Following the Lowest Energy Path of the Reaction of 2-Diazoethan-1-one

Potential energy change following the lowest energy path of the nitrogen loss reaction of 2-diazoethan-1-one is shown in Fig. 5. In contrast to the case of the cyclic 2-diazoketone, the first product obtained by loss of nitrogen is oxirene. Ring opening passes over a second saddle point of low energy to produce the final product, ketene. A ketocarbene-like structure appears in the process of the ring opening. However, the ketocarbene has no life time for reacting with any other molecule, since the structure does not exist at a minimum of the potential energy hypersurface. RHF level calculation using the 4-31G basis set<sup>10)</sup> and the same level calculation using the double-zeta plus polarization basis set (DZ+P)<sup>8)</sup> gave formylmethylene, a ketocarbene, at a minimum point. However, the minimum disappears in the higher level

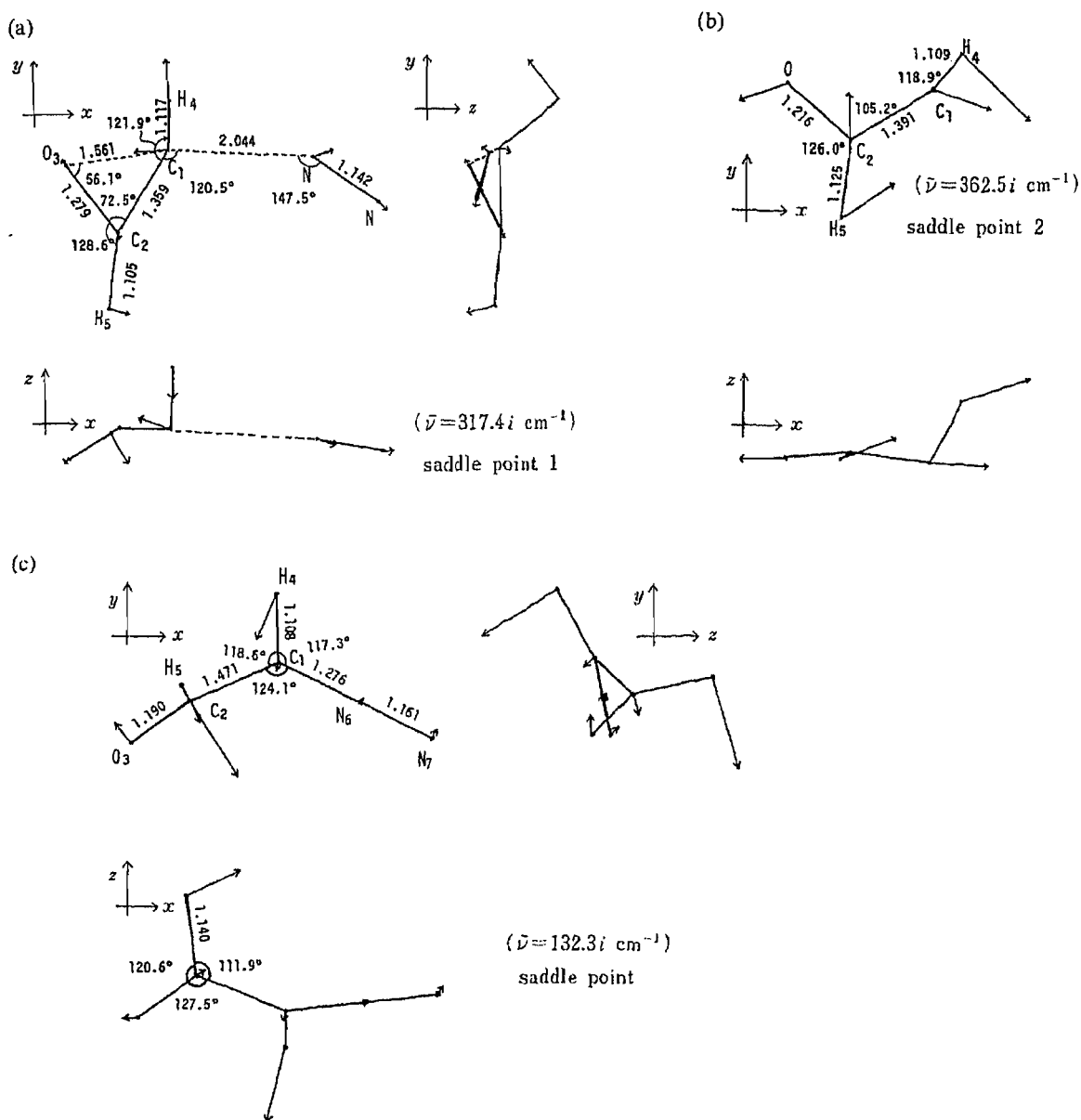


Fig. 6(a). The Structure of the Saddle Point 1 in Fig. 5  
 (b). The Structure of the Saddle Point 2 in Fig. 5  
 (c). The Structure of the Saddle Point in the *cis-trans* Isomerization of 2-Diazoethan-1-one in Fig. 7

calculation with CI(DZ+P),<sup>81</sup> where the ring opening of oxirene passes over a saddle point of low energy to give the final product, ketene. The results obtained by CI(DZ+P) agree with the conclusion of the present MINDO/3 calculation.

### Molecular Structure Change Following the Lowest Energy Path of the Reaction of 2-Diazoethan-1-one

The structure at the saddle point 1 is shown in Fig. 6(a), and is non-planar in spite of the planar structure of the starting reactant, 2-diazoethan-1-one. The non-planar structure is

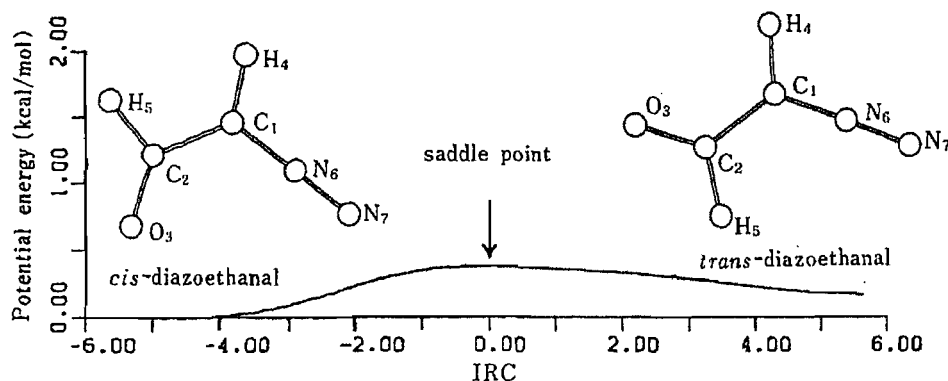


Fig. 7. The Lowest Potential Energy Change in the *cis-trans* Isomerization of 2-Diazoethan-1-one

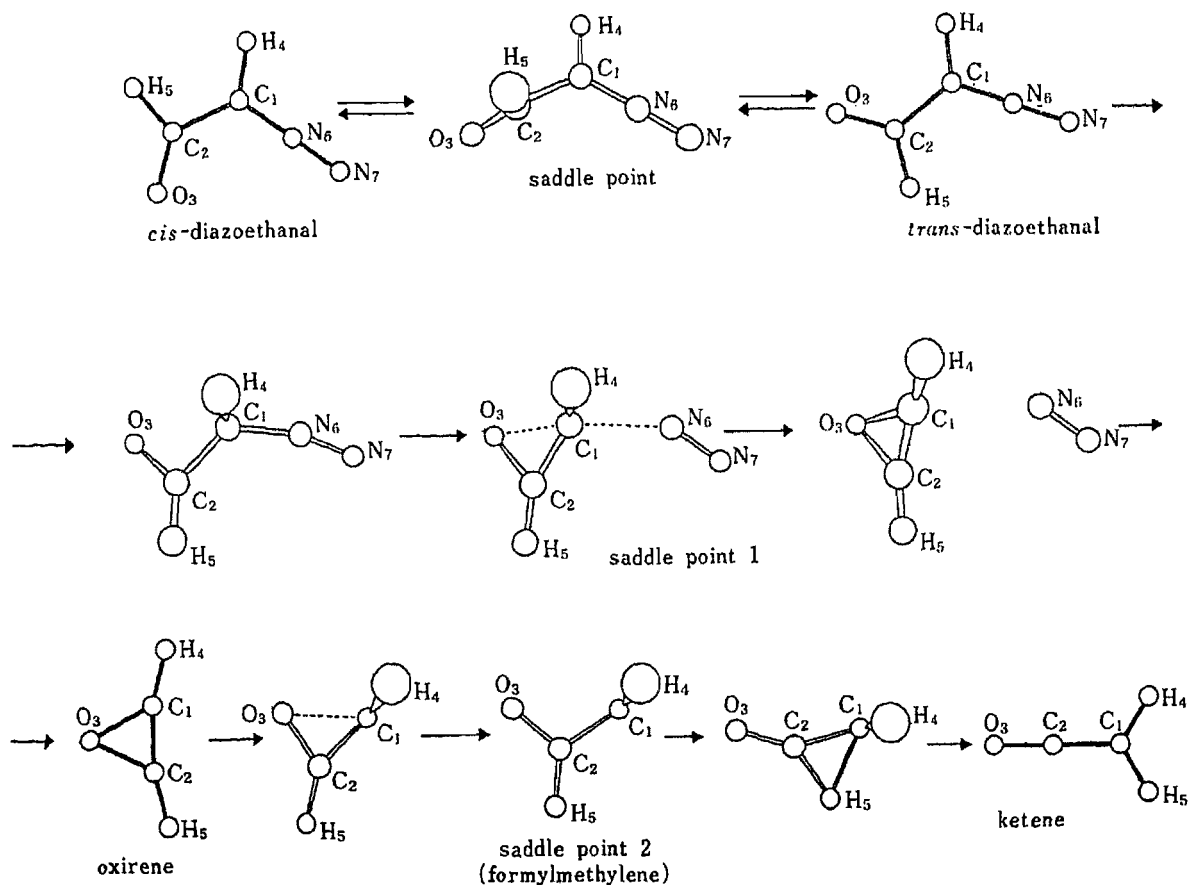


Fig. 8. Molecular Structure Change Following the Lowest Energy Path from the Reactant, 2-Diazoethan-1-one, to the Final Product, a Ketene

essential for oxirene formation. In the case of 2-diazobenzene-1-one, the oxirene formation may be inhibited because the benzene ring strongly maintains its planar structure. The produced oxirene is also non-planar. The structure at the saddle point 2 is shown in Fig. 6(b), and is a non-planar ketocarbene.

The structure at the saddle point in the *cis-trans* isomerization of 2-diazoethane-1-one is shown in Fig. 6(c), and is non-planar. The lowest potential energy change in the isomerization is shown in Fig. 7.

In Fig. 8, the isomerization process of 2-diazoethane-1-one is shown in the first line, and then the second and third lines show the molecular structure changes following the lowest potential energy path in Fig. 6. Starting from a planar *trans*-2-diazoethane-1-one, loss of a nitrogen molecule takes place with the torsion of the molecule around the C1-C2 bond, and oxirene is formed in a concerted fashion. The produced oxirene isomerizes to ketene via a formylmethylene structure at the saddle point. In contrast to the cyclic 2-diazoketone, the open-chain 2-diazoethane-1-one produces an oxirene at a minimum point of its potential energy hypersurface. Therefore, scrambling in the Wolff rearrangement is naturally observed in experiments by the carbon-13 labeling technique in the open-chain case (see Fig. 1), because of the long life time of the oxirene.

### Discussion

The results of many experiments on the Wolff rearrangement<sup>7-20)</sup> can be successfully explained, provided that the reaction proceeds through the lowest potential energy path which is shown in Fig. 2 for the cyclic 2-diazoketone and in Fig. 5 for the open-chain 2-diazoketone. These potential energy hypersurfaces are on the ground state where thermolysis occurs. However, a majority of the experiments involved photolysis. Why are the photochemical experiments explained by the potential energy hypersurface of the ground state? The reason is considered to be that the key steps of the photochemical reactions which give the observed products occur in the ground state and not in the excited states. In the simplest way, we can explain the results by assuming that the transition from the excited states to the ground state takes place at the right side of the saddle point of Fig. 2 or the saddle point 1 of Fig. 5. The elucidation of the exact mechanism of photolysis, however, must wait until the potential energy hypersurfaces of the excited states are calculated.

The highly reactive intermediate produced in the first step of the nitrogen elimination is ketene in the case of 2-diazobenzene-1-one, but phenyl cation in the case of benzene-diazonium.<sup>6)</sup> However, it is reasonable to consider that both ketene and phenyl cation may react with the amino group of guanine in deoxyribonucleic acid as the first step of mutagenesis or carcinogenesis.<sup>26)</sup>

**Acknowledgment** The main part of the computation was carried out at the Computer Centre, the University of Tokyo, and the Computer Center, Chiba University. The authors thank the Computer Center, Institute for Molecular Science, Okazaki, for the use of an M-200H computer in a part of the computation.

### References

- 1) M. Nagao, K. Wakabayashi and T. Sugimura, "Mutagenicity Testing in Environmental Pollution Control," ed. by F. K. Zimmerman and R. E. Taylor-Mayer, Wiley, New York, 1984, p. 69.
- 2) K. Wakabayashi, M. Nagao, M. Ochiai, M. Tsuda, Z. Yamaizumi, H. Saito and T. Sugimura, "N-Nitroso Compounds: Occurrence, Biological Effects and Relevance to Human Cancer," eds. by I. K. O'Neill, R. C. Von Borstel, C. T. Miller, J. Long and H. Bartsch, International Agency for Research on Cancer, Lyon, 1984, p. 17.
- 3) M. Ochiai, K. Wakabayashi, M. Nagao and T. Sugimura, *Gann*, **75**, 1 (1984); and a private communication from M. Nagao.
- 4) B. Toth, N. Nagel and A. Ross, *Brit. J. Cancer*, **46**, 417 (1982).

- 5) G. P. Ford and J. D. Scribner, *J. Am. Chem. Soc.*, **105**, 349 (1983).
- 6) S. Oikawa, M. Tsuda, A. Nogami, Y. Konno and Y. Fujimoto, *Phot. Sci. Eng.*, **27**, 123 (1983).
- 7) J. Bargon, K. Tanaka and M. Yoshimine, "Computational Methods in Chemistry," ed. by I. Bargon, Plenum, New York, 1980, p. 239.
- 8) K. Tanaka and M. Yoshimine, *J. Am. Chem. Soc.*, **102**, 7655 (1980); D. E. M. Siegbahn, M. Yoshimine and J. Pacansy, *J. Chem. Phys.*, **78**, 1384 (1983).
- 9) O. P. Strausz, R. K. Gosavi, A. S. Deves and I. G. Csizmadia, *J. Am. Chem. Soc.*, **98**, 4784 (1976).
- 10) O. P. Strausz, R. K. Gosavi and H. E. Gunning, *J. Chem. Phys.*, **67**, 3057 (1977).
- 11) S. A. Maltin and P. G. Sanames, *J. Chem. Soc., Perkin Trans. 1*, **1972**, 2623.
- 12) G. Frater and O. P. Strausz, *J. Am. Chem. Soc.*, **92**, 6654 (1970).
- 13) K. P. Zeller, H. Meier, H. Kolshorn and E. Muller, *Chem. Ber.*, **105**, 1875 (1972).
- 14) I. G. Csizmadia, J. Font and O. P. Strausz, *J. Am. Chem. Soc.*, **90**, 7360 (1968).
- 15) O. Süs, *Justus Liebigs Ann. Chem.*, **556**, 65, 85 (1944).
- 16) H. Zollinger, "Diazo and Azo Chemistry," 1961, p. 171.
- 17) L. Wolff, *Justus Liebigs Ann. Chem.*, **325**, 129 (1902); *idem, ibid.*, **394**, 24 (1912).
- 18) C. G. Wilson, "Introduction to Microlithography," ed. by L. F. Thompson, C. G. Wilson and M. J. Bowden, American Chemical Society, Washington D.C., 1983, p. 115.
- 19) Z. Majerski and C. S. Redvanly, *J. Chem. Soc., Chem. Commun.*, **1972**, 694.
- 20) K. P. Zeller, *J. Chem. Soc., Chem. Commun.*, **1975**, 317.
- 21) a) K. Fukui, *J. Phys. Chem.*, **74**, 4161 (1970); b) K. Fukui, S. Kato and H. Fujimoto, *J. Am. Chem. Soc.*, **97**, 1 (1975).
- 22) K. Ishida, K. Morokuma and A. Komornicki, *J. Chem. Phys.*, **66**, 2153 (1977).
- 23) S. Oikawa, M. Tsuda, Y. Okamura and T. Urabe, *J. Am. Chem. Soc.*, **106**, 6751 (1984).
- 24) R. C. Bingham, M. J. S. Dewar and D. H. Lo, *J. Am. Chem. Soc.*, **97**, 1285 (1975).
- 25) M. Tsuda and S. Oikawa, *Phot. Sci. Eng.*, **23**, 177 (1979).
- 26) C. Nagata, "Mechanism of Carcinogenesis (in Japanese)," Science-Sha, Tokyo, 1982, p. 86.

[Chem. Pharm. Bull.]  
[35(1) 9-22 (1987)]

**Dioxopyrrolines. XXXVI.<sup>1)</sup> [2+2] Photocycloaddition Reaction of  
4-Ethoxycarbonyl-5-phenyl-1*H*-pyrrole-2,3-dione to Acyclic  
Olefins. Structural and Stereochemical Assignment  
of the Photocycloadducts**

TAKEHIRO SANO,<sup>\*,a</sup> YOSHIE HORIGUCHI,<sup>a</sup> YOSHISUKE TSUDA,<sup>\*,b</sup>  
KIMIO FURUHATA,<sup>c</sup> HIROAKI TAKAYANAGI,<sup>c</sup>  
and HARUO OGURA<sup>c</sup>

*Showa College of Pharmaceutical Sciences,<sup>a</sup> Tsurumaki, Setagaya-ku, Tokyo 154, Japan,  
Faculty of Pharmaceutical Sciences, Kanazawa University,<sup>b</sup> 13-1 Takara-machi,  
Kanazawa 920, Japan, and School of Pharmaceutical Sciences,  
Kitasato University,<sup>c</sup> Minato-ku, Tokyo 108, Japan*

(Received May 8, 1986)

The photocycloaddition of the dioxopyrroline **1** to olefins with electron donating substituents proceeded with regio- and stereo-selectivity to give the 7-substituted 2-azabicyclo[3.2.0]heptane-3,4-diones **2** and **3**, together with, in a few instances, the dihydropyridone **4**. The stereochemistries of the [2+2] adducts were dependent on the nature of the olefins. Olefins carrying phenyl, vinyl, and alkyl substituents afforded the *exo*-adducts **2**, while olefins carrying an *O*-substituent afforded the *endo*-adducts **3**, predominantly. The structures of these cycloadducts were established by X-ray crystallographic analyses, chemical correlations, and spectroscopic means.

**Keywords**—photocycloaddition; 1*H*-pyrrole-2,3-dione; dioxopyrrolone; 2-azabicyclo[3.2.0]-heptane-3,4-dione; electron rich olefin; stereochemistry; [2+2] cycloadduct; X-ray analysis

2*H*-Pyrrole-2,3-dione (dioxopyrrolone) has been proved to be a versatile synthon for a variety of heterocycles. Diels-Alder reaction of dioxopyrrolone with butadienes gave hydroindoles,<sup>2)</sup> providing the key step in our total syntheses of Amaryllidaceae<sup>3)</sup> and Erythrina<sup>4)</sup> alkaloids. [2+2] Photocycloaddition of dioxopyrrolone with olefins gave 2-azabicyclo[3.2.0]heptane-3,4-diones, which are useful intermediates to other heterocycles such as azatropolones<sup>5)</sup> and dihydropyridines.<sup>6)</sup> In this paper, we describe in detail the photocycloaddition reactions of the dioxopyrrolone **1** to various acyclic olefins and the structural and stereochemical assignment of the photocycloadducts.

### Results and Discussion

Irradiation of a solution of the dioxopyrrolone **1** with various olefins in dimethoxyethane (DME) with  $\geq 300$  nm light gave two stereoisomeric cyclobutanes **2** and **3**, together with, in some instances, a minute amount of the dihydropyridone **4**. The results are collected in Table I. The ratio of each product was determined by chromatographic isolation or by inspection of the C<sub>7</sub>-H signal and/or methyl signal of COOCH<sub>2</sub>CH<sub>3</sub> in the <sup>1</sup>H-nuclear magnetic resonance (<sup>1</sup>H-NMR) spectrum of the product mixture. The yields of cyclobutanes and the ratios of stereoisomers were found to be greatly affected by the nature of the olefins. Olefins possessing electron-donating substituents (ethoxyethylene, isobutoxyethylene, cyclohexyloxyethylene, phenoxyethylene, vinyl acetate, isopropenyl acetate, and phenylthioethylene) smoothly underwent cycloaddition to **1** giving rise to the adducts with complete head-to-tail (HT)

regioselectivity and with high stereoselectivity. Olefins carrying  $\pi$ -substituents (styrene,  $\alpha$ -methylstyrene, butadiene, *cis*- and *trans*-pentadienes, and isoprene) also readily underwent cycloaddition in a regioselective manner to give the HT adducts, but with less stereoselectivity. Simple alkenes with a terminal double bond (1-butene) gave the cycloadducts in moderate yields. On the other hand, olefins possessing an electron-withdrawing group (methyl acrylate) and 1,2-substituted olefins (1,2-dichloroethylenes, 2-butenes, and 1-methyl-2-phenylethylene) did not undergo cycloaddition to **1** to any significant extent.

The structure and stereochemistry of the [2+2] adducts were elucidated as follows. Similar photoaddition of *N*-4'-bromophenyldioxopyrroline **5** to styrene gave a cycloadduct **6** as the sole isolable product. Butadiene also underwent cycloaddition to **5**, affording **7**. The structures of **6** and **7** were firmly established by X-ray crystallographic analysis as shown in Figs. 1 and 2, respectively,<sup>7)</sup> which indicate that they are the HT-adducts with *exo*-stereochemistry. Taking them as reference compounds, the <sup>1</sup>H-NMR spectra of the styrene

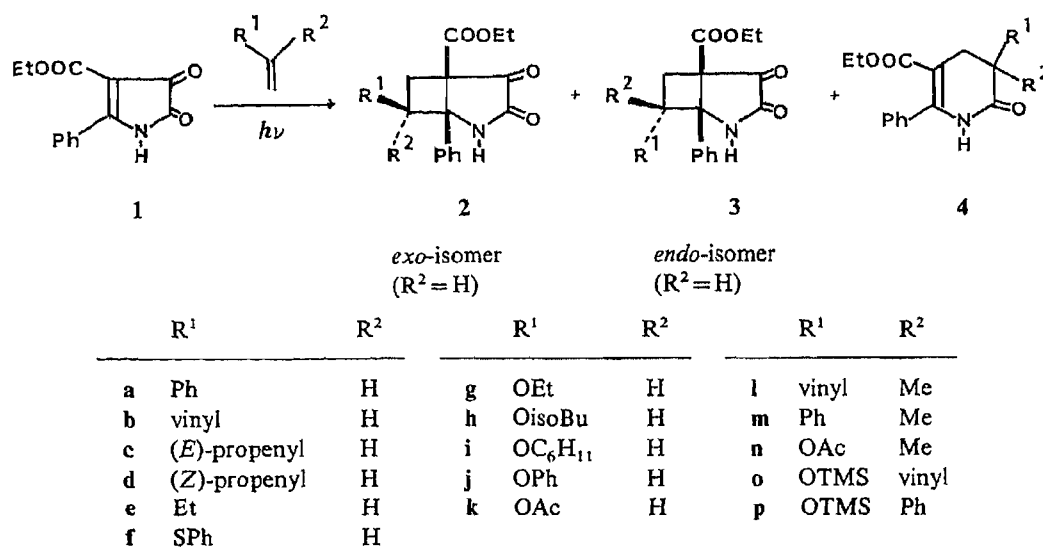
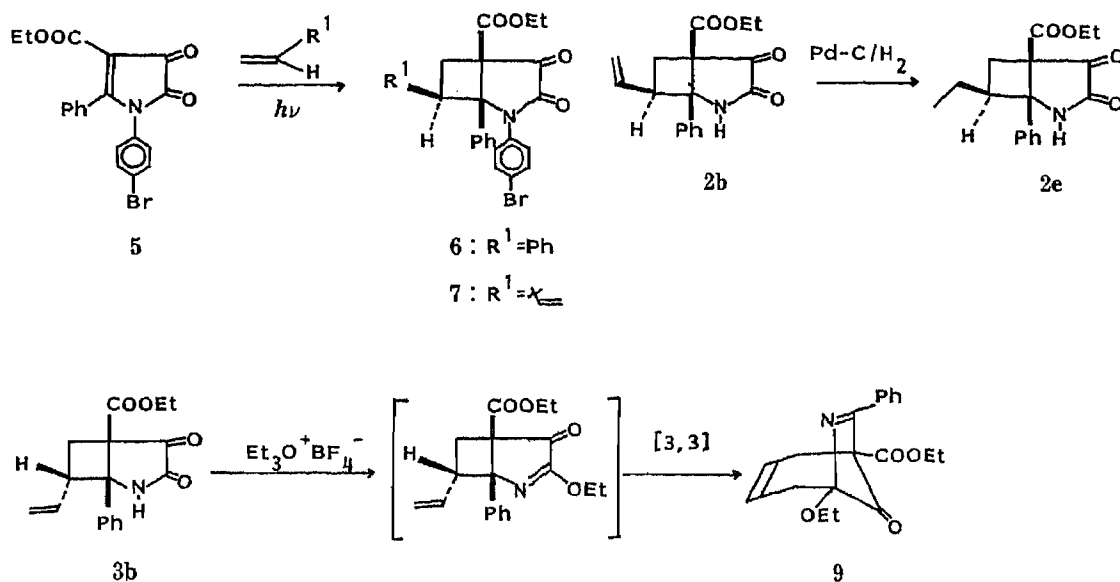


Chart 1

TABLE I. Yields (%) of Photoadducts of **1** to Olefins

Olefins	R <sup>1</sup>	R <sup>2</sup>	2	3	4
a Styrene	Ph	H	40	8	7
b Butadiene	Vinyl	H	48	20	2
c ( <i>E</i> )-1,3-Pentadiene	( <i>E</i> )-Propenyl	H	35	20	—
d ( <i>Z</i> )-1,3-Pentadiene	( <i>Z</i> )-Propenyl	H	27	18	—
e 1-Butene	Et	H	27	3	—
f Phenylthioethylene	SPh	H	36	13	—
g Ethoxyethylene	OEt	H	6	62	—
h Isobutoxyethylene	OisoBu	H	2	53	—
i Cyclohexyloxyethylene	OC <sub>6</sub> H <sub>11</sub>	H	—	67	4
j Phenoxyethylene	OC <sub>6</sub> H <sub>5</sub>	H	—	62	3
k Vinyl acetate	OAc	H	6	63	—
l Isoprene	Vinyl	Me	60	—	—
m $\alpha$ -Methylstyrene	Ph	Me	12	15	2
n Isopropenyl acetate	OAc	Me	6	36	5
o 1-OTMS butadiene	OTMS	Vinyl	—	70 <sup>(10)</sup>	—
p $\alpha$ -OTMS styrene	OTMS	Ph	—	70	—

TABLE II. Chemical Shifts ( $\delta_{\text{H}}$ ) of Cyclobutane Ring Protons in  $\text{CDCl}_3$ 

Cyclobutanes	R <sup>1</sup>	C <sub>6</sub> -H ( <i>exo</i> ) <sup>a)</sup>	C <sub>6</sub> -H ( <i>endo</i> ) <sup>a)</sup>	C <sub>7</sub> -H
<b>6</b>	Ph	2.75	3.72	4.18
<b>2a</b>	Ph	2.76	3.56	4.17
<b>3a</b>	Ph	2.49	3.39	4.83
<b>7</b>	Vinyl	2.60	3.30	3.60
<b>2b</b>	Vinyl	2.47	3.16	3.40
<b>3b</b>	Vinyl	2.19	3.19	4.10

a) For details of the assignments, see the accompanying paper.

TABLE III. Product Ratios of 2/3 in Photocycloaddition and Base-Catalyzed Equilibration

Olefin	Photocycloaddition 2 ( <i>exo</i> )/3 ( <i>endo</i> )	Equilibration 2 ( <i>exo</i> )/3 ( <i>endo</i> )
<b>a</b> Styrene	5/1	1/> 100
<b>g</b> Ethoxyethylene	1/10	1/6.5
<b>k</b> Vinyl acetate	1/10	1/8
<b>n</b> Isopropenyl acetate	1/6 <sup>a)</sup>	1.5/1 <sup>a)</sup>

a) 2: OAc-*exo*, Me-*endo*. 3: OAc-*endo*, Me-*exo*.

adducts and the butadiene adducts to 1 were compared with the spectra of **6** and **7** (Table II). The major adduct **2a** formed from styrene had the same spectral patterns (for C<sub>6</sub>-methylene and C<sub>7</sub>-methine protons) as those of **6**, and the major adduct **2b** formed from butadiene had similar spectral patterns to those of **7**. Thus, both products were concluded to be the HT adducts and *exo*-isomers **2a** and **2b**.

The major product from 1-butene was also identified as an *exo* isomer **2e**, since it was identical with the dihydro derivative **2e** obtained by catalytic hydrogenation of **2b**. The above assignment of the stereochemistry was supported by the following evidence. Upon base

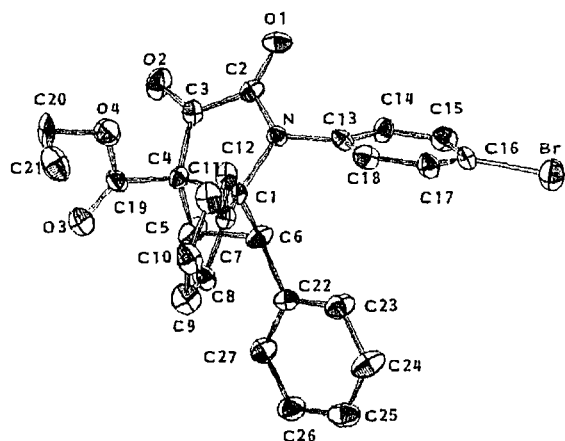


Fig. 1. Molecular Structure of Compound 6

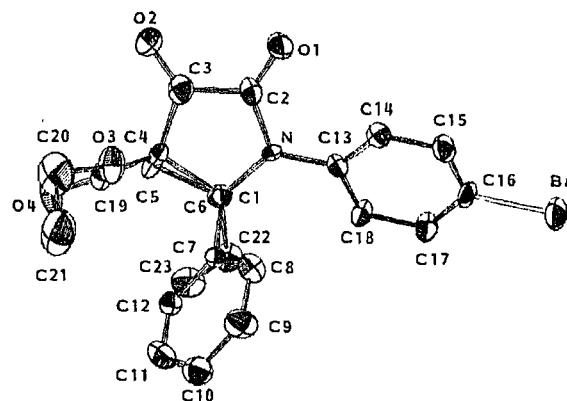


Fig. 2. Molecular Structure of Compound 7

treatment, the major adduct **2a** epimerized into an isomer which was found to be identical with the minor photoadduct **3a**, thus indicating that the latter is the thermodynamically more stable *endo*-isomer (Table III). The minor adduct **3b** formed from butadiene, when converted to the imidate **8**, underwent a [3, 3] sigmatropic rearrangement at room temperature to give an azanonane derivative **9** exclusively,<sup>81</sup> thus establishing the structure as the *endo*-isomer **3b**.

The *exo*- and *endo*-isomers are also distinguishable from their NMR spectra. In the <sup>1</sup>H-NMR spectra (Table IV), the C<sub>7</sub>-H (geminal to the substituent) of the *exo*-isomer **2a, b** (major product) resonates at higher field than that of the *endo*-isomer **3a, b** (minor product). The <sup>13</sup>C-NMR chemical shift of the 7-carbon also differentiates the two isomers; that of the *exo*-isomer resonates at lower field than that of the *endo*-isomer (Table IV). These relationships held for the adducts from olefins **c, d, e, and f**; the major products always gave the C<sub>7</sub>-H signals at higher field and 7-carbon signals at lower field than those of the corresponding minor products. Therefore, the major adducts from these olefins were concluded to be the *exo*-isomers **2** and the minor adducts to be the *endo*-isomers **3**. In contrast, the major adducts from olefins **g, h, and k** exhibit C<sub>7</sub>-H signals at lower field (by 0.6—0.9 ppm) and 7-carbon signals at higher field (by 9—10 ppm) than those of minor adducts. These olefins the major adducts are the *endo*-isomers **3** and the minor adducts are the *exo*-isomers **2**. The C<sub>7</sub>-H signals of the major adducts from olefins **i and j** appeared at lower field, comparable to those of **3g** and **3h** ( $\delta$  4.93 for **3i** and 5.36 for **3j**). Thus, they were concluded to be the *endo*-isomers. The above conclusion was confirmed by base-catalyzed epimerization experiments, where the major adduct from the olefins carrying an *O*-substituent was indicated to be the thermodynamically more stable *endo-O*-isomer **3** (Table III).

The adducts from 1,1-disubstituted olefins have no C<sub>7</sub>-H, and the difference of chemical shifts of the 7-carbon between the two isomers was too small to estimate their stereochemistry. The stereochemistries of the isopropenyl acetate adducts were clarified on the basis of a base-catalyzed equilibration experiment where the major product was shown to be thermodynamically less stable, thus proving that it is the *exo*-Me-*endo*-OAc isomer **3n**.<sup>91</sup> This assignment was supported by comparison of the chemical shift of the OAc group of each isomer with those of **2k** and **3k**; the signals of **2k** and **2n** appeared at  $\delta$  1.76 and 1.73, and those of **3k** and **3n** were at  $\delta$  2.10 and 2.05, respectively. In addition, the 6-*exo*-H signal of the minor adduct **2n** showed broadening ( $W_{1/2} = 1\text{--}2$  Hz), suggesting the presence of long-range coupling between 7-*endo*-Me and 6-*exo*-H, while the C<sub>6</sub>-protons of the major adduct **3n** appeared as a sharp doublet showing no long range coupling. The stereochemistry of two photoadducts **2m** and **3m** from  $\alpha$ -methylstyrene was elucidated from the fact that the 6-*exo*-H signal of **2m** showed a



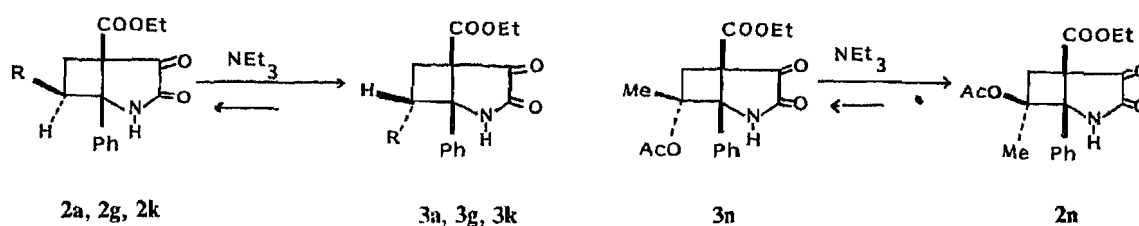


Chart 3

TABLE IV. Chemical Shifts of C<sub>7</sub>-H and C<sub>7</sub>-C in CDCl<sub>3</sub>

	$\delta_{\text{H}}$ of C <sub>7</sub> -H			$\delta_{\text{C}}$ of C <sub>7</sub> -C		
	2	3	$\Delta\delta_{\text{H}}$ (2-3)	2	3	$\Delta\delta_{\text{C}}$ (2-3)
a Ph	4.17	4.85	-0.66	54.3	43.3	11
b Vinyl	3.32	4.13	-0.79	52.1	41.6	10.5
c ( <i>E</i> )-Propenyl	3.3	4.04	-0.73	52.0	41.9	10.1
d ( <i>Z</i> )-Propenyl	3.5	4.33	-0.83	47.5	37.3	10.2
e Et	2.7	3.3	-0.6	52.1	42.7	9.3
f SPh	4.08	4.78	-0.70	56.1	48.6	7.5
g OEt	4.12	4.75	-0.63	83.3	75.6	7.7
h OisoBu	4.12	4.74	-0.62	83.2	75.1	8.1
i OC <sub>6</sub> H <sub>10</sub>	—	4.93	—	—	—	—
j OPh	—	5.36	—	—	—	—
k OAc	5.01	5.89	-0.88	—	—	—

long range coupling, while the C<sub>6</sub>-protons of **3m** appeared as a sharp double doublet. Isoprene gave a single adduct, whose 6-*exo*-H also showed long range coupling, thus suggesting that it is an *exo*-vinyl-*endo*-Me isomer **21**. The sole product from 1-trimethylsilyloxybutadiene was a 7-*exo*-vinyl-7-*endo*-OTMS derivative **3o**, the structure of which was unambiguously established by X-ray analysis.<sup>10)</sup>  $\alpha$ -Trimethylsilyloxystyrene also gave a single adduct which was identified, by analogy, as the 7-*exo*-phenyl-7-*endo*-OTMS isomer **3p**.

Summarizing the above results, the photocycloaddition of **1** to electron-rich olefins readily proceeded in a regioselective manner to give [2+2] adducts with HT-regiochemistry. The stereochemistry of the adducts is dependent on the nature of the olefins. Olefins carrying phenyl, vinyl, thiophenyl, and alkyl substituents afforded the *exo*-adducts **2**, while olefins carrying *O*-substituents such as alkoxy, acetoxy, and silyloxy groups afforded the *endo*-isomers **3**, predominantly.

The structure of the dihydropyridone **4** was elucidated by spectral comparisons<sup>6)</sup> with compound **11**, the photoproduct of **10** and cyclopentadiene, whose structure has been established by X-ray analysis.<sup>11)</sup>

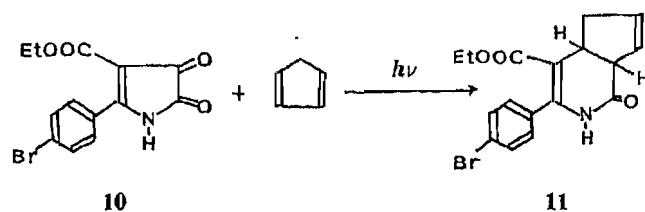


Chart 4

The detailed stereochemical pathways of this photocycloaddition reaction will be discussed in the accompanying paper.

### Experimental

Unless otherwise stated, the following procedures were adopted. Melting points were taken on a Yanagimoto micro hot-stage apparatus and are uncorrected. Infrared (IR) spectra were taken in Nujol mulls for solids and as liquid films for liquids with a Hitachi 260-10 spectrometer and are given in  $\text{cm}^{-1}$ . Ultraviolet (UV) spectra were recorded in dioxane with a Hitachi 200-10 spectrophotometer.  $^1\text{H-NMR}$  (100 MHz) and  $^{13}\text{C-NMR}$  (25.0 MHz) spectra were taken in  $\text{CDCl}_3$  solution with tetramethylsilane (TMS) as an internal standard on a JEOL FX-100 spectrometer. High-resolution mass spectra (MS) were recorded on a JEOL JMS-D300 mass spectrometer. For column chromatography, silica gel (Wako-gel C-200) was used. Thin layer chromatography (TLC) was performed on precoated Silica gel 60 F<sub>254</sub> plates (Merck). Medium-pressure liquid chromatography was performed on Kusano CIC prepacked silica gel columns. The photolysis solution was irradiated internally using a 300 W high-pressure mercury lamp (Eikosha Halos PIH 300) with a Pyrex filter.

#### General Procedure for the Photocycloaddition of 4-Ethoxycarbonyl-5-phenyl-1H-pyrrole-2,3-dione 1 to Olefins

A solution of **1** (3 g, 12 mmol) and an olefin (60 mmol) in dimethoxyethane (300 ml) was irradiated for 45 min under ice cooling. After removal of the solvent, the residue in benzene was chromatographed over silica gel. Elution with benzene gave the dihydropyridone **4**. Further elution with benzene- $\text{CH}_2\text{Cl}_2$  (1:1) gave a mixture of **2** and **3**, which were separated and purified by repeated recrystallization from hexane- $\text{CH}_2\text{Cl}_2$ -MeOH or by medium-pressure liquid column chromatography using hexane-AcOEt (3:1 and 1:1) as eluents.

#### Styrene Photoproducts

*rel*-(1*S*,5*R*,7*R*)-5-Ethoxycarbonyl-1,7-diphenyl-2-azabicyclo[3.2.0]heptane-3,4-dione (**2a**)—Colorless prisms, mp 202–204 °C. 1700 mg, 40%. IR: 1770, 1730, 1720. UV  $\lambda_{\text{max}}$  nm ( $\epsilon$ ): 260 (3900).  $^1\text{H-NMR}$   $\delta$ : 0.64 (3H, t,  $J=7$  Hz,  $\text{COOCH}_2\text{CH}_3$ ), 2.70 (1H, dd,  $J=10, 11$  Hz,  $\text{C}_6\text{-H}$ ), 3.56 (1H, t,  $J=11$  Hz,  $\text{C}_6\text{-H}$ ), 3.74 (2H, q,  $J=7$  Hz,  $\text{COOCH}_2\text{CH}_3$ ), 4.17 (1H, t,  $J=10$  Hz,  $\text{C}_7\text{-H}$ ), 7.1 (10H, m, Ar-H).  $^{13}\text{C-NMR}$  (ppm): 13.4 (q), 24.8 (t,  $\text{C}_6$ ), 54.3 (d,  $\text{C}_7$ ), 58.6 (s,  $\text{C}_3$ ), 61.9 (t), 69.4 (s,  $\text{C}_1$ ), 126.4 (d, 2C), 126.9 (d), 127.3 (d, 2C), 128.0 (d, 3C), 128.3 (d, 2C), 133.3 (s), 136.7 (s), 162.8 (s,  $\text{C}_3$ ), 165.7 (s), 196.7 (s,  $\text{C}_4$ ). Anal. Calcd for  $\text{C}_{21}\text{H}_{19}\text{NO}_4$ : C, 72.19; H, 5.48; N, 4.01. MS  $m/z$ : 349.1313. Found: C, 72.12; H, 5.28; N, 3.98. MS  $m/z$ : 349.1310.

*rel*-(1*S*,5*R*,7*S*)-5-Ethoxycarbonyl-1,7-diphenyl-2-azabicyclo[3.2.0]heptane-3,4-dione (**3a**)—Colorless prisms, mp 180–183 °C. 380 mg, 8%. IR: 1780, 1745, 1720. UV  $\lambda_{\text{max}}$  nm ( $\epsilon$ ): 255 (3600).  $^1\text{H-NMR}$   $\delta$ : 0.73 (3H, t,  $J=7$  Hz,  $\text{COOCH}_2\text{CH}_3$ ), 2.49 (1H, dd,  $J=9, 13$  Hz,  $\text{C}_6\text{-H}$ ), 3.39 (1H, dd,  $J=9, 13$  Hz,  $\text{C}_6\text{-H}$ ), 3.79 (2H, q,  $J=7$  Hz,  $\text{COOCH}_2\text{CH}_3$ ), 4.83 (1H, t,  $J=9$  Hz,  $\text{C}_7\text{-H}$ ), 7.1 (10H, m, Ar-H).  $^{13}\text{C-NMR}$  (ppm): 13.5 (q), 26.3 (t,  $\text{C}_6$ ), 43.3 (d,  $\text{C}_7$ ), 58.9 (s,  $\text{C}_3$ ), 62.1 (t), 66.8 (s,  $\text{C}_1$ ), 126.3 (d), 126.5 (d), 127.2 (d), 127.3 (d), 128.8 (d, 3C), 128.9 (d, 3C), 136.1 (s), 137.0 (s), 161.4 (s,  $\text{C}_3$ ), 166.4 (s), 193.7 (s,  $\text{C}_4$ ). Anal. Calcd for  $\text{C}_{21}\text{H}_{19}\text{NO}_4$ : C, 72.19; H, 5.48; N, 4.01. MS  $m/z$ : 349.1313. Found: C, 72.43; H, 5.40; N, 3.81. MS  $m/z$ : 349.1310.

5-Ethoxycarbonyl-3,6-diphenyl-3,4-dihydropyridin-2(1*H*)-one (**4a**)—Colorless needles, mp 134–136 °C. 92 mg, 7%. IR: 3200, 3100, 1690, 1670, 1640, 1600. UV  $\lambda_{\text{max}}$  nm ( $\epsilon$ ): 230 (10400), 283 (10300).  $^1\text{H-NMR}$   $\delta$ : 0.90 (3H, t,  $J=7$  Hz,  $\text{COOCH}_2\text{CH}_3$ ), 3.08 (1H, d,  $J=10$  Hz,  $\text{C}_4\text{-H}$ ), 3.14 (1H, d,  $J=7.5$  Hz,  $\text{C}_4\text{-H}$ ), 3.81 (1H, dd,  $J=7.5, 10$  Hz,  $\text{C}_3\text{-H}$ ), 3.93 (2H, q,  $J=7$  Hz,  $\text{COOCH}_2\text{CH}_3$ ), 7.3 (10H, m, Ar-H). Anal. Calcd for  $\text{C}_{20}\text{H}_{19}\text{NO}_3$ : C, 74.74; H, 5.96; N, 4.36. MS  $m/z$ : 321.1356. Found: C, 74.56; H, 5.75; N, 4.28. MS  $m/z$ : 321.1366.

#### Butadiene Photoproducts

*rel*-(1*S*,5*R*,7*R*)-5-Ethoxycarbonyl-1-phenyl-7-vinyl-2-azabicyclo[3.2.0]heptane-3,4-dione (**2b**)—Colorless plates, mp 165–166 °C. 1740 mg, 47.5%. IR: 3250, 1770, 1760, 1745, 1705. UV  $\lambda_{\text{max}}$  nm ( $\epsilon$ ): 262 (6800).  $^1\text{H-NMR}$   $\delta$ : 0.68 (3H, t,  $J=7$  Hz,  $\text{COOCH}_2\text{CH}_3$ ), 2.47 (1H, dd,  $J=9, 12$  Hz,  $\text{C}_6\text{-H}$ ), 3.16 (1H, dd,  $J=10, 12$  Hz,  $\text{C}_6\text{-H}$ ), 3.3–3.5 (1H, m,  $\text{C}_7\text{-H}$ ), 3.72 (2H, q,  $J=7$  Hz,  $\text{COOCH}_2\text{CH}_3$ ), 5.12 (1H, d,  $J=10$  Hz), 5.12 (1H, d,  $J=18$  Hz), 5.74 (1H, ddd,  $J=5, 10, 18$  Hz) olefinic-H, 7.2–7.4 (5H, m, Ar-H).  $^{13}\text{C-NMR}$  (ppm): 13.4 (q), 25.8 (t,  $\text{C}_6$ ), 52.1 (d,  $\text{C}_7$ ), 58.8 (s,  $\text{C}_3$ ), 61.9 (t), 68.2 (s,  $\text{C}_1$ ), 117.3 (t), 126.3 (d, 2C), 128.3 (d, 3C), 133.9 (s), 135.4 (d), 162.3 (s,  $\text{C}_3$ ), 165.9 (s), 196.7 (s,  $\text{C}_4$ ). Anal. Calcd for  $\text{C}_{17}\text{H}_{17}\text{NO}_4$ : C, 68.21; H, 5.73; N, 4.68. MS  $m/z$ : 299.1158. Found: C, 68.18; H, 5.61; N, 4.66. MS  $m/z$ : 299.1163.

*rel*-(1*S*,5*R*,7*S*)-5-Ethoxycarbonyl-1-phenyl-7-vinyl-2-azabicyclo[3.2.0]heptane-3,4-dione (**3b**)—Colorless prisms, mp 134–136 °C. 732 mg, 20%. IR: 3160, 3060, 1765, 1740, 1720. UV  $\lambda_{\text{max}}$  nm ( $\epsilon$ ): 257 (3500).  $^1\text{H-NMR}$   $\delta$ : 0.72 (3H, t,  $J=7$  Hz,  $\text{COOCH}_2\text{CH}_3$ ), 2.19 (1H, dd,  $J=8, 13$  Hz,  $\text{C}_6\text{-H}$ ), 3.19 (1H, dd,  $J=9, 13$  Hz,  $\text{C}_6\text{-H}$ ), 3.75 (2H, oct.,  $J=1, 7$  Hz,  $\text{COOCH}_2\text{CH}_3$ ), 3.98–4.24 (1H, m,  $\text{C}_7\text{-H}$ ), 5.18 (1H, d,  $J=17$  Hz), 5.28 (1H, d,  $J=11$  Hz), 5.94 (1H, ddd,  $J=6, 11, 17$  Hz) olefinic-H; 7.3–7.4 (5H, m, Ar-H).  $^{13}\text{C-NMR}$  (ppm): 13.4 (q), 26.2 (t,  $\text{C}_6$ ), 42.7 (d,  $\text{C}_7$ ), 58.5 (s,  $\text{C}_3$ ), 61.9 (t), 66.2 (s,  $\text{C}_1$ ), 119.1 (t), 126.1 (d, 2C), 128.8 (d, 2C), 128.9 (d), 133.6 (d), 136.6 (s), 162.2 (s,  $\text{C}_3$ ), 166.2 (s), 194.4 (s,  $\text{C}_4$ ). Anal. Calcd for  $\text{C}_{17}\text{H}_{17}\text{NO}_4$ : C, 68.21; H, 5.73; N, 4.68. MS  $m/z$ : 299.1158. Found: C, 68.27; H, 5.69; N, 4.69. MS  $m/z$ : 299.1178.

5-Ethoxycarbonyl-6-phenyl-3-vinyl-3,4-dihydropyridin-2(1*H*)-one (**4b**)—Colorless needles, mp 111–112 °C. 22 mg, 2%. IR: 3350, 3300, 1715, 1660, 1600. UV  $\lambda_{\text{max}}$  nm ( $\epsilon$ ): 286 (9600).  $^1\text{H-NMR}$   $\delta$ : 0.93 (3H, t,  $J=7$  Hz,  $\text{COOCH}_2\text{CH}_3$ ), 2.7–2.8 (2H, m,  $\text{C}_4\text{-H}$ ), 3.1–3.4 (1H, m,  $\text{C}_3\text{-H}$ ), 3.93 (2H, q,  $J=7$  Hz,  $\text{COOCH}_2\text{CH}_3$ ), 5.1–5.4 (2H, m), 5.8–6.3 (1H, m) olefinic-H, 7.35 (5H, m, Ar-H). MS  $m/z$ :  $\text{M}^+$  Calcd for  $\text{C}_{16}\text{H}_{17}\text{NO}_3$  271.1206. Found: 271.1190.

**(E)-Penta-1,3-diene Photoproducts**

*rel*-(1*S*,5*R*,7*R*)-5-Ethoxycarbonyl-1-phenyl-7-(*E*)-propenyl-2-azabicyclo[3.2.0]heptane-3,4-dione (**2c**)—Colorless needles, mp 165–166 °C. 1340 mg, 35%. IR: 1770, 1735 sh, 1725. UV  $\lambda_{\max}^{\text{EtOH}}$  nm ( $\epsilon$ ): 264 (2900).  $^1\text{H-NMR}$   $\delta$ : 0.70 (3H, t,  $J=7$  Hz,  $\text{COOCH}_2\text{CH}_3$ ), 1.47 (3H, d,  $J=6$  Hz, C- $\text{CH}_3$ ), 2.56 (1H, dd,  $J=10, 13$  Hz,  $\text{C}_6$ -H), 3.02 (1H, dd,  $J=10, 13$  Hz,  $\text{C}_6$ -H), 3.4–3.6 (1H, m,  $\text{C}_7$ -H), 3.72 (2H, q,  $J=7$  Hz,  $\text{COOCH}_2\text{CH}_3$ ), 5.4–5.5 (2H, m, olefinic-H), 7.35 (5H, s, Ar-H).  $^{13}\text{C-NMR}$  (ppm): 13.4 (q), 17.9 (q), 26.6 (t,  $\text{C}_6$ ), 52.0 (d,  $\text{C}_7$ ), 58.8 (s,  $\text{C}_5$ ), 61.9 (t), 68.4 (s,  $\text{C}_1$ ), 126.2 (d, 2C), 128.2 (d), 128.3 (d, 3C), 128.9 (d), 133.9 (s), 162.1 (s,  $\text{C}_3$ ), 166.0 (s), 196.6 (s,  $\text{C}_4$ ). *Anal.* Calcd for  $\text{C}_{18}\text{H}_{19}\text{NO}_4$ : C, 68.99; H, 6.11; N, 4.47. MS  $m/z$ : 313.1314. Found: C, 68.86; H, 6.08; N, 4.40. MS  $m/z$ : 313.1299.

*rel*-(1*S*,5*R*,7*S*)-5-Ethoxycarbonyl-1-phenyl-7-(*E*)-propenyl-2-azabicyclo[3.2.0]heptane-3,4-dione (**3c**)—Colorless needles, mp 152–156 °C. 770 mg, 20%. IR: 1760, 1740, 1720. UV  $\lambda_{\max}^{\text{EtOH}}$  nm ( $\epsilon$ ): 258 (3200).  $^1\text{H-NMR}$   $\delta$ : 0.73 (3H, t,  $J=7$  Hz,  $\text{COOCH}_2\text{CH}_3$ ), 1.62 (3H, d,  $J=7$  Hz, C- $\text{CH}_3$ ), 2.07 (1H, dd,  $J=8, 13$  Hz,  $\text{C}_6$ -H), 3.32 (1H, dd,  $J=10, 13$  Hz,  $\text{C}_6$ -H), 3.82 (2H, q,  $J=7$  Hz,  $\text{COOCH}_2\text{CH}_3$ ), 4.33 (1H, m,  $\text{C}_7$ -H), 5.3–5.8 (2H, m, olefinic-H), 7.39 (5H, br s, Ar-H), 8.53 (1H, br s, NH).  $^{13}\text{C-NMR}$  (ppm): 13.4 (q), 18.0 (q), 27.4 (t,  $\text{C}_6$ ), 41.9 (d,  $\text{C}_7$ ), 58.8 (s,  $\text{C}_5$ ), 61.9 (t), 66.4 (s,  $\text{C}_1$ ), 126.2 (d, 2C), 126.6 (d), 128.8 (d, 2C), 128.9 (d), 130.6 (d), 137.0 (s), 161.9 (s,  $\text{C}_3$ ), 166.3 (s), 194.4 (s,  $\text{C}_4$ ). *Anal.* Calcd for  $\text{C}_{18}\text{H}_{19}\text{NO}_4$ : C, 68.99; H, 6.11; N, 4.47. MS  $m/z$ : 313.1314. Found: C, 69.05; H, 6.06; N, 4.40. MS  $m/z$ : 313.1322.

**(Z)-Penta-1,3-diene Photoproducts**

*rel*-(1*S*,5*R*,7*R*)-5-Ethoxycarbonyl-1-phenyl-7-(*Z*)-propenyl-2-azabicyclo[3.2.0]heptane-3,4-dione (**2d**)—Colorless needles, mp 158–162 °C. 1034 mg, 27%. IR: 1770, 1740, 1720. UV  $\lambda_{\max}^{\text{EtOH}}$  nm ( $\epsilon$ ): 262 (3200).  $^1\text{H-NMR}$   $\delta$ : 0.68 (3H, t,  $J=7$  Hz,  $\text{COOCH}_2\text{CH}_3$ ), 1.60 (3H, d,  $J=5$  Hz, C- $\text{CH}_3$ ), 2.45 (1H, dd,  $J=9, 12$  Hz,  $\text{C}_6$ -H), 3.08 (1H, dd,  $J=10, 12$  Hz,  $\text{C}_6$ -H), 3.2–3.4 (1H, m,  $\text{C}_7$ -H), 3.78 (2H, q,  $J=7$  Hz,  $\text{COOCH}_2\text{CH}_3$ ), 5.2–5.7 (2H, m, olefinic-H), 7.35 (5H, s, Ar-H).  $^{13}\text{C-NMR}$  (ppm): 13.4 (q), 14.1 (q), 28.3 (t,  $\text{C}_6$ ), 47.5 (d,  $\text{C}_7$ ), 59.0 (s,  $\text{C}_5$ ), 61.9 (t), 69.5 (s,  $\text{C}_1$ ), 126.0 (d, 2C), 128.3 (d, 4C), 128.7 (d), 134.0 (s), 162.3 (s,  $\text{C}_3$ ), 166.0 (s), 196.7 (s,  $\text{C}_4$ ). *Anal.* Calcd for  $\text{C}_{18}\text{H}_{19}\text{NO}_4$ : C, 68.99; H, 6.11; N, 4.47. MS  $m/z$ : 313.1315. Found: C, 68.91; H, 6.05; N, 4.39. MS  $m/z$ : 313.1297.

*rel*-(1*S*,5*R*,7*S*)-5-Ethoxycarbonyl-1-phenyl-7-(*Z*)-propenyl-2-azabicyclo[3.2.0]heptane-3,4-dione (**3d**)—Colorless needles, mp 121–125 °C. 690 mg, 18%. IR: 1760, 1735, 1715. UV  $\lambda_{\max}^{\text{EtOH}}$  nm ( $\epsilon$ ): 259 (3100).  $^1\text{H-NMR}$   $\delta$ : 0.73 (3H, t,  $J=7$  Hz,  $\text{COOCH}_2\text{CH}_3$ ), 1.71 (3H, d,  $J=5$  Hz, C- $\text{CH}_3$ ), 2.14 (1H, dd,  $J=8.5, 13$  Hz,  $\text{C}_6$ -H), 3.20 (1H, dd,  $J=9.5, 13$  Hz,  $\text{C}_6$ -H), 3.85 (2H, q,  $J=7$  Hz,  $\text{COOCH}_2\text{CH}_3$ ), 4.03 (1H, m,  $\text{C}_7$ -H), 5.3–5.8 (2H, m, olefinic-H), 7.37 (5H, s, Ar-H), 8.52 (1H, br s, NH).  $^{13}\text{C-NMR}$  (ppm): 13.3 (q), 14.1 (q), 28.9 (t,  $\text{C}_6$ ), 37.3 (d,  $\text{C}_7$ ), 58.9 (s,  $\text{C}_5$ ), 61.9 (t), 66.6 (s,  $\text{C}_1$ ), 125.9 (d, 2C), 126.4 (d), 128.2 (d), 128.8 (d, 2C), 129.8 (d), 136.9 (s), 162.0 (s,  $\text{C}_3$ ), 166.3 (s), 194.6 (s,  $\text{C}_4$ ). MS  $m/z$ :  $\text{M}^+$  Calcd for  $\text{C}_{18}\text{H}_{19}\text{NO}_4$  331.1056. Found: 331.1071.

**1-Butene Photoproducts**

*rel*-(1*S*,5*R*,7*S*)-5-Ethoxycarbonyl-7-ethyl-1-phenyl-2-azabicyclo[3.2.0]heptane-3,4-dione (**2e**)—Colorless prisms, mp 156–158 °C. 1365 mg, 27%. IR: 3170, 1775, 1740, 1720. UV  $\lambda_{\max}$  nm ( $\epsilon$ ): 262 (3200).  $^1\text{H-NMR}$   $\delta$ : 0.66 (3H, t,  $J=7$  Hz,  $\text{CH}_2\text{CH}_3$ ), 0.73 (3H, t,  $J=7$  Hz,  $\text{COOCH}_2\text{CH}_3$ ), 1.39 (2H, quint,  $J=7$  Hz,  $\text{CH}_2\text{CH}_3$ ), 2.3–2.8 (3H, m,  $\text{C}_6$ -H,  $\text{C}_7$ -H), 3.85 (2H, q,  $J=7$  Hz,  $\text{COOCH}_2\text{CH}_3$ ), 7.4 (5H, m, Ar-H).  $^{13}\text{C-NMR}$  (ppm): 10.9 (q), 13.4 (q), 24.1 (t), 27.5 (t,  $\text{C}_6$ ), 52.1 (d,  $\text{C}_7$ ), 58.5 (s,  $\text{C}_5$ ), 61.8 (t), 67.8 (s,  $\text{C}_1$ ), 125.6 (d, 2C), 128.3 (d, 3C), 134.0 (s), 162.4 (s,  $\text{C}_3$ ), 166.3 (s), 197.0 (s,  $\text{C}_4$ ). *Anal.* Calcd for  $\text{C}_{17}\text{H}_{19}\text{NO}_4$ : C, 67.76; H, 6.36; N, 4.65. MS  $m/z$ : 301.1315. Found: C, 67.50; H, 6.42; N, 4.64. MS  $m/z$ : 301.1330.

*rel*-(1*S*,5*R*,7*R*)-5-Ethoxycarbonyl-7-ethyl-1-phenyl-2-azabicyclo[3.2.0]heptane-3,4-dione (**3e**)—Colorless prisms, mp 136–140 °C. 140 mg, 2.8%. IR: 3150, 1760, 1735 sh, 1720. UV  $\lambda_{\max}$  nm ( $\epsilon$ ): 258 (3550).  $^1\text{H-NMR}$   $\delta$ : 0.72 (3H, t,  $J=7$  Hz,  $\text{CH}_2\text{CH}_3$ ), 0.90 (3H, t,  $J=7$  Hz,  $\text{COOCH}_2\text{CH}_3$ ), 1.4–1.9 (2H, m,  $\text{CH}_2\text{CH}_3$ ), 1.65 (1H, m,  $\text{C}_6$ -H), 3.20 (1H, m,  $\text{C}_6$ -H), 3.33 (1H, m,  $\text{C}_7$ -H), 3.74 (2H, q,  $J=7$  Hz,  $\text{COOCH}_2\text{CH}_3$ ), 7.4 (5H, s, Ar-H).  $^{13}\text{C-NMR}$  (ppm): 11.0 (q), 13.4 (q), 24.2 (t), 27.5 (t,  $\text{C}_6$ ), 41.6 (d,  $\text{C}_7$ ), 58.7 (s,  $\text{C}_5$ ), 61.9 (t), 65.7 (s,  $\text{C}_1$ ), 126.0 (d, 3C), 128.7 (d, 2C), 137.1 (s), 162.7 (s,  $\text{C}_3$ ), 166.3 (s), 195.0 (s,  $\text{C}_4$ ). *Anal.* Calcd for  $\text{C}_{17}\text{H}_{19}\text{NO}_4$ : C, 67.76; H, 6.36; N, 4.65. MS  $m/z$ : 301.1315. Found: C, 67.45; H, 6.39; N, 4.74. MS  $m/z$ : 301.1337.

**Phenylthioethylene Photoproducts**

*rel*-(1*S*,5*R*,7*S*)-5-Ethoxycarbonyl-1-phenyl-7-phenylthio-2-azabicyclo[3.2.0]heptane-3,4-dione (**2f**)—Colorless needles, mp 183–186 °C. 1680 mg, 36%. IR: 1770, 1740, 1720. UV  $\lambda_{\max}$  nm ( $\epsilon$ ): 256 (5400).  $^1\text{H-NMR}$   $\delta$ : 0.67 (3H, t,  $J=7$  Hz,  $\text{COOCH}_2\text{CH}_3$ ), 3.14 (1H, dd,  $J=10, 13.5$  Hz,  $\text{C}_6$ -H), 3.80 (2H, q,  $J=7$  Hz,  $\text{COOCH}_2\text{CH}_3$ ), 4.08 (1H, t,  $J=10$  Hz,  $\text{C}_7$ -H), 7.0–7.2 (5H, m, Ar-H), 7.4 (5H, br s, Ar-H).  $^{13}\text{C-NMR}$  (ppm): 13.4 (q), 29.4 (s,  $\text{C}_6$ ), 56.1 (d,  $\text{C}_7$ ), 59.1 (s,  $\text{C}_5$ ), 62.2 (t), 69.5 (s,  $\text{C}_1$ ), 126.5 (d, 2C), 127.4 (d), 128.2 (d, 2C), 128.9 (d), 129.2 (d, 2C), 130.7 (d, 2C), 132.7 (s), 134.3 (s), 161.7 (s,  $\text{C}_3$ ), 165.3 (s), 195.4 (s,  $\text{C}_4$ ). *Anal.* Calcd for  $\text{C}_{21}\text{H}_{19}\text{NO}_4\text{S}$ : C, 66.12; H, 5.02; N, 3.67. MS  $m/z$ : 381.1035. Found: C, 66.04; H, 4.81; N, 3.58. MS  $m/z$ : 381.1058.

*rel*-(1*S*,5*R*,7*R*)-5-Ethoxycarbonyl-1-phenyl-7-phenylthio-2-azabicyclo[3.2.0]heptane-3,4-dione (**3f**)—Colorless prisms, mp 157–159 °C. 605 mg, 13%. IR: 1770, 1740 sh, 1725. UV  $\lambda_{\max}$  nm ( $\epsilon$ ): 253 (6000).  $^1\text{H-NMR}$   $\delta$ : 0.73 (3H, t,  $J=7$  Hz,  $\text{COOCH}_2\text{CH}_3$ ), 2.16 (1H, dd,  $J=7, 14$  Hz,  $\text{C}_6$ -H), 3.53 (1H, dd,  $J=9.5, 14$  Hz,  $\text{C}_6$ -H), 3.76 (2H, q,  $J=7$  Hz,  $\text{COOCH}_2\text{CH}_3$ ), 4.78 (1H, dd,  $J=9.5, 14$  Hz,  $\text{C}_7$ -H), 7.18 (5H, s, Ar-H), 7.36 (5H, s, Ar-H), 8.80 (1H, br s, NH).  $^{13}\text{C-NMR}$  (ppm): 13.4 (q), 29.9 (t,  $\text{C}_6$ ), 48.6 (d,  $\text{C}_7$ ), 59.1 (s,  $\text{C}_5$ ), 62.1 (t), 67.0 (s,  $\text{C}_1$ ), 125.9 (d, 2C), 127.5 (d), 129.0 (d, 2C), 129.2 (d), 129.4 (d, 2C), 130.6 (d, 2C), 133.6 (s), 136.0 (s), 161.7 (s,  $\text{C}_3$ ), 165.7 (s), 193.6 (s,  $\text{C}_4$ ). *Anal.* Calcd for

$C_{21}H_{19}NO_4S$ : C, 66.12; H, 5.02; N, 3.67. MS  $m/z$ : 381.1035. Found: C, 66.07; H, 4.92; N, 3.39. MS  $m/z$ : 381.1036.

#### Ethoxyethylene Photoproducts

*rel*-(1*S*,5*R*,7*S*)-7-Ethoxy-5-ethoxycarbonyl-1-phenyl-2-azabicyclo[3.2.0]heptane-3,4-dione (2g)——Colorless prisms, mp 149—152 °C. 225 mg, 5.8%. IR: 1760, 1740, 1725. UV  $\lambda_{max}$  nm ( $\epsilon$ ): 262 (2300).  $^1H$ -NMR  $\delta$ : 0.68 (3H,  $J=7$  Hz,  $COOCH_2CH_3$ ), 0.94 (3H, t,  $J=7$  Hz,  $OCH_2CH_3$ ), 2.59 (1H, dd,  $J=8, 14$  Hz,  $C_6-H$ ), 3.15 (1H, dd,  $J=8, 14$  Hz,  $C_6-H$ ), 3.16 (2H, m,  $OCH_2CH_3$ ), 3.81 (2H, q,  $J=7$  Hz,  $COOCH_2CH_3$ ), 4.12 (1H, t,  $J=8$  Hz,  $C_7-H$ ), 7.4 (5H, m, Ar-H).  $^{13}C$ -NMR (ppm): 13.5 (q), 14.6 (q), 29.7 (t,  $C_6$ ), 56.2 (s,  $C_5$ ), 62.2 (t), 65.6 (t), 69.7 (s,  $C_1$ ), 83.3 (d,  $C_7$ ), 126.4 (d, 2C), 128.4 (d, 3C), 132.3 (s), 161.7 (s,  $C_3$ ), 165.4 (s), 196.0 (s,  $C_4$ ). MS  $m/z$ :  $M^+$  Calcd for  $C_{17}H_{19}NO_5$  317.1261. Found: 317.1250.

*rel*-(1*S*,5*R*,7*R*)-7-Ethoxy-5-ethoxycarbonyl-1-phenyl-2-azabicyclo[3.2.0]heptane-3,4-dione (3g)——Colorless prisms, mp 149—152 °C. 2395 mg, 62%. IR: 1760, 1740, 1720. UV  $\lambda_{max}$  nm ( $\epsilon$ ): 255 (3300).  $^1H$ -NMR  $\delta$ : 0.72 (3H, t,  $J=7$  Hz,  $COOCH_2CH_3$ ), 1.17 (3H, t,  $J=7$  Hz,  $OCH_2CH_3$ ), 2.17 (1H, dd,  $J=6, 14$  Hz,  $C_6-H$ ), 3.33 (1H, dd,  $J=8, 14$  Hz,  $C_6-H$ ), 3.47 (2H, q,  $J=7$  Hz,  $OCH_2CH_3$ ), 3.73 (2H, q,  $J=7$  Hz,  $COOCH_2CH_3$ ), 4.75 (1H, dd,  $J=6, 8$  Hz,  $C_7-H$ ), 7.3 (5H, brs, Ar-H).  $^{13}C$ -NMR (ppm): 13.4 (q), 15.0 (q), 31.5 (t,  $C_6$ ), 56.3 (s,  $C_5$ ), 61.9 (t), 65.5 (t), 67.3 (s,  $C_1$ ), 75.6 (d,  $C_7$ ), 125.6 (d, 2C), 128.9 (d, 3C), 136.9 (s), 162.7 (s,  $C_3$ ), 166.1 (s), 193.9 (s,  $C_4$ ). Anal. Calcd for  $C_{17}H_{19}NO_5$ : C, 64.34; H, 6.04; N, 4.41. Found: C, 64.40; H, 6.06; N, 4.66.

3-Ethoxy-5-ethoxycarbonyl-6-phenyl-3,4-dihydropyridin-2(1*H*)-one (4g)——Colorless needles, mp 112—113 °C. 140 mg, 4%. IR: 3250, 1700, 1620, 1600. UV  $\lambda_{max}^{EtOH}$  nm ( $\epsilon$ ): 228 (8400), 284 (10500).  $^1H$ -NMR  $\delta$ : 0.93 (3H, t,  $J=7$  Hz,  $COOCH_2CH_3$ ), 1.23 (3H, t,  $J=7$  Hz,  $OCH_2CH_3$ ), 2.88 (1H, d,  $J=10$  Hz,  $C_4-H$ ), 2.92 (1H, d,  $J=7$  Hz,  $C_4-H$ ), 3.78 (2H, q,  $J=7$  Hz,  $OCH_2CH_3$ ), 3.83 (2H, m,  $COOCH_2CH_3$ ), 3.97 (1H, dd,  $J=7, 10$  Hz,  $C_3-H$ ), 7.2 (5H, s, Ar-H). MS  $m/z$ :  $M^+$  Calcd for  $C_{16}H_{19}NO_4$  289.1312. Found: 289.1252.

#### Isobutoxyethylene Photoproducts

*rel*-(1*S*,5*R*,7*S*)-5-Ethoxycarbonyl-7-isobutoxy-1-phenyl-2-azabicyclo[3.2.0]heptane-3,4-dione (2h)——Colorless prisms, mp 148—150.5 °C. 75 mg, 1.8%. IR: 3150, 1775, 1750, 1730. UV  $\lambda_{max}$  nm ( $\epsilon$ ): 262 (2700).  $^1H$ -NMR  $\delta$ : 0.66 (3H, d,  $J=5$  Hz, C- $CH_3$ ), 0.66 (3H, t,  $J=7$  Hz,  $COOCH_2CH_3$ ), 0.73 (3H, d,  $J=5$  Hz, C- $CH_3$ ), 1.63 (1H, hept,  $J=6$  Hz, C-CH), 2.59 (1H, dd,  $J=8, 13.5$  Hz,  $C_6-H$ ), 2.95 (2H, m,  $OCH_2-C$ ), 3.15 (1H, dd,  $J=8, 13.5$  Hz,  $C_6-H$ ), 3.50 (2H, dq,  $J=2, 7$  Hz,  $COOCH_2CH_3$ ), 4.12 (1H, t,  $J=8$  Hz,  $C_7-H$ ), 7.3—7.4 (3H, m, Ar-H), 7.5—7.6 (2H, m, Ar-H).  $^{13}C$ -NMR (ppm): 13.4 (q), 19.2 (q, 2C), 28.3 (d), 29.5 (t,  $C_6$ ), 56.0 (s,  $C_5$ ), 61.0 (s,  $C_1$ ), 62.1 (t), 77.0 (t), 83.2 (d,  $C_7$ ), 126.0 (d, 2C), 128.3 (d, 2C), 131.9 (s), 132.0 (d), 162.0 (s,  $C_3$ ), 165.4 (s), 196.4 (s,  $C_4$ ). MS  $m/z$ :  $M^+$  Calcd for  $C_{19}H_{23}NO_5$  345.1577. Found: 345.1613.

*rel*-(1*S*,5*R*,7*R*)-5-Ethoxycarbonyl-7-isobutoxy-1-phenyl-2-azabicyclo[3.2.0]heptane-3,4-dione (3h)——Colorless prisms, mp 133—136 °C. 2338 mg, 50.3%. IR: 3170, 1780, 1750, 1730. UV  $\lambda_{max}$  nm ( $\epsilon$ ): 259 (3000).  $^1H$ -NMR  $\delta$ : 0.71 (3H, t,  $J=7$  Hz,  $COOCH_2CH_3$ ), 0.87 (6H, d,  $J=7$  Hz, 2C- $CH_3$ ), 1.18 (1H, quint,  $J=7$  Hz, C-CH), 2.15 (1H, dd,  $J=6, 14$  Hz,  $C_6-H$ ), 3.19 (2H, hept,  $J=7$  Hz,  $OCH_2-C$ ), 3.33 (1H, dd,  $J=8, 14$  Hz,  $C_6-H$ ), 3.75 (2H, q,  $J=7$  Hz,  $COOCH_2CH_3$ ), 4.74 (1H, dd,  $J=6, 8$  Hz,  $C_7-H$ ), 7.40 (5H, s, Ar-H).  $^{13}C$ -NMR (ppm): 13.4 (q), 19.2 (q, 2C), 28.5 (d), 31.2 (t,  $C_6$ ), 56.3 (s,  $C_5$ ), 67.3 (s,  $C_1$ ), 76.5 (d,  $C_7$ ), 76.5 (t), 128.6 (d, 2C), 128.9 (d, 3C), 136.0 (s), 162.8 (s,  $C_3$ ), 166.0 (s), 194.1 (s,  $C_4$ ). MS  $m/z$ :  $M^+$  Calcd for  $C_{19}H_{23}NO_5$  345.1574. Found: 345.1571.

5-Ethoxycarbonyl-3-isobutoxy-6-phenyl-3,4-dihydropyridin-2(1*H*)-one (4h)——Colorless prisms, mp 100—104 °C. 80 mg, 2.1%. IR: 3200, 1700, 1660, 1620. UV  $\lambda_{max}$  nm ( $\epsilon$ ): 283 (10500).  $^1H$ -NMR  $\delta$ : 0.90 (3H, t,  $J=7$  Hz,  $COOCH_2CH_3$ ), 0.93 (6H, d,  $J=13$  Hz, 2C- $CH_3$ ), 1.88 (1H, hept,  $J=7$  Hz, C-CH), 2.90 (1H, d,  $J=9$  Hz,  $C_4-H$ ), 2.90 (1H, d,  $J=8$  Hz,  $C_4-H$ ), 3.40 (1H, dd,  $J=8, 9$  Hz,  $C_3-H$ ), 3.17—3.67 (2H, m,  $OCH_2-C$ ), 3.87 (2H, q,  $J=7$  Hz,  $COOCH_2CH_3$ ), 7.33 (5H, s, Ar-H). MS  $m/z$ :  $M^+$  Calcd for  $C_{18}H_{23}NO_4$  317.1624. Found: 317.1622.

#### Cyclohexyloxyethylene Photoproducts

*rel*-(1*S*,5*R*,7*R*)-7-Cyclohexyloxy-5-ethoxycarbonyl-1-phenyl-2-azabicyclo[3.2.0]heptane-3,4-dione (3i)——Colorless prisms, mp 195—197 °C. 3048 mg, 67.2%. IR: 3170, 1780, 1750, 1720. UV  $\lambda_{max}$  nm ( $\epsilon$ ): 260 (3000).  $^1H$ -NMR  $\delta$ : 0.72 (3H, t,  $J=7$  Hz,  $COOCH_2CH_3$ ), 1.1—1.8 (10H, m, 5C- $CH_2$ ), 2.18 (1H, dd,  $J=6, 13.5$  Hz,  $C_6-H$ ), 3.32 (1H, dd,  $J=8, 13.5$  Hz,  $C_6-H$ ), 3.3 (1H, m, OCH), 3.77 (2H, q,  $J=7$  Hz,  $COOCH_2CH_3$ ), 4.93 (1H, dd,  $J=6, 8$  Hz,  $C_7-H$ ), 7.38 (5H, s, Ar-H). MS  $m/z$ :  $M^+$  Calcd for  $C_{21}H_{25}NO_5$  371.1731. Found: 371.1725.

3-Cyclohexyloxy-5-ethoxycarbonyl-6-phenyl-3,4-dihydropyridin-2(1*H*)-one (4i)——Colorless needles, mp 194—196 °C. 170 mg, 4%. IR: 1660, 1640. UV  $\lambda_{max}$  nm ( $\epsilon$ ): 283 (9200).  $^1H$ -NMR  $\delta$ : 0.90 (3H, t,  $J=7$  Hz,  $COOCH_2CH_3$ ), 1.3—2.1 (10H, m, 5C- $CH_2$ ), 2.58 (1H, d,  $J=10$  Hz,  $C_4-H$ ), 2.60 (1H, d,  $J=8$  Hz,  $C_4-H$ ), 3.6 (1H, m, OCH), 3.92 (2H, q,  $J=7$  Hz,  $COOCH_2CH_3$ ), 4.15 (1H, dd,  $J=8, 10$  Hz,  $C_3-H$ ), 7.3 (5H, m). MS  $m/z$ :  $M^+$  Calcd for  $C_{20}H_{25}NO_4$  343.1781. Found: 343.1775.

#### Phenoxyethylene Photoproducts

*rel*-(1*S*,5*R*,7*R*)-5-Ethoxycarbonyl-7-phenoxy-1-phenyl-2-azabicyclo[3.2.0]heptane-3,4-dione (3j)——Colorless prisms, mp 177—182 °C. 2294 mg, 61.6%. IR: 3150, 1770, 1730, 1605. UV  $\lambda_{max}$  nm ( $\epsilon$ ): 259 (3000).  $^1H$ -NMR  $\delta$ : 0.73 (3H, t,  $J=7$  Hz,  $COOCH_2CH_3$ ), 2.36 (1H, dd,  $J=5, 14$  Hz,  $C_6-H$ ), 3.59 (1H, dd,  $J=7.5, 14$  Hz,  $C_6-H$ ), 3.77 (2H, q,  $J=7$  Hz,  $COOCH_2CH_3$ ), 5.36 (1H, dd,  $J=5, 7.5$  Hz,  $C_7-H$ ), 6.6—7.3 (5H, m, Ar-H), 7.40 (5H, s, Ar-H). MS  $m/z$ :  $M^+$  Calcd for  $C_{21}H_{19}NO_5$  365.1261. Found: 365.1260.

5-Ethoxycarbonyl-3-phenoxy-6-phenyl-3,4-dihydropyridin-2(1*H*)-one (4j)——Colorless needles, mp 117—

120°C. 84 mg, 2.4%. IR: 1720, 1680, 1640, 1600. UV  $\lambda_{\max}$  nm ( $\epsilon$ ): 278 (10700).  $^1\text{H-NMR}$   $\delta$ : 0.93 (3H, t,  $J=7$  Hz,  $\text{COOCH}_2\text{CH}_3$ ), 3.13 (1H, d,  $J=9.5$  Hz,  $\text{C}_4\text{-H}$ ), 3.15 (1H, d,  $J=8$  Hz,  $\text{C}_4\text{-H}$ ), 3.93 (2H, q,  $J=7$  Hz,  $\text{COOCH}_2\text{CH}_3$ ), 4.90 (1H, dd,  $J=8, 9.5$  Hz,  $\text{C}_3\text{-H}$ ), 7.0–7.5 (10H, m, Ar-H). MS  $m/z$ :  $\text{M}^+$  Calcd for  $\text{C}_{20}\text{H}_{19}\text{NO}_4$  337.1314. Found: 337.1321.

#### Vinyl Acetate Photoproducts

*rel*-(1*S*,5*R*,7*S*)-7-Acetoxy-5-ethoxycarbonyl-1-phenyl-2-azabicyclo[3.2.0]heptane-3,4-dione (2k)——Colorless prisms, mp 170–173°C. 243 mg, 6%. IR: 3400, 1780, 1640. UV  $\lambda_{\max}$  nm ( $\epsilon$ ): 257 (3500).  $^1\text{H-NMR}$   $\delta$ : 0.62 (3H, t,  $J=7$  Hz,  $\text{COOCH}_2\text{CH}_3$ ), 1.82 (3H, s, OAc), 2.66 (1H, dd,  $J=9, 14$  Hz,  $\text{C}_6\text{-H}$ ), 3.33 (1H, dd,  $J=9, 14$  Hz,  $\text{C}_6\text{-H}$ ), 3.72 (2H, q,  $J=7$  Hz,  $\text{COOCH}_2\text{CH}_3$ ), 4.97 (1H, t,  $J=9$  Hz,  $\text{C}_7\text{-H}$ ), 7.4 (5H, s, Ar-H). MS  $m/z$ :  $\text{M}^+$  Calcd for  $\text{C}_{17}\text{H}_{17}\text{NO}_6$  331.1056. Found: 331.1071.

*rel*-(1*S*,5*R*,7*R*)-7-Acetoxy-5-ethoxycarbonyl-1-phenyl-2-azabicyclo[3.2.0]heptane-3,4-dione (3k)——Colorless gum. 1460 mg, 36%. IR ( $\text{CH}_2\text{Cl}_2$ ): 3400, 1780, 1740. UV  $\lambda_{\max}$  nm ( $\epsilon$ ): 250 (3500).  $^1\text{H-NMR}$   $\delta$ : 0.73 (3H, t,  $J=7$  Hz,  $\text{COOCH}_2\text{CH}_3$ ), 2.09 (3H, s, OAc), 2.31 (1H, dd,  $J=6, 14$  Hz,  $\text{C}_6\text{-H}$ ), 3.46 (1H, dd,  $J=8, 14$  Hz,  $\text{C}_6\text{-H}$ ), 3.77 (2H, q,  $J=7$  Hz,  $\text{COOCH}_2\text{CH}_3$ ), 5.89 (1H, dd,  $J=6, 8$  Hz,  $\text{C}_7\text{-H}$ ), 7.4 (5H, s, Ar-H). MS  $m/z$ :  $\text{M}^+$  Calcd for  $\text{C}_{17}\text{H}_{17}\text{NO}_6$  331.1055. Found: 331.1075.

3-Acetoxy-5-ethoxycarbonyl-6-phenyl-3,4-dihydropyridin-2(1*H*)-one (4k)——Colorless needles, mp 142–146°C. 40 mg, 1%. IR: 3200, 3100, 1750, 1700, 1680. UV  $\lambda_{\max}$  nm ( $\epsilon$ ): 228 (12300), 282 (13200).  $^1\text{H-NMR}$   $\delta$ : 0.95 (3H, t,  $J=7$  Hz,  $\text{COOCH}_2\text{CH}_3$ ), 2.20 (3H, s, OAc), 2.89 (1H, dd,  $J=14, 16$  Hz,  $\text{C}_4\text{-H}$ ), 3.13 (1H, dd,  $J=7.5, 16$  Hz,  $\text{C}_4\text{-H}$ ), 3.96 (2H, q,  $J=7$  Hz,  $\text{COOCH}_2\text{CH}_3$ ), 5.58 (1H, dd,  $J=7.5, 14$  Hz,  $\text{C}_3\text{-H}$ ), 7.3 (5H, m, Ar-H). MS  $m/z$ :  $\text{M}^+$  Calcd for  $\text{C}_{16}\text{H}_{17}\text{NO}_5$  303.1105. Found: 303.1093.

#### Isoprene Photoproduct

*rel*-(1*S*,5*R*,7*R*)-5-Ethoxycarbonyl-7-methyl-1-phenyl-7-vinyl-2-azabicyclo[3.2.0]heptane-3,4-dione (21)——Colorless needles, mp 164–169°C. 2300 mg, 60%. IR: 1760, 1740, 1690. UV  $\lambda_{\max}^{\text{EtOH}}$  nm ( $\epsilon$ ): 260 (3500).  $^1\text{H-NMR}$   $\delta$ : 0.75 (3H, t,  $J=7$  Hz,  $\text{COOCH}_2\text{CH}_3$ ), 1.19 (3H, br s, C- $\text{CH}_3$ ), 2.24 (1H, d,  $J=7$  Hz,  $\text{C}_6\text{-H}$ ), 3.42 (1H, br d,  $J=7$  Hz,  $\text{C}_6\text{-H}$ ), 3.86 (2H, q,  $J=7$  Hz,  $\text{COOCH}_2\text{CH}_3$ ), 5.04 (1H, d,  $J=12$  Hz), 5.11 (1H, d,  $J=16$  Hz) and 5.56 (1H, dd,  $J=12, 16$  Hz) olefinic-H, 7.33 (5H, s, Ar-H).  $^{13}\text{C-NMR}$  (ppm): 13.4 (q), 25.3 (q), 34.6 (t,  $\text{C}_6$ ), 50.4 (s,  $\text{C}_7$ ), 57.4 (s,  $\text{C}_5$ ), 62.0 (t), 69.4 (s,  $\text{C}_1$ ), 113.9 (t), 126.5 (d, 2C), 128.0 (d, 3C), 134.4 (s), 142.0 (d), 163.6 (s,  $\text{C}_3$ ), 166.3 (s), 196.3 (s,  $\text{C}_4$ ). *Anal.* Calcd for  $\text{C}_{18}\text{H}_{19}\text{NO}_4$ : C, 68.99; H, 6.11; N, 4.47. MS  $m/z$ : 313.1312. Found: C, 68.76; H, 6.09; N, 4.40. MS  $m/z$ : 313.1300.

#### $\alpha$ -Methylstyrene Photoproducts

*rel*-(1*S*,5*R*,7*R*)-5-Ethoxycarbonyl-7-methyl-1,7-diphenyl-2-azabicyclo[3.2.0]heptane-3,4-dione (2m)——Colorless needles, mp 185–188°C. 533 mg, 12%. IR: 1762, 1735, 1720, 1605. UV  $\lambda_{\max}^{\text{EtOH}}$  nm ( $\epsilon$ ): 262 (3800).  $^1\text{H-NMR}$   $\delta$ : 0.60 (3H, t,  $J=7$  Hz,  $\text{COOCH}_2\text{CH}_3$ ), 1.40 (3H, br s, C- $\text{CH}_3$ ), 2.45 (1H, d,  $J=12$  Hz,  $\text{C}_6\text{-H}$ ), 3.60 (2H, q,  $J=7$  Hz,  $\text{COOCH}_2\text{CH}_3$ ), 3.68 (1H, br d,  $J=12$  Hz,  $\text{C}_6\text{-H}$ ), 7.0–7.2 (10H, m, Ar-H).  $^{13}\text{C-NMR}$  (ppm): 13.3 (q), 30.6 (q), 35.9 (t,  $\text{C}_6$ ), 53.5 (s,  $\text{C}_7$ ), 57.4 (s,  $\text{C}_5$ ), 62.0 (t), 70.5 (s,  $\text{C}_1$ ), 126.1 (d), 126.3 (d, 2C), 126.4 (d, 2C), 127.8 (d, 3C), 128.1 (d, 2C), 134.7 (s), 143.7 (s), 164.4 (s,  $\text{C}_3$ ), 165.7 (s), 196.6 (s,  $\text{C}_4$ ). MS  $m/z$ :  $\text{M}^+$  Calcd for  $\text{C}_{22}\text{H}_{21}\text{NO}_4$  363.1469. Found: 363.1459.

*rel*-(1*S*,5*R*,7*S*)-5-Ethoxycarbonyl-7-methyl-1,7-diphenyl-2-azabicyclo[3.2.0]heptane-3,4-dione (3m)——Colorless needles, mp 196–200°C. 670 mg, 15%. IR: 1770, 1725, 1605. UV  $\lambda_{\max}^{\text{EtOH}}$  nm ( $\epsilon$ ): 255 (4100).  $^1\text{H-NMR}$   $\delta$ : 1.16 (3H, t,  $J=7$  Hz,  $\text{COOCH}_2\text{CH}_3$ ), 1.43 (3H, s, C- $\text{CH}_3$ ), 2.82 (1H, d,  $J=13$  Hz,  $\text{C}_6\text{-H}$ ), 3.18 (1H, d,  $J=13$  Hz,  $\text{C}_6\text{-H}$ ), 4.18 (2H, q,  $J=7$  Hz,  $\text{COOCH}_2\text{CH}_3$ ), 6.9–7.6 (10H, m, Ar-H).  $^{13}\text{C-NMR}$  (ppm): 13.7 (q), 28.7 (q), 33.5 (t,  $\text{C}_6$ ), 51.8 (s,  $\text{C}_7$ ), 57.4 (s,  $\text{C}_5$ ), 62.3 (t), 69.9 (s,  $\text{C}_1$ ), 125.8 (d, 2C), 126.7 (d, 2C), 126.9 (d), 128.4 (d, 3C), 129.1 (d, 2C), 135.0 (s), 142.8 (s), 160.6 (s,  $\text{C}_3$ ), 167.7 (s), 195.4 (s,  $\text{C}_4$ ). *Anal.* Calcd for  $\text{C}_{22}\text{H}_{21}\text{NO}_4$ : C, 72.71; H, 5.82; N, 3.85. MS  $m/z$ : 363.1470. Found: C, 72.62; H, 5.76; N, 3.81. MS  $m/z$ : 363.1460.

5-Ethoxycarbonyl-3-methyl-3,6-diphenyl-3,4-dihydropyridin-2(1*H*)-one (4m)——Colorless prisms, mp 156–160°C. 82 mg, 2%. IR: 1700, 1680, 1640. UV  $\lambda_{\max}^{\text{EtOH}}$  nm ( $\epsilon$ ): 226 (10200), 284 (9400).  $^1\text{H-NMR}$   $\delta$ : 1.29 (3H, t,  $J=7$  Hz,  $\text{COOCH}_2\text{CH}_3$ ), 1.95 (3H, s, C- $\text{CH}_3$ ), 3.15 (1H, d,  $J=16$  Hz,  $\text{C}_4\text{-H}$ ), 3.39 (1H, d,  $J=16$  Hz,  $\text{C}_4\text{-H}$ ), 4.43 (2H, q,  $J=7$  Hz,  $\text{COOCH}_2\text{CH}_3$ ), 7.2–7.7 (10H, m, Ar-H). MS  $m/z$ :  $\text{M}^+$  Calcd for  $\text{C}_{21}\text{H}_{21}\text{NO}_3$  335.1520. Found: 335.1508.

#### Isopropenyl Acetate Photoproducts

*rel*-(1*S*,5*R*,7*S*)-7-Acetoxy-5-ethoxycarbonyl-7-methyl-1-phenyl-2-azabicyclo[3.2.0]heptane-3,4-dione (2n)——Colorless needles, mp 181–184°C. 250 mg, 6%. IR: 1780, 1750, 1730. UV  $\lambda_{\max}$  nm ( $\epsilon$ ): 258 (3500).  $^1\text{H-NMR}$   $\delta$ : 0.60 (3H, t,  $J=7$  Hz,  $\text{COOCH}_2\text{CH}_3$ ), 1.51 (3H, s, C- $\text{CH}_3$ ), 1.74 (3H, s, OAc), 2.44 (1H, d,  $J=14$  Hz,  $\text{C}_6\text{-H}$ ), 3.44 (1H, br d,  $J=14$  Hz,  $\text{C}_6\text{-H}$ ), 3.63 (2H, qd,  $J=2, 7$  Hz,  $\text{COOCH}_2\text{CH}_3$ ), 7.34 (5H, s, Ar-H).  $^{13}\text{C-NMR}$  (ppm): 13.3 (q), 20.8 (q), 22.5 (q), 38.2 (t,  $\text{C}_6$ ), 55.7 (s,  $\text{C}_5$ ), 62.1 (t), 70.5 (s,  $\text{C}_1$ ), 82.4 (s,  $\text{C}_7$ ), 125.8 (d, 2C), 128.0 (d, 2C), 128.3 (d), 133.6 (s), 161.9 (s,  $\text{C}_3$ ), 162.2 (s), 170.0 (s), 195.3 (s,  $\text{C}_4$ ). *Anal.* Calcd for  $\text{C}_{18}\text{H}_{19}\text{NO}_6$ : C, 62.60; H, 5.55; N, 4.06. Found: C, 62.70; H, 5.60; N, 4.20.

*rel*-(1*S*,5*R*,7*R*)-7-Acetoxy-5-ethoxycarbonyl-7-methyl-1-phenyl-2-azabicyclo[3.2.0]heptane-3,4-dione (3n)——Colorless prisms, mp 164–166°C. 1520 mg, 36%. IR: 1780, 1750 sh, 1730. UV  $\lambda_{\max}$  nm ( $\epsilon$ ): 258 (3400).  $^1\text{H-NMR}$   $\delta$ : 0.90 (3H, t,  $J=7$  Hz,  $\text{COOCH}_2\text{CH}_3$ ), 1.49 (3H, s, C- $\text{CH}_3$ ), 2.05 (3H, s, OAc), 2.59 (1H, d,  $J=14$  Hz,  $\text{C}_6\text{-H}$ ), 3.17 (1H, d,  $J=14$  Hz,  $\text{C}_6\text{-H}$ ), 4.01 (2H, q,  $J=7$  Hz,  $\text{COOCH}_2\text{CH}_3$ ), 7.37 (5H, s, Ar-H).  $^{13}\text{C-NMR}$  (ppm): 13.6 (q), 21.3 (q, 2C), 38.2 (t,  $\text{C}_6$ ), 56.8 (s,  $\text{C}_5$ ), 62.4 (t), 70.1 (s,  $\text{C}_1$ ), 84.5 (s,  $\text{C}_7$ ), 126.0 (d, 2C), 128.8 (d, 3C), 133.7 (s), 161.3 (s,  $\text{C}_3$ ), 166.3 (s),

170.8 (s), 194.3 (s, C<sub>4</sub>). *Anal.* Calcd for C<sub>18</sub>H<sub>19</sub>NO<sub>6</sub>: C, 62.60; H, 5.55; N, 4.06. Found: C, 62.71; H, 5.57; N, 4.06.

**3-Acetoxy-5-ethoxycarbonyl-3-methyl-6-phenyl-3,4-dihydropyridin-2(1H)-one (4n)**—Colorless gum. 135 mg, 3.5%. IR (CH<sub>2</sub>Cl<sub>2</sub>): 1750, 1730, 1640. UV  $\lambda_{\max}^{\text{EtOH}}$  nm ( $\epsilon$ ): 225 sh (9100), 282 (8600). <sup>1</sup>H-NMR  $\delta$ : 0.90 (3H, t,  $J=7$  Hz, COOCH<sub>2</sub>CH<sub>3</sub>), 1.60 (3H, s, C-CH<sub>3</sub>), 2.10 (3H, s, OAc), 2.77 (1H, d,  $J=16$  Hz, C<sub>4</sub>-H), 3.53 (1H, d,  $J=16$  Hz, C<sub>4</sub>-H), 3.95 (2H, q,  $J=7$  Hz, COOCH<sub>2</sub>CH<sub>3</sub>), 7.32 (5H, s, Ar-H). MS  $m/z$ : M<sup>+</sup> - CH<sub>3</sub>COOH Calcd for C<sub>15</sub>H<sub>15</sub>NO<sub>3</sub> 301.0012. Found: 301.0050.

#### $\alpha$ -Trimethylsilyloxystyrene Photoproduct

**rel-(1S,5R,7S)-5-Ethoxycarbonyl-1,7-diphenyl-7-trimethylsilyloxy-2-azabicyclo[3.2.0]heptane-3,4-dione (3p)**—Colorless prisms, mp 201–206 °C. 3480 mg, 65%. IR: 1770, 1745, 1725. <sup>1</sup>H-NMR  $\delta$ : 0.11 (9H, s, OSi(CH<sub>3</sub>)<sub>3</sub>), 0.83 (3H,  $J=7$  Hz, COOCH<sub>2</sub>CH<sub>3</sub>), 2.84 (1H, s,  $J=13$  Hz, C<sub>6</sub>-H), 3.93 (2H, oct,  $J=3$  Hz, COOCH<sub>2</sub>CH<sub>3</sub>), 4.01 (1H, d,  $J=13$  Hz, C<sub>6</sub>-H), 7.3 (10H, m, Ar-H). <sup>13</sup>C-NMR (ppm): 13.5 (q), 38.7 (t, C<sub>6</sub>), 57.5 (s, C<sub>5</sub>), 61.8 (t), 73.2 (s, C<sub>1</sub>), 84.5 (s, C<sub>7</sub>), 126.3 (d, 2C), 127.8 (d, 3C), 128.0 (d, 2C), 128.2 (d, 3C), 133.4 (s), 138.7 (s), 165.9 (s, C<sub>3</sub> and C\*OOEt), 195.4 (s, C<sub>4</sub>). MS  $m/z$ : M<sup>+</sup> Calcd for C<sub>24</sub>H<sub>27</sub>NO<sub>5</sub>Si 437.1658. Found: 437.1723.

#### Catalytic Hydrogenation of 2b

A solution of 2b (473 mg) in EtOH (30 ml) was hydrogenated over 5% Pd/C (500 mg) for 1 h at room temperature. After removal of the catalyst by filtration, the filtrate was evaporated, and the residue in CH<sub>2</sub>Cl<sub>2</sub> was purified through a short column of silica gel to give 2e (377 mg, 80%). Colorless prisms from CH<sub>2</sub>Cl<sub>2</sub>-Et<sub>2</sub>O, mp 156–158 °C.

#### Base Treatment of 2a

A solution of 2a (100 mg) and triethylamine (2 g) in benzene (20 ml) was refluxed for 4 h. Chromatography of the products over SiO<sub>2</sub> gave 3a (50 mg, 50%) from the benzene-CH<sub>2</sub>Cl<sub>2</sub> (1:1) eluate and 4-ethoxycarbonyl-3-hydroxy-6,7-diphenyl-1,5-dihydro-2H-azepin-2-one (10 mg, 10%) from the CH<sub>2</sub>Cl<sub>2</sub> eluate.<sup>5b</sup> Pale yellow needles, mp 226–236 °C. IR: 3200, 1670, 1600. UV  $\lambda_{\max}$  nm ( $\epsilon$ ): 226 (19200), 269 (17600). <sup>1</sup>H-NMR  $\delta$ : 1.03 (3H, t,  $J=7$  Hz, COOCH<sub>2</sub>CH<sub>3</sub>), 3.43 (2H, s, C<sub>5</sub>-H), 4.13 (2H, q,  $J=7$  Hz, COOCH<sub>2</sub>CH<sub>3</sub>), 7.12 (5H, s, Ar-H), 7.17 (5H, s, Ar-H). <sup>13</sup>C-NMR (ppm): 13.7 (q), 29.4 (t, C<sub>5</sub>), 61.6 (t), 109.4 (s, C<sub>4</sub>), 127.0 (d), 128.1 (d, 2C), 128.4 (d, 2C), 128.6 (s), 128.8 (d), 129.3 (d, 2C), 129.9 (d, 2C), 132.5 (s), 135.6 (s, C<sub>6</sub>), 139.1 (s, C<sub>7</sub>), 157.8 (s, C<sub>3</sub>), 164.2 (s, C<sub>2</sub>), 170.4 (s). *Anal.* Calcd for C<sub>21</sub>H<sub>19</sub>NO<sub>4</sub>: C, 72.19; H, 5.48; N, 4.01. MS  $m/z$ : 349.1313. Found: C, 71.90; H, 5.37; N, 4.02. MS  $m/z$ : 349.1313.

**Equilibration between 2 and 3 under Basic Conditions**—General Procedure: A solution of 2 or 3 (100 mg) in 10% (w/v) triethylamine-benzene (40 ml) was refluxed for an appropriate time. After evaporation of the solvent, each reaction mixture was subjected to <sup>1</sup>H-NMR measurement. The ratios of 2 and 3 were calculated from the intensity ratios of the methyl signals of COOEt. The ratios of 2k and 3k was calculated from the intensities of OAc signals. The results are given in Table III.

#### 1-(4'-Bromophenyl)-4-ethoxycarbonyl-5-phenyl-1H-pyrrole-2,3-dione (5)

A mixture of ethyl benzoylacetate (10 g) and *p*-bromoaniline (27 g) in ethanol (100 ml) was heated under reflux for 4 h. After evaporation of the solvent *in vacuo*, the residue was taken up in CH<sub>2</sub>Cl<sub>2</sub> and the organic layer was washed with 5% HCl and water, then dried over Na<sub>2</sub>SO<sub>4</sub>, and evaporated. Recrystallization of the residue from CH<sub>2</sub>Cl<sub>2</sub>-Et<sub>2</sub>O gave ethyl 3-(4'-bromophenylamino)-3-phenyl-2-propenoate (12 g, 62%) as pale yellow prisms, mp 108–112 °C. IR: 1660, 1605.

Oxalyl chloride (2.93 g) was slowly added to the propenoate (8.0 g) in dry ether (10 ml) at 0 °C under stirring. After addition of dioxane (10 ml), the reaction mixture was slowly warmed to 50 °C, and the ether was slowly distilled off to remove hydrogen chloride evolved during the reaction. Recrystallization of the product from CH<sub>2</sub>Cl<sub>2</sub>-benzene gave the dioxopyrrolone 5 (6.5 g, 70%) as red prisms. mp 168–169 °C. IR: 1775, 1722, 1710. UV  $\lambda_{\max}$  nm ( $\epsilon$ ): 250 (17200), 307 (5300), 405 (2700). MS  $m/z$ : M<sup>+</sup> Calcd for C<sub>19</sub>H<sub>14</sub>BrNO<sub>4</sub> 399.0106 and 401.0085. Found: 399.0158 and 401.0155.

#### Photocycloaddition of 5 to Styrene

A solution of 5 (1 g) and styrene (2.6 g, 10 eq) in dioxane-Et<sub>2</sub>O (1:1) (300 ml) was irradiated for 40 min and worked up as described in the general procedure to give *rel*-(1S,5R,7R)-2-(4'-bromophenyl)-5-ethoxycarbonyl-1,7-diphenyl-2-azabicyclo[3.2.0]heptane-3,4-dione (6, 252 mg, 20%). Colorless prisms from MeOH, mp 181–183 °C. IR: 1762, 1740, 1718. UV  $\lambda_{\max}$  nm ( $\epsilon$ ): 223 (19000), 260 sh (4800), 310 (6200). <sup>1</sup>H-NMR  $\delta$ : 0.85 (3H, t,  $J=7$  Hz, COOCH<sub>2</sub>CH<sub>3</sub>), 2.75 (1H, dd,  $J=10, 13$  Hz, C<sub>6</sub>-H), 3.72 (1H, dd,  $J=10, 13$  Hz, C<sub>6</sub>-H), 3.73 (2H, m, COOCH<sub>2</sub>CH<sub>3</sub>), 4.18 (1H, t,  $J=10$  Hz, C<sub>7</sub>-H), 6.9–7.5 (14H, m, Ar-H). MS  $m/z$ : M<sup>+</sup> Calcd for C<sub>27</sub>H<sub>22</sub>BrNO<sub>4</sub> 503.0728 and 505.0711. Found: 503.0671 and 505.0700. This product was subjected to X-ray analysis.

#### Photocycloaddition of 5 to Butadiene

Irradiation of 5 (1 g) and butadiene (5 ml) as above gave *rel*-(1S,5R,7R)-2-(4'-bromophenyl)-5-ethoxycarbonyl-1-phenyl-7-vinyl-2-azabicyclo[3.2.0]heptane-3,4-dione (7, 272 mg, 24%). Colorless prisms from MeOH, mp 193–195 °C. IR: 1772, 1741, 1720. <sup>1</sup>H-NMR  $\delta$ : 0.72 (3H, t,  $J=7$  Hz, COOCH<sub>2</sub>CH<sub>3</sub>), 2.60 (1H, dd,  $J=9, 12$  Hz, C<sub>6</sub>-H), 3.3 (1H, m, C<sub>6</sub>-H), 3.6 (3H, m, COOCH<sub>2</sub>CH<sub>3</sub>, C<sub>7</sub>-H), 5.1–5.5 (2H, m), 6.25–6.48 (1H, m) olefinic-H, 7.2–7.6 (9H, m, Ar-H). MS  $m/z$ : M<sup>+</sup> Calcd for C<sub>23</sub>H<sub>20</sub>BrNO<sub>4</sub> 453.0574 and 455.0522. Found: 453.0629 and 455.0490. This product was subjected to X-ray analysis.

#### Crystallographic Measurement

The crystal data were collected on a Rigaku Denki computer-controlled four-circle diffractometer using Cu- $K_{\alpha}$  radiation. The intensities of all the reflections with  $2\theta$  values up to  $140^{\circ}$  of  $(hkl)$ ,  $(\bar{h}kl)$ ,  $(h\bar{k}l)$  and  $(\bar{h}\bar{k}l)$  were measured by the  $\omega-2\theta$  scanning technique at a scan rate of 2 per minute. The scan range of  $\omega$  for each reflection was calculated by using the formula  $\omega = 1.10; 0.5 \tan \theta$ , and the backgrounds were measured at both ends of the scan range for 10.0 s. Three standard reflections were measured every 50 measurements, and showed to significant variation with time. The intensity data were corrected for the background count and for the usual Lorentz and polarization effects. In total, 1982 (for 6) and 2329 (for 7) independent non-zero reflections were measured visually.

**Crystal Data**—6:  $C_{27}H_{22}BrNO_4$ .  $M_r = 504.38$ . Triclinic.  $a = 11.384(5) \text{ \AA}$ ,  $b = 11.851(6) \text{ \AA}$ ,  $c = 9.321(1) \text{ \AA}$ ,  $\alpha = 109.49(11)^{\circ}$ ,  $\beta = 91.91(8)^{\circ}$ ,  $\gamma = 103.06(13)^{\circ}$ ,  $V = 1146.7 \text{ \AA}^3$ ,  $d_o = 1.43 \text{ g/cm}^3$ ,  $d_c = 1.464 \text{ g/cm}^3$ ,  $Z = 2$ . Space group  $P1$ . Crystal size,  $0.25 \times 0.20 \times 0.20 \text{ mm}^3$ . 7:  $C_{23}H_{20}BrNO_4$ .  $M_r = 454.314$ . Triclinic.  $a = 11.566(4) \text{ \AA}$ ,  $b = 12.238(7) \text{ \AA}$ ,  $c = 8.228(3) \text{ \AA}$ ,  $\alpha = 96.98(7)^{\circ}$ ,  $\beta = 103.45(52)^{\circ}$ ,  $\gamma = 104.90(60)^{\circ}$ ,  $V = 1033.8 \text{ \AA}^3$ ,  $d_o = 1.44 \text{ g/cm}^3$ ,  $d_c = 1.456 \text{ g/cm}^3$ ,  $Z = 2$ . Space group  $P1$ . Crystal size,  $0.30 \times 0.25 \times 0.25 \text{ mm}^3$ .

#### Structure Analysis and Refinement

The structures were established by the heavy atom method. From the Patterson map the position of the brom atom was determined and the whole structure of the molecule except for the hydrogen atoms was revealed from an electron density map calculated by the heavy atom method. At this stage, the  $R$  value was 0.54 for 6 and 0.48 for 7.

TABLE V. Positional Parameters ( $\times 10^4$ ) with Their Estimated Standard Deviations (in Parentheses) and Equivalent Isotropic Thermal Parameters ( $\text{Å}^2$ ) of 6 and 7

Atom	Compound 6				$B_{eq}$	Atom	Compound 7				$B_{eq}/B_{iso}$
	$x$	$y$	$z$				$x$	$y$	$z$		
Br	6203 (1)	-4280 (2)	-1557 (2)		5.5	Br	901 (1)	871 (1)	2231 (2)		6.0
O1	4450 (6)	549 (8)	3608 (8)		4.5	O1	3947 (6)	766 (6)	10382 (8)		5.0
O2	5595 (8)	2821 (8)	6079 (9)		5.4	O2	6371 (7)	1194 (7)	12780 (9)		5.8
O3	8531 (8)	4919 (9)	5454 (10)		6.0	O3	9137 (7)	3713 (7)	12748 (10)		7.1
O4	6709 (7)	4369 (8)	4096 (9)		4.8	O4	7190 (7)	3848 (6)	12810 (9)		6.0
N	6269 (7)	926 (8)	2599 (8)		2.6	N	5134 (6)	1882 (6)	8848 (8)		2.9
C1	7501 (8)	1803 (10)	3122 (9)		2.3	C1	6498 (7)	2479 (7)	9038 (10)		2.8
C2	5457 (9)	1195 (11)	3682 (10)		3.2	C2	4937 (8)	1347 (8)	10195 (12)		4.0
C3	6068 (10)	2346 (11)	4952 (11)		3.4	C3	6221 (9)	1579 (9)	11474 (12)		4.4
C4	7384 (9)	2837 (11)	4686 (10)		2.9	C4	7251 (8)	2327 (8)	10861 (11)		3.2
C5	8393 (11)	2521 (13)	5549 (11)		4.8	C5	8075 (9)	1724 (8)	10035 (11)		3.7
C6	8291 (9)	1306 (12)	4098 (10)		3.5	C6	7221 (8)	1679 (8)	8230 (12)		3.4
C7	8005 (9)	2335 (11)	1936 (10)		2.7	C7	6711 (7)	3723 (7)	8807 (11)		2.9
C8	9242 (10)	2905 (12)	2104 (11)		3.7	C8	7975 (9)	4384 (8)	8918 (12)		4.0
C9	9711 (11)	3518 (13)	1088 (12)		5.0	C9	8211 (10)	5448 (9)	8790 (14)		5.2
C10	8914 (13)	3538 (13)	-76 (12)		4.8	C10	7207 (11)	6060 (9)	8506 (15)		5.5
C11	7661 (11)	2992 (12)	-223 (12)		4.5	C11	5974 (11)	5391 (9)	8439 (17)		5.8
C12	7192 (10)	2409 (11)	812 (10)		3.4	C12	5716 (9)	4226 (9)	8540 (14)		4.8
C13	6157 (8)	-306 (11)	1569 (10)		2.8	C13	4139 (8)	1641 (7)	7311 (11)		3.2
C14	6412 (9)	-532 (12)	43 (11)		3.8	C14	4451 (8)	1659 (8)	5764 (11)		3.7
C15	6398 (10)	-1723 (11)	-898 (11)		3.5	C15	3491 (9)	1400 (9)	4241 (12)		4.3
C16	6147 (9)	-2658 (11)	-309 (11)		3.5	C16	2215 (8)	1185 (8)	4295 (12)		3.7
C17	5844 (10)	-2456 (12)	1203 (11)		3.9	C17	1896 (8)	1163 (8)	5816 (13)		4.2
C18	5859 (9)	-1288 (11)	2117 (11)		3.3	C18	2847 (9)	1425 (8)	7341 (13)		4.1
C19	7626 (9)	4153 (11)	4807 (11)		3.5	C19	7981 (9)	3408 (9)	12211 (12)		4.4
C20	6867 (13)	5690 (12)	4184 (16)		4.9	C20	7750 (16)	4815 (11)	14345 (18)		9.3
C21	7481 (14)	5792 (15)	2765 (15)		6.4	C21	7911 (18)	5830 (12)	13844 (22)		11.9
C22	9441 (8)	935 (11)	3588 (10)		3.0	C22	7850 (9)	2032 (9)	6874 (13)		4.4
C23	10492 (10)	1387 (12)	4606 (12)		4.2	C23	9081 (10)	2157 (10)	6900 (15)		5.5
C24	11548 (10)	974 (13)	4201 (14)		4.7						
C25	11513 (10)	82 (13)	2805 (13)		4.8						
C26	10453 (12)	-384 (15)	1772 (14)		5.7						

$$B_{eq} = \frac{4}{3} \sum_i \sum_j \beta_{ij} a_i a_j$$

TABLE VI. Bond Lengths (Å) and Bond Angles (°) with Estimated Standard Deviations in Parentheses of **6** and **7**

Compound <b>6</b>					
Atoms	Distance (Å)	Atoms	Distance (Å)	Atoms	Distance (Å)
Br-C(16)	1.902 (12)	O(1)-C(2)	1.213 (12)	O(2)-C(3)	1.221 (13)
O(3)-C(19)	1.193 (12)	O(4)-C(19)	1.336 (15)	O(4)-C(20)	1.508 (18)
N-C(1)	1.449 (11)	N-C(2)	1.339 (12)	N-C(13)	1.428 (13)
C(1)-C(4)	1.593 (12)	C(1)-C(6)	1.590 (17)	C(1)-C(7)	1.515 (15)
C(2)-C(3)	1.477 (13)	C(3)-C(4)	1.542 (14)	C(4)-C(5)	1.563 (19)
C(4)-C(19)	1.489 (19)	C(5)-C(6)	1.590 (15)	C(6)-C(22)	1.516 (15)
C(7)-C(8)	1.397 (14)	C(7)-C(12)	1.413 (16)	C(8)-C(9)	1.424 (19)
C(9)-C(10)	1.401 (19)	C(10)-C(11)	1.410 (17)	C(11)-C(12)	1.416 (18)
C(13)-C(14)	1.416 (14)	C(13)-C(18)	1.400 (19)	C(14)-C(15)	1.386 (17)
C(15)-C(16)	1.372 (20)	C(16)-C(17)	1.417 (15)	C(17)-C(18)	1.356 (17)
C(20)-C(21)	1.545 (22)	C(22)-C(23)	1.385 (14)	C(22)-C(27)	1.391 (14)
C(23)-C(24)	1.416 (18)	C(24)-C(25)	1.367 (16)	C(25)-C(26)	1.399 (16)
C(26)-C(27)	1.403 (20)				

Compound <b>6</b>			
Atoms	Angle (°)	Atoms	Angle (°)
C(19)-O(4)-C(20)	115.3 (9)	C(1)-N-C(2)	112.2 (8)
C(1)-N-C(13)	119.4 (8)	C(2)-N-C(13)	121.5 (8)
C(4)-C(1)-N	106.22 (7)	C(4)-C(1)-C(6)	87.88 (7)
C(4)-C(1)-C(7)	113.0 (8)	N-C(1)-C(6)	109.50 (8)
N-C(1)-C(7)	113.67 (8)	C(6)-C(1)-C(7)	122.8 (8)
C(3)-C(2)-O(1)	126.65 (11)	C(3)-C(2)-N	108.2 (9)
O(1)-C(2)-N	124.9 (12)	C(4)-C(3)-O(2)	124.9 (11)
C(4)-C(3)-C(2)	111.1 (9)	O(2)-C(3)-C(2)	124.0 (11)
C(5)-C(4)-C(1)	90.8 (8)	C(5)-C(4)-C(3)	116.2 (9)
C(5)-C(4)-C(19)	114.8 (9)	C(1)-C(4)-C(3)	101.8 (9)
C(1)-C(4)-C(19)	120.2 (9)	C(3)-C(4)-C(19)	111.3 (9)
C(6)-C(5)-C(4)	88.9 (8)	C(22)-C(6)-C(1)	122.2 (9)
C(22)-C(6)-C(5)	119.0 (9)	C(8)-C(7)-C(1)	119.4 (9)
C(1)-C(6)-C(5)	89.9 (8)	C(8)-C(7)-C(12)	120.9 (10)
C(1)-C(7)-C(12)	119.1 (9)	C(9)-C(8)-C(7)	120.2 (11)
C(10)-C(9)-C(8)	118.9 (12)	C(11)-C(10)-C(9)	121.0 (13)
C(12)-C(11)-C(10)	119.9 (11)	C(14)-C(13)-N	120.9 (9)
C(14)-C(13)-C(18)	119.9 (10)	N-C(13)-C(18)	119.1 (9)
C(15)-C(14)-C(13)	119.9 (10)	C(16)-C(15)-C(14)	118.8 (11)
C(17)-C(16)-Br	118.7 (8)	C(17)-C(16)-C(15)	122.1 (10)
Br-C(16)-C(15)	119.2 (9)	C(18)-C(17)-C(16)	118.3 (10)
C(21)-C(20)-O(4)	106.2 (12)	C(23)-C(22)-C(6)	119.9 (11)
C(23)-C(22)-C(27)	119.6 (13)	C(6)-C(22)-C(27)	120.1 (10)
C(24)-C(23)-C(22)	121.0 (11)	C(25)-C(24)-C(23)	119.3 (10)
C(26)-C(25)-C(24)	120.1 (12)	C(27)-C(26)-C(25)	120.6 (11)
O(3)-C(19)-O(4)	124.3 (12)	O(3)-C(19)-C(4)	124.0 (10)
O(4)-C(19)-C(4)	111.7 (9)	C(7)-C(12)-C(11)	118.9 (11)
C(13)-C(18)-C(17)	120.5 (12)	C(22)-C(27)-C(26)	119.4 (11)

The structure was refined by a diagonal-matrix least-squares procedure with isotropic temperature factors, until *R* values of 0.15 for **6** and 0.14 for **7** were reached. Further refinement was carried out by least-squares block-diagonal



TABLE VI. (continued)

Compound 7					
Atoms	Distance (Å)	Atoms	Distance (Å)	Atoms	Distance (Å)
Br-C(16)	1.887 (8)	C(1)-C(4)	1.598 (12)	C(1)-C(6)	1.597 (14)
C(1)-C(7)	1.520 (13)	C(1)-N	1.471 (10)	C(2)-C(3)	1.500 (12)
C(2)-O(1)	1.213 (11)	C(2)-N	1.385 (13)	C(3)-C(4)	1.502 (14)
C(3)-O(2)	1.217 (13)	C(4)-C(5)	1.540 (15)	C(4)-C(19)	1.521 (12)
C(5)-C(6)	1.550 (12)	C(6)-C(22)	1.499 (15)	C(7)-C(8)	1.409 (12)
C(7)-C(12)	1.388 (15)	C(8)-C(9)	1.409 (15)	C(9)-C(10)	1.405 (18)
C(10)-C(11)	1.393 (16)	C(11)-C(12)	1.396 (16)	C(13)-C(14)	1.395 (14)
C(13)-C(18)	1.403 (13)	C(13)-N	1.414 (10)	C(14)-C(15)	1.384 (12)
C(15)-C(16)	1.392 (14)	C(16)-C(17)	1.379 (15)	C(17)-C(18)	1.380 (12)
C(19)-O(3)	1.201 (12)	C(19)-O(4)	1.301 (15)	C(20)-C(21)	1.337 (22)
C(20)-O(4)	1.506 (14)	C(22)-C(23)	1.337 (16)		

Compound 7			
Atoms	Angle (°)	Atoms	Angle (°)
C(4)-C(1)-C(6)	87.2 (6)	C(4)-C(1)-C(7)	114.6 (7)
C(4)-C(1)-N	104.7 (7)	C(6)-C(1)-C(7)	121.1 (7)
C(6)-C(1)-N	113.1 (7)	C(7)-C(1)-N	112.4 (7)
C(3)-C(2)-O(1)	122.8 (9)	C(3)-C(2)-N	108.1 (8)
O(1)-C(2)-N	129.1 (9)	C(4)-C(3)-C(2)	109.2 (8)
C(4)-C(3)-O(2)	126.9 (9)	C(2)-C(3)-O(2)	123.8 (9)
C(5)-C(4)-C(1)	90.6 (7)	C(5)-C(4)-C(3)	116.9 (8)
C(5)-C(4)-C(19)	116.3 (8)	C(1)-C(4)-C(3)	104.1 (7)
C(1)-C(4)-C(19)	117.9 (8)	C(3)-C(4)-C(19)	109.5 (8)
C(6)-C(5)-C(4)	90.8 (7)	C(22)-C(6)-C(1)	119.8 (8)
C(22)-C(6)-C(5)	119.4 (8)	C(1)-C(6)-C(5)	90.1 (7)
C(8)-C(7)-C(1)	118.1 (8)	C(8)-C(7)-C(12)	119.6 (9)
C(1)-C(7)-C(12)	122.3 (8)	C(9)-C(8)-C(7)	119.4 (9)
C(10)-C(9)-C(8)	121.3 (10)	C(11)-C(10)-C(9)	118.0 (11)
C(12)-C(11)-C(10)	121.5 (11)	C(14)-C(13)-C(18)	120.0 (8)
C(14)-C(13)-N	119.6 (8)	C(18)-C(13)-N	120.4 (8)
C(15)-C(14)-C(13)	120.6 (9)	C(16)-C(15)-C(14)	118.5 (9)
C(17)-C(16)-Br	119.8 (7)	C(17)-C(16)-C(15)	121.2 (9)
Br-C(16)-C(15)	118.9 (7)	C(18)-C(17)-C(16)	120.5 (9)
O(3)-C(19)-C(4)	122.4 (9)	O(3)-C(19)-O(4)	126.1 (10)
C(4)-C(19)-O(4)	111.0 (8)	C(21)-C(20)-O(4)	109.9 (13)
C(23)-C(22)-C(6)	126.8 (10)	C(1)-N-C(2)	113.6 (7)
C(1)-N-C(13)	124.2 (7)	C(2)-N-C(13)	120.7 (7)
C(7)-C(12)-C(11)	120.2 (10)	C(13)-C(18)-C(17)	119.0 (9)
C(19)-O(4)-C(20)	118.1 (9)		

matrix approximations with anisotropic temperature factors, using 1928 (for 6) and 2292 (for 7) reflections. The  $R$  values were reduced to 0.085 for 6 and 0.078 for 7. The atomic parameters, bond lengths, and bond angles are given in Tables V and VI, and the structures are illustrated in Figs. 1 and 2.

**Acknowledgment** We thank Mr. Itatani and Miss Handa, Kanazawa University, for elementary analyses.

#### References and Notes

- 1) a) Preliminary communication: T. Sano, Y. Horiguchi, and Y. Tsuda, *Heterocycles*, **16**, 359 (1981); b) Part XXXV: T. Sano, Y. Horiguchi, K. Tanaka, and Y. Tsuda, *Chem. Pharm. Bull.*, **33**, 5197 (1985).

- 2) a) Y. Tsuda, K. Isobe, and A. Ukai, *J. Chem. Soc., Chem. Commun.*, **1971**, 1554; b) Y. Tsuda, Y. Horiguchi, and T. Sano, *Heterocycles*, **4**, 1355 (1976); c) T. Sano and Y. Tsuda, *ibid.*, **4**, 1361 (1976); d) T. Sano, J. Toda, N. Kashiwaba, and Y. Tsuda, *ibid.*, **16**, 1151 (1981); e) Y. Tsuda, T. Oshima, T. Sano, and J. Toda, *ibid.*, **19**, 2053 (1982).
- 3) a) Y. Tsuda and K. Isobe, *J. Chem. Soc., Chem. Commun.*, **1971**, 1555; b) Y. Tsuda, A. Ukai, and K. Isobe, *Tetrahedron Lett.*, **1972**, 3136.
- 4) T. Sano, J. Toda, and Y. Tsuda, *Heterocycles*, **18**, 229 (1982).
- 5) a) T. Sano, Y. Horiguchi, and Y. Tsuda, *Heterocycles*, **9**, 731 (1978); b) *Idem, ibid.*, **12**, 1427 (1979); c) T. Sano, Y. Horiguchi, S. Kambe, and Y. Tsuda, *ibid.*, **16**, 1463 (1981); d) Y. Horiguchi, T. Sano, and Y. Tsuda, *ibid.*, **23**, 1509 (1985).
- 6) T. Sano, Y. Horiguchi, and Y. Tsuda, *Heterocycles*, **6**, 889 (1981).
- 7) Preliminary communication: a) T. Sano, Y. Tsuda, H. Ogura, K. Furuhashi, and Y. Iitaka, *Heterocycles*, **4**, 1233 (1976); b) *Idem, ibid.*, 1367 (1976).
- 8) T. Sano, Y. Horiguchi, S. Kambe, J. Toda, J. Taga, and Y. Tsuda, *Heterocycles*, **16**, 893 (1981).
- 9) For the details of this reaction; see T. Sano, Y. Horiguchi, and Y. Tsuda, *Heterocycles*, **16**, 355 (1981).
- 10) T. Sano, J. Toda, Y. Tsuda, K. Yamaguchi, and S. Sakai, *Chem. Pharm. Bull.*, **32**, 3255 (1984).
- 11) Y. Tsuda, M. Kaneda, Y. Itatani, T. Sano, H. Horiguchi, and Y. Iitaka, *Heterocycles*, **9**, 153 (1978).

[Chem. Pharm. Bull.]  
35(1) 23-34 (1987)

## Dioxopyrrolines. XXXVII.<sup>1)</sup> Stereochemical Pathways of Dioxopyrroline-Olefin Photocycloaddition. Stereochemical Selection Rule for the Photocycloaddition of Enone-Olefin Pairs

TAKEHIRO SANO,\*<sup>a</sup> YOSHIE HORIGUCHI,<sup>a</sup> and YOSHISUKE TSUDA\*<sup>b</sup>

Showa College of Pharmaceutical Sciences,<sup>a</sup> Tsurumaki, Setagaya-ku, Tokyo 154, Japan,  
and Faculty of Pharmaceutical Sciences,<sup>b</sup> Kanazawa University,  
13-1 Takara-machi, Kanazawa 920, Japan

(Received May 8, 1986)

The photocycloaddition of 4-ethoxycarbonyl-5-phenyl-2*H*-pyrrole-2,3-dione **1** to (*Z*)- and (*E*)-*d*-styrenes proceeded in a stereoselective manner to give the compounds in which the styrene component added to **1** antarafacially as the major products. Including these results, the observed *exo*- or *endo*-stereoselectivity in the photocycloaddition of **1** to various acyclic olefins is well explained by assuming plural transition states, stepwise C-C bond formation, and a stereo-selection rule which may be stated as follows: 1) the first C-C bond formation always occurs suprafacially; 2) the second C-C bond formation in a polar enone-olefin pair (an enone and an olefin with a weak electron donating substituent) occurs antarafacially from the favored  $\pi$ -complex, while it occurs supra-selectively from the less favored transition state; and 3) in a very polar enone-olefin pair (an enone and an olefin with a strong electron donating group), the second C-C bond formation occurs supra-selectively from the favored  $\pi$ -complex and antarafacially from the less-favored transition state. Many other stereochemical results hitherto reported can be rationalized in terms of this stereo-selection rule.

**Keywords**—[2+2] photocycloaddition; 1*H*-pyrrole-2,3-dione; dioxopyrroline; (*Z*)-*d*-styrene; (*E*)-*d*-styrene; enone-olefin pair; stereochemistry; stereo-selection rule

The [2+2] photocycloaddition reaction of enones to olefins has been widely utilized for the construction of complex polycyclic compounds and many examples were reviewed.<sup>2)</sup> The broad outline of the reaction pathway appears to be generally accepted as shown in Chart 1.<sup>2a,3)</sup> The reaction involves a triplet excited state of the enone, which forms an excited  $\pi$ -complex with an olefin. This reactive species (an exciplex) then gives a 1,4-biradical by the formation of a covalent bond between either C $_{\alpha}$  or C $_{\beta}$  of the enone and one of the olefin carbons. The high regioselectivity in the formation of the head to tail (HT) adduct from an enone and an olefin (with an electron-donating substituent) pair is well explained by assuming that an "oriented  $\pi$ -complex or oriented exciplex" is formed from the encounter complex between the triplet excited enone and ground state olefin.<sup>4)</sup>

On the other hand, the stereochemical features of the reaction have remained obscure, although stereoselective addition of acyclic olefins to cyclic enones has often been observed

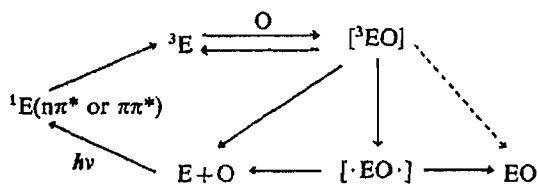


Chart 1. Generally Accepted Reaction Pathway of Enone-Olefin [2+2] Photocycloaddition Reaction

E: enone, O: olefin

<sup>1</sup>E: singlet excited enone

<sup>3</sup>E: triplet enone

<sup>3</sup>EO: exciplex

[·EO·]: 1,4-biradical intermediate

EO: cyclobutane product

(see below). In the photocycloaddition of 2-cyclohexenone to acyclic olefins, *trans*-fused bicyclo[4.2.0]octanes were usually obtained as the major product.<sup>4,5)</sup> As the reason for the formation of this strained product, the idea of rotational equilibration of the intermediate 1,4-biradicals<sup>2c)</sup> is hardly acceptable for such a cyclic compound. Instead of this idea, a mechanism involving initial complexation of a twisted enone triplet and the olefin leading to a twisted 1,4-biradical was suggested.<sup>6)</sup> However, the occurrence of this sort of highly strained intermediate is still uncertain.

Epiotis and Shaik theoretically concluded that the triplet [2+2] photoaddition of an enone-olefin pair preferentially occurs in a concerted [2s+2a] manner and suggested that the enone plays the role of the antarafacial component.<sup>7)</sup> From theoretical analyses of spin-inversion mechanisms leading to a final product, Shaik<sup>7b)</sup> further elaborated the above conclusion, indicating that the stereochemistry of olefin-olefin [2+2] photoaddition varies depending on the polarity (donor-acceptor relationship) of the olefin pair. When the olefin pair is nonpolar (*i.e.* both olefins are electron donors or electron acceptors) the [2s+2s] adduct is the main product. When the olefin pair is polar, the [2s+2a] adduct becomes the major product. When the olefin pair is very polar, the [2s+2s] adduct again becomes the main product. The formations of *trans*-fused and *cis*-fused cyclobutanes (shown in Chart 2) have been presented as examples of photocycloaddition of the polar<sup>4)</sup> and very polar olefin-olefin pairs.<sup>8)</sup>

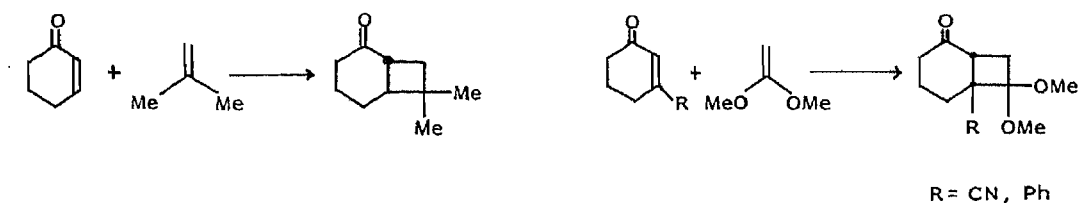


Chart 2. Examples of Polar and Very Polar Olefin-Olefin Pairs and Their Photocycloaddition (after Shaik)<sup>7b)</sup>

Few experimental data are available on the stereochemical pathway of the olefin component in photocycloaddition. This can only be elucidated when the stereochemistry of two termini of the olefin component in the product is established. One of the pioneering studies by de Mayo and Loutfy<sup>9)</sup> showed that the photoaddition of cyclopentenone to *cis*- and *trans*-dichloroethylenes afforded four stereoisomers in relative ratios shown in Chart 3. The result, as pointed out by the original authors,<sup>9)</sup> can not be rationalized in terms of rotational equilibration of 1,4-biradicals produced by bond formation at either the C<sub>α</sub> or C<sub>β</sub> position of the enone, since such an idea gives no adequate explanation for the preferred stereochemical inversions in the olefin component. Although their tentative interpretation is that both α- and β- bond formation pathways are operative, the data in Chart 3 rather imply that the reaction is controlled by some stereochemical selection rule. Contrary to de Mayo's result, both *cis*- and *trans*-2-butenes, in cycloaddition with a cyclohexenone derivative, often gave a mixture of the stereoisomers with almost identical relative ratios from either compound.<sup>4,10)</sup> The failure to retain the stereochemistry of the olefin moiety in the product was explained in terms of rotational equilibration of the 1,4-biradicals.<sup>4)</sup>

We have shown in the preceding paper<sup>1)</sup> that the photocycloaddition of the dioxopyrroline **1** to electron-rich olefins proceeds with high regio- and stereoselectivity to give the *cis*-fused cyclobutanes, 5-ethoxycarbonyl-1-phenyl-7-substituted-2-azabicyclo[3.2.0]heptane-3,4-diones **2** and **3**, with HT regiochemistry. The stereoselectivity in this reaction varies depending on the nature of the substituents of the olefins; olefins carrying phenyl, vinyl, thiophenyl, and

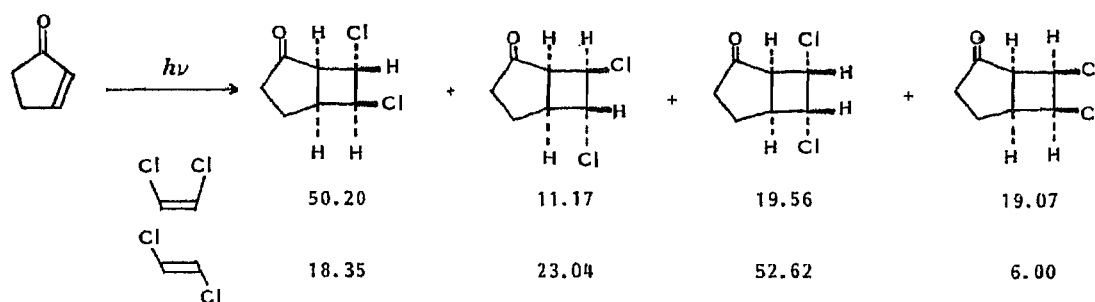


Chart 3. Photocycloaddition of Cyclopentenone to *cis*- and *trans*-Dichloroethylene (after Loufy and de Mayo)<sup>9)</sup>

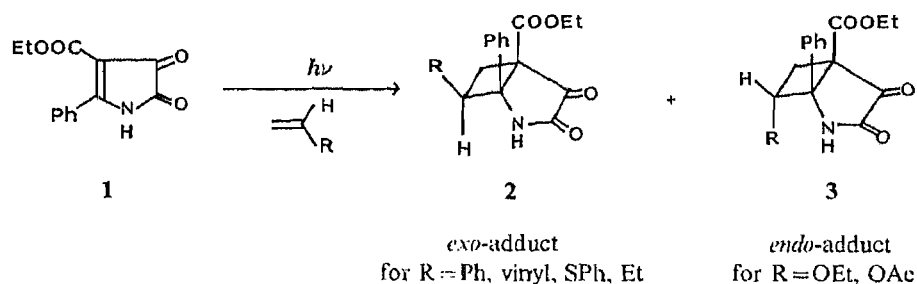


Chart 4. Photocycloaddition of Dioxopyrroline 1 to Acyclic Olefins<sup>1)</sup>

alkyl substituents gave the *exo*-adduct **2**, while olefins having *O*-substituents afforded the *endo*-adduct **3** as the major product. The *endo*-adduct **3**, irrespective of the nature of the C<sub>7</sub>-substituent, is thermodynamically more stable than the *exo*-isomer **2**.<sup>1)</sup> Therefore, the stereoselective formation of the thermodynamically less stable *exo*-isomer **2** can not be explained as a result of product developing control, but implies that the reaction is governed by some stereochemical selection rule.

It must be emphasized that in this cycloaddition reaction the stereochemistry of the ring junction and that of the C<sub>7</sub>-substituent in the adducts **2** and **3** do not disclose how the olefinic component underwent cycloaddition to the enone molecule. This can be established only when the stereochemistry at C<sub>6</sub> in the adduct is determined at the same time. In order to clarify this point we have carried out experiments using (*Z*)- and (*E*)-*d*-styrene.<sup>1)</sup>

In this paper we describe the stereochemical assignment of the photocycloadducts of dioxopyrroline to *d*-styrenes and discuss the stereochemical pathways of the dioxopyrroline-olefin photoannulation. We propose an empirical stereochemical selection rule for the enone-olefin photocycloaddition.

#### Photocycloaddition of Dioxopyrroline to (*Z*)- and (*E*)-*d*-Styrenes

Irradiation of **1** and (*Z*)-*d*-styrene in dimethoxyethane as described in the preceding paper<sup>1)</sup> afforded the *exo*-adduct **4Z** (22%) and the *endo*-adduct **5Z** (3%). That the deuterium is not lost in this photoreaction was evidenced by the mass and <sup>1</sup>H-nuclear magnetic resonance (<sup>1</sup>H-NMR) spectra of the products **4Z** and **5Z**. On the basis of the intensity ratio of the C<sub>6</sub>-*exo*-H and C<sub>6</sub>-*endo*-H signals (for stereochemical assignment, see below), **4Z** and **5Z** were identified as a 6 : 4 mixture of **4a** and **4b** and a 4 : 6 mixture of **5a** and **5b**, respectively, as shown in Fig. 1. The similar photoaddition of **1** to (*E*)-*d*-styrene afforded **4E** (40%) with 4 : 6 ratio of **4a** and **4b**, and **5E** (4%) with 6 : 4 ratio of **5a** and **5b**. Thus, the product distributions shown in Table I clearly indicate that the addition of (*Z*)- and (*E*)-*d*-styrene to **1** has proceeded in the same stereochemical manner.

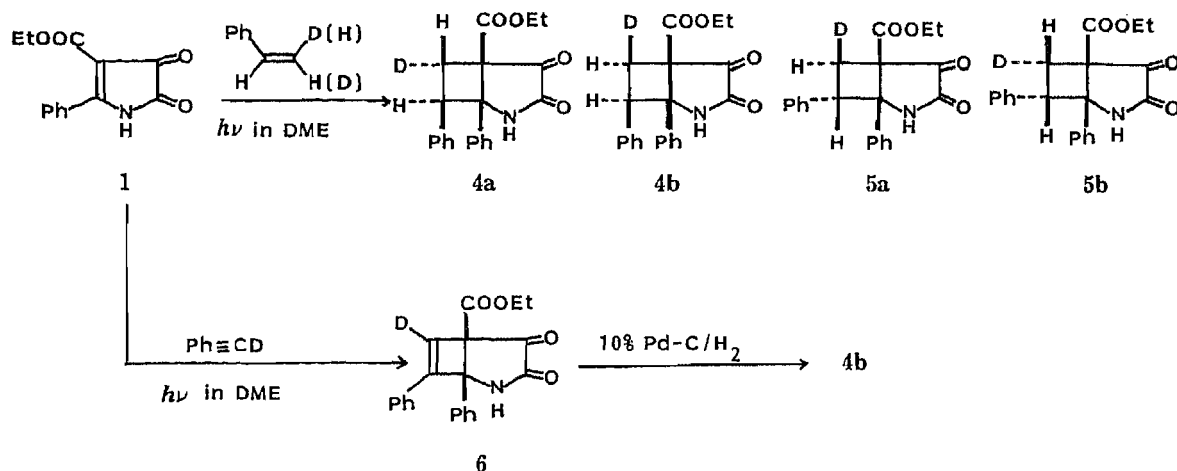
Chart 5. Photocycloaddition of 1 to (*Z*)- and (*E*)-*d*-Styrene

TABLE I. Product Ratios (%) of Photoadducts

Olefin	4a	4b	5a	5b
( <i>Z</i> )- <i>d</i> -Styrene	53	36	7	4
( <i>E</i> )- <i>d</i> -Styrene	36	54	4	6

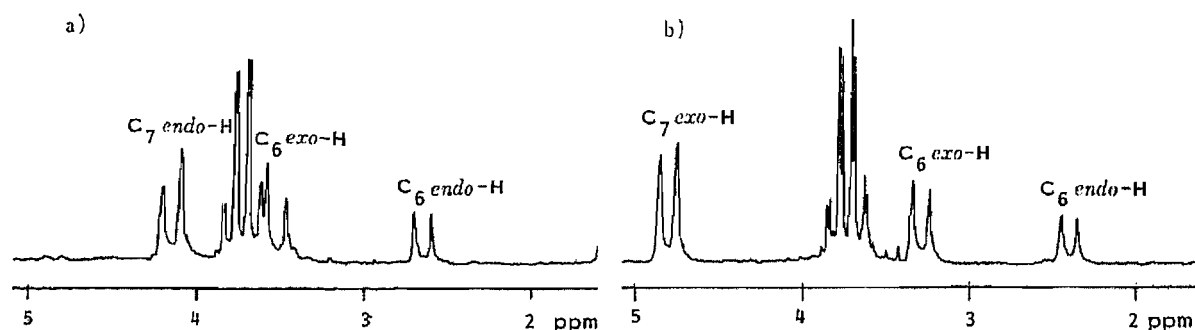


Fig. 1.  $^1\text{H-NMR}$  Spectra of *rel*-(1*S*,5*R*,7*R*)-6-Deutero-5-ethoxycarbonyl-1,7-diphenyl-2-azabicyclo[3.2.0]heptane-3,4-dione (**4Z**) and *rel*-(1*S*,5*R*,7*S*)-6-Deutero-5-ethoxycarbonyl-1,7-diphenyl-2-azabicyclo[3.2.0]heptane-3,4-dione (**5Z**)

a) **4Z**, b) **5Z**.

Formation of two isomers relating to the  $\text{C}_6$ -deuterium stereochemistry in **4Z** and **5Z** could not arise from either photo-isomerization of the olefin prior to photoaddition or that of the adducts, since (*Z*)-*d*-styrene did not isomerize to (*E*)-*d*-styrene under similar irradiation, and the ratio of **4a** and **4b** was independent of the reaction time. The above results therefore indicate that styrene undergoes cycloaddition to **1** in an antarafacial manner (or with inversion of configuration).

The stereochemical assignments of 6-*exo*- and 6-*endo*-H in **4Z** and **5Z** (and also in **4E** and **5E**) were achieved by nuclear Overhauser effect (NOE) observation as follows. The deuterated *exo*-adduct **4Z** exhibits the  $\text{C}_7$ -H (*endo*) signal at  $\delta$  4.19 and  $\text{C}_6$ -H signals at  $\delta$  2.68 (d) and 3.53

(d). Irradiation of the C<sub>7</sub>-*endo*-H at  $\delta$  4.19 enhanced the intensity of the C<sub>6</sub>-H signal at  $\delta$  2.68 by 16%, but had no effect on the intensity of the other C<sub>6</sub>-H signal at  $\delta$  3.53, indicating that the former proton is in *cis* relationship with C<sub>7</sub>-*endo*-H and the latter proton is *trans* to C<sub>7</sub>-H, corresponding to C<sub>6</sub>-H of **4a** and **4b**, respectively.

Similarly, the two C<sub>6</sub>-H signals at  $\delta$  2.48 and 3.36 in **5Z** were assigned as *endo* and *exo*, respectively, which correspond to the C<sub>6</sub>-H of **5a** and **5b**. When the signal at  $\delta$  4.83 due to the C<sub>7</sub>-*exo*-H was irradiated, an NOE enhancement (36%) was observed only in the signal at  $\delta$  3.36, indicating that it is in a *cis*-relationship with the C<sub>7</sub>-*exo*-H.

The above assignment was supported by the following chemical synthesis of **4b**. The photoaddition of **1** to deuterated phenylacetylene afforded the deuterated cyclobutene **6**. Catalytic hydrogenation of **6** over Pd-C afforded **4b** as a sole product, which showed the C<sub>6</sub>-H signal only at  $\delta$  2.69, confirming that in **4b** the stereochemistry of the C<sub>6</sub>-deuterium and C<sub>7</sub>-phenyl is *cis*.

### Stereoselection of Enone-Olefin Photocycloaddition

The regiochemistry of dioxopyrroline-olefin photocycloaddition is well explained by the concept of the oriented  $\pi$ -complex known for a usual enone-olefin photocycloaddition.<sup>4)</sup> Here we propose the following three assumptions to explain the stereochemical results of our reactions, which, we believe, are applicable not only to dioxopyrroline-olefin pairs but also to other enone-olefin pairs hitherto reported, as shown below.

1) The reaction proceeds through two or more transition states, equally or differently favored, which originate from (positionally or stereochemically) different modes of approach of the two components.

2) The two C-C bond formations in the oriented  $\pi$ -complex occur stepwise (though maybe only formally), at either the C <sub>$\alpha$</sub>  or C <sub>$\beta$</sub> -position of the enone in such a way that the first bond formation results in the formation of the most stable 1,4-biradical.

3) Selection rule of stereochemistry.

i) The first C-C bond formation always occurs suprafacially (or with retention of configuration in the  $\pi$ -complex). ii) In a polar pair (*i.e.* an enone and an olefin having weak an electron-donating group such as an alkene), the second C-C bond formation at the other terminus occurs *antara*-selectively (or with inversion of configuration) from the favored complex, and *supra*-selectively from the less favored transition. iii) In a very polar enone-olefin pair (*i.e.* an enone and an olefin having an *O*-substituent such as alkoxyethylene), the second bond formation occurs in a *supra*-selective manner from the favored complex and in an *antara*-selective manner from the less favored transition.

The first two assumptions may be *a priori* acceptable. The presence of plural transition states in photocycloaddition has often been considered or recognized.<sup>2c)</sup> Concomitant formations of regio-isomeric HH and HT adduct in some photocycloadditions are typical examples.<sup>12)</sup> The formations of *syn*- and *anti*-adduct in cycloaddition of a cyclic enone to a cycloalkene are examples where two assumed transitions are only stereochemically different.<sup>13)</sup> Those are considered to be *endo*- and *exo*-complexes, respectively.

The energy levels of the transition state are dependent on electronic factors such as orbital overlapping and dipole-dipole interaction and on steric hindrance to the approach. Generally the *endo* isomer would be favored because it would gain maximum orbital overlapping, unless steric interaction is excessive.<sup>14)</sup> The preferred formation of the *cis-syn-cis* adduct from the reaction of uracil and vinylene carbonate pair,<sup>13a)</sup> and the exclusive formation of the *cis-syn-cis* adduct from 4-hydroxycoumarin and cyclopentene pair<sup>15)</sup> show that the *endo*-complex is favored by the molecular orbital interaction. On the other hand, the adduct from cyclopentenone-cyclopentene pair<sup>16)</sup> usually has the *cis-anti-cis* stereochemistry, suggesting that the *endo*-complex is less favored than the *exo*-complex. The addition of 2-

acetoxycyclopentenone to 4,4-dimethylcyclopentene<sup>16d)</sup> leads to the nearly exclusive formation of the adduct with *cis-anti-cis* configuration, while dihydrofuran gives nearly equal amounts of the *syn*- and *anti*-isomers.<sup>2c)</sup> The presence of an oxygen atom in the ring system may reduce the steric hindrance and increase the molecular orbital interaction.

We should point out that in the reaction of a cyclic enone with monosubstituted olefins two stereoisomeric *exo*- and *endo*-exciplexes both leading to HT regiochemistry are possibly present. This has been overlooked in most cases, probably because the stereochemistry of the olefin moiety has seldom been established rigidly.

The second assumption is well known for the 1,4-biradical mechanism, although we do not envisage a clear biradical species but only assume the order of bond formation. The 1,4-biradical (A) formed from a complex of an enone and an olefin monosubstituted by an electron donating group due to coupling at C<sub>α</sub>, where the pair always gives the HT adduct, is obviously a more stable species than that formed by C<sub>β</sub>-coupling (B). In this case the first bond formation occurs at C<sub>α</sub>. The 1,4-biradical (C) formed by C<sub>β</sub>-coupling from a complex of an enone and an olefin 1,2-disubstituted by groups of the same or nearly the same electronic properties should be more stable than the biradical formed by C<sub>α</sub>-coupling (D), where the first bond formation would be at C<sub>β</sub>, although the energy differences between these two species might be small. [In the reaction of an enone and olefins monosubstituted by an electron withdrawing group, the first bond formation would occur at C<sub>β</sub>, since the 1,4-biradical (E) derived from the oriented π-complex leading to the HH adduct must be more stable than that in the case of C<sub>α</sub>-coupling (F). In some instances a re-orientation mechanism was proposed.<sup>17)</sup>] Our assumption does not conflict with the concerted mechanism. Even if the reaction is concerted, as suggested by Epiotis and Shaik,<sup>7a)</sup> the interpretation remains valid when a very short-lived biradical is considered in the course of a stepwise mechanism.

In contrast to assumptions 1) and 2), the third assumption (selection rule of stereochemistry) is purely empirical. The next section deals with this subject. Here we only point out the fact that *trans* stereochemistry in a cyclobutane adduct appears not only at the enone

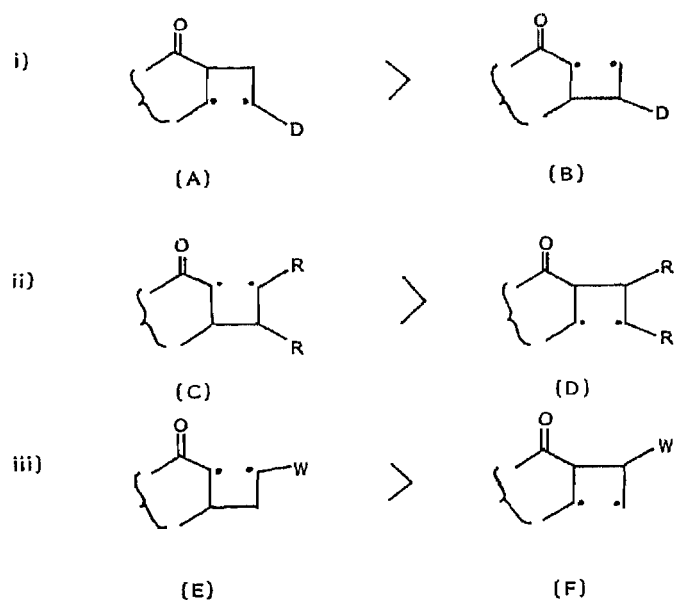


Chart 6. The Order of C-C Bond Formation

- i) Olefin monosubstituted by an electron-donating group.
- ii) Olefin 1,2-disubstituted by groups of the same or nearly the same electronic properties.
- iii) Olefin monosubstituted by an electron-withdrawing group.



component, but also, in some instances, at the olefin component.<sup>18)</sup> In cyclohexenone-olefin reactions, the antarafacial component, if present, is always the cyclohexenone. The triplet species in the encounter complex is undoubtedly the enone. However, in the oriented  $\pi$ -complex after intersystem crossing, either the enone or the olefin can be an antarafacial component. In fact, the reaction of cyclopentenones with cyclohexenes<sup>18a)</sup> and that of bicyclic enones with cyclohexenes,<sup>18b)</sup> where the enones are geometrically such that it is difficult or impossible to adopt *trans* configuration, afford the cyclobutanes having *trans*-stereochemistry at the olefin component.

### Interpretations of Stereochemical Results in Enone-Olefin Pairs

By adopting the above three assumptions, the stereochemical results of the enone-olefin photoannulations can be well interpreted. For the dioxopyrroline-(*Z*)- and (*E*)-*d*-styrene pairs, the product distribution can be explained as shown in Chart 7. The *endo*-complex **7** should be more favored than the *exo*-complex **8** as the oriented transition state formed from an encounter complex, because it has the least steric hindrance at the *endo* face and because of an orbital overlapping effect between the electron deficient dioxopyrroline ring and phenyl group, although the *exo*-complex **8** is not much less favored, because of phenyl-phenyl  $\pi$ - $\pi$  overlapping. These products are assumed to be formed in a ratio of 6:4. From the favored *endo*-complex **7**, the first C-C bond formation occurs suprafacially at  $C_\alpha$ , then the following bond formation at  $C_\beta$  with antarafacial selectivity to give the *exo*-adduct **4a** with 8-fold preference over **5b**, while from the less favored *exo*-complex **8**, supra-selective addition at  $C_\beta$  gives the *exo*-adduct **4b** with 8-fold preference over **5a**. The *exo*-selectivity observed in 1-butene, butadienes, and phenylthioethylene<sup>1)</sup> can be similarly rationalized in terms of the supra-

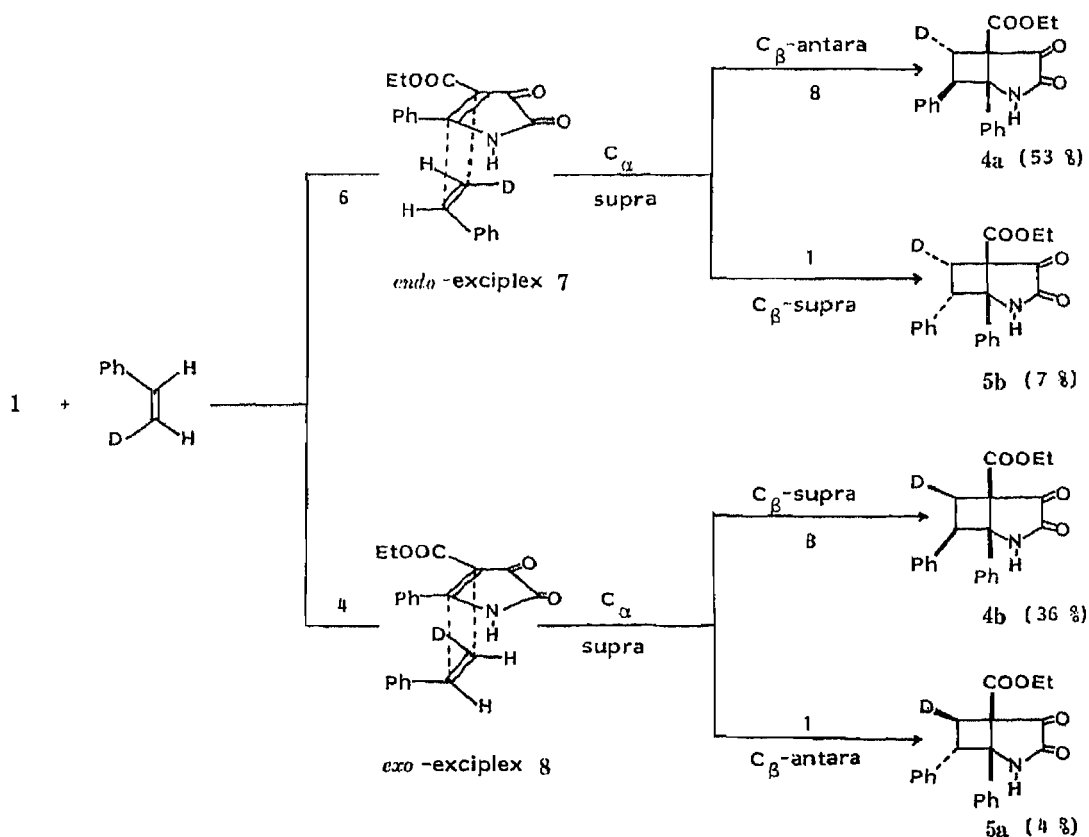


Chart 7. Interpretation of the Stereochemical Results of the Photocycloaddition Reaction of **1** to (*Z*)-*d*-Styrene in Terms of the Stereo-Selection Rule

selective addition at  $C_\alpha$  and antara-selective addition at  $C_\beta$  from the favored *endo*-complex. For those pairs, inversion always occurs at the olefin component, since the enone component can not invert its configuration due to the great strain of the five membered ring system.

Another explanation may be possible for this styrene addition; that is, either the 1,4-biradical **9** or **10** formed from the *endo* or *exo*-complex comes into rotational equilibrium to give the phenyl *exo*-oriented product **4Z** (**4E**) with 8-fold preference over **5Z** (**5E**) due to a phenyl-phenyl attractive interaction which produces a parallel array of the two phenyl groups. This mechanism can explain the *exo*-selectivity observed with butadiene, in which phenyl-vinyl attractive interaction is expected to operate in the biradical, leading to the *exo*-adduct **2**. However, this idea provides no basis for explaining the *exo*-selectivity observed with 1-butene and phenylthioethylene.

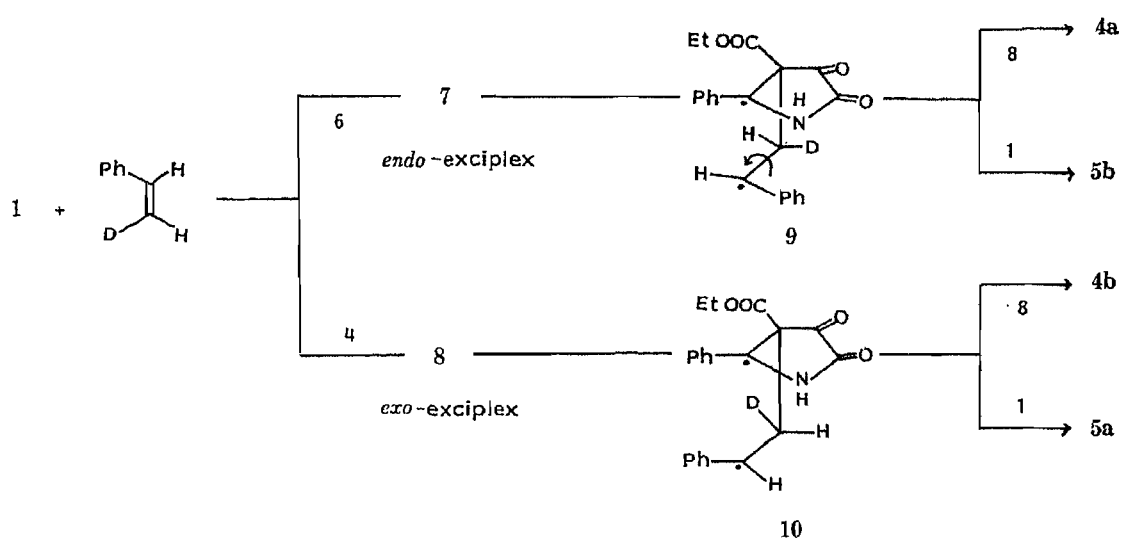


Chart 8. Attempted Interpretation of the Stereochemical Results of the Photocycloaddition Reaction of **1** to (*Z*)-*d*-Styrene in Terms of Rotational Equilibration of the Intermediate 1,4-Biradical

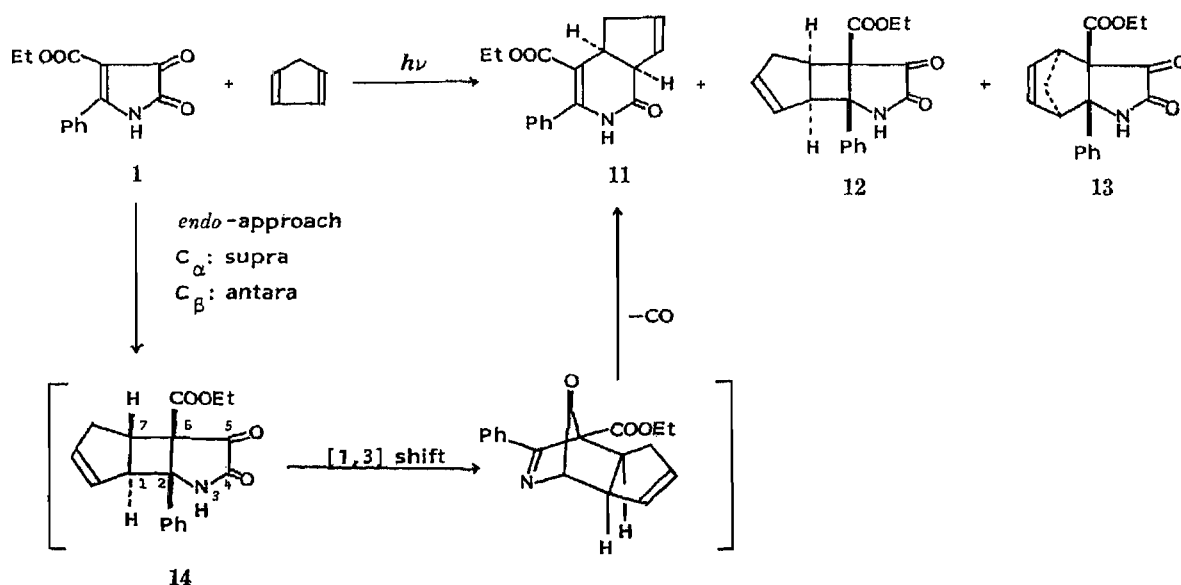


Chart 9. Photocycloaddition Reaction of **1** to Cyclopentadiene (after Tsuda *et al.*)<sup>23)</sup>

*endo*-Selectivity of the olefins carrying an *O*-substituent<sup>1)</sup> can be explained by considering that the pair is very polar, because the electron rich *O*-substituent and the dioxopyrrolone ring are expected to have strong attractive interactions. Thus, the *endo*-adduct **3** is formed supra-selectively from the favored *endo*-complex. An alternative explanation is that the intermediate formed from these pairs is a long lived biradical, so that the product is the thermodynamically more stable *endo*-isomer **3**. If we take this approach, the more stereo-selective addition of isopropenyl acetate (*endo*-*O*:*exo*-*O*=6:1) in contrast to the thermodynamic equilibration (*endo*-*O*:*exo*-*O*=2:3)<sup>1)</sup> in the above product is still to be explained. The intermediate from phenylthioethylene should be a similarly long-lived biradical. However, the result is different. Consequently, we can predict that as the polarity of the enone-olefin pair increases, the formation of the *endo*-adduct becomes preferred. In fact, ethoxyethylene affords the *endo*-

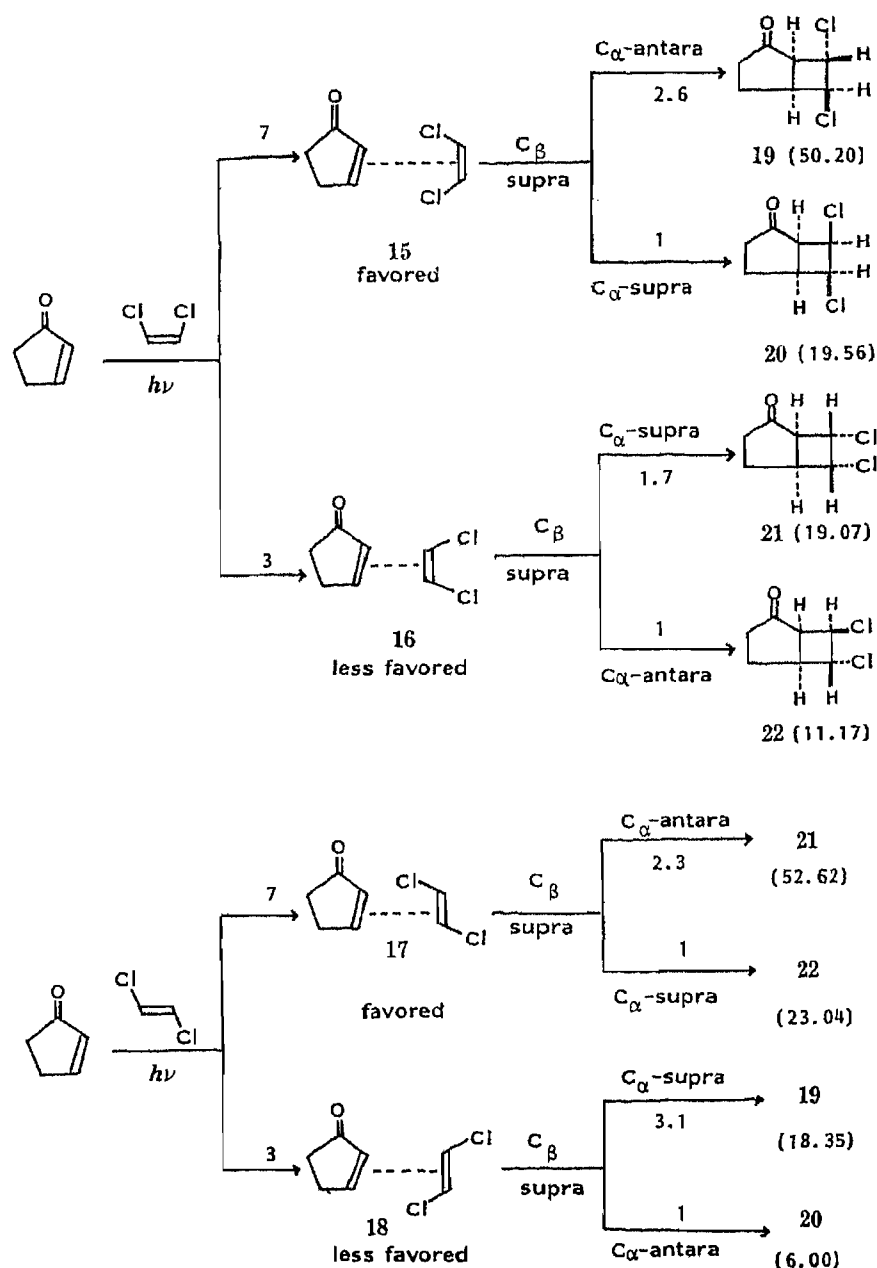


Chart 10. Interpretation of Loutfy and de Mayo's Results in Terms of the Stereo-Selection Rule

adduct **3** in 10-fold excess, while phenylthioethylene affords the *exo*-adduct **2** in 1.5-fold excess. The polarity of the latter pair is not as large as that of the former pair. In accordance with this interpretation a 1,1-disubstituted olefin carrying the *O*-tetramethylsilane (*O*-TMS) group exclusively afforded the *endo-O* adduct.<sup>19)</sup>

We have previously reported<sup>20)</sup> that the photoaddition of **1** to cyclopentadiene gave the dihydropyridone **11** as a major product, together with a cyclobutane **12**<sup>21)</sup> and a hydroindole **13** (Chart 9). This implies the intermediary formation of the unstable *trans*-fused cyclobutane **14**<sup>22)</sup> as a result of antarafacial addition of the cyclopentadiene component. This highly strained species would undergo 1,3-shift (either photochemically or thermally) of the C<sub>1</sub>-C<sub>7</sub> bond, followed by cheletropic loss of CO to afford **11**. Cyclopentene and indene also gave this type of photoadduct as a major product.<sup>23)</sup>

The above assumptions also give a reasonable explanation for the results of Loutfy and de Mayo (Chart 10).<sup>9)</sup> The cyclopentenone-*cis*- and *trans*- dichloroethylene pairs are considered to be polar. The favored oriented  $\pi$ -complexes formed from these pairs are those of **15** and **17**, where one chlorine atom is close to the carbonyl group, since the dipole-dipole interaction between C=O of the excited enone and C-Cl of the ground state olefin should be attractive. The product distributions indicate that the ratio of favored to less favored complexes (**15/16** and **17/18**) is 7/3 in both reactions. The first C-C bond formation occurs supra-selectively at C <sub>$\beta$</sub>  in all complexes, since both termini of the olefin are substituted by the same group. In *cis*-dichloroethylene the favored complex **15** yields cyclobutanes **19** and **20** with antarafacial coupling (2.6 times) at the  $\alpha$ -position, while the less favored complex **16** gives **21** and **22** with supra-selective coupling (1.7 times) at the  $\alpha$ -position. In the case of *trans*-dichloroethylene, **17** and **18** similarly form cyclobutanes with antarafacial (**21/22** = 2.3) and supra-selectivity (**19/20** = 3.1) at C <sub>$\alpha$</sub> , respectively.

The stereo-selection rule that we proposed here seems to work reliably for predicting the stereochemistry of [2 + 2] photocycloaddition of enone-olefin pairs. Although there are some exceptions,<sup>10,24)</sup> many examples hitherto reported in the literature, *i.e.* the *exo*- or *endo*-selectivity in photo-cycloaddition of cyclic enones to monosubstituted olefins,<sup>13,23)</sup> the *trans* addition of cyclohexenes to cyclopentenones<sup>18b,c)</sup> and the *trans* addition of cyclohexenones to cyclopentenones,<sup>5)</sup> can be rationalized in terms of this rule. However, we have to emphasize that at the present stage this rule is an empirical one, for which a theoretical background is awaited.

### Experimental

Unless otherwise stated, the following procedures were adopted. Melting points were taken on a Yanagimoto micro hot-stage apparatus, and are uncorrected. Infrared (IR) spectra were taken in Nujol mulls with a Hitachi 260-10 spectrometer and are given in cm<sup>-1</sup>. Ultraviolet (UV) spectra were recorded in dioxane with a Hitachi 200-10 spectrophotometer. <sup>1</sup>H-NMR (100 MHz) spectra were taken in CDCl<sub>3</sub> solution with TMS as an internal standard on a JEOL FX-100 spectrometer. High-resolution mass spectra (MS) were recorded on a JEOL JMS-D300 mass spectrometer. For column chromatography, silica gel (Wako-gel C-200) was used. Thin layer chromatography (TLC) was performed on precoated Silica gel 60 F<sub>254</sub> plates (Merck). The photolysis solution was irradiated internally using a 300 W high-pressure mercury lamp (Eikosha Halos PIH 300) with a Pyrex filter.

#### The Photocycloaddition of **1** to (*Z*)- and (*E*)-*d*-Styrene

(i) (*Z*)-*d*-Styrene—A solution of **1** (1 g, 4 mmol) and (*Z*)-*d*-styrene (1.3 g, 12 mmol) in dimethoxyethane (DME) (300 ml) was irradiated for 45 min under ice cooling. The residue obtained by evaporation of the solvent was crystallized from CH<sub>2</sub>Cl<sub>2</sub>-Et<sub>2</sub>O to give **4Z**. Chromatography of the mother liquor over SiO<sub>2</sub> in CH<sub>2</sub>Cl<sub>2</sub> and crystallization of the eluate from CH<sub>2</sub>Cl<sub>2</sub>-Et<sub>2</sub>O gave another crop of **4Z** and **5Z**.

**4Z**: Yield 310 mg, 22%, colorless prisms, mp 215–223 °C. IR: 1765, 1740 sh, 1720. <sup>1</sup>H-NMR  $\delta$ : 0.63 (3H, t, *J* = 7 Hz, COOCH<sub>2</sub>CH<sub>3</sub>), 2.68 (0.4H, d, *J* = 10 Hz, C<sub>6</sub>-H), 3.53 (0.6H, d, *J* = 10 Hz, C<sub>5</sub>-H), 3.73 (2H, q, *J* = 7 Hz, COOCH<sub>2</sub>CH<sub>3</sub>), 4.19 (1H, d, *J* = 10 Hz, C<sub>7</sub>-H), 7.1 (10H, m, Ar-H). MS *m/z*: M<sup>+</sup> Calcd for C<sub>21</sub>H<sub>18</sub>DNO<sub>4</sub> 350.1377. Found: 350.1372.

**5Z**: Yield 43 mg, 3%, colorless prisms, mp 173–185 °C. IR: 3310, 1765, 1735, 1710. <sup>1</sup>H-NMR  $\delta$ : 0.72 (3H, t, *J* =

7 Hz, COOCH<sub>2</sub>CH<sub>3</sub>), 2.48 (0.4H, d,  $J=9$  Hz, C<sub>6</sub>-H), 3.36 (0.6H, d,  $J=9$  Hz, C<sub>6</sub>-H), 3.78 (2H, q,  $J=7$  Hz, COOCH<sub>2</sub>CH<sub>3</sub>), 4.83 (1H, d,  $J=9$  Hz, C<sub>7</sub>-H), 7.0–7.5 (10H, m, Ar-H). MS  $m/z$ : M<sup>+</sup> Calcd for C<sub>21</sub>H<sub>18</sub>DNO<sub>4</sub> 350.1378. Found: 350.1415.

(ii) (*E*)-*d*-Styrene—A solution of **1** (1 g, 4 mmol) and (*E*)-*d*-styrene (1.3 g, 12 mmol) in DME (300 ml) was irradiated as above. Work-up as above gave **4E** and **5E**.

**4E**: Yield 570 mg, 40%, colorless prisms, mp 213–223 °C. <sup>1</sup>H-NMR  $\delta$ : 0.63 (3H, t,  $J=7$  Hz, COOCH<sub>2</sub>CH<sub>3</sub>), 2.68 (0.6H, d,  $J=10$  Hz, C<sub>6</sub>-H), 3.53 (0.4H, d,  $J=10$  Hz, C<sub>6</sub>-H), 3.73 (2H, q,  $J=7$  Hz, COOCH<sub>2</sub>CH<sub>3</sub>), 4.19 (1H, d,  $J=10$  Hz, C<sub>7</sub>-H), 7.1 (10H, m, Ar-H).

**5E**: Yield 57 mg, 4%, colorless prisms, mp 173–185 °C. <sup>1</sup>H-NMR  $\delta$ : 0.72 (3H, t,  $J=7$  Hz, COOCH<sub>2</sub>CH<sub>3</sub>), 2.48 (0.6H, d,  $J=9$  Hz, C<sub>6</sub>-H), 3.36 (0.4H, d,  $J=9$  Hz, C<sub>6</sub>-H), 3.78 (2H, q,  $J=7$  Hz, COOCH<sub>2</sub>CH<sub>3</sub>), 4.83 (1H, d,  $J=9$  Hz, C<sub>7</sub>-H), 7.0–7.5 (10H, m, Ar-H).

**Photocycloaddition of 1 to *d*-Phenylacetylene**—A solution of **1** (1 g, 4 mmol) and *d*-phenylacetylene (1.3 g, 12 mmol) in DME (300 ml) was irradiated for 45 min under ice cooling. After evaporation of the solvent, the residue in CH<sub>2</sub>Cl<sub>2</sub> was chromatographed over SiO<sub>2</sub> to give *rel*-(1*S*,5*R*)-6-deutero-5-ethoxycarbonyl-1,7-diphenyl-2-azabicyclo[3.2.0]hept-6-ene-3,4-dione **6** (200 mg, 14%) as pale yellow prisms from CH<sub>2</sub>Cl<sub>2</sub>-Et<sub>2</sub>O, mp 165–175 °C. IR: 1770, 1740, 1710. <sup>1</sup>H-NMR  $\delta$ : 0.79 (3H, t,  $J=7$  Hz, COOCH<sub>2</sub>CH<sub>3</sub>), 3.73 (2H, q,  $J=7$  Hz, COOCH<sub>2</sub>CH<sub>3</sub>), 7.27 (5H, br s, aromatic-H), 7.31 (5H, br s, Ar-H). UV  $\lambda_{max}$  nm ( $\epsilon$ ): 253 (15900). MS  $m/z$ : M<sup>+</sup> Calcd for C<sub>21</sub>H<sub>16</sub>DNO<sub>4</sub> 348.1220. Found: 348.1267.

**Catalytic Hydrogenation of 6**—The deuterated cyclobutene **6** (700 mg) in EtOH (40 ml) was hydrogenated over 10% Pd-C under 4.2 atmospheres pressure for 3 h at room temperature. The product in CH<sub>2</sub>Cl<sub>2</sub> was passed through a short column of SiO<sub>2</sub> and recrystallized from CH<sub>2</sub>Cl<sub>2</sub>-MeOH to give *rel*-(1*S*,5*R*,6*R*,7*R*)-6-deutero-5-ethoxycarbonyl-1,7-diphenyl-2-azabicyclo[3.2.0]heptane-3,4-dione **4b** (450 mg, 63%) as colorless prisms, mp 200–212 °C. IR: 1765, 1740 sh, 1720. <sup>1</sup>H-NMR  $\delta$ : 0.63 (3H, t,  $J=7$  Hz, COOCH<sub>2</sub>CH<sub>3</sub>), 2.68 (1H, d,  $J=10$  Hz, C<sub>6</sub>-H), 3.73 (2H, q,  $J=7$  Hz, COOCH<sub>2</sub>CH<sub>3</sub>), 4.19 (1H, d,  $J=10$  Hz, C<sub>7</sub>-H), 7.1 (10H, m, Ar-H). MS  $m/z$ : M<sup>+</sup> Calcd for C<sub>21</sub>H<sub>18</sub>DNO<sub>4</sub> 350.1377. Found: 350.1384.

#### References and Notes

- 1) Part XXXVI: T. Sano, Y. Horiguchi, Y. Tsuda, K. Furuhashi, H. Takayanagi, and H. Ogura, *Chem. Pharm. Bull.*, **35**, 9 (1987).
- 2) a) H. Meier, "Methoden Org. Chem." (Houben Weyl), 1975, 4/5b, p. 898; b) S. W. Baldwin, "Organic Photochemistry," Vol. 5, ed. by A. Padwa, Marcel Dekker, Inc., New York, 1981, p. 123; c) P. G. Bauslaugh, *Synthesis*, **1970**, 287; d) P. de Mayo, *Acc. Chem. Res.*, **4**, 41 (1971); e) P. Margaretha, *Chimia*, **29**, 203 (1975).
- 3) R. O. Loutfy and P. de Mayo, *J. Am. Chem. Soc.*, **97**, 3559 (1977).
- 4) E. J. Corey, J. D. Bass, R. LeMahieu, and R. B. Mitra, *J. Am. Chem. Soc.*, **86**, 5570 (1964).
- 5) a) G. R. Lenz, *J. Chem. Soc., Perkin Trans. 1*, **1984**, 2397; b) G. R. Lenz, *Tetrahedron*, **28**, 2195 (1972); c) M. Umehara, T. Oda, Y. Ikebe, and S. Hishida, *Bull. Chem. Soc. Jpn.*, **49**, 1075 (1976).
- 6) a) R. M. Bowman, C. Calvo, J. J. McCullough, P. W. Rasmussen, F. F. Snyder, *J. Org. Chem.*, **37**, 2084 (1972); b) D. I. Schuster, M. M. Greenberg, I. M. Nunez, and P. C. Tucker, *J. Org. Chem.*, **48**, 2615 (1983).
- 7) a) S. S. Shaik and N. D. Epiotis, *J. Am. Chem. Soc.*, **100**, 18 (1978); b) S. S. Shaik, *ibid.*, **101**, 3184 (1979).
- 8) a) T. S. Cantrell, W. S. Haller, and J. C. Williams, *J. Org. Chem.*, **34**, 509 (1969); b) T. S. Cantrell, *Tetrahedron*, **27**, 1227 (1971).
- 9) R. O. Loutfy and P. de Mayo, *Can. J. Chem.*, **50**, 3465 (1972).
- 10) a) N. P. Peet, R. L. Cargill, and D. F. Bushey, *J. Org. Chem.*, **38**, 1218 (1973); b) Y. Tobe, T. Hoshino, Y. Kawakami, Y. Sakai, K. Kimura, and Y. Odaira, *ibid.*, **43**, 4334 (1978); c) P. Margaretha, *Tetrahedron*, **29**, 1317 (1973).
- 11) K. E. Koenig and Wm. P. Weber, *J. Am. Chem. Soc.*, **95**, 3416 (1973).
- 12) T. Ogino, T. Kubota, and K. Manaka, *Chem. Lett.*, **1976**, 323.
- 13) a) D. E. Bergstrom and W. C. Agosta, *Tetrahedron Lett.*, **1974**, 1087; b) D. Termont, P. De Clereq, D. De Keukeleire, and M. Vandewalle, *Synthesis*, **1977**, 46.
- 14) Some examples of [2+2] photoaddition reactions of olefin-olefin pairs also showed the preferred formation of the *endo*-complex. [R. A. Caldwell and L. Smith, *J. Am. Chem. Soc.*, **96**, 2994 (1974) and F. D. Lewis, R. H. Hirsch, P. M. Roach, and D. E. Johnson, *ibid.*, **98**, 8438 (1976).]
- 15) H. Sugimoto, C. F. Liu, and A. Furusaki, *Chem. Lett.*, **1984**, 911.
- 16) a) K. Ohga and T. Matsuo, *Bull. Chem. Soc. Jpn.*, **49**, 1590 (1976); b) S. W. Baldwin and M. T. Crimmins, *J. Am. Chem. Soc.*, **102**, 1198 (1980); c) J. D. White and D. N. Gupta, *ibid.*, **90**, 6171 (1968); d) P. E. Eaton, *ibid.*, **84**, 2454 (1962).
- 17) T. Naito and C. Kaneko, *Yuki Gosei Kyokai Shi*, **42**, 51 (1984).
- 18) a) Y. Tobe, A. Doi, A. Kunai, K. Kimura, and Y. Odaira, *J. Org. Chem.*, **42**, 2523 (1977); b) H. Takeshita, R. Kikuchi, and Y. Shoji, *Bull. Chem. Soc. Jpn.*, **46**, 690 (1973); c) K. Tatsuta, K. Akimoto, and M. Kinoshita, *J.*

- Am. Chem. Soc.*, **101**, 6116 (1979).
- 19) T. Sano, J. Toda, Y. Tsuda, K. Yamaguchi, and S. Sakai, *Chem. Pharm. Bull.*, **32**, 3255 (1984).
  - 20) Y. Tsuda, M. Kaneda, Y. Itatani, T. Sano, H. Horiguchi, and Y. Iitaka, *Heterocycles*, **9**, 153 (1978).
  - 21) Although *cis-syn-cis* configuration was suggested<sup>20)</sup> for this compound, we now wish to revise the structure to *anti*-configuration on the basis of spectral and chemical evidence. The details will be reported elsewhere.
  - 22) This may be the first evidence that a cyclopentene component can undergo cycloaddition to an enone in an antarafacial manner.
  - 23) T. Sano, Y. Horiguchi, Y. Tsuda, and I. Itatani, *Heterocycles*, **9**, 161 (1978).
  - 24) a) J. S. Swenton, J. A. Hyatt, J. M. Lisy, and J. Clardy, *J. Am. Chem. Soc.*, **96**, 4885 (1974); b) A. Wexler, R. J. Balchunis, and J. S. Swenton, *J. Chem. Soc., Chem. Commun.*, **1975**, 602; c) K. Maruyama, T. Otsuki, and S. Tai, *Chem. Lett.*, **1984**, 371.
  - 25) a) K. Maruyama and N. Narita, *Bull. Chem. Soc. Jpn.*, **53**, 757 (1980); b) H. J. Liu and W. H. Chan, *Can. J. Chem.*, **58**, 2196 (1980); c) T. Chiba, T. Kato, A. Yoshida, R. Mori, N. Shimomura, Y. Momose, T. Naito, and C. Kaneko, *Chem. Pharm. Bull.*, **32**, 4707 (1984); d) A. Wexler and J. S. Swenton, *J. Am. Chem. Soc.*, **98**, 1602 (1976); e) D. Termont, D. De Keukeleire, and M. Vandewalle, *J. Chem. Soc., Perkin Trans. 1*, **1977**, 2349; f) H. Fujii, K. Shiba, and C. Kaneko, *J. Chem. Soc., Chem. Commun.*, **1980**, 537; g) T. Naito, Y. Makita, and C. Kaneko, *Chem. Lett.*, **1984**, 921.

[Chem. Pharm. Bull.]  
35(1) 35-45 (1987)

## 1,3-Dipolar Cycloaddition Reactions of Thiazolo[5,4-*d*]pyrimidine 1-Oxides with Acetylenic Esters Involving New Ring Transformations of the Thiazole Nucleus<sup>1)</sup>

HASHIME KANAZAWA,<sup>a</sup> MISUZU ICHIBA,<sup>a</sup> ZENZO TAMURA,<sup>a</sup>  
KEITARO SENGA,\*<sup>a</sup> KEN-ICHI KAWAI,<sup>b</sup>  
and HIROTAKE OTOMASU<sup>b</sup>

*Pharmaceutical Institute, School of Medicine, Keio University,<sup>a</sup> 35, Shinanomachi,  
Shinjuku-ku, Tokyo 160, Japan and Faculty of Pharmaceutical Sciences,  
Hoshi University,<sup>b</sup> Ebara 2-4-41, Shinagawa-ku, Tokyo 142, Japan*

(Received May 9, 1986)

The reaction of 2-(methoxycarbonyl)-4,6-dimethylthiazolo[5,4-*d*]pyrimidine-5,7(4*H*,6*H*)-dione 1-oxide (**1**) with dimethyl acetylenedicarboxylate resulted in a new ring transformation of the thiazole nucleus to give 5-[2-methoxalyl-1,2-bis(methoxycarbonyl)vinyl]imino-1,3-dimethyl-6-thiobarbituric acid (**4**), 6,7-bis(methoxycarbonyl)-1,3-dimethylpyrimido[4,5-*b*][1,4]thiazine-2,4-(1*H*,3*H*)-dione (**8**), 6,7-bis(methoxycarbonyl)-1,3-dimethylpyrrolo[3,2-*d*]pyrimidine-2,4(1*H*,3*H*)-dione (**9**), and anhydro-2-[1-methoxalyl-1-(*O*-sodiummethoxycarbonyl)]methyl-4,6-dimethylthiazolo[5,4-*d*]pyrimidine-5,7(4*H*,6*H*)-dione hydroxide (**11**). Analogously, the reaction of **1** with ethyl phenylpropionate gave 5-[2-benzoyl-2-(ethoxycarbonyl)-1-(methoxycarbonyl)vinyl]imino-1,3-dimethyl-6-thiobarbituric acid (**22**), 5-benzoyl-7-(ethoxycarbonyl)-6-(methoxycarbonyl)-1,3-dimethylpyrimido[4,5-*b*][1,4]thiazine-2,4(1*H*,3*H*)-dione (**23**), and 7-(ethoxycarbonyl)-6-(methoxycarbonyl)-1,3-dimethylpyrrolo[3,2-*d*]pyrimidine-2,4(1*H*,3*H*)-dione (**24**). The structures of these products were supported by their spectral [infrared (IR), mass (MS), ultraviolet (UV), proton nuclear magnetic resonance (<sup>1</sup>H-NMR) or carbon-13 nuclear magnetic resonance (<sup>13</sup>C-NMR)] data or by single-crystal X-ray diffraction analysis as well as by chemical transformations. The ring transformation of the thiazole nucleus can be best explained by taking into account the initial involvement of a 1,3-dipolar cycloaddition reaction.

**Keywords**—thiazolo[5,4-*d*]pyrimidine 1-oxide; acetylenic ester; 1,3-dipolar cycloaddition reaction; ring transformation; pyrimido[4,5-*b*][1,4]thiazine; pyrrolo[3,2-*d*]pyrimidine; crystal structure

The 1,3-dipolar cycloaddition reaction is a well known reaction for the construction of heterocyclic systems and its usefulness is comparable to that of the Diels-Alder reaction for the formation of carbocyclic systems.<sup>2)</sup> Although extensive studies have been carried out in this area, the 1,3-dipolar cycloaddition reactions of heterocyclic N-oxides, particularly those involving ring transformations, seem to be most important from the practical and mechanistic viewpoints.<sup>3)</sup> As one such reaction, we have previously reported that the reaction of pyrimido[5,4-*e*]-*as*-triazine 4-oxides with acetylenic esters resulted in the ring contraction of the *as*-triazine moiety to yield a variety of pyrrolo[3,2-*d*]pyrimidines (9-deazapurines) depending on the dipolarophile and solvent employed, as well as on the substituent at position 3 of the starting material.<sup>4)</sup>

On the basis of these findings, we were interested in the reactions of thiazolo[5,4-*d*]pyrimidine 1-oxides with acetylenic esters as a logical extension, since this heteroaromatic N-oxide system retains a conjugated  $\pi$ -system similar to that of the pyrimidotriazine N-oxide, though the  $\pi$ -electron deficient *as*-triazine nucleus is replaced by the  $\pi$ -electron excessive thiazole nucleus. We present here a detailed account of synthetic and mechanistic aspects of

the reactions of 2-(alkoxycarbonyl)-4,6-dimethylthiazolo[5,4-*d*]pyrimidine-5,7(4*H*,6*H*)-dione 1-oxides<sup>5</sup> with dimethyl acetylenedicarboxylate (DMAD) and ethyl phenylpropiolate (EPP) as well as with diethyl acetylenedicarboxylate (DEAD), in which the thiazole nucleus undergoes various hitherto-unknown transformations such as ring expansion and opening.<sup>11</sup>

### Results and Discussion

As depicted in Chart 1, heating of 2-(methoxycarbonyl)-4,6-dimethylthiazolo[5,4-*d*]pyrimidine-5,7(4*H*,6*H*)-dione 1-oxide (**1**)<sup>5</sup> with 2 eq of DMAD in MeOH for 7 h resulted in the formation of five products, *i.e.*, 6-thiobarbituric acid (**4**; 27%), pyrimido[4,5-*b*][1,4]thiazine (**8**; 21%), pyrrolo[3,2-*d*]pyrimidine (**9**; 10%), and thiazolo[5,4-*d*]pyrimidine salt (**11**; 3%) along with the deoxygenated starting material (**12**; 2%).<sup>6</sup> Among these compounds, **4** and **9** were readily precipitated from the reaction solution, while **8** and **12** were obtained by concentration of the filtrate, and **11** was isolated by column chromatography through activated alumina with MeOH.

Analogously, brief treatment of **1** with DEAD afforded the corresponding 6-thiobarbituric acid (**13**; 14%) and pyrrolo[3,2-*d*]pyrimidine (**14**; 26%), while the reaction of the thiazolo[5,4-*d*]pyrimidine 1-oxide (**15**)<sup>5</sup> with DMAD gave the corresponding 6-thiobarbituric acid (**16**; 29%), pyrimido[4,5-*b*][1,4]thiazine (**17**; 16%), and pyrrolo[3,2-*d*]pyrimidine (**18**; 12%).

The structures of **9** and **12** were confirmed by spectral (infrared: IR) comparison with the respective authentic samples,<sup>4a,5</sup> while those of others (**4**, **8**, and **11**) were supported by the following evidence. Namely, compound **4** was estimated as a 6-thiobarbituric acid derivative, particularly by the presence of an  $M^+ - 44$  ion (base peak) corresponding to the elimination of the C=S fragment in the mass spectrum (MS)<sup>7</sup> as well as by the observation of a signal at 179.05 ppm assignable to the C=S carbon in the <sup>13</sup>C nuclear magnetic resonance (<sup>13</sup>C-NMR) spectrum (Me<sub>2</sub>SO-*d*<sub>6</sub>). As shown in Chart 2, the structure was confirmed by the facts that the

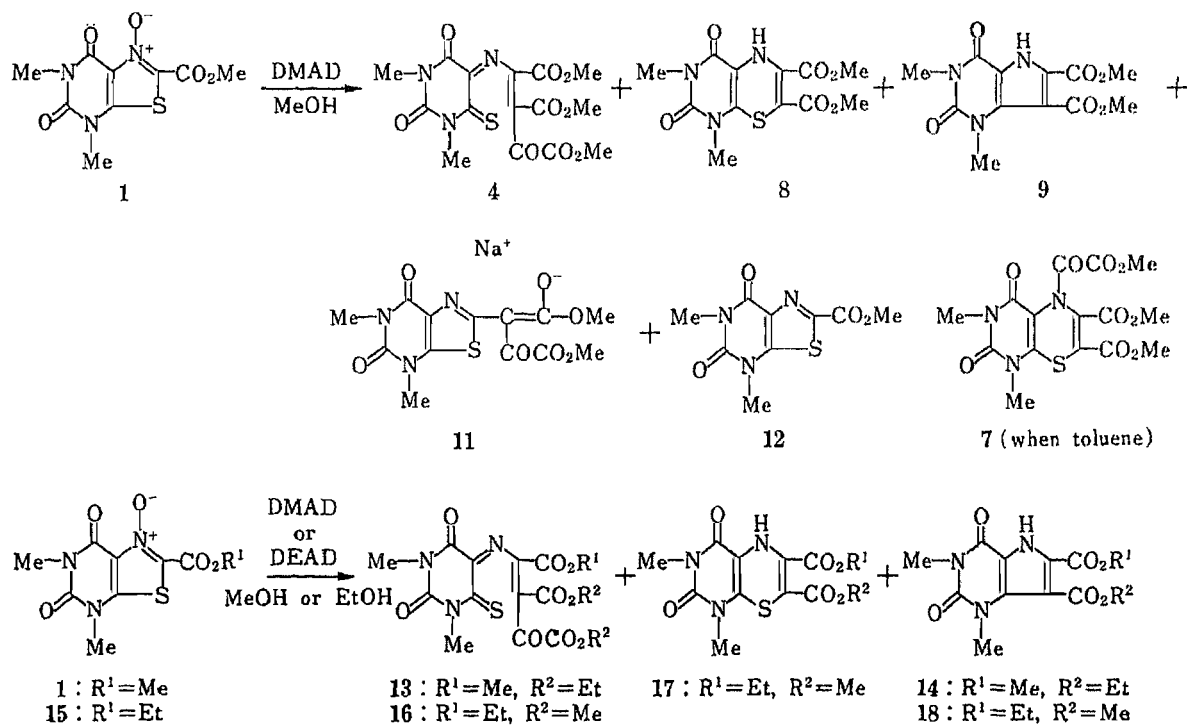
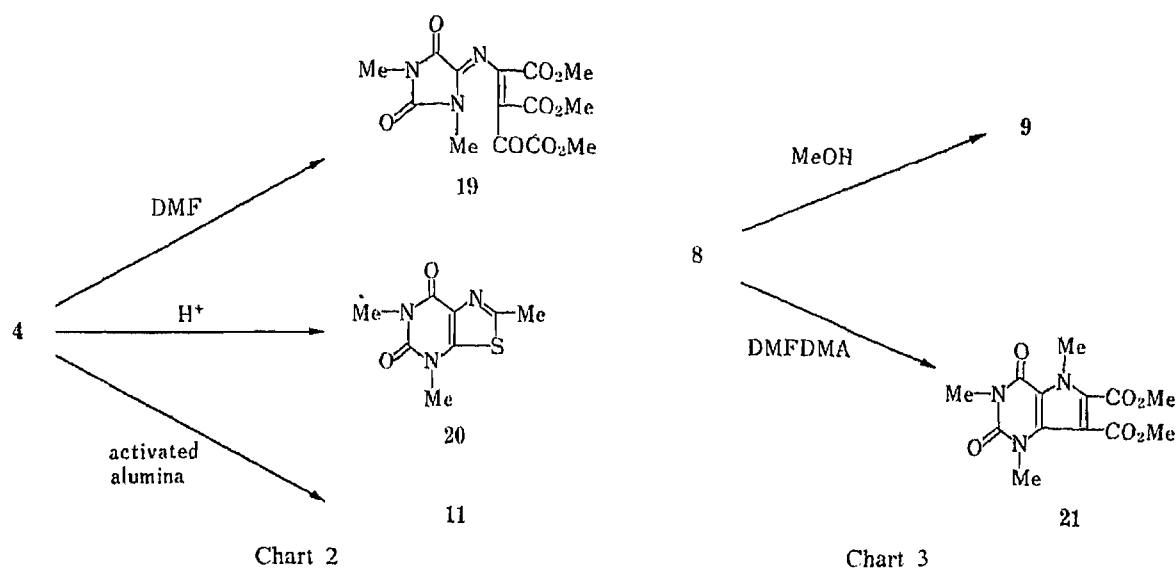


Chart 1





ring contraction of **4** occurred thermally under reflux in dimethylformamide (DMF) to give the parabanic acid derivative (**19**; 24%). Moreover, the presence of a 2-methoxallyl-1,2-bis(methoxycarbonyl)vinyl group was supported by the formation of the known 2-methylthiazolo[5,4-*d*]pyrimidine (**20**; 87%)<sup>8)</sup> on heating with ethanolic HCl.<sup>9)</sup>

Compound **8** was assigned as a pyrimido[4,5-*b*][1,4]thiazine derivative on the basis of the observation of an NH absorption at 3275 cm<sup>-1</sup> in the IR spectrum (Nujol), as well as the presence of an M<sup>+</sup> - 32 ion (base peak), attributable to the elimination of sulfur to give the pyrrolo[3,2-*d*]pyrimidine (**9**), in the MS.

In fact, as expected from the main characteristic of 1,3-dialkylpyrimido[4,5-*b*][1,4]thiazine-2,4(1*H*,3*H*)-diones,<sup>10)</sup> refluxing of **8** in MeOH caused ring contraction accompanied with desulfurization to give **9** (75%) (Chart 3). Moreover, heating of **8** with dimethylformamide dimethylacetal (DMFDMA) resulted in desulfurization and alkylation to give the known 5-methylpyrrolo[3,2-*d*]pyrimidine (**21**; 74%).<sup>4a,11)</sup> Theoretically, **8** could exist in either 5-H or 7-H tautomeric form,<sup>12)</sup> but no signal arising from the 7-H form could be observed in the <sup>1</sup>H-NMR spectrum (Me<sub>2</sub>SO-*d*<sub>6</sub>) and the signal attributable to the 5-H proton appeared at 9.13 ppm as a D<sub>2</sub>O exchangeable sharp singlet. The preference for 5-H form may be due to the methoxycarbonyl group at position 7, since the 7-unsubstituted pyrimido[4,5-*b*][1,4]thiazines, which are closely related to **8**, have been reported to exist in the 7-H form.<sup>10,13)</sup> The predominance of 5-H form was also reported in the case of 2-(ethoxycarbonyl)-3-methyl-4*H*-1,4-benzothiazine.<sup>14)</sup>

Although it was found that compound **11** could alternatively be obtained by the column chromatography of **4** in 24% yield, difficulties were encountered in the structural elucidation of **11**. For example, the <sup>1</sup>H-NMR spectrum (Me<sub>2</sub>SO-*d*<sub>6</sub>) only showed two sets of OMe and N-Me groups, and the MS did not exhibit appreciable parent or fragment ions, probably because of the low volatility of the compound. Therefore, a single-crystal X-ray diffraction study was undertaken.

As depicted in Fig. 1, the ORTEP<sup>15)</sup> drawing of **11** indicated that the compound is an unexpected sodium salt of thiazolo[5,4-*d*]pyrimidine in which the sodium binds to the oxygen of an extranuclear methoxycarbonyl group. However, consideration of the planarity and bond lengths of this molecule (shown in Fig. 2) did not rule out the possibility of additional interaction between N(3) and/or O(6) and sodium. The bonds N(7)-C(7a), C(3a)-C(4), C(3a)-N(3), N(3)-C(2), C(2)-S(1), S(1)-C(7a), C(2)-C(8), and C(8)-C(9) were considered to have double bond character, since the observed bond lengths are shorter than those expected

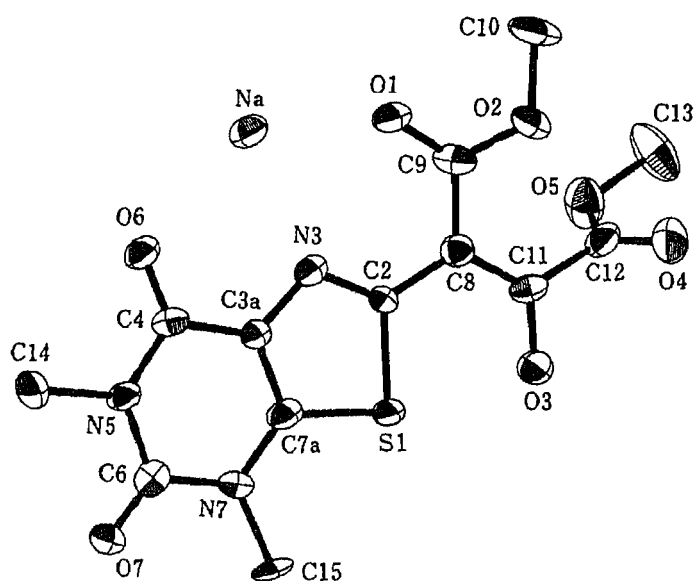


Fig. 1. An ORTEP Drawing of 11 with Thermal Ellipsoids at the 50% Probability Level

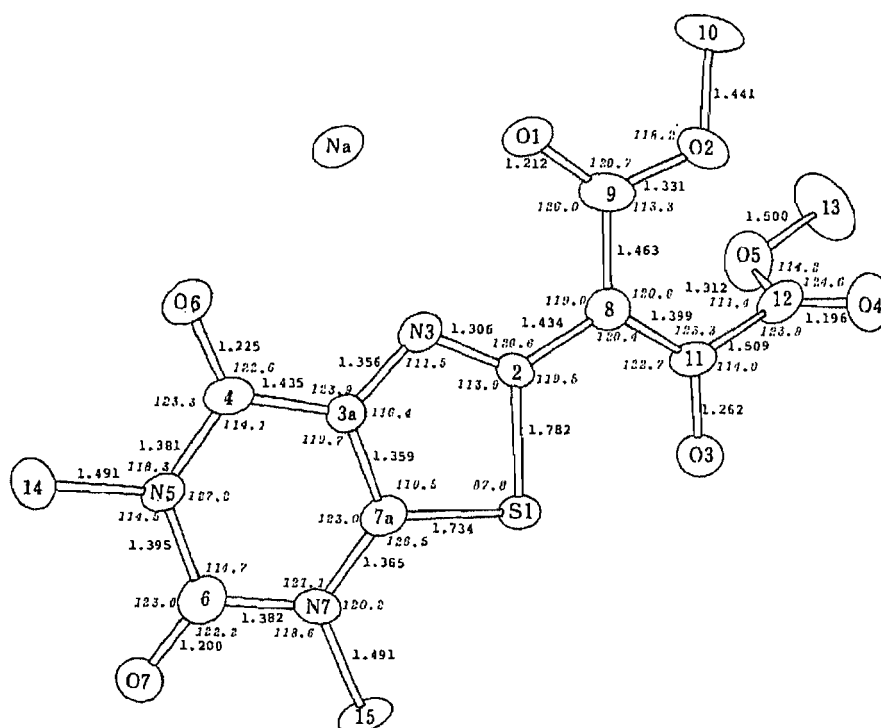


Fig. 2. Bond Angles and Bond Lengths of 11

for single bonds. The crystal data, final atomic parameters and equivalent thermal parameters, and anisotropic thermal parameters are listed in Tables I, II, and III, respectively.

In order to elucidate the mechanism of this reaction, we also investigated the influence of reaction solvent. Refluxing of 1 with DMAD in the presence of aqueous MeOH for 1 h caused a marked improvement in the yield of 8 (56%), and when the reaction period was prolonged to 10 h, the yield of 9 increased to 71%, apparently *via* the thermal desulfurization of 8 as described above. These findings suggested that a solvolytic process is involved in the

TABLE I. Crystal Data for 11<sup>a)</sup>

Formula	C <sub>13</sub> H <sub>12</sub> N <sub>3</sub> NaO <sub>7</sub> S
Formula weight	377.32
Crystal system	Monoclinic
Cell dimensions	$a = 12.674 (10) \text{ \AA}$ $b = 15.101 (9) \text{ \AA}$ $c = 14.738 (13) \text{ \AA}$ $\alpha = 90.03 (8)^\circ$ $\beta = 146.94 (5)^\circ$ $\gamma = 89.99 (7)^\circ$
Cell volume	1538.7 (28) $\text{\AA}^3$
Space group	$P2_1/C$
Calculated density	1.63 $\text{g cm}^{-3}$
Number of formula units in the unit cell	$Z = 4$

<sup>a)</sup> Final refinement value:  $R = 0.0777$  (the highest peak in the final difference Fourier was below  $0.25 \text{ e/\AA}^3$ ).

TABLE II. Final Atomic Parameters ( $\times 10^4$ ) and Equivalent Thermal Parameters with Estimated Standard Deviations in Parentheses

Atom	$x$	$y$	$z$	$B_{\text{eq}}$
S(1)	6765 (3)	4086 (2)	2154 (3)	2.35
Na	11676 (5)	4222 (3)	8227 (4)	2.82
C(2)	7705 (13)	4449 (6)	3895 (11)	2.02
C(3a)	10074 (14)	3599 (6)	5117 (11)	2.02
C(4)	11878 (13)	3130 (7)	6453 (11)	2.29
C(6)	10971 (13)	2431 (7)	4332 (12)	2.44
C(7a)	8878 (14)	3484 (7)	3533 (11)	2.68
C(8)	6580 (13)	5035 (7)	3638 (11)	2.39
C(9)	7428 (13)	5381 (7)	5086 (11)	2.50
C(10)	6951 (19)	6362 (9)	5986 (15)	4.99
C(11)	4670 (13)	5289 (6)	2026 (11)	2.25
C(12)	3325 (14)	5757 (7)	1663 (11)	2.98
C(13)	1424 (20)	5761 (10)	1627 (19)	6.26
C(14)	13997 (14)	2032 (8)	7241 (13)	3.39
C(15)	7949 (17)	2858 (9)	1373 (12)	4.51
O(1)	8893 (10)	5116 (6)	6504 (8)	4.19
O(2)	6456 (11)	6065 (5)	4730 (9)	4.28
O(3)	3910 (9)	4990 (5)	743 (7)	3.05
O(4)	2755 (12)	6486 (5)	1083 (10)	4.75
O(5)	2752 (11)	5281 (5)	1946 (10)	4.28
O(6)	13032 (9)	3220 (5)	7908 (7)	2.90
O(7)	11346 (9)	1925 (5)	3999 (8)	3.17
N(3)	9421 (11)	4135 (6)	5317 (9)	2.65
N(5)	12177 (10)	2561 (6)	5948 (9)	2.37
N(7)	9310 (12)	2940 (6)	3134 (10)	2.61

formation of 8. On the basis of this speculation, we next examined the effect of an aprotic solvent. Namely, heating of 1 with DMAD in toluene for 2 h resulted in the isolation of a new product, 5-methoxyalpyrimido[4,5-*b*][1,4]thiazine (7), albeit in a low yield (9%), along with 8 (41%). Compound 7 is highly susceptible to protic solvents, and heating of 7 in MeOH, for example, led to the ready formation of 8. Because of its lability, the purification of 7 was not successful. However, the spectral (IR and MS) similarity to the pyrimido[4,5-*b*][1,4]thiazine

TABLE III. Anisotropic Thermal Parameters ( $\times 10^4$ ) with Estimated Standard Deviations in Parentheses

Atom	$\beta_{11}$	$\beta_{22}$	$\beta_{33}$	$\beta_{12}$	$\beta_{13}$	$\beta_{23}$
S(1)	97 (5)	36 (1)	55 (4)	9 (2)	58 (4)	-1 (2)
Na	120 (8)	41 (2)	69 (6)	-3 (4)	72 (7)	-2 (3)
C(2)	113 (21)	27 (5)	77 (15)	14 (8)	82 (17)	5 (7)
C(3a)	96 (20)	25 (5)	65 (15)	4 (8)	65 (16)	0 (7)
C(4)	119 (22)	32 (5)	75 (16)	-9 (9)	82 (18)	-6 (7)
C(6)	118 (22)	27 (5)	92 (16)	-8 (9)	85 (18)	-2 (7)
C(7a)	107 (22)	38 (6)	59 (15)	2 (9)	60 (17)	-3 (8)
C(8)	113 (22)	29 (5)	83 (16)	-3 (9)	79 (17)	-2 (8)
C(9)	121 (22)	36 (5)	101 (17)	-28 (9)	99 (18)	-24 (8)
C(10)	318 (38)	64 (8)	171 (24)	-1 (14)	209 (28)	-30 (11)
C(11)	117 (22)	28 (5)	66 (15)	-17 (8)	73 (17)	-12 (7)
C(12)	112 (23)	46 (6)	69 (16)	12 (10)	67 (18)	11 (8)
C(13)	318 (41)	73 (9)	348 (37)	33 (16)	308 (37)	1 (15)
C(14)	146 (26)	43 (6)	111 (19)	26 (10)	102 (21)	6 (9)
C(15)	222 (31)	70 (8)	47 (17)	40 (13)	89 (21)	6 (9)
O(1)	185 (18)	68 (5)	80 (12)	44 (8)	99 (14)	12 (6)
O(2)	221 (20)	51 (5)	121 (13)	30 (8)	133 (15)	-7 (6)
O(3)	108 (15)	43 (4)	77 (11)	7 (6)	67 (12)	-6 (5)
O(4)	308 (24)	47 (5)	197 (17)	54 (9)	215 (19)	40 (7)
O(5)	195 (19)	51 (5)	196 (16)	23 (8)	171 (16)	21 (7)
O(6)	114 (15)	43 (4)	66 (11)	8 (7)	67 (12)	4 (5)
O(7)	159 (17)	39 (4)	91 (12)	18 (7)	97 (13)	-1 (5)
N(3)	121 (18)	38 (4)	70 (13)	13 (8)	75 (14)	7 (6)
N(5)	79 (17)	40 (5)	51 (12)	5 (7)	48 (13)	-1 (6)
N(7)	161 (20)	33 (4)	89 (13)	8 (8)	106 (15)	-2 (6)

(23) (*vide infra*), particularly the occurrence of a intense  $M^+ - 87$  ion due to the loss of a methoxalyl radical and the absence of an NH absorption, supported the indicated structure.

On the basis of these findings, we assumed that the reaction proceeds through the mechanism shown in Chart 4. Namely, the reaction of **1** with DMAD would produce the adduct (**2**) by 1,3-dipolar cycloaddition. The cleavage of the isoxazoline ring accompanied with C-S bond fission of **2**<sup>16)</sup> to **3**, and subsequent disproportionation by either path a<sup>17)</sup> or b would yield **5** and **4**, respectively. The cleavage of the cyclopropane ring of **5** to give **6**, followed by 1,2-migration of the methoxalyl group to **7**, and subsequent liberation of the methoxalyl group by the action of the protic solvent would yield **8**. Thus formed **8** would then undergo desulfurization to give **9** as a final product. Presumably, the last step can be regarded as stabilization by the transformation of the formally anti-aromatic 1,4-thiazine ring into the formally aromatic pyrrole ring. The anti-aromatic character of the 1,4-thiazine nucleus has been reported in certain pyrimido[4,5-*b*][1,4]thiazines.<sup>13)</sup> The formation of **12** would proceed by the thermal deoxygenation of **1**.<sup>2c)</sup> In contrast to these products, the formation of the salt (**11**) is apparently an artifact arising during the purification on activated alumina, as observed in the column chromatography of **4**, giving **11**. The reaction presumably proceeds through the initial cyclization to **10**, followed by liberation of the methoxycarbonyl group, and subsequent salt formation by the action of  $Na^+$  present in the alumina. Peculiar salt formation of this type has also been reported recently on the silica gel column chromatography of certain 1,2,4-triazines.<sup>18)</sup>

In order to support the mechanism shown in Chart 4, we have also investigated the reaction of **1** with EPP, which can be considered as a less reactive dipolarophile than DMAD.

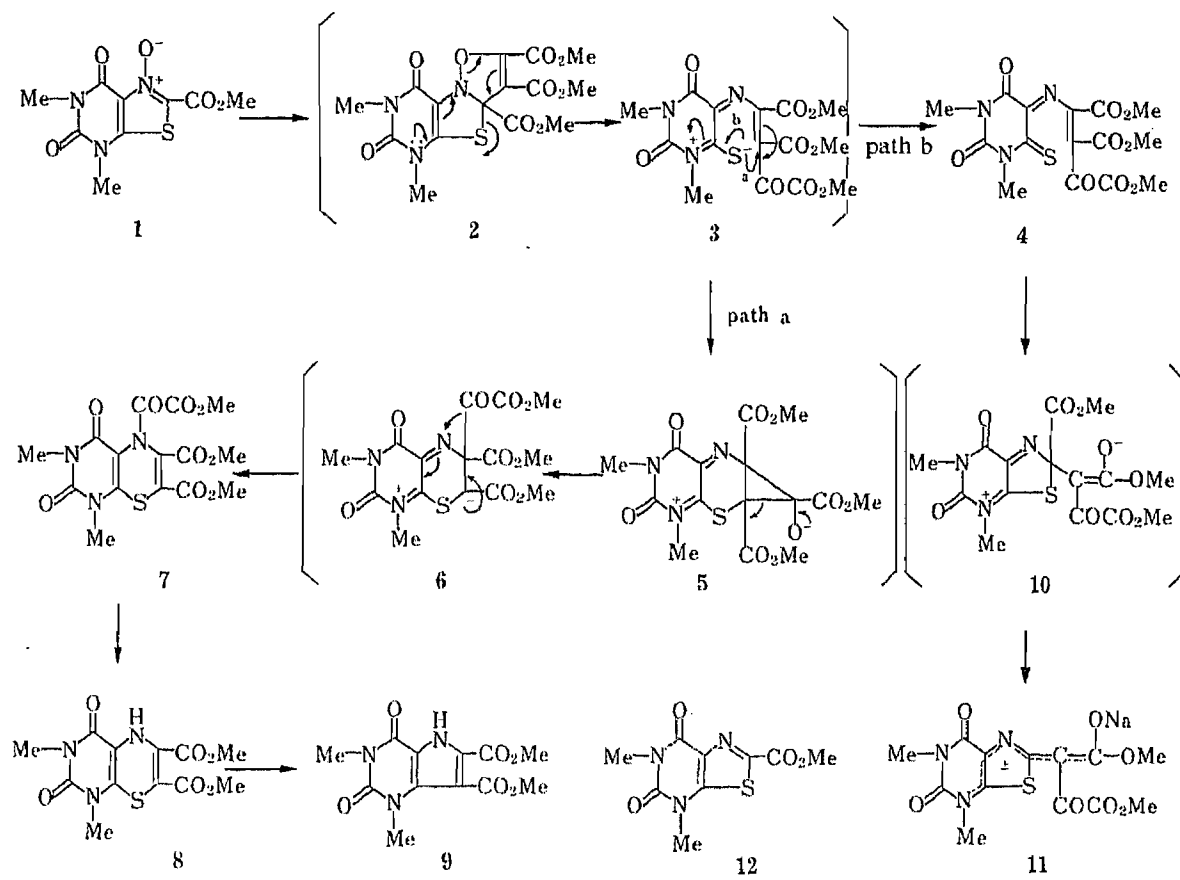


Chart 4

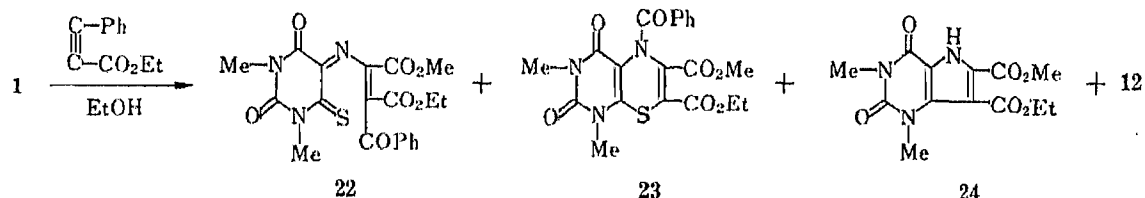


Chart 5

Namely, as depicted in Chart 5, heating of **1** with 2 eq of EPP in EtOH for 10 h gave the 6-thiobarbituric acid (**22**; 5%), pyrimido[4,5-*b*][1,4]thiazine (**23**; 30%), and pyrrolo[3,2-*d'*]pyrimidine (**24**; trace) along with the deoxygenated starting material (**12**; trace). In contrast to **7**, compound **23** was stable enough to permit recrystallization, even from protic solvents.

The structure of **22** was supported by the presence of an  $M^+ - 44$  ion in the MS and by its conversion to **20** as in the case of **4**, while that of **24** was corroborated by the spectral (IR and MS) resemblance to **9**. On the other hand, the structure of **23** was deduced from the following evidence. Namely, the IR spectrum (Nujol) lacked an NH absorption and the MS showed a strong  $M^+ - 105$  fragment ion attributable to the liberation of a benzoyl radical. Moreover, the <sup>13</sup>C-NMR spectrum (Me<sub>2</sub>SO-*d*<sub>6</sub>) showed a signal at 188.6 ppm which is attributable to a carbonyl carbon of the benzamide structure. The successful isolation of **23** supported the validity of the proposed mechanism (Chart 4).

### Experimental

Melting points were taken on a Yanaco micro-hot-stage melting point apparatus and are uncorrected. IR spectra

TABLE IV. Analytical Data

Compd. No.	Formula	Calcd (%)			Found (%)		
		C	H	N	C	H	N
4	C <sub>15</sub> H <sub>15</sub> N <sub>3</sub> O <sub>9</sub> S	43.58	3.66	10.17	43.50	3.63	10.19
8	C <sub>12</sub> H <sub>13</sub> N <sub>3</sub> O <sub>6</sub> S	44.03	4.01	12.84	44.23	4.00	12.57
11	C <sub>13</sub> H <sub>12</sub> N <sub>3</sub> NaO <sub>7</sub> S	41.38	3.21	11.14	41.58	3.16	11.15
13	C <sub>17</sub> H <sub>19</sub> N <sub>3</sub> O <sub>9</sub> S	46.25	4.35	9.52	46.53	4.39	9.47
16	C <sub>16</sub> H <sub>17</sub> N <sub>3</sub> O <sub>9</sub> S	44.96	4.02	9.83	44.81	3.92	9.71
17	C <sub>13</sub> H <sub>15</sub> N <sub>3</sub> O <sub>6</sub> S	45.73	4.43	12.31	45.50	4.35	12.17
18	C <sub>13</sub> H <sub>15</sub> N <sub>3</sub> O <sub>6</sub>	50.48	4.89	13.59	50.37	4.75	13.73
19	C <sub>14</sub> H <sub>15</sub> N <sub>3</sub> O <sub>9</sub> <sup>a)</sup>	44.44	4.27	11.11	44.83	3.97	11.35
20	C <sub>8</sub> H <sub>9</sub> N <sub>3</sub> O <sub>2</sub> S	45.48	4.30	19.89	45.66	4.26	20.02
22	C <sub>20</sub> H <sub>19</sub> N <sub>3</sub> O <sub>7</sub> S	53.92	4.31	9.43	53.88	4.35	9.67
23	C <sub>20</sub> H <sub>19</sub> N <sub>3</sub> O <sub>7</sub> S	53.92	4.31	9.43	53.66	4.21	9.43
24	C <sub>13</sub> H <sub>15</sub> N <sub>3</sub> O <sub>6</sub>	50.48	4.90	13.59	50.47	4.87	13.56

a) As a hemihydrate.

were recorded on a JASCO A-100 spectrophotometer from samples mulled in Nujol. <sup>1</sup>H-NMR spectra were determined at 90 MHz with a Varian EM-390 spectrometer with tetramethylsilane as an internal standard and <sup>13</sup>C-NMR spectra were measured on a JEOL JMS-PS-100 spectrometer by using tetramethylsilane as an internal standard. Ultraviolet (UV) spectra were obtained on a Hitachi 124 spectrophotometer in EtOH. The molecular weights of all compounds were confirmed by mass spectroscopy with a JEOL JMS D-300 spectrometer with a direct-inlet system at 70 eV. Elemental analyses (C, H, and N) for all new compounds were in agreement with the assigned structures to within ±0.4% as shown in Table IV.

**Reaction of 1 with DMAD in MeOH**—A mixture of 2-(methoxycarbonyl)-4,6-dimethylthiazolo[5,4-*d*]pyrimidine-5,7(4*H*,6*H*)-dione 1-oxide (1)<sup>5)</sup> (0.542 g, 0.002 mol) and DMAD (0.568 g, 0.004 mol) in MeOH (10 ml) was refluxed for 7 h, then left to stand overnight at room temperature. The precipitates were filtered off and the products were separated into three parts depending on the color and shape of crystals.

The pale yellow powder was recrystallized from EtOH to give 5-[2-methoxalyl-1,2-bis(methoxycarbonyl)-vinyl]imino-1,3-dimethyl-6-thiobarbituric acid (4: 0.227 g, 27%) as colorless prisms, mp 194–196 °C. <sup>1</sup>H-NMR (Me<sub>2</sub>SO-*d*<sub>6</sub>) δ: 3.28 (s, 3H, Me), 3.55 (s, 3H, Me), 3.87 (s, 3H, Me), 3.92 (s, 3H, Me), 4.00 (s, 3H, Me). UV λ<sub>max</sub> nm (log ε): 280 (3.65), 345 (4.33). MS *m/z*: 413 (M<sup>+</sup>), 369 (M<sup>+</sup> - C=S).

The off-white crystals were recrystallized from EtOH to give 6,7-bis(methoxycarbonyl)-1,3-dimethylpyrrolo[3,2-*d*]pyrimidine-2,4(1*H*,3*H*)-dione (9: 0.06 g, 10%) as colorless needles, mp 248–249 °C. This product was identical with an authentic sample by the reaction of fervenulin 4-oxide with DMAD in EtOH.<sup>4a)</sup>

The pale yellow globules (trace) were identified as sulfur from the IR spectrum.

The filtrate after removal of 4, 9, and sulfur was evaporated *in vacuo* and the residue was covered with MeOH (5 ml). The insoluble violet crystals were recrystallized from EtOAc to give 6,7-bis(methoxycarbonyl)-1,3-dimethylpyrimido[4,5-*b*][1,4]thiazine-2,4(1*H*,3*H*)-dione (8: 0.135 g, 21%) as violet needles, mp 168–169 °C. <sup>1</sup>H-NMR (Me<sub>2</sub>SO-*d*<sub>6</sub>) δ: 3.13 (s, 3H, Me), 3.26 (s, 3H, Me), 3.59 (s, 3H, Me), 3.70 (s, 3H, Me), 9.13 (s, 1H, NH, D<sub>2</sub>O exchangeable). UV λ<sub>max</sub> nm (log ε): 258 (3.89), 313 (3.89), 370 (3.43). MS *m/z*: 327 (M<sup>+</sup>), 295 (M<sup>+</sup> - S).

The filtrate after removal of 8 was again evaporated *in vacuo* and the residue was covered with MeOH (5 ml). The insoluble material was filtered off and recrystallized from EtOH to give 2-(methoxycarbonyl)-4,6-dimethylthiazolo[5,4-*d*]pyrimidine-5,7(4*H*,6*H*)-dione (12: 0.008 g, 2%) as colorless needles. This product was identical with an authentic sample.<sup>5)</sup>

The filtrate was evaporated *in vacuo* and the residue was chromatographed through activated alumina using MeOH as an eluent. The eluate (ca. 50 ml) was evaporated *in vacuo* and the resulting residue was recrystallized from MeOH to give anhydro-2-[1-methoxalyl-1-(*O*-sodiummethoxycarbonyl)]methyl-4,6-dimethylthiazolo[5,4-*d*]pyrimidine-5,7(4*H*,6*H*)-dione hydroxide (11: 0.023 g, 3%) as colorless prisms, mp > 300 °C. <sup>1</sup>H-NMR (Me<sub>2</sub>SO-*d*<sub>6</sub>) δ: 3.28 (s, 3H, Me), 3.50 (s, 3H, Me), 3.57 (s, 3H, Me), 3.68 (s, 3H, Me). UV λ<sub>max</sub> nm (log ε): 322.5 (5.08), 282.5 (4.88).

**4-[2-Methoxalyl-1,2-bis(methoxycarbonyl)vinyl]imino-1,3-dimethylparabanic Acid (19)**—A solution of 4 (0.08 g, 0.00019 mol) in DMF (1.5 ml) was refluxed for 2 h. The reaction mixture was evaporated *in vacuo* and the residue was covered with EtOH. The insoluble material was filtered off and recrystallized from MeOH to give 19 (0.017 g, 24%), mp 267–268 °C. MS *m/z*: 369 (M<sup>+</sup>).

**2,4,6-Trimethylthiazolo[5,4-*d*]pyrimidine-5,7(4*H*,6*H*)-dione (20)**—A suspension of **4** (0.124 g, 0.0003 mol) in a mixture of 1 *N* HCl (5 ml) and EtOH (5 ml) was refluxed for 10 h. The reaction mixture was evaporated *in vacuo* and the residue was covered with EtOH. The insoluble material was filtered off and recrystallized from EtOH to give **20** (0.055 g, 87%)<sup>81</sup> as colorless needles, mp 202–203 °C. <sup>1</sup>H-NMR (Me<sub>2</sub>SO-*d*<sub>6</sub>) δ: 2.63 (s, 3H, Me), 3.21 (s, 3H, Me), 3.43 (s, 3H, Me). MS *m/z*: 211 (M<sup>+</sup>).

Similar treatment of **22** (0.128 g, 0.0003 mol) in a mixture of 1 *N* HCl and EtOH gave **20** (0.047 g, 75%).

**Conversion of 8 to 9**—A suspension of **8** (0.327 g, 0.001 mol) in MeOH (5 ml) was refluxed for 3 h and the reaction mixture was evaporated *in vacuo*. The residue was recrystallized from EtOH to give **9** (0.22 g, 75%) as colorless needles, mp 248–249 °C. This product was identical with an authentic sample.<sup>4a)</sup>

**6,7-Bis(methoxycarbonyl)-1,3,5-trimethylpyrrolo[3,2-*d*]pyrimidine-2,4(1*H*,3*H*)-dione (21)**—A mixture of **8** (0.327 g, 0.001 mol) and DMFDMA (2 ml) was heated at 95 °C for 1 h and the reaction mixture was evaporated *in vacuo*. The residue was recrystallized from EtOH to give **21** (0.229 g, 74%), mp 149–150 °C. This product was identical with an authentic sample.<sup>4a)</sup>

**Column Chromatography of 4**—A CHCl<sub>3</sub> solution of **4** (0.083 g, 0.002 mol) was chromatographed through activated alumina<sup>14)</sup> with MeOH. The eluate (*ca.* 50 ml) was collected and evaporated *in vacuo*. The resulting residue was recrystallized from MeOH to give **11** (0.018 g, 24%). This product was identical with the sample obtained by the reaction of **1** with DMAD.

**Reaction of 1 with DMAD in Aqueous MeOH**—A mixture of **1** (0.271 g, 0.001 mol) and DMAD (0.142 g, 0.001 mol) in MeOH (3 ml) containing H<sub>2</sub>O (0.05 ml) was refluxed for 8 h. After cooling, the precipitates were filtered off and recrystallized from EtOAc to give **8** (0.18 g, 56%). This product was identical with the sample obtained by the reaction of **1** with DMAD in MeOH.

When the reaction was carried out for 10 h, **9** was obtained in 71% yield.

**Reaction of 1 with DMAD in Toluene**—A mixture of **1** (0.136 g, 0.0005 mol) and DMAD (0.071 g, 0.0005 mol) in dry toluene (2 ml) was heated at 95 °C for 2 h. After cooling to the ambient temperature, the precipitates were filtered off to give 5-methoxalyl-6,7-bis(methoxycarbonyl)-1,3-dimethylpyrimido[4,5-*b*][1,4]thiazine-2,4(1*H*,3*H*)-dione (**7**; 0.019 g, 9%) as a yellow powder, mp 205–206 °C. MS *m/z*: 413 (M<sup>+</sup>), 326 (M<sup>+</sup> – COCO<sub>2</sub>Me).

This compound is quite unstable toward various organic solvents, therefore, further purification could not be achieved.

The filtrate after removal of **7** was evaporated *in vacuo* and the residue was recrystallized from EtOAc to give **8** (0.067 g, 41%). This product was identical with the sample obtained by the reaction of **1** with DMAD.

**Reaction of 1 with DEAD**—A mixture of **1** (0.271 g, 0.001 mol) and DEAD (0.34 g, 0.002 mol) in EtOH (15 ml) was refluxed for 7 h. The reaction mixture was evaporated *in vacuo* and the residue was covered with MeOH. The insoluble material was filtered off and recrystallized from EtOH to give 5-[2-ethoxalyl-2-(ethoxycarbonyl)-1-(methoxycarbonyl)vinyl]imino-1,3-dimethyl-6-thiobarbituric acid (**13**; 0.06 g, 14%) as colorless needles, mp 170–172 °C. MS *m/z*: 441 (M<sup>+</sup>), 397 (M<sup>+</sup> – C=S).

The filtrate after removal of **13** was again evaporated *in vacuo* and the residue was covered with MeOH to obtain the insoluble material. This operation was repeated 5 times and the resulting crystals were recrystallized from EtOH to give 5-benzoyl-7-(ethoxycarbonyl)-6-(methoxycarbonyl)-1,3-dimethylpyrimido[4,5-*b*][1,4]thiazine-2,4(1*H*,3*H*)-**1** with EPP.

**Reaction of 1 with EPP**—A mixture of **1** (0.271 g, 0.001 mol) and EPP (0.348 g, 0.002 mol) in EtOH (20 ml) was refluxed for 20 h and the reaction mixture was evaporated *in vacuo*. The residue was recrystallized from EtOH to give 5-[2-benzoyl-2-(ethoxycarbonyl)-1-(methoxycarbonyl)vinyl]imino-1,3-dimethyl-6-thiobarbituric acid (**22**; 0.02 g, 5%) as colorless needles, mp 205–206 °C. <sup>1</sup>H-NMR (Me<sub>2</sub>SO-*d*<sub>6</sub>) δ: 1.03 (t, 3H, Me, *J* = 7 Hz), 3.30 (s, 3H, Me), 3.54 (s, 3H, Me), 4.17 (q, 2H, CH<sub>2</sub>, *J* = 7 Hz), 7.52 (s, 5H, Ph). UV λ<sub>max</sub> nm (log ε): 331 (4.59). MS *m/z*: 445 (M<sup>+</sup>), 401 (M<sup>+</sup> – C=S).

The mother liquor of this recrystallization was evaporated *in vacuo* and the residue was recrystallized from EtOH to give 5-benzoyl-7-(ethoxycarbonyl)-6-(methoxycarbonyl)-1,3-dimethylpyrimido[4,5-*b*][1,4]thiazine-2,4(1*H*,3*H*)-dione (**23**; 0.13 g, 30%) as yellow needles, mp 175–176 °C. <sup>1</sup>H-NMR (Me<sub>2</sub>SO-*d*<sub>6</sub>) δ: 1.03 (t, 3H, Me, *J* = 7 Hz), 3.23 (s, 3H, Me), 3.78 (s, 3H, Me), 4.23 (q, 2H, CH<sub>2</sub>, *J* = 7 Hz), 7.33–7.93 (m, 5H, Ph). UV λ<sub>max</sub> nm (log ε): 366 (4.68), 256 (4.68). MS *m/z*: 455 (M<sup>+</sup>), 350 (M<sup>+</sup> – C=O). Ph).

The filtrate was again evaporated *in vacuo* and the residue was chromatographed through activated alumina with CHCl<sub>3</sub>. The first eluate was collected and evaporated *in vacuo* to give a trace of **12**, which was identical with an authentic sample.<sup>5)</sup> The second eluate was similarly treated to give a trace of 7-(ethoxycarbonyl)-6-(methoxycarbonyl)-1,3-dimethylpyrrolo[3,2-*d*]pyrimidine-2,4(1*H*,3*H*)-dione (**24**), which was identical with the sample obtained by the reaction of **1** with DEAD (*vide infra*).

**Reaction of 15 with DMAD**—A mixture of 2-(ethoxycarbonyl)-4,6-dimethylthiazolo[5,4-*d*]pyrimidine-5,7(4*H*,6*H*)-dione 1-oxide (**15**; 0.57 g, 0.002 mol)<sup>5)</sup> and DMAD (0.284 g, 0.002 mol) in MeOH (5 ml) was refluxed for 2 h. After standing overnight at room temperature, the precipitates were filtered off and recrystallized from EtOH to give 5-[1-(ethoxycarbonyl)-2-methoxalyl-2-(methoxycarbonyl)vinyl]imino-1,3-dimethyl-6-thiobarbituric acid (**16**; 0.245 g, 29%) as colorless needles, mp 173–175 °C. <sup>1</sup>H-NMR (Me<sub>2</sub>SO-*d*<sub>6</sub>) δ: 1.33 (t, 3H, Me, *J* = 6 Hz), 3.25 (s, 3H,

Me), 3.50 (s, 3H, Me), 3.82 (s, 3H, Me), 3.87 (s, 3H, Me), 4.39 (q, 2H, CH<sub>2</sub>, *J* = 6 Hz). MS *m/z*: 427 (M<sup>+</sup>), 383 (M<sup>+</sup> - C=S).

The filtrate after removal of 16 was evaporated *in vacuo* and the residue was covered with MeOH (3 ml). The insoluble material was filtered off and recrystallized from EtOAc to give 6-(ethoxycarbonyl)-7-(methoxycarbonyl)-1,3-dimethylpyrimido[4,5-*b*][1,4]thiazine-2,4(1*H*,3*H*)-dione (17: 0.11 g, 16%) as orange plates, mp 173–175 °C. <sup>1</sup>H-NMR (Me<sub>2</sub>SO-*d*<sub>6</sub>) δ: 1.23 (t, 3H, Me, *J* = 6 Hz), 3.13 (s, 3H, Me), 3.28 (s, 3H, Me), 3.60 (s, 3H, Me), 4.17 (q, 2H, CH<sub>2</sub>, *J* = 6 Hz), 9.13 (s, 1H, NH, D<sub>2</sub>O exchangeable). MS *m/z*: 341 (M<sup>+</sup>), 309 (M<sup>+</sup> - S).

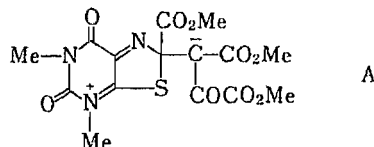
The filtrate after removal of 17 was again evaporated *in vacuo* and the residue was recrystallized from EtOH to give 6-(ethoxycarbonyl)-7-(methoxycarbonyl)-1,3-dimethylpyrrolo[3,2-*d*]pyrimidine-2,4(1*H*,3*H*)-dione (18: 0.075 g, 12%) as colorless needles, mp 143–145 °C. <sup>1</sup>H-NMR (Me<sub>2</sub>SO-*d*<sub>6</sub>) δ: 1.30 (t, 3H, Me, *J* = 6 Hz), 3.30 (s, 3H, Me), 3.37 (s, 3H, Me), 3.87 (s, 3H, Me), 12.90 (br, 1H, NH, D<sub>2</sub>O exchangeable). UV λ<sub>max</sub> nm (log ε): 228 (4.55), 273 (4.27), 305 (4.20). MS *m/z*: 309 (M<sup>+</sup>).

**X-Ray Crystallographic Analysis of 11**—A single crystal (colorless prism) of 11 was obtained by recrystallization from MeOH. The crystal data, final atomic parameters and equivalent thermal parameters, and anisotropic thermal parameters are listed in Tables I, II, and III, respectively. The lattice constants and intensity data were measured by using graphite-monochromated Mo K<sub>α</sub> radiation (λ 0.71070 Å) on a Rigaku AFC-5 four-circle diffractometer at 293 K. A total of 2028 unique reflections with [|F<sup>o</sup>| > 3(|F<sup>c</sup>|)] were obtained by using the θ - 2θ scanning method with a 2θ scan speed of 4 °/min up to 2θ = 45 °. The structure was solved by the direct method with the MULTAN program<sup>19)</sup> and refined by the block-matrix least squares method. The structure and bond lengths and angles are shown in Figs. 1 and 2, respectively.<sup>20)</sup> The contribution of H atoms was not considered in the ORTEP drawing.

**Acknowledgement** We are indebted to Dr. K. Nagahara of Kitasato University for the <sup>1</sup>H- and <sup>13</sup>C-NMR spectra and to Dr. K. Saito and Mr. H. Yamanaka of this school for the MS.

#### References and Notes

- 1) Preliminary report: K. Senga, M. Ichiba, H. Kanazawa, and S. Nishigaki, *J. Chem. Soc., Chem. Commun.*, **1981**, 278.
- 2) For reviews on the 1,3-dipolar cycloaddition reactions of nitrones and cyclic nitrones, see a) D. St. C. Black, R. F. Crozier, and V. C. Davis, *Synthesis*, **1975**, 205; b) E. Ochiai, "Aromatic Amine Oxides," Elsevier, New York, 1967, pp. 256–259; c) A. R. Katritzky and J. M. Lagowski, "Chemistry of Heterocyclic N-Oxides," ed. by A. T. Blomquist, Academic Press, New York, 1971, pp. 330–335.
- 3) For a recent report on the 1,3-dipolar cycloaddition reaction involving ring transformation, see J. P. Freeman, D. J. Duchamp, C. G. Chidester, G. Slomp, J. Szmuszkowicz, and M. Raban, *J. Am. Chem. Soc.*, **104**, 1380 (1982) and references cited therein.
- 4) a) K. Senga, M. Ichiba, and S. Nishigaki, *J. Org. Chem.*, **44**, 3830 (1979); b) S. Nishigaki, H. Kanazawa, Y. Kanamori, M. Ichiba, and K. Senga, *J. Heterocycl. Chem.*, **19**, 1309 (1982); c) H. Kanazawa, M. Ichiba, N. Shimizu, Z. Tamura, and K. Senga, *J. Org. Chem.*, **50**, 2413 (1985).
- 5) K. Senga, M. Ichiba, H. Kanazawa, and S. Nishigaki, *J. Heterocycl. Chem.*, **19**, 77 (1982).
- 6) In addition to these products, sulfur was also isolated from the reaction mixture.
- 7) The elimination of C=S fragment has also been observed in 6-thiotheophylline, see M. Chaigneau, G. Valdener, and J. Seyden-Penne, *C. R. Acad. Sci.*, **1965**, 3965.
- 8) G. P. Hager and C. Kaiser, *J. Am. Pharm. Assoc.*, **44**, 193 (1955).
- 9) The reaction probably proceeds through the initial formation of an intermediate A, followed by exhaustive hydrolytic decarboxylation.



- 10) H. Fenner and H. Motschall, *Tetrahedron Lett.*, **1971**, 4185.
- 11) The expected 6,7-bis(methoxycarbonyl)-1,3,5-trimethylpyrimido[4,5-*b*][1,4]thiazine-2,4(1*H*,3*H*)-dione could not be obtained.
- 12) For a review on the 1,4-thiazines, see R. J. Stoodley, "Advances in Heterocyclic Chemistry," Vol. 24, ed. by R. J. Stoodley, Academic Press, New York, 1979, pp. 294–361.
- 13) H. Fenner, H. Motschall, S. Ghisla, and P. Hemmerich, *Justus Liebigs Ann. Chem.*, **1974**, 1793.
- 14) Y. Maki, M. Suzuki, and T. Yamada, *Chem. Pharm. Bull.*, **14**, 770 (1966).
- 15) C. K. Johnson, "ORTEP," Report ORNL-3794, Oak Ridge National Laboratory, Tennessee, 1965.



- 
- 16) The cleavage of adduct (2) is presumably initiated by the contribution of an electron-releasing N-methyl group, as shown in the chart.
  - 17) Although the intermediate 3 resonates with 4, failure to obtain 7, 8 or 9 from 4 strongly suggested the involvement of path a.
  - 18) V. L. Styles and R. W. Morrison Jr., *J. Org. Chem.*, **50**, 347 (1985).
  - 19) G. Germain, P. Main, and M. M. Woolfson, *Acta Crystallogr., Sect. B*, **26**, 91 (1970).
  - 20) Further crystallographic details are available upon request.

[Chem. Pharm. Bull.]  
35(1) 46-52 (1987)]

**Studies on the Constituents of Leguminous Plants. IX.<sup>1)</sup> The Structure of a New Triterpenoid Saponin from the Fruits of *Gymnocladus chinensis* BAILLON**

TAKAO KONOSHIMA,<sup>\*,a</sup> MUTSUO KOZUKA,<sup>a</sup> TOKUNOSUKE SAWADA<sup>a</sup> (deceased) and TAKEATSU KIMURA<sup>b</sup>

*Kyoto Pharmaceutical University,<sup>a</sup> Nakauchi-cho, Misasagi, Yamashina-ku, Kyoto 607, Japan and Daiichi College of Pharmaceutical Sciences,<sup>b</sup> Tamagawa-cho 22-1, Minami-ku, Fukuoka 815, Japan*

(Received May 29, 1986)

A new triterpenoid saponin, gymnocladus saponin G (1), having a glycosyl monoterpene carboxyl moiety and a 2-methylbutyloyl group, was isolated from the fruits of *Gymnocladus chinensis* BAILLON. On the basis of chemical and physicochemical evidence, its structure was characterized as 2 $\beta$ ,23-dihydroxy-3-*O*-[ $\beta$ -D-xylopyranosyl-(1 $\rightarrow$ 2)- $\alpha$ -L-arabinopyranosyl-(1 $\rightarrow$ 6)- $\beta$ -D-glucopyranosyl]-21-*O*-{(6*S*)-2-*trans*-2,6-dimethyl-6-[3-*O*-( $\beta$ -D-glucopyranosyl)-4-*O*-(2-methylbutyryl)- $\alpha$ -L-arabinopyranosyloxy]-2,7-octadienoyl}acacic acid 28-*O*- $\beta$ -D-xylopyranosyl-(1 $\rightarrow$ 3)- $\beta$ -D-xylopyranosyl-(1 $\rightarrow$ 4)- $\alpha$ -L-rhamnopyranosyl-(1 $\rightarrow$ 2)-[ $\alpha$ -L-rhamnopyranosyl-(1 $\rightarrow$ 6)]- $\beta$ -D-glucopyranoside.

**Keywords**—*Gymnocladus chinensis*; Leguminosae; gymnocladus saponin G; 2 $\beta$ ,23-dihydroxyacacic acid; triterpenoid; saponin; monoterpene glycoside

In previous papers,<sup>1-3)</sup> we reported the structure elucidations of two monoterpene glycosides (2 and 3), and four triterpenoid saponins, gymnocladus saponins A (4), B (5), C (6) and D (7), isolated from the fruits of *Gymnocladus chinensis* BAILLON. Compounds 4, 5 and 6 were 3-*O*-glycosides of 2 $\beta$ ,23-dihydroxyacacic acid lactone (8), and 7 was a 3,28-bisglycoside of 2 $\beta$ ,23-dihydroxyacacic acid (9), as shown in Chart 1. A new saponin, named gymnocladus saponin G (1) has now been isolated from the most polar fraction of the same source, and characterized as a 3,28-bisglycoside of 9, bearing a glycosyl monoterpene carboxylate as an acyl side-chain, on the basis of carbon-13 nuclear magnetic resonance (<sup>13</sup>C-NMR) spectrometry and some chemical degradations.

Gymnocladus saponin G (1) was isolated from the crude saponin fraction by repeated chromatography on silica gel columns, gel filtration on Sephadex LH20, and finally high-performance liquid chromatography (HPLC), as a white powder, C<sub>100</sub>H<sub>160</sub>O<sub>53</sub>·H<sub>2</sub>O, [ $\alpha$ ]<sub>D</sub><sup>26</sup> -4.8°.

In the infrared (IR) spectrum (1680 cm<sup>-1</sup>) and the ultraviolet (UV) spectrum ( $\lambda_{\max}$  217 nm), the saponin G (1) showed the presence of a conjugated acyl group, and in the <sup>13</sup>C-NMR spectrum, 1 showed three singlet signals of carbonyl carbons at  $\delta$  176.7, 174.7 and 167.8, and four olefinic carbons at  $\delta$  143.7, 142.2, 128.6 and 115.2, in addition to  $\delta$  123.9 (C-12) and 143.3 (C-13). On acid hydrolysis of 1 with 10% H<sub>2</sub>SO<sub>4</sub>, 2 $\beta$ ,23-dihydroxyacacic acid lactone (8)<sup>3)</sup> and four kinds of sugars, glucose, xylose, arbinose and rhamnose, were obtained and identified by comparison with authentic samples.

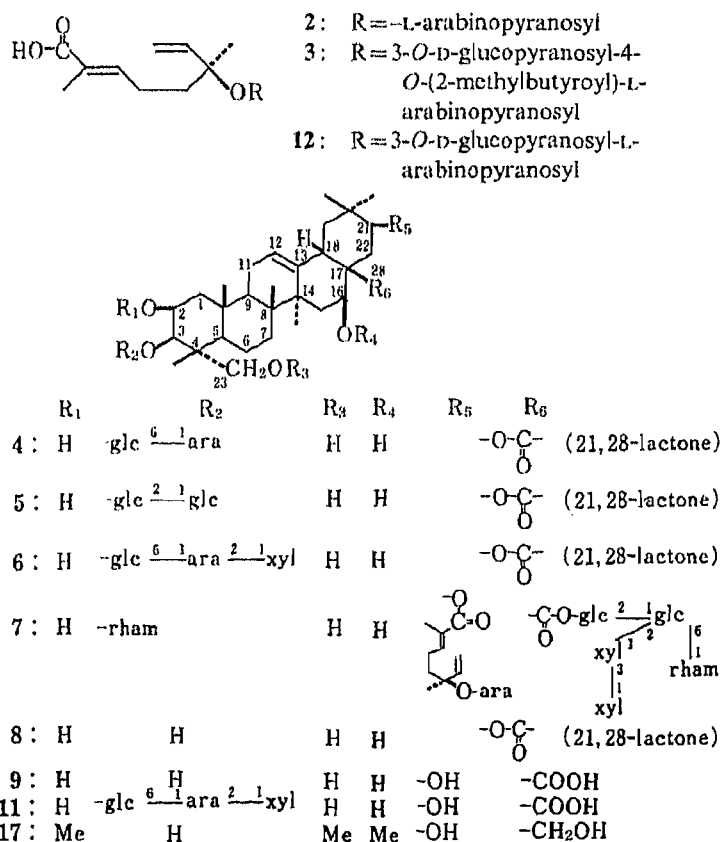
On alkaline hydrolysis of 1 with 2% NaHCO<sub>3</sub> in ethanol, a partially deacylated compound (10) was obtained as a white powder, C<sub>95</sub>H<sub>152</sub>O<sub>52</sub>·3H<sub>2</sub>O, [ $\alpha$ ]<sub>D</sub><sup>27</sup> -23.2°. The IR spectrum (1680 cm<sup>-1</sup>), the UV spectrum ( $\lambda_{\max}$  216 nm) and the <sup>13</sup>C-NMR spectrum (signals at

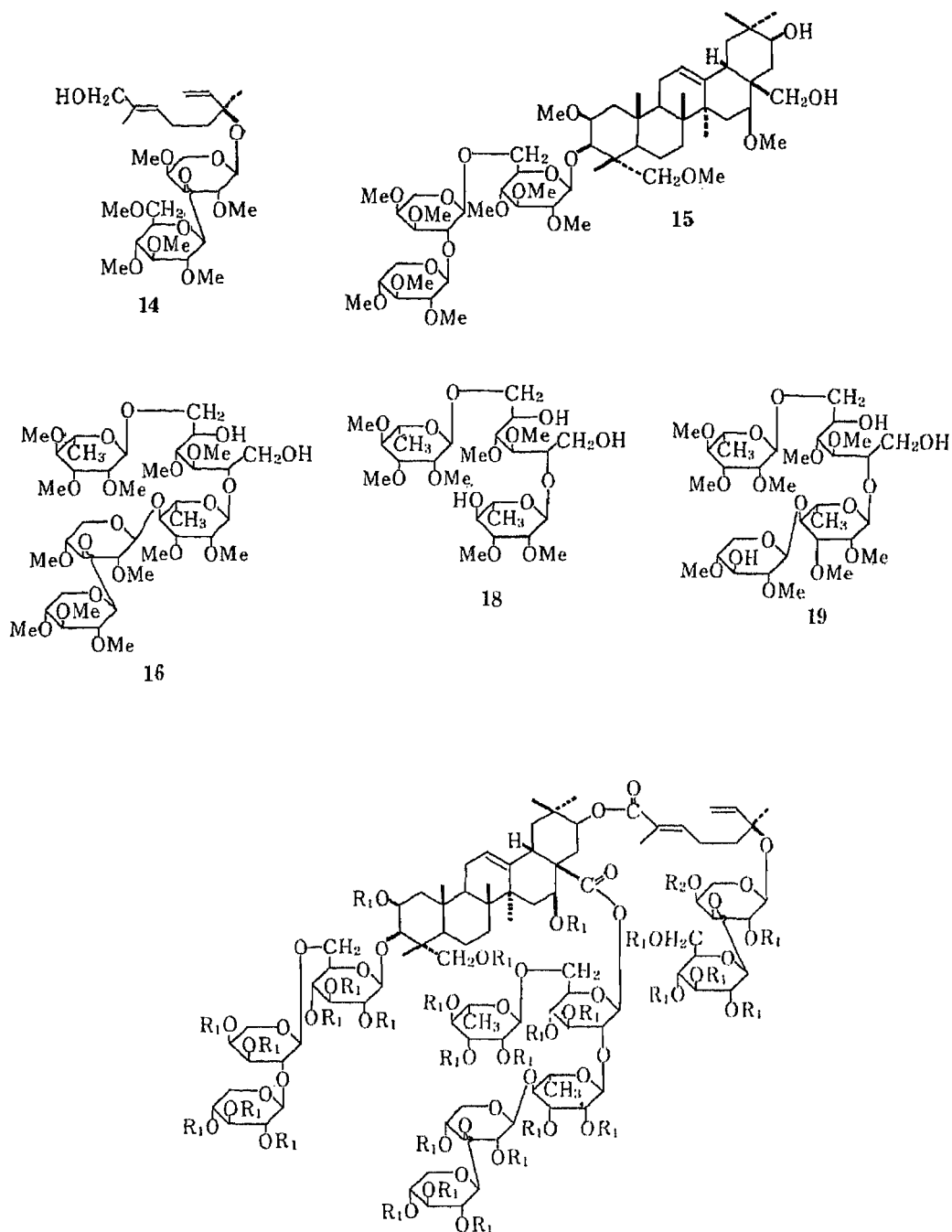
$\delta$  174.7 and 167.8 due to carbonyl carbons, and at  $\delta$  144.0, 142.3, 128.5 and 115.1 due to olefinic carbons) of **10** suggested the presence of a conjugated acyl group, which was not hydrolysed under the conditions used.

On hydrolysis of **1** with 10% KOH in ethanol, two prosapogenins, (**6**) and (**11**), and a monoterpene-glycoside (**12**) were obtained. The prosapogenin (**6**) was found to be identical with gymnocladus saponin C,<sup>3)</sup> based on thin layer chromatography (TLC), IR and <sup>13</sup>C-NMR. In the <sup>13</sup>C-NMR of **11**, a signal assigned to carbonyl carbon at  $\delta$  179.6 was found instead of the signal due to the lactone group in **4**, **5** and **6**, and the chemical shifts of the sugar carbons and the A, B ring residue of the triterpene moiety closely resembled those of **6**.<sup>3)</sup> Therefore, **6** is a cyclization product of **11**. The sugar moiety at C-3 of the saponin G (**1**) was also characterized as a  $\beta$ -D-xylopyranosyl-(1 $\rightarrow$ 2)- $\alpha$ -L-arabinopyranosyl-(1 $\rightarrow$ 6)- $\beta$ -D-glucopyranosyl group. The monoterpene glycoside (**12**) showed four olefinic carbons at  $\delta$  144.0, 141.5, 129.6 and 115.0, and two anomeric carbons at  $\delta$  106.0 and 99.9 in the <sup>13</sup>C-NMR, and was identical with the deacyl monoterpene glycoside<sup>2)</sup> obtained from **3** by alkaline hydrolysis with 1% KOH.

On methylation by Hakomori's method,<sup>4)</sup> **1** and **10** gave the same permethylate (**13**), showing an absorption maximum at 212 nm in the UV spectrum, and signals due to a terminal olefin at  $\delta$  5.13 (dd,  $J=18.0$ , 2.5 Hz), 5.20 (dd,  $J=11.5$ , 2.5 Hz) and 5.82 (dd,  $J=18.0$ , 11.5 Hz), and ten anomeric protons of sugars at  $\delta$  4.19 (d,  $J=7.5$  Hz), 4.24 (d,  $J=7.5$  Hz), 4.43 (d,  $J=6.5$  Hz), 4.45 (d,  $J=7.0$  Hz), 4.54 (d,  $J=3.5$  Hz), 4.61 (d,  $J=7.0$  Hz), 4.69 (d,  $J=7.5$  Hz), 4.83 (brs), 5.10 (brs) and 5.58 (d,  $J=7.0$  Hz) in the <sup>1</sup>H-NMR spectrum.

On reduction with lithium aluminum hydride (LiAlH<sub>4</sub>), **13** gave a mixture of a monoterpene glycoside (**14**), a triterpene glycoside (**15**) and an oligosaccharide alcohol (**16**). On the basis of spectral comparisons, the monoterpene glycoside (**14**) was shown to be





- 1:  $R_1 = H$ ,  $R_2 = 2\text{-methylbutyryl}$  (gymnocladus saponin G)  
 10:  $R_1 = H$ ,  $R_2 = H$   
 13:  $R_1 = Me$ ,  $R_2 = Me$

identical with the permethylate of (6*S*)-2-*trans*-6-[ $\beta$ -D-glucopyranosyl-(1 $\rightarrow$ 3)- $\alpha$ -L-arabinopyranosyloxy]-2,6-dimethyl-2,7-octadienol, which was derived from the acid (3).<sup>2)</sup>

The triterpene glycoside (15) was methanolized with 2N hydrogen chloride (HCl) in methanol to afford methyl 2,3,4-tri-*O*-methyl-D-xylopyranoside, methyl 3,4-di-*O*-methyl-L-arabinopyranoside, methyl 2,3,4-tri-*O*-methyl-D-glucopyranoside and a triterpene alcohol (17). The triterpene alcohol (17) was identical with an authentic sample of olean-12-ene-2 $\beta$ ,16 $\beta$ ,23-tri-*O*-methyl-3 $\beta$ ,21 $\beta$ ,28-triol (17) derived from the saponin D (7),<sup>1)</sup> on the basis of

TABLE I.  $^{13}\text{C}$ -NMR Chemical Shifts ( $\delta$ ) of the Triterpene Moiety and Sugars at C-3 in Pyridine- $d_5^a$ 

Carbon	11	10 $\Delta\delta$ 10-11	1 $\Delta\delta$ 1-10	Carbon	11	10 $\Delta\delta$ 10-11	1 $\Delta\delta$ 1-10
1	44.0	44.0 ( $\pm 0$ )	44.1 (+0.1)	26	17.6 <sup>c)</sup>	17.5 <sup>a)</sup> (-0.1)	17.5 <sup>a)</sup> ( $\pm 0$ )
2	70.4	70.4 ( $\pm 0$ )	70.4 ( $\pm 0$ )	27	27.3	27.2 (-0.1)	27.1 (-0.1)
3	83.3	83.5 (+0.2)	83.5 ( $\pm 0$ )	28	179.6	174.7	174.7 ( $\pm 0$ )
4	42.7	42.7 ( $\pm 0$ )	42.7 ( $\pm 0$ )	29	30.0	29.2 (-0.8)	29.1 (-0.1)
5	47.6 <sup>b)</sup>	47.5 <sup>b)</sup> (-0.1)	47.5 <sup>b)</sup> ( $\pm 0$ )	30	18.4	19.2 (+0.8)	19.2 ( $\pm 0$ )
6	18.0	18.2 (+0.2)	18.3 (+0.1)	glc			
7	33.2	33.2 ( $\pm 0$ )	33.2 ( $\pm 0$ )	1	105.6	105.6 ( $\pm 0$ )	105.6 ( $\pm 0$ )
8	40.0	40.2 (+0.2)	40.2 ( $\pm 0$ )	2	75.4	75.4 ( $\pm 0$ )	75.4 ( $\pm 0$ )
9	47.7 <sup>b)</sup>	47.8 <sup>b)</sup> (+0.1)	47.7 <sup>b)</sup> (-0.1)	3	78.1	78.1 ( $\pm 0$ )	78.1 ( $\pm 0$ )
10	36.9	37.0 (+0.1)	37.0 ( $\pm 0$ )	4	71.6	71.6 ( $\pm 0$ )	71.5 (-0.1)
11	24.1	24.1 ( $\pm 0$ )	24.1 ( $\pm 0$ )	5	75.9	76.0 (+0.1)	75.9 (-0.1)
12	122.8	123.9 (+1.1)	123.9 ( $\pm 0$ )	6	68.4	68.4 ( $\pm 0$ )	68.3 (-0.1)
13	144.5	143.3 (-1.2)	143.3 ( $\pm 0$ )	ara			
14	42.2	42.2 ( $\pm 0$ )	42.2 ( $\pm 0$ )	1	101.6	101.5 (-0.1)	101.5 ( $\pm 0$ )
15	35.8	35.9 (+0.1)	35.9 ( $\pm 0$ )	2	79.3	79.4 (+0.1)	79.3 (-0.1)
16	73.6	73.4 (-0.2)	73.4 ( $\pm 0$ )	3	72.2	72.2 ( $\pm 0$ )	72.2 ( $\pm 0$ )
17	51.8	51.8 ( $\pm 0$ )	51.7 (-0.1)	4	67.3	67.4 (+0.1)	67.3 (-0.1)
18	41.0	40.9 (-0.1)	40.8 (-0.1)	5	63.6	63.6 ( $\pm 0$ )	63.6 ( $\pm 0$ )
19	48.5	47.9 (-0.6)	48.0 (+0.1)	xyf			
20	36.7	35.4 (-1.3)	35.3 (-0.1)	1	105.7	105.8 (+0.1)	105.7 (-0.1)
21	74.7	77.0 (+2.6)	77.0 ( $\pm 0$ )	2	75.0	75.0 ( $\pm 0$ )	74.9 (-0.1)
22	41.8	36.4 (-5.4)	36.5 (+0.1)	3	77.9	77.9 ( $\pm 0$ )	77.9 ( $\pm 0$ )
23	65.4	65.5 (+0.1)	65.6 (+0.1)	4	70.8	70.7 (-0.1)	70.7 ( $\pm 0$ )
24	15.0	15.0 ( $\pm 0$ )	15.0 ( $\pm 0$ )	5	67.0	67.0 ( $\pm 0$ )	67.0 ( $\pm 0$ )
25	17.3 <sup>a)</sup>	17.3 <sup>a)</sup> ( $\pm 0$ )	17.3 <sup>a)</sup> ( $\pm 0$ )				

a) Measured with TMS as an internal standard, at 75.0 MHz, on a Varian XL 300. b, c) Assignments may be interchanged in each column.

TLC behavior, and IR and  $^1\text{H}$ -NMR spectral comparisons. These observations indicate the position of the glycosyl monoterpene carboxylate group in the saponin G (1) to be C-21.

The  $^1\text{H}$ -NMR spectrum of the methylated oligosaccharide (16) showed four anomeric protons at  $\delta$  4.59 (d,  $J=8.0$  Hz), 4.70 (d,  $J=8.3$  Hz), 4.88 (d,  $J=2.1$  Hz) and 5.06 (d,  $J=3.2$  Hz). On partial methanolysis of 16 with 1 N HCl in methanol, two oligosaccharides, 18 and 19 were obtained. In the  $^1\text{H}$ -NMR spectrum, 18 showed two signals of anomeric protons at  $\delta$  4.87 (d,  $J=1.7$  Hz) and 5.08 (d,  $J=1.6$  Hz), and 19 showed three signals of anomeric protons at  $\delta$  4.67 (d,  $J=7.5$  Hz), 4.87 (d,  $J=1.5$  Hz) and 5.05 (d,  $J=1.5$  Hz). Comparisons of TLC, optical rotation, and IR and  $^1\text{H}$ -NMR spectra showed that 16, 18 and 19 were identical with authentic samples obtained from gleditsia saponin C, which was isolated from the fruits of *Gleditsia japonica*.<sup>5)</sup> The oligosaccharide moiety at C-28 in the saponin G (1) was thus characterized as  $\beta$ -D-xylopyranosyl-(1 $\rightarrow$ 3)- $\beta$ -D-xylopyranosyl-(1 $\rightarrow$ 4)- $\alpha$ -L-rhamnopyranosyl-(1 $\rightarrow$ 2)-[ $\alpha$ -L-rhamnopyranosyl-(1 $\rightarrow$ 6)]- $\beta$ -D-glucopyranosyl. It has been noted from the biogenetic point of view that the saponin G (1) and gleditsia saponin C have the same sugar moieties, including configurations and sequences, at C-3 and C-28.

As shown in Tables I and II, in the  $^{13}\text{C}$ -NMR spectrum of 1, the signals assigned to the triterpene moiety, and the oligosaccharide moieties at C-3 and C-28, were superimposable with those of 10 within  $\pm 0.1$  ppm, except for the signals of the glycosylated monoterpene moiety. The  $^{13}\text{C}$ -NMR spectrum of 3 was very similar to those of the monoterpene glycoside moiety of the saponin G (1). The signals attributable to C-3, C-4 and C-5 of the arabinose at  $\delta$  83.9, 69.1 and 66.6, respectively, in 10, were found to be shifted  $-2.7$ ,  $+2.6$  and  $-2.4$  ppm, respectively, in the saponin G(1). The five prominent signals at  $\delta$  176.7, 41.2, 27.0, 11.5 and

TABLE II. Carbon-13 NMR Chemical Shifts ( $\delta$ ) of the Monoterpene Glycoside Moiety and Sugars at C-28 in Pyridine- $d_5$ <sup>a)</sup>

Carbon	3' <sup>b)</sup>	12	10 $\Delta\delta$ 10-12	1 $\Delta\delta$ 1-10	Carbon	10	1 $\Delta\delta$ 1-10
					C-28 glc		
1	168.4	171.2	167.8 (-3.4)	167.8 ( $\pm 0$ )	1	95.0	95.0 ( $\pm 0$ )
2	127.7	129.6	128.5 (-1.1)	128.6 (+0.1)	2	78.9	78.9 ( $\pm 0$ )
3	143.0	141.5	142.3 (+0.8)	142.2 (-0.1)	3	77.8	77.9 (+0.1)
4	23.6	23.7	23.6 (-0.1)	23.6 ( $\pm 0$ )	4	71.3	71.4 (+0.1)
5	40.3	40.6	40.4 (-0.2)	40.3 (-0.1)	5	76.6	76.5 (-0.1)
6	79.8	79.7	79.7 ( $\pm 0$ )	79.9 (+0.2)	6	66.8	66.8 ( $\pm 0$ )
7	143.0	144.0	144.0 ( $\pm 0$ )	143.7 (-0.3)	rham		
8	115.2	115.0	115.1 (+0.1)	115.2 (+0.1)	1	101.4	101.4 ( $\pm 0$ )
9	12.4	12.9	12.7 (-0.2)	12.7 ( $\pm 0$ )	2	71.7	71.8 (+0.1)
10	23.7	23.7	23.7 ( $\pm 0$ )	23.7 ( $\pm 0$ )	3	72.4	72.4 ( $\pm 0$ )
ara					4	84.1	84.1 ( $\pm 0$ )
1	99.7	99.9	99.9 ( $\pm 0$ )	99.8 (-0.1)	5	68.3	68.2 (-0.1)
2	71.7	71.5	71.5 ( $\pm 0$ )	71.7 (+0.2)	6	18.6	18.6 ( $\pm 0$ )
3	81.4	84.0	83.9 (-0.1)	81.2 (-2.7)	xyl		
4	71.6	69.1	69.1 (+0)	71.7 (+2.6)	1	106.3	106.2 (-0.1)
5	64.1	66.6	66.6 (+0)	64.2 (-2.4)	2	75.0	74.9 (-0.1)
glc					3	87.7	87.7 ( $\pm 0$ )
1	106.1	106.0	106.0 ( $\pm 0$ )	106.1 (+0.1)	4	68.9	68.9 ( $\pm 0$ )
2	75.5	75.6	75.6 ( $\pm 0$ )	75.6 ( $\pm 0$ )	5	67.1	67.1 ( $\pm 0$ )
3	78.4	78.6	78.5 (-0.1)	78.3 (-0.2)	xyl		
4	71.5	71.5	71.5 ( $\pm 0$ )	71.6 (+0.1)	1	105.9	106.0 (+0.1)
5	78.2	78.2	78.2 ( $\pm 0$ )	78.2 ( $\pm 0$ )	2	75.1	75.1 ( $\pm 0$ )
6	62.9	62.6	62.6 ( $\pm 0$ )	63.0 (+0.4)	3	78.1	78.1 ( $\pm 0$ )
2-Methylbutyroyl					4	70.7	70.7 ( $\pm 0$ )
1	176.7			176.6	5	67.3	67.2 (-0.1)
2	41.2			41.2	rham		
3	27.0			27.0	1	102.0	101.9 (-0.1)
4	11.5			11.5	2	72.0	72.0 ( $\pm 0$ )
5	16.5			16.5	3	72.6	72.6 ( $\pm 0$ )
					4	73.9	73.9 ( $\pm 0$ )
					5	69.6	69.6 ( $\pm 0$ )
					6	18.6	18.6 ( $\pm 0$ )

a) Measured with TMS as an internal standard, at 75.0 MHz, on a Varian XL 300. b) Methyl ester of 3 (diazomethane).

16.6 in 1 correspond to the 2-methylbutyroyl group of 3.<sup>2)</sup> On the basis of the acylation shift rule,<sup>6)</sup> it was concluded that the 2-methylbutyroyl group was located at C-4 of the arabinose, as in 3.

Based on all of the above results, the structure of gymnocladus saponin G (1) was characterized as 2 $\beta$ ,23-dihydroxy-3-*O*-[ $\beta$ -D-xylopyranosyl-(1 $\rightarrow$ 2)- $\alpha$ -L-arabinopyranosyl-(1 $\rightarrow$ 6)- $\beta$ -D-glucopyranosyl]-21-*O*-{(6*S*)-2-*trans*-2,6-dimethyl-6-[3-*O*-( $\beta$ -D-glucopyranosyl)-4-*O*-(2-methylbutyroyl)- $\alpha$ -L-arabinopyranosyloxy]-2,7-octadienoyl}acacic acid 28-*O*- $\beta$ -D-xylopyranosyl-(1 $\rightarrow$ 3)- $\beta$ -D-xylopyranosyl-(1 $\rightarrow$ 4)- $\alpha$ -L-rhamnopyranosyl-(1 $\rightarrow$ 2)-[ $\alpha$ -L-rhamnopyranosyl-(1 $\rightarrow$ 6)]- $\beta$ -D-glucopyranoside.

#### Experimental

Unless otherwise stated, <sup>1</sup>H-NMR spectra were measured on a Varian XL-300 NMR spectrometer in CDCl<sub>3</sub> at 300 MHz with tetramethylsilane (TMS) as an internal standard. UV spectra were measured on a Shimadzu UV 240 spectrometer in 95% EtOH. HPLC were carried out on  $\mu$ -Bondapak C-18 (Waters Ltd.), 7.8 mm  $\times$  30 cm, solvent flow rate 1.6 ml/min. Conditions of TLC and gas liquid chromatography (GLC) for identification of methylated

monosaccharides were reported in the previous papers.<sup>3,5)</sup>

**Purification and Properties of Gymnocladus Saponin G (1)**—The crude saponin fraction<sup>3)</sup> was chromatographed repeatedly on silica gel columns with  $\text{CHCl}_3 : \text{MeOH} : \text{H}_2\text{O} = 65 : 35 : 10$  (lower layer). The major fraction was subjected to gel filtration on Sephadex LH20 with MeOH, and purified by preparative HPLC with  $\text{MeOH} : \text{H}_2\text{O} = 68 : 32$  to afford **1** as a hygroscopic white powder (Yield: 0.015% from the dried fruits).  $[\alpha]_D^{27} - 4.8^\circ$  ( $c = 1.20$ , MeOH). IR  $\nu_{\text{max}}^{\text{KBr}} \text{cm}^{-1}$ : 3400–3600 (OH), 1680, 1730 (COOR). UV  $\lambda_{\text{max}}^{\text{EtOH}} \text{nm}$  ( $\epsilon$ ): 217 (18000).  $^{13}\text{C-NMR}$ : Tables I and II. *Anal.* Calcd for  $\text{C}_{100}\text{H}_{160}\text{O}_{53} \cdot \text{H}_2\text{O}$ : C, 53.90; H, 7.33. Found: C, 53.74; H, 7.50.

**Hydrolysis of 1 with 10%  $\text{H}_2\text{SO}_4$** —A solution of **1** (100 mg) in EtOH (10 ml) and 10%  $\text{H}_2\text{SO}_4$  (10 ml) was refluxed for 2.5 h and neutralized with Amberlite IRA 450. The reaction mixture was concentrated to half the initial volume *in vacuo*, and then extracted with EtOAc. The organic layer was evaporated, and the residue was recrystallized from MeOH– $\text{H}_2\text{O}$  to afford 2 $\beta$ ,23-dihydroxyacacic acid lactone (**8**, 20 mg) as colorless needles (mp 187–189°C); this product was identical with an authentic sample obtained from gymnocladus saponin A (**4**)<sup>3)</sup> on the basis of TLC, IR and  $^1\text{H-NMR}$  comparisons and mixed melting point determination. From the water layer, glucose, xylose, rhamnose and arabinose were identified by paper partition chromatography (PPC).

**Hydrolysis of 1 with 2%  $\text{NaHCO}_3$** —A solution of **1** (160 mg) in EtOH (30 ml) and 2%  $\text{NaHCO}_3$  (30 ml) was refluxed for 1.5 h. The reaction mixture was neutralized with Dowex 50W  $\times 8$ , and evaporated to dryness *in vacuo*. The residue showed two major spots on TLC ( $R_f$ : 0.20 and 0.15) ( $\text{CHCl}_3 : \text{MeOH} : \text{H}_2\text{O} = 65 : 35 : 10$ , lower layer). The mixture was separated and purified by HPLC ( $\text{MeOH} : \text{H}_2\text{O} = 7 : 3$ ) to give 40 mg of **1** ( $R_f$  0.20) and 80 mg of **10** ( $R_f$  0.15) as a hygroscopic white powder.  $[\alpha]_D^{26} - 23.2^\circ$  ( $c = 0.64$ , MeOH). IR  $\nu_{\text{max}}^{\text{KBr}} \text{cm}^{-1}$ : 3400–3600 (OH), 1680, 1720 (COOR). UV  $\lambda_{\text{max}}^{\text{EtOH}} \text{nm}$ : 216.  $^{13}\text{C-NMR}$ : Tables I and II. *Anal.* Calcd for  $\text{C}_{95}\text{H}_{152}\text{O}_{52} \cdot 3\text{H}_2\text{O}$ : C, 52.32; H, 7.30. Found: C, 52.11; H, 7.48.

**Hydrolysis of 1 with 10% KOH**—A solution of **1** (500 mg) in EtOH (15 ml) and KOH (15 ml) was refluxed for 3 h, and neutralized with Dowex 50W  $\times 8$ . The solution was evaporated to half the initial volume, and extracted with *n*-BuOH saturated with  $\text{H}_2\text{O}$ . The organic layer was evaporated to dryness to give a brown oily residue (280 mg). The residue showed three major spots on TLC ( $R_f$ : 0.55, 0.45 and 0.21,  $\text{CHCl}_3 : \text{MeOH} : \text{H}_2\text{O} = 65 : 35 : 10$ , lower layer). The mixture was subjected to chromatography on a silica gel column ( $\text{CHCl}_3 : \text{MeOH} : \text{H}_2\text{O} = 8 : 3 : 1$ , lower layer) to afford three major fractions, and each fraction was purified by HPLC ( $\text{MeOH} : \text{H}_2\text{O} = 66 : 34$ ) to give 45 mg of **6**, corresponding to the product of  $R_f$  0.55. This product was identified with an authentic sample of gymnocladus saponin C on the basis of TLC, IR and  $^{13}\text{C-NMR}$ , comparisons. From the second fraction, **12** (35 mg) was obtained as a white amorphous powder.  $[\alpha]_D^{26} - 4.8^\circ$  ( $c = 0.81$ , MeOH), UV  $\lambda_{\text{max}}^{\text{EtOH}} \text{nm}$ : 215. IR  $\nu_{\text{max}}^{\text{KBr}} \text{cm}^{-1}$ : 3400–3500 (OH), 1680 (COOR).  $^{13}\text{C-NMR}$ : Table II. This product was identical with an authentic sample of deacyl monoterpene glycoside (**12**) obtained from **3** on the basis of TLC, IR and  $^{13}\text{C-NMR}$ <sup>2)</sup> comparisons. From the third fraction, compound **11** (110 mg) corresponding to the product of  $R_f$  0.21 was obtained as a white powder.  $[\alpha]_D^{26} - 1.5^\circ$  ( $c = 0.74$ , MeOH). IR  $\nu_{\text{max}}^{\text{KBr}} \text{cm}^{-1}$ : 3400–3500 (OH), 1680 (COOH).  $^{13}\text{C-NMR}$ : Table I. *Anal.* Calcd for  $\text{C}_{46}\text{H}_{74}\text{O}_{20} \cdot 2\text{H}_2\text{O}$ : C, 56.20; H, 8.00. Found: C, 56.49; H, 8.09.

**Permethylolation of 1 and 10**—According to Hakomori's method,<sup>4)</sup> the reagent mixture (20 ml) [prepared from NaH (2 g) and DMSO (50 ml)] was added to a solution of **1** (400 mg) in DMSO (10 ml). The mixture was stirred for 1 h at room temperature under an  $\text{N}_2$  stream. After addition of  $\text{CH}_3\text{I}$  (25 ml), the reaction mixture was stirred for 3 h at room temperature, then poured into ice-water and extracted with  $\text{Et}_2\text{O}$ . The  $\text{Et}_2\text{O}$  layer was washed with  $\text{H}_2\text{O}$ , dried over  $\text{MgSO}_4$  and evaporated to give a yellow oily product (505 mg). This oily product was purified by chromatography on a silica gel column (benzene : acetone = 7 : 3) to give the permethylate (**13**, 150 mg) as a colorless syrup.  $[\alpha]_D^{26} - 9.5^\circ$  ( $c = 0.85$ ,  $\text{CHCl}_3$ ). IR  $\nu_{\text{max}}^{\text{CHCl}_3} \text{cm}^{-1}$ : 1720 (COOR), 1100 (C–O–C).  $^1\text{H-NMR}$   $\delta$ : 0.76, 0.83, 0.92, 1.00, 1.20, 1.25 (3H, each s,  $\text{CH}_3 \times 6$ ), 4.19 (1H, d,  $J = 7.5$  Hz, anomeric H), 4.24 (1H, d,  $J = 7.5$  Hz, anomeric H), 4.43 (1H, d,  $J = 6.5$  Hz, anomeric H), 4.45 (1H, d,  $J = 7.0$  Hz, anomeric H), 4.54 (1H, d,  $J = 3.5$  Hz, anomeric H), 4.61 (1H, d,  $J = 7.0$  Hz, anomeric H), 4.69 (1H, d,  $J = 7.5$  Hz, anomeric H), 4.83 (1H, brs, anomeric H), 5.10 (1H, brs, anomeric H), 5.13 (1H, dd,  $J = 18.0, 2.5$  Hz,  $\text{H}_R > \text{C} = \text{C} < \text{H}_H$ ), 5.20 (1H, dd,  $J = 11.5, 2.5$  Hz,  $\text{H}_R > \text{C} = \text{C} < \text{H}_H$ ), 5.58 (1H, d,  $J = 7.0$  Hz, anomeric H), 5.82 (1H, dd,  $J = 18.0, 11.5$  Hz,  $\text{H}_R > \text{C} = \text{C} < \text{H}_H$ ). *Anal.* Calcd for  $\text{C}_{124}\text{H}_{210}\text{O}_{53} \cdot \text{H}_2\text{O}$ : C, 58.02; H, 8.32. Found: C, 57.85; H, 8.30. This permethylate (**13**) was also obtained from **10** in the same manner.

**Methanolysis of 13**—A solution of **13** (20 mg) in 2N methanolic HCl (20 ml) was refluxed for 3 h, then neutralized with  $\text{Ag}_2\text{CO}_3$  and filtered. The filtrate was evaporated and residue was examined by TLC and GLC. Nine different methylated monosaccharides, methyl 2,3,4-tri-*O*-methyl-D-xylopyranoside, methyl 2,4-di-*O*-methyl-D-xylopyranoside, methyl 2,4-di-*O*-methyl-L-arabinopyranoside, methyl 3,4-di-*O*-methyl-L-arabinopyranoside, methyl 2,3,4-tri-*O*-methyl-L-rhamnopyranoside, methyl 2,3-di-*O*-methyl-L-rhamnopyranoside, methyl 2,3,4,6-tetra-*O*-methyl-D-glucopyranoside, methyl 2,3,4-tri-*O*-methyl-D-glucopyranoside and methyl 3,4-di-*O*-methyl-D-glucopyranoside were identified by comparison with authentic samples.

**Reductive Cleavage of Permethylate (13) with  $\text{LiAlH}_4$** —A solution of the permethylate (**13**, 200 mg) in anhydrous tetrahydrofuran (THF) (15 ml) was treated with  $\text{LiAlH}_4$  (150 mg), and the mixture was refluxed for 3 h. The excess  $\text{LiAlH}_4$  was decomposed with wet  $\text{Et}_2\text{O}$  and the mixture was extracted with  $\text{Et}_2\text{O}$  and EtOAc successively.

The Et<sub>2</sub>O extract was chromatographed on a silica gel column (benzene : acetone = 7 : 3), and purified by preparative TLC (benzene : acetone = 5 : 4) to give 30 mg of **14** as a colorless syrup.  $[\alpha]_D^{25} + 17.1^\circ$  ( $c = 1.70$ , CHCl<sub>3</sub>). IR  $\nu_{\max}^{\text{CHCl}_3} \text{cm}^{-1}$ : 3500 (OH), 1100 (C-O-C). <sup>1</sup>H-NMR  $\delta$ : 0.98 (3H, d,  $J = 1.9$  Hz, CH<sub>3</sub>), 1.32 (3H, s, CH<sub>3</sub>), 3.36, 3.44, 3.52, 3.58, 3.62, 3.63 (3H, each s, OCH<sub>3</sub> × 6), 4.26 (1H, d,  $J = 7.1$  Hz, anomeric H), 4.44 (1H, d,  $J = 6.8$  Hz, anomeric H), 5.15 (1H, dd,  $J = 18.0, 2.0$  Hz,  $\begin{matrix} \text{H} \\ | \\ \text{C}=\text{C} \\ | \\ \text{H} \end{matrix}$ ), 5.21 (1H, dd,  $J = 11.2, 2.0$  Hz,  $\begin{matrix} \text{H} \\ | \\ \text{C}=\text{C} \\ | \\ \text{H} \end{matrix}$ ), 5.84 (1H, dd,  $J = 18.0, 11.2$  Hz,  $\begin{matrix} \text{H} \\ | \\ \text{C}=\text{C} \\ | \\ \text{H} \end{matrix}$ ). From the second fraction, a triterpenoid glycoside alcohol (**15**, 35 mg) was obtained as an amorphous powder. IR  $\nu_{\max}^{\text{CHCl}_3} \text{cm}^{-1}$ : 3450 (OH), 1100 (C-O-C). <sup>1</sup>H-NMR  $\delta$ : 0.87, 0.91, 0.94, 0.96, 1.22, 1.29 (3H, each s, CH<sub>3</sub> × 6), 3.23, 3.31, 3.35, 3.41, 3.45, 3.47, 3.53, 3.58, 3.61, 3.62, 3.63 (3H, each s, OCH<sub>3</sub> × 11), 4.19 (1H, d,  $J = 8.0$  Hz, anomeric H), 4.43 (1H, d,  $J = 7.3$  Hz, anomeric H), 4.53 (1H, d,  $J = 4.8$  Hz, anomeric H), 5.28 (1H, t like, C-12-H), 4.12 (1H, dd,  $J = 15.0, 7.3$  Hz, C-18-H). The EtOAc extract was purified by preparative TLC (benzene : acetone = 9 : 10) to give an oligosaccharide alcohol (**16**, 15 mg) as a colorless oil.  $[\alpha]_D^{25} - 67.4^\circ$  ( $c = 1.40$ , CHCl<sub>3</sub>). IR  $\nu_{\max}^{\text{CHCl}_3} \text{cm}^{-1}$ : 3450 (OH), 1100 (C-O-C). <sup>1</sup>H-NMR  $\delta$ : 1.30, 1.32 (3H, each d,  $J = 6.3$  Hz, CH<sub>3</sub> × 2), 3.45, 3.46, 3.48, 3.49 (3H, each s, OCH<sub>3</sub> × 4), 3.50 (6H, s, OCH<sub>3</sub> × 2), 3.51, 3.55, 3.75, 3.61 (3H, each s, OCH<sub>3</sub> × 4), 3.62 (6H, s, OCH<sub>3</sub> × 2), 4.59 (1H, d,  $J = 8.0$  Hz, anomeric H), 4.70 (1H, d,  $J = 8.3$  Hz, anomeric H), 4.88 (1H, d,  $J = 2.1$  Hz, anomeric H), 5.06 (1H, d,  $J = 3.2$  Hz, anomeric H).

**Methanolysis of 15**—A solution of **15** (10 mg) in 2N methanolic HCl (10 ml) was refluxed for 3 h. The reaction mixture was treated in the same manner as described above, to give three different methylated monosaccharides and a triterpene alcohol (**17**, 5 mg). **17** was identical with the corresponding alcohol, olean-12-ene-2 $\beta$ ,16 $\beta$ ,23-tri-*O*-methyl-3 $\beta$ ,21 $\beta$ ,28-triol, obtained from gymnocladus saponin D (**7**) in the same manner, on the basis of TLC, IR and <sup>1</sup>H-NMR<sup>1)</sup> comparisons.

**Partial Methanolysis of 16**—A solution of **16** (90 mg) in 2N methanolic HCl (30 ml) was allowed to stand at room temperature for 24 h. After being neutralized with Ag<sub>2</sub>CO<sub>3</sub>, the mixture was filtered, the filtrate was evaporated and the residue was purified by preparative TLC (benzene : acetone = 5 : 4) to give **18** and **19** as colorless syrups. These methylated oligosaccharides were identical with the previously reported samples.<sup>5)</sup>

**Methanolysis of 16**—A solution of **16** in methanolic HCl was refluxed for 2 h, and treated in the usual manner as described above. All of the methylated monosaccharides were identical with authentic samples on the basis of TLC and GLC comparisons.<sup>5)</sup>

**Acknowledgement** The authors are grateful to Mr. Y. Fujiwara, Kyoto Pharmaceutical University, for <sup>1</sup>H- and <sup>13</sup>C-NMR measurements, and to Miss M. Takahashi of Kyoto Pharmaceutical University for MS measurements. They are also indebted to the members of the Analytical Center of Kyoto University for microanalysis.

#### References

- 1) Part VIII: T. Konoshima, T. Sawada and T. Kimura, *Chem. Pharm. Bull.*, **33**, 4732 (1985).
- 2) T. Konoshima and T. Sawada, *Chem. Pharm. Bull.*, **32**, 2617 (1984).
- 3) T. Konoshima, T. Sawada and T. Kimura, *Chem. Pharm. Bull.*, **32**, 4833 (1984).
- 4) S. Hakomori, *J. Biochem. (Tokyo)*, **55**, 205 (1964).
- 5) T. Konoshima, H. Inui, K. Sato, M. Yonezawa and T. Sawada, *Chem. Pharm. Bull.*, **28**, 3473 (1980).
- 6) H. Ishii, K. Tori, T. Tojo and Y. Yoshimura, *Chem. Pharm. Bull.*, **26**, 678 (1978).



[Chem. Pharm. Bull.]  
35(1) 53-59 (1987)

## Structures of Sesquiterpenes from *Curcuma aromatica* SALISB.

MASANORI KUROYANAGI,<sup>\*,a</sup> AKIRA UENO,<sup>a</sup> KAORU UJIE<sup>a</sup>  
and SADA O SATO<sup>b</sup>

*Shizuoka College of Pharmacy,<sup>a</sup> 2-2-1 Oshika, Shizuoka 422, Japan and  
Analytical and Metabolic Research Laboratories, Sankyo Co., Ltd.,<sup>b</sup>  
1-2-58 Hiromachi, Shinagawa-ku, Tokyo 140, Japan*

(Received June 5, 1986)

Three new sesquiterpenes, isozedoarondiol (**8**), methylzedoarondiol (**9**) and neocurdione (**10**), were isolated along with germacrone (**1**), curdione (**2**), (4*S*,5*S*)-germacrone 4,5-epoxide (**3**), dehydrocurdione (**4**), procurcumenol (**5**), zedoarondiol (**6**) and curcumenone (**7**) from *Curcuma aromatica* SALISB. The absolute configuration of **6** was determined by X-ray analysis and chemical correlation with **3**. The structures of **8**, **9** and **10** were also determined.

**Keywords**—*Curcuma aromatica*; sesquiterpene; germacrane-type sesquiterpene; guaiane-type sesquiterpene; zedoarondiol; isozedoarondiol; neocurdione; (4*S*,5*S*)-germacrone 4,5-epoxide; X-ray analysis

Rhizomes of *Curcuma* spp. (Zingiberaceae), such as *C. longa*, *C. zedoaria*, *C. xanthorrhiza* and *C. aromatica*, are used as oriental traditional medicines in China, Japan and southeastern Asia. From these plants, many kinds of sesquiterpenes have been isolated, but there have been few reports on the constituents of *C. aromatica* SALISB.<sup>1)</sup>

The fresh rhizomes of the title plant, cultivated at the medicinal plants garden of this college, were extracted and treated as described in the experimental section to give three new sesquiterpenes, isozedoarondiol (**8**), methylzedoarondiol (**9**) and neocurdione (**10**), along with germacrone (**1**), curdione (**2**), (4*S*,5*S*)-germacrone 4,5-epoxide (**3**), dehydrocurdione (**4**), procurcumenol (**5**), zedoarondiol (**6**) and curcumenone (**7**).<sup>2)</sup> This paper deals with the isolation and structural elucidation of these sesquiterpenes. Further, the absolute configuration of **6** was determined by X-ray analysis and chemical derivatization from **3**.

The proton and carbon-13 nuclear magnetic resonance (<sup>1</sup>H- and <sup>13</sup>C-NMR) spectra, and the other physicochemical data of **1**, **3**, **4** and **5** showed that these compounds were identical with germacrone,<sup>3)</sup> (4*S*,5*S*)-germacrone 4,5-epoxide,<sup>4)</sup> dehydrocurdione<sup>5)</sup> and procurcumenol,<sup>6)</sup> respectively.

The spectral data of **2**, mp 61–62 °C, C<sub>15</sub>H<sub>24</sub>O<sub>2</sub>, indicated that it was curdione,<sup>7)</sup> and **2** was confirmed to be identical with an authentic sample. The <sup>1</sup>H- and <sup>13</sup>C-NMR spectra of **10**, mp 45–47 °C, C<sub>15</sub>H<sub>24</sub>O<sub>2</sub>, showed signal patterns similar to those of **2**, including three secondary methyl groups [ $\delta$  0.97 (3H, d, *J* = 6.8 Hz), 1.03 (3H, d, *J* = 6.8 Hz), 0.92 (3H, d, *J* = 6.6 Hz)], a vinyl methyl group [ $\delta$  1.67 (3H, s)], a tri-substituted olefin group [ $\delta$  5.18 (H, br t, *J* = 7.0 Hz)] and two carbonyl groups ( $\delta$  210.2, 212.5). These results indicated that **2** and **10** are diastereomers. The olefin groups of **2** and **10** were determined to be *trans* by nuclear Overhauser effect (NOE) experiments; in both compounds, irradiation at 9-CH<sub>2</sub> gave a 14% increase in the intensity of 1-H. Therefore, **2** and **10** might be epimers at C-4 or at C-7. The absolute structure of curdione has been reported as **2**.<sup>7)</sup> The circular dichroism (CD) spectra of **2** and **10** are shown in Fig. 1. Curdione and neocurdione showed opposite CD Cotton effects attributable to the  $\beta,\gamma$ -unsaturated ketone groups<sup>8)</sup> (Fig. 1). An isopropyl group has a

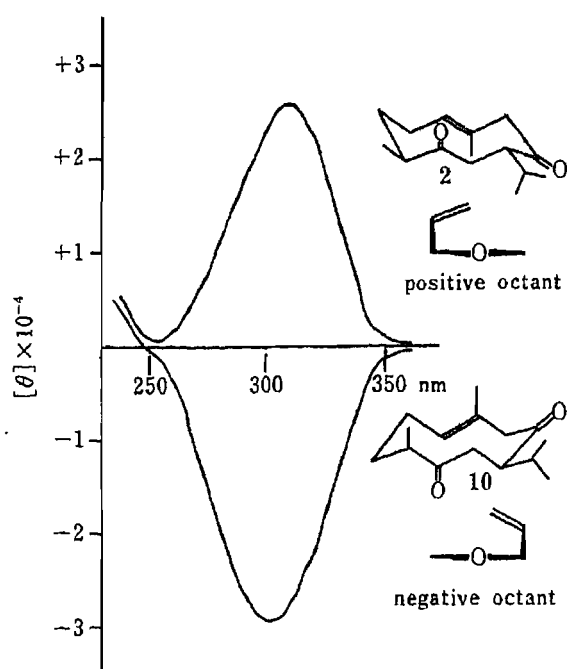


Fig. 1. CD Spectra of Curdione (2) and Neocurdione (10) in  $\text{CDCl}_3$

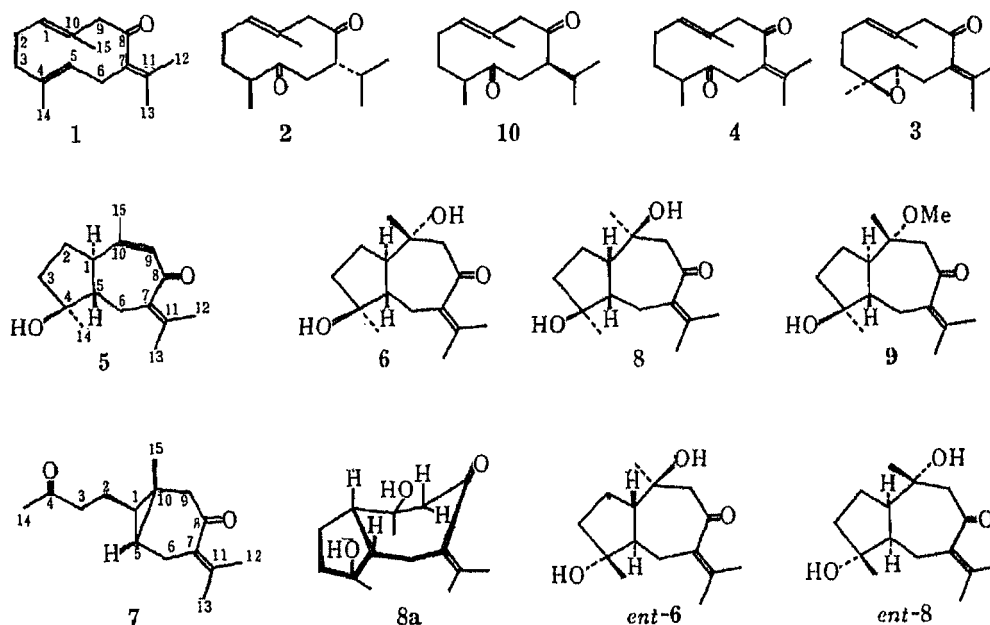


Chart 1

greater effect than a methyl group on the conformation so the isopropyl group at C-7 of **10** may have the opposite configuration from that of **2**,<sup>7)</sup> but unequivocal confirmation is needed for the determination of the configurations at C-4 and C-7 of **10**.

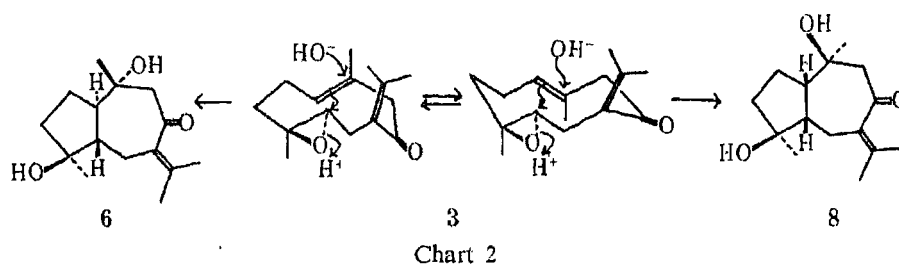
The  $^1\text{H-NMR}$  spectrum of compound **7**, mp  $28^\circ\text{C}$ ,  $\text{C}_{15}\text{H}_{22}\text{O}_2$ , showed that the structure of **7** was identical with that of curcumenone isolated from *C. zedoaria* by Asakawa *et al.*<sup>9)</sup> The enantiomer of **7** has been isolated from *Asarum calescense* MAXIM.<sup>10)</sup> This seco-guaiane-type compound having a cyclopropane ring is the secondary case after carabrone<sup>11)</sup> isolated from *Carpesium abrotanoides*.

The  $^1\text{H-}$  and  $^{13}\text{C-NMR}$  spectra of zedoarondiol (**6**), mp  $134^\circ\text{C}$ ,  $\text{C}_{15}\text{H}_{24}\text{O}_3$ ,  $[\alpha]_D -44.0^\circ$ , showed the presence of two tertiary methyl groups [ $\delta$  1.18 (s), 1.20 (s), and 20.6, 22.7] on

TABLE I.  $^{13}\text{C}$ -NMR Data for the Sesquiterpenes<sup>a)</sup>

	1	2	3	4	5	6	7	8	9	10
C-1	132.5	131.5	129.7	132.7	50.5	55.9	29.8	53.4	51.6	131.1
C-2	24.0	26.4	24.5	26.2	26.9	22.9	24.2	25.2	22.9	25.5
C-3	38.0	34.1	37.7	34.1	28.6	28.5	43.8	27.4	28.7	32.8
C-4	126.7	46.8	60.4	46.4	80.2	79.9	208.2	82.4	79.7	45.8
C-5	125.4	211.0	64.3	210.6	54.0	52.0	24.3	51.7	48.4	210.2
C-6	29.1	44.2	29.7	43.4	39.9	39.7	28.0	37.0	39.9	42.1
C-7	129.0	53.5	126.7	129.4	136.6 <sup>b)</sup>	134.6	128.0	134.0	135.0	52.6
C-8	207.2	214.2	204.3	206.4	199.0	202.9	201.2	203.0	203.3	212.5
C-9	55.8	55.9	55.4	56.8	129.2	59.8	48.9	50.2	53.9	55.3
C-10	134.7	129.8	133.7	130.0	136.3 <sup>b)</sup>	72.7	20.0	73.2	76.8	129.1
C-11	137.3	30.0	133.9	136.9	155.1	142.1	146.9	143.7	141.5	30.9
C-12	19.8	19.9 <sup>b)</sup>	20.3	20.9	21.2	21.9	23.4	22.1	21.9	20.2 <sup>b)</sup>
C-13	22.2	21.1 <sup>b)</sup>	22.6	22.0	22.4	22.2	23.4	22.8	22.2	21.1 <sup>b)</sup>
C-14	15.5	18.5 <sup>b)</sup>	15.8	18.3	23.3	22.7	23.2	25.0	22.6	18.2 <sup>b)</sup>
C-15	16.6	16.6 <sup>b)</sup>	17.0	16.2	24.3	20.6	18.9	32.2	17.1	18.2 <sup>b)</sup>
OMe									53.4	

a) Measured in  $\text{CDCl}_3$ . b) Assignments may be interchanged in each column.



carbinyl carbons ( $\delta$  79.9, 72.7), and an isopropylidene group [ $\delta$  1.84 (s), 1.94 (s), and 21.9, 22.2, 134.6, 142.1] conjugated with a carbonyl group ( $\delta$  202.9). The presence of conjugated enone system was supported by the ultraviolet (UV) spectrum [ $\lambda$  258 nm (3.86)]. The  $^1\text{H}$ - and  $^{13}\text{C}$ -NMR of isozedoarondiol (**8**), mp 150–156 °C,  $\text{C}_{15}\text{H}_{24}\text{O}_3$ ,  $[\alpha]_{\text{D}} -147.2^\circ$ , UV 252 nm (3.94), also showed the presence of the same functional groups as in **6** [ $\delta$  1.23 (s), 1.42 (s), 1.86 (s), 2.03 (s), and 22.1, 22.8, 25.0, 32.2, 134.0, 143.7, 203.0] ( $^{13}\text{C}$ -NMR data for **6** and **8** are listed in Table I). These data suggested that **6** and **8** had the same plane structure, having a guaiane-type skeleton, and might be diastereomers. From the transannular cyclization reaction mechanism, **6** and **8** should be formed from **3** as shown in Chart 2.

To elucidate the relative stereostructure of **6**, X-ray analysis was carried out. The X-ray crystallographical data are as follows:  $\text{C}_{15}\text{H}_{24}\text{O}_3$ ,  $M_r = 252.4$ , monoclinic,  $P2_1$ ,  $a = 9.397(1)$ ,  $b = 8.405(1)$ ,  $c = 10.201(2)$  Å,  $\beta = 110.44(1)^\circ$ ,  $U = 754.9$  Å<sup>3</sup>,  $Z = 2$ ,  $D_x = 1.11$  g·cm<sup>-3</sup>. Intensity data to  $\theta = 64^\circ$  were recorded on a Rigaku AFC-5R diffractometer, using graphite-monochromated  $\text{CuK}_\alpha$  radiation. A total of 1346 independent reflections were corrected for Lorentz and polarization factors but not for absorption. The structure was solved by MULTAN<sup>12)</sup> and refined by block-diagonal least-squares methods. Hydrogen atoms were located in difference syntheses. The final least-squares refinement with anisotropic temperature factors for the non-hydrogen atoms and isotropic temperature factors for the hydrogen atoms lowered the  $R$ -value to 0.076 for 1153 observed reflections ( $F_o$ ,  $2\sigma F_o$ ).

The geometry of the molecule thus obtained is shown in Fig. 2 with the atomic numbering. Compound **6** is biosynthesized from **3** in the plant. Zedoarondiol was formed

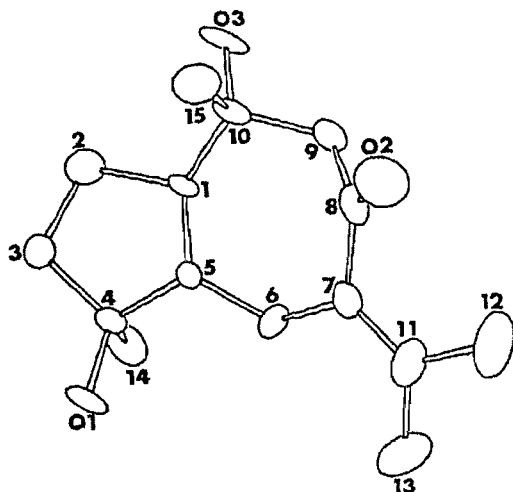


Fig. 2. A Perspective Drawing of **6**

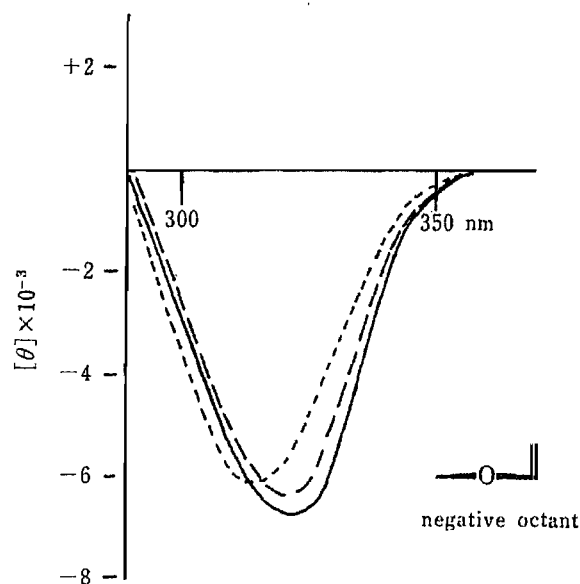


Fig. 3. CD Spectra of Zedoarondiol (**6**), Isozedoarondiol (**8**) and Methylzedoarondiol (**9**) in MeOH  
**6**, ---; **8**, - - - -; **9**, —.

from **3** along with **8** by treatment with  $\text{H}_2\text{SO}_4$  in dioxane-water. Thus, its absolute configuration is that shown in **6**.

The five-membered ring occurs in an envelope conformation with C(4) as the flap at  $-0.65$  (4) Å out of the best plane formed by the other four atoms. The fusion to the seven-membered ring is *trans* with torsion angles of  $30.0$  ( $9^\circ$ ) and  $-76.0$  ( $10^\circ$ ) for C(4)-C(5)-C(1)-C(2) and C(10)-C(1)-C(5)-C(6), respectively. The seven-membered ring has a twist-chair conformation. The torsion angles agree well with the theoretical values for the twist-chair form of the cycloheptane ring.<sup>13)</sup> The two hydroxyl groups attached to C(4) and C(10) are *cis* with respect to the neighboring bridgehead H atom, and participate in intermolecular hydrogen bonds: O(1) H $\cdots$ O(2) (O(1) $\cdots$ O(2)=2.810(11) Å) and O(3)H $\cdots$ O(1) (O(3) $\cdots$ O(1)=2.826(10) Å), respectively.

The  $^1\text{H-NMR}$  spectrum of **6** showed the presence of a long-range coupling between 15- $\text{CH}_3$  [ $\delta$  1.18 (3H, s)] and  $9\alpha\text{-H}$  [ $\delta$  2.98 (H, d,  $J=13.0$  Hz)], which was confirmed by a decoupling experiment. Thus, 15- $\text{CH}_3$  was decoupled to sharpen the broad doublet of  $9\alpha\text{-H}$ , while  $9\alpha\text{-H}$  was decoupled to increase the height of the 15- $\text{CH}_3$  signal. The CD spectrum of **6** showed a negative Cotton effect (Fig. 3) ( $[\theta]_{321} -6463$ ) attributed to  $n \rightarrow \pi^*$  transition of an  $\alpha, \beta$ -unsaturated ketone.<sup>14)</sup> These data accord with the absolute structure obtained from the X-ray analysis (Fig. 2). The  $^1\text{H-NMR}$  spectrum of **8** showed the presence of long-range coupling between 15- $\text{CH}_3$  [ $\delta$  1.42 (3H, s)] and  $9\beta\text{-H}$  [ $\delta$  2.42 (H, d,  $J=16.0$  Hz)]. The CD spectrum of **8** also showed negative Cotton effect (Fig. 3) ( $[\theta]_{313} -6323$ ). These data suggested that the absolute configuration of isozedoarondiol is **8** and its conformation might be as shown in **8a**, having an antiparallel relationship between 15- $\text{CH}_3$  and  $9\beta\text{-H}$ , and anticlockwise helicity of the conjugated enone system.

Endo and Itokawa<sup>10)</sup> isolated the *ent*-type compounds **6** and **8**, from *A. caulescens* MAXIM. The  $^1\text{H-NMR}$  data and infrared (IR) data of **6** and **8** were identical with those of *ent*-**6** and *ent*-**8**, but the optical properties, such as optical rotations and CD spectra, were opposite. The structures of *ent*-**6** and *ent*-**8** have been reported to be the interchanged structures, so they should be revised as shown in Chart 1.

Methylzedoarondiol (**9**), mp  $83\text{--}85^\circ\text{C}$ ,  $\text{C}_{16}\text{H}_{26}\text{O}_3$ , showed the presence of a methoxyl

group [ $\delta$  3.20 (3H, s) and 51.9] and the same functional groups as those of **6** (Table I), which indicated that **9** was a mono-methylether of **6**. In the  $^1\text{H-NMR}$  spectrum, the carbon at C-10 was shifted to lower field and the carbons at C-1 and C-9 were shifted to higher field compared with those of **6** ( $\delta$  72.7 $\rightarrow$ 76.8 for C-10, 55.9 $\rightarrow$ 51.9 for C-1 and 59.8 $\rightarrow$ 53.9 for C-9, respectively). Other carbon signals were almost the same as those of **6**. These results indicated that the structure of **9** was the methyl ether of **6** at C-10. Methylzedoarondiol also showed the same negative optical rotation ( $[\alpha]_D -43.1^\circ$ ) and CD spectrum (Fig. 3) ( $[\theta]_{322} -6742$ ) as **6**. Further, **9** was derived from **3** by treatment with  $\text{H}_2\text{SO}_4/\text{MeOH}$ . The synthetic **9** was identical with the natural one ( $^1\text{H-NMR}$ ,  $^{13}\text{C-NMR}$ , thin layer chromatography (TLC), high-performance liquid chromatography (HPLC) and optical rotation).

Kawano and Kouno isolated zedoarondiol,<sup>15)</sup> from *C. zedoaria*, but the optical properties have not been reported. From *C. zedoaria*, (4*S*,5*S*)-germacrone 4,5-epoxide (**3**) has also been isolated, so the absolute configuration of zedoarondiol, isolated by Kawano and Kouno might be identical with that of **6**, isolated from *C. aromatica*.

The biogenetic pathway of these sesquiterpenes, isolated from *C. aromatica*, was considered to be as follows, (4*S*,5*S*)-germacrone 4,5-epoxide (**3**) acts as a key intermediate in the pathway. Germacrone (**1**) is epoxidated to give the key intermediate (**3**). Then hydrolysis and dehydration of **3** give dehydrocurdione (**4**), which is further hydrogenated to give curdione (**2**) and neocurdione (**10**). On the other hand **3** is also transformed by transannular cyclization *via* a cationic intermediate to procuremenol (**5**), zedoarondiol (**6**), isozedoarondiol (**8**), methylzedoarondiol (**9**) and curcumenone (**7**).

### Experimental

All melting points were determined on a Yanagimoto micro melting point apparatus and are uncorrected. IR spectra were recorded on a JASCO A-202 grating infrared spectrometer. UV spectra were recorded on a Hitachi model 200-10 spectrometer. Optical rotations were recorded on a JASCO DIP-140 digital polarimeter. CD spectra were recorded on a JASCO J-20A spectropolarimeter.  $^1\text{H}$ - and  $^{13}\text{C}$ -NMR spectra were recorded on a JEOL JNM-FX 90Q NMR spectrometer with tetramethylsilane as an internal standard ( $\delta$  value, ppm). Mass spectra (MS) were recorded on JEOL JMS D-100 and JEOL JMS 01SG-2 mass spectrometers. TLC was performed on precoated Silica gel 60F<sub>254</sub> plates (Merck). Preparative thin layer chromatography (PTLC) was performed on Silica gel PF<sub>254</sub> (Merck, 200  $\times$  200  $\times$  0.7 mm). Column chromatography was performed on Silica gel type 60 (Merck).

**Isolation of the Constituents**-----The fresh rhizomes of *C. aromatica* (2 kg) were extracted with MeOH at room temperature to give the MeOH extract. The residue was extracted with chloroform ( $\text{CHCl}_3$ ) at room temperature to give the  $\text{CHCl}_3$  extract. The MeOH extract was suspended in water and extracted with  $\text{CHCl}_3$  to give the  $\text{CHCl}_3$ -soluble fraction. The  $\text{CHCl}_3$  fraction and  $\text{CHCl}_3$  extract were combined to give the  $\text{CHCl}_3$ -soluble extract (37 g). The extract was chromatographed on a silica gel column using a benzene-ethyl acetate (AcOEt) gradient solvent system to give five fractions, Fr. I (3.8 g), II (10.2 g), III (5.4 g), IV (5.9 g) and V (6.2 g). Fraction II was chromatographed on a silica gel column using the hexane-AcOEt gradient solvent system to give germacrone (**1**) (550 mg), curdione (**2**) (720 mg) and (4*S*,5*S*)-germacrone 4,5-epoxide (**3**) (300 mg). Fraction III was chromatographed on a silica gel column using the same solvent system to give dehydrocurdione (**4**) (90 mg), neocurdione (**10**) (150 mg) and curcumenone (**7**) (800 mg). Fraction IV was repeatedly chromatographed on a silica gel column using  $\text{CHCl}_3$ -MeOH gradient and hexane-AcOEt gradient solvent systems to give procuremenol (**5**) (210 mg) and methylzedoarondiol (**9**) (160 mg). Fraction V was chromatographed on a silica gel column using the  $\text{CHCl}_3$ -MeOH gradient solvent system, followed by PTLC using benzene-AcOEt-MeOH (2:2:1) to give zedoarondiol (**6**) (250 mg) and isozedoarondiol (**8**) (80 mg).

**Germacrone (1)**: Colorless prisms. mp 53 $\text{--}54^\circ\text{C}$  (MeOH). MS  $m/z$ : 218 ( $\text{M}^+$ ) ( $\text{C}_{15}\text{H}_{22}\text{O}$ ). IR  $\nu_{\text{max}}^{\text{KBr}}$   $\text{cm}^{-1}$ : 1679, 1665, 1445, 1294, 1135.  $^{13}\text{C-NMR}$  was shown in Table I.

**Curdione (2)**: Colorless prisms. mp 61 $\text{--}62^\circ\text{C}$  (pet. ether). MS  $m/z$ : 236 ( $\text{M}^+$ ) ( $\text{C}_{15}\text{H}_{24}\text{O}_2$ ). IR  $\nu_{\text{max}}^{\text{KBr}}$   $\text{cm}^{-1}$ : 1690, 1460, 1420, 1170, 1060.  $[\alpha]_D^{23} +214.0^\circ$  ( $c=1.6$ , MeOH). CD ( $c=0.033$ ,  $\text{CHCl}_3$ ):  $[\theta]_{309} +26655$ .  $^{13}\text{C-NMR}$  data are shown in Table I.

**(4*S*,5*S*)-Germacrone 4,5-Epoxide (3)**: Colorless prisms. mp 63.5 $\text{--}64^\circ\text{C}$  (hexane). MS  $m/z$ : 234 ( $\text{M}^+$ ) ( $\text{C}_{15}\text{H}_{22}\text{O}_2$ ).  $[\alpha]_D^{23} +306.1^\circ$  ( $c=0.5$ , MeOH). IR  $\nu_{\text{max}}^{\text{KBr}}$   $\text{cm}^{-1}$ : 1710, 1694, 1662, 1440, 1250. CD ( $c=0.006$ , MeOH):  $[\theta]_{309} +14900$ ,  $[\theta]_{253} +14900$ ,  $[\theta]_{227} -13590$ .  $^{13}\text{C-NMR}$  data are shown in Table I.

**Dehydrocurdione (4)**: Colorless needles. mp 40 $\text{--}42^\circ\text{C}$  (hexane). MS  $m/z$ : 234 ( $\text{M}^+$ ) ( $\text{C}_{15}\text{H}_{22}\text{O}_2$ ).  $[\alpha]_D^{23} +147.5^\circ$

( $c=1.1$ , MeOH). CD ( $c=0.004$ , MeOH):  $[\theta]_{303} +13671$ .  $^{13}\text{C-NMR}$  data are shown in Table I.

Procurcumenol (5): Viscous oil. MS  $m/z$ : 234 ( $\text{M}^+$ ) ( $\text{C}_{15}\text{H}_{22}\text{O}_2$ ). IR  $\nu_{\text{max}}^{\text{liq}} \text{cm}^{-1}$ : 3430, 1650, 1440, 1377.  $[\alpha]_{\text{D}}^{23} +60.9^\circ$  ( $c=0.8$ ,  $\text{CHCl}_3$ ).  $^{13}\text{C-NMR}$  data are shown in Table I.

Zedoarandiol (6): Colorless needles. mp  $134^\circ\text{C}$  ( $\text{CHCl}_3$ ). MS  $m/z$ : 252 ( $\text{M}^+$ ) ( $\text{C}_{15}\text{H}_{24}\text{O}_3$ ). IR  $\nu_{\text{max}}^{\text{KBr}} \text{cm}^{-1}$ : 3420, 1662, 1604. UV  $\lambda_{\text{max}}^{\text{MeOH}} \text{nm}$  (log  $\epsilon$ ): 258 (3.86).  $[\alpha]_{\text{D}}^{23} -44^\circ$  ( $c=1.0$ , MeOH). CD ( $c=0.03$ , MeOH):  $[\theta]_{321} -6468$ .  $^1\text{H-NMR}$  ( $\text{CDCl}_3$ ): 1.18 (3H, s, 14 or 15- $\text{CH}_3$ ), 1.20 (3H, s, 15 or 14- $\text{CH}_3$ ), 1.84 (3H, s, 12 or 13- $\text{CH}_3$ ), 1.94 (3H, s, 13 or 12- $\text{CH}_3$ ), 2.60 (H, d,  $J=13.0$  Hz, 9 $\beta$ -H), 2.98 (H, d,  $J=13.0$  Hz, 9 $\alpha$ -H).  $^{13}\text{C-NMR}$  data are shown in Table I.

Curcumenone (7): Colorless needles. mp  $28^\circ\text{C}$  (hexane). MS  $m/z$ : 234.1621 ( $\text{M}^+$ ) (Calcd. for  $\text{C}_{15}\text{H}_{22}\text{O}_2$  234.1618). IR  $\nu_{\text{max}}^{\text{KBr}} \text{cm}^{-1}$ : 1718, 1675, 1600, 1360, 1170. UV  $\lambda_{\text{max}}^{\text{MeOH}} \text{nm}$  (log  $\epsilon$ ): 234 (3.82).  $[\alpha]_{\text{D}}^{23} -6.1^\circ$  ( $c=0.5$ , MeOH). CD ( $c=0.007$ , MeOH):  $[\theta]_{314} +1884$ .  $^{13}\text{C-NMR}$  data are shown in Table I.

Isozedoarandiol (8): Colorless needles. mp  $150\text{--}156^\circ\text{C}$  ( $\text{CHCl}_3$ ). IR  $\nu_{\text{max}}^{\text{KBr}} \text{cm}^{-1}$ : 3500, 3330, 1662, 1598, 1378, 1304, 1170. UV  $\lambda_{\text{max}}^{\text{MeOH}} \text{nm}$  (log  $\epsilon$ ): 252 (3.94).  $[\alpha]_{\text{D}}^{23} -147.2^\circ$  ( $c=0.8$ , MeOH). CD ( $c=0.003$ , MeOH):  $[\theta]_{313} -6323$ . Anal. Calcd for  $\text{C}_{15}\text{H}_{24}\text{O}_3$ : C, 71.39; H, 9.59. Found: C, 71.65; H, 9.52.  $^1\text{H-NMR}$  ( $\text{CDCl}_3$ ): 1.23 (3H, s, 14- $\text{CH}_3$ ), 1.42 (3H, s, 15- $\text{CH}_3$ ), 1.86 (3H, s, 12 or 13- $\text{CH}_3$ ), 2.03 (3H, s, 13 or 12- $\text{CH}_3$ ), 2.42 (H, d,  $J=16.0$  Hz, 9 $\beta$ -H), 3.21 (H, d,  $J=16.0$  Hz, 9 $\alpha$ -H).  $^{13}\text{C-NMR}$  data are shown in Table I.

Methylzedoarandiol (9): Colorless needles, mp  $83\text{--}85^\circ\text{C}$  (hexane). IR  $\nu_{\text{max}}^{\text{KBr}} \text{cm}^{-1}$ : 3330, 3300, 1676, 1652, 1579, 1300.  $[\alpha]_{\text{D}}^{23} -43.1^\circ$  ( $c=0.2$ , MeOH). CD ( $c=0.007$ , MeOH):  $[\theta]_{322} -6742$ . Anal. Calcd for  $\text{C}_{16}\text{H}_{26}\text{O}_3$ : C, 72.14; H, 9.84. Found: C, 72.29; H, 9.89.  $^1\text{H-NMR}$  ( $\text{CDCl}_3$ ): 1.12 (3H, s, 14 or 15- $\text{CH}_3$ ), 1.20 (3H, s, 15 or 14- $\text{CH}_3$ ), 1.84 (3H, s, 12 or 13- $\text{CH}_3$ ), 1.95 (3H, s, 13 or 12- $\text{CH}_3$ ), 3.20 (3H, s, OMe).  $^{13}\text{C-NMR}$  data are shown in Table I.

Neocardione (10): Colorless needles. mp  $45\text{--}47^\circ\text{C}$  (hexane). MS  $m/z$ : 236.1763 ( $\text{M}^+$ ) (Calcd for  $\text{C}_{15}\text{H}_{24}\text{O}_2$  236.1777). IR  $\nu_{\text{max}}^{\text{KBr}} \text{cm}^{-1}$ : 1696, 1682, 1395, 1282. UV  $\lambda_{\text{max}}^{\text{MeOH}} \text{nm}$  (log  $\epsilon$ ): 203 (3.73).  $[\alpha]_{\text{D}}^{23} -190.6^\circ$  ( $c=2.1$ ,  $\text{CHCl}_3$ ). CD ( $c=0.022$ , MeOH):  $[\theta]_{301} -29230$ .  $^1\text{H-NMR}$  ( $\text{CDCl}_3$ ): 0.92 (3H, d,  $J=6.6$  Hz, 14- $\text{CH}_3$ ), 0.98 (3H, d,  $J=6.8$  Hz, 12 or 13- $\text{CH}_3$ ), 1.03 (3H, d,  $J=6.8$  Hz, 13 or 12- $\text{CH}_3$ ), 1.67 (3H, s, 15- $\text{CH}_3$ ), 5.18 (1H, br t,  $J=7.0$  Hz).  $^{13}\text{C-NMR}$  data are shown in Table I.

**Transformation from 3 to 10**—One drop of conc.  $\text{H}_2\text{SO}_4$  was added to 280 mg of 3 in MeOH (4 ml). The reaction solution was stirred for 1 h at room temperature. The reaction solution was poured into ice-water and extracted with  $\text{CHCl}_3$ . The  $\text{CHCl}_3$  solution was dried and evaporated. The reaction products were purified by PLC to give 9 (80 mg), which was identical with the natural compound in terms of spectra.

**Transformation from 3 to 6 and 8**—One drop of conc.  $\text{H}_2\text{SO}_4$  was added to 234 mg of 3 in dioxane (2 ml) and water (2 ml). The solution was stirred for 4 h at room temperature. The reaction solution was poured into ice-water and extracted with  $\text{CHCl}_3$ . The  $\text{CHCl}_3$  solution was dried and evaporated. The reaction products were purified with PTLC to give 6 (19 mg) and 8 (15 mg). The synthetic 6 and 8 were identical with the natural compounds in terms of TLC behavior,  $^1\text{H-NMR}$  signals and optical rotation.

**Acknowledgements** We wish to thank Dr. A. Ogiso, Sankyo Co., Ltd., and Dr. K. Yoshihira, National Institute of Hygienic Sciences, for their valuable suggestions, and Prof. S. Inayama, Pharmaceutical Institute, School of Medicine, Keio University, for the identification of curdione and valuable discussions. We also thank Dr. M. Uchida and Mrs. H. Kitamura of the Analysis Center of this College for mass spectral measurement and elemental analysis.

## References

- 1) R. Hegnauer "Chemotaxonomie der Pflanzen," Band II, Birkhauser Verlag Basel und Stuttgart, 1963, p. 451.
- 2) M. Kuroyanagi, K. Ujiie, S. Fukushima and K. Nishi, Abstracts of Papers, 31st Annual Meeting of the Japanese Society of Pharmacognosy, Tokyo, 1984, p. 55; M. Kuroyanagi, K. Ujiie, A. Ueno, S. Fukushima and K. Nishi, Symposium Papers, 29th Symposium on the Chemistry of Terpenes, Essential Oils and Aromatics, Mie, 1985, p. 268.
- 3) F. Bohlmann and C. Zdero, *Chem. Ber.*, **106**, 3614 (1973).
- 4) M. Yoshihara, H. Shibuya, E. Kitano, K. Yanagi and I. Kitagawa, *Chem. Pharm. Bull.*, **32**, 2059 (1984).
- 5) H. Hikino, C. Konno and T. Takemoto, *Chem. Pharm. Bull.*, **20**, 987 (1972).
- 6) H. Hikino, Y. Sakurai and T. Takemoto, *Chem. Pharm. Bull.*, **16**, 1605 (1968); M. Yoshihara, C. Yong, C. Zheng, H. Shibuya, Y. Hamamoto, N. Tanaka and I. Kitagawa, *Chem. Pharm. Bull.*, **34**, 434 (1986).
- 7) S. Inayama, J.-F. Gao, K. Harimaya, Y. Itaka, Y.-T. Guo and T. Kawamata, *Chem. Pharm. Bull.*, **33**, 1323 (1985).
- 8) E. Bunnenberg, C. Djerassi, K. Mislow and A. Moskowitz, *J. Am. Chem. Soc.*, **84**, 2823 (1962).
- 9) Y. Shiobara, Y. Asakawa, M. Kodama, K. Yasuda and T. Takemoto, *Phytochemistry*, **24**, 2629 (1985).
- 10) J. Endo and H. Itokawa, Symposium Papers, 21st Symposium on the Chemistry of Natural Products, Sapporo, 1978, p. 401.
- 11) H. Minato and I. Horibe, *J. Chem. Soc. C*, **1968**, 2131.

- 
- 12) P. Main, L. Lessinger, M. M. Woolfson, G. Germain and T. P. Declercq, 1974. MULTAN 74. A System of Computer Programs for the Automatic Solution of Crystal Structures from X-Ray Diffraction Data, Universities of York, England, and Louvain, Belgium.
  - 13) J. B. Hendrickson, *J. Am. Chem. Soc.*, **89**, 7036 (1967).
  - 14) G. Sratzke, *Tetrahedron*, **21**, 413, 421, 439 (1965).
  - 15) I. Kouno and N. Kawano, *Phytochemistry*, **24**, 1845 (1985).

[Chem. Pharm. Bull.]  
35(1) 60-71 (1987)

## Synthesis of a 37-Residue Peptide Amide Corresponding to the Entire Amino Acid Sequence of $\alpha$ -Form of Rat Calcitonin Gene-Related Peptide ( $\alpha$ -rCGRP)<sup>1)</sup>

KENSHI ANDO,<sup>a</sup> KOUKI KITAGAWA,<sup>\*a</sup> SHINYA KIYAMA,<sup>a</sup> TATSUHIKO KAWAMOTO,<sup>a</sup>  
TADASHI AKITA,<sup>a</sup> ITSUO YAMAMOTO,<sup>b</sup>  
and KANJI TORIZUKA<sup>b</sup>

*Faculty of Pharmaceutical Sciences, Tokushima University,<sup>a</sup> Sho-machi, Tokushima 770,  
Japan and Faculty of Medicine, Kyoto University,<sup>b</sup>  
Sakyo-ku, Kyoto 606, Japan*

(Received June 5, 1986)

The heptatriacontapeptide amide corresponding to the entire amino acid sequence of  $\alpha$ -form of rat calcitonin gene-related peptide ( $\alpha$ -rCGRP) was synthesized by the conventional solution method. All protecting groups employed were removed by treatment with 1 M trifluoromethanesulfonic acid-thioanisole-trifluoroacetic acid, and the deprotected peptide was subjected to air-oxidation to form the intramolecular disulfide bond. After purification by gel-filtration on Sephadex G-50, followed by reversed-phase high performance liquid chromatography, a highly purified sample of synthetic  $\alpha$ -rCGRP was obtained. In terms of suppression of bone <sup>45</sup>Ca-release stimulated by synthetic human parathyroid hormone (1-34), synthetic  $\alpha$ -rCGRP was as active as synthetic human CGRP.

**Keywords**—rat calcitonin gene-related peptide synthesis; aminosuccinimide formation;  $\beta$ -cycloheptylaspartate; thioanisole-mediated acidolysis; trifluoromethanesulfonic acid deprotection; intramolecular disulfide bond formation; <sup>45</sup>Ca-release suppression

The existence of a novel peptide, referred to as calcitonin gene-related peptide (CGRP), was predicted on the basis of structural analysis of the rat calcitonin gene by Rosenfeld *et al.*<sup>2)</sup> Subsequently, human CGRP (hCGRP)<sup>3)</sup> and porcine CGRP<sup>4)</sup> were isolated from human medullary thyroid carcinoma and porcine spinal cord, respectively. It has become evident that the calcitonin gene generates at least two messenger ribonucleic acids (mRNAs), one encoding the precursor of calcitonin in thyroid C-cells and the second encoding the precursor of a novel structurally related neuropeptide, CGRP, which predominates in the brain. In 1984, Rosenfeld *et al.*,<sup>5)</sup> detected the presence of yet another CGRP, referred to as  $\beta$ -CGRP in the rat, and thus raised the possibility that a single neuropeptide gene generates multiple RNA products. This  $\beta$ -form of rat CGRP ( $\beta$ -rCGRP) differs in sequence from  $\alpha$ -rCGRP by an internal amino acid residue at position 35 (Lys instead of Glu), as shown in Fig. 1.

Following the synthesis of hCGRP,<sup>6)</sup> which was conducted in collaboration with Fujii *et al.*, we wish to report the solution synthesis of a 37-residue peptide corresponding to the entire amino acid sequence of  $\alpha$ -rCGRP, the sequence of which was first deduced from the rat gene by Rosenfeld *et al.*, in 1983.<sup>2d)</sup>

The TFA-labile Z(OMe) or Boc group was employed for  $N^{\alpha}$ -protection, and amino acid derivatives bearing protecting groups removable by 1 M TFMSA-thioanisole in TFA<sup>7)</sup> were employed, *i.e.*, Asp(OChp),<sup>8)</sup> Glu(OBzl), Ser(Bzl), Lys(Z), Arg(Mts),<sup>9)</sup> and Cys(MBzl). Structurally different from hCGRP, rCGRP contains the Asp-Asn linkage at position 25-26, which is known to be particularly susceptible to base-catalyzed succinimide formation.<sup>10)</sup> Thus, Asp(OChp), which is known to suppress this side reaction, was employed. In the



H- 1 -Cys- 3 -Thr-Ala-Thr-Cys-Val-Thr-His-Arg-Leu-Ala-  
 Gly-Leu-Leu-Ser-Arg-Ser-Gly-Gly-Val-Val-Lys- 25 -Asn-  
 Phe-Val-Pro-Thr-Asn-Val-Gly-Ser- 35 -Ala-Phe-NH<sub>2</sub>

	1	3	25	35
rat $\alpha$	Ser	Asn	Asp	Glu
rat $\beta$	Ser	Asn	Asp	Lys
human	Ala	Asp	Asn	Lys

Fig. 1. Amino Acid Sequences of Rat and Human CGRPs

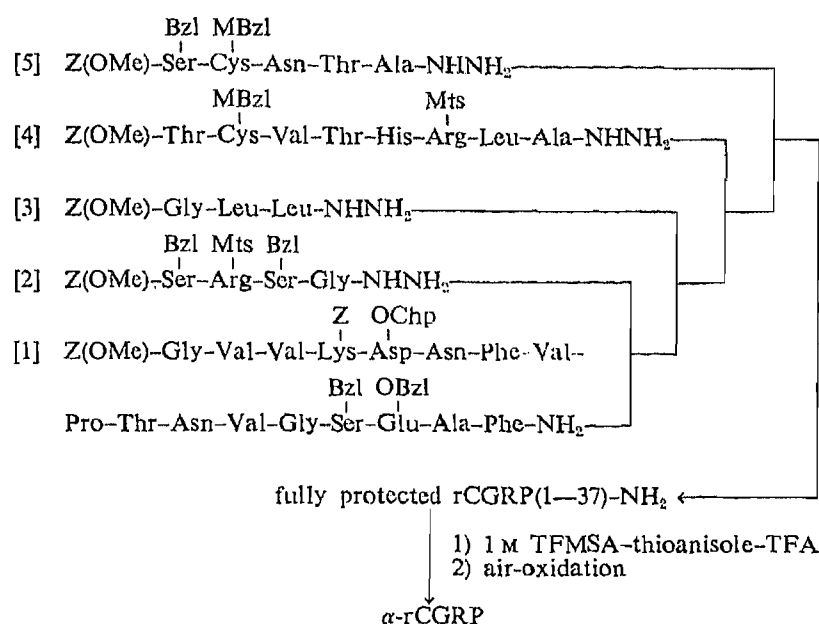


Fig. 2. Synthetic Route to Rat  $\alpha$ -CGRP

hCGRP synthesis, the S-adamantyl group<sup>11)</sup> was employed for the protection of the sulfhydryl function of Cys. However, in the present synthesis, a readily available derivative, Cys(MBzl),<sup>12)</sup> was employed.

In order to construct the entire peptide backbone of  $\alpha$ -rCGRP, five fragments were prepared as building blocks, as shown in Fig. 2. Of these, fragments [2] and [3] are identical with those employed for the synthesis of hCGRP.<sup>6)</sup> Fragments [1], [4] and [5], which cover the areas of species variation between these CGRPs (positions 1, 3, 25, and 35 in Fig. 1), were newly synthesized.

Fragment [1] was prepared according to the scheme shown in Fig. 3. First, the C-terminal dodecapeptide amide was prepared by the azide condensation<sup>13)</sup> of two subunits, the hepta- and pentapeptide units. The former heptapeptide amide, Boc-Asn-Val-Gly-Ser(Bzl)-Glu(OBzl)-Ala-Phe-NH<sub>2</sub>, was prepared in a stepwise manner starting with H-Phe-NH<sub>2</sub>.<sup>14)</sup> The active ester procedure, such as Su<sup>15)</sup> or Np<sup>16)</sup> procedure, was employed for elongation of the peptide chain. To prepare the latter peptide unit, Boc-Phe-Val-Pro-Thr-OMe was first synthesized by the DCC + HOBT<sup>17)</sup> condensation of the known tripeptide, Boc-Phe-Val-Pro-OH<sup>18)</sup> and H-Thr-OMe. After the usual TFA treatment, Boc-Asn-OH was introduced by the Np method to afford Boc-Asn-Phe-Val-Pro-Thr-OMe, which was converted to the corresponding hydrazide by the usual hydrazinolysis. The dodecapeptide amide thus constructed was further elongated to [1] in a stepwise manner by the active ester procedure.

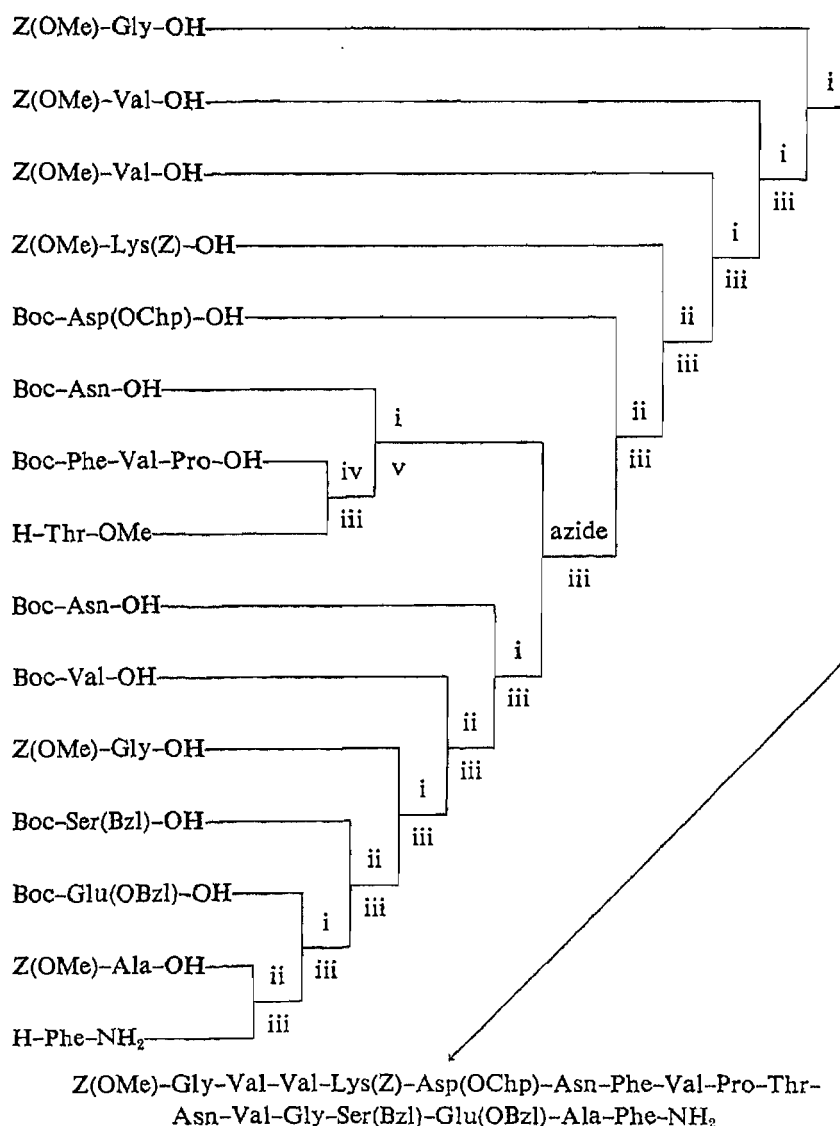


Fig. 3. Synthetic Scheme for the Protected Heptapeptide Amide; Fragment [1]  
 i, Np; ii, Su; iii, TFA; iv, DCC+HOBt; v,  $\text{NH}_2\text{NH}_2$ .

Preliminarily, after introduction of the Asp(OChp) residue, we tried the azide condensation of  $\text{Z(OMe)-Gly-Val-Val-Lys(Z)-NHNH}_2$ , a fragment used in the hCGRP synthesis,<sup>6)</sup> with this tridecapeptide amide. However, despite the use of the acyl component in excess (10 to 15 eq) and a long reaction time (7 d), amino acid analysis of the product showed an insufficient incorporation of the acyl component (*ca.* 65%). The bulkiness of the Chp group at the N-terminal residue of the amino component may account for this unsatisfactory azide reaction. On the other hand, the satisfactory incorporation of  $\text{Z(OMe)-Lys(Z)-OH}$  into the tridecapeptide amide by the Su method was ascertained by thin layer chromatography (TLC) and amino acid analysis. Each product was purified by reprecipitation from DMSO-DMF with MeOH and its homogeneity was confirmed by TLC, elemental analysis, and amino acid analysis. In the latter instance, after the incorporation of the bulky Val-Val sequence (positions 22-23), the recovery of Val on amino acid analysis became slightly low, due to the resistance to acid hydrolysis.

Fragment [4] was synthesized according to the scheme shown in Fig. 4. In the hCGRP synthesis, to construct the peptide backbone corresponding to positions 6 to 13, two

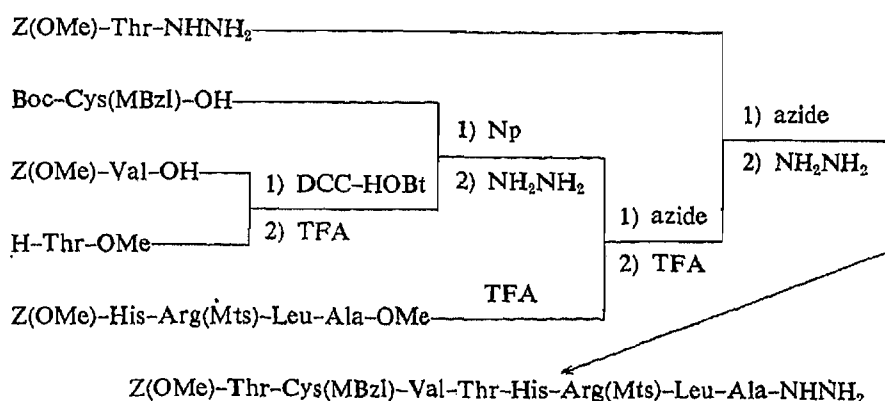


Fig. 4. Synthetic Scheme for the Protected Octapeptide Hydrazide; Fragment [4]

fragments, (6—9) and (10—13), were employed.<sup>6)</sup> Considering the good solubility of  $Z(\text{OMe})\text{-His-Arg}(\text{Mts})\text{-Leu-Ala-OMe}$ ,<sup>6)</sup> we decided to elongate this peptide chain and establish the peptide backbone by condensation of one fragment, [4].  $Z(\text{OMe})\text{-Cys}(\text{MBzl})\text{-Val-Thr-OMe}$ , prepared by DCC+HOBt condensation followed by the Np method, was converted to the corresponding hydrazide and the resulting hydrazide was next condensed with a TFA-treated sample of  $Z(\text{OMe})\text{-His-Arg}(\text{Mts})\text{-Leu-Ala-OMe}$ <sup>6)</sup> by the azide method to afford  $\text{Boc-Cys}(\text{MBzl})\text{-Val-Thr-His-Arg}(\text{Mts})\text{-Leu-Ala-OMe}$ . Subsequent introduction of  $Z(\text{OMe})\text{-Thr-NHNH}_2$ , *via* the azide, afforded  $Z(\text{OMe})\text{-Thr-Cys}(\text{MBzl})\text{-Val-Thr-His-Arg}(\text{Mts})\text{-Leu-Ala-OMe}$ , which was smoothly converted to [4] by the usual hydrazine treatment. In the previous hCGRP synthesis, the azide condensation of  $Z(\text{OMe})\text{-Thr-Cys}(\text{Ad})\text{-Val-Thr-NHNH}_2$  with the relatively large amino component (positions 10—37) was performed at lower temperature ( $-15^\circ\text{C}$ ) than usual ( $-4^\circ\text{C}$ ) in order to minimize the Curtius rearrangement.<sup>19)</sup> In this fragment synthesis, the condensation between Thr (position 9) and His (position 10) could be performed as usual without particular attention. The employment of the altered fragment, namely that corresponding to positions 6 to 13 of the peptide backbone, was effective to avoid the problem of the Curtius rearrangement at the larger peptide level.

The synthetic scheme for fragment [5] is shown in Fig. 5.  $Z(\text{OMe})\text{-Ser}(\text{Bzl})\text{-Cys}(\text{MBzl})\text{-Asn-Thr-OMe}$ , prepared in a stepwise manner by the Np or the Su active ester procedures, was converted to the corresponding hydrazide. The azide condensation of the resulting hydrazide with  $\text{H-Ala-OMe}$  afforded  $Z(\text{OMe})\text{-Ser}(\text{Bzl})\text{-Cys}(\text{MBzl})\text{-Asn-Thr-Ala-OMe}$ , which was converted to the corresponding hydrazide [5] as usual.

The five fragments thus obtained, [1] to [5], were successively assembled by the azide procedure according to the scheme shown in Fig. 2. Each condensation was performed in a mixture of HMPA-DMF (5:1) at  $-4^\circ\text{C}$  and the amount of acyl component was increased from 6 to 10 eq as the peptide chain was elongated in order to ensure completion of the coupling reaction. Each product was purified by precipitation from HMPA-DMF (5:1) with MeOH and its homogeneity was confirmed by amino acid analysis after 6 N HCl hydrolysis, in which Phe was selected as a diagnostic amino acid. By comparison of the recovery of Phe with those of newly incorporated amino acids, satisfactory incorporation of each fragment was ascertained in each condensation step. The results of amino acid analyses are listed in Table I.

In the final step, the fully protected  $\alpha$ -rCGRP was treated with 1 M TFMSA-thioanisole in TFA in the presence of *m*-cresol<sup>20)</sup> ( $0^\circ\text{C}$ , 4 h) to remove all protecting groups. The deprotected peptide was reduced with 2-mercaptoethanol in Tris-HCl buffer containing 6 M guanidine-HCl (pH 8.0) and applied to a column of Sephadex G-25. The main fraction was submitted to air-oxidation to form the intramolecular disulfide bond as follows: a diluted

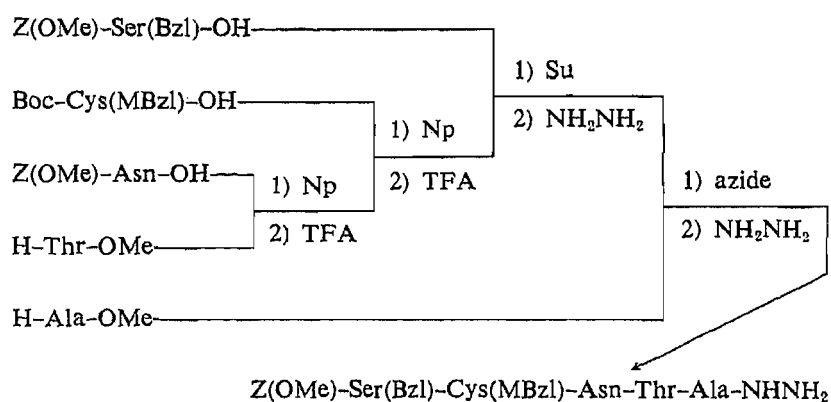


Fig. 5. Synthetic Scheme for the Protected Pentapeptide Hydrazide; Fragment [5]

TABLE I. Amino Acid Ratios in 6N HCl Hydrolysates of Synthetic  $\alpha$ -rCGRP and Its Intermediates

Amino acid	Protected peptides					Synthetic $\alpha$ -rCGRP
	20--37	17--37	14--37	6--37	1--37	
Asp	2.73 (3)	2.93 (3)	3.00 (3)	3.00 (3)	4.09 (4)	4.02 (4)
Thr	0.77 (1)	0.94 (1)	0.87 (1)	2.76 (3)	3.82 (4)	3.85 (4)
Ser	0.73 (1)	2.23 (3)	2.19 (3)	2.68 (3)	3.56 (4)	3.89 (4)
Glu	1.06 (1)	1.05 (1)	1.04 (1)	1.06 (1)	1.22 (1)	1.18 (1)
Pro	1.00 (1)	0.97 (1)	0.92 (1)	0.90 (1)	1.05 (1)	1.08 (1)
Gly	1.89 (2)	2.61 (3)	3.59 (4)	4.00 (4)	4.22 (4)	4.37 (4)
Ala	1.00 (1)	1.04 (1)	1.03 (1)	2.25 (2)	3.40 (3)	3.23 (3)
Cys					N.D.	0.75 (1)
Val	3.34 (4)	3.32 (4)	3.63 (4)	4.64 (5)	4.74 (5)	4.48 (5)
Leu			1.76 (2)	3.32 (3)	3.44 (3)	3.17 (3)
Phe	2.00 (2)	2.00 (2)	2.00 (2)	2.00 (2)	2.00 (2)	2.00 (2)
Lys	0.88 (1)	0.95 (1)	0.87 (1)	0.95 (1)	1.00 (1)	1.07 (1)
His				1.20 (1)	1.18 (1)	1.05 (1)
Arg		0.87 (1)	0.90 (1)	2.33 (2)	2.09 (2)	2.05 (2)
Recovery (%)	88	83	83	85	82	90

solution of the desired eluate (1 l) in 5% AcONH<sub>4</sub> (pH 7.5) was kept standing at room temperature for 4 d, while the progress of air-oxidation was monitored by the use of Ellman's reagent.<sup>21)</sup> The oxidized product, after removal of the solvent by lyophilization, was purified by gel-filtration on Sephadex G-50, followed by reversed-phase high performance liquid chromatography (HPLC) on a Nucleosil 7C<sub>18</sub> column using gradient elution with CH<sub>3</sub>CN (30% to 40% for 50 min) in 0.2% TFA (Fig. 7-a). The purity of the product thus obtained was confirmed by analytical HPLC (Fig. 7-b), TLC in three different solvent systems, amino acid analyses after acid hydrolysis (Table I) and enzymic hydrolysis (papain + LAP). The excellent recoveries of Asp (1.02) and Asn (3.03) in enzymic hydrolysate confirm the absence of the contaminant derived from ring closure at the Asp<sup>25</sup>-Asn<sup>26</sup> linkage. In addition, our synthetic  $\alpha$ -rCGRP was confirmed to be monomeric by HPLC using a TSKgel G 2000SW column (Fig. 8).

Synthetic  $\alpha$ -rCGRP ( $1 \times 10^{-7}$  M) suppressed the <sup>45</sup>Ca-release from bone stimulated by a synthetic sample of human parathyroid hormone (1-34),<sup>22)</sup> purchased from Toyo Jozo Co. Its potency was estimated to be at the same level as that of synthetic hCGRP.

### Experimental

General experimental procedures employed in this study were as follows.

**N<sup>α</sup>-Deprotection**—The N<sup>α</sup>-protecting group, Z(OMe) or Boc, was removed with TFA (ca. 2–3 ml per 1 g of the protected peptide) in the presence of anisole (2 mol eq or more) under ice-cooling for 60 min. After evaporation of TFA *in vacuo* at 30 °C or less, the residue was treated with dry ether. If a powder was obtained, it was collected by filtration, dried over KOH pellets *in vacuo* and used for the next coupling reaction. If an oily precipitate was obtained, it was washed with *n*-hexane, dried over KOH pellets *in vacuo* and used for the coupling reaction.

**Coupling Reactions**—The DCC and the active ester couplings were carried out at room temperature. The azide coupling was carried out according to the method of Honzl and Rudinger<sup>14)</sup> using isoamyl nitrite with stirring in a cold room (–4 °C). Mixed anhydrides were prepared using ethyl chloroformate.

**Purification**—Unless otherwise mentioned, products were purified by one of the following procedures. Procedure A; for the purification of protected peptide esters soluble in AcOEt, the extract was washed with 5% citric acid, 5% Na<sub>2</sub>CO<sub>3</sub> and H<sub>2</sub>O–NaCl, dried over Na<sub>2</sub>SO<sub>4</sub> and concentrated. The residue was crystallized or precipitated from appropriate solvents. Procedure B; for the purification of protected peptides less soluble in AcOEt, the crude product was washed with 5% citric acid, 5% NaHCO<sub>3</sub> and H<sub>2</sub>O, then crystallized or precipitated from appropriate solvents.

The melting points are uncorrected. Optical rotations were determined with a Union PM-201 polarimeter. Acid hydrolyses were carried out in 6N HCl in a sealed tube, and amino acid analyses were performed on an IRICA model A-3300 amino acid analyzer. LAP (Lot. 15F-0402) and papain (Lot. 102F-8160) were purchased from Sigma Chemical Co.

TLC was carried out on silica gel (precoated Silica gel 60 F<sub>254</sub>, Merck) or cellulose (precoated Cellulose F, Merck). Solvent systems used were as follows; *R*<sub>f1</sub> = CHCl<sub>3</sub>–MeOH–H<sub>2</sub>O (8 : 3 : 1), *R*<sub>f2</sub> = *n*-BuOH–AcOH–pyridine–H<sub>2</sub>O (4 : 1 : 1 : 2), *R*<sub>f3</sub> = *n*-BuOH–AcOH–pyridine–H<sub>2</sub>O (30 : 20 : 6 : 24), and *R*<sub>f4</sub> = *n*-BuOH–AcOH–pyridine–H<sub>2</sub>O (30 : 6 : 20 : 24).

HPLC was conducted with a Shimadzu LC 4A instrument equipped with a Chemopak column (Nucleosil 7C<sub>18</sub>, 4.8 × 250 mm).

**Z(OMe)–Ala–Phe–NH<sub>2</sub>**—A TFA-treated sample of Z(OMe)–Phe–NH<sub>2</sub> (6.60 g, 20 mmol) was dissolved in DMF (100 ml), together with Et<sub>3</sub>N (5.60 ml, 40 mmol) and Z(OMe)–Ala–OSu (7.70 g, 22 mmol). The mixture was stirred for 24 h, and DMF was removed by evaporation. The residue was triturated with MeOH and the resulting solid was purified by procedure B, followed by recrystallization from MeOH with ether. Yield 6.70 g (84%), mp 220–222 °C, [α]<sub>D</sub><sup>25</sup> –20.2° (*c* = 1.0, DMF), *R*<sub>f1</sub> 0.60. *Anal.* Calcd for C<sub>21</sub>H<sub>25</sub>N<sub>3</sub>O<sub>5</sub>: C, 63.14; H, 6.31; N, 10.52. Found: C, 62.79; H, 6.28; N, 10.47.

**Boc–Glu(OBzl)–Ala–Phe–NH<sub>2</sub>**—A TFA-treated sample of Z(OMe)–Ala–Phe–NH<sub>2</sub> (8.00 g, 20 mmol) was dissolved in DMF (100 ml), together with Et<sub>3</sub>N (6.20 ml, 44 mmol) and Boc–Glu(OBzl)–ONp (11.0 g, 24 mmol). The mixture was stirred for 48 h, and DMF was removed by evaporation. Addition of MeOH to the residue afforded a powder, which was purified by procedure B, followed by reprecipitation from DMF with ether. Yield 10.0 g (90%), mp 174–177 °C, [α]<sub>D</sub><sup>25</sup> –30.0° (*c* = 1.0, MeOH), *R*<sub>f1</sub> 0.58. *Anal.* Calcd for C<sub>29</sub>H<sub>38</sub>N<sub>4</sub>O<sub>7</sub>: C, 62.80; H, 6.91; N, 10.10. Found: C, 62.70; H, 6.97; N, 10.28.

**Boc–Ser(Bzl)–Glu(OBzl)–Ala–Phe–NH<sub>2</sub>**—A TFA-treated sample of Boc–Glu(OBzl)–Ala–Phe–NH<sub>2</sub> (8.90 g, 16 mmol) was dissolved in DMF (100 ml), together with Et<sub>3</sub>N (5.00 ml, 35.2 mmol) and Boc–Ser(Bzl)–OSu (7.53 g, 19.2 mmol). The mixture was stirred for 24 h, and DMF was removed by evaporation. The residue was triturated with ether and the resulting solid was purified by procedure B, followed by reprecipitation from DMF with ether. Yield 11.12 g (95%), mp 199–201 °C, [α]<sub>D</sub><sup>25</sup> –14.0° (*c* = 1.0, MeOH), *R*<sub>f1</sub> 0.74. *Anal.* Calcd for C<sub>39</sub>H<sub>49</sub>N<sub>5</sub>O<sub>9</sub>: C, 64.00; H, 6.75; N, 9.57. Found: C, 63.77; H, 6.65; N, 9.40.

**Z(OMe)–Gly–Ser(Bzl)–Glu(OBzl)–Ala–Phe–NH<sub>2</sub>**—A TFA-treated sample of Boc–Ser(Bzl)–Glu(OBzl)–Ala–Phe–NH<sub>2</sub> (9.60 g, 13 mmol) was dissolved in DMF (200 ml), together with Et<sub>3</sub>N (4.00 ml, 28.6 mmol) and Z(OMe)–Gly–ONp (5.60 g, 15.6 mmol). The mixture was stirred for 24 h, and DMF was removed by evaporation. The residue was triturated with ether and the resulting solid was purified by procedure B, followed by reprecipitation from DMF with ether. Yield 10.42 g (94%), mp 203–206 °C, [α]<sub>D</sub><sup>25</sup> –16.1° (*c* = 1.1, DMF), *R*<sub>f1</sub> 0.67. *Anal.* Calcd for C<sub>45</sub>H<sub>52</sub>N<sub>6</sub>O<sub>11</sub> · 1/2H<sub>2</sub>O: C, 62.70; H, 6.20; N, 9.75. Found: C, 62.66; H, 6.04; N, 9.47.

**Boc–Val–Gly–Ser(Bzl)–Glu(OBzl)–Ala–Phe–NH<sub>2</sub>**—A TFA-treated sample of Z(OMe)–Gly–Ser(Bzl)–Glu(OBzl)–Ala–Phe–NH<sub>2</sub> (9.00 g, 11 mmol) was dissolved in DMF (150 ml), together with Et<sub>3</sub>N (3.40 ml, 25.3 mmol) and Boc–Val–OSu (4.30 g, 14.3 mmol). The mixture was stirred for 24 h, and DMF was removed by evaporation. The residue was triturated with ether and the resulting solid was purified by procedure B, followed by reprecipitation from DMF with ether. Yield 8.50 g (91%), mp 231–234 °C, [α]<sub>D</sub><sup>25</sup> –5.5° (*c* = 1.3, DMF), *R*<sub>f1</sub> 0.85. *Anal.* Calcd for C<sub>46</sub>H<sub>61</sub>N<sub>7</sub>O<sub>11</sub>: C, 62.21; H, 6.92; N, 10.93. Found: C, 62.06; H, 6.86; N, 11.26.

**Boc–Asn–Val–Gly–Ser(Bzl)–Glu(OBzl)–Ala–Phe–NH<sub>2</sub>**—A TFA-treated sample of Boc–Val–Gly–Ser(Bzl)–Glu(OBzl)–Ala–Phe–NH<sub>2</sub> (4.50 g, 5 mmol) was dissolved in DMF (100 ml), together with Et<sub>3</sub>N (0.70 ml, 5 mmol), Boc–Asn–ONp (2.30 g, 6.5 mmol), HOBt (0.68 g, 5 mmol), and NMM (1.27 ml, 11.5 mmol). The mixture was stirred

for 5 h, and the solution was poured into cold MeOH (500 ml). The precipitate was purified by procedure B, followed by reprecipitation from DMF with cold MeOH. Yield 4.00 g (80%), mp > 240 °C (dec.),  $[\alpha]_D^{25} - 14.0^\circ$  ( $c=0.6$ , DMF),  $R_f$  0.58. Anal. Calcd for  $C_{50}H_{67}N_9O_{13}$ : C, 59.92; H, 6.74; N, 12.58. Found: C, 59.61; H, 6.68; N, 12.21. Amino acid ratios in 6 N HCl hydrolysate: Asp 0.98, Ser 0.97, Glu 1.00, Gly 0.93, Ala 1.00, Val 0.87, Phe 1.09 (recovery of Ala; 92%).

**Boc-Phe-Val-Pro-Thr-OMe**—Boc-Phe-Val-Pro-OH<sup>(18)</sup> (3.30 g, 7.1 mmol) was dissolved in AcOEt (50 ml) and, to this ice-chilled solution, DCC (1.70 g, 8.17 mmol), HOBt (0.92 g, 7.1 mmol) and H-Thr-OMe [prepared from 1.50 g (8.52 mmol) of the hydrochloride with Et<sub>3</sub>N (1.20 ml, 8.52 mmol) in DMF (20 ml)] were added. The mixture was stirred at room temperature for 24 h, the precipitated urea derivative was removed by filtration, and the filtrate was concentrated *in vacuo*. The residue was purified by procedure A, followed by recrystallization from AcOEt with petroleum ether. Yield 3.50 g (87%), mp 96–101 °C,  $[\alpha]_D^{25} - 85.0^\circ$  ( $c=1.0$ , MeOH),  $R_f$  0.73. Anal. Calcd for  $C_{29}H_{44}N_4O_8$ : C, 60.40; H, 7.69; N, 9.72. Found: C, 60.27; H, 7.91; N, 9.64.

**Boc-Asn-Phe-Val-Pro-Thr-OMe**—A TFA-treated sample of Boc-Phe-Val-Pro-Thr-OMe (10.90 g, 17 mmol) was dissolved in DMF (100 ml), together with Et<sub>3</sub>N (2.40 ml, 17 mmol), Boc-Asn-ONp (7.20 g, 20.4 mmol), HOBt (2.20 g, 17 mmol) and NMM (4.00 ml, 37.4 mmol). The mixture was stirred for 24 h, and DMF was removed by evaporation. The product was purified by procedure A, followed by recrystallization from AcOEt with ether twice. Yield 9.70 g (83%), mp 124–134 °C,  $[\alpha]_D^{25} - 75.0^\circ$  ( $c=1.0$ , MeOH),  $R_f$  0.73. Anal. Calcd for  $C_{33}H_{50}N_6O_{10} \cdot 1/2H_2O$ : C, 56.64; H, 7.35; N, 12.01. Found: C, 56.79; H, 7.30; N, 12.00.

**Boc-Asn-Phe-Val-Pro-Thr-NHNH<sub>2</sub>**—Boc-Asn-Phe-Val-Pro-Thr-OMe (6.90 g, 10 mmol) dissolved in MeOH (100 ml) was treated with 80% hydrazine hydrate (6.20 ml, 100 ml) at room temperature for 24 h. The MeOH was evaporated off *in vacuo* and the residue was dissolved in *n*-BuOH and washed with H<sub>2</sub>O–NaCl. The solution was dried over MgSO<sub>4</sub>, and *n*-BuOH was removed by evaporation. The residue was triturated with ether and the resulting solid was recrystallized from MeOH with ether twice. Yield 4.00 g (59%), mp 198–201 °C,  $[\alpha]_D^{25} - 44.0^\circ$  ( $c=1.0$ , DMF),  $R_f$  0.60. Anal. Calcd for  $C_{32}H_{50}N_6O_9 \cdot H_2O$ : C, 54.22; H, 7.40; N, 15.81. Found: C, 54.10; H, 7.52; N, 15.89. Amino acid ratios in 6 N HCl hydrolysate: Asp 0.95, Thr 0.92, Pro 0.90, Val 0.83, Phe 1.00 (recovery of Phe; 87%).

**Boc-Asn-Phe-Val-Pro-Thr-Asn-Val-Gly-Ser(Bzl)-Glu(OBzl)-Ala-Phe-NH<sub>2</sub>**—A TFA-treated sample of Boc-Asn-Val-Gly-Ser(Bzl)-Glu(OBzl)-Ala-Phe-NH<sub>2</sub> (4.00 g, 4 mmol) was dissolved in DMF–DMSO (2:1, 50 ml) containing Et<sub>3</sub>N (0.56 ml, 4 mmol). To this ice-chilled solution, the azide [prepared from 5.60 g (8 mmol) of Boc-Asn-Phe-Val-Pro-Thr-NHNH<sub>2</sub> in DMF (50 ml)] and NMM (1.30 ml, 12 mmol) were added. The mixture was stirred at –4 °C for 48 h, then additional azide (2 mmol) and NMM (3.6 mmol) were added and the reaction mixture was further stirred at –4 °C for 48 h. DMF was removed by evaporation and the residue was poured into H<sub>2</sub>O (500 ml). The precipitate was collected and washed with hot MeOH well, then reprecipitated from DMSO with MeOH. Yield 5.20 g (83%), mp > 200 °C (dec.),  $[\alpha]_D^{25} - 13.5^\circ$  ( $c=0.5$ , DMSO),  $R_f$  0.44. Anal. Calcd for  $C_{77}H_{105}N_{15}O_{20} \cdot 2H_2O$ : C, 57.92; H, 6.88; N, 13.16. Found: C, 58.18; H, 6.99; N, 13.12. Amino acid ratios in 6 N HCl hydrolysate: Asp 1.97, Thr 0.95, Ser 0.99, Glu 1.06, Pro 1.01, Gly 1.04, Ala 1.06, Val 1.84, Phe 2.00 (recovery of Phe, 89%).

**Boc-Asp(OChp)-Asn-Phe-Val-Pro-Thr-Asn-Val-Gly-Ser(Bzl)-Glu(OBzl)-Ala-Phe-NH<sub>2</sub>**—A TFA-treated sample of the above-prepared dodecapeptide amide (4.20 g, 2.7 mmol) was dissolved in DMF–DMSO (1:1, 100 ml), together with Et<sub>3</sub>N (0.38 ml, 2.7 mmol), Boc-Asp(OChp)-OSu (1.60 g, 3.7 mmol), HOBt (0.35 g, 2.7 mmol) and NMM (0.75 ml, 6.8 mmol). The mixture was stirred for 48 h, and this solution was poured into H<sub>2</sub>O (500 ml). The precipitate was collected and washed with hot MeOH, then reprecipitated from DMSO with MeOH. Yield 4.20 g (89%), mp > 230 °C (dec.),  $[\alpha]_D^{25} - 7.8^\circ$  ( $c=0.6$ , DMSO),  $R_f$  0.53. Anal. Calcd for  $C_{88}H_{122}N_{16}O_{23} \cdot 2H_2O$ : C, 58.46; H, 7.02; N, 12.40. Found: C, 58.15; H, 7.02; N, 12.63. Amino acid ratios in 6 N HCl hydrolysate: Asp 2.75, Thr 0.92, Ser 0.98, Glu 1.07, Pro 1.03, Gly 0.98, Ala 1.04, Val 2.14, Phe 2.00 (recovery of Phe, 86%).

**Z(OMe)-Lys(Z)-Asp(OChp)-Asn-Phe-Val-Pro-Thr-Asn-Val-Gly-Ser(Bzl)-Glu(OBzl)-Ala-Phe-NH<sub>2</sub>**—A TFA-treated sample of the above-prepared tridecapeptide amide (4.20 g, 2.4 mmol) was dissolved in DMF–DMSO (1:4, 100 ml), together with Et<sub>3</sub>N (0.34 ml, 2.4 mmol), Z(OMe)-Lys(Z)-OSu (2.00 g, 3.6 mmol) and NMM (0.60 ml, 3.6 mmol). The mixture was stirred for 48 h, and the solution was poured into H<sub>2</sub>O (200 ml). The precipitate was collected and washed with hot MeOH, then reprecipitated from DMSO with MeOH. Yield 4.00 g (80%), mp > 250 °C (dec.),  $[\alpha]_D^{25} + 90.8^\circ$  ( $c=0.8$ , DMSO),  $R_f$  0.64. Anal. Calcd for  $C_{106}H_{140}N_{18}O_{27} \cdot 5H_2O$ : C, 58.17; H, 6.91; N, 11.53. Found: C, 58.09; H, 6.66; N, 11.64. Amino acid ratios in 6 N HCl hydrolysate: Asp 2.71, Thr 0.86, Ser 0.89, Glu 1.08, Pro 1.07, Gly 1.05, Ala 1.05, Val 2.00, Phe 2.00, Lys 0.89 (recovery of Phe, 90%).

**Z(OMe)-Val-Lys(Z)-Asp(OChp)-Asn-Phe-Val-Pro-Thr-Asn-Val-Gly-Ser(Bzl)-Glu(OBzl)-Ala-Phe-NH<sub>2</sub>**—A TFA-treated sample of the above-prepared tetradecapeptide amide (4.00 g, 1.9 mmol) was dissolved in DMF–DMSO (1:4, 100 ml), together with Et<sub>3</sub>N (0.80 ml, 5.7 mmol) and Z(OMe)-Val-ONp (1.60 g, 3.8 mmol). The mixture was stirred for 48 h, and the solution was poured into H<sub>2</sub>O (500 ml). The precipitate was collected and washed well with hot MeOH, then reprecipitated from DMSO with MeOH. Yield 3.20 g (79%), mp > 250 °C (dec.),  $[\alpha]_D^{25} + 112.1^\circ$  ( $c=0.6$ , DMSO),  $R_f$  0.59. Anal. Calcd for  $C_{111}H_{149}N_{19}O_{28} \cdot 3H_2O$ : C, 59.21; H, 6.94; N, 11.82. Found: C, 58.80; H, 6.63; N, 11.95. Amino acid ratios in 6 N HCl hydrolysate: Asp 2.92, Thr 1.01, Ser 1.01, Glu 1.07, Pro 1.09, Gly 0.98, Ala 1.09, Val 2.85, Phe 2.00, Lys 0.91 (recovery of Phe, 87%).

**Z(OMe)-Val-Val-Lys(Z)-Asp(OChp)-Asn-Phe-Val-Pro-Thr-Asn-Val-Gly-Ser(Bzl)-Glu(OBzl)-Ala-Phe-**

**NH<sub>2</sub>**—A TFA-treated sample of the above-prepared pentadecapeptide amide (3.20 g, 1.5 mmol) was dissolved in DMF–DMSO (1:4, 100 ml), together with Et<sub>3</sub>N (0.63 ml, 4.5 mmol) and Z(OMe)–Val–ONp (1.20 g, 3.0 mmol). The mixture was stirred for 48 h, and the solution was poured into H<sub>2</sub>O (500 ml). The precipitate was collected and washed well with hot MeOH, then reprecipitated from DMSO with MeOH. Yield 2.70 g (80%), mp >250 °C (dec.),  $[\alpha]_D^{25} + 71.4^\circ$  ( $c=0.2$ , DMSO),  $R_f$  0.80. *Anal.* Calcd for C<sub>116</sub>H<sub>158</sub>N<sub>20</sub>O<sub>29</sub>·3 1/2H<sub>2</sub>O: C, 59.04; H, 7.05; N, 11.87. Found: C, 59.09; H, 6.93; N, 12.05. Amino acid ratios in 6 N HCl hydrolysate: Asp 2.80, Thr 0.92, Ser 0.83, Glu 1.00, Pro 1.17, Gly 1.00, Ala 0.94, Val 3.40, Phe 2.00, Lys 0.76 (recovery of Phe, 86%).

**Z(OMe)–Gly–Val–Val–Lys(Z)–Asp(OChp)–Asn–Phe–Val–Pro–Thr–Asn–Val–Gly–Ser(Bzl)–Glu(OBzl)–Ala–Phe–NH<sub>2</sub>; [1]**—A TFA-treated sample of the above-prepared hexadecapeptide amide (2.70 g, 1.2 mmol) was dissolved in DMF–DMSO (1:4, 100 ml), together with Et<sub>3</sub>N (0.67 ml, 4.8 mmol) and Z(OMe)–Gly–ONp (1.30 g, 3.6 mmol). The mixture was stirred for 48 h, and the solution was poured into MeOH (500 ml). The precipitate was collected and washed well with hot MeOH, then reprecipitated from DMSO with MeOH. Yield 2.20 g (78%), mp >250 °C (dec.),  $[\alpha]_D^{25} + 60.1^\circ$  ( $c=0.3$ , DMSO),  $R_f$  0.60. *Anal.* Calcd for C<sub>118</sub>H<sub>161</sub>N<sub>21</sub>O<sub>30</sub>·3H<sub>2</sub>O: C, 58.86; H, 6.94; N, 12.22. Found: C, 58.73; H, 6.96; N, 12.26.

**Boc–Cys(MBzl)–Val–Thr–OMe**—A TFA-treated sample of Z(OMe)–Val–Thr–OMe<sup>6)</sup> (4.80 g, 12 mmol) was dissolved in DMF (30 ml), together with Et<sub>3</sub>N (3.36 ml, 24 mmol) and Boc–Cys(MBzl)–ONp (5.36 g, 12 mmol). The mixture was stirred for 24 h, and DMF was removed by evaporation. The product was purified by procedure A, followed by recrystallization from AcOEt with petroleum ether. Yield 5.75 g (86%), mp 130–132 °C,  $[\alpha]_D^{25} - 8.2^\circ$  ( $c=0.9$ , DMF),  $R_f$  0.69. *Anal.* Calcd for C<sub>26</sub>H<sub>41</sub>N<sub>3</sub>O<sub>8</sub>S: C, 56.19; H, 7.43; N, 7.56. Found: C, 56.24; H, 7.54; N, 7.55.

**Boc–Cys(MBzl)–Val–Thr–NHNH<sub>2</sub>**—Boc–Cys(MBzl)–Val–Thr–OMe (9.50 g, 17 mmol) dissolved in MeOH (150 ml) was treated with 80% hydrazine hydrate (10.0 ml, 170 mmol) at room temperature for 72 h. The precipitate was collected and washed well with cold MeOH. Yield 8.50 g (89%), mp 205–207 °C,  $[\alpha]_D^{25} - 2.0^\circ$  ( $c=1.0$ , DMSO),  $R_f$  0.68. *Anal.* Calcd for C<sub>25</sub>H<sub>41</sub>N<sub>5</sub>O<sub>7</sub>S·1/2H<sub>2</sub>O: C, 53.17; H, 7.50; N, 12.40. Found: C, 53.55; H, 7.46; N, 12.35.

**Boc–Cys(MBzl)–Val–Thr–His–Arg(Mts)–Leu–Ala–OMe**—A TFA-treated sample of Z(OMe)–His–Arg(Mts)–Leu–Ala–OMe<sup>6)</sup> (4.30 g, 5 mmol) was dissolved in DMF (50 ml) containing Et<sub>3</sub>N (0.70 ml, 5 mmol). To this ice-chilled solution, the azide [prepared from 2.50 g (5 mmol) of Boc–Cys(MBzl)–Val–Thr–NHNH<sub>2</sub> in DMF (30 ml)] and Et<sub>3</sub>N (0.70 ml, 5.0 mmol) were added. The mixture was stirred at –4 °C for 48 h, and DMF was removed by evaporation. The residue was dissolved in *n*-BuOH and washed with 10% citric acid, 5% NaHCO<sub>3</sub> and H<sub>2</sub>O–NaCl. The solution was dried over MgSO<sub>4</sub>, and *n*-BuOH was removed by evaporation. The residue was triturated with ether and the resulting solid was recrystallized from MeOH with ether twice. Yield 3.80 g (49%), mp 195–199 °C,  $[\alpha]_D^{25} - 6.9^\circ$  ( $c=1.0$ , DMSO),  $R_f$  0.68. *Anal.* Calcd for C<sub>56</sub>H<sub>86</sub>N<sub>12</sub>O<sub>16</sub>S<sub>2</sub>·H<sub>2</sub>O: C, 54.53; H, 7.13; N, 13.63. Found: C, 54.44; H, 7.30; N, 12.98.

**Z(OMe)–Thr–Cys(MBzl)–Val–Thr–His–Arg(Mts)–Leu–Ala–OMe**—A TFA-treated sample of Boc–Cys(MBzl)–Val–Thr–His–Arg(Mts)–Leu–Ala–OMe (7.00 g, 5.8 mmol) was dissolved in DMF (50 ml) containing Et<sub>3</sub>N (0.81 ml, 5.8 mmol). To this ice-chilled solution, the azide [prepared from 2.10 g (14 mmol) of Z(OMe)–Thr–NHNH<sub>2</sub> in DMF (30 ml)] and Et<sub>3</sub>N (2.00 ml, 14 mmol) were added. The mixture was stirred at –4 °C for 48 h, and DMF was removed by evaporation. The residue was triturated with ether and the resulting solid was purified by procedure B, followed by reprecipitation from DMF with ether. Yield 5.00 g (71%), mp 178–180 °C,  $[\alpha]_D^{25} - 1.4^\circ$  ( $c=0.7$ , DMSO),  $R_f$  0.69. *Anal.* Calcd for C<sub>66</sub>H<sub>93</sub>N<sub>13</sub>O<sub>17</sub>S<sub>2</sub>·4H<sub>2</sub>O: C, 52.91; H, 7.00; N, 12.54. Found: C, 53.05; H, 6.79; N, 12.35.

**Z(OMe)–Thr–Cys(MBzl)–Val–Thr–His–Arg(Mts)–Leu–Ala–NHNH<sub>2</sub>; [4]**—The above-prepared methyl ester (5.00 g, 3.6 mmol) dissolved in DMF (50 ml) was treated with 80% hydrazine hydrate (2.20 ml, 35 mmol) at room temperature for 24 h. DMF was removed by evaporation and the residue was triturated with H<sub>2</sub>O. The resulting solid was collected and washed well with H<sub>2</sub>O and cold MeOH. Yield 4.50 g (90%), mp 216–218 °C,  $[\alpha]_D^{25} + 3.9^\circ$  ( $c=0.8$ , DMSO),  $R_f$  0.49. *Anal.* Calcd for C<sub>63</sub>H<sub>93</sub>N<sub>15</sub>O<sub>16</sub>S<sub>2</sub>·2 1/2H<sub>2</sub>O: C, 53.07; H, 6.92; N, 14.74. Found: C, 53.34; H, 6.83; N, 14.46. Amino acid ratios in 6 N HCl hydrolysate: Thr 1.55, Ala 1.00, Val 1.08, Leu 1.00, His 1.00, Arg 1.03 (recovery of Leu, 87%).

**Z(OMe)–Asn–Thr–OMe**—Z(OMe)–Asn–ONp (8.40 g, 20 mmol) and NMM (2.50 ml, 23.0 mmol) were added to a solution of H–Thr–OMe [prepared from 4.30 g (25 mmol) of the hydrochloride with 3.50 ml (25 mmol) of Et<sub>3</sub>N in DMF (75 ml)], and the reaction mixture was stirred for 24 h. DMF was removed by evaporation and the residue was dissolved in *n*-BuOH. The organic layer was washed with 5% citric acid, 5% NaHCO<sub>3</sub> and H<sub>2</sub>O–NaCl. The solution was dried over MgSO<sub>4</sub>, and *n*-BuOH was removed by evaporation. The residue was triturated with ether and the resulting solid was recrystallized from MeOH with ether twice. Yield 4.60 g (55%), mp 136–137 °C,  $[\alpha]_D^{25} - 3.0^\circ$  ( $c=1.0$ , MeOH),  $R_f$  0.58. *Anal.* Calcd for C<sub>18</sub>H<sub>25</sub>N<sub>3</sub>O<sub>8</sub>: C, 52.55; H, 6.13; N, 10.21. Found: C, 52.26; H, 5.85; N, 10.16.

**Boc–Cys(MBzl)–Asn–Thr–OMe**—A TFA-treated sample of Z(OMe)–Asn–Thr–OMe (4.10 g, 10 mmol) was dissolved in DMF (50 ml), together with Et<sub>3</sub>N (1.40 ml, 10 mmol), Boc–Cys(MBzl)–ONp (5.40 g, 10 mmol) and NMM (1.30 ml, 12 mmol). The mixture was stirred for 24 h, and DMF was removed by evaporation. The residue was triturated with ether and the resulting solid was purified by procedure B, followed by recrystallization from MeOH with ether. Yield 5.80 g (92%), mp 202–203 °C,  $[\alpha]_D^{25} - 19.0^\circ$  ( $c=1.0$ , DMF),  $R_f$  0.66. *Anal.* Calcd for C<sub>29</sub>H<sub>38</sub>N<sub>4</sub>O<sub>10</sub>S: C, 54.88; H, 6.04; N, 8.83. Found: C, 54.99; H, 6.15; N, 8.83.

**Z(OMe)–Ser(Bzl)–Cys(MBzl)–Asn–Thr–OMe**—A TFA-treated sample of Boc–Cys(MBzl)–Asn–Thr–OMe

(5.00 g, 8 mmol) was dissolved in DMF (50 ml), together with Et<sub>3</sub>N (1.20 ml, 8 mmol), Z(OMe)-Ser(Bzl)-OSu (3.65 g, 8 mmol) and NMM (1.00 ml, 9.0 mmol). The mixture was stirred for 24 h, and DMF was removed by evaporation. The residue was triturated with ether and the resulting solid was purified by procedure B, followed by recrystallization from DMF with ether. Yield 5.20 g (94%), mp 196–199 °C,  $[\alpha]_D^{25}$   $-8.0^\circ$  ( $c=1.0$ , DMF),  $R_f$  0.72. *Anal.* Calcd for C<sub>39</sub>H<sub>49</sub>N<sub>5</sub>O<sub>12</sub>S·1/2H<sub>2</sub>O: C, 57.06; H, 6.14; N, 8.53. Found: C, 57.06; H, 6.13; N, 8.24.

**Z(OMe)-Ser(Bzl)-Cys(MBzl)-Asn-Thr-NHNH<sub>2</sub>**—The above-prepared methyl ester (4.50 g, 3.7 mmol) dissolved in DMF-DMSO (1:1, 70 ml) was treated with 80% hydrazine hydrate (3.50 ml, 37 mmol) at room temperature for 24 h. The solvent was concentrated *in vacuo* and poured into H<sub>2</sub>O (200 ml). The precipitate was collected and washed well with H<sub>2</sub>O and MeOH. Yield 4.00 g (89%), mp 219–221 °C,  $[\alpha]_D^{25}$   $+6.0^\circ$  ( $c=0.5$ , DMF),  $R_f$  0.48. *Anal.* Calcd for C<sub>38</sub>H<sub>49</sub>N<sub>7</sub>O<sub>11</sub>S·1/2H<sub>2</sub>O: C, 55.60; H, 6.14; N, 11.94. Found: C, 55.36; H, 6.19; N, 11.83.

**Z(OMe)-Ser(Bzl)-Cys(MBzl)-Asn-Thr-Ala-OMe**—The azide [prepared from 2.00 g (2.5 mmol) of Z(OMe)-Ser(Bzl)-Cys(MBzl)-Asn-Thr-NHNH<sub>2</sub> in DMF (30 ml)] and Et<sub>3</sub>N (0.35 ml, 2.5 mmol) were added to an ice-chilled solution of H-Ala-OMe [prepared from 0.52 g (3.7 mmol) of the hydrochloride with Et<sub>3</sub>N (0.52 ml, 3.7 mmol) in DMF (50 ml)]. The mixture was stirred at 4 °C for 24 h, and DMF was removed by evaporation. The residue was triturated with H<sub>2</sub>O and the resulting solid was purified by procedure B, followed by recrystallization from DMF with ether. Yield 1.80 g (81%), mp 203–205 °C,  $[\alpha]_D^{25}$   $-13.9^\circ$  ( $c=1.0$ , DMSO),  $R_f$  0.61. *Anal.* Calcd for C<sub>42</sub>H<sub>54</sub>N<sub>6</sub>O<sub>13</sub>S: C, 57.13; H, 6.16; N, 9.52. Found: C, 57.05; H, 6.40; N, 9.28.

**Z(OMe)-Ser(Bzl)-Cys(MBzl)-Asn-Thr-Ala-NHNH<sub>2</sub>; [5]**—Z(OMe)-Ser(Bzl)-Cys(MBzl)-Asn-Thr-Ala-OMe (1.70 g, 2.1 mmol) dissolved in DMF-DMSO (1:1, 50 ml) was treated with 80% hydrazine hydrate (1.2 ml, 20 mmol) and the mixture was stirred at room temperature for 24 h, then concentrated *in vacuo*. The residue was poured into H<sub>2</sub>O (200 ml). The precipitate was collected and washed well with H<sub>2</sub>O and MeOH. Yield 1.50 g (88%), mp >225 °C (dec.),  $[\alpha]_D^{25}$   $-7.9^\circ$  ( $c=0.9$ , DMSO),  $R_f$  0.49. *Anal.* Calcd for C<sub>41</sub>H<sub>54</sub>N<sub>6</sub>O<sub>12</sub>S·3H<sub>2</sub>O: C, 52.55; H, 6.45; N, 11.96. Found: C, 52.38; H, 6.10; N, 11.77. Amino acid ratios in 6N HCl hydrolysate: Asp 0.97, Thr 0.90, Ser 0.75, Ala 1.00 (recovery of Ala, 85%).

**Z(OMe)-Ser(Bzl)-Arg(Mts)-Ser(Bzl)-Gly-Gly-Val-Val-Lys(Z)-Asp(OChp)-Asn-Phe-Val-Pro-Thr-Asn-Val-Gly-Ser(Bzl)-Glu(OBzl)-Ala-Phe-NH<sub>2</sub>; Z(OMe)-rCGRP(17–37)-NH<sub>2</sub>**—A TFA-treated sample of the protected heptadecapeptide amide [1] (1.00 g, 0.42 mmol) was dissolved in HMPA-DMF (5:1, 50 ml) containing Et<sub>3</sub>N (0.06 ml, 0.42 mmol). To this ice-chilled solution, the azide [prepared from 1.10 g (1.3 mmol) of Z(OMe)-Ser(Bzl)-Arg(Mts)-Ser(Bzl)-Gly-NHNH<sub>2</sub><sup>6)</sup> in DMF (30 ml)] and Et<sub>3</sub>N (0.18 ml, 1.4 mmol) were added. The mixture was stirred at -4 °C for 48 h, then additional azide (1.30 mmol) and Et<sub>3</sub>N (1.4 mmol) were added, and stirring was continued for 48 h. The reaction mixture was poured into H<sub>2</sub>O (300 ml) and the precipitate was collected and washed with hot MeOH, then reprecipitated from HMPA-DMF (5:1) with MeOH. Yield 1.10 g (83%), mp >230 °C (dec.),  $[\alpha]_D^{25}$   $-2.1^\circ$  ( $c=0.5$ , DMSO),  $R_f$  0.60. *Anal.* Calcd for C<sub>155</sub>H<sub>208</sub>N<sub>28</sub>O<sub>38</sub>S·3H<sub>2</sub>O: C, 58.96; H, 6.83; N, 12.46. Found: C, 59.03; H, 6.84; N, 12.29.

**Z(OMe)-Gly-Leu-Leu-Ser(Bzl)-Arg(Mts)-Ser(Bzl)-Gly-Gly-Val-Val-Lys(Z)-Asp(OChp)-Asn-Phe-Val-Pro-Thr-Asn-Val-Gly-Ser(Bzl)-Glu(OBzl)-Ala-Phe-NH<sub>2</sub>; Z(OMe)-rCGRP(14–37)-NH<sub>2</sub>**—A TFA-treated sample of Z(OMe)-rCGRP(17–37)-NH<sub>2</sub> (1.10 g, 0.35 mmol) was dissolved in HMPA-DMF (5:1, 50 ml) containing Et<sub>3</sub>N (0.05 ml, 0.35 mmol). To this ice-chilled solution, the azide [prepared from 0.84 g (1.75 mmol) of Z(OMe)-Gly-Leu-Leu-NHNH<sub>2</sub><sup>6)</sup> in DMF (20 ml)] and Et<sub>3</sub>N (0.24 ml, 1.75 mmol) were added. The mixture was stirred at -4 °C for 48 h, additional azide (1.75 mmol) and Et<sub>3</sub>N (1.75 mmol) were added, and stirring was continued for 48 h. The reaction mixture was poured into cold H<sub>2</sub>O (300 ml) and the precipitate was collected and washed with hot MeOH, then reprecipitated from HMPA-DMF (5:1) with MeOH. Yield 1.00 g (84%), mp >235 °C (dec.),  $[\alpha]_D^{25}$   $+8.0^\circ$  ( $c=0.3$ , DMSO),  $R_f$  0.65. *Anal.* Calcd for C<sub>169</sub>H<sub>233</sub>N<sub>31</sub>O<sub>41</sub>S·3H<sub>2</sub>O: C, 58.99; H, 7.00; N, 12.62. Found: C, 58.79; H, 7.02; N, 12.84.

**Z(OMe)-Thr-Cys(MBzl)-Val-Thr-His-Arg(Mts)-Leu-Ala-Gly-Leu-Leu-Ser(Bzl)-Arg(Mts)-Ser(Bzl)-Gly-Gly-Val-Val-Lys(Z)-Asp(OChp)-Asn-Phe-Val-Pro-Thr-Asn-Val-Gly-Ser(Bzl)-Glu(OBzl)-Ala-Phe-NH<sub>2</sub>; Z(OMe)-rCGRP(6–37)-NH<sub>2</sub>**—The above-prepared Z(OMe)-rCGRP(14–37)-NH<sub>2</sub> (0.35 g, 0.11 mmol) was treated with TFA-anisole (1.0 ml–0.2 ml) for 60 min with ice-cooling twice and dried over KOH pellets *in vacuo*. The dried TFA salt was dissolved in HMPA-DMF (5:1, 30 ml) containing Et<sub>3</sub>N (15 μl, 0.11 mmol) and, to this ice-chilled solution, the azide [prepared from 0.69 g (0.5 mmol) of Z(OMe)-Thr-Cys(MBzl)-Val-Thr-His-Arg(Mts)-Leu-Ala-NHNH<sub>2</sub> in DMF (10 ml)] and Et<sub>3</sub>N (70 μl, 0.5 mmol) were added. The mixture was stirred at -4 °C for 48 h, additional azide (0.5 mmol) and Et<sub>3</sub>N (0.5 mmol) were added, and stirring was continued for 48 h. The reaction mixture was poured into cold H<sub>2</sub>O (200 ml) and the precipitate was collected and washed with hot MeOH, then reprecipitated from HMPA-DMF (5:1) with MeOH. Yield 0.32 g (68%), mp >235 °C (dec.),  $[\alpha]_D^{25}$   $+25.0^\circ$  ( $c=0.4$ , DMSO),  $R_f$  0.54. *Anal.* Calcd for C<sub>223</sub>H<sub>314</sub>N<sub>44</sub>O<sub>54</sub>S<sub>3</sub>·10H<sub>2</sub>O: C, 56.37; H, 7.09; N, 12.97. Found: C, 56.72; H, 7.03; N, 12.89.

**Z(OMe)-Ser(Bzl)-Cys(MBzl)-Asn-Thr-Ala-Thr-Cys(MBzl)-Val-Thr-His-Arg(Mts)-Leu-Ala-Gly-Leu-Leu-Ser(Bzl)-Arg(Mts)-Ser(Bzl)-Gly-Gly-Val-Val-Lys(Z)-Asp(OChp)-Asn-Phe-Val-Pro-Thr-Asn-Val-Gly-Ser(Bzl)-Glu(OBzl)-Ala-Phe-NH<sub>2</sub>; Z(OMe)-rCGRP(1–37)-NH<sub>2</sub>**—The above-prepared Z(OMe)-rCGRP(6–37)-NH<sub>2</sub> (0.30 g, 70 μmol) was treated with TFA-anisole (1.0 ml–0.1 ml) for 60 min with ice-cooling twice and



then dried over KOH pellets *in vacuo*. The dried TFA salt was dissolved in HMPA-DMF (5:1, 30 ml) containing Et<sub>3</sub>N (9.8  $\mu$ l, 70  $\mu$ mol) and, to this ice-chilled solution, the azide [prepared from 0.29 g (350  $\mu$ mol) of Z(OMe)-Ser(Bzl)-Cys(MBzl)-Asn-Thr-Ala-NHNH<sub>2</sub> in DMF (10 ml)] and Et<sub>3</sub>N (50  $\mu$ l, 350  $\mu$ mol) were added. The mixture was stirred at -4 °C for 48 h, additional azide (350  $\mu$ mol) and Et<sub>3</sub>N (350  $\mu$ mol) were added, and stirring was continued for 48 h. The reaction mixture was poured into H<sub>2</sub>O (200 ml) and the precipitate was collected and washed well with hot MeOH. Yield 0.19 g (52%), mp >250 °C (dec.),  $[\alpha]_D^{25}$  -12.1° (*c*=0.3, DMSO), *R*<sub>f</sub> 0.59. *Anal.* Calcd for C<sub>255</sub>H<sub>356</sub>N<sub>50</sub>O<sub>63</sub>S<sub>4</sub>·7 1/2H<sub>2</sub>O: C, 56.79; H, 6.93; N, 12.99. Found: C, 56.77; H, 6.58; N, 12.81.

H-Ser-Cys-Asn-Thr-Ala-Thr-Cys-Val-Thr-His-Arg-Leu-Ala-Gly-Leu-Leu-Ser-Arg-Ser-Gly-Gly-Val-Val-Lys-Asp-Asn-Phe-Val-Pro-Thr-Asn-Val-Gly-Ser-Glu-Ala-Phe-NH<sub>2</sub>;  $\alpha$ -rCGRP----The above-prepared Z(OMe)-rCGRP(1-37)-NH<sub>2</sub> (95 mg, 18  $\mu$ mol) was treated with 1 M TFMSA-thioanisole in TFA (7.30 ml) in the presence of *m*-cresol (0.38 ml, 200 eq) for 4 h with ice-cooling, then dry ether was added. The precipitate was collected by centrifugation, washed with ether three times and dissolved in a solution of 0.1 M Tris-HCl buffer containing 6 M guanidine-HCl (pH 8.0, 4 ml). After the pH was adjusted to 8.0 with 5% methylamine, the solution was incubated with 2-mercaptoethanol (0.20 ml) at 30 °C for 24 h under an N<sub>2</sub> gas atmosphere. The insoluble material formed during incubation was removed by centrifugation and the supernatant solution was applied to a column of Sephadex G-25 (2.2  $\times$  110 cm), which was eluted with 1 N AcOH. The ultraviolet (UV) absorption at 275 nm was determined in each fraction (7.0 ml) and the fractions corresponding to the main peak (tube Nos. 32-43) were combined. The combined solution was diluted with ice-chilled H<sub>2</sub>O (1000 ml, peptide concentration 0.07 mg/ml). The pH of this solution was adjusted to 7.5 with 5% NH<sub>4</sub>OH and the solution was kept standing at room temperature for 4 d; during this time, the Ellman test value (UV absorption at 412 nm) dropped from 0.153 to a constant value of 0.013. The solution was then stirred gently for an additional 24 h. The pH was adjusted to 6.6 with 1 N AcOH, and the solution was lyophilized. The residue was dissolved in 1 N AcOH (4.0 ml) and applied to a column of Sephadex G-50 (2.7  $\times$  100 cm), which was eluted with 1 N AcOH. The UV absorption at 275 nm was determined in each fraction (6.0 ml), then the fractions corresponding to the main peak (tube Nos. 66-97, Fig. 6) were combined and the solvent was removed by lyophilization to afford a white fluffy powder, 33 mg (48% from deprotection).

A part of this sample (25 mg, *ca.* 0.7 mg each) was purified by HPLC on a Nucleosil 7C<sub>18</sub> (4.8  $\times$  250 mm) column using a gradient of CH<sub>3</sub>CN (from 30% to 40% in 50 min) in 0.2% TFA. The eluate corresponding to the main peak (*t*<sub>R</sub>: 39.80 min, Fig. 7-a) was pooled. The rest of the sample was similarly purified and the combined eluates were repeatedly lyophilized to afford a white fluffy powder, 7.5 mg (30% recovery on HPLC).  $[\alpha]_D^{25}$  -44.0° (*c*=0.4, 5% AcOH), *R*<sub>f</sub> 0.21, *R*<sub>f</sub> 0.41, *R*<sub>f</sub> 0.84. Amino acid ratios in the 6 N HCl hydrolysate are listed in Table I. Amino acid ratios in papain plus LAP digest (numbers in parentheses are theoretical values): Asp 1.02 (1), Thr 3.73 (4), Ser 3.54 (4), Asn 3.03 (3), Glu 1.00 (1), Gly 4.38 (4), Ala 3.15 (3), Val 4.41 (5), Leu 3.38 (3), Phe 2.00 (2), Lys 1.03 (1), His 0.94 (1), Arg 2.18 (2), Pro 0.76 (1), Cys was not determined (recovery of Phe, 75%). HPLC *t*<sub>R</sub>: 39.80 min (Fig. 7-b). Molecular weight estimation was conducted by HPLC on a TSKgel G 2000SW column (7.5  $\times$  600 mm), upon which

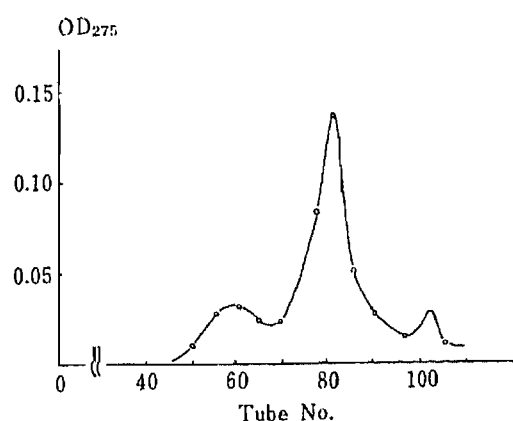


Fig. 6. Purification of the Air-Oxidized Crude Peptide on Sephadex G-50

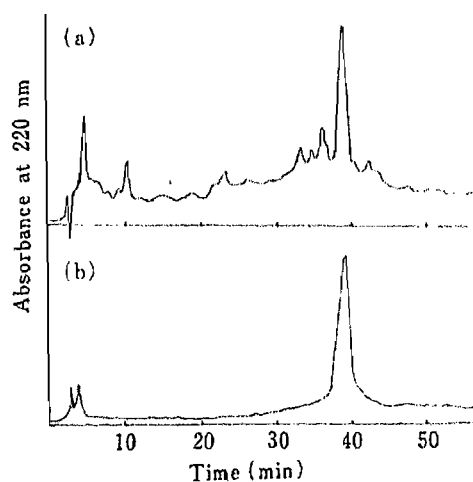


Fig. 7. HPLC of Sephadex G-50 Purified Product (a) and Finally Purified  $\alpha$ -rCGRP (b)

HPLC was performed on a reversed-phase column (Chemopak, Nucleosil 7C<sub>18</sub>, 4.8  $\times$  250 mm). Isocratic elution with (A) (10 min) was followed by linear gradient elution from (A) to (B) (50 min) at a flow rate 1 ml/min. (A): 30% CH<sub>3</sub>CN (0.2% TFA). (B): 40% CH<sub>3</sub>CN (0.2% TFA).



Fig. 8. Elution of Synthetic  $\alpha$ -rCGRP from a TSKgel G 2000SW Column ( $7.5 \times 600$  mm)

Sample, synthetic  $\alpha$ -rCGRP ( $M_r = ca. 3800$ ,  $50 \mu\text{g}$ ); eluent,  $0.1 \text{ M AcONH}_4$  (pH 4.2); flow rate,  $0.5 \text{ ml/min}$ ; absorbance,  $230 \text{ nm}$ .

synthetic  $\alpha$ -rCGRP ( $M_r = ca. 3800$ ,  $t_R$  43.17 min) was eluted between human growth hormone releasing factor (hGRF) derivative ( $M_r = ca. 4500$ ,  $t_R$  42.18 min) and human atrial natriuretic peptide (hANP) derivative ( $M_r = ca. 2000$ ,  $t_R$  49.72 min) (Fig. 8).

**Acknowledgement** We wish to express our gratitude to Professor Haruaki Yajima and Dr. Nobutaka Fujii of Kyoto University for their encouragement and helpful discussions during the course of this investigation. Thanks are also extended to Professor Yoshiaki Kiso and Dr. Masanori Shimokura of Kyoto College of Pharmacy for the molecular weight estimation of the synthetic peptide by HPLC.

#### References and Notes

- 1) Amino acids, peptides and their derivatives in this paper are of L-configuration. Abbreviations used are those recommended by the I.U.P.A.C.-I.U.B. Commission on Biochemical Nomenclature: *J. Biol. Chem.*, **247**, 977 (1972). Z = benzyloxycarbonyl, Z(OMe) = *p*-methoxybenzyloxycarbonyl, Boc = *tert*-butyloxycarbonyl, Bzl = benzyl, Mts = mesitylenesulfonyl, Chp = cycloheptyl, MBzl = *p*-methoxybenzyl, Ad = adamantyl, Np = *p*-nitrophenyl, Su = *N*-hydroxysuccinimidyl, DCC = *N,N'*-dicyclohexylcarbodiimide, HOBt = *N*-hydroxybenzotriazole, TFA = trifluoroacetic acid, TFMSA = trifluoromethanesulfonic acid,  $\text{Et}_3\text{N}$  = triethylamine, NMM = *N*-methylmorpholine, DMF = dimethylformamide, DMSO = dimethylsulfoxide, HMPA = hexamethylphosphoramide, MeOH = methanol, AcOEt = ethyl acetate, AcOH = acetic acid, LAP = leucine aminopeptidase.
- 2) a) M. G. Rosenfeld, S. G. Amara, B. A. Roos, E. S. Ong, and R. M. Evans, *Nature* (London), **290**, 63 (1981); b) M. G. Rosenfeld, C. R. Lin, S. G. Amara, L. Stolarsky, B. A. Roos, E. S. Ong, and R. M. Evans, *Proc. Natl. Acad. Sci. U.S.A.*, **79**, 1717 (1982); c) S. G. Amara, V. Jonas, M. G. Rosenfeld, E. S. Ong, and R. M. Evans, *Nature* (London), **298**, 240 (1982); d) M. G. Rosenfeld, J.-J. Mermod, S. G. Amara, L. W. Swanson, P. E. Sawchenko, J. Rivier, W. W. Vale, and R. M. Evans, *ibid.*, **304**, 129 (1983).
- 3) H. R. Morris, M. Panico, T. Etienne, J. Tippins, S. I. Girgis, and I. MacIntyre, *Nature* (London), **308**, 746 (1984).
- 4) S. Kimura, Y. Shigematsu, Y. Yamashita, Y. Sugita, K. Goto, I. Kanazawa, and E. Munekata, Abstracts of the 58th Annual Meeting of the Japanese Biochemical Society, *Seikagaku*, **57**, 1128 (1985).
- 5) M. G. Rosenfeld, S. G. Amara, and R. M. Evans, *Science*, **225**, 1315 (1985).
- 6) a) N. Fujii, H. Yajima, A. Otaka, S. Funakoshi, M. Nomizu, K. Akaji, I. Yamamoto, K. Torizuka, K. Kitagawa, T. Akita, K. Ando, T. Kawamoto, Y. Shimonishi, and T. Takao, *J. Chem. Soc., Chem. Commun.*, **1985**, 602; b) N. Fujii, A. Otaka, S. Funakoshi, M. Nomizu, K. Akaji, H. Yajima, K. Kitagawa, T. Akita, K. Ando, and T. Kawamoto, *Chem. Pharm. Bull.*, **34**, 603 (1986); c) N. Fujii, A. Otaka, S. Funakoshi, M. Nomizu, K. Akaji, H. Yajima, I. Yamamoto, K. Torizuka, K. Kitagawa, T. Akita, K. Ando, T. Kawamoto, Y. Shimonishi, and T. Takao, *ibid.*, **34**, 613 (1986).
- 7) a) H. Yajima, N. Fujii, H. Ogawa, and H. Kawatani, *J. Chem. Soc., Chem. Commun.*, **1974**, 107; b) H. Yajima and N. Fujii, *J. Am. Chem. Soc.*, **103**, 5867 (1981).
- 8) a) S. Futaki, K. Akaji, S. Katakura, M. Sakurai, N. Fujii, and H. Yajima, in "Peptide Chemistry 1984," ed. by N. Izumiya, Protein Research Foundation, Osaka, 1985, p. 23; b) N. Fujii, M. Nomizu, S. Futaki, A. Otaka, S. Funakoshi, K. Akaji, K. Watanabe, and H. Yajima, *Chem. Pharm. Bull.*, **34**, 864 (1986).
- 9) H. Yajima, M. Takeyama, J. Kanaki, and K. Mitani, *J. Chem. Soc., Chem. Commun.*, **1978**, 482.
- 10) a) M. Bodanszky and J. Z. Kwei, *Int. J. Peptide Protein Res.*, **12**, 69 (1978); b) M. Bodanszky, J. C. Tolle, S. S. Deshmane, and A. Bodanszky, *ibid.*, **12**, 57 (1978); c) I. Schön and L. Kisfaludy, *ibid.*, **14**, 485 (1979).
- 11) a) O. Nishimura, C. Kitada, and M. Fujino, *Chem. Pharm. Bull.*, **26**, 1576 (1978); b) N. Fujii, A. Otaka, S. Funakoshi, H. Yajima, O. Nishimura, and M. Fujino, *ibid.*, **34**, 869 (1986).
- 12) S. Akabori, S. Sakakibara, Y. Shimonishi, and Y. Nobuhara, *Bull. Chem. Soc., Jpn.*, **37**, 433 (1964).
- 13) J. Honzl and J. Rudinger, *Coll. Czech. Chem. Commun.*, **26**, 2333 (1961).
- 14) S. Funakoshi, H. Yajima, C. Shigeno, I. Yamamoto, R. Morita, and K. Torizuka, *Chem. Pharm. Bull.*, **30**, 1738 (1982).
- 15) G. W. Anderson, J. E. Aimmerman, and F. Callahan, *J. Am. Chem. Soc.*, **85**, 3039 (1963).
- 16) M. Bodanszky and V. du Vigneaud, *J. Am. Chem. Soc.*, **81**, 5688 (1959).

- 
- 17) W. König and R. Geiger, *Chem. Ber.*, **103**, 788 (1970).
  - 18) K. Kitagawa, K. Yoneto, S. Kiyama, K. Ando, T. Kawamoto, T. Akita, A. Inoue, and T. Segawa, *Chem. Pharm. Bull.*, **33**, 3307 (1985).
  - 19) a) K. Inoue and K. Watanabe, *J. Chem. Soc., Perkin Trans. 1*, **1977**, 1911; b) K. Akaji, N. Fujii, H. Yajima, M. Moriga, A. Takagi, K. Mizuta, M. Noguchi, and T. J. McDonald, *Int. J. Peptide Protein Res.*, **20**, 276 (1982).
  - 20) a) H. Yajima, M. Takeyama, J. Kanaki, and K. Mitani, *J. Chem. Soc., Chem. Commun.*, **1978**, 482; b) H. Yajima, M. Takeyama, J. Kanaki, O. Nishimura, and M. Fujino, *Chem. Pharm. Bull.*, **26**, 3752 (1978).
  - 21) G. L. Ellman, *Arch. Biochem. Biophys.*, **82**, 70 (1959).
  - 22) The method of <sup>45</sup>Ca-release assay was described in ref. 6c.

[Chem. Pharm. Bull.]  
35(1) 72-79 (1987)

## Direct C-8 Lithiation of Naturally-Occurring Purine Nucleosides. A Simple Method for the Synthesis of 8-Carbon-Substituted Purine Nucleosides<sup>1)</sup>

HIROYUKI HAYAKAWA, KAZUHIRO HARAGUCHI, HIROMICHI TANAKA,  
and TADASHI MIYASAKA\*

*School of Pharmaceutical Sciences, Showa University,  
Hatanodai 1-5-8, Shinagawa-ku, Tokyo 142, Japan*

(Received June 6, 1986)

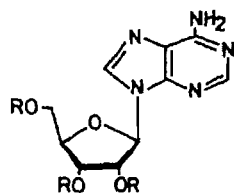
The sugar moiety of adenosine, inosine, or guanosine was protected with a *tert*-butyldimethylsilyl group. The C-8 lithiation of these protected nucleosides was carried out with lithium diisopropylamide in tetrahydrofuran at below  $-70^{\circ}\text{C}$ . The reactions of the C-8-lithiated species with MeI,  $\text{HCO}_2\text{Me}$ , and  $\text{ClCO}_2\text{Me}$  were examined. The resulting products having a carbon substituent at the C-8 position were converted to the corresponding 8-carbon-substituted purine nucleosides by treatment with tetrabutylammonium fluoride. The whole sequence constitutes a simple method for the preparation of 8-carbon-substituted purine nucleosides from intact purine nucleosides.

**Keywords**—lithiation; purine nucleoside; LDA; 8-carbon-substituted purine nucleoside; *tert*-butyldimethylsilyl group

Our recent studies on the lithiation of nucleosides<sup>2)</sup> have demonstrated the effectiveness of this approach for the introduction of a variety of functionalities into the base moiety. In an earlier paper, we reported the use of 6-chloro-9-(2,3-*O*-isopropylidene- $\beta$ -D-ribofuranosyl)purine as a starting material in the lithiation approach to the synthesis of 8-carbon-substituted adenosines, 6-thioinosines, and nebularines.<sup>3,4)</sup>

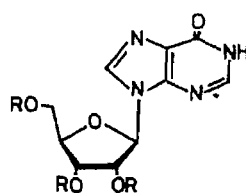
In connection with our continuing studies on the lithiation chemistry of nucleosides, we would like to report here the direct C-8 metallation of naturally-occurring purine nucleosides—adenosine (1), inosine (2), and guanosine (3)—which provides a simple method for the preparation of their 8-carbon-substituted derivatives.

Although the preparation of purine nucleosides having carbon substituent at the C-8 position has ample precedent in the literature, most methods are based on either radical reaction, which suffers from the problem of regioselectivity,<sup>5)</sup> or nucleophilic displacement, in which only cyanide ion or ethyl sodioacetoacetate can be used as a nucleophile.<sup>6)</sup> An alternative method, palladium-catalyzed condensation of Grignard reagents with trimethyl-



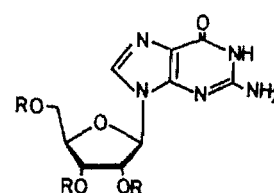
1: R=H  
4: R=TBDMS

Fig. 1



2: R=H  
5: R=TBDMS

Fig. 2



3: R=H  
6: R=TBDMS

Fig. 3

silyl derivatives of 8-bromopurine nucleosides,<sup>7)</sup> is far from satisfactory in synthesis due to its poor yields.

The above facts prompted us to carry out the present work. There have been two reports on the lithiation of purine nucleosides other than those cited in references 3 and 4. Barton and his co-workers described, for the first time in studies on the lithiation of purine nucleosides, the C-8 metallation and successive methylation of *N*<sup>6</sup>-methyl-2',3'-*O*-isopropylideneadenosine to obtain *N*<sup>6</sup>,*N*<sup>6</sup>-dimethyl-8-methyl-2',3'-*O*-isopropylideneadenosine in 35% yield.<sup>8)</sup> Halogen-lithium exchange reaction of 8-bromopurine nucleosides has also been used for the modification of the C-8 position.<sup>9)</sup> However, the direct C-8 lithiation of "intact purine nucleosides" is unprecedented to our knowledge.

A major concern in the lithiation of nucleosides is the problem of protection of hydroxyl groups and selection of a suitable lithiating agent. In our previous studies, the use of a combination of acid-labile protecting groups such as 5'-*O*-methoxymethyl/2',3'-*O*-isopropylidene and 5'-*O*-*tert*-butyldimethylsilyl (TBDMS)/2',3'-*O*-methoxymethylidene was successful in effecting lithiation of uridine<sup>2a)</sup> and an imidazole nucleoside.<sup>2b)</sup> However, these are not suitable for purine nucleosides, since their glycosidic bonds undergo acid-catalyzed hydrolysis.<sup>10)</sup> The TBDMS group would meet our requirements because of its stability under strongly basic conditions and its easy cleavage under neutral conditions with fluoride anion.<sup>11)</sup>

When adenosine (1), inosine (2), and guanosine (3) were treated with TBDMSCl (3.5, 5.0, and 6.0 eq, respectively) in *N,N*-dimethylformamide (DMF) containing imidazole (7–10 eq) at room temperature overnight, the corresponding 2',3',5'-tris-*O*-TBDMS derivatives (4,<sup>12)</sup> 5, and 6<sup>13)</sup> were obtained as crystals in high yields. We then examined the C-8 lithiation of these protected nucleosides (4–6). As purine nucleosides are known to undergo hydrogen exchange at the C-8 position<sup>14)</sup> and as the C-8 hydrogen was considered to be rather acidic, lithium diisopropylamide (LDA)<sup>15)</sup> was used in the present investigation.

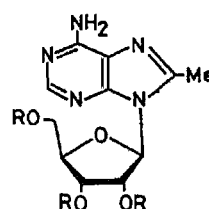
When 4 in tetrahydrofuran (THF) was added to a THF solution of LDA (3 eq) at below –70 °C, a clear solution of the lithiated species resulted. After keeping the mixture below –70 °C for 1.5 h, CD<sub>3</sub>OD was added to the solution and the resulting deuterated product was isolated by short-column chromatography on silica gel. The proton nuclear magnetic resonance (<sup>1</sup>H-NMR) spectrum of the deuterated 4 in CDCl<sub>3</sub> showed, by comparison of the integrals of the H-2 (δ 8.33 ppm) and H-8 (δ 8.15 ppm) signals with that of the H-1' signal (δ 6.02 ppm), that the metallation took place at the C-8 position in a regiospecific manner in 68% yield. As can be seen from Table I, a higher deuterium incorporation was observed when the above reaction was performed by using 5 eq of LDA. In a similar manner, LDA lithiation of 5 and 6 was examined by deuteration and the results are summarized in Table I. In an attempt to increase the lithiation levels, lithium 2,2,6,6-tetramethylpiperidide (LTMP), which is a more basic lithiating agent than LDA,<sup>16)</sup> was also examined but no practical advantage could be found in the use of this expensive reagent. Thus, throughout this study, 5 eq of LDA was used for the C-8 lithiation of 4–6.

Methylation at the C-8 position of 4 was first carried out. When the lithiated 4 prepared by using 5 eq of LDA as mentioned above was reacted with MeI (3 eq) for 2 h at below –70 °C, 2',3',5'-tris-*O*-TBDMS-8-methyladenosine (7) was isolated in 45% yield and most of the starting material (4) was left unchanged after quenching with AcOH. Although Barton *et al.*<sup>8)</sup> have reported the simultaneous methylation at the N-6 and C-8 positions in the reaction of lithiated *N*<sup>6</sup>-methyl-2',3'-*O*-isopropylideneadenosine, the N<sup>6</sup>-methylated product of 7 was not detected even in a trace amount in our reaction. The absence of such an undesired product could be attributed to the lower reaction temperature, which decreases the nucleophilicity of the N<sup>6</sup>-anion. Treatment of 7 with tetrabutylammonium fluoride (TBAF) in THF for 2 h at room temperature gave 8-methyladenosine (8)<sup>5d)</sup> in 85% yield.

A similar methylation of the lithiated 5 (5 eq of MeI, 3 h), on the other hand, gave a

TABLE I. Deuterium Incorporation (%)  
 at the C-8 Position of 4–6

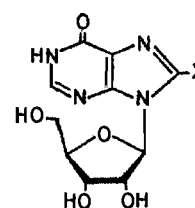
Compd.	LDA			LTMP
	3 eq	4 eq	5 eq	5 eq
4	68	67	77	83
5	75	89	91	87
6	42	45	66	57



7: R = TBDMS

8: R = H

Fig. 4



9: X = Me

10: X = Et

11: X = CHMe<sub>2</sub>

Fig. 5

mixture of products which could not be separated at this stage. After removal of the TBDMS groups, 8-methyl- (9),<sup>5d)</sup> 8-ethyl- (10), and 8-isopropylinosines (11) were obtained by preparative thin layer chromatography (TLC) in 21%, 16%, and 15% yields, respectively. The formation of 10 and 11 apparently results from further methylation of the initially formed 8-methyl derivative and this is in accord with our earlier observation in the case of 6-chloropurine nucleoside.<sup>3)</sup>

A functionalized alkyl group, the hydroxymethyl group, can be introduced by electrophilic reaction of HCO<sub>2</sub>Me followed by reduction of the resulting formyl derivative with NaBH<sub>4</sub>. Thus, when HCO<sub>2</sub>Me (5 eq, 3 h) was added to the lithiated 4, the 8-formyladenosine derivative (12) was produced. Subsequent reduction of 12 with NaBH<sub>4</sub> in MeOH gave the 8-hydroxymethyladenosine derivative (13) in 62% yield from 4. Deprotection of 13 gave 8-hydroxymethyladenosine (14) in 87% yield as crystals (mp 209–210 °C). This compound has been reported recently but not in a crystalline form.<sup>6c)</sup> The lithiated 5 also followed the above reaction sequence, giving the 8-formylinosine derivative (15) in 71% yield and then its 8-hydroxymethyl derivative (16) in 92% yield. 8-Hydroxymethylinosine (17) was obtained as crystals (mp >290 °C) upon TBAF treatment of 16. Similarly, the 8-formyl derivative (18) of guanosine was prepared in 41% yield. Although the yield of 18 was not quite satisfactory, it is noteworthy that the lithiation reaction could work with such a polar substrate as 6. Reduction of 18 followed by deprotection gave 8-hydroxymethylguanosine (19: 86% from 18, mp 212–214 °C).

The reactions with ClCO<sub>2</sub>Me were next examined. Treatment of the lithiated 4 with 5 eq of ClCO<sub>2</sub>Me (3 h, below –70 °C) gave two products. Both products, isolated by column chromatography, had one D<sub>2</sub>O-exchangeable proton and one aromatic proton in their <sup>1</sup>H-NMR spectra measured in CDCl<sub>3</sub>, indicating that one amino proton and a proton at the C-8

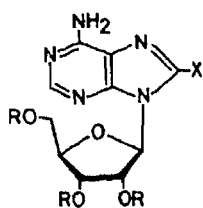
12: R = TBDMS,  
X = CHO13: R = TBDMS,  
X = CH<sub>2</sub>OH14: R = H,  
X = CH<sub>2</sub>OH

Fig. 6

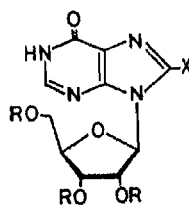
15: R = TBDMS,  
X = CHO16: R = TBDMS,  
X = CH<sub>2</sub>OH17: R = H,  
X = CH<sub>2</sub>OH

Fig. 7

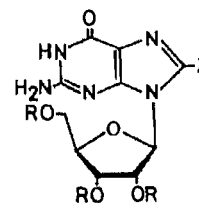
18: R = TBDMS,  
X = CHO19: R = H,  
X = CH<sub>2</sub>OH

Fig. 8

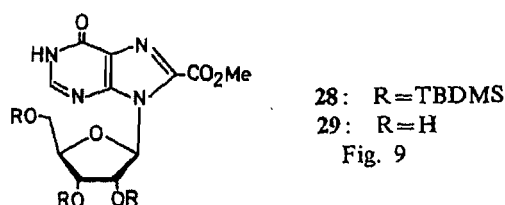
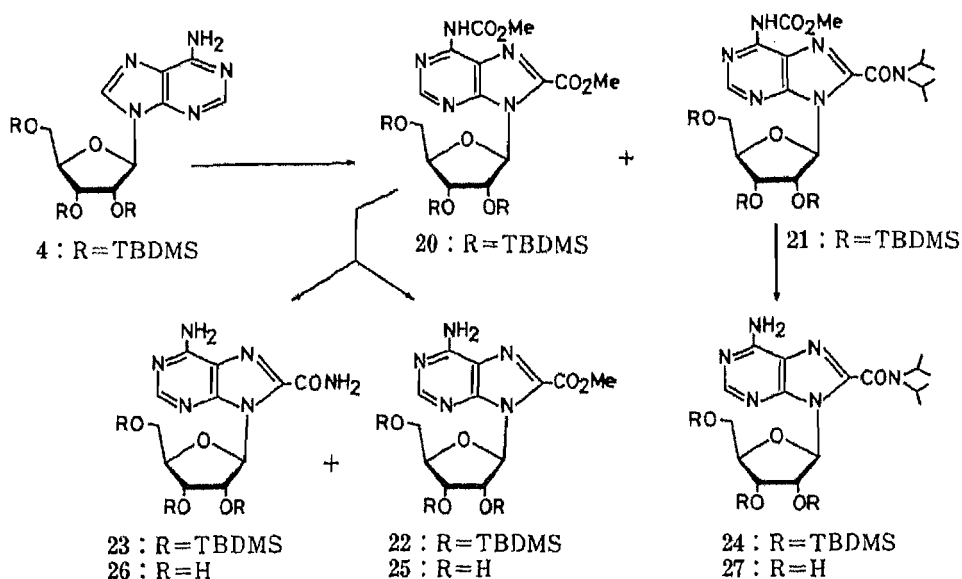
position had been displaced during this reaction. The  $^1\text{H-NMR}$  spectrum of the slower-moving product showed two  $\text{CO}_2\text{Me}$  signals at 3.88 and 4.07 ppm, which was suggestive of the structure **20**, while that of the faster-moving one indicated the presence of two fixed isopropyl groups (1.24 and 1.57 ppm, each as a double doublet) and one  $\text{CO}_2\text{Me}$  group (3.89 ppm, singlet).

Since LDA was apparently the origin of the two isopropyl groups and since such nucleophilic attack of diisopropylamide anion was considered to be less favored at  $\text{N}^6\text{-CO}_2\text{Me}$  than at  $\text{C}^8\text{-CO}_2\text{Me}$ , the structure **21** was assigned to the latter product. The yield of **20** and **21** were 27% and 50%, respectively.

From the result of methylation of the lithiated **4**, we assumed that regioselective reaction at the C-8 position might be possible by using a limited amount of  $\text{ClCO}_2\text{Me}$ . However, when this reaction was conducted with 1 eq of the electrophile, **21** was the sole product (20% yield). The structures of **20** and **21** were eventually further confirmed by  $\text{NH}_3/\text{MeOH}$  treatment (at room temperature, overnight) which gave **22** (24%) plus **23** (46%) and **24** (79%), respectively, as shown in Chart 1.

Although we have no clear explanation for the attack of diisopropylamide anion in the above methoxycarbonylation of **4**, the acylation at the N-6 position should be responsible for this result, since LDA (5 eq) treatment of **22** under similar conditions did not furnish **24**. Compounds **22**—**24** were converted to the corresponding free nucleosides (**25**—**27**) in high yields by TBAF treatment.

Finally, the reaction of the lithiated **5** with  $\text{ClCO}_2\text{Me}$  (3 eq, 2 h, below  $-70^\circ\text{C}$ ) was carried out. The corresponding 8-methoxycarbonyl derivative (**28**) was isolated in 61% yield as the sole product. In contrast to the case of adenosine, it is interesting that the 8- $\text{CO}_2\text{Me}$  group survived completely during this reaction. Deprotection of **28** gave 8-methoxycarbonyl-



inosine (**29**) in 73% yield.

### Experimental

Melting points were determined with a Yanagimoto micro melting point apparatus and are uncorrected. <sup>1</sup>H-NMR spectra were measured with tetramethylsilane (TMS) as an internal standard, with a JEOL JNM-FX 100 NMR spectrometer. The abbreviations used are as follows: s, singlet; d, doublet; dd, double doublet; t, triplet; m, multiplet; br, broad. Mass spectra (MS) were taken on a JEOL JMS-D 300 spectrometer. Ultraviolet (UV) spectra were recorded on a Shimadzu UV-240 spectrophotometer. Reactions at low temperature were performed using a CryoCool CC-100 (NESLAB Instrument, Inc.). Butyllithium in hexane was titrated before use by using diphenylacetic acid in THF. THF was distilled from sodium benzophenone ketyl. Column chromatography was carried out either on silica gel (Wakogel<sup>®</sup> C-200) or on magnesium silicate (Florisil<sup>®</sup>). TLC was performed on silica gel (precoated Silica gel plates 60 F<sub>254</sub>, Merck).

**2',3',5'-Tris-*O*-(*tert*-butyldimethylsilyl)adenosine (4)**—Compound **1** (267 mg, 1.0 mmol) was added to a mixture of TBDMSCl (528 mg 3.5 mmol) and imidazole (340 mg, 5.0 mmol) in DMF (2 ml), and the resulting solution was stirred at room temperature overnight. The mixture was poured into EtOAc–H<sub>2</sub>O and the organic layer was separated, dried (Na<sub>2</sub>SO<sub>4</sub>) and evaporated to dryness. Column chromatographic purification (benzene : EtOAc = 4 : 1) of the residue gave **4** (532 mg, 86%). Crystallization from MeOH–H<sub>2</sub>O gave an analytical sample (mp 143–144 °C, lit.<sup>12</sup> mp 142–144 °C). *Anal.* Calcd for C<sub>28</sub>H<sub>55</sub>N<sub>5</sub>O<sub>4</sub>Si<sub>3</sub>: C, 55.16; H, 9.09; N, 11.49. Found: C, 55.10; H, 9.15; N, 11.41. MS *m/z*: 594 (M–Me), 552 (M–Bu-*tert*), 135 (B+1). UV λ<sub>max</sub><sup>MeOH</sup> nm (ε): 260 (15600), λ<sub>min</sub><sup>MeOH</sup> nm (ε): 229 (2900). <sup>1</sup>H-NMR (CDCl<sub>3</sub>) δ: 0.10–0.13 (18H, m, SiMe), 0.79–0.95 (27H, m, SiBu-*tert*), 3.80 (1H, m, H-4'), 3.96–4.18 (2H, m, CH<sub>2</sub>-5'), 4.32 (1H, dd, H-3'), 4.69 (1H, dd, H-2'), 5.80 (2H, br, NH<sub>2</sub>), 6.02 (1H, d, H-1'), 8.15 (1H, s, H-8), 8.33 (1H, s, H-2).

**2',3',5'-Tris-*O*-(*tert*-butyldimethylsilyl)inosine (5)**—This compound was prepared from **2** (1.07 g, 4.0 mmol), TBDMSCl (3.02 g, 20 mmol), and imidazole (1.91 g, 28 mmol) in DMF (5 ml) by the same procedure as used for the preparation of **4**. Silica gel column chromatography (benzene : EtOAc = 2 : 1) gave **5** (2.21 g, 91%). Crystallization from MeOH gave an analytical sample (mp 248–249 °C). *Anal.* Calcd for C<sub>28</sub>H<sub>54</sub>N<sub>4</sub>O<sub>5</sub>Si<sub>3</sub>: C, 55.07; H, 8.91; N, 9.17. Found: C, 55.29; H, 9.15; N, 9.40. MS *m/z*: 595 (M–Me), 553 (M–Bu-*tert*), 136 (B+1). UV λ<sub>max</sub><sup>MeOH</sup> nm (ε): 247 (11300), λ<sub>shoulder</sub><sup>MeOH</sup> nm (ε): 260 (6500), λ<sub>min</sub><sup>MeOH</sup> nm (ε): 225 (4500). <sup>1</sup>H-NMR (CDCl<sub>3</sub>) δ: 0.10–0.15 (18H, m, SiMe), 0.82–0.97 (27H, m, SiBu-*tert*), 3.74–4.56 (5H, m, H-2', H-3', H-4', CH<sub>2</sub>-5'), 6.02 (1H, d, *J* = 4.9 Hz, H-1'), 8.17 (1H, s, H-2), 8.24 (1H, s, H-8), 13.21 (1H, br, NH).

**2',3',5'-Tris-*O*-(*tert*-butyldimethylsilyl)guanosine (6)**—This compound was prepared from **3** (1.13 g, 4.0 mmol), TBDMSCl (3.62 g, 24 mmol), and imidazole (2.72 g, 40 mmol) in DMF (20 ml) by the procedure as used for the preparation of **4**. Silica gel column chromatography (6% EtOH in CHCl<sub>3</sub>) gave **6** (2.10 g, 86%). Crystallization from MeOH–H<sub>2</sub>O gave an analytical sample (mp 255–257 °C, lit.<sup>13</sup> mp > 245 °C, dec.). *Anal.* Calcd for C<sub>28</sub>H<sub>55</sub>N<sub>5</sub>O<sub>5</sub>Si<sub>3</sub>·1/2H<sub>2</sub>O: C, 52.97; H, 8.89; N, 11.03. Found: C, 53.09; H, 8.97; N, 11.13. MS *m/z*: 568 (M–Bu-*tert*), 151 (B+1). UV λ<sub>max</sub><sup>MeOH</sup> nm (ε): 256 (20000), λ<sub>shoulder</sub><sup>MeOH</sup> nm (ε): 266 (16200), λ<sub>min</sub><sup>MeOH</sup> nm (ε): 223 (1900). <sup>1</sup>H-NMR (CDCl<sub>3</sub>) δ: 0.02–0.14 (18H, m, SiMe), 0.87–0.96 (27H, m, SiBu-*tert*), 3.74–4.49 (5H, m, H-2', H-3', H-4', CH<sub>2</sub>-5'), 5.83 (1H, d, *J* = 3.9 Hz, H-1'), 6.29 (2H, br, NH<sub>2</sub>), 7.90 (1H, s, H-8), 12.03 (1H, br, NH).

**2',3',5'-Tris-*O*-(*tert*-butyldimethylsilyl)-8-methyladenosine (7)**—LDA (7.5 mmol) in THF (15 ml) was placed in a three-necked flask equipped with a gas-inlet adaptor, thermometer, and rubber septum. To this, a solution of **4** (915 mg, 1.5 mmol) in THF (15 ml) was added, under positive pressure of dry argon, at such a rate that the temperature did not exceed –70 °C. The mixture was stirred for 1.5 h at below –70 °C, MeI (0.28 ml, 4.5 mmol) was added and the whole was stirred for a further 3 h. The reaction was then quenched by adding AcOH (0.43 ml, 7.5 mmol). Evaporation of the solvent followed by chromatography on a silica gel column (0.5% EtOH in CHCl<sub>3</sub>) gave **7** (417 mg, 45%). Crystallization from EtOH gave an analytical sample (mp 170–172 °C). *Anal.* Calcd for C<sub>29</sub>H<sub>57</sub>N<sub>5</sub>O<sub>4</sub>Si<sub>3</sub>: C, 55.85; H, 9.21; N, 11.23. Found: C, 55.80; H, 9.33; N, 11.10. MS *m/z*: 567 (M–Bu-*tert*), 149 (B+1). UV λ<sub>max</sub><sup>MeOH</sup> nm (ε): 260 (17100), λ<sub>min</sub><sup>MeOH</sup> nm (ε): 229 (4100). <sup>1</sup>H-NMR (CDCl<sub>3</sub>) δ: 0.04–0.16 (18H, m, SiMe), 0.77–0.97 (27H, m, SiBu-*tert*), 2.62 (3H, s, 8-Me), 3.76 (1H, m, H-4'), 3.98–4.12 (2H, m, CH<sub>2</sub>-5'), 4.51 (1H, dd, H-3'), 5.43–5.53 (3H, m, H-2', NH<sub>2</sub>), 5.79 (1H, d, *J* = 6.3 Hz, H-1'), 8.24 (1H, s, H-2).

**8-Methyladenosine (8)**—TBAF·3H<sub>2</sub>O (265 mg, 0.84 mmol) was added to a solution of **7** (150 mg, 0.24 mmol) in THF (7 ml) and the mixture was stirred at room temperature for 2 h. After evaporation of the solvent, the resulting residue was chromatographed on a Florisil column (15% EtOH in CHCl<sub>3</sub>). This afforded **8** (58 mg, 86%), which was crystallized from MeOH–H<sub>2</sub>O to give an analytical sample (mp 199–202 °C, sintering at 132 °C; lit.<sup>5d</sup> mp 130–133 °C). *Anal.* Calcd for C<sub>11</sub>H<sub>15</sub>N<sub>5</sub>O<sub>4</sub>: C, 46.97; H, 5.37; N, 24.90. Found: C, 46.91; H, 5.38; N, 24.63. MS *m/z*: 149 (B+1). UV λ<sub>max</sub><sup>H<sub>2</sub>O</sup> nm (ε): 261 (14500), λ<sub>min</sub><sup>H<sub>2</sub>O</sup> nm (ε): 227 (800). <sup>1</sup>H-NMR (CD<sub>3</sub>OD) δ: 2.64 (3H, s, 8-Me), 3.75–3.85 (2H, m, CH<sub>2</sub>-5'), 4.18 (1H, m, H-4'), 4.31 (1H, m, H-3'), 4.92 (1H, dd, H-2'), 5.90 (1H, d, *J* = 3.9 Hz, H-1'), 8.10 (1H, s, H-2).

**8-Alkylinosines (9, 10, and 11)**—The C-8 alkylation of **5** (916 mg, 1.5 mmol) with MeI (0.47 ml, 7.5 mmol) was carried out for 3 h by the same procedure as used for the preparation of **7**. Silica gel column chromatography (2%



EtOH in  $\text{CHCl}_3$ ) gave a mixture of products, which was treated with  $\text{TBAF} \cdot 3\text{H}_2\text{O}$  (1.66 g, 5.3 mmol) in THF (15 ml) for 2 h. Column chromatography on Florisil (40% EtOH in  $\text{CHCl}_3$ ) gave a mixture of **9**, **10**, and **11**. Purification by preparative TLC (silica gel, 6% EtOH in  $\text{CHCl}_3$ ) gave **9** (91 mg, 21%), **10** (72 mg, 16%), and **11** (71 mg, 15%).

Physical data for **9** are as follows. mp 163–165 °C (MeOH– $\text{H}_2\text{O}$ ). *Anal.* Calcd for  $\text{C}_{11}\text{H}_{14}\text{N}_4\text{O}_5 \cdot \text{H}_2\text{O}$ : C, 44.00; H, 5.37; N, 18.66. Found: C, 43.98; H, 5.18; N, 18.52. MS  $m/z$ : 150 (B+1). UV  $\lambda_{\text{max}}^{\text{H}_2\text{O}}$  nm ( $\epsilon$ ): 251 (12400),  $\lambda_{\text{min}}^{\text{H}_2\text{O}}$  nm ( $\epsilon$ ): 226 (4600).  $^1\text{H-NMR}$  (DMSO- $d_6$ )  $\delta$ : 2.51 (overlapped with DMSO, 8-Me), 3.58–3.62 (2H, m,  $\text{CH}_2$ -5'), 3.91–3.94 (1H, m, H-4'), 4.13 (1H, m, H-3'), 4.65–4.84 (1H, m, H-2'), 5.04–5.42 (3H, m, 2'-OH, 3'-OH, 5'-OH), 5.78 (1H, d,  $J=6.8$  Hz, H-1'), 8.01 (1H, s, H-2), 12.37 (1H, br, NH).

Physical data for **10** (obtained as a foam) are as follows. MS  $m/z$ : 164 (B+1). UV  $\lambda_{\text{max}}^{\text{H}_2\text{O}}$  nm: 250,  $\lambda_{\text{min}}^{\text{H}_2\text{O}}$  nm: 232.  $^1\text{H-NMR}$  (DMSO- $d_6$ )  $\delta$ : 1.28 (3H, t,  $\text{CH}_2\text{CH}_3$ ), 2.86 (2H, q,  $\text{CH}_2\text{CH}_3$ ), 3.58–3.62 (2H, m,  $\text{CH}_2$ -5'), 3.94 (1H, m, H-4'), 4.15 (1H, dd, H-3'), 4.82 (1H, dd, H-2'), 5.11 (3H, br, 2'-OH, 3'-OH, 5'-OH), 5.78 (1H, d,  $J=6.8$  Hz, H-1'), 8.01 (1H, s, H-2). Compound **10** was converted to its triacetate, whose high-resolution MS was measured. High-resolution MS  $m/z$ : 422.1436 ( $\text{M}^+$ ) Calcd for  $\text{C}_{18}\text{H}_{22}\text{N}_4\text{O}_8$  422.1436.  $^1\text{H-NMR}$  ( $\text{CDCl}_3$ )  $\delta$ : 1.46 (3H, t, 8- $\text{CH}_2\text{CH}_3$ ), 2.06, 2.09, and 2.16 (9H, each as s, Ac), 2.91 (2H, q, 8- $\text{CH}_2\text{CH}_3$ ), 4.30–4.39 (2H, m,  $\text{CH}_2$ -5'), 4.49 (1H, m, H-4'), 5.79 (1H, dd, H-3'), 5.96 (1H, d,  $J=5.1$  Hz, H-1'), 6.19 (1H, dd, H-2'), 8.03 (1H, s, H-2), 12.80 (1H, br, NH).

Physical data for **11** are as follows. mp 143–145 °C (MeOH– $\text{H}_2\text{O}$ ). *Anal.* Calcd for  $\text{C}_{13}\text{H}_{18}\text{N}_4\text{O}_5 \cdot 1/2\text{H}_2\text{O}$ : C, 48.89; H, 5.99; N, 17.55. Found: C, 48.63; H, 6.07; N, 17.31. MS  $m/z$ : 178 (B+1), 163 (B+1–Me). UV  $\lambda_{\text{max}}^{\text{H}_2\text{O}}$  nm ( $\epsilon$ ): 252 (14000),  $\lambda_{\text{min}}^{\text{H}_2\text{O}}$  nm ( $\epsilon$ ): 224 (3800).  $^1\text{H-NMR}$  (DMSO- $d_6$ , after addition of  $\text{D}_2\text{O}$ )  $\delta$ : 1.30 (6H, d,  $\text{CHMe}_2$ ), 3.14–3.48 (2H, m,  $\text{CH}_2$ -5'), 3.63 (1H, q,  $\text{CHMe}_2$ ), 3.95 (1H, m, H-4'), 4.17 (1H, dd, H-3'), 4.90 (1H, dd, H-2'), 5.82 (1H, d,  $J=6.8$  Hz, H-1'), 8.02 (1H, s, H-2).

**2',3',5'-Tris-*O*-(*tert*-butyldimethylsilyl)-8-hydroxymethyladenosine (13)**—The C-8 formylation of **4** (766 mg, 1.26 mmol) with  $\text{HCO}_2\text{Me}$  (0.46 ml, 7.5 mmol) was carried out for 3 h by the same procedure as used for the preparation of **7**. The reaction mixture containing **12** was diluted with MeOH and treated with  $\text{NaBH}_4$ . After being quenched with AcOH, the mixture was evaporated to dryness. The resulting mixture was taken up into  $\text{CHCl}_3$ – $\text{H}_2\text{O}$ . The organic layer was separated, dried ( $\text{Na}_2\text{SO}_4$ ), and chromatographed on a silica gel column (4% EtOH in  $\text{CHCl}_3$ ) to give **13** (245 mg, 61%) as a foam. *Anal.* calcd for  $\text{C}_{29}\text{H}_{57}\text{N}_5\text{O}_7\text{Si}_3$ : C, 54.45; H, 8.98; N, 10.95. Found: C, 54.74; H, 9.20; N, 10.75. MS  $m/z$ : 583 (M–Bu-*tert*), 165 (B+1). UV  $\lambda_{\text{max}}^{\text{MeOH}}$  nm ( $\epsilon$ ): 262 (15900),  $\lambda_{\text{min}}^{\text{MeOH}}$  nm ( $\epsilon$ ): 231 (4100).  $^1\text{H-NMR}$  ( $\text{CDCl}_3$ )  $\delta$ : 0.02–0.16 (18H, m, SiMe), 0.75–0.83 (27H, m, SiBu-*tert*), 3.57–3.80 (1H, m, H-4'), 3.94–4.07 (2H, m,  $\text{CH}_2$ -5'), 4.50 (1H, dd, H-3'), 4.91 (2H, s, 8- $\text{CH}_2\text{OH}$ ), 5.34 (1H, dd, H-2'), 5.92 (1H, d,  $J=5.9$  Hz, H-1'), 8.27 (1H, s, H-2).

**8-Hydroxymethyladenosine (14)**—Compound **13** (176 mg, 0.28 mmol) was deprotected with  $\text{TBAF} \cdot 3\text{H}_2\text{O}$  (309 mg, 0.96 mmol) in THF (15 ml) as described for the preparation of **8**. Florisil column chromatography (30% EtOH in  $\text{CHCl}_3$ ) gave **14** (72 mg, 87%). Crystallization from EtOH– $\text{H}_2\text{O}$  gave an analytical sample (mp 209–210 °C). *Anal.* Calcd for  $\text{C}_{11}\text{H}_{15}\text{N}_5\text{O}_5$ : C, 44.44; H, 5.09; N, 23.56. Found: C, 44.56; H, 5.11; N, 23.30. MS  $m/z$ : 166 (B+2). UV  $\lambda_{\text{max}}^{\text{H}_2\text{O}}$  nm ( $\epsilon$ ): 263 (15000),  $\lambda_{\text{min}}^{\text{H}_2\text{O}}$  nm ( $\epsilon$ ): 230 (2500).  $^1\text{H-NMR}$  (DMSO- $d_6$ , after addition of  $\text{D}_2\text{O}$ )  $\delta$ : 3.58 (2H, m,  $\text{CH}_2$ -5'), 4.01 (1H, m, H-4'), 4.18 (1H, dd, H-3'), 4.61, 4.72 (2H, each as d, 8- $\text{CH}_2\text{OH}$ ), 4.82 (1H, dd, H-2'), 6.02 (1H, d,  $J=7.3$  Hz, H-1'), 8.10 (1H, s, H-2).

**2',3',5'-Tris-*O*-(*tert*-butyldimethylsilyl)-8-formylinosine (15)**—The C-8 formylation of **5** (916 mg, 1.5 mmol) with  $\text{HCO}_2\text{Me}$  (0.46 ml, 7.5 mmol) was carried out for 3 h by the same procedure as used for the preparation of **7**. Silica gel column chromatography (benzene : EtOAc = 4 : 1) gave **15** (680 mg, 71%), which was crystallized from MeOH (mp 210–212 °C). *Anal.* Calcd for  $\text{C}_{29}\text{H}_{54}\text{N}_4\text{O}_6\text{Si}_3$ : C, 54.53; H, 8.52; N, 8.77. Found: C, 54.84; H, 8.85; N, 8.49. MS  $m/z$ : 581 (M–Bu-*tert*), 164 (B+1). IR ( $\text{CHCl}_3$ )  $\text{cm}^{-1}$ : 1690 (CHO). UV  $\lambda_{\text{max}}^{\text{MeOH}}$  nm ( $\epsilon$ ): 251 (8600),  $\lambda_{\text{shoulder}}^{\text{MeOH}}$  nm ( $\epsilon$ ): 263 (6900),  $\lambda_{\text{min}}^{\text{MeOH}}$  nm ( $\epsilon$ ): 226 (5100).  $^1\text{H-NMR}$  ( $\text{CDCl}_3$ )  $\delta$ : 0.04–0.16 (18H, m, SiMe), 0.76–0.98 (27H, m, SiBu-*tert*), 3.69–4.06 (3H, m, H-4',  $\text{CH}_2$ -5'), 4.51 (1H, m, H-3'), 5.20 (1H, dd, H-2'), 6.86 (1H, d,  $J=6.1$  Hz, H-1'), 8.28 (1H, s, H-2), 9.99 (1H, s, 8-CHO), 12.95 (1H, br, NH).

**2',3',5'-Tris-*O*-(*tert*-butyldimethylsilyl)-8-hydroxymethylinosine (16)**—Compound **15** (639 mg, 1.0 mmol) in MeOH (20 ml) was treated with  $\text{NaBH}_4$  (82 mg, 2.2 mmol) at room temperature for 15 min. After being quenched with AcOH, the mixture was evaporated to dryness. Chromatographic purification of the residue (2% EtOH in  $\text{CHCl}_3$ ) gave **16** (589 mg, 92%), which was crystallized from MeOH (mp 250–251 °C). *Anal.* Calcd for  $\text{C}_{29}\text{H}_{56}\text{N}_4\text{O}_6\text{Si}_3$ : C, 54.36; H, 8.81; N, 8.74. Found: C, 54.48; H, 8.99; N, 8.74. MS  $m/z$ : 584 (M–Bu-*tert*), 166 (B+1). UV  $\lambda_{\text{max}}^{\text{MeOH}}$  nm ( $\epsilon$ ): 252 (13400),  $\lambda_{\text{shoulder}}^{\text{MeOH}}$  nm ( $\epsilon$ ): 264 (7700),  $\lambda_{\text{min}}^{\text{MeOH}}$  nm ( $\epsilon$ ): 227 (6000).  $^1\text{H-NMR}$  ( $\text{CDCl}_3$ )  $\delta$ : 0.06–0.15 (18H, m, SiMe), 0.76–0.96 (27H, m, SiBu-*tert*), 3.69–3.94 (3H, m,  $\text{CH}_2$ -5', 8- $\text{CH}_2\text{OH}$ ), 4.11 (1H, m, H-4'), 4.40 (1H, dd, H-3'), 4.91–5.04 (3H, m, H-2', 8- $\text{CH}_2\text{OH}$ ), 6.00 (1H, d,  $J=6.4$  Hz, H-1'), 8.15 (1H, s, H-2), 13.06 (1H, br, NH).

**8-Hydroxymethylinosine (17)**—Compound **16** (322 mg, 0.5 mmol) was deprotected with  $\text{TBAF} \cdot 3\text{H}_2\text{O}$  (552 mg, 1.75 mmol) in THF (15 ml) as described for the preparation of **8**. Florisil column chromatography (50% EtOH in  $\text{CHCl}_3$ ) gave **17** (122 mg, 82%), which was crystallized from MeOH (mp >290 °C). *Anal.* calcd for  $\text{C}_{11}\text{H}_{14}\text{N}_4\text{O}_6 \cdot 2/3\text{H}_2\text{O}$ : C, 42.58; H, 4.98; N, 18.05. Found: C, 42.60; H, 4.68; N, 17.78. MS  $m/z$ : 152 (B+1). UV  $\lambda_{\text{max}}^{\text{H}_2\text{O}}$  nm ( $\epsilon$ ): 252 (12000),  $\lambda_{\text{min}}^{\text{H}_2\text{O}}$  nm ( $\epsilon$ ): 225 (3400).  $^1\text{H-NMR}$  (DMSO- $d_6$ , after addition of  $\text{D}_2\text{O}$ )  $\delta$ : 3.46–3.50 (2H, m,  $\text{CH}_2$ -5'), 3.94 (1H, m, H-4'), 4.16 (1H, m, H-3'), 4.59, 4.67 (2H, each as d, 8- $\text{CH}_2\text{OH}$ ), 4.74 (1H, dd, H-2'), 5.99 (1H,

d,  $J=6.3$  Hz, H-1'), 8.05 (1H, s, H-2).

**2',3',5'-Tris-*O*-(*tert*-butyldimethylsilyl)-8-formylguanosine (18)**—The C-8 formylation of **6** (614 mg, 1.0 mmol) with  $\text{HCO}_2\text{Me}$  (0.3 ml, 5.0 mmol) was carried out for 2 h by the same procedure as used for the preparation of **7**. Silica gel column chromatography (3% EtOH in  $\text{CHCl}_3$ ) gave **18** (262 mg, 41%). MS  $m/z$ : 596 (*M* - Bu-*tert*), 179 (*B* + 1). UV  $\lambda_{\text{max}}^{\text{MeOH}}$  nm: 337, 258,  $\lambda_{\text{shoulder}}^{\text{MeOH}}$  nm: 266,  $\lambda_{\text{min}}^{\text{MeOH}}$  nm: 291, 231.  $^1\text{H-NMR}$  ( $\text{CDCl}_3$ )  $\delta$ : 0.04–0.16 (18H, m, SiMe), 0.78–0.98 (27H, m, SiBu-*tert*), 3.71–3.94 (2H, m,  $\text{CH}_2$ -5'), 4.05 (1H, m, H-4'), 4.46 (1H, m, H-3'), 5.09 (1H, t, H-2'), 6.64 (1H, d,  $J=5.6$  Hz, H-1'), 6.79 (2H, br,  $\text{NH}_2$ ), 9.98 (1H, s, 8-CHO), 12.15 (1H, s, NH).

**8-Hydroxymethylguanosine (19)**—Compound **18** (134 mg, 0.21 mmol) in MeOH (4 ml) and THF (1 ml) was treated with  $\text{NaBH}_4$  (22 mg, 0.6 mmol) at room temperature for 15 min. After being quenched with AcOH, the mixture was evaporated to dryness. The resulting residue was dissolved in  $\text{CHCl}_3$  and the solution was washed with  $\text{H}_2\text{O}$ . The organic layer was separated, dried ( $\text{Na}_2\text{SO}_4$ ), filtered, and evaporated. The residue thus obtained was treated with  $\text{TBAF} \cdot 3\text{H}_2\text{O}$  (231 mg, 0.73 mmol) in THF (5 ml) as described for the preparation of **8**. Florisil column chromatography (40% EtOH in  $\text{CHCl}_3$ ) gave **19** (57 mg, 86%), which was crystallized from MeOH- $\text{H}_2\text{O}$  (mp 212–214 °C). Anal. Calcd for  $\text{C}_{11}\text{H}_{15}\text{N}_5\text{O}_6 \cdot 1/2\text{H}_2\text{O}$ : C, 40.99; H, 5.17; N, 21.73. Found: C, 41.22; H, 5.39; N, 21.43. MS  $m/z$ : 181 (*B* + 1). UV  $\lambda_{\text{max}}^{\text{H}_2\text{O}}$  nm ( $\epsilon$ ): 259 (7200),  $\lambda_{\text{shoulder}}^{\text{H}_2\text{O}}$  nm ( $\epsilon$ ): 270 (5900),  $\lambda_{\text{min}}^{\text{H}_2\text{O}}$  nm ( $\epsilon$ ): 226 (2300).  $^1\text{H-NMR}$  ( $\text{DMSO}-d_6$ , after addition of  $\text{D}_2\text{O}$ )  $\delta$ : 2.53–2.57 (2H, m,  $\text{CH}_2$ -5'), 3.89 (1H, m, H-4'), 4.13 (1H, dd, H-3'), 4.43, 4.61 (2H, each as d, 8- $\text{CH}_2\text{OH}$ ), 5.84 (1H, d,  $J=6.8$  Hz, H-1').

**2',3',5'-Tris-*O*-(*tert*-butyldimethylsilyl)-*N*<sup>6</sup>,8-bis(methoxycarbonyl)adenosine (20) and 2',3',5'-Tris-*O*-(*tert*-butyldimethylsilyl)-8-(*N,N*-diisopropylcarbamoyl)-*N*<sup>6</sup>-methoxycarbonyl-adenosine (21)**—The methoxycarbonylation of **4** (915 mg, 1.5 mmol) with  $\text{ClCO}_2\text{Me}$  (0.58 ml, 7.5 mmol) was carried out for 3 h by the same procedure as used for the preparation of **7**. Silica gel column chromatography ( $\text{CHCl}_3$ ) gave **20** (288 mg, a syrup, 27%) and **21** (503 mg, a foam, 50%).

Physical data for **20** are as follows. MS  $m/z$ : 670 (*M* + 1 - Bu-*tert*), 638 (*M* + 1 - Bu-*tert* - OMe), 220 (*B* + 1 - OMe). UV  $\lambda_{\text{max}}^{\text{MeOH}}$  nm: 280,  $\lambda_{\text{min}}^{\text{MeOH}}$  nm: 242.  $^1\text{H-NMR}$  ( $\text{CDCl}_3$ )  $\delta$ : 0.03–0.16 (18H, m, SiMe), 0.77–0.97 (27H, m, SiBu-*tert*), 3.67–4.19 (3H, m, H-4',  $\text{CH}_2$ -5'), 3.88, 4.07 (6H, each as s, *N*<sup>6</sup>- $\text{CO}_2\text{Me}$ , 8- $\text{CO}_2\text{Me}$ ), 4.57 (1H; m, H-3'), 5.58 (1H, dd, H-2'), 6.83 (1H, d, H-1'), 8.24 (1H, br, NH), 8.79 (1H, s, H-2).

Physical data for **21** are as follows. MS  $m/z$ : 320 (*B* + 1), 261 (*B* + 1 -  $\text{CO}_2\text{Me}$ ). UV  $\lambda_{\text{max}}^{\text{MeOH}}$  nm: 270,  $\lambda_{\text{min}}^{\text{MeOH}}$  nm: 235.  $^1\text{H-NMR}$  ( $\text{CDCl}_3$ )  $\delta$ : 0.08–0.23 (18H, m, SiMe), 0.78–0.94 (27H, m, SiBu-*tert*), 1.24, 1.57 (12H, each as dd,  $\text{CHMe}_2$ ), 3.53–4.07 (5H, m, H-4',  $\text{CH}_2$ -5',  $\text{CHMe}_2$ ), 4.59 (1H, m, H-3'), 5.53 (1H, dd, H-2'), 5.85 (1H, d,  $J=5.9$  Hz, H-1'), 8.01 (1H, br, NH), 8.73 (1H, s, H-2).

**2',3',5'-Tris-*O*-(*tert*-butyldimethylsilyl)-8-methoxycarbonyl-adenosine (22) and 2',3',5'-Tris-*O*-(*tert*-butyldimethylsilyl)-adenosine-8-carboxamide (23)**—Compound **20** (288 mg, 0.4 mmol) was treated with  $\text{NH}_3/\text{MeOH}$  (15 ml) overnight. After evaporation of the solvent, the residue was chromatographed on a silica gel column (1–2% EtOH in  $\text{CHCl}_3$ ). This afforded **22** (63 mg, a foam, 24%) and **23** (119 mg, a powder, 46%).

Physical data for **22** are as follows. MS  $m/z$ : 611 (*M* - Bu-*tert*), 162 (*B* + 1 - OMe). UV  $\lambda_{\text{max}}^{\text{MeOH}}$  nm: 278,  $\lambda_{\text{min}}^{\text{MeOH}}$  nm: 244.  $^1\text{H-NMR}$  ( $\text{CDCl}_3$ )  $\delta$ : 0.02–0.16 (18H, m, SiMe), 0.77–0.96 (27H, m, SiBu-*tert*), 3.61–4.09 (3H, m, H-4',  $\text{CH}_2$ -5'), 3.91 (3H, s, 8- $\text{CO}_2\text{Me}$ ), 4.62 (1H, m, H-3'), 5.51 (1H, dd, H-2'), 5.76 (2H, br,  $\text{NH}_2$ ), 7.16 (1H, d,  $J=5.4$  Hz, H-1'), 8.76 (1H, s, H-2).

Physical data for **23** are as follows. MS  $m/z$ : 176 (*B* + 1). UV  $\lambda_{\text{max}}^{\text{MeOH}}$  nm: 285,  $\lambda_{\text{min}}^{\text{MeOH}}$  nm: 246.  $^1\text{H-NMR}$  ( $\text{CDCl}_3$ )  $\delta$ : 0.02–0.16 (18H, m, SiMe), 0.79–0.97 (27H, m, SiBu-*tert*), 3.74 (1H, m, H-4'), 4.05 (2H, m,  $\text{CH}_2$ -5'), 4.67 (1H, dd, H-3'), 5.51 (1H, dd, H-2'), 5.78 (2H, br,  $\text{NH}_2$ ), 7.13 (1H, d,  $J=4.9$  Hz, H-1'), 8.34 (1H, s, H-2).

**2',3',5'-Tris-*O*-(*tert*-butyldimethylsilyl)-8-(*N,N*-diisopropylcarbamoyl)-adenosine (24)**—Compound **21** (503 mg, 0.68 mmol) was treated with  $\text{NH}_3/\text{MeOH}$  (20 ml) overnight. After evaporation of the solvent, the residue was chromatographed on a silica gel column (1% EtOH in  $\text{CHCl}_3$ ). This afforded **24** (393 mg, 79%) as a foam. MS  $m/z$ : 680 (*M* + 1 - Bu-*tert*), 263 (*B* + 2), 162 (*B* + 1 -  $\text{NPr}_2$ ). UV  $\lambda_{\text{max}}^{\text{MeOH}}$  nm: 270,  $\lambda_{\text{min}}^{\text{MeOH}}$  nm: 235.  $^1\text{H-NMR}$  ( $\text{CDCl}_3$ )  $\delta$ : 0.08–0.23 (18H, m, SiMe), 0.89–1.02 (27H, m, SiBu-*tert*), 1.29, 1.65 (12H, each as dd,  $\text{CHMe}_2$ ), 3.67–4.24 (5H, m, H-4',  $\text{CH}_2$ -5',  $\text{CHMe}_2$ ), 4.72 (1H, m, H-3'), 5.62 (1H, dd, H-2'), 5.77 (2H, br,  $\text{NH}_2$ ), 5.90 (1H, d,  $J=5.9$  Hz, H-1'), 8.38 (1H, s, H-2).

**8-Methoxycarbonyl-adenosine (25)**—Compound **22** (39 mg, 0.06 mmol) was deprotected with  $\text{TBAF} \cdot 3\text{H}_2\text{O}$  (66 mg, 0.21 mmol) in THF (4 ml) as described for the preparation of **8**. Florisil column chromatography (8% EtOH in  $\text{CHCl}_3$ ) gave **25** (16 mg, 82%), which was crystallized from MeOH (mp 200–201 °C, lit.<sup>6b</sup>) mp 199–200 °C). UV  $\lambda_{\text{max}}^{\text{MeOH}}$  nm: 278,  $\lambda_{\text{min}}^{\text{MeOH}}$  nm: 246.  $^1\text{H-NMR}$  ( $\text{DMSO}-d_6$ , after addition of  $\text{D}_2\text{O}$ )  $\delta$ : 2.54 (3H, s, 8- $\text{CO}_2\text{Me}$ ), 3.51–3.64 (2H, m,  $\text{CH}_2$ -5'), 4.00 (1H, m, H-4'), 4.14 (1H, m, H-3'), 4.83 (1H, dd, H-2'), 5.77 (1H, d,  $J=7.3$  Hz, H-1'), 8.05 (1H, s, H-2).

**Adenosine-8-carboxamide (26)**—Compound **23** (93 mg, 0.14 mmol) was deprotected with  $\text{TBAF} \cdot 3\text{H}_2\text{O}$  (155 mg, 0.49 mmol) in THF (5 ml) as described for the preparation of **8**. Florisil column chromatography (40% EtOH in  $\text{CHCl}_3$ ) gave **26** (38 mg, 86%), which was crystallized from EtOH (mp 250–251 °C, lit.<sup>6b</sup>) mp 249–251 °C). MS  $m/z$ : 181 (*B* + 1). UV  $\lambda_{\text{max}}^{\text{H}_2\text{O}}$  nm: 289,  $\lambda_{\text{min}}^{\text{H}_2\text{O}}$  nm: 245.  $^1\text{H-NMR}$  ( $\text{DMSO}-d_6$ )  $\delta$ : 3.49–3.71 (2H, m,  $\text{CH}_2$ -5'), 3.94 (1H, m, H-4'), 4.17–4.20 (1H, m, H-3'), 4.94–4.98 (1H, m, H-2'), 5.08–5.60 (3H, m, 2'-OH, 3'-OH, 5'-OH), 6.77 (1H, d,  $J=6.6$  Hz, H-1'), 7.58 (2H, br,  $\text{NH}_2$ ), 8.00 (2H, br, 8- $\text{CONH}_2$ ), 8.18 (1H, s, H-2).

**Adenosine-8-(*N,N*-diisopropyl)carboxamide (27)**—Compound **24** (153 mg, 0.2 mmol) was deprotected with TBAF·3H<sub>2</sub>O (221 mg, 0.7 mmol) in THF (7 ml) as described for the preparation of **8**. Florisil column chromatography (8% EtOH in CHCl<sub>3</sub>) gave **27** (64 mg, 81%), which was crystallized from EtOH-H<sub>2</sub>O (mp 238–240 °C). *Anal.* Calcd for C<sub>17</sub>H<sub>26</sub>N<sub>6</sub>O<sub>5</sub>: C, 51.77; H, 6.64; N, 21.31. Found: C, 52.02; H, 6.83; N, 21.37. MS *m/z*: 263 (B+2), 262 (B+1), 162 (B+1-NPr<sub>2</sub>). UV λ<sub>max</sub><sup>H<sub>2</sub>O</sup> nm (ε): 268 (15600), λ<sub>min</sub><sup>H<sub>2</sub>O</sup> nm (ε): 239 (7400). <sup>1</sup>H-NMR (DMSO-*d*<sub>6</sub>, after addition of D<sub>2</sub>O) δ: 1.21, 1.49 (12H, each as dd, CHMe<sub>2</sub>), 3.59–3.81 (4H, m, CH<sub>2</sub>-5', CHMe<sub>2</sub>), 4.01 (1H, m, H-4'), 4.19 (1H, dd, H-3'), 4.97 (1H, dd, H-2'), 5.65 (1H, d, *J* = 6.8 Hz, H-1'), 8.20 (1H, s, H-2).

**2',3',5'-Tris-*O*-(*tert*-butyldimethylsilyl)-8-methoxycarbonylinosine (28)**—The methoxycarbonylation of **5** (611 mg, 1.0 mmol) with ClCO<sub>2</sub>Me (0.39 ml, 5.0 mmol) was carried out for 1 h by the same procedure as used for the preparation of **7**. Silica gel column chromatography (1% EtOH in CHCl<sub>3</sub>) gave **28** (418 mg, 61%) as a syrup. MS *m/z*: 612 (M-Bu-*tert*), 208 (B+1). UV λ<sub>max</sub><sup>MeOH</sup> nm: 287, λ<sub>min</sub><sup>MeOH</sup> nm: 240. <sup>1</sup>H-NMR (CDCl<sub>3</sub>) δ: 0.02–0.16 (18H, m, SiMe), 0.80–0.97 (27H, m, SiBu-*tert*), 3.78 (1H, m, H-4'), 4.01 (3H, s, 8-CO<sub>2</sub>Me), 4.03 (2H, m, CH<sub>2</sub>-5'), 4.51 (1H, m, H-3'), 5.38 (1H, dd, H-2'), 6.84 (1H, d, H-1'), 8.26 (1H, s, H-2), 12.89 (1H, br, NH).

**8-Methoxycarbonylinosine (29)**—Compound **28** (305 mg, 0.46 mmol) was deprotected with TBAF·3H<sub>2</sub>O (497 mg, 1.6 mmol) in THF (10 ml) as described for the preparation of **8**. Florisil column chromatography (15% EtOH in CHCl<sub>3</sub>) gave **29** (109 mg, 73%), which was crystallized from EtOH (mp 189–190 °C, dec.). *Anal.* calcd for C<sub>12</sub>H<sub>14</sub>N<sub>4</sub>O<sub>7</sub>: C, 44.18; H, 4.32; N, 17.17. Found: C, 44.51; H, 4.50; N, 16.81. MS *m/z*: 194 (B+1), 134 (B+1-CO<sub>2</sub>Me). UV λ<sub>max</sub><sup>H<sub>2</sub>O</sup> nm (ε): 284 (13200), λ<sub>min</sub><sup>H<sub>2</sub>O</sup> nm (ε): 240 (3500). <sup>1</sup>H-NMR (DMSO-*d*<sub>6</sub>) δ: 3.50–3.63 (2H, m, CH<sub>2</sub>-5'), 3.93 (3H, s, 8-CO<sub>2</sub>Me), 4.19–4.27 (2H, m, H-3', H-4'), 4.87–4.96 (2H, m, H-2', 5'-OH), 5.13, 5.33 (2H, each as d, 2'-OH, 3'-OH), 6.58 (1H, d, *J* = 5.9 Hz, H-1'), 8.20 (1H, s, H-2), 12.69 (1H, br, NH).

**Acknowledgement** The authors thank Dr. A. Yamazaki, Ajinomoto Co., Inc., for his private communication of physical data for 8-methylinosine.

#### References

- 1) This paper is dedicated to Professor Morio Ikehara on the occasion of his retirement from Osaka University in March, 1986.
- 2) a) H. Tanaka, H. Hayakawa, and T. Miyasaka, *Tetrahedron*, **38**, 2635 (1982); b) H. Tanaka, A. Matsuda, S. Iijima, H. Hayakawa, and T. Miyasaka, *Chem. Pharm. Bull.*, **31**, 2164 (1983); c) H. Tanaka, H. Hayakawa, S. Iijima, K. Haraguchi, and T. Miyasaka, *Tetrahedron*, **41**, 861 (1985); d) H. Hayakawa, H. Tanaka, and T. Miyasaka, *ibid.*, **41**, 1675 (1985); e) H. Hayakawa, H. Tanaka, Y. Maruyama, and T. Miyasaka, *Chem. Lett.*, **1985**, 1401; f) H. Tanaka, H. Hayakawa, K. Obi, and T. Miyasaka, *Tetrahedron Lett.*, **26**, 6229 (1985); g) H. Tanaka, M. Hirayama, M. Suzuki, T. Miyasaka, A. Matsuda, and T. Ueda, *Tetrahedron*, **42**, 1971 (1986).
- 3) H. Tanaka, Y. Uchida, M. Shinozaki, H. Hayakawa, A. Matsuda, and T. Miyasaka, *Chem. Pharm. Bull.*, **31**, 787 (1983).
- 4) The reaction of the C-8 lithiated species of a 6-chloropurine ribonucleoside with diethyl chlorophosphate has also been reported: T. Maruyama, S. Kimura, M. Horikawa, Y. Sato, and M. Honjo, *Nucleic Acids Symposium Series*, **12**, 43 (1983).
- 5) a) H. Steinmaus, I. Rosenthal, and D. Elad, *J. Org. Chem.*, **36**, 3594 (1971); b) M. Maeda, K. Nushi, and Y. Kawazoe, *Tetrahedron*, **30**, 2677 (1974); c) L. F. Christensen, R. B. Meyer, Jr., J. P. Miller, L. N. Simon, and R. K. Robins, *Biochemistry*, **14**, 1490 (1975); d) M. Ikehara, W. Limn, and T. Fukui, *Chem. Pharm. Bull.*, **25**, 2702 (1977); e) Y. Maki, K. Kameyama, M. Sako, and K. Hirota, *Tetrahedron Lett.*, **24**, 799 (1983).
- 6) a) T. Naka and M. Honjo, *Chem. Pharm. Bull.*, **24**, 2052 (1976); b) A. Matsuda, Y. Nomoto, and T. Ueda, *ibid.*, **27**, 183 (1979); c) T. Ueda, Y. Nomoto, and A. Matsuda, *ibid.*, **33**, 3263 (1985).
- 7) N. Công-Danh, J.-P. Beaucourt, and L. Pichat, *Tetrahedron Lett.*, **1979**, 3159.
- 8) D. H. R. Barton, C. J. R. Hedgcock, E. Lederer, and W. B. Motherwell, *Tetrahedron Lett.*, **1979**, 279.
- 9) N. Công-Danh, J.-P. Beaucourt, and L. Pichat, *Tetrahedron Lett.*, **1979**, 2385.
- 10) R. Romero, R. Stein, H. G. Bull, and E. H. Cordes, *J. Am. Chem. Soc.*, **100**, 7620 (1978) and references cited therein.
- 11) T. W. Greene, "Protective Groups in Organic Synthesis," John Wiley and Sons, Inc., New York, Chichester, Brisbane, Toronto, 1981, p. 44.
- 12) K. K. Ogilvie, S. L. Beaucage, A. L. Schiffman, N. Y. Theriault, and K. L. Sadana, *Can. J. Chem.*, **56**, 2768 (1978).
- 13) K. K. Ogilvie, A. L. Schiffman, and C. L. Penney, *Can. J. Chem.*, **57**, 2230 (1979).
- 14) M. Maeda, M. Saneyoshi, and Y. Kawazoe, *Chem. Pharm. Bull.*, **19**, 1641 (1971) and references cited therein.
- 15) LDA is thought to act through an "acid-base mechanism." H. W. Gschwend and H. R. Rodriguez, "Organic Reactions," Vol. 26, ed. by W. G. Dauben, John Wiley and Sons, Inc., New York, Chichester, Brisbane, Toronto, 1979, pp. 1–360.
- 16) LTMP is reported to be 1.6 pK units more basic than LDA: R. R. Fraser, A. Baignée, M. Breese, and K. Hata, *Tetrahedron Lett.*, **23**, 4195 (1982).

[Chem. Pharm. Bull.]  
35(1) 80-89 (1987)

## Synthesis of Novel Pyridotriazepinones as Antisecretory Agents

SHIN-ICHI KODATO,\*<sup>a</sup> HIROSHI WADA,<sup>a</sup> SEIICHI SAITO,<sup>a</sup> MIKIO TAKEDA,<sup>a</sup>  
YOSHIHIKO NISHIBATA,<sup>a</sup> KEIICHI AOE,<sup>a</sup> TADAMASA DATE,<sup>a</sup>  
YUICHI ONODA,<sup>b</sup> and HAJIME TAMAKI<sup>b</sup>

*Organic Chemistry Research Laboratory<sup>a</sup> and Biological Research Laboratory,<sup>b</sup>  
Tanabe Seiyaku Co., Ltd., 2-2-50, Kawagishi, Toda-shi,  
Saitama 335, Japan*

(Received June 6, 1986)

In connection with the known antisecretory activity of the benzotriazepinone (1) and the pyridylurea (2), novel pyridotriazepinones (3 and 4) have been synthesized. They were prepared from aminopyridinecarboxylic acids *via* several steps, and their structures were confirmed by X-ray crystallographic analysis. Attempts to synthesize the positional isomer (24) resulted in formation of the pyridotriazine (25 or 26). Some of these compounds showed moderate antisecretory activity in rats.

**Keywords**—pyrido[2,3-*f*]-1,2,4-triazepinone; pyrido[2,3-*e*]-1,2,4-triazepinone; X-ray analysis; 1,3,4-oxadiazole; pyridotriazine; antisecretory activity; ring contraction

Some antisecretory compounds have their origins in psychotropic agents.<sup>1)</sup> Among such compounds, 1,4-dihydro-4-methyl-5*H*-benzo-1,2,4-triazepin-5-one (1) is known to have antisecretory activity with diminished central nervous system (CNS) activity.<sup>2)</sup> On the other hand, a number of pyridine derivatives were recently reported to inhibit gastric acid secretion, as exemplified by the pyridylurea derivative (2).<sup>3)</sup> In the course of our continuing studies on antisecretory agents, we were interested in the activities of 1,4-dihydro-4-methyl-5*H*-pyrido[2,3-*f*]-1,2,4-triazepin-5-one (3) and 1,4-dihydro-4-methyl-5*H*-pyrido[2,3-*e*]-1,2,4-triazepin-5-one (4), which are pyrido analogues of 1. No reports have appeared on the synthesis and biological activity of pyridotriazepinones, in contrast with benzotriazepinone derivatives.<sup>4)</sup> We describe here the syntheses of the new pyridotriazepinones (3, 4) and the results of several attempts to synthesize the other positional isomer (24). Since structural assignment for benzotriazepinones has sometimes been erroneous and has been intensively discussed in recent papers,<sup>5)</sup> the structures of the pyrido analogues (3, 4) and related products in this study were confirmed by X-ray crystallographic analysis. The antisecretory activity of the resulting compounds determined in rats is also presented.

The pyrido[2,3-*f*]-1,2,4-triazepinone (3) was synthesized through the sequence of reactions outlined in Chart 1. 3-Aminopicolinic acid (5a) was converted to the *N*-carbobenzyloxy (CBZ) derivative (5b), which in turn was condensed with dimethyl methylamino-malonate by the use of 1*H*-benzotriazol-1-ol (HOBt) and dicyclohexylcarbodiimide (DCC) to give the amide (6a). Reductive removal of the CBZ group afforded the amino-amide (6b) as an unstable oil. On diazotization by the method of Bianchi *et al.*,<sup>2)</sup> 6b readily underwent cyclization, giving the 1,2,4-triazepinone (7) in 77% yield. Treatment of 7 with 2 molar equivalents of aqueous NaOH in MeOH gave the monocarboxylic acid (8) in 52% yield. Decarboxylation of 8 readily occurred in dioxane at 80°C and gave the desired 1,2,4-triazepinone (3) in 94% yield. The structure of 3 was unequivocally confirmed by X-ray crystallographic analysis. A perspective drawing of 3 is shown in Fig. 1.

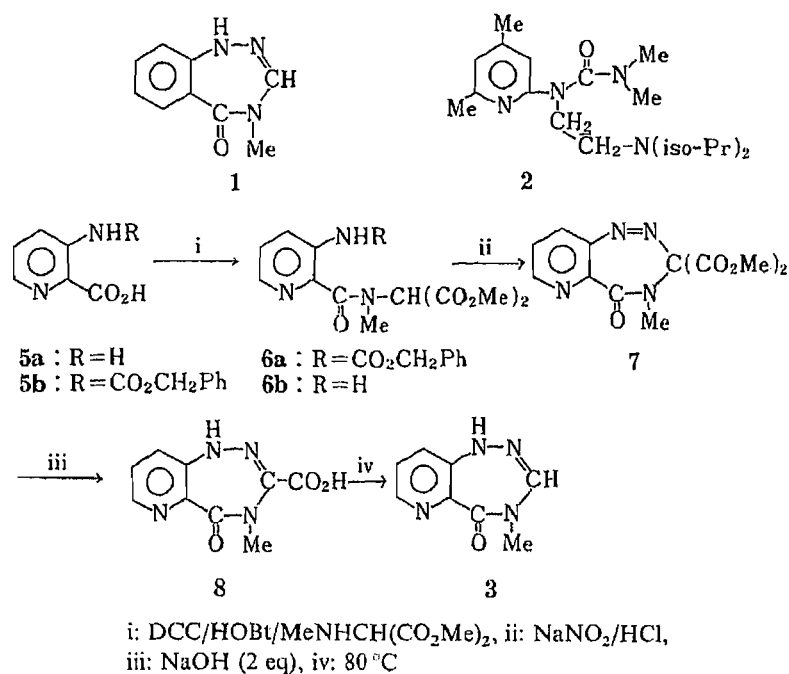


Chart 1

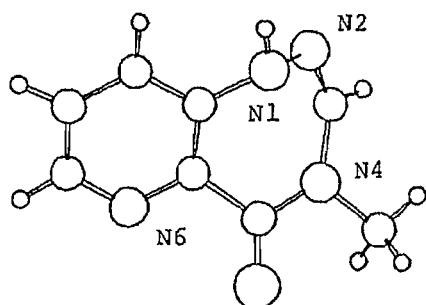
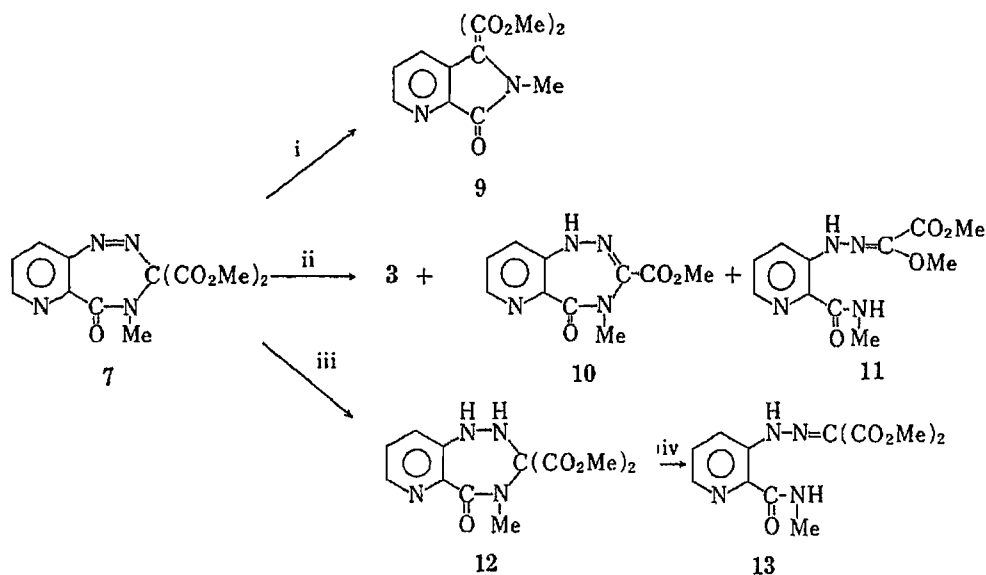


Fig. 1. A Perspective Drawing of 3

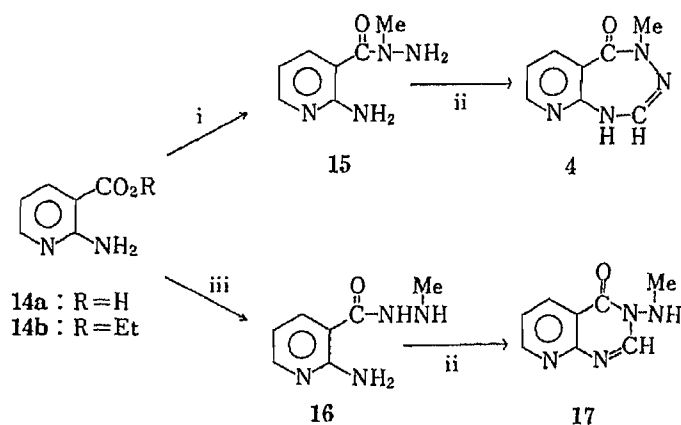
The results of other unsuccessful attempts to obtain 3 from 7 are summarized in Chart 2. On heating at 110 °C in dimethylsulfoxide (DMSO) in the presence of NaCl,<sup>6)</sup> 7 gave only the ring-contracted product (9) in 26% yield. In the mass spectrum (MS), 9 showed the molecular ion peak at  $m/e$  264 indicating loss of a nitrogen molecule from 7. The proton nuclear magnetic resonance (<sup>1</sup>H-NMR) spectrum of 9 showed signals due to the geminal methoxycarbonyl groups at  $\delta$  3.82 (6H, s) and the N-methyl group at  $\delta$  3.29 (3H, s) together with three aromatic protons at  $\delta$  7.46–8.82. In the infrared spectrum (IR), a five-membered lactam carbonyl band appeared at 1725 cm<sup>-1</sup> together with ester carbonyl bands at 1740 cm<sup>-1</sup>.

On treatment with 1 molar equivalent of NaOH in MeOH, 7 gave a mixture of the monoester (10), the ring-fissioned product (11), and the triazepinone (3) in yields of 6, 4.3, and 13%, respectively. The spectral data and elemental analysis of 10 were compatible with the assigned structure and are given in the experimental section. The <sup>1</sup>H-NMR spectrum of 11 showed, in addition to two OMe signals ( $\delta$  4.06 and 4.10), the signal due to the NMe group in the secondary amide at  $\delta$  2.95 as a doublet, which collapsed to a singlet on addition of D<sub>2</sub>O. In its IR spectrum, 11 showed strong carbonyl bands at 1675 and 1720 cm<sup>-1</sup> assignable to amide and ester groups. Compound 11 was correctly analyzed for C<sub>11</sub>H<sub>14</sub>N<sub>4</sub>O<sub>4</sub> and showed the molecular ion peak at  $m/e$  266. On the basis of these data, we tentatively assigned the ring-fissioned structure (11) to this compound. Susceptibility to cleavage of the C<sub>3</sub>-N<sub>4</sub> bond of



i: 110 °C, NaCl/DMSO, ii: NaOH (1 eq)/MeOH,  
 iii: H<sub>2</sub> (1 eq)/Pd-C, iv: heat/EtOH

Chart 2



i: DCC/HOBt/MeNHNH<sub>2</sub>, ii: HC(OEt)<sub>3</sub>, iii: MeNHNH<sub>2</sub>/150 °C

Chart 3

1,2,4-triazepinones was also observed for the dihydro derivative (12), obtained by catalytic hydrogenation of 7. When heated in boiling EtOH for 7 h, 12 readily gave the ring-fissioned product (13) in 89% yield. Compound 13 showed spectroscopic data similar to those of 11 (see Experimental).

The pyrido[2,3-*e*]-1,2,4-triazepinone (4), a positional isomer of 3, was synthesized from 2-aminonicotinic acid (14a) (Chart 3). Treatment of 14a with methylhydrazine by the use of HOBt and DCC yielded the amide (15). Reaction of 15 with triethyl orthoformate (HC(OEt)<sub>3</sub>) in boiling EtOH gave the desired product (4) in 52% yield. Since the pyridopyrimidone (17) is also a possible product of this sequence of reactions,<sup>7)</sup> 17 was synthesized independently. Heating of ethyl 2-aminonicotinate (14b) with methylhydrazine yielded the secondary amide (16), which is isomeric with 15. The <sup>1</sup>H-NMR spectrum of 16 showed the NMe signal at  $\delta$  2.71 as a doublet, which collapsed to a singlet on addition of D<sub>2</sub>O. On the other hand, the NMe signal of 15 appeared at  $\delta$  3.25 as a singlet.<sup>8)</sup> Cyclization of 16 with

HC(OEt)<sub>3</sub> gave **17** in 79% yield. The difference between the <sup>1</sup>H-NMR spectra of **4** and **17** is consistent with their assigned structures. While the signal due to the NMe group of **4** appeared at  $\delta$  3.17 as a singlet, that of **17** appeared at  $\delta$  2.92 as a doublet and collapsed to a singlet on addition of D<sub>2</sub>O. The vinyl proton signal of **4** was observed at  $\delta$  6.92 as a doublet, which changed to a singlet on addition of D<sub>2</sub>O. On the other hand, the vinyl proton of **17** appeared at  $\delta$  8.49 as a singlet. Further structural confirmation of **4**, including the position of the double bond, was obtained by X-ray crystallographic analysis (Fig. 2).

We next planned to prepare pyrido-1,2,4-triazepinones (**19a, b**) having an amino group at C<sub>2</sub> by the cyclodesulfurization<sup>9)</sup> of the thiosemicarbazide (**18a, b**). However, treatment of **18a, b**<sup>10)</sup> with DCC in pyridine only yielded the 1,3,4-oxadiazole (**20a, b**) (Chart 4). Similar formation of oxadiazole derivatives was reported for the corresponding benzo analogues by Peet *et al.*<sup>11)</sup> The structural assignments of **20a, b** were based on the presence of signals due to a primary amino group in the <sup>1</sup>H-NMR spectra and the characteristic MS fragmentation pattern. These spectral data are quite similar to those reported for 2-(2-aminophenyl)-1,3,4-oxadiazole derivatives.<sup>11)</sup>

Synthesis of the 3-substituted pyrido-1,2,5-triazepinone (**24**) was also attempted (Chart 5). Condensation of 3-nitro-2-pyridylhydrazines (**21a, b**)<sup>12)</sup> with ethyl pyruvate or ethyl phenylglyoxylate gave the corresponding nitro-hydrazones (**22a—d**).<sup>13)</sup> Catalytic hydrogenation of the nitro-hydrazones (**22a, b**) afforded a mixture of the corresponding amino-

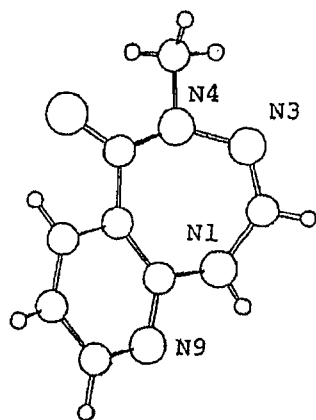


Fig. 2. A Perspective Drawing of **4**

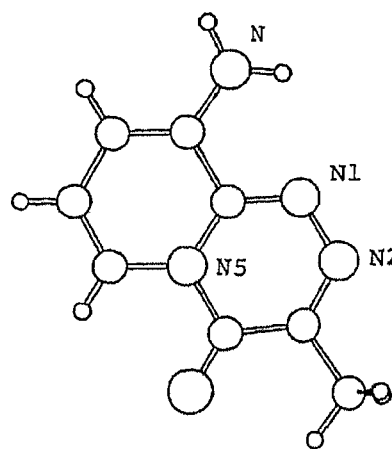
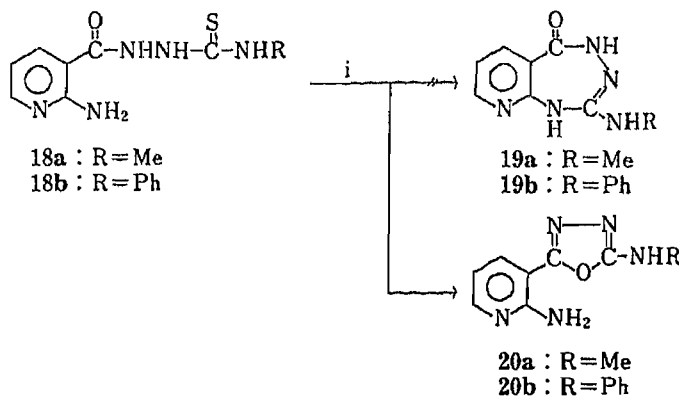


Fig. 3. A Perspective Drawing of **25a**



i: DCC/60–80 °C

Chart 4

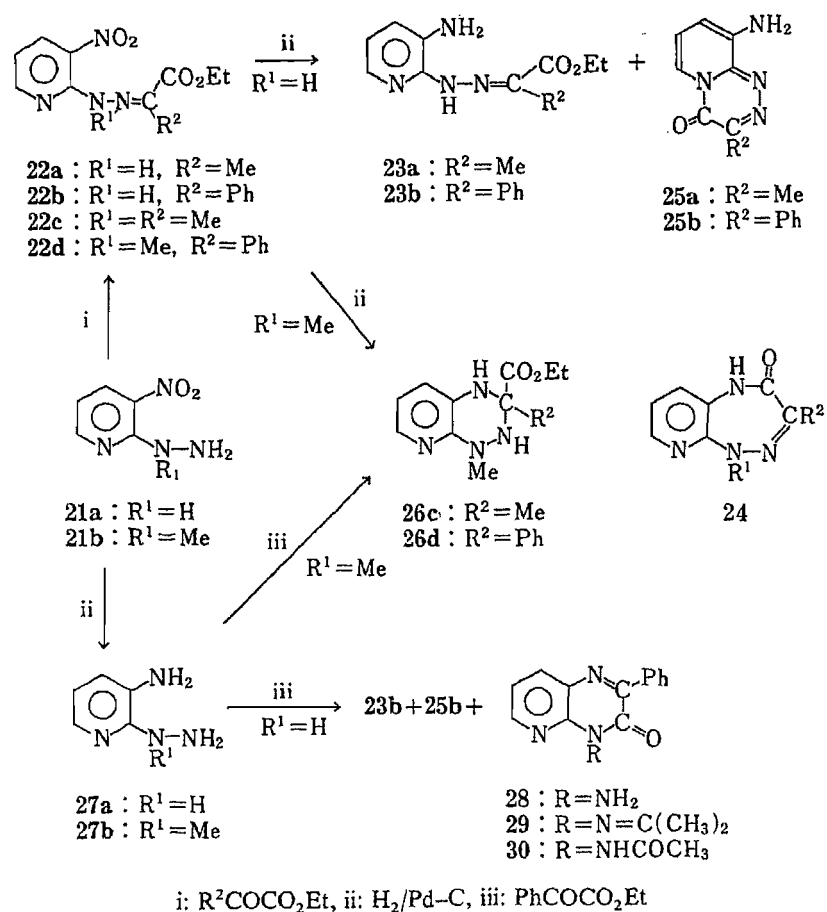


Chart 5

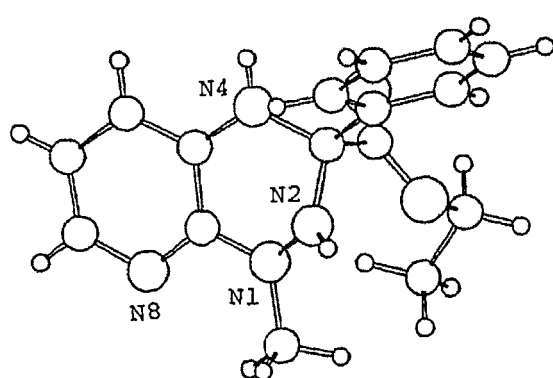


Fig. 4. A Perspective Drawing of 26d

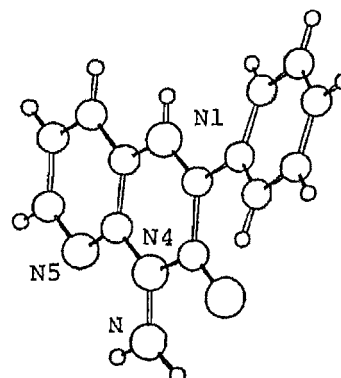


Fig. 5. A Perspective Drawing of 28

hydrazones (23a, b) and pyrido[2,1-c]triazines (25a, b) instead of the desired triazepinone (24). Since the formation of 25a, b from 23a, b might be due to a tautomeric contribution of the hydrogen on the hydrazone group, catalytic hydrogenation of the corresponding N-methyl derivative (22c) was attempted. In this case, however, the animal (26c) was obtained in 87% yield. Several attempts to convert 26c to 24 ( $R^1=R^2=Me$ ) under acidic or alkaline conditions were unsuccessful. Similarly, catalytic hydrogenation of 22d gave 26d in 59% yield. Alternatively, 26d could be obtained by the reaction of 1-(3-amino-2-pyridyl)-1-methylhydrazine (27b)<sup>12)</sup> with ethyl phenylglyoxylate in 68% yield.



TABLE I. The Antisecretory Activity of Pyridotriazepinones

Compound No.	Antisecretory activity % inhibition rat i.p.	
	at 30 mg/kg	at 100 mg/kg
3	31	59
4	51	59
7		15
8		44
10		0
12		-16
1	48	

TABLE II. Crystal Data

	3	4	25a	26d	28
Crystal system	Monoclinic	Monoclinic	Orthorhombic	Monoclinic	Orthorhombic
Space group	$P2_1/c$	$P2_1/a$	$Pbca$	$Cc$	$P2_12_12_1$
$a$ (Å)	11.190 (1)	14.183 (3)	14.446 (4)	8.735 (1)	12.810 (2)
$b$ (Å)	7.210 (4)	14.967 (3)	12.881 (3)	22.005 (5)	14.686 (3)
$c$ (Å)	10.677 (7)	3.788 (1)	8.674 (2)	9.136 (1)	5.889 (1)
$\beta$ (°)	101.128 (4)	99.58 (1)	—	118.99 (1)	—
Volume (Å <sup>3</sup> )	845.2 (1)	792.9 (3)	1614.0 (4)	1536.0 (3)	1107.9 (2)
$Z$	4	4	8	4	4
$D_c$ (g cm <sup>-3</sup> )	1.384	1.476	1.450	1.290	1.428
No. of unique reflections	1448	1351	1071	1109	1119
No. of reliable reflections $ F_o  \geq 3\sigma( F_o )$	1187	1047	1068	1086	1099
Final $R$	0.051	0.073	0.063	0.049	0.073

As an alternative route to **24** ( $R^1 = H$ ,  $R^2 = Ph$ ), condensation of the aminohydrazine (**27a**)<sup>12)</sup> with ethyl phenylglyoxylate was also attempted. The major product (51%) in this reaction, however, was the pyrido[2,3-*b*]pyrazine (**28**), compounds **23b** and **25b** being also isolated in low yields. The presence of the primary amino group in **28** was demonstrated by its conversion to the isopropylidene derivative (**29**) and the *N*-acetate (**30**). The structures of the pyridotriazines (**25a** and **26d**) and the pyridopyrazine (**28**) were unequivocally confirmed by X-ray crystallographic analysis, and perspective drawings are shown in Figs. 3, 4, and 5, respectively.

### Pharmacology

The pyridotriazepinone derivatives and related compounds obtained in this study were tested for antisecretory activity in rats after intraperitoneal (i.p.) administration by the method reported previously.<sup>14)</sup> The results are summarized in Table I together with comparative data for the benzotriazepinone (**1**). The antisecretory activity of the pyridotriazepinones (**3** and **4**) is of the same order as that of the benzo analogue (**1**).

### Experimental

All melting points are uncorrected. IR spectra were recorded in Nujol mulls on a Hitachi IR-215 spectrometer.

$^1\text{H-NMR}$  spectra were taken in  $\text{CDCl}_3$  or  $\text{DMSO-}d_6$  at 60 MHz on a JEOL PMX-60 spectrometer with tetramethylsilane (TMS) as an internal reference. The following abbreviations are used: s=singlet, d=doublet, t=triplet, q=quartet, m=multiplet, and br=broad. MS were measured with a Hitachi RMU-6M instrument. Ultraviolet (UV) spectra were measured with a Hitachi 323 spectrometer. X-Ray crystallographic analyses were performed on a Rigaku AFC-5 diffractometer.

**3-Benzyloxycarbonylamino-picolinic Acid (5b)**—A solution of benzyl chloroformate (1.30 g, 7.71 mmol) in tetrahydrofuran (THF, 2 ml) and an aqueous (aq.) solution of LiOH (0.9 N, 9 ml) were added alternately to an ice-cooled mixture of 3-aminopicolinic acid (**5a**, 0.691 g, 5 mmol), aq. LiOH (0.9 N, 6 ml), and THF (8 ml) over a period of 30 min. After being stirred at 0–5 °C for 1 h and then at room temperature for 4 h, the mixture was diluted with  $\text{H}_2\text{O}$  and washed with  $\text{Et}_2\text{O}$ . The aq. solution was then acidified (pH 2–3) with dil. HCl and extracted with  $\text{CHCl}_3$ . The  $\text{CHCl}_3$  extracts were dried over  $\text{Na}_2\text{SO}_4$  and concentrated. The residue was recrystallized from benzene to give **5b** (1.137 g, 83%), mp 174–177 °C. IR (Nujol): 1730, 1660  $\text{cm}^{-1}$ . MS *m/e*: 272 ( $\text{M}^+$ ), 228, 166. *Anal.* Calcd for  $\text{C}_{14}\text{H}_{12}\text{N}_2\text{O}_4$ : C, 61.76; H, 4.44; N, 10.29. Found: C, 61.66; H, 4.26; N, 10.41.

**Dimethyl [3-(Benzyloxycarbonylamino)-N-methylpicolinamido]malonate (6a)**—DCC (21.95 g, 106.38 mmol) and HOBt (16.3 g, 106.4 mmol) were added to an ice-cold solution of **5b** (28.95 g, 106.3 mmol) in dimethylformamide (DMF, 250 ml), and the mixture was stirred at 0 °C for 30 min. A solution of dimethyl methylaminomalonate (20.6 g, 127.8 mmol) in DMF (30 ml) was then added dropwise. After the mixture had been stirred at room temperature for 62 h, insoluble materials were filtered off, and the filtrate was concentrated *in vacuo*. The residue was diluted with  $\text{H}_2\text{O}$  and extracted with EtOAc. The EtOAc extracts were dried over  $\text{MgSO}_4$  and concentrated. The residue was purified by chromatography ( $\text{SiO}_2$ , hexane : EtOAc = 1 : 1) and recrystallized from  $\text{Et}_2\text{O}$  to give **6a** (33.9 g, 76.7%), mp 95–96 °C. IR (Nujol): 3300, 1740, 1635  $\text{cm}^{-1}$ . MS *m/e*: 415 ( $\text{M}^+$ ), 384, 356, 165.  $^1\text{H-NMR}$  ( $\text{CDCl}_3$ )  $\delta$ : 3.17 (3H, s, N-Me), 3.81 (6H, s, OMe). *Anal.* Calcd for  $\text{C}_{20}\text{H}_{21}\text{N}_3\text{O}_7$ : C, 57.83; H, 5.10; N, 10.12. Found: C, 57.81; H, 5.05; N, 9.91.

**Dimethyl (3-Amino-N-methylpicolinamido)malonate (6b)**—A mixture of **6a** (0.89 g, 2.14 mmol), 10% Pd-C (0.1 g), and MeOH (20 ml) was stirred for 2 h at room temperature under a stream of hydrogen. After removal of Pd-C, the mixture was evaporated *in vacuo* below 40 °C to give **6b** (0.69 g) as an oil. IR (liq.): 3460–3230, 1740, 1635  $\text{cm}^{-1}$ . MS *m/e*: 281 ( $\text{M}^+$ ).

**Dimethyl 4,5-Dihydro-4-methyl-5-oxo-3H-pyrido[2,3-f]-1,2,4-triazepine-3,3-dicarboxylate (7)**—A solution of  $\text{NaNO}_2$  (0.15 g, 2.17 mmol) in  $\text{H}_2\text{O}$  (2 ml) was added dropwise to a mixture of conc. HCl (4.2 ml) and ice-sticks (17 g). Next, a solution of **6b** (0.6 g, 2.12 mmol) in MeOH (6 ml) was added dropwise at –10 °C. After being stirred at 0 °C for 2 h and then at room temperature for 2 h, the mixture was made alkaline (pH 9) with conc.  $\text{NH}_4\text{OH}$  and extracted with  $\text{CHCl}_3$ . The  $\text{CHCl}_3$  extracts were dried over  $\text{Na}_2\text{SO}_4$  and concentrated *in vacuo*. The residue was purified by chromatography ( $\text{SiO}_2$ ,  $\text{CHCl}_3$ ) and recrystallized from hexane–benzene to give **7** (0.48 g, 77%), mp 138–140 °C (dec.). IR (Nujol): 1750, 1680  $\text{cm}^{-1}$ . MS *m/e*: 294 ( $\text{M}^+ + 2$ ), 264. *Anal.* Calcd for  $\text{C}_{12}\text{H}_{12}\text{N}_4\text{O}_5$ : C, 49.31; H, 4.14; N, 19.17. Found: C, 49.61; H, 4.05; N, 18.95.

**4,5-Dihydro-4-methyl-5-oxo-1H-pyrido[2,3-f]-1,2,4-triazepine-3-carboxylic Acid (8)**—Aqueous NaOH solution (10%, 1.7 ml, 4.25 mmol) was added to a solution of **7** (0.64 g, 2.19 mmol) in MeOH (7 ml) under ice-cooling (below 8 °C). The solvent was removed (below 18 °C), then the residue was diluted with  $\text{H}_2\text{O}$  and acidified with cold aq. 10% HCl (pH 2). The yellow crystalline precipitate was collected by filtration, washed with  $\text{H}_2\text{O}$ , and dried to give **8** (0.3 g, 52%), mp 100–102 °C (dec.). IR (Nujol): 3500–3280, 1710, 1665  $\text{cm}^{-1}$ . MS *m/e*: 176 ( $\text{M}^+ - \text{CO}_2$ ), 135, 107.  $^1\text{H-NMR}$  ( $\text{CDCl}_3$ )  $\delta$ : 3.08 (3H, s), 9.16 (1H, s, NH). *Anal.* Calcd for  $\text{C}_9\text{H}_8\text{N}_4\text{O}_3 \cdot 2\text{H}_2\text{O}$ : C, 42.19; H, 4.72; N, 21.87. Found: C, 42.28; H, 4.49; N, 21.56.

**1,4-Dihydro-4-methyl-5H-pyrido[2,3-f]-1,2,4-triazepin-5-one (3)**—Compound **8** (0.2 g, 0.91 mmol) was suspended in dioxane (10 ml), and the mixture was heated at 80 °C for 20 min. The solvent was removed and the residue was recrystallized from EtOAc to give **3** (0.15 g, 94%) as yellow needles, mp 179 °C (dec.). IR (Nujol): 3275, 1650  $\text{cm}^{-1}$ . MS *m/e*: 176 ( $\text{M}^+$ ), 135, 107.  $^1\text{H-NMR}$  ( $\text{CDCl}_3 + \text{DMSO-}d_6$ )  $\delta$ : 3.25 (3H, s), 6.71 (1H, s), 7.48 (1H, br s). UV  $\lambda_{\text{max}}^{\text{EtOH}}$  nm ( $\epsilon$ ): 247 (6300), 288 (4100). *Anal.* Calcd for  $\text{C}_8\text{H}_8\text{N}_4\text{O}$ : C, 54.54; H, 4.58; N, 31.80. Found: C, 54.42; H, 4.47; N, 31.79.

**Dimethyl 6,7-Dihydro-6-methyl-7-oxo-5H-pyrrolo[3,4-b]pyridine-5,5-dicarboxylate (9)**—A mixture of **7** (0.292 g, 1 mmol), NaCl (0.117 g, 2 mmol), and DMSO (3 ml) was heated at 110 °C for 10 min. After cooling, the mixture was diluted with  $\text{H}_2\text{O}$  (10 ml) and extracted with EtOAc. The EtOAc extracts were dried over  $\text{MgSO}_4$  and evaporated. The residue was purified by chromatography ( $\text{SiO}_2$ , hexane : EtOAc = 1 : 1) and digested with hexane– $\text{Et}_2\text{O}$  to give **9** (0.07 g, 26%), mp 105 °C (dec.). IR (Nujol): 1740, 1725  $\text{cm}^{-1}$ . MS *m/e*: 264 ( $\text{M}^+$ ), 220, 205, 177.  $^1\text{H-NMR}$  ( $\text{CDCl}_3$ )  $\delta$ : 3.29 (3H, s), 3.82 (6H, s), 7.46 (1H, dd,  $J_1 = 4.6$  Hz,  $J_2 = 7.6$  Hz), 8.05 (1H, dd,  $J_1 = 1.5$  Hz,  $J_2 = 7.6$  Hz), 8.82 (1H, dd,  $J_1 = 1.5$  Hz,  $J_2 = 4.6$  Hz). *Anal.* Calcd for  $\text{C}_{12}\text{H}_{12}\text{N}_2\text{O}_5$ : C, 54.54; H, 4.58; N, 10.60. Found: C, 54.21; H, 4.47; N, 11.04.

**Treatment of 7 with NaOH (1 eq)**—Aqueous NaOH (10%, 1.95 ml, 4.87 mmol) was added dropwise to a solution of **7** (1.47 g, 5.03 mmol) in MeOH (20 ml) under ice-cooling (below 8 °C). The solvent was removed, and the residue was acidified with 10% aq. HCl and then made alkaline with conc.  $\text{NH}_4\text{OH}$ . The aqueous layer was extracted with  $\text{CHCl}_3$ , and the  $\text{CHCl}_3$  extracts were dried over  $\text{MgSO}_4$  and concentrated. The residue was purified by chromatography ( $\text{SiO}_2$ ,  $\text{CHCl}_3$  : MeOH = 50 : 1) to yield methyl 4,5-dihydro-4-methyl-5-oxo-1H-pyrido[2,3-f]-1,2,4-

triazepine-3-carboxylate (**10**, 0.071 g, 6%) and methyl 2-methoxy-2-(2-methylcarbamoyl-3-pyridylhydrazono)acetate (**11**, 0.058 g, 4.3%).

Physical data for **10**, mp 168 °C (dec.) (from MeOH-Et<sub>2</sub>O-hexane): IR (Nujol): 3200, 1730, 1670, 1650 cm<sup>-1</sup>. MS *m/e*: 234 (M<sup>+</sup>), 219, 206, 203, 175. <sup>1</sup>H-NMR (DMSO-*d*<sub>6</sub>) δ: 3.07 (3H, s), 3.82 (3H, s), 9.32 (1H, s, NH). *Anal.* Calcd for C<sub>10</sub>H<sub>10</sub>N<sub>4</sub>O<sub>3</sub>: C, 51.28; H, 4.30; N, 23.92. Found: C, 53.20; H, 5.23; N, 21.73.

Physical data for **11**, mp 147–148 °C (from benzene-hexane): IR (Nujol): 3450, 3300, 1720, 1675 cm<sup>-1</sup>. MS *m/e*: 266 (M<sup>+</sup>), 234, 207, 193, 175, 152, 148. <sup>1</sup>H-NMR (CDCl<sub>3</sub>) δ: 2.95 (3H, d, *J* = 5 Hz; s, in D<sub>2</sub>O, NH-Me), 4.06 (3H, s), 4.10 (3H, s), 4.79 (1H, brs, NH). UV λ<sub>max</sub><sup>EtOH</sup> nm (ε): 262 (6400), 367 (15400). *Anal.* Calcd for C<sub>11</sub>H<sub>14</sub>N<sub>4</sub>O<sub>4</sub>: C, 49.62; H, 5.30; N, 21.04. Found: C, 49.26; H, 5.14; N, 20.81.

The aqueous layer described above was evaporated to dryness and extracted with a mixture of boiling EtOH-Me<sub>2</sub>CO. The EtOH-Me<sub>2</sub>CO extracts were concentrated, and the residue was purified by chromatography (SiO<sub>2</sub>, CHCl<sub>3</sub>) to give **3** (0.117 g, 13%).

**Dimethyl 1,2,4,5-Tetrahydro-4-methyl-5-oxo-3H-pyrido[2,3-*f*]-1,2,4-triazepine-3,3-dicarboxylate (12)**—Compound **7** (2.92 g, 10 mmol) was hydrogenated in MeOH (160 ml) in the presence of 10% Pd-C (0.2 g) under ordinary pressure and temperature. After 1 molar equivalent of hydrogen had been absorbed, Pd-C and the solvent were removed. The residue was recrystallized from Et<sub>2</sub>O-MeOH to give **12** (2.5 g, 85%), mp 176 °C (dec.). IR (Nujol): 3260, 1750, 1610 cm<sup>-1</sup>. MS *m/e*: 294 (M<sup>+</sup>), 263, 235, 204. <sup>1</sup>H-NMR (CDCl<sub>3</sub>+DMSO-*d*<sub>6</sub>) δ: 3.10 (3H, s), 3.85 (6H, s), 5.02 (1H, s, NH), 7.19 (1H, s, NH). *Anal.* Calcd for C<sub>12</sub>H<sub>14</sub>N<sub>4</sub>O<sub>5</sub>: C, 48.98; H, 4.80; N, 19.04. Found: C, 49.08; H, 4.82; N, 19.08.

**Dimethyl 2-[2-(Methylcarbamoyl)-3-pyridylhydrazono]malonate (13)**—A solution of **12** (0.81 g, 2.75 mmol) in EtOH (20 ml) was heated under reflux for 7 h. The solvent was removed, and the residue was purified by chromatography (SiO<sub>2</sub>, CHCl<sub>3</sub>) and recrystallized from CHCl<sub>3</sub>-MeOH to yield **13** (0.723 g, 89%) as needles, mp 200–203 °C. IR (Nujol): 3350, 3120, 1740, 1650 cm<sup>-1</sup>. MS *m/e*: 294, 263, 234, 204, 175, 150, 149, 136, 121. <sup>1</sup>H-NMR (CDCl<sub>3</sub>) δ: 3.0 (3H, d, *J* = 5.1 Hz; s in D<sub>2</sub>O), 3.87, 3.96 (each 3H, s). UV λ<sub>max</sub><sup>EtOH</sup> nm (ε): 342 (26000). *Anal.* Calcd for C<sub>12</sub>H<sub>14</sub>N<sub>4</sub>O<sub>5</sub>: C, 48.98; H, 4.80; N, 19.04. Found: C, 49.03; H, 4.81; N, 19.07.

**2-Aminonicotino-*N*-methylhydrazide (15)**—2-Aminonicotinic acid (**14a**, 2.76 g, 20 mmol) was condensed with methylhydrazine (1.11 g, 24 mmol) using HOBt (3.37 g, 22 mmol), DCC (4.54 g, 22 mmol), Et<sub>3</sub>N (4.05 g, 40 mmol), and DMF (30 ml) in the same manner as described for **6a** to yield **15** (0.72 g, 22%) as an oil. IR (liq.): 3450–3200, 1610, 1570 cm<sup>-1</sup>. MS *m/e*: 166 (M<sup>+</sup>). <sup>1</sup>H-NMR (CDCl<sub>3</sub>) δ: 3.25 (3H, s).

**1,4-Dihydro-4-methyl-5H-pyrido[2,3-*e*]-1,2,4-triazepin-5-one (4)**—A solution of **15** (0.64 g, 3.85 mmol), and HC(OEt)<sub>3</sub> (1.72 g, 11.61 mmol) in EtOH (30 ml) was refluxed for 2 h. After cooling, separated crystals were collected by filtration to give **4** (0.351 g, 52%) as yellow needles, mp 229–231 °C (from EtOH). IR (Nujol): 3220–3075, 1675 (w), 1630, 1610 cm<sup>-1</sup>. MS *m/e*: 176 (M<sup>+</sup>), 148, 133. <sup>1</sup>H-NMR (DMSO-*d*<sub>6</sub>) δ: 3.17 (3H, s), 6.92 (1H, d, *J* = 4.8 Hz; s in D<sub>2</sub>O), 6.99 (1H, dd, *J*<sub>1</sub> = 4.8 Hz, *J*<sub>2</sub> = 7.6 Hz), 8.08 (1H, dd, *J*<sub>1</sub> = 1.9 Hz, *J*<sub>2</sub> = 7.8 Hz), 8.23 (1H, dd, *J*<sub>1</sub> = 1.9 Hz, *J*<sub>2</sub> = 4.8 Hz), 9.21 (1H, brs, NH). UV λ<sub>max</sub><sup>EtOH</sup> nm (ε): 251 (6700), 285 (3700). *Anal.* Calcd for C<sub>8</sub>H<sub>8</sub>N<sub>4</sub>O: C, 54.54; H, 4.58; N, 31.80. Found: C, 54.05; H, 4.50; N, 31.67.

**2-Aminonicotino-*N'*-methylhydrazide (16)**—A mixture of ethyl 2-aminonicotinate (2.36 g, 14.2 mmol) and methylhydrazine (1.3 g, 28 mmol) was heated at 150 °C for 4 h and then at 120 °C for 16 h. Volatile materials were removed by evaporation, and the residue was purified by chromatography (SiO<sub>2</sub>, CHCl<sub>3</sub>:MeOH = 20:1) and recrystallized from hexane-EtOAc to give **16** (0.753 g, 32%), mp 122–124 °C. IR (Nujol): 3280, 1630, 1575 cm<sup>-1</sup>. MS *m/e*: 166 (M<sup>+</sup>). <sup>1</sup>H-NMR (CDCl<sub>3</sub>) δ: 2.71 (3H, d; s in D<sub>2</sub>O). *Anal.* Calcd for C<sub>7</sub>H<sub>10</sub>N<sub>4</sub>O: C, 50.59; H, 6.07; N, 33.72. Found: 50.62; H, 6.02; N, 33.73.

**3-Methylamino-pyrido[2,3-*d*]pyrimidin-4(3H)-one (17)**—A solution of **16** (0.68 g, 4.09 mmol) and HC(OEt)<sub>3</sub> (1.82 g, 12.28 mmol) in EtOH (15 ml) was refluxed for 19 h. After cooling, the solution was treated with charcoal and concentrated to yield **17** (0.57 g, 79%), mp 187 °C (from EtOH). IR (Nujol): 3250, 1680, 1590 cm<sup>-1</sup>. MS *m/e*: 176 (M<sup>+</sup>), 147, 133. <sup>1</sup>H-NMR (CDCl<sub>3</sub>) δ: 2.92 (3H, d, *J* = 5.3 Hz; s in D<sub>2</sub>O), 5.73 (1H, d, *J* = 5.3 Hz, NH), 8.49 (1H, s). *Anal.* Calcd for C<sub>8</sub>H<sub>8</sub>N<sub>4</sub>O: C, 54.54; H, 4.58; N, 31.80. Found: C, 54.29; H, 4.51; N, 31.66.

**3-(5-Methylamino-1,3,4-oxadiazol-2-yl)-2-pyridinamine (20a)**—A mixture of **18a** (2.65 g, 11.76 mmol), DCC (3.64 g, 17.64 mmol), and pyridine (200 ml) was heated at 80 °C for 29 h. After cooling, the separated solid was collected by filtration and extracted with MeOH. The MeOH was removed by evaporation, and the residue was crystallized from benzene to yield **20a** (0.757 g, 33%), mp 197–199 °C. IR (Nujol): 3420, 3220, 1680, 1640 cm<sup>-1</sup>. MS *m/e*: 191 (M<sup>+</sup>), 175, 134, 121, 119, 105. <sup>1</sup>H-NMR (DMSO-*d*<sub>6</sub>) δ: 2.88 (3H, d, *J* = 4.6 Hz; s in D<sub>2</sub>O), 7.05 (2H, brs, NH<sub>2</sub>). *Anal.* Calcd for C<sub>8</sub>H<sub>9</sub>N<sub>5</sub>O: C, 50.25; H, 4.74; N, 36.63. Found: C, 50.27; H, 4.75; N, 36.64.

**3-(5-Phenylamino-1,3,4-oxadiazol-2-yl)-2-pyridinamine (20b)**—A mixture of **18b** (2.94 g, 10.23 mmol), DCC (3.17 g, 15.36 mmol), and pyridine (50 ml) was heated at 60 °C for 1 h. The pyridine was evaporated off, and the residue was recrystallized from benzene, and then from MeOH to give **20b** (2.15 g, 83%), mp 237–239 °C (dec.). IR (Nujol): 3460, 3360, 1670, 1630 cm<sup>-1</sup>. MS *m/e*: 253 (M<sup>+</sup>), 237, 211, 196, 169, 161, 134, 121, 119. <sup>1</sup>H-NMR (DMSO-*d*<sub>6</sub>) δ: 7.20 (2H, brs, NH<sub>2</sub>), 10.70 (1H, s, NH). *Anal.* Calcd for C<sub>13</sub>H<sub>11</sub>N<sub>5</sub>O: C, 61.65; H, 4.38; N, 27.66. Found: C, 61.48; H, 4.25; N, 27.60.

**Ethyl 2-(3-Nitro-2-pyridylhydrazono)propionate (22a)**—A solution of 3-nitro-2-pyridylhydrazine<sup>12)</sup> (**21a**, 6.17 g,

40 mmol), ethyl pyruvate (4.75 g, 40 mmol),  $H_3PO_4$  (85%, 4 ml), and EtOH (60 ml) was heated for 2 h under reflux. After cooling, the separated crystalline solid was collected by filtration and recrystallized from EtOH to yield **22a** (7.56 g, 75%), mp 121–127 °C. IR (Nujol): 3225, 3080, 1690, 1600  $cm^{-1}$ . MS *m/e*: 253 ( $M^+ + 1$ ), 207. *Anal.* Calcd for  $C_{10}H_{12}N_4O_4$ : C, 47.62; H, 4.80; N, 22.22. Found: C, 47.41; H, 4.76; N, 22.21.

**Ethyl 2-(3-Nitro-2-pyridylhydrazono)phenylacetate (22b)**—This compound was prepared by the reaction of **21a** and ethyl phenylglyoxylate in the same manner as described above to give **22b** (68%), mp 135–137 °C (from EtOH). IR (Nujol): 3220, 1725, 1705, 1680, 1590  $cm^{-1}$ . MS *m/e*: 315 ( $M^+ + 1$ ), 269, 241. *Anal.* Calcd for  $C_{15}H_{14}N_4O_4$ : C, 57.32; H, 4.49; N, 17.83. Found: C, 57.03; H, 4.42; N, 17.80.

**Ethyl 2-[Methyl(3-nitro-2-pyridyl)hydrazono]propionate (22c)**—A mixture of **21b**<sup>12)</sup> (3.37 g, 20 mmol), ethyl pyruvate (2.37 g, 20 mmol),  $H_3PO_4$  (85%, 2 ml), and EtOH (30 ml) was stirred at room temperature for 15 h and then poured onto ice-sticks. The mixture was extracted with  $CHCl_3$ . The  $CHCl_3$  extracts were washed with aq. NaCl and dried over  $Na_2SO_4$ . The solvent was evaporated, and the residue was recrystallized from aq. EtOH to give **22c** (4.14 g, 78%), mp 76–82 °C. IR (Nujol): 1700, 1580, 1560  $cm^{-1}$ . MS *m/e*: 267 ( $M^+ + 1$ ), 251, 236.  $^1H$ -NMR ( $CDCl_3$ )  $\delta$ : 2.31 (3H, s), 3.58 (3H, s). *Anal.* Calcd for  $C_{11}H_{14}N_4O_4$ : C, 49.62; H, 5.30; N, 21.04. Found: C, 49.66; H, 5.34; N, 21.27.

**Ethyl 2-[Methyl(3-nitro-2-pyridyl)hydrazono]phenylacetate (22d)**<sup>13)</sup>—Compound **21b** (2.53 g, 15 mmol) and  $H_3PO_4$  (85%, 1.5 ml) were added to a solution of ethyl phenylglyoxylate (2.68 g, 15 mmol) in EtOH (25 ml). After being stirred for 3.5 h at room temperature and then heated for 50 min under reflux, the mixture was poured onto  $H_2O$  and extracted with  $CHCl_3$ . The  $CHCl_3$  extracts were washed with aq. NaCl and dried over  $Na_2SO_4$ . The solvent was evaporated off, and the residue was chromatographed ( $SiO_2$ , benzene :  $CHCl_3$  = 1 : 1) repeatedly to yield **22d** ( $\alpha$  isomer, 1.76 g, 36%) and **22d** ( $\beta$  isomer, 1.45 g, 29%). Physical data for **22d**- $\alpha$ , mp 75–78 °C (recrystallized from hexane-iso- $Pr_2O$ ): IR (Nujol): 1720, 1595, 1560  $cm^{-1}$ . MS *m/e*: 329 ( $M^+ + 1$ ), 298, 283, 255.  $^1H$ -NMR ( $CDCl_3$ )  $\delta$ : 1.45 (3H, t,  $J=7.1$  Hz), 3.75 (3H, s), 4.50 (2H, q,  $J=7.1$  Hz), 7.30–7.47 (5H, m), 6.99 (1H, dd,  $J_1=4.8$  Hz,  $J_2=8.1$  Hz), 7.85 (1H, dd,  $J_1=1.7$  Hz,  $J_2=8.1$  Hz), 8.40 (1H, dd,  $J_1=1.7$  Hz,  $J_2=4.8$  Hz). *Anal.* Calcd for  $C_{16}H_{16}N_4O_4$ : C, 58.53; H, 4.91; N, 17.07. Found: C, 58.49; H, 4.93; N, 17.00.

Physical data for **22d**- $\beta$ , mp 134–135 °C (recrystallized from aq. EtOH): IR (Nujol): 1700, 1590, 1560  $cm^{-1}$ . MS *m/e*: 329 ( $M^+ + 1$ ), 298, 283, 255.  $^1H$ -NMR ( $CDCl_3$ )  $\delta$ : 1.36 (3H, t,  $J=7.2$  Hz), 3.16 (3H, s), 4.29 (2H, q,  $J=7.2$  Hz), 7.45 (5H, s-like), 7.02 (1H, dd,  $J_1=4.8$  Hz,  $J_2=7.8$  Hz), 8.0 (1H, dd,  $J_1=1.8$  Hz,  $J_2=8.0$  Hz), 8.38 (1H, dd,  $J_1=1.8$  Hz,  $J_2=4.8$  Hz).

**Ethyl 2-(3-Amino-2-pyridylhydrazono)propionate (23a) and 9-Amino-3-methyl-4H-pyrido[2,1-c]-1,2,4-triazin-4-one (25a)**—Compound **22a** (1.88 g, 7.45 mmol) was hydrogenated in EtOH (50 ml) in the presence of 10% Pd-C (0.15 g) under 2.5 atm pressure. After 50 min, Pd-C and the solvent were removed. The residue was purified by chromatography ( $SiO_2$ ,  $CHCl_3$  : MeOH = 100 : 1) to yield **23a** (0.312 g, 19%) and **25a** (0.304 g, 23%).

Physical data for **23a**, mp 93 °C (from benzene-hexane): IR (Nujol): 3460–3255, 1700  $cm^{-1}$ . MS *m/e*: 222 ( $M^+$ ), 207, 177, 176. NMR ( $CDCl_3$ )  $\delta$ : 2.13 (3H, s). *Anal.* Calcd for  $C_{10}H_{14}N_4O_2$ : C, 54.04; H, 6.35; N, 25.21. Found: C, 53.95; H, 6.34; N, 25.18.

Physical data for **25a**, mp 193–195 °C (from benzene): IR (Nujol): 3480, 3340, 1670, 1620, 1600  $cm^{-1}$ .  $^1H$ -NMR ( $DMSO-d_6$ )  $\delta$ : 2.67 (3H, s), 5.78 (2H, brs,  $NH_2$ ), 6.82–7.19 (2H, m), 8.20 (1H, dd,  $J_1=1.6$  Hz,  $J_2=6.4$  Hz). UV  $\lambda_{max}^{EtOH}$  nm ( $\epsilon$ ): 286 (3300), 342 (8900), 400 (10000). *Anal.* Calcd for  $C_8H_8N_4O$ : C, 54.54; H, 4.58; N, 31.80. Found: C, 54.37; H, 4.50; N, 31.59.

**Ethyl 2-(3-Amino-2-pyridylhydrazono)phenylacetate (23b) and 9-Amino-3-phenyl-4H-pyrido[2,1-c]-1,2,4-triazin-4-one (25b)**—These compounds were prepared from **22b** (0.3 g, 0.96 mmol) in the same manner as described above to give **23b** (0.08 g, 30%) and **25b** (0.08 g, 30%).

Physical data for **23b**, mp 151–153 °C (from benzene-hexane): IR (Nujol): 3400–3150, 1700  $cm^{-1}$ . MS *m/e*: 284 ( $M^+$ ), 238, 212, 211. *Anal.* Calcd for  $C_{15}H_{16}N_4O_2$ : C, 63.36; H, 5.67; N, 19.71. Found: C, 63.56; H, 5.58; N, 19.65.

Physical data for **25b**, mp 181–182 °C (from benzene): IR (Nujol): 3430–3200, 1670, 1630  $cm^{-1}$ . MS *m/e*: 238 ( $M^+$ ), 210, 181.  $^1H$ -NMR ( $CDCl_3$  +  $DMSO-d_6$ )  $\delta$ : 5.77 (2H, brs,  $NH_2$ ), 6.8–7.7 (5H, aromatic H), 8.20–8.46 (3H). UV  $\lambda_{max}^{EtOH}$  nm ( $\epsilon$ ): 222 sh. (13100), 250 (8500), 309 (6800), 352 (9600), 427 (17200). *Anal.* Calcd for  $C_{13}H_{10}N_4O$ : C, 65.53; H, 4.23; N, 23.52. Found: C, 65.31; H, 4.02; N, 23.54.

**Ethyl 1,2,3,4-Tetrahydro-1,3-dimethylpyrido[3,2-e]-1,2,4-triazine-3-carboxylate (26c)**—This compound was prepared by hydrogenation of **22c** (3.52 g, 13.32 mmol) in the same manner as described for **25a** to give **26c** (2.7 g, 87%), mp 115–117 °C (from benzene-hexane). IR (Nujol): 3370, 3160, 1720  $cm^{-1}$ . MS *m/e*: 236 ( $M^+$ ),  $^1H$ -NMR ( $CDCl_3$ )  $\delta$ : 1.28 (3H, t,  $J=7.1$  Hz), 1.52 (3H, s), 3.22 (3H, s), 4.24 (2H, q,  $J=7.1$  Hz). UV  $\lambda_{max}^{EtOH}$  nm ( $\epsilon$ ): 266 (6500), 326 (9700). *Anal.* Calcd for  $C_{11}H_{16}N_4O_2$ : C, 55.91; H, 6.83; N, 23.72. Found: C, 56.03; H, 6.88; N, 23.74.

**Ethyl 1,2,3,4-Tetrahydro-1-methyl-3-phenylpyrido[3,2-e]-1,2,4-triazine-3-carboxylate (26d)**—This compound was prepared by hydrogenation of **22d**- $\alpha$  (3.28 g, 10 mmol) in the same manner as described for **25a** to give **26d** (1.76 g, 59%), mp 113–116 °C (from iso- $Pr_2O$ ). IR (Nujol): 3380, 3140, 1720  $cm^{-1}$ . MS *m/e*: 298 ( $M^+$ ), 225, 122.  $^1H$ -NMR ( $CDCl_3$ )  $\delta$ : 1.22 (3H, t,  $J=7$  Hz), 3.21 (3H, s), 4.20 (2H, dd,  $J=7$  Hz), 4.20, 5.10 (each 1H, brs,  $NH_2$ ), 6.56 (1H, dd,  $J_1=5$  Hz,  $J_2=8$  Hz), 6.87 (1H, dd,  $J_1=2$  Hz,  $J_2=8$  Hz), 7.28–7.75 (6H, m). UV  $\lambda_{max}^{EtOH}$  nm ( $\epsilon$ ): 262 (5400), 328 (8000). *Anal.* Calcd for  $C_{16}H_{18}N_4O_2$ : C, 64.41; H, 6.08; N, 18.78. Found: C, 64.26; H, 6.03; N, 18.78.

Hydrogenation of **22d**- $\alpha$  also gave **26d** in comparable yield.

Compound **26d** was also prepared as follows. Ethyl phenylglyoxylate (1.53 g, 8.59 mmol) and AcOH (0.3 ml) were added to a cold solution of 1-(3-amino-2-pyridyl)-1-methylhydrazine (**27b**, 1.18 g, 8.54 mmol) in EtOH (15 ml). The mixture was stirred at room temperature for 4 d under an argon atmosphere, then the solvent was removed. The residue was dissolved in iso-Pr<sub>2</sub>O, treated with charcoal, and concentrated to give **26d** (1.73 g, 68%), which has physical data identical with those described above.

**4-Amino-2-phenylpyrido[2,3-*b*]pyrazin-3(4*H*)-one (28)**—3-Amino-2-pyridylhydrazine<sup>12)</sup> (**27a**, 3.73 g, 30 mmol) and AcOH (0.5 ml) were added to a solution of ethyl phenylglyoxylate (5.35 g, 30 mmol) in EtOH (5 ml). After being heated at 50 °C for 3 min, the mixture was concentrated. The residue was diluted with H<sub>2</sub>O and extracted with CHCl<sub>3</sub>. The CHCl<sub>3</sub> extracts were washed with aq. NaHCO<sub>3</sub> and aq. NaCl successively and dried over Na<sub>2</sub>SO<sub>4</sub>. Evaporation of the solvent and purification of the residue by chromatography (SiO<sub>2</sub>, CHCl<sub>3</sub> : MeOH = 100 : 1) gave **23b** (0.716 g, 8.4%), **25b** (0.86 g, 12%), and **28** (3.65 g, 51%), mp 155–156 °C (from benzene). IR (Nujol): 3300, 3230, 1640 cm<sup>-1</sup>. MS *m/e*: 238 (M<sup>+</sup>). UV λ<sub>max</sub><sup>EtOH</sup> nm (ε): 230 (12200), 265 sh. (4300), 303 (4200), 372 (7800). *Anal.* Calcd. for C<sub>13</sub>H<sub>10</sub>N<sub>4</sub>O: C, 65.53; H, 4.23; N, 23.52. Found: C, 65.42; H, 4.15; N, 23.71.

**4-Isopropylideneamino-2-phenylpyrido[2,3-*b*]pyrazin-3(4*H*)-one (29)**—A mixture of **28** (0.1 g, 0.42 mmol), Me<sub>2</sub>CO (5 ml), and AcOH (0.5 ml) was heated for 2 h under reflux. After cooling, the mixture was concentrated, and the residue was recrystallized from Me<sub>2</sub>CO–hexane to give **29** (0.07 g, 60%) as pale yellow needles, mp 151–152 °C. IR (Nujol): 1650, 1580 cm<sup>-1</sup>. MS *m/e*: 278 (M<sup>+</sup>), 235. *Anal.* Calcd. for C<sub>16</sub>H<sub>14</sub>N<sub>4</sub>O: C, 69.05; H, 5.07; N, 20.13. Found: C, 68.70; H, 4.98; N, 20.22.

**4-Acetamido-2-phenylpyrido[2,3-*b*]pyrazin-3(4*H*)-one (30)**—Compound **28** (0.784 g, 3.29 mmol) was dissolved in Ac<sub>2</sub>O (30 ml), and the mixture was stirred at room temperature overnight. Ac<sub>2</sub>O was evaporated, and the residue was recrystallized from a mixture of AcOEt and hexane to yield **30** (0.732 g, 79%), mp 176–178 °C. IR (Nujol): 3250, 1690, 1645 cm<sup>-1</sup>. MS *m/e*: 280 (M<sup>+</sup>), 238. *Anal.* Calcd. for C<sub>15</sub>H<sub>12</sub>N<sub>4</sub>O<sub>2</sub>: C, 64.27; H, 4.32; N, 19.99. Found: C, 64.20; H, 4.31; N, 19.77.

**X-Ray Crystallographic Analysis**—The structures of compounds **3**, **4**, **25a**, **26d** and **28** were solved by the direct method using MULTAN and refined by the block-diagonal least-squares method. The crystal data are summarized in Table II.

**Acknowledgement** The authors wish to thank the staff of the Analytical Division of this laboratory for measurement of spectra and elemental analyses. Thanks are also due to Dr. H. Nakajima, Director of the Biological Research Laboratory, for his interest and encouragement.

#### References and Notes

- 1) a) J. Myren and A. Berstad, *Scand. J. Gastroenterol.*, **10**, 817 (1975); b) W. Eberlein, G. Sohmidt, A. Reuter, and E. Kutter, *Arzneim.-Forsch.*, **27**, 356 (1977).
- 2) M. Bianchi, A. Butti, S. Rossi, F. Barzaghi, and V. Marcaria, *Eur. J. Med. Chem.*, **12**, 263 (1977).
- 3) W. A. Bolhofer, A. A. Deana, C. N. Habecker, J. M. Hoffman, N. P. Gould, A. M. Pietruszkiewicz, J. O. I Prugh, M. L. Torchiana, E. J. Cragoe, Jr., and R. Hirschmann, *J. Med. Chem.*, **26**, 538 (1983).
- 4) N. P. Peet, "The Chemistry of Heterocyclic Compounds," Vol. 43, ed. by A. Weissberger, E. C. Taylor, and A. Rosowsky, John Wiley and Sons, Inc., New York, 1984, p. 719.
- 5) See references 7 and 11.
- 6) a) A. P. Krapcho and A. J. Lovey, *Tetrahedron Lett.*, **1973**, 957; b) A. P. Krapcho, J. F. Weimaster, J. M. Eldridge, E. G. E. Jahngen, Jr., A. J. Lovey, and W. P. Stephens, *J. Org. Chem.*, **43**, 138 (1978).
- 7) a) N. P. Peet and S. Sunder, *J. Heterocycl. Chem.*, **21**, 1807 (1984); b) P. Scheiner, L. Frank, I. Giusti, S. Arwin, S. A. Pearson, F. Excellent, and A. P. Harper, *ibid.*, **21**, 1817 (1984); c) R. W. Leiby, *ibid.*, **21**, 1825 (1984).
- 8) 2-Aminonicotino-*N,N'*-dimethylhydrazide showed signals due to the methyl groups at δ 3.17 (3H, s) and δ 2.63 (3H, d, changed to s on addition of D<sub>2</sub>O).
- 9) A.-M. M. E. Omar, F. A. Ashour, and J. J. Boudais, *J. Heterocycl. Chem.*, **16**, 1435 (1979).
- 10) These compounds were prepared by the method of Omar *et al.* (see reference 9).
- 11) S. Sunder, N. P. Peet, and R. J. Barbuch, *J. Heterocycl. Chem.*, **18**, 1601 (1981).
- 12) A. Lewis and R. G. Shepherd, *J. Heterocycl. Chem.*, **8**, 41 (1971).
- 13) Isolation of the geometrical isomers (*syn* and *anti*) of these hydrazones (**22a–c**) was unsuccessful. In the case of **22d**, two isomers (α, β) could be isolated, but their geometry was not ascertained. See Experimental.
- 14) H. Wada, S. Kodato, M. Kawamori, T. Morikawa, H. Nakai, M. Takeda, S. Saito, Y. Onoda, and H. Tamaki, *Chem. Pharm. Bull.*, **33**, 1472 (1985).

[Chem. Pharm. Bull.]  
35(1) 90-96 (1987)

## Synthesis and Reactions of 2,3-Dihydrothiazolo[3,2-*a*]pyrimidine Derivatives

TOSHIO KINOSHITA,\* YASUJI UESHIMA, KOUJI SAITOH,  
YASUFUMI YOSHIDA, and SUNAO FURUKAWA

*Faculty of Pharmaceutical Sciences, Nagasaki University,  
1-14 Bunkyo-machi, Nagasaki 852, Japan*

(Received June 9, 1986)

The reaction of 2-amino-2-thiazoline (1) with acetylene carboxylates (2) afforded 5-substituted 2,3-dihydro-7*H*-thiazolo[3,2-*a*]pyrimidin-7-ones (3). 7-Bromomethyl-2,3-dihydro-5*H*-thiazolo[3,2-*a*]pyrimidin-5-one (10) was obtained by the reaction of 1 with  $\gamma$ -bromoacetoacetyl bromide. Treatment of 10 with *N*-bromosuccinimide provided the 6-bromo compound (12). The 7-bromomethyl compounds (10 and 12) were converted to 7-morpholinomethyl derivatives by treatment with morpholine. When 3a (unsubstituted-), 3b (5-ethoxycarbonyl-), and 3c (5-hydroxymethyl-) were treated with 5% hydrochloric acid, covalent hydration occurred across the 5,6-carbon-carbon bond, giving 5-hydroxy-2,3,5,6-tetrahydro-7*H*-thiazolo[3,2-*a*]pyrimidin-7-one derivatives (16a, 16b, and 16c). On the other hand, in the case of 11 (7-methyl-) and 17 (5-phenyl-), the dihydrothiazole ring was cleaved to give 3(and 1)-(2-mercaptoethyl)-6-methyl(and phenyl)-2,4(1*H*,3*H*)-pyrimidinedione (19 and 18).

**Keywords**—dihydrothiazolo[3,2-*a*]pyrimidine;  $\gamma$ -bromoacetoacetyl bromide; 2-amino-2-thiazoline; covalent hydration; ring cleavage; bromination; cyclization; acetylene carboxylate

Various syntheses have been reported of 2,3-dihydrothiazolo[3,2-*a*]pyrimidine derivatives, some of which have analgesic, antithrombic and antiinflammatory activities. The compounds have been synthesized in two ways, when classified in terms of the starting materials. One involves cyclization of 2-thiouracil with 1,2-dibromoethane,<sup>1)</sup> ethyl  $\gamma$ -chloroacetoacetate,<sup>2)</sup> or ethyl chloroacetate,<sup>3)</sup> or intramolecular cyclization of 1-(2-hydroxyethyl)-thiouracil with methanesulfonyl chloride<sup>4)</sup> or of 1-allylthiouracil with iodine.<sup>5)</sup> The other consists of the reaction of 2-amino-2-thiazoline (1) with diketene,<sup>6)</sup> acetoacetic esters,<sup>7)</sup> ethoxymethylenemalonic esters,<sup>1b)</sup> ethoxymethylenecyanoacetamide,<sup>8)</sup> acetylene carboxylic ester,<sup>9)</sup> ethyl malonyl chloride<sup>10)</sup> or diethyl malonate.<sup>11)</sup> In this paper we describe the synthesis of 2,3-dihydrothiazolo[3,2-*a*]pyrimidine derivatives from 2-amino-2-thiazoline (1) as a starting material, and some reactions of the thiazolopyrimidines.

The reaction of 2-amino-2-thiazoline (1) with ethyl propiolate (2a, R=H) and diethyl acetylenedicarboxylate (2b, R=COOEt) gave unsubstituted 2,3-dihydro-7*H*-thiazolo[3,2-*a*]pyrimidin-7-one (3a) and 2,3-dihydro-5-ethoxycarbonyl-7*H*-thiazolo[3,2-*a*]pyrimidin-7-one (3b). Similarly, the 5-hydroxymethyl compound (3c) was obtained in 62.0% yield by treatment with ethyl  $\gamma$ -hydroxytetrolate (2c)<sup>12)</sup> in ethanol. The structures of the above products (3a, 3b, and 3c) are supported by the infrared (IR) and ultraviolet (UV) spectral data.<sup>1b)</sup>

Compound 3b was converted to the carboxamide (4) by reaction with ethanolic ammonia in a flask sealed by a stopcock at room temperature. The reaction of 3c with acetic anhydride afforded the corresponding acetoxy compound (5). For the preparation of the 5-halomethyl compounds (8 and 10'), 3c was treated with thionyl chloride, phosphorus oxychloride or phosphorus tribromide under various conditions; however, no reaction occurred and the starting material was recovered.

6-Hydroxymethyl-2-thioxo-1,3-thiazin-4-one (6)<sup>12)</sup> was converted to 2,3-dihydro-1-(2-

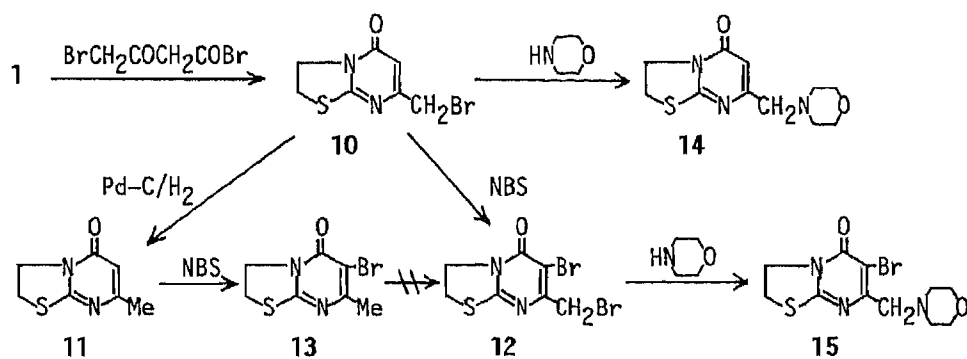
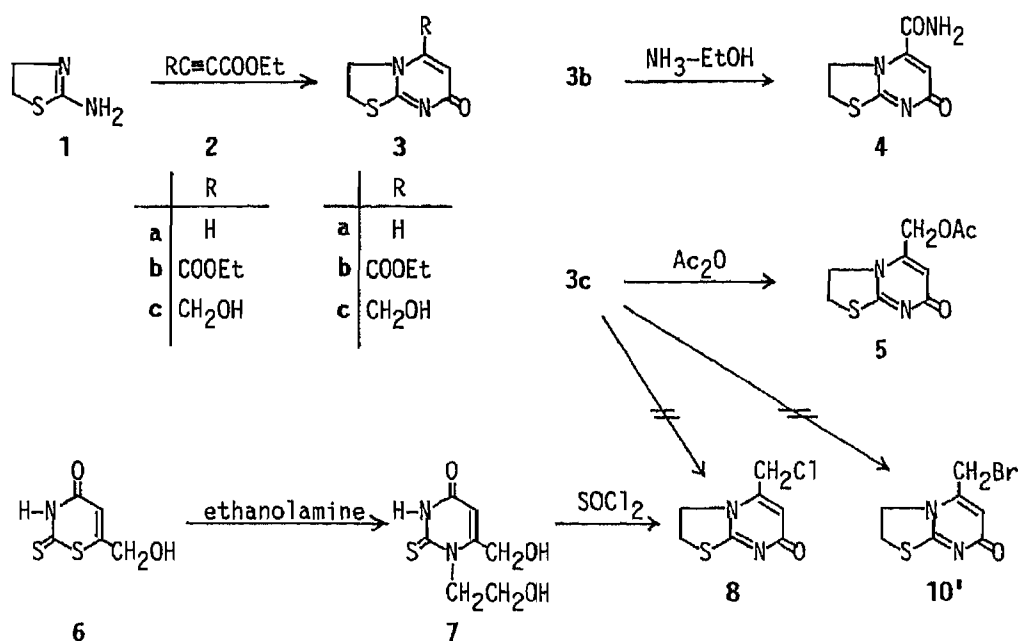


Chart 1

hydroxyethyl)-6-hydroxymethyl-2-thioxo-4(1*H*)-pyrimidinone (7) by reaction with 2-aminoethanol. In order to prepare 1-(2-chloroethyl)-6-chloromethyl-2-thioxo-4(3*H*)-pyrimidinone, 7 was treated with thionyl chloride, but the cyclized product 8 was obtained.

It has been reported that the reaction of acid chlorides with 2-aminoethiazole or 2-amino-2-thiazoline (1) gives 2-acylaminothiazole<sup>13)</sup> or 2-acylamino-2-thiazoline.<sup>12)</sup> Therefore we expected that the reaction of  $\gamma$ -bromoacetoacetyl bromide (9)<sup>14)</sup> with 1 would afford 2-( $\gamma$ -bromoacetoacetyl-amino)-2-thiazoline, followed by ring closure to yield 5-bromomethyl-2,3-dihydro-7*H*-thiazolo[3,2-*a*]pyrimidin-7-one (10'). However, we found that the product is 7-bromomethyl-2,3-dihydro-5*H*-thiazolo[3,2-*a*]pyrimidin-5-one (10). The structure of 10 was confirmed by IR and UV spectral data and chemical evidence. Compound 10 was converted to 7-methyl-2,3-dihydro-5*H*-thiazolo[3,2-*a*]pyrimidin-5-one (11)<sup>1b,6)</sup> by catalytic hydrogenolysis over palladium-carbon catalyst.

With *N*-bromosuccinimide in ethanol, 10 was converted to the corresponding 6-bromo compound 12. Similarly, 11 was converted to the 6-bromo compound 13 by treatment with *N*-bromosuccinimide or bromine in acetic acid.<sup>1b)</sup> The position of the bromine substituent was determined from the proton nuclear magnetic resonance (<sup>1</sup>H-NMR) spectra of 12 and 13, in which no olefinic protons were not observed. It is well known that 5-bromo-1,3-disubstituted-

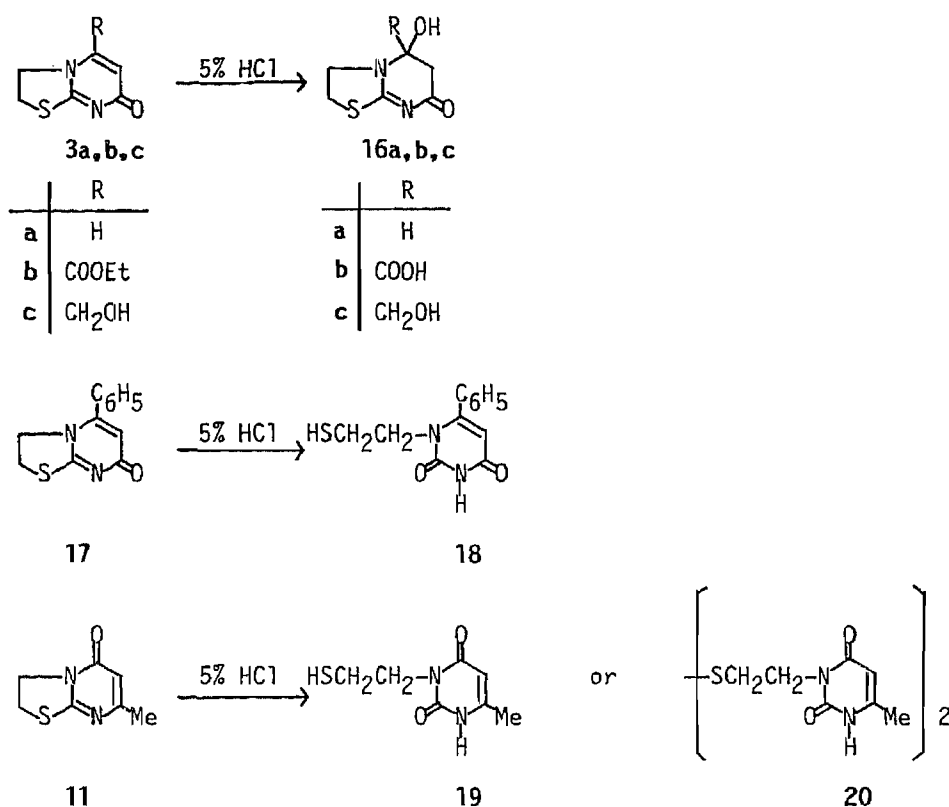


Chart 2

6-methyl-2,4(1*H*,3*H*)-pyrimidinediones are converted to the 6-bromomethyl derivatives by reaction with bromine in acetic acid.<sup>15)</sup> However, in the case of **13**, no reaction occurred under these conditions. The reaction of the 7-bromomethyl compound (**10** and **12**) with morpholine yielded the corresponding 7-morpholinomethyl derivatives (**14** and **15**).

For the preparation of 1-(2-mercaptoethyl)-6-hydroxymethyl-2,4(1*H*,3*H*)-pyrimidinedione, **3c** was treated with 5% hydrochloric acid according to Falch and Natvig.<sup>16)</sup> The product (**16**) was found to have the molecular formula C<sub>7</sub>H<sub>10</sub>N<sub>2</sub>O<sub>3</sub> by elemental microanalysis, but the UV spectrum showed no absorption maximum and was different from those of 2,4-(1*H*,3*H*)-pyrimidinedione derivatives.<sup>17)</sup>

The carbon-13 nuclear magnetic resonance (<sup>13</sup>C-NMR) spectrum of **16b** indicated the presence of three methylene groups at  $\delta$  48.93, 40.80, and 28.77. The former two signals are assignable to the carbons of the dihydrothiazole ring by comparison with those of the starting material (**3b**). Further structural assignment was possible from the <sup>1</sup>H-NMR (270 MHz) spectrum, which exhibited signals due to one isolated methylene moiety at  $\delta$  3.70 and 3.18 as doublets, complicated ethylene signals at  $\delta$  4.32, 4.13, and 3.5–3.3 and a characteristic broad singlet signal at  $\delta$  9.48 due to a hydroxyl group.

The structure of **16b**, based on the above spectral data, was assumed to 5-carboxy-5-hydroxy-2,3,5,6-tetrahydro-7*H*-thiazolo[3,2-*a*]pyrimidin-7-one, which corresponded to covalent hydration across the 5,6-carbon-carbon double bond of **3b**. Similarly, **3a** and **3c** were converted to the covalent hydration products **16a** and **16c**. However, under the same reaction conditions, no covalent hydration was observed in the case of compounds **17** and **11**; instead, the dihydrothiazole ring was cleaved to afford **18** and **19**, as described by Falch and Natvig.<sup>16)</sup> The UV spectra of the reaction products (**18** and **19**) showed absorption maxima at 275 and 264 nm, and the IR spectra showed SH stretching absorptions at 2530 and 2555 cm<sup>-1</sup>. The



$^1\text{H-NMR}$  spectrum of **18** showed signals at  $\delta$  1.48, 2.80, and 4.14 due to  $\text{NCH}_2\text{CH}_2\text{SH}$  and  $\delta$  5.91 due to ring proton. Similarly, **19** exhibited signals at  $\delta$  1.19, 2.64, and 3.83 due to  $\text{NCH}_2\text{CH}_2\text{SH}$  and  $\delta$  5.63 due to a ring proton in the  $^1\text{H-NMR}$  spectrum. On the basis of the above data, the structures of **18** and **19** were concluded to be 1-(2-mercaptoethyl)-6-phenyl-2,4-(1*H*,3*H*)-pyrimidinedione and 3-(2-mercaptoethyl)-6-methyl-2,4-(1*H*,3*H*)-pyrimidinedione, respectively. When **11** was treated with 5% hydrochloric acid for 7 h, an alternative product **20** was obtained which showed an absorption maximum at 263 nm in the UV spectrum (similar to that of **19**). The  $^1\text{H-NMR}$  spectrum exhibited two double-doublet signals due to an ethylene group ( $\delta$  4.33 and 2.97) and no peak due to an SH group. Furthermore, fast atom bombardment mass spectrometry (FAB-MS) showed the hydrogenated molecular ion peak  $[(M+1)^+]$  at  $m/z$  371. Therefore, **20** was concluded to be 3,3'-bis[6-methyl-1,2,3,4-tetrahydro-2,4-dioxypyrimidinyl]diethyldisulfide. When **19** was treated with iodine in ethanol, **20** was obtained in good yield.

### Experimental

Melting points reported here are uncorrected. IR spectra were recorded on JASCO IRA-2 and IR-810 spectrophotometer. UV spectra were recorded in ethanol on a Hitachi 323 spectrophotometer. The NMR spectra were obtained on Hitachi R-600 (60 MHz, for  $^1\text{H}$ ), JEOL JNM FX-90Q (90 MHz for  $^1\text{H}$  and 22.5 MHz for  $^{13}\text{C}$ ) and JEOL JNM GX-270 (270 MHz, for  $^1\text{H}$ ) spectrometers. Chemical shifts are reported in ppm ( $\delta$ ) relative to tetramethylsilane as an internal standard. Mass spectra were obtained on a JEOL JMS-DX-303 spectrometer by the electron impact (EI) or fast atom bombardment (FAB) ionization method.

**2,3-Dihydro-7*H*-thiazolo[3,2-*a*]pyrimidin-7-one (3a)**—A solution of 2-amino-2-thiazoline (**1**) (0.51 g, 5.0 mmol) and ethyl propiolate (**2a**) (0.5 g, 5.0 mmol) in EtOH (20 ml) was refluxed for 9 h. The reaction mixture was concentrated to dryness *in vacuo* and the residue was washed with ether. The insoluble material was crystallized from MeOH, giving 0.53 g (68.8%) of colorless needles, mp 225 °C (lit.<sup>10</sup> mp 227–228 °C).  $^1\text{H-NMR}$  ( $\text{CDCl}_3$ )  $\delta$ : 7.27 (1H, d,  $J=7.8$  Hz, C(5)-H), 6.02 (1H, d,  $J=7.8$  Hz, C(6)-H), 4.34 (2H, t,  $J=6.8$  Hz, N- $\text{CH}_2$ ), 3.50 (2H, t,  $J=6.8$  Hz, S- $\text{CH}_2$ ). MS  $m/z$ : 154 ( $M^+$ ).

**2,3-Dihydro-5-ethoxycarbonyl-7*H*-thiazolo[3,2-*a*]pyrimidin-7-one (3b)**—A solution of **1** (0.5 g, 5.0 mmol) and diethyl acetylenedicarboxylate (**2b**) (0.85 g, 5.0 mmol) in EtOH (20 ml) was refluxed for 3 h. The reaction mixture was concentrated to dryness *in vacuo*, and the residue was recrystallized from AcOEt, giving 0.61 g (61.0%) of colorless needles, mp 121–122 °C. *Anal.* Calcd for  $\text{C}_9\text{H}_{10}\text{N}_2\text{O}_3\text{S}$ : C, 47.79; H, 4.42; N, 12.39; S, 14.16. Found: C, 47.53; H, 4.43; N, 12.43; S, 14.27. IR (KBr): 1724, 1625 ( $\text{C}=\text{O}$ )  $\text{cm}^{-1}$ . UV  $\lambda_{\text{max}}^{\text{ethanol}}$  nm (log  $\epsilon$ ): 239 (4.34), 290 (3.68).  $^1\text{H-NMR}$  ( $\text{CDCl}_3$ )  $\delta$ : 6.70 (1H, s, C(6)-H), 4.80 (2H, t,  $J=7.5$  Hz, N- $\text{CH}_2$ ), 4.38 (2H, q,  $J=7.2$  Hz,  $\text{C}[\text{H}_2\text{C}(\text{H})_3$ ]), 3.48 (2H, t,  $J=7.5$  Hz, S- $\text{CH}_2$ ), 1.39 (3H, t,  $J=7.2$  Hz,  $\text{CH}_2\text{C}(\text{H})_3$ ). FAB-MS  $m/z$ : 227 [ $(M+1)^+$ ].

**2,3-Dihydro-5-hydroxymethyl-7*H*-thiazolo[3,2-*a*]pyrimidin-7-one (3c)**—A solution of **1** (0.25 g, 2.5 mmol) and ethyl  $\gamma$ -hydroxytetrolate (**2c**) (0.32 g, 2.5 mmol) in MeOH (10 ml) was refluxed for 3 h. The reaction mixture was concentrated to dryness *in vacuo*, and the residue was crystallized from MeOH, giving 0.28 g (62.0%) of colorless needles, mp 267–269 °C. *Anal.* Calcd for  $\text{C}_7\text{H}_8\text{N}_2\text{O}_2\text{S}$ : C, 45.65; H, 4.38; N, 15.21; S, 17.40. Found: C, 45.79; H, 4.50; N, 15.14; S, 17.32. IR (KBr): 3210 (OH), 1632 ( $\text{C}=\text{O}$ )  $\text{cm}^{-1}$ . UV  $\lambda_{\text{max}}^{\text{ethanol}}$  nm (log  $\epsilon$ ): 232.5 (4.45), *ca.* 268 (sh, 4.00).  $^1\text{H-NMR}$  ( $\text{DMSO-}d_6$ - $\text{CF}_3\text{COOH}=1:1$ )  $\delta$ : 6.27 (1H, s, C(6)-H), 5.48 (1H, s, OH), 4.78 (2H, dd,  $J=7.6, 8.3$  Hz, N- $\text{CH}_2$ ), 4.74 (2H, s, O- $\text{CH}_2$ ), 3.85 (2H, dd,  $J=7.6, 8.3$  Hz, S- $\text{CH}_2$ ). FAB-MS  $m/z$ : 185 [ $(M+1)^+$ ].

**5-Carbamoyl-2,3-dihydro-7*H*-thiazolo[3,2-*a*]pyrimidin-7-one (4)**—A solution of **3b** (0.1 g, 0.44 mmol) in  $\text{NH}_3$ -EtOH (saturated, 20 ml) was sealed in a flask with a stopcock and allowed to stand at room temperature overnight. The separated crystalline mass was collected and recrystallized from MeOH, giving 70 mg (61.0%) of colorless needles, mp 289–290 °C. *Anal.* Calcd for  $\text{C}_7\text{H}_7\text{N}_3\text{O}_2\text{S}$ : C, 42.63; H, 3.58; N, 21.30; S, 16.26. Found: C, 42.33; H, 3.64; N, 21.08; S, 16.04. IR (KBr): 3440, 3320 ( $\text{NH}_2$ ), 1695 ( $\text{C}=\text{O}$ )  $\text{cm}^{-1}$ . UV  $\lambda_{\text{max}}^{\text{ethanol}}$  nm (log  $\epsilon$ ): 236 (4.42), 286 (sh, 3.88).  $^1\text{H-NMR}$  ( $\text{DMSO-}d_6$ - $\text{CF}_3\text{COOH}=1:1$ )  $\delta$ : 8.41 (1H, brs, NH), 8.00 (1H, brs, NH), 6.77 (1H, s, C(6)-H), 4.87 (2H, t,  $J=7.9$  Hz, N- $\text{CH}_2$ ), 3.74 (2H, t,  $J=7.9$  Hz, S- $\text{CH}_2$ ). FAB-MS  $m/z$ : 198 [ $(M+1)^+$ ].

**5-Acetoxymethyl-2,3-dihydro-7*H*-thiazolo[3,2-*a*]pyrimidin-7-one (5)**—A mixture of **3c** (1.8 g, 9.8 mmol) and acetic anhydride (30 ml) was refluxed for 3 h. The reaction mixture was concentrated to dryness *in vacuo*, and the residue was crystallized from acetone, giving 2.0 g (90.3%) of colorless needles, mp 137–138 °C. *Anal.* Calcd for  $\text{C}_9\text{H}_{10}\text{N}_2\text{O}_3\text{S}$ : C, 47.77; H, 4.46; N, 12.38; S, 14.17. Found: C, 47.84; H, 4.44; N, 12.49; S, 13.88. IR (KBr): 1740, 1630 ( $\text{C}=\text{O}$ )  $\text{cm}^{-1}$ . UV  $\lambda_{\text{max}}^{\text{ethanol}}$  nm (log  $\epsilon$ ): 233 (4.38), *ca.* 268 (sh, 3.82).  $^1\text{H-NMR}$  ( $\text{CDCl}_3$ )  $\delta$ : 6.00 (1H, s, C(6)-H), 4.58 (2H, s, O- $\text{CH}_2$ ), 4.38 (2H, dd,  $J=6.8, 7.9$  Hz, N- $\text{CH}_2$ ), 3.49 (2H, dd,  $J=6.8, 7.9$  Hz, S- $\text{CH}_2$ ), 2.17 (3H, s, CO- $\text{CH}_3$ ). FAB-MS  $m/z$ : 227 [ $(M+1)^+$ ].

**2,3-Dihydro-1-(2-hydroxyethyl)-6-hydroxymethyl-2-thioxo-4(1*H*)-pyrimidinone (7)**—A solution of **6**<sup>(12)</sup> (2.4 g,

13.7 mmol) and ethanolamine (1.6 g, 26.5 mmol) in EtOH (10 ml) was refluxed for 1 h. After cooling, the mixture was acidified with 10% HCl, and left to stand in a refrigerator overnight. After concentration, the separated crystalline mass was collected and recrystallized from EtOH, giving 1.05 g (37.9%) of colorless prisms, mp 199–200 °C. *Anal.* Calcd for  $C_7H_{10}N_2O_3S$ : C, 41.58; H, 4.98; N, 13.85; S, 15.85. Found: C, 41.45; H, 4.99; N, 13.71; S, 15.78. IR (KBr): 1650 (C=O)  $cm^{-1}$ . UV  $\lambda_{max}^{ethanol}$  nm (log  $\epsilon$ ): 221 (4.25), 278 (4.21).  $^1H$ -NMR ( $CDCl_3$ )  $\delta$ : 12.44 (1H, brs, NH), 5.98 (1H, s, ring), 4.51 (2H, brs, C(6)- $CH_2$ ), 4.29 (2H, t,  $J=5.5$  Hz, N- $CH_2$ ), 3.74 (2H, q,  $J=5.5$  Hz, S- $CH_2$ ).

**5-Chloromethyl-2,3-dihydro-7H-thiazolo[3,2-a]pyrimidin-7-one (8)**—A mixture of **7** (0.3 g, 14.9 mmol) and thionyl chloride (4.9 g, 41.2 mmol) with 2 drops of pyridine as a catalyst was stirred at room temperature for 5 h. The reaction mixture was poured onto ice, then neutralized with 5%  $NaHCO_3$ . The mixture was extracted with  $CHCl_3$ , and the extract was dried over  $Na_2SO_4$ . After evaporation of the solvent, the residue was crystallized from acetone, giving 50 mg (16.7%) of colorless needles, mp 174–175 °C. *Anal.* Calcd for  $C_7H_7ClN_2OS$ : C, 41.49; H, 3.48; N, 13.82; S, 15.82. Found: C, 41.74; H, 3.68; N, 13.57; S, 15.74. UV  $\lambda_{max}^{ethanol}$  nm (log  $\epsilon$ ): 234 (4.40), ca. 270 (sh, 3.85).  $^1H$ -NMR ( $CDCl_3$ )  $\delta$ : 6.30 (1H, s, C(6)-H), 4.59 (2H, t,  $J=7.5$  Hz, N- $CH_2$ ), 3.55 (2H, t,  $J=7.5$  Hz, S- $CH_2$ ), 3.06 (2H, s,  $CH_2$ -Cl).

**7-Bromomethyl-2,3-dihydro-5H-thiazolo[3,2-a]pyrimidin-5-one (10)**—A solution of bromine (6.4 g, 40 mmol) in  $CCl_4$  (15 ml) was added to a solution of diketene (3.36 g, 40 mmol) in  $CCl_4$  (30 ml) under ice cooling with stirring, and the temperature was maintained for 2 h. The reaction mixture was added to a solution of **1** (2.04 g, 20 mmol) in  $CHCl_3$  (30 ml) under ice cooling with stirring, and the whole was maintained at the same temperature for 2 h, then at room temperature for 3 h. The separated crystalline mass was collected and recrystallized from MeOH, giving 2.4 g (36.5%) of brown prisms, mp 299–300 °C (HBr salt). These crystals were dissolved in 5%  $NaHCO_3$ , and the solution was extracted with  $CHCl_3$ . The extract was dried over  $MgSO_4$ . After evaporation of the solvent, the residue was crystallized from MeOH, giving 0.9 g (18.2%) of colorless needles, mp 98–99 °C. *Anal.* Calcd for  $C_7H_7BrN_2OS$ : C, 34.02; H, 2.85; Br, 32.34; N, 11.34; S, 12.97. Found: C, 34.18; H, 2.87; Br, 31.87; N, 11.32; S, 12.97. IR (KBr): 1660 (C=O)  $cm^{-1}$ . UV  $\lambda_{max}^{ethanol}$  nm (log  $\epsilon$ ): 233 (3.94), 298 (3.81).  $^1H$ -NMR ( $CDCl_3$ )  $\delta$ : 6.25 (1H, s, C(6)-H), 4.47 (2H, t,  $J=7.5$  Hz, N- $CH_2$ ), 4.14 (2H, s,  $CH_2$ -Br), 3.47 (2H, t,  $J=7.5$  Hz, S- $CH_2$ ). MS  $m/z$ : 248 and 246 ( $M^+$ ).

**Hydrogenolysis of 10**—A mixture of **10** (60 mg, 0.24 mmol) and 5% Pd-C (50 mg) in EtOH (20 ml) was stirred under a hydrogen atmosphere at room temperature for 8 h. The reaction mixture was filtered, and the filtrate was concentrated to dryness *in vacuo*. The residue was treated with 5%  $NaHCO_3$ , then extracted with  $CHCl_3$ . The extract was dried over  $MgSO_4$  and filtered. The filtrate was evaporated to dryness and the residue was crystallized from AcOEt, giving **11**, 40 mg (99.2%) of colorless needles, mp 126–127 °C (lit.<sup>1b</sup>) mp 127–128 °C.

**6-Bromo-7-bromomethyl-2,3-dihydro-5H-thiazolo[3,2-a]pyrimidine-5-one (12)**—A solution of **10** (247 mg, 1.00 mmol) and *N*-bromosuccinimide (200 mg, 1.12 mmol) in EtOH (20 ml) was refluxed for 9 h. The reaction mixture was concentrated to dryness *in vacuo*, and the residue was crystallized from MeOH, giving 200 mg (61.3%) as colorless needles, mp 166–167 °C. *Anal.* Calcd for  $C_7H_6Br_2N_2OS$ : C, 25.79; H, 1.86; N, 8.59; Br, 49.02. Found: C, 25.96; H, 2.00; N, 8.57; Br, 48.57. IR (KBr): 1661 (C=O)  $cm^{-1}$ . UV  $\lambda_{max}^{ethanol}$  nm (log  $\epsilon$ ): 245 (3.94), 317 (3.94).  $^1H$ -NMR ( $CDCl_3$ )  $\delta$ : 4.52 (2H, t,  $J=7.9$  Hz, N- $CH_2$ ), 4.39 (2H, s,  $CH_2$ -Br), 3.52 (2H, t,  $J=7.9$  Hz, S- $CH_2$ ). MS  $m/z$ : 328, 326, and 324 ( $M^+$ ).

**6-Bromo-2,3-dihydro-7-methyl-5H-thiazolo[3,2-a]pyrimidin-5-one (13)**—a) A solution of **11** (168 mg, 1.00 mmol) and *N*-bromosuccinimide (200 mg, 1.12 mmol) in EtOH (20 ml) was refluxed for 4.5 h. The reaction mixture was ice-cooled and the separated crystalline mass was collected, then crystallized from MeOH, giving 100 mg (40.0%) of colorless prisms, mp 209–210 °C. *Anal.* Calcd for  $C_7H_7BrN_2OS$ : C, 34.02; H, 2.86; Br, 32.34; N, 11.34; S, 12.97. Found: C, 33.90; H, 2.93; Br, 32.34; N, 11.26; S, 13.06. IR (KBr): 1662 (C=O)  $cm^{-1}$ . UV  $\lambda_{max}^{ethanol}$  nm (log  $\epsilon$ ): 250 (3.78), 304 (3.99).  $^1H$ -NMR ( $CDCl_3$ )  $\delta$ : 4.51 (2H, t,  $J=7.5$  Hz, N- $CH_2$ ), 3.50 (2H, t,  $J=7.5$  Hz, S- $CH_2$ ), 2.43 (3H, s,  $CH_3$ ). MS  $m/z$ : 248 and 246 ( $M^+$ ).

b) A solution of bromine (0.3 ml) in acetic acid (1 ml) was added to a solution of **11** (340 mg, 2.02 mmol) in acetic acid (7 ml) with stirring; a reddish brown crystalline mass immediately separated. The mixture was heated at 90–95 °C for 2 h. After cooling, the separated crystalline mass was collected and recrystallized from MeOH, giving 340 mg (68.1%) of colorless prisms, mp 209–210 °C.

**2,3-Dihydro-7-morpholinomethyl-5H-thiazolo[3,2-a]pyrimidin-5-one (14)**—A solution of **10** (1.0 g, 4.0 mmol) and morpholine (0.7 g, 8.0 mmol) in EtOH (80 ml) was refluxed for 6 h. The reaction mixture was concentrated to dryness *in vacuo*. The residue was crystallized from MeOH, giving 0.9 g (87.9%) of colorless plates, mp 163–164 °C. *Anal.* Calcd for  $C_{11}H_{15}N_3O_2S$ : C, 52.15; H, 5.97; N, 16.59; S, 12.66. Found: C, 51.94; H, 6.00; N, 16.55; S, 12.72. IR (KBr): 1675, 1653 (C=O)  $cm^{-1}$ . UV  $\lambda_{max}^{ethanol}$  nm (log  $\epsilon$ ): 230 (3.89), 292 (3.85).  $^1H$ -NMR ( $CDCl_3$ )  $\delta$ : 6.29 (1H, s, C(6)-H), 4.47 (2H, t,  $J=7.9$  Hz, N- $CH_2$ ), 3.74 (4H, m, 2  $\times$  O- $CH_2$ ), 3.46 (2H, t,  $J=7.9$  Hz, S- $CH_2$ ), 3.33 (2H, s, C(7)- $CH_2$ ), 2.52 (4H, m, 2  $\times$  N- $CH_2$ ). MS  $m/z$ : 253 ( $M^+$ ).

**6-Bromo-2,3-dihydro-7-morpholinomethyl-5H-thiazolo[3,2-a]pyrimidin-5-one (15)**—A solution of **12** (652 mg, 2.0 mmol) and morpholine (348 mg, 4.0 mmol) in EtOH (60 ml) was refluxed for 3 h. The reaction mixture was concentrated, and the separated crystalline mass was collected and recrystallized from MeOH-AcOEt, giving 300 mg (45.2%) of colorless needles, mp 141–142 °C. *Anal.* Calcd for  $C_{11}H_{14}BrN_3O_2S$ : C, 39.77; H, 4.25; N, 12.65. Found: C, 39.85; H, 4.07; N, 12.53. IR (KBr): 1661 (C=O)  $cm^{-1}$ . UV  $\lambda_{max}^{ethanol}$  nm (log  $\epsilon$ ): 242 (3.84), 308 (3.94).  $^1H$ -NMR

(CDCl<sub>3</sub>)  $\delta$ : 4.52 (2H, t,  $J=7.8$  Hz, N-CH<sub>2</sub>), 3.74 (4H, m,  $2 \times$  O-CH<sub>2</sub>), 3.61 (2H, s, C(7)-CH<sub>2</sub>), 3.49 (2H, t,  $J=7.8$  Hz, S-CH<sub>2</sub>), 2.60 (4H, m,  $2 \times$  N-CH<sub>2</sub>). MS  $m/z$ : 333 and 331 (M<sup>+</sup>).

**5-Hydroxy-2,3,5,6-tetrahydro-7H-thiazolo[3,2-*a*]pyrimidin-7-one (16a)**—A solution of **3a** (1.0 g, 6.49 mmol) in 5% HCl (20 ml) was heated at 95–100 °C for 9 h. The reaction mixture was concentrated to dryness *in vacuo*. Water was added to the residue, and the mixture was evaporated to dryness *in vacuo*. The crystalline residue was recrystallized from H<sub>2</sub>O, giving 720 mg (64.5%) of colorless prisms, mp 211–213 °C. *Anal.* Calcd for C<sub>6</sub>H<sub>8</sub>N<sub>2</sub>O<sub>2</sub>S: C, 41.85; H, 4.68; N, 16.27; S, 18.62. Found: C, 41.86; H, 4.48; N, 16.16; S, 18.81. IR (KBr): 3400, 3170 (OH), 1700 (br) (C=O) cm<sup>-1</sup>. UV: no absorption maximum. <sup>1</sup>H-NMR (270 MHz: CDCl<sub>3</sub> and 3 drops of CF<sub>3</sub>COOH)  $\delta$ : 9.23 (1H, s, OH), 5.02 (1H, dd,  $J=4.4, 12.6$  Hz, C(5)-H), 4.16 (1H, dt,  $J=6.6, 6.6, 11.5$  Hz, N-CH), 3.85 (1H, quintet,  $J=5.5, 5.5, 11.5$  Hz, N-CH), 3.3–3.15 (2H, m, S-CH<sub>2</sub>), 3.14 (1H, dd,  $J=4.4, 17.0$  Hz, C(6)-H), 2.92 (1H, dd,  $J=12.6, 17.0$  Hz, C(6)-H). <sup>13</sup>C-NMR (pyridine-*d*<sub>5</sub>)  $\delta$ : 169.29 (s, C(7 or 1a)), 151.33 (s, C(1a or 7)), 57.43 (d, C(5)), 48.82 (t, C(3)), 38.44 (t, C(2)), 29.28 (t, C(6)). FAB-MS  $m/z$ : 173 [(M+1)<sup>+</sup>].

**5-Carboxy-2,3,5,6-tetrahydro-5-hydroxy-7H-thiazolo[3,2-*a*]pyrimidin-7-one (16b)**—A solution of **3b** (0.56 g, 2.48 mmol) in 5% HCl (6 ml) was heated at 90–95 °C for 8 h. The reaction mixture was worked up as described above, giving 0.4 g (74.7%, H<sub>2</sub>O) of colorless powder, mp 236 °C (sub.). *Anal.* Calcd for C<sub>7</sub>H<sub>8</sub>N<sub>2</sub>O<sub>4</sub>S: C, 38.88; H, 3.73; N, 12.96; S, 14.83. Found: C, 38.18; H, 3.66; N, 12.98; S, 14.88. IR (KBr): 3245 (OH), 1738, 1720 (sh), 1659 (C=O) cm<sup>-1</sup>. UV: no absorption maximum. <sup>1</sup>H-NMR (270 MHz: CDCl<sub>3</sub> and 3 drops of CF<sub>3</sub>COOH)  $\delta$ : 9.48 (1H, s, OH), 4.32 (1H, dt,  $J=6.9, 6.9, 11.5$  Hz, N-CH), 4.13 (1H, ddd,  $J=5.0, 6.9, 11.5$  Hz, N-CH), 3.70 (1H, d,  $J=17.0$  Hz, C(6)-H), 3.5–3.3 (2H, m, S-CH<sub>2</sub>), 3.18 (1H, d,  $J=17.0$  Hz, C(6)-H). <sup>13</sup>C-NMR (DMSO-*d*<sub>6</sub>)  $\delta$ : 171.43 (s, COOH), 167.47 (s, C(7 or 1a)), 149.43 (s, C(1a or 7)), 67.08 (s, C(5)), 48.93 (t, C(3)), 40.80 (t, C(2)), 28.77 (t, C(6)). FAB-MS  $m/z$ : 217 [(M+1)<sup>+</sup>].

**5-Hydroxy-5-hydroxymethyl-2,3,5,6-tetrahydro-7H-thiazolo[3,2-*a*]pyrimidin-7-one (16c)**—A solution of **3c** (300 mg, 1.63 mmol) in 5% HCl (8 ml) was heated at 95–100 °C for 6 h. The reaction mixture was worked up as described above, giving 190 mg (57.7%, H<sub>2</sub>O) of colorless prisms, mp 210–212 °C. *Anal.* Calcd for C<sub>7</sub>H<sub>10</sub>N<sub>2</sub>O<sub>3</sub>S: C, 41.58; H, 4.98; N, 13.85. Found: C, 41.50; H, 4.85; N, 13.71. IR (KBr): 3395, 3190 (OH), 1710 (sh), 1695 (C=O) cm<sup>-1</sup>. UV  $\lambda_{\text{max}}^{\text{ethanol}}$  nm (log  $\epsilon$ ): 262 (sh, 3.45). <sup>1</sup>H-NMR (270 MHz: CDCl<sub>3</sub> and 3 drops of CF<sub>3</sub>COOH)  $\delta$ : 9.32 (1H, s, OH), 4.44 (1H, ddd,  $J=5.0, 7.0, 12.1$  Hz, N-CH), 3.96 (1H, d,  $J=12.6$  Hz, C(6)-H), 3.80 (1H, dt,  $J=6.6, 7.0, 12.1$  Hz, N-CH), 3.78 (1H, d,  $J=12.6$  Hz, C(6)-H), 3.3–3.15 (2H, m, S-CH<sub>2</sub>), 3.23 (2H, s, O-CH<sub>2</sub>). <sup>13</sup>C-NMR (pyridine-*d*<sub>5</sub>)  $\delta$ : 169.4 (s, C(7)), 151.5 (s, C(1a)), 71.5 (s, C(5)), 69.0 (t, CH<sub>2</sub>OH), 48.4 (t, C(3)), 41.8 (t, C(2)). FAB-MS  $m/z$ : 203 [(M+1)<sup>+</sup>].

**1-(2-Mercaptoethyl)-6-phenyl-2,4(1H,3H)-pyrimidinedione (18)**—A solution of **17** (0.5 g, 2.17 mmol) in 5% HCl (10 ml) was refluxed for 4 h. The reaction mixture was worked up as described above, giving 0.30 g (55.8%, AcOEt) of colorless needles, mp 164–165 °C. *Anal.* Calcd for C<sub>12</sub>H<sub>12</sub>N<sub>2</sub>O<sub>2</sub>S: C, 58.05; H, 4.87; N, 11.28. Found: C, 58.35; H, 4.97; N, 11.06. IR (KBr): 2530 (SH), 1702 (C=O) cm<sup>-1</sup>. UV  $\lambda_{\text{max}}^{\text{ethanol}}$  nm (log  $\epsilon$ ): 275 (4.05). <sup>1</sup>H-NMR (CDCl<sub>3</sub>)  $\delta$ : 9.4 (1H, br s, NH), 7.6–7.2 (5H, m, C<sub>6</sub>H<sub>5</sub>), 5.63 (1H, s, ring), 3.83 (2H, dd,  $J=7.25, 5.27$  Hz, N-CH<sub>2</sub>), 2.63 (2H, m, S-CH<sub>2</sub>), 1.19 (1H, t,  $J=8.8$  Hz, SH).

**3-(2-Mercaptoethyl)-6-methyl-2,4(1H,3H)-pyrimidinedione (19)**—A solution of **11** (1.0 g, 5.95 mmol) in 5% HCl (20 ml) was refluxed for 2 h. The reaction mixture was worked up as described above, giving 0.65 g (58.1%, H<sub>2</sub>O) of colorless prisms, mp 203 °C. *Anal.* Calcd for C<sub>7</sub>H<sub>10</sub>N<sub>2</sub>O<sub>2</sub>S · 1/10H<sub>2</sub>O: C, 44.71; H, 5.47; N, 14.90. Found: C, 44.76; H, 5.30; N, 14.67. IR (KBr): 2555 (SH), 1725, 1705, 1642 (C=O) cm<sup>-1</sup>. UV  $\lambda_{\text{max}}^{\text{ethanol}}$  nm (log  $\epsilon$ ): 264 (4.08). FAB-MS  $m/z$ : 187 [(M+1)<sup>+</sup>]. <sup>1</sup>H-NMR (CDCl<sub>3</sub> and 5 drops of CF<sub>3</sub>COOH)  $\delta$ : 10.37 (1H, br s, NH), 5.91 (1H, q,  $J=0.88$  Hz, ring), 4.14 (2H, dd,  $J=7.03, 5.71$  Hz, N-CH<sub>2</sub>), 2.80 (2H, m, S-CH<sub>2</sub>), 2.26 (3H, d,  $J=0.88$  Hz, CCH<sub>3</sub>), 1.41 (1H, t,  $J=8.7$  Hz, CH<sub>2</sub>SH). <sup>13</sup>C-NMR (DMSO-*d*<sub>6</sub>)  $\delta$ : 162.43 (C(4)), 151.27 (C(2 or 6)), 151.16 (C(6 or 2)), 98.18 (C(5)), 41.77 (CH<sub>2</sub>N), 21.02 (CH<sub>2</sub>SH), 17.93 (CH<sub>3</sub>).

**3,3'-Bis[6-methyl-1,2,3,4-tetrahydro-2,4-dioxypyrimidinyl]diethyldisulfide (20)**—A solution of **11** (336 mg, 2.00 mmol) in 5% HCl (30 ml) was heated at 95–100 °C for 7 h. The reaction mixture was concentrated to dryness *in vacuo*. Water was added to the residue, and the mixture was evaporated to dryness *in vacuo*. The residue was treated with 5% NaHCO<sub>3</sub>, and the insoluble crystalline mass was collected and recrystallized from MeOH, giving 100 mg (26.6%) of colorless powder, mp 283–285 °C. *Anal.* Calcd for C<sub>14</sub>H<sub>18</sub>N<sub>4</sub>O<sub>4</sub>S<sub>2</sub> · 0.3H<sub>2</sub>O: C, 44.74; H, 4.99; N, 14.91. Found: C, 44.69; H, 4.95; N, 14.50. IR (KBr): 3550, 3430 (NH), 1730, 1707 (sh), 1645 (C=O) cm<sup>-1</sup>. UV  $\lambda_{\text{max}}^{\text{ethanol}}$  nm (log  $\epsilon$ ): 263 (4.36). FAB-MS  $m/z$ : 371 [(M+1)<sup>+</sup>]. <sup>1</sup>H-NMR (CDCl<sub>3</sub> and 3 drops of CF<sub>3</sub>COOH)  $\delta$ : 5.92 (2H, s, 2 × ring), 4.33 (4H, dd,  $J=7.91, 6.59$  Hz,  $2 \times$  N-CH<sub>2</sub>), 2.97 (4H, dd,  $J=7.91, 6.59$  Hz,  $2 \times$  S-CH<sub>2</sub>), 2.28 (6H, s,  $2 \times$  CH<sub>3</sub>).

**Acknowledgement** The authors are grateful to Mr. Y. Kinoshita, Kissei Pharmaceutical Industry, for measuring the <sup>1</sup>H-NMR (270 MHz) spectra. Thanks are also due to Mrs. H. Mazume, Mr. M. Ohwatari, Mr. K. Inada, and Mr. N. Yamaguchi for elemental analysis, IR, UV, NMR, and mass spectra.

#### References

- 1) a) N. G. Pashkurov and V. S. Reznik, *Khim. Geterotsikl. Soedin*, **1968**, 918 [*Chem. Abstr.*, **71**, 13088 (1969)]; b)

- G. R. Brown and W. R. Dyson, *J. Chem. Soc. C*, **1971**, 1527.
- 2) a) E. Campaigne, J. C. Huffman, and T. P. Selby, *J. Heterocycl. Chem.*, **16**, 725 (1979); b) E. Campaigne, K. Folting, J. C. Huffman, and T. P. Selby, *ibid.*, **18**, 575 (1981).
  - 3) M. Szajda and E. Wyrzykiewicz, *Pol. J. Chem.*, **57**, 1027 (1983).
  - 4) G. Shaw and R. N. Warrener, *J. Chem. Soc.*, **1959**, 50.
  - 5) a) S. Giambone, *Bull. Sci. Fac. Chim. Ind. Bologna*, **11**, 86 (1953) [*Chem. Abstr.*, **49**, 4662 (1955)]; b) V. Škarić, D. Škarić, and A. Čižmek, *J. Chem. Soc., Perkin Trans. I*, **1984**, 2221; c) M. Mizutani, Y. Sanemitsu, Y. Tamura, and Z. Yoshida, *J. Org. Chem.*, **50**, 764 (1985).
  - 6) T. Kato, N. Katagiri, U. Izumi, Y. Miura, T. Yamazaki, and Y. Hirai, *Heterocycles*, **15**, 399 (1981).
  - 7) a) M. Seperic, Ger Offen. 2140601 [*Chem. Abstr.*, **77**, 5516 (1972)]; b) J. Baetz, Brit. Patent 1334628 [*Chem. Abstr.*, **80**, 48028 (1974)]; c) SEPERIC, Fr. Demande, 2173668 [*Chem. Abstr.*, **80**, 96015 (1974)]; d) SEPERIC, Neth. Appl. 7600885 [*Chem. Abstr.*, **87**, 85046 (1977)]; e) SEPERIC, Bel. 778911 [*Chem. Abstr.*, **80**, 48028 (1974)].
  - 8) K. D. Kampe, *Angew. Chem.*, **94**, 543 (1982).
  - 9) H. N. Al-Jallo and M. A. Muniem, *J. Heterocycl. Chem.*, **15**, 849 (1978).
  - 10) R. A. Glennon, R. G. Bass, and E. Schubert, *J. Heterocycl. Chem.*, **16**, 903 (1979).
  - 11) a) N. Okamura, T. Toru, T. Tanaka, K. Watanabe, K. Bannai, S. Kurozumi, T. Naruchi, and K. Kamoriya, Eur. Pat. Appl., EP 49902 [*Chem. Abstr.*, **97**, 92311 (1982)]; b) Teijin Ltd., Jpn. Kokai Tokkyo Koho JP 83 24590 [*Chem. Abstr.*, **98**, 215611 (1983)]; c) Teijin Ltd., Jpn. Kokai Tokkyo Koho JP 84 88491 [*Chem. Abstr.*, **101**, 230562 (1984)].
  - 12) R. N. Warrener and E. N. Cain, *Aust. J. Chem.*, **24**, 785 (1971).
  - 13) D. W. Dunwell and D. Evans, *J. Chem. Soc. C*, **1971**, 2094.
  - 14) K. Tabei, E. Kawashima, T. Takeda, and T. Kato, *Chem. Pharm. Bull.*, **30**, 3987 (1982).
  - 15) K. Hirota, Y. Yamada, Y. Kitade, and S. Senda, *J. Chem. Soc., Perkin Trans. I*, **1981**, 2943.
  - 16) E. Falch and T. Natvig, *Acta Chem. Scand.*, **24**, 1423 (1970).
  - 17) T. Kinoshita, H. Tanaka, and S. Furukawa, *Chem. Pharm. Bull.*, **34**, 1809 (1986).

[Chem. Pharm. Bull.]  
[35(1) 97-107 (1987)]

## New Acylated Flavonol Glucosides in *Allium tuberosum* ROTTLER

TAKATOSHI YOSHIDA,\* TAKASHI SAITO, and SHIZUO KADOYA

Research Institute, Daiichi Seiyaku Co., Ltd., 16-13, Kitakusai  
1-chome, Edogawa-ku, Tokyo 134, Japan

(Received June 12, 1986)

Six flavonoids (1-6) were isolated from the leaves of *Allium tuberosum* ROTTLER (Liliaceae). Their structures were characterized as 3-*O*- $\beta$ -sophorosyl-7-*O*- $\beta$ -D-(2-*O*-feruloyl)glucosylkaempferol (1), 3,4'-di-*O*- $\beta$ -D-glucosyl-7-*O*- $\beta$ -D-(2-*O*-feruloyl)glucosylkaempferol (2), 3-*O*- $\beta$ -D-(2-*O*-feruloyl)-glucosyl-7,4'-di-*O*- $\beta$ -D-glucosylkaempferol (3), 3,4'-di-*O*- $\beta$ -D-glucosylkaempferol (4), 3,4'-di-*O*- $\beta$ -D-glucosylquercetin (5) and 3-*O*- $\beta$ -sophorosylkaempferol (6) by examination of their physico-chemical properties. On partial acid hydrolysis, 1 gave 7-*O*- $\beta$ -D-(2-*O*-feruloyl)glucosylkaempferol (10), and on enzymatic hydrolysis, 1 and 3 afforded 3-*O*- $\beta$ -D-glucosyl-7-*O*- $\beta$ -D-(2-*O*-feruloyl)-glucosylkaempferol (11) and 3-*O*- $\beta$ -D-(2-*O*-feruloyl)glucosylkaempferol (14), respectively. At pH 7.0 or at pH 11.0, or both, the 2-*O*-feruloyl group of 1, 2, 10 and 11 migrated to give the corresponding 6-*O*-feruloyl derivatives (15, 17, 16 and 18). Compounds 1-3 and their derivatives 10, 11, 14, 15, 16, 17 and 18 are new acylated flavonol glucosides.

**Keywords**—*Allium tuberosum*; Liliaceae; flavonol; kaempferol; quercetin; ferulic acid; glucoside; acylated flavonol glucoside; acyl migration

*Allium tuberosum* ROTTLER (Liliaceae) is a perennial herb which has been cultivated widely and whose leaves have been used as food. Various sulfide derivatives,<sup>1)</sup> linalool<sup>1)</sup> and 3-*O*-rhamnogalactosyl-7-*O*-rhamnosylkaempferol<sup>2)</sup> have been isolated from the leaves of *A. tuberosum*. According to the dictionary of Chinese drugs,<sup>3)</sup> they have been used for treatment of abdominal pain, diarrhea, hematemesis, snake-bite and asthma. We have attempted to

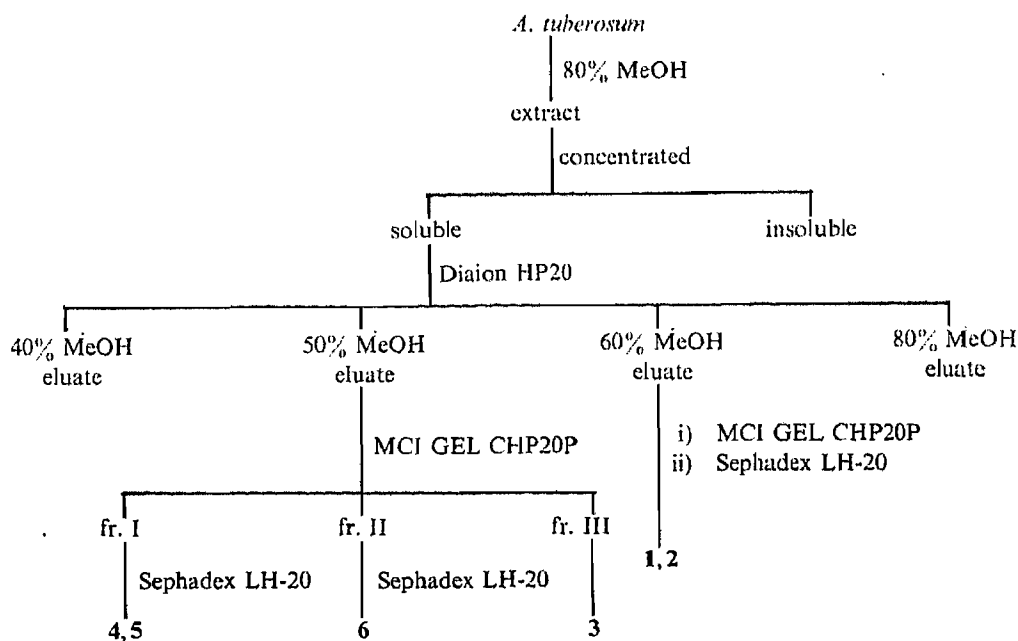


Chart 1

isolate anti-allergic agents from *A. tuberosum*, and have obtained three new acylated flavonol glucosides together with three known flavonol glucosides. This paper deals with the isolation and structural elucidation of these compounds, and the acyl migration of acylated flavonol glucosides.

Commercially available fresh leaves of *A. tuberosum* were extracted with 80% methanol, and the extract was treated as shown in Chart 1 to isolate compounds 1–6.

Compound 1 exhibited absorption maxima at 233, 269 and 333 nm in the ultraviolet (UV) spectrum, and its field desorption mass spectrum (FD-MS) showed  $[M^+ + K]$  at  $m/z$  987 and  $[M^+ + Na]$  at  $m/z$  971. On acid hydrolysis, 1 gave kaempferol and D-glucose, and on alkaline hydrolysis it afforded ferulic acid and kaempferol glucoside (8). Methylation of 1 according to Hakomori's method<sup>4)</sup> followed by hydrolysis gave, in a ratio of 2:1, 2,3,4,6-tetra-*O*-methylglucose and 3,4,6-tri-*O*-methylglucose, which were identified as alditol acetates by gas liquid chromatography (GLC) and GLC-mass spectrometry (GLC-MS). Acetylation of 1 afforded a tridecaacetate, the proton nuclear magnetic resonance (<sup>1</sup>H-NMR) spectrum of which showed the signals of three aromatic and ten aliphatic acetoxy protons. From these data 1 was found to contain a D-glucosyl (1→2)-D-glucose moiety and a D-glucose moiety attached to kaempferol, and a feruloyl moiety attached to D-glucose.

In the UV spectrum the diagnostic shifts<sup>5)</sup> of 8 on addition of sodium acetate, sodium methoxide or aluminum chloride showed that glucose was linked to kaempferol at C-3 and -7.<sup>6)</sup> The <sup>1</sup>H-NMR spectrum of 8, as shown in Table I, exhibited the signals of β-anomeric protons at 4.66, 5.10 and 5.72 ppm, which could be assigned to the anomeric protons of glucose linked to C-2 of glucose, and to C-3 and -7 of kaempferol, respectively. In the <sup>13</sup>C-nuclear magnetic resonance (<sup>13</sup>C-NMR) spectrum, as shown in Table II, the signals due to C-3 and -7 were shifted upfield, and the signals due to C-2, -4, -6, -8 and -10 were shifted downfield from those of kaempferol.<sup>7)</sup> On partial acid hydrolysis with 1% sulfuric acid, 8 gave 7-*O*-β-D-glucosylkaempferol (9) and sophorose.<sup>8a,b)</sup> On enzymatic hydrolysis with β-glucosidase, 8 afforded 3-*O*-β-sophorosylkaempferol (6).<sup>8a,b)</sup> These results suggested that 8 is 3-*O*-β-sophorosyl-7-*O*-β-D-glucosylkaempferol.<sup>8b)</sup>

The linkage between the feruloyl group and glucose in 1 was determined from the <sup>1</sup>H-

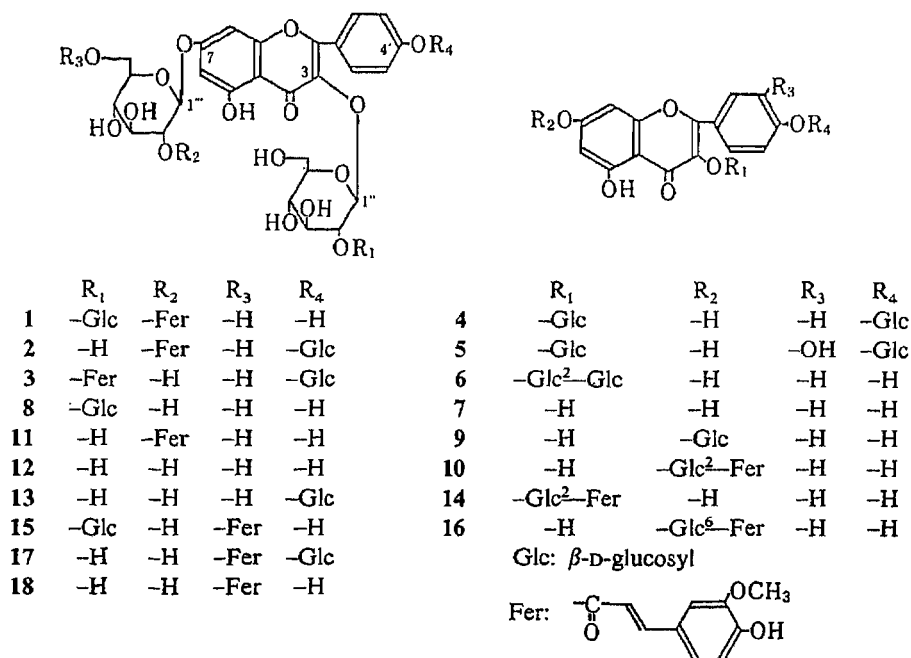


Chart 2

TABLE I. <sup>1</sup>H-NMR Spectral Data for Kaempferol Glucosides (in DMSO-*d*<sub>6</sub>-D<sub>2</sub>O, *J*=Hz)

	Kaempferol moiety				Sugar moiety						Feruloyl moiety						
	6 d, <i>J</i> =2	8 d, <i>J</i> =2	2',6' d, <i>J</i> =8	3',5' d, <i>J</i> =8	1-K3 <sup>a)</sup> d, <i>J</i> =8	2-K3 t, <i>J</i> =8	1-G2 d, <i>J</i> =8	1-K7 d, <i>J</i> =8	2-K7 t, <i>J</i> =8	6-K7 dd, d <sup>b)</sup>	1-K4' d, <i>J</i> =8	2 d, <i>J</i> =16	3 d, <i>J</i> =16	2' d, <i>J</i> =2	5' d, <i>J</i> =8	6' dd <sup>c)</sup>	OMe s
1	6.41	6.80	8.11	6.95	5.69 <sup>d)</sup>		4.65	5.46	4.97			6.50	7.64	7.31	6.83	7.16 <sup>d)</sup>	3.80
2	3.42	6.83	8.16	7.19	5.50			5.48	4.97	5.05		6.49	7.62	7.32	6.81	7.14 <sup>d)</sup>	3.80
3	6.49	6.86	8.18	7.21	5.80	4.92		5.10		5.10		6.53	7.64	7.34	6.84	7.16	3.83
4	6.29	6.53	8.16	7.20	5.51					5.06							
6	6.27	6.51	8.10	6.96	5.71 <sup>d)</sup>		4.65										
7	6.28	6.54	8.10	7.00													
8	6.48	6.84	8.12	6.97	5.72 <sup>d)</sup>		4.66	5.10									
9	6.48	6.86	8.12	6.99				5.09									
10	6.40	6.81	8.11	6.98				5.47	4.98			6.47	7.64	7.30	6.82	7.15	3.80
11	6.42	6.80	8.10	6.93	5.48			5.48	4.98			6.50	7.64	7.32	6.82	7.15	3.80
12	6.49	6.84	8.10	6.94	5.51			5.10									
13	6.51	6.87	8.19	7.21	5.54			5.12		5.07							
14	6.22	6.46	8.07	6.94	5.79	4.90						6.51	7.62	7.32	6.83	7.14	3.83
15	6.55	6.85	8.12	6.93	5.70 <sup>d)</sup>		4.66	5.18		4.21, 4.52		6.47	7.59	7.27	6.82	7.08	3.80
16	6.52	6.82	8.09	6.94				5.18		4.19, 4.54		6.42	7.53	6.94	6.72	7.18	3.76
17	6.59	6.85	8.16	7.18	5.48			5.19		4.21, 4.51	5.03	6.46	7.57	7.23	6.82	7.06 <sup>d)</sup>	3.81
18	6.57	6.82	8.09	6.92	5.49			5.19		4.20, 4.49		6.47	7.56	7.27	6.80	7.06 <sup>d)</sup>	3.80

a) Position of glucose proton; the linkage position of glucose to kaempferol (K) or glucose (G) is shown after the hyphen. b) Coupling constant: dd, *J*=12, 8; d, *J*=8. c) *J*=8, 2. d) Broad.

TABLE II.  $^{13}\text{C}$ -NMR Spectral Data for Kaempferol Glucosides (in  $\text{DMSO-}d_6$ )

Carbon	1	2	3	7	8	13	15	Carbon	1	2	3	8	13	15
<b>Kaempferol moiety</b>								<b>3-O-Sugar moiety</b>						
2	155.7 <sup>a)</sup>	155.9 <sup>a)</sup>	156.0 <sup>a)</sup>	146.8	155.8 <sup>a)</sup>	156.0	155.8 <sup>a)</sup>	1	97.7	100.6	98.1	97.8	100.6	97.9
3	133.1	133.9	133.3	135.7	133.1	133.9	133.1	2	82.4	74.1	74.0 <sup>b)</sup>	82.3	74.1	82.5
4	177.5	177.6	177.4	175.9	177.5	177.6	177.6	3	76.5	76.6 <sup>b)</sup>	73.9 <sup>b)</sup>	76.5	76.3	76.5
5	160.9	160.9	160.7	160.7	160.8	160.8	161.0	4	69.6	69.7 <sup>c)</sup>	70.1 <sup>c)</sup>	69.6	69.8 <sup>a)</sup>	69.5 <sup>b)</sup>
6	98.9	99.1	99.4	98.3	99.2	99.4	99.0	5	77.4 <sup>b)</sup>	77.5 <sup>d)</sup>	77.8 <sup>d)</sup>	77.4 <sup>b)</sup>	77.5 <sup>b)</sup>	77.4
7	161.9	162.1	162.8	164.0	162.6	162.8	162.5	6	60.6 <sup>c)</sup>	60.8 <sup>e)</sup>	60.5	60.7 <sup>c)</sup>	60.8 <sup>c)</sup>	60.5 <sup>c)</sup>
8	94.5	94.5	94.4	93.5	94.3	94.3	94.5	1'	104.1			104.0		104.1
9	156.1 <sup>a)</sup>	156.2 <sup>a)</sup>	156.1 <sup>a)</sup>	156.2	156.1 <sup>a)</sup>	156.0	156.1 <sup>a)</sup>	2'	74.3			74.3		74.3
10	105.7	105.9	105.6	103.0	105.5	105.7	105.6	3'	76.5			76.5		76.5
1'	120.6	123.4	123.1	121.7	120.6	123.5	120.7	4'	69.6			69.6		69.6 <sup>b)</sup>
2'	131.0	130.6	130.6	129.5	130.9	130.5	130.9	5'	76.9			76.9		76.9
3'	115.2	115.7	115.7	115.4	115.3	115.7	115.2	6'	60.8 <sup>c)</sup>			61.0 <sup>c)</sup>		60.8 <sup>c)</sup>
4'	160.2	159.3	159.6	159.2	160.1	159.2	160.0	<b>7-O-Sugar moiety</b>						
5'	115.2	115.7	115.7	115.4	115.3	115.7	115.2	1	97.3	97.3	99.9 <sup>e)</sup>	99.7	99.9 <sup>d)</sup>	99.6
6'	131.0	130.6	130.6	129.5	130.9	130.5	130.9	2	73.0 <sup>d)</sup>	73.1 <sup>f)</sup>	73.1 <sup>f)</sup>	73.0	73.1 <sup>e)</sup>	73.0
<b>Feruloyl moiety</b>								3	73.9 <sup>d)</sup>	73.8 <sup>f)</sup>	76.4 <sup>g)</sup>	76.5	76.3	76.1
1	165.6	165.6	165.8				166.5	4	69.6	69.6 <sup>c)</sup>	69.5 <sup>c)</sup>	69.6	69.5 <sup>a)</sup>	69.5 <sup>b)</sup>
2	114.2	114.2	114.5				114.1	5	77.3 <sup>b)</sup>	77.3 <sup>d)</sup>	77.0 <sup>d)</sup>	77.1 <sup>b)</sup>	77.0 <sup>b)</sup>	73.9
3	145.4	145.5	145.3				145.2	6	60.4 <sup>c)</sup>	60.7 <sup>e)</sup>	60.5	60.6 <sup>c)</sup>	60.7 <sup>c)</sup>	63.1
1'	125.5	125.4	125.5				125.4	<b>4'-O-Sugar moiety</b>						
2'	111.0	110.9	111.0				111.0	1		99.8	99.6 <sup>e)</sup>		99.6 <sup>d)</sup>	
3'	147.9	147.9	147.8				147.8	2		73.0 <sup>f)</sup>	72.9 <sup>f)</sup>		72.9 <sup>e)</sup>	
4'	149.3	149.3	149.2				149.3	3		76.4 <sup>b)</sup>	76.3 <sup>g)</sup>		76.3	
5'	115.4	115.4	115.4				115.4	4		69.5 <sup>c)</sup>	69.5 <sup>c)</sup>		69.5 <sup>a)</sup>	
6'	123.2	123.2	123.2				123.1	5		77.0 <sup>d)</sup>	77.0 <sup>d)</sup>		77.0 <sup>b)</sup>	
OMe	55.6	55.6	55.6				55.6	6		60.6 <sup>e)</sup>	60.5		60.6 <sup>c)</sup>	

a—g) Assignments may be interchangeable within the same column.



and  $^{13}\text{C}$ -NMR spectra. The  $^1\text{H}$ -NMR spectrum of **1** exhibited signals ascribable to kaempferol and feruloyl moieties, along with those of three  $\beta$ -anomeric protons of glucose linked to C-2'', -7 and -3 at 4.65, 5.46 and 5.69 ppm, respectively, and a triplet signal due to a proton on carbon bearing an acyl group at 4.97 ppm. This triplet signal was found to be coupled with H-1''' by spin decoupling. The acylation shifts<sup>7,9)</sup> in  $^{13}\text{C}$ -NMR spectroscopy are useful for determining the positions of acyl groups in partially acylated glycosides. In the  $^{13}\text{C}$ -NMR spectrum of **1**, the signals due to C-1''' and -3''' were shifted upfield in comparison with those of **8**, while other signals remained almost unaffected. These data suggested that the feruloyl group was linked to C-2''. In order to confirm this assumption, partial and enzymatic hydrolyses of **1** were examined.

On partial acid hydrolysis with 5% sulfuric acid, **1** afforded kaempferol glucoside (**10**). On hydrolysis with 1% potassium hydroxide, **10** gave ferulic acid and **9**. Acetylation of **10** gave a heptaacetate, the  $^1\text{H}$ -NMR spectrum of which showed the signals of four aromatic and three aliphatic acetoxy protons. The  $^1\text{H}$ -NMR spectrum of **10** exhibited the signal of a  $\beta$ -anomeric proton of glucose attached to C-7 at 5.47 ppm and a triplet due to a proton on carbon bearing an acyl group at 4.98 ppm, coupled with each other. Consequently, **10** was established to be 7-*O*- $\beta$ -D-(2-*O*-feruloyl)glucosylkaempferol.

On enzymatic hydrolysis with crude hesperidinase, **1** afforded kaempferol glucoside (**11**). Treatment of **11** with 1% potassium hydroxide gave ferulic acid and 3,7-di-*O*- $\beta$ -D-glucosylkaempferol (**12**), which was identified on the basis of the diagnostic shifts<sup>6)</sup> in the UV spectrum, and the  $^1\text{H}$ -NMR spectrum. Acetylation of **11** afforded a decaacetate, the  $^1\text{H}$ -NMR spectrum of which showed the signals of three aromatic and seven aliphatic acetoxy protons. The  $^1\text{H}$ -NMR spectrum of **11** exhibited the signals of two  $\beta$ -anomeric protons and a triplet due to a proton on carbon bearing an acyl group. Therefore, **11** was established to be 3-*O*- $\beta$ -D-glucosyl-7-*O*- $\beta$ -D-(2-*O*-feruloyl)glucosylkaempferol.

On the basis of the above results, the structure of compound **1** was established as 3-*O*- $\beta$ -sophorosyl-7-*O*- $\beta$ -D-(2-*O*-feruloyl)glucosylkaempferol.

Compounds **2** and **3** exhibited similar absorption maxima in the UV spectrum, and their FD-MS showed  $[\text{M}^+ + 1]$  at  $m/z$  949. On acetylation **2** and **3** afforded a tridecaacetate, whose  $^1\text{H}$ -NMR spectra showed the signals of two aromatic and eleven aliphatic acetoxy protons. Acid hydrolysis of **2** and **3** gave kaempferol and D-glucose, and alkaline hydrolysis afforded ferulic acid and kaempferol glucoside (**13**). These observations indicated that **2** and **3** are isomers in which the positions of the feruloyl group on **13** differ.

Enzymatic hydrolysis of **13** with  $\beta$ -glucosidase gave kaempferol. In the  $^1\text{H}$ -NMR spectrum of **13**, the signals of three  $\beta$ -anomeric protons of glucose linked to phenolic oxygen were observed at 5.07, 5.12 and 5.54 ppm, the H-3' and -5' signals were shifted downfield in comparison with those of **8**, and a hydrogen-bonded 5-OH proton signal was observed at 12.61 ppm in dimethyl sulfoxide- $d_6$  (DMSO- $d_6$ ). In the  $^{13}\text{C}$ -NMR spectrum, the C-1' signal was shifted upfield<sup>7)</sup> from that of **8**. From these results and the diagnostic shifts in the UV spectrum, **13** was established to be 3,7,4'-tri-*O*- $\beta$ -D-glucosylkaempferol, a rare flavonol glycoside that has been isolated only as the *p*-coumarate from *Crambe cordifolia*.<sup>10)</sup>

The  $^1\text{H}$ -NMR spectrum of **2** showed the signals of  $\beta$ -anomeric protons at 5.05, 5.48 and 5.50 ppm, and a triplet due to a proton on carbon bearing an acyl group at 4.97 ppm, coupled with the anomeric proton at 5.48 ppm. In the  $^{13}\text{C}$ -NMR spectrum of **2**, the signals due to C-1 and -3 of glucose linked to C-7 or -4' were shifted upfield compared with those of **13**. Moreover, partial acid hydrolysis of **2** afforded **5**. These data suggested that a feruloyl group is linked to C-2''. Thus, compound **2** was deduced to be 3,4'-di-*O*- $\beta$ -D-glucosyl-7-*O*- $\beta$ -D-(2-*O*-feruloyl)glucosylkaempferol.

The  $^1\text{H}$ -NMR spectrum of **3** exhibited three  $\beta$ -anomeric signals, and a triplet due to a proton on carbon bearing an acyl group, coupled with the H-1'' proton. In the  $^{13}\text{C}$ -NMR

spectrum, the signals due to C-1'' and -3'' were shifted upfield in comparison with those of 13, while other signals remained almost unaffected.

Enzymatic hydrolysis of 3 with  $\beta$ -glucosidase yielded kaempferol glucoside (14), and its FD-MS showed  $[M^+ + 1]$  at  $m/z$  625. Acetylation of 14 afforded a heptaacetate, the  $^1\text{H-NMR}$  spectrum of which exhibited the signals of four aromatic and three aliphatic acetoxy protons. These results showed the elimination of two glucose molecules from 3. The  $^1\text{H-NMR}$  spectrum of 14 exhibited the signal of a  $\beta$ -anomeric proton of glucose attached to C-3 at 5.79 ppm, coupled with the triplet signal at 4.90 ppm. In this way, 14 was deduced to be 3-*O*- $\beta$ -D-(2-*O*-feruloyl)glucosylkaempferol.

The above results established compound 3 as 3-*O*- $\beta$ -D-(2-*O*-feruloyl)glucosyl-7,4'-di-*O*- $\beta$ -D-glucosylkaempferol.

Compound 4 exhibited absorption maxima at 267 and 344 nm in the UV spectrum, and its FD-MS showed  $[M^+ + 1]$  at  $m/z$  611. Acid hydrolysis of 3 afforded kaempferol and D-glucose. In the  $^1\text{H-NMR}$  spectrum two  $\beta$ -anomeric proton signals were observed at 5.06 and 5.51 ppm, and the signals due to H-3' and -5' were shifted downfield in comparison with those of 7. From these data and the diagnostic shifts in the UV spectrum, glucose is linked to C-3 and -4'. Compound 4 was thus established to be 3,4'-di-*O*- $\beta$ -D-glucosylkaempferol.<sup>11)</sup>

Compound 5 exhibited absorption maxima at 267 and 348 nm in the UV spectrum, and its FD-MS showed  $[M^+ + 1]$  at  $m/z$  627. On acid hydrolysis, 5 afforded quercetin and D-glucose. In the  $^1\text{H-NMR}$  spectrum two  $\beta$ -anomeric proton signals were observed at 4.92 and 5.53 ppm, and the signal due to H-5' was shifted downfield from that of quercetin. These data and the diagnostic shifts in the UV spectrum showed that glucose is linked to quercetin at C-3 and -4'. Consequently, compound 5 was established to be 3,4'-di-*O*- $\beta$ -D-glucosylquercetin, which has been isolated from *Allium cepa*,<sup>8a,12)</sup> *Allium ascalonicum*,<sup>13)</sup> and *Ribes* species.<sup>14)</sup>

Compound 6 was identified as 3-*O*- $\beta$ -sophorosylkaempferol, which was obtained from 8 by enzymatic hydrolysis with  $\beta$ -glucosidase.

As compound 1 seemed to be unstable during the process of separation, the stability of 1 was examined. Compound 1 was dissolved in pH 3.2, 7.0 and 8.0 buffer solutions and the stability at 100 °C was checked by high-performance liquid chromatography (HPLC). After heating for 3 h, the chromatogram of the pH 3.2 solution was not changed, but at pH 7.0, as shown in Fig. 1, the peak of 1 at  $t_R$  7.8 min disappeared, and peaks a and b were observed at  $t_R$  3.7 and 11.7 min. At pH 8.0, the peak of 1 disappeared and peak a, which was identified as 8 formed by alkaline hydrolysis of 1, was recognized.

The product in peak b was obtained as colorless needles (15), whose UV spectrum closely resembled that of 1. The  $^1\text{H-NMR}$  spectrum of its acetate showed the signals of three

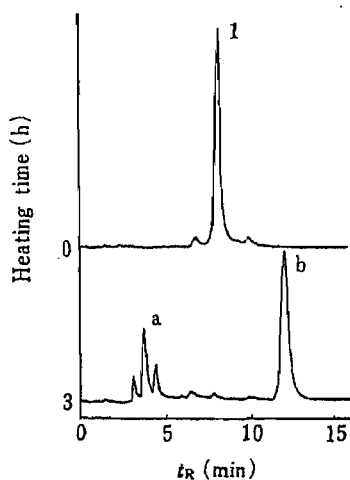


Fig. 1. Chromatogram of 1 before and after Heating at 100 °C at pH 7.0

Column, Nucleosil  $\mu\text{C}_{18}$  (4.6  $\times$  250 mm); mobile phase, MeOH-H<sub>2</sub>O (45:55); flow rate, 1.0 ml/min; detection, UV 254 nm; oven temperature, 40 °C.

aromatic and ten aliphatic acetoxy protons. On alkaline hydrolysis, **15** afforded ferulic acid and **8**. These results indicated that **15** is an isomer of **1** whose feruloyl position on **8** differs from that of **1**. In the  $^1\text{H-NMR}$  spectrum of **15**, doublet and double doublet proton signals at 4.21 and 4.52 ppm coupled with each other ( $J=12\text{ Hz}$ ) were observed instead of a triplet signal in the  $^1\text{H-NMR}$  spectrum of **1**. In the  $^{13}\text{C-NMR}$  spectrum, the signals due to C-5 and -6 of one of the glucosyl moieties were shifted upfield and downfield, respectively, from those of **8**. These data suggested that the feruloyl group was linked to C-6 of glucose.

In order to clarify the linkage between the feruloyl and glucose moieties, partial acid hydrolysis of **15** was performed. Hydrolysis of **15** with 5% sulfuric acid afforded kaempferol glucoside (**16**). Acetylation of **16** gave a heptaacetate, the  $^1\text{H-NMR}$  spectrum of which showed the signals of four aromatic and three aliphatic acetoxy protons. On alkaline hydrolysis, **16** yielded ferulic acid and **9**. In the  $^1\text{H-NMR}$  spectrum of **16**, doublet and double doublet proton signals due to H-6'' were observed at 4.19 and 4.54 ppm. Compound **16** was thus deduced to be 7-*O*- $\beta$ -D-(6-*O*-feruloyl)glucosylkaempferol.

From the above, **15** was established to be 3-*O*- $\beta$ -sophorosyl-7-*O*- $\beta$ -D-(6-*O*-feruloyl)-glucosylkaempferol, so that the feruloyl group had migrated from C-2''' to C-6''' of the same molecule. Acyl migration in partially acylated carbohydrates is known<sup>15)</sup> under various conditions, especially under mild alkaline conditions. Therefore, **1** was treated with pH 11.0 buffer at room temperature to afford **15**.

A similar acyl migration was observed in **2**, **10** and **11**—in the case of **10** and **11**, only in buffer at pH 11.0, on account of the low solubility of these compounds in pH 7.0 buffer solution—to afford the corresponding 6-*O*-feruloylates **17**, **16** and **18**, respectively. The structures of these substances were elucidated by FD-MS, UV spectra and  $^1\text{H-NMR}$  spectra.

Six flavonol glycosides were isolated from *A. tuberosum*, four of them being rare C-4' glycosides. Compounds **1**, **2**, **3**, **10**, **11**, **14**, **15**, **16**, **17** and **18** are new acylated flavonol glycosides. Compounds **1**, **2**, **10**, **11**, **15** and **16** have significant inhibitory effects on the homologous passive cutaneous anaphylaxis reaction in rats at the dose of 2.5 mg/kg (i.v.). Further biological studies are in progress.

### Experimental

All melting points were determined on a Yanagimoto micromelting point apparatus and are uncorrected. UV spectra were measured on a Hitachi 323 or 228 spectrophotometer.  $^1\text{H-}$  and  $^{13}\text{C-NMR}$  spectra were taken at 200 and 50.3 MHz, respectively, with a Varian XL-200 spectrometer, and chemical shifts are expressed in  $\delta$  (ppm) values with tetramethylsilane as an internal standard (s, singlet; d, doublet; t, triplet; m, multiplet; br, broad). FD-MS were obtained on a JEOL JMS-01SG2 spectrometer. Optical rotation was measured on a Perkin-Elmer 141 or Horiba SEPA 200 polarimeter. GLC was performed on a Hitachi 163 apparatus with a flame ionization detector using a glass column (3 mm i.d.  $\times$  2 m) packed with 3% OV-225 on Gas Chrom Q (100—200 mesh); injection temperature, 280 °C; column temperature, 170 °C; carrier gas,  $\text{N}_2$  55 ml/min. GLC mass spectrometry (GLC-MS) was performed with the chromatographic column coupled to a JEOL JMS D-300 mass spectrometer. HPLC was carried out on a Hewlett-Packard 1084B apparatus. TLC was performed on Kieselgel 60F<sub>254</sub> (Merck) using the following solvents: (A) EtOAc saturated with  $\text{H}_2\text{O}$ ; (B) BuOH-AcOH- $\text{H}_2\text{O}$  (4:1:5, upper); (C) BuOH-iso-PrOH- $\text{H}_2\text{O}$  (5:3:1). The spots were detected by UV irradiation,  $\text{FeCl}_3$  reagent or *p*-anisaldehyde- $\text{H}_2\text{SO}_4$  reagent. D-Glucose was detected by using glucose oxidase (Sigma) followed by bromphenol blue. Acetylation was carried out with acetic anhydride-pyridine in the usual way.

**Extraction and Separation**—Commercially available fresh leaves of *Allium tuberosum* ROTTLER (Liliaceae, 59 kg) were extracted with 80% MeOH (300 l) at room temperature for 12 d, and the extract was concentrated in order to remove MeOH. The residual solution was allowed to stand overnight, and the resulting precipitate was filtered off. The filtrate was passed through a Diaion HP20 (Mitsubishi Chemical Industry Ltd.) column. The column was washed with  $\text{H}_2\text{O}$  and then eluted with an  $\text{H}_2\text{O}$ -MeOH stepwise gradient. The 60% MeOH eluate was repeatedly chromatographed on MCI GEL CHP20P (Mitsubishi Chemical Industry Ltd.) with a linear gradient from 40% MeOH to 80% MeOH, and on Sephadex LH-20 with 50% MeOH to yield **1** (1.04 g) and **2** (0.29 g). The 50% MeOH eluate was rechromatographed on MCI GEL CHP20P with a linear gradient from 30% MeOH to 60% MeOH to give

three fractions (fractions I to III). Fraction III was concentrated to afford **3** (0.24 g). Fractions I and II were rechromatographed on Sephadex LH-20 with 50% MeOH to yield **4** (0.25 g) and **5** (0.14 g) from fraction I, and **6** (0.13 g) from fraction II.

**Properties of 1**—Yellow amorphous powder, mp 212–215 °C (H<sub>2</sub>O–EtOH).  $[\alpha]_D^{22} -84.9^\circ$  ( $c = 1.00$ , pyridine). *Anal.* Calcd for C<sub>43</sub>H<sub>48</sub>O<sub>24</sub>·H<sub>2</sub>O: C, 53.42; H, 5.21. Found: C, 53.27; H, 4.98. FD-MS  $m/z$ : 987 (M<sup>+</sup> + K), 971 (M<sup>+</sup> + Na). UV  $\lambda_{\text{max}}^{\text{EtOH}}$  nm (log  $\epsilon$ ): 233 (4.36), 246 (4.27), 269 (4.31), 333 (4.42). <sup>1</sup>H-NMR: Table I. <sup>13</sup>C-NMR: Table II.

**Acetate of 1**—Colorless amorphous powder, mp 129–130 °C (EtOH). *Anal.* Calcd for C<sub>69</sub>H<sub>74</sub>O<sub>37</sub>·H<sub>2</sub>O: C, 54.76; H, 5.06. Found: C, 54.38; H, 4.88. <sup>1</sup>H-NMR (CDCl<sub>3</sub>)  $\delta$ : 1.89–2.10 (30H, each s, OAc  $\times$  10), 2.34, 2.36, 2.44 (each 3H, s, Ar–OAc), 3.88 (3H, s, OCH<sub>3</sub>), 5.82 (1H, d,  $J = 8$  Hz, H-1'' anomeric), 6.38 (1H, d,  $J = 16$  Hz, CH = CHCO), 6.70 (1H, d,  $J = 2$  Hz, H-6), 7.00 (1H, d,  $J = 2$  Hz, H-8), 7.25 (2H, d,  $J = 8$  Hz, H-3',5'), 7.73 (1H, d,  $J = 16$  Hz, CH = CHCO), 8.01 (2H, d,  $J = 8$  Hz, H-2',6').

**Acid Hydrolysis of 1**—A solution of **1** (3 mg) in 1 N HCl (1 ml) was heated at 100 °C for 5 h. After cooling, the reaction mixture was extracted with EtOAc. The organic layer was washed with H<sub>2</sub>O and dried over Na<sub>2</sub>SO<sub>4</sub>, then concentrated to dryness to yield a yellow powder, which was identified as kaempferol by comparison with an authentic sample. The aqueous layer was neutralized with Dowex 1-X2 (CO<sub>3</sub><sup>2-</sup>) and concentrated to obtain D-glucose which was identified by TLC comparison with an authentic sample.

**Alkaline Hydrolysis of 1**—A solution of **1** (20 mg) in 1% KOH was allowed to stand overnight. After acidification with 1 N HCl, the reaction mixture was extracted with ether. The organic layer was concentrated to dryness and the residue was recrystallized from H<sub>2</sub>O to yield colorless needles (2 mg), which were identified as ferulic acid by comparison with an authentic sample. The aqueous layer was passed through an MCI GEL CHP20P column (pH 3.0 HCl), which was washed successively with pH 3.0 HCl and H<sub>2</sub>O, then eluted with 80% MeOH. The eluate was concentrated to dryness and the residue was recrystallized from EtOH to yield a pale yellow amorphous powder **8** (13 mg), mp 207–209 °C. *Anal.* Calcd for C<sub>33</sub>H<sub>40</sub>O<sub>21</sub>·3H<sub>2</sub>O: C, 47.94; H, 5.61. Found: C, 48.33; H, 5.27. FD-MS  $m/z$ : 811 (M<sup>+</sup> + K), 795 (M<sup>+</sup> + Na). UV  $\lambda_{\text{max}}^{\text{EtOH}}$  nm (log  $\epsilon$ ): 267 (4.42), 349 (4.38);  $\lambda^{\text{NaOAc}}$ : 267 (4.42), 351 (4.35);  $\lambda^{\text{NaOMe}}$ : 276 (4.41), 395 (4.46);  $\lambda^{\text{AlCl}_3}$ : 275 (4.41), 302 (4.13), 348 (4.33), 395 (4.21). <sup>1</sup>H-NMR: Table I. <sup>13</sup>C-NMR: Table II.

**Partial Acid Hydrolysis of 8**—A solution of **8** (30 mg) in 1% H<sub>2</sub>SO<sub>4</sub> (2 ml) was heated at 100 °C for 45 min. After cooling, the reaction mixture was extracted with EtOAc. The organic layer was chromatographed on silica gel with EtOAc–EtOH (1 : 1) to yield 7-O- $\beta$ -D-glucosylkaempferol (**9**, 4 mg) as a yellow amorphous powder, which was identified on the basis of diagnostic shifts in the UV spectrum,<sup>6)</sup> and the <sup>1</sup>H-NMR spectrum (Table I). The aqueous layer was neutralized with Dowex 1-X2 (CO<sub>3</sub><sup>2-</sup>) and concentrated to obtain sophorose which was identified by TLC comparison with an authentic sample.

**Enzymatic Hydrolysis of 8**—A solution of **8** (20 mg) and  $\beta$ -glucosidase (20 mg, from almond, Sigma) in pH 5.0 MacIlvaine buffer (20 ml) was incubated at 37 °C for 5 h. After cooling, the reaction mixture was extracted with BuOH. The organic layer was washed with water and concentrated to dryness to yield 3-O- $\beta$ -sophorosylkaempferol (**6**, 12 mg) as a yellow amorphous powder which was identified on the basis of the diagnostic shifts in the UV spectrum,<sup>6)</sup> and the <sup>1</sup>H-NMR spectrum (Table I).

**Methylation Analysis of 1**—A solution of **1** (3 mg) and sodium methylsulfinylmethide (0.5 mM) in DMSO (0.5 ml) was allowed to stand overnight at room temperature. Methyl iodide (0.1 ml) was added and the reaction mixture was stirred at room temperature for 90 min. After dilution with water, the reaction mixture was extracted with CHCl<sub>3</sub>, and the dried organic layer was concentrated to dryness. The residue was hydrolyzed with 90% formic acid at 100 °C for 2 h, and with 0.5 N H<sub>2</sub>SO<sub>4</sub> (1 ml) at 100 °C for 16 h. After neutralization with BaCO<sub>3</sub> solution, the reaction mixture was centrifuged and the supernatant was concentrated to dryness. The residue was reduced with 0.5% sodium borohydride (0.5 ml) at room temperature for 1 h. Boric acid was removed by distillation with MeOH and the residue was acetylated with acetic anhydride–pyridine (1 : 1, 0.5 ml) at 100 °C for 2 h. The reaction mixture was concentrated to dryness and the residue was examined by GLC and GLC-MS, which indicated the presence of 2,3,4,6-tetra-O-methyl-1,5-O-diacetylglycitol ( $t_R$  7.1 min) and 3,4,6-tri-O-methyl-1,2,5-O-triacetylglycitol ( $t_R$  12.9 min) in a ratio of 2 : 1.

**Partial Acid Hydrolysis of 1**—A solution of **1** (50 mg) in 5% H<sub>2</sub>SO<sub>4</sub> was heated at 100 °C for 100 min. After cooling, the resulting precipitate was filtered to give a yellow-brown powder, which was recrystallized from EtOH to afford **10** (10 mg) as a pale yellow amorphous powder, mp 215–217 °C.  $[\alpha]_D^{22} + 32.0^\circ$  ( $c = 0.20$ , pyridine). *Anal.* Calcd for C<sub>31</sub>H<sub>28</sub>O<sub>14</sub>·2H<sub>2</sub>O: C, 56.37; H, 4.88. Found: C, 56.82; H, 4.71. FD-MS  $m/z$ : 625 (M<sup>+</sup> + 1). UV  $\lambda_{\text{max}}^{\text{EtOH}}$  nm (log  $\epsilon$ ): 235 (4.26), 248 (4.34), 271 (4.26), 330 (4.41), 378 sh (4.28). <sup>1</sup>H-NMR: Table I. Alkaline hydrolysis of **10** afforded ferulic acid and **9**.

**Acetate of 10**—Colorless amorphous powder, mp 131–133 °C (EtOH). *Anal.* Calcd for C<sub>45</sub>H<sub>42</sub>O<sub>21</sub>·1/2H<sub>2</sub>O: C, 58.25; H, 4.67. Found: C, 58.21; H, 4.83. <sup>1</sup>H-NMR (CDCl<sub>3</sub>)  $\delta$ : 2.04, 2.07, 2.08 (each 3H, s, OAc), 2.31, 2.32, 2.36, 2.42 (each 3H, s, Ar–OAc), 3.88 (3H, s, OCH<sub>3</sub>), 6.38 (1H, d,  $J = 16$  Hz, CH = CHCO), 6.76 (1H, d,  $J = 2$  Hz, H-6), 7.02 (1H, d,  $J = 2$  Hz, H-8), 7.37 (2H, d,  $J = 8$  Hz, H-3',5'), 7.73 (1H, d,  $J = 16$  Hz, CH = CHCO), 7.84 (2H, d,  $J = 8$  Hz, H-2',6').

**Enzymatic Hydrolysis of 1**—A solution of **1** (100 mg) and crude hesperidinase (200 mg, Tanabe Seiyaku Co.,

Ltd.) in pH 4.0 MacIlvaine buffer (25 ml) was incubated at 37 °C for 40 h. After cooling, the resulting precipitate was collected and washed with water to yield **11** (61 mg) as a yellow amorphous powder, mp 200–205 °C.  $[\alpha]_D^{22} -48.7^\circ$  ( $c=0.27, 0.1 \text{ N NaOH}$ ). *Anal.* Calcd for  $\text{C}_{37}\text{H}_{38}\text{O}_{19} \cdot 2\text{H}_2\text{O}$ : C, 54.02; H, 5.15. Found: C, 53.77; H, 5.03. FD-MS  $m/z$ : 787 ( $\text{M}^+ + 1$ ). UV  $\lambda_{\text{max}}^{\text{EtOH}}$  nm (log  $\epsilon$ ): 233 (4.39), 246 (4.33), 269 (4.34), 333 (4.47).  $^1\text{H-NMR}$ : Table I. Alkaline hydrolysis of **11** afforded ferulic acid and 3,7-di-*O*- $\beta$ -D-glucosylkaempferol (**12**).  $^1\text{H-NMR}$ : Table I.

**Acetate of 11**—Colorless amorphous powder, mp 155–157 °C (EtOH). *Anal.* Calcd for  $\text{C}_{57}\text{H}_{58}\text{O}_{29} \cdot 2\text{H}_2\text{O}$ : C, 55.07; H, 5.03. Found: C, 55.38; H, 4.64.  $^1\text{H-NMR}$  ( $\text{CDCl}_3$ )  $\delta$ : 1.91, 1.99, 2.01, 2.04, 2.08, 2.08, 2.10 (each 3H, s, OAc), 2.32, 2.34, 2.43 (each 3H, s, Ar-OAc), 3.87 (3H, s,  $\text{OCH}_3$ ), 5.56 (1H, d,  $J=8 \text{ Hz}$ , H-1'' anomeric), 6.36 (1H, d,  $J=16 \text{ Hz}$ ,  $\text{CH}=\text{CHCO}$ ), 6.70 (1H, d,  $J=2 \text{ Hz}$ , H-6), 7.00 (1H, d,  $J=2 \text{ Hz}$ , H-8), 7.23 (2H, d,  $J=8 \text{ Hz}$ , H-3',5'), 7.71 (1H, d,  $J=16 \text{ Hz}$ ,  $\text{CH}=\text{CHCO}$ ), 8.03 (2H, d,  $J=8 \text{ Hz}$ , H-2',6').

**Properties of 2**—Pale yellow amorphous powder, mp 214–217 °C ( $\text{H}_2\text{O}$ -EtOH).  $[\alpha]_D^{22} -39.9^\circ$  ( $c=0.26$ , pyridine). *Anal.* Calcd for  $\text{C}_{43}\text{H}_{44}\text{O}_{24} \cdot 2\text{H}_2\text{O}$ : C, 52.44; H, 5.32. Found: C, 52.75; H, 5.52. FD-MS  $m/z$ : 949 ( $\text{M}^+ + 1$ ). UV  $\lambda_{\text{max}}^{\text{EtOH}}$  nm (log  $\epsilon$ ): 232 (4.38), 268 (4.37), 328 (4.47).  $^1\text{H-NMR}$ : Table I.  $^{13}\text{C-NMR}$ : Table II. Acid hydrolysis of **2** gave kaempferol and D-glucose, and partial acid hydrolysis afforded **10**.

**Acetate of 2**—Colorless needles, mp 201–205 °C (EtOH). *Anal.* Calcd for  $\text{C}_{69}\text{H}_{74}\text{O}_{37} \cdot 1/2\text{H}_2\text{O}$ : C, 55.09; H, 5.03. Found: C, 54.81; H, 5.56.  $^1\text{H-NMR}$  ( $\text{CDCl}_3$ )  $\delta$ : 1.90–2.12 (33H, each s, OAc  $\times$  11), 2.34, 2.44 (each 3H, s, Ar-OAc), 3.88 (3H, s,  $\text{OCH}_3$ ), 5.82 (1H, d,  $J=8 \text{ Hz}$ , H-1'' anomeric), 6.38 (1H, d,  $J=16 \text{ Hz}$ ,  $\text{CH}=\text{CHCO}$ ), 6.70 (1H, d,  $J=2 \text{ Hz}$ , H-6), 7.00 (1H, d,  $J=2 \text{ Hz}$ , H-8), 7.25 (2H, d,  $J=8 \text{ Hz}$ , H-3',5'), 7.73 (1H, d,  $J=16 \text{ Hz}$ ,  $\text{CH}=\text{CHCO}$ ), 8.01 (2H, d,  $J=8 \text{ Hz}$ , H-2',6').

**Properties of 3**—Colorless amorphous powder, mp 235–238 °C ( $\text{H}_2\text{O}$ ).  $[\alpha]_D^{22} -206^\circ$  ( $c=0.22$ , pyridine). *Anal.* Calcd for  $\text{C}_{43}\text{H}_{44}\text{O}_{24} \cdot 3\text{H}_2\text{O}$ : C, 51.50; H, 5.43. Found: C, 51.64; H, 5.31. FD-MS  $m/z$ : 949 ( $\text{M}^+ + 1$ ). UV  $\lambda_{\text{max}}^{\text{EtOH}}$  nm (log  $\epsilon$ ): 232 (4.47), 269 (4.55), 327 (4.66).  $^1\text{H-NMR}$ : Table I.  $^{13}\text{C-NMR}$ : Table II. Acid hydrolysis of **3** afforded kaempferol and D-glucose.

**Acetate of 3**—Colorless amorphous powder, mp 186–188 °C (EtOH). *Anal.* Calcd for  $\text{C}_{69}\text{H}_{74}\text{O}_{37} \cdot \text{H}_2\text{O}$ : C, 54.76; H, 5.06. Found: C, 54.55; H, 4.91.  $^1\text{H-NMR}$  ( $\text{CDCl}_3$ )  $\delta$ : 1.94–2.14 (33H, each s, OAc  $\times$  11), 2.35, 2.43 (each 3H, s, Ar-OAc), 3.90 (3H, s,  $\text{OCH}_3$ ), 5.86 (1H, d,  $J=8 \text{ Hz}$ , H-1'' anomeric), 6.38 (1H, d,  $J=16 \text{ Hz}$ ,  $\text{CH}=\text{CHCO}$ ), 6.69 (1H, d,  $J=2 \text{ Hz}$ , H-6), 6.95 (1H, d,  $J=2 \text{ Hz}$ , H-8), 7.70 (1H, d,  $J=16 \text{ Hz}$ ,  $\text{CH}=\text{CHCO}$ ), 8.02 (2H, d,  $J=8 \text{ Hz}$ , H-2',6').

**Alkaline Hydrolysis of 3**—A solution of **3** (158 mg) was hydrolyzed with 1% KOH (30 ml) and worked up in the same way as **1** to obtain ferulic acid and **13** (61 mg) as a pale yellow amorphous powder, mp 210–213 °C ( $\text{H}_2\text{O}$ -EtOH).  $[\alpha]_D^{22} -91.0^\circ$  ( $c=0.22$ , pyridine). *Anal.* Calcd for  $\text{C}_{33}\text{H}_{44}\text{O}_{21} \cdot 2\text{H}_2\text{O}$ : C, 49.01; H, 5.48. Found: C, 49.41; H, 5.35. FD-MS  $m/z$ : 773 ( $\text{M}^+ + 1$ ). UV  $\lambda_{\text{max}}^{\text{EtOH}}$  nm (log  $\epsilon$ ): 268 (4.35), 321 (4.18), 347 (4.18);  $\lambda^+ \text{NaOAc}$ : 268 (4.36), 321 (4.21), 347 (4.18);  $\lambda^+ \text{NaOMe}$ : 287 (4.35), 391 (3.88);  $\lambda^+ \text{AlCl}_3$ : 278 (4.30), 338 (4.23), 394 (3.96).  $^1\text{H-NMR}$  ( $\text{DMSO}-d_6$ )  $\delta$ : 12.61 (1H, s, 5-OH); ( $\text{DMSO}-d_6$ - $\text{D}_2\text{O}$ ): Table I.  $^{13}\text{C-NMR}$ : Table II. Enzymatic hydrolysis of **13** with  $\beta$ -glucosidase afforded kaempferol.

**Alkaline Hydrolysis of 2**—A solution of **2** was hydrolyzed with 1% KOH and worked up in the same way as **1** to identify ferulic acid and **13**.

**Enzymatic Hydrolysis of 3**—A solution of **3** (40 mg) and  $\beta$ -glucosidase (120 mg) in pH 5.0 MacIlvaine buffer (80 ml) was incubated at 37 °C for 3 d. The reaction mixture was extracted with EtOAc and the organic layer was concentrated to yield a brown residue, which was chromatographed on a Sephadex LH-20 column with MeOH to yield **10** (7 mg) as pale yellow prisms, mp 183–185 °C (EtOH). *Anal.* Calcd for  $\text{C}_{31}\text{H}_{28}\text{O}_{14} \cdot 2\text{H}_2\text{O}$ : C, 56.37; H, 4.88. Found: C, 56.17; H, 4.83. FD-MS  $m/z$ : 625 ( $\text{M}^+ + 1$ ). UV  $\lambda_{\text{max}}^{\text{EtOH}}$  nm (log  $\epsilon$ ): 236 (4.32), 268 (4.31), 330 (4.45).  $^1\text{H-NMR}$ : Table I.

**Properties of 4**—Pale yellow amorphous powder, mp 207–210 °C. *Anal.* Calcd for  $\text{C}_{27}\text{H}_{30}\text{O}_{16} \cdot \text{H}_2\text{O}$ : C, 51.60; H, 5.13. Found: C, 51.37; H, 5.13. FD-MS  $m/z$ : 611 ( $\text{M}^+ + 1$ ). UV  $\lambda_{\text{max}}^{\text{MeOH}}$  nm (log  $\epsilon$ ): 267 (4.39), 344 (4.19);  $\lambda^+ \text{NaOAc}$ : 276 (4.54), 371 (4.11);  $\lambda^+ \text{NaOMe}$ : 276 (4.51), 372 (4.14);  $\lambda^+ \text{AlCl}_3$ : 276 (4.35), 302 (4.17), 343 (4.24), 393 (4.10).  $^1\text{H-NMR}$ : Table I. Acid hydrolysis of **4** afforded kaempferol and D-glucose.

**Properties of 5**—Yellow amorphous powder, mp 208–212 °C. *Anal.* Calcd for  $\text{C}_{27}\text{H}_{30}\text{O}_{17} \cdot \text{H}_2\text{O}$ : C, 50.32; H, 5.00. Found: C, 50.26; H, 4.86. FD-MS  $m/z$ : 627 ( $\text{M}^+ + 1$ ). UV  $\lambda_{\text{max}}^{\text{EtOH}}$  nm (log  $\epsilon$ ): 268 (4.31), 349 (4.24);  $\lambda^+ \text{NaOAc}$ : 276 (4.45), 323 (4.13), 366 (4.16);  $\lambda^+ \text{NaOMe}$ : 275 (4.46), 382 (4.14);  $\lambda^+ \text{AlCl}_3$ : 277 (4.34), 298 (4.10), 351 (4.18), 396 (4.13);  $\lambda^+ \text{NaOAc} + \text{H}_3\text{BO}_4$ : 268 (4.21), 353 (4.20);  $\lambda^+ \text{AlCl}_3 + \text{HCl}$ : 278 (4.35), 347 (4.21), 395 (4.08).  $^1\text{H-NMR}$  ( $\text{DMSO}-d_6$ - $\text{D}_2\text{O}$ )  $\delta$ : 4.92 (1H, d,  $J=8 \text{ Hz}$ , H-1''' anomeric), 5.53 (1H, d,  $J=8 \text{ Hz}$ , H-1'' anomeric), 6.25 (1H, d,  $J=2 \text{ Hz}$ , H-6), 6.49 (1H, d,  $J=2 \text{ Hz}$ , H-8), 7.25 (1H, d,  $J=8 \text{ Hz}$ , H-5'), 7.65 (1H, br dd,  $J=8, 2 \text{ Hz}$ , H-6'), 7.68 (1H, d,  $J=2 \text{ Hz}$ , H-2'). Acid hydrolysis of **5** afforded quercetin and D-glucose.

**Properties of 6**—Yellow needles, mp 195–198 °C (EtOH). *Anal.* Calcd for  $\text{C}_{27}\text{H}_{30}\text{O}_{16} \cdot 2\text{H}_2\text{O}$ : C, 50.16; H, 5.30. Found: C, 50.50; H, 4.96. FD-MS  $m/z$ : 611 ( $\text{M}^+ + 1$ ). UV  $\lambda_{\text{max}}^{\text{EtOH}}$  nm (log  $\epsilon$ ): 267 (4.38), 350 (4.30);  $\lambda^+ \text{NaOAc}$ : 275 (4.33), 300 (4.11), 365 (4.10);  $\lambda^+ \text{NaOMe}$ : 276 (4.54), 328 (4.29), 406 (4.52);  $\lambda^+ \text{AlCl}_3$ : 277 (4.38), 304 (4.21), 348 (4.30), 397 (4.26).  $^1\text{H-NMR}$ : Table I.

**Stability Test of Compound 1**—A 0.1% solution of compound **1** at pH 3.2 (0.1 M acetate buffer), pH 7.0 or pH 8.0 (0.1 M phosphate buffer) was heated at 100 °C for 3 h, and the stability of **1** was checked by HPLC.

**Procedures of Acyl Migration**—i) A solution of 1% 2-*O*-acylated flavonol glucoside in 0.1 M pH 7.0 phosphate buffer was heated at 100 °C for 3 h, and allowed to stand overnight at 5 °C. The resulting precipitate was collected by centrifugation and washed with water to afford 6-*O*-acylated flavonol glucoside.

ii) A solution of 0.1% 2-*O*-acylated flavonol glucoside in 0.1 M pH 11.0 Na<sub>2</sub>HPO<sub>4</sub>-NaOH buffer was allowed to stand at room temperature for 3–8 h, and the solution was acidified with 1 N HCl. The resulting precipitate was collected by centrifugation and washed with water to afford 6-*O*-acylated flavonol glucoside.

**Properties of 15**—Compound 15 was obtained from 1 by methods i and ii above. Colorless needles, mp 214–217 °C (MeOH-H<sub>2</sub>O).  $[\alpha]_D^{22}$  -212° (*c*=0.26, pyridine). *Anal.* Calcd for C<sub>43</sub>H<sub>48</sub>O<sub>24</sub>·2H<sub>2</sub>O: C, 52.44; H, 5.32. Found: C, 52.38; H, 5.09. FD-MS *m/z*: 987 (M<sup>+</sup>+K), 971 (M<sup>+</sup>+Na). UV  $\lambda_{\max}^{\text{EtOH}}$  nm (log  $\epsilon$ ): 233 (4.31), 247 (4.21), 268 (4.22), 333 (4.33). <sup>1</sup>H-NMR: Table I. <sup>13</sup>C-NMR: Table II. Alkaline hydrolysis of 15 afforded ferulic acid and 8.

**Acetate of 15**—Colorless amorphous powder, mp 129–131 °C (EtOH). *Anal.* Calcd for C<sub>69</sub>H<sub>74</sub>O<sub>37</sub>·2H<sub>2</sub>O: C, 54.12; H, 5.13. Found: C, 53.93; H, 4.64. <sup>1</sup>H-NMR (CDCl<sub>3</sub>)  $\delta$ : 1.90–2.11 (30H, each s, OAc  $\times$  10), 2.34, 2.36, 2.41 (each 3H, s, Ar-OAc), 3.88 (3H, s, OCH<sub>3</sub>), 5.79 (1H, d, *J*=8 Hz, H-1'' anomeric), 6.40 (1H, d, *J*=16 Hz, CH=CHCO), 6.70 (1H, d, *J*=2 Hz, H-6), 6.98 (1H, d, *J*=2 Hz, H-8), 7.24 (2H, d, *J*=8 Hz, H-3',5'), 7.68 (1H, d, *J*=16 Hz, CH=CHCO), 8.02 (2H, d, *J*=8 Hz, H-2',6').

**Partial Acid Hydrolysis of 15**—A solution of 15 (78 mg) in 5% H<sub>2</sub>SO<sub>4</sub>-EtOH (1:1, 20 ml) was refluxed for 100 min, then the reaction mixture was concentrated and the resulting precipitate was filtered and recrystallized from EtOH to afford 16 (23 mg) as yellow needles, mp 238–243 °C.  $[\alpha]_D^{22}$  -128° (*c*=0.13, MeOH). *Anal.* Calcd for C<sub>31</sub>H<sub>28</sub>O<sub>14</sub>·2H<sub>2</sub>O: C, 56.37; H, 4.88. Found: C, 56.73; H, 4.44. FD-MS *m/z*: 625 (M<sup>+</sup>+1). UV  $\lambda_{\max}^{\text{EtOH}}$  nm (log  $\epsilon$ ): 235 (4.35), 247 (4.35), 270 (4.45), 329 (4.57), 376 sh (4.47). <sup>1</sup>H-NMR: Table I. Compound 16 was also obtained from 10 by acyl migration by method ii. Alkaline hydrolysis of 16 afforded ferulic acid and 9.

**Acetate of 16**—Colorless needles, mp 189–191 °C (EtOH). *Anal.* Calcd for C<sub>45</sub>H<sub>42</sub>O<sub>21</sub>·2H<sub>2</sub>O: C, 56.61; H, 4.86. Found: C, 57.06; H, 4.43. <sup>1</sup>H-NMR (CDCl<sub>3</sub>)  $\delta$ : 2.06 (3H, s, OAc), 2.09 (6H, s, OAc  $\times$  2), 2.32, 2.34, 2.36, 2.38 (each 3H, s, Ar-OAc), 3.84 (3H, s, OCH<sub>3</sub>), 6.37 (1H, d, *J*=16 Hz, CH=CHCO), 6.76 (1H, d, *J*=2 Hz, H-6), 7.22 (2H, d, *J*=8 Hz, H-3',5'), 7.65 (1H, d, *J*=16 Hz, CH=CHCO), 7.82 (2H, d, *J*=8 Hz, H-2',6').

**Properties of 17**—17 was obtained from 2 by acyl migration by methods i and ii. Pale yellow amorphous powder, mp 233–236 °C (MeOH).  $[\alpha]_D^{22}$  -149° (*c*=0.20, pyridine). *Anal.* Calcd for C<sub>43</sub>H<sub>48</sub>O<sub>24</sub>·4H<sub>2</sub>O: C, 50.59; H, 5.53. Found: C, 50.23; H, 5.09. FD-MS *m/z*: 949 (M<sup>+</sup>+1). UV  $\lambda_{\max}^{\text{EtOH}}$  nm (log  $\epsilon$ ): 232 (4.59), 243 (4.59), 269 (4.63), 328 (4.71). <sup>1</sup>H-NMR: Table I. <sup>13</sup>C-NMR: Table II.

**Acetate of 17**—Colorless amorphous powder, mp 179–180 °C (EtOH). *Anal.* Calcd for C<sub>69</sub>H<sub>74</sub>O<sub>37</sub>: C, 55.40; H, 4.99. Found: C, 55.18; H, 4.93. <sup>1</sup>H-NMR (CDCl<sub>3</sub>)  $\delta$ : 1.90–2.13 (33H, each s, OAc  $\times$  11), 2.36, 2.39 (each 3H, s, Ar-OAc), 3.88 (3H, s, OCH<sub>3</sub>), 5.63 (1H, d, *J*=8 Hz, H-1'' anomeric), 6.43 (1H, d, *J*=16 Hz, CH=CHCO), 6.73 (1H, d, *J*=2 Hz, H-6), 7.02 (1H, d, *J*=2 Hz, H-8), 7.70 (1H, d, *J*=16 Hz, CH=CHCO), 8.02 (2H, d, *J*=8 Hz, H-2',6').

**Properties of 18**—Compound 18 was obtained from 11 by acyl migration by method i. Colorless amorphous powder, mp 253–255 °C (EtOH).  $[\alpha]_D^{22}$  -157° (*c*=0.20, pyridine). *Anal.* Calcd for C<sub>37</sub>H<sub>38</sub>O<sub>19</sub>·4H<sub>2</sub>O: C, 51.75; H, 5.40. Found: C, 51.45; H, 5.40. FD-MS *m/z*: 787 (M<sup>+</sup>+1). UV  $\lambda_{\max}^{\text{EtOH}}$  nm (log  $\epsilon$ ): 234 (4.32), 244 (4.34), 267 (4.31), 332 (4.43). <sup>1</sup>H-NMR: Table I.

**Acetate of 18**—Colorless amorphous powder, mp 128–132 °C (EtOH). *Anal.* Calcd for C<sub>57</sub>H<sub>58</sub>O<sub>29</sub>·H<sub>2</sub>O: C, 54.29; H, 5.12. Found: C, 54.06; H, 4.72. <sup>1</sup>H-NMR (CDCl<sub>3</sub>)  $\delta$ : 1.92, 2.00, 2.02, 2.06, 2.08, 2.08, 2.11 (each 3H, s, OAc), 2.33, 2.34, 2.38 (each 3H, s, Ar-OAc), 3.86 (3H, s, OCH<sub>3</sub>), 5.56 (1H, d, *J*=8 Hz, H-1'' anomeric), 6.38 (1H, d, *J*=16 Hz, CH=CHCO), 6.70 (1H, d, *J*=2 Hz, H-6), 6.98 (1H, d, *J*=2 Hz, H-8), 7.66 (1H, d, *J*=16 Hz, CH=CHCO), 8.02 (2H, d, *J*=8 Hz, H-2',6').

## References

- 1) H. Kameoka and A. Miyake, *Nippon Nogeikagaku Kaishi*, **48**, 385 (1974); A. I. Mackenzie and D. A. Ferns, *Phytochemistry*, **16**, 763 (1977).
- 2) M. Kaneta, H. Hikichi, S. Endo, and N. Sugiyama, *Agric. Biol. Chem.*, **44**, 1405 (1980).
- 3) Shanghai Science and Technologic Publisher and Shougakukan, "The Dictionary of Chinese Drugs," (中藥大辭典), Vol. I, Shougakukan, Tokyo, 1985, p. 449.
- 4) S. Hakomori, *J. Biochem.* (Tokyo), **55**, 205 (1964).
- 5) T. J. Mabry, K. R. Markham, and M. B. Thomas, "The Systematic Identification of Flavonoids," Springer-Verlag, Inc., New York, 1970.
- 6) N. A. M. Saleh, W. Majak, and G. H. N. Towers, *Phytochemistry*, **11**, 1095 (1972).
- 7) K. R. Markham, B. Terniai, R. Stanley, H. Geiger, and T. J. Mabry, *Tetrahedron*, **34**, 1389 (1978).
- 8) a) J. B. Harborn, *Phytochemistry*, **4**, 107 (1965); b) N. A. M. Saleh, *ibid.*, **14**, 286 (1975).
- 9) K. Yamasaki, R. Kasai, Y. Masaki, M. Okihara, O. Tanaka, H. Oshio, S. Takagi, M. Yamaki, K. Masuda, G. Nonaka, M. Tuboi, and I. Nishioka, *Tetrahedron Lett.*, **1977**, 1231; H. Ishii, S. Seo, K. Tori, T. Tozoy, and Y. Yoshimura, *ibid.*, **1977**, 1227; V. M. Chari, M. Jordan, H. Wagner, and P. W. Thies, *Phytochemistry*, **16**, 1110 (1977).

- 10) I. Aguinagalde and M. A. P. Martinez, *Phytochemistry*, **21**, 2875 (1982).
- 11) N. Ishikura and S. Hayashida, *Agric. Biol. Chem.*, **43**, 1923 (1979); W. Henning and K. Harmann; *Z. Lebensm. Unters. Forsch.*, **170**, 433 (1980); M. A. P. Martinez and I. Aguinagalde, *Parodiana*, **1**, 287 (1982) [*Chem. Abstr.*, **97**, 159508w (1982)]; A. Ulubelen, H. Abdolmaleky, and T. J. Mabry, *J. Nat. Prod.*, **45**, 507 (1982); F. Imperato, *Chem. Ind. (London)*, **1983**, 204.
- 12) B. J. Brandwein, *J. Food Sci.*, **30**, 680 (1965).
- 13) L. Bezanger-Beauquesne and A. Delelis, *C. R. Acad. Sci., Paris, Ser. D*, **265**, 2118 (1967) [*Chem. Abstr.*, **68**, 75713x (1968)].
- 14) S. Fred, G. Rudolf, and H. Karl, *Z. Lebensm. Unters. Forsch.*, **179**, 315 (1984).
- 15) L. Brikofer, C. Kaiser, H. Kosmol, G. Romussi, M. Donike, and G. Michelis, *Justus Liebigs Ann. Chem.*, **669**, 223 (1966); D. Sato and J. Morita, *Chem. Pharm. Bull.*, **17**, 1456 (1969); T. Konishi, A. Tada, J. Shoji, R. Kasai, and O. Tanaka, *ibid.*, **26**, 668 (1978); K. Yoshimoto and Y. Tsuda, *ibid.*, **31**, 4324 (1983).

[Chem. Pharm. Bull.]  
35(1) 108-111 (1987)

## Constituents of *Wikstroemia sikokiana*. II.<sup>1)</sup> Absolute Configurations of 1,5-Diphenylpentane-1,3-diols

MASATAKE NIWA,\* PEI-FENG JIANG,<sup>2)</sup> and YOSHIMASA HIRATA

Faculty of Pharmacy, Meijo University, Tempaku-ku, Nagoya 468, Japan

(Received June 20, 1986)

Further examination of the chemical constituents of *Wikstroemia sikokiana* FRANCH. *et* SAV. (Thymelaeaceae) afforded (+)-chamaejasmenin B (C-3/C-3''-biflavanone) and (–)-*erythro*-1,5-diphenylpentane-1,3-diol. The unsettled absolute configuration of the 1,3-diol was established as 1(*S*) and 3(*S*) on the basis of a synthesis using chiral styrene oxide as a starting material.

**Keywords**—Thymelaeaceae; *Wikstroemia sikokiana*; biflavanone; chamaejasmenin B; 1,5-diphenylpentane-1,3-diol; absolute configuration; (*R*)-styrene oxide; chiral epoxide

### Introduction

In the previous paper,<sup>1)</sup> we reported two new C-3/C-3''-biflavanones from the roots of *Wikstroemia sikokiana* FRANCH. *et* SAV. (Ganpi in Japanese) (Thymelaeaceae). We further examined the chemical constituents of the same plant and isolated two known compounds: (+)-chamaejasmenin B (1), which is a C-3/C-3''-biflavanone,<sup>3)</sup> and (–)-*erythro*-1,5-diphenylpentane-1,3-diol (2).<sup>4)</sup> In order to establish the absolute configuration of the latter compound, a chiral synthesis was carried out. In this paper, we wish to report the isolation of (+)-chamaejasmenin B and (–)-*erythro*-1,5-diphenylpentane-1,3-diol from the above plant and the syntheses of optically active (–)-*erythro*-1,5-diphenylpentane-1,3-diol and its epimer using the commercially available chiral epoxide as a starting material.

### Results and Discussion

#### Isolation and Identification

The benzene-soluble fraction described in the previous paper<sup>1)</sup> was separated by a combination of column chromatography and preparative thin layer chromatography (TLC) to give two compounds. One was identified as chamaejasmenin B (1), a C-3/C-3''-biflavanone isolated from the root of *Stellera chamaejasme* L. (Thymelaeaceae), by direct comparison of the infrared (IR) and proton nuclear magnetic resonance (<sup>1</sup>H-NMR) spectra with those of an authentic sample.<sup>3)</sup>

The IR, <sup>1</sup>H-NMR and <sup>13</sup>C-NMR spectra of the other compound, mp 91–92 °C, [ $\alpha$ ]<sub>D</sub> –19.2° and its diacetate (4) suggested that it was *erythro*-1,5-diphenylpentane-1,3-diol (2) isolated from the wood of *Flindersia laevis* C. T. WHITE *et* FRANCIS (Rutaceae)<sup>4)</sup> or *threo*-1,5-diphenylpentane-1,3-diol (3) isolated from the bark of the same plant.<sup>5)</sup> The stereochemistry between the C-1 and C-3 positions was established by the following experiments. Treatment of the natural diol (2) with acetone in the presence of camphorsulfonic acid afforded the corresponding acetonide (5). The <sup>1</sup>H-NMR spectrum of 5 showed two methyl protons at  $\delta$  1.53 (3H, s) and 1.54 (3H, s) and two methine protons at  $\delta$  3.96 (1H, m) and 4.86 (1H, dd,  $J=11.7, 2.7$  Hz). The coupling constant ( $J=11.7$  Hz) indicated that 1-H must be in an axial configuration. In a nuclear Overhauser effect (NOE) experiment on the acetonide (5),



irradiation of the methine signal at  $\delta$  3.96 (3-H) caused a 9.4% enhancement of the signal at  $\delta$  4.86 (1-H). This result suggested the relationship between 1-H and 3-H in **5** to be *syn*. Therefore, the original diol should be *erythro*-1,5-diphenylpentane-1,3-diol (**2**).

### Synthesis

In order to establish the absolute configuration of the *erythro*-diol, an asymmetric synthesis of the diol was carried out as follows. Dithiane (**6**),<sup>6)</sup> which was prepared from 3-phenylpropionaldehyde and propane-1,3-dithiol by using chloroform as a solvent and boron trifluoride etherate as a catalyst, was converted into 2-lithiodithiane by adding a 1.1-fold molar excess of *n*-butyllithium to a tetrahydrofuran (THF) solution of **6**, and then the 2-lithiodithiane was reacted with the commercially available chiral epoxide, (*R*)-styrene oxide (**7**),  $[\alpha]_D^{25} + 32.5$ <sup>7)</sup> to afford the adduct (**8**). The presence of a hydroxy group was indicated by the following spectral data;  $\nu$  3570 and 3460  $\text{cm}^{-1}$ ;  $\delta$  5.10 (1H, dt,  $J=9$ , 4 Hz, changed to a double doublet ( $J=9$ , 2 Hz) on addition of deuterium oxide). The adduct was subjected to hydrolysis with mercuric chloride and mercuric oxide in aqueous methanol to give a mixture of the dimethylacetal (**9**), mp 66–67°C,  $[\alpha]_D - 8.5^\circ$  and the ketone (**10**) as an oil,  $[\alpha]_D - 28^\circ$  in 38 and 57% yields, respectively. The <sup>1</sup>H-NMR spectrum of **9** showed two methoxyl groups ( $\delta$  3.18 (3H, s) and 3.25 (3H, s)). The structure of the ketone (**10**) was supported by the IR and <sup>1</sup>H-NMR data ( $\nu$  3450 and 1710  $\text{cm}^{-1}$ ,  $\delta$  5.10 (1H, m, changed to a double doublet ( $J=5$ , 7 Hz) on addition of deuterium oxide). Next, the ketone (**10**) was reduced with sodium borohydride in THF to afford a mixture of two diols separable by reversed-phase high-performance liquid chromatography (HPLC). One, mp 89.5–91°C,  $[\delta]_D - 23.0^\circ$ , having the larger retention time ( $t_R$ ) on HPLC, was identical with natural (–)-*erythro*-1,5-diphenyl-

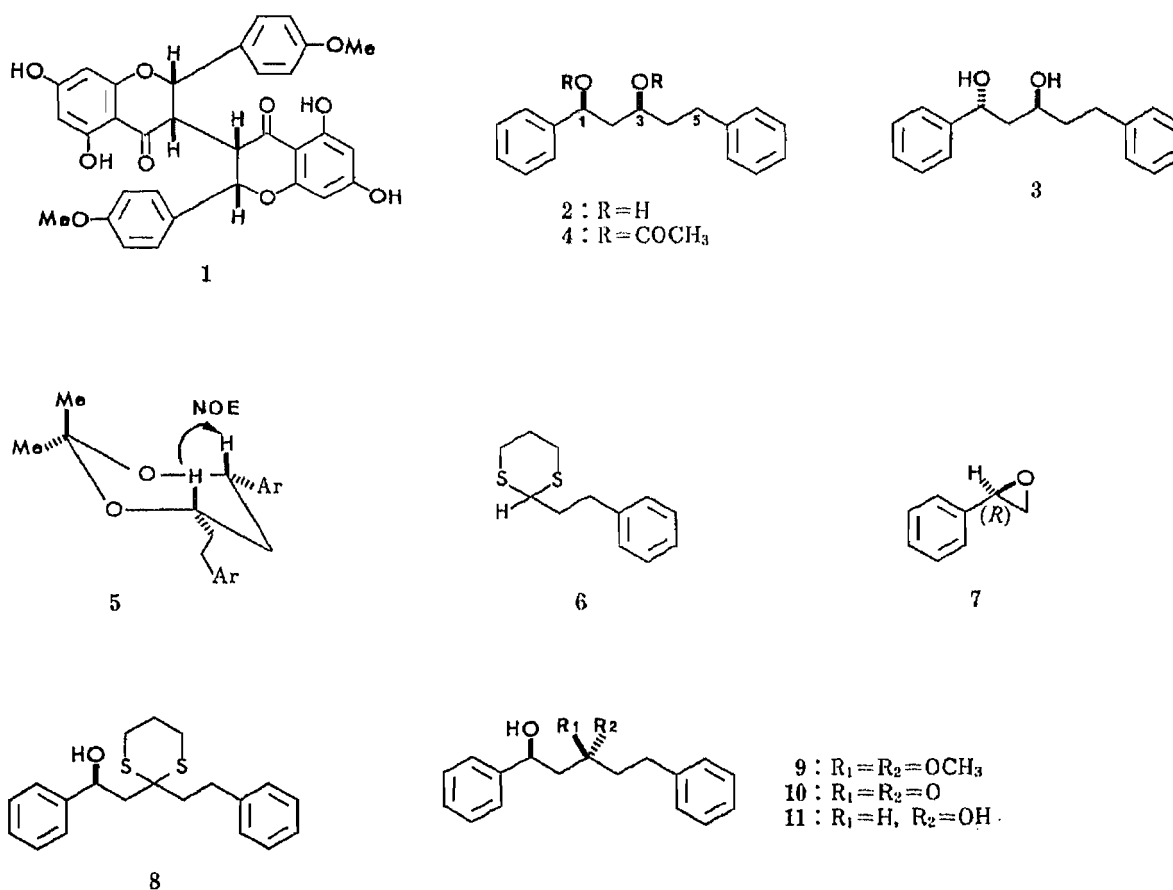


Fig. 1

pentane-1,3-diol (**2**) isolated from *Wikstroemia sikokiana*, by IR,  $^1\text{H-NMR}$ , and HPLC comparisons. Consequently, the stereochemistry of **2** should be 1(*S*) and 3(*S*). Finally, the other diol, mp 91–92 °C,  $[\alpha]_{\text{D}} -23.3^\circ$ , having the smaller  $t_{\text{R}}$  on HPLC should be the *threo*-isomer (**11**). The sign of the optical rotation of the natural *threo*-diol (**3**) ( $[\alpha]_{\text{D}} +29.8^\circ$ ) isolated from the bark of *Flindersia laevis* C. T. WHITE *et* FRANCIS<sup>5</sup>) was opposite to that of the optical rotation of the synthetic diol (**11**) ( $[\alpha]_{\text{D}} -23.3^\circ$ ), whose absolute configuration should be 1(*S*) and 3(*R*). Consequently, the absolute configuration of natural (+)-*threo*-1,5-diphenylpentane-1,3-diol (**3**) is 1(*R*) and 3(*S*).

### Experimental

Optical rotations were measured on JASCO DIP-181 and DIP-360 digital polarimeters. Infrared (IR) spectra were taken on a JASCO IR-2 spectrometer.  $^1\text{H}$ - and  $^{13}\text{C}$ -NMR spectra were taken on JEOL GX-400 and/or FX-100 spectrometers in  $\text{CDCl}_3$  unless otherwise stated. Chemical shifts are given in ppm relative to internal tetramethylsilane (TMS). Mass spectra (MS) were obtained on a Hitachi M-80 spectrometer operating at an ionization potential of 70 eV. Column chromatography (CC) and preparative TLC were performed with silica gel. HPLC was carried out with a JASCO TRIROTAR-V (detector: JASCO UVIDEC-100-V, 254 nm).

**Isolation**—The benzene soluble fraction (7.5 g) reported in the previous paper,<sup>1</sup> was chromatographed (Merck 7734, 200 g) with mixtures of benzene and AcOEt (9:1, 7:3 and 5:5) (each 1000 ml) to afford five fractions (0.67, 1.93, 2.14, 0.53 and 0.28 g). The second fraction (1.93 g) eluted with the first half (500 ml) of benzene–AcOEt (7:3) was subsequently separated by CC (Merck 7734, 60 g,  $\text{CHCl}_3$ –AcOEt (9:1)), medium-pressure liquid chromatography (MPLC) (Fuji gel, CQ-3,  $\phi 3 \times 23$  cm,  $\text{CHCl}_3$ –AcOEt (7:3)) and preparative TLC (Merck 13895,  $\text{CHCl}_3$ –AcOEt (1:1)) to afford 1,5-diphenylpentane-1,3-diol (**2**) (100 mg, 0.003%) as colorless needles, mp 91–92 °C (hexane–Et<sub>2</sub>O).  $[\alpha]_{\text{D}} -19.2^\circ$  ( $c=0.52$ , MeOH). MS  $m/z$ : 238 ( $\text{M}^+ - \text{H}_2\text{O}$ ). IR  $\nu_{\text{max}}^{\text{KBr}}$ : 3310  $\text{cm}^{-1}$ .  $^1\text{H-NMR}$   $\delta$ : 1.6–1.9 (4H, complex), 2.5–2.8 (2H, complex), 3.44 (2H, brs, OH, disappeared on addition of D<sub>2</sub>O), 3.90 (1H, complex), 4.89 (1H, dd,  $J=10.0$ , 2.9 Hz), 7.0–7.4 (10H, complex).  $^{13}\text{C-NMR}$   $\delta$ : 31.6 (t), 39.5 (t), 45.2 (t), 71.8 (d), 75.1 (d), 125.6 (d  $\times 2$ ), 125.8 (d), 127.5 (d), 128.4 (d  $\times 6$ ), 141.9 (s), 144.4 (s). *Anal.* Calcd for  $\text{C}_{17}\text{H}_{20}\text{O}_2$ : C, 79.65; H, 7.87. Found: C, 79.30; H, 7.93. The third fraction (2.14 g) eluted with the latter half (500 ml) of  $\text{CHCl}_3$ –AcOEt (7:3) was subsequently separated by CC (Katayama Chemical K230, 60 g,  $\text{CHCl}_3$ –AcOEt (7:3)) and preparative TLC (Merck 13895,  $\text{CHCl}_3$ –AcOEt (1:1)) to afford chamaejasmenin B (**1**) (51 mg, 0.006%) as an amorphous powder,  $[\alpha]_{\text{D}} +143.9^\circ$  ( $c=0.57$ , MeOH), which was identified by comparison of the IR and  $^1\text{H-NMR}$  spectra with those of an authentic sample.<sup>3</sup>

**Acetylation of the Diol (2)**—A mixture of **2** (5 mg), Ac<sub>2</sub>O (0.5 ml) and pyridine (0.5 ml) was left to stand at room temperature overnight. After concentration, the residue was purified by preparative TLC (Merck 5715,  $\text{CHCl}_3$ ) to afford **4** (4 mg) as a colorless oil. High-resolution MS Found  $m/z$ : 280.1459 ( $\text{M}^+ - \text{CH}_3\text{COOH}$ );  $\text{C}_{19}\text{H}_{20}\text{O}_2$  requires 280.1461. IR  $\nu_{\text{max}}^{\text{film}}$ : 1735  $\text{cm}^{-1}$ .  $^1\text{H-NMR}$   $\delta$ : 1.95 (3H, s), 2.01 (3H, s), 4.85 (1H, m), 5.79 (1H, t,  $J=7$  Hz), 7.0–7.4 (10H, complex).

**Acetalization of the Diol (2)**—A solution of **2** (13 mg) and camphorsulfonic acid (2 mg) in acetone (3 ml) was left to stand at room temperature overnight. After evaporation of acetone, the residue was separated by preparative TLC (Merck 5715,  $\text{CHCl}_3$ –hexane (2:1)) to afford an acetonide (**5**) (6 mg) as a colorless oil. High-resolution MS Found  $m/z$ : 281.1555 ( $\text{M}^+ - \text{CH}_3$ );  $\text{C}_{19}\text{H}_{21}\text{O}_2$  requires 271.1541. IR  $\nu_{\text{max}}^{\text{film}}$ : 1600, 1495  $\text{cm}^{-1}$ .  $^1\text{H-NMR}$   $\delta$ : 1.53 (3H, s), 1.54 (3H, s), 3.96 (1H, m), 4.86 (1H, dd,  $J=11.7$ , 2.7 Hz), 7.1–7.4 (10H, complex).

**Preparation of 2-(2-Phenylethyl)-1,3-dithiane (6)**—A solution of 3-phenylpropionaldehyde (2.56 g, 18.5 mmol), propane-1,3-dithiol (2.20 g, 20.3 mmol) and  $\text{BF}_3 \cdot \text{Et}_2\text{O}$  (1.0 ml) in  $\text{CHCl}_3$  (50 ml) was kept at  $-10^\circ\text{C}$  for 30 min and then at room temperature for 3 h. The  $\text{CHCl}_3$  solution was washed with brine, dried over  $\text{Na}_2\text{SO}_4$  and evaporated under reduced pressure. The residue was purified by CC (Merck 7734, 190 g, hexane–benzene (2:1)) to afford **6** (4.21 g, 81%). The spectral data were in good agreement with the reported values.<sup>6</sup>

**Reaction of (*R*)-Styrene Oxide (7) with 6**—A solution of **6** (2.028 g, 8.9 mmol) in THF (50 ml) was cooled to  $-40^\circ\text{C}$  under argon, treated with 15% *n*-butyllithium in hexane (4.2 ml, 9.7 mmol) and kept at  $-40^\circ\text{C}$  for 30 min and then at  $-20^\circ\text{C}$  for 30 min. The solution was cooled to  $-50^\circ\text{C}$ , treated with (*R*)-styrene oxide (**7**) (1.068 g, 8.9 mmol) in THF (10 ml), kept at  $-50^\circ\text{C}$  for 30 min and at  $-20^\circ\text{C}$  at 1 h, and diluted with AcOEt (100 ml). The solution was successively washed with aqueous  $\text{NH}_4\text{Cl}$ , water and brine. The organic phase was dried over  $\text{Na}_2\text{SO}_4$  and concentrated. The residue was separated by CC (Merck 7734, 150 g,  $\text{CHCl}_3$ ) to afford the unreacted dithiane (**6**) (0.610 g, 30.1%) and the adduct (**8**) (1.996 g, 65.0%) as colorless needles, mp 103–104 °C from hexane–ether.  $[\alpha]_{\text{D}} -31.3^\circ$  ( $c=0.54$ , MeOH). IR  $\nu_{\text{max}}^{\text{KBr}}$ : 3570, 3460  $\text{cm}^{-1}$ .  $^1\text{H-NMR}$   $\delta$ : 3.52 (1H, d,  $J=2$  Hz, disappeared on addition of D<sub>2</sub>O), 5.10 (1H, dt,  $J=9$ , 4 Hz, changed to a double doublet ( $J=9$ , 2 Hz) on addition of D<sub>2</sub>O).  $^{13}\text{C-NMR}$   $\delta$ : 24.9 (t), 26.0 (t), 26.3 (t), 30.7 (t), 41.7 (t), 47.2 (t), 52.2 (s), 71.2 (d), 125.6 (d  $\times 2$ ), 125.9 (d), 127.4 (d), 128.4 (d  $\times 6$ ), 141.6 (s), 144.7 (s). *Anal.* Calcd for  $\text{C}_{20}\text{H}_{24}\text{OS}_2$ : C, 69.72; H, 7.02. Found: C, 69.72; H, 7.14.

**Hydrolysis of the Adduct (8)**—Mercuric oxide (820 mg, 3.8 mmol) and mercuric chloride (1030 mg, 3.8 mmol) were added to an efficiently stirred solution of **8** (800 mg, 2.3 mmol) in aqueous 90% MeOH at room temperature. The mixture was stirred at the same temperature for 2 h and filtered through Super Cel. The filter cake was washed thoroughly with MeOH and the filtrate was concentrated. The residue was separated by CC (Merck 7734, 50 g, CHCl<sub>3</sub>-AcOEt (15:1)) to afford the dimethylacetal (**9**) (260 mg, 38%) as colorless needles and the ketone (**10**) (330 mg, 57%) as an oil.

**The Dimethylacetal (9)**—Colorless needles from hexane-ether, mp 66–67 °C.  $[\alpha]_D -8.5^\circ$  ( $c=1.0$ , MeOH). IR  $\nu_{\text{max}}^{\text{KBr}}$ : 3480 cm<sup>-1</sup>. <sup>1</sup>H-NMR  $\delta$ : 3.18 (3H, s), 3.25 (3H, s), 3.95 (1H, d,  $J=1$  Hz, disappeared on addition of D<sub>2</sub>O), 4.90 (1H, br d,  $J=10$  Hz, changed to a sharp double doublet ( $J=10, 3$  Hz) on addition of D<sub>2</sub>O). *Anal.* Calcd for C<sub>19</sub>H<sub>24</sub>O<sub>3</sub>: C, 75.97; H, 8.05. Found: C, 75.94; H, 8.25.

**The Ketone (10)**— $[\alpha]_D -28.0^\circ$  ( $c=1.0$ , MeOH). High-resolution MS Found  $m/z$ : 254.1340 (M<sup>+</sup>); C<sub>17</sub>H<sub>18</sub>O<sub>2</sub> requires 254.1306. IR  $\nu_{\text{max}}^{\text{film}}$ : 3450, 1710 cm<sup>-1</sup>. <sup>1</sup>H-NMR  $\delta$ : 3.21 (1H, d,  $J=3$  Hz, disappeared on addition of D<sub>2</sub>O), 5.10 (1H, m, changed to a double doublet ( $J=7, 5$  Hz) on addition of D<sub>2</sub>O).

**Reduction of the Ketone (10)**—**10** (300 mg) in THF (20 ml) was reduced with NaBH<sub>4</sub> (20 mg) at room temperature for 2 h. The mixture was concentrated under reduced pressure, diluted with AcOEt (40 ml) and washed with water and then with brine. The organic phase was dried over Na<sub>2</sub>SO<sub>4</sub> and concentrated under reduced pressure. The residue was roughly separated by preparative TLC (Merck 13895, CHCl<sub>3</sub>-AcOEt (10:1)) using the method of repeated developments (3 times) to afford two fractions. Each fraction was further separated by preparative HPLC (Develosil ODS-5,  $\phi 10 \times 250$  mm, MeOH-H<sub>2</sub>O (75:25)) to afford the diols **11** (61 mg) and **2** (118 mg), as colorless needles, respectively. HPLC analyses of the synthetic diols **2** and **11** were performed under the following conditions: column, Wakogel ODS-5K,  $\phi 4.6 \times 250$  mm; solvent, MeOH-H<sub>2</sub>O (70:30); flow rate, 0.7 ml/min; chart speed, 10 mm/min.

**2**: mp 89.5–91 °C from hexane-ether.  $[\alpha]_D -23.0^\circ$  ( $c=1.0$ , MeOH).  $t_R$  12.6 min.

**11**: mp 91–92 °C from hexane-ether.  $[\alpha]_D -23.3^\circ$  ( $c=1.0$ , MeOH).  $t_R$  12.1 min. MS  $m/z$ : 238 (M<sup>+</sup> - H<sub>2</sub>O). IR  $\nu_{\text{max}}^{\text{KBr}}$ : 3350 cm<sup>-1</sup>. <sup>1</sup>H-NMR  $\delta$ : 1.65–1.95 (4H, complex), 2.56 (1H, complex), 2.70 (1H, complex), 3.13 (1H, br s, disappeared on addition of D<sub>2</sub>O), 3.61 (1H, br s, disappeared on addition of D<sub>2</sub>O), 3.84 (1H, complex), 4.97 (1H, dd,  $J=8.2, 3.4$  Hz), 7.10–7.30 (10H, complex). <sup>13</sup>C-NMR  $\delta$ : 32.0 (t), 39.0 (t), 44.7 (t), 68.6 (d), 71.4 (d), 125.5 (d × 2), 125.8 (d), 127.2 (d), 128.4 (d × 6), 141.9 (s), 144.4 (s). *Anal.* Calcd for C<sub>17</sub>H<sub>20</sub>O<sub>2</sub>: C, 79.65; H, 7.87. Found: C, 79.50; H, 7.93.

**Acknowledgement** The authors wish to thank Mrs. H. Kato (Kato Seishi, Ishikawa Prefecture) for collection of the plant. They are also indebted to Drs. H. Tanino, M. Haruna, Miss T. Sakai and Mr. K. Masuda (this University) for NOE experiments, elemental analyses and high-resolution MS, respectively.

#### References and Notes

- 1) Part I: M. Niwa, P.-F. Jiang and Y. Hirata, *Chem. Pharm. Bull.*, **34**, 3631 (1986).
- 2) Permanent address: *Beijing College of Traditional Chinese Medicine, Beijing, China.*
- 3) G.-Q. Liu, H. Tatematsu, M. Kurokawa, M. Niwa and Y. Hirata, *Chem. Pharm. Bull.*, **32**, 362 (1984).
- 4) G. J. W. Breen, E. Ritchie and W. C. Taylor, *Aust. J. Chem.*, **15**, 819 (1962).
- 5) K. Picker, E. Ritchie and W. C. Taylor, *Aust. J. Chem.*, **29**, 2023 (1976).
- 6) E. J. Corey and B. W. Erickson, *J. Org. Chem.*, **36**, 3553 (1971).
- 7) The chiral epoxide is available from Nihon Kogyo Co., Ltd., Tokyo.

[Chem. Pharm. Bull.]  
35(1) 112-123 (1987)

**Cycloadditions in Syntheses. XXXII.<sup>1)</sup> Intramolecular  
Photocycloaddition of 4-( $\omega$ -Alkenyloxy)quinolin-  
2(1*H*)-one: Synthesis of 2-Substituted  
Cyclobuta[*c*]quinolin-3(4*H*)-ones**

CHIKARA KANEKO,<sup>\*,a</sup> TAKESHI SUZUKI,<sup>a</sup> MASAYUKI SATO,<sup>a</sup>  
and TOSHIHIKO NAITO<sup>b,2)</sup>

*Pharmaceutical Institute, Tohoku University,<sup>a</sup> Aobayama, Sendai 980, Japan and  
Faculty of Pharmaceutical Sciences, Kanazawa University,<sup>b</sup>  
Takara-machi, Kanazawa 920, Japan*

(Received June 26, 1986)

Irradiation of 4-allyloxy-2-quinolone and 4-(pent-4-enyloxy)-2-quinolone gave corresponding cross and parallel adducts specifically, whereas 4-(but-3-enyloxy)-2-quinolone led to a mixture of cross and parallel adducts. Regioselectivity in these photoreactions was not affected by the introduction of substituents into 4-( $\omega$ -alkenyloxy)-2-quinolones.

These cross adducts were transformed to 2-substituted 1,2-dihydrocyclobuta[*c*]quinolin-3(4*H*)-ones, whose synthesis could not be achieved by using so-far known intermolecular photocycloaddition of 4-alkoxy-2-quinolone to olefins (the Kaneko-Naito method). Preliminary experiments demonstrated that these 2-substituted derivatives could be used as synthons for 7,8-disubstituted phenanthridin-6(5*H*)-ones by an application of the benzocyclobutene method.

**Keywords**—photocycloaddition; photochemical synthesis; cyclobuta[*c*]quinolin-3(4*H*)-one, 2-substituted; 2-oxabicyclo[2.1.1]hexane; long-range coupling; 4-( $\omega$ -alkenyloxy)-2-quinolone; benzocyclobutene method; phenanthridin-6(5*H*)-one, 7,8-disubstituted

Previously, we have developed a novel synthetic method for 1,2-dihydrocyclobuta[*c*]quinolin-3(4*H*)-one and its 1-substituted derivatives (**C**), through regioselective photoaddition of 4-alkoxy-2-quinolones (**A**) to olefins followed by an elimination of the alcohol from the adducts (**B**),<sup>3-5)</sup> and we termed this two-step cyclobutane annelation to 2-quinolone and related heteroaromatic compounds as the Kaneko-Naito method.<sup>6,7)</sup> These 1-substituted cyclobuta[*c*]quinolin-3(4*H*)-ones (**C**) can be converted to a variety of polycyclic compounds (**D—G**) mostly by the use of the so-called benzocyclobutene method.<sup>8)</sup>

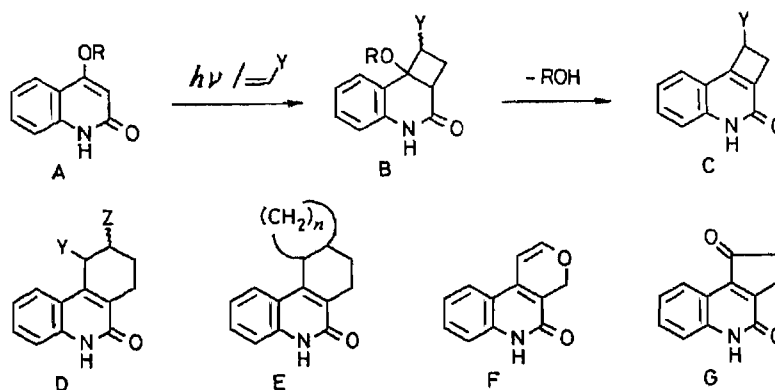


Chart 1

Since the synthesis of corresponding 2-substituted derivatives of 1,2-dihydrocyclobuta[*c*]quinolin-3(4*H*)-one has not been attained by this method, we examined the photochemical behavior of 4-( $\omega$ -alkenyloxy)-2-quinolones and the reactions of the photo-adducts thus obtained.

In this paper, we report the intramolecular photoaddition of 4-( $\omega$ -alkenyloxy)-2-quinolones in detail.<sup>9)</sup> A facile and efficient synthesis of 2-substituted 1,2-dihydrocyclobuta[*c*]quinolin-3(4*H*)-ones from 4-allyloxy-2-quinolone and its derivatives is also described. A successful use of these compounds in the synthesis of 7,8-disubstituted phenanthridin-6(5*H*)-ones is presented.

### Intramolecular Photocycloaddition of 4-( $\omega$ -Alkenyloxy)-2-quinolones

4-( $\omega$ -Alkenyloxy)-2-quinolones (**1**–**3**) were prepared from 4-chloroquinoline-1-oxide by replacing the chlorine atom with the corresponding primary and secondary  $\omega$ -alkenol followed by 2-quinolone formation either by thermal<sup>10)</sup> or photochemical rearrangement reaction.<sup>11)</sup> Because photochemical rearrangement of 4-alkoxyquinoline-1-oxides to the corresponding 4-alkoxy-2-quinolones proceeded in almost quantitative yield in a protic solvent,<sup>11,12)</sup> one can directly use these 1-oxides as the starting materials.

In general, a solution of 4-( $\omega$ -alkenyloxy)-2-quinolones (**1**–**3**) in a transparent solvent was irradiated by a 400 W high-pressure mercury lamp with a Pyrex filter until the starting material disappeared [the reaction was followed by thin-layer chromatography (TLC)]. If the 1-oxides were used as the starting material, methanol is the solvent of choice<sup>1,1,12)</sup> and the

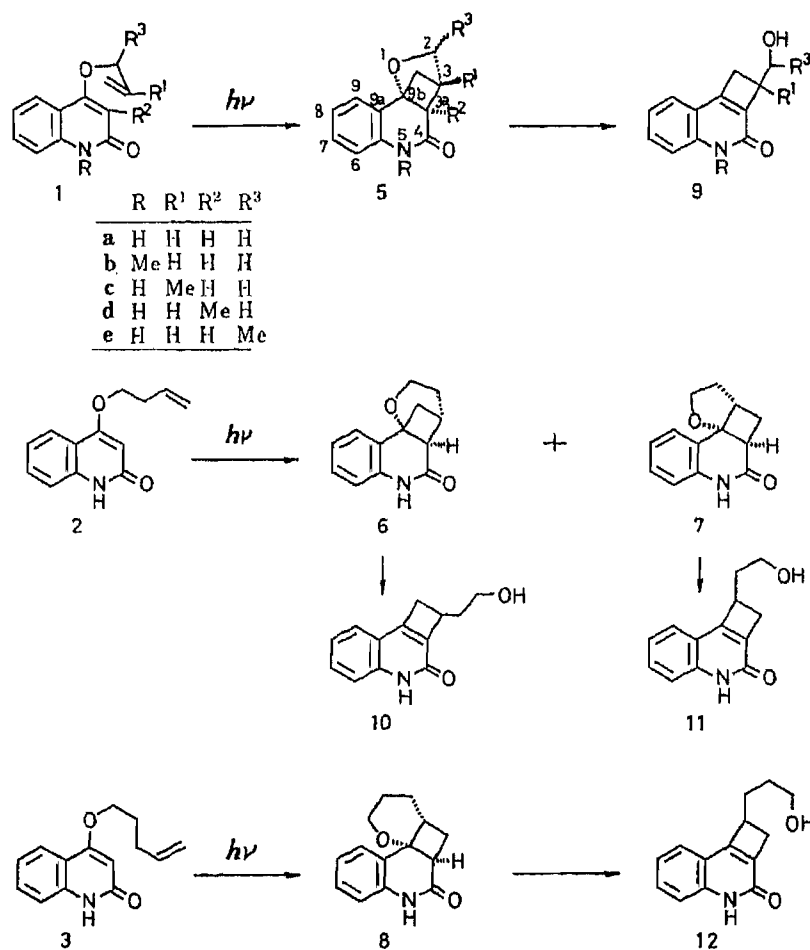
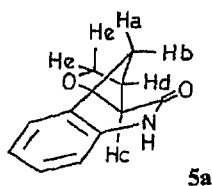


Chart 2

irradiation should be continued until the 2-quinolones formed as the primary product have disappeared. After removal of the solvent, the crude material was directly recrystallized from an appropriate solvent or if necessary, subjected to column chromatography.

Irradiation of 4-allyloxy-2-quinolone (**1a**) in methanol resulted in regio- and stereo-specific formation of the tetracyclic compound (**5a**) in 93% yield. If the corresponding 1-oxide was used as the starting material, the same product (**5a**) was obtained in 88% yield, showing that the photochemical 2-quinolone formation from the 1-oxide in methanol proceeded almost quantitatively. The structure of **5a** was assigned to be the cross adduct on the basis of the proton nuclear magnetic resonance ( $^1\text{H-NMR}$ ) spectrum showing the presence of a typical 2-oxabicyclo[2.1.1]hexane system (see formula in Table I). A long-range coupling between  $\text{H}_a$  and  $\text{H}_c$  ( $J_{ac}=9.5\text{ Hz}$ ) shows clearly that these two protons are in a *W*-configuration in the cyclobutane ring.<sup>13)</sup> In contrast to the regiospecific addition observed with **1a**, irradiation of

TABLE I.  $^1\text{H-NMR}$  Spectral Data for the Cross Adducts (**5a**—**e**) in  $\text{CDCl}_3$



Compd.	Chemical shift ( $\delta$ )					Coupling const. <sup>a)</sup> (Hz)		
	$\text{H}_a$	$\text{H}_b$	$\text{H}_c$	$\text{H}_d$	$\text{H}_e$	$J_{ac}$	$J_{nb}$	$J_{bd}$
<b>a</b>	1.68 dd	2.66 dd	2.79 d	3.47 d	4.14 s	9.5	8.5	3.0
<b>b</b>	1.57 dd	2.46 dd	2.60 d	3.33 d	4.00 s	9.5	8.0	3.0
<b>c</b>	1.69 dd	2.44 d	2.60 d	—	3.87 s	9.5	8.5	—
<b>d</b>	1.56 dd	2.47 d	—	3.19 d	4.00 s	—	8.5	3.0
<b>e</b> <sup>b)</sup>	1.73 t	2.51 dd	2.87 d	3.18 d	4.49 q	9.0	9.0	3.0

a)  $J_{ad}=J_{de}=J_{cd}=0$ . b) Major diastereomer.

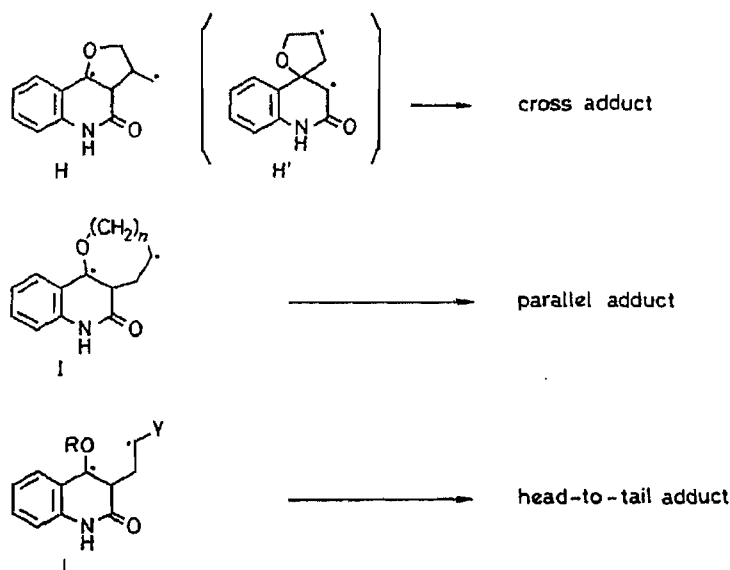


Chart 3

4-(but-3-enyloxy)-2-quinolone (**2**) in methanol led to a mixture of two adducts (**6** and **7**, in a ratio of *ca.* 1:7) in 81% yield. Only the minor adduct (**6**) was the cross adduct as evidenced from the NMR spectrum, in which the same long-range coupling was observed.

Irradiation of 4-(pent-4-enyloxy)-2-quinolone (**3**) again afforded a single product (**8**) in high yield. However, it was the parallel adduct. Its NMR spectrum was similar to that of **7** and did not show the long-range coupling.

The regioselectivity of **1a** was not affected by the introduction of a substituent either on the 2-quinolone ring or in the side-chain. Thus, as shown in Table I, all of the adducts (**5**) obtained from **1** have the 2-oxabicyclo[2.1.1]hexane system.

The above results revealed clearly that the regioselectivity of the intramolecular addition reactions of 4-( $\omega$ -alkenyloxy)-2-quinolones was dependent only upon the length of the methylene chain in the alkenyloxy group and not upon the substituent pattern either on the side chain or in the quinolone ring.<sup>14)</sup> We feel it reasonable to assume that selective formation of the cross adduct (**5**) from **1** occurs *via* the unstable biradical intermediate (**H** or **H'**)<sup>15)</sup> which is formed under kinetic control with favorable entropy assistance. The regiospecific formation of the cross adducts (**5**) from **1** fits well to the so-called "rule of five," which states that the preferred orientation of the adduct formed from 1,5-diene systems in photochemical reactions is the cross adduct rather than the parallel adduct.<sup>16)</sup>

The selective formation of the parallel adduct (**8**) from **3** may be due to the presence of two extra methylenes in the chain as compared to **1** which may facilitate the formation of a stable biradical intermediate (**I**:  $n=3$ ), owing to the steric flexibility of **3**. Thus, just as in the corresponding intermolecular addition reactions<sup>3,4)</sup> which proceed *via* a stable biradical (**J**), the parallel adduct (**8**) is formed selectively. Concomitant formation of both cross (**6**) and parallel adducts (**7**) from **2** supports this view.

#### Synthesis of 2-Substituted 1,2-Dihydrocyclobuta[*c*]quinolin-3(4*H*)-ones

Just as was found with the intermolecular adducts obtained from 4-methoxy-2-quinolone and olefins, all of the adducts (**5**–**8**) obtained from **1**–**3** afforded upon treatment with base the corresponding cyclobuta[*c*]quinolin-3(4*H*)-ones (**9**–**12**) in almost quantitative yields. From the cross adducts (**5** and **6**), 2-substituted derivatives (**9** and **10**) were obtained, whereas 1-substituted ones (**11** and **12**) were obtained from the parallel adducts (**7** and **8**). The products from the parallel adducts are identical with those (**11** and **12**) synthesized from 4-methoxy-2-

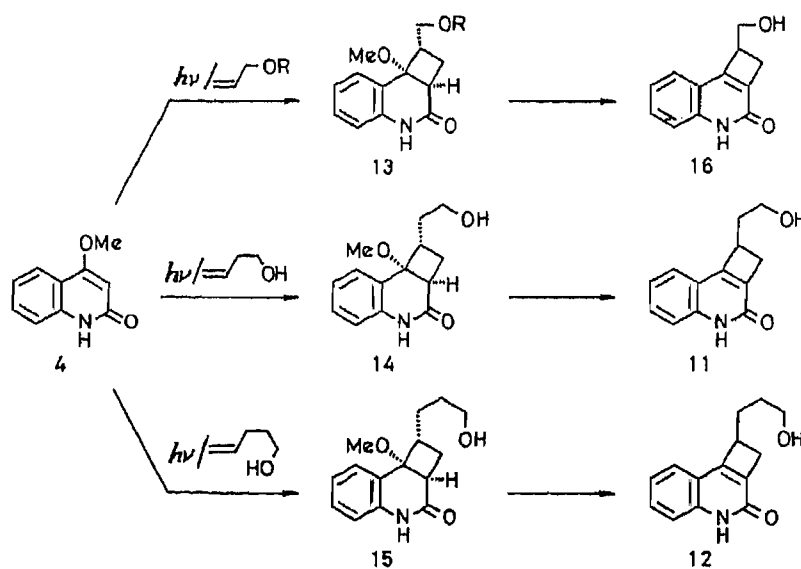


Chart 4

quinolone by the application of the Kaneko–Naito method (Chart 4). This fact as well as the non-identity between **9a** and **16** shows clearly that the structure assignments of **5–8** made by  $^1\text{H-NMR}$  spectroscopy (*vide supra*) are valid.

We chose compound **5a** as a representative of the cross adducts and the following reactions were carried out in order to obtain 2-substituted cyclobuta[*c*]quinolin-3(4*H*)-ones.

When the adduct (**5a**) was treated with conc. hydrobromic acid at room temperature, the 2-bromomethyl derivative (**17a**) was obtained as the major product. With hydrochloric acid, the corresponding chloro derivative (**18a**) was obtained. In both reactions, 2-hydroxymethyl derivative (**9a**) was obtained as a by-product. Since **9a** was stable under these conditions, it is clear that the reactions proceeded *via* the intermediate (**K**) formed by acid-catalyzed  $S_N2$  replacement at the C-3 position by a halide ion ( $X^-$ ) followed by elimination of water. On treatment with potassium *tert*-butoxide in dimethylformamide (DMF) at room temperature, the 2-chloromethyl derivatives (**18a**) afforded the exocyclic methylene compound (**19a**) in high yield. This compound (**19a**) on methylation under usual conditions gave the *N*-methyl derivative (**19b**). Though **19b** was obtained previously from 4-methoxy-1-methyl-2-quinolone (**4b**) by an application of the Kaneko–Naito method using allene (or diketene) as an olefin, the yield was less than 10%.<sup>17)</sup> This is because the major product in the photoaddition step is the 1-methylene derivative (reminiscent of the intermolecular addition reactions of **4**). The halogen atom in these 2-halomethyl derivatives (**17** and **18**) could also be replaced with an appropriate nucleophile. Thus, by usual operation (treatment by potassium phthalimide in DMF, followed by reaction with hydrazine), **18b** was converted to the 2-aminomethyl derivative (**20b**). As is evident from the above experiments, the cross adduct (**5**) obtained from 4-allyloxy-2-quinolone (**1**) serves as an effective nice synthon for 1,2-dihydrocyclobuta[*c*]quinolin-3(4*H*)-ones having a variety of  $C_1$ -units at the 2-position.

Finally, in order to clarify the effect of the substituent at the 2-position of 1,2-dihydrocyclobuta[*c*]quinolin-3(4*H*)-ones in the reaction with olefins (the so-called benzocyclobutene method), reaction of the 2-acetoxymethyl derivative (**21**) with methyl methacrylate was examined. When **21** was heated in xylene in the presence of the acrylate, three products (**22<sub>cis</sub>**, **22<sub>trans</sub>**, and **23**) were obtained in high yield in a ratio of *ca.* 35, 8, and 4. Though the chromatographic separation of the former two compounds (epimeric to each other) had failed, treatment of the mixture with 10% hydrochloric acid at 80 °C afforded the cyclized product, again as an inseparable mixture of two stereoisomers (**24<sub>cis</sub>** and **24<sub>trans</sub>**) in *ca.* 4:1

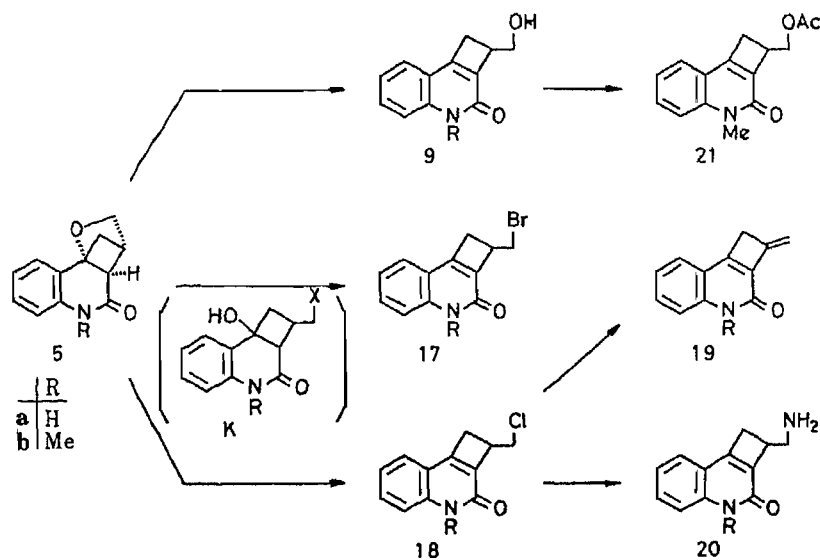


Chart 5



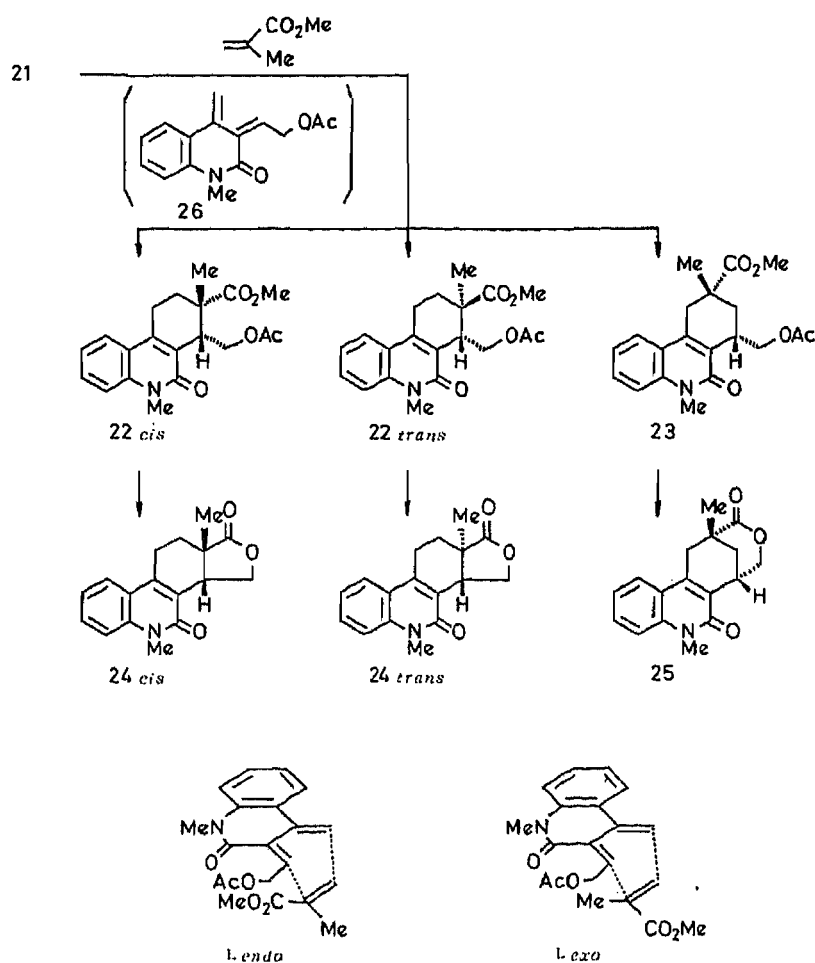


Chart 6

ratio. The infrared (IR) spectrum of the mixture showed the carbonyl absorption at  $1765\text{ cm}^{-1}$  due to the 5-membered lactone. The stereochemistries of the two adducts (**24<sub>cis</sub>** and **24<sub>trans</sub>**) were assigned on the basis of <sup>1</sup>H-NMR signals due to the C-methyl protons. The methyl protons in the major isomer (**24<sub>cis</sub>**) appear at  $\delta$  1.38, while those of the minor isomer (**24<sub>trans</sub>**) are in the shielding cone of the aromatic ring and the signal appears at the relatively highfield position of  $\delta$  1.11.<sup>18)</sup> Hence, it is evident that the cycloadditions of the quinodimethane species (**26**) derived from **21** to the acrylate proceed through the *endo* transition state (*L<sub>endo</sub>*) in preference to the *exo* transition state (*L<sub>exo</sub>*). The same *endo*-selectivity was also evident in the selective formation of **23**, because **23** cyclized to the  $\delta$ -lactone (**25**) under the same conditions.

The high regioselectivity in this reaction to give **22** deserves comment. Previously we have demonstrated that, while 1,2-dihydrocyclobuta[*c*]quinolin-3(4*H*)-one cycloadds to olefins to give two regio-isomers in *ca.* 1 : 1 ratio, 1-substituted derivatives afford only the head-to-head adduct [9,10-disubstituted phenanthridin-6(5*H*)-ones: **D**] regioselectively, and we pointed out that the presence of the 1-substituent plays an important role in this selectivity.<sup>7a,19)</sup> In the present case, it is clearly demonstrated that the presence of the acetoxymethyl group at the 2-position is essential for the formation of 7,8-disubstituted phenanthridone (**22**). The 7,9-disubstituted product (**23**), though obtained, was only the minor product (*ca.* 1/10 of the major regio-isomer).

## Conclusions

The present study has shown that intramolecular photoaddition of 4-( $\omega$ -alkenyloxy)-2-quinolones proceeds to give either the cross or parallel adducts and the regioselectivity of these addition reactions is dependent solely upon the length of the methylene chain in the alkenyloxy side chain. The cross adducts (**5**) obtained from 4-allyloxy-2-quinolones (**1**) were converted successfully to the cyclobuta[*c*]quinolin-3(4*H*)-ones having a variety of C-1 units at the 2-position, whose synthesis could not be achieved by the known method. Further, as evidenced by the cycloaddition of **21** to methyl methacrylate, these 2-substituted derivatives could be effective as nice synthons for 7,8-substituted phenanthridin-6(5*H*)-one derivatives.

## Experimental

All melting points were determined on a micro-hot stage (Yanagimoto) and are uncorrected. IR spectra were recorded on a Shimadzu IR-420 spectrometer, ultraviolet (UV) spectra with a Hitachi 323 spectrometer, and <sup>1</sup>H-NMR spectra on a JEOL JNM-PMX60 or JEOL JNM-FX-100 spectrometer (with tetramethylsilane as an internal standard). Mass spectra (MS) were taken either with a Hitachi M-80 spectrometer or with a JEOL JMS-01SG-2 spectrometer.

Silica gel used for column chromatography was 100–200 mesh, purchased from Kanto Chemical Co., Inc., and alumina was *ca.* 300 mesh from Wako Junyaku Co., Ltd. Preparative thin-layer chromatography (PTLC) was performed on Merck Aluminium Oxide GF<sub>254</sub> (type 60/E, Al<sub>2</sub>O<sub>3</sub>) or Silica Gel GF<sub>254</sub> (type 60, SiO<sub>2</sub>).

**Irradiation Conditions**—a) Irradiation at  $\geq 300$  nm: The photolyses were carried out in a Pyrex immersion apparatus equipped with an Ushio 400W or Toshiba 400P high-pressure mercury lamp.

b) Irradiation at 300 nm (for small-scale intramolecular photoaddition reactions): The photolyses were performed in a quartz vessel using a Rayonet photochemical reactor lamp (RPR-3000 Å).

**Synthesis of 4-( $\omega$ -Alkenyloxy)quinoline 1-Oxides by Reaction of 4-Chloroquinoline 1-Oxides with Primary Alcohols**—Synthesis of 4-Allyloxy-3-methylquinoline 1-Oxide as a Typical Example: A solution of 4-chloro-3-methylquinoline 1-oxide<sup>10</sup> (500 mg, 2.58 mmol) and allyl alcohol (600 mg, 4 mol eq) in tetrahydrofuran (THF 10 ml) containing powdered KOH (290 mg, 2 mol eq) was refluxed for 10 h. After evaporation of the solvent *in vacuo*, the residue was taken up in CH<sub>2</sub>Cl<sub>2</sub>, washed with water and dried over Na<sub>2</sub>SO<sub>4</sub>. The crude product was chromatographed on alumina. Elution with CH<sub>2</sub>Cl<sub>2</sub> afforded 390 mg (70%) of the 4-allyloxyquinoline 1-oxide. Colorless prisms, mp 93–94°C (Et<sub>2</sub>O). <sup>1</sup>H-NMR (CDCl<sub>3</sub>)  $\delta$ : 2.34 (3H, s), 4.49 (2H, dt, *J* = 5.2, 1.0 Hz), 5.25 (1H, ddt, *J* = 9.5, 2.0, 1.0 Hz), 5.32 (1H, ddt, *J* = 16.5, 2.0, 1.0 Hz), 6.10 (1H, ddt, *J* = 16.5, 9.5, 5.2 Hz), 7.35–8.10 (4H, m), 8.28 (1H, s), 8.45–8.70 (1H, m). *Anal.* Calcd for C<sub>13</sub>H<sub>13</sub>NO<sub>2</sub>: C, 72.54; H, 6.09; N, 6.51. Found: C, 72.48; H, 6.01; N, 6.38.

The following compounds were prepared in the same manner from 4-chloroquinoline 1-oxide<sup>10</sup> and their structures were supported by acceptable spectral data and combustion or accurate mass data.

4-Allyloxyquinoline 1-Oxide: Yield 78%. Colorless prisms, mp 133–136°C (hexane-acetone). *Anal.* Calcd for C<sub>12</sub>H<sub>11</sub>NO<sub>2</sub>: C, 71.62; H, 5.51; N, 6.96. Found: C, 71.58; H, 5.49; N, 6.99.

4-(2-Methylallyloxy)quinoline 1-Oxide: Yield 95%. Colorless needles, mp 87–87.5°C (hexane-acetone). UV  $\lambda_{\text{max}}^{\text{MeOH}}$  nm (log  $\epsilon$ ): 222 (4.16), 247 (4.24), 340 (4.03). <sup>1</sup>H-NMR (CDCl<sub>3</sub>)  $\delta$ : 1.75 (3H, s), 4.61 (2H, s), 5.09 (2H, br s), 6.56 (1H, d, *J* = 7.0 Hz), 7.35–7.90 (2H, m), 8.05–8.40 (1H, m), 8.34 (1H, d, *J* = 7.0 Hz), 8.66 (1H, br d, *J* = 7.0 Hz). *Anal.* Calcd for C<sub>13</sub>H<sub>13</sub>NO<sub>2</sub> · 1/2H<sub>2</sub>O: C, 69.62; H, 6.29; N, 6.25. Found: C, 69.22; H, 6.24; N, 6.06.

4-(3-Butenyloxy)quinoline 1-Oxide: Yield 76%. Colorless oil. <sup>1</sup>H-NMR (CDCl<sub>3</sub>)  $\delta$ : 2.70 (2H, br q, *J* = 6.5 Hz), 4.23 (2H, t, *J* = 6.5 Hz), 5.16 (1H, br d, *J* = 9.2 Hz), 5.21 (1H, br d, *J* = 17.2 Hz), 5.93 (1H, ddt, *J* = 17.2, 9.2, 6.5 Hz), 6.61 (1H, d, *J* = 6.8 Hz), 8.44 (1H, d, *J* = 6.8 Hz), 7.35–7.90 (3H, s), 8.67 (1H, br d, *J* = 7.0 Hz). High-resolution MS *m/z*: M<sup>+</sup> Calcd C<sub>13</sub>H<sub>13</sub>NO<sub>2</sub>: 215.0946. Found: 215.0930.

4-(4-Pentyloxy)quinoline 1-Oxide: Yield 81%. Colorless oil. <sup>1</sup>H-NMR (CDCl<sub>3</sub>)  $\delta$ : 1.70–2.60 (4H, m), 4.15 (2H, t, *J* = 6.0 Hz), 5.00 (1H, br d, *J* = 9.0 Hz), 5.07 (1H, br d, *J* = 17.5 Hz), 5.84 (1H, ddd, *J* = 17.5, 9.0, 5.5 Hz), 6.53 (1H, d, *J* = 7.0 Hz), 7.30–7.90 (2H, m), 8.14 (1H, m), 8.34 (1H, d, *J* = 7.0 Hz), 8.63 (1H, br d, *J* = 7.0 Hz). High-resolution MS *m/z*: M<sup>+</sup> Calcd C<sub>14</sub>H<sub>15</sub>NO<sub>2</sub>: 229.1102. Found: 229.1101.

**4-(1-Methylallyloxy)quinoline 1-Oxide**—A solution of 3-buten-2-ol (102 mg, 1.4 mol eq) in hexamethylphosphoramide (HMPA, 2 ml) containing 60% NaH (50 mg, 1.2 mol eq) was stirred for 1 h at room temperature. Under stirring, 4-chloroquinoline 1-oxide (180 mg, 1 mmol) was added to the above solution and the whole was stirred for 15 h at room temperature. After evaporation of the solvent *in vacuo*, the residue was taken up in CH<sub>2</sub>Cl<sub>2</sub>. The organic layer was washed with water, and dried over MgSO<sub>4</sub>. The residue obtained after evaporation of the solvent was chromatographed on silica gel. Elution with MeOH–CH<sub>2</sub>Cl<sub>2</sub> (5:95, v/v) gave 99 mg (46%) of the 1-oxide

as an oil. High-resolution MS  $m/z$ :  $M^+$  Calcd  $C_{13}H_{13}NO_2$ : 215.0946. Found: 215.0948.

**4-( $\omega$ -Alkenyloxy)quinolin-2(1H)-ones**—a) By Photochemical Rearrangement of the 1-Oxides: A solution of 4-(2-methylallyloxy)quinoline-1-oxide (506 mg) in MeOH (230 ml) was irradiated at  $\geq 300$  nm for 5 min under an argon atmosphere. The residue obtained after evaporation of the solvent was chromatographed on alumina. Elution with  $CH_2Cl_2$  gave first 18 mg (4%) of **5c** (*vide infra*) and then 404 mg (83%) of 4-(2-methylallyloxy)quinolin-2(1H)-one (**1e**). Colorless prisms, mp 132.5–133°C (MeOH–Et<sub>2</sub>O). UV  $\lambda_{max}^{MeOH}$  nm (log  $\epsilon$ ): 227 (4.68), 266 (3.83), 275 (3.82), 315 (3.77), 328 (3.67). <sup>1</sup>H-NMR (CDCl<sub>3</sub>)  $\delta$ : 1.90 (3H, s), 4.54 (2H, s), 5.15 (2H, brs), 5.94 (1H, s), 6.90–7.60 (3H, m), 7.86 (1H, brd,  $J=7.0$  Hz), 12.24 (1H, brs). IR (CHCl<sub>3</sub>)  $cm^{-1}$ : 3400–2700, 1650 (br), 1610. Anal. Calcd for  $C_{13}H_{13}NO_2$ : C, 72.54; H, 6.09; N, 6.51. Found: C, 72.52; H, 6.00; N, 6.81.

The following compounds were prepared in the same manner and the structures were supported by acceptable spectroscopic data.

4-Allyloxyquinolin-2(1H)-one (**1a**): Yield 85% (8% of **5a** was obtained at the same time). Colorless prisms, mp 173–174°C (MeOH). Anal. Calcd for  $C_{12}H_{11}NO_2$ : C, 71.62; H, 5.51; N, 6.96. Found: C, 71.52; H, 5.38; N, 6.74.

4-(3-Butenyloxy)quinolin-2(1H)-one (**2**): Yield 82% (6% of a mixture of **6** and **7** was also obtained). Colorless prisms, mp 186–186.5°C (MeOH). Anal. Calcd for  $C_{13}H_{13}NO_2$ : C, 72.54; H, 6.09; N, 6.51. Found: C, 72.34; H, 6.25; N, 6.65.

b) By Rearrangement under Thermal Conditions: Tosyl chloride (160 mg, 1.1 mol eq) was added to a solution of 4-allyloxy-3-methylquinoline 1-oxide (163 mg) in  $CHCl_3$  (3 ml) and the whole was refluxed for 5 min. After cooling, 5 ml of 10% Na<sub>2</sub>CO<sub>3</sub> was added and the mixture was stirred for 30 min. The precipitates were collected by filtration and washed with water to give 111 mg (68%) of 4-allyloxy-3-methylquinolin-2(1H)-one (**1d**). Colorless needles, mp 133–134°C (AcOEt–MeOH).<sup>12)</sup>

4-(4-Pentyloxy)quinolin-2(1H)-one (**3**) was prepared in the same manner. Yield 77%. Colorless prisms, mp 149–150°C (MeOH–Et<sub>2</sub>O). High-resolution MS  $m/z$ :  $M^+$  Calcd  $C_{14}H_{15}NO_2$ : 229.1102. Found: 229.1100.

1-Methyl-4-(allyloxy)quinolin-2(1H)-one (**1b**)—Powdered NaOH (350 mg) and MeI (0.4 ml) were added to a solution of **1a** (416 mg) in iso-PrOH (15 ml) and the whole was refluxed for 2 h. After evaporation of the solvent *in vacuo* and addition of water, the product was taken up in  $CH_2Cl_2$  and dried over Na<sub>2</sub>SO<sub>4</sub>. Short column chromatography on silica gel (3% MeOH– $CH_2Cl_2$ ) afforded 440 mg (quant.) of **1b**. mp 86–86.5°C (hexane–Et<sub>2</sub>O).<sup>12)</sup>

**Synthesis of 3,3a,4,5-Tetrahydro-3,9b-methanofuro[3,2-c]quinolin-4(2H)-ones (5a–e)**—A) Irradiation of 4-Allyloxyquinolin-2(1H)-one and Its Derivatives (**1a–d**): A solution of 4-allyloxyquinolin-2(1H)-one (**1a**: 604 mg) in MeOH (305 ml) was irradiated at  $\geq 300$  nm for 25 min. The residue obtained after evaporation of the solvent was chromatographed on alumina. Elution with  $CH_2Cl_2$  gave 561 mg (93%) of the cross adduct (**5a**). Colorless needles, mp 178–179°C (MeOH). UV  $\lambda_{max}^{MeOH}$  nm (log  $\epsilon$ ): 215 (4.47), 259 (3.89), 269 (3.83). IR (KBr)  $cm^{-1}$ : 1670. <sup>1</sup>H-NMR (CDCl<sub>3</sub>)  $\delta$ : 6.80–7.50 (4H, m), 9.60 (1H, brs) and signals shown in Table I. Anal. Calcd for  $C_{12}H_{11}NO_2$ : C, 71.62; H, 5.51; N, 6.96. Found: C, 71.88; H, 5.33; N, 7.12.

The following compounds were obtained in the same manner and their structures were supported by acceptable NMR (Table I) and other spectral data.

**5b**: Yield 85%. Colorless prisms, mp 64–65°C (hexane–Et<sub>2</sub>O). Anal. Calcd for  $C_{13}H_{13}NO_2$ : C, 72.54; H, 6.09; N, 6.51. Found: C, 72.66; H, 6.22; N, 6.38.

**5c**: Yield 67%. Colorless needles, mp 209–211°C (MeOH). Anal. Calcd for  $C_{13}H_{13}NO_2$ : C, 72.54; H, 6.09; N, 6.51. Found: C, 72.64; H, 6.14; N, 6.50.

**5d**: Yield 77%. Colorless oil. High-resolution MS  $m/z$ :  $M^+$  Calcd for  $C_{13}H_{13}NO_2$ : 215.0946. Found: 215.0936.

b) Irradiation of 4-(1-Methylallyloxy)quinoline 1-Oxide (**1e**): A solution of **1e** (70 mg) in MeOH (40 ml) was irradiated at 300 nm for 1 h. The residue obtained after evaporation of the solvent was chromatographed on silica gel. Elution with AcOEt–hexane (1 : 1, v/v) afforded 67 mg (96%) of *ca.* 4 : 1 mixture of the cross adducts (**5e**), from which the major isomer was obtained in pure form by recrystallization from a mixture of acetone–hexane. Major isomer of **5e**. Colorless needles, mp 165–168°C. <sup>1</sup>H-NMR (CDCl<sub>3</sub>)  $\delta$ : 1.31 (3H, d,  $J=6.0$  Hz) and other signals shown in Table I. <sup>1</sup>H-NMR of the minor isomer of **5e** (CDCl<sub>3</sub>)  $\delta$ : 1.28 (3H, d,  $J=6.0$  Hz) and other signals shown in Table I, among which two signals due to H<sub>a</sub> and H<sub>b</sub> appear downfield from those of the major isomer by 0.03 and 0.05 ppm, respectively.

In the same manner, the cross adduct (**5a**) was obtained in 88% yield, when 4-allyloxyquinoline 1-oxide was used as the starting material.

**Irradiation of 4-(3-Butenyloxy)quinolin-2(1H)-one (2)**—A solution of **2** (216 mg) in MeOH (320 ml) was irradiated at  $\geq 300$  nm for 25 min. The residue obtained after evaporation of the solvent was chromatographed on silica gel. Elution with  $CH_2Cl_2$  gave 20 mg (9%) of the cross adduct (**6**). Elution with 0.5% MeOH– $CH_2Cl_2$  gave 148 mg (69%) of the parallel adduct (**7**) and then the recovered 2-quinolone [2.6 mg (3%)].

2,3,4,4a,6,10b-Hexahydro-4,10b-methanopyrano[3,2-c]quinolin-5(5H)-one (**6**): Colorless prisms, mp 193–194°C (MeOH). UV  $\lambda_{max}^{MeOH}$  nm (log  $\epsilon$ ): 213 (4.46), 248 sh (3.86), 258 (3.91), 268 sh (3.84), 283 sh (3.49). IR (KBr)  $cm^{-1}$ : 1675. <sup>1</sup>H-NMR (CDCl<sub>3</sub>)  $\delta$ : 2.10–2.25 (2H, m), 2.17 (1H, dd,  $J=11.0, 7.8$  Hz), 2.58 (1H, dd,  $J=11.0, 5.5$  Hz), 2.91 (1H, d,  $J=7.8$  Hz), 3.10 (1H, m), 4.10–4.55 (2H, m), 6.75–7.45 (4H, m), 9.50 (1H, brs). Anal. Calcd for  $C_{13}H_{13}NO_2$ : C, 72.54; H, 6.09; N, 6.51. Found: C, 72.54; H, 5.88; N, 6.39.

**1,9,10,10a-Tetrahydro-3H-furo[2',3':2,3]cyclobuta[1,2-c]quinolin-2(1aH)-one (7):** Colorless prisms, mp 195—195.5°C (MeOH). UV  $\lambda_{\text{max}}^{\text{MeOH}}$  nm (log  $\epsilon$ ): 215 (4.46), 248 (3.91), 257 (3.92), 268 sh (3.79), 288 (3.45). IR (KBr)  $\text{cm}^{-1}$ : 1682.  $^1\text{H-NMR}$  ( $\text{CDCl}_3$ )  $\delta$ : 1.70—1.95 (1H, m), 1.95—2.55 (3H, m), 2.92 (1H, m), 3.34 (1H, ddd,  $J=11.0, 7.0, 1.5$  Hz), 4.05—4.55 (2H, m), 6.70—7.30 (4H, m), 9.30 (1H, brs). *Anal.* Calcd for  $\text{C}_{13}\text{H}_{13}\text{NO}_2$ : C, 72.54; H, 6.09; N, 6.51. Found: C, 72.40; H, 6.02; N, 6.35.

**Irradiation of 4-(4-Pentenyl)oxyquinolin-2(1H)-one (3)**—A solution of 3 (132 mg) in MeOH (210 ml) was irradiated at  $\geq 300$  nm for 20 min. The residue obtained after chromatography ( $\text{SiO}_2$ , 1% MeOH- $\text{CH}_2\text{Cl}_2$ ) gave 116 mg (88%) of the parallel adduct (**8**: benz[*k*]-10-aza-2-oxatricyclo[6.4.0.0<sup>1,6</sup>]undecan-9-one). Colorless prisms, mp 204.5—205.5°C (MeOH). UV  $\lambda_{\text{max}}^{\text{MeOH}}$  nm (log  $\epsilon$ ): 250 (4.05), 284 (3.45), 293 sh (3.35). IR (KBr)  $\text{cm}^{-1}$ : 1675.  $^1\text{H-NMR}$  ( $\text{CDCl}_3$ )  $\delta$ : 1.50—2.10 (5H, m), 2.10—2.65 (2H, m), 3.60—4.05 (3H, m), 6.70—7.50 (4H, m), 9.50 (1H, brs). *Anal.* Calcd for  $\text{C}_{14}\text{H}_{15}\text{NO}_2$ : C, 73.34; H, 6.59; N, 6.11. Found: C, 73.28; H, 6.65; N, 5.93.

**2-Substituted 1,2-Dihydrocyclobuta[*c*]quinolin-3(4H)-ones (9 and 10)**—By Base Treatment of the Cross Adducts (**5** and **6**): Synthesis of the 2-Hydroxymethyl Derivative (**9a**) as a Typical Example: A solution of **5a** (61 mg) in NaOMe-MeOH [prepared from Na (60 mg) and MeOH (7 ml)] was refluxed for 2 h. After evaporation of the solvent and addition of water, the product was taken up in 2% MeOH- $\text{CH}_2\text{Cl}_2$  and dried over  $\text{Na}_2\text{SO}_4$ . The residue obtained after evaporation of the solvent was chromatographed on silica gel. Elution with 2% MeOH- $\text{CH}_2\text{Cl}_2$  afforded 60 mg (quant.) of **9a**. Colorless needles, mp 198—199°C (MeOH). UV  $\lambda_{\text{max}}^{\text{MeOH}}$  nm (log  $\epsilon$ ): 228 (4.56), 245 (4.05), 272 (3.84), 281 (3.80), 323 (3.92), 336 (3.81). IR (KBr)  $\text{cm}^{-1}$ : 3350, 1645.  $^1\text{H-NMR}$  ( $\text{CD}_3\text{OD-CDCl}_3$ ; 1:10)  $\delta$ : 2.80—3.50 (2H, m), 3.55—4.20 (3H, m), 6.95—7.65 (4H, m). *Anal.* Calcd for  $\text{C}_{12}\text{H}_{11}\text{NO}_2$ : C, 71.62; H, 5.51; N, 6.96. Found: C, 71.88; H, 5.33; N, 7.12.

The following compounds were prepared in the same manner.

**9b:** Yield 95%. Colorless needles, mp 180—181°C (hexane- $\text{CH}_2\text{Cl}_2$ ). *Anal.* Calcd for  $\text{C}_{13}\text{H}_{13}\text{NO}_2$ : C, 72.54; H, 6.09; N, 6.51. Found: C, 72.45; H, 5.82; N, 6.43.

**9c:** Yield quant. Colorless prisms, mp 216—216.5°C (MeOH). *Anal.* Calcd for  $\text{C}_{13}\text{H}_{13}\text{NO}_2$ : C, 72.54; H, 6.09; N, 6.51. Found: C, 72.54; H, 6.22; N, 6.36.

**10:** Yield quant. Colorless prisms, mp 174—175°C (acetone). High-resolution MS  $m/z$ :  $M^+$  Calcd  $\text{C}_{13}\text{H}_{13}\text{NO}_2$ : 215.0946. Found: 215.0945.

**Synthesis of 1-Substituted 1,2-Dihydrocyclobuta[*c*]quinolin-3(4H)-ones**—a) By Base Treatment of the Parallel Adducts (**7** and **8**): A solution of **7** (103 mg) in NaOMe/MeOH [prepared from Na (50 mg) in MeOH (10 ml)] was refluxed for 2 h. After evaporation of the solvent *in vacuo*, the residue was acidified by the addition of 10% HCl. The precipitates were collected by filtration to give 83 mg (81%) of the 1-(2-hydroxyethyl)cyclobutaquinolinone (**11**). Colorless needles, mp 190—191°C (MeOH). UV  $\lambda_{\text{max}}^{\text{MeOH}}$  nm: 226, 245, 271, 280, 322, 334. IR (KBr)  $\text{cm}^{-1}$ : 3370, 1655.  $^1\text{H-NMR}$  ( $\text{DMSO-}d_6$ )  $\delta$ : 2.00 (2H, q,  $J=6.5$  Hz), 2.62 (1H, dd,  $J=14.0, 1.5$  Hz), 3.16 (1H, dd,  $J=14.0, 4.0$  Hz), 3.50 (1H, m), 6.90—7.60 (4H, m), 11.35 (1H, brs). *Anal.* Calcd for  $\text{C}_{13}\text{H}_{13}\text{NO}_2$ : C, 72.54; H, 6.09; N, 6.51. Found: C, 72.38; H, 5.82; N, 6.33.

The 1-(3-hydroxypropyl)derivative (**12**) was prepared from **8** in the same manner. Yield quant. Colorless needles, mp 180—180.5°C (MeOH). *Anal.* Calcd for  $\text{C}_{14}\text{H}_{15}\text{NO}_2$ : C, 73.34; H, 6.59; N, 6.11. Found: C, 73.19; H, 6.52; N, 6.02.

b) By the Kaneko-Naito Method Using 4-Methoxyquinolin-2(1H)-one (**4**)<sup>21</sup> as the Starting Material: Synthesis of 1-Hydroxymethyl-1,2-dihydrocyclobuta[*c*]quinolin-3(4H)-one (**16**) as a Typical Example: A solution of **4** (179 mg) in MeOH (170 ml) containing allyl acetate 86.0 ml, 50 mol eq) was irradiated at  $\geq 300$  nm for 30 min. The residue after evaporation of the solvent was recrystallized from acetone to give 180 mg of the major stereoisomer of **13** ( $R=Ac$ ). The mother liquor was chromatographed on silica gel. Elution with 9% MeOH- $\text{CH}_2\text{Cl}_2$  afforded 54 mg of a mixture of diastereoisomers of **13** ( $R=Ac$ ) in a ratio of *ca.* 5:1. Total yield of the adduct (**13**:  $R=Ac$ ) was 234 mg (83%). The major adduct had the *exo*-acetoxymethyl group at the 1-position (*vide infra*). Colorless prisms, mp 174—175°C (acetone).  $^1\text{H-NMR}$  ( $\text{CDCl}_3$ )  $\delta$ : 1.80—2.40 (2H, m), 2.07 (3H, s), 2.65—2.95 (1H, m), 2.93 (3H, s), 3.38 (1H, t,  $J=9.5$  Hz), 4.30 (1H, dd,  $J=11.5, 7.6$  Hz), 9.60 (1H, brs). *Anal.* Calcd for  $\text{C}_{15}\text{H}_{17}\text{NO}_4$ : C, 65.44; H, 6.22; N, 5.09. Found: C, 65.29; H, 6.35; N, 5.05.

The *exo*-adduct (**13**: 59 mg) was refluxed in NaOMe-MeOH [prepared from Na (50 mg) and MeOH (6 ml)] for 45 min. After evaporation of the solvent and addition of 10% HCl, the precipitates were collected by filtration and washed with water to give 36 mg (84%) of **16**. Colorless prisms, mp 231—232°C (MeOH). IR (KBr)  $\text{cm}^{-1}$ : 3300, 1650.  $^1\text{H-NMR}$  ( $\text{CD}_3\text{OD}$ )  $\delta$ : 2.83 (1H, dd,  $J=14.2, 1.5$  Hz), 3.21 (1H, dd,  $J=14.2, 4.5$  Hz), 3.65—4.05 (3H, m), 7.00—7.55 (3H, m), 7.67 (1H, brd,  $J=7.2$  Hz). *Anal.* Calcd for  $\text{C}_{12}\text{H}_{11}\text{NO}_2$ : C, 71.62; H, 5.51; N, 6.96. Found: C, 71.58; H, 5.24; N, 6.80. The same product (**16**) was also obtained in a comparable yield (80%) when the mixture of stereoisomers (**13**:  $R=Ac$ ) was used as the starting material.

The following compounds were prepared in the same manner.

**14** [obtained as a single monoacetate by photoaddition of **4** to 3-buten-1-ol, followed by acetylation ( $\text{Ac}_2\text{O}$ -pyridine)]: Yield 78%. Colorless prisms, mp 128—131°C (hexane- $\text{Et}_2\text{O}$ ).  $^1\text{H-NMR}$  ( $\text{CDCl}_3$ )  $\delta$ : 1.55—2.30 (4H, m), 1.99 (3H, s), 2.30—2.75 (1H, m), 2.90 (3H, s), 3.28 (1H, t,  $J=9.3$  Hz), 4.14 (2H, t,  $J=6.3$  Hz), 6.70—7.45 (4H, m), 9.70 (1H, brs). MS  $m/z$ : 289 ( $M^+$ ).

**11:** Yield 87%. The compound was identical with **11** obtained from the parallel adduct (**7**).

**15** (obtained as a single isomer): Yield, quant. Colorless oil.  $^1\text{H-NMR}$  ( $\text{CDCl}_3$ )  $\delta$ : 1.10—4.20 (10H, m), 2.90 (3H, s), 6.70—7.50 (4H, m), 9.01 (1H, br s). Treatment of **15** with  $\text{Ac}_2\text{O}$  and pyridine afforded the acetate of **15**. Yield 94%. Colorless needles, mp 127—128 °C (hexane-acetone).  $^1\text{H-NMR}$  ( $\text{CDCl}_3$ )  $\delta$ : 1.30—2.85 (7H, m), 2.03 (3H, s), 2.91 (3H, s), 3.29 (1H, t,  $J=9.5$  Hz), 4.04 (2H, t,  $J=6.0$  Hz), 6.75—7.45 (4H, m), 9.78 (1H, br s). *Anal.* Calcd for  $\text{C}_{17}\text{H}_{21}\text{NO}_2$ : C, 67.31; H, 6.98; N, 4.62. Found: C, 67.30; H, 7.12; N, 4.41.

**12:** Yield 90%. This compound was identical with **12** obtained from the parallel adduct (**8**).

**Synthesis of 2-Hydroxymethyl-4-methyl-1,2-dihydrocyclobuta[*c*]quinolin-3(4*H*)-one (9b) from 4-Methoxy-1-methylquinolin-2(1*H*)-one and Allyl Alcohol by the Kaneko-Naito Method**—a) Photocycloaddition Step: A solution of 4-methoxy-1-methylquinolin-2(1*H*)-one (290 mg, 1.5 mmol)<sup>22)</sup> in MeOH (130 ml) containing allyl alcohol (1.8 g, 30 mmol) was irradiated at  $\geq 300$  nm for 2.5 h. After evaporation of the solvent, the residue was chromatographed on silica gel. Elution with hexane-ether (1:1, v/v) afforded first 343 mg (90%) of the *exo*-adduct and then 21 mg (6%) of the *endo*-adduct.

*exo*-Adduct: Colorless prisms, mp 100—100.5 °C (hexane-AcOEt).  $^1\text{H-NMR}$  ( $\text{CDCl}_3$ )  $\delta$ : 1.55—2.3 (2H, m), 2.4—3.0 (1H, m), 2.89 (3H, s), 3.35 (3H, s), 3.45 (1H, t,  $J=9.8$  Hz), 3.5—4.3 (2H, m), 6.75—7.55 (4H, m).

*endo*-Adduct: Colorless prisms, mp 151—152 °C (hexane-AcOEt).  $^1\text{H-NMR}$  ( $\text{CDCl}_3$ )  $\delta$ : 1.0—1.8 (2H, m), 2.0—3.0 (1H, m), 2.90 (3H, s), 3.0—3.7 (2H, m), 3.24 (1H, t,  $J=9.0$  Hz), 3.33 (3H, s), 6.8—7.6 (4H, m).

Both adducts were converted to the known acetates.<sup>23)</sup> In their NMR spectra, the  $\text{CH}_2\text{OAc}$  signal of the *endo*-adduct appeared at a higher field region ( $\delta$ : 3.80, d,  $J=6.8$  Hz) than that ( $\delta$ : 4.21, dd,  $J=11.0$  and 7.2 Hz and 4.50, dd,  $J=11.0$  and 6.8 Hz) of the *exo*-adduct.

b) Base Treatment of the Adducts: Treatment of the adducts with 2% NaOH-MeOH (reflux, 2 h) afforded **9b** in almost quantitative yield, irrespective of the stereo-chemistry. Colorless needles, mp 145—147 °C ( $\text{CH}_2\text{Cl}_2$ -hexane).  $^1\text{H-NMR}$  ( $\text{CDCl}_3$ )  $\delta$ : 2.53 (1H, s), 2.78 (1H, dd,  $J=13.5$ , 1.5 Hz), 3.21 (1H, dd,  $J=13.5$ , 3.8 Hz), 3.50—4.20 (3H, m), 3.59 (3H, s), 6.90—7.45 (3H, m), 7.54 (1H, br d,  $J=7.0$  Hz). *Anal.* Calcd for  $\text{C}_{13}\text{H}_{13}\text{NO}_2$ : C, 72.54; H, 6.09; N, 6.51. Found: C, 72.55; H, 6.23; N, 6.40.

**2-Bromomethyl-1,2-dihydrocyclobuta[*c*]quinolin-3(4*H*)-one (17a)**—A solution of **5a** (100 mg) in 48% HBr (2 ml) was stirred at room temperature for 1 h. After evaporation of the solvent and addition of sat.  $\text{NaHCO}_3$ , the product was taken up in 5% MeOH- $\text{CH}_2\text{Cl}_2$  and dried over  $\text{MgSO}_4$ . The product obtained after evaporation of the solvent was chromatographed on silica gel. Elution with hexane-AcOEt (1:2, v/v) gave 126 mg (96%) of **17a**. Elution with AcOEt afforded a trace amount of **9a**.

**17a:** Colorless needles, mp 208—209 °C (AcOEt).  $^1\text{H-NMR}$  ( $\text{DMSO}-d_6$ )  $\delta$ : 2.7—4.3 (5H, m), 6.9—8.0 (4H, m), 11.63 (1H, br s, NH). *Anal.* Calcd for  $\text{C}_{12}\text{H}_{10}\text{BrNO}_2$ : C, 54.57; H, 3.82; Br, 30.25; N, 5.30. Found: C, 54.53; H, 3.59; Br, 30.65; N, 5.42.

A mixture of **17a** (112 mg), MeI (0.5 g),  $\text{K}_2\text{CO}_3$  (0.5 g) and acetone (10 ml) was stirred at room temperature overnight. Next day, the same amounts of MeI and  $\text{K}_2\text{CO}_3$  were added and the whole was again stirred for 1 d. After evaporation of the solvent, the product was taken up in  $\text{CH}_2\text{Cl}_2$ , washed with water and dried over  $\text{MgSO}_4$ . The residue obtained after evaporation of the solvent was chromatographed on silica gel. Elution with hexane-AcOEt (5:1) afforded 115 mg (97%) of **17b**. Colorless needles, mp 138—139 °C (acetone-hexane). *Anal.* Calcd for  $\text{C}_{13}\text{H}_{12}\text{BrNO}$ : C, 56.16; H, 4.35; Br, 28.73; N, 5.04. Found: C, 56.16; H, 4.11; Br, 28.57; N, 4.95.  $^1\text{H-NMR}$  ( $\text{CDCl}_3$ )  $\delta$ : 2.7—4.2 (5H, m), 3.70 (3H, s), 7.0—7.9 (4H, m).

**2-Chloromethyl-1,2-dihydrocyclobuta[*c*]quinolin-3(4*H*)-one (18a) and Its 4-Methyl Derivative (18b)**—A solution of **5a** (1.17 g) in conc. HCl (10 ml) was heated at 80 °C on a water bath for 2 h. After evaporation of the solvent and addition of sat.  $\text{NaHCO}_3$ , the product was taken up in 5% MeOH- $\text{CH}_2\text{Cl}_2$  and dried over  $\text{MgSO}_4$ . The residue obtained after evaporation of the solvent was chromatographed on silica gel. Elution with hexane-AcOEt (1:2, v/v) afforded 972 mg (76%) of **18a**. Further elution with ethyl acetate afforded 108 mg (9.3%) of **9a**.

**18a:** Colorless needles, mp 195—196 °C (MeOH). High-resolution MS  $m/z$ :  $M^+$  Calcd  $\text{C}_{12}\text{H}_{10}\text{ClNO}$ : 219.0451. Found: 219.0454.

The methylation of **18a** as above gave the 4-methyl derivative (**18b**) in nearly quantitative yield. Colorless needles, mp 131—132 °C ( $\text{CH}_2\text{Cl}_2$ -hexane).  $^1\text{H-NMR}$  ( $\text{CDCl}_3$ )  $\delta$ : 3.05 (1H, br d,  $J=14.0$  Hz), 3.45 (1H, dd,  $J=14.0$ , 3.0 Hz), 3.5—4.6 (3H, m), 3.73 (3H, s), 7.0—7.8 (4H, m). High-resolution MS  $m/z$ :  $M^+$  Calcd  $\text{C}_{13}\text{H}_{12}\text{ClNO}$ : 233.0604. Found: 233.0601.

**2-Methylene-1,2-dihydrocyclobuta[*c*]quinolin-3(4*H*)-one (19a)**—A solution of **18a** (404 mg) in DMF (10 ml) containing *tert*-BuOK (0.62 g) was stirred at room temperature for 2 h. After addition of water (1 ml), the solvent was evaporated off *in vacuo* and the residue was dissolved in 5% MeOH- $\text{CH}_2\text{Cl}_2$ , washed with water and dried over  $\text{MgSO}_4$ . The product obtained after evaporation of the solvent was recrystallized from MeOH to give 252 mg (75%) of **19a**. Colorless prisms, mp  $> 300$  °C (turns brown when heated at about 230 °C) (MeOH).  $^1\text{H-NMR}$  ( $\text{CDCl}_3$ - $\text{DMSO}-d_6$ , 2:1, v/v)  $\delta$ : 3.61 (2H, s), 4.95 (1H, s), 5.33 (1H, s), 7.0—8.1 (4H, m), 11.6 (1H, br s, NH). *Anal.* Calcd for  $\text{C}_{12}\text{H}_9\text{NO}$ : C, 78.68; H, 4.95; N, 7.65. Found: C, 78.32; H, 4.94; N, 7.24.

The methylation of **19a** as above afforded the 4-methyl derivative (**19b**: mp 132—134 °C)<sup>17)</sup> in almost quantitative yield.

**2-Aminomethyl-4-methyl-1,2-dihydrocyclobuta[*c*]quinolin-3(4*H*)-one (20b)**—a) A solution of **18b** (260 mg, 1.1 mmol) and potassium phthalimide (257 mg, 1.2 mol eq) in DMF (10 ml) was heated at 80 °C for 5 h and then at 110 °C for 12 h. After evaporation of the solvent, the product was taken up in CH<sub>2</sub>Cl<sub>2</sub> and dried over MgSO<sub>4</sub>. The residue obtained after evaporation of the solvent was chromatographed on silica gel. Elution with hexane–AcOEt (3:1, v/v) afforded 88 mg (40%) of **19b**. Elution with hexane–AcOEt (1:1, v/v) gave 202 mg (58%) of the phthalimide. Colorless needles, mp 201–202 °C (CH<sub>2</sub>Cl<sub>2</sub>–hexane). *Anal.* Calcd for C<sub>21</sub>H<sub>16</sub>N<sub>2</sub>O<sub>3</sub>: C, 73.24; H, 4.68; N, 8.13. Found: C, 73.07; H, 4.46; N, 7.91.

b) Treatment of the Phthalimide with Hydrazine: A solution of the phthalimide (240 mg, 0.7 mmol) and hydrazine hydrate (42 mg, 1.2 mmol) in EtOH (5 ml) was refluxed for 4.5 h. After cooling, the precipitates were removed by filtration. The residue obtained after evaporation of the solvent was chromatographed on a short alumina column. Elution with 5% MeOH–CH<sub>2</sub>Cl<sub>2</sub> gave 120 mg (80%) of **20b** as a semi-solid. <sup>1</sup>H-NMR (CDCl<sub>3</sub>) δ: 1.30 (2H, s, NH<sub>2</sub>), 2.6–3.9 (5H, m), 3.71 (3H, s), 6.9–7.8 (4H, m). High-resolution MS *m/z*: M<sup>+</sup> C<sub>13</sub>H<sub>14</sub>N<sub>2</sub>O: 214.1105. Found: 214.1097.

**2-Acetoxymethyl-4-methyl-1,2-dihydrocyclobuta[*c*]quinolin-3(4*H*)-one (21)**—A solution of **9b** (60 mg) in acetic anhydride (2 ml) containing 2 drops of pyridine was warmed slightly and then kept standing at room temperature for 3 h. After evaporation of the solvent, the residue was taken up in CH<sub>2</sub>Cl<sub>2</sub>, washed with sat. NaHCO<sub>3</sub>, and dried over MgSO<sub>4</sub>. The product obtained after evaporation of the solvent was chromatographed on silica gel. Elution with hexane–AcOEt (3:1, v/v) afforded 61 mg (85%) of **21**. Colorless needles, mp 114–115 °C (CH<sub>2</sub>Cl<sub>2</sub>–hexane). <sup>1</sup>H-NMR (CDCl<sub>3</sub>) δ: 2.08 (3H, s), 2.92 (1H, dd, *J* = 14.5, 2.0 Hz), 3.35 (1H, dd, *J* = 14.5, 4.0 Hz), 3.67 (3H, s), 3.8–4.1 (1H, m), 4.2–4.9 (2H, m), 7.1–7.9 (4H, m). *Anal.* Calcd for C<sub>15</sub>H<sub>15</sub>NO<sub>3</sub>: C, 70.02; H, 5.88; N, 5.44. Found: C, 70.05; H, 5.81; N, 5.35.

**Reaction of 21 with Methyl Methacrylate**—A solution of **21** (45 mg) and methyl methacrylate (530 mg, 30 mol eq) in xylene (10 ml) was refluxed for 10 h. The residue obtained after evaporation of the solvent was chromatographed on silica gel. Elution with hexane–AcOEt (3:1, v/v) gave first a mixture of **23** and **22** and then 30 mg of pure **22**. The mixture was separated by PTLC (developing solvent: hexane–AcOEt, 2:1, v/v) to give 4 mg of **23** (the less polar adduct) and 13 mg of **22** (the more polar adduct). The combined yields of **22** and **23** are 43 mg (69%) and 4 mg (6.5%). The NMR spectra of **22** and **23** showed that the former was a mixture of two isomers (*cis/trans* ratio: *ca.* 4:1) and the latter was a single isomer.

**22**: Oil. IR (CHCl<sub>3</sub>) cm<sup>-1</sup>: 1725, 1635. <sup>1</sup>H-NMR (CDCl<sub>3</sub>) δ: 1.20 (2.4H, s, C–CH<sub>3</sub>), 1.40 (0.6H, s, C–CH<sub>3</sub>), 1.97 (2.4H, s, COCH<sub>3</sub>), 1.99 (0.6H, s, COCH<sub>3</sub>), 3.56 (0.6H, s, OCH<sub>3</sub>), 3.74 (0.6H, s, N–CH<sub>3</sub>), 3.77 and 3.79 (each 2.4H, s, OCH<sub>3</sub> and N–CH<sub>3</sub>). High-resolution MS *m/z*: M<sup>+</sup> Calcd C<sub>20</sub>H<sub>23</sub>NO<sub>5</sub>: 357.1574. Found: 357.1557.

**23**: Colorless needles, mp 139–141 °C (CH<sub>2</sub>Cl<sub>2</sub>–hexane). IR (CHCl<sub>3</sub>) cm<sup>-1</sup>: 1725, 1630. <sup>1</sup>H-NMR (CDCl<sub>3</sub>) δ: 1.29 (3H, s, C–CH<sub>3</sub>), 2.02 (3H, s, COCH<sub>3</sub>), 1.8–2.4 (2H, m), 2.83 (1H, d, *J* = 18.0 Hz), 3.3–3.7 (1H, m), 3.40 (1H, d, *J* = 18.0 Hz), 3.75 (6H, s, OCH<sub>3</sub> and N–CH<sub>3</sub>), 4.20 (1H, dd, *J* = 11.0, 8.0 Hz), 4.56 (1H, dd, *J* = 11.0, 4.0 Hz), 7.1–7.7 (3H, m), 7.82 (1H, br d, *J* = 8.0 Hz). High-resolution MS *m/z*: M<sup>+</sup> Calcd C<sub>20</sub>H<sub>23</sub>NO<sub>5</sub>: 357.1574. Found: 357.1542.

**Conversion of the Adducts (22 and 23) to the Lactones (24 and 25)**—Formation of **24** as a Typical Example: A solution of **22** (*ca.* 4:1 mixture of *cis* and *trans* isomers; 30 mg) in 10% HCl (3 ml) was heated at 80 °C for 5 h. After the reaction, the mixture was basified by addition of sat. NaHCO<sub>3</sub>, extracted with CH<sub>2</sub>Cl<sub>2</sub>, and dried over MgSO<sub>4</sub>. Evaporation of the solvent afforded the  $\gamma$ -lactone (**24**) in a quantitative yield as a mixture of two inseparable isomers (the *cis/trans* ratio was *ca.* 4:1 as judged from the NMR spectrum). IR (CHCl<sub>3</sub>) cm<sup>-1</sup>: 1765, 1635. <sup>1</sup>H-NMR (CDCl<sub>3</sub>) δ: 1.11 (0.6H, s, C–CH<sub>3</sub>), 1.38 (2.4H, s, C–CH<sub>3</sub>), 3.72 (0.6H, s, N–CH<sub>3</sub>), 3.75 (2.4H, N–CH<sub>3</sub>).

Recrystallization of the product from acetone–hexane afforded **24** (*cis/trans* ratio: *ca.* 3:1) as colorless needles, mp 158–169 °C. High-resolution MS *m/z*: M<sup>+</sup> Calcd C<sub>17</sub>H<sub>17</sub>NO<sub>3</sub>: 283.1209. Found: 283.1212.

Under the same conditions as above, **23** gave the  $\delta$ -lactone (**25**) in a quantitative yield. Colorless needles, mp 268–270 °C (CH<sub>2</sub>Cl<sub>2</sub>–hexane). IR (CHCl<sub>3</sub>) cm<sup>-1</sup>: 1723, 1635. <sup>1</sup>H-NMR (CDCl<sub>3</sub>) δ: 1.60 (3H, s, C–CH<sub>3</sub>), 1.89 (1H, br d, *J* = 13.0 Hz), 2.27 (1H, br d, *J* = 13.0 Hz), 2.80 (1H, d, *J* = 19.0 Hz), 3.35 (1H, d, *J* = 19.0 Hz), 3.70 (br s), 3.77 (3H, s, N–CH<sub>3</sub>), 4.56 (2H, m), 7.1–7.8 (4H, m). High-resolution MS *m/z*: M<sup>+</sup> Calcd C<sub>17</sub>H<sub>17</sub>NO<sub>3</sub>: 283.1209. Found: 283.1196.

**Acknowledgements** We thank Mr. K. Kawamura, Miss K. Mushiake, Miss K. Koike, and Miss E. Niwa of the Central Analysis Room of this Institute for elemental analyses and spectral measurements. This work was supported by Ministry of Education, Science and Culture, Grant-in-Aid for Special Project Research No. 61123005.

#### References and Notes

- 1) Part XXXI: C. Kaneko, K. Kasai, H. Watanabe, and N. Katagiri, *Chem. Pharm. Bull.*, **34**, 4955 (1986).
- 2) Present address: Eisai Co., Ltd., Tokodai 5-chome, Toyosato-machi, Tsukuba-gun, Ibaraki 300–26, Japan.
- 3) C. Kaneko and T. Naito, *Chem. Pharm. Bull.*, **27**, 2254 (1979).
- 4) The two possible orientations for the cycloaddition of an enone to an unsymmetrical alkene are commonly referred to as the head-to-tail and head-to-head orientations, respectively, with the “head” of the enone bearing

the carbonyl group and the "head" of the alkene being the more substituted of the alkene carbons.

- 5) C. Kaneko, T. Naito, Y. Momose, H. Fujii, N. Nakayama, and I. Koizumi, *Chem. Pharm. Bull.*, **30**, 519 (1982).
- 6) T. Naito, Y. Makita, S. Yazaki, and C. Kaneko, *Chem. Pharm. Bull.*, **34**, 1505 (1986).
- 7) Reviews on this topics: a) C. Kaneko and T. Naito, *Heterocycles*, **19**, 2183 (1982); b) T. Naito and C. Kaneko, *Yuki Gosei Kagaku Kyokai Shi*, **42**, 51 (1984).
- 8) T. Kametani and K. Fukumoto, *Heterocycles*, **3**, 29 (1975); W. Oppolzer, *Synthesis*, **1978**, 793.
- 9) Some data on the intramolecular reaction of 4-( $\omega$ -alkenyloxy)-2-quinolones were presented in a communication: C. Kaneko, T. Naito, and M. Somei, *J. Chem. Soc., Chem. Commun.*, **1979**, 804.
- 10) E. Ochiai, *J. Org. Chem.*, **18**, 549 (1953); *idem*, "Aromatic Amine Oxides," Elsevier Pub. Co., Amsterdam, 1967, p. 247.
- 11) C. Kaneko, *Yuki Gosei Kagaku Kyokai Shi*, **26**, 758 (1968); G. G. Spence, E. C. Taylor, and O. Buchardt, *Chem. Rev.*, **1974**, 241.
- 12) C. Kaneko, T. Naito, M. Hashiba, H. Fujii, and M. Somei, *Chem. Pharm. Bull.*, **27**, 1813 (1979).
- 13) K. B. Wiberg, B. R. Lowry, and B. J. Nist, *J. Am. Chem. Soc.*, **84**, 1594 (1962); J. W. Gibson and W. F. Erman, *J. Org. Chem.*, **37**, 1148 (1972); Y. Tamura, H. Ishibashi, M. Hirai, Y. Kita, and M. Ikeda, *ibid.*, **40**, 2702 (1975).
- 14) It was reported that while intramolecular photocycloaddition reaction of 4-(but-3-enyloxy)- and 4-(pent-4-enyloxy)-coumarins afforded only the parallel adducts, none of the cycloadduct was formed from 4-allyloxy-coumarin: D. J. Haywood and S. T. Reid, *Tetrahedron Lett.*, **1979**, 2637.
- 15) Recently, Ikeda *et al.* reported the photochemical formation of 2-azabicyclo[2.1.1]hexane derivatives (the cross adducts) from 2-[*N*-acyl-*N*-(2-propenyl)amino]cyclohex-2-enones and suggested that the biradical corresponding to H was a more probable intermediate than the one corresponding to H': M. Ikeda, T. Uchino, M. Takahashi, H. Ishibe, Y. Tamura, and M. Kido, *Chem. Pharm. Bull.*, **33**, 3279 (1985).
- 16) R. Srinivasan and K. H. Carlough, *J. Am. Chem. Soc.*, **89**, 4932 (1967); S. Wolff and W. C. Agosta, *ibid.*, **105**, 1292, 1299 (1983); W. Oppolzer, *Acc. Chem. Res.*, **15**, 135 (1982).
- 17) C. Kaneko, N. Shimomura, Y. Momose, and T. Naito, *Chem. Lett.*, **1983**, 1239; T. Chiba, T. Kato, A. Yoshida, R. Moroi, N. Shimomura, Y. Momose, T. Naito, and C. Kaneko, *Chem. Pharm. Bull.*, **32**, 4707 (1984).
- 18) K. Shishido, S. Shimada, K. Fukumoto, and T. Kametani, *Chem. Pharm. Bull.*, **32**, 922 (1984).
- 19) C. Kaneko, T. Naito, and M. Ito, *Tetrahedron Lett.*, **19**, 2183 (1982).
- 20) Y. Kawazoe and M. Tachibana, *Chem. Pharm. Bull.*, **15**, 1 (1967).
- 21) F. Arndt, L. Ergener, and O. Kutlu, *Chem. Ber.*, **86**, 951 (1953).
- 22) P. Beak, T. S. Woods, and D. S. Mueller, *Tetrahedron*, **28**, 5507 (1972).
- 23) T. Naito and C. Kaneko, *Chem. Pharm. Bull.*, **31**, 366 (1983).

[Chem. Pharm. Bull.]  
35(1) 124-135 (1987)

**Marine Natural Products. XVII.<sup>1)</sup> Nephtheoxydiol, a New Cytotoxic Hydroperoxy-Germacrane Sesquiterpene, and Related Sesquiterpenoids from an Okinawan Soft Coral of *Nephthea* sp. (Nephtheidae)**

ISAO KITAGAWA,\*<sup>a</sup> ZHENG CUI,<sup>a</sup> BYENG WHA SON,<sup>a</sup>  
MOTOMASA KOBAYASHI,<sup>a</sup> and YOSHIMASA KYOGOKU<sup>b</sup>

*Faculty of Pharmaceutical Sciences, Osaka University,<sup>a</sup> 1-6, Yamada-oka, Suita, Osaka 565, Japan and Institute for Protein Research, Osaka University,<sup>b</sup> 3-2, Yamada-oka, Suita, Osaka 565, Japan*

(Received June 30, 1986)

A new cytotoxic hydroperoxy-germacrane sesquiterpene named nephtheoxydiol (**8**) and several related sesquiterpenoids, *ent*-oplopanone (**2**), nephthenol (**6**), and nephthediol (**9**), were isolated from an Okinawan soft coral of *Nephthea* sp. (Nephtheidae), together with a new cadinane-type sesquiterpene named nephthene (**17**). Based on chemical reactions and physical data analyses, the absolute stereostructures of *ent*-oplopanone (**2**), nephthenol (**6**), nephtheoxydiol (**8**), nephthediol (**9**), and nephthene (**17**) have been determined as (+)-oplopanone (**2**), (4*R*,7*S*)-germacra-1(10)*E*,5*E*-dien-4-ol (**6**), (1*S*,4*R*,7*S*)-1-hydroperoxygermacra-5*E*,10(15)-dien-4-ol (**8**), (1*S*,4*R*,7*S*)-germacra-5*E*,10(15)-diene-1,4-diol (**9**), and (1*S*,7*R*,10*S*)-cadina-4(14),5-diene (**17**), respectively.

**Keywords**—soft coral; *Nephthea* sp.; Nephtheidae; nephtheoxydiol; germacrane sesquiterpene hydroperoxylated; nephthenol; nephthediol; *ent*-oplopanone; nephthene; cytotoxic activity

During the course of our studies on bioactive constituents of marine organisms,<sup>2)</sup> we isolated a trinorsesquiterpene named clavukerin C (**1**) from the Okinawan stoloniferan soft coral *Clavularia koellikeri* and determined the absolute stereostructure, which was characterized by the presence of a hydroperoxy function.<sup>3)</sup> In a continuing study on chemical constituents of an Okinawan soft coral of *Nephthea* sp. (family: Nephtheidae, order: Alcyonacea), we have isolated a new cytotoxic germacrane-sesquiterpene named nephtheoxydiol (**8**) and several related sesquiterpenoids, *ent*-oplopanone (**2**), nephthenol (**6**), and nephthediol (**9**), together with a new cadinane-type sesquiterpene named nephthene (**17**). This paper deals with the structure elucidation of these sesquiterpenoids.<sup>4)</sup>

The acetone extract of a fresh soft coral, collected in July 1984 at Iriomote-jima, Okinawa Prefecture, was partitioned into an ethyl acetate-water mixture. The ethyl acetate-soluble portion was subjected to silica gel column chromatography and high-performance liquid chromatography (HPLC) to furnish nephthene (**17**), nephthenol (**6**), nephtheoxydiol (**8**), *ent*-oplopanone (**2**), and nephthediol (**9**) in 11.0, 6.5, 1.5, 0.4, and 0.5% yields (from the ethyl acetate-soluble portion).

*ent*-Oplopanone (**2**) was obtained as colorless needles. The physicochemical properties of **2** except for the sign of its specific rotation were found to be identical with those reported for oplopanone (**3**), which was previously isolated from a terrestrial plant, *Oplopanax japonicus* (Araliaceae).<sup>5)</sup> Furthermore, a dehydration product (**4**), which was prepared by phosphorus oxychloride treatment of *ent*-oplopanone (**2**), was found to be identical with (–)-anhydrooplopanone (**5**), previously isolated from another terrestrial plant, *Rugelia nudicaulis* (Compositae),<sup>6)</sup> in all respects except for the sign of the specific rotation. Therefore, we



concluded that *ent*-oplopanone (**2**) isolated from a soft coral of *Nephthea* sp. is an enantiomer of oplopanone (**3**) found in a terrestrial plant.

Nephthenol (**6**) is a sesquiterpene alcohol. The proton nuclear magnetic resonance ( $^1\text{H-NMR}$ ) spectrum of **6** showed the presence of a *transoid* disubstituted double bond ( $\delta$  5.25, 1H, d,  $J=16.0$  Hz;  $\delta$  5.18, 1H, dd,  $J=16.0, 9.5$  Hz), a trisubstituted double bond ( $\delta$  4.95, 1H, brd,  $J=ca. 11.5$  Hz), an olefinic methyl group ( $\delta$  1.54, 3H, s), a tertiary methyl group geminal to a hydroxyl group ( $\delta$  1.19, 3H, s), and an isopropyl moiety ( $\delta$  0.79, 0.83, both 3H, d,  $J=7.0$  Hz). In addition to these findings, detailed analysis of the carbon-13 nuclear magnetic resonance ( $^{13}\text{C-NMR}$ ) spectrum of **6** led us to formulate nephthenol as **6**, except for its configuration.

Oxidation of nephthenol (**6**) with *m*-chloroperbenzoic acid (*m*-Cl-PBA) in chloroform provided *ent*-oplopanone (**2**). This conversion is considered to proceed successively *via*: i) epoxidation at the 1(10) double bond, ii) epoxide-ring opening concerted with the 1(6) bond formation, followed by another epoxide-ring formation, and iii) ring contraction constructing a five-membered ring with a methylketone moiety (*cf.* i, ii). Therefore, it has become clear that nephthenol (**6**) is a germacrane-type sesquiterpene having a 1(10)*E*,5*E*-dien-4-ol moiety and a 7*S* configuration.

In order to determine the C-4 configuration of nephthenol (**6**), **6** was oxidized with *tert*-butyl hydroperoxide in the presence of vanadium(IV) oxyacetylacetonate [ $\text{VO}(\text{acac})_2$ ]<sup>7</sup> to afford an  $\alpha$ -glycol derivative (**7**). The  $\alpha$ -glycol (**7**) was presumably formed *via*: i) initial  $\alpha$ -epoxidation at the 5(6) double bond, ii) epoxide-ring opening followed by 1(6) bond formation, and finally iii) deprotonation at C-15 to generate the 10(15) terminal methylene moiety (*cf.* iii).

In a nuclear Overhauser effect (NOE) experiment on **7**, irradiation of 4- $\text{CH}_3$  ( $\delta$  1.07) resulted in increased signal intensities of 1 $\beta$ -H ( $\delta$  1.40, dd-like,  $J=ca. 12.0, 10.0$  Hz) (9%) and

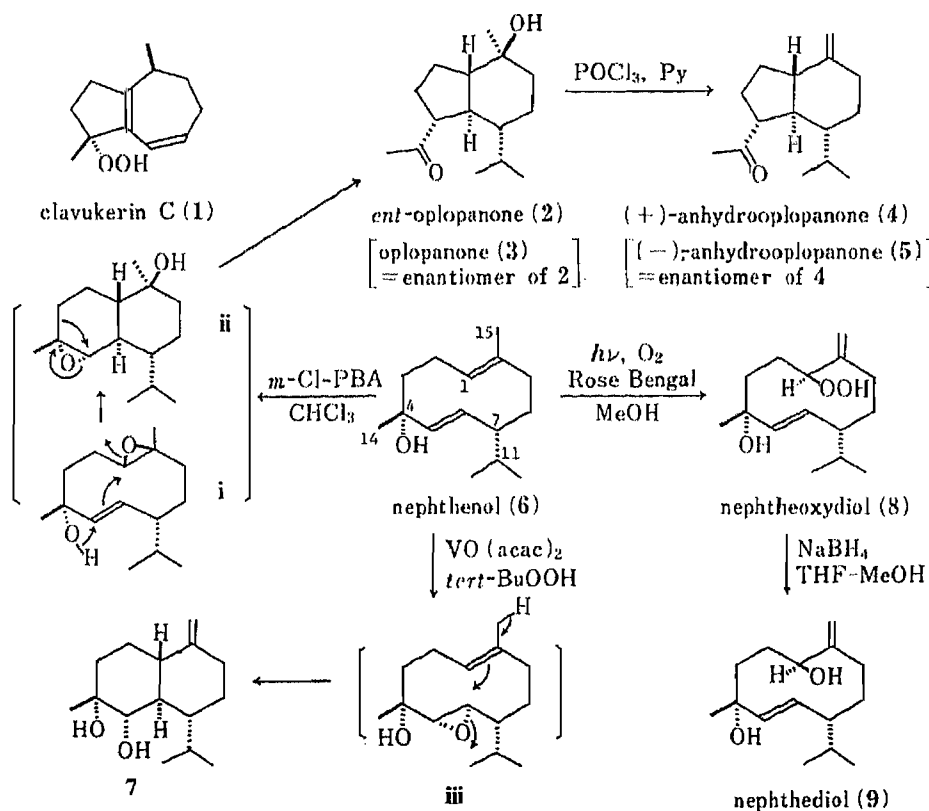


Chart 1

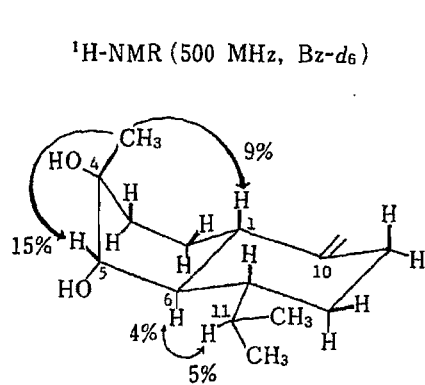


Fig. 1. NOE (%) of 7  
Bz=benzene.

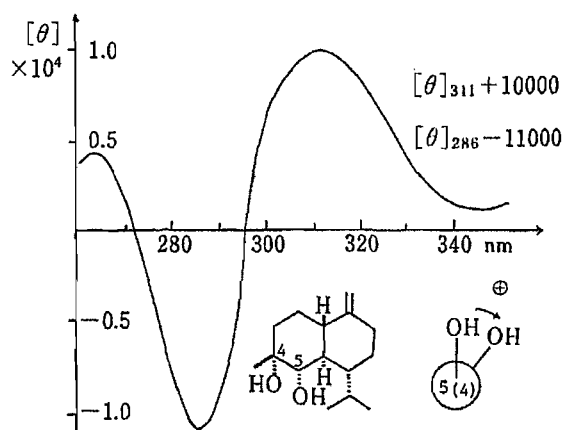


Fig. 2. The CD Curve of a Mixture of 7 ( $1.5 \times 10^{-4}$  M) and  $\text{Eu}(\text{fod})_3$  ( $1.5 \times 10^{-4}$  M)

$5\beta\text{-H}$  ( $\delta$  2.85, br dd-like) (15%), whereas irradiation of  $6\alpha\text{-H}$  ( $\delta$  1.29, ddd,  $J_{6,1} = J_{6,5} = 9.0$  Hz,  $J_{6,7} = 10.5$  Hz) resulted in a 5% increase of  $11\text{-H}$  ( $\delta$  2.67, m) and a 4% increase was observed for  $6\text{-H}$  upon irradiation of  $11\text{-H}$  (Fig. 1). These findings show that the A-ring with the  $\alpha$ -glycol moiety in 7 takes a boat-like conformation in solution. The circular dichroism (CD) spectrum of 7 taken by the  $\alpha$ -glycol chirality method<sup>8)</sup> showed a positive first Cotton effect:  $[\theta]_{311} + 10000$  (Fig. 2), indicating the  $4R$  configuration in 7 and consequently in nephthenol (6). Thus, we concluded that the structure of nephthenol is  $4R,7S$ -germacra-1(10)*E*,  $5E$ -dien-4-ol (6).

Nephtheoxydiol (8) has a hydroperoxy residue in its molecule as shown by its positive responses to the *N,N*-dimethyl-*p*-phenylenediammonium dichloride reagent<sup>3,9)</sup> and the ferrous thiocyanate reagent.<sup>3,10)</sup> The chemical ionization mass spectrum (CI-MS) of 8 gave the ( $M^+ + H$ ) ion peak at  $m/z$  255, which shows that 8 is a sesquiterpene having one hydroxyl group and one hydroperoxyl group.

The  $^1\text{H-NMR}$  spectrum of nephtheoxydiol (8) showed the presence of a *transoid* disubstituted double bond ( $\delta$  5.38, 1H, d,  $J = 15.5$  Hz;  $\delta$  5.70, 1H, dd,  $J = 15.5, 10.0$  Hz), a tertiary methyl residue geminal to a hydroxyl group ( $\delta$  1.47, 3H, s), an isopropyl residue ( $\delta$  0.83, 0.87, both 3H, d,  $J = 6.5$  Hz), a terminal methylene moiety ( $\delta$  5.14, 5.42, both 1H, s), and a secondary hydroperoxyl residue ( $\delta$  4.55, 1H, br d,  $J = ca. 6.5$  Hz). The  $^{13}\text{C-NMR}$  spectrum of 8 also showed signals due to a carbon bearing a secondary hydroperoxyl residue [ $\delta_c$  93.0 (d)].<sup>3)</sup> It was presumed therefore that nephtheoxydiol (8) is an oxygenated derivative of nephthenol (6). In order to verify this presumption, nephthenol (6) was subjected to photosensitized oxygenation in the presence of Rose Bengal in a Pyrex tube.<sup>3,11)</sup> The product obtained in high yield was shown to be identical with nephtheoxydiol (8). Thus, it has become clear that the structure of nephtheoxydiol corresponds to 8 having a 1-hydroperoxy-10(15)-ene moiety, except for its C-1 configuration.

Nephthediol (9) is a sesquiterpene diol. The  $^1\text{H-}$  and  $^{13}\text{C-NMR}$  spectra of 9 were very similar to those of nephtheoxydiol (8) except that the former showed signals due to H-1 and C-1 at  $\delta$  3.93 (1H, dd,  $J = 9.0, 3.0$  Hz) and  $\delta_c$  78.7 (d), respectively. Therefore, nephthediol (9) appears to be the 1-hydroxy counterpart of nephtheoxydiol (8). In fact, sodium borohydride reduction of 8 afforded 9 quantitatively. Thus, the structure of nephthediol can be formulated as 9, except for the C-1 configuration. This formulation of 9 was further supported by the fact that oxidation of nephthediol under Moffatt conditions<sup>12)</sup> provided 4, the anhydro derivative of *ent*-oplopanone (2). The conversion from nephthediol (9) to 4 is considered to proceed *via*: i) initial elimination of the 1-OH group followed by 1(6) bond formation and epoxide-ring

formation, and ii) ring contraction constructing a five-membered ring with a methylketone moiety (*cf.* iv, v).

In order to determine the C-4 configuration of nephthediol (**9**), **9** was epoxidized with *m*-Cl-PBA to afford the 5,6-epoxide (**10**). In the NOE experiments on **10**, irradiation of 4-CH<sub>3</sub> ( $\delta$  1.27) increased by 11% the signal intensity of 5-H ( $\delta$  2.54, d,  $J$  = 2.0 Hz) whereas irradiation of 5-H increased by 7% the signal intensity of 7-H ( $\delta$  1.18, m). Furthermore, irradiation of 7-H resulted in 9% NOE for 5-H while irradiation of the two 11-CH<sub>3</sub> signals ( $\delta$  0.97, 3H, d,  $J$  = 6.5 Hz;  $\delta$  0.98, 3H, d,  $J$  = 7.0 Hz) caused 7% NOE for 6-H ( $\delta$  2.93, dd,  $J$  = 9.5, 2.0 Hz). These results substantiate the 4*R* configuration in nephthediol (**9**) and consequently in nephthenol (**6**) and nephtheoxydiol (**8**).

Next, the C-1 configuration in nephtheoxydiol (**8**) and nephthediol (**9**) was investigated. Acetylation of nephthediol (**9**) followed by dehydration with phosphorus oxychloride afforded a trienol acetate (**11**). Deacetylation of **11** furnished the trienol (**12**). Examination in detail of the <sup>1</sup>H-NMR spectrum of **12** allowed us to assign all the proton signals (see Experimental). Furthermore, in the NOE experiments on **12**, irradiation of 1-H ( $\delta$  4.08, dd,  $J$  = 11.5, 4.0 Hz) caused 5% increases of 5-H ( $\delta$  6.01, d,  $J$  = 16.0 Hz) and 9-Hb ( $\delta$  1.79, ddd,  $J$  = 14.0, 12.0, *ca.* 2.0 Hz), whereas irradiation of 5-H increased signals due to 1-H (3%), 14-Ha ( $\delta$  4.96, s) (5%), and 7-H ( $\delta$  1.67, dddd,  $J$  = 10.5, 10.5, 6.5, 4.5 Hz) (8%). Further detailed NOE experiments on **12**, indicated that the conformation of **12** is as shown in Fig. 3, and consequently the 1*S* configuration has been determined. This conclusion was further supported by applying Horeau's method<sup>13)</sup> to nephthediol (**9**) and **12**, where recovered  $\alpha$ -phenylbutyric acid showed  $[\alpha]_D -13.5^\circ$  (from **9**) and  $[\alpha]_D -2.5^\circ$  (from **12**).

Based on the above evidence, the absolute stereostructures of nephtheoxydiol and nephthediol were concluded to be (1*S*,4*R*,7*S*)-1-hydroperoxygermacra-5*E*,10(15)-dien-4-ol (**8**) and (1*S*,4*R*,7*S*)-germacra-5*E*,10(15)-diene-1,4-diol (**9**), respectively.

A sesquiterpene dienediol (**13**) was isolated from the red alga *Laurencia subopposita*<sup>14)</sup>

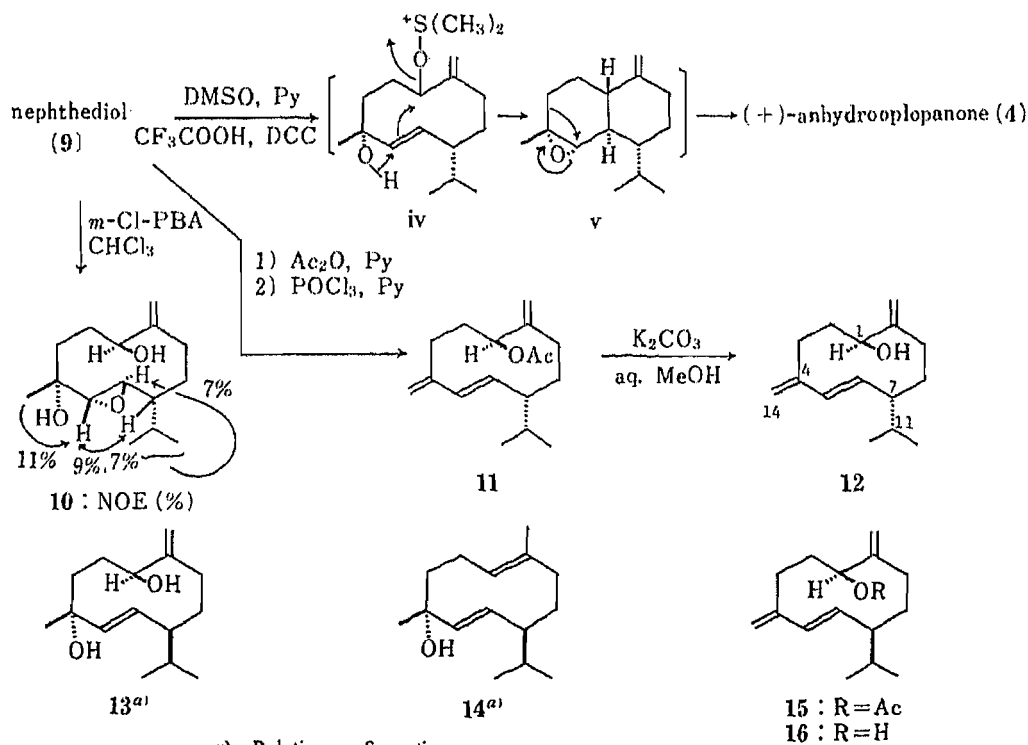


Chart 2

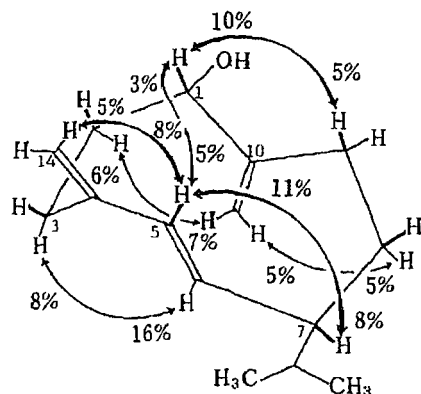
$^1\text{H-NMR}$  [500 MHz,  $\text{Bz-d}_6$ - $\text{Py-d}_5$  (1 : 1)]

Fig. 3. NOE (%) of **12**  
Py=pyridine

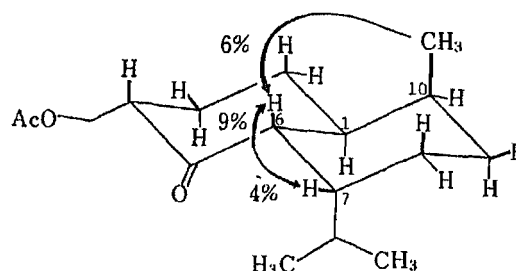
 $^1\text{H-NMR}$  (500 MHz,  $\text{Bz-d}_6$  or  $\text{Py-d}_5$ )

Fig. 4. NOE (%) of **21**

and a sesquiterpene diol (**14**) was isolated from the soft coral *Lemnalia africana*,<sup>15)</sup> and their relative configurations were proposed to be as shown.<sup>14,15)</sup> Physical data reported for **13** and **14** including the signs of  $[\alpha]_D$  values were found to be identical with those of present nephthediol (**9**) and nephthenol (**6**), respectively. Therefore, re-examination of the structures proposed for **13** and **14** seems to be necessary. Furthermore, there was a report on the structure elucidation of a germacrane-type trienol acetate (**15**), which was isolated from the brown alga *Dilophus fuscicola*.<sup>16)</sup> The structures proposed for **15** and its deacetylated product (**16**) are diastereomeric to the present trienol acetate (**11**) and its deacetylated product (**12**), respectively. Since there is some ambiguity in the presentation<sup>16)</sup> and the reported data for **15** and **16** are similar to those for **11** and **12** except for the sign of the specific rotation, re-examination of the structure proposed for **15** also seems to be appropriate.

Nephthene (**17**) is a cadinane-type sesquiterpene having a conjugated diene chromophore, as shown by its ultraviolet (UV) maximum at 240 nm ( $\epsilon=20000$ ). The  $^1\text{H-NMR}$  spectrum of nephthene (**17**) showed the presence of a terminal methylene moiety ( $\delta$  4.63, 4.68, both 1H, s), a trisubstituted double bond ( $\delta$  5.99, 1H, s), an isopropyl residue ( $\delta$  0.76, 0.93, both 3H, d,  $J=6.5$  Hz), and a secondary methyl residue ( $\delta$  0.87, 3H, d,  $J=6.0$  Hz). Thus, nephthene (**17**) has a bicarbocyclic skeleton.

Dehydrogenation of nephthene (**17**) with 10% palladium-carbon in boiling diethylene-glycol dimethyl ether provided cadalene (**18**).<sup>17)</sup> Oxidation of nephthene (**17**) with osmium tetroxide-sodium periodate yielded the norenone (**19**). In the  $^1\text{H-NMR}$  spectrum of **19**, irradiation of  $1\alpha\text{-H}$  ( $\delta$  2.59, dddd,  $J=5.0, 5.0, 5.0, 2.0$  Hz) resulted in 5% NOE for  $10\alpha\text{-H}$  ( $\delta$  2.17, m) whereas irradiation of  $10\alpha\text{-H}$  caused 7% NOE for  $1\alpha\text{-H}$ . Thus, the relative configurations of  $1\alpha\text{-H}$  and  $10\alpha\text{-H}$  were determined.

Hydroboration-oxidation of nephthene (**17**) furnished a diol (**20**). In the  $^1\text{H-NMR}$  spectrum of **20**, both  $J_{4,5}$  and  $J_{5,6}$  were observed at 9.5 Hz, so that the *trans*-diaxial correlations of 4-H/5-H and 5-H/6-H were established. Mild acetylation of **20** followed by pyridinium chlorochromate (PCC) oxidation yielded a keto-alcohol acetate (**21**). In the  $^1\text{H-NMR}$  spectrum of **21**, the coupling constant between  $6\beta\text{-H}$  and  $1\alpha\text{-H}$  was 12.5 Hz whereas the  $J$  value between  $6\beta\text{-H}$  and  $7\beta\text{-H}$  was 3.5 Hz, so that the *trans*-diaxial correlation of  $1\alpha\text{-H}$  and  $6\beta\text{-H}$  and the axial-equatorial correlation of  $6\beta\text{-H}$  and  $7\beta\text{-H}$  were proven. Furthermore, irradiation of  $6\beta\text{-H}$  caused 4% NOE for  $7\beta\text{-H}$  and irradiation of  $7\beta\text{-H}$  resulted in 9% NOE for  $6\beta\text{-H}$  (in benzene- $d_6$ ). Irradiation of  $10\beta\text{-CH}_3$  ( $\delta$  0.80, d,  $J=7.0$  Hz) caused 6% NOE for  $6\beta\text{-H}$  ( $\delta$  2.18, dd,  $J=12.5, 3.5$  Hz) in pyridine- $d_5$  (Fig. 4). The CD spectrum of **21** showed

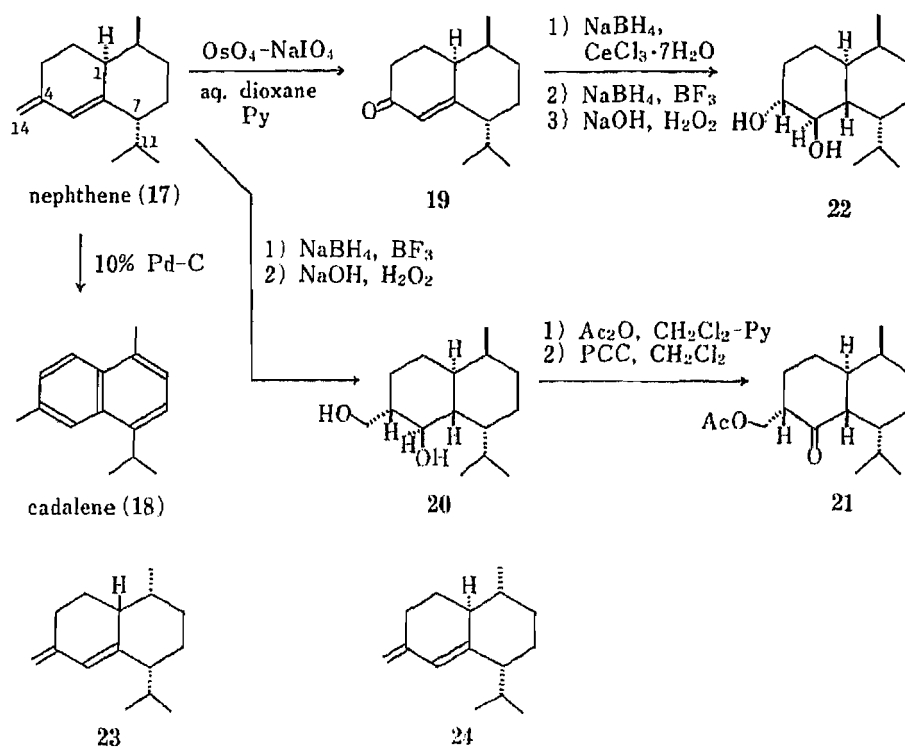


Chart 3

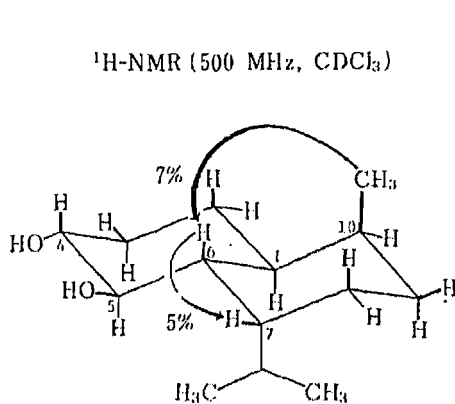
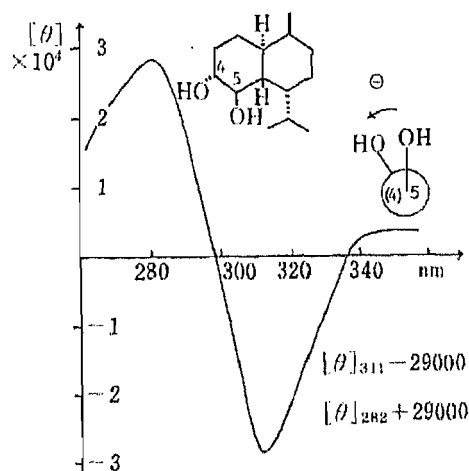


Fig. 5. NOE (%) of 22

Fig. 6. The CD Curve of a Mixture of 22 ( $1.5 \times 10^{-4} \text{ M}$ ) and  $\text{Eu}(\text{fod})_3$  ( $1.5 \times 10^{-4} \text{ M}$ )

a positive maximum:  $[\theta]_{297} + 4000$  due to the 5-CO moiety. These results established the 1*S*, 4*S*, 6*S*, 7*R*, and 10*S* configurations in 21.

Reduction of the norenone (19) with sodium borohydride in the presence of cerous chloride hydrate and subsequent hydroboration-oxidation, provided the nor-*trans*- $\alpha$ -glycol (22). The  $^1\text{H-NMR}$  spectrum of 22 showed signals due to  $1\alpha\text{-H}$  ( $\delta$  1.63, ddd,  $J = 12.0, 10.5, 4.5$  Hz),  $4\beta\text{-H}$  ( $\delta$  3.34, ddd,  $J = 11.0, 10.0, 4.5$  Hz),  $5\alpha\text{-H}$  ( $\delta$  3.40, dd,  $J = 10.0, 9.0$  Hz),  $6\beta\text{-H}$  ( $\delta$  1.54, ddd,  $J = 12.0, 9.0, 5.0$  Hz), and  $7\beta\text{-H}$  ( $\delta$  1.79, m). The coupling constants between 4-H and 5-H (10.0 Hz), between 5-H and 6-H (9.0 Hz), between 1-H and 6-H (12.0 Hz), and between 6-H and 7-H (5.0 Hz), indicated *trans*-diaxial correlations of 4-H/5-H, 5-H/6-H, and

1-H/6-H, and the axial-equatorial correlation of 6-H/7-H. Furthermore, irradiation of 10-CH<sub>3</sub> ( $\delta$ 0.87, d,  $J=7.0$  Hz) caused 7% NOE for 6-H (Fig. 5). The CD spectrum of **22** taken by the  $\alpha$ -glycol chirality method<sup>8)</sup> showed a negative first Cotton effect ( $[\theta]_{311} - 29000$ ) (Fig. 6). Thus, **22** has 1*S*, 4*R*, 5*R*, 6*S*, 7*R*, and 10*S* configurations, and consequently, the absolute configuration of **21** has been further substantiated.

Based on the above evidence, the absolute stereostructure of nephtene is 1*S*,7*R*,10*S*-cadina-4(14),5-diene (**17**).

Several examples of naturally occurring sesquiterpenes having a cadina-4(14),5-diene structure are known: e.g. bicyclosesquiphellandrene (**23**)<sup>18)</sup> from the terrestrial plant *Piper cubeba* (Piperaceae)<sup>19)</sup> and 1-*epi*-bicyclosesquiphellandrene (**24**)<sup>18)</sup> from the terrestrial plant *Ocimum basilicum* (Labiatae)<sup>19)</sup> and from the brown alga *Dilophus fasciola*.<sup>20)</sup> It should be pointed out here that nephteoxydiol (**8**) having a hydroperoxyl function was found to exhibit a significant growth-inhibitory effect on B-16 melanoma cells (IC<sub>50</sub> 0.1  $\mu$ g/ml). However, the other four sesquiterpenes described in this paper did not exhibit such an effect, so that the physiological function of the hydroperoxyl residue may be an interesting subject for future study.

### Experimental

The instruments used to obtain physical data and the experimental conditions for chromatography were the same as described in our previous paper.<sup>1)</sup>

**Isolation of Nephtene (17), Nephtenol (6), Nephteoxydiol (8), ent-Oplopanone (2), and Nephtediol (9)**—The fresh, soft coral (360 g) of *Nephtea* sp. (Neph-84-IRI-1),<sup>21)</sup> which was collected at Iriomote-jima, Okinawa Prefecture, in July 1984, was cut finely and immersed in acetone at room temperature (25 °C). The acetone solution was concentrated under reduced pressure at below 30 °C. The acetone extract thus obtained was partitioned into an AcOEt-H<sub>2</sub>O mixture. Removal of the solvent under reduced pressure from the AcOEt-soluble portion afforded the AcOEt extract (4 g). Column chromatography (SiO<sub>2</sub> 200 g, 60—230 mesh, Merck) of the AcOEt extract furnished a nephtene fraction (600 mg) (by eluting with *n*-hexane), a nephtenol fraction (300 mg) (by eluting with *n*-hexane-AcOEt=20:1), a nephteoxydiol fraction (100 mg) and an *ent*-oplopanone fraction (80 mg) (by eluting with *n*-hexane-AcOEt=2:1), and a nephtediol fraction (60 mg) (by eluting with *n*-hexane-AcOEt=1:1). The fraction containing nephtene (600 mg) was purified with a Lobar column [LiChroprep Si 60 (40—63  $\mu$ m), *n*-hexane] to furnish nephtene (**17**) (460 mg). The nephtenol containing fraction (300 mg) was purified by HPLC (Semi Prep Zorbax SIL, *n*-hexane-AcOEt=20:1) to furnish nephtenol (**6**) (270 mg). The fraction containing nephteoxydiol (100 mg) was purified by column chromatography (SiO<sub>2</sub> 40 g, *n*-hexane-AcOEt=2:1) again and then by HPLC (Semi Prep Zorbax ODS, MeOH-H<sub>2</sub>O=8:1) to afford nephteoxydiol (**8**) (60 mg). The *ent*-oplopanone fraction (80 mg) was also purified by column chromatography (SiO<sub>2</sub> 30 g, *n*-hexane-AcOEt=2:1) again and then by HPLC (Semi Prep Zorbax ODS, MeOH-H<sub>2</sub>O=6:1) to afford *ent*-oplopanone (**2**) (14 mg). The nephtediol fraction (60 mg) was purified again by column chromatography (SiO<sub>2</sub> 20 g, *n*-hexane-AcOEt=1:1) and then by HPLC (Semi Prep Zorbax SIL, *n*-hexane-AcOEt=1:1) to furnish nephtediol (**9**) (20 mg). Nephtene (**17**), colorless oil,  $[\alpha]_D^{20} - 9^\circ$  ( $c=5.3$ , CHCl<sub>3</sub>). High-resolution MS: Found 204.188. Calcd for C<sub>15</sub>H<sub>24</sub> (M<sup>+</sup>)=204.188. IR  $\nu_{\text{max}}^{\text{CHCl}_3}$  cm<sup>-1</sup>: 1637, 1600, 893. UV  $\lambda_{\text{max}}^{\text{MeOH}}$  nm ( $\epsilon$ ): 240 (20000). CD ( $c=3.3 \times 10^{-2}$ , MeOH):  $[\theta]_{265}^0$  0,  $[\theta]_{240}^0 - 17000$  (neg. max.),  $[\theta]_{215}^0$  0,  $[\theta]_{200}^0 + 21000$ ! <sup>1</sup>H-NMR (500 MHz, CDCl<sub>3</sub>,  $\delta$ ): 2.33 (2H, overlapped, 1,7-H), 5.99 (1H, s, 5-H), 1.96 (1H, m, 10-H), 0.76, 0.93 [both 3H, d,  $J=6.5$  Hz, 11-(CH<sub>3</sub>)<sub>2</sub>], 0.87 (3H, d,  $J=6.0$  Hz, 10-CH<sub>3</sub>), 4.63, 4.68 (both 1H, s, 14-H<sub>2</sub>). <sup>13</sup>C-NMR (22.5 MHz, CDCl<sub>3</sub>,  $\delta_c$ ): 144.2 (s), 144.0 (s), 126.8 (d), 51.3 (d), 37.2 (d), 34.9 (d), 27.4 (d), 108.1 (t), 29.7 (t), 29.5 (t), 27.3 (t), 22.9 (t), 21.8 (q), 21.3 (q), 14.8 (q). MS  $m/z$  (%): 204 (M<sup>+</sup>, 18), 161 (M<sup>+</sup>-C<sub>3</sub>H<sub>7</sub>, 100). Nephtenol (**6**), colorless oil,  $[\alpha]_D^{20} + 184^\circ$  ( $c=3.1$ , CHCl<sub>3</sub>). High-resolution MS: Found 222.196. Calcd for C<sub>15</sub>H<sub>26</sub>O (M<sup>+</sup>)=222.196. IR  $\nu_{\text{max}}^{\text{MeOH}}$  cm<sup>-1</sup>: 3470. CD ( $c=3.7 \times 10^{-2}$ , MeOH):  $[\theta]_{265}^0$  0,  $[\theta]_{229}^0 + 48000$  (pos. max.),  $[\theta]_{200}^0 + 10000$ ! <sup>1</sup>H-NMR (500 MHz, CDCl<sub>3</sub>,  $\delta$ ): 4.95 (1H, br d,  $J=11.5$  Hz, 1-H), 5.25 (1H, d,  $J=16.0$  Hz, 5-H), 5.18 (1H, dd,  $J=16.0, 9.5$  Hz, 6-H), 1.19 (3H, s, 4-CH<sub>3</sub>), 1.54 (3H, s, 10-CH<sub>3</sub>), 0.79, 0.83 [both 3H, d,  $J=7.0$  Hz, 11-(CH<sub>3</sub>)<sub>2</sub>]. <sup>13</sup>C-NMR (22.5 MHz, CDCl<sub>3</sub>,  $\delta_c$ ): 129.0 (d, C-1), 23.7 (t, C-2), 41.3 (t, C-3), 72.9 (s, C-4), 140.0 (d, C-5), 125.9 (d, C-6), 52.9 (d, C-7), 39.7 (t, C-8), 26.1 (t, C-9), 132.3 (s, C-10), 33.0 (d, C-11), 19.0 (q, C-12), 20.6 (q, C-13), 30.9 (q, C-14), 16.6 (q, C-15). MS  $m/z$  (%): 222 (M<sup>+</sup>, 4), 207 (M<sup>+</sup>-CH<sub>3</sub>, 16), 204 (M<sup>+</sup>-H<sub>2</sub>O, 11), 179 (M<sup>+</sup>-C<sub>3</sub>H<sub>7</sub>, 5), 161 (M<sup>+</sup>-H<sub>2</sub>O-C<sub>3</sub>H<sub>7</sub>, 30), 81 (100). Nephteoxydiol (**8**), colorless amorphous,  $[\alpha]_D^{21} + 14^\circ$  ( $c=1.2$ , CHCl<sub>3</sub>). High-resolution MS: Found 236.180. Calcd for C<sub>15</sub>H<sub>24</sub>O<sub>2</sub> (M<sup>+</sup>-H<sub>2</sub>O)=236.178. IR  $\nu_{\text{max}}^{\text{CHCl}_3}$  cm<sup>-1</sup>: 3600, 3530, 3312 (br). CD ( $c=2.9 \times 10^{-2}$ , MeOH):  $[\theta]_{248}^0$  0,  $[\theta]_{215}^0 - 21000$  (neg. max.),  $[\theta]_{208}^0$  0. <sup>1</sup>H-NMR (500 MHz, pyridine-*d*<sub>5</sub>,  $\delta$ ): 4.55 (1H, br d,  $J=ca. 6.5$  Hz, 1-H), 5.38 (1H, d,  $J=15.5$  Hz, 5-H), 5.70 (1H, dd,  $J=15.5, 10.0$  Hz, 6-H), 5.14, 5.42 (both 1H, s, 15-H<sub>2</sub>), 0.83, 0.87 [both 3H, d,

$J=6.5$  Hz, 11-(CH<sub>3</sub>)<sub>2</sub>], 1.47 (3H, s, 4-CH<sub>3</sub>). <sup>13</sup>C-NMR (22.5 MHz, CDCl<sub>3</sub>, δ<sub>c</sub>): 149.1 (s, C-10), 72.5 (s, C-4), 137.0, 131.3 (both d, C-5, 6), 93.0 (d, C-1), 50.9 (d, C-7), 32.3 (d, C-11), 114.8 (t, C-15), 40.3, 33.0, 32.3, 25.5 (all t, C-2, 3, 8, 9), 29.8 (q, C-14), 20.7, 20.3 (both q, C-12, 13). CI-MS (isobutane)  $m/z$  (%): 255 (M<sup>+</sup> + H, 2), 237 (255 - H<sub>2</sub>O, 17), 221 (255 - H<sub>2</sub>O<sub>2</sub>, 22), 219 (255 - 2H<sub>2</sub>O, 35). *ent*-Oplopanone (2), colorless needles (from petr. ether), mp 83–84 °C, [α]<sub>D</sub><sup>25</sup> + 19° ( $c=0.8$ , dioxane). High-resolution MS: Found 238.195. Calcd for C<sub>15</sub>H<sub>26</sub>O<sub>2</sub> (M<sup>+</sup>) = 238.193. IR ν<sub>max</sub><sup>CHCl<sub>3</sub></sup> cm<sup>-1</sup>: 3600, 1700. CD ( $c=1.3 \times 10^{-1}$ , dioxane): [θ]<sub>286</sub> + 3400 (pos. max.), [θ]<sub>237</sub> 0. <sup>1</sup>H-NMR (500 MHz, CDCl<sub>3</sub>, δ): 2.65 (1H, ddd,  $J=10.5, 10.5, 5.5$  Hz, 3-H), 2.19 (3H, s, 4-CH<sub>3</sub>), 1.20 (3H, s, 9-CH<sub>3</sub>), 0.69, 0.89 [both 3H, d,  $J=7.0$  Hz, 11-(CH<sub>3</sub>)<sub>2</sub>]. <sup>13</sup>C-NMR (22.5 MHz, CDCl<sub>3</sub>, δ<sub>c</sub>): 211.2 (s, C-4), 73.0 (s, C-9), 57.2, 55.9, 46.8 (all d, C-3, 5, 10), 49.6 (d, C-6), 29.6 (d, C-11), 42.2, 28.7, 25.4, 23.1 (all t, C-1, 2, 7, 8), 29.5 (q, C-14), 22.0, 15.7 (both q, C-12, 13), 20.4 (q, C-15). MS  $m/z$  (%): 238 (M<sup>+</sup>, 8), 223 (M<sup>+</sup> - CH<sub>3</sub>), 220 (M<sup>+</sup> - H<sub>2</sub>O, 2), 205 (M<sup>+</sup> - CH<sub>3</sub> - H<sub>2</sub>O, 2), 177 (M<sup>+</sup> - C<sub>3</sub>H<sub>7</sub> - H<sub>2</sub>O, 7), 153 (100). Nephthediol (9), colorless amorphous, [α]<sub>D</sub><sup>21</sup> + 82° ( $c=1.2$ , CHCl<sub>3</sub>). High-resolution MS: Found 238.195. Calcd for C<sub>15</sub>H<sub>26</sub>O<sub>2</sub> (M<sup>+</sup>) = 238.193. IR ν<sub>max</sub><sup>CHCl<sub>3</sub></sup> cm<sup>-1</sup>: 3600, 3440 (br). CD ( $c=2.7 \times 10^{-2}$ , MeOH): [θ]<sub>230</sub> 0, [θ]<sub>218</sub> - 5000 (neg. max.), [θ]<sub>212</sub> 0. <sup>1</sup>H-NMR (500 MHz, CDCl<sub>3</sub>, δ): 3.93 (1H, dd,  $J=9.0, 3.0$  Hz, 1-H), 5.21 (1H, d,  $J=15.5$  Hz, 5-H), 5.29 (1H, dd,  $J=15.5, 10.0$  Hz, 6-H), 4.89, 5.12 (both 1H, s, 15-H<sub>2</sub>), 1.26 (3H, s, 4-CH<sub>3</sub>), 0.84, 0.89 [both 3H, d,  $J=6.5$  Hz, 11-(CH<sub>3</sub>)<sub>2</sub>]. <sup>13</sup>C-NMR (22.5 MHz, CDCl<sub>3</sub>, δ<sub>c</sub>): 151.1 (s, C-10), 72.3 (s, C-4), 137.7, 129.9 (both d, C-5, 6), 78.7 (d, C-1), 49.9 (d, C-7), 32.4 (d, C-11), 111.4 (t, C-15), 38.7, 30.0, 28.4, 28.4 (all t, C-2, 3, 8, 9), 29.5 (q, C-14), 20.6, 20.6 (both q, C-12, 13). MS  $m/z$  (%): 238 (M<sup>+</sup>, 2), 220 (M<sup>+</sup> - H<sub>2</sub>O, 10), 205 (M<sup>+</sup> - H<sub>2</sub>O - CH<sub>3</sub>, 9), 202 (M<sup>+</sup> - 2H<sub>2</sub>O, 7), 177 (M<sup>+</sup> - C<sub>3</sub>H<sub>7</sub> - H<sub>2</sub>O, 49), 81 (100).

**Dehydration of *ent*-Oplopanone (2) Giving (+)-Anhydrooplopanone (4)**—An ice-cooled solution of 2 (13 mg) in dry pyridine (1 ml) was treated with POCl<sub>3</sub> (3 drops) under a nitrogen atmosphere and stirred for 30 min. The reaction mixture was stirred at room temperature (15 °C) for a further 8 h, then poured into water. The whole was extracted with AcOEt. The AcOEt extract was washed with aq. sat. NaCl and dried over MgSO<sub>4</sub>. Removal of the solvent under reduced pressure from the AcOEt extract afforded a product, which was purified by column chromatography (SiO<sub>2</sub> 2 g, *n*-hexane-AcOEt = 8 : 1) to furnish (+)-anhydrooplopanone (4) (9 mg). 4, colorless needles (from petr. ether), mp 70–71 °C, [α]<sub>D</sub><sup>18</sup> + 14° ( $c=0.5$ , CHCl<sub>3</sub>). High-resolution MS: Found 220.182. Calcd for C<sub>15</sub>H<sub>24</sub>O (M<sup>+</sup>) = 220.183. IR ν<sub>max</sub><sup>CCl<sub>4</sub></sup> cm<sup>-1</sup>: 3075, 1711, 1651, 891. <sup>1</sup>H-NMR (500 MHz, CDCl<sub>3</sub>, δ): 4.56, 4.67 (both 1H, d,  $J=2.0$  Hz, 15-H<sub>2</sub>), 2.19 (3H, s, 4-CH<sub>3</sub>), 0.91 (3H, d,  $J=7.0$  Hz, 11-CH<sub>3</sub>), 0.66 (3H, d,  $J=6.5$  Hz, 11-CH<sub>3</sub>). <sup>13</sup>C-NMR (22.5 MHz, CDCl<sub>3</sub>, δ<sub>c</sub>): 211.6 (s, C-4), 150.9 (s, C-9), 56.2 (d, C-3), 52.2 (d, C-5), 52.0 (d, C-10), 49.5 (d, C-6), 29.7 (d, C-11), 103.6 (t, C-15), 35.4 (t, C-8), 28.6 (t, C-2), 27.4 (t, C-1), 26.7 (t, C-7), 28.9 (q, C-14), 22.0, 15.8 (both q, C-12, 13). MS  $m/z$  (%): 220 (M<sup>+</sup>, 12), 205 (M<sup>+</sup> - CH<sub>3</sub>, 7), 187 (M<sup>+</sup> - CH<sub>3</sub> - H<sub>2</sub>O), 177 (M<sup>+</sup> - C<sub>3</sub>H<sub>7</sub>, 85), 43 (100).

**Oxidation of Nephthenol (6) with *m*-Cl-PBA Giving *ent*-Oplopanone (2)**—An ice-cooled solution of 6 (40 mg) in CHCl<sub>3</sub> (1 ml) was treated with *m*-Cl-PBA (118 mg, 1.5 eq) and stirred for 2 h. The reaction mixture was poured into ice-water and the whole was extracted with AcOEt. The AcOEt extract was washed with aq. sat. NaCl and dried over MgSO<sub>4</sub>. Removal of the solvent under reduced pressure from the AcOEt extract gave a product, which was purified first by column chromatography (SiO<sub>2</sub> 5 g, *n*-hexane-AcOEt = 2 : 1) and then with a Lobar column (LiChroprep Si 60, *n*-hexane-AcOEt = 2 : 1) to furnish *ent*-oplopanone (2) (8 mg). 2 thus obtained was shown to be identical with an authentic sample by mixed melting point determination and [α]<sub>D</sub>, <sup>1</sup>H-NMR (90 MHz, CDCl<sub>3</sub>), and <sup>13</sup>C-NMR (22.5 MHz, CDCl<sub>3</sub>) comparisons.

**Oxidation of Nephthenol (6) with VO(acac)<sub>2</sub>-*tert*-BuOOH Giving 7**—A solution of 6 (50 mg) in benzene (1 ml) was treated with VO(acac)<sub>2</sub> (0.6 mg, 0.01 eq) and then with a solution of aq. 70% *tert*-BuOOH (32 mg, 1.1 eq) in benzene (1 ml) and the whole mixture was stirred at room temperature (25 °C) for 3 h. Work-up of the reaction mixture as described above for *m*-Cl-PBA oxidation yielded a product, which was purified by column chromatography (SiO<sub>2</sub> 6 g, *n*-hexane-AcOEt = 7 : 1) and HPLC (Semi Prep Zorbax ODS, MeOH-H<sub>2</sub>O = 10 : 1) to furnish the α-glycol (7) (15 mg). 7, colorless amorphous, [α]<sub>D</sub><sup>25</sup> + 4.5° ( $c=0.9$ , CHCl<sub>3</sub>). High-resolution MS: Found 220.184. Calcd for C<sub>15</sub>H<sub>24</sub>O (M<sup>+</sup> - H<sub>2</sub>O) = 220.183. IR ν<sub>max</sub><sup>CCl<sub>4</sub></sup> cm<sup>-1</sup>: 3620, 3560 (br), 3457 (br), 1644, 893. <sup>1</sup>H-NMR (500 MHz, benzene-*d*<sub>6</sub>, δ): 1.40 (1H, dd-like,  $J=ca, 12.0, 10.0$  Hz, 1-H), 2.85 (1H, br dd-like, 5-H), 1.29 (1H, ddd,  $J=10.5, 9.0, 9.0$  Hz, 6-H), 1.22 (1H, dddd,  $J=10.5, 10.5, 3.0, 3.0$  Hz, 7-H), 2.67 (1H, m, 11-H), 0.98 (3H, d,  $J=7.0$  Hz, 11-CH<sub>3</sub>), 0.86 (3H, d,  $J=6.5$  Hz, 11-CH<sub>3</sub>), 4.69, 4.77 (both 1H, d,  $J=1.5$  Hz, 15-H<sub>2</sub>), 1.07 (3H, s, 4-CH<sub>3</sub>). <sup>1</sup>H-NMR (500 MHz, CDCl<sub>3</sub>, δ): 1.64 (2H overlapped, 1-H), 3.22 (1H, dd,  $J=9.0, 8.5$  Hz, 5-H), 2.15 (1H, d,  $J=8.5$  Hz, 5-OH). <sup>13</sup>C-NMR (22.5 MHz, CDCl<sub>3</sub>, δ<sub>c</sub>): 152.2 (s), 72.3 (s), 79.2 (d), 49.3 (d), 48.4 (d), 45.5 (d), 28.6 (d), 104.5 (t), 37.2 (t), 35.5 (t), 26.0 (t), 23.2 (t), 28.0 (q), 22.3 (q), 16.8 (q). MS  $m/z$  (%): 220 (M<sup>+</sup> - H<sub>2</sub>O, 100), 202 (M<sup>+</sup> - 2H<sub>2</sub>O, 25), 177 (M<sup>+</sup> - H<sub>2</sub>O - C<sub>3</sub>H<sub>7</sub>, 25), 159 (M<sup>+</sup> - 2H<sub>2</sub>O - C<sub>3</sub>H<sub>7</sub>, 51).

**CD Spectrum of 7 Taken by the α-Glycol Chirality Method**—7 (0.357 mg, 1.5 × 10<sup>-4</sup> M) was dissolved in a solution of tris(6,6,7,7,8,8,8-heptafluoro-2,2-dimethyl-3,5-octane-dionato)europium [Eu(fod)<sub>3</sub>] (1.5 × 10<sup>-4</sup> M) in CCl<sub>4</sub> (10 ml) [prepared from Eu(fod)<sub>3</sub> (155 mg) and dry CCl<sub>4</sub> (10 ml)]. After 30 min, the CD spectrum of the solution was measured. CD ( $c=1.6 \times 10^{-1}$ , CCl<sub>4</sub>): [θ]<sub>311</sub> + 10000 (pos. max.), [θ]<sub>295</sub> 0, [θ]<sub>286</sub> - 11000 (neg. max.), [θ]<sub>272</sub> 0.

**Photosensitized Oxygenation of Nephthenol (6) Giving Nephthoxydiol (8)**—A solution of 6 (20 mg) and Rose Bengal (5 mg) in MeOH (5 ml) was put in a Pyrex tube and cooled (0 °C). While bubbling with a stream of oxygen, the cooled solution was irradiated with a 100 W high-pressure Hg lamp for 10 min. The residue, obtained by removal of the solvent, was purified by column chromatography (SiO<sub>2</sub> 5 g, *n*-hexane-AcOEt = 2 : 1) and then with a Lobar

column [LiChroprep Si 60 (40--63  $\mu\text{m}$ ), *n*-hexane-AcOEt = 3:1) to furnish nephtheoxydiol (8) (20 mg). Nephtheoxydiol (8) thus obtained was shown to be identical with an authentic sample by  $[\alpha]_D$ , MS,  $^1\text{H-NMR}$  (90 MHz,  $\text{CDCl}_3$ ), and  $^{13}\text{C-NMR}$  (22.5 MHz,  $\text{CDCl}_3$ ) comparisons.

**$\text{NaBH}_4$  Reduction of Nephtheoxydiol (8) Giving Nephthediol (9)**—An ice-cooled solution of 8 (20 mg) in tetrahydrofuran (THF)-MeOH (2:1) (1 ml) was treated under a nitrogen atmosphere with  $\text{NaBH}_4$  (10 mg) and stirred for 30 min. The reaction mixture was poured into ice-water and the whole was extracted with AcOEt. The AcOEt extract was washed with aq. sat. NaCl and dried over  $\text{MgSO}_4$ . Removal of the solvent under reduced pressure from the AcOEt extract gave a product, which was purified by column chromatography ( $\text{SiO}_2$  5 g, *n*-hexane-AcOEt = 1:1) to furnish nephthediol (9) (14 mg). Nephthediol (9) obtained here was shown to be identical with an authentic sample by  $[\alpha]_D$ , MS,  $^1\text{H-NMR}$  (90 MHz,  $\text{CDCl}_3$ ), and  $^{13}\text{C-NMR}$  (22.5 MHz,  $\text{CDCl}_3$ ) comparisons.

**Oxidation of Nephthediol (9) under Moffatt Conditions Giving (+)-Anhydrooplopanone (4)**—Under a nitrogen atmosphere, 9 (50 mg) was dissolved in dry  $\text{CH}_2\text{Cl}_2$  (850  $\mu\text{l}$ ) and the solution was treated successively with dimethyl sulfoxide (distilled before use, 850  $\mu\text{l}$ ), pyridine (distilled before use, 15  $\mu\text{l}$ ),  $\text{CF}_3\text{COOH}$  (10  $\mu\text{l}$ ), and dicyclohexylcarbodiimide (DCC) (125 mg). The whole was stirred at room temperature (25  $^\circ\text{C}$ ) for 10 h. The reaction mixture was concentrated under reduced pressure, and the resulting product was purified by column chromatography ( $\text{SiO}_2$  10 g, *n*-hexane-AcOEt = 10:1) and then with a Lobar column (LiChroprep Si 60, *n*-hexane-AcOEt = 10:1) to furnish (+)-anhydrooplopanone (4) (33 mg). 4 thus obtained was shown to be identical with an authentic sample (prepared above) by mixed melting point determination and by  $[\alpha]_D$ , MS,  $^1\text{H-NMR}$  (90 MHz,  $\text{CDCl}_3$ ), and  $^{13}\text{C-NMR}$  (22.5 MHz,  $\text{CDCl}_3$ ) comparisons.

**Epoxidation of Nephthediol (9) Giving 10**—A solution of 9 (60 mg) in  $\text{CHCl}_3$  (2 ml) was treated with *m*-Cl-PBA (86 mg) and the whole mixture was stirred at room temperature (24  $^\circ\text{C}$ ) for 6 h. Work-up of the reaction mixture as described above for *m*-Cl-PBA oxidation of nephthenol (6) gave a product, which was purified by column chromatography ( $\text{SiO}_2$  10 g, *n*-hexane-AcOEt = 1:1) and HPLC (Semi Prep Zorbax ODS, MeOH- $\text{H}_2\text{O}$  = 3:1) and then with a Lobar column (LiChroprep Si 60, *n*-hexane-AcOEt = 2:1) to furnish the 5,6-epoxide (10) (16 mg). 10, colorless amorphous,  $[\alpha]_D^{25} + 48^\circ$  ( $c = 0.7$ ,  $\text{CHCl}_3$ ). High-resolution MS: Found 236.180. Calcd for  $\text{C}_{15}\text{H}_{24}\text{O}_2$  ( $\text{M}^+ - \text{H}_2\text{O}$ ) = 236.178. IR  $\nu_{\text{max}}^{\text{CHCl}_3} \text{cm}^{-1}$ : 3410 (br), 900.  $^1\text{H-NMR}$  (500 MHz,  $\text{CDCl}_3$ ,  $\delta$ ): 4.15 (1H, dd,  $J = 9.0, 3.5$  Hz, 1-H), 2.54 (1H, d,  $J = 2.0$  Hz, 5-H), 2.93 (1H, dd,  $J = 9.5, 2.0$  Hz, 6-H), 1.18 (1H, m, 7-H), 5.08, 4.98 (both 1H, s, 15- $\text{H}_2$ ), 1.27 (3H, s, 4- $\text{CH}_3$ ), 0.98 (3H, d,  $J = 7.0$  Hz, 11- $\text{CH}_3$ ), 0.97 (3H, d,  $J = 6.5$  Hz, 11- $\text{CH}_3$ ).  $^{13}\text{C-NMR}$  (22.5 MHz,  $\text{CDCl}_3$ ,  $\delta_c$ ): 149.8 (s), 69.0 (s), 77.2 (d), 65.4 (d), 57.3 (d), 45.5 (d), 30.6 (d), 111.3 (t), 33.5 (t), 27.7 (t), 27.7 (t), 23.1 (t), 28.4 (q), 20.1 (q), 18.2 (q). MS  $m/z$  (%): 236 ( $\text{M}^+ - \text{H}_2\text{O}$ , 1), 221 ( $\text{M}^+ - \text{H}_2\text{O} - \text{CH}_3$ , 3), 203 ( $\text{M}^+ - 2\text{H}_2\text{O} - \text{CH}_3$ , 3), 81 (100).

**Acetylation of Nephthediol (9) Followed by Dehydration Giving the Trienol Acetate (11)**—A solution of 9 (11 mg) in pyridine (1 ml) was treated with  $\text{Ac}_2\text{O}$  (2 drops) and the whole mixture was stirred at room temperature (20  $^\circ\text{C}$ ) for 6 h. Work-up of the reaction mixture in the usual manner gave a product which was purified by column chromatography ( $\text{SiO}_2$  2 g, *n*-hexane-AcOEt = 5:1) to furnish the monoacetate (8 mg) and 4 (recovered, 3 mg). The monoacetate (8 mg) was dissolved in dry pyridine (1 ml) and under a nitrogen atmosphere, the ice-cooled solution was treated with  $\text{POCl}_3$  (2 drops). The whole was stirred at room temperature for 3 h. The reaction mixture was poured into water and the whole was extracted with AcOEt. Work-up of the AcOEt extract in the usual manner gave a product, which was purified by column chromatography ( $\text{SiO}_2$  2 g, *n*-hexane-AcOEt = 10:1) to furnish the trienol acetate (11) (2 mg). 11, colorless oil,  $[\alpha]_D^{21} + 102^\circ$  ( $c = 0.35$ ,  $\text{CHCl}_3$ ). High-resolution MS: Found 262.194. Calcd for  $\text{C}_{17}\text{H}_{26}\text{O}_2$  ( $\text{M}^+$ ) = 262.193. IR  $\nu_{\text{max}}^{\text{CHCl}_3} \text{cm}^{-1}$ : 1720, 1243 (br). UV  $\lambda_{\text{max}}^{\text{MeOH}} \text{nm}$  ( $\epsilon$ ): 237 (17000).  $^1\text{H-NMR}$  (500 MHz,  $\text{CDCl}_3$ ,  $\delta$ ): 5.05 (1H, dd,  $J = 12.0, 4.0$  Hz, 1-H), 6.10 (1H, d,  $J = 16.0$  Hz, 5-H), 5.44 (1H, dd,  $J = 16.0, 10.5$  Hz, 6-H), 0.82, 0.90 [both 3H, d,  $J = 6.5$  Hz, 11-( $\text{CH}_3$ )<sub>2</sub>], 4.89, 5.14 (both 1H, s, 15- $\text{H}_2$ ), 4.93, 5.36 (both 1H, s, 14- $\text{H}_2$ ), 1.97 (3H, s,  $\text{OCOCH}_3$ ).  $^{13}\text{C-NMR}$  (22.5 MHz,  $\text{CDCl}_3$ ,  $\delta_c$ ): 170.4 (s,  $\text{OCOCH}_3$ ), 149.3 (s, C-10), 146.1 (s, C-4), 138.2 (d, C-6), 129.6 (d, C-5), 77.5 (d, C-1), 52.5 (d, C-7), 31.8 (d, C-11), 113.9, 113.3 (both t, C-14, 15), 35.9, 34.5, 33.0, 29.7 (all t, C-2, 3, 8, 9), 21.4, 20.7, 20.5 (all q, C-12, 13,  $\text{OCOCH}_3$ ). MS  $m/z$  (%): 262 ( $\text{M}^+$ , 1), 202 ( $\text{M}^+ - \text{AcOH}$ , 29), 187 ( $\text{M}^+ - \text{AcOH} - \text{CH}_3$ , 13), 159 ( $\text{M}^+ - \text{AcOH} - \text{C}_3\text{H}_7$ , 100).

**Deacetylation of Trienol Acetate (11) Giving the Trienol (12)**—A solution of 11 (18 mg) in 0.1 M  $\text{K}_2\text{CO}_3$  (aq. 85% MeOH) (1 ml) was stirred at room temperature (20  $^\circ\text{C}$ ) for 3 h. The reaction mixture was poured into water and the whole was extracted with AcOEt. The AcOEt extract was washed with aq. sat. NaCl and dried over  $\text{MgSO}_4$ . A product, obtained by evaporation of the solvent under reduced pressure, was purified by column chromatography ( $\text{SiO}_2$  5 g, *n*-hexane-AcOEt = 3:1) to furnish the trienol (12) (13 mg). 12, colorless solid,  $[\alpha]_D^{20} + 200^\circ$  ( $c = 0.5$ ,  $\text{CHCl}_3$ ). High-resolution MS: Found 220.182. Calcd for  $\text{C}_{15}\text{H}_{24}\text{O}$  ( $\text{M}^+$ ) = 220.182. IR  $\nu_{\text{max}}^{\text{CHCl}_3} \text{cm}^{-1}$ : 3600, 3425 (br). UV  $\lambda_{\text{max}}^{\text{MeOH}} \text{nm}$  ( $\epsilon$ ): 238 (16000).  $^1\text{H-NMR}$  (500 MHz, benzene- $d_6$ ,  $\delta$ ): 3.71 (1H, dd,  $J = 11.5, 4.0$  Hz, 1-H), 1.86 (1H, dddd,  $J = 13.0, 11.5, 5.0, 3.0$  Hz, 2- $\text{H}_a$ ), 1.68 (1H, dddd,  $J = 13.0, 13.0, 5.5, 4.0$  Hz, 2- $\text{H}_b$ ), 2.34 (1H, ddd,  $J = 13.0, 13.0, 5.0$  Hz, 3- $\text{H}_a$ ), 2.04 (1H, ddd,  $J = 13.0, 5.5, 3.0$  Hz, 3- $\text{H}_b$ ), 5.87 (1H, d,  $J = 16.0$  Hz, 5-H), 5.37 (1H, dd,  $J = 16.0, 10.5$  Hz, 6-H), 1.55 (2H, overlapped, 7-H, 9- $\text{H}_b$ ), 1.77 (1H, dddd,  $J = 13.0, 6.5, 4.5, 2.0$  Hz, 8- $\text{H}_a$ ), 1.42 (1H, dddd,  $J = 13.0, 12.0, 10.5, 2.0$  Hz, 8- $\text{H}_b$ ), 2.47 (1H, ddd,  $J = 14.0, 6.5, 2.0$  Hz, 9- $\text{H}_a$ ), 1.33 (1H, oct,  $J = 6.5$  Hz, 11-H), 0.80, 0.83 [both 3H, d,  $J = 6.5$  Hz, 11-( $\text{CH}_3$ )<sub>2</sub>], 4.84, 4.88 (both 1H, s, 14- $\text{H}_2$ ), 4.77, 5.03 (both 1H, s, 15- $\text{H}_2$ ).  $^1\text{H-NMR}$  [500 MHz, benzene- $d_6$ -pyridine- $d_5$  (1:1),  $\delta$ ]: 4.08 (1H, dd,  $J = 11.5, 4.0$  Hz, 1-H), 2.31 (1H, dddd,  $J = 13.0, 11.5, 5.0, 3.0$  Hz, 2- $\text{H}_a$ ), 1.98 (1H, dddd,  $J = 13.0, 13.0, 5.5, 4.0$  Hz, 2- $\text{H}_b$ ), 2.54 (1H, ddd,  $J = 13.0, 13.0, 5.0$  Hz, 3- $\text{H}_a$ ), 2.20 (1H, ddd,  $J = 13.0, 5.5,$



3.0 Hz, 3-H<sub>b</sub>), 6.01 (1H, d,  $J = 16.0$  Hz, 5-H), 5.56 (1H, dd,  $J = 16.0, 10.5$  Hz, 6-H), 1.67 (1H, dddd,  $J = 10.5, 10.5, 6.5, 4.5$  Hz, 7-H), 1.87 (1H, dddd,  $J = 13.0, 6.5, 4.5, 2.0$  Hz, 8-H<sub>a</sub>), 1.58 (1H, dddd,  $J = 13.0, 12.0, 10.5, 2.0$  Hz, 8-H<sub>b</sub>), 2.66 (1H, ddd,  $J = 14.0, 6.5, 2.0$  Hz, 9-H<sub>a</sub>), 1.79 (1H, ddd,  $J = 14.0, 12.0, ca. 2.0$  Hz, 9-H<sub>b</sub>), 1.39 (1H, oct,  $J = 6.5$  Hz, 11-H), 0.81, 0.85 [both 3H, d,  $J = 6.5$  Hz, 11-(CH<sub>3</sub>)<sub>2</sub>], 4.96, 4.90 (both 1H, s, 14-H<sub>2</sub>), 5.37, 5.02 (both 1H, s, 15-H<sub>2</sub>). <sup>13</sup>C-NMR (22.5 MHz, CDCl<sub>3</sub>, δ<sub>c</sub>): 153.6 (s, C-10), 146.8 (s, C-4), 137.9 (d, C-6), 129.7 (d, C-5), 76.0 (d, C-1), 52.6 (d, C-7), 31.8 (d, C-11), 112.8, 110.5 (both t, C-14, 15), 36.2, 36.2, 34.5, 30.0 (all t, C-2, 3, 8, 9), 20.7, 20.5 (both q, C-12, 13). MS  $m/z$  (%): 220 (M<sup>+</sup>, 7), 202 (M<sup>+</sup> - H<sub>2</sub>O, 25), 177 (M<sup>+</sup> - C<sub>3</sub>H<sub>7</sub>, 29), 159 (M<sup>+</sup> - C<sub>3</sub>H<sub>7</sub> - H<sub>2</sub>O, 51), 109 (100).

**Application of Horeau's Method to Nephthediol (9)**—A solution of 9 (29 mg) in pyridine (1 ml) was treated with (±)-α-phenylbutyric anhydride (42 mg) and the whole mixture was stirred under a nitrogen atmosphere at room temperature (21 °C) for 14 h. The reaction mixture was then treated with H<sub>2</sub>O (1 ml) and stirred further for 1 h. The whole mixture was partitioned into an AcOEt-aq. sat. NaHCO<sub>3</sub> mixture. The AcOEt phase was washed with aq. sat. NaCl and dried over MgSO<sub>4</sub>. A product, obtained after work-up in the usual manner, was purified by column chromatography (SiO<sub>2</sub> 5 g, *n*-hexane-AcOEt = 5:1) to furnish the ester (28 mg) and 9 (recovered, 12 mg). The aq. NaHCO<sub>3</sub> phase was acidified with aq. 2N HCl and the whole was extracted with AcOEt. Work-up of the AcOEt extract in the usual manner afforded the recovered acid, which was purified by HPLC (Semi Prep Cosmosil 5C<sub>18</sub>, MeOH = H<sub>2</sub>O = 8:1) to furnish α-phenylbutyric acid (26 mg) of  $[\alpha]_D^{25} = -13.5^\circ$  ( $c = 0.8$ , benzene). The ester, colorless oil. High-resolution MS: Found 384.267. Calcd for C<sub>25</sub>H<sub>30</sub>O<sub>3</sub> (M<sup>+</sup>) = 384.266. IR  $\nu_{\max}^{\text{CHCl}_3} \text{ cm}^{-1}$ : 3600, 1720, 1265. <sup>1</sup>H-NMR (90 MHz, CDCl<sub>3</sub>, δ): 5.07 (3H, overlapped, 1-H, 15-H<sub>2</sub>), 5.30 (2H, overlapped, 5, 6-H), 1.27 (3H, s, 4-CH<sub>3</sub>), 0.86 (9H, overlapped), 7.26 (5H, s), 3.38 (1H, t,  $J = 7.5$  Hz). MS  $m/z$  (%): 384 (M<sup>+</sup>, 0.4), 341 (M<sup>+</sup> - C<sub>3</sub>H<sub>7</sub>, 0.4), 91 (100).

**Application of Horeau's Method to the Trienol (12)**—A solution of 12 (13 mg) in pyridine (1 ml) was treated with (±)-α-phenylbutyric anhydride (21 mg) and the whole mixture was stirred under a nitrogen atmosphere at room temperature (19 °C) for 19 h. Work-up of the reaction mixture as described above furnished the ester (10 mg), 12 (recovered, 5 mg) and α-phenylbutyric acid (15 mg). α-Phenylbutyric acid:  $[\alpha]_D^{20} = -2.5^\circ$  ( $c = 0.4$ , benzene). The ester, colorless oil. High-resolution MS: Found 366.254. Calcd for C<sub>25</sub>H<sub>34</sub>O<sub>2</sub> (M<sup>+</sup>) = 366.256. IR  $\nu_{\max}^{\text{CHCl}_3} \text{ cm}^{-1}$ : 1718, 1264. <sup>1</sup>H-NMR (90 MHz, CDCl<sub>3</sub>, δ): 5.00 (1H, m, 1-H), 5.49 (1H, d,  $J = 9.0$  Hz, 5-H), 5.31 (1H, dd,  $J = 9.0, ca. 3.0$  Hz, 6-H), 0.80, 0.88 [both 3H, d,  $J = 7.0$  Hz, 11-(CH<sub>3</sub>)<sub>2</sub>], 5.99, 6.16 (both 1H, s, 14-H<sub>2</sub>), 4.87, 5.14 (both 1H, s, 15-H<sub>2</sub>), 3.36 (1H, t,  $J = 7.5$  Hz), 0.85 (3H, t,  $J = 7.5$  Hz), 7.26 (5H, s). MS  $m/z$  (%): 366 (M<sup>+</sup>, 3), 323 (M<sup>+</sup> - C<sub>3</sub>H<sub>7</sub>, 0.5), 159 (100).

**Dehydrogenation of Nephthene (17)**—A solution of 17 (50 mg) in diethyleneglycol dimethyl ether (3 ml) was treated with 10% Pd-C (10 mg) and the whole mixture was heated under reflux for 25 h. After cooling to room temperature (25 °C), the reaction mixture was filtered. The filtrate was poured into water and the whole was extracted with AcOEt. The AcOEt extract was washed with water several times and with aq. sat. NaCl, then dried over MgSO<sub>4</sub>. A product, obtained after removal of the solvent under reduced pressure, was purified by column chromatography (SiO<sub>2</sub> 5 g, *n*-hexane) to furnish eadalene (18) (9 mg). 18, colorless oil. High-resolution MS: Found 198.143. Calcd for C<sub>15</sub>H<sub>18</sub> (M<sup>+</sup>) = 198.141. IR  $\nu_{\max}^{\text{CHCl}_3} \text{ cm}^{-1}$ : 1625, 1600, 1508. UV  $\lambda_{\max}^{\text{MeOH}} \text{ nm}$  ( $\epsilon$ ): 231 (45000), 290 (6000), 325 (800). <sup>1</sup>H-NMR (90 MHz, CCl<sub>4</sub>, δ): 2.54 (3H, s), 2.61 (3H, s), 1.36 (6H, d,  $J = 7.0$  Hz), 7.81 (2H, overlapped), 7.20 (3H, overlapped). <sup>13</sup>C-NMR (22.5 MHz, CDCl<sub>3</sub>, δ<sub>c</sub>): 142.2 (s), 134.7 (s), 131.9 (s), 131.6 (s), 131.2 (s), 127.2 (d), 125.6 (d), 124.8 (d), 123.0 (d), 121.5 (d), 28.3 (d), 23.7 (q), 23.7 (q), 22.0 (q), 19.4 (q). MS  $m/z$  (%): 198 (M<sup>+</sup>, 33), 183 (M<sup>+</sup> - CH<sub>3</sub>, 100), 168 (M<sup>+</sup> - 2C<sub>2</sub>H<sub>5</sub>, 42), 155 (M<sup>+</sup> - C<sub>3</sub>H<sub>7</sub>, 12), 153 (M<sup>+</sup> - 3C<sub>2</sub>H<sub>5</sub>, 30).

**Oxidation of Nephthene (17) with OsO<sub>4</sub>-NaIO<sub>4</sub> Giving the Norenone (19)**—A solution of 17 (30 mg) in dioxane-H<sub>2</sub>O (1.8:0.5) (2.3 ml) was treated with a solution of OsO<sub>4</sub> (12 mg) in pyridine-H<sub>2</sub>O (1:1) (0.5 ml) and the whole mixture was stirred at room temperature (20 °C) for 10 min. The reaction mixture was then treated with NaIO<sub>4</sub> (190 mg) in small portions over a period of 10 min and stirred at room temperature for further 2 h. The reaction mixture was poured into water and the whole was extracted with AcOEt. The AcOEt extract was washed with aq. sat. NaCl and worked up in the usual manner. A product thus obtained was purified by column chromatography (SiO<sub>2</sub> 7 g, *n*-hexane-AcOEt = 5:1) to furnish the norenone (19) (15 mg). 19, colorless oil,  $[\alpha]_D^{25} = +45^\circ$  ( $c = 1.5$ , CHCl<sub>3</sub>). High-resolution MS: Found 206.166. Calcd for C<sub>14</sub>H<sub>22</sub>O (M<sup>+</sup>) = 206.167. IR  $\nu_{\max}^{\text{CHCl}_3} \text{ cm}^{-1}$ : 1675, 1611. UV  $\lambda_{\max}^{\text{MeOH}} \text{ nm}$  ( $\epsilon$ ): 244 (15000). CD ( $c = 1.8 \times 10^{-2}$ , MeOH):  $[\theta]_{220}^{20} + 3000$  (pos. max.),  $[\theta]_{268}^{20} 0$ ,  $[\theta]_{241}^{20} - 15000$  (neg. max.),  $[\theta]_{226}^{20} 0$ ,  $[\theta]_{208}^{20} + 30000$  (pos. max.),  $[\theta]_{210}^{20} + 20000$ . <sup>1</sup>H-NMR (500 MHz, CDCl<sub>3</sub>, δ): 2.59 (1H, dddd,  $J = 5.0, 5.0, 5.0, 2.0$  Hz, 1-H), 5.92 (1H, d,  $J = 2.0$  Hz, 5-H), 2.17 (1H, m, 10-H), 0.95 (3H, d,  $J = 7.5$  Hz, 10-CH<sub>3</sub>), 0.76, 0.98 [both 3H, d,  $J = 6.0$  Hz, 11-(CH<sub>3</sub>)<sub>2</sub>]. <sup>13</sup>C-NMR (22.5 MHz, CDCl<sub>3</sub>, δ<sub>c</sub>): 199.7 (s), 167.8 (s), 127.6 (d), 52.0 (d), 37.7 (d), 36.0 (d), 27.8 (d), 36.0 (t), 29.0 (t), 25.5 (t), 23.1 (t), 21.6 (q), 21.1 (q), 14.9 (q). MS  $m/z$  (%): 206 (M<sup>+</sup>, 49), 191 (M<sup>+</sup> - CH<sub>3</sub>, 11), 164 (M<sup>+</sup> - C<sub>3</sub>H<sub>6</sub>, 100), 163 (M<sup>+</sup> - C<sub>3</sub>H<sub>7</sub>, 46), 149 (M<sup>+</sup> + 1 - C<sub>3</sub>H<sub>7</sub> - CH<sub>3</sub>, 49).

**Hydroboration-Oxidation of Nephthene (17) Giving the Diol (20)**—Under a nitrogen atmosphere, a solution of 17 (40 mg) in dry THF (1 ml) was treated with NaBH<sub>4</sub> (23 mg) and then cooled to -25 °C. The cooled mixture was then treated with a solution of BF<sub>3</sub>-etherate (0.5 ml) in THF (1 ml) over a period of 10 min. The reaction mixture was stirred at room temperature (20 °C) for a further 1.5 h, then treated with H<sub>2</sub>O (0.5 ml). After adjusting weakly alkaline with aq. 2N NaOH (1.5 ml), the reaction mixture was treated with aq. 30% H<sub>2</sub>O<sub>2</sub> (0.5 ml) and the whole mixture was stirred at room temperature for 1 h, then poured into water. The whole was extracted with AcOEt and work-up of the AcOEt extract in the usual manner gave a product. Purification of the product by column

chromatography (SiO<sub>2</sub> 10 g, *n*-hexane–AcOEt = 2:1) and HPLC (Semi Prep Zorbax SIL, *n*-hexane–AcOEt = 2:1) gave the diol (**20**) (11 mg). **20**, colorless solid,  $[\alpha]_D^{18} + 66^\circ$  ( $c = 0.6$ , CHCl<sub>3</sub>). High-resolution MS: Found 222.200. Calcd for C<sub>15</sub>H<sub>26</sub>O (M<sup>+</sup> – H<sub>2</sub>O) = 222.198. IR  $\nu_{\max}^{\text{CHCl}_3} \text{ cm}^{-1}$ : 3455 (br). <sup>1</sup>H-NMR (500 MHz, CDCl<sub>3</sub>,  $\delta$ ): 3.58 (1H, dd,  $J = 9.5, 9.5$  Hz, 5-H), 2.02 (1H, m, 11-H), 0.89 (3H, d,  $J = 7.0$  Hz, 10-CH<sub>3</sub>), 1.05, 1.01 [both 3H, d,  $J = 6.5$  Hz, 11-(CH<sub>3</sub>)<sub>2</sub>], 3.68 (2H, overlapped, 14-H<sub>2</sub>). <sup>13</sup>C-NMR (22.5 MHz, CDCl<sub>3</sub>,  $\delta_c$ ): 76.9 (d), 46.5 (d), 45.6 (d), 37.9 (d), 37.3 (d), 32.0 (d), 26.3 (d), 69.0 (t), 30.6 (t), 30.3 (t), 26.4 (t), 21.3 (t), 25.0 (q), 22.1 (q), 13.2 (q). MS  $m/z$  (%): 222 (M<sup>+</sup> – H<sub>2</sub>O, 16), 191 (222 – CH<sub>2</sub>OH, 21), 179 (222 – C<sub>3</sub>H<sub>7</sub>, 33), 161 (222 – C<sub>3</sub>H<sub>7</sub> – H<sub>2</sub>O, 36).

**Acetylation of the Diol (20) Followed by Oxidation Giving 21**—Under a nitrogen atmosphere, a solution of **20** (30 mg) in CH<sub>2</sub>Cl<sub>2</sub>–pyridine (2:1) (3 ml) was treated with Ac<sub>2</sub>O (5 drops) at –20 °C.

The mixture was stirred for 3 h while the reaction temperature was raised from –20 °C to room temperature (25 °C). The reaction mixture was poured into water and the whole was extracted with AcOEt. Work-up of the AcOEt extract in the usual manner gave a product, which was purified by column chromatography (SiO<sub>2</sub> 7 g, *n*-hexane–AcOEt = 4:1) to furnish the monoacetate (22 mg) and **20** (recovered, 5 mg). The monoacetate (22 mg) was dissolved in CH<sub>2</sub>Cl<sub>2</sub> (2 ml) and the solution was treated with PCC (30 mg). The mixture was stirred at room temperature for 30 h and filtered. The filtrate was poured into water and the whole was extracted with AcOEt. Work-up of the AcOEt extract in the usual manner gave a product, which was purified by column chromatography (SiO<sub>2</sub> 7 g, *n*-hexane–AcOEt = 7:1 → 5:1) to furnish the keto-alcohol acetate (**21**) (5 mg) and the monoacetate (recovered, 14 mg). **21**, colorless oil,  $[\alpha]_D^{20} + 112^\circ$  ( $c = 0.9$ , CHCl<sub>3</sub>). High-resolution MS: Found 280.205. Calcd for C<sub>17</sub>H<sub>28</sub>O<sub>3</sub> (M<sup>+</sup>) = 280.204. IR  $\nu_{\max}^{\text{CHCl}_3} \text{ cm}^{-1}$ : 1737 (sh), 1725, 1250 (br). CD ( $c = 4.0 \times 10^{-1}$ , MeOH):  $[\theta]_{331}^0$ ,  $[\theta]_{297}^0 + 4000$  (pos. max.),  $[\theta]_{225}^0$ . <sup>1</sup>H-NMR (500 MHz, benzene-*d*<sub>6</sub>,  $\delta$ ): 1.65 (1H, overlapped, 1-H), 2.57 (1H, dddd,  $J = 7.0, 7.0, 6.0, 5.5$  Hz, 4-H), 1.96 (1H, dd,  $J = 12.5, 3.5$  Hz, 6-H), 2.26 (1H, dddd,  $J = 10.0, 3.5, 3.0, 2.5$  Hz, 7-H), 4.30 (A in ABX,  $J_{AB} = 11.0, J_{AX} = 6.0$  Hz, 14-H<sub>a</sub>), 4.15 (B in ABX,  $J_{AB} = 11.0, J_{BX} = 7.0$  Hz, 14-H<sub>b</sub>), 0.66 (3H, d,  $J = 7.0$  Hz, 10-CH<sub>3</sub>), 0.76, 0.89 [both 3H, d,  $J = 6.5$  Hz, 11-(CH<sub>3</sub>)<sub>2</sub>], 1.67 (3H, s, OCOCH<sub>3</sub>). <sup>1</sup>H-NMR (500 MHz, pyridine-*d*<sub>5</sub>,  $\delta$ ): 1.91 (1H, dddd,  $J = 12.5, 11.5, 4.5, 4.5$  Hz, 1-H), 2.83 (1H, dddd,  $J = 7.0, 7.0, 6.0, 5.5$  Hz, 4-H), 2.18 (1H, dd,  $J = 12.5, 3.5$  Hz, 6-H), 2.23 (1H, dddd,  $J = 10.0, 3.5, 3.0, 2.5$  Hz, 7-H), 4.43 (A in ABX,  $J_{AB} = 11.0, J_{AX} = 6.0$  Hz, 14-H<sub>a</sub>), 4.29 (B in ABX,  $J_{AB} = 11.0, J_{BX} = 7.0$  Hz, 14-H<sub>b</sub>), 0.80 (3H, d,  $J = 7.0$  Hz, 10-CH<sub>3</sub>), 0.76, 0.88 [both 3H, d,  $J = 6.5$  Hz, 11-(CH<sub>3</sub>)<sub>2</sub>], 2.00 (3H, s, OCOCH<sub>3</sub>). <sup>13</sup>C-NMR (22.5 MHz, CDCl<sub>3</sub>,  $\delta_c$ ): 213.7 (s), 170.9 (s), 51.2 (d), 46.5 (d), 41.9 (d), 36.5 (d), 32.3 (d), 26.0 (d), 65.1 (t), 28.2 (t), 25.2 (t), 24.8 (t), 24.2 (t), 23.6 (q), 22.0 (q), 20.9 (q), 12.5 (q). MS  $m/z$  (%): 280 (M<sup>+</sup>, 10), 220 (M<sup>+</sup> – AcOH, 80), 177 (M<sup>+</sup> – AcOH – C<sub>3</sub>H<sub>7</sub>, 14), 109 (100).

**Synthesis of the Nor-trans- $\alpha$ -Glycol (22) from the Norenone (19)**—Under a nitrogen atmosphere, a solution of **19** (100 mg) in dry THF–MeOH (2:1) (2 ml) was treated with CeCl<sub>3</sub>·7H<sub>2</sub>O (181 mg) and NaBH<sub>4</sub> (30 mg) and the mixture was stirred at room temperature (22 °C) for 1 h. The reaction mixture was poured into water and the whole was extracted with AcOEt. Work-up of the AcOEt extract in the usual manner gave a mixture of 4-ol-5-ene derivatives (100 mg). The product (100 mg) was dissolved in dry THF (2 ml) and the solution was treated under a nitrogen atmosphere with NaBH<sub>4</sub> (28 mg) and then with a solution of BF<sub>3</sub>–etherate (0.3 ml) in THF (2 ml) at –70 °C. The reaction mixture was stirred for 4 h while the reaction temperature was raised from –70 °C to room temperature (25 °C), then treated with H<sub>2</sub>O (1 ml). The reaction mixture was made weakly alkaline with aq. 2 N NaOH, and treated with aq. 30% H<sub>2</sub>O<sub>2</sub> (0.5 ml). The whole mixture was stirred at room temperature for 4 h and poured into water. The whole was then extracted with AcOEt and the AcOEt extract was worked up in the usual manner. The product was purified by column chromatography (SiO<sub>2</sub> 30 g, *n*-hexane–AcOEt = 2:1) and HPLC (Semi Prep Zorbax ODS, MeOH–H<sub>2</sub>O = 7:1) to furnish the nor-trans- $\alpha$ -glycol (**22**) (10 mg). **22**, colorless oil,  $[\alpha]_D^{22} + 43^\circ$  ( $c = 0.7$ , CHCl<sub>3</sub>). High-resolution MS: Found 208.183. Calcd for C<sub>14</sub>H<sub>24</sub>O (M<sup>+</sup> – H<sub>2</sub>O) = 208.183. IR  $\nu_{\max}^{\text{CHCl}_3} \text{ cm}^{-1}$ : 3586, 3425 (br). CD ( $c = 1.6 \times 10^{-1}$ , CCl<sub>4</sub>):  $[\theta]_{311}^0 - 29000$  (neg. max.),  $[\theta]_{297}^0$ ,  $[\theta]_{282}^0 + 29000$  (pos. max.). <sup>1</sup>H-NMR (500 MHz, CDCl<sub>3</sub>,  $\delta$ ): 1.63 (1H, ddd,  $J = 12.0, 10.5, 4.5$  Hz, 1-H), 3.34 (1H, ddd,  $J = 11.0, 10.0, 4.5$  Hz, 4-H), 3.40 (1H, dd,  $J = 10.0, 9.0$  Hz, 5-H), 1.54 (1H, ddd,  $J = 12.0, 9.0, 5.0$  Hz, 6-H), 1.79 (1H, m, 7-H), 1.82 (1H, m, 10-H), 2.01 (1H, m, 11-H), 0.87 (3H, d,  $J = 7.0$  Hz, 10-CH<sub>3</sub>), 1.00, 1.04 [both 3H, d,  $J = 7.0$  Hz, 11-(CH<sub>3</sub>)<sub>2</sub>]. <sup>13</sup>C-NMR (22.5 MHz, CDCl<sub>3</sub>,  $\delta_c$ ): 76.4 (d), 76.3 (d), 43.2 (d), 37.9 (d), 37.8 (d), 31.8 (d), 26.4 (d), 31.8 (t), 30.2 (t), 28.9 (t), 21.1 (t), 25.0 (q), 22.2 (q), 13.2 (q). CI-MS (isobutane)  $m/z$  (%): 227 (M<sup>+</sup> + H, 0.3), 209 (227 – H<sub>2</sub>O, 43), 191 (227 – 2H<sub>2</sub>O, 47).

**CD Spectrum of 22 Measured by the  $\alpha$ -Glycol Chirality Method**—**22** (0.339 mg) was dissolved in a  $1.5 \times 10^{-4}$  M solution of Eu(fod)<sub>3</sub> in CCl<sub>4</sub> (10 ml) [prepared from Eu(fod)<sub>3</sub> 1.55 mg in CCl<sub>4</sub> 10 ml] and after 30 min, the CD spectrum of the solution ( $1.5 \times 10^{-4}$  M **22**) was measured. CD ( $c = 1.6 \times 10^{-1}$ , CCl<sub>4</sub>):  $[\theta]_{311}^0 - 29000$  (neg. max.),  $[\theta]_{297}^0$ ,  $[\theta]_{282}^0 + 29000$  (pos. max.).

**Acknowledgement** The authors are grateful to the Ministry of Education, Science, and Culture of Japan for financial support (Grant No. 59470121). One of the authors (Z. C.) is grateful to the State Education Commission, the People's Republic of China for giving him the opportunity to study at Osaka University.

#### References and Notes

- 1) Part XVI: I. Kitagawa, Z. Cui, Y. Cai, M. Kobayashi, and Y. Kyogoku, *Chem. Pharm. Bull.*, **34**, 4641 (1986).

- 2) *E.g.* A recent publication from this laboratory: I. Kitagawa, M. Kobayashi, N. K. Lee, H. Shibuya, Y. Kawata, and F. Sakiyama, *Chem. Pharm. Bull.*, **34**, 2664 (1986).
- 3) M. Kobayashi, B. W. Son, Y. Kyogoku, and I. Kitagawa, *Chem. Pharm. Bull.*, **32**, 1667 (1984).
- 4) a) M. Kobayashi, B. W. Son, I. Kitagawa, and Y. Kyogoku, presented at the 105th Annual Meeting of the Pharmaceutical Society of Japan, Kanazawa, April 1985, Abstracts of Papers, p. 491; b) I. Kitagawa, presented at the 51st Annual Meeting of the Chemical Society of Japan, Kanazawa, Oct. 1985, Abstracts of Papers, p. I-462.
- 5) K. Takeda, H. Minato, and M. Ishikawa, *Tetrahedron Suppl.*, No. 7, 219 (1966).
- 6) F. Bohlmann, R. K. Gupta, J. Jakupovic, R. M. King, and H. Robinson, *Phytochemistry*, **21**, 1665 (1982).
- 7) K. B. Sharpless and R. C. Michaelson, *J. Am. Chem. Soc.*, **95**, 6136 (1973).
- 8) K. Nakanishi and J. Dillon, *J. Am. Chem. Soc.*, **93**, 4058 (1971).
- 9) E. Knappe and D. Peteri, *Z. Anal. Chem.*, **190**, 386 (1962).
- 10) M. H. Abraham, A. G. Davies, D. R. Llewellyn, and E. M. Thain, *Anal. Chim. Acta*, **17**, 499 (1957).
- 11) A. A. Frimer, *Chem. Rev.*, **79**, 359 (1979).
- 12) J. G. Moffatt, *Org. Synth.*, **47**, 25 (1967).
- 13) A. Horeau, *Tetrahedron Lett.*, **1961**, 506.
- 14) S. J. Wratten and D. J. Faulkner, *J. Org. Chem.*, **42**, 3343 (1977).
- 15) R. R. Izac, M. M. Bandurraga, J. M. Wasyluk, F. W. Dunn, and W. Fenical, *Tetrahedron*, **38**, 301 (1982).
- 16) E. Fattorusso, S. Magno, L. Mayol, V. Amico, G. Oriente, M. Piattelli, and C. Tringali, *Tetrahedron Lett.*, **1978**, 4149.
- 17) a) T. Irie, K. Yamamoto, and T. Masamune, *Bull. Chem. Soc. Jpn.*, **37**, 1053 (1964); b) K. Adachi, *Nippon Kagaku Kaishi*, **1972**, 985.
- 18) M. V. Rangaishenvi, S. V. Hiremath, and S. N. Kulkarni, *Indian J. Chem.*, **21B**, 678 (1982).
- 19) S. J. Terhune, J. W. Hogg, and B. M. Lawrence, *Phytochemistry*, **13**, 1183 (1974).
- 20) V. Amico, G. Oriente, M. Piattelli, C. Tringali, E. Fattorusso, S. Magno, and L. Mayol, *Experientia*, **35**, 450 (1979).
- 21) Since the soft coral investigated in this work has not yet been identified, the specimen reported here is designated as Neph-84-IRI-1, which indicates that it is a sample of *Nephthea* sp. collected at Iriomote-jima in July 1984, as described in our previous paper.<sup>22)</sup>
- 22) Part XV: I. Kitagawa, M. Kobayashi, Z. Cui, Y. Kiyota, and M. Ohnishi, *Chem. Pharm. Bull.*, **34**, 4590 (1986).

[Chem. Pharm. Bull.]  
35(1) 136-141 (1987)

## Spirolactones of Xanthene. IV.<sup>1)</sup> New Method of Xanthone Synthesis by Oxidation of Novel Spirolactones of Dibenzo[*c,h*]xanthene and Xanthenes

MICHIO KIMURA\* and ICHIZO OKABAYASHI

*Niigata College of Pharmacy 5829 Kamishin'ei-cho,  
Niigata 950-21, Japan*

(Received July 2, 1986)

Dibenzo[*c,h*]xanthone and halogen- and methyl-substituted xanthenes have been synthesized by the oxidation of novel spirolactones of dibenzo[*c,h*]xanthene and xanthene, which were prepared by a new condensation reaction of 1-naphthol or phenol derivatives with oxalic acid in the presence of sulfuric acid. The oxidation was carried out by using potassium permanganate in the presence of aqueous potassium hydroxide. The dibenzo[*c,h*]xanthone and xanthenes were identical with samples obtained by another synthetic route.

**Keywords**—spirolactone; dibenzo[*c,h*]xanthone; xanthone; 1-naphthol; phenol; X-ray analysis

In previous papers,<sup>1-5)</sup> it has been reported that the reaction of 1-naphthol (1) with oxalic and sulfuric acids occurred with the loss of four molecules of water to give a novel spirolactone (2) of dibenzo[*c,h*]xanthene in excellent yield (70–75%). The molecular structure of 2 has been established by the X-ray diffraction method (Fig. 1). In the course of further investigation of this novel reaction, we found that the reaction proceeds when substituted phenols are used in place of 1-naphthol to give novel spirolactones (6, 10, 14 and 18) of xanthene as shown in Chart 1. The molecular structure of 14 was also determined by the X-ray diffraction method (Fig. 2).<sup>3)</sup> Recently, we have found that these novel spirolactones give the dibenzo[*c,h*]xanthone (3) and xanthenes (7, 11, 15 and 19) on potassium permanganate

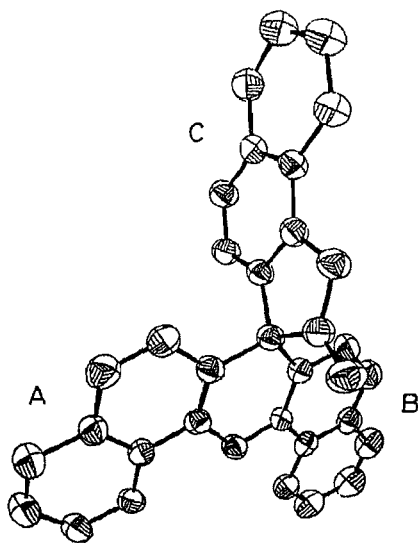


Fig. 1. ORTEP Drawing of Compound 2<sup>1,2)</sup>

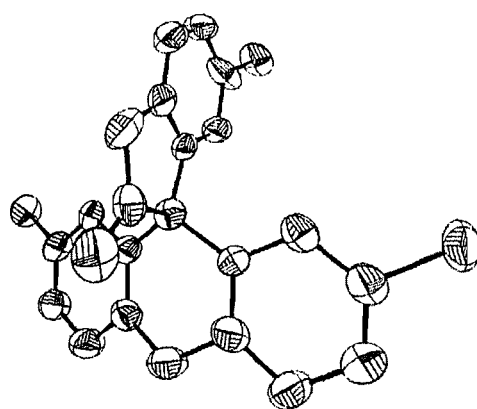


Fig. 2. ORTEP Drawing of Compound 14<sup>3)</sup>

( $\text{KMnO}_4$ ) oxidation in the presence of aqueous potassium hydroxide. This reaction appears to have generality to form xanthone derivatives bearing various substituents, which can not be obtained easily by the other synthetic method, that is, the use of the Ullmann reaction<sup>4)</sup> followed by cyclization using sulfuric acid, polyphosphoric acid (PPA), or phosphoric acid. The structures of the resulting dibenzo[*c,h*]xanthone and xanthenes were proved by confirming their identity with authentic samples obtained *via* another synthetic method, *i.e.*, the cyclization reaction of diphenyl ether derivatives obtained by the Ullmann reaction<sup>4)</sup> of 2-chlorobenzoic acid and phenol derivatives by the use of PPA, phosphoric acid, or sulfuric acid.<sup>5,6)</sup>

### Results and Discussion

The spirolactones (2, 6, 10, 14 and 18) prepared in this study are outlined in Charts 1, 2 and 3. The reactions were carried out by treating 1 mol of 1-naphthol (1) or substituted phenols (5, 9, 13 and 17) with 1 mol or less of oxalic acid in the presence of 1 mol of sulfuric acid at 130–145°C for 3–5 h. The reactions were also successfully carried out by using mesitylene or xylene as solvents, but generally the use of no solvent led to a good yield of the desired spirolactone. The spirolactones were detected easily by thin-layer chromatography (TLC) after the reaction because of their high *R<sub>f</sub>* values, as mentioned in the experimental section. The resulting reaction mixtures were purified by column chromatography on silica gel using chloroform or ethyl acetate as an eluent, or by preparative TLC (silica gel and chloroform eluate), and then recrystallized from xylene, toluene, benzene, chloroform or nitrobenzene. Regarding the formation of the spirolactones, the yields were high except for some cases involving sterically hindered substituents or halides on the phenol ring. A methyl group attached to the 3- or 4-position in the phenol ring (5 and 9) did not particularly affect the formation of the spirolactones. However, this reaction did not result in the formation of the desired spirolactone when the unsubstituted phenol was used, because the sulfonation reaction of phenol proceeded initially. In addition, a bulky substituent in the phenol ring, such as ethyl, propyl, *tert*-butyl, trimethylene, or phenyl, prevented the formation of the desired spirolactones.

The structures of the spirolactones were supported by the results of infrared (IR), proton and carbon-13 nuclear magnetic resonance ( $^1\text{H}$ - and  $^{13}\text{C}$ -NMR) spectroscopy as well as mass (MS) spectrometry after isolation of the products. The IR spectra of the spirolactones showed the strong absorption ( $1790\text{--}1810\text{cm}^{-1}$ ) characteristic of the lactone moiety. In the  $^1\text{H}$ -NMR spectra, the presence of sharp singlet signals in the range of  $\delta 2.0\text{--}2.5$  confirmed the

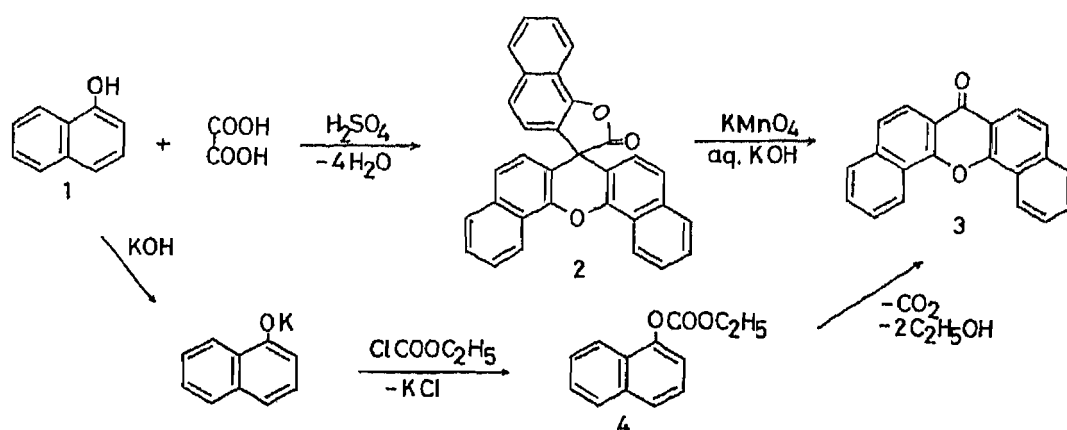


Chart 1

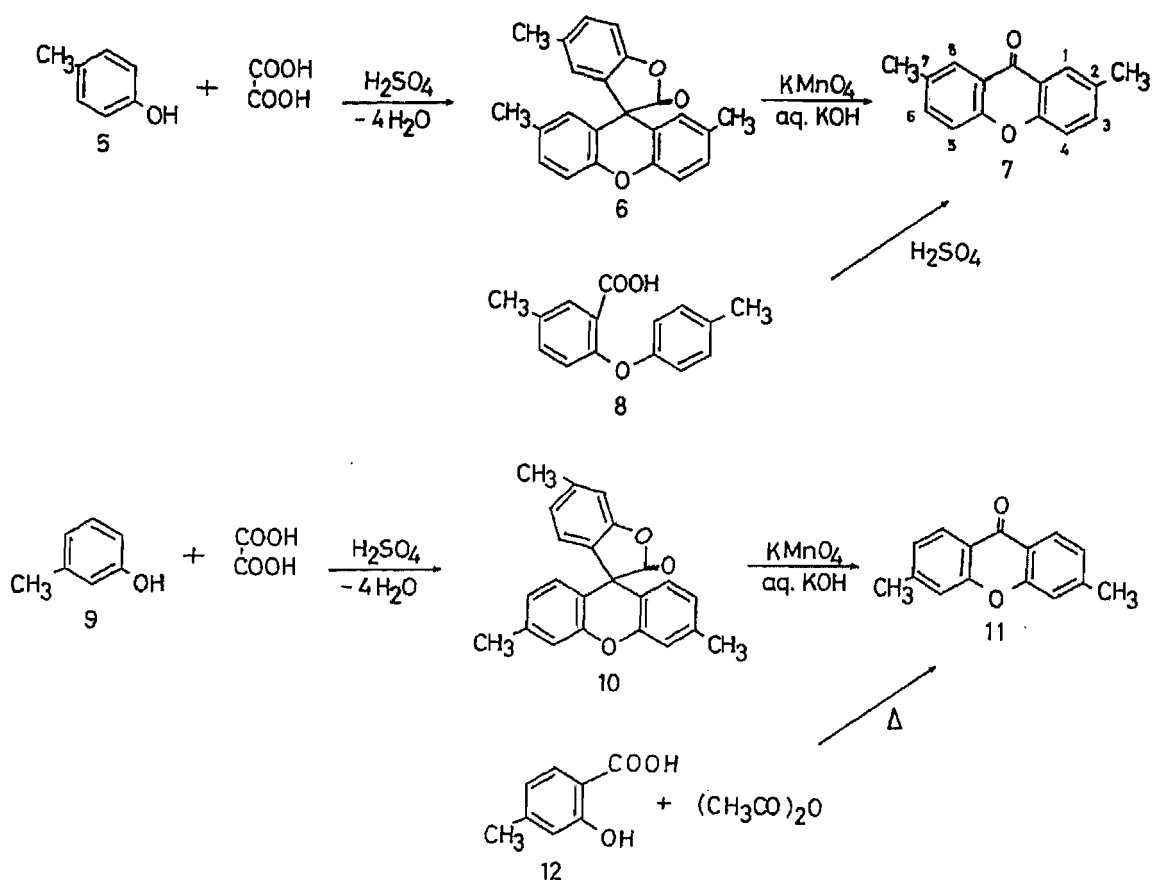


Chart 2

presence of a methyl groups on a benzene ring. The <sup>13</sup>C-NMR spectra contained three kinds of signals: the aromatic carbons appear at *ca.*  $\delta$  105–150, the spiro carbon (C-3) is observed at *ca.*  $\delta$  51, and the carbonyl carbon is observed at *ca.*  $\delta$  175. With regard to MS spectrometry, all the compounds exhibited a common fragmentation pattern corresponding to the molecular ion ( $M^+$ ),  $M^+ - CO$ , and  $M^+ - CO - OH$ , which assisted in confirming the structures. The elemental analyses and high-resolution mass (HR-MS) spectra of the spiro-lactones were in good agreement with the calculated values.

According to the molecular structure established by X-ray analysis, compound 2 possesses a  $\psi$ -like shape composed of three naphthalene rings fused by the spiro-lactone. The most interesting feature may be the dihedral angles of the naphthalene planes; 5.9° between rings A and B, 86.9° between rings A and C, and 81.4° between rings B and C. These dihedral angles may be compared with the corresponding values in the reported molecular structure of 2',5,7'-trichlorospiro[benzofuran-3(2*H*),9'-[9*H*]xanthen]-2-one (14)<sup>3)</sup>: 22.8, 83.6, and 73.6°, respectively. The great difference in the butterfly angles of the benzoxanthene ring in 2 and 14 (5.9 and 22.8°) seems to be caused by the interaction between the carbonyl group of the lactone moiety and the oxygen atom of the xanthen ring, which is induced by the electron-withdrawing effects of the chloride atoms. Another reason may be the lesser steric hindrance of the phenyl ring of 14 in comparison with the bulky naphthalene ring of 2.

The preparation of dibenzo[*c,h*]xanthone (3) and xanthones (7, 11, 15, and 19) was successfully carried out by refluxing 1 mol of the spiro-lactone with 9 mol of potassium permanganate in aqueous potassium hydroxide solution for 15–20 h. The termination of the reaction could be checked by fading of the red color of potassium permanganate, or by

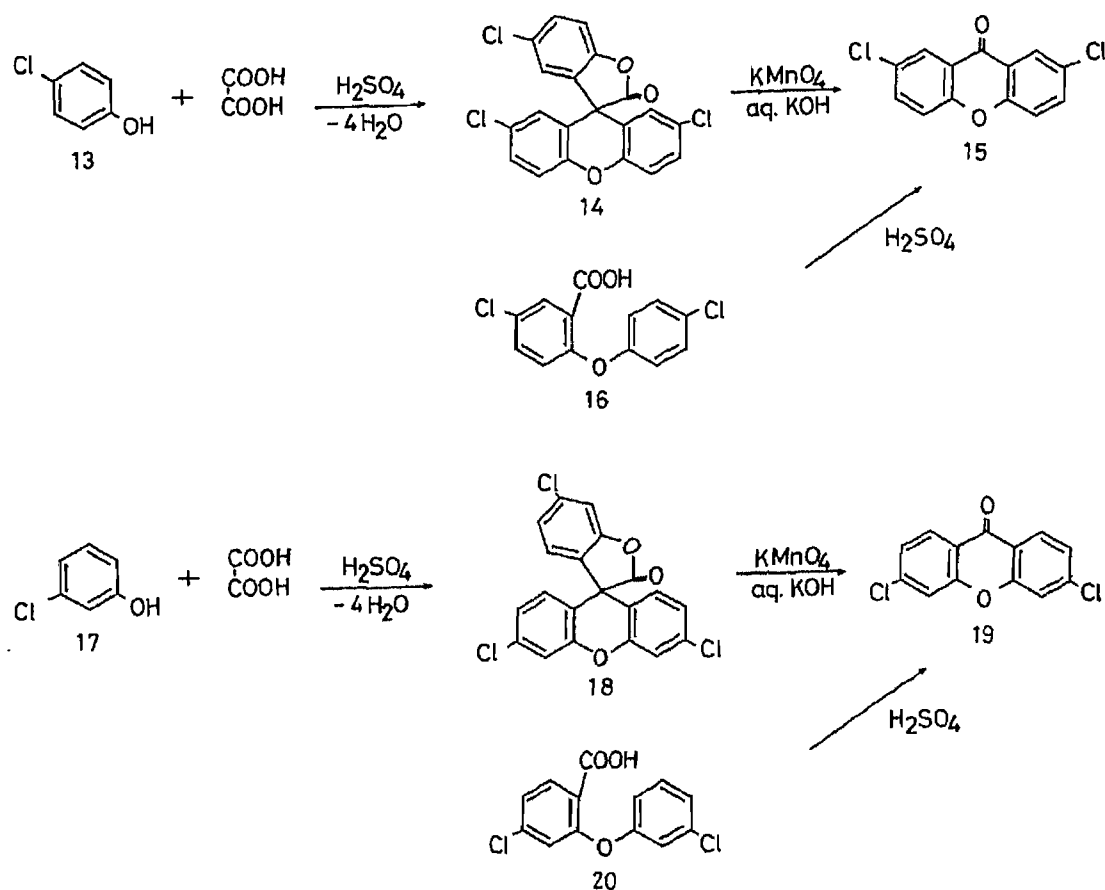


Chart 3

TLC (lower  $R_f$  values than the corresponding spiro-lactones). The structures of the desired xanthenes (3, 7, 11, 15 and 19) were established by IR,  $^1\text{H-NMR}$ ,  $^{13}\text{C-NMR}$  and MS spectral investigation.

The molecular structure of 3 was proved by its identity with the unequivocal product obtained by cyclization<sup>7)</sup> of 1-ethoxycarbonyloxynaphthalene (4), which was obtained from 1-naphthol (1) and ethyl chloroformate as shown in Chart 1. Spirolactone (10) was also oxidized to 3,6-dimethylxanthone (11), which was proved by reference to unequivocal product obtained by cyclization of 2-hydroxy-4-methylbenzoic acid (12) under reflux with acetic anhydride, as shown in Chart 2. On the other hand, spiro-lactones (6, 14 and 18) of xanthenes formed by the condensation of the corresponding phenols (5, 13 and 17) with oxalic and sulfuric acids gave the corresponding xanthenes (7, 15 and 19) by a similar procedure using potassium permanganate oxidation in the presence of aqueous potassium hydroxide. The structures of these xanthenes were proved by reference to unequivocal materials obtained in high yields by cyclization of substituted 2-carboxy diphenyl ethers, which were formed by Ullmann condensation of 2-chlorobenzoic acids with phenol derivatives.<sup>4)</sup> This cyclization to xanthenes was carried out successfully by using PPA, sulfuric acid or phosphoric acid.

The main advantage of this route for the synthesis of dibenzo[*c,h*]xanthone and xanthenes is the use of simple starting materials, such as phenol derivatives, and the ease of manipulation. This route is particularly suitable for the synthesis of symmetrically substituted xanthenes, which are not obtainable in good yields by other synthetic methods, as described in the experimental sections. The present method should also be effective for obtaining symmetrical thioxanthenes.

### Experimental

**Spectroscopy**—The  $^1\text{H-NMR}$ , totally decoupled and off-resonance decoupled  $^{13}\text{C-NMR}$  spectra were measured in  $\text{CDCl}_3$  solution in 5 mm tubes on a JEOL FX-200 spectrometer. Chemical shifts are relative to tetramethylsilane. The IR spectra were measured on a JASCO A-3 spectrometer. The electron impact (EI) MS spectra were obtained on a Hitachi RMU-7M mass spectrometer.

**Chromatography**—The TLC was performed on Merck Kieselgel 60  $F_{254}$  strips,  $9.5 \times 3.5$  cm, and thickness, 0.25 mm with  $\text{CHCl}_3$  or ethyl acetate (EtOAc). The preparative TLC was carried out on Merck Kieselgel 60  $F_{254}$  plate,  $20 \times 20$  cm, and thickness 2 mm with  $\text{CHCl}_3$  as an eluent.

**Melting Points**—The melting points were measured with a Yanagimoto micro-melting point apparatus and are uncorrected.

**Spiro[7*H*-dibenzo[*c,h*]xanthen-7,3'(2'*H*)-naphtho[1,2-*b*]furan]-2'-one (2)**—The reported method<sup>1,2)</sup> was used to obtain 2 from 7 g of 1-naphthol (0.049 mol), 3.5 g of oxalic acid (0.039 mol) and 4.4 g of conc. sulfuric acid (0.046 g).

**2',5,7'-Trimethylspiro[benzofuran-3(2*H*),9'-[9*H*]xanthen-2-one (6)**—The reported method<sup>1,2)</sup> was used to obtain 6 from 11 g of 4-methylphenol (0.1 mol), 8 g of oxalic acid (0.09 mol), and 8 g of conc. sulfuric acid (0.08 mol).

**3',6,6'-Trimethylspiro[benzofuran-3(2*H*),9'-[9*H*]xanthen]-2-one (10)**—Compound 10 (23.3 g; 65% yield) was synthesized from 11 g of 3-methylphenol (0.1 mol) and 8 g of oxalic acid (0.09 mol) with 8 g of conc. sulfuric acid (0.08 mol) by the same procedure as above except that the product was isolated by preparative TLC with  $\text{CHCl}_3$  as the developer. mp 205–208 °C. IR (KBr): 2920, 1810 (C=O), 1620, 1600, 1500  $\text{cm}^{-1}$ .  $^1\text{H-NMR}$  ( $\text{CDCl}_3$ )  $\delta$ : 2.31 (s, 6H), 2.42 (s, 3H), 6.50 (d, 2H), 6.72 (d, 2H), 6.84–7.40 (m, 5H).  $^{13}\text{C-NMR}$  ( $\text{CDCl}_3$ )  $\delta$ : 21.09, 21.75, 51.13 (C-3), 108.17, 111.26, 117.20, 117.68, 117.76, 124.59, 124.71, 125.05, 126.15, 126.68, 126.83, 127.20, 129.73, 140.01, 140.11, 140.43, 150.89, 153.86, 176.55 (C=O). MS  $m/z$  (relative intensity, %): 342 (35,  $\text{M}^+$ ), 314 (97,  $\text{M}^+ - \text{CO}$ ), 299 (100), 269 (5). HR-MS  $m/z$ : Calcd for  $\text{C}_{23}\text{H}_{18}\text{O}_3$  342.1241. Found: 342.1254. TLC ( $\text{CHCl}_3$ )  $R_f$  = 0.72.

**3',6,6'-Trichlorospiro[benzofuran-3(2*H*),9'-[9*H*]xanthen]-2-one (18)**—Compound 18 (7.9 g; 23% yield) was synthesized from 11 g of 3-chlorophenol (0.17 mol) and 8 g of oxalic acid (0.09 mol) with 8 g of sulfuric acid (0.08 mol) by the same procedure as above. mp 233–235 °C. IR (KBr): 1810, 1610, 1590, 1470, 1400  $\text{cm}^{-1}$ .  $^1\text{H-NMR}$  ( $\text{CDCl}_3$ )  $\delta$ : 6.29 (d, 1H), 6.48 (d, 1H), 6.49 (d, 1H), 7.08–7.20 (m, 6H for aromatic ring protons).  $^{13}\text{C-NMR}$  ( $\text{CDCl}_3$ )  $\delta$ : 50.74 (C-3), 112.11, 117.64, 118.00, 124.71, 126.25, 126.34, 128.34, 129.87, 135.83, 136.17, 151.08, 154.05, 174.48 (C=O). MS  $m/z$  (relative intensity, %): 402 (10,  $\text{M}^+$ ), 374 (50,  $\text{M}^+ - \text{CO}$ ), 339 (100,  $\text{M}^+ - \text{CO} - \text{OH} - \text{H}_2\text{O}$ ), 276 (15), 162 (23), 106 (25). TLC ( $\text{CHCl}_3$ )  $R_f$  = 0.60. Anal. Calcd for  $\text{C}_{20}\text{H}_9\text{Cl}_3\text{O}_3$ : C, 59.51; H, 2.25; Cl, 26.35. Found: C, 59.30; H, 2.40; Cl, 26.13.

**Dibenzo[*c,h*]xanthone (3)**—A solution of 10 g (0.063 mol) of potassium permanganate in 200 ml of water was added dropwise at 100 °C to a mixture of 3 g (0.007 mol) of spiro[7*H*-dibenzo[*c,h*]xanthen-7,3'(2'*H*)-naphtho[1,2-*b*]furan]-2'-one (2) and 3 g (0.053 mol) of potassium hydroxide in 50 ml of water, and the whole was refluxed for 13 h. The reaction mixture was then allowed to cool to room temperature, and 50 ml of ethanol was added to the reaction mixture. The precipitates were collected, washed with water, and extracted with 100 ml of ethanol. The filtrate was kept at room temperature for a further 5 h, and the precipitates that appeared were collected to obtain 3. The ethanol extract was concentrated to obtain the residual products, including 3. The combined crude 3 was recrystallized from ethanol to obtain pure crystals of 3, 0.66 g (31%). The melting point was 248–250 °C alone and on admixture with unequivocal material obtained from 1-ethoxycarbonyloxynaphthalene (4) by Bender's method.<sup>7)</sup> (lit.<sup>7)</sup>, mp 245 °C; 17% in yield). They showed identical IR,  $^1\text{H-NMR}$ ,  $^{13}\text{C-NMR}$ , and MS spectra as follows. IR (KBr): 3050, 1650, 1630, 1620, 1500, 1460  $\text{cm}^{-1}$ .  $^1\text{H-NMR}$  ( $\text{CDCl}_3$ )  $\delta$ : 7.48–7.60 (m, 6H), 7.7 (q, 2H), 8.12 (d, 2H), 8.46 (q, 2H).  $^{13}\text{C-NMR}$  ( $\text{CDCl}_3$ )  $\delta$ : 118.20 (C-6a), 121.31, 122.40, 124.06 (C-2a), 124.30, 126.83, 127.97, 129.21, 136.12 (C-1a), 152.66 (C-14a), 176.23 (C=O). MS  $m/z$ : 296 (100,  $\text{M}^+$ ), 268 (10,  $\text{M}^+ - \text{CO}$ ), 267 (8,  $\text{M}^+ - \text{CHO}$ ).

**2,7-Dimethylxanthone (7)**—Compound 7 (1.79 g; 34.7% yield) was synthesized from 8 g of 2',5,7'-trimethylspiro[benzofuran-3(2*H*),9'-[9*H*]xanthen]-2-one (6) (0.023 mol) and 10 g (0.0179 mol) of potassium hydroxide in 160 ml of water, and 35.2 g (0.223 mol) of potassium permanganate in 670 ml of water, by the same procedure as described above. The melting point was 150–151 °C alone and on admixture with an authentic sample obtained by the cyclization of 2-carboxy-4,4'-dimethyldiphenyl ether (8) with sulfuric acid according to Granoth and Pownall<sup>8)</sup> (lit.<sup>8)</sup>, mp 141 °C; 65% yield). They showed identical IR,  $^1\text{H-NMR}$ ,  $^{13}\text{C-NMR}$  and MS spectrometry as follows. IR (KBr): 1660, 1620, 1610, 1480  $\text{cm}^{-1}$ .  $^1\text{H-NMR}$  ( $\text{CDCl}_3$ )  $\delta$ : 2.42 (6H, s,  $2 \times \text{CH}_3$ ), 7.30 (2H, d,  $J = 9$  Hz, H-4, H-5), 7.45 (2H, dd,  $J = 9, 2$  Hz, H-3, H-6), 8.08 (2H, d,  $J = 2$  Hz, H-1, H-8).  $^{13}\text{C-NMR}$  ( $\text{CDCl}_3$ )  $\delta$ : 20.77 ( $\text{CH}_3$ ), 117.68, 121.43 (C-2), 125.98, 133.37 (C-1a), 135.81, 154.39 (C-4a), 177.21 (C-9). MS  $m/z$  (relative intensity, %): 224 ( $\text{M}^+$ ), 195 (23,  $\text{M}^+ - \text{CHO}$ ), 181 (13,  $\text{M}^+ - \text{CO} - \text{CH}_3$ ).

**3,6-Dimethylxanthone (11)**—Compound 11 (0.3 g; 35.2% yield) was synthesized from 1.8 g of 3',6,6'-trimethylspiro[benzofuran-3(2*H*),9'-[9*H*]xanthen]-2-one (10) (0.005 mol) and 2.2 g (0.039 mol) of potassium hydroxide in 36 ml of water, and 7.8 g (0.049 mol) of potassium permanganate in 150 ml of water, by the same procedure as described above. The melting point was 169–171 °C alone and in admixture with unequivocal materials obtained from 2-hydroxy-4-methylbenzoic acid (12)<sup>9)</sup> by Weber's method (lit.<sup>9)</sup> mp 166 °C; 4% yield). Both are also identified



by means of IR,  $^1\text{H-NMR}$ ,  $^{13}\text{C-NMR}$  and MS spectrometry as follows. IR (KBr): 1650, 1620, 1610, 1420  $\text{cm}^{-1}$ .  $^1\text{H-NMR}$  ( $\text{CDCl}_3$ )  $\delta$ : 2.44 (6H, s,  $2 \times \text{CH}_3$ ), 7.18 (2H, dd,  $J=9, 1.5$  Hz, H-2 and H-7), 7.26 (2H, d,  $J=1.5$  Hz, H-4 and H-5), 8.12 (2H, d,  $J=9$  Hz, H-1 and H-8).  $^{13}\text{C-NMR}$  ( $\text{CDCl}_3$ )  $\delta$ : 21.87, 117.61, 119.58 (C-3), 125.18, 126.32, 145.88 (C-1a), 156.12 (C-4a), 176.62 (C-9). TLC (benzene)  $R_f=0.19$ .

**2,7-Dichloroxanthone (15)**—Compound 15 (0.7 g; 24.8% yield) was synthesized from 5 g of 2',5,7'-trichlorospiro[benzofuran-3(2H),9'-[9H]xanthen]-2-one (14)<sup>3)</sup> (0.012 mol) and 5.1 g (0.091 mol) of potassium hydroxide in 85 ml of water, and 17 g (0.11 mol) of potassium permanganate in 340 ml of water, by the same procedure as described above. The melting point was 228–230 °C alone and in admixture with an authentic sample obtained by the cyclization of 4,4'-dichlorodiphenyl ether according to Granoth and Pownall<sup>8)</sup> (lit.<sup>8)</sup> mp 219 °C; 45% yield). Both were identified by means of IR,  $^1\text{H-NMR}$ ,  $^{13}\text{C-NMR}$  and MS spectrometry as follows. IR (KBr): 3080, 1670, 1610, 1600, 1460  $\text{cm}^{-1}$ .  $^1\text{H-NMR}$  ( $\text{CDCl}_3$ )  $\delta$ : 7.42 (2H, d,  $J=9$  Hz, H-4 and H-5), 7.65 (2H, dd,  $J=9, 2$  Hz, H-3 and H-6), 8.24 (2H, d,  $J=2$  Hz, H-1 and H-8).  $^{13}\text{C-NMR}$  ( $\text{CDCl}_3$ )  $\delta$ : 119.78, 122.31 (C-2), 126.08, 130.19 (C-1a), 135.28, 154.34 (C-4a), 174.95 (C-9). TLC (benzene)  $R_f=0.48$ .

**3,6-Dichloroxanthone (19)**—Compound 19 (0.84 g; 26.3% yield) was synthesized from 5 g of 3',6,6'-trichlorospiro[benzofuran-3(2H),9'-[9H]xanthen]-2-one (18) (0.012 mol) and 5.1 g (0.09 mol) of potassium hydroxide in 85 ml of water, and 17 g (0.11 mol) of potassium permanganate in 340 ml of water, by the same procedure as described above. The melting point was 190–191 °C alone and in admixture with unequivocal material obtained from 3,3'-dichloro-6-carboxydiphenyl ether according to Goldberg and Wragg<sup>6)</sup> (lit.<sup>6)</sup> mp 184–186 °C; 21% yield). Both were also identified by means of IR,  $^1\text{H-NMR}$ ,  $^{13}\text{C-NMR}$  and MS spectrometry as follows. IR (KBr): 3100, 1670, 1610, 1600, 1420  $\text{cm}^{-1}$ .  $^1\text{H-NMR}$  ( $\text{CDCl}_3$ )  $\delta$ : 7.33 (2H, dd,  $J=9, 2$  Hz, H-2 and H-7), 7.44 (2H, d,  $J=2$  Hz, H-4 and H-5), 8.20 (2H, d,  $J=9$  Hz, H-1 and H-8).  $^{13}\text{C-NMR}$  ( $\text{CDCl}_3$ )  $\delta$ : 118.00, 120.32 (C-3), 125.20, 128.10, 141.16 (C-1a), 156.12 (C-4a), 175.29 (C-9). TLC (benzene)  $R_f=0.41$ .

#### References

- 1) Part III: M. Kimura, *J. Heterocycl. Chem.*, in press.
- 2) M. Kimura and I. Okabayashi, *Chem. Pharm. Bull.*, **31**, 3357 (1983).
- 3) M. Kimura, *Bull. Chem. Soc. Jpn.*, **58**, 905 (1985).
- 4) F. Jourdan, *Ber.*, **18**, 1444 (1885); F. Ullmann, *ibid.*, **36**, 2382 (1903); I. Goldberg, *ibid.*, **39**, 1691 (1906); *idem*, *ibid.*, **40**, 4541 (1907); A. A. Goldberg and A. H. Walker, *J. Chem. Soc.*, **1953**, 1348.
- 5) A. A. Goldberg and A. H. Wragg, *J. Chem. Soc.*, **1958**, 4227.
- 6) A. A. Goldberg and A. H. Wragg, *J. Chem. Soc.*, **1958**, 4234.
- 7) G. Bender, *Ber.*, **13**, 696 (1880); *idem*, *ibid.*, **19**, 2265 (1886).
- 8) I. Granoth and H. J. Pownall, *J. Org. Chem.*, **40**, 2088 (1975).
- 9) O. Weber, *Ber.*, **25**, 1737 (1892).
- 10) H. E. Faith, M. E. Bahler and H. J. Florestano, *J. Am. Chem. Soc.*, **77**, 543 (1955).

[Chem. Pharm. Bull.]  
[35(1) 142-148 (1987)]

## Synthesis in the Diazasteroid Group. XX.<sup>1)</sup> Synthesis of the 5,14-Diazasteroid System<sup>2)</sup>

KATSUhide MATOBA,\* YOSHIRO HIRAI, MINORU TOKIZAWA, YUKO WAKUI,  
MASANORI NAGATA, and TAKAO YAMAZAKI

Faculty of Pharmaceutical Sciences, Toyama Medical & Pharmaceutical University,  
Sugitani, Toyama 930-01, Japan

(Received July 2, 1986)

*trans*-2-Quinolizidinone (I) was treated with methyl 2-pyrrolidylacetate (III) to give a mixture of two isomers, 5,14-diaza-1,6-cyclo-1,10-secogon-8-en-11-one (IV) and 5,14-diazagon-8-en-11-one (Va) in 8.6 and 2.7% yields, respectively. 1,2,3,3a,4,5,6,7,8,9-Decahydro-7-benzoylpyrrolo[1,2-*a*]-[1,6]-naphthyridin-5-one (VIb) [prepared from 1-benzoyl-4-piperidone (IIb) and III] was hydrolyzed and then allowed to react with methyl vinyl ketone to give a Michael adduct (VIc). It was treated with mercuric acetate to afford regio- and stereoselectively 5,14-diazagon-8-ene-2,11-dione (Vb), whose angular protons at the C<sub>10</sub> and C<sub>13</sub> were *anti* to each other. The structure of Vb was determined by X-ray crystallographic analysis. Compound Vb was converted to Va via a thio-ketal (Vc).

**Keywords**—diazasteroid; 5,14-diazasteroid; oxidative cyclization; mercuric acetate; X-ray crystallographic analysis

In our laboratory, a variety of diazasteroids have been synthesized for examination of their biological activity.<sup>1)</sup> In this paper, we will describe a synthesis of the 5,14-diazasteroid system which has not hitherto been synthesized, starting with *trans*-2-quinolizidinone (I) or 1-substituted 4-piperidone (II) and methyl 2-pyrrolidylacetate (III), as shown in Chart 1. Compound I was prepared by the known method<sup>3)</sup> in two steps from piperidine and methyl vinyl ketone (MVK). Compound III was synthesized in four steps from 2-pyrrolidone.<sup>4)</sup> A solution of I and III in toluene was refluxed in the presence of a catalytic amount of trifluoroacetic acid (TFA), using a Dean-Stark water separator. The reaction mixture showed four spots on thin layer chromatography (TLC), and each product was separated by column chromatography and preparative TLC. The first-eluted product was the starting material, I (34.9%), and the second-eluted product, mp 143–144 °C, was suggested to be 5,14-diaza-1,6-cyclo-1,10-secogon-8-en-11-one (IV), which exhibited characteristic AB-type ( $J=14$  Hz) signals at  $\delta$  2.72 and 3.74 in the nuclear magnetic resonance (NMR) spectrum due to the C<sub>10</sub>-protons interposed between the nitrogen atom and carbonyl group. Compound IV exhibited in the mass spectrum (MS) a strong peak at  $m/e$  163 due to the fragment produced by retro Diels-Alder reaction (extrusion of piperidene). The third-eluted product, mp 148–151 °C, showed similar physical data to IV and was considered to be a diastereomer of IV. The last-eluted product, which could not be crystallized, showed a strong peak due to M<sup>+</sup> (parent peak) – 1, but a weak fragment peak at  $m/e$  163 in the MS. This product was supposed to be a crude 5,14-diazagon-8-en-11-one (Va), which was confirmed later (*vide infra*). The yields of IV, a diastereomer of IV, and Va were 6.3, 2.3, and 2.7%, respectively. The poor yield of Va was ascribed to the formation of 2-(2-methoxycarbonylmethylpyrrolidyl)-*trans*-quinolizidin-2-ene in preference to the corresponding quinolizidin-1-ene as an intermediate. The preferential formation of 2-ene rather than 1-ene has already been found in *trans*-2-decalone.<sup>5)</sup>

Because of the preferential formation of IV rather than Va and the poor yields of IV and

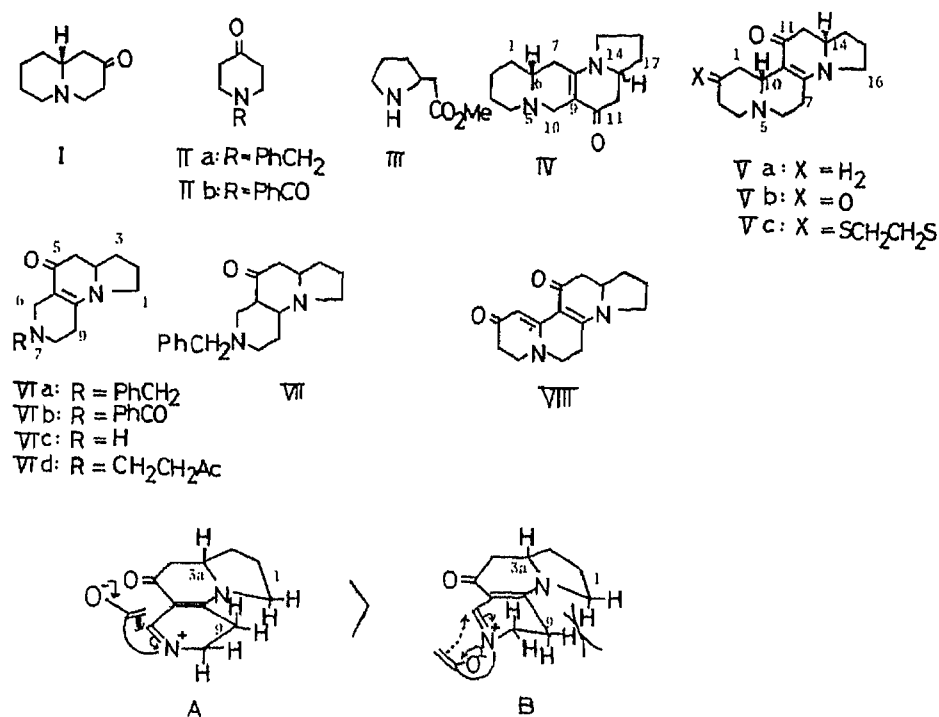


Chart 1

Va, we tried to obtain the 5,14-diazasteroid system from II. 1-Benzyl-4-piperidone (IIa) is commercially available and was treated with III in the presence of TFA as a catalyst in benzene to give 1,2,3,3a,4,5,6,7,8,9-decahydro-7-benzylpyrrolo[1,2-a][1,6]naphthyridin-5-one (VIa) in 33.3% yield accompanied with recovery of IIa (49.2%). The NMR spectrum of VIa showed an AB-type signal at  $\delta$  2.99 and 3.47 due to the C<sub>6</sub>-methylene protons, and a carbonyl band at 1605 cm<sup>-1</sup> was detected in the infrared (IR) spectrum. When *p*-toluenesulfonic acid (*p*-TsOH) was used as a catalyst, the yield of VIa was 28.4%, and the recovery of IIa was 40.9%. Trials of catalytic debenzoylation using Adams' catalyst<sup>6)</sup> gave an inseparable mixture and the catalytic reduction of VIa-hydrochloride using palladium-carbon<sup>7)</sup> gave a perhydro compound, 7-benzylperhydropyrrolo[1,2-a][1,6]naphthyridin-5-one (VII), mp 107–108 °C, which exhibited a carbonyl band at 1705 cm<sup>-1</sup> in the IR spectrum. The stereochemistry of the ring junctures could not be determined.

As attempts to debenzylate VIa failed, a similar reaction was carried out by using 1-benzoyl-4-piperidone (IIb) instead of IIa. Compound IIb was prepared in five steps starting with ethyl acrylate and liquid ammonia.<sup>8)</sup> Compound IIb was treated with III in the presence of a catalytic amount of TFA in benzene to give VIb in 55.6% yield accompanied with recovery of IIb (34.6%). When acetic acid was used as a catalyst, VIb was obtained in better yield in a reasonably pure state without using column chromatography. The NMR spectrum of VIb showed AB-type signals at  $\delta$  4.04 and 4.33 due to the C<sub>6</sub>-methylene protons and multiplet signals at  $\delta$  4.3–4.6 due to the C<sub>3a</sub> proton. Debenzoylation of VIb was performed with 20% sodium hydroxide-ethanol solution under reflux to give VIc in 98.4% yield. Compound VIc was treated with MVK at room temperature to afford a Michael addition product (VI d), which showed a singlet signal at  $\delta$  2.17 due to the methyl protons in the NMR spectrum and a carbonyl band at 1705 and 1605 cm<sup>-1</sup> in the IR spectrum. The cyclization of VI d was effected by mercuric acetate in 10% acetic acid followed by treatment with hydrogen sulfide to give a cyclized product, mp 190–191 °C, in 86.4% yield. Analyses using carbon-13 nuclear magnetic resonance (<sup>13</sup>C-NMR) spectroscopy and high-performance liquid chroma-

tography (HPLC) revealed that the product was diastereomerically pure. The NMR spectrum exhibited an octet-like signal at  $\delta$  3.5—3.8 due to the  $C_{13}$  proton. This product showed absorptions at 2880—2770, 1710, and 1605  $\text{cm}^{-1}$  due to the Bohlmann, carbonyl, and vinylogous lactam bands, respectively, in the IR spectrum. The Bohlmann bands suggested that the fusion of the A/B ring is *trans*. To establish the structure of the cyclized product, dehydrogenation was carried out. When treated with mercuric acetate for a long time, Vb gave a product in 70.5% yield, whose NMR spectrum showed a sharp singlet signal at  $\delta$  6.61 due to the vinylic proton. From the above data, the cyclized product and its dehydrogenation product were suggested to be 5,14-diazagon-8-ene-2,11-dione (Vb) and 5,14-diazagona-1(10),8-diene-2,11-dione (VIII), respectively. X-Ray crystallographic analysis of Vb was carried out to determine the stereochemistry, and it was revealed that the angular protons at the  $C_{10}$  and  $C_{13}$  were *anti* to each other, as shown in Fig. 1. Thus, the cyclization reaction of VI<sub>d</sub> using mercuric acetate proceeded regio- and stereoselectively to afford Vb. We considered that the conformer of the intermediate in the oxidative ring closure on VI<sub>d</sub> is probably A, which may involve less steric repulsion between  $C_1$  and  $C_9$  methylene protons than in B, and the enolate may approach the iminium ion from the sterically less hindered side, or the same side with respect to the  $C_{3a}$ -proton, maintaining maximum overlap of the orbitals of the enolate and iminium ion.<sup>9)</sup>

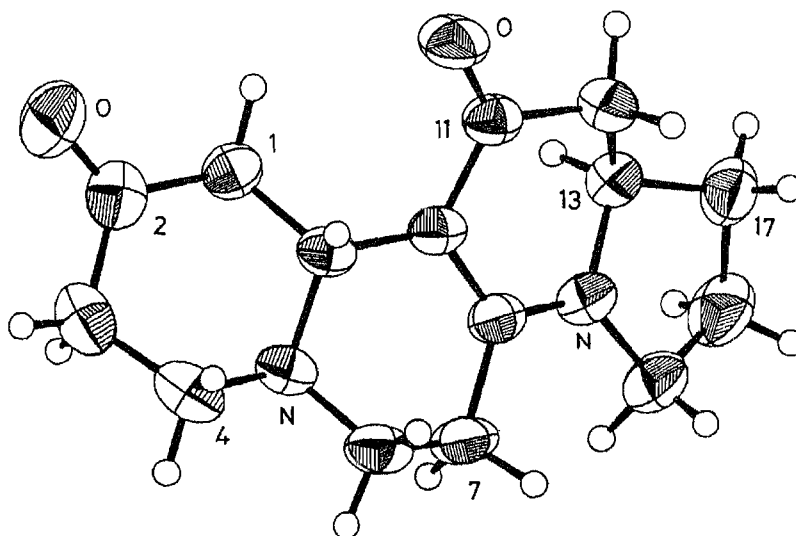


Fig. 1. ORTEP Drawing of Compound V<sub>b</sub>

Compound Vb was treated with ethanedithiol and borontrifluoride etherate at 60 °C for 2 h to afford a thioketal (Vc) in 93.4% yield. Compound Vc was then desulfurized with Raney nickel in dry ethanol at 60 °C for 2 h to give Va in 67.3% yield. The product was identified as the target compound on the basis of the elemental analysis, MS, and IR and NMR spectra. These physical data were nearly identical with those of the minor product obtained from I and III.

The biological activities of these synthesized compounds are now being examined.

#### Experimental

All melting points (taken on a Kofler block) and boiling points (bath temperature) are uncorrected. IR spectra were determined for solutions in  $\text{CHCl}_3$  by using a JASCO A 102 diffraction grating spectrophotometer; absorption data are given in  $\text{cm}^{-1}$ . Ultraviolet (UV) spectra were obtained in MeOH with a Hitachi 220 spectrometer, and

absorption maxima are given in nm. HPLC was carried out on a Shimadzu LC-3A apparatus equipped with a column packed with RP-select B and MeOH/0.035 M phosphate buffer (pH 6.9) = 60/40 as the eluent (flow rate: 1.0 ml/min). NMR spectra measured in  $\text{CDCl}_3$  were recorded on a Varian XL-200 spectrometer with tetramethylsilane as an internal standard. The chemical shifts and coupling constants ( $J$ ) are given in  $\delta$  and Hz, respectively. MS were measured with a JEOL D-200 or D-300 (70 eV, direct inlet system) spectrometer. All solvents were removed by evaporation under reduced pressure after drying of the solution over anhydrous  $\text{K}_2\text{CO}_3$ .

**Condensation of *trans*-2-Quinolizidinone (I) and Methyl 2-Pyrrolidylacetate (III)**—A mixture of I<sup>31</sup> (0.766 g, 5 mmol) and III<sup>41</sup> (0.939 g, 6.6 mmol), TFA (0.086 ml, 1.1 mmol), and toluene (30 ml) was heated to boiling in a flask equipped with a Dean-Stark water separator. After about 4 h, the mixture was cooled and washed with saturated aq.  $\text{NaHCO}_3$  and brine. The oily product obtained after removal of the solvent was fractionated through an  $\text{SiO}_2$  column. I (267 mg, 34.9%), 5,14-diaza-1,6-cyclo-1,10-secoogon-8-en-11-one (IV, 77.6 mg, 6.3%), a diastereoisomer of IV (28.2 mg, 2.3%), and 5,14-diazagon-8-en-11-one (Va, 33.5 mg, 2.7%) were eluted with 2, 3, 3, and 5% MeOH- $\text{CHCl}_3$ , respectively. IV: mp 143–144°C (recrystallized from isopropyl ether). IR:  $\nu_{\text{C}=\text{O}}$  1620, 1560. UV  $\lambda_{\text{max}}$ : 336. NMR: 1.1–2.8 (17H, m), 2.72 (1H, d,  $J=14$ ,  $\text{C}_{10}$ -H), 3.11 (1H, d,  $J=12$ ), 3.2–3.9 (2H, m,  $\text{C}_6$ -H and  $\text{C}_{13}$ -H), 3.74 (1H, d,  $J=14$ ,  $\text{C}_{10}$ -H). MS  $m/e$  (%): 246 ( $\text{M}^+$ , 53), 245 ( $\text{M}^+ - 1$ , 100), 203 ( $\text{M}^+ - 1 - \text{CH}_3\text{CO}$ , 16), 163 ( $\text{M}^+ - \text{piperidene}$ , 29). Anal. Calcd for  $\text{C}_{15}\text{H}_{22}\text{N}_2\text{O} \cdot 2/5\text{H}_2\text{O}$ : C, 71.06; H, 9.06; N, 11.05. Found: C, 71.02; H, 9.11; N, 10.94. High resolution MS, Calcd for  $\text{C}_{15}\text{H}_{22}\text{N}_2\text{O}$ : 246.1731. Found: 246.1718. Diastereomer of IV: mp 148–151°C (recrystallized from petr. ether). IR:  $\nu_{\text{C}=\text{O}}$  1625, 1565. UV  $\lambda_{\text{max}}$ : 334. NMR: 1.1–2.8 (17H, m), 2.74 (1H, d,  $J=14$ ,  $\text{C}_{10}$ -H), 3.11 (1H, d,  $J=12$ ), 3.3–3.5 (1H, m,  $\text{C}_6$ -H), 3.4–3.9 (1H, m,  $\text{C}_{13}$ -H), 3.75 (1H, d,  $J=14$ ,  $\text{C}_{10}$ -H). MS  $m/e$  (%): 246 ( $\text{M}^+$ , 53), 245 ( $\text{M}^+ - 1$ , 100), 203 ( $\text{M}^+ - 1 - \text{CH}_3\text{CO}$ , 20), 163 ( $\text{M}^+ - \text{piperidene}$ , 24). Anal. Calcd for  $\text{C}_{15}\text{H}_{22}\text{N}_2\text{O} \cdot 0.15\text{H}_2\text{O}$ : C, 72.34; H, 9.03; N, 11.25. Found: C, 72.35; H, 8.86; N, 11.06. Va (crude, *vide infra*): IR:  $\nu_{\text{C}=\text{O}}$  2810, 2750 (Bohlmann band),  $\nu_{\text{C}=\text{O}}$  1600. MS  $m/e$  (%): 246 ( $\text{M}^+$ , 53), 245 ( $\text{M}^+ - 1$ , 100), 217 ( $\text{M}^+ - 1 - \text{CO}$ , 39), 204 ( $\text{M}^+ - \text{CH}_3\text{CO}$ , 12), 190 ( $\text{M}^+ - \text{C}_4\text{H}_9$ , 29), 163 ( $\text{M}^+ - \text{piperidene}$ , 4). High-resolution MS, calcd for  $\text{C}_{15}\text{H}_{22}\text{N}_2\text{O}$ : 246.1731. Found: 246.1704.

**Condensation of 1-Benzyl-4-piperidone (IIa) and III**—A benzene solution of IIa (2.64 g, 14 mmol), III (2 g, 14 mmol), and TFA (0.1 ml, 1.3 mmol) was refluxed in a flask equipped with a Dean-Stark water separator for 20 h. The reaction mixture was cooled and washed with saturated  $\text{NaHCO}_3$  and brine. The crude product obtained after removal of the solvent was fractionated by  $\text{SiO}_2$  column chromatography. IIa (1.30 g, 49.2%) and 1,2,3,3a,4,5,6,7,8,9-decahydro-7-benzylpyrrolo[1,2-*a*][1,6]naphthyridin-5-one (VIa, 1.31 g, 33.3%) were eluted with  $\text{CHCl}_3$  and 2% MeOH- $\text{CHCl}_3$ , respectively. VIa: bp 112°C (1.5 mmHg). IR:  $\nu_{\text{C}=\text{O}}$  1605. UV  $\lambda_{\text{max}}$ : 338. NMR: 1.4–2.8 (10H, m), 2.99 (1H, d,  $J=13$ ,  $\text{C}_6$ -H), 3.34 (2H, t,  $J=8$ ,  $\text{C}_8$ -H), 3.47 (1H, d,  $J=13$ ,  $\text{C}_6$ -H), 3.56 (2H, d like,  $J=14$ ,  $\text{PhCH}_2$ -), 3.6–3.7 (1H, m,  $\text{C}_{3a}$ -H), 7.1–7.4 (5H, m, Ph). MS  $m/e$  (%): 282 ( $\text{M}^+$ , 24), 281 ( $\text{M}^+ - 1$ , 22), 191 ( $\text{M}^+ - \text{PhCH}_2$ , 100), 91 ( $\text{PhCH}_2^+$ , 82). Anal. Calcd for  $\text{C}_{18}\text{H}_{22}\text{N}_2\text{O} \cdot 1/10\text{H}_2\text{O}$ : C, 76.08; H, 7.87; N, 9.86. Found: C, 75.97; H, 7.98; N, 9.90.

**Catalytic Reduction of VIa**—VIa-hydrochloride, prepared from VIa (200 mg, 0.7 mmol) and HCl gas in  $\text{Et}_2\text{O}$ , was dissolved in dry MeOH. The methanolic solution was stirred in the presence of Pd-C (10%, 0.3 g) at room temperature under high pressure (80 atm) for 14 h. The filtrate was basified with  $\text{Et}_3\text{N}$  and concentrated. The residue was fractionated through an  $\text{SiO}_2$  column. 7-Benzylperhydropyrrolo[1,2-*a*][1,6]naphthyridin-5-one (VII) was eluted with 2% MeOH- $\text{CHCl}_3$ , 43 mg (21.3%), mp 107–108°C (recrystallized from  $\text{H}_2\text{O}$ ). IR:  $\nu_{\text{C}=\text{O}}$  2970, 2800,  $\nu_{\text{C}-\text{O}}$  1705. NMR: 1.4–2.1 (10H, m), 2.2–3.0 (4H, m), 3.0–3.3 (2H, m,  $\text{C}_{3a}$ -H and  $\text{C}_{5a}$ -H), 3.4–3.6 (1H, m,  $\text{C}_{3a}$ -H), 3.50 (2H, d like,  $J=4$ ,  $\text{CH}_2$ -Ph), 6.1–6.3 (5H, m, Ph). MS  $m/e$  (%): 284 ( $\text{M}^+$ , 37), 193 ( $\text{M}^+ - \text{CH}_2$ -Ph, 63), 91 ( $\text{PhCH}_2$ , 100). Anal. Calcd for  $\text{C}_{18}\text{H}_{24}\text{N}_2\text{O} \cdot 1/10\text{H}_2\text{O}$ : C, 75.54; H, 8.52; N, 9.79. Found: C, 75.46; H, 8.36; N, 9.73.

**Condensation of 1-Benzoyl-4-piperidone (IIb) with III**—A benzene solution (100 ml) of IIb<sup>31</sup> (12.7 g, 89 mmol), III (16 g, 79 mmol), and AcOH (20 ml) was refluxed using the same apparatus as mentioned above for 15 h. The cooled mixture was washed with saturated aq.  $\text{NaHCO}_3$  and brine. The solid obtained after removal of the organic solvent was recrystallized from acetone to give 7-benzoyl-1,2,3,3a,4,5,6,7,8,9-decahydropyrrolo[1,2-*a*][1,6]naphthyridin-5-one (VIb). The mother liquor was concentrated and fractionated by  $\text{SiO}_2$  column chromatography. IIb (0.94 g, 5.9%) and VIb were eluted with  $\text{CH}_2\text{Cl}_2$  and 3% MeOH- $\text{CH}_2\text{Cl}_2$ , respectively. The combined yield of VIb was 17 g (72.9%), mp 144–145°C (colorless needles). IR:  $\nu_{\text{C}=\text{O}}$  1605, 1545. NMR: 1.5–2.7 (8H, m), 3.1–3.4 (1H, m,  $\text{C}_4$ -H), 3.44 (2H, t,  $J=8$ ,  $\text{C}_8$ -H), 3.5–3.8 (1H, m,  $\text{C}_4$ -H), 4.04 and 4.33 (each 1H, d,  $J=14$ ,  $\text{C}_6$ -H), 4.3–4.6 (1H, m,  $\text{C}_{3a}$ -H), 7.38 (5H, br s, aromatic H). MS  $m/e$  (%): 296 ( $\text{M}^+$ , 29), 191 ( $\text{M}^+ - \text{PhCO}$ , 63), 149 ( $m/e$  191- $\text{C}_2\text{H}_4\text{N}$ , 100), 105 ( $\text{PhCO}^+$ , 50). Anal. Calcd for  $\text{C}_{18}\text{H}_{20}\text{N}_2\text{O}_2$ : C, 72.95; H, 6.80; N, 9.45. Found: C, 72.90; H, 6.79; N, 9.45.

**1,2,3,3a,4,5,6,7,8,9-Decahydropyrrolo[1,2-*a*][1,6]naphthyridin-5-one (VIc)**—NaOH (20% aq. solution, 20 ml) was added to an ethanolic solution (20 ml) of VIb (4.5 g, 15.3 mmol), and then the mixture was heated under reflux for 2 h. The residue obtained after removal of the solvent was dissolved in  $\text{CH}_2\text{Cl}_2$ , and the solution was washed with water. The residue obtained after removal of the solvent was recrystallized from  $\text{CH}_2\text{Cl}_2$  to give pure VIc. mp 119–120°C (colorless needles). The yield was 2.9 g (98.4%). NMR: 1.0–2.8 (9H, m), 2.97 and 3.07 (each 1H, d,  $J=13$ ,  $\text{C}_6$ -H), 3.2–4.3 (5H, m). MS  $m/e$  (%): 192 ( $\text{M}^+$ , 61), 191 ( $\text{M}^+ - 1$ , 100), 163 ( $\text{M}^+ - 1 - \text{CO}$ , 25).

**7-(3-Oxo-1-butyl)-1,2,3,3a,4,5,6,7,8,9-decahydropyrrolo[1,2-*a*][1,6]naphthyridin-5-one (VIId)**—MVK (1.05 g, 15.1 mmol) was added to a solution of VIc (2.9 g, 15.1 mmol) in  $\text{CH}_2\text{Cl}_2$  (10 ml), and the mixture was stirred at room

temperature for 12 h. The residue obtained after removal of the solvent was recrystallized from isopropyl alcohol to give VI<sub>d</sub> (2.9 g, 74%). mp 73–75°C. IR:  $\nu_{\text{CH}}$  2880, 2810, 2770 (Bohlmann band),  $\nu_{\text{C=O}}$  1705, 1605. NMR: 1.5–2.5 (6H, m), 2.17 (3H, s, CH<sub>3</sub>CO), 2.47 and 2.74 (each 2H, t,  $J=5$ , –COCH<sub>2</sub>CH<sub>2</sub>N<), 2.6–2.8 (4H, m, C<sub>4</sub>- and C<sub>9</sub>-H), 2.96 and 3.47 (each 1H, d,  $J=13$ , C<sub>6</sub>-H), 3.3–3.6 (2H, m, C<sub>8</sub>-H), 3.5–3.8 (1H, octet like, C<sub>3a</sub>-H). MS  $m/e$  (%): 262 (M<sup>+</sup>, 33), 261 (M<sup>+</sup>–1, 82), 204 (M<sup>+</sup>–acetone, 84), 192 (VI<sub>c</sub>, 45), 191 (100). Anal. Calcd for C<sub>15</sub>H<sub>22</sub>N<sub>2</sub>O<sub>2</sub>: C, 68.07; H, 8.45; N, 10.68. Found: C, 68.61; H, 8.22; N, 10.54.

**5,14-Diazagon-8-ene-2,11-dione (Vb)**—VI<sub>d</sub> (0.49 g, 1.9 mmol) was added to a solution of Hg(OAc)<sub>2</sub> (2.4 g, 7.5 mmol) in 10% AcOH (35 ml). The mixture was heated at 100°C for 2.5 h. The precipitated Hg<sub>2</sub>(OAc)<sub>2</sub> was filtered off and then H<sub>2</sub>S gas was bubbled into the filtrate. The resulting mixture was filtered through celite and concentrated. The residue was treated with aq. NH<sub>3</sub> and the alkaline solution was extracted with CH<sub>2</sub>Cl<sub>2</sub> (20 ml × 3). The combined organic layer was washed with brine and concentrated. The residue was recrystallized from acetone to give Vb (0.42 g, 86.4%). mp 190–191°C (colorless needles). HPLC:  $t_R$  3.71 min. IR:  $\nu_{\text{CH}}$  2880, 2820, 2770 (Bohlmann band),  $\nu_{\text{C=O}}$  1710, 1605. UV  $\lambda_{\text{max}}$  ( $\epsilon$ ): 332 (16000). NMR: 1.4–3.2 (16H, m), 3.32 and 3.50 (each 1H, dd,  $J=15$ , 5, C<sub>1</sub>-H), 3.46 (1H, m, C<sub>10</sub>-H), 3.5–3.8 (1H, octet like, C<sub>13</sub>-H). <sup>13</sup>C-NMR: 212.2 (C<sub>2</sub>), 188.0 (C<sub>11</sub>), 157.4 (C<sub>8</sub>), 106.1 (C<sub>9</sub>), 58.7, 57.4, 53.9, 48.5, 47.1, 46.6, 42.3, 41.0, 32.5, 29.0, 23.8. MS  $m/e$  (%): 260 (M<sup>+</sup>, 51), 259 (M<sup>+</sup>–1, 100), 217 (M<sup>+</sup>–1–CH<sub>2</sub>CO, 31), 190 (M<sup>+</sup>–C<sub>4</sub>H<sub>6</sub>O, 86), 175 (41), 163 (M<sup>+</sup>–piperidone, 4). Anal. Calcd for C<sub>15</sub>H<sub>22</sub>N<sub>2</sub>O<sub>2</sub>: C, 69.20; H, 7.74; N, 10.76. Found: C, 69.05; H, 7.78; N, 10.61.

**5,14-Diazagona-1(10),8-diene-2,11-dione (VIII)**—Vb (1 g, 3.9 mmol) was added to a solution of Hg(OAc)<sub>2</sub> (4.9 g, 15 mmol) in 10% AcOH (50 ml), and then the mixture was heated at 100°C for 8.5 h. The resulting mixture was saturated with H<sub>2</sub>S and filtered through celite. The filtrate was concentrated and basified with aq. NH<sub>3</sub>. The alkaline solution was extracted with CH<sub>2</sub>Cl<sub>2</sub> (50 ml × 3). The organic layer was washed with brine and concentrated. The residue was fractionated through an SiO<sub>2</sub> column. Vb (110 mg, 11.1%) and VIII (700 mg, 70.5%) were eluted successively with CHCl<sub>3</sub>. VIII: mp 223–225°C (recrystallized from CH<sub>2</sub>Cl<sub>2</sub>, colorless needles). IR:  $\nu_{\text{C=O}}$  1625, 1600. UV  $\lambda_{\text{max}}$  ( $\epsilon$ ): 355 (36000). NMR: 1.7–3.8 (16H, m), 3.7–4.0 (1H, octet like, C<sub>13</sub>-H), 6.61 (1H, s, C<sub>1</sub>-H). MS  $m/e$  (%): 259 (M<sup>+</sup>+1, 20), 258 (M<sup>+</sup>, 100), 257 (M<sup>+</sup>–1, 35), 230 (M<sup>+</sup>–CO, 40), 229 (75), 175 (M<sup>+</sup>–2-methylenepyrrolidine, 25), 108 (*N*-methylene-4-pyridone, 27). Anal. Calcd for C<sub>15</sub>H<sub>18</sub>N<sub>2</sub>O<sub>2</sub>: C, 69.74; H, 7.02; N, 10.85. Found: C, 69.47; H, 7.15; N, 10.60.

**Vb-2-ethanedithioketal (Vc)**—BF<sub>3</sub>·Et<sub>2</sub>O (47%, 3.5 ml 32.2 mmol) was added at 0°C to a mixture of Vb (0.5 g, 1.9 mmol) and ethanedithiol (2 ml, 23.8 mmol), and then the mixture was heated at 60°C for 2 h. The reaction mixture basified with 5% K<sub>2</sub>CO<sub>3</sub> was extracted with CH<sub>2</sub>Cl<sub>2</sub> (50 ml × 3). The organic layer was washed with brine and then dried over CaSO<sub>4</sub>. The viscous syrup obtained after removal of the solvent was fractionated through an SiO<sub>2</sub> column. Vc (0.6 g, 93.4%) was eluted with 1% MeOH–CHCl<sub>3</sub> and recrystallized from acetone. mp 230–235°C (colorless needles). IR:  $\nu_{\text{CH}}$  2950, 2830, 2770 (Bohlmann band),  $\nu_{\text{C=O}}$  1600, 1540. NMR: 3.35 (4H, s like, –CH<sub>2</sub>–S–). <sup>13</sup>C-NMR: 189.2 (C<sub>11</sub>), 158.4 (C<sub>8</sub>), 106.8 (C<sub>9</sub>). MS  $m/e$  (%): 336 (M<sup>+</sup>, 33), 275 (M<sup>+</sup>–C<sub>2</sub>H<sub>5</sub>S, 63), 243 (M<sup>+</sup>–C<sub>2</sub>H<sub>5</sub>S<sub>2</sub>, 39), 204 ( $m/e$  243–C<sub>3</sub>H<sub>3</sub>, 100). Anal. Calcd for C<sub>17</sub>H<sub>24</sub>N<sub>2</sub>OS<sub>2</sub>: C, 60.68; H, 7.19; N, 8.32. Found: C, 60.38; H, 7.24; N, 8.09.

**5,14-Diazagon-8-en-11-one (Va)**—An ethanolic solution of Vc (0.49 g, 2.0 mmol) and Raney-Ni (9.8 g) was heated at 50°C for 9 h. The catalyst was removed and the filtrate was concentrated to give a viscous syrup, which was fractionated through an Al<sub>2</sub>O<sub>3</sub> column. Va (238 mg, 67.3%) was eluted with CHCl<sub>3</sub> and recrystallized from Et<sub>2</sub>O. mp 104–106°C (colorless needles). IR:  $\nu_{\text{CH}}$  2810, 2750 (Bohlmann band),  $\nu_{\text{C=O}}$  1600. UV  $\lambda_{\text{max}}$  ( $\epsilon$ ): 332 (11000). NMR: 0.9–2.7 (12H, m), 2.78 (2H, t,  $J=6$ , C<sub>7</sub>-H), 2.94 (2H, brs, C<sub>12</sub>-H), 3.46 (2H, t,  $J=6$ , C<sub>6</sub>-H), 3.4–3.6 (1H, m, C<sub>10</sub>-H), 3.4–3.8 (1H, octet like, C<sub>13</sub>-H). <sup>13</sup>C-NMR: 188.7 (C<sub>11</sub>), 158.0 (C<sub>8</sub>), 98.8 (C<sub>9</sub>), 61.1, 57.2, 56.3, 50.0, 46.5, 42.9, 32.5, 31.3, 29.1, 25.9, 25.2, 23.9. MS  $m/e$  (%): 246 (M<sup>+</sup>, 57), 245 (M<sup>+</sup>–1, 100), 217 (M<sup>+</sup>–1–CO or M<sup>+</sup>–1–C<sub>2</sub>H<sub>4</sub>, 39), 204 (M<sup>+</sup>–CH<sub>2</sub>CO, 12), 190 (M<sup>+</sup>–C<sub>4</sub>H<sub>6</sub>O, 25), 163 (M<sup>+</sup>–piperidene, null). Anal. Calcd for C<sub>15</sub>H<sub>22</sub>N<sub>2</sub>O: C, 73.13; H, 9.00; N, 11.37. Found: C, 73.07; H, 8.99; N, 11.19.

**X-Ray Analysis of Compound Vb**—Intensity measurements were performed with a Rigaku AFC 5R automatic

TABLE I. Crystal Data for Compound V<sub>b</sub>

Molecular formula	C <sub>15</sub> H <sub>20</sub> N <sub>2</sub> O <sub>2</sub>
Molecular weight	260.33
Crystal system	Triclinic
Space group	$P\bar{1}$
Cell dimensions	$a$ 11.80 (3) Å
	$b$ 13.56 (9)
	$c$ 8.55 (7)
	$v$ 1332.5 (4) Å <sup>3</sup>
	$z$ 4
	$D_x$ 1.298 g cm <sup>-3</sup>
Final $R$ value	5.1%

TABLE II. Fractional Coordinates of Non-hydrogen Atoms with Estimated Standard Deviations in Parenthesis

Atom	x	y	z	B
C(1)	-0.618 (3)	-0.405 (9)	-0.160 (3)	0.006 (5)
C(2)	-0.707 (0)	-0.381 (8)	-0.059 (4)	0.007 (9)
C(3)	-0.659 (3)	-0.353 (2)	0.113 (6)	0.010 (1)
C(4)	-0.556 (2)	-0.288 (3)	0.136 (8)	0.011 (2)
N(5)	-0.469 (7)	-0.332 (3)	0.050 (5)	0.008 (3)
C(6)	-0.362 (4)	-0.280 (2)	0.089 (7)	0.010 (6)
C(7)	-0.267 (7)	-0.340 (8)	0.028 (2)	0.007 (7)
C(8)	-0.310 (4)	-0.375 (7)	-0.144 (8)	0.006 (7)
C(9)	-0.426 (7)	-0.364 (1)	-0.218 (2)	0.006 (4)
C(10)	-0.518 (4)	-0.334 (5)	-0.123 (2)	0.007 (0)
C(11)	-0.459 (4)	-0.365 (9)	-0.391 (4)	0.007 (0)
C(12)	-0.362 (9)	-0.391 (7)	-0.480 (7)	0.007 (8)
C(13)	-0.270 (6)	-0.460 (1)	-0.387 (3)	0.006 (6)
N(14)	-0.231 (7)	-0.416 (0)	-0.224 (0)	0.005 (7)
C(15)	-0.107 (0)	-0.434 (4)	-0.160 (5)	0.005 (7)
C(16)	-0.069 (2)	-0.503 (0)	-0.289 (8)	0.006 (3)
C(17)	-0.157 (1)	-0.480 (2)	-0.444 (0)	0.007 (4)
O(2)	-0.810 (5)	-0.387 (8)	-0.114 (0)	0.007 (3)
O(10)	-0.558 (3)	-0.342 (0)	-0.466 (2)	0.007 (6)

TABLE III. Bond Distances (Å) for the Non-hydrogen Atoms

C(1)-C(2)	1.505 (3)	C(1)-C(10)	1.538 (2)	C(2)-C(3)	1.497 (3)
C(2)-O(2)	1.214 (2)	C(3)-C(4)	1.515 (3)	C(4)-N(5)	1.462 (3)
N(5)-C(6)	1.450 (3)	N(5)-C(10)	1.471 (2)	C(6)-C(7)	1.513 (3)
C(7)-C(8)	1.508 (2)	C(8)-C(9)	1.383 (2)	C(8)-N(14)	1.337 (2)
C(9)-C(10)	1.511 (3)	C(9)-C(11)	1.446 (2)	C(11)-C(12)	1.516 (3)
C(11)-O(11)	1.238 (2)	C(12)-C(13)	1.511 (2)	C(13)-N(14)	1.469 (2)
C(13)-C(17)	1.525 (3)	N(14)-C(15)	1.466 (2)	C(15)-C(16)	1.520 (4)
C(16)-C(17)	1.526 (3)				

TABLE IV. Valence Angles (°) for the Non-hydrogen Atoms

C(10)-C(1)-C(2)	112.82 (15)	C(1)-C(2)-C(3)	111.43 (19)
C(1)-C(2)-O(2)	122.04 (18)	C(3)-C(2)-O(2)	122.21 (21)
C(2)-C(3)-C(4)	112.43 (19)	C(3)-C(4)-N(5)	110.82 (16)
C(4)-N(5)-C(10)	109.66 (13)	C(4)-N(5)-C(6)	112.23 (14)
C(6)-N(5)-C(10)	110.47 (14)	N(5)-C(6)-C(7)	110.03 (15)
C(6)-C(7)-C(8)	110.51 (14)	C(7)-C(8)-C(9)	120.69 (16)
C(7)-C(8)-N(14)	117.52 (14)	C(9)-C(8)-N(14)	121.77 (14)
C(8)-C(9)-C(10)	121.69 (14)	C(8)-C(9)-C(11)	119.07 (16)
C(10)-C(9)-C(11)	118.60 (14)	C(1)-C(10)-C(9)	111.76 (13)
C(1)-C(10)-N(5)	107.77 (14)	C(9)-C(10)-N(5)	111.60 (13)
C(9)-C(11)-C(12)	116.43 (14)	C(9)-C(11)-O(11)	123.33 (17)
C(12)-C(11)-O(11)	120.08 (15)	C(11)-C(12)-C(13)	111.00 (15)
C(12)-C(13)-C(17)	118.39 (17)	C(12)-C(13)-N(14)	108.84 (15)
N(14)-C(13)-C(17)	102.89 (14)	C(8)-N(14)-C(13)	119.44 (13)
C(8)-N(14)-C(15)	127.40 (15)	C(13)-N(14)-C(15)	112.64 (16)
N(14)-C(15)-C(16)	103.38 (16)	C(15)-C(16)-C(17)	104.86 (19)
C(16)-C(17)-C(13)	103.09 (19)		

4-circle diffractometer using monochromated Cu- $K_{\alpha}$  radiation. Colorless single crystals of Vb for X-ray study were obtained from acetone. The crystal data for Vb are listed in Table I. Intramolecular bond distances (Å) and valence angles ( $^{\circ}$ ) for the non-hydrogen atoms are given in Tables II and III, respectively.

**Acknowledgement** The authors thank Dr. C. Katayama of the analytical center of Rigaku Denki Co., Ltd., and also Mr. M. Morikoshi and Mr. M. Ogawa for the measurements of  $^{13}\text{C}$ -NMR spectra and elemental analyses, respectively.

#### References and Notes

- 1) K. Matoba, M. Shibata, and T. Yamazaki, *Chem. Pharm. Bull.*, **30**, 1718 (1982).
- 2) A part of this work was presented at the 64th Meeting of the Hokuriku Branch of the Pharmaceutical Society of Japan, Kanazawa, November 1984.
- 3) S. F. Mason, K. Schofield, and R. J. Wells, *J. Chem. Soc. (C)*, **1967**, 626.
- 4) T. Yamazaki, K. Matoba, M. Yajima, and M. Nagata, *J. Heterocycl. Chem.*, **12**, 973 (1975).
- 5) H. O. House and B. M. Trost, *J. Org. Chem.*, **30**, 1341 (1965).
- 6) J. S. Buck and R. Baltzly, *J. Am. Chem. Soc.*, **63**, 1964 (1941).
- 7) T. Shono, H. Hamaguchi, M. Sasaki, S. Fujita, and K. Nagami, *J. Org. Chem.*, **48**, 1621 (1983).
- 8) S. M. McElvain and R. E. McMahon, *J. Am. Chem. Soc.*, **71**, 901 (1949).
- 9) P. Deslongchamps, "Streolectronic Effects in Organic Chemistry," Pergamon Press, Inc., New York, 1983, pp. 211—221.



[Chem. Pharm. Bull.]  
35(1) 149-155 (1987)

## Tannins and Related Compounds. L.<sup>1)</sup> Structures of Proanthocyanidin A-1 and Related Compounds

GEN-ICHIRO NONAKA,<sup>a</sup> SATOSHI MORIMOTO,<sup>a</sup> JUN-EI KINJO,<sup>b</sup>  
TOSHIHIRO NOHARA,<sup>b</sup> and ITSUO NISHIOKA\*<sup>a</sup>

*Faculty of Pharmaceutical Sciences, Kyushu University,<sup>a</sup> 3-1-1 Maidashi, Higashi-ku, Fukuoka 812,  
Japan and Faculty of Pharmaceutical Sciences, Kumamoto University,<sup>b</sup>  
Oe-honmachi 5-1, Kumamoto 862, Japan*

(Received July 2, 1986)

The structures of proanthocyanidin A-1 (**2**) and two related proanthocyanidins, tentatively named A-4 (**3**) and A-5' (**4**), have been established unambiguously on the basis of spectroscopic evidence and chemical correlations with the structurally known proanthocyanidin A-2 (**1**). Chemical transformation of singly linked proanthocyanidin B-1 (**6**) into **2** also confirmed the stereostructure of **2**.

**Keywords**—proanthocyanidin A-1; A-type proanthocyanidin; chemical correlation; epimerization; enantiomer; diastereoisomer; polyphenol; flavan-3-ol; catechin

Proanthocyanidins, the oligomers and polymers of which have long been referred to as "condensed tannins or non-hydrolyzable tannins," fall into three distinct classes. One of these consists of flavan-3-ol units linked singly through carbon-carbon linkages at C(4)-C(8) or C(4)-C(6), and is readily convertible by heating with mineral acids into the common anthocyanidins, pelargonidin, cyanidin and delphinidin (the dimers and trimers of this class are designated as proanthocyanidin B-<sup>2)</sup> and C-types,<sup>3)</sup> respectively, and are the most commonly present in the vegetable tissues of plants). Another class possesses structures in which two flavan-3-ol units are joined doubly by ether and carbon-carbon linkages, and it is decomposed by acid treatment with the production of a mixture of uncharacterized flavylum salts (the dimers are designated as proanthocyanidin A-type).<sup>2)</sup> The third class, related to the second in complex anthocyanidin formation, includes a series of compounds containing a substituent, such as a C<sub>6</sub>-C<sub>3</sub> or a chalcane moiety, which is attached to the flavan-3-ol framework (*e.g.*, cinchonans,<sup>4)</sup> kandelins<sup>5)</sup> and gambiriins).<sup>6)</sup>

The chemistry and structures of the lower-molecular-weight proanthocyanidins of the first class, especially those of the dimers and trimers, have been almost entirely elucidated during the past few years.<sup>3,5,7-9)</sup> In contrast, much of the chemistry of the second group of proanthocyanidins still remains unclarified, although proanthocyanidins of this type are found as relatively common constituents among plant polyphenolics.

The A-type proanthocyanidins (A-1, A-2 and A-3) were first isolated as methyl ethers by Weinges and his collaborators from *Vaccinium vitis-idaea* and *Aesculus hippocastanum*.<sup>2)</sup> The structure **1** of proanthocyanidin A-2 was later deduced by Haslam and his co-workers based mainly on spectroscopic evidence,<sup>10)</sup> and more recently, the structure was unequivocally established by X-ray crystallography.<sup>11)</sup> As for proanthocyanidins A-1 and A-3, there is no report on their structures except that the same structure **1** as that of A-2 was formerly proposed for A-1.<sup>12)</sup>

In the course of chemical examination of vegetable tannins, we have isolated proanthocyanidin A-1 (**2**) and two related proanthocyanidins (**3** and **4**) (tentatively named A-4

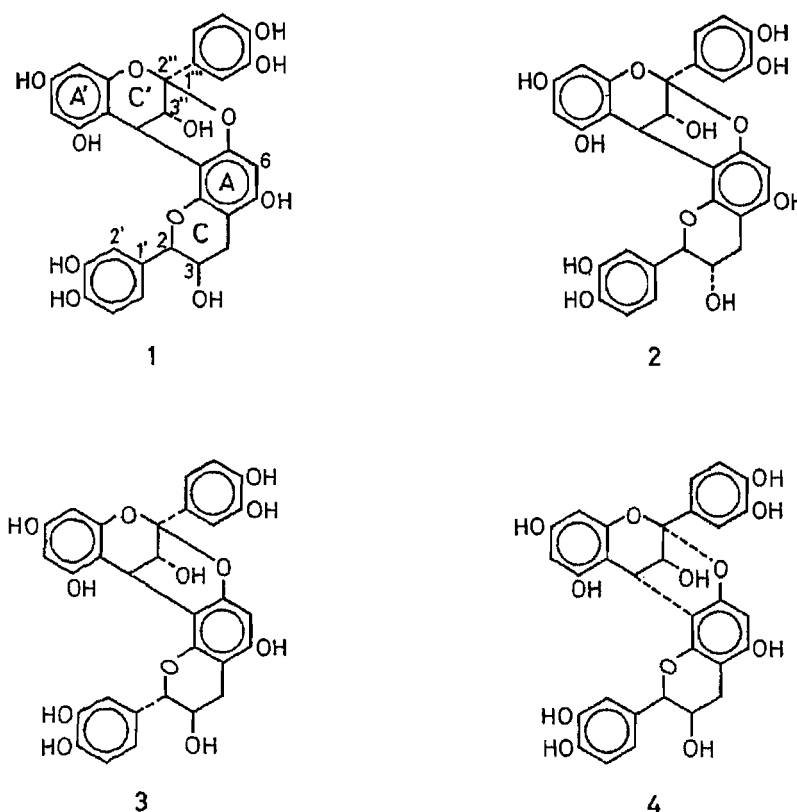


Chart 1

and A-5') from various plant sources, and chemical correlations between A-2 (1) and these compounds have now established their structures. Here, we wish to present unequivocal proof of the structures.

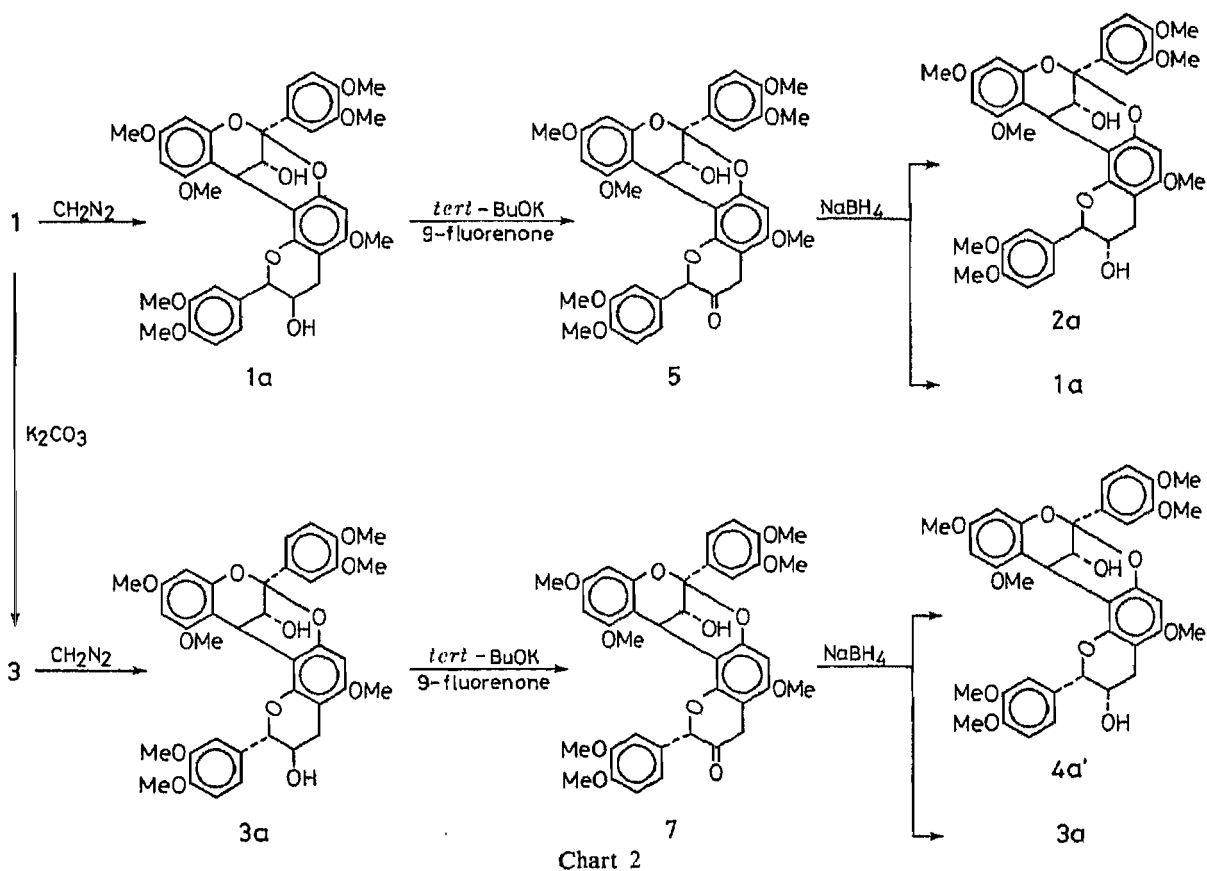
Proanthocyanidin A-1 (2) was isolated in a crystalline form from *Areca catechu*,<sup>7)</sup> *Vaccinium vitis-idaea*, *Cinnamomum sieboldii* and *C. camphora*. The proton-nuclear magnetic resonance (<sup>1</sup>H-NMR) spectrum of 2 resembled that of A-2 (1), but differed in flavan C-ring signals. The appearance of a doublet ( $J=8$  Hz) at  $\delta$  4.73 due to C(2)-H suggested the presence of a flavan-3-ol moiety with 2,3-*trans* (catechin-type) stereochemistry. This was supported by the carbon-13 nuclear magnetic resonance (<sup>13</sup>C-NMR) chemical shift ( $\delta$  84.1) of C(2), which is consistent with that ( $\delta$  82.3) observed in catechin.<sup>3)</sup> Methylation of 2 with diazomethane yielded the heptamethyl ether (2a). The <sup>1</sup>H-NMR spectrum of 2a showed, together with six methoxyl signals at  $\delta$  3.6—3.9, one upfield methoxyl signal at  $\delta$  3.32 assignable to the C(5'')-methoxyl on the basis of nuclear Overhauser effect (NOE) measurements. This unusual upfield shift may be interpreted in terms of a through-space interaction of the lower flavan B-ring, thus suggesting that the two flavan units are linked through the C(4'')- and C(8)-positions. The chemical shift of the above-mentioned C(2)-H signal in 2 also supports the location of the interflavanoid linkage at C(4'')-C(8); a lower field shift of this signal than that of catechin ( $\delta$  4.57) implies the presence of steric interaction between C(2)-H and the upper flavan aromatic ring.<sup>7)</sup> On the basis of these observations, A-1 was presumed to be formulated as 2.

To determine the structure unequivocally, derivation of A-1 from A-2 (1) was attempted. Selective oxidation of one of two alcoholic hydroxyl groups in the heptamethyl ether (1a) was achieved by the modified Oppenauer method using potassium *tert*-butoxide and 9-fluorenone.<sup>13)</sup> Other oxidation methods using chromium trioxide, dimethyl sulfoxide-acetic

TABLE I.  $^{13}\text{C}$ -NMR Chemical Shifts of A, C-Ring Carbons in A-Type Proanthocyanidins

Carbon No.	1 <sup>a)</sup>	2 <sup>a)</sup>	3 <sup>a)</sup>	4 <sup>a)</sup>	1a <sup>b)</sup>	2a <sup>b)</sup>	3a <sup>b)</sup>	4a <sup>b)</sup>	5 <sup>b)</sup>	7 <sup>b)</sup>
2	81.1	84.1	83.6	80.6	78.3	80.8	81.4	78.1	83.6	83.1
3	65.7	66.9	67.9	66.6	65.5	67.1	68.7	66.6	205.2	205.9
4	28.5	28.6	— <sup>d)</sup>	— <sup>d)</sup>	28.7	29.1	28.4	28.1	33.0	34.3
2''	103.6	103.5	103.8	103.9	103.9	103.6	103.4	104.0	103.3	103.5 <sup>c)</sup>
3''	67.1	67.3	67.2	67.3	67.5	67.1	67.1	67.2	67.2	67.2
4''	28.7	29.5	— <sup>d)</sup>	— <sup>d)</sup>	27.7	27.4	27.4	27.6	27.6	27.6
4a	99.5	99.6	100.0	100.1	99.0	99.0	99.0	99.2	99.4	99.3
4a''	102.0	102.8	102.6	101.7	101.7	101.4	102.8	101.3	102.1	103.7 <sup>c)</sup>
6,8,6''	96.0 (2C)	96.0 (2C)	96.2	96.2	92.1	91.6	91.8	92.2	92.6	93.0
	97.7	97.6	96.5	96.4	93.2	92.5	92.3	92.7	93.2	93.4
			97.9	97.7	93.5	92.9	92.8	93.1	93.4	94.1
8''	106.3	106.2	106.3	106.5	106.7	105.8	106.0	106.5	107.3	108.2
5,7,9,	151.2 (2C)	150.8	150.5	150.9	151.2	152.4	150.8	151.0	151.2	151.3
5'',7'',9''	153.4	151.3	151.8	151.6	151.6	153.1	151.2	151.3	151.9	152.2
	155.6	153.5	153.9	154.0	152.9	154.9	152.8	153.1	153.3	152.9
	156.0	155.2	155.6	156.1	157.6	157.0	156.8	157.7	156.5	156.4
	157.2	155.8	156.4	156.6	159.0	158.2	158.3	158.7	158.5	158.6
		157.3	157.9	157.9	159.9	159.5	159.5	159.8	160.1	160.1

a) Measured in acetone- $d_6$  +  $\text{D}_2\text{O}$ . b) Measured in  $\text{CDCl}_3$ . c) Assignments may be interchanged. d) Overlapped with solvent signals.



anhydride, dimethyl sulfoxide-dicyclohexylcarbodiimide and phosphorus pentoxide-dimethyl formamide, yielded a complex mixture of products. The structure of the mono-ketone (**5**) was confirmed by  $^1\text{H}$ - and  $^{13}\text{C}$ -NMR measurements, which clearly indicate the presence of a

carbonyl ( $\delta$  205.2), an isolated methine ( $\delta$  5.31, s) and a methylene ( $\delta$  3.32 and 3.59, each d,  $J=16$  Hz). Subsequent reduction of **5** with sodium borohydride afforded two products in the ratio of *ca.* 1:3, found to be identical with **2a** and **1a**. Thus, the structure of A-1 was established unequivocally to be **2**.

It should be noted that **2** was obtainable from procyanidin B-1 (**6**), a singly linked proanthocyanidin, by oxidation with hydrogen peroxide in a weakly alkaline medium. This fact clearly indicates that the stereostructure including absolute configuration can be represented as **2**.

The new dimeric proanthocyanidin, A-4 (**3**), was obtained as colorless prisms from the seed shells of *Aesculus hippocastanum*. It formed a heptamethyl ether (**3a**) on methylation with diazomethane. The  $^1\text{H-NMR}$  spectrum of **3** was almost indistinguishable from that of **2**, but comparison of the  $^1\text{H-NMR}$  spectra of their methyl ethers **3a** and **2a** permitted the differentiation of these compounds. The chemical shifts for the methoxyls and the lower C-ring protons in **3a** were different from those in **2a**. The unusual upfield shift ( $\delta$  3.12) of one methoxyl group, similar to that observed in **2a**, was consistent with the C(4'')-C(8) linkage of two flavan units. From these observations, **3** was assumed to be a diastereoisomer of **2**. The structure of **3** was further confirmed by successful epimerization of C(2) in **1** with weak alkali (potassium carbonate in acetone), providing **3** in a fairly good yield.

Another new proanthocyanidin, A-5' (**4**) was isolated from a commercial *Ephedra* plant (Japanese name: Maō). The  $^1\text{H-NMR}$  spectrum was closely correlated with that of **1**, showing a similar broad singlet due to C(2)-H at  $\delta$  5.08. A characteristic upfield shift of one methoxyl signal was also observed at  $\delta$  3.14 in the  $^1\text{H-NMR}$  spectrum of the heptamethyl ether (**4a**). Accordingly, **4** was considered to be an epimer of **1** with respect to the C(2)- and C(3)-

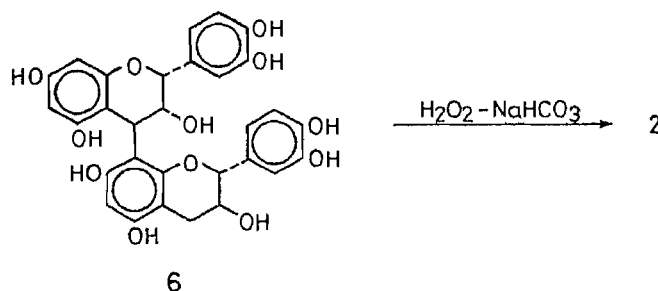
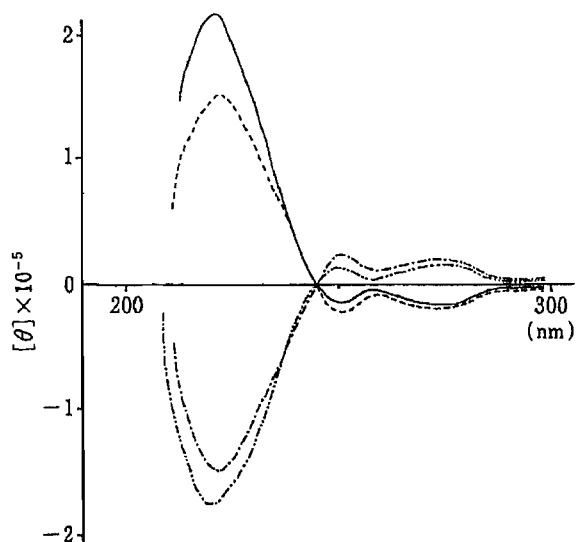


Chart 3

Fig. 1. CD Spectra of **3a**, **3a'**, **4a** and **4a'** (in MeOH)

—, **4a'**; - - - -, **3a**; ·····, **3a'**; - · - ·, **4a**.

positions.

Further structural confirmation was obtained by similar synthetic methods. The methyl ether (3a) was subjected to the above-mentioned modified Oppenauer oxidation followed by sodium borohydride reduction to yield two products, of which one was identified as the starting material 3a. Although the  $^1\text{H}$ - and  $^{13}\text{C}$ -NMR spectra of the other product were found to be identical with those of the heptamethyl ether (4a) of A-5', the specific optical rotation and the Cotton effects in the circular dichroism (CD) spectrum (Fig. 1) showed opposite signs, indicating that the synthetic sample is an enantiomer of 4a. Based on these chemical and spectroscopic findings, the structure of A-5' was established to be 4.

The enantiomers (3' and 1') of proanthocyanidins A-4 and A-2, though 1' is slightly racemic, were also obtained from the *Ephedra* plant. It is interesting from the viewpoint of plant physiology that only the plant belonging to Gymnospermae characteristically produces such enantiomorphous compounds in the secondary metabolism.

### Experimental

Melting points were determined on a Yanagimoto micro-melting point apparatus and are uncorrected. Optical rotations were measured with a JASCO DIP-4 digital polarimeter (cell length: 0.5 dm). Field-desorption (FD-) and electron-impact (EI-) mass spectra (MS) were recorded with JEOL D-300 and JEOL DX-300 spectrometers.  $^1\text{H}$  (100 MHz)- and  $^{13}\text{C}$  (25.05 MHz)-NMR spectra were taken with JEOL PS-100 and JEOL FX-100 spectrometers, respectively, with tetramethylsilane as an internal standard; chemical shifts are given on a  $\delta$ (ppm) scale. CD data were obtained in methanol with a JASCO J-20 spectropolarimeter. Column chromatography was carried out with Sephadex LH-20 (25–100  $\mu$ , Pharmacia Fine Chemical Co., Ltd.), Bondapak/C<sub>18</sub> Porasil b (37–75  $\mu$ , Waters Associates, Inc.) and Kieselgel 60 (70–230 mesh, Merck). Thin-layer chromatography (TLC) was performed on precoated Kieselgel 60 F<sub>254</sub> plates (0.20 mm, Merck) with benzene-ethyl formate-formic acid (2:7:1) (for phenolics) and benzene-acetone (4:1) (for methyl ethers), and the spots were detected by observing their fluorescence under ultraviolet (UV) light and by the use of 10% sulfuric acid and ferric chloride reagent sprays.

**Proanthocyanidin A-1 (2)**—This compound was isolated from the seeds of *Areca catechu*,<sup>21</sup> the leaves of *Vaccinium vitis-idaea*, the root bark of *Cinnamomum sieboldii* and the bark of *Cinnamomum camphora*,<sup>14b</sup> and its identity with authentic A-1 was confirmed by comparison of the physical data and the  $^1\text{H}$ -NMR spectrum of its heptamethyl diacetyl derivative with those reported in the literature.<sup>21</sup> Colorless needles (H<sub>2</sub>O), mp > 300°C,  $[\alpha]_D^{25} + 62.9^\circ$  ( $c = 1.4$ , acetone).  $^1\text{H}$ -NMR (acetone- $d_6$ ): 2.58 (1H, dd,  $J = 8, 16$  Hz, 4-H), 3.04 (1H, dd,  $J = 6, 16$  Hz, 4-H), 4.15 (1H, d,  $J = 4$  Hz, 3''-H), 4.22 (1H, d,  $J = 4$  Hz, 4''-H), 4.30 (1H, m, 3-H), 4.73 (1H, d,  $J = 8$  Hz, 2-H), 5.97 (1H, d,  $J = 2$  Hz, 6''-H), 6.09 (1H, d,  $J = 2$  Hz, 8''-H), 6.15 (1H, s, 6-H), 6.7–7.3 (6H in total, B, B'-ring H).

**Methylation of 2**—2 (100 mg) was methylated overnight with ethereal diazomethane. Work-up was done as usual, and the product was purified by silica gel chromatography with benzene-acetone (17:3) to yield the heptamethyl ether (2a) (60 mg). A white amorphous powder,  $[\alpha]_D^{25} + 12.5^\circ$  ( $c = 1.2$ , acetone).  $^1\text{H}$ -NMR (CDCl<sub>3</sub>): 2.64–2.76 (2H, m, 4-H), 3.32, 3.62, 3.72, 3.74, 3.86, 3.89, 3.90 (OMe), 4.22 (1H, m, 3-H), 4.87 (1H, d,  $J = 4$  Hz, 4''-H), 4.98 (1H, d,  $J = 6$  Hz, 2-H), 6.03 (1H, d,  $J = 2$  Hz, 6''-H), 6.20 (1H, s, 6-H), 6.29 (1H, d,  $J = 2$  Hz, 8''-H), 6.7–7.3 (6H in total, B, B'-ring H).

**Methylation of 1**—Proanthocyanidin A-2 (1), colorless needles (H<sub>2</sub>O), mp > 300°C,  $[\alpha]_D^{19} + 51.2^\circ$  ( $c = 1.1$ , acetone), isolated from the seed shells of *Aesculus hippocastanum*, was methylated with ethereal diazomethane. Work-up as described above yielded the heptamethyl ether (1a). Colorless needles (*n*-hexane-ethyl acetate), mp 212°C,  $[\alpha]_D^{25} + 31.2^\circ$  ( $c = 1.1$ , acetone).  $^1\text{H}$ -NMR (CDCl<sub>3</sub>): 2.70 (1H, dd,  $J = 4, 16$  Hz, 4-H), 2.95 (1H, dd,  $J = 5, 16$  Hz, 4-H), 3.45, 3.72 ( $\times 2$ ), 3.80, 3.98 ( $\times 2$ ), 3.99 (OMe), 4.22 (1H, d,  $J = 4$  Hz, 3''-H), 4.44 (1H, m, 3-H), 4.92 (1H, d,  $J = 4$  Hz, 4''-H), 4.99 (1H, s, 2-H), 6.05 (1H, d,  $J = 2$  Hz, 6''-H), 6.20 (1H, s, 6-H), 6.29 (1H, d,  $J = 2$  Hz, 8''-H), 6.88–7.36 (6H in total, B, B'-ring H).

**Oxidation of 1a**—A mixture of 1a (300 mg), 9-fluorenone (1.0 g) and potassium *tert*-butoxide (160 mg) in dry benzene (40 ml) was heated under reflux for 9 h. The reaction mixture was neutralized with 1 N hydrochloric acid, and the benzene layer was washed with water, dried over sodium sulfate and concentrated under reduced pressure. The residue was chromatographed over silica gel with benzene-acetone (7:1) to give the mono-ketone (5) (150 mg). A white amorphous powder,  $[\alpha]_D^{25} - 12.5^\circ$  ( $c = 1.1$ , acetone). *Anal.* Calcd for C<sub>37</sub>H<sub>36</sub>O<sub>12</sub>: C, 66.06; H, 5.39. Found: C, 66.00; H, 5.60. EI-MS *m/z*: 672 ( $M^+$ ).  $^1\text{H}$ -NMR (CDCl<sub>3</sub>): 3.32 (1H, d,  $J = 16$  Hz, 4-H), 3.59 (1H, d,  $J = 16$  Hz, 4-H), 3.29, 3.60, 3.73 ( $\times 2$ ), 3.83, 3.88, 3.90 (OMe), 4.25 (1H, t-like,  $J = 4$  Hz, 3''-H, on addition of D<sub>2</sub>O, this signal changed into a doublet,  $J = 4$  Hz), 4.91 (1H, d,  $J = 4$  Hz, 4''-H), 5.31 (1H, s, 2-H), 5.96 (1H, d,  $J = 2$  Hz, 6''-H), 6.30 (2H, br s, 8''- and 6-H), 6.7–7.4 (6H in total, B, B'-ring H).

**Reduction of 5**—A solution of 5 (100 mg) in methanol was treated with sodium borohydride (20 mg) at room

temperature for 5 min. The reaction mixture was neutralized with Amberlite IR-120B ( $H^+$  form), and concentrated to dryness under reduced pressure. The residue was subjected to silica gel chromatography with benzene-acetone (17:3) to furnish the A-1 heptamethyl ether (**2a**) (15 mg) and the A-2 methyl ether (**1a**) (48 mg).

**Oxidation of 6**—A mixture of **6** (200 mg), sodium bicarbonate (50 mg) and hydrogen peroxide (0.5 ml) in ethanol (20 ml) was left at room temperature for 13 h. The reaction mixture was neutralized with Amberlite IR-120B ( $H^+$  form), and the solvent was evaporated off under reduced pressure. The residue was chromatographed over Sephadex LH-20 with 80% aqueous methanol to give A-1 (**1**) (25 mg).

**Proanthocyanidin A-4 (3)**—This compound was isolated from the seed shells of *Aesculus hippocastanum*.<sup>14)</sup> Colorless needles ( $H_2O$ ), mp  $>300^\circ C$ ,  $[\alpha]_D^{21} + 63.2^\circ$  ( $c=1.1$ , acetone). *Anal.* Calcd for  $C_{30}H_{24}O_{12} \cdot 5/2H_2O$ : C, 57.97; H, 4.70. Found: C, 57.78; H, 4.34. FD-MS  $m/z$ : 576 ( $M^+$ ).  $^1H$ -NMR (acetone- $d_6 + D_2O$ ): 2.58 (1H, dd,  $J=8$ , 16 Hz, 4-H), 3.01 (1H, dd,  $J=6$ , 16 Hz, 4-H), 4.10 (1H, m, 3''-H), 4.24 (2H, br s, 3- and 4''-H), 4.77 (1H, d,  $J=8$  Hz, 2-H), 5.95 (1H, d,  $J=2$  Hz, 6''-H), 6.10 (1H, d,  $J=2$  Hz, 8''-H), 6.16 (1H, s, 6-H), 6.76—7.24 (6H in total, B, B'-ring H).

**Methylation of 3**—**3** (300 mg) was methylated with ethereal diazomethane. Work-up as before yielded the heptamethyl ether (**3a**) (220 mg). Colorless needles (EtOH), mp  $173$ — $174^\circ C$ ,  $[\alpha]_D^{22} + 80.2^\circ$  ( $c=1.1$ , acetone). *Anal.* Calcd for  $C_{37}H_{38}O_{12} \cdot 1/2H_2O$ : C, 65.00; H, 5.75. Found: C, 65.16; H, 6.04. EI-MS  $m/z$ : 674 ( $M^+$ ).  $^1H$ -NMR ( $CDCl_3$ ): 2.53 (1H, dd,  $J=9$ , 16 Hz, 4-H), 3.12 (1H, dd,  $J=6$ , 16 Hz, 4-H), 3.12, 3.72, 3.74, 3.91 ( $\times 4$ ) (OMe), 4.28 (1H, t-like,  $J=4$  Hz, 3''-H, on addition of  $D_2O$ , this signal changed into a doublet,  $J=4$  Hz), 4.54 (1H, d,  $J=8$  Hz, 2-H), 4.87 (1H, d,  $J=4$  Hz, 4''-H), 5.99 (1H, d,  $J=2$  Hz, 6''-H), 6.19 (1H, s, 6-H), 6.26 (1H, d,  $J=2$  Hz, 8''-H), 6.84—7.40 (6H in total, B, B'-ring H).

**Epimerization of 1**—A mixture of **1** (600 mg) and potassium carbonate (150 mg) in acetone (30 ml) was heated under reflux for 10 min. After removal of potassium carbonate by filtration, the filtrate was concentrated to dryness under reduced pressure. The residue was subjected to Bondapak/ $C_{18}$  Porasil B chromatography to afford A-4 (**3**) (450 mg).

**Proanthocyanidin A-5' (4)**—This compound was isolated from a commercial *Ephedra* plant (Maō). Colorless fine needles ( $H_2O$ ), mp  $>300^\circ C$ ,  $[\alpha]_D^{26} - 111.0^\circ$  ( $c=1.6$ , MeOH). *Anal.* Calcd for  $C_{30}H_{24}O_{12} \cdot 2H_2O$ : C, 58.82; H, 4.61. Found: C, 59.13; H, 4.88. FD-MS  $m/z$ : 576 ( $M^+$ ).  $^1H$ -NMR (acetone- $d_6 + D_2O$ ): 2.88 (2H, br s,  $J=3$  Hz, 4-H), 4.24 (1H, d,  $J=4$  Hz, 3''-H), 4.28 (1H, br s, 3-H), 4.36 (1H, d,  $J=4$  Hz, 4''-H), 5.08 (1H, s, 2-H), 5.90 (1H, d,  $J=2$  Hz, 6''-H), 6.07 (1H, d,  $J=2$  Hz, 8''-H), 6.14 (1H, s, 6-H), 6.7—7.3 (6H in total, B, B'-ring H).

**Methylation of 4**—**4** was methylated in the same way as described above to give the heptamethyl ether (**4a**). Colorless needles (MeOH), mp  $151$ — $153^\circ C$ ,  $[\alpha]_D^{26} - 12.3^\circ$  ( $c=1.3$ , acetone). *Anal.* Calcd for  $C_{37}H_{38}O_{12} \cdot 1/2H_2O$ : C, 65.00; H, 5.75. Found: C, 64.74; H, 5.67. EI-MS  $m/z$ : 674 ( $M^+$ ), 494, 465, 342 (base peak).  $^1H$ -NMR ( $CDCl_3 + D_2O$ ): 2.92 (2H, br s, 4-H), 3.14, 3.72 ( $\times 2$ ), 3.92 ( $\times 4$ ) (OMe), 4.24 (1H, m, 3-H), 4.32 (1H, d,  $J=4$  Hz, 3''-H), 4.94 (1H, s, 2-H), 4.99 (1H, d,  $J=4$  Hz, 4''-H), 5.99 (1H, d,  $J=2$  Hz, 6''-H), 6.20 (1H, s, 6-H), 6.27 (1H, d,  $J=2$  Hz, 8''-H), 6.8—7.4 (6H in total, B, B'-ring H).

**Oxidation of 3a**—A mixture of **3a** (200 mg), 9-fluorenone (700 mg) and potassium *tert*-butoxide (400 mg) in dry benzene (30 ml) was heated under reflux for 9 h. The reaction mixture was worked-up as above to yield the mono-ketone (**7**) (105 mg). A white amorphous powder,  $[\alpha]_D^{25} + 11.2^\circ$  ( $c=1.2$ , acetone). *Anal.* Calcd for  $C_{37}H_{36}O_{12}$ : C, 66.06; H, 5.39. Found: C, 66.35; H, 5.00. EI-MS  $m/z$ : 672 ( $M^+$ ).  $^1H$ -NMR ( $CDCl_3$ ): 3.34 (1H, d,  $J=16$  Hz, 4-H), 3.71 (1H, d,  $J=16$  Hz, 4-H), 3.37, 3.75 ( $\times 2$ ), 3.89, 3.92 ( $\times 2$ ), 3.93 (OMe), 4.28 (1H, dd,  $J=4$ , 6 Hz, 3''-H, on addition of  $D_2O$ , this signal changed into a doublet,  $J=4$  Hz), 5.00 (1H, d,  $J=4$  Hz, 4''-H), 5.12 (1H, s, 2-H), 6.07 (1H, d,  $J=2$  Hz, 6''-H), 6.30 (1H, d,  $J=2$  Hz, 8''-H), 6.32 (1H, s, 6-H), 6.86—7.40 (6H in total, B, B'-ring H).

**Reduction of 7**—A solution of **7** (100 mg) in methanol was treated with sodium borohydride (20 mg) at room temperature for 10 min. Work-up as described above yielded the enantiomer (**4a'**) (14 mg) of **4a** and the A-4 heptamethyl ether (**3a**) (24 mg). **4a'**: Colorless needles (EtOH), mp  $151$ — $152^\circ C$ ,  $[\alpha]_D^{21} + 10.5^\circ$  ( $c=1.1$ , acetone). *Anal.* Calcd for  $C_{37}H_{38}O_{12} \cdot 1/2H_2O$ : C, 65.00; H, 5.75. Found: C, 65.16; H, 5.62. EI-MS  $m/z$ : 674 ( $M^+$ ). The  $^1H$ - and  $^{13}C$ -NMR spectra of **4a'** were identical with those of **4a**.

**Acknowledgement** We are grateful to Mr. Y. Tanaka, Miss K. Soeda and Mr. R. Isobe for  $^{13}C$ -,  $^1H$ -NMR and MS measurements, respectively, and to the staff of the Central Analysis Room of this University for elemental analyses.

#### References and Notes

- 1) Part XLIX: E. Furuichi, G. Nonaka, I. Nishioka, and K. Hayashi, *Agric. Biol. Chem.*, in press.
- 2) K. Weinges, W. Kaltenhäuser, H.-D. Marx, E. Nader, J. Perner, and D. Seiler, *Ann. Chem.*, **711**, 184 (1968).
- 3) R. S. Thompson, D. Jacques, E. Haslam, and R. J. N. Tanner, *J. Chem. Soc., Perkin Trans. 1*, **1972**, 1387.
- 4) G. Nonaka, O. Kawahara, and I. Nishioka, *Chem. Pharm. Bull.*, **30**, 4277 (1982).
- 5) F.-L. Hsu, G. Nonaka, and I. Nishioka, *Chem. Pharm. Bull.*, **33**, 3142 (1985).

- 
- 6) G. Nonaka and I. Nishioka, *Chem. Pharm. Bull.*, **28**, 3145 (1980).
  - 7) G. Nonaka, F.-L. Hsu, and I. Nishioka, *J. Chem. Soc., Chem. Commun.*, **1981**, 781.
  - 8) G. Nonaka, I. Nishioka, T. Nagasawa, and H. Oura, *Chem. Pharm. Bull.*, **29**, 2862 (1981).
  - 9) G. Nonaka, M. Muta, and I. Nishioka, *Phytochemistry*, **22**, 237 (1983); R. W. Hemingway, L. Y. Foo, and L. J. Porter, *J. Chem. Soc., Perkin Trans. 1*, **1982**, 1209; T. Tanaka, G. Nonaka, and I. Nishioka, *Phytochemistry*, **22**, 2575 (1983); G. Nonaka, O. Kawahara, and I. Nishioka, *Chem. Pharm. Bull.*, **31**, 3906 (1983); F.-L. Hsu, G. Nonaka, and I. Nishioka, *Chem. Pharm. Bull.*, **33**, 3293 (1985).
  - 10) D. Jacques, E. Haslam, G. R. Bedford, and D. Greatbanks, *J. Chem. Soc., Perkin Trans. 1*, **1974**, 2663.
  - 11) H. Otsuka, S. Fujioka, T. Komiya, E. Mizuta, and M. Takemoto, *Yakugaku Zasshi*, **102**, 162 (1982).
  - 12) R. B. Woodward, N. L. Wendler, and F. J. Brutschy, *J. Am. Chem. Soc.*, **67**, 1425 (1945).
  - 13) Details of the isolation procedures will be reported elsewhere.

[Chem. Pharm. Bull.]  
35(1) 156-169 (1987)

## Preparation of New Nitrogen-Bridged Heterocycles. XIV.<sup>1)</sup> Further Investigation of the Desulfurization and the Rearrangement of Pyrido[1,2-*d*]-1,3,4-thiadiazine Intermediates

AKIKAZU KAKEHI,\* SUKETAKA ITO, KENJI NAGATA,  
NAOSUMI KINOSHITA, and NOBORU KAKINUMA

*Department of Industrial Chemistry, Faculty of Engineering,  
Shinshu University, Wakasato, Nagano 380, Japan*

(Received July 8, 1986)

The formation of pyrazolo[1,5-*a*]pyridine derivatives *via* the desulfurization and the rearrangement of pyrido[1,2-*d*]-1,3,4-thiadiazine intermediates having various substituents at the 2- and 4-positions was investigated, and the wide applicability of this approach to the syntheses of pyrazolo[1,5-*a*]pyridines was established. The substituent effect in these reactions was also clarified. The possibility of the extension of this reaction to other heterocyclic systems such as pyrido[1,2-*b*]pyridazine and pyrido[2,1-*f*]-1,2,4-triazine was examined, but only pyridinium 1-aminide and 1,2,4-triazolo[1,5-*a*]pyridine were obtained instead of the expected heterocyclic compounds.

**Keywords**—desulfurization; rearrangement; pyrazolo[1,5-*a*]pyridine; pyrido[1,2-*d*]-1,3,4-thiadiazine; pyridinium 1-(thiocarbonyl)aminide; 1,2,4-triazolo[1,5-*a*]pyridine; pyridinium 1-aminide; 1-[(methylthio)methyleneamino]pyridinium bromide

Recently, we developed a new convenient method for the preparation of 2-alkylthio-3-cyano-, 3-acyl- and 3-(arylthio)pyrazolo[1,5-*a*]pyridine derivatives, involving the desulfurization and the rearrangement of transient pyrido[1,2-*d*]-1,3,4-thiadiazines generated *in situ* by the alkaline treatment of 1-[substituted (methylthio)methyleneamino]pyridinium halides.<sup>2)</sup> Mechanistically, this reaction can be considered to be the same as that described in the conversion of a 1,3,4-thiadiazinyl anion to the desulfurized pyrazole and the rearranged 5-mercaptopyrazole,<sup>3)</sup> since the neutral pyrido[1,2-*d*]-1,3,4-thiadiazine (A) is a high-energy 12 $\pi$  bicyclic species and has a contributing structure (B) isoelectronic with the 1,3,4-thiadiazinyl anion (C), as shown in Fig. 1.

In particular, we were interested in the generality of this reaction and the substituent effect, since there is no precedent for the migration of a group other than a hydrogen onto the sulfur atom in this type of reaction, and the factors affecting this reaction are still uncertain. In this paper we wish to report the generations of pyrido[1,2-*d*]-1,3,4-thiadiazine intermediates possessing various substituents at the 2- and 4-positions, and an examination of the behavior of the desulfurization and the rearrangement. Some attempts to extend the reaction to other heterocyclic systems such as pyrido[1,2-*b*]pyridazine and pyrido[2,1-*f*]-1,2,4-triazine are also described.

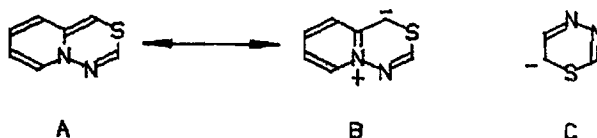


Fig. 1



## Results and Discussion

### Preparation of Pyridinium 1-Aminides

We selected alkyl, aryl, amino, alkoxy groups as the 2-substituent of pyrido[1,2-*d*]-1,3,4-thiadiazine and cyano, ester, and aroyl groups as the 4-substituent, in order to examine the generality of this reaction and the substituent effect. From the nature of the reaction,<sup>2)</sup> the 2-substituent is generally derived from pyridinium 1-aminide as a starting material. We prepared the corresponding pyridinium 1-(thiocarbonyl)aminides (**8—19**) in good yields from the reactions of *N*-unsubstituted pyridinium 1-aminides, generated *in situ* by the alkaline treatment of 1-aminopyridinium iodides (**1—3**), with methyl dithiocarboxylates (**4, 5, and 7**), and thiocarbamoyl chloride (**6**) (Chart 1). The structures of these pyridinium 1-(thiocarbonyl)aminides (**8—19**) were determined on the basis of elementary analyses, spectral comparisons with other pyridinium 1-aminides,<sup>4)</sup> and the comparison of **17** with an authentic sample.<sup>5)</sup>

### Preparation and Reaction of 1-[(Substituted Methylthio)methyleneamino]pyridinium Bromides

Since the 4-substituent of the pyridothiadiazine is derived from the alkylating agent used, we employed bromoacetonitrile (**20**), ethyl bromoacetate (**21**), phenacyl bromide (**22**), and *p*-chlorophenacyl bromide (**23**) as alkylating agents for the purpose of introducing cyano, ester, and aroyl groups. Treatment of pyridinium 1-[(ethyl)thiocarbonyl]aminides (**8—10**) with alkylating agents (**20—23**) in chloroform at room temperature gave the corresponding 1-[(substituted methylthio)methyleneamino]pyridinium bromides (**24—35**) in quantitative yields. The reactions of the pyridinium salts (**24—35**) with excess anhydrous potassium carbonate in chloroform at room temperature for 1 d afforded the desulfurized 3-cyano- (**36—38**) and 3-ethoxycarbonyl-2-ethylpyrazolo[1,5-*a*]pyridines (**39—41**) and the rearranged 3-aryloxythio-2-ethylpyrazolo[1,5-*a*]pyridines (**42—47**), respectively. Similarly, the alkylations of pyridinium 1-[(phenyl)thiocarbonyl]aminides (**11—13**) and 1-[(dimethylamino)thiocarbonyl]aminides (**14—16**) with **20—23** followed by the alkaline treatment of the resulting pyridinium bromides (**48—59** and **72—83**) at room temperature provided 2-phenyl- (**60—71**) and 2-(dimethylamino)pyrazolo[1,5-*a*]pyridine derivatives (**84—95**) in good yields (Chart 2). On the other hand, the reactions of pyridinium salts (**96—107**), obtained from pyridinium 1-[(ethoxy)thiocarbonyl]aminides (**17—19**) and **20—23**, with base at room temperature gave only complex mixtures and no pyrazolopyridine product could be isolated. When the alkaline treatment of pyridinium salts (**96—107**) was performed in an ice bath under stirring for 3 d, however, the expected 2-ethoxypyrazolo[1,5-*a*]pyridines (**108—113** and **120—125**) were

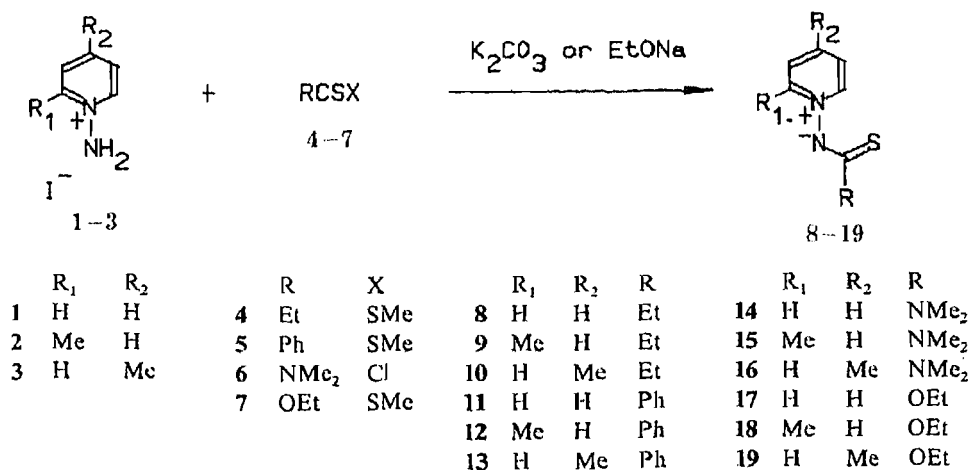


Chart 1

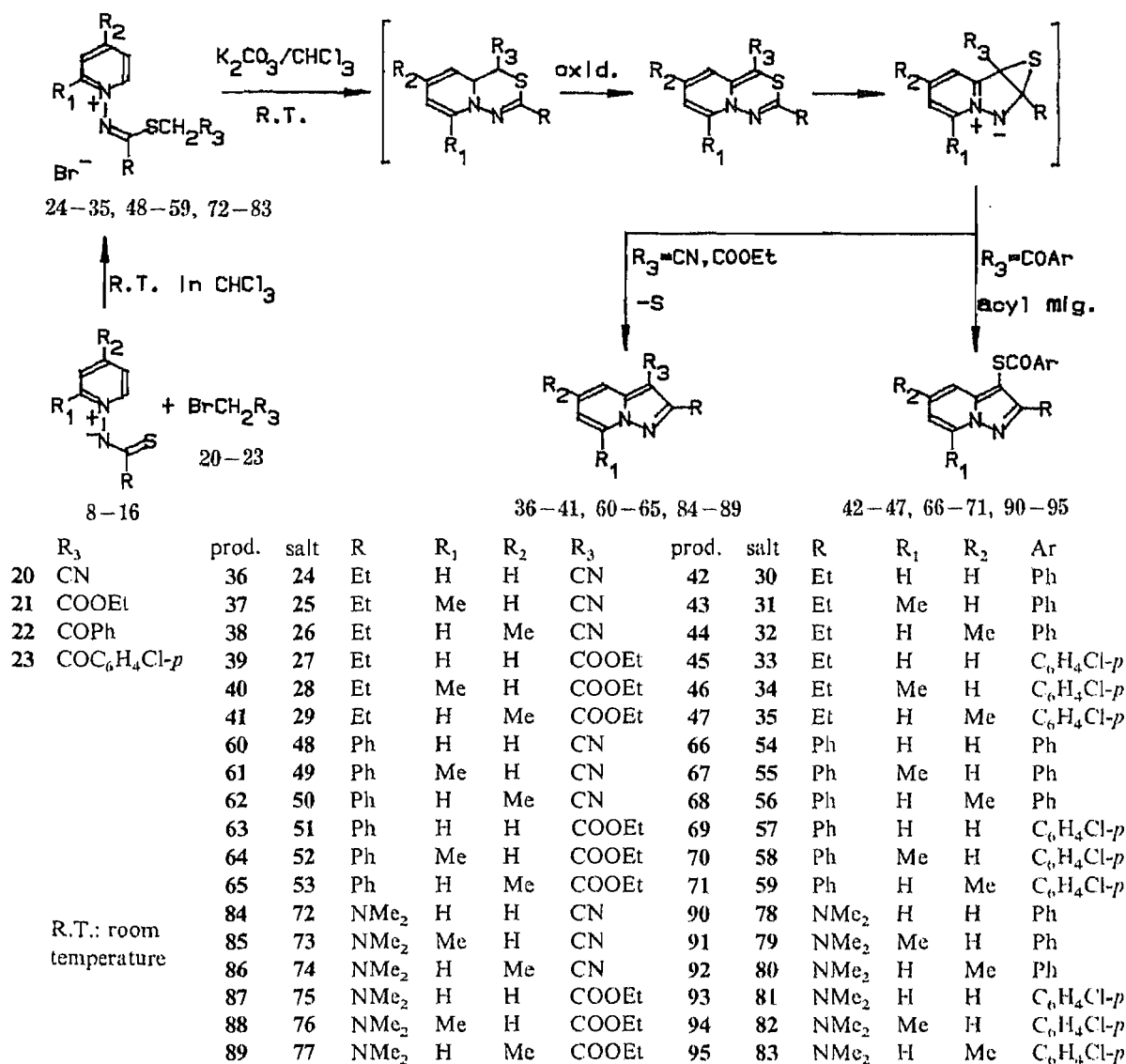


Chart 2

obtained in low yields, together with pyridinium 1-[(substituted methylthio)carbonyl]aminides (114—119 and 126—131). The same pyridinium 1-aminides (114—119 and 126—131) were also formed in good yields by keeping the corresponding salts (96—107) in chloroform at room temperature or by heating them at 50—60 °C in a water bath, respectively (Chart 3).

The structures of these pyrazolo[1,5-*a*]pyridines were determined from their molecular compositions and their infrared (IR) and proton nuclear magnetic resonance (<sup>1</sup>H-NMR) spectra. For example, the IR spectra each exhibit characteristic absorption bands at 2196—2210 cm<sup>-1</sup> ( $\alpha,\beta$ -unsaturated cyano group), at 1670—1708 cm<sup>-1</sup> ( $\alpha,\beta$ -unsaturated ester carbonyl group), and at 1654—1688 cm<sup>-1</sup> (aryl carbonyl group). In particular, the positions of the absorption bands due to the cyano or the carbonyl group in the 3-substituents on the pyrazolopyridine skeleton are almost the same as those of 2-(alkylthio)pyrazolopyridines reported earlier by us.<sup>2)</sup> As can be seen in Table I, the chemical shifts and the signal patterns are very similar to those of 2-(alkylthio)pyrazolo[1,5-*a*]pyridines<sup>2)</sup> and other pyrazolo[1,5-*a*]pyridines.<sup>4a,6)</sup> Furthermore, ethyl 2-phenylpyrazolo[1,5-*a*]pyridine-3-carboxylates (63 and 65) were identical with authentic samples prepared independently.<sup>7)</sup>

The extent of the desulfurization and the rearrangement observed above were all the

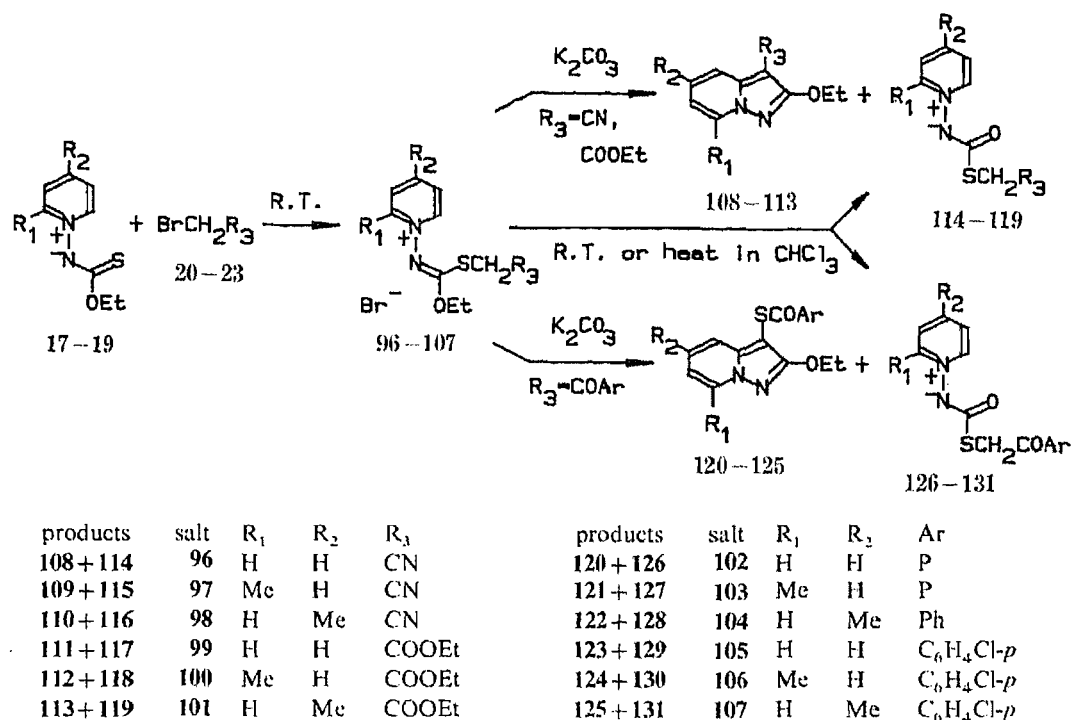


Chart 3

same as in the case of the 2-(alkylthio)pyrazolo[1,5-*a*]pyridines described earlier by us,<sup>2)</sup> and this indicates that the course of this reaction depends on only the 4-substituent in the pyridothiadiazine intermediates but not at all on the 2-substituent.

On the other hand, the structural assignment of pyridinium 1-[substituted (methylthio)carbonyl]aminides (114--119 and 126--131) was accomplished on the basis of elementary analyses and <sup>1</sup>H-NMR spectral inspection. In particular, the chemical shifts and the signal patterns due to the protons on the pyridine ring in the <sup>1</sup>H-NMR spectra (Table II) of these compounds (114--119 and 126--131) are quite different from those in the pyrazolo[1,5-*a*]pyridine derivatives (36--47, 60--71, 84--89, 108--113, and 120--125) but the same as those (Table II) of pyridinium 1-(thiocarbonyl)aminides (8--19) and other pyridinium 1-aminides.<sup>4)</sup> The absence of ethoxy proton signals and the presence of the proton signals derived from the *S*-alkyl moiety also represent strong evidence for the proposed ylidic structure.

#### Attempts to Extend the Reaction to Other Heterocyclic Systems

Since the generality and wide applicability of this reaction were well established, its extension to other heterocyclic systems containing no sulfur atom was examined. Pyrido[1,2-*b*]pyridazine and pyrido[2,1-*f*]-1,2,4-triazine were selected as model compounds, and the corresponding pyridinium salts (135--138) were prepared by alkylations of pyridinium 1-vinylaminides (132 and 133)<sup>8)</sup> and 1-imidoylaminide (134)<sup>9)</sup> with bromoacetonitrile (20) and ethyl bromoacetate (21). The alkaline treatment of these pyridinium salts (135--138), however, did not give the expected compounds (139) and/or the pyrazolopyridines formed *via* 139 at all: for example, the reaction of the salt 135 with base gave only the *N*-unsubstituted pyridinium 1-aminide (140), whose structure was confirmed by formation of its *N*-benzoyl derivative (142, 13%, mp 177--179°C), while the similar treatment of salt 136 afforded only an intractable tarry product. On the other hand, the treatment of the salts 137 and 138 with 1,8-diazabicyclo[5.4.0]-7-undecene (DBU) yielded the same product, 7-methyl-2-phenyl-1,2,4-

TABLE I. <sup>1</sup>H-NMR Spectral Data for Pyrazolo[1,5-*a*]pyridines in CDCl<sub>3</sub>

Compd. <sup>a)</sup>	C-4	C-5	C-6	C-7	R		R <sub>3</sub>	
36	7.75 brd	7.48 brt	7.00 dt	8.56 brd	1.42 t	2.99 q	—	
37	7.62 brd	7.47 q	6.80 brd	2.79 s	1.41 t	3.01 q	—	
38	7.49 brs	2.49 s	6.81 dd	8.41 d	1.42 t	2.99 q	—	
39	8.18 brd	7.41 brt	6.90 dt	8.51 brd	1.38 t	3.16 q	1.43 t	4.42 q
40	8.08 d	7.38 q	6.75 brd	2.77 s	1.38 t	3.18 q	1.43 t	4.42 q
41	7.93 brs	2.43 s	6.72 dd	8.37 d	1.32 t	3.10 q	1.40 t	4.39 q
42	<sup>b)</sup>	7.21 brt	6.81 dt	8.52 brd	1.33 t	2.89 q	7.3—8.3 m	
43	<sup>b)</sup>	7.09 q	6.60 brt	2.70 s	1.33 t	2.90 q	7.6—8.3 m	
44	7.18 brs	2.31 s	6.58 dd	8.36 d	1.33 t	2.85 q	7.3—8.3 m	
45	<sup>b)</sup>	7.23 brt	6.82 dt	8.51 brd	1.32 t	2.87 q	7.3—8.3 m	
46	7.40 d	7.18 q	6.70 brd	2.78 s	1.33 t	2.89 q	7.4—8.3 m	
47	7.20 brs	2.37 s	6.67 dd	8.39 d	1.32 t	2.83 q	7.4—8.3 m	
60	<sup>b)</sup>	<sup>b)</sup>	6.97 dt	8.54 brd	7.2—8.3 m		—	
61	<sup>b)</sup>	<sup>b)</sup>	6.83 brd	2.82 s	7.1—8.4 m		—	
62	<sup>b)</sup>	2.47 s	6.83 dd	8.47 d	7.3—8.3 m		—	
63	8.27 brd	<sup>b)</sup>	6.97 dt	8.55 brd	7.3—8.0 m		1.33 t	4.33 q
64	8.15 d	<sup>b)</sup>	6.78 brd	2.79 s	7.1—8.0 m		1.27 t	4.28 q
65	8.03 brd	2.47 s	6.79 dd	8.45 d	7.3—8.0 m		1.28 t	4.31 q
66	<sup>b)</sup>	<sup>b)</sup>	6.85 dt	8.56 brd	7.0—8.3 m		7.0—8.3 m	
67	<sup>b)</sup>	7.10 q	6.64 brd	2.75 s	7.2—8.3 m		7.2—8.3 m	
68	7.27 brs	2.42 s	6.71 dd	8.47 d	7.2—8.3 m		7.2—8.3 m	
69	<sup>b)</sup>	<sup>b)</sup>	6.85 dt	8.55 brd	7.0—8.3 m		7.0—8.3 m	
70	<sup>b)</sup>	<sup>b)</sup>	6.73 brd	2.81 s	7.0—8.3 m		7.0—8.3 m	
71	7.27 brs	2.37 s	6.73 dd	8.48 d	7.2—8.3 m		7.2—8.3 m	
84	7.0—7.5 m		6.76 dt	8.21 brd	3.18 s	—		
85	7.0—7.4 m		6.59 brd	2.62 s	3.19 s	—		
86	7.14 brs	2.36 s	6.55 dd	8.05 d	3.14 s	—		

TABLE I. (continued)

Compd. <sup>a)</sup>	C-4	C-5	C-6	C-7	R	R <sub>3</sub>		
87	8.03 brd	7.33 brt	6.80 dt	8.36 brd	3.09 s	1.42 t	4.39 q	
88	7.91 brd	7.24 q	6.66 brd	2.67 s	3.08 s	1.40 l	4.38 q	
89	7.77 brs	2.39 s	6.56 dd	8.22 d	3.06 s	1.40 t	4.36 q	
90	<sup>b)</sup>	<sup>b)</sup>	6.67 dt	8.32 brd	3.13 s	7.1—8.3 m		
91	6.9—7.4 m		6.57 brd	2.70 s	3.16 s	7.4—8.3 m		
92	6.98 brs	2.32 s	6.47 dd	<sup>b)</sup>	3.12 s	7.4—8.3 m		
93	<sup>b)</sup>	<sup>b)</sup>	6.67 dt	8.33 brd	3.12 s	7.1—8.2 m		
94	6.8—7.3 m		6.54 brd	2.66 s	3.11 s	7.3—8.3 m		
95	6.98 brs	2.33 s	6.49 dd	8.18 d	3.11 s	7.3—8.3 m		
108	7.64 brd	7.47 brt	6.92 dt	8.38 brd	1.49 t	4.49 q	—	
109	7.1—7.7 m		6.76 brd	2.69 s	1.48 t	4.51 q	—	
110	7.29 brs	2.43 s	6.67 dd	8.16 d	1.47 t	4.42 q	—	
111	7.98 brd	7.34 brt	6.80 dt	8.28 d	1.50 t	4.49 q	1.40 t	4.37 q
112	7.88 brd	7.27 q	6.65 brd	2.65 s	1.49 t	4.52 q	1.37 t	4.37 q
113	7.80 brs	2.41 s	6.65 dd	8.19 d	1.51 t	4.49 q	1.40 t	4.38 q
120	<sup>b)</sup>	<sup>b)</sup>	6.71 dt	8.33 brd	1.45 t	4.47 q	7.0—8.3 m	
121	6.9—7.4 m		6.63 brd	2.71 s	1.46 t	4.55 q	7.3—8.3 m	
122	7.10 brs	2.36 s	6.60 dd	<sup>b)</sup>	1.44 t	4.47 q	7.0—8.3 m	
123	<sup>b)</sup>	<sup>b)</sup>	6.76 m	8.33 brd	1.44 t	4.47 q	7.0—8.3 m	
124	6.9—7.4 m		6.61 brd	2.69 s	1.46 t	4.53 q	7.3—8.3 m	
125	7.04 brs	2.33 s	6.55 dd	8.20 d	1.41 t	4.44 q	7.3—8.3 m	

a) The coupling constants are as follows:  $J_{4,5}=9.0$ ,  $J_{5,6}=J_{6,7}=7.0$ ,  $J_{5,7}=2.0$ , and  $J_{6,8}=7.0$  Hz. b) Overlapped with the phenyl proton signals.

triazolo[1,5-a]pyridine (**143**), in 11% and 72% yields, respectively, together with ethyl cyanoacetate (**144**) and diethyl malonate (**145**) (confirmed by gas chromatographic (GLC) monitoring of the reaction mixtures). The use of potassium carbonate as a base in the reaction of **137** also afforded the same product (**143**) in 11% yield.

Compounds **142** and **143** were identical with authentic samples.<sup>4c,9)</sup>

### Reaction Mechanisms

The mechanism for the formations of 2-ethyl- (**36—47**), 2-phenyl- (**60—71**), 2-

TABLE II. <sup>1</sup>H-NMR Spectral Data for Pyridinium 1-Aminides in CDCl<sub>3</sub>

Compd. <sup>a)</sup>	C-2	C-3	C-4	C-5	C-6	Others		
8	8.42 br d	————	7.6—8.3 m	————	8.45 br d	1.36 t	2.85 q	
9	2.61 s	————	7.5—8.2 m	————	8.28 br d	1.40 t	2.88 q	
10	8.29 br d	7.63 br d	2.59 s	7.63 br d	8.29 br d	1.34 t	2.82 q	
11	————	————	————	7.3—9.3 m	————	————	————	
12	2.66 s	————	————	7.3—8.4 m	————	————	————	
13	7.2—8.5 m	————	2.51 s	————	7.2—8.5 m	————	————	
14	8.38 br d	————	7.4—8.2 m	————	8.38 br d	3.30 s	————	
15	2.58 s	————	7.3—8.1 m	————	8.28 br d	3.30 s	————	
16	8.21 br d	7.40 br d	2.50 s	7.40 br d	8.21 br d	3.29 s	————	
17	8.69 br d	————	7.8—8.6 m	————	8.69 br d	1.41 t	4.55 q	
18	2.70 s	————	7.6—8.4 m	————	8.50 br d	1.43 t	4.51 q	
19	8.51 br d	7.74 br d	2.67 s	7.74 br d	8.51 br d	1.43 t	4.56 q	
114	8.85 br d	————	7.5—8.1 m	————	8.85 br d	3.68 s	————	
115	2.73 s	————	7.3—8.3 m	————	8.64 br d	3.72 s	————	
116	8.62 br d	7.51 br d	2.55 s	7.51 br d	8.62 br d	3.65 s	————	
117	8.86 br d	————	7.5—8.2 m	————	8.86 br d	3.73 s	1.30 t	4.22 q
118	2.71 s	————	7.4—8.2 m	————	8.66 br d	3.72 s	1.27 t	4.21 q
119	8.68 br d	7.51 br d	2.56 s	7.51 br d	8.68 br d	3.71 s	1.27 t	4.21 q
126	8.83 br d	————	7.3—8.3 m	————	8.83 br d	4.37 s	7.3—8.3 m	
127	2.67 s	————	7.3—8.3 m	————	8.63 br d	4.39 s	7.3—8.3 m	
128	8.65 br d	<sup>b)</sup>	2.55 s	<sup>b)</sup>	8.65 br d	4.38 s	7.3—8.3 m	
129	8.84 br d	————	7.3—8.3 m	————	8.84 br d	4.31 s	7.3—8.3 m	
130	2.68 s	————	7.3—8.3 m	————	8.61 br d	4.32 s	7.3—8.3 m	
131	8.66 br d	<sup>b)</sup>	2.55 s	<sup>b)</sup>	8.66 br d	4.33 s	7.3—8.3 m	

<sup>a)</sup> The coupling constants are as follows:  $J_{2,3}=J_{5,6}=7.0$ , and  $J_{E1}=7.0$  Hz. <sup>b)</sup> Overlapped with the phenyl proton signals.

dimethylamino- (84—95), and 2-ethoxypyrazolo[1,5-*a*]pyridines (108—113 and 120—125) must be the same as that proposed for the formation of 2-(alkylthio)pyrazolo[1,5-*a*]pyridine derivatives.<sup>2)</sup> On the other hand, the formation of pyridinium 1-aminides (114—119 and

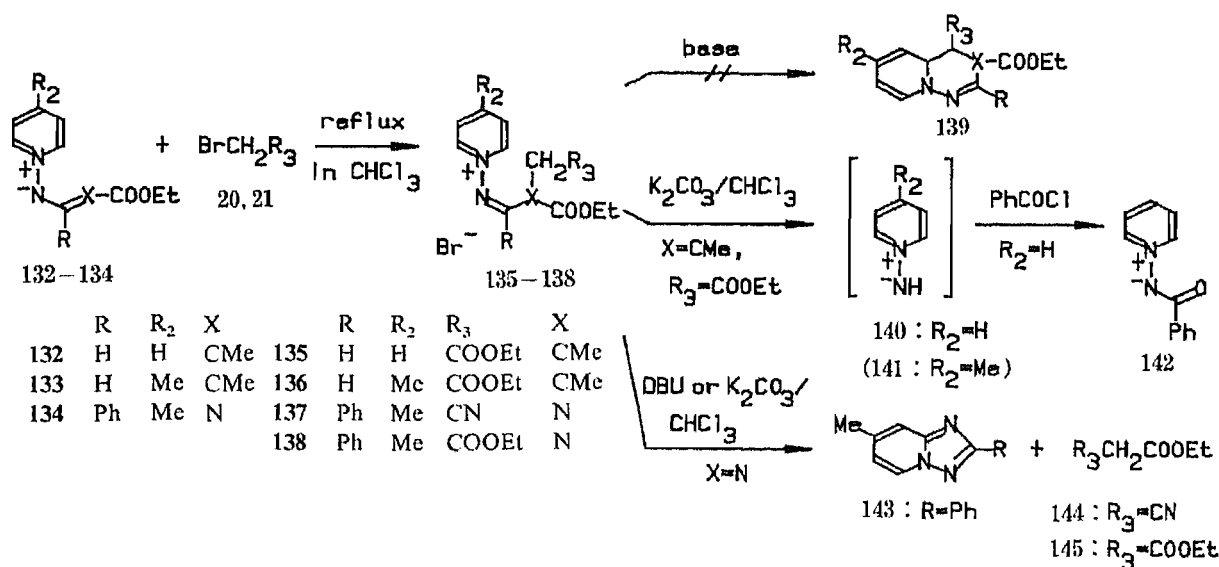


Chart 4

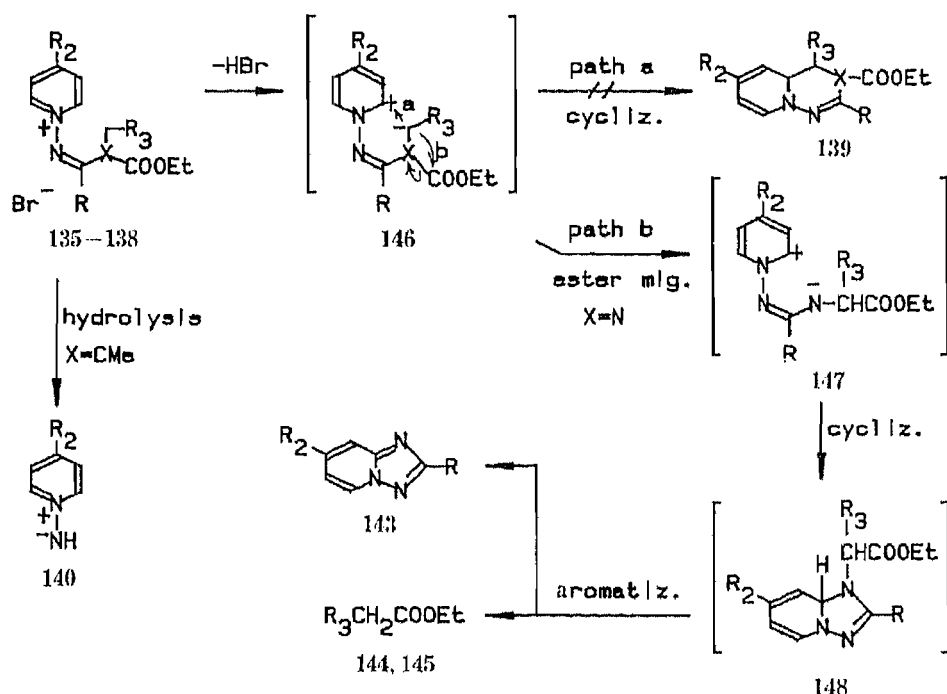


Chart 5

126—131) from the salts (96—107) seems to proceed *via* the nucleophilic dealkylation of the corresponding pyridinium salts (96—107) by the bromide ion and not *via* hydrolysis, since these reactions could be carried out in dry chloroform, and similar dealkylations of pyridinium salts<sup>5)</sup> and sulfonium salts<sup>10)</sup> have been reported recently. Interestingly, pyridinium 1-aminides (114—119 and 126—131) could not be alkylated at all by usual alkyl halides such as 20—23 and methyl iodide even under more drastic conditions (refluxing in chloroform for a week).

The possible mechanisms of formation of pyridinium 1-aminide (140) and 1,2,4-triazolo[1,5-*a*]pyridine (143) are summarized in Chart 5. Pyridinium 1-aminide (140) must be

formed by the hydrolysis of the carbon–nitrogen double bond in the 1-substituent of the salt **135**, though its counterpart, malonaldehydic ester, could not be detected in the reaction mixture. The low yield of **140** and the absence of **141** in the reaction of the salt **136**, however, mean that this route is not predominant. Finally, it seems that the main route in the reactions of salts **135** and **136** can not lead to any stabilized system such as aromatic pyrazolo[1,5-*a*]pyridine. On the other hand, 1,2,4-triazolo[1,5-*a*]pyridine (**143**) should be produced *via* the initial formation of the 1,6-zwitterion (**146**) followed by the migration of the ester group to the anionic center (path b) rather than the cyclization of **146** to 4,4a-dihydropyrido[2,1-*f*]-1,2,4-triazine (**139**) (path a), and the subsequent 1,5-dipolar cyclization of **147** and the aromatization of 1,8a-dihydro-1,2,4-triazolo[1,5-*a*]pyridine (**148**) to the final product (**143**) with the elimination of active methylene compounds (**144** and **145**).

Since anionic 1,2-sigmatropic suprafacial shift in this mechanism is a symmetry forbidden process,<sup>11)</sup> an aziridine intermediate may be involved *via* the nucleophilic attack of the anionic center on the ester carbonyl carbon in **146**. However, it is still uncertain why the ester rearrangement (path b) took place prior to the 1,6-cyclization (path a) to **139**.

### Experimental<sup>12)</sup>

**Pyridinium 1-Aminides (8–19 and 132–134)**—General Method A: An ethanolic solution (60 ml) of 1-aminopyridinium iodide (10 mmol) and methyl dithiopropionate (**4**, 12 mmol)<sup>13)</sup> or *N,N*-dimethylthiocarbamoyl chloride (**6**, 12 mmol) was treated with ethanolic sodium ethoxide (10 mmol in 10 ml of ethanol or 20 mmol in 20 ml of ethanol) under stirring at a room temperature for 1 d. The resulting solution was filtered to remove insoluble inorganic substances and the filtrate was concentrated under reduced pressure. The residue was separated by column chromatography on alumina using ether and chloroform as eluents, and the chloroform layer was concentrated under reduced pressure. The crude pyridinium 1-aminide thus obtained was purified by recrystallization from chloroform–

TABLE III. Some Data for Pyridinium 1-(Thiocarbonyl)aminides

Compd. No.	Reactants	Yield (%)	mp (°C)	$\nu_{\max}^{\text{KBr}}$ cm <sup>-1</sup>	Formula	Analysis (%)		
						Calcd	(Found)	
						C	H	N
<b>8</b>	1 4	62	116–118	1421 1169	C <sub>8</sub> H <sub>10</sub> N <sub>2</sub> S	a)		
<b>9</b>	2 4	64	115–116	1425 1170	C <sub>9</sub> H <sub>12</sub> N <sub>2</sub> S	a)		
<b>10</b>	3 4	72	114–116	1406 1164	C <sub>9</sub> H <sub>12</sub> N <sub>2</sub> S	a)		
<b>11</b>	1 5	75	152–153	1382 986	C <sub>12</sub> H <sub>10</sub> N <sub>2</sub> S	67.26	4.70	13.07
						(67.30)	4.53	13.07)
<b>12</b>	2 5	76	110–112	1400 982	C <sub>13</sub> H <sub>12</sub> N <sub>2</sub> S	68.39	5.30	12.27
						(68.18)	5.55	12.33)
<b>13</b>	3 5	96	135–137	1382 988	C <sub>13</sub> H <sub>12</sub> N <sub>2</sub> S	68.39	5.30	12.27
						(68.31)	5.34	12.31)
<b>14</b>	1 6	70	137–138	1325 1114	C <sub>8</sub> H <sub>11</sub> N <sub>3</sub> S	53.01	6.12	23.18
						(53.32)	6.11	22.88)
<b>15</b>	2 6	87	98–99	1337 1117	C <sub>9</sub> H <sub>13</sub> N <sub>3</sub> S	55.35	6.71	21.52
						(55.25)	6.67	21.66)
<b>16</b>	3 6	88	136–137	1330 1103	C <sub>9</sub> H <sub>13</sub> N <sub>3</sub> S	55.35	6.71	21.52
						(55.51)	6.79	21.28)
<b>17</b>	1 7	92	129–130 <sup>b)</sup>	1401 1199	Known compound <sup>b)</sup>			
<b>18</b>	2 7	93	105–106	1434 1200	C <sub>9</sub> H <sub>12</sub> N <sub>2</sub> OS	54.79	6.13	14.20
						(54.96)	6.05	14.36)
<b>19</b>	3 7	99	135–136	1411 1182	C <sub>9</sub> H <sub>12</sub> N <sub>2</sub> OS	54.79	6.13	14.20
						(54.98)	6.30	14.34)

a) Elemental analysis could not be performed because the compound sublimed readily. b) 130–131°C, see ref. 5.



TABLE IV. Some Data for Pyrazolo[1,5-*a*]pyridines

Product <sup>a)</sup> No.	Salt (S.M. <sup>b)</sup> )	Yield (%)	mp (°C)	$\nu_{\text{max}}^{\text{KBr}}$ $\text{cm}^{-1}$	Formula	Analysis (%)		
						Calcd (Found)		
						C	H	N
36	24 (8, 20)	87	74—76	2206	$\text{C}_{10}\text{H}_9\text{N}_3$	70.16 (70.17)	5.30 (5.21)	24.54 (24.63)
37	25 (9, 20)	79	80—82	2201	$\text{C}_{11}\text{H}_{11}\text{N}_3$	71.33 (71.46)	5.99 (6.01)	22.69 (22.54)
38	26 (10, 20)	89	74—76	2208	$\text{C}_{11}\text{H}_{11}\text{N}_3$	71.33 (71.03)	5.99 (6.12)	22.69 (22.86)
39	27 (8, 21)	92	95—97	1670	$\text{C}_{12}\text{H}_{14}\text{N}_2\text{O}_2$	66.04 (66.23)	6.47 (6.56)	12.84 (12.55)
40	28 (9, 21)	81	54—56	1685	$\text{C}_{13}\text{H}_{16}\text{N}_2\text{O}_2$	67.22 (67.14)	6.94 (7.05)	12.06 (12.03)
41	29 (10, 21)	85	83—85	1690	$\text{C}_{13}\text{H}_{16}\text{N}_2\text{O}_2$	67.22 (67.30)	6.94 (6.95)	12.06 (11.97)
42	30 (8, 22)	71	109—111	1675	$\text{C}_{16}\text{H}_{14}\text{N}_2\text{OS}$	68.06 (67.90)	5.00 (5.13)	9.92 (9.95)
43	31 (9, 22)	68	116—118	1660	$\text{C}_{17}\text{H}_{16}\text{N}_2\text{OS}$	<sup>c)</sup>		
44	32 (10, 22)	79	106—108	1676	$\text{C}_{17}\text{H}_{16}\text{N}_2\text{OS}$	68.89 (68.96)	5.44 (5.58)	9.45 (9.37)
45	33 (8, 23)	78	136—137	1688	$\text{C}_{16}\text{H}_{13}\text{ClN}_2\text{OS}$	60.66 (60.67)	4.14 (4.03)	8.84 (8.94)
46	34 (9, 23)	75	97—98	1671	$\text{C}_{17}\text{H}_{15}\text{ClN}_2\text{OS}$	61.72 (61.69)	4.57 (4.64)	8.47 (8.43)
47	35 (10, 23)	71	111—113	1672	$\text{C}_{17}\text{H}_{15}\text{ClN}_2\text{OS}$	61.72 (61.47)	4.57 (4.67)	8.47 (8.62)
60	48 (11, 20)	90	143—145	2210	$\text{C}_{14}\text{H}_9\text{N}_3$	76.70 (76.71)	4.14 (4.14)	19.17 (19.26)
61	49 (12, 20)	91	96—97	2196	$\text{C}_{15}\text{H}_{11}\text{N}_3$	77.23 (77.29)	4.75 (4.66)	18.01 (18.04)
62	50 (13, 20)	96	143—145	2202	$\text{C}_{15}\text{H}_{11}\text{N}_3$	77.23 (77.40)	4.75 (4.60)	18.01 (17.76)
63	51 (11, 21)	97	82—84 <sup>d)</sup>	1700	Known compound <sup>d)</sup>			
64	52 (12, 21)	95	97—98	1675	$\text{C}_{17}\text{H}_{16}\text{N}_2\text{O}_2$	72.84 (72.82)	5.75 (5.71)	9.99 (10.05)
65	53 (13, 21)	78	90—91 <sup>e)</sup>	1708	Known compound <sup>e)</sup>			
66	54 (11, 22)	67	97—99	1670	$\text{C}_{20}\text{H}_{14}\text{N}_2\text{OS}$	72.70 (72.68)	4.27 (4.27)	8.48 (8.66)
67	55 (12, 22)	65	79—81	1675	$\text{C}_{21}\text{H}_{16}\text{N}_2\text{OS}$	73.23 (73.07)	4.68 (4.70)	8.13 (8.27)
68	56 (13, 22)	73	128—129	1673	$\text{C}_{21}\text{H}_{16}\text{N}_2\text{OS}$	73.23 (73.27)	4.68 (4.67)	8.13 (8.10)
69	57 (11, 23)	80	141—143	1673	$\text{C}_{20}\text{H}_{13}\text{ClN}_2\text{OS}$	65.84 (65.79)	3.59 (3.62)	7.68 (7.70)
70	58 (12, 23)	72	86—88	1671	$\text{C}_{21}\text{H}_{15}\text{ClN}_2\text{OS}$	66.57 (66.61)	3.99 (4.20)	7.39 (7.24)
71	59 (13, 23)	67	172—174	1654	$\text{C}_{21}\text{H}_{15}\text{ClN}_2\text{OS}$	66.57 (66.87)	3.99 (3.96)	7.39 (7.13)
84	72 (14, 20)	86	127—128	2200	$\text{C}_{10}\text{H}_{10}\text{N}_4$	64.50 (64.55)	5.41 (5.59)	30.09 (29.86)
85	73 (15, 20)	75	127	2199	$\text{C}_{11}\text{H}_{12}\text{N}_4$	65.98 (65.90)	6.04 (5.89)	27.98 (28.20)
86	74 (13, 21)	85	121—123	2200	$\text{C}_{11}\text{H}_{12}\text{N}_4$	65.98 (65.79)	6.04 (5.94)	27.98 (28.27)

TABLE IV. (continued)

Product <sup>a)</sup> No.	Salt (S.M. <sup>b)</sup> )	Yield (%)	mp (°C)	$\nu_{\max}^{\text{KBr}} \text{ cm}^{-1}$	Formula	Analysis (%)		
						Calcd	(Found)	
						C	H	N
87	75 (14, 21)	93	79—80	1686	C <sub>12</sub> H <sub>15</sub> N <sub>3</sub> O <sub>2</sub>	61.79 (61.56)	6.48 (6.53)	18.01 (18.19)
88	76 (15, 21)	88	78—79	1681	C <sub>13</sub> H <sub>17</sub> N <sub>3</sub> O <sub>2</sub>	63.14 (62.89)	6.93 (6.91)	16.99 (17.27)
89	77 (16, 21)	82	81—83	1673	C <sub>13</sub> H <sub>17</sub> N <sub>3</sub> O <sub>2</sub>	63.14 (63.17)	6.93 (7.02)	16.99 (16.87)
90	78 (14, 22)	65	125—127	1675	C <sub>16</sub> H <sub>15</sub> N <sub>3</sub> OS	64.62 (64.60)	5.08 (5.10)	14.13 (14.12)
91	79 (15, 22)	78	102—103	1672	C <sub>17</sub> H <sub>17</sub> N <sub>3</sub> OS	65.57 (65.77)	5.50 (5.49)	13.49 (13.30)
92	80 (16, 22)	83	129—131	1670	C <sub>17</sub> H <sub>17</sub> N <sub>3</sub> OS	65.57 (65.54)	5.50 (5.45)	13.49 (13.57)
93	81 (14, 23)	76	138—140	1675	C <sub>16</sub> H <sub>14</sub> ClN <sub>3</sub> OS	57.91 (57.69)	4.25 (4.27)	12.66 (12.87)
94	82 (15, 23)	73	140—142	1670	C <sub>17</sub> H <sub>16</sub> ClN <sub>3</sub> OS	59.04 (58.74)	4.66 (4.74)	12.15 (12.37)
95	83 (16, 23)	84	148—149	1672	C <sub>17</sub> H <sub>16</sub> ClN <sub>3</sub> OS	59.04 (58.74)	4.66 (4.84)	12.15 (12.37)
108 (114)	96 (17, 20)	26 (6)	126—127	2205	C <sub>10</sub> H <sub>9</sub> N <sub>3</sub> O	64.16 (63.98)	4.85 (4.93)	22.45 (22.56)
109 (115)	97 (18, 20)	22 (34)	109—111	2203	C <sub>11</sub> H <sub>11</sub> N <sub>3</sub> O	65.66 (65.43)	5.51 (5.56)	20.88 (21.06)
110 (116)	98 (19, 20)	22 (36)	101—103	2207	C <sub>11</sub> H <sub>11</sub> N <sub>3</sub> O	65.66 (65.64)	5.51 (5.68)	20.88 (20.73)
111 (117)	99 (17, 21)	37 (33)	85—86	1705	C <sub>12</sub> H <sub>14</sub> N <sub>2</sub> O <sub>3</sub>	61.53 (65.35)	6.02 (6.03)	11.96 (11.67)
112 (118)	100 (18, 21)	27 (18)	87—89	1703	C <sub>13</sub> H <sub>16</sub> N <sub>2</sub> O <sub>3</sub>	62.89 (63.17)	6.50 (6.48)	11.28 (11.02)
113 (119)	101 (19, 21)	33 (29)	63—64	1697	C <sub>13</sub> H <sub>16</sub> N <sub>2</sub> O <sub>3</sub>	62.89 (62.60)	6.50 (6.39)	11.28 (11.05)
120 (126)	102 (17, 22)	36 (13)	82—84	1671	C <sub>16</sub> H <sub>14</sub> N <sub>2</sub> O <sub>2</sub> S	64.41 (64.46)	4.73 (4.72)	9.39 (9.21)
121 (127)	103 (18, 22)	34 (24)	95—97	1672	C <sub>17</sub> H <sub>16</sub> N <sub>2</sub> O <sub>2</sub> S	65.36 (65.39)	5.16 (5.26)	8.97 (9.03)
122 (128)	104 (19, 22)	33 (20)	89—90	1671	C <sub>17</sub> H <sub>16</sub> N <sub>2</sub> O <sub>2</sub> S	65.36 (65.52)	5.16 (5.15)	8.97 (8.82)
123 (129)	105 (17, 23)	48 (35)	136—138	1669	C <sub>16</sub> H <sub>13</sub> ClN <sub>2</sub> O <sub>2</sub> S	57.74 (57.98)	3.94 (3.78)	8.42 (8.34)
124 (130)	106 (18, 23)	22 (40)	137—139	1674	C <sub>17</sub> H <sub>15</sub> ClN <sub>2</sub> O <sub>2</sub> S	58.87 (58.77)	4.36 (4.28)	8.08 (8.22)
125 (131)	107 (19, 23)	39 (30)	116—118	1670	C <sub>17</sub> H <sub>15</sub> ClN <sub>2</sub> O <sub>2</sub> S	58.87 (58.86)	4.36 (4.31)	8.08 (8.14)

a) Physical and analytical data for pyridinium 1-aminides (114—119 and 126—131) are listed in Table V. b) Starting materials. c) The elementary analysis of this compound could not be performed because it sublimed readily. d) 73—75°C, see ref. 6. e) 88—90°C, see ref. 6.

ether. Pyridinium 1-(thiocarbonyl)aminides (8—10 and 14—16) were prepared by this method.

General Method B: An ethanolic solution (60 ml) of 1-aminopyridinium iodide (10 mmol) and methyl dithiobenzoate<sup>13)</sup> (5, 12 mmol) or methyl xanthogenate (7, 12 mmol)<sup>5)</sup> was treated with anhydrous potassium carbonate (10 g) as a base at room temperature for 1 d under stirring. The isolation and the purification of pyridinium 1-aminide from the reaction mixture were accomplished according to the procedure mentioned in method A. By this method, pyridinium 1-(thiocarbonyl)aminides (11—13 and 17—19) were prepared.

These pyridinium 1-(thiocarbonyl)aminides were obtained as colorless prisms (8—10) or colorless needles (11—19), and compound 17 was identical with an authentic sample.<sup>5)</sup> Some data for these compounds (8—19) are listed in Tables II and III.

On the other hand, pyridinium 1-vinylaminides (132 and 133) and 1-imidoylaminide (134) were prepared according to the literature.<sup>8,9)</sup>

**1-[(Substituted Methylthio)methyleneamino]pyridinium Bromides (24—35, 48—59, 72—83, and 96—107)**—General Method: A chloroform solution (20 ml) of pyridinium 1-aminide (2 mmol) and an alkylating agent (2.5 mmol) such as bromoacetonitrile (20), ethyl bromoacetate (21), phenacyl bromide (22), or *p*-chlorophenacyl bromide (23) was kept at room temperature for 1—10 d until the pyridinium 1-aminide employed here was completely consumed (determined by thin layer chromatographic (TLC) monitoring). The resulting solution was concentrated under reduced pressure and the residue was washed three times with ether to remove the excess alkylating agent. Since all of the pyridinium salts were obtained quantitatively in an almost pure state, they were used directly for a subsequent reaction without further purification.

**2-Ethyl- (36—47), 2-Phenyl- (60—71), 2-Dimethylamino- (84—95), and 2-Ethoxypyrazolo[1,5-*a*]pyridines (108—113 and 120—125)**—General Method A: Pyridinium salt (2 mmol) was dissolved in chloroform (40 ml) and anhydrous potassium carbonate (5 g) was added. The reaction solution was stirred at room temperature for 1 d and then filtered to remove inorganic substances. The filtrate was concentrated under reduced pressure and the residue was separated by column chromatography (alumina) using hexane, ether, and chloroform as eluents. The combined ether and chloroform layer was concentrated under reduced pressure and the crude pyrazolopyridine was recrystallized from ethanol. By this route, 2-ethyl (36—47), 2-phenyl- (60—71), and 2-(dimethylamino)pyrazolo[1,5-*a*]pyridines (84—95) were prepared.

General Method B: A chloroform solution (40 ml) of pyridinium salt (2 mmol) was treated with anhydrous potassium carbonate (5 g) in an ice bath under stirring for 3 d. Work-up of the resulting reaction mixture was carried out according to the procedure described in general method A. By this method, 2-ethoxypyrazolo[1,5-*a*]pyridines (108—113 and 120—125) were formed together with pyridinium 1-[(substituted methylthio)carbonyl]aminides (114—119 and 126—131).

TABLE V. Some Data for Pyridinium 1-Aminides

Compd.	Salt	Yield (%)	mp (°C)	$\nu_{\text{max}}^{\text{KBr}}$ $\text{cm}^{-1}$	Formula	Analysis (%)		
						Calcd (Found)		
						C	H	N
114	96	79	130—132	2233 1603	$\text{C}_8\text{H}_7\text{N}_3\text{OS}$	49.73 (49.47)	3.65 (3.57)	21.75 (21.63)
115	97	99	87—89	2241 1609	$\text{C}_9\text{H}_9\text{N}_3\text{OS}$	52.16 (52.47)	4.38 (4.46)	20.28 (20.02)
116	98	100	156—157	2238 1605	$\text{C}_9\text{H}_9\text{N}_3\text{OS}$	52.16 (51.87)	4.38 (4.32)	20.28 (20.33)
117	99	80	61—62	1729 1603	$\text{C}_{10}\text{H}_{12}\text{N}_2\text{O}_3\text{S}$	49.99 (50.20)	5.03 (4.84)	11.66 (11.64)
118	100	95	58—59	1734 1601	$\text{C}_{11}\text{H}_{14}\text{N}_2\text{O}_3\text{S}$	51.95 (51.65)	5.55 (5.47)	11.02 (11.30)
119	101	89	122—123	1741 1609	$\text{C}_{11}\text{H}_{14}\text{N}_2\text{O}_3\text{S}$	51.95 (51.73)	5.55 (5.47)	11.02 (11.32)
126	102	83	142—143	1690 1600	$\text{C}_{14}\text{H}_{12}\text{N}_2\text{O}_2\text{S}$	61.75 (61.74)	4.44 (4.50)	10.29 (10.24)
127	103	93	146—148 <sup>a)</sup>	1682 1594 <sup>b)</sup>	$\text{C}_{21}\text{H}_{17}\text{N}_5\text{O}_6\text{S}^{a)}$	48.93 (48.71)	3.32 (3.25)	13.59 (13.43)
128	104	77	139—140	1690 1598	$\text{C}_{15}\text{H}_{14}\text{N}_2\text{O}_2\text{S}$	62.92 (63.21)	4.93 (4.88)	9.78 (9.48)
129	105	87	125—126	1684 1580	$\text{C}_{14}\text{H}_{11}\text{ClN}_2\text{O}_2\text{S}$	54.81 (54.71)	3.61 (3.60)	9.13 (9.19)
130	106	63	113—114	1693 1598	$\text{C}_{15}\text{H}_{13}\text{ClN}_2\text{O}_2\text{S}$	56.16 (55.89)	4.08 (4.03)	8.73 (8.53)
131	107	82	138—140	1690 1601	$\text{C}_{15}\text{H}_{13}\text{ClN}_2\text{O}_2\text{S}$	56.16 (56.00)	4.08 (4.02)	8.73 (8.84)

a) Its picrate. b) Neat.

The application of method A to 1-(ethoxymethyleneamino)pyridinium bromides (96—107) gave only small amounts of pyridinium 1-aminides (114—119 and 126—131); the desulfurized 2-ethoxypyrazolopyridines (108—113) and the rearranged products, 2-arylthio-2-ethoxypyrazolopyridines (120—125), could not be obtained.

The products were obtained as colorless needles (36—41, 44, 60—68, 84—89, and 108—113) or pale yellow needles (42, 43, 45—47, 69—71, 90—95, and 120—125) and some data for the products other than pyridinium 1-aminides (114—119 and 126—131, see Tables II and V) are summarized in Tables I and IV.

**Pyridinium 1-[Substituted (Methylthio)carbonyl]aminides (114—119 and 126—131)**—General Method: A chloroform solution (30 ml) of pyridinium salt (2 mmol) was heated at 50—60 °C in a water bath until the spot of the salt had completely disappeared (about 5—10 d, by TLC monitoring). The reaction mixtures were purified by work-up as mentioned above to afford the corresponding pyridinium 1-aminides (117—119 and 126—131). On the other hand, the reactions of pyridinium salts (96—98) possessing a cyano group could be accomplished only by keeping them at room temperature for 2 d.

These compounds were obtained as colorless needles (114—117, 126, 128, 129, and 131) and colorless prisms (118, 119, and 130) from chloroform–ether. Some data are summarized in Tables II and V.

**1-Propylideneamino- (135 and 136) and 1-(Aminomethyleneamino)pyridinium Bromides (137 and 138)**—Pyridinium 1-vinylaminides (132 and 133) and 1-imidoylaminide (134) did not react at all with alkylating agents such as 20—23 under the conditions described for the preparations of 1-[(substituted methylthio)methyleneamino]pyridinium bromides. However, the alkylations of 132—134 (2 mmol) with 20 or 21 (10 mmol) were accomplished in refluxing chloroform to afford the corresponding pyridinium salts (135—138) in quantitative yields. These salts were used in the next reactions without further purification.

**Pyridinium 1-Aminide and Pyridinium 1-Benzoylaminide**—A chloroform solution (30 ml) of 1-propylideneaminopyridinium bromide (135) (2 mmol) was treated with anhydrous potassium carbonate (5 g) under stirring at room temperature for 3 h. The reaction solution gradually turned blue, indicating the generation of pyridinium 1-aminide (140). When benzoyl chloride (0.28 g, 2 mmol) was added to the blue solution, the color changed to red. The solution was stirred for a further 2 h and then filtered. The filtrate was concentrated and the residual oil was separated by column chromatography on alumina using ether and chloroform. The chloroform layer was concentrated and recrystallization of the residue from ether–chloroform gave pyridinium 1-benzoylaminide (142, 52 mg, 13%, mp 177—179 °C (lit.<sup>4c</sup>) 179—180.5 °C). Compound 142 was identical with an authentic sample.<sup>4c</sup>

On the other hand, the reaction of the salt 136 with base afforded only a polymeric tar and no significant product could be isolated.

**1,2,4-Triazolo[1,5-*a*]pyridine**—General Method: A chloroform solution (30 ml) of 1-(aminomethyleneamino)pyridinium bromide (2 mmol) was treated with DBU (0.30 g, 2 mmol) under stirring at room temperature for 1 d and the dark brown solution was concentrated under reduced pressure. The residue was separated by column chromatography on alumina using hexane and ether. The ether layer was concentrated and recrystallization of the residue from hexane gave 7-methyl-2-phenyl-1,2,4-triazolo[1,5-*a*]pyridine (143, mp 140—142 °C (lit.<sup>9</sup>) 140—142 °C). Concentration of the hexane layer yielded an active methylene compound 144 or 145 which could be identified by GLC monitoring.

By this method, 143 was formed in 11% and 72% yields from the salts 137 and 138, respectively. In the reaction of 137 with potassium carbonate as a base, triazolopyridine (143) was obtained in 11% yield.

#### References and Notes

- 1) For part XIII of this series, see A. Kakehi, S. Ito, and T. Yotsuya, *Chem. Pharm. Bull.*, **34**, 2435 (1986).
- 2) a) A. Kakehi, S. Ito, M. Ito, and T. Yotsuya, *Heterocycles*, **22**, 2237 (1984); b) A. Kakehi, S. Ito, M. Ito, T. Yotsuya, and K. Nagata, *Bull. Chem. Soc. Jpn.*, **58**, 1432 (1985).
- 3) a) H. Beyer, *Z. Chem.*, **9**, 361 (1969); b) H. Beyer, H. Honeck, and L. Reichelt, *Justus Liebigs Ann. Chem.*, **741**, 45 (1970); c) R. R. Schmidt, *Angew. Chem. Int. Ed. Engl.*, **14**, 581 (1975); d) R. R. Schmidt and H. Huth, *Tetrahedron Lett.*, **1975**, 33; e) K. Kaji, H. Nagashima, S. Nagao, K. Tabashi, and H. Oda, *Chem. Pharm. Bull.*, **32**, 4437 (1984); f) K. Kaji, H. Nagashima, Y. Ohta, S. Nagao, Y. Hirose, and H. Oda, *Heterocycles*, **22**, 479 (1984).
- 4) a) K. Hafner, D. Zinser, and K. L. Moritz, *Tetrahedron Lett.*, **1964**, 1733; b) T. Sasaki, K. Kanematsu, A. Kakehi, I. Ichikawa, and K. Hayakawa, *J. Org. Chem.*, **35**, 426 (1970); c) A. Balasubramanian, J. M. McIntosh, and V. Snieckus, *ibid.*, **35**, 433 (1970).
- 5) H. Yoshida, K. Urushibata, and T. Ogata, *Bull. Chem. Soc. Jpn.*, **56**, 1561 (1983).
- 6) a) R. Huisgen, R. Grashey, and R. Krischke, *Tetrahedron Lett.*, **1962**, 387; b) V. Boeckelheide and N. A. Fedruk, *J. Org. Chem.*, **33**, 2062 (1968); c) T. Sasaki, K. Kanematsu, and A. Kakehi, *J. Org. Chem.*, **37**, 3106 (1972); d) Y. Tamura, A. Yamagami, and M. Ikeda, *Yakugaku Zasshi*, **91**, 1154 (1971); e) Y. Tamura, W. Tujimoto, Y. Sumida, and M. Ikeda, *Tetrahedron*, **28**, 21 (1972); f) Y. Tamura, Y. Sumida, Y. Miki, and M. Ikeda, *J. Chem. Soc., Perkin Trans. 1*, **1975**, 406.
- 7) a) A. Kakehi and S. Ito, *J. Org. Chem.*, **39**, 1542 (1974); b) P. L. Anderson, J. P. Hasak, A. D. Kahle, N. A.

- 
- Paolella, and M. T. Shapiro, *J. Heterocycl. Chem.*, **18**, 1149 (1981).
- 8) T. Sasaki, K. Kanematsu, and A. Kakehi, *Tetrahedron Lett.*, **1972**, 5245.
  - 9) A. Kakehi, S. Ito, K. Uchiyama, Y. Konno, and K. Kondo, *J. Org. Chem.*, **42**, 443 (1977).
  - 10) E. Vedejs, *Acc. Chem. Res.*, **17**, 358 (1984).
  - 11) R. B. Woodward and R. Hoffmann, "The Conservation of Orbital Symmetry," Academic Press Inc., 1970, p. 115.
  - 12) Melting points were measured with a Yanagimoto micromelting point apparatus and are uncorrected. Microanalyses were carried out on a Perkin-Elmer 240 elemental analyzer. The <sup>1</sup>H-NMR spectra were determined with a Varian EM360A spectrometer in deuteriochloroform with tetramethylsilane as an internal standard. The IR spectra were taken with a Hitachi 260-10 infrared spectrophotometer.
  - 13) J. Meijer, P. Vermeer, and L. Brandsma, *Recl. Trav. Chim. Pays-Bas*, **92**, 601 (1973).

[Chem. Pharm. Bull.]  
[35(1) 170-181 (1987)]

## A Quantitative Analysis of Nuclear Magnetic Relaxation: The Configuration and the Conformation of ML-236B(Mevastatin) Metabolites

HIDEYUKI HARUYAMA\* and MICHIO KONDO

*Analytical and Metabolic Research Laboratories,  
Sankyo Company Ltd., 1-2-58, Hiromachi,  
Shinagawa-ku, Tokyo 140, Japan*

(Received July 10, 1986)

A quantitative treatment of proton spin-lattice relaxation time ( $T_1$ ) and nuclear Overhauser effect (NOE) has been applied to the conformational analysis of two ML-236B (mevastatin) metabolites, 4 $\beta$ ,6 $\alpha$ -dihydroxy ML-236B (**1**) and 3 $\beta$ -hydroxy ML-236B (**2**) in solution. The  $T_1$  values and NOE factors predicted for several candidate conformers were compared with the observed ones.

For **1**, the best agreements between observed and calculated values were obtained when the A ring of its octalin moiety was assumed to adopt a chair conformation, and the B ring, a 7 $\beta$ -sofa conformation. In addition it was found that the  $\delta$ -lactone side chain should be confined to some limited orientations to give calculated values consistent with the observed  $T_1$  values and NOEs. Based on the X-ray derived geometry, a similar analysis was done for **2**, to check the validity of the method and to characterize the conformation of the  $\delta$ -lactone side chain in solution. The  $\delta$ -lactone side chain of **2** was concluded to have the same conformation as in the crystal state.

The applicability of the distance geometry method to calculate the coordinates of small organic molecules was confirmed.

**Keywords**—ML-236B metabolite; mevastatin;  $^1\text{H-NMR}$ ; spin-lattice relaxation time; NOE; distance geometry; conformation analysis

### Introduction

Nuclear Overhauser effect (NOE) and spin-lattice relaxation time ( $T_1$ ) reflect the inter-nuclear distances in a molecule through the dipole-dipole relaxation mechanism, and the quantitative analysis of these relaxation parameters has been expected to provide the three-dimensional geometries of the molecules in solution.<sup>1)</sup> The recent development of superconducting high-resolution nuclear magnetic resonance (NMR) spectrometers, has made it possible to apply this method to rather complex natural products. In a previous paper, we have reported an application of this method to structural studies of saframycin A.<sup>2)</sup>

In a study of the metabolism of ML-236B,<sup>3)</sup> a competitive inhibitor of 3-hydroxy-3-methyl glutaryl coenzyme A (HMG-CoA) reductase, two metabolites (4 $\beta$ ,6 $\alpha$ -dihydroxy ML-236B (**1**) and 3 $\beta$ -hydroxy ML-236B (**2**)), have been isolated from the urine of ML-236B-treated dogs.<sup>4)</sup> These compounds were also obtained by microbial conversion of ML-236B.<sup>5)</sup> These metabolites inhibit HMG-CoA reductase, but their potencies are quite different. The metabolite **2** shows a more potent inhibitory activity against HMG-CoA reductase than does the parent compound ML-236B, while the potency of **1** is only one-fifth of that of ML-236B.<sup>3)</sup> This suggests that the hexalin portion of ML-236B should play an important role in binding to HMG-CoA reductase,<sup>6)</sup> and prompted us to examine the conformational differences between **1** and **2**.

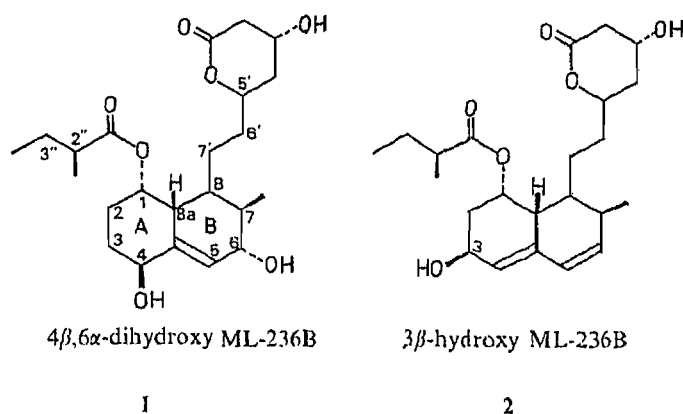


Chart 1

The X-ray analysis of ML-236B<sup>7)</sup> and **2**<sup>4)</sup> has been already done, but that of **1** has not been possible due to the unavailability of good crystals. We will show here that in such a case the quantitative analysis of  $T_1$  values and NOE factors can provide the three-dimensional geometry of the molecule in a quantitative manner which is substantially equivalent to X-ray analysis.

For the analysis of **1**, the distance geometry method<sup>8)</sup> has been applied with some modification to generate possible and chemically reasonable geometries of the octalin ring moiety.  $T_1$ s and NOEs expected for these geometries were calculated and compared with the observed values. The following conclusions were reached: (1) the *S* configurations of the two hydroxyl groups at  $C_4$  and  $C_6$  have been confirmed<sup>4)</sup>; (2) in the octalin ring moiety, the B ring adopted a  $7\beta$ -sofa conformation, while the A ring took a chair conformation; (3) the dihedral angles which determine the orientation of the  $\delta$ -lactone side chain,  $\psi_1$  ( $=C_5-C_6-C_7-C_8$ ) and  $\psi_2$  ( $=C_6-C_7-C_8-C_7$ ), were estimated to be  $180^\circ$  and  $120^\circ$ , respectively.

The above conclusions were supported by the satisfactory agreement between observed and calculated  $T_1$  values of **2**, for which the calculation was carried out with the coordinates derived from X-ray analysis.<sup>4)</sup> The two dihedral angles,  $\psi_1$  and  $\psi_2$ , were varied to search for the optimal agreement. The final values,  $\psi_1 = 180^\circ$  and  $\psi_2 = 50^\circ$ , are very similar to the values observed in the crystal ( $\psi_1 = 176.3^\circ$  and  $\psi_2 = 55.1^\circ$ ).

### Experimental

**Samples**—Di (**1**), and mono (**2**)-hydroxylated derivatives obtained by microbial conversion of ML-236B<sup>5)</sup> were supplied by Dr. Serizawa, Bio-science Research Laboratories of Sankyo Co.

A small amount of  $CD_3OD$  was added to the samples and freeze-dried two or three times to substitute deuterium for each labile proton. The samples for  $^1H$ -NMR measurements were prepared at concentrations, of 0.05 M for **1** and 0.03 M for **2** in  $CD_3OD$ , and they were sealed after five freeze-pump-thaw cycles. A similar method was applied to a chloroform solution of ML-236B (0.1 M) for  $^{13}C$ - $T_1$  measurement.

**Spectroscopy**— $^1H$ - and  $^{13}C$ -NMR spectra were obtained on a JEOL GX-400 spectrometer operating at 399.6 MHz ( $^1H$ ) and 100.5 MHz ( $^{13}C$ ), respectively. The measurements of  $^1H$ - $T_1$  were made by the inversion recovery method ( $180^\circ$ - $\tau$ - $90^\circ$  pulse sequence) at ambient temperature ( $24.5 \pm 0.5^\circ C$ ) while varying the variable  $\tau$  in range from 0.1 to 2.0 s. Sixty-four free induction decays (FIDs) were accumulated for each experiment with 16 K data points and  $T_1$ s were obtained by linear least-squares fitting to the initial part of the recovery curves (up to 50%).  $^{13}C$ - $T_1$ s were obtained by a similar procedure, where 640 FIDs were accumulated and non-linear least-squares fitting was applied.

The NOE was measured in the difference spectral mode.<sup>9)</sup> The eight FIDs irradiated off-resonance were subtracted from the eight FIDs irradiated at a certain signal, and the resulting difference FID was accumulated until a sufficient *S/N* ratio could be attained. The pre-irradiation time, 7 s, was used for complete saturation. Signal enhancement was given by the ratio of the integrated intensity of the observed signal in the difference spectra to that of the saturated one.

**Geometry Generation by the Distance Geometry Method**—The distance geometry (DG) method is an algorithm

to calculate the three-dimensional coordinates of a molecule which satisfy constraints given in the form of upper and lower bounds to interatomic distances.<sup>8)</sup> A distance matrix, the elements of which are interatomic distances randomly given, satisfying the preliminary bounds, was prepared for a certain model conformation and was converted to a metric matrix, the elements of which are scalar products of the vectors  $r_i$  and  $r_j$ . The three-dimensional coordinates of the model conformation were calculated from the largest three eigenvalues and eigenvectors of this metric matrix. At this stage, the resulting coordinates do not always satisfy the preliminarily given constraints, and corrections were made by minimizing appropriate error functions.

In the present work, four different conditions of interatomic bounds were used. A typical set of constraints and one of the resulting geometries is explained in Table III. The applied error function  $F_{\text{err}}$  is given by Eq. 1.

$$F_{\text{err}} = \frac{1}{2} \sum_{i < j} (d_{ij}^2 - u_{ij}^2)^2 + \frac{1}{2} \sum_{k < l} (l_{kl}^2 - d_{kl}^2)^2 + \sum_{\text{chiral}} (f_{\text{oh}} - f_{\text{ch}}^*)^2 + \sum_{\varphi} (\varphi_1 - \varphi)^2 + \sum_{\varphi} (\varphi_u - \varphi)^2 \quad (1)$$

The last two terms of  $F_{\text{err}}$  were newly added to ensure the convergence to chemically reasonable structures. These terms act so as to maintain the planarity of the double bonds and to set the dihedral angles in the range,  $\varphi_1 \leq \varphi \leq \varphi_u$  including signs. The definitions of the other terms were given in the literature.<sup>8)</sup>

The minimization of  $F_{\text{err}}$  was done in two steps. At the first step, the chirality and dihedral constraints (third to fifth terms) were minimized and at the second step, all of the terms were minimized. The resulting geometries were further optimized by molecular mechanics calculation.<sup>10)</sup>

**Calculation of the Relaxation Parameters**—Except for the treatment of the internal rotation of the methyl group,  $T_1$ s and NOEs were calculated by the same procedure as described previously.<sup>2)</sup> The effective correlation time of methyl protons ( $\tau_c^{\text{eff}}$ ) and the effective interproton distances between the methyl protons and other protons in the rigid part of the molecules were defined according to the formulation of Heatley *et al.*<sup>12)</sup> as shown in Eqs. 2 and 3, respectively.

$$\tau_c^{\text{eff}} = \tau_c \left[ \frac{1}{4} (3 \cos^2 \theta - 1) + \frac{3}{4} (\sin^2 2\theta + \sin^4 \theta) \cdot \frac{1}{1 + \alpha} \right] \quad (2)$$

$$\left\langle \frac{1}{r_{ij}^6} \right\rangle_{\text{eff}} = \frac{1}{9} \left[ (A + 2B) + 2(A - B) \cdot \frac{1}{1 + \alpha} \right] \quad (3)$$

$$A = \sum_{m=1}^3 (r_{ij}^{(m)})^{-6}$$

$$B = \sum_{m=1}^2 \sum_{n < m}^3 \frac{1}{2} (3 \cos^2 \beta_{ij}^{(mn)} - 1) \times \frac{1}{(r_{ij}^{(m)} \cdot r_{ij}^{(n)})^3}$$

In Eq. 2,  $\theta$  is the angle between the interatomic vectors and the axis of internal rotation ( $\theta = 90^\circ$ , for the relaxation of methyl protons and  $\theta = 109.5^\circ$  for the relaxation of methyl carbons), and  $\alpha$  is the ratio of the correlation time for overall molecular tumbling ( $\tau_c$ ) to that for internal rotation of the methyl group ( $\tau_{\text{int}}$ ). In Eq. 3,  $r_{ij}^{(m)}$  is the interproton distance between  $H_i$  and  $H_j$ , where  $H_i$  is one of the methyl protons in one of the three different potential minima while  $H_j$  is a proton on a rigid molecular frame, and  $\beta_{ij}^{(mn)}$  is the angle between  $r_{ij}^{(m)}$  and  $r_{ij}^{(n)}$ .

## Results and Discussion

### 4 $\beta$ ,6 $\alpha$ -Dihydroxy ML-236B (1)

**<sup>1</sup>H-NMR**—Most of the proton signals of the  $\Delta^{4a}$  octalin ring moiety have been assigned<sup>4)</sup> on the basis of extensive decoupling experiments as shown in Fig. 1. A large coupling constant of 14 Hz between  $H_{2a}$  (2.08 ppm) and  $H_{3b}$  (1.83 ppm) requires their antiperiplanar arrangement, and relatively small coupling constants between  $H_1$  and adjacent vicinal protons,  $H_{8a}$ ,  $H_{2a}$  and  $H_{2b}$ , suggest that  $H_1$  is in a *gauche* relation to these protons.

The above observations are consistent with a chair conformation of the A ring, while some ambiguity exists concerning the B ring conformation. For the B ring, a 7 $\beta$ , 8 $\alpha$  half-chair or half-boat conformation is possible, while the possibility of a 7 $\alpha$ , 8 $\beta$  half-chair conformation can be ruled out, because the vicinal coupling constant between  $H_8$  and  $H_{8a}$  ( $J = 7.4$  Hz) indicates that these two protons should be in quasi-axial positions. Further information about



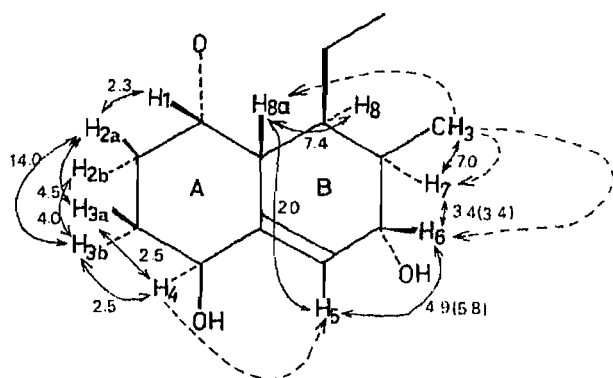


Fig. 1. Vicinal Coupling Constants and NOEs for the Octalin Ring Moiety of **1**

—, indicating the presence of vicinal coupling; ---, indicating the presence of NOE. The values in the figure are the vicinal coupling constants (Hz). Those enclosed by parentheses are the calculated values based on the Karplus equation, assuming the G1-SS geometry.

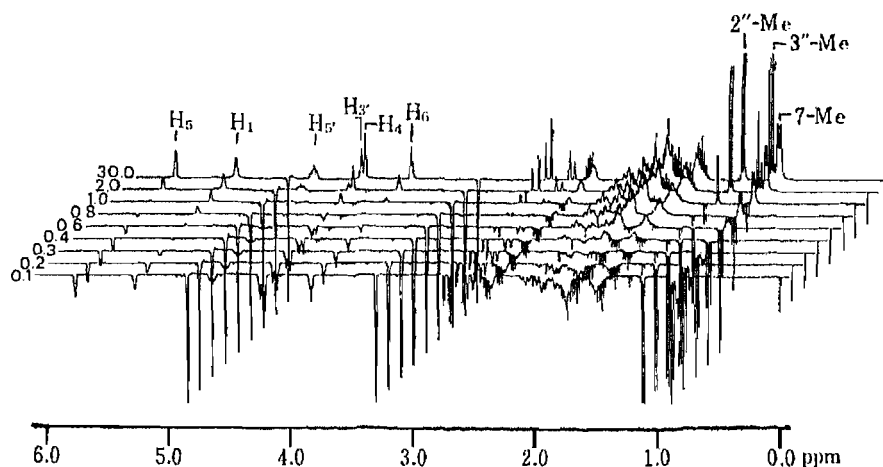


Fig. 2. Non-selective Partially Relaxed Spectra for **1**

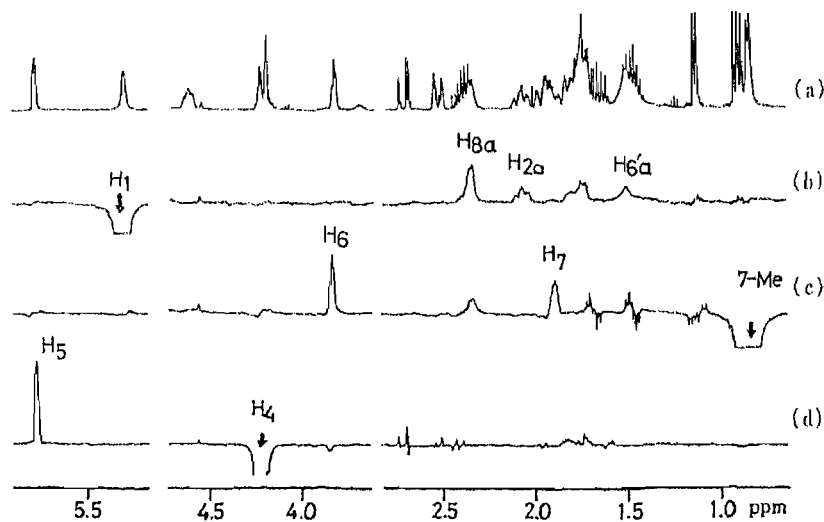


Fig. 3. NOE Difference Spectra for **1**

(a), control; (b), (c), and (d), H<sub>1</sub>, 7-Me, and H<sub>4</sub> were irradiated.

the conformation of the B ring could be obtained from the quantitative analysis of  $T_1$ s and NOEs.

Figure 2 shows typical partially relaxed Fourier transform spectra for **1**, and the observed  $T_1$  values are given in the first column of Table I. Figure 3 shows NOE difference spectra, and

the results are summarized in Table II. The 10% signal enhancement of H<sub>6</sub> on irradiating the 7-methyl protons suggests  $\alpha$  configuration of the hydroxyl group at C<sub>6</sub>. The large NOE observed between H<sub>4</sub> and H<sub>5</sub> supports  $\beta$  configuration of another hydroxyl group at C<sub>4</sub>. The quantitative analysis of these data was carried out by the following procedure.

**Geometry**—The conformations of the octalin ring moiety and the  $\delta$ -lactone side chain should be taken into account for the quantitative interpretation of the above relaxation

TABLE I. Observed and Calculated  $T_1$  Values for 1

	H <sub>1</sub>	H <sub>4</sub>	H <sub>5</sub>	H <sub>6</sub>	H <sub>7</sub>	H <sub>8a</sub>	7-Me	$q^a$
Obs.	0.60	1.00	1.28	1.08	0.72	0.65	0.57	
Calc.								
G1-SS	0.66	0.92	1.27	1.21	0.74	0.67	0.54	0.07
G1-SR	0.66	0.91	1.59	1.49	0.72	0.67	0.56	0.14
G1-RR	0.66	1.42	3.91	1.48	0.72	0.61	0.56	0.30
G1-RS	0.66	1.42	2.55	1.19	0.74	0.61	0.54	0.23
G2-SS	0.60	0.98	1.26	1.23	0.67	0.59	0.50	0.09
G2-SR	0.60	0.97	1.43	1.37	0.62	0.59	0.52	0.12
G2-RR	0.60	1.39	3.36	1.35	0.62	0.55	0.52	0.29
G2-RS	0.60	1.38	2.64	1.21	0.67	0.55	0.50	0.24
G3-SS	0.54	1.23	1.66	1.17	0.80	0.57	0.51	0.15
G3-SR	0.54	1.23	1.77	1.34	0.69	0.57	0.54	0.16
G3-RR	0.53	1.40	3.33	1.33	0.69	0.52	0.54	0.29
G3-RS	0.53	1.40	2.98	1.16	0.80	0.52	0.52	0.27
G4-SS	0.58	1.23	1.75	1.09	0.75	0.56	0.48	0.16
G4-SR	0.58	1.23	1.73	1.33	0.62	0.56	0.50	0.17
G4-RR	0.58	1.41	3.22	1.32	0.62	0.50	0.50	0.30
G4-RS	0.58	1.40	3.27	1.09	0.75	0.50	0.48	0.29
G5-SS	0.62	1.41	2.77	0.99	0.84	0.74	0.52	0.25
G5-SR	0.62	1.43	1.91	1.43	0.71	1.22	0.52	0.26
G5-RR	0.61	1.51	2.53	1.38	0.72	1.13	0.50	0.29
G5-RS	0.62	1.50	4.18	1.04	0.86	0.70	0.50	0.30

$$a) \quad q = \sqrt{\frac{1}{n} \sum_{i=1}^n [(1/T_{1,obs}^i - 1/T_{1,calc}^i) / 1/T_{1,obs}^i]^2}$$

for details of the definition, see reference.<sup>2)</sup>

TABLE II. Observed and Calculated NOE Factors for 1

Irr.	7-Me	H <sub>6</sub>	H <sub>7</sub>	H <sub>8a</sub>	H <sub>4</sub>	H <sub>6</sub>	H <sub>8a</sub>	H <sub>1</sub>	H <sub>2a</sub>	H <sub>6'a</sub>
Obs.	H <sub>5</sub>	H <sub>6</sub>	H <sub>7</sub>	H <sub>8a</sub>	H <sub>5</sub>	H <sub>6</sub>	H <sub>8a</sub>	H <sub>8a</sub>	H <sub>2a</sub>	H <sub>6'a</sub>
Obs.	0.00	0.10	0.11	0.06	0.16	-0.02	0.00	0.08	0.03	0.06
Calc.										
G1-SS	0.00	0.14	0.11	0.07	0.25	-0.03	0.00	0.05	0.03	0.08
G1-SR	0.03	0.00	0.12	0.07	0.30	-0.02	0.00	0.05	0.03	0.08
G1-RR	0.08	0.00	0.12	0.06	0.07	0.00	0.04	0.05	0.04	0.08
G1-RS	0.01	0.14	0.11	0.06	0.05	0.00	0.04	0.05	0.04	0.08
G2-SS	0.00	0.15	0.10	0.11	0.26	-0.03	0.00	0.06	0.04	0.04
G3-SS	-0.01	0.19	0.11	0.18	0.26	-0.03	0.00	0.05	0.03	0.04
G4-SS	-0.02	0.21	0.11	0.18	0.22	-0.02	0.00	0.05	0.04	0.04
G5-SS	0.00	0.05	0.17	0.00	0.22	0.00	0.00	0.12	0.03	0.02

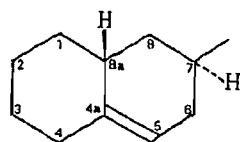


Fig. 4

TABLE III. Typical Constraints Applied to the Distance Geometry Generated Structure for the  $A^{4a}$ -Octalinal Unit of 1

	Constraints	Results	
<b>Bond lengths (Å)</b>			
$C_{sp^3}-C_{sp^3}$	1.54	$1.56 \pm 0.04$	$(1.55 \pm 0.01)^a$
$C_{sp^3}-C_{sp^2}$	1.53	$1.45 \pm 0.09$	$(1.53 \pm 0.03)^a$
$C_{sp^2}-C_{sp^2}$	1.34	1.49	$(1.35)^a$
<b>Bond angles (<math>^\circ</math>)</b>			
$C_{sp^3}-C_{sp^3}-C_{sp^3}$	110.0	$110.9 \pm 4.9$	$(110.8 \pm 1.7)^a$
$C_{sp^3}-C_{sp^2}-C_{sp^3}$	120.0	$122.2 \pm 2.7$	$(122.9)^a$
<b>Inter atomic distances (Å)</b>			
$C_1-C_4$	2.8—3.0	2.86	
$C_2-C_{4a}$	2.8—3.0	2.96	
$C_3-C_{8a}$	2.8—3.0	2.98	
$C_{4a}-C_7$	2.9—3.1	2.91	
$C_2-C_5$	4.5—5.5	4.35	
$C_3-C_7$	4.5—5.5	5.15	
$C_3-C(7-Me)$	5.8—6.2	6.41	
<b>Dihedral angles (<math>^\circ</math>)</b>			
$C_{8a}-C_{4a}-C_5-C_6$	-5.0—5.0	3.3	
$C_2-C_1-C_{8a}-C_{4a}$	50.0—70.0	33.3	
$C_1-C_2-C_3-C_4$	50.0—70.0	64.2	
$C_6-C_7-C_8-C_{8a}$	50.0—70.0	65.5	
$C_{8a}-C_1-C_2-C_3$	-70.0—-50.0	-54.0	
<b>Chirality constraint</b>			
$f_{ch}(C_{8a})$	-8.8		
$F_{err}$		0.440	

a) Values after energy minimization.

parameters. Generally it is difficult to construct three-dimensional structural models, especially for cyclic systems. In the present work, instead of the conventional model projection technique, the distance geometry method was applied to the preparation of the coordinates for the possible octalinal ring conformations, and the  $\delta$ -lactone side chain was added later.

Figure 4 shows the 13 atoms of the octalinal ring moiety with the numbering scheme, to which the distance geometry method was applied. A typical set of constraints is presented in Table III. Standard bond lengths and bond angles were used to specify the 1-2 (bond length) and 1-3 (separated by two bonds) distances.

To keep the A ring in chair form and to maintain the planarity of the double bond,  $C_{4a}-C_5$ , the ranges of several dihedral angles were explicitly given. These values could be easily converted to upper and lower bounds of the corresponding 1-4 distances (separated by three successive bonds). For the other 1-4 distances, the dihedral angles were not explicitly given, but the lower and upper bound distances were set to the distance between the two end atoms in the *cis* and *trans* forms, respectively.

For the non-bonded distances separated more than four bonds, the lower default bound

was set to 2.0 Å and the upper bound to the fully extended bond lengths. Several non-bonded distances estimated from Dreiding models were explicitly given as constraints, which were proved to be essential to generate chemically reasonable geometries.<sup>13)</sup> The chirality constraints are given for C<sub>8a</sub> only.

The constraint values after applying the distance geometry method are also given in Table III. The bond lengths and bond angles of the resulting geometry are within normal values. Four of the five dihedral angles converged within the initially given range. To correct

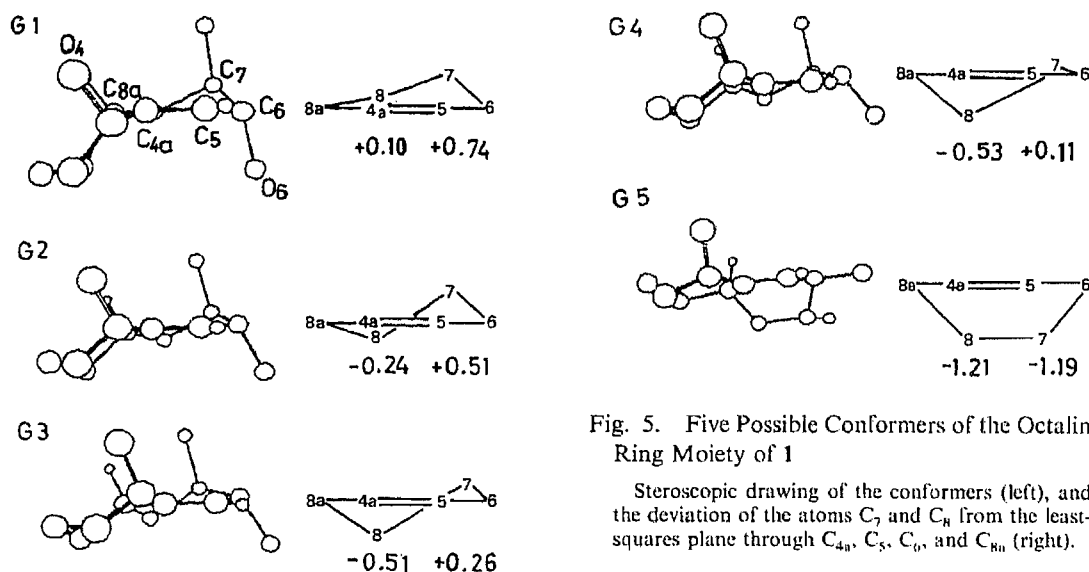


Fig. 5. Five Possible Conformers of the Octalin Ring Moiety of 1

Stereoscopic drawing of the conformers (left), and the deviation of the atoms C<sub>4a</sub>, C<sub>5</sub>, C<sub>6</sub>, and C<sub>8a</sub> from the least-squares plane through C<sub>4a</sub>, C<sub>5</sub>, C<sub>6</sub>, and C<sub>8a</sub> (right).

TABLE IV. Geometries Generated by the Distance Geometry Method for the Δ<sup>4a</sup>-Octalin Unit of 1

	G1	G2	G3	G4	G5
Bond lengths (Å)					
C <sub>sp<sup>3</sup></sub> -C <sub>sp<sup>3</sup></sub>	1.56	1.52	1.55	1.55	1.55
C <sub>sp<sup>3</sup></sub> -C <sub>sp<sup>2</sup></sub>	1.53	1.51	1.53	1.52	1.52
C <sub>sp<sup>2</sup></sub> -C <sub>sp<sup>2</sup></sub>	1.35	1.32	1.35	1.35	1.35
Bond angles (°)					
C <sub>sp<sup>3</sup></sub> -C <sub>sp<sup>3</sup></sub> -C <sub>sp<sup>3</sup></sub>	111.6	110.9	110.8	111.5	111.3
C <sub>sp<sup>3</sup></sub> -C <sub>sp<sup>2</sup></sub> -C <sub>sp<sup>3</sup></sub>	123.5	123.8	122.9	122.9	115.7
C <sub>4</sub> -C <sub>4a</sub> -C <sub>8a</sub>	114.7	115.5	113.2	113.2	118.2
Dihedral angles (°)					
C <sub>1</sub> -C <sub>2</sub> -C <sub>3</sub> -C <sub>4</sub>	52.0	60.0	57.5	57.5	64.9
C <sub>2</sub> -C <sub>3</sub> -C <sub>4</sub> -C <sub>4a</sub>	-45.3	-52.4	-56.1	-56.1	-55.9
C <sub>3</sub> -C <sub>4</sub> -C <sub>4a</sub> -C <sub>8a</sub>	46.0	47.7	56.2	56.2	31.9
C <sub>4</sub> -C <sub>4a</sub> -C <sub>8a</sub> -C <sub>1</sub>	-51.2	-47.7	-55.0	-55.0	-19.4
C <sub>4a</sub> -C <sub>8a</sub> -C <sub>1</sub> -C <sub>2</sub>	60.1	54.7	55.6	55.6	32.4
C <sub>8a</sub> -C <sub>1</sub> -C <sub>2</sub> -C <sub>3</sub>	-61.5	-62.3	-58.1	-58.1	-54.9
C <sub>8a</sub> -C <sub>4a</sub> -C <sub>5</sub> -C <sub>6</sub>	-2.0	5.5	3.8	3.6	-2.0
C <sub>4a</sub> -C <sub>5</sub> -C <sub>6</sub> -C <sub>7</sub>	32.1	15.3	6.5	0.4	-53.6
C <sub>5</sub> -C <sub>6</sub> -C <sub>7</sub> -C <sub>8</sub>	-55.5	-47.9	-38.0	-27.9	50.4
C <sub>6</sub> -C <sub>7</sub> -C <sub>8</sub> -C <sub>8a</sub>	54.4	62.2	61.8	52.7	1.0
C <sub>7</sub> -C <sub>8</sub> -C <sub>8a</sub> -C <sub>4a</sub>	-25.0	-40.2	-52.1	-48.6	-51.3
C <sub>8</sub> -C <sub>8a</sub> -C <sub>4a</sub> -C <sub>5</sub>	-2.4	7.5	18.8	20.1	22.8

G1; 7β-sofa, G2, G3; 7β,8α-half-chair, G4; 8α-sofa, and G5; half-boat. S.D. for bond lengths=0.01--0.02 Å, S.D. for bond angles=1.0--3.0°.

the distortion of the geometry, energy minimization was carried out after hydrogen atoms were added.

The processes described above were applied to four sets of constraints.<sup>14)</sup> For each set, about ten different distance matrixes were generated. Among the resulting geometries, those shown in Fig. 5 were selected as candidates for the possible octalin ring conformations. The B ring of these geometries adopts half-chair conformations with different extents of distortion or a half-boat conformation, while the A ring adopts a chair conformation. The geometrical parameters are summarized in Table IV.

**Correlation Time**—The calculation of the relaxation parameters was carried out on the assumption that the motion of the octalin ring moiety can be described by a single correlation time, except for the 7-methyl group. The  $\tau_c = 0.8 \times 10^{-10}$  s gave a satisfactory agreement between observed and calculated  $T_1$  values of methylene protons, H<sub>2a</sub> and H<sub>3b</sub>, which are insensitive to the geometry, while the effective  $\tau_c$  value of the 7-methyl group,  $\tau_c^{\text{eff}} = 0.32 \times 10^{-10}$  s, was obtained on the assumption that the  $^1\text{H}-T_1$  value of methyl protons is practically determined by the mutual dipole-dipole interaction.<sup>15)</sup> Putting the correlation times,  $\tau_c$  and  $\tau_c^{\text{eff}}$ , into Eq. 2, the ratio of  $\tau_c/\tau_{\text{int}}$  ( $=\alpha$ ) was calculated as 4.0.

To check the validity of the above treatment,  $^{13}\text{C}-T_1$  measurements of ML-236B were made and the correlation times for the individual C-H vectors were calculated (Fig. 6). The averaged correlation times for the octalin ring moiety, the  $\delta$ -lactone side chain, and the 2-methyl butanoyl group are  $0.69 \pm 0.1 \times 10^{-10}$  s,  $0.43 \pm 0.1 \times 10^{-10}$  s and  $0.20 \pm 0.1 \times 10^{-10}$  s, respectively. This supports the assumption of a localized correlation time for the octalin ring moiety.

Putting the correlation time,  $\tau_c = 0.69 \times 10^{-10}$  s, and the effective correlation time of the 7-methyl group,  $\tau_c^{\text{eff}} = 0.16 \times 10^{-10}$  s, into Eq. 2, the ratio  $\alpha$  was calculated as 6.4. The effective interproton distances between 7-methyl protons and the protons on the rigid molecular frame were calculated by introducing  $\alpha = 4.0$  into Eq. 3, or alternatively by introducing  $\alpha = 6.4$ . As the difference of the calculated interproton distances between these two cases were very small,  $\alpha = 6.4$  was used in the following analysis, which gave a better agreement of the observed and calculated  $T_1$  value for the 7-methyl protons.

**Calculation of  $T_1$ s and NOEs**—Relaxational parameters were calculated for twenty cases, which are combinations of the five possible octalin ring conformations and the four configurations about two hydroxyl groups at C<sub>4</sub> and C<sub>6</sub>. The motional parameters,  $\tau_c = 0.8 \times 10^{-10}$  s and the ratio  $\alpha = \tau_c/\tau_{\text{int}} = 6.4$ , were used. Interproton distances were directly obtained from the geometries given above except those between the 7-methyl protons and protons on the rigid molecular frame, to which the effective values were given as described above.

The  $T_1$  value of a certain proton given by the initial slope approximation is practically determined by the dipolar contribution from the neighboring protons located within 3.0 Å. This means that the observed set of  $T_1$  values reflects the overall spatial distribution of the protons, *i.e.*, the configuration and the conformation of the molecule.

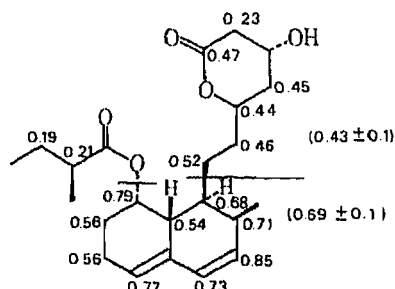


Fig. 6. Correlation Times of the C-H Vectors of ML-236B ( $\times 10^{10}$  s)

The values were derived from  $^{13}\text{C}-T_1$  values according to Eq. 4.

$1/T_1(^{13}\text{C}) = N_{\text{H}} \gamma_{\text{H}}^2 \gamma_{\text{C}}^2 \tau_c(\text{CH}) / r_{\text{CH}}^6$  (4)  
where  $N_{\text{H}}$  is the number of directly bonded protons and  $\tau_c(\text{CH})$  is the rotational correlation time for the CH internuclear vector. Taking the internuclear distance  $r_{\text{CH}} = 1.10$  Å,  $\tau_c(\text{CH})$  can be obtained from the observed  $T_1(^{13}\text{C})$  values.

As can be readily understood from an inspection of the geometries,  $T_1$  values for  $H_4$ ,  $H_5$ , and  $H_6$  are expected to depend on the configuration of the two hydroxyl groups and the conformation of the octalin ring, while  $T_1$  values for  $H_1$ ,  $H_7$ ,  $H_8$ , and  $H_{8a}$  should receive significant contributions from the protons on the  $\delta$ -lactone side chain. In fact,  $T_1$  values for  $H_1$ ,  $H_7$ , and  $H_{8a}$  could not be explained in a preliminary calculation which neglected the contribution of the  $\delta$ -lactone side chain. On the other hand, the contribution of the 2-methylbutanoyl group should be negligible, because the protons on 2-methylbutanoyl group are always more than 3.0 Å from the protons on the octalin ring moiety.

Therefore, calculation was carried out for the spin-system consisting of the non-exchangeable protons on the octalin ring, including the methylene protons on  $C_6$  and  $C_7$ . Two dihedral angles  $\psi_1 = C_5-C_6-C_7-C_8$  and  $\psi_2 = C_6-C_7-C_8-C_7$  were varied in the ranges given in Fig. 8 to search for values which give satisfactory agreement between the observed and calculated  $T_1$  values. The results of the calculations are summarized in Table I together with  $q$  values, as an index of the agreement between the observed and calculated  $T_1$  values. In Fig. 7, the  $q$  values are presented as a function of the geometries. Figure 8 is a  $q$ -value map relating the two dihedral angles and the resulting  $q$  values. The NOE factors were calculated by using the same motional and geometrical parameters. The results are given in Table II.

**The Configuration of the Hydroxyl Groups**—The interproton distance,  $d_{H_4, H_5}$ , was estimated as *ca.* 2.3 Å in the case of 4 $\beta$ -hydroxyl configuration, while it becomes more than 3.0 Å in the case of 4 $\alpha$ -hydroxyl configuration. Similarly,  $d_{H_6, 7-Me}$  depends on the configuration of the 6-hydroxyl group. Therefore,  $T_1$  values for  $H_4$ ,  $H_5$ , and  $H_6$  are sensitive to the configurations at  $C_4$  and  $C_6$ .

Configuration dependence of the agreement factors is clearly displayed in Fig. 7, which shows that most satisfactory agreement has been obtained for the geometry G1-SS. The  $S$  configurations of the two hydroxyl groups at  $C_4$  and  $C_6$  could be confirmed. The NOEs observed between  $H_6$  and 7-Me, and between  $H_4$  and  $H_5$ , support this conclusion quantitatively (see Table II).

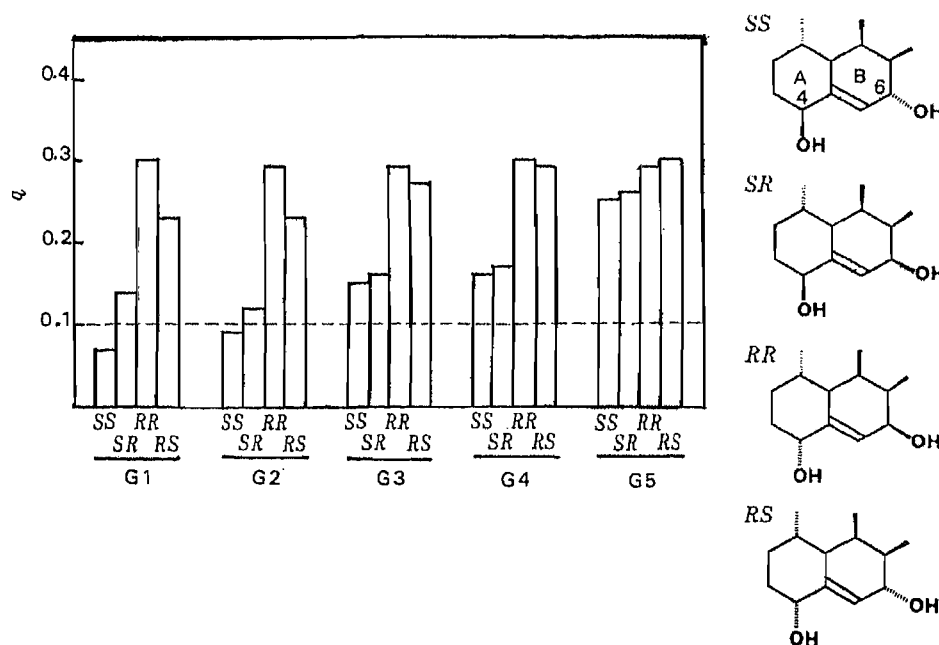


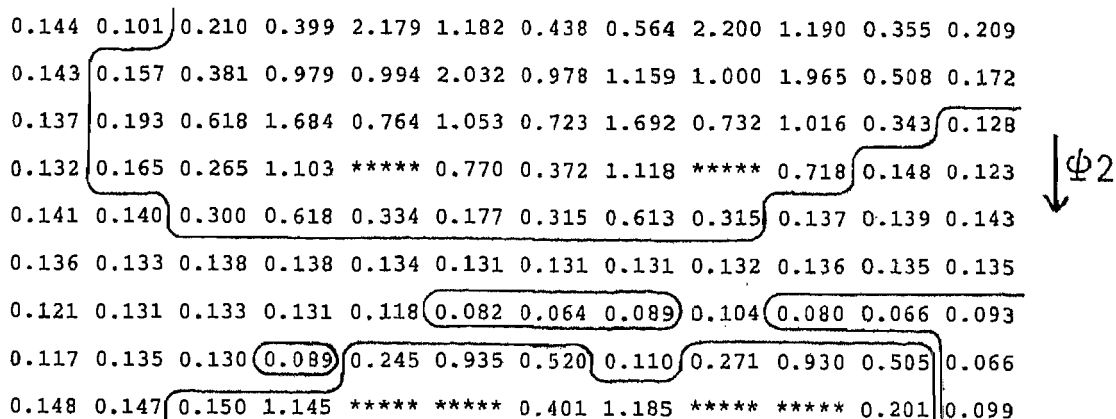
Fig. 7. Dependence of the  $q$ -Values on the Configuration and the Conformation of the Octalin Ring Moiety of 1

G1 to G5 refer to the octalin ring conformations presented in Fig. 5. In each conformer, four possible diastereomers about two hydroxyl groups at  $C_4$  and  $C_6$  were assumed.

==  $q$ -value scanning ==

VP 1 C05' -- C06' -- C07' -- C008 from 0.0000 to 300.0003 by 30.0000

VP 2 C06' -- C07' -- C008 -- C007 from -60.0000 to 180.0002 by 30.0000



end of  $T_1$  calc 22:19:44  $\Phi_1 \longrightarrow$

Fig. 8. Contour Plot of the  $q$ -Values as a Function of Dihedral Angles  $\Psi_1$  and  $\Psi_2$

$\Psi_1 (=C_5-C_6-C_7-C_8)$  and  $\Psi_2 (=C_6-C_7-C_8-C_7)$  were varied in the range given in the figure in steps of  $30^\circ$ C.

**The Conformation of the Octalin Ring**—Figure 7 shows clearly that the agreement between observed and calculated  $T_1$  values also depends on the octalin ring conformation. The possibility that the B ring adopts a half-boat conformation could be completely excluded because of the poor agreement between the observed and calculated  $T_1$  values. Among the half-chair conformations of the B ring affording relatively good agreements, the most satisfactory result has been given by the G1-conformation ( $7\beta$ -sofa). This suggests that the B ring favors the  $7\beta$ -sofa conformation. The calculation, assuming a boat conformation of the A ring, gave a poor agreement (data not shown). Thus, the A ring may be concluded to adopt a chair conformation.

The deviation of the B ring conformation from normal half chair to  $7\beta$ -sofa may be ascribed to the non-bonding repulsion between  $H_{8a}$  and the 7-methyl protons, which can be reduced in the B ring with  $7\beta$ -sofa conformation.

**The Conformation of the  $\delta$ -Lactone Side Chain**—It is found from Fig. 8 that the  $\psi_1$  and the  $\psi_2$ , which reproduce the observed  $T_1$  values, are restricted to narrow ranges. The best agreement was achieved at  $\psi_1 = 120^\circ$  and  $\psi_2 = 180^\circ$ . In this conformation,  $H_1$  is so close to  $H_{6'a}$  that NOE between  $H_1$  and  $H_{6'a}$  might be expected. Actually, 6% signal enhancement of  $H_{6'a}$  was observed on irradiation of  $H_1$ , and this was quantitatively reproduced by the calculation (Table II).<sup>16)</sup>

An inspection of the CPK model of this configuration reveals that the motional freedom of the  $\delta$ -lactone side chain is significantly reduced by the presence of the 2-methylbutanoyl group at  $C_1$  and the methyl group at  $C_7$ . This is consistent with the above observation that the orientation of the  $\delta$ -lactone side chain seems to be restricted in solution.

### 3 $\beta$ -Hydroxy ML-236B (2)

To check the validity of the above discussion as well as to compare the conformation of

TABLE V. Observed and Calculated  $T_1$  Values for 2

	H <sub>1</sub>	H <sub>2</sub>	H <sub>3</sub>	H <sub>4</sub>	H <sub>5</sub>	H <sub>6</sub>	7-Me	$q$
Obs.	0.60	0.42	1.87	2.09	1.55	1.39	0.61	
Calc.								
C-1	0.60	0.40	1.80	1.73	1.35	1.36	0.53	0.11
C-2	0.54	0.42	1.15	1.74	1.35	1.36	0.53	0.26

C-1, 3 $\beta$ -hydroxyl; C-2, 3 $\alpha$ -hydroxyl.

the  $\delta$ -lactone side chain in solution with that in the crystal, the same analysis of  $T_1$  values was applied to compound 2, although its X-ray analysis has already been done.<sup>4)</sup> The calculation was carried out on the spin system consisting of the non-exchangeable protons on the bisdehydroxy-decalin ring, including methylene protons on C<sub>6</sub>' and C<sub>7</sub>' (on the  $\delta$ -lactone side chain). Two dihedral angles,  $\psi_1 = C_5-C_6-C_7-C_8$  and  $\psi_2 = C_6-C_7-C_8-C_7$ , were changed to search for the values minimizing the  $q$ -index. The 2-methylbutanoyl group was neglected, as in the analysis of 1. Ring conformation was assumed to be similar to that in the crystal. The correlation times,  $\tau_c = 0.8 \times 10^{-10}$  s and  $\tau_c/\tau_{int} = 6.4$  were used as in the case of 1.

Table V shows the results of the calculation carried out for two epimers about the 3-hydroxyl group. In each case, the dihedral angles  $\psi_1$  and  $\psi_2$  have been optimized to the values giving the most satisfactory agreement. The agreement between observed and calculated  $T_1$  value for H<sub>3</sub>, which was sensitive to the configuration at C<sub>3</sub>, was found to be satisfactory for the epimer with the 3 $\beta$ -hydroxyl group. This is consistent with the configuration established by the X-ray analysis.<sup>4)</sup> Additionally, the optimal dihedral angles,  $\psi_1 = 180^\circ$  and  $\psi_2 = 50^\circ$ , are very similar to the values observed in the crystal,  $\psi_1 = 176.3^\circ$  and  $\psi_2 = 55.1^\circ$ . This indicates that the motional freedom of the  $\delta$ -lactone side chain is also restricted in solution, as in the case of 1.

According to the currently accepted interaction mode of ML-236B derivatives with HMG-CoA reductase presented by Nakamura *et al.*,<sup>6)</sup> the  $\delta$ -lactone part, which is cleaved to 3 $\beta$ -hydroxyheptanoic acid by hydrolysis and binds to the active site of the enzyme, must be connected in a specified orientation to the decalin moiety to exert its activity, because the decalin moiety is supposed to act as an anchor by binding to a hydrophobic pocket assumed to be located near the active site. Thus, the relative position of these two parts in space must be optimal in a potent inhibitor. The observed conformational difference of the decalin moiety between 1 and 2 necessarily leads to a difference of the location of the  $\delta$ -lactone side chain in space relative to the decalin moiety. This must be responsible for the observed difference in the inhibitory potency between these two compounds. The diminished activity of ML-236A may be explained along the same line; the  $\delta$ -lactone side chain may not be kept in a proper orientation due to the loss of the 2-methylbutanoyl group at C<sub>1</sub>.

### Conclusion

A quantitative evaluation of spin-lattice relaxation times and steady-state NOE factors has been made. By comparing the observed relaxation parameters with those calculated for several possible geometries, the configurations of the two hydroxyl groups at C<sub>4</sub> and C<sub>6</sub>, as well as the most probable conformation of the octalin ring system in 1, could be determined. The motional freedom of the  $\delta$ -lactone side chain was proved to be restricted; the dihedral angles,  $\psi_1$  and  $\psi_2$ , which characterize the conformation of the  $\delta$ -lactone side chain, are consistent with the observed relaxation parameters only when they are limited to narrow ranges of values.



The validity of the above conclusion was confirmed by the results of a similar analysis carried out on **2**. The availability of the distance geometry method to generate coordinates for small molecules was confirmed.

**Acknowledgement** The authors wish to thank Dr. Nobufusa Serizawa for supplying the materials, ML-236B, 4 $\beta$ ,6 $\alpha$ -dihydroxy ML-236B and 3 $\beta$ -hydroxy ML-236B.

#### References and Notes

- 1) J. H. Noggle and R. E. Schirmer, "The Nuclear Overhauser Effect," Academic Press, New York, 1971, p. 25.
- 2) H. Haruyama, H. Kurihara and M. Kondo, *Chem. Pharm. Bull.*, **33**, 905 (1985).
- 3) M. Tanaka, T. Nishigaki, E. Nakajima, E. Shigehara, E. Sato and Y. Tsujita, in preparation.
- 4) H. Haruyama, H. Kuwano, T. Kinoshita, A. Terahara, T. Nishigaki and C. Tamura, *Chem. Pharm. Bull.*, **34**, 1459 (1986).
- 5) N. Serizawa, K. Nakagawa, K. Hamano, Y. Tsujita, A. Terahara and H. Kuwano, *J. Antibiot.*, **36**, 604 (1983).
- 6) C. E. Nakamura and R. H. Abeles, *Biochemistry*, **24**, 1364 (1985).
- 7) C. Tamura, unpublished data.
- 8) G. M. Crippen, "Distance Geometry and Conformational Calculations," Research Studies Press-Wiley, New York, 1981, p. 25.
- 9) L. D. Hall and J. K. M. Sanders, *J. Am. Chem. Soc.*, **102**, 5703 (1980).
- 10) A molecular mechanics program based on the MM2 force field<sup>11</sup> was incorporated into our RSCA system, so that the geometries generated by the distance geometry method could be successively subjected to energy minimization.
- 11) N. L. Allinger, *J. Am. Chem. Soc.*, **99**, 8127 (1977).
- 12) F. Heatley, L. Akhter and R. T. Brown, *J. Chem. Soc., Perkin Trans. 2*, **1980**, 919.
- 13) P. K. Weiner, S. Profeta, Jr., G. Wipff, T. Havel, I. D. Kuniz, R. Langridge and P. A. Kollman, *Tetrahedron*, **39**, 1113 (1983).
- 14) The number and the range of the values for the dihedral constraints and non-bonding distances were changed in a trial and error manner. In our experience, the selection of these constraint sets was critical to generate chemically reasonable conformers.
- 15) L. D. Colebrook and L. D. Hall, *Org. Magn. Reson.*, **21**, 532 (1983).
- 16) If the conformation of the  $\delta$ -lactone side chain is fixed as mentioned in the text, other signal enhancements would be expected on H<sub>7 $\alpha$</sub>  (one of the methylene protons on C<sub>7</sub>) and H<sub>8</sub> on irradiating H<sub>1</sub>. Although these signals were discernible near 1.8 ppm in the difference spectrum (Fig. 3(b)), quantitative treatment of these signals were not done due to the serious overlapping.

[Chem. Pharm. Bull.]  
[35(1) 182-187 (1987)]

**Corianin from *Coriaria japonica* A. GRAY, and Sesquiterpene  
Lactones from *Loranthus parasiticus* MERR. Used for  
Treatment of Schizophrenia**

TAKUO OKUDA,<sup>\*,a</sup> TAKASHI YOSHIDA,<sup>a</sup> XIN-MIN CHEN,<sup>b</sup>  
JING-XI XIE,<sup>c</sup> and MAKOTO FUKUSHIMA<sup>d</sup>

*Faculty of Pharmaceutical Sciences, Okayama University,<sup>a</sup> Tsushima, Okayama 700, Japan,  
Chengdu Institute of Biology, The Chinese Academy of Sciences,<sup>b</sup> Chengdu, China,  
Institute of Materia Medica, Chinese Academy of Medical Sciences,<sup>c</sup> Beijing,  
China, and Laboratories, Pola Corporation,<sup>d</sup> Takashimadai,  
Kanagawa-ku, Yokohama 221, Japan*

(Received July 21, 1986)

Pseudotutin previously isolated from *Coriaria japonica* A. GRAY was revealed to be a molecular compound consisting of equimolar tutin (2) and a new related sesquiterpene lactone, corianin (3). Corianin was also isolated together with coriamyrtin (1), tutin (2) and coriatin (4), from *Loranthus parasiticus* MERR., a parasitic plant that grows on the twigs of *Coriaria sinica* MAXIM. The structure of corianin was elucidated on the basis of nuclear magnetic resonance and chemical evidence. The previously proposed structure (4) for coriatin was also substantiated.

**Keywords**—*Coriaria japonica*; Coriariaceae; *Loranthus parasiticus*; Loranaceae; pseudotutin; corianin; tutin; molecular compound; coriatin

*Coriaria japonica* A. GRAY (Coriariaceae) is known to produce several sesquiterpene lactones including coriamyrtin (1) and tutin (2), which are the main toxic principles.<sup>1)</sup> Among them, pseudotutin, which was previously isolated from the fruit extract and analyzed as C<sub>15</sub>H<sub>18</sub>O<sub>6</sub>,<sup>2)</sup> was reexamined and shown to be a molecular compound composed of tutin (2) and a new related sesquiterpene lactone named corianin (3).<sup>3)</sup>

We have also isolated corianin, together with three sesquiterpene lactones, during an investigation of the active principles of *Loranthus parasiticus* MERR. (Chinese name: mā sāng jìshēng, basō-kisei in Japanese pronunciation) (Loranthaceae), a parasitic plant that grows on the twigs of *Coriaria sinica* MAXIM. (Chinese name: mā sāng, basō in Japanese pronunciation) (Coriariaceae), which is distributed in the south and southwest parts of China and is a folk medicine used as a shock therapy for schizophrenia in the southwest area of China. In this paper we present a detailed account of the isolation and characterization of sesquiterpene lactones of *L. parasiticus*, and of the structure elucidation of corianin (3).

Although pseudotutin obtained by recrystallization from water has a constant, sharp melting point (184 °C)<sup>2)</sup> and was regarded as a single compound, it has been found to give two spots on a thin-layer chromatogram (TLC), and two constituents have been separated by recrystallization from chloroform. The one which crystallized first was identified as tutin (2), and the other component, corianin (3), deposited from the mother liquor, showed mp 214—216 °C and analyzed as C<sub>15</sub>H<sub>18</sub>O<sub>6</sub> (M<sup>+</sup> 294.1160). Comparisons of the melting points of 2, 3 and their mixtures indicated that pseudotutin is a molecular compound composed of equimolar 2 and 3 as found for picrotoxin.<sup>4)</sup> Namely, the crystals obtained upon evaporation of the aqueous solution of 1 : 1 mixture of 2 and 3 displayed a melting point and infrared (IR) spectrum identical with those of pseudotutin, while the mixtures of different ratios near 1 : 1

showed lower melting points.

The sesquiterpene lactones including corianin of *L. parasiticus* were isolated from the chloroform-soluble portion of the ethanol extract of the dried leaves. The mixture of sesquiterpene lactones was separated into four compounds by column chromatography over polyamide and then on silicic acid, followed by recrystallization. Among them, two components which showed strong convulsive action in mice, were identified as coriamyrtin (1) and tutin (2) and the other two were identified as corianin (3) and coriatin (4), by direct comparison with authentic specimens obtained from *Coriaria japonica*. The aqueous extractive of the plant, or a mixture of these crystalline sesquiterpenes including nontoxic corianin and coriatin, which gives effects comparable to insulin or electric shock, is currently used by muscle injection for the treatment of catatonia in hospitals in diverse areas of China.<sup>5)</sup> The results described above show that coriamyrtin and tutin are the active ingredients of *L. parasiticus* for this therapy. The isolation of these sesquiterpenoids from *Coriaria sinica*,<sup>6)</sup> suggests that these compounds have been transported from the host plant to the parasitic one, and accumulated in the latter without being metabolized.

Coriatin (4), C<sub>15</sub>H<sub>20</sub>O<sub>6</sub>, a hydroxycoriamyrtin, was first isolated from the fruit juice of *Coriaria japonica* in 1961, and its structure (4) was proposed based mainly on the IR spectrum.<sup>7)</sup> Further evidence of the structure has now been provided by the proton and carbon-13 nuclear magnetic resonance (<sup>1</sup>H- and <sup>13</sup>C-NMR (Table I)) spectra which are very similar to those of coriamyrtin (1)<sup>8)</sup> except that they show three tertiary methyl signals [ $\delta_{11}$  1.16, 1.30 and 1.43;  $\delta_C$  22.97, 30.17 and 28.39], and that the signals attributable to the

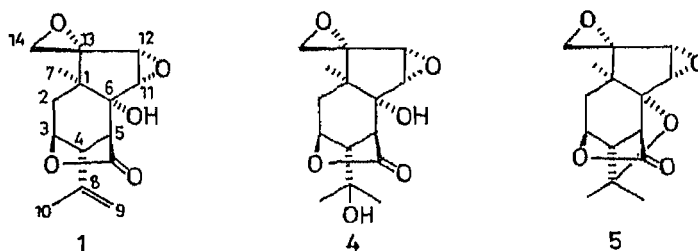


Chart 1

TABLE I. <sup>13</sup>C-NMR Data for Coriamyrtin (1), Tutin (2), Corianin (3) and Coriatin (4) in Pyridine-d<sub>5</sub>

Carbon	1	4	2	3
1	39.71 (s)	39.98 (s)	45.94 (s)	55.58 (s)
2	30.93 (t)	31.80 (t)	72.16 (d)	81.86 (d)
3	78.61 (d)	78.82 (d)	84.40 (d)	85.38 (d)
4	48.59 (d)	49.57 (d)	49.95 (d)	48.81 (d)
5	50.06 (d)	52.60 (d)	50.76 (d)	50.17 (d)
6	76.38 (s)	75.41 (s)	77.90 (s)	75.30 (s)
7	23.35 (q)	22.97 (q)	22.97 (q)	22.86 (q)
8	142.58 (s)	68.37 (s)	142.69 (s)	140.69 (s)
9	110.46 (t)	30.17 (q)	110.46 (t)	112.36 (t)
10	23.02 (q)	28.39 (q)	21.29 (q)	22.21 (q)
11	61.54 (d)	61.22 (d)	61.00 (d)	63.92 (d)
12	58.89 (d)	58.45 (d)	60.19 (d)	60.78 (d)
13	66.36 (s)	67.07 (s)	65.98 (s)	90.20 (s)
14	52.17 (t)	52.17 (t)	52.06 (t)	77.74 (t)
15	175.20 (s)	175.36 (s)	175.63 (s)	175.68 (s)

isopropenyl group are missing. The mass spectrum (MS) exhibited a fragment ion peak  $[(\text{Me})_2\text{C}=\text{OH}]^+$  at  $m/z$  59 as the base peak, whereas the base peak in coriamyrtin is at  $m/z$  41  $[\text{CH}_3\text{C}=\text{CH}_2]^+$ . Finally, the structure **4** was proved by the chemical conversion of coriatin into apocoriamyrtin (**5**)<sup>9</sup> by treatment with  $\text{POCl}_3$ . Therefore, the established structure of coriatin, including the absolute configuration, is represented by **4**.

The structure **3** is assigned to corianin on the basis of the following observations. The IR spectrum (KBr) shows absorption bands at 3450 (hydroxyl), 1760 and 1740  $[\text{1750 cm}^{-1}$  in  $\text{CHCl}_3$ ;  $\gamma$ -lactone], and  $1640 \text{ cm}^{-1}$  (double bond). The  $^{13}\text{C}$ -NMR spectrum exhibits the lactone carbonyl carbon signal at  $\delta$  175.68 and resonances due to a terminal methylene at  $\delta$  140.69 (s) and 112.36 (t), and does not show any other signals in the  $sp^2$  carbon region (Table I). The terminal methylene signal in the  $^1\text{H}$ -NMR spectrum (pyridine- $d_5$ ) is a 2H broad singlet at  $\delta$  4.94, which is coupled with a methyl signal at  $\delta$  2.08. The double bond is thus in the isopropenyl group. An AB quartet at  $\delta$  3.84 and 4.27 ( $J=3 \text{ Hz}$ ), which is analogous to the epoxide protons at C-11 and C-12 of tutin (**2**), is observed. The rest of the proton signals of **3** are also similar to those of **2**, with the exception that the AB quartet of the terminal epoxide

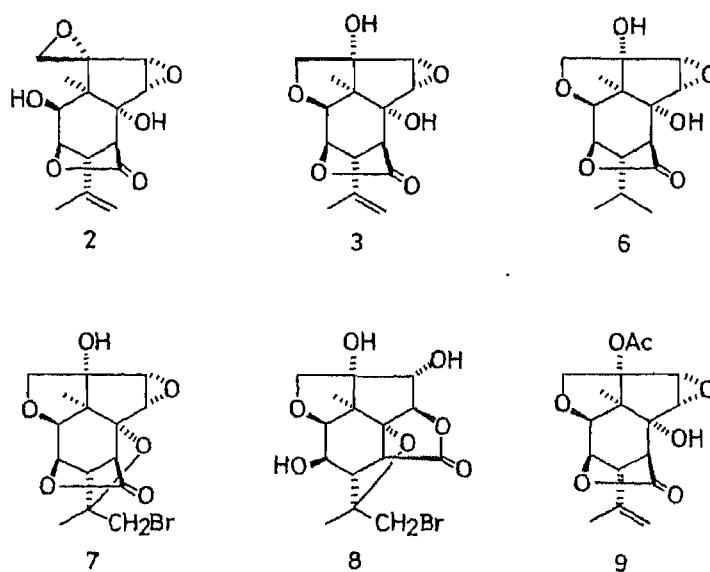


Chart 2

TABLE II.  $^1\text{H}$ -NMR Data for Tutin (**2**) and Corianin (**3**) in Pyridine- $d_5$ 

Proton	Tutin ( <b>2</b> )	Corianin ( <b>3</b> )
H-2	4.75 <sup>a)</sup>	4.65 (d, $J=4 \text{ Hz}$ )
H-3	5.23 (dt, $J=4, 1 \text{ Hz}$ )	5.28 (dt, $J=4, 1 \text{ Hz}$ )
H-4	3.43 (m)	3.40 (m)
H-5	3.43 (m)	3.48 (dd, $J=4, 1 \text{ Hz}$ )
H-7 ( $\text{CH}_3$ )	1.93 (s)	1.60 (s)
H-9 ( $\text{CH}_2$ )	4.75 <sup>a)</sup>	4.94 (2H, brs)
	4.91 (brs)	
H-10 ( $\text{CH}_3$ )	2.13 (brs)	2.08 (brs)
H-11	3.53 (d, $J=3 \text{ Hz}$ )	3.84 (d, $J=3 \text{ Hz}$ )
H-12	4.11 (d, $J=3 \text{ Hz}$ )	4.27 (d, $J=3 \text{ Hz}$ )
H-14	3.10 (d, $J=6 \text{ Hz}$ )	4.32 (d, $J=10 \text{ Hz}$ )
	4.70 (d, $J=6 \text{ Hz}$ )	4.46 (d, $J=10 \text{ Hz}$ )

a) Overlapped.

[ $\delta$  4.70 and 3.10 ( $J=6$  Hz)] in **2** is replaced in **3** by an AB quartet [ $\delta$  4.32 and 4.46] with a larger coupling constant  $J=10$  Hz (Table II).

Hydrogenation of corianin (**3**) over Adams catalyst afforded dihydrocorianin (**6**),  $C_{15}H_{20}O_6$  ( $M^+$  296), whose  $^1H$ -NMR spectrum ( $CDCl_3$ ) shows doublets at  $\delta$  0.98 ( $J=6$  Hz) and 1.08 ( $J=6$  Hz) due to an isopropyl group. Upon the treatment of corianin with bromine water, bromocorianin (**7**),  $C_{15}H_{17}O_6Br$  ( $M^+$  372 and 374) was produced. Formation of an ether ring between the isopropenyl and a hydroxyl group upon the bromination is indicated by the  $^1H$ -NMR spectrum of **7**, wherein the methyl and olefinic proton signals of the isopropenyl group observed in **3** are replaced by a methyl singlet at  $\delta$  1.56 and a singlet at  $\delta$  4.02 attributable to the bromomethyl group. These chemical and spectroscopic analogies between corianin and tutin lead to the assumption that corianin possesses a structure similar to tutin, on the same carbon skeleton. The difference between corianin and tutin is in the region of the terminal epoxide and C-2 oxygen function in tutin: in the  $^{13}C$ -NMR spectrum of **3** (Table I), the signals due to C-13 and C-14 appear at  $\delta$  90.20 and 77.74, respectively, which are shifted downfield by 24.22 and 25.68 ppm from the corresponding signals of **2**, indicating the absence of the "spiro" epoxide ring in corianin. Significant downfield shifts of C-1 and C-2 in **3** compared with **2** are also observed. The other signals are virtually identical in chemical shifts as well as multiplicity with the signals of **2**.

In the  $^1H$ -NMR spectrum measured in  $DMSO-d_6$ , the protons which are replaced by deuterium upon addition of  $D_2O$  appear as two singlets at  $\delta$  5.14 and 5.09 for corianin, while they appear as a singlet at  $\delta$  5.60 and a doublet at  $\delta$  5.16 for tutin. Corianin, therefore, should have two tertiary hydroxyl groups, the locations of which should be C-6 and C-13. Chemical evidence for this assumption was provided by the fairly high resistance to acetylation in a usual manner and to Jones oxidation. However, upon acetylation at an elevated temperature ( $80^\circ C$ ), corianin gave a monoacetate (**9**),  $C_{17}H_{20}O_7$  ( $M^+$  336.1180). The  $^1H$ -NMR spectrum ( $CDCl_3$ ) of **9** showed relatively large downfield shifts of one of the C-14 methylene proton signals and the H-12 signal, which can be explained by the deshielding effect of the acetyl group which is located spatially close to the hydrogens concerned.

As the presence of the oxygen function at C-2 and C-14 is evidenced by the  $^1H$ - and  $^{13}C$ -NMR spectra, these carbons should be in the five-membered ether ring, as in the structure **3**, which is compatible with the previously mentioned large coupling constant ( $J=10$  Hz) of the C-14 proton signals.

The stereochemical relationship among the functional groups, *i.e.*,  $\gamma$ -lactone, C-4 isopropenyl group and C-6 hydroxyl group, on the cyclohexane ring has been established to be identical with that of tutin, as demonstrated by the formation of the ether bridge at C-6-O-C-8 on bromination, and also by the coupling constants of the H-2--H-5 signals which are analogous to those of tutin. The epoxide at C-11-C-12 in corianin (**3**) is hardly available for intermolecular nucleophilic attack, as found for tutin and coriamyrtin.<sup>8)</sup> This stability can be rationalized in terms of protection of the epoxide moiety from backside attack by the  $\gamma$ -lactone group, and hence the epoxide at C-11-C-12 is *trans* to the  $\gamma$ -lactone. This assignment was chemically supported as follows: bromination of corianin afforded, in addition to **7**, a

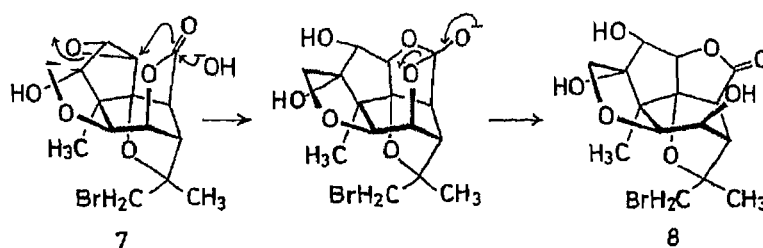


Chart 3

byproduct, isobromocorianin (**8**),  $C_{15}H_{19}O_7Br$  ( $M^+$  390, 392), which retains the  $\gamma$ -lactone as indicated by an IR absorption band at  $1750\text{ cm}^{-1}$ . The  $^1\text{H-NMR}$  spectrum ( $\text{CDCl}_3$ ) of **8** indicates the presence of the C-6-O-C-8 ether bridge [AB quartet at  $\delta$  3.46 and 3.56 ( $J=14\text{ Hz}$ ) ( $\text{CH}_2\text{Br}$ ); 1.54 (3H, s)]. The H-3 signal is shifted upfield by 0.64 ppm from the corresponding signal of **7**, while a part of the AB quartet due to H-11 and H-12 showed a significant downfield shift. These spectral data, considered in conjunction with a molecular model, are consistent with the structure **8** for isobromocorianin. The transesterification during bromination is presumed to occur by intramolecular rearward attack on the epoxide by the lactone carbonyl oxygen, as illustrated in Chart 3.

The optical rotatory dispersion (ORD) curve of corianin is almost superposable on that of tutin. The absolute configuration of corianin is consequently represented by **3**.

### Experimental

IR spectra were recorded on a Perkin-Elmer 683 spectrometer, optical rotations on a Perkin-Elmer 241 polarimeter, and MS on a ZAB-2F mass spectrometer or a Shimadzu LKB-9000 GC-MS spectrometer. NMR spectra were recorded on a Hitachi R-22FTS or a JEOL FX-90Q, with tetramethylsilane (TMS) as internal standard. Chemical shifts are given in  $\delta$  (ppm) values. TLC was performed on Kieselgel PF<sub>254</sub> plates (Merck), and spots were visualized under ultraviolet (UV) light or by exposure to iodine vapor.

**Separation of Tutin (2) and Corianin (3) from Pseudotutin**—Pseudotutin, 184–185 °C, was recrystallized twice from  $\text{CHCl}_3$  to give white crystals of mp 208–210 °C, which were identical with tutin (mixed melting point and IR comparison). Repeated recrystallization of the crystals obtained from the mother liquor afforded corianin (**3**), as colorless needles, mp 214–216 °C ( $\text{CHCl}_3$ ), mp 224–225 °C (from EtOH),  $[\alpha]_D^{25} +26.8^\circ$  ( $c=1.1$ , EtOH– $\text{H}_2\text{O}$ ). IR (KBr)  $\text{cm}^{-1}$ : 3500, 3080, 1760, 1740, 1640, 1230, 1190, 1170, 1050, 917, 900, 860, 820. Accurate MS  $m/z$ : Calcd for  $C_{15}H_{18}O_6$ : 294.1103; Found: 294.1160. MS  $m/z$  (relative intensity, %): 279 (4), 248 (8), 250 (13), 217 (6), 205 (8), 165 (20), 125 (30), 124 (28), 95 (100), 41 (75). The  $^1\text{H}$ - and  $^{13}\text{C}$ -NMR spectra; see Tables I and II. ORD ( $c=0.08$ , MeOH);  $[M]_{237}^{25} +4185^\circ$ . Anal. Calcd for  $C_{15}H_{18}O_6$ : C, 61.21; H, 6.17. Found: C, 61.47; H, 6.16.

**Relation of the Composition and Melting Point of Tutin (2) and Corianin (3)**—A mixture of **2** and **3** in several amount ratios was dissolved in hot  $\text{H}_2\text{O}$ , and then the solvent was evaporated off. The melting point of each crystalline mixture thus obtained was determined and compared with those of **2**, **3** and pseudotutin. The results are as follows: mp 209–212 °C (2:3, 10:0); mp 152–160 °C (2:3, 7:3); mp 184–186 °C (2:3, 1:1); mp 160–170 °C (2:3, 3:7); mp 215–216 °C (2:3, 0:10). The crystals consisting of equimolar **2** and **3** were identical with pseudotutin as judged by comparison of the IR spectra.

**Isolation of the Sesquiterpene Lactones from *Loranthus parasiticus***—Dried leaves (32 kg) of *L. parasiticus*, collected at Ning nan Xian, Sichuan, China, were percolated in 95% EtOH (125 l) for 3 months. The solvent was concentrated under reduced pressure, and the precipitate was filtered off. The filtrate was extracted with  $\text{CHCl}_3$ . The  $\text{CHCl}_3$  layer was evaporated to give a residue (50.5 g) which was chromatographed over polyamide (5.6  $\times$  106 cm). The eluates with  $\text{H}_2\text{O}$  and  $\text{H}_2\text{O}$ –EtOH (9:1) were combined and concentrated. The deposited crystals (24.5 g) were recrystallized from EtOH to give coriatin (**4**) (6 g). The mother liquor of the crude crystals and also of the recrystallization gave tutin (**2**) (11.2 g) after concentration followed by crystallization from EtOH. The residue obtained from this mother liquor was finally purified by column chromatography on silicic acid to afford coriamyrtin (**1**) (2.7 g) and corianin (**3**) (0.45 g). The identities of these compounds were confirmed by direct comparisons of the physico-chemical data with those of authentic samples.

**Preparation of Apocoriamyrtin (5) from Coriatin (4)**—A mixture of **4** (145 mg) and  $\text{POCl}_3$  (0.45 ml) in pyridine (10 ml) was left standing at room temperature for 24 h. The reaction mixture was poured into ice-water, and extracted with  $\text{CHCl}_3$ . The  $\text{CHCl}_3$  layer was washed with 10% HCl and 5%  $\text{Na}_2\text{CO}_3$ , and dried over  $\text{Na}_2\text{SO}_4$ . Removal of the solvent gave an orange oily residue (90 mg). Purification by prep. TLC using cyclohexane–EtOAc–MeOH (8:2:0.5) gave apocoriamyrtin (**5**) (20 mg), mp 207–210 °C, which was identical with an authentic sample.<sup>9)</sup>

**Dihydrocorianin (6)**—A solution of corianin (**3**) (43 mg) in AcOH (10 ml) was hydrogenated over prehydrogenated  $\text{PtO}_2$  (10 mg) at room temperature for 1 h. After removal of the catalyst by filtration, the solvent was removed to give a crystalline residue. Recrystallization from EtOH afforded dihydrocorianin (**4**) (36 mg) as colorless needles, mp 249–251 °C. IR (KBr)  $\text{cm}^{-1}$ : 3450, 1735, 916, 770.  $^1\text{H-NMR}$  ( $\text{CDCl}_3$ )  $\delta$ : 1.20 (3H, s,  $\text{C}_7\text{-CH}_3$ ), 0.98, 1.08 [3H each, d,  $J=7\text{ Hz}$ ,  $\text{C}_8\text{-(CH}_3)_2$ ], 1.70–2.04 (1H, m, H-8), 2.10–2.30 (1H, m, H-5), 3.62, 4.16 (AB q,  $J=3\text{ Hz}$ , H-11 and H-12), 4.02 (2H, s, H-14), 3.88 (1H, d,  $J=4\text{ Hz}$ , H-2), 4.80 (1H, t,  $J=4\text{ Hz}$ , H-3), 3.00 (1H, d,  $J=4\text{ Hz}$ , H-5), 1.70–2.36 (OH). MS  $m/z$  (relative intensity, %): 296 ( $M^+$ , 15), 276 (15), 253 (78), 235 (18), 124 (42), 111 (36), 97 (78), 85 (38), 43 (80), 41 (100). Anal. Calcd for  $C_{15}H_{20}O_6$ : C, 60.80; H, 6.80. Found: C, 61.03; H, 6.78.

**Bromination of Corianin (3)**—Bromine water was added to a solution of corianin (**3**) (27 mg) in hot water (1 ml)

until the color of bromine was persistent, and the reaction mixture was heated at 100 °C for 30 min, then allowed to stand further at room temperature for 2 d. The products were extracted with EtOAc and purified by prep. TLC (cyclohexane-EtOAc-MeOH 5:5:0.8). Fractions of *R<sub>f</sub>* 0.65 and 0.45 yielded bromocorianin (7) and isobromocorianin (8), respectively. Bromocorianin (7): white needles, mp 129–131 °C from MeOH. <sup>1</sup>H-NMR (CDCl<sub>3</sub>) δ: 1.30 (3H, s, C<sub>1</sub>-CH<sub>3</sub>), 1.56 (3H, s, C<sub>8</sub>-CH<sub>3</sub>), 3.44, 3.56 (ABq, *J* = 10 Hz, C<sub>8</sub>-CH<sub>2</sub>Br), 3.58, 3.84 (ABq, *J* = 3 Hz, H-11 and H-12), 4.02 (2H, s, H-14), 4.06 (1H, d, *J* = 4.5 Hz, H-2), 5.02 (1H, dt, *J* = 4.5, 2 Hz, H-3), 3.22 (1H, t, *J* = 4.5 Hz, H-4), 3.32 (1H, d, *J* = 4.5 Hz, H-5). MS *m/z* (relative intensity, %): 372 (2), 374 (2) (M<sup>+</sup>), 344 (17), 346 (17), 293 (8), 265 (70), 219 (17), 95 (80), 43 (100). *Anal.* Calcd for C<sub>15</sub>H<sub>17</sub>BrO<sub>6</sub>: C, 48.27; H, 4.59. Found: C, 48.01; H, 4.87. Isobromocorianin (8): white long plates from MeOH, mp 180–183 °C (dec.). IR (KBr) cm<sup>-1</sup>: 3520, 3380, 1740, 1720, 1360, 1155, 1045, 825. IR (CHCl<sub>3</sub>) cm<sup>-1</sup>: 1750. <sup>1</sup>H-NMR (CDCl<sub>3</sub>) δ: 1.18 (3H, s, C<sub>1</sub>-CH<sub>3</sub>), 1.54 (3H, s, C<sub>8</sub>-CH<sub>3</sub>), 3.46, 3.56 (ABq, *J* = 14 Hz, C<sub>8</sub>-CH<sub>2</sub>Br), 3.44, 4.34 (ABq, *J* = 3 Hz, H-11 and H-12), 3.83, 4.26 (ABq, *J* = 7 Hz, H-14), 4.43 (1H, s, H-2), 4.38 (1H, d, *J* = 4 Hz, H-3), 2.84 (1H, t, *J* = 4 Hz, H-4), 2.98 (1H, d, *J* = 4 Hz, H-5). MS *m/z* (relative intensity, %): 390 (1.5), 392 (1.5) (M<sup>+</sup>), 372 (11), 374 (11), 293 (13), 195 (20), 82 (93), 80 (100).

**Acetylcorianin (9)**—Corianin (3) (27 mg) was dissolved in pyridine (0.5 ml), and Ac<sub>2</sub>O (1 ml) was added. After 2 d at room temperature, the reaction mixture was further allowed to stand at 80 °C for 5 h, and then poured into ice-water. The crystals deposited were collected and recrystallized from aq. EtOH to give colorless needles of acetylcorianin (7) (15 mg), mp 95–97 °C. <sup>1</sup>H-NMR (CDCl<sub>3</sub>) δ: 1.16 (3H, s, C<sub>1</sub>-CH<sub>3</sub>), 1.92 (3H, s, C<sub>8</sub>-CH<sub>3</sub>), 2.12 (3H, s, OAc), 3.97, 4.20 (ABq, *J* = 3 Hz, H-11 and H-12), 4.06, 4.32 (ABq, *J* = 11 Hz, H-14), 4.82, 5.00 (1H each, br s, H-9), 4.25 (1H, d, *J* = 4 Hz, H-2), 3.18–3.22 (2H, m, H-4 and H-5), 5.02 (1H, t, *J* = 4 Hz, H-3). Accurate MS *m/z*: Calcd for C<sub>17</sub>H<sub>20</sub>O<sub>7</sub>: 336.1208; Found: 336.1180. MS *m/z* (relative intensity, %): 276 (58), 43 (100), 41 (46).

#### References

- 1) T. Okuda and T. Yoshida, *Chem. Pharm. Bull.*, **15**, 1955 (1967).
- 2) T. Okuda, *Chem. Pharm. Bull.*, **2**, 185 (1954).
- 3) The structure of corianin was outlined in a preliminary report, T. Okuda and T. Yoshida, *Tetrahedron Lett.*, **1971**, 4499.
- 4) E. J. Hansen and B. Jerslev, *Dansk Tidsskr. Farm.*, **28**, 25 (1954) [*Chem. Abstr.*, **49**, 2376c (1955)].
- 5) D.-J. Yuan, *Zhonghua Shenjingjingshenke Zazhi*, **12**, 196 (1979).
- 6) X.-M. Chen, *Chinese Medicinal Herbs Communications*, **11**, 34 (1977).
- 7) T. Okuda, *Chem. Pharm. Bull.*, **9**, 178 (1961).
- 8) T. Okuda and T. Yoshida, *Chem. Pharm. Bull.*, **15**, 1697 (1967).
- 9) T. Okuda and T. Yoshida, *Chem. Pharm. Bull.*, **15**, 1687 (1967).

[Chem. Pharm. Bull.  
35(1) 188-194 (1987)]

## Two-Dimensional Nuclear Magnetic Resonance Spectra of Selected Tricyclic Antidepressants

DAVID J. CRAIK,\* JON G. HALL and SHARON L. A. MUNRO

*School of Pharmaceutical Chemistry, Victorian College of Pharmacy Ltd.,  
381 Royal Parade, Parkville, Victoria, Australia 3052*

(Received July 23, 1986)

Two-dimensional nuclear magnetic resonance (2D NMR) spectroscopy has been used to assign  $^{13}\text{C}$  spectra of the tricyclic antidepressants imipramine and chlorimipramine. The 2D-INADEQUATE method was used to unambiguously assign the aromatic spectral region for the former compound. Errors in previous literature assignments based on 1D methods were corrected. For chlorimipramine the pitfalls of classical substituent chemical shift arguments for  $^{13}\text{C}$  assignments and the difficulties of 1D selective  $^1\text{H}$  irradiation in overlapped systems are contrasted with the power and relative simplicity of the 2D- $^{13}\text{C}$ ,  $^1\text{H}$ -correlated and  $^{13}\text{C}$ ,  $^1\text{H}$  RELAY methods.

**Keywords**—NMR; 2D NMR; imipramine; chlorimipramine; antidepressants; spectral assignment;  $^{13}\text{C}$ -NMR

### Introduction

Tricyclic antidepressants (TCA's) are widely used in the treatment of depression. This action is thought to be related, at least in part, to their ability to inhibit re-uptake of amine neurotransmitters into presynaptic nerve endings, although the detailed mechanism by which TCA's exert their effects remains unknown. Nuclear magnetic resonance (NMR) spectroscopy has the potential to increase our knowledge of the molecular events involved in antidepressant action, since it provides a means of examining interactions between drugs and membranes or receptor proteins.<sup>1)</sup> However, before such studies can be contemplated a thorough understanding of the solution properties and spectral assignments of the antidepressants is required. Unfortunately, some of the early studies in this area<sup>2,3)</sup> have been marred by incorrect assignments due largely to the inadequacies of conventional assignment techniques. In this paper these errors are corrected and the power of modern two-dimensional (2D) methods in the assignment of  $^1\text{H}$ - and  $^{13}\text{C}$ -NMR spectra of representative antidepressants is discussed.

The 2D NMR methods of interest are 2D-INADEQUATE,<sup>4)</sup> carbon-hydrogen correlated spectroscopy<sup>5)</sup> and carbon-hydrogen relayed coherence transfer (RELAY).<sup>6)</sup>

The 2D-INADEQUATE<sup>4)</sup> experiment is potentially the most powerful technique available for deducing connectivities in molecular frameworks as it provides direct detection of one-bond carbon-carbon couplings. Such couplings are observable only in molecules containing two adjacent  $^{13}\text{C}$  nuclei (*i.e.*, 1 in every 10000 molecules at natural abundance) and thus in a conventional  $^{13}\text{C}$  spectrum would appear as satellite signals centred about the hundred-fold stronger resonance arising from molecules containing a single  $^{13}\text{C}$  nucleus. Limitations of dynamic range and resolution make observation of these satellite signals difficult in practical cases, except with a technique such as INADEQUATE,<sup>7)</sup> which uses phase cycling of the applied radio frequency pulses to suppress the strong central band. For carbons attached to more than one other carbon, significant overlap of the separate satellites



could be expected in a 1D experiment, but in the 2D-INADEQUATE method an appropriate pulse sequence separates the satellites according to the double quantum frequency of the coupled nuclei. The resultant 2D spectrum has the carbon chemical shift as one axis ( $F_2$ ) and the double quantum frequency, which is the sum of the chemical shifts of the coupled nuclei (relative to the carrier frequency) as the second axis ( $F_1$ ). While this technique provides very direct connectivity information, it has the disadvantage of being time-consuming in terms of data acquisition because only molecules containing two adjacent  $^{13}\text{C}$  nuclei are detected.

The heteronuclear shift-correlated 2D pulse experiment provides a rapid method for correlating the chemical shift of proton-bearing carbons with the chemical shift of their respective protons. Heteronuclear shift-correlated 2D spectra are normally represented in contour form, with the  $^{13}\text{C}$  chemical shift ( $\delta\text{C}$ ) along the horizontal ( $F_2$ ) axis and the proton chemical shift ( $\delta\text{H}$ ) along the vertical ( $F_1$ ) axis. Correlations appear at  $(\delta\text{C}, \delta\text{H})$ . A major advantage of this method is that it uses the carbon chemical shift dispersion to resolve the proton spectrum and in so doing, it has the potential to reveal overlapping proton multiplicities and coupling constants.

Detection of remote carbon-proton connectivities may be achieved by the 2D technique of relayed coherence transfer heteronuclear correlated spectroscopy (RELAY). The resultant 2D spectrum correlates the chemical shifts of  $^{13}\text{C}$  nuclei (along the  $F_2$  axis) with the  $^1\text{H}$  chemical shifts of both directly coupled neighbouring protons and the remote protons which are coupled to the neighbouring protons. The 2D spectrum therefore displays not only neighbouring cross-peaks of two protonated carbons, A and B, at  $(\delta\text{C}_A, \delta\text{H}_A)$  and  $(\delta\text{C}_B, \delta\text{H}_B)$ , similar to the CH correlated 2D spectrum, but in addition relayed cross-peaks at  $(\delta\text{C}_A, \delta\text{H}_B)$  and  $(\delta\text{C}_B, \delta\text{H}_A)$ . These four signals appear at the corners of a rectangle in the 2D spectrum and provide evidence that the two carbon signals at  $\delta\text{C}_A$  and  $\delta\text{C}_B$  are from sites in the immediate vicinity of each other within the molecular framework. The method thus directly provides connectivity information, as does 2D-INADEQUATE, but is more sensitive since it does not rely on natural abundance double- $^{13}\text{C}$  labelling.

### Experimental

**Materials**—Imipramine hydrochloride was a generous gift from Ciba-Geigy. Chlorimipramine hydrochloride was kindly donated by Dr. D. Taylor, Victorian College of Pharmacy Ltd. Deuteriochloroform (99.8% D) was supplied by Aldrich Chemical Co., Michigan, U.S.A.

**NMR Spectroscopy**— $^1\text{H}$ - and  $^{13}\text{C}$ -NMR spectra were recorded on a Bruker AM 300WB spectrometer operating at 300.13 and 75.48 MHz respectively. Fourier transform (FT)  $^1\text{H}$ -NMR spectra were normally recorded with a  $60^\circ$  pulse (3  $\mu\text{s}$ ), repetition time 3 s, spectral width 3 kHz, and 16 k data points. 16 transients were accumulated. Chemical shifts are referenced to the residual chloroform resonance at 7.24 parts per million (ppm).

1D  $^{13}\text{C}$ -NMR spectra were obtained with a  $45^\circ$  pulse (6  $\mu\text{s}$ ), repetition time 2 s, spectral width 16 kHz and 8 K data points. Proton decoupling was achieved using low-power Waltz decoupling.<sup>6)</sup> Free-induction decays (FID's) were zero-filled to 16 K data points, and 2 Hz exponential line-broadening was applied before Fourier transformation. Chemical shifts were referenced to the centre peak of deuteriochloroform at 77.0 ppm.

2D-INADEQUATE spectra<sup>4)</sup> were obtained with the pulse sequence  $90^\circ-\tau-180^\circ-\tau-90^\circ-t_1-135^\circ$  FID ( $t_2$ ) with spectral widths  $F_1 = 5000$ ,  $F_2 = 2500$  Hz, a  $90^\circ$  pulse of 13.5  $\mu\text{s}$ , quadrature detection in both dimensions, Waltz proton decoupling,  $\tau = 1/4J(\text{C}-\text{C}) = 4.2$  ms, a repetition time of 1.2 s, a  $128 \times 2048$  word data matrix, and a total acquisition time of 12 h. The data was processed as a  $256 \times 2048$  word data matrix with a sine-bell window function in both dimensions.

The 2D- $^1\text{H}$ ,  $^{13}\text{C}$  CORRELATED spectra<sup>5)</sup> were acquired with the pulse sequence

$^1\text{H}$ :  $90-t_1/2- -t_1/2-\tau_1-90-\tau_2$ -Waltz decoupling

$^{13}\text{C}$ : 180 90 -FID ( $t_2$ )

with spectral widths  $F_1 \pm 100$  Hz,  $F_2 = 2000$  Hz, quadrature detection in both dimensions,  $\tau_1 = \tau_2 = 1/2 J(\text{CH}) = 3$  ms, a  $128 \times 2048$  word data matrix, and a repetition time of 4 s. The data were processed as a  $512 \times 2048$  word data matrix with a sine-bell window in  $F_1$  and 2 Hz exponential line-broadening in  $F_2$ .

The 2D- $^1\text{H}$ ,  $^1\text{H}$ ,  $^{13}\text{C}$  RELAYED spectra<sup>6)</sup> were acquired with the pulse sequence

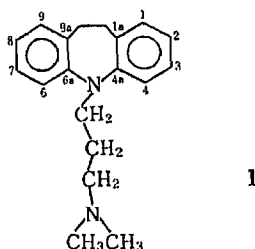
$^1\text{H}$ :  $90-t_1/2- -t_1/2-90-t_m/2-180-t_m/2-\tau_1-90-\tau_2$ -Waltz decoupling

$^{13}\text{C}$ : 180 90 FID ( $t_2$ )

with the same spectral and acquisition parameters used in the  $^1\text{H}$ ,  $^{13}\text{C}$  correlated spectra. The mixing time,  $t_m$ , was 16 ms and total acquisition time 15 h. The data were processed as a  $256 \times 2048$  word data matrix with a sine-bell window in  $F_1$  and a 2 Hz exponential line-broadening in  $F_2$ .

## Results and Discussion

Imipramine (1) was the first of the TCA's to be developed and it is still in widespread clinical use.



Its  $^{13}\text{C}$ -NMR spectrum in the aromatic region is shown in Fig. 1 with proposed assignments of Abraham *et al.*<sup>2)</sup> and Saito and coworkers.<sup>1)</sup> The original assignments of Abraham, which were presumably based on model compounds, appear to be plausible; however, very recently Saito and coworkers used selective  $^1\text{H}$  decoupling to reassign the  $^{13}\text{C}$  shifts for protonated carbons. In this technique each proton is separately irradiated during acquisition of the  $^{13}\text{C}$  spectrum and hence only the carbon attached to the irradiated proton appears as a sharp singlet. Other carbons are only partially decoupled and appear as multiplets or broadened peaks. The results of these experiments suggested that the original  $\text{C}_2$  and  $\text{C}_4$  assignments should be reversed.

This  $^{13}\text{C}$  assignment technique of course requires a prior assignment of the aromatic region of the  $^1\text{H}$ -NMR spectrum, which in the case of imipramine consists of two doublets and two triplets due to *ortho* coupling (*meta* coupling was not resolved in the spectra shown by Saito and coworkers). The doublets were assigned to  $\text{H}_1$  and  $\text{H}_4$  and the connectivity of the peaks was determined by selective  $^1\text{H}$  homonuclear decoupling. To complete the assignment a determination of which of the doublets was  $\text{H}_1$  and which  $\text{H}_4$  was required, and this was made from chemical shift arguments relating to the central nitrogen's effect on  $\text{H}_1$ . Such arguments must, however, be used with caution since the substituent effect of a nitrogen varies markedly with its state of protonation (*e.g.*,  $\text{NH}_2$  induces an upfield shift of  $-0.8$  ppm at the *ortho* proton in aniline relative to benzene, while for  $\text{NH}_3^+$  the shift is opposite in sign,  $+0.4$  ppm.<sup>9)</sup> To some extent this ambiguity was resolved by noting that on treatment with  $\text{DCl}$ , the  $^1\text{H}$ -NMR signals from  $\text{H}_2$  and  $\text{H}_4$  disappeared, as expected for sites *ortho* and *para* to the nitrogen, but again this relies on assumptions about the chemical-directing effect of this group, which may well change with protonation.

Another difficulty with Saito's assignment is that  $\text{C}_{1a}$  is shown to be the most downfield peak, in contrast to Abraham's assignment and to expectations based on the inductive effect of the nitrogen having its major effect on  $\text{C}_{4a}$ . In Saito and coworkers' discussion of this assignment, it was suggested that the peak assigned to  $\text{C}_{1a}$  is broadened by unresolved long-range coupling to the benzylic bridge protons. While this is reasonable, it would be equally valid to argue that  $\text{C}_{4a}$  should be broadened due to rapid quadrupolar relaxation of the adjacent nitrogen, and hence peak broadening cannot be used as an assignment criterion.

To overcome the difficulties noted above, and to resolve the anomalies in the two literature assignments of imipramine, we have applied a technique which requires no assumptions and does not require specific isotope labelling. This is the 2D-INADEQUATE method. A contour plot of the 2D-INADEQUATE spectrum for the aromatic region of imipramine is shown in Fig. 2. In this figure the  $F_2$  dimension shows pairs of AX doublets arising from molecules containing two adjacent  $^{13}\text{C}$  nuclei, while the  $F_1$  dimension resolves these doublet pairs according to their double quantum frequency (equal to the sum of the shifts of A and X with respect to the radio frequency carrier).

The assignment proceeds by noting that the only doublet (marked X on Fig. 2) which has a coupling partner outside the spectral range must be  $\text{C}_{1a}$ , since it is the only aromatic carbon coupled to an aliphatic carbon. In addition, this peak shows couplings to two aromatic carbons, one of which is a quaternary carbon and thus must be  $\text{C}_{4a}$ , and the other is thus  $\text{C}_1$ . The coupling network can be further traced around the ring, as shown in the figure, to provide a completely unambiguous assignment. Our results show that the assignments of Saito *et al.* are correct for the protonated aromatic carbons but that the non-protonated aromatic carbon assignments should be reversed to correspond with the original assignment of Abraham *et al.* The correct assignments are summarized in Fig. 1.

Imipramine represents a favourable case for the 2D-INADEQUATE experiment in that it has a low molecular weight and is relatively soluble, so that sensitivity problems can be

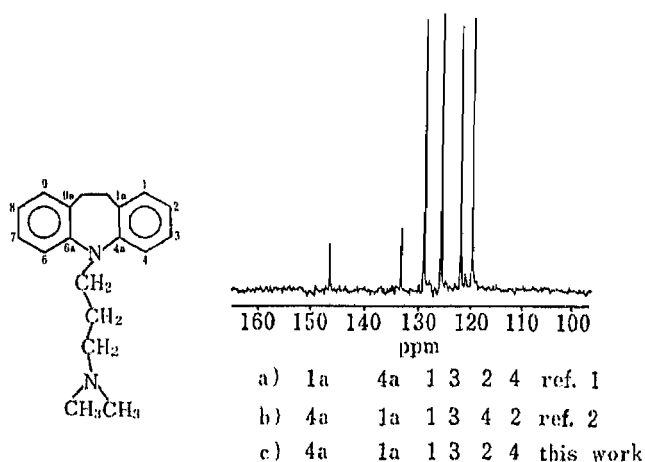


Fig. 1. The Aromatic Region of the  $^{13}\text{C}$ -NMR Spectrum of Imipramine with Proposed Assignments of (a) Saito and Coworkers,<sup>11</sup> (b) Abraham *et al.*,<sup>21</sup> and (c) This Work Based on the 2D-INADEQUATE Technique

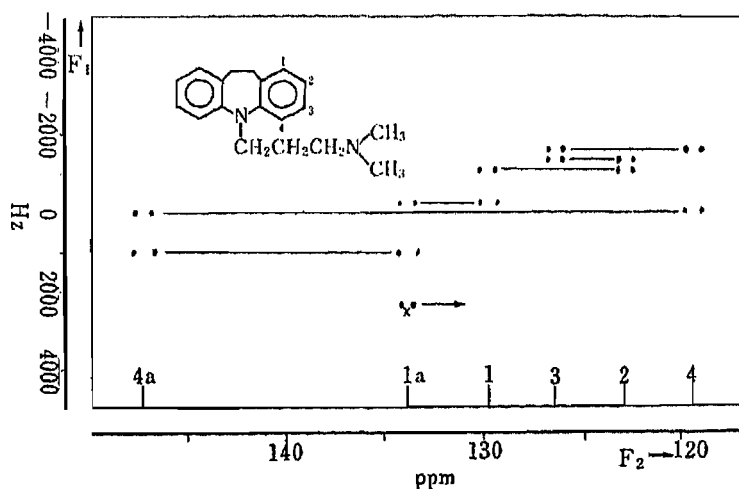
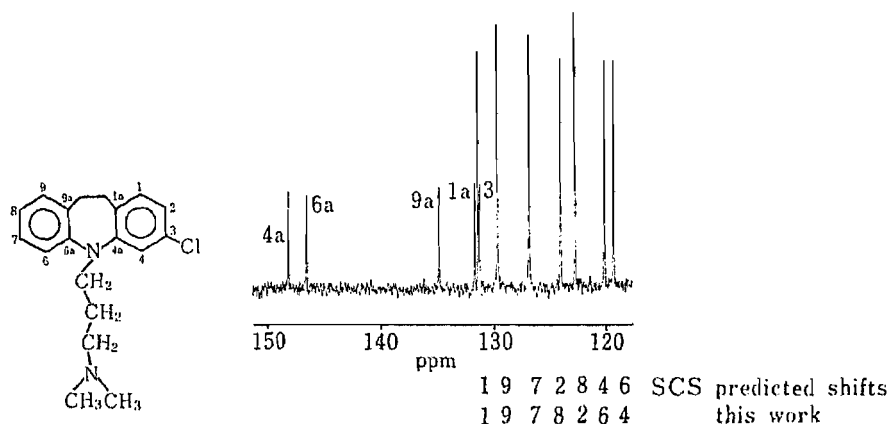


Fig. 2. 2D-INADEQUATE  $^{13}\text{C}$  Spectrum of the Aromatic Region of Imipramine

TABLE I. Predicted  $^{13}\text{C}$  Shifts for Chlorimipramine

Carbon number	Imipramine shifts (ppm)	Cl-SCS (ppm)	Predicted chlorimipramine shifts (ppm)	Observed chlorimipramine shifts (ppm)
1	129.9	1.3	131.2	131.4
2	123.1	0.4	123.5	122.7
3	126.5	6.2	132.7	131.4
4	119.5	0.4	119.9	119.4
6	119.5	—	119.5	120.2
7	126.5	—	126.5	126.8
8	123.1	—	123.1	124.0
9	129.9	—	129.9	129.7
1a	133.9	-1.9	132.0	131.7
4a	147.1	1.3	148.4	148.2
6a	147.1	—	147.1	146.5
9a	133.9	—	133.9	134.9

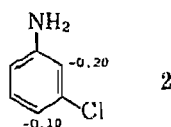
Fig. 3.  $^{13}\text{C}$ -NMR Spectrum of the Aromatic Region of Chlorimipramine

alleviated by using relatively concentrated solutions. (In the case above the concentration was 150 mg/ml.) The symmetry of the molecule on the NMR time-scale also doubles the effective concentration of each aromatic carbon, thus reducing the accumulation time by a factor of four relative to a similarly sized non-symmetrical TCA such as chlorimipramine.

In this case, the relative insensitivity of the 2D-INADEQUATE technique is compounded by chlorimipramine's lower solubility relative to imipramine and thus alternative assignment methods are of interest. The usual technique for assignment of a substituted derivative when that of the parent is available, as in this case, is the use of substituent chemical shifts<sup>10)</sup> (SCS) to predict  $^{13}\text{C}$  shifts in the substituted derivative. Using standard SCS values (derived from chlorobenzene) for a Cl substituent, the predicted shifts for chlorimipramine are shown in Table I. It can be seen that predicted shifts produced in this way are sufficiently close to observed shifts (Figure 3) to assign the non-protonated carbons as well as  $\text{C}_1$ ,  $\text{C}_3$ ,  $\text{C}_7$  and  $\text{C}_9$ , but the pairs  $\text{C}_2$ ,  $\text{C}_8$  and  $\text{C}_4$ ,  $\text{C}_6$  remain ambiguous. Indeed, when the shifts are compared with those established to be correct by 2D NMR (see below), it is seen (Table I) that predictions that  $\text{C}_2$  should be downfield of  $\text{C}_8$ , and  $\text{C}_4$  downfield of  $\text{C}_6$  are incorrect. This occurs because SCS values of a given substituent may be significantly different in a polysubstituted benzene from those in mono-substituted benzenes.<sup>11)</sup>

It is interesting to note, for example, that better predictions for  $\text{C}_2$ ,  $\text{C}_8$  and  $\text{C}_4$ ,  $\text{C}_6$  can

be obtained by using chlorine SCS increments derived from aniline and *m*-chloroaniline.<sup>12)</sup> These SCS values are shown in structure (2).



Using these values, the predicted shifts ( $C_2$ , 123.0;  $C_8$ , 123.1;  $C_4$ , 119.3;  $C_6$ , 119.5) now show the correct order. Even with these improvements, however, SCS values are not generally a totally conclusive assignment aid and other methods to distinguish the pairs  $C_2$ ,  $C_8$  and  $C_4$ ,  $C_6$  are required. The 2D- $^{13}\text{C}$ ,  $^1\text{H}$  correlated spectrum in Fig. 4 provides this distinction.

In the  $F_1$  ( $^1\text{H}$ ) dimension,  $H_4$  should be the only peak to show just *meta* coupling and hence this unique coupling pattern in the contour plot identifies the most upfield peak (119.4 ppm) as being due to the carbon correlated with  $H_4$ , *i.e.*,  $C_4$ . The peak at 120.2 ppm must therefore be due to  $C_6$ . Similarly, of the remaining ambiguous peaks for  $C_2/H_2$ ,  $C_8/H_8$  at 122.7 and 124.0 ppm, the lower field carbon signal appears as an *ortho* doublet with *meta* coupling, *i.e.*, it is connected to  $H_2$  and is hence  $C_2$ . The peak at 124.0 ppm is thus  $C_8$ .

The projection of the 2D- $^{13}\text{C}$ ,  $^1\text{H}$  correlated spectrum in the proton dimension provides the conventional proton spectrum (Fig. 4), which is heavily overlapped in the  $H_8$ ,  $H_1$ ,  $H_4$ ,  $H_6$  region. This would make the traditional technique of selective  $^1\text{H}$  irradiation to assign the carbon spectrum difficult and, indeed, is the reason why Saito *et al.* were unable to unambiguously assign the spectra of the structurally related compound chlorpromazine. The 2D- $^{13}\text{C}$ ,  $^1\text{H}$ -correlated technique overcomes the problem of overlap in the  $^1\text{H}$  spectrum by spreading it into a second dimension based on  $^{13}\text{C}$  chemical shifts.

It should be noted that although the 2D- $^{13}\text{C}$ ,  $^1\text{H}$ -correlated technique was extremely valuable in distinguishing between  $C_2$  and  $C_8$ , and between  $C_4$  and  $C_6$ , the assignment is not without assumption, since chemical shift arguments were used to roughly predict shifts for  $C_1$ ,  $C_9$ ,  $C_7$ ,  $C_8/C_2$  and  $C_6/C_4$ . Such chemical shift arguments can break down and, for example, the 2D-correlated spectrum alone could not be used to distinguish between  $C_7$  and  $C_8$ , since both have similar  $^1\text{H}$  multiplicity. In principle 1D-selective homonuclear decoupling experiments could be used to further assign the 1D proton spectrum, which would then lead to an assignment of the  $^{13}\text{C}$  spectrum *via* the 2D- $^{13}\text{C}$ ,  $^1\text{H}$ -correlated spectrum. However, in the

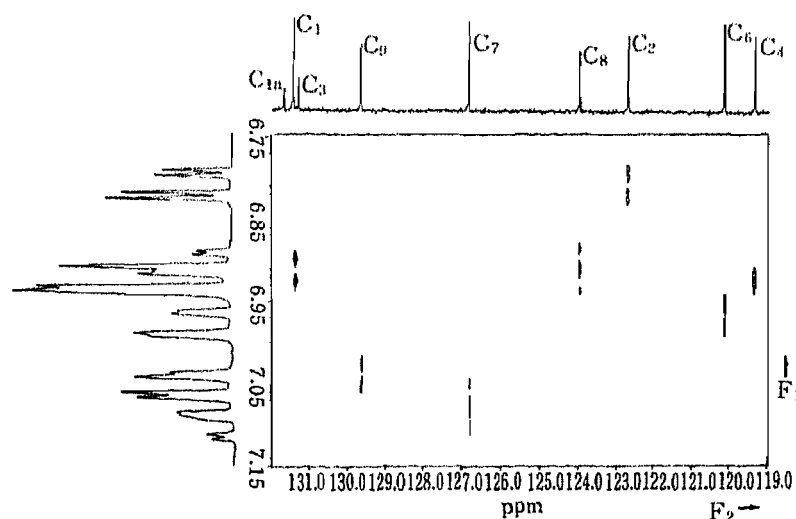


Fig. 4. 2D-Carbon-Hydrogen-Correlated Spectrum of the Aromatic Region of Chlorimipramine

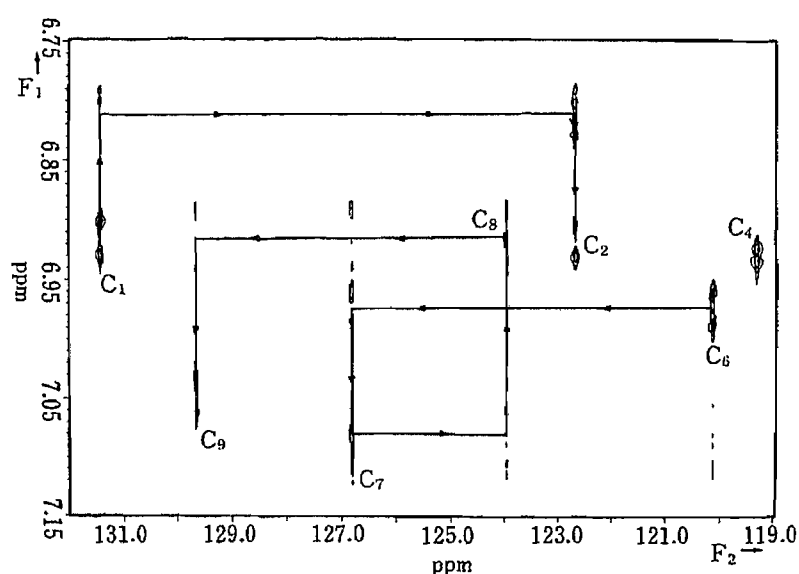


Fig. 5. 2D-RELAY Spectrum of the Aromatic Region of Chlorimipramine

current case the 1D  $^1\text{H}$  spectrum is significantly overlapped, making the selective  $^1\text{H}$  irradiation time-consuming and subject to substantial interpretation.

The RELAY technique can be used to overcome these difficulties and provides an assignment essentially free of assumption. The RELAY spectrum of the aromatic region of chlorimipramine shown in Fig. 5 displays all of the peaks noted in Fig. 4, but in addition contains cross-peaks indicative of two carbons sharing a common  $^1\text{H}$  coupling partner. The way in which this provides connectivity information can be seen by noting that once, say,  $\text{C}_6$  is assigned, then connection to, and hence assignment of,  $\text{C}_7$ , then  $\text{C}_8$ , and then  $\text{C}_9$  is immediately established. Similarly, connection between the protonated carbons  $\text{C}_1$  and  $\text{C}_2$  is established.

In summary, it can be seen that even for relatively simple compounds of pharmaceutical interest, 1D methods are often inadequate for NMR spectral assignment. On the other hand, 2D methods are now easy to implement and have proven useful in correcting previous ambiguous assignments.

**Acknowledgement** This work was supported by the Australian Research Grants Scheme.

#### References

- 1) R. Tabeta, S. Mahajan, M. Maeda and H. Saito, *Chem. Pharm. Bull.*, **33**, 1793 (1985).
- 2) R. J. Abraham, L. J. Kricka and A. Ledwith, *J. Chem. Soc., Perkin Trans. 2*, **1964**, 1977.
- 3) A. A. Al Badr, "Analytical Profiles of Drug Substances," Vol. 2, ed. by K. Florey, Academic Press, London, 1983.
- 4) A. Bax, R. Freeman, T. A. Frenkiel and M. H. Levitt, *J. Magn. Reson.*, **43**, 478 (1981).
- 5) R. Freeman and G. A. Morris, *J. Chem. Soc., Chem. Commun.*, **1978**, 684; A. A. Maudsley and R. R. Ernst, *Chem. Phys. Lett.*, **50**, 368 (1977).
- 6) P. H. Bolton, *J. Magn. Reson.*, **48**, 336 (1982).
- 7) A. Bax, R. Freeman and S. P. Kempell, *J. Am. Chem. Soc.*, **102**, 4849 (1980).
- 8) A. J. Shaka, J. Keeler, T. Frenkiel and R. Freeman, *J. Magn. Reson.*, **52**, 335 (1983); *idem, ibid.*, **53**, 313 (1983).
- 9) D. W. Mathieson (ed.), "Nuclear Magnetic Resonance for Organic Chemists," Academic Press, New York, 1967, p. 184.
- 10) G. C. Levy, G. L. Nelson and R. L. Lichter, "Carbon-13 Nuclear Magnetic Resonance Spectroscopy for Organic Chemists," Wiley, New York, 1980.
- 11) J. Bromilow, R. T. C. Brownlee, D. J. Craik, M. Sadek and R. W. Taft, *J. Org. Chem.*, **45**, 2429 (1980).
- 12) J. Bromilow, R. T. C. Brownlee, D. J. Craik and M. Sadek, *Magn. Reson. in Chem.*, **24**, 862 (1986).

[Chem. Pharm. Bull.]  
35(1) 195-199 (1987)

## Chemical Transformation of Protoberberines. XI.<sup>1)</sup> A Novel Synthesis of 2,3,10,11-Tetraoxygenated Protoberberine Alkaloids from Corresponding 2,3,9,10-Tetraoxygenated Protoberberine Alkaloids<sup>2)</sup>

MIYOJI HANAOKA,\* WON JEA CHO, MARI MARUTANI,  
and CHISATO MUKAI

Faculty of Pharmaceutical Sciences, Kanazawa University,  
Takara-machi, Kanazawa 920, Japan

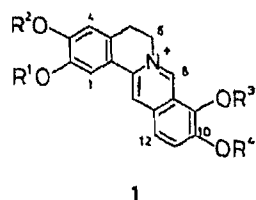
(Received July 24, 1986)

2,3,9,10-Tetraoxygenated protoberberin alkaloids, berberine (**1a**), palmatine (**1b**), and coptisine (**1c**), were efficiently converted into the corresponding 12-hydroxy-2,3,10,11-tetraoxygenated protoberberines (**6a**, **6b**, **6c**) through an oxidative C<sub>8</sub>-C<sub>8a</sub> bond cleavage with *m*-chloroperbenzoic acid, followed by the enamide photo-cyclization. On successive treatment with diethyl chlorophosphate and sodium in liquid ammonia, the 12-hydroxy derivatives (**6a**, **6b**, **6c**) underwent reductive dehydroxylation to produce the corresponding 2,3,10,11-tetraoxygenated protoberberines, tetrahydropseudoberberine (**4a**), (±)-xylopinine (**4b**), and tetrahydropseudooptisine (**4c**), respectively.

**Keywords**—2,3,9,10-tetraoxygenated protoberberine; 2,3,10,11-tetraoxygenated protoberberine; berberine; palmatine; coptisine; tetrahydropseudoberberine; xylopinine; tetrahydropseudooptisine; photo-induced cyclization; oxidative C<sub>8</sub>-C<sub>8a</sub> bond fission

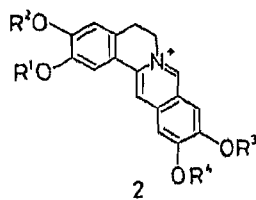
Tetraoxygenated protoberberine alkaloids can be classified into two groups, naturally abundant 2,3,9,10-tetraoxygenated protoberberines and 2,3,10,11-tetraoxygenated ones, according to the substitution patterns of oxygen functions in ring A as well as ring D.<sup>3)</sup> Some of the latter type of alkaloids, pseudoberberine (**2a**), pseudooptisine (**2c**), *etc.*, have recently been isolated.<sup>4)</sup> 1,2,10,11-Tetraoxygenated protoberberine alkaloids,<sup>5)</sup> caseadine and caseamine, are also known. These protoberberine alkaloids have been shown to be the biogenetic precursors of related alkaloids such as benzo[*c*]phenanthridine,<sup>6)</sup> spirobenzylisoquinoline,<sup>7)</sup> and phthalideisoquinoline<sup>8)</sup> alkaloids.

2,3,9,10-tetraoxygenated  
protoberberine



1

2,3,10,11-tetraoxygenated  
protoberberine



2

a: R<sup>1</sup> + R<sup>2</sup> = CH<sub>2</sub>, R<sup>3</sup> = R<sup>4</sup> = Me    b: R<sup>1</sup> = R<sup>2</sup> = R<sup>3</sup> = R<sup>4</sup> = Me    c: R<sup>1</sup> + R<sup>2</sup> = R<sup>3</sup> + R<sup>4</sup> = CH<sub>2</sub>

Chart 1

In the course of our continuing studies<sup>1,9)</sup> on the transformation of protoberberines to benzo[*c*]phenanthridine alkaloids *via* a proposed biogenetic route,<sup>6)</sup> we required the pseudoberberine (**2a**), a 2,3,10,11-tetraoxygenated protoberberine, for a synthesis of nitidine,<sup>10,11)</sup>

which has attracted much attention because of its strong antileukemic activity. Although several methods for the synthesis of protoberberines have so far been developed<sup>12)</sup> and pseudoberberine (**2a**) has been synthesized by conventional means,<sup>13)</sup> a simple conversion of berberine (**1a**) into **2a** would be of great value as an alternative synthesis of **2a** because of the easy access to the starting material.

The strategy of our transformation is outlined in Chart 2, and is based on the consideration that pseudoberberine (**2a**) is the ring D-inverted product<sup>14)</sup> of berberine (**1a**). Therefore, conversion of **1a** to **3** via C<sub>8</sub>-C<sub>8a</sub> bond cleavage followed by recyclization between the original C<sub>8</sub> and C<sub>12</sub> positions and subsequent removal of the substituent X at C<sub>8a</sub> will afford tetrahydropseudoberberine (**4a**).

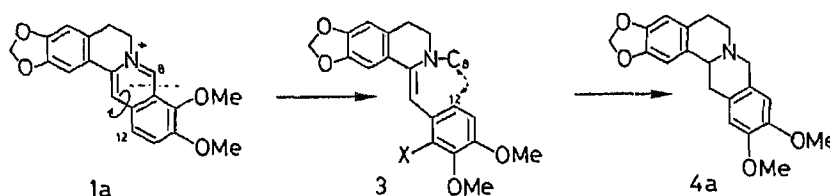


Chart 2

Polyberberine has recently been isolated from *Berberis valdiviana* PHIL.<sup>15)</sup> and found to be the oxidative C<sub>8</sub>-C<sub>8a</sub> bond cleavage product (**3**: C<sub>8</sub>=CHO, X=OH) of berberine. Though polyberberine has been derived from **1a** by treatment with *m*-chloroperbenzoic acid (*m*-CPBA) only in low yield (20%),<sup>16,17)</sup> this product seems to be a suitable candidate for our strategy.

Treatment of well-dried berberine (**1a**) with 1.3 eq of *m*-CPBA in dry tetrahydrofuran (THF) in the presence of 2 eq of sodium hydride in a stream of nitrogen at room temperature for 1 h afforded polyberberine (**5a**) in 76% yield. The yield was considerably improved by adjusting the reaction conditions. The spectral data of **5a** thus obtained are in good agreement with those described in the literature.<sup>16)</sup> Irradiation<sup>18)</sup> of polyberberine (**5a**) in ethanol with a 400 W high-pressure mercury lamp in a stream of nitrogen for 2 h, followed by reduction of the resulting quaternary base with sodium borohydride (NaBH<sub>4</sub>), afforded 12-hydroxytetrahydropseudoberberine (**6a**) in 79% yield. The salient feature of **6a** in the mass spectrum (MS) is the peaks at *m/z* 176 and 180 arising from the retro Diels-Alder reaction.<sup>12)</sup> The proton nuclear magnetic resonance (<sup>1</sup>H-NMR) spectrum showed only three signals at  $\delta$  6.81, 6.57, and 6.20 ppm as singlets in the aromatic region. The hydroxy group at the C<sub>12</sub> position in **6a** was, as expected, easily methylated with diazomethane to produce a novel protoberberine, 12-methoxytetrahydropseudoberberine (**7a**) in 91% yield; the structure of this product was supported by spectral evidence.

Finally reductive removal of the hydroxy group at the C<sub>12</sub> position in **6a** was realized *via* the corresponding phosphate (**8a**). A solution of **6a** in THF was treated with diethyl chlorophosphate to provide the phosphate (**8a**) which, without purification, was exposed to sodium in liquid ammonia<sup>19)</sup> at -70 °C to furnish tetrahydropseudoberberine (**4a**) in 53% overall yield from **6a**. The synthetic tetrahydropseudoberberine was proved to be identical with an authentic specimen<sup>13)</sup> by comparison of their spectra and thin-layer chromatographic behavior. Thus, we have succeeded in the development of a convenient method for the synthesis of tetrahydropseudoberberine from easily available berberine.

We next examined the generality of the above transformation method. Similar treatment of palmatine (**1b**) and coptisine (**1c**) with *m*-CPBA in THF yielded polycarpine (**5b**)<sup>16,20)</sup> and the enamide (**5c**)<sup>21)</sup> in 44 and 39% yields,<sup>22)</sup> respectively, though these yields are lower than that in the case of **5a**. The structures of **5b** and **5c** were easily determined on the basis of spectral evidence. On exposure to sequential irradiation with a high-pressure mercury lamp



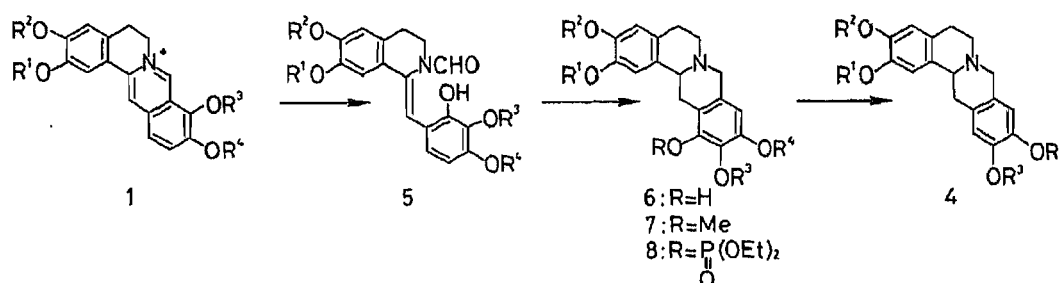


Chart 3

and reduction with  $\text{NaBH}_4$ , polycarpine (**5b**) and **5c** underwent photo-induced cyclization to give 12-hydroxyxylopinine (**6b**) and 12-hydroxytetrahydropseudocoptisine (**6c**) in 70 and 65% yields, respectively. Both tetrahydroprotoberberines (**6b** and **6c**) exhibited diagnostic fragmentation peaks at  $m/z$  180 and 192, and at  $m/z$  164 and 176, respectively, in their MS. The hydroxy group at the  $\text{C}_{12}$  position in **6b** and **6c** was reductively removed *via* **8b** and **8c** by the same procedure as described for conversion of **6a** to **4a**, to afford ( $\pm$ )-xylopinine (**4b**) and tetrahydropseudocoptisine (**4c**) in 62 and 44% overall yields from **6b** and **6c**, respectively. The synthetic ( $\pm$ )-xylopinine and tetrahydropseudocoptisine were identical with authentic samples.<sup>23,24)</sup>

Thus, we have accomplished a novel and convenient synthesis of 2,3,10,11-tetraoxygenated protoberberine alkaloids from the corresponding 2,3,9,10-tetraoxygenated ones. The present method provides an alternative route for the synthesis of 2,3,10,11-tetraoxygenated protoberberines, especially pseudoberberine (**2a**), because of the easy access to the starting material, berberine (**1a**).

### Experimental

Melting points were determined on a Yanagimoto micro melting point apparatus and are uncorrected. Alumina (Aluminiumoxid 90, Aktivitätsstufe II --III, 70--230 mesh, Merck) and silica gel (Kieselgel 60, 70--230 mesh, Merck) were used for column chromatography. Organic extracts were dried over anhydrous  $\text{Na}_2\text{SO}_4$ . Infrared (IR) spectra were measured with a JASCO A-102 spectrometer, MS with a Hitachi M-80 mass spectrometer, ultraviolet (UV) spectra with a Hitachi 323 spectrometer in MeOH, and  $^1\text{H-NMR}$  spectra with a JEOL FX-100 spectrometer in  $\text{CDCl}_3$  using tetramethylsilane as an internal standard, unless otherwise stated. Irradiation was carried out with a 100 or 400 W high-pressure mercury lamp equipped with a Pyrex filter (Riko Kagaku Co.).

**Polyberbine (5a)**—Well-dried berberine chloride (**1a**) (2.1 g, 5.7 mmol) was added portionwise to a stirred suspension of sodium hydride (50% in oil; 550 mg, 11.4 mmol) in dry THF (70 ml) in a stream of nitrogen at room temperature. After 1 h, *m*-CPBA (1.6 g, 7.4 mmol) in dry THF (30 ml) was added to the reaction mixture at  $0^\circ\text{C}$ , and the solution was stirred at room temperature for an additional 1 h. Saturated sodium thiosulfate solution (15 ml) and saturated sodium bicarbonate solution (15 ml) were added at once to the reaction mixture and the THF layer was separated. The water layer was extracted with chloroform, and the combined organic layers were washed with water and brine, dried, and concentrated to dryness. Chromatography of the residue on silica gel with ethyl acetate-hexane (1:1) gave polyberbine (**5a**, 1.59 g, 76%), mp  $165\text{--}166^\circ\text{C}$  (MeOH). IR  $\nu_{\text{max}}^{\text{CHCl}_3}$   $\text{cm}^{-1}$ : 3500 (OH), 1660 (amide).  $^1\text{H-NMR}$   $\delta$ : 8.10 (1H, s, CHO), 7.27 (1H, s, olefinic proton), 6.99, 6.46 (2H, AB-q,  $J=9$  Hz,  $\text{C}_6\text{-H}$  and  $\text{C}_5\text{-H}$ ), 6.85, 6.58 (each 1H, s,  $\text{C}_8\text{-H}$  and  $\text{C}_5\text{-H}$ ), 5.96 (2H, s,  $\text{OCH}_2\text{O}$ ), 3.95 (2H, t,  $J=6$  Hz,  $\text{CH}_2\text{CH}_2\text{N}$ ), 3.89, 3.85 (each 3H, s,  $\text{OMe} \times 2$ ), 2.85 (2H, t,  $J=6$  Hz,  $\text{CH}_2\text{CH}_2\text{N}$ ). UV  $\lambda_{\text{max}}$  nm (log  $\epsilon$ ): 335 (4.30), 221 (4.56). MS  $m/z$ : 369 ( $\text{M}^+$ , 100%), 352 (30), 341 (41), 326 (35), 324 (36), 308 (54). *Anal.* Calcd for  $\text{C}_{20}\text{H}_{19}\text{NO}_6$ : C, 65.03; H, 5.19; N, 3.79. Found: C, 65.20; H, 5.36; N, 3.76.

**Polycarpine (5b)**—Palmitine chloride (**1b**) (379 mg, 1.0 mmol) was oxidized with *m*-CPBA (280 mg, 1.3 mmol) in THF (total 70 ml) in the presence of sodium hydride (60% in oil; 82 mg, 2.1 mmol). The reaction mixture was treated as described for **5a** to give **5b** (175 mg, 44%), mp  $176\text{--}177^\circ\text{C}$  (MeOH) (lit.<sup>16)</sup>  $179\text{--}180^\circ\text{C}$ ). IR  $\nu_{\text{max}}^{\text{CHCl}_3}$   $\text{cm}^{-1}$ : 3500 (OH), 1660 (amide).  $^1\text{H-NMR}$   $\delta$ : 8.13 (1H, s, CHO), 7.26 (1H, s, olefinic proton), 7.01, 6.71 (2H, AB-q,  $J=9$  Hz,  $\text{C}_6\text{-H}$  and  $\text{C}_5\text{-H}$ ), 6.88, 6.60 (each 1H, s,  $\text{C}_8\text{-H}$  and  $\text{C}_5\text{-H}$ ), 3.98, (2H, t,  $J=6$  Hz,  $\text{CH}_2\text{CH}_2\text{N}$ ), 3.94, 3.90, 3.89, 3.85 (each 3H, s,  $\text{OMe} \times 4$ ), 2.88 (2H, t,  $J=6$  Hz,  $\text{CH}_2\text{CH}_2\text{N}$ ). UV  $\lambda_{\text{max}}$  nm (log  $\epsilon$ ): 330 (4.32), 268 (4.12), 222 (4.56). MS  $m/z$ : 385 ( $\text{M}^+$ , 100%), 368 (37), 357 (53), 342 (48), 340 (43), 324 (82). *Anal.* Calcd for  $\text{C}_{21}\text{H}_{23}\text{NO}_6$ : C, 65.44; H, 6.02; N,

3.63. Found: C, 65.30; H, 6.08; N, 3.51.

**(Z)-1,2,3,4-Tetrahydro-1-(2-hydroxy-3,4-methylenedioxyphenylethylidene)-2-formyl-6,7-methylenedioxyquinoline (5c)**—Coptisine chloride (**1c**) (195 mg, 0.55 mmol) was oxidized with *m*-CPBA (593 mg, 2.75 mmol) in THF (total 40 ml) in the presence of sodium hydride (60% in oil; 113 mg, 2.81 mmol). The reaction mixture was treated as described for **5a** to give **5c** (75 mg, 39%) as an amorphous mass. IR  $\nu_{\max}^{\text{CHCl}_3}$   $\text{cm}^{-1}$ : 3200 (OH), 1660 (amide).  $^1\text{H-NMR}$   $\delta$ : 8.03 (1H, s, CHO), 7.24 (1H, s, olefinic proton), 6.78, 6.58 (each 1H, s, C<sub>8</sub>-H and C<sub>5</sub>-H), 6.76, 6.44 (2H, AB-q,  $J=8$  Hz, C<sub>6</sub>-H and C<sub>5</sub>-H), 5.96, 5.90 (each 2H, s, OCH<sub>2</sub>O  $\times$  2), 3.90 (2H, t,  $J=6$  Hz, CH<sub>2</sub>CH<sub>2</sub>N), 2.84 (2H, t,  $J=6$  Hz, CH<sub>2</sub>CH<sub>2</sub>N). MS (chemical ionization mass)  $m/z$ : 354 ( $\text{M}^+ + 1$ , 81%), 353 ( $\text{M}^+$ , 65), 336 (36), 326 (100), 325 (99), 308 (56).

**5,8,13,14-Tetrahydro-12-hydroxy-10,11-dimethoxy-2,3-methylenedioxy-6H-dibenzo[*a,g*]quinolizine (6a)**—A solution of **5a** (553 mg, 1.5 mmol) in ethanol (500 ml) was irradiated with a 400 W high-pressure mercury lamp in a stream of nitrogen at room temperature for 2 h. The solution was concentrated to half volume (about 250 ml), and NaBH<sub>4</sub> (635 mg, 17 mmol) was added. The reaction mixture was stirred at room temperature for 2 h. After evaporation of the solvent, the residue was neutralized with 10% hydrochloric acid solution and extracted with methylene chloride. The extract was washed with water and brine, dried, and concentrated to dryness. The residue was chromatographed on silica gel with ethyl acetate-hexane (1:1) to afford **6a** (429 mg, 79%), mp 219–220 °C (MeOH). IR  $\nu_{\max}^{\text{CHCl}_3}$   $\text{cm}^{-1}$ : 3550 (OH).  $^1\text{H-NMR}$   $\delta$ : 6.81, 6.57, 6.20 (each 1H, s, aromatic protons), 5.91 (2H, s, OCH<sub>2</sub>O), 3.86, 3.83 (each 3H, s, OMe  $\times$  2). UV  $\lambda_{\max}$  nm (log  $\epsilon$ ): 292 (3.79), 234 (4.13). MS  $m/z$ : 355 ( $\text{M}^+$ , 41%), 180 (61), 176 (100). Anal. Calcd for C<sub>20</sub>H<sub>21</sub>NO<sub>5</sub>: C, 67.59; H, 5.96; N, 3.94. Found: C, 67.36; H, 6.02; N, 3.89.

**5,8,13,14-Tetrahydro-12-hydroxy-2,3,10,11-tetramethoxy-6H-dibenzo[*a,g*]quinolizine (6b)**—Polycarpine (**5b**) (170 mg, 0.44 mmol) in ethanol (250 ml) was irradiated with a 100 W high-pressure mercury lamp and reduced with NaBH<sub>4</sub> (202 mg, 5.46 mmol) as described for **6a** to give **6b** (115 mg, 70%) as an oil. IR  $\nu_{\max}^{\text{CHCl}_3}$   $\text{cm}^{-1}$ : 3520 (OH).  $^1\text{H-NMR}$   $\delta$ : 6.80, 6.61, 6.20 (each 1H, s, aromatic protons), 3.89, 3.83 (each 3H, s, OMe  $\times$  2), 3.86 (6H, s, OMe  $\times$  2). MS  $m/z$ : 371 ( $\text{M}^+$ , 32%), 192 (100), 180 (62). High-resolution mass Calcd for C<sub>21</sub>H<sub>25</sub>NO<sub>5</sub>: 371.1731. Found: 371.1711.

**5,8,13,14-Tetrahydro-12-hydroxy-2,3,10,11-bismethylenedioxy-6H-dibenzo[*a,g*]quinolizine (6c)**—A solution of **5c** (169 mg, 0.48 mmol) in ethanol (250 ml) was irradiated with a 100 W high-pressure mercury lamp and reduced with NaBH<sub>4</sub> (283 mg, 7.56 mmol) as described for **6a** to give the crude product, which was chromatographed on silica gel with ethyl acetate-methanol (99:1) to afford **6c** (105 mg, 65%), mp 232–233 °C (dec.) (AcOEt). IR  $\nu_{\max}^{\text{CHCl}_3}$   $\text{cm}^{-1}$ : 3400 (OH).  $^1\text{H-NMR}$   $\delta$  [(CD<sub>3</sub>)<sub>2</sub>SO]: 6.88, 6.65, 6.22 (each 1H, s, aromatic protons), 5.93 (2H, s, OCH<sub>2</sub>O), 5.90, 5.89 (2H, AB-q,  $J=1$  Hz, OCH<sub>2</sub>O). MS  $m/z$ : 339 ( $\text{M}^+$ , 41%), 176 (100), 164 (43). Anal. Calcd for C<sub>19</sub>H<sub>17</sub>NO<sub>5</sub>: C, 67.25; H, 5.05; N, 4.13. Found: C, 67.42; H, 5.03; N, 4.24.

**5,8,13,14-Tetrahydro-10,11,12-trimethoxy-2,3-methylenedioxy-6H-dibenzo[*a,g*]quinolizine (7a)**—A solution of diazomethane in ether (ca. 2% solution; 10 ml) was added dropwise to a solution of **6a** (40 mg, 0.11 mmol) in methanol (20 ml) at room temperature and the reaction mixture was allowed to stand for 6 h. The solvent was evaporated off and the resulting solid was recrystallized from methanol to give **7a** (38 mg, 91%), mp 127–128 °C.  $^1\text{H-NMR}$   $\delta$ : 6.79, 6.59, 6.40 (each 1H, s, aromatic protons), 5.92 (2H, s, OCH<sub>2</sub>O), 3.86, 3.85, 3.83 (each 3H, s, OMe  $\times$  3). UV  $\lambda_{\max}$  nm (log  $\epsilon$ ): 285 (3.72), 231 (sh, 4.14). MS  $m/z$ : 369 ( $\text{M}^+$ , 36%), 194 (100), 179 (36). Anal. Calcd for C<sub>21</sub>H<sub>23</sub>NO<sub>5</sub> · 1/2MeOH: C, 67.00; H, 6.53; N, 3.63. Found: C, 67.17; H, 6.26; N, 3.60.

**Tetrahydropseudoberberine (4a)**—A solution of **6a** (201 mg, 0.57 mmol) in dry THF (10 ml) was added dropwise to a stirred suspension of sodium hydride (60% in oil; 38 mg, 0.94 mmol) in dry THF (10 ml) at 0 °C and the resulting THF solution was stirred for 30 min at the same temperature. A solution of diethyl chlorophosphate (149 mg, 0.87 mmol) was added to the THF solution and stirring was continued for 1 h. Saturated ammonium chloride solution was added to the reaction mixture and the THF layer was separated. The water layer was extracted with methylene chloride, and the combined organic layers were washed with water and brine, dried, and concentrated to leave the crude phosphate (**8a**). A solution of **8a** in dry THF (10 ml) was added to liquid ammonia (50 ml) at –70 °C, and then sodium (58 mg, 2.5 mmol) was added. The reaction mixture was stirred for 4 h at the same temperature and solid ammonium chloride (1.5 g) was added to the reaction mixture, which was then warmed to room temperature. Water was added to the THF solution and the THF layer was separated. The water layer was extracted with methylene chloride, and the combined organic layers were washed with water and brine, dried, and concentrated to dryness. Chromatography of the residue on silica gel with methylene chloride-methanol (98:2) provided **4a** (100 mg, 53%), mp 177–178.5 °C (MeOH) (lit.<sup>13</sup>) 177 °C). The synthetic tetrahydropseudoberberine was proved to be identical with an authentic specimen<sup>13</sup>) by comparison of their IR and  $^1\text{H-NMR}$  spectra, and thin-layer chromatographic behavior.

**(±)-Xylopinine (4b)**—A solution of **6b** (144 mg, 0.39 mmol) in THF was treated with sodium hydride (60% in oil; 24 mg, 0.59 mmol) and diethyl chlorophosphate (110 mg, 0.63 mmol) and then with sodium (16 mg  $\times$  2, total 1.38 mmol) in liquid ammonia as described for **4a** to give **4b** (95 mg, 62%), mp 157–159 °C (EtOH) (lit.<sup>23</sup>) 156–159 °C). The synthetic (±)-xylopinine was proved to be identical with an authentic sample<sup>23</sup>) by comparison of their IR and  $^1\text{H-NMR}$  spectra, and thin-layer chromatographic behavior.

**Tetrahydropseudooptisine (4c)**—A solution of **6c** (42 mg, 0.12 mmol) in THF was treated with *n*-BuLi in hexane (0.7 ml, 1.1 mmol) (instead of sodium hydride) and diethyl chlorophosphate (20 mg, 1.2 mmol) and then with

sodium (10 mg  $\times$  2, total 0.9 mmol) in liquid ammonia as described for **4a** to give **4c** (22 mg, 44%), mp 213–214 °C (EtOH) (lit.<sup>24)</sup> 214–215 °C). The synthetic tetrahydropseudocoptisine was proved to be identical with an authentic sample<sup>24)</sup> by comparison of their IR and <sup>1</sup>H-NMR spectra, and thin-layer chromatographic behavior.

**Acknowledgement** The authors are grateful to Mr. Y. Itatani and Misses K. Handa and E. Fukui of this Faculty for elemental analyses and mass spectral measurements. Financial support from the Ministry of Education, Science, and Culture of Japan in the form of a Grant-in-Aid for Scientific Research is also gratefully acknowledged.

#### References and Notes

- 1) Part X: M. Hanaoka, N. Kobayashi, K. Shimada, and C. Mukai, *J. Chem. Soc., Perkin Trans. 1*, **1987**, in press.
- 2) A part of this work was published in a preliminary communication: M. Hanaoka, M. Marutani, K. Saitoh, and C. Mukai, *Heterocycles*, **23**, 2927 (1985).
- 3) T. Kametani, "The Chemistry of the Isoquinoline Alkaloids," Vol. 2, Kinkodo Publishing Company, Sendai, 1974, pp. 189–209.
- 4) C. Moulis, J. Gleye, and E. Stanislas, *Phytochemistry*, **16**, 1283 (1977).
- 5) C. Y. Chen, D. B. MacLean, and R. H. F. Manske, *Tetrahedron Lett.*, **1968**, 349.
- 6) E. Leete and S. J. B. Murrill, *Phytochemistry*, **6**, 231 (1967); A. Yagi, G. Nonaka, S. Nakayama, and I. Nishioka, *ibid.*, **16**, 1197 (1977); A. R. Battersby, J. Staunton, H. C. Summers, and R. Southgate, *J. Chem. Soc., Perkin Trans. 1*, **1979**, 45; N. Takao, M. Kamiguchi, and M. Okada, *Helv. Chim. Acta*, **66**, 473 (1983) and references cited therein.
- 7) H. L. Holland, M. Castillo, D. B. MacLean, and I. D. Spenser, *Can. J. Chem.*, **52**, 2818 (1974); H. L. Holland, P. W. Jeffs, T. M. Capps, and D. B. MacLean, *ibid.*, **57**, 1588 (1979).
- 8) A. R. Battersby, J. Staunton, H. R. Wiltshire, R. J. Francis, and R. Southgate, *J. Chem. Soc., Perkin Trans. 1*, **1975**, 1147.
- 9) M. Hanaoka, T. Motonishi, and C. Mukai, *J. Chem. Soc., Chem. Commun.*, **1984**, 718; *idem*, *J. Chem. Soc., Perkin Trans. 1*, **1986**, 2253; M. Hanaoka, H. Yamagishi, M. Marutani, and C. Mukai, *Tetrahedron Lett.*, **25**, 5169 (1984); M. Hanaoka, H. Yamagishi, and C. Mukai, *Chem. Pharm. Bull.*, **33**, 1763 (1985).
- 10) M. E. Wall, M. C. Wani, and H. L. Taylor, 162nd American Chemical Society National Meeting, Washington, D.C., MEDI-34, 1971.
- 11) M. Suffness and G. A. Cordell, "The Alkaloids," Vol. 25, ed. by A. Brossi, Academic Press, New York, 1985, pp. 333–338.
- 12) T. Kametani, "The Total Synthesis of Natural Products," Vol. 3, ed. by J. ApSimon, John Wiley and Sons, New York, 1977, p. 1.
- 13) R. D. Haworth, W. H. Perkin, Jr., and J. Rankin, *J. Chem. Soc.*, **125**, 1686 (1924).
- 14) M. Hanaoka, M. Inoue, M. Takahashi, and S. Yasuda, *Chem. Pharm. Bull.*, **32**, 4431 (1984).
- 15) S. Firdous, A. J. Freyer, M. Shamma, and A. Urzúa, *J. Am. Chem. Soc.*, **106**, 6099 (1984).
- 16) a) N. Murugesan and M. Shamma, *Tetrahedron Lett.*, **1979**, 4521; b) Cf. H. Ishii, T. Ishikawa, S.-T. Lu, and I.-S. Chen, *ibid.*, **1976**, 1203; H. Ishii and T. Ishikawa, *J. Chem. Soc., Perkin Trans. 1*, **1984**, 1769.
- 17) The reaction was carried out in methylene chloride at –78 °C in the presence of sodium bicarbonate.<sup>16a)</sup>
- 18) G. R. Lenz, *J. Org. Chem.*, **42**, 1117 (1977).
- 19) R. A. Rossi and J. K. Bunnett, *J. Org. Chem.*, **38**, 2314 (1973).
- 20) A. Jossang, M. Leboeuf, A. Cáva, M. Damak, and C. Riche, *C. R. Acad. Sci., Ser. C*, **284**, 467 (1977).
- 21) N. Murugesan and M. Shamma, *Heterocycles*, **14**, 585 (1980).
- 22) M. Shamma obtained **5b**<sup>16a)</sup> and **5c**<sup>21)</sup> in 40 and 40–50% yields, respectively.
- 23) T. Kametani, M. Takeshita, F. Satoh, and K. Nyu, *Yukugaku Zasshi*, **94**, 478 (1974).
- 24) R. M. Sotelo and D. Giacomello, *Aust. J. Chem.*, **25**, 385 (1972).

[Chem. Pharm. Bull.]  
35(1) 200—210 (1987)

**Studies on the Constituents of Orchidaceous Plants. VII.<sup>1)</sup> The C-24 Stereochemistry of Cyclohomonervilol and 24-Isopropenylcholesterol, Non-conventional Side Chain Triterpene and Sterol, from *Nervilia purpurea* SCHLECHTER<sup>2)</sup>**

SHIGETOSHI KADOTA, TAKEHIKO SHIMA, and TOHRU KIKUCHI\*

Research Institute for Wakan-Yaku (Oriental Medicines), Toyama Medical and Pharmaceutical University, 2630 Sugitani, Toyama 930-01, Japan

(Received July 25, 1986)

The C-24 stereochemistry of cyclohomonervilol, a non-conventional side chain triterpene isolated from *Nervilia purpurea*, was determined to be 24*S* by chemical transformation to 24*S*-dihydrocyclofuntumienol. Separation of a 24-epimeric mixture of chemically synthesized 24-isopropenylcholesterol was effectively achieved by reversed-phase high-performance liquid chromatography (HPLC), and the C-24 stereochemistry of each epimer was determined on the basis of chemical correlation with sitosterol or clionasterol. Then, 24*ξ*-isopropenylcholesterol, isolated from *N. purpurea*, was identified as 24*S*-isopropenylcholesterol by proton nuclear magnetic resonance and HPLC comparisons with the synthetic sample.

**Keywords**—*Nervilia purpurea*; Orchidaceae; cyclohomonervilol; 24*S*-isopropenylcholesterol; reversed-phase HPLC; stereochemistry; triterpene; sterol; 2D-NMR

In previous papers,<sup>3)</sup> we reported the isolation of cyclohomonervilol and 24*ξ*-isopropenylcholesterol, non-conventional side chain triterpene and sterol, from *Nervilia purpurea* SCHLECHTER (Orchidaceae) and proposed the structures **1a** and **3a**, respectively, but the stereochemistry at the C-24 position of these compounds remained uncertain. Isopropenylcholesterol has recently been obtained as a 24-epimeric mixture (**4a**) from Caribbean sponge, *Verongia cauriformis*, by a combination of silver nitrate-silica gel thin-layer chromatography (TLC), reversed-phase high-performance liquid chromatography (HPLC), and preparative gas chromatography (GC) by Djerassi and co-workers,<sup>4)</sup> who also synthesized **4a** starting from fucosterol (**5a**) and isolated one of the C-24 epimers in an almost pure state. However, the stereochemistry at the C-24 position of that epimer was not determined. In this paper we wish to present full details of the stereochemical assignments of cyclohomonervilol (**1a**) and 24*ξ*-isopropenylcholesterol (**3a**) and also to describe the effective separation of an epimeric mixture of 24-isopropenylcholesterol.

Cyclohomonervilol (**1a**) was converted to the benzoate (**1b**) for practical convenience for TLC and HPLC analyses. Oxidation of **1b** with osmium tetroxide gave a diol (**6**) as an amorphous material, which showed the molecular ion peak at  $m/z$  592 ( $C_{39}H_{60}O_4$ ) in the mass spectrum (MS). Brief treatment of **6** with hydrogen periodate in aqueous dioxane and subsequent reduction with sodium borohydride afforded a mixture of epimeric alcohols, which could be separated by preparative TLC to give **7a**, mp 144.5—146.5 °C, MS  $m/z$ : 562 ( $M^+$ ,  $C_{38}H_{58}O_3$ ), and **8a**, mp 150—152 °C, MS  $m/z$ : 562 ( $M^+$ ,  $C_{38}H_{58}O_3$ ). Then, we examined the transformation of the alcohols, **7a** and **8a**, into the 24-ethyl compound (**9**), which is distinguishable from its C-24 epimer by the chemical shift difference of the 29-methyl signals and the reversed-phase HPLC behavior.<sup>3a,5)</sup>

First, an attempt at the reductive desulfurization of **7a** mesylate with sodium iodide-zinc

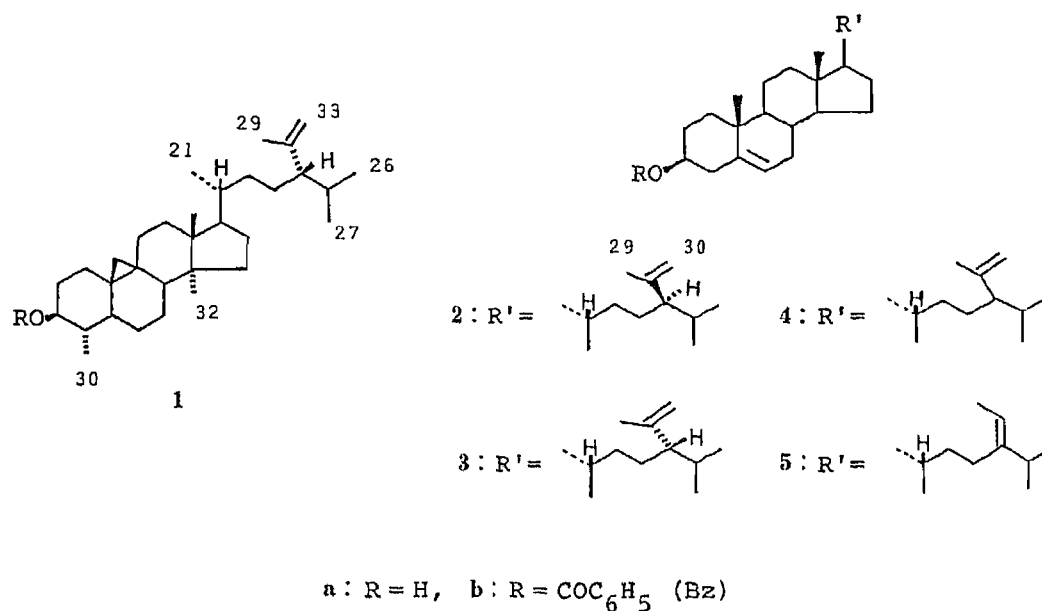


Chart 1

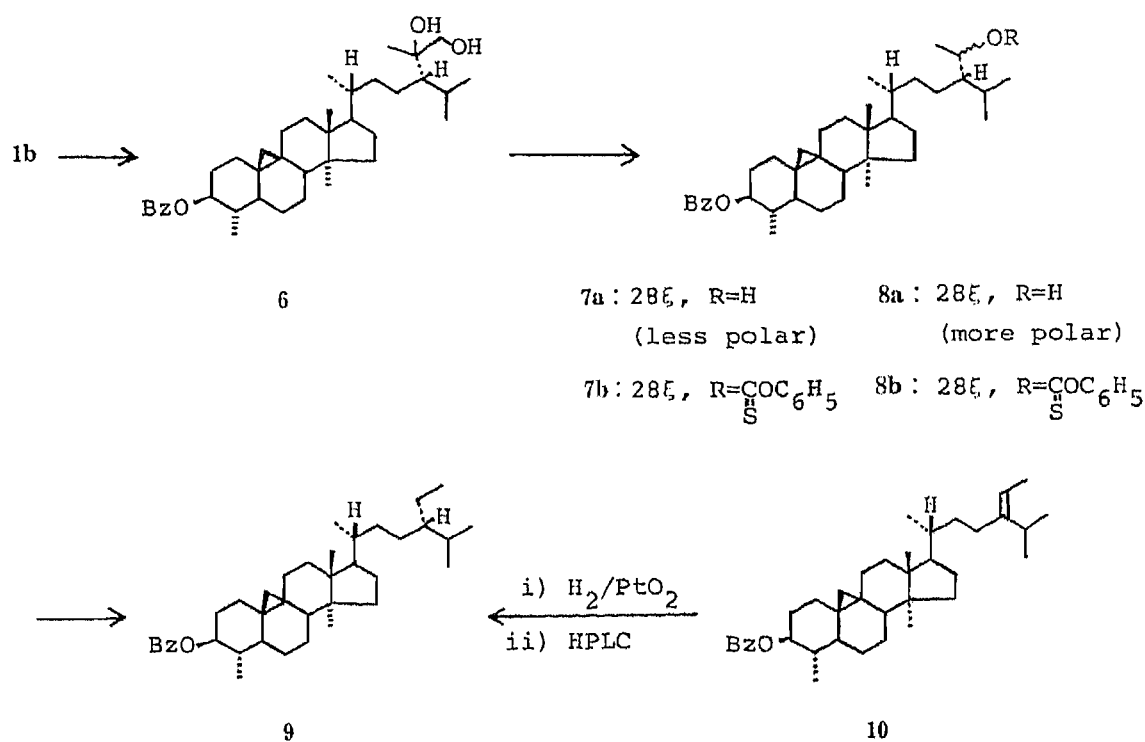


Chart 2

powder<sup>6)</sup> did not give the desired compound, but only a mixture of elimination products. Then, the alcohol **7a** was derived to the phenoxythiocarbonate (**7b**) and subsequently reduced with tributyltin hydride<sup>7)</sup> in toluene to yield a crystalline material, which showed four peaks (in an approximate ratio of 7:8:7:78) on HPLC with a reversed-phase column using chloroform-acetonitrile (2:8) as the eluting solvent (Fig. 1). Each of these peaks could be isolated by repeated preparative HPLC; the fourth peak (main product) was found to be identical with 24*S*-dihydrocyclofuntumienol benzoate (**9**),<sup>3a)</sup> prepared from cyclofuntumienol

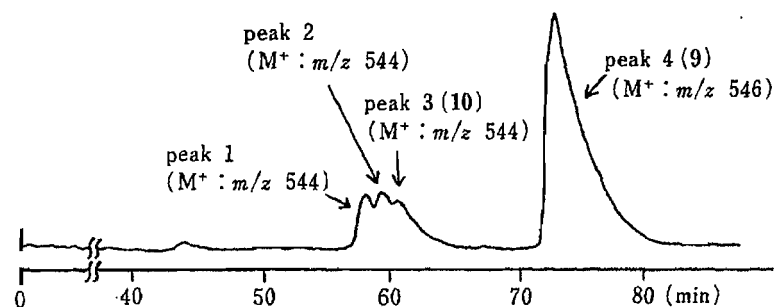


Fig. 1. HPLC Chromatogram of the Reductive Deoxygenation Products of the Thiocarbonate (7b)

Conditions: column, TSK-GEL ODS-120A (25 cm  $\times$  4.6 mm i.d.); solvent,  $\text{CHCl}_3$ - $\text{CH}_3\text{CN}$  (2 : 8); flow rate, 0.6 ml/min; temperature, 20  $^\circ\text{C}$ ; detector setting, UV 240 nm.

bezoate (10), by MS, proton nuclear magnetic resonance ( $^1\text{H-NMR}$ ), and HPLC comparisons. The other peaks were considered to be elimination products on the basis of their MS data ( $\text{M}^+$  peak at  $m/z$  544). Among them, the third peak was assigned to 10 by MS and HPLC analyses.

The other alcohol (8a) was also deoxygenated in the same way as above and the products were separated by preparative HPLC to give 9 as the main product and 10 as a minor product. Identification of these compounds was achieved by MS and HPLC comparisons with authentic samples.

From the above results, the stereochemistry at the C-24 position of cyclohomonervilol (1a) was determined to be *S*.

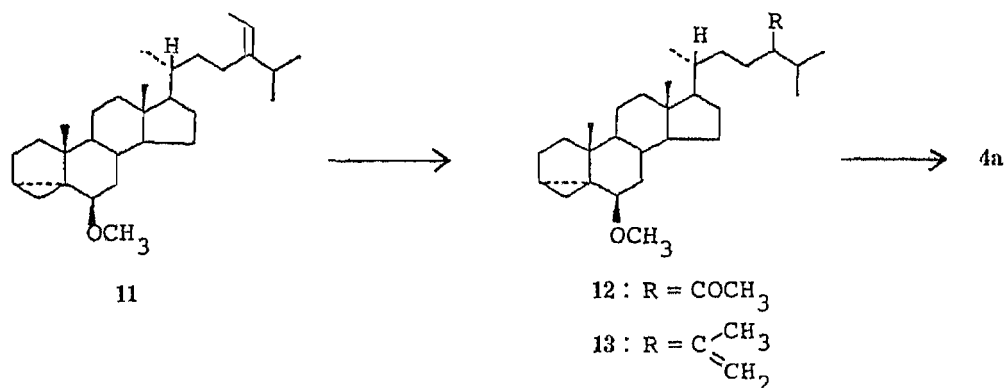


Chart 3

Next, we examined the effective separation of a C-24 epimeric mixture of 24-isopropenylcholesterol (4a) and the stereochemical assignment of each eimer.

24-Isopropenylcholesterol (4a) was prepared from fucosterol (5a) according to Djerassi's description.<sup>4)</sup> Benzoylation of 4a yielded the benzoate (4b), which showed two peaks in an approximate ratio of 51 : 49 on reversed-phase HPLC using a TSK-GEL ODS-120A column (developed with chloroform-acetonitrile 2 : 8) as illustrated in Fig. 2. Thus, preparative HPLC of this mixture gave each epimer; the more mobile epimer (2b) showed mp 130—131  $^\circ\text{C}$  and the less mobile one (3b), mp 150—151  $^\circ\text{C}$ .

Alkaline hydrolyses of these epimeric benzoates (2b and 3b) afforded the corresponding alcohols, 2a, 141—142  $^\circ\text{C}$ ,  $[\alpha]_D -38.8^\circ$  (chloroform), and 3a, 135—135.5  $^\circ\text{C}$ ,  $[\alpha]_D -39.8^\circ$  (chloroform), respectively, whose MS patterns were identical with each other. Further, the  $^1\text{H-NMR}$  spectra of 2a and 3a, and those of 2b and 3b closely resembled each other, except for

TABLE I. 200 MHz <sup>1</sup>H-NMR Spectral Data for Synthetic 24*R*- and 24*S*-Isopropenylcholesterols and Natural 24*S*-Isopropenylcholesterol from *Nervilia purpurea* and Their Benzoates ( $\delta$  Values in CDCl<sub>3</sub> and Coupling Constants in Hz)

Compound (C-24 config.)	3-H	6-H	18-CH <sub>3</sub>	19-H <sub>3</sub>	21-CH <sub>3</sub>	26-CH <sub>3</sub> ,	27-CH <sub>3</sub> <sup>a)</sup>	29-CH <sub>3</sub>	30-H <sub>2</sub>	Others		
<b>2a (synthetic)<sup>b)</sup></b> ( <i>R</i> / $\alpha$ )	3.53 m	5.36 br d (5.4)	0.673 s	1.006 s	0.906 d (5.8)	0.904, d (6.6)	0.798 d (6.4)	1.560 br s	4.62, br s	4.74 br s		
<b>3a (synthetic)</b> ( <i>S</i> / $\beta$ )	3.52 m	5.35 br d (5.1)	0.666 s	1.006 s	0.922 d (6.6)	0.911, d (6.0)	0.802 d (6.0)	1.565 br s	4.60, br s	4.74 br s		
<b>3a (natural)</b> ( <i>S</i> / $\beta$ )	3.52 m	5.35 br d (5.5)	0.666 s	1.006 s	0.922 d (6.2)	0.911, d (5.8)	0.802 d (6.4)	1.566 br s	4.60, br s	4.73 br s		
<b>2b (synthetic)</b> ( <i>R</i> / $\alpha$ )	4.89 m	5.44 br d (4.3)	0.684 s	1.067 s	0.911 d (6.0)	0.911, d (6.0)	0.802 d (6.2)	1.563 br s	4.63, br s	4.76 br s	7.47, m	8.08 (phenyl) m
<b>3b (synthetic)</b> ( <i>S</i> / $\beta$ )	4.88 m	5.44 br d (4.3)	0.676 s	1.067 s	0.929 d (6.4)	0.914, d (6.0)	0.804 d (6.2)	1.566 br s	4.61, br s	4.75 br s	7.47, m	8.08 (phenyl) m
<b>3b (natural)</b> ( <i>S</i> / $\beta$ )	4.88 m	5.44 br d (4.5)	0.678 s	1.068 s	0.930 d (6.4)	0.915, d (6.0)	0.806 d (6.2)	1.569 br s	4.61, br s	4.75 br s	7.47, m	8.08 (phenyl) m

a) The higher-field signal was arbitrarily assigned to the 27-methyl group. b) The <sup>1</sup>H-NMR signals of this compound are identical with those of Djerassi's synthetic 24 $\xi$ -isopropenylcholesterol obtained in an almost pure state; see ref. 4.

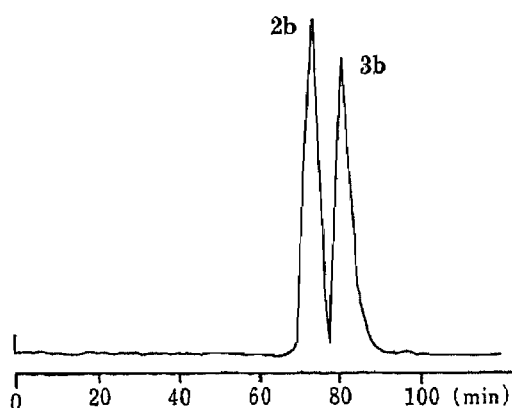


Fig. 2. HPLC Chromatogram of 24-Isopropenylcholesterol Benzoate (**4b**)

Conditions: the same as given in Fig. 1.

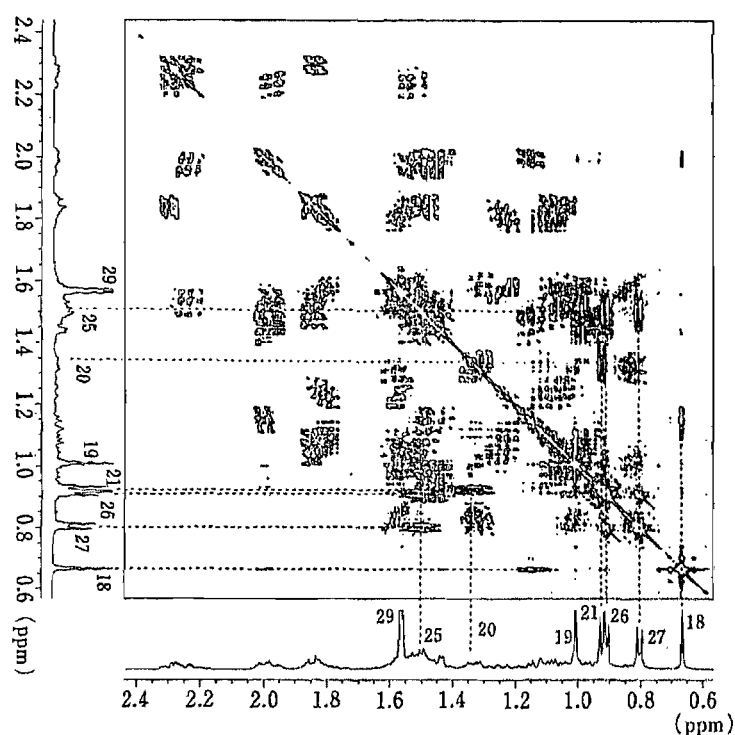


Fig. 3. Contour Map of the  $^1\text{H}$ - $^1\text{H}$  Shift Correlated Spectrum of 24*S*-Isopropenylcholesterol (**3a**) in the Upfield Region

very slight differences between the chemical shifts of their methyl signals, as shown in Table I. Assignments of three *sec*-methyl signals in these compounds were done with the aid of the two-dimensional  $^1\text{H}$ - $^1\text{H}$  shift correlation spectrum of **3a** (Fig. 3), in which two doublets at  $\delta$  0.911 and 0.802, correlated with a proton multiplet at  $\delta$  1.51, were assigned to the 26- and 27-methyls, and the remaining doublet at  $\delta$  0.922 was assigned to the 21-methyl.

In order to determine the stereochemistry at the C-24 position in **2a** and **3a**, we then examined the transformation of **2b** and **3b** into the corresponding 24-ethyl compounds, sitosterol benzoate (**17**) and clionasterol benzoate (**21**), respectively. These sterols (**17** and **21**) are distinguishable from each other by their relative HPLC mobilities, as reported in our previous paper.<sup>8)</sup>

Osmium tetroxide oxidation of **2b** under controlled conditions gave a diol (**14**), whose MS showed the molecular ion peak at  $m/z$  564 ( $\text{C}_{37}\text{H}_{56}\text{O}_4$ ). Treatment of **14** with hydrogen periodate in aqueous dioxane for a short time, followed by reduction with sodium



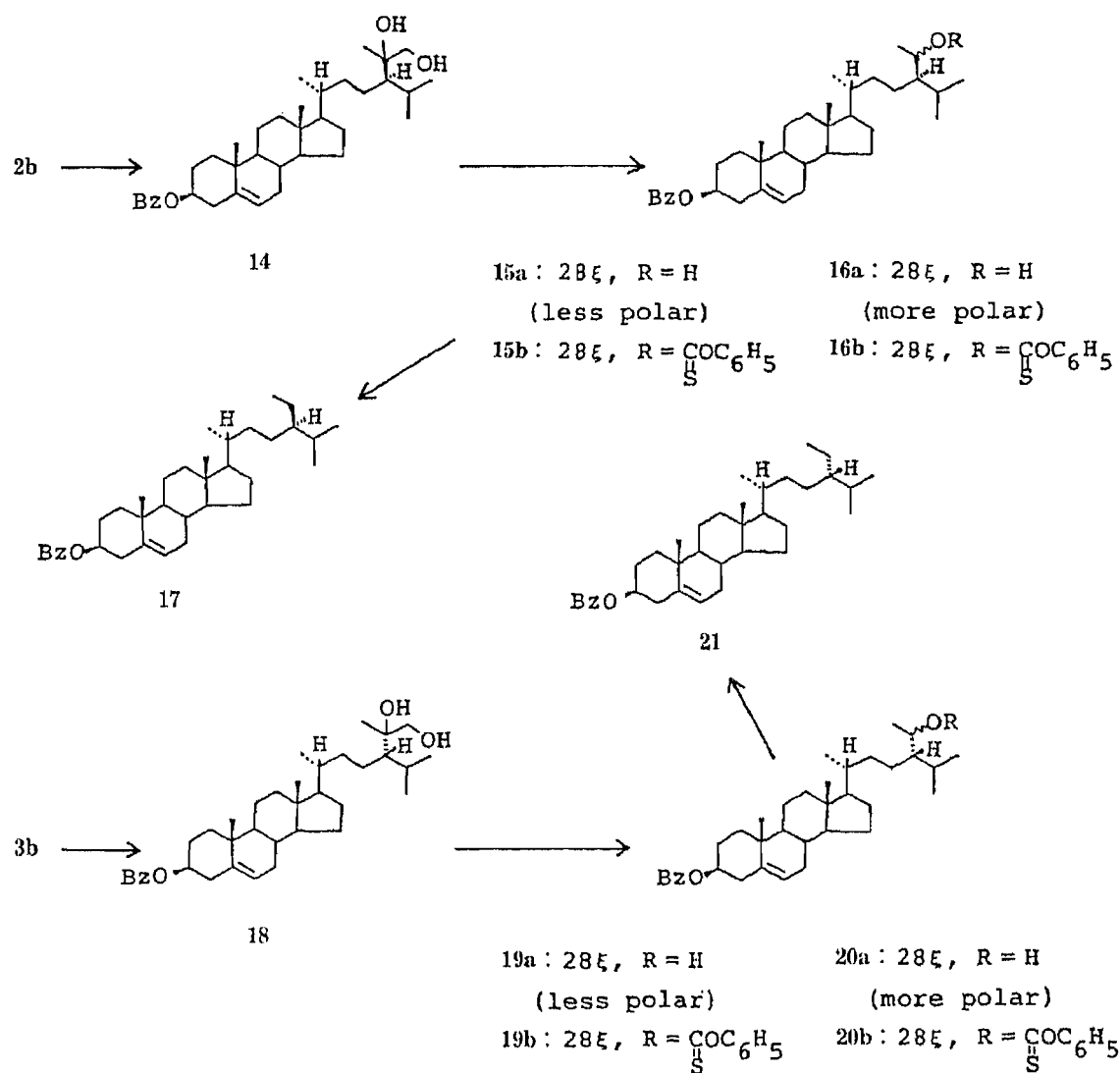


Chart 4

borohydride, gave the 28-epimeric alcohols, **15a** and **16a**, which could be separated by preparative TLC.

The less polar alcohol (**15a**), mp 131–133°C, was converted to the phenoxythiocarbonate (**15b**) and subsequently reduced with tributyltin hydride to yield a crystalline material, which showed three peaks (in an approximate ratio of 25:38:37) on HPLC (Fig. 4a). Separation of these products was successfully performed by preparative HPLC; the third peak was proved to be identical with sitosterol benzoate (**17**) by MS and HPLC comparisons. The other peaks must be elimination products, based on their MS data ( $M^+ - C_6H_5COOH$  peak at  $m/z$  396). Of these, the second peak was assigned to fucosterol benzoate (**5b**) by HPLC analysis.

The more polar alcohol (**16a**) was also deoxygenated in the same manner and the crude product was separated by preparative HPLC to give **17** (the major product) and **5b**. Identification of these compounds was done by MS and HPLC comparisons with authentic samples.

Similarly, treatment of the less mobile epimer (**3b**) with osmium tetroxide in pyridine

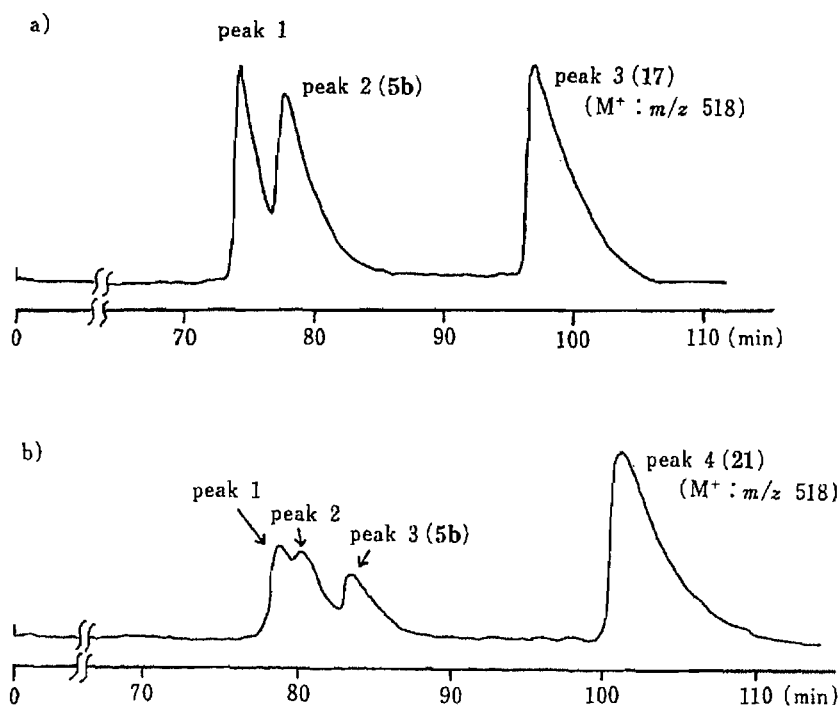


Fig. 4. HPLC Chromatograms of the Reductive Deoxygenation Products of the Phenoxythiocarbonates (**15b** and **19b**)

a) Deoxygenation products of **15b** (at 18°C) and b) deoxygenation products of **19b** (at 17°C).

Conditions: the same as given in Fig. 1, except for the operating temperature.

gave a diol (**18**), MS  $m/z$ : 564 ( $M^+$ ,  $C_{37}H_{56}O_4$ ). Subsequent oxidation of **18** with hydrogen periodate, followed by sodium borohydride reduction, led to a mixture of 28-epimeric alcohols, which on preparative TLC gave **19a** (less polar), mp 161–161.5°C, and **20a** (more polar), mp 132–132.5°C.

When both of **19a** and **20a** were subjected to the deoxygenation reaction in the same manner as above and the crude products were separated by preparative HPLC (Fig. 4b), the same compound (**21**) was obtained as the major product; it was found to be identical with authentic clionasterol benzoate (**21**) by means of MS and HPLC. Also, one of the minor products in both cases was identified as **5b**.

From the foregoing results, the stereochemistry at the C-24 position of **2a** and **3a** was proved to be 24 ( $R/\alpha$ ) and 24 ( $S/\beta$ ), respectively. It is noteworthy that the 24 $\alpha$ -epimer (**2b**) is eluted faster than the corresponding 24 $\beta$ -isomer (**3b**), as in the case of typical C-24 epimers of sterol benzoate.<sup>8)</sup>

Turning now to the stereochemistry of 24 $\xi$ -isopropenylcholesterol (**3a**) isolated from *Nervilia purpurea*, the MS and <sup>1</sup>H-NMR spectra of the free sterol and the benzoate (**3b**) were found to be identical with those of the synthetic **3a** and **3b**, respectively (see Table I). This was further substantiated by comparison of the HPLC behaviors of both benzoates. Therefore, the natural sterol was proved to be 24( $S/\beta$ )-isopropenylcholesterol (**3a**). On the other hand, Djerassi's synthetic specimen,<sup>4)</sup> obtained in an almost pure state, must be the 24 ( $R/\alpha$ )-epimer (**2a**), since the reported <sup>1</sup>H-NMR data are substantially identical with those of our synthetic **2a**.

It is of interest from the biosynthetic viewpoint that no trace of the epimeric counterparts of **1a** and **3a** could be found in the extracts of *Nervilia* species, while both of the 24-epimers occur<sup>4)</sup> in the marine sterol.

### Experimental

Melting points were determined with a Kofler-type apparatus and are uncorrected. Optical rotations were measured in chloroform solutions on a JASCO DIP-4 automatic polarimeter at 22 °C. NMR spectra were taken on Varian Associates XL-200 and JEOL JNM-GX 400 spectrometers in CDCl<sub>3</sub> solutions with tetramethylsilane as an internal standard; chemical shifts are recorded in  $\delta$  values. MS measurements were done on a JEOL D-300 mass spectrometer using a direct inlet system; ionization energy, 70 eV; accelerating voltage, 3 kV. HPLC and preparative HPLC were performed on a Waters Associates ALC/GPC 201 D compact-type liquid chromatograph using a TSK-GEL ODS-120A column (column size 25 cm  $\times$  4.6 mm i.d.; detector setting, UV 240 nm) with CHCl<sub>3</sub>-CH<sub>3</sub>CN (2:8) as the eluent (flow rate 0.6 ml/min). Preparative TLC was carried out on Merck Kieselgel GF<sub>254</sub> with CHCl<sub>3</sub> or CHCl<sub>3</sub>-hexane (1:1 and 2:8) and plates were examined under ultraviolet (UV) light (for UV-absorbing material). Extraction of substances from silica gel was done with MeOH-CHCl<sub>3</sub> (1:9) and solutions were concentrated *in vacuo*. Mallinckrodt silica gel was used for ordinary column chromatography. For drying of organic solutions, anhydrous MgSO<sub>4</sub> was used.

**Benzoylation of Cyclohomonervilol (1a)**—Cyclohomonervilol (1a) (4 mg) was treated with benzoyl chloride (0.01 ml) and pyridine (0.2 ml) overnight at room temperature and the reaction mixture was worked up as usual. Recrystallization of the product from MeOH gave cyclohomonervilol benzoate (1b) (5 mg), colorless needles, mp 156–158 °C. MS *m/z*: 558 (M<sup>+</sup>, C<sub>39</sub>H<sub>58</sub>O), 436 (M<sup>+</sup> - C<sub>6</sub>H<sub>5</sub>COOH), 421, 381, 283. <sup>1</sup>H-NMR  $\delta$ : 0.20, 0.45 (each 1H, d, *J* = 4.0 Hz, 19-H<sub>2</sub>), 0.82 (3H, d, *J* = 6.0 Hz, 26- or 27-CH<sub>3</sub>), 0.85 (3H, d, *J* = 6.0 Hz, 21-CH<sub>3</sub>), 0.92 (3H, d, *J* = 6.0 Hz, 26- or 27-CH<sub>3</sub>), 0.90 (3H, s, 32-CH<sub>3</sub>), 0.96 (3H, s, 18-CH<sub>3</sub>), 1.57 (3H, brs, 29-CH<sub>3</sub>), 4.62, 4.75 (each 1H, m, C = CH<sub>2</sub>), 4.76 (1H, m, 3-H), 7.50 (3H, m, phenyl), 8.08 (2H, m, phenyl).

**Osmium Tetroxide Oxidation of Cyclohomonervilol Benzoate (1b)**—Osmium tetroxide (10 mg) was added to a solution of 1b (5 mg) in pyridine (0.5 ml) and the mixture was allowed to stand overnight with stirring at room temperature. Then, a solution of sodium bisulfite (0.2 g) in water (1 ml) was added and the whole was stirred for 1 h, poured into ice water, basified with Na<sub>2</sub>CO<sub>3</sub>, and extracted with CH<sub>2</sub>Cl<sub>2</sub>. The CH<sub>2</sub>Cl<sub>2</sub> solution was washed successively with 2% HCl and dil. Na<sub>2</sub>CO<sub>3</sub>, dried, and concentrated *in vacuo*. Silica gel column chromatography of the residue with MeOH-CH<sub>2</sub>Cl<sub>2</sub> (5:95) gave a diol (6) (5.5 mg), an amorphous material. MS *m/z*: 592 (M<sup>+</sup>, C<sub>39</sub>H<sub>60</sub>O<sub>4</sub>), 470 (M<sup>+</sup> - C<sub>6</sub>H<sub>5</sub>COOH), 452 (M<sup>+</sup> - C<sub>6</sub>H<sub>5</sub>COOH - H<sub>2</sub>O) (base peak), 437, 410, 344, 283.

**Periodate Oxidation of the Diol (6) Followed by Sodium Borohydride Reduction**—The above diol (6) (5.5 mg) was dissolved in dioxane (0.5 ml) and the solution was cooled in an ice-water bath. To this solution was added a solution of HIO<sub>4</sub> (3 mg) in H<sub>2</sub>O (30  $\mu$ l) under vigorous stirring, and the stirring was continued for 8 min. Then, MeOH (0.2 ml) and NaBH<sub>4</sub> (7 mg) were added and the stirring was continued for a further 30 min. Acetic acid (30  $\mu$ l) was added to the above reaction mixture and the solution was concentrated *in vacuo*. The residue was extracted with CH<sub>2</sub>Cl<sub>2</sub> and the CH<sub>2</sub>Cl<sub>2</sub> extract was washed with brine, dried, and concentrated to give a crystalline residue (9 mg), which was separated by preparative TLC with hexane-CHCl<sub>3</sub> (1:1) into two fractions. The less polar fraction (1.8 mg) was recrystallized from MeOH to give colorless needles (7a), mp 144.5–146.5 °C. MS *m/z*: 562 (M<sup>+</sup>, C<sub>38</sub>H<sub>58</sub>O<sub>3</sub>), 544, 529, 422 (base peak), 407, 283. <sup>1</sup>H-NMR  $\delta$ : 0.194, 0.449 (each 1H, d, *J* = 4.2 Hz, 19-H<sub>2</sub>), 0.890–0.960 (CH<sub>3</sub>  $\times$  5), 0.983 (3H, s, 18-CH<sub>3</sub>), 1.193 (3H, d, *J* = 6.3 Hz, 29-CH<sub>3</sub>), 3.97 (1H, m, 28-H), 4.80 (1H, m, 3-H), 7.50 (3H, m, phenyl), 8.08 (2H, m, phenyl).

The more polar fraction (2.0 mg) was recrystallized from MeOH to give colorless needles (8a), mp 150–152 °C. MS *m/z*: 562 (M<sup>+</sup>, C<sub>38</sub>H<sub>58</sub>O<sub>3</sub>), 544, 529, 422 (base peak), 407, 283. <sup>1</sup>H-NMR  $\delta$ : 0.193, 0.450 (each 1H, d, *J* = 4.0 Hz, 19-H<sub>2</sub>), 0.890–0.924 (CH<sub>3</sub>  $\times$  5), 0.979 (3H, s, 18-CH<sub>3</sub>), 3.84 (1H, m, 28-H), 4.78 (1H, m, 3-H), 7.50 (3H, m, phenyl), 8.08 (2H, m, phenyl).

**Conversion of the Alcohols, 7a and 8a, to 24S-Dihydrocyclofuntumienol Benzoate (9)**—The alcohol 7a (1.0 mg) was treated with phenyl chlorothionocarbonate (5  $\mu$ l) in pyridine (0.1 ml) with stirring for 12 h at room temperature. The reaction mixture was separated by preparative TLC to give the thiocarbonate (7b) (3.5 mg). MS *m/z*: 560 (M<sup>+</sup> - C<sub>6</sub>H<sub>5</sub>OCS - H), 544 (M<sup>+</sup> - C<sub>6</sub>H<sub>5</sub>OCSOH), 529, 440, 422, 407, 283. This was dissolved in toluene (0.8 ml), tributyltin hydride (40  $\mu$ l) was added, and the mixture was heated at 130 °C in an oil bath for 4 h. Evaporation of the solvent *in vacuo* gave an oily residue, which was purified by preparative TLC with CHCl<sub>3</sub>-hexane (2:8) to give a crystalline mass (1.0 mg). This product was subjected to preparative HPLC on a TSK-GEL ODS-120A column with CHCl<sub>3</sub>-CH<sub>3</sub>CN (2:8) as the eluent to give four components. The first peak (0.01 mg), MS *m/z*: 544 (M<sup>+</sup>), and the second peak (0.01 mg), MS *m/z*: 544 (M<sup>+</sup>), were unidentified, and the third peak (0.01 mg), MS *m/z*: 544 (M<sup>+</sup>), was identified as cyclofuntumienol benzoate (10) by MS and HPLC analyses. The fourth peak gave colorless needles (9) (0.5 mg), mp 149–151 °C. MS *m/z*: 546 (M<sup>+</sup>, C<sub>38</sub>H<sub>58</sub>O<sub>2</sub>). <sup>1</sup>H-NMR  $\delta$ : 0.19, 0.45 (each 1H, d, *J* = 4.0 Hz, 19-H<sub>2</sub>), 0.82, 0.84 (each 3H, d, *J* = 6.8 Hz, 26- and 27-CH<sub>3</sub>), 0.86 (3H, t, *J* = 7.5 Hz, 29-CH<sub>3</sub>), 0.88 (3H, d, *J* = 6.6 Hz, 21-CH<sub>3</sub>), 0.91 (3H, d, *J* = 6.4 Hz, 30-CH<sub>3</sub>), 0.92, 0.98 (each 3H, s, 32- and 18-CH<sub>3</sub>), 4.80 (1H, m, 3-H), 7.50 (3H, m, phenyl), 8.08 (2H, m, phenyl). This compound was found to be identical with 24S-dihydrocyclofuntumienol benzoate (9)<sup>30</sup> by MS, <sup>1</sup>H-NMR, and HPLC comparisons.

The other alcohol (8a) (1.0 mg) was also deoxygenated in the same manner as above and the product was separated by preparative HPLC to give 10 (0.01 mg) and 9 (0.2 mg). Identification of these compounds was confirmed

by MS and HPLC comparisons with authentic samples.

**Hydroboration of *i*-Fucosterol Methyl Ether (11) Followed by Collins Oxidation**—Fucosterol (5a) was derived to the *i*-methyl ether (11) in the usual way. To a solution of 11 (198 mg) in tetrahydrofuran (THF) (13 ml), 1 M borane-THF complex (4 ml) was added slowly under stirring. Stirring was continued for 10 h at room temperature, and water was added to destroy the excess reagent. Then, 6 N aq. NaOH and 30% H<sub>2</sub>O<sub>2</sub> (3 ml) were added dropwise over a period for 10 min with stirring under ice-cooling, and the mixture was stirred for a further 1.5 h at room temperature. The mixture was saturated with K<sub>2</sub>CO<sub>3</sub> (10 g) and the organic layer was separated from the aqueous layer, which was washed with ether. The combined organic layer was dried over MgSO<sub>4</sub> and concentrated. The residue (256 mg) was chromatographed on silica gel (4 g) with hexane and CHCl<sub>3</sub>-hexane (4:6) to give the alcohol (180 mg) as a colorless oil.

Collins reagent (1 g) was added to a solution of the above alcohol (180 mg) in dry CH<sub>2</sub>Cl<sub>2</sub> (5 ml) and the mixture was stirred for 16 h at room temperature. After removal of the reagent, the product was chromatographed on silica gel (5 g) with CH<sub>2</sub>Cl<sub>2</sub> to afford the ketone (12) (160 mg) as an oil. MS *m/z*: 442 (M<sup>+</sup>, C<sub>30</sub>H<sub>50</sub>O<sub>2</sub>), 427, 410, 387, 255. <sup>1</sup>H-NMR δ: 0.7–1.05 (CH<sub>3</sub> × 5), 2.10 (3H, s, CH<sub>3</sub>-CO-), 2.75 (1H, m, 6-H), 3.33 (3H, s, OCH<sub>3</sub>).

**Witting Reaction of the Ketone (12)**—A solution of methyltriphenylphosphonium bromide (5 g) in dimethylsulfoxide (DMSO 5 ml) was added to a solution of oil-free KH (570 mg) in DMSO (5 ml) under argon gas and the mixture was stirred for 1 h. Then, a solution of 12 (130 mg) in ether-DMSO (1:1) (1 ml) was added slowly under vigorous stirring, and the whole was stirred for 3 h at room temperature. Silica gel column chromatography of the reaction mixture with hexane and ether-hexane (5:95) gave the olefin (13) (97 mg) as an oil. MS *m/z*: 440 (M<sup>+</sup>, C<sub>31</sub>H<sub>52</sub>O), 425, 408, 385, 255, 253.

**Acid Hydrolysis of the Olefin (13)**—A solution of 13 (97 mg) and *p*-toluenesulfonic acid (3 mg) in aqueous dioxane (10 ml) was refluxed for 30 min. After cooling, the mixture was neutralized with aq. Na<sub>2</sub>CO<sub>3</sub> and extracted with CH<sub>2</sub>Cl<sub>2</sub>. The extract was dried and concentrated. The residue was purified by preparative TLC [developed with MeOH-CHCl<sub>3</sub> (1:99)] to give 24-isopropenylcholesterol (4a) (56 mg), colorless needles (from MeOH), mp 119–122 °C. MS *m/z*: 426 (M<sup>+</sup>, C<sub>30</sub>H<sub>50</sub>O), 408, 393, 383, 328, 314, 299, 271, 255.

Benzoate (4b): colorless needles (from MeOH-isopropyl ether), mp 123–126 °C. MS *m/z*: 530 (M<sup>+</sup>, C<sub>37</sub>H<sub>54</sub>O<sub>2</sub>), 408, 368, 253.

**Separation of the Epimeric Mixture of 24-Isopropenylcholesterol Benzoate (4b) by HPLC**—The benzoate mixture (4b) (43 mg) was subjected repeatedly to preparative HPLC on a TSK-GEL ODS-120A column with CHCl<sub>3</sub>-CH<sub>3</sub>CN (2:8) as the eluent at 20 °C. The more mobile fraction afforded 24 (*R*/α)-isopropenylcholesterol benzoate (2b) (19 mg), colorless needles (from MeOH-isopropyl ether), mp 130–131 °C, [α]<sub>D</sub> -15.4° (*c*=0.82). <sup>1</sup>H-NMR δ: see Table I. The less mobile fraction gave the 24 (*S*/β) epimer (3b) (18 mg), colorless needles (from MeOH-isopropyl ether), mp 150–151 °C, [α]<sub>D</sub> -19.2° (*c*=0.78). <sup>1</sup>H-NMR δ: see Table I.

**24(*R*/α)-Isopropenylcholesterol (2a)**—Compound 2b (9 mg) was refluxed with 5% KOH-MeOH (0.5 ml) for 1.5 h and the reaction mixture was worked up as usual. Recrystallization of the product from MeOH gave 2a (6.5 mg), colorless needles, mp 141–142 °C, [α]<sub>D</sub> -38.8° (*c*=0.4). MS *m/z*: 426 (M<sup>+</sup>, 408, 393, 383, 328, 314, 299, 271, 255. High-resolution MS *m/z*: Found 426.3910, Calcd for C<sub>30</sub>H<sub>50</sub>O (M<sup>+</sup>) 426.3861. <sup>1</sup>H-NMR δ: see Table I.

**24(*S*/β)-Isopropenylcholesterol (3a)**—The benzoate 3b (7.5 mg) was hydrolyzed in the same manner as above and the product was recrystallized from MeOH to give 3a (5.4 mg), colorless plates, mp 135–135.3 °C, [α]<sub>D</sub> -39.8° (*c*=0.44). MS *m/z*: 426 (M<sup>+</sup>, 408, 393, 383, 328, 314, 299, 271, 255. High-resolution MS *m/z*: Found 426.3910, Calcd for C<sub>30</sub>H<sub>50</sub>O (M<sup>+</sup>) 426.3861. <sup>1</sup>H-NMR δ: see Table I.

**Osmium Tetroxide Oxidation of 24(*R*/α)-Isopropenylcholesterol Benzoate (2b)**—Osmium tetroxide (20 mg) was added to a solution of 2b (10 mg) in anhydrous ether (200 μl) and anhydrous benzene (100 μl) and the mixture was allowed to stand overnight with stirring at room temperature. After removal of the solvent by evaporation, a solution of sodium bisulfite (0.2 g) in water (1 ml) and ethyl alcohol (1 ml) was added to the reaction mixture and the whole was stirred for 1 h. Then, the mixture was concentrated *in vacuo*, and the product was taken up in CH<sub>2</sub>Cl<sub>2</sub>. The CH<sub>2</sub>Cl<sub>2</sub> solution was concentrated and the residue was purified by preparative TLC (developed with CHCl<sub>3</sub>) to give a diol (14) (10 mg) as an amorphous material. MS *m/z*: 564 (M<sup>+</sup>, C<sub>37</sub>H<sub>56</sub>O<sub>4</sub>), 442 (M<sup>+</sup> - C<sub>6</sub>H<sub>5</sub>COOH), 440 (M<sup>+</sup> - C<sub>6</sub>H<sub>5</sub>COOH - H<sub>2</sub>), 424, 410, 395, 255.

**Periodate Oxidation of the Diol (14) Followed by Sodium Borohydride Reduction**—A solution of HIO<sub>4</sub> (4.5 mg) in H<sub>2</sub>O (45 μl) was added to a stirred solution of the diol 14 (10 mg) in dioxane (0.5 ml) and the mixture was stirred for 5 min under ice-cooling. Then, MeOH (0.2 ml) and NaBH<sub>4</sub> (10 mg) were added to the mixture and stirring was continued for 30 min. After decomposition of the excess reagent by addition of acetic acid (30 μl) under stirring, the reaction mixture was concentrated *in vacuo*. The product was taken up in CH<sub>2</sub>Cl<sub>2</sub>, and the CH<sub>2</sub>Cl<sub>2</sub> solution was washed with brine, dried, and concentrated. The residue (3.2 mg) was separated by preparative TLC with CHCl<sub>3</sub> into two fractions. The less polar fraction (0.8 mg) was recrystallized from MeOH to give the alcohol 15a, colorless needles, mp 131–133 °C. <sup>1</sup>H-NMR δ: 0.692 (3H, s, 18-CH<sub>3</sub>), 0.890 (3H, d, *J*=6.7 Hz, 27-CH<sub>3</sub>), 0.943 (3H, d, *J*=6.8 Hz, 26-CH<sub>3</sub>), 0.965 (3H, d, *J*=6.3 Hz, 21-CH<sub>3</sub>), 1.070 (3H, s, 19-CH<sub>3</sub>), 1.188 (3H, d, *J*=6.4 Hz, 29-CH<sub>3</sub>), 3.95 (1H, m, 28-H), 4.89 (1H, m, 3-H), 5.45 (1H, br d, *J*=5.1 Hz, 6-H), 7.47 (3H, m, phenyl), 8.08 (2H, m, phenyl).

The more polar fraction (1.2 mg) was recrystallized from MeOH to give colorless needles (16a), mp 136–138 °C.

$^1\text{H-NMR}$   $\delta$ : 0.693 (3H, s, 18- $\text{CH}_3$ ), 0.885 (3H, d,  $J=6.6$  Hz, 27- $\text{CH}_3$ ), 0.913 (3H, d,  $J=6.7$  Hz, 26- $\text{CH}_3$ ), 0.954 (3H, d,  $J=7.0$  Hz, 21- $\text{CH}_3$ ), 1.071 (3H, s, 19- $\text{CH}_3$ ), 1.194 (3H, d,  $J=6.3$  Hz, 29- $\text{CH}_3$ ), 3.83 (1H, m, 28-H), 4.89 (1H, m, 3-H), 5.44 (1H, br d,  $J=5.1$  Hz, 6-H), 7.47 (3H, m, phenyl), 8.08 (2H, m, phenyl).

**Conversion of the Alcohols, 15a and 16a, to Sitosterol Benzoate (17)**—The alcohol 15a (0.8 mg) was dissolved in pyridine (40  $\mu\text{l}$ ) and treated with phenyl chlorothionocarbonate (20  $\mu\text{l}$ ) for 14 h under stirring at room temperature. The reaction mixture was separated by preparative TLC to give the thiocarbonate (15b) (2.9 mg). MS  $m/z$ : 548 ( $\text{M}^+ - \text{C}_6\text{H}_5\text{COOH}$ ), 516 ( $\text{M}^+ - \text{C}_6\text{H}_5\text{OCSOH}$ ), 394, 296, 283, 255. This was reduced with tributyltin hydride (60  $\mu\text{l}$ ) in toluene (0.5 ml) at 130  $^\circ\text{C}$  in an oil bath for 5 h. Evaporation of the solvent *in vacuo* gave an oily residue, which was purified by preparative TLC with hexane- $\text{CHCl}_3$  (1:1) to give a crystalline material (1 mg). This product was subjected to preparative HPLC on a TSK-GEL ODS-120A column with  $\text{CHCl}_3$ - $\text{CH}_3\text{CN}$  (2:8) to give three components. The first eluate (*ca.* 0.08 mg) was considered to be an elimination product on the basis of the MS data, MS  $m/z$ : 394 ( $\text{M}^+ - \text{C}_6\text{H}_5\text{COOH}$ ), but was not identified. The second eluate (*ca.* 0.1 mg), MS  $m/z$ : 394 ( $\text{M}^+ - \text{C}_6\text{H}_5\text{COOH}$ ), was identified as fucosterol benzoate (5b) by MS and HPLC analyses. The third eluate gave sitosterol benzoate (17) (0.1 mg), MS  $m/z$ : 518 ( $\text{M}^+$ ), 396 ( $\text{M}^+ - \text{C}_6\text{H}_5\text{COOH}$ ). Its identity was confirmed by MS and HPLC comparisons with an authentic sample.

The alcohol 16a (1.2 mg) was also treated with phenyl chlorothionocarbonate (20  $\mu\text{l}$ ) in pyridine (40  $\mu\text{l}$ ) and the resulted thiocarbonate (16b) (2.5 mg) was deoxygenated with tributyltin hydride (60  $\mu\text{l}$ ) in the same manner as above. Separation of the product by HPLC gave fucosterol benzoate (5b) (0.2 mg) and sitosterol benzoate (17) (0.3 mg). Their identities were confirmed by MS and HPLC comparisons with authentic samples.

**Osmium Tetroxide Oxidation of 24(S/ $\beta$ )-Isopropenylcholesterol Benzoate (3b)**—The benzoate 3b (10 mg) was allowed to react with osmium tetroxide (20 mg) in anhydrous ether (200  $\mu\text{l}$ ) and anhydrous benzene (100  $\mu\text{l}$ ) overnight at room temperature and the reaction mixture was treated in the same manner as described for 2b. Purification of the product by preparative TLC (developed with  $\text{CHCl}_3$ ) afforded a diol (18) (7 mg) as an amorphous material. MS  $m/z$ : 564 ( $\text{M}^+$ ,  $\text{C}_{37}\text{H}_{56}\text{O}_4$ ), 442 ( $\text{M}^+ - \text{C}_6\text{H}_5\text{COOH}$ ), 440, 424, 410, 395, 255.

**Periodate Oxidation of the Diol (18) Followed by Sodium Borohydride Reduction**—The above diol (18) (7 mg) was dissolved in dioxane (0.4 ml) and a solution of  $\text{HIO}_4$  (4.0 mg) in  $\text{H}_2\text{O}$  (40  $\mu\text{l}$ ) was added under vigorous stirring. Stirring was continued for 5 min under ice-cooling, then MeOH (0.16 ml) and  $\text{NaBH}_4$  (7 mg) were added and the mixture was stirred for 30 min. Then, the excess reagent was decomposed by addition of acetic acid (30  $\mu\text{l}$ ) and the reaction mixture was concentrated *in vacuo*. The product was extracted with  $\text{CH}_2\text{Cl}_2$  and the  $\text{CH}_2\text{Cl}_2$  extract was washed with brine, dried, and concentrated. The residue (5.1 mg) was separated by preparative TLC with  $\text{CHCl}_3$  into two fractions. The less polar fraction (0.9 mg) was recrystallized from MeOH to give the alcohol 19a, colorless needles, mp 161–161.5  $^\circ\text{C}$ .  $^1\text{H-NMR}$   $\delta$ : 0.689 (3H, s, 18- $\text{CH}_3$ ), 0.905 (3H, d,  $J=6.8$  Hz, 27- $\text{CH}_3$ ), 0.941 (3H, d,  $J=7.1$  Hz, 26- $\text{CH}_3$ ), 0.960 (3H, d,  $J=6.2$  Hz, 21- $\text{CH}_3$ ), 1.068 (3H, s, 19- $\text{CH}_3$ ), 1.187 (3H, d,  $J=6.5$  Hz, 29- $\text{CH}_3$ ), 3.95 (1H, m, 28-H), 4.87 (1H, m, 3-H), 5.43 (1H, br d,  $J=5.0$  Hz, 6-H), 7.47 (3H, m, phenyl), 8.08 (2H, m, phenyl).

The more polar fraction (1.0 mg) was recrystallized from MeOH to give the alcohol 20a, colorless needles, mp 132–132.5  $^\circ\text{C}$ .  $^1\text{H-NMR}$   $\delta$ : 0.688 (3H, s, 18- $\text{CH}_3$ ), 0.903 (3H, d,  $J=6.8$  Hz, 27- $\text{CH}_3$ ), 0.913 (3H, d,  $J=6.9$  Hz, 26- $\text{CH}_3$ ), 0.955 (3H, d,  $J=6.4$  Hz, 21- $\text{CH}_3$ ), 1.069 (3H, s, 19- $\text{CH}_3$ ), 1.183 (3H, d,  $J=6.4$  Hz, 29- $\text{CH}_3$ ), 3.84 (1H, m, 28-H), 4.89 (1H, m, 3-H), 5.44 (1H, br d,  $J=5.0$  Hz, 6-H), 7.47 (3H, m, phenyl), 8.08 (2H, m, phenyl).

**Conversion of the Alcohols, 19a and 20a, to Clionasterol Benzoate (21)**—Phenyl chlorothionocarbonate (20  $\mu\text{l}$ ) was added to a solution of the alcohol 19a (0.9 mg) in pyridine (40  $\mu\text{l}$ ) and the mixture was stirred for 18 h at room temperature. The reaction mixture was separated by preparative TLC to give the thiocarbonate (19b) (3.0 mg). This was dissolved in toluene (0.5 ml), then tributyltin hydride (50  $\mu\text{l}$ ) was added and the mixture was heated at 130  $^\circ\text{C}$  in an oil bath for 5 h. Evaporation of the solvent *in vacuo* gave an oily residue, which was purified by preparative TLC with hexane- $\text{CHCl}_3$  (1:1) to give a crystalline material (0.6 mg). This was subjected to preparative HPLC on a TSK-GEL ODS-120A column with  $\text{CHCl}_3$ - $\text{CH}_3\text{CN}$  (2:8) as the eluent to give four components. The first and second eluates (*ca.* 0.1 mg each) were considered to be elimination products on the basis of the MS data, MS  $m/z$ : 394 ( $\text{M}^+ - \text{C}_6\text{H}_5\text{COOH}$ ), but were not identified. The third eluate (*ca.* 0.05 mg), MS  $m/z$ : 394 ( $\text{M}^+ - \text{C}_6\text{H}_5\text{COOH}$ ), was identified as fucosterol benzoate (5b) by MS and HPLC analyses. The fourth eluate gave clionasterol benzoate (21) (0.2 mg), MS  $m/z$ : 518 ( $\text{M}^+$ ), 396 ( $\text{M}^+ - \text{C}_6\text{H}_5\text{COOH}$ ), which was identified by MS and HPLC comparisons with an authentic sample.

The more polar alcohol (20a) (0.8 mg) was also treated with phenyl chlorothionocarbonate (20  $\mu\text{l}$ ) in pyridine (40  $\mu\text{l}$ ) and the resulting thiocarbonate (20b) (2.5 mg) was deoxygenated with tributyltin hydride (50  $\mu\text{l}$ ) in the same manner as above. Separation of the products by HPLC gave fucosterol benzoate (5b) (0.1 mg) and clionasterol benzoate (21) (0.15 mg). Their identities were confirmed by MS and HPLC comparisons with authentic samples.

**Acknowledgement** This work was supported in part by a Grant-in-Aid for Scientific Research from the Ministry of Education, Science, and Culture, which is gratefully acknowledged.

#### References and Notes

- 1) Part VI: S. Kadota, S. Kanomi (née Matsuda), T. Shima, and T. Kikuchi, *Chem. Pharm. Bull.*, **34**, 3244 (1986).

- 2) Preliminary reports of this work have appeared. a) T. Kikuchi, S. Kadota, and T. Shima, *Chem. Pharm. Bull.*, **33**, 2609 (1985); b) T. Kikuchi, S. Kadota, and T. Shima, *Tetrahedron Lett.*, **26**, 3817 (1985).
- 3) a) T. Kikuchi, S. Kadota, H. Suehara, and T. Shima, *Chem. Pharm. Bull.*, **33**, 1914 (1985); b) T. Kikuchi, S. Kadota, H. Suehara, and T. Namba, *ibid.*, **33**, 2235 (1985).
- 4) W. C. M. C. Kokke, C. S. Pak, W. Fenical, and C. Djerassi, *Helv. Chim. Acta*, **62**, 1310 (1979).
- 5) The stereochemistry at the C-24 position of **9** and its epimer was determined from the HPLC behavior compared with that of analogous sterols, the 24 $\alpha$ -epimers of which are usually eluted faster than the 24 $\beta$ -epimers; see ref. 8.
- 6) F. Fujimoto and T. Tatsuno, *Tetrahedron Lett.*, **17**, 3325 (1976).
- 7) M. J. Robins, J. S. Wilson, and F. Hansske, *J. Am. Chem. Soc.*, **105**, 4059 (1983).
- 8) T. Kikuchi, S. Kadota, T. Shima, N. Ikekawa, and Y. Fujimoto, *Chem. Pharm. Bull.*, **32**, 3779 (1984).

[Chem. Pharm. Bull.]  
35(1) 211—216 (1987)

## Structure–Activity Relationship of Brassinosteroids with Respect to the A/B-Ring Functional Groups<sup>1)</sup>

SUGURU TAKATSUTO,<sup>\*,a</sup> NOBUO IKEKAWA,<sup>b</sup> TADASHI MORISHITA,<sup>c</sup>  
and HIROSHI ABE<sup>c</sup>

*Department of Chemistry, Joetsu University of Education,<sup>a</sup> Joetsu, Niigata 943, Japan,  
Department of Chemistry, Tokyo Institute of Technology,<sup>b</sup> Ookayama, Meguro-ku,  
Tokyo 152, Japan, and Department of Plant Protection, Tokyo University  
of Agriculture and Technology,<sup>c</sup> Fuchu-shi, Tokyo 183, Japan*

(Received July 25, 1986)

In order to examine the biological role of the A/B-ring functional groups of plant-growth-promoting brassinosteroids, twenty-three brassinosteroids with some modifications at rings A and B (1—15 and 22—29) were bioassayed by means of the rice-lamina inclination test. The results showed that 1) removal of one or two hydroxyl groups from the A-ring reduced the biological activity of the steroids; 2) the 7-oxalactone brassinosteroids were almost as active as the corresponding 6-oxo steroids and they were much more active than their regioisomeric 6-oxalactone counterparts; 3) introduction of a double bond at the C-7 position and a hydroxyl group at the C-5 position of 6-oxo brassinosteroids significantly decreased the biological activity of the hormonal steroids. These data suggest that the presence of a 2 $\alpha$ ,3 $\alpha$ -diol, 7-oxalactone or 6-oxo group, and the A/B-*trans* ring junction are important for high biological activity.

**Keywords**—plant growth promoter; brassinosteroid; structure–activity relationship; rice-lamina inclination test

### Introduction

Since the discovery of brassinolide as a new plant growth promoter, a number of related steroids have been isolated and identified in higher plants.<sup>2)</sup> These steroids and their synthetic analogues (termed brassinosteroids) constitute a new class of plant growth promoters. Recently, our group and the USDA scientists have independently investigated the structure–activity relationship of brassinosteroids with particular emphasis on the 22,23-vicinal diol and the 24-alkyl group, and disclosed some stringent structural requirements for high activity.<sup>3)</sup>

However, little is known about the importance of the A/B ring functional groups of the steroids. Wada *et al.* have examined this point by employing several brassinosteroids with the unnatural (22*S*,23*S*)-stereochemistry in the side chain.<sup>4)</sup> To obtain further insight into the structural requirements for the A/B ring part, we have synthesized fifteen (22*R*,23*R*)-28-homobrasinosteroids (1—15)<sup>5)</sup> (Fig. 1) and four new 24-epibrassinosteroids (22—25) (Fig. 2). In this paper we report the structure–activity relationship of these brassinosteroids with respect to the A/B-ring functional groups examined by means of the rice-lamina inclination test.

### Experimental

Melting points were determined on a hot stage microscope and are uncorrected. Proton nuclear magnetic resonance (<sup>1</sup>H-NMR) spectra were recorded on a Hitachi R-24A (60 MHz) spectrometer with tetramethylsilane as an internal standard. Mass spectra (MS) were taken with a Shimadzu LKB-9000S mass spectrometer at 70 eV. Ultraviolet (UV) spectra were run with a Shimadzu UV-200 double beam spectrophotometer. Column chromatography was

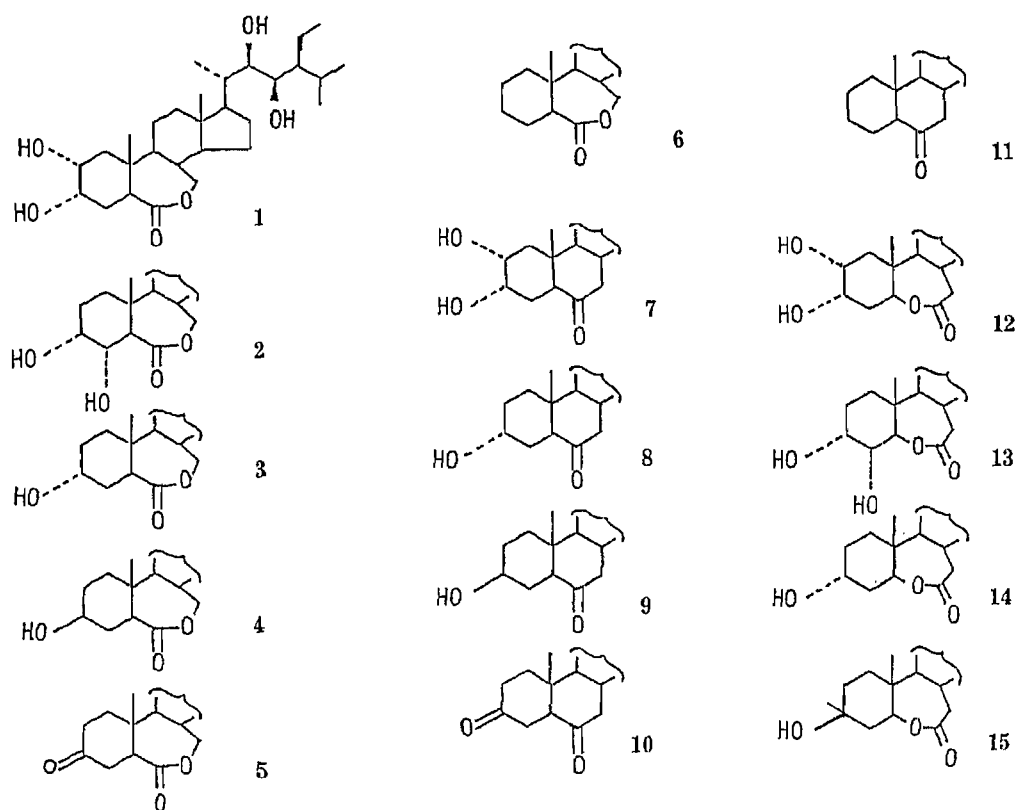


Fig. 1

effected with silica gel (Merck, Kieselgel 60, 70—230 mesh), and preparative and analytical thin layer chromatographies (TLC) were carried out on precoated silica gel plates (Merck, Kieselgel 60 F<sub>254</sub>, 0.25 mm thickness). Work-up refers to dilution with water, extraction with the organic solvent indicated in parenthesis, washing of the extract to neutrality, drying over anhydrous MgSO<sub>4</sub>, filtration, and removal of the solvent under reduced pressure.

**(22*E*,24*R*)-5 $\alpha$ -Hydroxyergosta-2,7,22-trien-6-one (20)**—The known (22*E*,24*R*)-3 $\beta$ -acetoxy-5 $\alpha$ -hydroxyergosta-7,22-dien-6-one (**16**)<sup>6</sup> (1.17 g, 2.49 mmol) in tetrahydrofuran (THF, 50 ml) was treated with 5% KOH/MeOH (10 ml) at room temperature for 1 h. Work-up (CH<sub>2</sub>Cl<sub>2</sub>) and recrystallization from EtOAc gave the 3 $\beta$ ,5 $\alpha$ -diol **17** (439 mg). The mother liquor was concentrated and chromatographed on silica gel (40 g) with CHCl<sub>3</sub>-MeOH (20 : 1) to give additional diol **17** (240 mg). The total amount of **17** was 679 mg (64%), mp 252—253 °C (EtOAc). UV  $\lambda_{\text{max}}^{\text{EtOH}}$ : 248 nm. <sup>1</sup>H-NMR (CDCl<sub>3</sub>)  $\delta$ : 0.68 (3H, s, 18-H<sub>3</sub>), 0.86 (3H, s, 19-H<sub>3</sub>), 3.90 (1H, m, 3-H), 5.20 (2H, m, 22-H and 23-H), 5.62 (1H, m, 7-H). The diol **17** (626 mg, 1.46 mmol) in pyridine (10 ml) was treated with *p*-toluenesulfonyl chloride (800 mg, 4.2 mmol) at room temperature overnight. Work-up (EtOAc) gave the tosylate **18** (828 mg), which was further treated with lithium carbonate (400 mg, 5.41 mmol) and dimethylformamide (10 ml) at 150 °C for 45 min. Work-up (EtOAc) and chromatography on silica gel (50 g) with benzene-EtOAc (80 : 1) gave the trienone **20** (227 mg, 38%), mp 204—205 °C (MeOH). UV  $\lambda_{\text{max}}^{\text{EtOH}}$ : 248 nm ( $\epsilon$  11500). <sup>1</sup>H-NMR (CDCl<sub>3</sub>)  $\delta$ : 0.70 (3H, s, 18-H<sub>3</sub>), 0.87 (3H, s, 19-H<sub>3</sub>), 5.20 (2H, m, 22-H and 23-H), 5.68 (3H, m, 2-H, 3-H, and 7-H). Anal. Calcd for C<sub>28</sub>H<sub>42</sub>O<sub>2</sub>: C, 81.90; H, 10.31. Found: C, 82.19; H, 10.26.

**(22*E*,24*R*)-5 $\alpha$ -Ergosta-2,7,22-trien-6-one (21)**—The known (22*E*, 24*R*)-3 $\beta$ -acetoxy-5 $\alpha$ -ergosta-7,22-dien-6-one (**5a**)<sup>6</sup> (1.8 g, 3.96 mmol) was transformed, as described for **16**, into the trienone **21** (455 mg, 41%), mp 138—140 °C (MeOH). UV  $\lambda_{\text{max}}^{\text{EtOH}}$ : 244 nm ( $\epsilon$  11100). <sup>1</sup>H-NMR (CDCl<sub>3</sub>)  $\delta$ : 0.89 (3H, s, 18-H<sub>3</sub>), 1.00 (3H, s, 19-H<sub>3</sub>), 5.25 (2H, m, 22-H and 23-H), 5.65 (2-H, m, 2-H and 3-H), 5.83 (1H, d, *J* = 3 Hz, 7-H). Anal. Calcd for C<sub>28</sub>H<sub>42</sub>O: C, 85.22; H, 10.73. Found: C, 85.10; H, 10.77.

**(22*R*,23*R*,23*R*)- and (22*S*,23*S*,24*R*)-2 $\alpha$ ,3 $\alpha$ ,5 $\alpha$ ,22,23-Pentahydroxyergost-7-en-6-one (22 and 23)**—The trienone **20** (251 mg, 0.611 mmol) in *tert*-BuOH-THF-H<sub>2</sub>O (10 : 3 : 1, 10 ml) was treated with osmium tetroxide (20 mg) and *N*-methylmorpholine *N*-oxide (420 mg, 3.11 mmol) at room temperature for 63 h. Work-up (CH<sub>2</sub>Cl<sub>2</sub>) gave crude products (290 mg), which showed two main spots on TLC (CHCl<sub>3</sub>-MeOH, 10 : 1, developed twice) with *R*<sub>f</sub> values of 0.26 and 0.20. These two products were purified by preparative TLC (CHCl<sub>3</sub>-MeOH, 10 : 1, developed three times) to give the less polar (22*S*,23*S*)-pentaol **23** (75 mg, 26%), mp 229—231 °C (dec., EtOAc), UV  $\lambda_{\text{max}}^{\text{EtOH}}$ : 248 nm ( $\epsilon$  11100), <sup>1</sup>H-NMR (CDCl<sub>3</sub>-CD<sub>3</sub>OD)  $\delta$ : 0.72 (3H, s, 18-H<sub>3</sub>), 0.88 (3H, s, 19-H<sub>3</sub>), 5.70 (1H, m, 7-H), Anal. Calcd for C<sub>28</sub>H<sub>46</sub>O<sub>6</sub>: C, 70.26; H, 9.69. Found: C, 70.09; H, 9.81, and the more polar (22*R*,23*R*)-pentaol **22** (68 mg, 23%), mp 245—246 °C



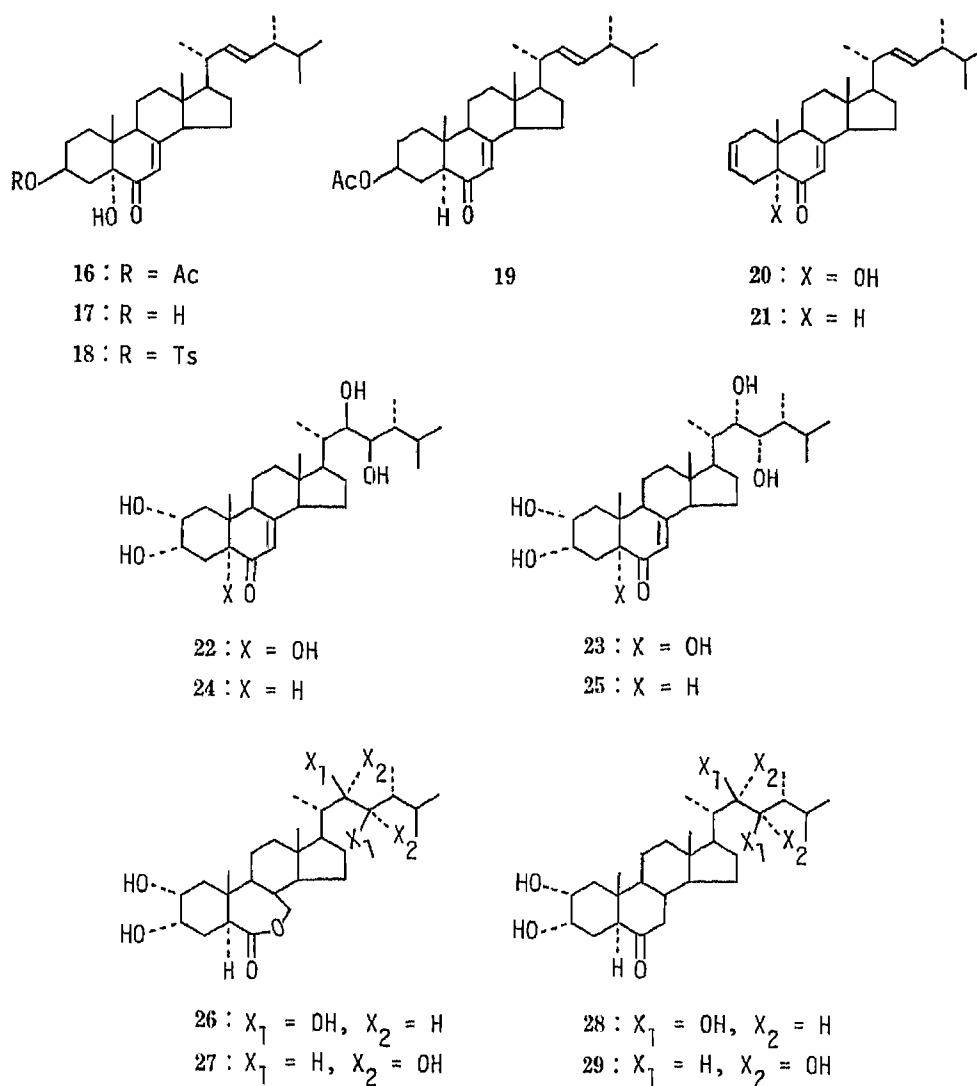


Fig. 2

(EtOAc), UV  $\lambda_{\text{max}}^{\text{EtOH}}$ : 248 nm ( $\epsilon$  11100),  $^1\text{H-NMR}$  ( $\text{CDCl}_3\text{-CD}_3\text{OD}$ )  $\delta$ : 0.71 (3H, s, 18- $\text{H}_3$ ), 0.87 (3H, s, 19- $\text{H}_3$ ), 5.68 (1H, m, 7-H), *Anal.* Calcd for  $\text{C}_{28}\text{H}_{46}\text{O}_6$ : C, 70.26; H, 9.69. Found: C, 70.12; H, 9.72.

**(22*R*,23*R*,24*R*)- and (22*S*,23*S*,24*R*)-2 $\alpha$ ,3 $\alpha$ ,22,23-Tetrahydroxy-5 $\alpha$ -ergost-7-en-6-one (24 and 25)**—The trienone 21 (201 mg, 0.509 mmol) was hydroxylated with osmium tetroxide, as described for 20, to give the less polar (22*S*,23*S*)-tetraol 25 (42 mg, 18%), amorphous solid, UV  $\lambda_{\text{max}}^{\text{EtOH}}$ : 244 nm ( $\epsilon$  11100),  $^1\text{H-NMR}$  ( $\text{CDCl}_3\text{-CD}_3\text{OD}$ )  $\delta$ : 0.71 (3H, s, 18- $\text{H}_3$ ), 5.82 (1H, m, 7-H), and the more polar (22*R*,23*R*)-tetraol 24 (40 mg, 17%), mp 250–251 °C (EtOAc), UV  $\lambda_{\text{max}}^{\text{EtOH}}$ : 244 nm ( $\epsilon$  11100),  $^1\text{H-NMR}$  ( $\text{CDCl}_3\text{-CD}_3\text{OD}$ )  $\delta$ : 0.72 (3H, s, 18- $\text{H}_3$ ), 5.82 (1H, m, 7-H). Gas chromatography-mass spectrometry (GC-MS) analysis of the bismethaneboronates<sup>7)</sup> of 24 and 25 was carried out; Shimadzu LKB 9000S; column, 1% OV-17 (3 mm i.d.  $\times$  1 m); column temp., 280 °C, carrier gas, helium; flow rate, 30 ml/min. The retention times of the bismethaneboronates of 24 and 25 were 17.0 and 15.5 min, respectively. Electron impact-mass spectra (EI-MS) of the bismethaneboronates of 24 and 25 were identical and were as follows;  $m/z$  510 ( $\text{M}^+$ , 23%), 495 (6), 468 (13), 450 (4), 439 (3), 411 (5), 397 (10), 367 (7), 356 (6), 355 (6), 327 (29), 301 (42), 285 (6), 233 (15), 155 (36), 95 (100), 85 (68), 71 (39), 43 (88).

It is well known that upon osmium tetroxide oxidation of a 5 $\alpha$ -2-ene steroid, the bulky osmium tetroxide approaches stereoselectively from the less hindered  $\alpha$ -face to afford the 2 $\alpha$ ,3 $\alpha$ -diol steroid.<sup>8)</sup> However, the stereochemical assignment of 22, 23, 24, and 25 at the C-22,23 position was only tentative, based on the mobilities on TLC. Many examples have been reported showing that (22*S*,23*S*)-brassinosteroids are less polar than their (22*R*,23*R*)-stereoisomers on normal-phase TLC.<sup>3e,f)</sup>

**Brassinosteroids**—The (22*R*,23*R*)-28-homobrassinosteroids 1–15 and the 24-epibrassinosteroids 26–29 were prepared as described in our previous papers.<sup>5,9)</sup>

**Rice-Lamina Inclination Test**—The bioassay was carried out according to the reported method<sup>3a)</sup> using

etiolated seedlings of rice (*Oryza sativa* L. cv Arborio J1).

### Results and Discussion

For the investigation of the importance of the A/B-ring functionalities of brassinosteroids, fifteen (22*R*,23*R*,24*S*)-28-homobrassinosteroids with modifications at rings A and B were synthesized as described in our previous paper.<sup>5)</sup> They have the same stereochemistry in the side chain that brassinolide has. The bioassay was carried out using the rice-lamina inclination test, which was originally developed as an auxin bioassay system and has recently been found to be a highly sensitive and specific bioassay for brassinosteroids.<sup>3a,4)</sup> The results are summarized in Table I. 28-Homobrassinolide (1), having the same activity as brassinolide in this bioassay,<sup>3a)</sup> was used as a standard compound and 28-homobrassinolide (1), giving *ca.* 140° bending angle between laminae and sheaths at 0.01 μg/ml, showed the strongest activity among the 28-homobrassinosteroids tested. The tetrahydroxy steroid 2 having a 3α,4α-diol moiety instead of 2α,3α-diol was slightly less active than 28-homobrassinolide (1), judging from the concentration giving *ca.* 140° bending angle. The 2-deoxy-3α-hydroxylactone 3

TABLE I. Activities of 28-Homobrassinosteroids in the Rice-Lamina Inclination Test

Concentration (μg/ml)	Compounds							
	1	2	3	4	5	6	7	8
10		180		180		180		180
1	180	163 ± 13	171 ± 15	149 ± 9	180	164 ± 23	180	165 ± 21
0.1	180	169 ± 11	128 ± 16	138 ± 19	127 ± 5	127 ± 5	173 ± 9	141 ± 12
0.01	142 ± 17	119 ± 17	120 ± 19	101 ± 11	114 ± 11	99 ± 3	144 ± 23	123 ± 15
0.001	129 ± 16	117 ± 9	120 ± 9	100 ± 11	97 ± 10	102 ± 18	126 ± 10	121 ± 12
Control	102 ± 16							

Concentration (μg/ml)	Compounds						
	9	10	11	12	13	14	15
10		180	144 ± 8	180	163 ± 15	180	180
1	180	138 ± 20	113 ± 15	180	140 ± 23	161 ± 13	154 ± 10
0.1	146 ± 11	103 ± 9	118 ± 11	117 ± 19	130 ± 13	120 ± 10	114 ± 12
0.01	118 ± 11	100 ± 13	109 ± 17	117 ± 18	110 ± 11	117 ± 11	124 ± 11
0.001	119 ± 14	94 ± 6	105 ± 9	109 ± 12	100 ± 14	117 ± 12	115 ± 15
Control	102 ± 16						

Concentration (μg/ml)	Compounds							
	26	27	28	29	22	23	24	25
10					135 ± 6	114 ± 10	180	144 ± 12
1	180		180	180	106 ± 7	101 ± 6	170 ± 11	110 ± 4
0.1	159 ± 5	180	175 ± 9	140 ± 18	109 ± 8	93 ± 2	136 ± 22	107 ± 7
0.01	139 ± 2	131 ± 2	146 ± 11	105 ± 10	98 ± 6		117 ± 12	
0.001	121 ± 12	100 ± 1	128 ± 7	104 ± 5				
Control	97 ± 5							

Values in the table are angles (in degrees) between the lamina and sheath (± standard error).

showed almost the same activity as its  $3\beta$ -isomer **4** and they were about one-tenth as active as the standard **1**, indicating that the hydroxyl group at  $2\alpha$ -position is not indispensable to elicit the biological activity, although its absence reduced the activity. It is of interest that the 3-ketolactone **5** and the 2,3-dideoxylactone **6** possessed *ca.* 5% of the activity of the native steroidal lactone **1**. Among the 6-oxo steroids, the 28-homologue **7** of castasterone induced the strongest response, the activity being almost equal to that of 28-homograssinolide (**1**). The  $3\alpha$ - and  $3\beta$ -hydroxy ketones **8** and **9** were equally active and were about one-tenth as active as the reference steroid **1**. These ketones have similar activity to the corresponding 7-oxalactones **3** and **4**. The 3-keto steroid **10** was *ca.* 10 times less active than the corresponding  $3\alpha$ - and  $3\beta$ -hydroxy steroids **8** and **9**. The activity of the 2,3-dideoxy ketone **11** was *ca.* 100 times less than that of the 2,3-dideoxylactone **6**, suggesting that the 7-oxalactone group plays a more important role in the plant growth-promoting activity than the 6-oxo group. In the case of 28-homocastasterone (**7**), it may bind to the receptor as effectively as 28-homobrassinolide (**1**) and may be rapidly metabolized to the corresponding lactone **1**, exhibiting high biological activity. The regioisomeric 6-oxalactone compounds **12** and **13** were found to be less active than the corresponding 7-oxalactones **1** and **2**, respectively, indicating that the 7-oxalactone group in the B-ring, as in brassinolide, cannot be replaced by the 6-oxalactone group. However, it is interest to note that the 2-deoxy 6-oxalactones **14** and **15** were almost as active as the 2-deoxy 7-oxalactone counterparts **3** and **4**, respectively.

The biological activity of the new 24-epibrassinosteroids **22**—**25** prepared in this paper was also evaluated by using the rice-lamina inclination test. The results are summarized in Table I, along with the biological results for 24-epibrassinolide (**26**), 24-epicastasterone (**28**), and their (22*S*,23*S*)-stereoisomers **27**, and **29**. 24-Epibrassinolide (**26**), giving *ca.* 140° bending angle at 0.01  $\mu\text{g/ml}$ , was several times more active than the (22*S*,23*S*)-lactone stereoisomer **27**. 24-Epicasterone (**28**) was found to be as highly active as 24-epibrassinolide (**26**), while its (22*S*,23*S*)-stereoisomer **29** was about ten times less active than the corresponding lactone **27**. These relations are in good agreement with our previous findings, in which a number of brassinosteroids with modified side chains were bioassayed by using the rice-lamina inclination test.<sup>3a)</sup>

It is of interest that the (22*R*,23*R*)-7-en-6-one compound **24**, which has an additional double bond at the C-7 position, gave *ca.* 140° bending angle at 0.1  $\mu\text{g/ml}$  and was estimated to be about ten times less active than 24-epicastasterone (**28**), because these two steroidal ketones could be considered to be almost identical in terms of steric and conformational factors. The (22*R*,23*R*)-5 $\alpha$ -hydroxyenone **22** was found to be *ca.* 10<sup>3</sup> times less active than the native 24-epicastasterone (**28**), judging from the concentration giving *ca.* 140° bending angle. The (22*S*,23*S*)-brassinosteroids **23** and **25** were weakly active and were less active than the corresponding (22*R*,23*R*)-stereoisomers **22** and **23**, respectively. These results showed that introduction of a double bond at the C-7 position and a hydroxyl group at the C-5 position markedly decreased the activity of brassinosteroids.

On the other hand, Yokota *et al.* have recently isolated 6-deoxocasterone, which lacks the 6-oxo functional group of castasterone, and they reported that it was *ca.* 100 times less active than castasterone in the rice-lamina inclination test.<sup>10)</sup> Our present results and the reported data lead us to conclude that the 7-oxalactone or 6-oxo functionality, as in brassinolide or castasterone, is allowed as a B-ring functionality of brassinosteroids for high plant growth-promoting activity, in addition to the presence of the  $2\alpha,3\alpha$ -diol in the A-ring and the A/B *trans* ring junction.

#### References and Notes

- 1) A part of this work was presented at the Symposium on Chemical Regulation of Plants, Nagoya, October 1983,

- p. 26.
- 2) a) T. Yokota, The 20th Symposium on Phytochemistry, Tokyo, January 1983, p. 68; b) N. Ikekawa and S. Takatsuto, *Mass Spectroscopy*, **32**, 55 (1984).
  - 3) a) S. Takatsuto, N. Yazawa, N. Ikekawa, T. Morishita, and H. Abe, *Phytochemistry*, **22**, 1393 (1983); b) S. Takatsuto, N. Yazawa, N. Ikekawa, T. Takematsu, T. Takeuchi, and M. Koguchi, *ibid.*, **22**, 2437 (1983); c) K. Wada, S. Marumo, K. Mori, S. Takatsuto, M. Morisaki, and N. Ikekawa, *Agric. Biol. Chem.*, **47**, 1139 (1983); d) S. Takatsuto, N. Yazawa, and N. Ikekawa, *Phytochemistry*, **23**, 525 (1984); e) M. J. Thompson, N. B. Mandava, W. J. Meudt, W. R. Lusby, and D. W. Spaulding, *Steroids*, **38**, 567 (1981); f) M. J. Thompson, W. J. Meudt, N. B. Mandava, S. R. Dutky, W. R. Lusby, and D. W. Spaulding, *ibid.*, **39**, 89 (1982).
  - 4) K. Wada and S. Marumo, *Agric. Biol. Chem.*, **45**, 2579 (1981).
  - 5) S. Takatsuto and N. Ikekawa, *J. Chem. Soc., Perkin Trans. 1*, **1984**, 439.
  - 6) D. H. R. Barton and C. H. Robinson, *J. Chem. Soc.*, **1954**, 3045.
  - 7) S. Takatsuto, B. Ying, M. Morisaki, and N. Ikekawa, *J. Chromatogr.*, **239**, 233 (1982).
  - 8) L. F. Fieser and M. Fieser, "Steroids," Reinhold, New York, 1959, p. 274.
  - 9) S. Takatsuto and N. Ikekawa, *Chem. Pharm. Bull.*, **32**, 2001 (1984).
  - 10) T. Yokota, M. Morita, and N. Takahashi, *Agric. Biol. Chem.*, **47**, 2149 (1983).

[Chem. Pharm. Bull.  
35(1) 217-220 (1987)]

**Tannins and Related Compounds. LI.<sup>1)</sup> Elucidation of the Stereochemistry of the Triphenoyl Moiety in Castalagin and Vescalagin, and Isolation of 1-O-Galloyl Castalagin from *Eugenia grandis***

GEN-ICHIRO NONAKA,<sup>a</sup> KANJI ISHIMARU,<sup>a</sup> MICHIO WATANABE,<sup>a</sup> ITSUO NISHIOKA,<sup>\*a</sup>  
TATSUO YAMAUCHI,<sup>b</sup> and ALFRED S. C. WAN<sup>c</sup>

*Faculty of Pharmaceutical Sciences, Kyushu University,<sup>a</sup> 3-1-1 Maidashi, Higashi-ku,  
Fukuoka 812, Japan, Faculty of Pharmaceutical Sciences, Fukuoka University,<sup>b</sup>  
Nanakuma Jonan-ku, Fukuoka 814-01, Japan, and Department of Pharmacy,  
Faculty of Science, National University of Singapore,<sup>c</sup>  
Lower Kent Ridge Road 0511, Singapore*

(Received July 26, 1986)

The chirality of the nonahydroxytriphenoyl group in castalagin (**1**) and vescalagin (**2**) was determined to be in the *S,S*-series on the basis of circular dichroism analysis. In addition, a new ellagitannin (**4**) has been isolated from the leaves of *Eugenia grandis* (Myrtaceae), and the structure was established to be 1-*O*-galloyl castalagin on the basis of chemical and spectroscopic evidence.

**Keywords**—castalagin; vescalagin; C-glycosidic ellagitannin; atropisomerism; absolute stereochemistry; nonahydroxytriphenoyl group; flavogallonic acid; *Eugenia grandis*; 1-*O*-galloyl castalagin

Castalagin (**1**) and vescalagin (**2**) are hydrolyzable tannins which were first isolated from the woods of the Fagaceous plants, *Castanea sativa* and *Quercus sesseliflora*,<sup>2)</sup> and have now been found to be distributed widely in the plant kingdom. Their structures were elucidated on the basis of hydrolytic studies combined with <sup>1</sup>H-nuclear magnetic resonance (<sup>1</sup>H-NMR) analysis as novel C-glycosidic ellagitannins possessing an open-chain glucose core and a unique nonahydroxytriphenoyl group in each molecule,<sup>3)</sup> although the atropisomerism of the triphenoyl moiety remains to be solved. Previously, we isolated from the leaves of *Terminalia catappa* (Combretaceae) a novel ellagitannin, terflavin A (**3**), which contains a similar triphenoyl (flavogallonyl) group in the molecule.<sup>4)</sup> During this work, the chirality of the flavogallonyl group was determined by circular dichroism (CD) analysis. Comparison of the CD data of the triphenoyl derivatives prepared individually from **1** and **3** has now established the atropisomerism of the triphenoyl group in **1**. This paper presents the results of these experiments. In addition, the isolation and characterization of a new ellagitannin (**4**) from the leaves of *Eugenia grandis* are described.

The model triphenoyl compound (**5**) of known absolute stereochemistry, as well as the accompanying optically inactive meso-type compound (**6**), was prepared by three-step methylation (involving hydrolysis) of **3** as shown in Chart 2. The molecular formula of **5** was confirmed by electron-impact mass spectrometry (EI-MS) ( $M^+$   $m/z$ : 674) and elemental analysis. The <sup>1</sup>H-NMR data were consistent with the structure **5**, showing a symmetrical signal pattern. Since the chirality of the flavogallonyl group in **3** had formerly been shown to be in the *S*-series,<sup>4)</sup> the symmetrical pattern of the molecule, coupled with the fact that **5** is optically active [ $-25.1^\circ$  (acetone)], indicated that **5** possesses the *S,S*-configuration.

On the other hand, the triphenoyl derivative (**7**) was obtained by drastic methylation of

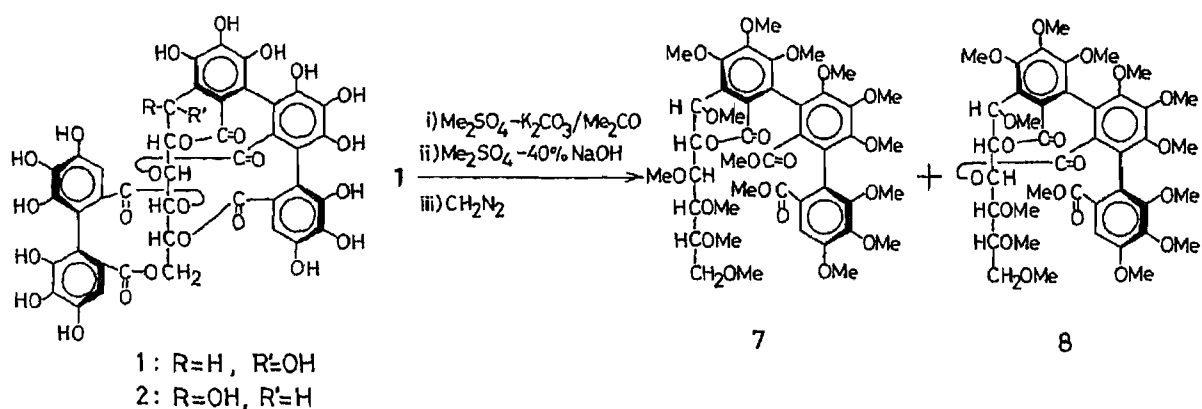


Chart 1

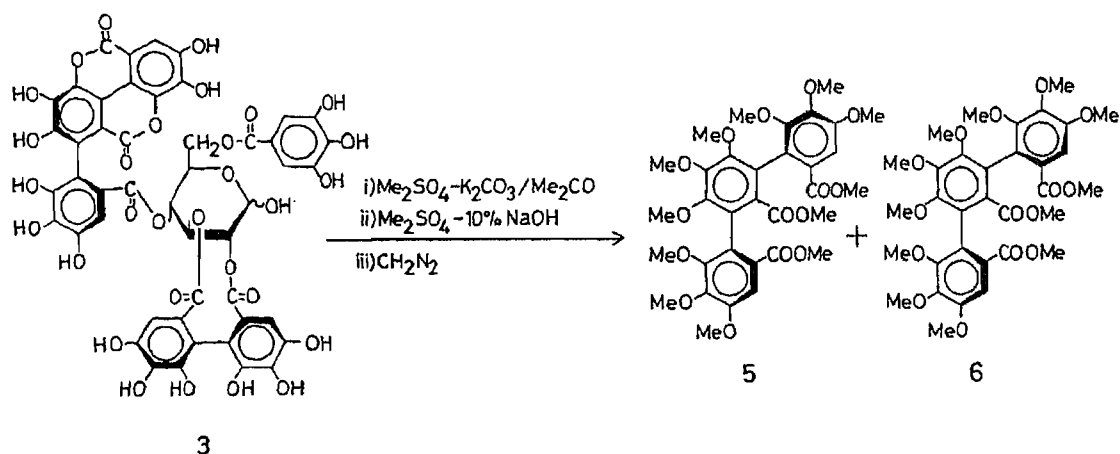


Chart 2

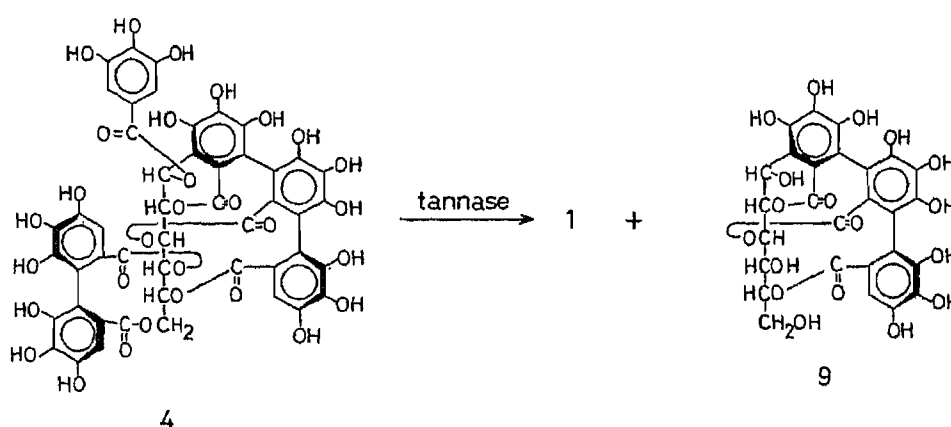


Chart 3

castalagin pentadecamethyl ether with dimethyl sulfate in a strongly alkaline medium, followed by diazomethane methylation. The field-desorption mass spectrum (FD-MS) and  $^1\text{H-NMR}$  data were consistent with the proposed structure. It should be noted that all attempts to cleave the remaining ester linkage (at the glucose C-2 position) were unsuccessful. The CD spectrum of 7 showed a strong negative couplet at 230 nm and a positive one at 252 nm, which were in agreement with those found in 5 (Fig. 1). Based on these observations, the atropisomerism of the triphenoyl group in 1 was concluded to be in the *S,S*-series. Since

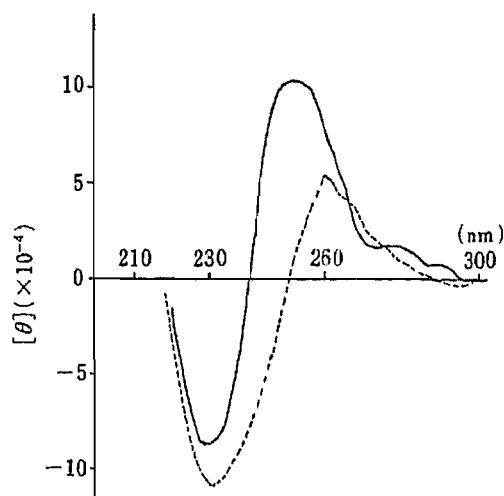


Fig. 1. CD Spectra of 5 and 7  
 -----, 5; ———, 7.

earlier work had demonstrated that **2** is obtainable from **1** upon heating in an aqueous solution (only epimerization at the glucose C-1 position takes place),<sup>3)</sup> the triphenoyl moiety in **2** is also shown to have the same *S,S*-configuration.

A new ellagitannin (**4**) was isolated, together with **2** and a large quantity of **1**, as colorless needles, mp 230 °C (dec.),  $[\alpha]_D^{20}$   $-105.0^\circ$  (MeOH), from the leaves of *Eugenia grandis* (Myrtaceae). The <sup>1</sup>H-NMR spectrum showed well-defined lowfield signals due to sugar protons, and their coupling pattern was closely related to that of **1**. Aromatic signals appeared at  $\delta$  6.57, 6.61 and 6.78 as one-proton singlets and at  $\delta$  7.12 as a two-proton singlet. The former three signals were assignable to the protons of hexahydroxydiphenoyl and nonahydroxytriphenoyl groups, and the latter to those of a galloyl group. These observations were supported by the results of negative fast atom bombardment mass spectrometry (FAB-MS) [(M-H)<sup>-</sup> *m/z*: 1085] and also by <sup>13</sup>C-nuclear magnetic resonance (<sup>13</sup>C-NMR) spectroscopy which showed the presence of six ester carbonyl groups. The presence of the above-mentioned odd aromatic one-proton singlets in the <sup>1</sup>H-NMR spectrum suggested that **4** is a C-glycosidic ellagitannin related to **1** and **2**.

The constitution was confirmed by enzymatic hydrolysis of **4** with tannase, which afforded **1** and gallic acid, together with a small amount of castalin (**9**).<sup>5)</sup> The notable lowfield shift ( $\delta$  6.82) of the glucose C-1 proton signal in the <sup>1</sup>H-NMR spectrum of **4** established the position of the galloyl group. Thus, **4** was characterized as 1-*O*-galloyl castalagin.

### Experimental

Details of the instruments and chromatographic conditions used in this work were essentially the same as described in the previous paper.<sup>6)</sup>

**Preparation of the Triphenoyl Compounds (5 and 6)**—A mixture of terflavin A heptadecamethyl ether<sup>4)</sup> (223 mg) and dimethyl sulfate (2 ml) in 10% NaOH was heated under reflux for 40 min. After cooling, the reaction mixture was acidified with 1N HCl and extracted with ether. The ether layer was washed with H<sub>2</sub>O and dried over Na<sub>2</sub>SO<sub>4</sub>. Evaporation of the solvent left a residue, which was treated with ethereal diazomethane for 10 min. After removal of the solvent by evaporation, the residue was chromatographed on a silica gel. Elution with benzene-acetone (97:3) yielded methyl trimethoxybenzoate as colorless prisms (MeOH) (32 mg), mp 81–82 °C, dimethyl (*S*)-hexamethoxydiphenoate as a colorless syrup (61 mg),  $[\alpha]_D^{20}$   $-27.3^\circ$  ( $c=1.0$ , CHCl<sub>3</sub>) and the trimethyl nonamethoxytriphenoates [**5** (17 mg) and **6** (13 mg)]. **5**: Colorless syrup,  $[\alpha]_D^{20}$   $-25.1^\circ$  ( $c=1.0$ , acetone). *Anal.* Calcd for C<sub>33</sub>H<sub>38</sub>O<sub>15</sub>: C, 58.75; H, 5.68. Found: C, 58.98; H, 5.83. EI-MS *m/z*: 674 (M<sup>+</sup>). UV  $\lambda_{\max}^{\text{MeOH}}$  nm: 293, 220. <sup>1</sup>H-NMR (CDCl<sub>3</sub>): 3.58, 3.68, 3.76, 3.88, 3.92, 3.96 (12 × OMe), 7.24 (2H, s, aromatic H). **6**: Colorless prisms, mp 130–132 °C (MeOH),  $[\alpha]_D^{20}$   $0^\circ$  ( $c=1.3$ , acetone). *Anal.* Calcd for C<sub>33</sub>H<sub>38</sub>O<sub>15</sub>: C, 58.75; H, 5.68. Found: C, 58.82; H, 5.66. EI-MS *m/z*: 674 (M<sup>+</sup>). <sup>1</sup>H-NMR (CDCl<sub>3</sub>): 3.62, 3.68, 3.78, 3.90, 3.92, 3.96 (12 × OMe), 7.24 (2H, s, aromatic H).

**Preparation of the Triphenoyl Compound (7)**—A mixture of castalagin pentadecamethyl ether<sup>3)</sup> (1.0 g) and

dimethyl sulfate (6 ml) in 40% NaOH (10 ml) was refluxed for 1 h. The reaction mixture was made acidic by adding 6N HCl, and extracted with ether. The ether layer was washed with H<sub>2</sub>O, dried over Na<sub>2</sub>SO<sub>4</sub> and concentrated to yield a pale brown residue, which was subjected to silica gel chromatography. Elution with benzene–acetone (9:1) afforded dimethyl (S)-hexamethoxydiphenoate (180 mg). Further elution with benzene–acetone (4:1) furnished the hexadecamethyl ether (7) (32 mg) and the tetradecamethyl ether (8) (120 mg). 7: A white amorphous powder,  $[\alpha]_D^{25} -46.0^\circ$  ( $c=0.7$ , acetone). *Anal.* Calcd for C<sub>43</sub>H<sub>56</sub>O<sub>20</sub>: C, 57.83; H, 6.32. Found: C, 57.44; H, 6.30. FD-MS *m/z*: 892 (M<sup>+</sup>). UV  $\lambda_{\text{max}}^{\text{MeOH}}$  nm: 297, 219. <sup>1</sup>H-NMR (CDCl<sub>3</sub>): 3.08, 3.20, 3.34, 3.46, 3.48, 3.64, 3.68, 3.72, 3.76, 3.86, 3.92 (16 × OMe), 5.28 (1H, d,  $J=4$  Hz, glc. 2-H), 7.36 (1H, s, aromatic H). 8: A white amorphous powder,  $[\alpha]_D^{25} +20.9^\circ$  ( $c=1.6$ , acetone). *Anal.* Calcd for C<sub>40</sub>H<sub>50</sub>O<sub>19</sub>: C, 57.54; H, 6.03. Found: C, 57.81; H, 5.85. FD-MS *m/z*: 846 (M<sup>+</sup>). UV  $\lambda_{\text{max}}^{\text{MeOH}}$  nm: 300, 218. <sup>1</sup>H-NMR (CDCl<sub>3</sub>): 3.16, 3.32, 3.46, 3.52, 3.60, 3.62, 3.68, 3.70, 3.74, 3.90, 3.92, 3.94, 3.96 (14 × OMe), 4.10–4.36 (3H, m, glc. 1-, 4- and 5-H), 4.90 (1H, br d,  $J=4$  Hz, glc. 3-H), 5.32 (1H, d,  $J=4$  Hz, glc. 2-H), 7.32 (1H, s, aromatic H).

**Isolation of the Ellagitannin (4)**—The air-dried leaves (2.3 kg) of *Eugenia grandis* (collected in Singapore) were extracted with 60% aqueous acetone at room temperature. The acetone was removed by evaporation under reduced pressure (*ca.* 40 °C) and the resulting precipitates, consisting mainly of chlorophylls and waxes, were removed by filtration. The filtrate was concentrated under reduced pressure, and applied to a column of Sephadex LH-20. Elution with H<sub>2</sub>O containing increasing amounts of MeOH furnished five fractions (I–V). Fraction III was subjected to rechromatography over Sephadex LH-20 with EtOH to yield castalagin (1) as colorless fine needles (H<sub>2</sub>O) (*ca.* 9 g). Fraction IV was chromatographed successively over Sephadex LH-20 (EtOH), MCI-gel CHP-20P (H<sub>2</sub>O–MeOH), Fuji-gel ODS-G3 (H<sub>2</sub>O–MeOH) and Bondapak C<sub>18</sub>/Porasil B (H<sub>2</sub>O–MeOH) to give vescalagin (2) as colorless fine needles (H<sub>2</sub>O) (0.5 g) and the ellagitannin (4) as colorless needles (H<sub>2</sub>O) (0.15 g). 4: mp 230 °C (*dec.*),  $[\alpha]_D^{25} -105.0^\circ$  ( $c=1.0$ , MeOH). *Anal.* Calcd for C<sub>48</sub>H<sub>30</sub>O<sub>30</sub> · 7H<sub>2</sub>O: C, 47.53; H, 3.82. Found: C, 47.33; H, 3.53. Negative FAB-MS *m/z*: 1085 (M–H)<sup>–</sup>, 915 (M–gallic acid)<sup>–</sup>. <sup>1</sup>H-NMR (acetone-*d*<sub>6</sub>): 4.03 (1H, d,  $J=12$  Hz, glc. 6-H), 4.87 (1H, dd,  $J=3, 12$  Hz, glc. 6-H), 5.19 (1H, s, glc. 3-H), 5.22 (1H, d,  $J=5$  Hz, glc. 4-H), 5.37 (1H, d,  $J=6$  Hz, glc. 2-H), 5.66 (1H, dd-like,  $J=3, 6$  Hz, glc. 5-H), 6.51, 6.61, 6.78 (each 1H, s, aromatic H), 6.82 (1H, d,  $J=6$  Hz, glc. 1-H), 7.12 (2H, s, galloyl H). <sup>13</sup>C-NMR (acetone-*d*<sub>6</sub>): 65.6 (t, glc. 6-C), 66.9, 67.9, 69.7, 71.1, 71.5 (each d, glc. C), 107.8, 108.3, 108.9 (each d, aromatic C), 110.5 (d, galloyl C), 163.6, 165.4, 165.6, 166.4, 166.9, 169.0 (–COO–).

**Enzymatic Hydrolysis of 4 with Tannase**—A solution of 4 (50 mg) in H<sub>2</sub>O was incubated with tannase at 37 °C for 2 h. Evaporation of the solvent afforded a gum, which was treated with EtOH. The EtOH-soluble portion was chromatographed over MCI-gel CHP-20P with H<sub>2</sub>O containing increasing amounts of MeOH to yield gallic acid, castalagin (1) (15 mg) and castalin (9) (5 mg).

**Acknowledgements** We are grateful to Mr. T. Tanaka, Sankyo Co., Ltd. for the provision of tannase. Thanks are also due to Mr. Y. Tanaka, Miss K. Soeda and Mr. R. Isobe for <sup>13</sup>C-NMR, <sup>1</sup>H-NMR and MS measurements, respectively. This work was supported in part by a Grant-in-Aid from the Ministry of Education, Science and Culture, Japan.

#### References and Notes

- 1) Part L: G. Nonaka, S. Morimoto, J. Kinjo, T. Nohara, and I. Nishioka, *Chem. Pharm. Bull.*, **35**, 149 (1987).
- 2) W. Mayer, W. Gabler, A. Riester, and H. Korger, *Ann. Chem.*, **707**, 177 (1967).
- 3) W. Mayer, H. Seitz, and J. C. Jochims, *Ann. Chem.*, **721**, 186 (1969); W. Mayer, H. Seitz, J. C. Jochims, K. Schauerer, and G. Schilling, *ibid.*, **751**, 60 (1971).
- 4) T. Tanaka, G. Nonaka, and I. Nishioka, *Chem. Pharm. Bull.*, **34**, 1039 (1986).
- 5) W. Mayer, A. Einwiller, and J. C. Jochims, *Ann. Chem.*, **707**, 182 (1967).
- 6) T. Tanaka, G. Nonaka, and I. Nishioka, *Chem. Pharm. Bull.*, **34**, 650 (1986).



[Chem. Pharm. Bull.  
35(1) 221-228 (1987)]

## Syntheses and Antitumor Activities of 1*R*,2*R*-Cyclohexanediamine Pt(II) Complexes Containing Dicarboxylates

MASAHIDE NOJI,<sup>\*a</sup> KENJIRO SUZUKI,<sup>b</sup> TAZUKO TASHIRO,<sup>c</sup> MAKOTO SUZUKI,<sup>d</sup>  
KEN-ICHI HARADA,<sup>d</sup> KATSUYOSHI MASUDA<sup>d</sup> and YOSHINORI KIDANI<sup>a</sup>

Faculty of Pharmaceutical Sciences, Nagoya City University,<sup>a</sup> 3-1 Tanabe-dori, Mizuho-ku,  
Nagoya 467, Japan, Department of Pharmacy, Tokai Teishin Hospital,<sup>b</sup> 2-17-5  
Matsubara-cho, Naka-ku, Nagoya 460, Japan, Division of Experimental  
Chemotherapy, Cancer Chemotherapy Center,<sup>c</sup> 1-37-1 Kami-  
Ikebukuro, Toshima-ku, Tokyo 170, Japan and Faculty  
of Pharmacy, Meijo University,<sup>d</sup> Yagoto,  
Tempaku-ku, Nagoya 468, Japan

(Received May 13, 1986)

New 1*R*,2*R*-cyclohexanediamine(=1*R*,2*R*-dach) Pt(II) complexes containing dicarboxylate ions, *i.e.*, ketomalonate, malate, saccharate, glutarate, diphenate, and  $\alpha,\beta$ -diphenylsuccinate were synthesized and tested against leukemia L1210 *in vivo*. All of the dicarboxylato Pt(II) complexes showed relatively high antitumor activities with T/C% values of more than 200 at optimal doses. In particular, mucato and  $\alpha,\beta$ -diphenylsuccinato Pt(II) complexes exhibited excellent antitumor activities with T/C% values of 348 and 369, respectively, with 3 cured mice out of six.

The dicarboxylato Pt(II) complexes were determined by elemental analyses to contain dicarboxylates : Pt : 1*R*,2*R*-dach in a ratio of 1 : 1 : 1. The molecular secondary ion mass spectra of saccharato and glutarate Pt(II) complexes indicate that these complexes exist in a binuclear form together with a mononuclear form in aqueous solution.

**Keywords**—dicarboxylato Pt(II) complex; 1*R*,2*R*-cyclohexanediamine Pt(II) complex; mass spectrum; binuclear complex; antitumor activity

*cis*-Diamminedichloroplatinum(II) (cisplatin) has been used clinically as an antitumor agent effective against testicular, ovarian, and bladder cancers, although it causes severe renal toxicity, nausea and vomiting.<sup>1)</sup> Recently, much effort has been devoted to developing more antitumor-active Pt complexes with less toxicity. New antitumor Pt complexes, diammine(1,1-cyclobutanedicarboxylato)platinum(II)<sup>2)</sup> and *cis*-dichloro-*trans*-dihydroxobis(isopropylamine)platinum(IV),<sup>3)</sup> are now under clinical trial.

We have reported that Pt(II) complexes containing 1*R*,2*R*-cyclohexanediamine (=1*R*,2*R*-dach) showed the highest antitumor activity against leukemia L1210 and P 388 among Pt(II) complexes containing 1*S*,2*S*- or 1*R*,2*S*-dach as a carrier ligand.<sup>4,5)</sup> We have introduced D-glucuronate and D-gluconate as leaving groups into dach Pt(II) complexes in order to increase the water-solubility, since antitumor dach Pt(II) complexes containing chloride, oxalate, or malonate ions are difficult to dissolve in water. These water-soluble Pt(II) complexes showed remarkable antitumor activity against leukemia L1210 *in vivo*, but they are relatively unstable in water.<sup>4,6,7)</sup>

Thus, we have designed more water-stable Pt(II) complexes by introducing dicarboxylates as leaving groups. The dicarboxylates adopted were ketomalonate, malate, saccharate and glutarate anions. Such compounds were expected to show moderate water-solubility. Diphenate and  $\alpha,\beta$ -diphenylsuccinate anions were also used as leaving groups, and were expected to provide lipo-solubility.

In this paper, syntheses and antitumor activities of the dicarboxylato Pt(II) complexes of

1*R*,2*R*-dach are described and the structures of these compounds are discussed on the basis of the infrared IR and molecular secondary ion mass (SIMS) spectral data.

### Experimental

#### Syntheses of Pt(II) Complexes

**Ketomalonato- or Saccharato(1*R*,2*R*-dach)platinum(II); [Pt(ketomal)(1*R*,2*R*-dach)] or [Pt(sac)(1*R*,2*R*-dach)]**—Pt(NO<sub>3</sub>)<sub>2</sub>(1*R*,2*R*-dach) (1.0 g) was dissolved in 10 ml of H<sub>2</sub>O by heating, then an equimolar amount of ketomalonic acid monohydrate (0.31 g) or potassium hydrogen saccharate (0.57 g) dissolved in 10 ml of H<sub>2</sub>O was added. The resultant solution was filtered and the pH of the filtrate was adjusted to 5 with a 5% NaOH solution. After several days at room temperature, white precipitates deposited were collected by filtration, and washed with H<sub>2</sub>O and EtOH.

**Mucato(1*R*,2*R*-dach)platinum(II); [Pt(muc)(1*R*,2*R*-dach)]**—Pt(NO<sub>3</sub>)<sub>2</sub>(1*R*,2*R*-dach) (1.0 g) was dissolved in 10 ml of H<sub>2</sub>O by heating, then an equimolar amount of mucic acid (0.49 g) dissolved in 10 ml of H<sub>2</sub>O with a minimum amount of a 5% NaOH solution was added. The pH of the resultant solution was adjusted to 5 with a 5% NaOH solution. After 4 d of standing at room temperature, white precipitates gradually deposited and they were collected by filtration and washed with H<sub>2</sub>O and EtOH.

**Malato- or Glutarato(1*R*,2*R*-dach)platinum(II); [Pt(mala)(1*R*,2*R*-dach)] or [Pt(glut)(1*R*,2*R*-dach)]**—Pt(NO<sub>3</sub>)<sub>2</sub>(1*R*,2*R*-dach) (1.0 g) was dissolved in 10 ml of H<sub>2</sub>O by heating, then 2 eq of malic acid (0.62 g) or glutaric acid (0.61 g) dissolved in 15 ml of H<sub>2</sub>O was added. The resultant solution was adjusted to pH 5 with a 5% NaOH solution, and after 2 weeks at room temperature, white precipitates gradually deposited and were collected by filtration. They were washed with H<sub>2</sub>O and EtOH.

**Diphenato- or  $\alpha,\beta$ -Diphenylsuccinato(1*R*,2*R*-dach)platinum(II); [Pt(diphen)(1*R*,2*R*-dach)] or [Pt(diphsuc)(1*R*,2*R*-dach)]**—One gram of Pt(NO<sub>3</sub>)<sub>2</sub>(1*R*,2*R*-dach) was dissolved in 10 ml of H<sub>2</sub>O by heating. An equimolar amount of diphenic acid (0.56 g) or diphenylsuccinic acid (0.62 g) was dissolved in 100 ml of H<sub>2</sub>O by the addition of a 5% NaOH solution under pH 7. These solutions were mixed and the pH of the resultant solution was adjusted to ca. 7. After standing overnight at room temperature, white precipitates were collected by filtration.

All Pt(II) complexes thus synthesized were dried under reduced pressure at 60°C. The results of elemental analyses are shown in Table I together with the yields.

#### Measurements

The solubilities of the dicarboxylato Pt(II) complexes in H<sub>2</sub>O were measured by suspending them in 5 ml of H<sub>2</sub>O with constant agitation at 37°C. After incubation for 2 d, the suspensions were filtered and the Pt contents of the filtrates were determined with a Shimadzu AA-607G flameless atomic absorption spectrometer.

**MS spectrometry**—SIMS spectrometry was performed using a double focusing Hitachi M-80 B mass spectrometer fitted with a high-field magnet (M-8089), SIMS source and M-0101 data system. Operating conditions were; primary ion, Xe<sup>+</sup>; accelerating voltage, 8 kV (primary) and 3 kV (secondary); source temperature, 35°C. Samples were dissolved in H<sub>2</sub>O in the concentration range of 0.9–3.4 mg/ml. Each sample solution (0.5–1  $\mu$ l) was loaded on a silver target. About 1  $\mu$ l of matrix material was added to the sample on the target. Calibration was achieved by using glycerol-derived oligomers. Linked-field scanning was performed in the B/E mode with a Hitachi linked-scan unit (M-8084).

TABLE I. Elemental Analyses of 1*R*,2*R*-Cyclohexanediamine Pt(II) Complexes Containing Dicarboxylates

Complexes	Found (%)			Calcd (%)			Yield (%)
	C	H	N	C	H	N	
Pt(ketomalonato)(dach)·4H <sub>2</sub> O	21.93	4.32	5.92	21.73	4.46	5.63	30
Pt( <i>dl</i> -malto)(dach)·3H <sub>2</sub> O	24.12	4.76	5.61	24.24	4.88	5.65	50
Pt( <i>d</i> -malato)(dach)·3H <sub>2</sub> O	24.09	4.77	5.40	24.24	4.88	5.65	60
Pt( <i>l</i> -malato)(dach)·2.5H <sub>2</sub> O	24.52	4.76	5.94	24.70	4.77	5.77	50
Pt(glutarato)(dach)·2H <sub>2</sub> O	27.76	4.69	6.04	27.78	5.09	5.89	21
Pt(saccharato)(dach)·H <sub>2</sub> O	26.95	4.60	5.15	26.92	4.52	5.23	67
Pt(mucato)(dach)·3H <sub>2</sub> O	25.10	4.81	5.03	25.22	4.94	4.90	58
Pt(diphenato)(dach)·3H <sub>2</sub> O	39.88	4.36	4.94	39.80	4.68	4.64	30
Pt( $\alpha,\beta$ -diphenylsuccinato)(dach)·3H <sub>2</sub> O	41.96	4.81	4.72	41.84	5.11	4.43	48

dach = 1*R*,2*R*-cyclohexanediamine.

### Evaluation of Antitumor Activity

Antitumor activities of the Pt(II) complexes were tested according to the protocols for routine screening at the National Cancer Institute (Bethesda, Md.). L1210 cells ( $10^5$ ) were transplanted intraperitoneally into CDF<sub>1</sub> mice (each group consisted of 6 mice) on day 0, and the samples were given intraperitoneally on days 1, 5, and 9. From the mean survival times (d) of treated (T) and control (C) mice, T/C% values were calculated. Samples with T/C% values that exceeded 125 were evaluated as antitumor-active. A dose at which the T/C% value was less than 85% was designated as a toxic dose.

### Results and Discussion

Judging from the elemental analyses shown in Table I, these dicarboxylato Pt(II) complexes were composed of the dicarboxylates, 1*R*,2*R*-cyclohexanediamine (= 1*R*,2*R*-dach), and Pt(II) in a ratio of 1:1:1. Based upon the infrared spectral data shown in Table II, the dicarboxylates and dach coordinated through the carboxyl and amino groups, respectively. For example, the IR spectrum of Pt(sac)(1*R*,2*R*-dach) exhibited absorption peaks at 3200 and 3100  $\text{cm}^{-1}$  due to the asymmetric and symmetric stretching frequencies of the amino groups, being shifted toward higher frequencies compared with those of the hydrogen chloride salt of 1*R*,2*R*-dach. Two strong peaks at 1610 and 1340  $\text{cm}^{-1}$  were assigned to asymmetric and symmetric stretching frequencies of the carboxyl groups, respectively, being shifted toward the lower frequency side due to the coordination to the central metal ions, compared with those of saccharic acid.

Other dicarboxylato Pt(II) complexes showed IR spectral behavior similar to that of Pt(sac)(1*R*,2*R*-dach), exhibiting coordination of the carboxyl and amino groups.

### Solubility of the Dicarboxylato Pt(II) Complexes in Water

Expecting water-solubility, we had chosen saccharic and mucic acids, which have four hydroxyl groups, as leaving groups, but in fact the solubilities of the complexes in H<sub>2</sub>O were rather poor (3.38 and 2.58 mg/ml at 37°C, respectively, as shown in Table III).

However, the glutarato Pt(II) complex has a solubility of 2.91 mg/ml in H<sub>2</sub>O, indicating that the water-solubility is not proportional to the numbers of hydroxyl groups.

The diphenato and  $\alpha,\beta$ -diphenylsuccinato (mixture of *meso* and *racemic* forms) Pt(II) complexes were hardly soluble in either H<sub>2</sub>O or organic solvents such as chloroform benzene, and ethanol.

TABLE II. Vibrational Frequencies of Dicarboxylato Pt(II) Complexes of 1*R*,2*R*-Cyclohexanediamine ( $\text{cm}^{-1}$ )

Complexes	$\nu_{\text{OH}}$	$\nu_{\text{NH}}$	$\nu_{\text{CH}}$	$\nu_{\text{C=O}}$	$\nu_{\text{C-O}}$
Pt(ketomalonato)(dach)	3400 (s, br)	3200 (s) 3100 (s)	2920 (m) 2850 (w)	1610 (s)	1350 (s)
Pt(malato)(dach)	3400 (s, br)	3200 (s, br)	2920 (m) 2850 (w)	1600 (s)	1370 (s)
Pt(glutarato)(dach)	3400 (s, br)	3200 (s) 3100 (s)	2920 (m) 2850 (w)	1600 (s)	1350 (s)
Pt(saccharato)(dach)	3400 (s, br)	3200 (s) 3100 (s)	2920 (m) 2850 (w)	1610 (s)	1340 (s)
Pt(mucato)(dach)	3400 (s, br)	3200 (s) 3100 (s)	2920 (m) 2850 (w)	1610 (s)	1340 (s)
Pt(diphenato)(dach)	3400 (s, br)	3200 (s) 3100 (s)	2920 (m) 2850 (w)	1600 (s)	1350 (s)
Pt( $\alpha,\beta$ -diphenylsuccinato)(dach)	3400 (s, br)	3250 (s)	2920 (m) 2850 (w)	1600 (s)	1340 (s)

Abbreviations: s, m, w, and br mean strong, medium, weak, and broad.

TABLE III. Solubilities of Dicarboxylato Pt(II) Complexes in H<sub>2</sub>O (37 °C)

Complexes	Solubility (mg/ml)
Pt(ketomalonato)(dach)	2.7
Pt( <i>l</i> -malato)(dach)	0.9
Pt(glutarato)(dach)	2.9
Pt(saccharato)(dach)	3.4
Pt(mucato)(dach)	2.6
Pt(diphenato)(dach)	0.1
Pt( $\alpha,\beta$ -diphenylsuccinato)(dach)	0.2

TABLE IV. Antitumor Activities of Dicarboxylato Pt(II) Complexes of 1*R,2R*-Cyclohexanediamine against Leukemia L1210

Complexes	Dose (mg/kg)					
	100	50	25	12.5	6.25	3.12
	T/C%					
Pt(ketomalonato)(dach)	0	0	<u>229</u> (2)			
Pt( <i>d</i> -malato)(dach)		<u>177</u> (1)	<u>236</u> (1)	<u>250</u> (1)		
Pt( <i>d</i> -malato)(dach)		78 <sup>a)</sup>	<u>293</u> (1)	<u>210</u>		
Pt( <i>l</i> -malato)(dach)		<u>193</u> (1)	<u>273</u> (1)	<u>214</u>		
Pt(glutarato)(dach)		<u>238</u> (1)	<u>176</u>	<u>172</u>		
Pt(saccharato)(dach)	<u>134</u> <sup>a)</sup>	<u>231</u> (2)	<u>302</u> (1)	<u>210</u> (1)	<u>134</u>	<u>118</u>
Pt(mucato)(dach)	<u>112</u> <sup>a)</sup>	<u>348</u> (3)	<u>247</u>	<u>240</u>	<u>148</u>	<u>132</u>
Pt(diphenato)(dach)		<u>238</u> (1)	<u>208</u> (2)	<u>133</u>		
Pt( $\alpha,\beta$ -diphenylsuccinato)(dach)		<u>176</u>	<u>369</u> (3)	<u>145</u>		
Pt(1,1-cyclobutanedicarboxylato)(dach)			<u>235</u>	<u>177</u>	<u>125</u>	

Underlined figures indicate significant antitumor activity (T/C%  $\geq$  125). <sup>a)</sup> Indicates toxicity. 10<sup>5</sup> cells/mouse were transplanted i.p. into CDF<sub>1</sub> mice (6 mice/group), and the test samples were administered i.p. on days 1, 5 and 9.

### Antitumor Activity

The antitumor activities of the dicarboxylato Pt(II) complexes of 1*R,2R*-dach were tested against leukemia L1210, and the results are shown in Table IV, together with those of 1,1-cyclobutanedicarboxylato(1*R,2R*-cyclohexanediamine)platinum(II). All of the Pt(II) complexes exhibited relatively high antitumor activities as compared with cisplatin, with T/C% values of more than 200 at the optimal doses. The optical isomers of malic acids as leaving groups did not show much difference as far as antitumor activities were concerned, but Pt(*d*-malato)(1*R,2R*-dach) showed toxicity at the dose of 50 mg/kg, while *l*-malato Pt(II) did not. However, mucato and saccharato are diastereomers and their Pt(II) complexes showed different antitumor activities with T/C% values of 348 and 302 at the optimal doses, respectively.

Among the dicarboxylato Pt(II) complexes examined,  $\alpha,\beta$ -diphenylsuccinato Pt(II) complex showed the highest antitumor activity against L1210 with a T/C% value of 369, and gave three cured mice out of six.

### MS Spectra by Molecular SIMS Method

The dicarboxylato Pt(II) complexes were suspended in H<sub>2</sub>O and continuously stirred overnight at room temperature. The suspensions were filtered, portions of the filtrates were mixed well with glycerol, and the mixtures were introduced to a MS spectrometer as samples. Among 7 dicarboxylato Pt(II) complexes examined, only 3 complexes, *i.e.*, saccharato,

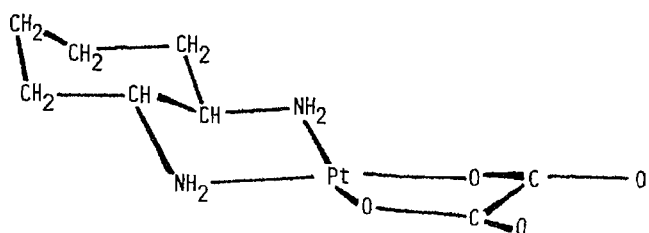


Fig. 1. Structure of  $[Pt(ox)(1R,2R-dach)]$  Determined by X-Ray Anomalous Scattering Techniques

TABLE V. MS Spectral Data for Dicarboxylato Pt(II) Complexes of 1R,2R-Cyclohexanediamine

Complexes	$m/z$ values and relative ion abundances (%)		
	$[PtLC_1C_2]^+$	$[Pt_2LC_3C_1]^+$	$[Pt_2L_2C_1C_2]^+$
Pt(ox)(1R,2R-dach)	401 (24)	707 (0.6)	797 (0.4)
	399 (79)	706 (0.7)	796 (0.5)
	398 (100)	705 (0.8)	795 (0.5)
	397 (82)	704 (0.7)	794 (0.4)
		703 (0.4)	793 (0.2)
Pt( <i>l</i> -mala)(1R,2R-dach)	443 (130)	751 (7)	
	442 (100)	750 (14)	
	441 (120)	749 (17)	
		748 (11)	
Pt(sac)(1R,2R-dach)	519 (67)	827 (28)	1037 (30)
	518 (100)	826 (31)	1036 (31)
	517 (80)	825 (45)	1035 (60)
		824 (31)	1034 (43)
		823 (12)	1033 (18)
Pt(glut)(1R,2R-dach)	441 (94)	749 (13)	881 (9)
	440 (100)	748 (13)	880 (11)
	439 (100)	747 (12)	879 (11)
		746 (4)	878 (8)
		745 (3)	877 (5)

L denotes dicarboxylate anions.  $C_1$  represents neutral 1R,2R-dach ( $C_6H_{14}N_2$ ).  $C_2$  denotes protonated 1R,2R-dach ( $C_6H_{15}N_2$ ).  $C_3$  denotes deprotonated 1R,2R-dach ( $C_6H_{13}N_2$ ). Numbers in parentheses indicate ion abundances in per cent, taking mononuclear ions containing  $^{195}Pt$  as a standard.

glutarato, and malato Pt(II) exhibited MS spectra. The other complexes did not show the spectra due to their low solubilities in  $H_2O$ .

### Pt(oxalato)(1R,2R-dach)

As a standard sample, Pt(ox)(1R,2R-dach)(ox = oxalate) was taken since it is stable in an aqueous solution. Its absolute structure was determined by X-ray diffraction analyses to be square planar and monomeric, as shown in Fig. 1.<sup>8)</sup> Pt(ox)(1R,2R-dach) exhibited MS spectrum with 4 peaks at  $m/z$  values of 401, 399, 398, and 397; such a pattern is expected for a complex containing naturally abundant Pt isotopes, i.e.,  $^{198}Pt$  (7.2%),  $^{196}Pt$  (25.2%),  $^{195}Pt$  (33.8%) and  $^{194}Pt$  (32.9%). These peaks were assigned to the molecular ion of  $[Pt(ox)(1R,2R-dachH)]^+$  (dachH denotes protonated dach). The peaks due to the less abundant Pt isotopes, i.e.,  $^{190}Pt$  (0.01%) and  $^{191}Pt$  (0.8%), were not observed in the spectrum.

In addition, the oxalato complex showed two groups of peaks around  $m/z$  values of 705 and 795 with very low intensities, each of which consists of 5 peaks. Their patterns were characteristic of binuclear Pt complexes. Since the solubility of the complex in  $H_2O$  was limited, the peaks due to the less abundant Pt isotopes, i.e.,  $^{190}Pt$ ,  $^{191}Pt$ , and  $^{198}Pt$  were not observed. These peaks may be assigned to binuclear complexes, where an oxalate ion bridges two Pt ions through the carboxyl groups. The mass number of  $[^{195}Pt_2(ox)_2(1R,2R-dach)-$

$[1R,2R\text{-dachH}]^+$  is 795 and that of  $[^{195}\text{Pt}_2(\text{ox})(1R,2R\text{-dach})(1R,2R\text{-dach-H})]^+$  (dach-H denotes deprotonated dach) is 705. These binuclear Pt complexes may be formed by recombinations of fragments, judging from their extremely low intensities.

The MS spectral data of oxalato Pt(II) complex are summarized in Table V, together with those of other dicarboxylato Pt(II) complexes; relative peak intensities are expressed in per cent taking the corresponding mononuclear species containing  $^{195}\text{Pt}$  as a standard.

### Pt(sac)(1R,2R-dach)

In contrast to the oxalato Pt(II) complex, Pt(sac)(1R,2R-dach) gave a somewhat different MS spectrum as shown in Fig. 2. Three peaks were observed at  $m/z$  values of 517, 518, and 519, which may be assignable to mononuclear  $[\text{Pt}(\text{sac})(1R,2R\text{-dach})(1R,2R\text{-dachH})]^+$  containing  $^{194}\text{Pt}$ ,  $^{195}\text{Pt}$ , and  $^{196}\text{Pt}$  isotopes, respectively. In the higher mass region, two groups of peaks each consisting of five peaks were also observed around  $m/z$  values of 1035 and 825 with high relative intensities, and these may be assignable to binuclear Pt complexes. The peaks at  $m/z$  values of 1033, 1034, 1035, 1036, 1037 correspond to  $[\text{Pt}_2(\text{sac})_2(1R,2R\text{-dach})(1R,2R\text{-dachH})]^+$  and the peaks at  $m/z$  values of 823, 824, 825, 826, and 827 are assignable to  $[\text{Pt}_2(\text{sac})(1R,2R\text{-dach})(1R,2R\text{-dach-H})]^+$ , which may be formed by cleavage of a saccharate ion from the former complex. In both binuclear complexes, saccharate ions bridge two different Pt ions.

Fragmentation of a binuclear complex, *i.e.*,  $[\text{Pt}_2(\text{sac})_2(1R,2R\text{-dach})(1R,2R\text{-dachH})]^+$ , may occur as shown in Fig. 3, where a saccharate anion was cleaved first with resultant

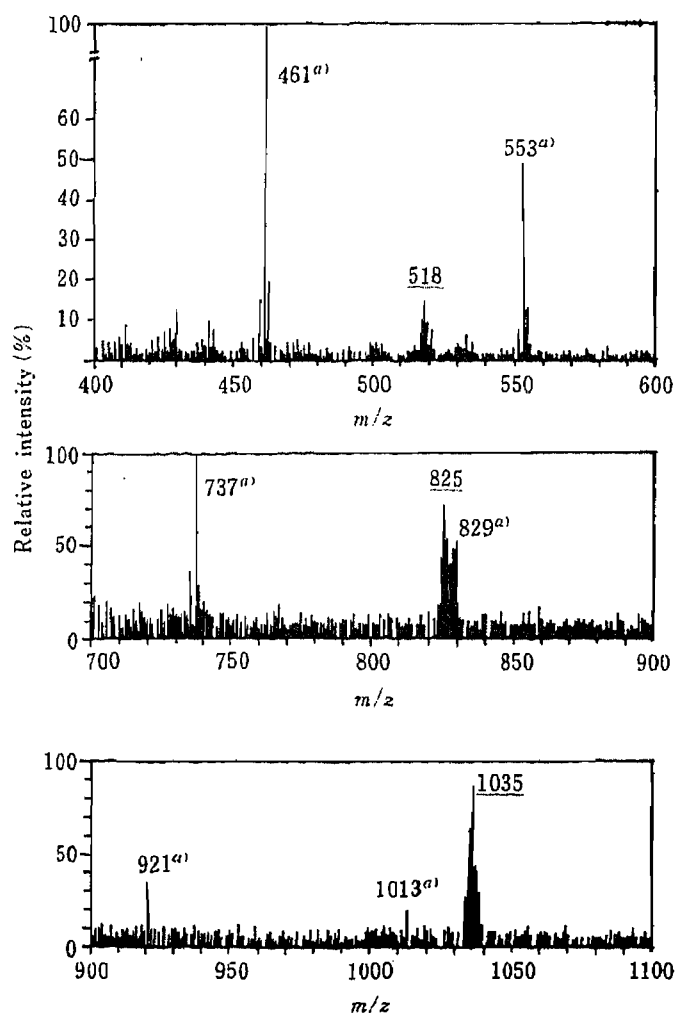


Fig. 2. MS Spectrum of Pt(sac)(1R,2R-dach) Complex Obtained by the Molecular SIMS Method

Figures with *a*) indicate peaks due to background glycerol. Underlined figures denote the most intense peaks due to the dacharato Pt(II) complex.

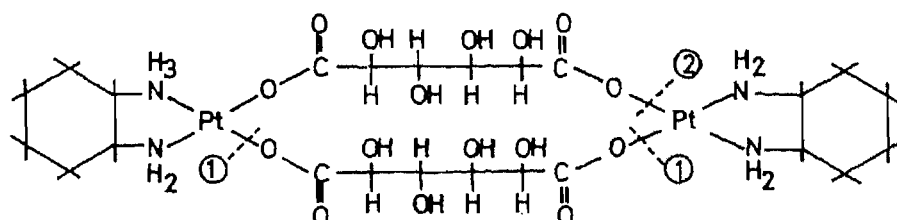
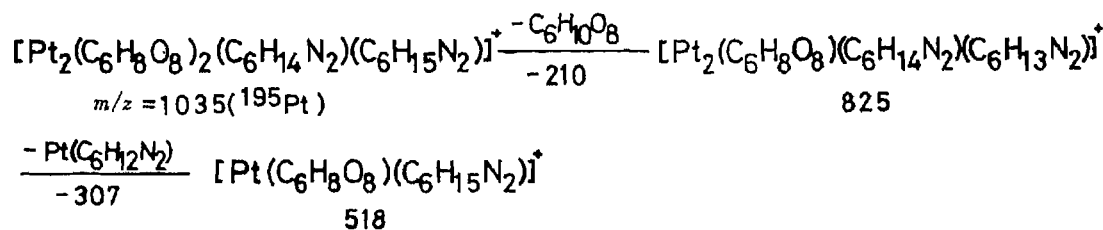


Fig. 3. Proposed Fragmentation of Pt(sac)(1*R*,2*R*-dach) Complex and the Positions of Bond Breakages

formation of  $[\text{Pt}_2(\text{sac})(1*R*,2*R*\text{-dach})(1*R*,2*R*\text{-dach-H})]^+$ . The latter ion was decomposed into the mononuclear  $[\text{Pt}(\text{sac})(1*R*,2*R*\text{-dachH})]^+$  with further dissociation of a sac ion. However, there is a possibility that the binuclear complex dissociates into  $[\text{Pt}_2(\text{sac})(1*R*,2*R*\text{-dach})_2]$  and  $[\text{Pt}(\text{sac})(1*R*,2*R*\text{-dach})]$  in a dilute aqueous solution, and these complexes are expected to show MS spectra similar to that illustrated in Fig. 2. In reality, both processes may contribute to the observed MS spectrum.

At this stage we can not distinguish whether the solid saccharato Pt(II) complex exists as a binuclear form or a mixture of mono- and binuclear forms, since in both cases similar spectra will be obtained. However, considering its low solubility in  $\text{H}_2\text{O}$  and the very slow formation of its precipitates in the process of synthesis, we speculate that saccharato Pt(II) complex exists as a binuclear form.

#### Pt(glut)(1*R*,2*R*-dach)

Glutarato Pt(II) complex exhibited a MS spectrum similar to that of saccharato Pt(II) complex, except that the peak intensities around  $m/z$  values of 879 and 747 (originated from the binuclear glutarato Pt(II) complexes) were lower than those of saccharato complex. Moreover, the peak intensities of  $[\text{Pt}_2(\text{glut})(1*R*,2*R*\text{-dach})(1*R*,2*R*\text{-dach-H})]^+$  were less than those of  $[\text{Pt}_2(\text{glut})_2(1*R*,2*R*\text{-dach})(1*R*,2*R*\text{-dachH})]^+$ , indicating a lower abundance of the former complex in an aqueous solution. The most intense peaks were observed at  $m/z$  values of 439, 440, and 441, which were assigned to the mononuclear  $[\text{Pt}(\text{glut})(1*R*,2*R*\text{-dachH})]^+$  ions.

#### Pt(*l*-mala)(1*R*,2*R*-dach)

In the case of the *l*-malato Pt(II) complex, its MS spectrum lacked the expected peaks at  $m/z$  values around 883, which may be assignable to binuclear species, *i.e.*,  $[\text{Pt}_2(\textit{l}\text{-mala})_2(1*R*,2*R*\text{-dach})(1*R*,2*R*\text{-dachH})]^+$ , but only exhibited four peaks around  $m/z$  values of 749, which may originate from  $[\text{Pt}_2(\textit{l}\text{-mala})(1*R*,2*R*\text{-dach})(1*R*,2*R*\text{-dach-H})]^+$ . The mononuclear species showed three peaks at  $m/z$  values of 441, 442, and 443, whose intensities were not proportional to the natural abundances of Pt isotopes; this may be due to over-lapping background peaks.

These SIMS spectral data give very important information as to the species existing in aqueous solutions. In the case of saccharato Pt(II) complex, the binuclear species is relatively abundant in an aqueous solution (comparable to the mononuclear species). From the MS spectral data we could not confirm whether the saccharato Pt(II) complex exists as a

mononuclear or binuclear species in the solid state, but in an aqueous solution it may coexist in three states, *i.e.*,  $[\text{Pt}_2(\text{sac})_2(1R,2R\text{-dach})_2]$ ,  $[\text{Pt}_2(\text{sac})(1R,2R\text{-dach})_2]$ , and  $[\text{Pt}(\text{sac})(1R,2R\text{-dach})]$ , of which the last species is the most stable. The *l*-malato Pt(II) complex did not exist in the form of  $[\text{Pt}_2(l\text{-mala})_2(1R,2R\text{-dach})_2]$ , which may be unstable in an aqueous solution and may dissociate mainly into  $[\text{Pt}(l\text{-mala})(1R,2R\text{-dach})]$  and partly into  $[\text{Pt}_2(l\text{-mala})(1R,2R\text{-dach})_2]$ . These SIMS spectral data offer valuable information as to the species of the dicarboxylato Pt(II) complexes existing in aqueous solutions, and may help to identify the antitumor-active Pt(II) species.

**Acknowledgements** This work was supported in part by Grants-in-Aid from the Ministry of Health and Welfare of Japan. We are also grateful to Tanaka Kikinzoku Kogyo K. K. for financial support.

#### References

- 1) A. W. Prestayko, S. T. Crooke and S. K. Carter (eds.), "Cisplatin," Academic Press, Inc., New York, 1980.
- 2) a) C. Sessa, F. Cavalli, S. Kaye, A. Howell, W. T. B. Huinink, T. Wagener, H. Pinedo and J. Vermorken, *Proc. Am. Soc. Clin. Oncol.*, **4**, 116 (1985); b) V. H. C. Bramwell, D. Crowther, S. O'Malley, R. Swindell, R. Johnson, E. H. Cooper, N. Thatcher and A. Howell, *Cancer Treat. Rep.*, **69**, 409 (1985); c) W. S. F. Wong, V. R. Tindall, J. Wagstaff, V. Bramwell and D. Crowther, *J. R. Soc. Med.*, **78**, 203 (1985).
- 3) a) A. H. Calvert, S. J. Harland, D. R. Newell, Z. H. Siddik, A. C. Jones, T. J. McElwain, S. Raju, E. Wiltshaw, I. E. Smith, J. M. Baker, M. J. Peckham and K. R. Harrap, *Cancer Chemother. Pharmacol.*, **9**, 140 (1982); b) G. A. Curt, J. J. Grygiel, B. J. Corden, R. F. Ozols, R. B. Weiss, D. T. Tell, C. E. Myers and J. M. Collins, *Cancer Res.*, **43**, 4470 (1983); c) M. J. Egorin, D. A. Van Echo, M. Y. Whitacre, E. A. Olman and J. Aisner, *Proc. Am. Soc. Clin. Oncol.*, **2**, 28 (1983); d) B. D. Evans, K. S. Raju, A. H. Calvert, S. J. Harland and E. Wiltshaw, *Cancer Treat. Rep.*, **67**, 997 (1984); e) S. Kaplan, R. Joss, C. Sessa, A. Goldhirsch, M. Cattaneo and F. Cavalli, *Proc. Am. Assoc. Cancer Res.*, **24**, 132 (1983); f) J. M. Koeller, R. H. Earhart, T. E. Davis, D. L. Trump and D. C. Tormey, *ibid.*, **24**, 162 (1983).
- 4) Y. Kidani, M. Noji and T. Tashiro, *Gann*, **71**, 637 (1980).
- 5) M. Noji, K. Okamoto, Y. Kidani and T. Tashiro, *J. Med. Chem.*, **24**, 508 (1981).
- 6) M. Noji, K. Achiwa, A. Kondo and Y. Kidani, *Chem. Lett.*, **1982**, 1757.
- 7) Y. Kidani, K. Achiwa, H. Ono, K. Tomatsu, K. Zaikokuji, M. Noji and T. Tashiro, *J. Clin. Oncol. Hematol.*, **15**, 35 (1985).
- 8) M. A. Bruck, R. Bau, M. Noji, K. Inagaki and Y. Kidani, *Inorg. Chim. Acta*, **92**, 279 (1984).



[Chem. Pharm. Bull.  
35(1) 229-234 (1987)]

## Constituent of Pollen. XIII.<sup>1)</sup> Constituents of *Cedrus deodara* LOUD. (2)

TAICHI OHMOTO,\* KEFKO KANATANI (née INAGAKI),  
and KYOKO YAMAGUCHI

School of Pharmaceutical Sciences, Toho University,  
Funabashi, Chiba 274, Japan

(Received May 30, 1986)

From the pollen grains of *Cedrus deodara* LOUD., five known compounds, dehydroabietic acid (I), 15-hydroxydehydroabietic acid (II), 7 $\alpha$ ,18-dihydroxydehydroabietanol (IV), naringenin (VI) and  $\beta$ -sitosteryl  $\beta$ -D-glucoside (VII), and two new compounds, 7 $\beta$ ,15-dihydroxydehydroabietic acid (III) and hexadecane-1,16-diol 7-caffeoyl ester (V), were isolated. The structures of III and V were elucidated on the basis of spectroscopic studies and chemical evidence.

**Keywords**—*Cedrus deodara*; Pinaceae; pollen grains; 7 $\beta$ ,15-dihydroxydehydroabietic acid; hexadecane-1,16-diol 7-caffeoyl ester

As a part of our continuing studies on pollen grains, this paper deals with the chemical constituents of the pollen grains of *Cedrus deodara* LOUD. (Himarayasugi in Japanese). *Cedrus deodara* LOUD. is an evergreen monoecious tree of the family Pinaceae, which is distributed in the southernmost states and in the tropics. The constituents so far isolated from the wood are centdarol,<sup>2)</sup> isocentdarol,<sup>3)</sup> himachalol and allohimachalol,<sup>4)</sup> and from the stem-bark, deodarin<sup>5)</sup> and its 4'-glucoside. In part VI of this series,<sup>6)</sup> we reported the isolation of several amino acids, hydrocarbons, campesterol,  $\beta$ -sitosterol, *d*-pinitol, and others.

The pollen grains of *Cedrus deodara* LOUD. were extracted with ether and fractionated into acidic, phenolic and neutral fractions. Column chromatography of the acidic fraction resulted in the isolation of compounds I–III. Two of them were identical with the known diterpenoids, dehydroabietic acid (I)<sup>7)</sup> and 15-hydroxydehydroabietic acid (II),<sup>8)</sup> on the basis of infrared (IR) and proton nuclear magnetic resonance (<sup>1</sup>H-NMR) data. The phenolic fraction, on column chromatography, yielded compound V. The neutral fraction, on column chromatography, furnished 7 $\alpha$ ,18-dihydroxydehydroabietanol (IV). The methanol extract of the pollen grains which had been extracted with ether was subjected to column chromatography to give naringenin (VI) and  $\beta$ -sitosteryl  $\beta$ -D-glucoside (VII).

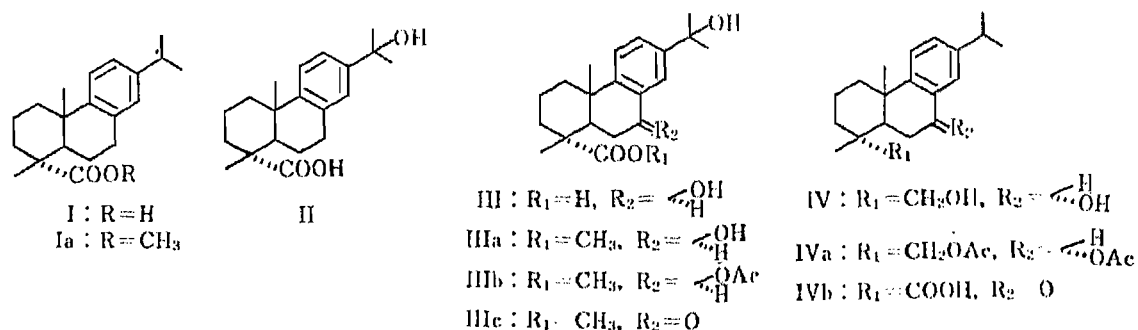


Fig. 1

TABLE I.  $^{13}\text{C}$ -NMR Chemical Shifts of Ia, II, III and IIIa

Carbon No.	Ia <sup>a)</sup>	II <sup>b)</sup>	III <sup>c)</sup>	IIIa <sup>d)</sup>
1	38.0	38.5	39.4	38.0
2	18.6	18.2	19.5	18.4
3	36.7	37.1	37.8	36.5
4	47.7	47.4	47.4	47.3
5	44.9	45.3	45.0	43.5
6	21.7	22.1	33.4	32.7
7	30.0	30.5	72.9	70.5
8	134.7	136.2	138.8	137.7
9	146.9	148.2	148.7	147.6
10	37.0	37.3	38.7	37.6
11	124.1	124.2	124.9	124.0
12	123.9	122.9	124.9	123.4
13	145.7	147.7	148.1	146.9
14	126.9	125.7	124.9	128.4
15	33.5	71.3	71.3	72.5
16	24.0	32.5	31.9	31.6
17	24.0	32.5	31.9	31.6
18	179.1	180.8	182.2	178.8
19	16.5	17.0	17.0	16.5
20	25.1	25.2	25.8	25.5
-OCH <sub>3</sub>	51.9			52.1

a) Run at 100 MHz in  $\text{CDCl}_3$  solution. b) Run at 100 MHz in  $\text{C}_5\text{D}_5\text{N}$  solution. c) Run at 100 MHz in  $\text{CD}_3\text{OD}$  solution.

Compound III was obtained as colorless needles, mp 166–168 °C, and had the composition  $\text{C}_{20}\text{H}_{28}\text{O}_4$  on the basis of the high-resolution mass spectrum (MS) ( $\text{M}^+$ ,  $m/z$  332.2022). The ultraviolet (UV) spectrum showed absorption maxima at 216, 266 and 274 nm. The IR spectrum showed hydroxyl ( $3400\text{ cm}^{-1}$ ) and carbonyl group ( $1700\text{ cm}^{-1}$ ) absorptions. The carbon-13 nuclear magnetic resonance ( $^{13}\text{C}$ -NMR) spectrum of III showed a pattern similar to that of II, except for C-6 to C-8 (Table I). Detailed examination of these data suggested that III might be a dehydroabiatic acid derivative possessing two hydroxyl groups. On methylation with diazomethane, III gave a monomethylester (IIIa) as colorless needles, mp 90–92 °C. The acetylation of IIIa yielded a monoacetate (IIIb) as a white powder, mp 91–93 °C, whose IR spectrum showed an absorption due to a tertiary hydroxyl group ( $3500\text{ cm}^{-1}$ ). From this result and the diagnostic MS fragment ion peaks at  $m/z$  59 and 43, the presence of a hydroxyisopropyl group was established. Oxidation of IIIa with chromium trioxide in pyridine afforded a colorless oil (IIIc), which showed a bathochromic shift to 296 from 274 nm due to a newly formed conjugated carbonyl, indicating that the secondary hydroxyl group was located at C-7. The  $\beta$ -configuration of the hydroxyl group at C-7 was determined from the  $^1\text{H}$ -NMR spectrum, in which a 1H triplet at  $\delta$  4.72 ( $J=8.5\text{ Hz}$ ) due to a hydroxymethine proton was observed<sup>9)</sup> (Table II). From the above results, III was identified as  $7\beta$ , 15-dihydroxydehydroabiatic acid.

Compound IV was obtained as colorless needles, mp 89 °C, and had the composition  $\text{C}_{20}\text{H}_{30}\text{O}_2$  on the basis of the high-resolution MS ( $\text{M}^+$ ,  $m/z$  302.2246). Comparison of the spectral data of IV with those of III indicated that both compounds possess the same skeleton. The  $^1\text{H}$ -NMR spectrum of IV also exhibited signals due to a carbinol proton. Spectral data of the diacetate (IVa) suggested that IV was dehydroabietane, having primary and secondary hydroxyl groups. Oxidation of IV with chromium trioxide in pyridine afforded a monoketone (IVb), whose UV spectrum showed absorption maxima at 216, 252, and 298 nm. The

TABLE II. <sup>1</sup>H-NMR Spectral Data for Compounds I—III and IIIa (ppm) (*J* in Hz)

Proton No.	I <sup>a)</sup>	II <sup>b)</sup>	III <sup>b)</sup>	IIIa <sup>b)</sup>
7	2.94 (2H, t, <i>J</i> =3)	2.93 (2H, m)	4.72 (1H, t, <i>J</i> =8.5)	4.75 (1H, t, <i>J</i> =8.5)
11	7.16 (1H, d, <i>J</i> =9)		7.16 (1H, d, <i>J</i> =9)	7.18 (1H, d, <i>J</i> =9)
12	6.94 (1H, dd, <i>J</i> =2, 9)	7.24 (1H × 3, d, <i>J</i> =7.5)	7.31 (1H, dd, <i>J</i> =2, 9)	7.35 (1H, dd, <i>J</i> =2, 9)
14	6.88 (1H, d, <i>J</i> =2)		7.59 (1H, d, <i>J</i> =2)	7.62 (1H, d, <i>J</i> =2)
16	1.26 (3H × 2, d, <i>J</i> =2)	1.53 (3H × 2, s)	1.48 (3H × 2, s)	1.51 (3H × 2, s)
17				
19	1.21 (3H, s)	1.30 (3H, s)	1.26 (3H × 2, s)	1.30 (3H × 2, s)
20	1.18 (3H, s)	1.23 (3H, s)		
-OCH <sub>3</sub>				3.68 (3H, s)

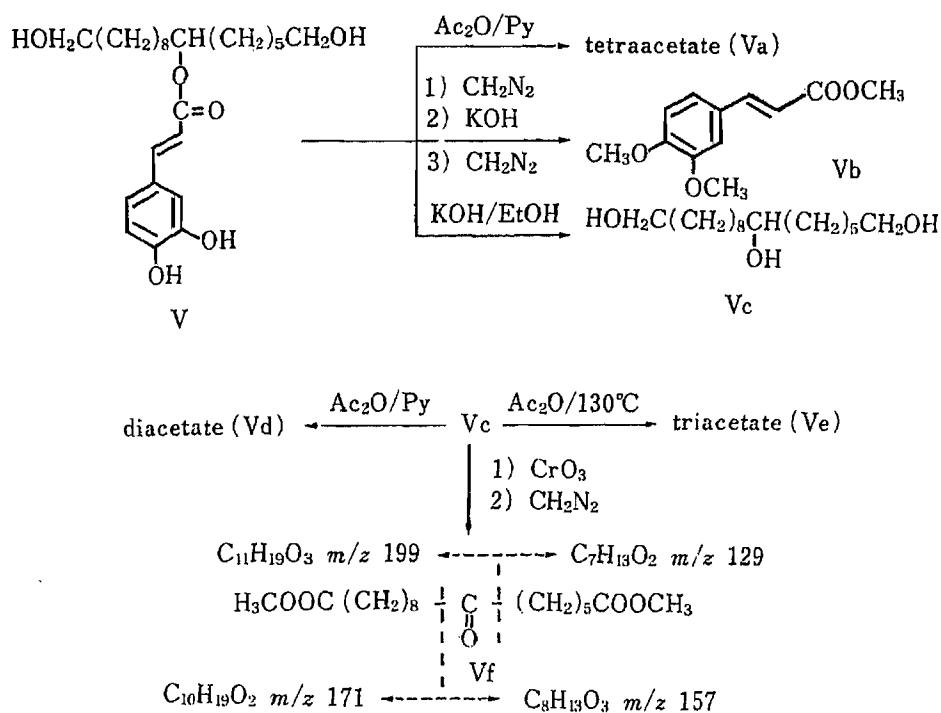
a) Run at 90 MHz in CDCl<sub>3</sub> solution. b) Run at 90 MHz in CD<sub>3</sub>OD solution.

secondary hydroxyl group was located at C-7, and its  $\alpha$ -configuration was indicated by the <sup>1</sup>H-NMR spectrum,<sup>10)</sup> based on the observation of the hydroxymethine proton signal at  $\delta$  4.61 (1H, br s,  $W_{1/2}$  = 7 Hz). Thus IV was identified as 7 $\alpha$ , 18-dihydroxydehydroabietanol. Compound IV is known as a synthetic intermediate,<sup>11)</sup> but this is the first time that IV has been isolated from a natural source.

Compound V was obtained as a yellow oil, which was positive in the FeCl<sub>3</sub> reaction. The UV spectrum showed absorption maxima at 220, 238, 246, 316 and 334 nm. The IR spectrum showed hydroxyl (3320 cm<sup>-1</sup>) and ester (1690, 1260 cm<sup>-1</sup>) absorptions. The <sup>1</sup>H-NMR spectrum showed a broad singlet at  $\delta$  1.30 due to the methylenes, a triplet at  $\delta$  3.53 (2H × 2, *J* = 6 Hz) due to the primary alcohols, and a triplet at  $\delta$  4.98 (1H, *J* = 7 Hz) due to the methine bearing the ester group, as well as signals due to the 1,2,4-trisubstituted benzene protons at  $\delta$  6.86 (1H, d, *J* = 9 Hz), 7.01 (1H, dd, *J* = 2, 9 Hz) and 7.06 (1H, d, *J* = 2 Hz), and two 1 H doublets at  $\delta$  6.25 (*J* = 16 Hz) and 7.54 (*J* = 16 Hz) due to *trans* olefinic protons. The acetylation of V yielded a tetraacetate (Va). Thus, V was deduced to be an ester of caffeic acid with a secondary hydroxyl group of an aliphatic triol. Compound V was methylated with diazomethane and then hydrolyzed with alkali. Subsequent methylation yielded Vb, which was identified as 3,4-dimethoxycaffeic acid methyl ester by comparison with an authentic sample on gas liquid chromatography (GLC). Alkaline hydrolysis of V gave an alcohol (Vc), which was acetylated by the usual method at room temperature to give a diacetate (Vd). On heating with acetic anhydride at 130 °C, Vc gave a triacetate (Ve). Compound Vc was oxygenated with chromium trioxide and then methylated with diazomethane to give Vf, whose MS showed characteristic peaks at *m/z* 129, 157, 171 and 199, as shown in Chart 1. These results indicated that caffeic acid might be linked by an ester bond to C-7 of Vc. Therefore, V was determined to be hexadecane-1,16-diol 7-caffeoyl ester.

Compounds VI and VII were identified as naringenin and  $\beta$ -sitosteryl  $\beta$ -D-glucoside by direct comparison of the IR spectra with those of corresponding authentic samples,<sup>12,13)</sup> and by mixed melting point determination.

In conclusion, seven compounds (I—VII) were isolated from the pollen grains of *Cedrus deodara*. In comparison with the constituents of other parts of the tree, it is interesting that



diterpenes of dehydroabietane type were isolated from the pollen grains, whereas the sesquiterpenes have been mainly reported from wood and stem-bark.

### Experimental

All melting points were determined on a Yanagimoto micro melting point apparatus and are uncorrected. The UV and IR spectra were recorded with Hitachi 139 and Hitachi 295 spectrophotometers, respectively. The field desorption mass spectra (FD-MS) and MS were run on JEOL JMS-01-SG-2 and JEOL JMS-D-300 mass spectrometers, respectively. The  $^1\text{H}$ - and  $^{13}\text{C}$ -NMR spectra were measured with Hitachi R-900 and JEOL GX-400 spectrometers. Chemical shifts are expressed in  $\delta$  (ppm) downfield from tetramethylsilane as an internal standard, and coupling constants in Hz. Optical rotations were measured with a JASCO DIP-4 digital polarimeter. GLC was carried out on a Hitachi 063 gas liquid chromatograph using a stainless steel column (3 mm  $\times$  1 m) packed with 2% SE-30 and 10% SE-30 on Chromosorb-W (60–80 mesh) with  $\text{N}_2$  carrier gas at a flow rate of 30 ml/min. Alumina (Wako, 300 mesh) and silica gel (Wako, C-200) were used for column chromatography. Thin layer chromatography (TLC) was performed on precoated silica gel plates (Merck, silica gel), which were generally developed with  $\text{CHCl}_3$ -AcOEt (1:4, v/v) for IV,  $\text{CHCl}_3$ -MeOH (9:1, v/v) for I, II, VI and VII,  $\text{CHCl}_3$ -MeOH (7:1, v/v) for III and  $\text{CHCl}_3$ -MeOH (5:1, v/v) for V. The spots were detected by spraying of 5%  $\text{FeCl}_3$  or 10%  $\text{H}_2\text{SO}_4$  followed by heating.

**Extraction and Fractionation of Components**—Pollen grains (4090 g) of *Cedrus deodara* collected in November, 1979 and 1980, at Toho University, were extracted with ether in a Soxhlet apparatus for 27 h, then the residue was extracted with hot MeOH. The ether extract (686 g) was dissolved in ether and shaken with 5%  $\text{NaHCO}_3$ , 5%  $\text{Na}_2\text{CO}_3$  and 5% NaOH successively.

**Isolation of I–III**—The 5%  $\text{Na}_2\text{CO}_3$  extract was acidified with dil. HCl and extracted with ether. The ether extract was dried over  $\text{Na}_2\text{SO}_4$ , and the ether was evaporated off. The residue (172 g) was chromatographed on silica gel (200 g, upper layer) and alumina (500 g, bottom layer). The column was eluted successively with hexane, benzene,  $\text{CHCl}_3$  and MeOH. The fraction (7.6 g) eluted with hexane–benzene (1:1) was rechromatographed on silica gel with hexane–benzene (1:1) to give I (2.1 g). The fraction (6 g) eluted with  $\text{CHCl}_3$ -MeOH (99:1) was subjected to rechromatography on silica gel with benzene- $\text{CHCl}_3$  (7:3) and  $\text{CHCl}_3$  to give II (210 mg) and III (110 mg).

**Dehydroabietic Acid (I)**—I was recrystallized from ether and MeOH to give colorless needles, mp  $174^\circ\text{C}$ .  $[\alpha]_D^{20} + 66^\circ$  ( $c=0.60$ , EtOH). High-resolution MS  $m/z$ : Calcd for  $\text{C}_{20}\text{H}_{28}\text{O}_2$ : 300.2082. Found: 300.2049. UV  $\lambda_{\text{max}}^{\text{EtOH}}$  nm: 218, 243, 252, 270, 278. IR  $\nu_{\text{max}}^{\text{KBr}}$   $\text{cm}^{-1}$ : 3400, 1695, 1492, 1275, 878, 814. MS  $m/z$ : 300 ( $\text{M}^+$ , 39), 286 (23), 285 (100), 240 (12), 197 (20), 47 (10).  $^1\text{H}$ -NMR: Table I.

**Methylation of I**—I was dissolved in MeOH and methylated with diazomethane for 14 h. After removal of the

solvent, the residue was recrystallized from benzene to give colorless needles (Ia). mp 61—61.5 °C. IR  $\nu_{\max}^{\text{KBr}} \text{cm}^{-1}$ : 1750, 1490, 1244, 884, 818. MS  $m/z$ : 314 ( $M^+$ , 22), 299 (17), 239 (100), 197 (32).  $^1\text{H-NMR}$  ( $\text{CDCl}_3$ )  $\delta$ : 1.21 (3H, s), 1.23 (3H, s), 1.27 (3H  $\times$  2, d,  $J=2$  Hz), 2.93 (2H, t,  $J=3$  Hz), 3.66 (3H, s), 6.88 (1H, d,  $J=2$  Hz), 6.99 (1H, dd,  $J=2, 9$  Hz), 7.18 (1H, d,  $J=9$  Hz).  $^{13}\text{C-NMR}$ : Table II.

**15-Hydroxydehydroabietic Acid (II)**—II was recrystallized from acetone to give colorless needles. mp 191—192 °C.  $[\alpha]_D^{20} + 57.6^\circ$  ( $c=1.04$ , MeOH). High-resolution MS  $m/z$ : Calcd for  $\text{C}_{20}\text{H}_{28}\text{O}_3$ : 316.2038. Found: 316.2020. UV  $\lambda_{\max}^{\text{EtOH}}$  nm: 216, 268, 276. IR  $\nu_{\max}^{\text{KBr}} \text{cm}^{-1}$ : 3420, 1690, 1490, 878, 820. MS  $m/z$ : 316 ( $M^+$ , 29), 301 (100), 255 (24), 197 (41), 131 (25), 59 (35), 43 (67).  $^1\text{H-}$  and  $^{13}\text{C-NMR}$ : Tables I and II.

**7 $\beta$ ,15-Dihydroxydehydroabietic Acid (III)**—III was recrystallized from benzene- $\text{CHCl}_3$  (1:1) to give colorless needles. mp 166—168 °C.  $[\alpha]_D^{20} + 24.1^\circ$  ( $c=0.28$ , EtOH). High-resolution MS  $m/z$ : Calcd for  $\text{C}_{20}\text{H}_{28}\text{O}_4$ : 332.2022. Found: 332.1988. UV  $\lambda_{\max}^{\text{EtOH}}$  nm: 216, 266, 274. IR  $\nu_{\max}^{\text{KBr}} \text{cm}^{-1}$ : 3400, 1700, 1500, 880, 830. MS  $m/z$ : 332 ( $M^+$ , 19), 317 (100), 314 (32), 235 (28), 195 (32), 59 (24), 43 (51).  $^1\text{H-}$  and  $^{13}\text{C-NMR}$ : Tables I and II.

**Methylation of III**—III (30 mg) was dissolved in MeOH and methylated with diazomethane for 14 h. After removal of the solvent, the residue was recrystallized from benzene to give colorless needles (IIIa, 28 mg). mp 90—92 °C.  $[\alpha]_D^{20} + 57.5^\circ$  ( $c=0.11$ , MeOH). High-resolution MS  $m/z$ : Calcd for  $\text{C}_{21}\text{H}_{30}\text{O}_4$ : 346.2144. Found: 346.2170. UV  $\lambda_{\max}^{\text{EtOH}}$  nm: 216, 268, 276. IR  $\nu_{\max}^{\text{KBr}} \text{cm}^{-1}$ : 3350, 1720, 1490, 1250, 890, 820. MS  $m/z$ : 346 ( $M^+$ , 29), 332 (35), 331 (100), 328 (32), 253 (41), 195 (20), 59 (27), 43 (49).  $^1\text{H-}$  and  $^{13}\text{C-NMR}$ : Tables I and II.

**Acetylation of 7 $\beta$ ,15-Dihydroxydehydroabietic Acid Methyl Ester (IIIa)**—IIIa (20 mg) was acetylated with  $\text{Ac}_2\text{O}$  (1 ml) in pyridine (1 ml) at room temperature for 10 h. The product (21 mg) was recrystallized from hexane and  $\text{CHCl}_3$  to give the monoacetate (IIIb) as a white powder. mp 91—93 °C. IR  $\nu_{\max}^{\text{KBr}} \text{cm}^{-1}$ : 3500, 1720, 1240.  $^1\text{H-NMR}$  ( $\text{CDCl}_3$ )  $\delta$ : 1.28 (3H, s, H-20), 1.30 (3H, s, H-19), 1.55 (3H  $\times$  2, s, H-16, H-17), 2.13 (3H, s, -OAc), 3.69 (3H, s, -OCH<sub>3</sub>), 6.07 (1H, t,  $J=8.5$  Hz, H-7), 7.23 (1H, d,  $J=9$  Hz, H-11), 7.30 (1H, d,  $J=2$  Hz, H-14), 7.36 (1H, dd,  $J=2, 9$  Hz, H-12).

**Oxidation of IIIa**—IIIa (8 mg) was dissolved in pyridine (0.5 ml) and allowed to stand with  $\text{CrO}_3$ -pyridine (27 mg in 1 ml) overnight at room temperature, then poured into aq. MeOH. The product gave IIIc (7 mg) as a colorless oil. UV  $\lambda_{\max}^{\text{EtOH}}$  nm: 216, 250, 296. IR  $\nu_{\max}^{\text{liq.}} \text{cm}^{-1}$ : 3450, 1720, 1680, 1250. MS  $m/z$ : 344 ( $M^+$ , 13), 330 (28), 329 (100), 269 (20), 59 (11), 43 (29).  $^1\text{H-NMR}$  ( $\text{CDCl}_3$ )  $\delta$ : 1.28 (3H, s, H-20), 1.35 (3H, s, H-19), 1.59 (3H  $\times$  2, s, H-16, H-17), 3.66 (3H, s, -OCH<sub>3</sub>), 7.36 (1H, d,  $J=9$  Hz, H-11), 7.74 (1H, dd,  $J=2, 9$  Hz, H-12), 8.06 (1H, d,  $J=2$  Hz, H-14).

**Isolation of IV**—The ether layer was washed with water, dried over  $\text{Na}_2\text{SO}_4$ , and concentrated to give a neutral fraction (110 g) which was passed through a column packed with alumina (1000 g). The column was eluted successively with hexane, benzene,  $\text{CHCl}_3$  and MeOH. The fraction (6.6 g) eluted with benzene- $\text{CHCl}_3$  (2:3) was rechromatographed on silica gel with benzene- $\text{CHCl}_3$  (7:3) to give IV (40 mg).

**7 $\alpha$ ,18-Dihydroxydehydroabietanol (IV)**—IV was recrystallized from acetone to give colorless needles. mp 89 °C.  $[\alpha]_D^{20} - 3.3^\circ$  ( $c=0.46$ , EtOH). High-resolution MS  $m/z$ : Calcd for  $\text{C}_{20}\text{H}_{30}\text{O}_2$ : 302.2246. Found: 302.2254. UV  $\lambda_{\max}^{\text{EtOH}}$  nm: 216, 266, 274. IR  $\nu_{\max}^{\text{KBr}} \text{cm}^{-1}$ : 3300, 1500, 1460, 1380, 1050, 878, 820. MS  $m/z$ : 302 ( $M^+$ , 18), 254 (97), 251 (48), 197 (29), 155 (22), 85 (72), 83 (100), 47 (31), 43 (18).  $^1\text{H-NMR}$  ( $\text{CDCl}_3$ )  $\delta$ : 0.72 (3H, s), 1.13 (3H, s), 1.23 (3H  $\times$  2, d,  $J=6$  Hz), 2.87 (1H, d,  $J=9$  Hz), 3.45 (1H, d,  $J=9$  Hz), 4.61 (1H, brs,  $W_{1/2}=7$  Hz), 6.98 (2H, brs), 7.24 (1H, brs).  $^{13}\text{C-NMR}$  ( $\text{CDCl}_3$ )  $\delta$ : 147.4 (C-9), 146.2 (C-13), 136.0 (C-8), 128.0 (C-14), 126.4 (C-11), 124.4 (C-12), 70.4 (C-18), 68.2 (C-7), 38.2 (C-5), 37.7 (C-4), 37.4 (C-1), 37.1 (C-10), 34.6 (C-3), 33.6 (C-15), 27.9 (C-6), 24.4 (C-20), 23.9 (C-16), C-17), 18.7 (C-2), 17.8 (C-19).

**Acetylation of IV**—IV (30 mg) was acetylated with  $\text{Ac}_2\text{O}$  (0.5 ml) and pyridine (1 ml) to give a diacetate (IVa, 32.6 mg) as a colorless powder. mp 97 °C. IR  $\nu_{\max}^{\text{KBr}} \text{cm}^{-1}$ : 1720, 1270, 1100, 1060, 880.  $^1\text{H-NMR}$  ( $\text{CDCl}_3$ )  $\delta$ : 0.91 (3H, s), 1.15 (3H, s), 1.20 (3H  $\times$  2, d,  $J=6$  Hz), 2.01 (3H  $\times$  2, s, -OAc), 3.65 (1H, d,  $J=9$  Hz), 3.93 (1H, d,  $J=9$  Hz), 5.96 (1H, t,  $J=3$  Hz), 6.99 (2H, brs), 7.18 (1H, brs).

**Oxidation of IV**—IV (15 mg) was dissolved in pyridine (1 ml) and allowed to stand with  $\text{CrO}_3$ -pyridine (27 mg in 1 ml) overnight at room temperature, then poured into aq. MeOH to give IVb (2 mg) as a colorless oil. UV  $\lambda_{\max}^{\text{EtOH}}$  nm: 216, 252, 298. IR  $\nu_{\max}^{\text{liq.}} \text{cm}^{-1}$ : 3420, 1730, 1680. MS  $m/z$ : 314 ( $M^+$ , 3), 300 (37), 285 (24), 267 (32), 187 (100), 43 (25).

**Isolation of V**—The 5% NaOH extract was acidified with dil. HCl and extracted with ether. The ether extract was dried over  $\text{Na}_2\text{SO}_4$ , and the ether was evaporated off. The residue (148 g) was chromatographed on silica gel (150 g, upper layer) and alumina (500 g, bottom layer). The column was eluted successively with hexane, benzene,  $\text{CHCl}_3$  and MeOH. The fraction (5.3 g) eluted with  $\text{CHCl}_3$ -MeOH (4:1) was rechromatographed on silica gel with  $\text{CHCl}_3$ -MeOH (4:1) to give V (1.2 g).

**Hexadecane-1,16-diol 7-Caffeoyl Ester (V)**—Yellow oil.  $[\alpha]_D^{20} + 3.6^\circ$  ( $c=0.28$ , MeOH). UV  $\lambda_{\max}^{\text{EtOH}}$  nm: 220, 238, 246, 316, 334. IR  $\nu_{\max}^{\text{liq.}} \text{cm}^{-1}$ : 3320, 1690, 1600, 1515, 1445, 1260. MS  $m/z$ : 436 ( $M^+$ , 4), 257 (10), 180 (100), 173 (28), 163 (34), 131 (44), 95 (89), 81 (45), 69 (46), 57 (36), 55 (51), 43 (38).  $^1\text{H-NMR}$  ( $\text{CD}_3\text{OD}$ )  $\delta$ : 1.30 (brs), 3.53 (2H  $\times$  2, t,  $J=6$  Hz, H-1, H-16), 4.98 (1H, t,  $J=7$  Hz, H-7), 6.25 (1H, d,  $J=16$  Hz, H-7'), 6.86 (1H, d,  $J=9$  Hz, H-5'), 7.01 (1H, dd,  $J=2, 9$  Hz, H-6'), 7.06 (1H, d,  $J=2$  Hz, H-2'), 7.54 (1H, d,  $J=16$  Hz, H-8').  $^{13}\text{C-NMR}$  ( $\text{CD}_3\text{OD}$ )  $\delta$ : 168.9 (C-9'), 149.2 (C-4'), 146.5 (C-3', C-7'), 127.4 (C-1'), 122.7 (C-6'), 116.3 (C-5'), 115.3 (C-8'), 115.0 (C-2'), 75.2 (C-7), 62.8 (C-1, C-16).

**Acetylation of V**—V (116 mg) was acetylated with  $\text{Ac}_2\text{O}$  (1 ml) in pyridine (1 ml) at room temperature for 10 h to give a tetracetate (Va 121 mg) as a colorless oil. MS  $m/z$ : 604 ( $\text{M}^+$ , 2), 562 (25), 520 (59), 341 (100), 180 (62), 163 (42), 95 (25), 83 (22), 69 (25), 43 (42).  $^1\text{H-NMR}$  ( $\text{CDCl}_3$ )  $\delta$ : 1.28 (br s), 2.02 (3H  $\times$  2, s, -OAc), 2.28 (3H  $\times$  2, s, -OAc), 4.03 (2H  $\times$  2, t,  $J=5$  Hz, H-1, H-16), 4.98 (1H, t,  $J=6$  Hz, H-7), 6.36 (1H, d,  $J=16$  Hz, H-7'), 7.19 (1H, dd,  $J=2, 9$  Hz, H-6'), 7.34 (1H, d,  $J=9$  Hz, H-5'), 7.37 (1H, d,  $J=2$  Hz, H-2'), 7.58 (1H, d,  $J=16$  Hz, H-8').

**Identification of 3,4-Dimethoxycaffeic Acid Methyl Ester (Vb)**—V (26 mg) was methylated with diazomethane and a solution of the product (10.5 mg) in EtOH (1 ml) containing KOH-EtOH (150 mg in 2 ml) was refluxed for 3 h. The reaction mixture was acidified with dil. HCl and extracted with ether. Methylation of the ether extract with diazomethane yielded Vb (4 mg), which was identified as 3,4-dimethoxycaffeic acid methyl ester by comparison with an authentic sample on GLC.

**Hydrolysis of V**—A solution of V (50 mg) in EtOH (1 ml) containing KOH-EtOH (250 mg in 4 ml) was refluxed for 3 h. The reaction mixture was acidified with dil. HCl and extracted with ether. The ether extract gave hexadecane-1,7,16-triol (Vc) as a colorless oil. FD-MS  $m/z$ : 274 ( $\text{M}^+$ ).  $^1\text{H-NMR}$  ( $\text{CD}_3\text{OD}$ )  $\delta$ : 1.32 (br s), 3.53 (2H  $\times$  2, t,  $J=6$  Hz).

**Acetylation of Vc**—i) Diacetate of Vc: Vc (12 mg) was acetylated with  $\text{Ac}_2\text{O}$  (0.5 ml) in pyridine (1 ml) at room temperature to give a diacetate (Vd, 13.2 mg) as a colorless oil. MS  $m/z$ : 358 ( $\text{M}^+$ , 3), 357 (17), 280 (31), 257 (27), 215 (97), 173 (67), 95 (55), 81 (45), 69 (48), 55 (44), 43 (100), 18 (29).  $^1\text{H-NMR}$  ( $\text{CDCl}_3$ )  $\delta$ : 1.27 (br s), 2.03 (3H  $\times$  2, s, -OAc), 4.03 (2H  $\times$  2, t,  $J=6$  Hz, H-1, H-16), 4.85 (1H, t,  $J=6$  Hz, H-7).  $^{13}\text{C-NMR}$  ( $\text{CDCl}_3$ )  $\delta$ : 171.2 (-O $\text{C}=\text{OCH}_3$ ), 171.0 (-O $\text{C}=\text{OCH}_3$ ), 74.3 (C-7), 64.6 (C-1, C-16), 21.3 (-O $\text{C}=\text{OCH}_3$ ), 21.0 (-O $\text{C}=\text{OCH}_3$ ).

ii) Triacetate of Vc: Vc (10 mg) was dissolved in  $\text{Ac}_2\text{O}$  (3 ml) and heated at 130 °C for 3 h to give a triacetate (Ve, 12.6 mg) as a colorless oil. FD-MS  $m/z$ : 400 ( $\text{M}^+$ ).  $^1\text{H-NMR}$  ( $\text{CDCl}_3$ )  $\delta$ : 1.28 (br s), 2.04 (3H  $\times$  3, s, -OAc), 4.01 (2H  $\times$  2, t,  $J=6$  Hz, H-1, H-16), 4.80 (1H, t,  $J=6$  Hz, H-7).

**Oxidation of Vc**—Vc (6 mg) was dissolved in pyridine (0.5 ml) and allowed to stand with  $\text{CrO}_3$ -pyridine (15 mg in 1 ml) overnight at room temperature, then poured into aq. MeOH to give 7-ketohexadecane-1,16-dicarboxylic acid. This acid was methylated with diazomethane to give 7-ketohexadecane-1,16-dicarboxylic acid methyl ester (VI) as a colorless oil. MS  $m/z$ : 328 ( $\text{M}^+$ , 3), 214 (57), 199 (30), 185 (17), 172 (100), 171 (18), 157 (48), 140 (62), 129 (31).

**Isolation of VI and VII**—The MeOH extract (16.7 g) was chromatographed on silica gel with hexane, benzene,  $\text{CHCl}_3$  and MeOH, successively. The  $\text{CHCl}_3$  eluate gave VI (20 mg), and the  $\text{CHCl}_3$ -MeOH (9:1) eluate gave VII (102 mg).

**Naringenin (VI)**—Pale yellow needles. mp 249–250 °C. IR  $\nu_{\text{max}}^{\text{KBr}}$   $\text{cm}^{-1}$ : 3200, 1640, 1600, 1515, 1490, 1460, 1310, 1250, 1160, 1080, 890, 830. The melting point on admixture of VI with an authentic sample of naringenin showed no depression, and the IR spectra and TLC properties of the two samples were identical.

**$\beta$ -Sitosterol  $\beta$ -D-Glucoside (VII)**—White powder. mp 264–265 °C (dec.). IR  $\nu_{\text{max}}^{\text{KBr}}$   $\text{cm}^{-1}$ : 3430, 3000, 2960, 2900, 1470, 1380, 1370, 1170, 1120, 1090, 1040. The IR spectrum was identical with that of an authentic sample of  $\beta$ -sitosterol  $\beta$ -D-glucoside.

**Acknowledgement** We are grateful to Mr. H. Miyamoto (Nissan Chem. Ind. Co.) for measuring the FD-MS spectra, to Miss Y. Sakamoto for the NMR spectra, and to Mr. M. Takayama for the MS.

#### References and Notes

- 1) A part of this study was presented at the 104th Annual Meeting of the Pharmaceutical Society of Japan, Sendai, April 1984. This paper forms part XIII of "Constituents of Pollen." Part XII: T. Ohmoto, M. Udagawa and K. Yamaguchi, *Shoyakugaku Zasshi*, **40**, 172 (1986).
- 2) D. K. Kulshreshtha and R. P. Rastogi, *Phytochemistry*, **14**, 2237 (1975).
- 3) D. K. Kulshreshtha and R. P. Rastogi, *Phytochemistry*, **15**, 557 (1976).
- 4) S. C. Bisarya and Sukh Dev, *Tetrahedron*, **24**, 3869 (1968).
- 5) D. Adinarayana and T. R. Seshadri, *Tetrahedron*, **21**, 3727 (1965).
- 6) T. Ohmoto, T. Nikaido and M. Ikuse, *Shoyakugaku Zasshi*, **34**, 87 (1980).
- 7) G. Stork and J. W. Schulenberg, *J. Am. Chem. Soc.*, **78**, 250 (1956).
- 8) Y. S. Cheng and S. B. Lu, *J. Chinese Chem. Soc.*, **25**, 47 (1978).
- 9) J. F. Biellmann, G. Branlant, M. Gero-Robert and M. Poiret, *Tetrahedron*, **29**, 1237 (1973).
- 10) S. Valverde, J. C. Lopez, R. M. Rabanal and J. Escudero, *Tetrahedron*, **42**, 573 (1986).
- 11) G. D. Duchateau, *Bull. Soc. Chim. Fr.*, **7**, 1469 (1964).
- 12) T. Ohmoto and O. Yoshida, *Chem. Pharm. Bull.*, **31**, 919 (1983).
- 13) F. Aylward and B. W. Nichols, *Nature* (London), **181**, 1064 (1958).

[Chem. Pharm. Bull.]  
[35(1) 235—240 (1987)]

## Determination of L-3,4-Dihydroxyphenylalanine in Plasma and Urine by High-Performance Liquid Chromatography with Fluorescence Detection

MYUNGKOO LEE,<sup>a</sup> HITOSHI NOHTA,<sup>a</sup> KENJI OHTSUBO,<sup>b</sup>  
BEONGTAE YOO<sup>c</sup> and YOSUKE OHKURA<sup>\*a</sup>

*Faculty of Pharmaceutical Sciences<sup>a</sup> and Hospital Pharmacy, Faculty of Medicine,<sup>b</sup>  
Kyushu University, Maidashi, Higashi-ku, Fukuoka 812, Japan, and College of  
Pharmacy, Chungnam National University,<sup>c</sup> Gung-dong,  
Chung-ku, Daejeon 300-31, Korea*

(Received July 8, 1986)

A simple and highly sensitive method for the determination of L-3,4-dihydroxyphenylalanine (L-DOPA) in human plasma and urine is described which employs high-performance liquid chromatography with fluorescence detection. After cation-exchange chromatography on a Toyopak IC-SP S cartridge, L-DOPA and  $\alpha$ -methyldopa (an internal standard) in 300  $\mu$ l of plasma or 10  $\mu$ l of urine are converted into the corresponding fluorescent compounds by reaction with 1,2-diphenylethylenediamine. These compounds are separated by reversed-phase chromatography on a TSK gel ODS-120T column with isocratic elution. The detection limit for L-DOPA is 10 fmol in a 100- $\mu$ l injection volume.

**Keywords**—L-3,4-dihydroxyphenylalanine;  $\alpha$ -methyldopa; 1,2-diphenylethylenediamine; HPLC; fluorescence detection; human plasma; urine

L-3,4-Dihydroxyphenylalanine (L-DOPA), a catechol  $\alpha$ -amino acid, is synthesized by the hydroxylation of tyrosine, and it acts as an important intermediate in the catecholamine biosynthetic pathway.<sup>1,2)</sup> As L-DOPA has been introduced for the treatment of Parkinson's disease,<sup>3)</sup> many methods for the determination of L-DOPA in biological materials have been developed: colorimetric,<sup>4)</sup> fluorimetric,<sup>5-7)</sup> gas chromatographic,<sup>8,9)</sup> radioenzymatic<sup>10-13)</sup> and high-performance liquid chromatographic (HPLC) methods with ultraviolet,<sup>14)</sup> fluorescence (FID)<sup>15)</sup> and electrochemical (ECD) detections.<sup>16-23)</sup> Although those methods permit the monitoring of therapeutic L-DOPA, endogenous L-DOPA in plasma can be determined only by radioenzymatic<sup>11-13)</sup> and HPLC-ECD methods.<sup>20-23)</sup> The radioenzymatic methods are complicated and time-consuming to carry out, and the HPLC-ECD methods are sensitive but require rather complicated sample clean-up procedures.

We have developed a highly sensitive and simple HPLC-FID method for the determination of L-DOPA, based on precolumn derivatization with 1,2-diphenylethylenediamine (DPE), a fluorogenic reagent for catechol compounds.<sup>24,25)</sup> L-DOPA in plasma and urine, (with  $\alpha$ -methyldopa as an internal standard), after cation-exchange chromatography on a cartridge for sample clean-up, are converted into the corresponding fluorescent compounds by reaction with DPE. These products are separated by reversed-phase HPLC with isocratic elution.

### Experimental

**Reagents and Solutions**—L-DOPA and  $\alpha$ -methyldopa were purchased from Sigma (St. Louis, U.S.A.). DPE

was synthesized as described previously.<sup>24)</sup> All other chemicals were of reagent grade. Deionized and distilled water was used. DPE solution (0.1 M; pH 6.5–6.7) was prepared in 0.1 M hydrochloric acid. A Toyopak IC-SP S (strong cation-exchanger, sulfopropyl resin, Na<sup>+</sup> form; Toyo Soda, Tokyo, Japan) cartridge (35 × 4 mm i.d.) was washed successively with 1 ml of 2 M sodium hydroxide, 5 ml of water, 1 ml of 2 M hydrochloric acid and 5 ml of water, and equilibrated with 2 ml of 0.2 M sodium phosphate buffer (pH 6.0). The used cartridge could be regenerated by treating in the same way, and could be used more than five times. Heparinized blood (5 ml) from healthy volunteers (21–55 years of age) was taken into chilled polyethylene tubes and centrifuged at 1000g for 20 min at 4°C. The plasma was stored at –70°C until assay.

**Apparatus and HPLC Conditions**—An Eyela LP-1 liquid chromatograph (Tokyo Rika, Tokyo, Japan) was used, equipped with a Rheodyne 7125 sample injector valve (100- $\mu$ l loop) and a Hitachi 650-10 LC spectrofluorimeter fitted with a 18- $\mu$ l flow cell operated at an emission wavelength of 475 nm and an excitation wavelength of 350 nm; spectral bandwidths of 10 nm were used both for excitation and emission. For the measurement of uncorrected fluorescence excitation and emission spectra of the eluate, a Hitachi 850 fluorescence spectrophotometer fitted with a 20- $\mu$ l flow cell was used; the spectral bandwidths in the excitation and emission monochromators were both 5 nm. A TSK gel ODS-120T column (particle size 5  $\mu$ m, 150 × 4.6 mm i.d.; Toyo Soda) was used. The column temperature was ambient (20–25°C). The mobile phase was a mixture of acetonitrile, methanol and 0.1 M acetate buffer (pH 5.0) (1:1:2, v/v) and the flow-rate was 1.0 ml/min.

When conventional spectrofluorimetry was required, uncorrected fluorescence excitation and emission spectra and intensities were measured with a Hitachi MPF-4 spectrofluorimeter using quartz cells (*ca.* 1.2-ml cell volume; 0.3 × 1.0 cm optical pathlengths). The excitation and emission bandwidths were both set at 10 nm.

**Procedures for Clean-up of Samples**—a) Plasma: A 300- $\mu$ l aliquot of plasma was mixed with 30  $\mu$ l of 1 nmol/ml  $\alpha$ -methyldopa (internal standard) and 500  $\mu$ l of 0.5 M perchloric acid, and the mixture was centrifuged at 1000g for 10 min at 4°C. The supernatant (600  $\mu$ l) was poured onto a Toyopak IC-SP S cartridge. The cartridge was washed with 5 ml of water, 1 ml of 0.02 M sodium phosphate buffer (pH 6.0); 1 ml of water and 1 ml of aqueous 60% ethanol. The adsorbed L-DOPA and  $\alpha$ -methyldopa were eluted with 1 ml of a mixture of ethanol, 2 M sodium perchlorate and 2 M sodium hydroxide (7:3:0.1, v/v). The eluate was used for the fluorescence derivatization.

b) Urine: A 10- $\mu$ l aliquot of urine was mixed with 30  $\mu$ l of 1 nmol/ml  $\alpha$ -methyldopa and 500  $\mu$ l of 0.5 M perchloric acid. The mixture was poured onto a Toyopak IC-SP S cartridge and then treated as described for plasma.

**Procedure for the Fluorescence Derivatization**—The eluate (*ca.* 1 ml) from the Toyopak IC-SP S cartridge was mixed with 200  $\mu$ l of DPE solution, 20  $\mu$ l of 0.5 M sodium carbonate (to adjust the pH to 6.5–6.9) and 50  $\mu$ l of 0.6 mM potassium hexacyanoferrate (III). The mixture was allowed to stand at 25°C for 20 min and then 100  $\mu$ l of 0.4 M sodium sulfite was added to decompose the excess hexacyanoferrate. A 100- $\mu$ l aliquot of the mixture was injected into the chromatograph. The amount of L-DOPA was calculated by the internal standard method.

## Results and Discussion

### Fluorescence Derivatization

L-DOPA and  $\alpha$ -methyldopa did not give very intense fluorescence under the conditions used for the reaction of catecholamines (epinephrine, norepinephrine and dopamine) with DPE.<sup>24,25)</sup> Therefore, the reaction conditions for the derivatization of L-DOPA and  $\alpha$ -methyldopa were investigated, mostly by conventional spectrofluorimetry.

The derivatization reaction of L-DOPA was strongly affected by the concentration of potassium hexacyanoferrate (III) and the reaction temperature (Fig. 1). At higher concentrations of potassium hexacyanoferrate (III) the reaction proceeded more rapidly. At 200  $\mu$ M, however, the fluorescence intensity decreased more rapidly. The reaction occurred even at 0°C. Higher temperatures allowed the fluorescence to develop more rapidly, but caused a decrease in the intensity with time. Maximum and constant fluorescence intensity was attained by warming at 20–25°C for 20–40 min in the presence of 15–30  $\mu$ M potassium hexacyanoferrate (III) in the reaction mixture: warming for 20 min at 25°C and a potassium hexacyanoferrate (III) concentration of 25  $\mu$ M gave reproducible results.

Ethanol accelerated the derivatization reaction of L-DOPA and gave maximum intensity at concentrations of 50–65% (v/v) in the reaction mixture: 55% was selected. Ethanol was actually used as a component of the eluent in the chromatography for sample clean-up. The optimum pH for the reaction of L-DOPA was 6.5–7.0. DPE in the concentration range of 10–30 mM in the reaction mixture gave almost maximum fluorescence intensity: 15 mM was



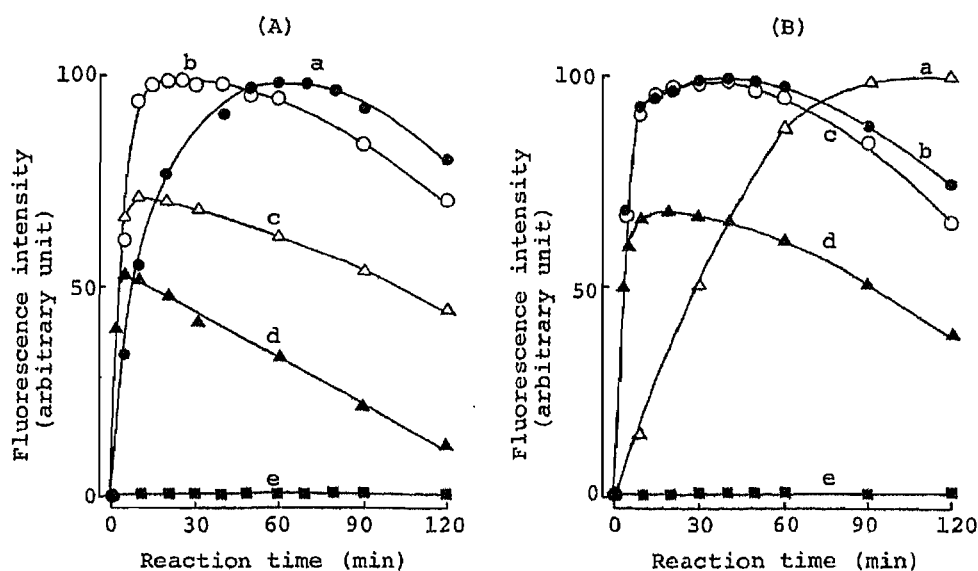


Fig. 1. Effects of (A) the Concentration of Potassium Hexacyanoferrate(III) and the Reaction Time, and (B) the Reaction Temperature and the Time on the Fluorescence Development from L-DOPA

Aliquots (1 ml) of a mixture of ethanol and sodium perchlorate (7:3, v/v) containing L-DOPA (1 nmol) were treated according to the procedure for the derivatization.

(A) Concentrations of potassium hexacyanoferrate(III) ( $\mu\text{M}$ ) in the reaction mixtures: a, 5; b, 24; c, 100; d, 200; e, the reagent blanks for a—d. (B) Reaction temperatures ( $^{\circ}\text{C}$ ): a, 0; b, 20; c, 25; d, 37; e, the reagent blanks for a—d.

selected. The optimum conditions for the derivatization reaction of  $\alpha$ -methyldopa were closely similar to those for L-DOPA.

The excitation and emission maxima for the fluorescent products from L-DOPA and  $\alpha$ -methyldopa were at 350 and 475 nm, respectively, in each case. The fluorescence intensities from L-DOPA and  $\alpha$ -methyldopa decreased slightly with time if potassium hexacyanoferrate (III) that remained unreacted was not decomposed with sodium sulfite. The fluorescence obtained under the recommended derivatization conditions was stable for at least 12 h at room temperature, even in daylight.

#### HPLC Conditions

Figure 2 shows a typical chromatogram obtained with a standard mixture of L-DOPA and  $\alpha$ -methyldopa. The retention times for the DPE derivatives of L-DOPA and  $\alpha$ -methyldopa were 3.6 and 4.7 min, respectively. The DPE derivatives in the eluates from peaks 1 and 2 showed the fluorescence excitation and emission maxima at 350 and 475 nm, respectively.

A mixture of methanol and 0.1 M acetate buffer (pH 5.0) (1:1, v/v) as a mobile phase resulted in relatively long elution times with broadening of the peaks (retention times for L-DOPA and  $\alpha$ -methyldopa, 12 and 19.3 min, respectively). A mixture of acetonitrile and the buffer (4:6, v/v) afforded short elution times but did not give satisfactory resolution of the peaks (retention times for L-DOPA and  $\alpha$ -methyldopa, 2.6 and 2.9 min, respectively). In these solvent systems, the pH values (5.0—6.0) and concentrations (0.05—1.0 M) of acetate buffer had almost no effect on the retention times and peak heights for L-DOPA and  $\alpha$ -methyldopa. However, at lower pH values (3.0—4.0) of the buffer, the peak heights were lowered with broadening of the peaks and delay of the elution. Finally, a mixture of acetonitrile, methanol and 0.1 M acetate buffer (pH 5.0) (1:1:2, v/v) was found to give rapid and complete separation.

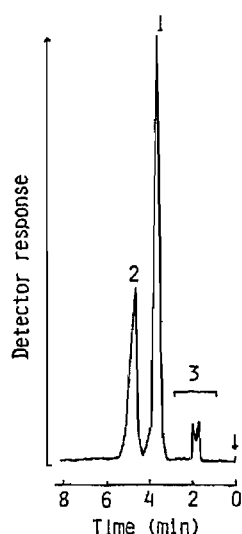


Fig. 2. Chromatogram Obtained with a Standard Mixture of L-DOPA and  $\alpha$ -Methyl-dopa

An aliquot (1 ml) of a standard mixture of L-DOPA and  $\alpha$ -methyl-dopa (0.1 nmol/ml each) in the eluent for the chromatography in the clean-up procedure was treated according to the standard procedures for derivatization and HPLC. Peaks: 1, L-DOPA; 2,  $\alpha$ -methyl-dopa; 3, unidentified. Detector sensitivity: 1.

DPE also reacts with catecholamines<sup>24)</sup> under the derivatization conditions, though their peaks in the chromatogram are small. The DPE derivatives of these compounds could be separated under the HPLC conditions: the retention times (min) were 6.1 (norepinephrine), 15.8 (epinephrine), 17.6 (dopamine).

#### Determination of L-DOPA in Plasma and Urine

Figure 3 (A) and (B) shows typical chromatograms obtained with a normal plasma and a normal urine, respectively. The peaks for L-DOPA, norepinephrine, epinephrine and dopamine (peaks 1, 5, 6 and 7) were identified on the basis of their retention times and the fluorescence excitation and emission spectra of the eluates in comparison with those of standard compounds and also by co-chromatography of the standards and the samples. The peaks for epinephrine and dopamine could not be clearly detected in normal plasma because their concentrations are extremely low as compared with those in urine and the derivatization conditions are not suitable for the catecholamines.

A Toyopak IC-SP S cartridge was easily applied for the sample clean-up after being equilibrated with 0.2M sodium phosphate buffer (pH 6.0). The adsorbed amines could be eluted by using a mixture of ethanol, 2M sodium perchlorate and 2M sodium hydroxide (7:3:0.1, v/v). Sodium chloride (2M) has an elution power comparable to 2M sodium perchlorate, but it caused turbidity in the final reaction mixture in the fluorescence derivatization procedure.

Recoveries of L-DOPA (30 pmol per the prescribed sample sizes) added to plasma and urine ( $n=5$  in each case) were  $61.1 \pm 4.2$  and  $61.3 \pm 2.7\%$ , respectively. In addition, the values for  $\alpha$ -methyl-dopa (30 pmol) added to plasma and urine ( $n=5$  in each case) were almost the same as those for L-DOPA ( $60.0 \pm 1.8$  and  $65.4 \pm 2.5\%$ , respectively). This result indicates that  $\alpha$ -methyl-dopa is suitable as an internal standard.

The calibration plots between the peak height ratios of L-DOPA and  $\alpha$ -methyl-dopa and the amounts of L-DOPA added to plasma and urine were linear in the range of 0.5—150 pmol.

The detection limit for L-DOPA was 0.66 pmol/ml in plasma and 20 pmol/ml in urine (10 fmol per 100- $\mu$ l injection volume, respectively) at a signal-to-noise ratio of 2. This sensitivity is comparable to the best sensitivity in the HPLC-ECD method.<sup>22)</sup> The precision was established by repeated determinations using a normal plasma and a normal urine. The coefficients of variation for L-DOPA were 4.6 and 6.2% at mean concentrations of 9.8 pmol/ml of plasma and 280 pmol/ml of urine, respectively ( $n=7$  in each case).

The L-DOPA concentrations in plasma from healthy volunteers were assayed by the

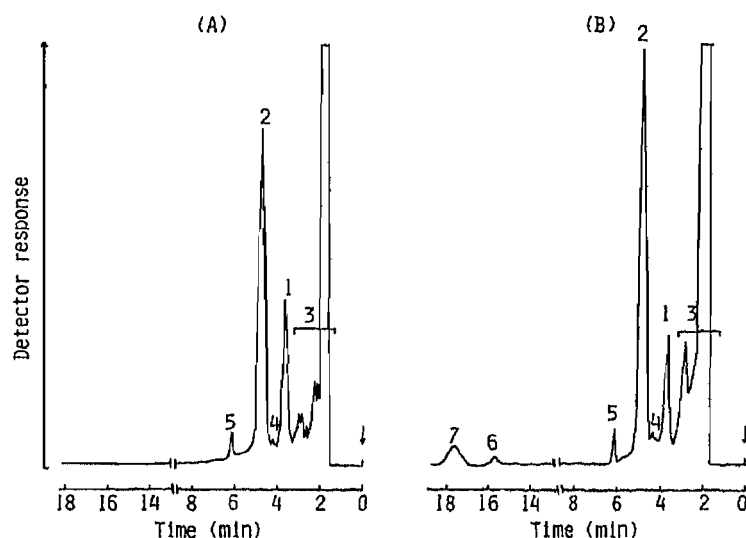


Fig. 3. Chromatograms Obtained with (A) Plasma and (B) Urine

Peaks: 1, 2 and 3, see Fig. 2; 4, unidentified; 5, norepinephrine; 6, epinephrine; 7, dopamine. Detector sensitivity: 10. Concentrations (pmol/ml) of L-DOPA: A, 18.4; B, 313.

TABLE I. Concentrations of L-DOPA in Plasma<sup>a)</sup>

Sex <sup>b)</sup>	Age	Concentration (pmol/ml) <sup>c)</sup>
M	55	17.6
M	39	18.3
M	34	14.7
M	31	9.9
M	29	18.4
M	27	12.8
M	26	10.2
M	23	11.5
M	23	17.8
F	23	14.4
F	22	19.0
F	21	18.7
Mean $\pm$ S.D.		15.3 $\pm$ 3.5

a) Blood samples were collected at 9:00–10:00 a.m. from healthy volunteers who had a light breakfast at ca. 8:00 a.m. b) M, male; F, female. c) Mean of duplicate determinations.

present method (Table I). The values are in good agreement with data obtained by other workers<sup>20,23)</sup> but slightly higher than other reported data.<sup>11,13,21,22)</sup> The L-DOPA concentrations in urine samples from six healthy, non-fasted men (23–31 years of age) were  $410 \pm 164$  pmol/ml.

This method is highly sensitive and simple enough to allow the assay of ten samples within 4 h, with small sample sizes of plasma and urine. The method should be useful for biological, biomedical and clinical investigations of L-DOPA.

**Acknowledgement** We thank Miss M. Kuroki for her skillful assistance and also Toyo Soda for the generous gifts of Toyopak IC-SP S cartridge and TSK gel ODS-120T column.

#### References

- 1) S. Udenfriend and J. B. Wyngaarden, *Biochim. Biophys. Acta*, **20**, 48 (1956).

- 2) T. Nagatsu, M. Levitt and S. Udenfriend, *J. Biol. Chem.*, **239**, 2910 (1964).
- 3) M. D. Yahr, R. C. Ouvoisin, M. J. Shear, R. E. Barrett and M. M. Hoehn, *Arch. Neurol.*, **21**, 343 (1969).
- 4) T. A. Hare and W. H. Vogel, *Biochem. Med.*, **4**, 277 (1970).
- 5) F. Eichhorn, A. Rutenberg and E. Kott, *Clin. Chem.*, **17**, 296 (1971).
- 6) S. Fahn, A. L. N. Prasad and R. Delesie, *Anal. Biochem.*, **46**, 557 (1972).
- 7) J. M. Cottet-Emard and L. Peyrin, *J. Neural Trans.*, **41**, 145 (1977).
- 8) K. Imai, M. Sugiura, H. Kubo, Z. Tamura, K. Ohya, N. Tsunakawa, K. Hirayama and H. Narabayashi, *Chem. Pharm. Bull.*, **20**, 759 (1972).
- 9) K. Imai, N. Arizumi, M. Wang, S. Yoshiue and Z. Tamura, *Chem. Pharm. Bull.*, **20**, 2436 (1972).
- 10) M. N. Rossor, J. Watkins, M. J. Brown, J. L. Reid and C. T. Dollery, *J. Neurol. Sci.*, **46**, 385 (1980).
- 11) G. A. Johnson, J. M. Gren and R. Kupiecki, *Clin. Chem.*, **24**, 1927 (1978).
- 12) G. Zürcher and M. D. Prada, *J. Neurochem.*, **33**, 631 (1979).
- 13) M. J. Brown and C. T. Dollery, *Br. J. Clin. Pharmac.*, **11**, 79 (1981).
- 14) J. Mitchell and C. T. Coscia, *J. Chromatogr.*, **145**, 295 (1978).
- 15) J. Seki, Y. Arakawa, K. Imai, Z. Tamura, S. Yoshiue, Y. Mizuno, K. Yamada, M. Tatué and H. Narabayashi, *Chem. Pharm. Bull.*, **29**, 789 (1981).
- 16) R. M. Riggan, R. L. Alcorn and P. T. Kissinger, *Clin. Chem.*, **22**, 782 (1976).
- 17) E. Nissinen and J. Taskinen, *J. Chromatogr.*, **231**, 459 (1982).
- 18) R. C. Causon, M. J. Brown, K. L. Leenders and L. Wolfson, *J. Chromatogr.*, **277**, 115 (1983).
- 19) M. F. Beers, M. Stern, H. Hurtig, G. Melvin and A. Scarpa, *J. Chromatogr.*, **336**, 380 (1984).
- 20) A. Shum, G. R. V. Loon and M. J. Sole, *Life Sci.*, **31**, 1541 (1982).
- 21) Z. L. Rossetti, G. Mercurio and C. A. Rivano, *Life Sci.*, **33**, 2387 (1983).
- 22) S. Ito, T. Kato, K. Maruta, K. Fujita and T. Kurahashi, *J. Chromatogr.*, **311**, 154 (1984).
- 23) D. S. Goldstein, R. Stull, R. Zimlichman, P. D. Levinson, H. Smith and H. R. Keiser, *Clin. Chem.*, **30**, 815 (1984).
- 24) H. Nohta, A. Mitsui and Y. Ohkura, *Anal. Chim. Acta*, **165**, 171 (1984).
- 25) A. Mitsui, H. Nohta and Y. Ohkura, *J. Chromatogr.*, **344**, 61 (1985).

[Chem. Pharm. Bull.]  
35(1) 241-248 (1987)

## Chronic Effects of Ginseng Saponin, Glycyrrhizin and Flavin Adenine Dinucleotide on Adrenal and Thymus Weight in Normal and Dexamethasone-Treated Rats

SUSUMU HIAI,\*<sup>a</sup> YUICHI SASAYAMA<sup>b</sup> and CHITARU OGURO<sup>b</sup>

Research Institute for WAKAN-YAKU, Toyama Medical and Pharmaceutical University,<sup>a</sup>  
2630 Sugitani, Toyama 930-01, Japan and Department of Biology, Faculty of  
Science, Toyama University,<sup>b</sup> Gofuku, Toyama 930, Japan

(Received March 7, 1986)

The effects of chronic treatment with ginseng saponin, saikosaponin, glycyrrhizin and flavin adenine dinucleotide (FAD) on the adrenal and thymus weight, and the size of the adrenal cortex and medulla were determined in intact or hypophysectomized rats. A high dose of ginseng saponin significantly decreased the thymus weight, although ginseng saponin and a low dose of adrenocorticotropic (ACTH) induced insignificant hypertrophy of the adrenals. Ginseng saponin evoked a significant increase in the relative thickness of the adrenal cortex. Saikosaponin d increased the area of the adrenal cortex, but not that of the medulla, and induced adrenal hypertrophy and thymus atrophy, whereas saikosaponin c did not affect the weight of either. A high dose of glycyrrhetic acid, like ginseng saponin, induced thymus atrophy, but not adrenal hypertrophy. FAD evoked adrenal hypertrophy in dexamethasone-treated rats but not in control rats. In hypophysectomized rats these effects of ginseng saponin, saikosaponin d and FAD disappeared, while a low dose of dexamethasone or ACTH induced thymus atrophy or adrenal hypertrophy, respectively.

**Keywords**—ginseng saponin; saikosaponin; glycyrrhizin; glycyrrhetic acid; flavin adenine dinucleotide; ACTH; adrenal hypertrophy; adrenal cortex thickness; thymus atrophy; hypophysectomized rat

A number of studies on the effects of *Panax ginseng* C.A. MEYER on wet weight and the function of the adrenal cortex have been done. Petkov and Staneva reported that repeated administration of ginseng extract increased the relative weight of the adrenals, reduced eosinophils in peripheral blood in intact or unilaterally adrenalectomized rats, and increased urinary corticosteroid.<sup>1)</sup> In anti-stress studies Brekhman and Dardymov showed that panaxoside C or ginseng saponin inhibited stress-induced increase in the wet weight of the adrenals.<sup>2)</sup> Kim *et al.* found that in normal rats, extract of ginseng did not affect adrenal weight, and it induced an insignificant increase in the thickness of the adrenal cortex but induced a significant increase in the thickness of the zona fasciculata at the expense of the zona reticularis.<sup>3)</sup> Recently Bombardelli *et al.* observed that a purified mixture of ginseng saponin evoked a decrease in the wet weight of the thymus and a decrease in body weight gain accompanied with a decrease in food and water intake.<sup>4)</sup> Tanizawa *et al.* showed that total saponin of ginseng antagonized the cortisone acetate-induced decrease in both remaining adrenal weight and relative weight of the thymus in unilaterally adrenalectomized and cortisone-treated rats.<sup>5)</sup>

Saikosaponin d (but not c) of *Bupleurum falcatum* L. had an antigranulomatous action,<sup>6)</sup> and a potentiating action on the antigranulomatous action of dexamethasone,<sup>7)</sup> whereas it did not affect the relative weight of the adrenals or the basal level of plasma 11-OH corticosteroid,<sup>6)</sup> and it was slightly hypertrophic to the adrenals in control rats, but atrophic in dexamethasone-treated rats.<sup>7)</sup> Glycyrrhizin of *Glycyrrhiza* sp. induced inhibition of  $\Delta^4$ -5 $\beta$ -

reduction of corticoids in the liver, which "potentiated" and prolonged the action of corticosteroids.<sup>8,9)</sup> Glycyrrhizin antagonized cortisone-induced suppression of adrenocorticotropin (ACTH) synthesis in adrenalectomized rats, and cortisone-induced suppression of compensatory adrenal hypertrophy in unilaterally adrenalectomized rats.<sup>10)</sup> Tanizawa *et al.* showed that glycyrrhizin antagonized cortisone-induced atrophy of both adrenal and thymus in unilaterally adrenalectomized and cortisone-treated rats.<sup>5)</sup> In intact rats, glycyrrhetic acid sapogenin of glycyrrhizin evoked marked inhibition of  $5\beta$ -reductase<sup>9)</sup> and antigranulomatous action.<sup>11)</sup> Ono *et al.* reported that flavin adenine dinucleotide (FAD) simultaneously administered with dexamethasone phosphate prevented the dexamethasone-induced decrease in relative weight of the adrenals in intact rats,<sup>12)</sup> and FAD did not affect the relative weight of the adrenals in hypophysectomized rats, which had not been treated with dexamethasone.<sup>13)</sup>

Triterpenoidal saponins from *P. ginseng*,<sup>14-16)</sup> *B. falcatum*<sup>17,18)</sup> and *Platycodon grandiflorum* A. DC.<sup>19)</sup> and total saponins from several other crude drugs<sup>20)</sup> increased plasma ACTH and corticosterone in acute experiments, whereas a high dose of saikosaponin c from *B. falcatum*<sup>17)</sup> or glycyrrhizin<sup>15)</sup> did not. A high dose of ginseng saponin partially antagonized dexamethasone-induced blocking of (ACTH and) corticosterone secretion,<sup>21)</sup> and a high dose of saikosaponin a or d completely released dexamethasone-induced blocking of the pituitary in an acute experiment.<sup>22)</sup> Chronic treatment with a moderate dose of saikosaponin d induced hypertrophy of the adrenals and atrophy of the thymus, and in rats treated with a high dose of saikosaponin alone long term or with a high dose of dexamethasone, saikosaponin induced slight atrophy of the adrenals and marked atrophy of the thymus.<sup>23)</sup> The present study was undertaken to examine the effect of ginseng saponin, saikosaponins d and c, glycyrrhizin, glycyrrhetic acid, and FAD on the wet weight of the adrenal and thymus, the histologically determined size of the cortex and medulla of the adrenal gland, and the body weight in rats.

#### Materials and Methods

Four-week-old Wistar male rats initially weighing 85–95 g were used. Hypophysectomized male Wistar rats weighing 135–155 (5-week-old) or 95–115 g (4-week-old) were from Nippon Hypox, Yamanashi. They were fed on laboratory chow (CE-2, CLEA Japan Inc., Tokyo) and tap water *ad libitum*, and maintained with artificial light (light on: 0700 to 1900 h) for more than 7 or 12 d. Rats were "gentled" by handling and weighing every morning and evening. After conditioning for 3 or 7 d they were injected intraperitoneally with 5 ml/kg of saline (pyrogen-free saline or 2.5% ethanol-saline) or test substance once a day in the evening just after weighing for 4 or 5 successive days; this time was chosen in relation to the circadian rhythm of plasma corticosterone level in rats. At 15 or 24 h after the final injection, they were decapitated with a guillotine. Immediately after this, the adrenal glands and thymus were rapidly excised, put into ice-cold saline, and then weighed after being cleaned in cold saline and blotted on filter paper.

Immediately after weighing, the adrenal gland was fixed with formalin-acetic acid-ethanol solution (10:5:85), then dehydrated, embedded in paraffin and sectioned serially at 20  $\mu$ m according to routine procedures. Serial sections were stained with Delafield's hematoxylin and eosin. The area of the adrenal cortex and medulla of one specified section among the serial sections was measured by the use of a camera lucida essentially as described in the previous paper.<sup>24)</sup>

Ginseng saponin fraction 4 or 6 contained 36 and 45% protopanaxadiol equivalent sapogenin, respectively, and ginsenosides Rb<sub>1</sub>, Rb<sub>2</sub>, Rc, Rc<sub>2</sub>, Rd, Re and Rg<sub>1</sub>. They were obtained as described in the previous paper.<sup>25)</sup> Saikosaponins d and c were kindly supplied by Drs. K. Takeda and K. Sakurai of Shionogi Research Laboratories, Shionogi and Co., Ltd., Osaka. Glycyrrhizin and glycyrrhetic acid were from Tokyo Kasei Kogyo Co., Ltd. and Fluka AG Chemische Fabrik, Switzerland, respectively; they were dissolved in an appropriate volume of ethanol and neutralized with NaOH solution, and then saline was added to the solution just before use to form a gel-like suspension. The disodium salt of flavin adenine dinucleotide was from Nakarai Chemicals Ltd., Kyoto. Cortrosyn z injection as corticotropin was from N. V. Organon, Netherlands. Other chemicals were of reagent grade.

#### Results

##### Effect of Ginseng Saponin on Body Weight Gain, and Adrenal and Thymus Weight

In order to avoid possible superficial influence on the weight of the adrenals and thymus

due to differences of body weight and body weight change during the experimental period, the relative weight with respect to the initial body weight in the evening of day 0 was adopted as a criterion.<sup>23)</sup> As shown in Table Ia in rats treated with ginseng saponin mixture fraction 4 for 4 d, a low dose of ginseng saponin (30 or 60 mg/kg/d) did not affect body weight gain, or the relative weight of the adrenals and thymus. In dexamethasone-treated rats, 60 mg/kg/d of ginseng saponin also insignificantly affected body weight gain, and the relative weight of the adrenals and thymus.

The ED<sub>50</sub> value of fraction 6 saponin on corticosterone secretion-inducing activity was 15 mg/kg.<sup>15)</sup> In rats treated with a high dose of fraction 6 saponin (125 mg/kg/d) for 5 d, ginseng saponin significantly decreased the daily body weight gain, tended to increase the relative weight of the adrenals, but significantly decreased the relative weight of the thymus (Table Ia). The decrease in body weight gain was probably a result of the decrease in food intake, which was observed with ginseng saponin mixture by Bombardelli *et al.*<sup>4)</sup> and with ginsenoside Rb<sub>1</sub> by Takagi.<sup>26)</sup> In dexamethasone-treated rats, ginseng saponin induced a significant decrease in body weight gain, as in dexamethasone-untreated rats, but it tended to evoke adrenal hypertrophy and thymus atrophy. ACTH (4 U or 0.1 mg/kg/d) tended to increase adrenal weight and to decrease thymus weight. Dexamethasone (0.025 mg/kg/d) was atrophic on both the adrenals and thymus (in experiment 2, *vs.* saline,  $p < 0.05$  and  $p < 0.01$ ).

TABLE Ia. Effect of Ginseng Saponin (GS) on Adrenal and Thymus Weight

Treatment <sup>a)</sup> (mg/kg/d)	Body weight (g)		Weight (mg/100 g BWi <sup>b)</sup> )	
	Initial	Final	Adrenal	Thymus
Exp. 1: 4-d treatment				
Saline (6)	105.6 ± 2.3	133.0 ± 3.1	29.6 ± 0.7	385 ± 25
+GS 30 (6)	105.4 ± 1.7	132.6 ± 2.4	30.5 ± 1.3	411 ± 14
+GS 60 (6)	106.8 ± 2.3	132.4 ± 4.1	29.0 ± 1.4	406 ± 31
Dex 0.025 (6)	107.9 ± 2.2	129.3 ± 2.4	26.9 ± 1.0	335 ± 15
+GS 60 (6)	109.1 ± 2.2	126.5 ± 2.5	27.0 ± 1.1	301 ± 14
Exp. 2: 5-d treatment				
Saline (6)	97.3 ± 0.9	128.8 ± 1.5	32.1 ± 1.1	509 ± 39
+GS 125 (6)	95.6 ± 1.6	109.0 ± 1.2 <sup>c)</sup>	35.5 ± 1.6	359 ± 17 <sup>d)</sup>
+ACTH 0.1 (6)	95.5 ± 1.3	125.6 ± 1.7	34.4 ± 0.9	432 ± 25
Dex 0.025 (6)	96.5 ± 1.7	122.8 ± 2.9	28.2 ± 1.2	318 ± 16
+GS 125 (6)	96.8 ± 1.8	108.3 ± 2.1 <sup>d)</sup>	29.6 ± 1.3	286 ± 19

a) Numbers of rats are shown in parentheses. Each value is the mean ± S.E. Saline: 5 ml/kg/d of saline. GS: fraction 4 and fraction 6 saponin in experiments 1 and 2, respectively. Dex: dexamethasone. b) BWi: body weight in the evening of day 0. c)  $p < 0.001$ , d)  $p < 0.01$  *vs.* saline or dexamethasone.

TABLE Ib. Histological Estimation of the Effects of Ginseng Saponin (GS) on the Adrenal Cortex (C) and Medulla (M)

Treatment <sup>a)</sup> (mg/kg/d × 5 d)	Area (mm <sup>2</sup> )		Length $\sqrt{C+M/M}$	Volume $\sqrt{C+M/M}^3$
	Cortex	Medulla		
Saline (6)	2.97 ± 0.13	0.313 ± 0.024	3.11 ± 0.10 <sup>b)</sup>	30.5 ± 2.8 <sup>b)</sup>
+GS 125 (6)	3.12 ± 0.19	0.266 ± 0.026	3.60 ± 0.14 <sup>c)</sup>	48.6 ± 5.0 <sup>c)</sup>
+ACTH 0.1 (6)	3.38 ± 0.16 <sup>d)</sup>	0.323 ± 0.012	3.39 ± 0.08 <sup>d)</sup>	39.4 ± 3.1 <sup>d)</sup>
Dex 0.025 (6)	2.79 ± 0.15	0.338 ± 0.039	3.10 ± 0.11	30.7 ± 3.7
+GS 125 (6)	2.85 ± 0.11	0.313 ± 0.022	3.20 ± 0.11	33.5 ± 3.8

a) For details, see Table Ia. b)  $N = 5$ . c)  $p < 0.05$ , d)  $p < 0.1$ .

### Quantitative Histological Study of Ginseng Saponin Action on the Adrenal Cortex and Medulla

One section of the adrenal gland, which had the largest area, was selected among the serial sections on the basis of microscopic determination of the length and width. Because the thickness of the adrenal cortex was markedly uneven even in the same section, the area of the adrenal cortex of the section was determined by using a camera lucida, and its square root was calculated to estimate the mean thickness equivalent of the adrenal cortex. In addition to this, in order to avoid superficial influence due to difference of body weight, the relative thickness of the cortex with respect to the thickness or radius of the medulla as an internal standard in the same section was adopted.

In control and dexamethasone-treated rats, ginseng saponin and ACTH tended to increase the cortex area of the adrenal but did not affect the medulla area (Table Ib). In control rats, ginseng saponin significantly increased the relative thickness and volume of the cortex, but in dexamethasone-treated rats, the effect of the same dose of ginseng saponin on both length and volume was insignificant. These results suggested that effect of ginseng saponin on the adrenal cortex was roughly parallel to that on the relative weight of the adrenals (Table Ia and b).

### Effect of Saikosaponins d and c on the Adrenal Cortex

The ED<sub>50</sub> value of saikosaponin d on corticosterone secretion-inducing activity was 0.33 mg/kg, but 100 mg/kg of saikosaponin c was not effective.<sup>17,18)</sup> Treatment with 2.5 mg/kg/d of saikosaponin d for 5 d significantly increased the adrenal weight and decreased the thymus weight.<sup>23)</sup> The same treatment with saikosaponin d significantly increased the area of the cortex but not that of the medulla (Table II).

TABLE II. Histological Estimation of the Effects of Saikosaponin d (Sd) on Growth of the Adrenal Cortex (C) and Medulla (M)

Treatment <sup>a)</sup> (mg/kg/d × 5 d)	Area (mm <sup>2</sup> )		Length $\sqrt{C+M/M}$	Volume <sup>3</sup> $\sqrt{C+M/M}$
	Cortex	Medulla		
Saline (6)	3.24 ± 0.09	0.392 ± 0.021	3.05 ± 0.07	28.8 ± 2.0
+Sd 2.5 (6)	3.68 ± 0.12 <sup>b)</sup>	0.405 ± 0.026	3.19 ± 0.08	32.9 ± 2.7
+ACTH 0.1 (6)	3.49 ± 0.22	0.353 ± 0.036	3.32 ± 0.07 <sup>b)</sup>	37.2 ± 2.5 <sup>b)</sup>
Dex 0.025 (5)	3.05 ± 0.21	0.382 ± 0.028	3.00 ± 0.03	27.1 ± 1.0
+Sd (5)	3.08 ± 0.06	0.380 ± 0.029	3.04 ± 0.12	28.8 ± 3.7

a) For details, see Table Ia. b)  $p < 0.05$ .

TABLE III. Effects of Saikosaponins d and c (Sd and Sc) on the Adrenal and Thymus Weight

Treatment <sup>a)</sup> (mg/kg/d × 4 d)	Body weight (g)		Weight (mg/100 g BW <sup>b)</sup> )	
	Initial	Final	Adrenal	Thymus
Saline (6)	103.4 ± 1.8	129.0 ± 2.9	30.4 ± 1.3	449 ± 14
+Sd 1.0 (6)	103.4 ± 1.5	124.9 ± 2.1	31.1 ± 1.1	394 ± 29
+Sd 2.5 (6)	101.6 ± 2.4	116.0 ± 2.5 <sup>c)</sup>	37.7 ± 0.7 <sup>d)</sup>	275 ± 18 <sup>d)</sup>
Saline (5)	101.0 ± 3.8	129.9 ± 4.5	27.1 ± 0.9	376 ± 12
+Sc 7.5 (6)	100.8 ± 2.8	127.0 ± 3.8	25.7 ± 0.5	384 ± 22
Dex 0.025 (6)	101.6 ± 1.7	124.2 ± 1.5	21.0 ± 0.5	294 ± 15
+Sc 7.5 (5)	101.8 ± 2.9	124.2 ± 3.2	23.0 ± 0.8 <sup>c)</sup>	280 ± 8
+ACTH 0.2 (6)	101.8 ± 2.3	121.5 ± 2.7	28.6 ± 0.8 <sup>d)</sup>	224 ± 13 <sup>c)</sup>

a, b) For details, see Table Ia. c)  $p < 0.01$ , d)  $p < 0.001$ , e)  $p < 0.1$ .



In the experiment with the 4-d treatment, 2.5 mg/kg/d of saikosaponin d significantly increased the adrenal weight and decreased the thymus weight, while 7.5 mg/kg/d of saikosaponin c did not affect body weight gain, or the adrenal or thymus weight in control or dexamethasone-treated rats. A high dose of ACTH induced marked adrenal hypertrophy and thymus atrophy in dexamethasone-treated rats (Table III).

#### Effects of Glycyrrhizin and Glycyrrhetic Acid on the Adrenal and Thymus Weight

Acute treatment with 100 mg/kg of glycyrrhizin induced no increase in plasma corticosterone.<sup>15)</sup> Treatment with 100 mg/kg/d of glycyrrhizin for 4 d also did not affect body weight, the adrenal weight or the thymus weights in control or dexamethasone-treated rats. A high dose of dexamethasone (0.05 mg/kg/d) markedly reduced both adrenal and thymus weights ( $p < 0.001$ ,  $p < 0.001$  vs. saline, Table IV).

In chronic treatment with glycyrrhetic acid, the sapogenin of glycyrrhizin, for 4 d, low doses had no effect, but the high dose (50 mg/kg/d) significantly decreased daily body weight gain and the thymus weight, but it did not induce adrenal hypertrophy as saikosaponin d did. The decrease in body weight gain was accompanied with a decrease in food and water intake (144 g/kg body weight and 210 ml/kg body weight to 71 g/kg and 120 ml/kg, respectively, during the 1st 24 h period, and 141 g/kg and 205 ml/kg to 126 g/kg and 200 ml/kg, respectively, during the 2nd 24 h period).

#### Effect of FAD on the Adrenal and Thymus Weight in Control and Dexamethasone-Treated Rats

In rats treated with 70 mg/kg/d of FAD for 4 d, FAD did not affect body weight gain, and it tended to increase the adrenal weight and to decrease the thymus weight (Table V). In another experiment, treatment with 70 mg/kg/d of FAD induced a decrease in daily body

TABLE IV. Effects of Glycyrrhizin (GL) and Glycyrrhetic Acid (GA) on the Adrenal and Thymus Weight

Treatment <sup>a)</sup> (mg/kg/d × 4 d)	Body weight (g)		Weight (mg/100 g BW) <sup>b)</sup>	
	Initial	Final	Adrenal	Thymus
Saline (6)	106.6 ± 2.5	136.3 ± 4.2	28.0 ± 0.9	390 ± 17
+ GL 100 (6)	107.2 ± 2.2	132.9 ± 2.0	28.9 ± 2.3	342 ± 15 <sup>c)</sup>
Dex 0.05 (6)	108.3 ± 1.8	126.0 ± 2.0	21.6 ± 0.7	183 ± 13
+ GL 100 (6)	107.6 ± 1.6	127.3 ± 2.8	21.5 ± 1.1	193 ± 18
Saline (6)	103.1 ± 2.4	133.0 ± 3.8	30.6 ± 1.6	421 ± 19
+ GA 2 (6)	102.5 ± 2.3	130.3 ± 3.2	32.2 ± 0.5	416 ± 14
+ GA 10 (6)	103.0 ± 3.4	132.6 ± 4.4	32.3 ± 0.9	425 ± 23
+ GA 50 (6)	103.3 ± 3.3	119.4 ± 4.3 <sup>d)</sup>	33.3 ± 1.5	331 ± 32 <sup>d)</sup>

a, b) For details, see Table Ia. c)  $p < 0.1$ , d)  $p < 0.05$ .

TABLE V. Effect of Flavin Adenine Dinucleotide (FAD) on the Adrenal and Thymus Weight

Treatment <sup>a)</sup> (mg/kg/d × 4 d)	Body weight (g)		Weight (mg/100 g BW) <sup>b)</sup>	
	Initial	Final	Adrenal	Thymus
Saline (6)	111.9 ± 2.0	136.2 ± 3.2	28.2 ± 1.1	415 ± 33
+ FAD 70 (6)	111.4 ± 3.0	134.8 ± 2.2	30.3 ± 1.0	347 ± 11 <sup>c)</sup>
Dex 0.05 (6)	113.6 ± 1.9	135.3 ± 2.7	23.7 ± 0.5	226 ± 7
+ FAD 14 (6)	112.0 ± 1.9	127.0 ± 2.7 <sup>c)</sup>	25.3 ± 0.8	237 ± 9
+ FAD 70 (6)	111.1 ± 1.4	126.2 ± 2.5 <sup>d)</sup>	26.8 ± 1.2 <sup>d)</sup>	215 ± 12

a, b) For details, see Table Ia. c)  $p < 0.1$ , d)  $p < 0.05$ .

TABLE VI. Effects of Ginseng Saponin (GS) and Flavin Adenine Dinucleotide (FAD) on the Adrenal and Thymus Weight in Hypophysectomized Rats

Treatment <sup>a)</sup> (mg/kg/d × 5 d)	Body weight (g)		Weight (mg/100 g BW <sup>i</sup> <sup>b)</sup> )	
	Initial	Final	Adrenal	Thymus
Exp. 1				
Saline (7)	130.6 ± 3.8	129.1 ± 4.2	12.3 ± 0.6	256 ± 28
+Sd 2.5 (6)	132.2 ± 2.9	126.1 ± 3.2	12.9 ± 0.4	250 ± 8
+ACTH 0.1 (6)	134.0 ± 3.9	132.3 ± 3.5	16.1 ± 0.6 <sup>f)</sup>	256 ± 18
+Dex 0.025 (7)	130.6 ± 3.9	123.1 ± 3.2	12.2 ± 0.5	139 ± 15 <sup>f)</sup>
Exp. 2 <sup>c)</sup>				
Saline (6)	109.0 ± 3.7	111.4 ± 2.9	13.9 ± 0.5	263 ± 13
+GS 120 (3) <sup>d)</sup>	110.6 ± 5.7	101.5 ± 7.2	15.4 ± 0.4	265 ± 14
+FAD 70 (5)	113.4 ± 1.2	110.9 ± 3.4	15.1 ± 0.2	257 ± 28
+Dex 0.05 (6)	109.9 ± 2.9	107.0 ± 2.3	15.8 ± 0.6 <sup>g)</sup>	125 ± 8 <sup>h)</sup>
+ACTH 0.2 (5) <sup>e)</sup>	109.0 ± 3.0	113.4 ± 1.8	20.8 ± 0.7 <sup>h)</sup>	238 ± 13

*a, b)* For details, see Table Ia. *c)* During conditioning for 7 d, one rat among 35 lost body weight and died. After 7 d of conditioning, 29 rats whose body weights did not increase or decrease markedly during the conditioning were selected among 34 and used. *d)* Fraction 4 saponin. One rat lost body weight and died on day 4. Two rats lost body weight and died on day 5. *e)* One rat among 6 showed a marked decrease of body weight and died on day 5. *f)*  $p < 0.01$ , *g)*  $p < 0.05$ , *h)*  $p < 0.001$ .

weight gain, which was accompanied with a slight decrease in food intake (1st 24 h, 123 g/kg body weight to 115 g/kg; 2nd 24 h, 138 to 141 g/kg; 3rd 24 h, 134 to 110 g/kg). In dexamethasone-treated rats, FAD simultaneously administered with dexamethasone induced a significant decrease in daily body weight gain, and clearly antagonized the atrophic effect of dexamethasone on the adrenals, though it did not affect thymus weight (Table V).

#### Effects of Ginseng Saponin, FAD and Dexamethasone on the Adrenal and Thymus Weight in Hypophysectomized Rats

In hypophysectomized rats, 2.5 mg/kg/d of saikosaponin d did not affect adrenal or thymus weight, but 0.1 mg/kg/d of ACTH markedly increased adrenal weight, whereas in intact rats the former was more effective than the latter (Tables VI, III and Ia). In hypophysectomized rats, treatment with a high dose of ginseng saponin markedly decreased the body weight, as in intact rats. In hypophysectomized rats, a high dose of ginseng saponin or FAD had no effect on adrenal or thymus weight, while in intact rats they markedly decreased the thymus weight (Tables VI, Ia and V). In hypophysectomized rats, a high dose of dexamethasone (0.05 mg/kg/d) did not decrease the adrenal weight, but a low dose decreased the thymus weight, while a high dose of ACTH did not decrease the thymus weight (Table VI).

#### Discussion

Daily treatment with ginseng saponin, saikosaponin d, glycyrrhetic acid, and FAD, but not saikosaponin c or glycyrrhizin, for 4 or 5 d induced thymus atrophy resembling that observed with dexamethasone, and a tendency for adrenal hypertrophy like that caused by ACTH in intact rats. In hypophysectomized rats, however, these effects of ginseng saponin and FAD as well as saikosaponin d were completely lost, whereas the effect of ACTH on the adrenal weight was exaggerated. These results suggested that ginseng saponin and FAD as well as saikosaponin d primarily acted on the hypothalamic-pituitary system to secrete ACTH, which stimulated adrenal growth, and the secretion and synthesis of corticosterone in the adrenal cortex, which ultimately resulted in thymus atrophy.

In the acute experiment, in fact, ginseng saponin increased plasma ACTH and corticosterone,<sup>15)</sup> and adrenal cyclic adenosine monophosphate (cAMP) in intact rats but not in hypophysectomized rats.<sup>27)</sup> These acute and chronic effects of ginseng saponin coincided with those of ginseng extract and saponin reported by Petkov and Staneva,<sup>1)</sup> Kim *et al.*<sup>3)</sup> and Bombardelli *et al.*,<sup>4)</sup> but not with those on the thymus weight reported by Tanizawa *et al.*<sup>5)</sup> or on the adrenal weight found by Brekhman and Dardymov.<sup>2)</sup> In the report of Tanizawa *et al.* the adrenal weight was expressed relative to the adrenal initially excised, but the thymus weight seemed to be expressed as the relative weight with respect to final body weight in cortisone-treated and unilaterally adrenalectomized rats. This may be the main cause of the difference between their results and ours. Brekhman and Dardymov reported that ginseng panaxoside antagonized stress-induced adrenal hypertrophy. In previous papers we showed that saikosaponin d induced secretion of ACTH and corticosterone,<sup>15)</sup> and had a hypertrophic action on the adrenals,<sup>23)</sup> while it was rather atrophic to the adrenals and its action was additive to the atrophic effect of dexamethasone in dexamethasone-treated rats.<sup>23)</sup> Therefore, if ginseng panaxoside, like saikosaponin d, was hypertrophic to the adrenals in non-stressed rats, and if stress markedly stimulated secretion of corticosterone and ACTH, the contradiction can be resolved.

It may be suggested that ginseng saponin and saikosaponin d, which induced secretion of ACTH and corticosterone,<sup>15,17)</sup> stimulated hypertrophy and hyperplasia of the cortex, but not the medulla, of the adrenals through N-terminal peptides of proopiomelanocortin<sup>28)</sup> co-secreted with ACTH from the corticotroph, and that ginseng saponin- and saikosaponin d-induced thymus atrophy resulted from stimulation of the function of the cortex but not the medulla. Tanizawa *et al.* showed in a histological section that ginseng saponin antagonized the cortisone-induced decrease in thickness of the adrenal cortex in a cortisone-treated and unilaterally adrenalectomized rats. In a quantitative histological study Kim *et al.* observed that ginseng extract induced a significant increase in the thickness of the zona fasciculata at the expense of the zona reticularis, while it induced no increase in the adrenal weight and induced an insignificant increase in the thickness of the adrenal cortex.<sup>3)</sup> In the present study, we determined the area of the cortex and medulla of one specified section of the adrenal by a quantitative histological method, and estimated the mean thickness of the cortex in the section, and then the relative thickness of the cortex to the radius of the medulla in the section. The effect of ginseng saponin and saikosaponin d on the histological size of the cortex was determined by this method. From the results it was clear that the ginseng saponin- and saikosaponin d-induced increase in the adrenal weight was accompanied with an increase in the size of the cortex of the adrenals but not the medulla.

In rats treated with glycyrrhizin for 4 d, glycyrrhizin tended to induce thymus atrophy. This result is compatible with the inhibition of  $5\beta$  reduction of corticoids in the liver<sup>9)</sup> and stimulation of the pituitary-adrenal cortex system. However, glycyrrhizin did not induce corticosterone secretion,<sup>15)</sup> so it probably did not induce ACTH secretion. Therefore, the glycyrrhizin-induced tendency for thymus atrophy may be due to inhibition of  $5\beta$ -reductase by glycyrrhizin. In rats treated with glycyrrhetinic acid, glycyrrhetinic acid clearly induced thymus atrophy and a tendency for adrenal hypertrophy. These effects of glycyrrhetinic acid were compatible with both the inhibition of  $5\beta$ -reductase and antigranulomatous action of glycyrrhetinic acid,<sup>11)</sup> but they seemed to reflect stimulation of the pituitary-adrenal cortex system. However, it remains to be determined whether the mechanism of action of glycyrrhetinic acid differs from that of glycyrrhizin.

FAD induced thymus atrophy and a tendency for adrenal hypertrophy in rats not treated with dexamethasone, while it evoked significant adrenal hypertrophy in dexamethasone-treated rats. These effects of FAD disappeared in hypophysectomized rats. The results were in agreement with those of Ono *et al.*<sup>12,13)</sup> This suggested that FAD as well as saikosaponin d

and ginseng saponin acted on the hypothalamic-pituitary system. However, in riboflavin-deficient baboons, Foy *et al.*<sup>29)</sup> observed a decrease in urinary corticosteroids, a markedly diminished response of plasma and urinary steroids to ACTH, and a fibrotic state of the adrenals. This suggested that riboflavin and also FAD have some direct action on the adrenals, which may differ from that of ACTH. Therefore, the mechanism of action of FAD on histological and functional changes in the adrenal cortex remains to be elucidated.

#### References

- 1) W. Petkov and D. Staneva, *Arzneim.-Forsch.*, **13**, 1078 (1963).
- 2) I. I. Brekhman and I. V. Dardymov, *Lloydia*, **32**, 46 (1969).
- 3) C. Kim, C. C. Kim, M. S. Kim, C. Y. Hu and J. S. Rhe, *Lloydia*, **33**, 43 (1970).
- 4) E. Bombardelli, A. Cristoni and A. Lietti, *Proc. Intern. Ginseng Symposium*, **3**, 9 (1980).
- 5) H. Tanizawa, H. Numada, T. Odani, Y. Takino, T. Hayashi and S. Arichi, *Yakugaku Zasshi*, **101**, 169 (1981).
- 6) M. Yamamoto, A. Kumagai and Y. Yamamura, *Arzneim.-Forsch.*, **25**, 1021 (1975).
- 7) H. Abe, M. Sakaguchi and S. Arichi, *Nippon Yakurigaku Zasshi*, **80**, 155 (1982).
- 8) A. Kumagai, S. Yano and M. Otomo, *Endocrinol. Jpn.*, **4**, 17 (1957).
- 9) Y. Tamura, T. Nishikawa, K. Yamada, M. Yamamoto and A. Kumagai, *Arzneim.-Forsch.*, **29**, 647 (1979).
- 10) A. Kumagai, Y. Asano, S. Yano, K. Takeuchi, Y. Morimoto, T. Uemura and Y. Yamamura, *Endocrinol. Jpn.*, **13**, 234 (1966).
- 11) R. S. H. Finney and G. F. Somers, *J. Pharm. Pharmacol.*, **10**, 613 (1958).
- 12) S. Ono, H. Hirano and K. Obara, *J. Nutr. Sci. Vitaminol.*, **19**, 287 (1973).
- 13) S. Ono, S. Hamajima, H. Hirano and K. Obara, *Jpn. J. Exp. Med.*, **44**, 115 (1974).
- 14) S. Hiai, H. Yokoyama, H. Oura and Y. Kawashima, *Chem. Pharm. Bull.*, **31**, 168 (1983).
- 15) S. Hiai, H. Yokoyama, H. Oura and S. Yano, *Endocrinol. Jpn.*, **26**, 661 (1979).
- 16) S. Hiai, H. Yokoyama and H. Oura, *Endocrinol. Jpn.*, **26**, 737 (1979).
- 17) S. Hiai, H. Yokoyama, T. Nagasawa and H. Oura, *Chem. Pharm. Bull.*, **29**, 495 (1981).
- 18) H. Yokoyama, S. Hiai and H. Oura, *Chem. Pharm. Bull.*, **29**, 500 (1981).
- 19) H. Yokoyama, S. Hiai and H. Oura, *Yakugaku Zasshi*, **102**, 1192 (1982).
- 20) H. Yokoyama, S. Hiai, H. Oura and T. Hayashi, *Yakugaku Zasshi*, **102**, 555 (1982).
- 21) S. Hiai, H. Yokoyama and H. Oura, *Proc. Symp. Wakan-Yaku*, **12**, 23 (1979).
- 22) H. Yokoyama, S. Hiai and H. Oura, *Chem. Pharm. Bull.*, **32**, 1224 (1984).
- 23) S. Hiai and H. Yokoyama, *Chem. Pharm. Bull.*, **34**, 1195 (1986).
- 24) Y. Sasayama and H. Takahashi, *Bull. Faculty of Fisheries, Hokkaido University*, **25**, 273 (1975).
- 25) H. Oura, S. Hiai, Y. Odaka and T. Yokozawa, *J. Biochem. (Tokyo)*, **77**, 1057 (1975).
- 26) K. Takagi, *Proc. Intern. Ginseng Symposium*, **1**, 119 (1974).
- 27) S. Hiai, S. Sasaki and H. Oura, *Planta Medica*, **37**, 119 (1979).
- 28) F. E. Estivariz, F. Iturriza, C. McLean, J. Hope and P. J. Lowry, *Nature (London)*, **297**, 419 (1982).
- 29) H. Foy, A. Kondi and Z. H. M. Verjee, *J. Nutr.*, **102**, 571 (1972).

[Chem. Pharm. Bull.]  
35(1) 249—255 (1987)

## The Structure and Physiological Activity of a Glycoprotein Secreted from Conidia of *Mycosphaerella pinodes*. II<sup>1)</sup>

MACHIKO MATSUBARA\* and HISATORA KURODA

*Kobe Women's College of Pharmacy, Motoyama-kita-machi,  
Higashinada-ku, Kobe 658, Japan*

(Received March 17, 1986)

The chemical structure of a glycoprotein secreted from conidia of *Mycosphaerella pinodes* into the medium during germination was investigated, and its elicitor activity to induce pisatin synthesis in peas was examined. The glycoprotein showed a higher elicitor activity than the intra-conidial polysaccharide. The glycoprotein, whose molecular weight is about  $130 \times 10^4$ , has a partial structure in which a reducing terminal mannosyl residue of a trisaccharide  $^1\text{Man}^6 \xrightarrow{\alpha} ^1\text{Man}^6 \xrightarrow{\beta} ^1\text{Glu}$  is *O*-glycosidically attached to serine in the protein portion.

**Keywords**—*Mycosphaerella pinodes*; fungal spore; conidia; glycoprotein; pisatin; phytoalexin; elicitor activity

Plants sometimes synthesize *de novo* antibiotic substances, when exposed to invasion by certain species of microbes. An antibiotic substance accumulated in the plant by this protecting mechanism is called a phytoalexin, while the microbial component which induces its synthesis is called an elicitor. It was shown in the previous paper<sup>1)</sup> that a polysaccharide extracted and purified from conidia of *Mycosphaerella pinodes*, a pathogen of peas causing brown spots, acts as an elicitor for peas to synthesize a phytoalexin, pisatin. Oku *et al.*<sup>2)</sup> have reported that the germinating conidia of this microbe secrete a substance having a higher elicitor activity into the culture medium. The authors, therefore, tried to isolate and elucidate the structure of the elicitor-active substance secreted by the germinating conidia of this microbe into its culture medium.

### Materials and Methods

**Microorganism**—The strain of fungus (*Mycosphaerella pinodes*) and the harvesting procedure of the conidia were as described previously.<sup>1)</sup>

**Germination of Conidia**—Conidia, suspended in a small amount of water, were put on a large Petri dish and allowed to stand at 26°C for 24 h. The germination culture broth was filtered through Toyo No. 5B filter paper and the filtrate was freeze-dried.

**Purification of Glycoprotein**—The freeze-dried substance was dissolved in a small amount of distilled water and subjected to Sepharose 4B column chromatography (2.5 × 40 cm). The column was eluted with distilled water, and fractions (5 ml) were collected. Fractions containing both sugars and proteins simultaneously eluted immediately after the void volume were collected, and freeze-dried. The crude secretion was dissolved in 10 mM phosphate buffer (pH 7.0) and charged on a diethylaminoethyl (DEAE) Sephadex A-50 column (2.5 × 20 cm). The column was eluted with phosphate buffer and fractions (5 ml) were collected. After the removal of non-absorbed materials by washing out with the same buffer, absorbed materials were eluted with the same buffer containing 0.1 M NaCl. The fractions containing both sugars and proteins were collected, freeze-dried and rechromatographed on a Sepharose 4B column (2.5 × 40 cm). The column was eluted with distilled water and fractions (5 ml) were collected. The freeze-dried precipitate served as the glycoprotein fraction, amounting to about 0.20% of the freeze-dried weight of secretion during germination.

**Release of Sugar Chains**—The glycoprotein was dissolved in 0.1 N NaOH at a concentration of 0.03%, the solution was allowed to stand at 26°C for 20 h and, after evaporation, the residue was subjected to Sephadex G-25

column chromatography (2.5 × 25 cm). The column was eluted with distilled water and fractions (5 ml) were collected.

**Determination of Sugar and Protein**—Sugar content was determined by the phenol-sulfuric acid method, and protein content was determined either by measuring the absorbance at 280 nm or by Lowry's method.

**Electrophoresis**—i) Paper Electrophoresis: The same procedures as reported in the previous paper<sup>1)</sup> were employed.

ii) Disk Electrophoresis: A well known method described in a technical book<sup>3)</sup> was employed. For staining sugar and protein, Schiff's reagent and 1% amide black 10B, respectively, were used.

**Paper Chromatography**—The filter paper sheet (Whatman No. 1) was developed with *n*-BuOH-pyridine-H<sub>2</sub>O (6:4:3). The spots were made visible by heating the paper after spraying with aniline hydrogen phthalic acid.

**Methylation Analysis**—The same method as reported in the previous paper<sup>1)</sup> was used.

**Enzyme Digestion**—The same method as reported in the previous paper<sup>1)</sup> was used. The reaction conditions of  $\beta$ -glucosidase were as follows: substrate, 1.0 mg;  $\beta$ -glucosidase (from almonds, Sigma) 1.0 mg; 0.05 M acetate buffer (pH 5.25), 0.5 ml; 37 °C for 18 h.

**Amino Acid Analysis**—A portion of the glycoprotein was hydrolyzed by heating in a sealed tube with 6 N HCl at 105 °C for 24 h and analyzed for amino acid composition. Another portion was mixed with 0.1 N NaOH and allowed to stand at 26 °C for 20 h to release sugar-chains, and, after being neutralized, was hydrolyzed in a similar way and analyzed. The amino acid analysis was conducted using a Hitachi 835-30 amino acid analyzer.

**Measurement of Molecular Weight**—The molecular weight was measured by gel filtration using Sepharose 4B and Sephadex G-10 columns as shown in Figs. 3 and 4. Field desorption-mass spectrum (FD-MS) was also used. FD-MS analysis was carried out in a Hitachi M-80 apparatus with a carbon emitter at 20 mA.

**Methanolysis, Reduction and Acetylation**—A sample was methanolized with 5% HCl in MeOH in a sealed tube at 100 °C for 5 h. HCl was removed by evaporation with toluene-ethanol (1:1). The methanolized sample was then dissolved in distilled water (1 mg/250  $\mu$ l), and a 50  $\mu$ l aliquot was mixed with 0.22 M NaBH<sub>4</sub> (50  $\mu$ l) and allowed to stand at 26 °C for 3 h. Excess NaBH<sub>4</sub> was decomposed with AcOH, then MeOH was added, and AcOH was removed by evaporation. The dried sample was acetylated by heating with 50  $\mu$ l of pyridine and 50  $\mu$ l of anhydrous acetic acid at 100 °C for 30 min.

**Gas Chromatography and GLC-MS Analysis**—The methanolized and acetylated sample was analyzed for sugar composition by gas liquid chromatography (GLC). The chromatographic conditions were as follows: column length, 3 mm × 1.0 m; column temp., 150 °C (1 min) then 1 °C/min to max. 200 °C; packing, 5% SE-30 on Shimalite W; N<sub>2</sub> flow rate, 40 ml/min; detector, flame ionization detector (FID); detector temp., 250 °C; injection temp., 250 °C; H<sub>2</sub> flow rate, 40 ml/min. On GLC analysis, methyl 2,3,4,6-tetra-*O*-acetyl mannoside (*t*<sub>R</sub>: 30 min) and methyl 2,3,4,6-tetra-*O*-acetyl glucoside (*t*<sub>R</sub>: 31.2 min) were identified. For analysis of the methylated sugar, an aliquot of the methylated oligosaccharide, after hydrolysis with 1.5 N HCl at 100 °C for 4 h, was reduced, acetylated and then subjected to GLC under the conditions shown in Fig. 6. Another aliquot was used for GLC-MS analysis (JMS-OISG, Nihon Denshi Co.). For examination of the bonding of the sugars to the protein, the glycoprotein sample was divided into two portions. One portion, after the sugar chains had been released by alkali treatment, was reduced, methanolized and acetylated, and then subjected to GLC under the conditions shown in Fig. 5. The other portion was subjected to GLC after reduction, alkali treatment, methanolysis and acetylation in the order mentioned.

**Elicitor Activity**—The activity was measured under the conditions shown in Chart 1.

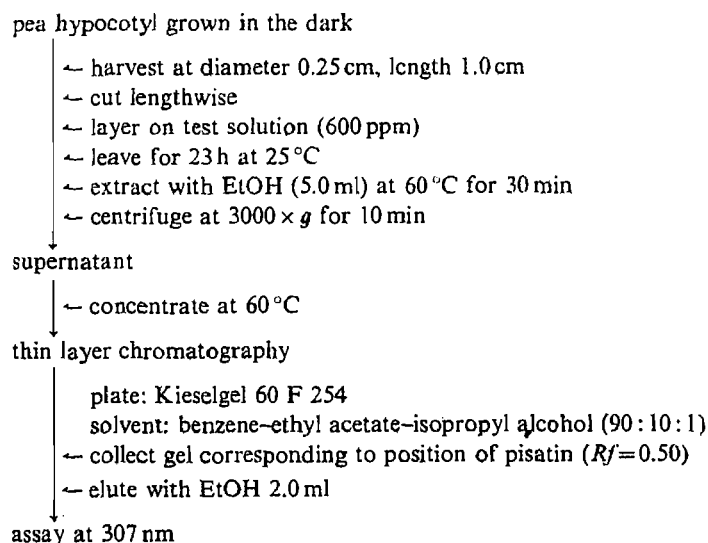


Chart 1. Method of Bioassay for Elicitor Activity

### Results and Discussion

Figure 1 shows a Sepharose 4B column chromatogram of the glycoprotein from culture filtrate of the germinating *M. pinodes* conidia. Fractions in which sugars and proteins coexisted were collected (Nos. 11—16) and assayed for elicitor activity. The results are presented in Table I. The activity of glycoprotein from germinating conidia was about 6.5 times higher than that of the intraconidial polysaccharide.<sup>1)</sup> Thus, a chemical structural analysis of the substances contained in this fraction was undertaken. This fraction gave a single spot in high-pressure paper electrophoresis and also gave a single band at the same position in disk electrophoresis after being stained with Schiff's reagent or with 1% amide black 10 B, respectively, suggesting that the chemical nature of the substance in this fraction is glycoprotein. The optical rotation was  $[\alpha]_D^{25} - 122^\circ$  ( $c=1$ , water). The ratio of the sugar moiety to the protein moiety of this glycoprotein was determined to be 1:2.8. For the purpose of estimating the linkages of this glycoprotein, it was dissolved in 0.1N NaOH to give a concentration of 0.02% and the change of OD at 241 nm during standing at 26°C was followed. An *O*-glycosidic glycoprotein, under weakly alkaline conditions, readily undergoes a  $\beta$ -elimination reaction releasing sugar chains, whereby double bonds are newly formed at the linking sites of the protein portion, resulting in an increased absorbance at 241 nm. As can be seen in Fig. 2, the absorbance at 241 nm of the weakly alkaline solution of this glycoprotein continued to increase over a period of about 17 h. No glycoprotein was detected when this substance was subjected to disk electrophoresis after treatment with alkali for 20 h. Therefore, all the sugar-chain portion of this glycoprotein is *O*-glycosidically linked to the protein. The molecular weight was estimated to be about  $1.3 \times 10^6$  by gel filtration. On GLC analysis after methanolysis, mannose ( $t_R$ : 30 min) and glucose ( $t_R$ : 31.2 min) were detected in the ratio of

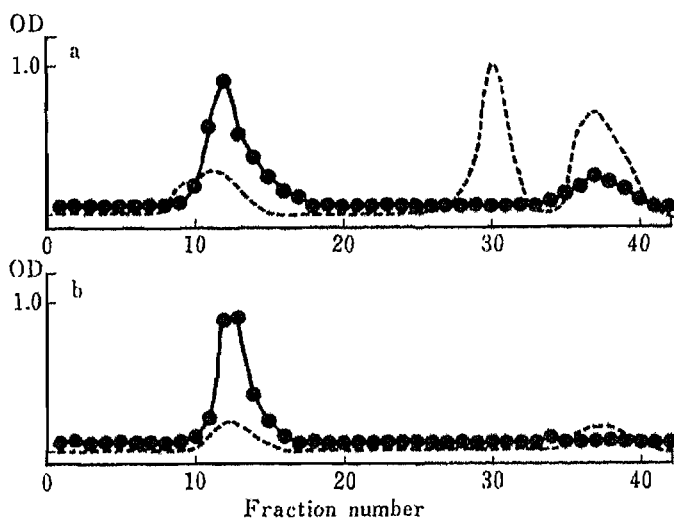


Fig. 1. Sepharose 4B Column Chromatography of the Crude and Purified Secreted Materials from Conidia

a, crude material; b, purified material. The column ( $2.5 \times 40$  cm) was eluted with distilled water and fractions (5 ml) were collected. Carbohydrate contents were determined by the phenol- $H_2SO_4$  method ( $\bullet \cdots \bullet$ ). Protein contents were determined by measuring  $OD_{280}$  ( $-\cdots-$ ).

TABLE I. Elicitor Activities of Glycoprotein Fractions Obtained from Conidia of *Mycosphaerella pinodes*

Fraction	Accumulated pisatin $\mu\text{g}/\text{cm}^2$ hypocotyl
$H_2O$ (control)	17.9
Endogenous polysaccharide of conidia	37.4
Secreted glycoprotein from germinating conidia	241.1

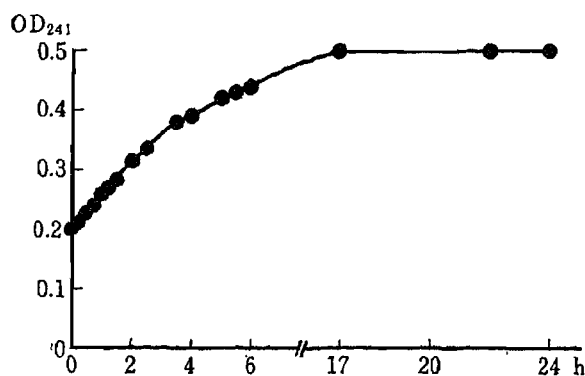


Fig. 2. Change of OD<sub>241</sub> of Glycoprotein on Treatment with Alkali

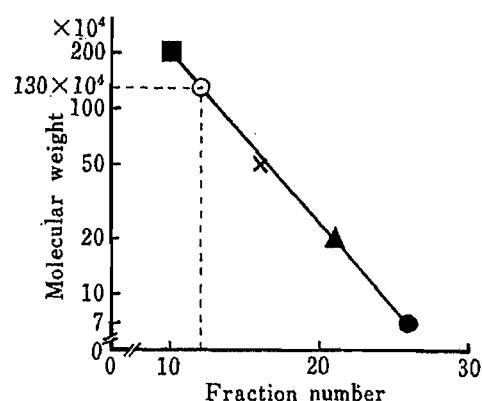


Fig. 3. Estimation of the Molecular Weight of the Glycoprotein by Column Chromatography

Glycoprotein (○) and dextran [■,  $M_r$  200 × 10<sup>4</sup>]; (×,  $M_r$  50 × 10<sup>4</sup>); (▲,  $M_r$  20 × 10<sup>4</sup>), (●,  $M_r$  7 × 10<sup>4</sup>)] were placed on a Sepharose 4B column (2.5 × 40 cm, 5 ml). Eluted compounds were detected by the phenol-H<sub>2</sub>SO<sub>4</sub> method.

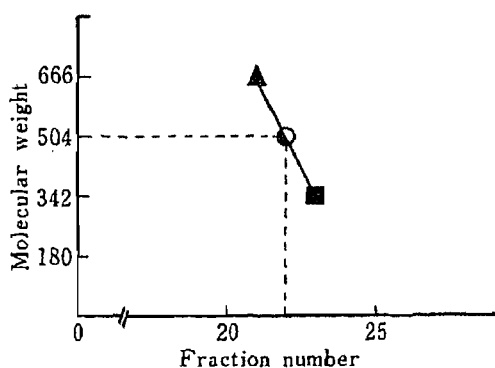


Fig. 4. Estimation of the Molecular Weight of the Oligosaccharide by Column Chromatography

Oligosaccharide (●), maltotetraose (▲), maltotriose (○) and gentiobiose (■) were placed on a Sephadex G-10 column (2 × 38 cm, 2.5 ml). Eluted compounds were detected by the phenol-H<sub>2</sub>SO<sub>4</sub> method.

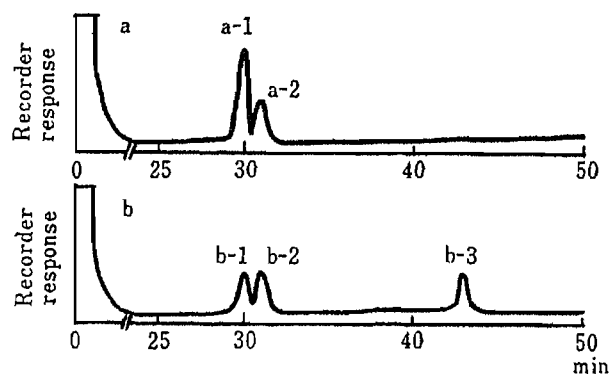


Fig. 5. Gas Chromatogram of Oligosaccharide Released from the Glycoprotein

Conditions: column length, 3 mm × 1.0 m; column temp., 150 °C (1 min) then 1 °C/min to max. 200 °C; packing, 5% SE-30 on Shimalite W; N<sub>2</sub> flow rate, 40 ml/min; detector, FID; detector temp., 250 °C; injection temp., 250 °C; H<sub>2</sub> flow rate, 40 ml/min.

Peaks: a-1, b-1, methyl 2,3,4,6-tetra-*O*-acetyl mannoside; a-2, b-2, methyl 2,3,4,6-tetra-*O*-acetyl glucoside; b-3, 1,2,3,4,6-penta-*O*-acetyl mannitol.

Retention times (min): a-1, b-1, 30; a-2, b-2, 31.2; b-3, 43. The following acetylated sugars were prepared by the same procedure for use as authentic compounds: glucose, mannose, sorbitol, mannitol. Before acetylation, authentic glucose and mannose were heat-treated with 5% HCl in MeOH in a sealed tube at 100 °C for 4 h.

2:1.

Next, for the purpose of clarifying the sugar-chain structure, the glycoprotein was treated with alkali and its sugar-chain portion was fractionated by Sephadex G-25 column chromatography. Sugars were eluted in fractions Nos. 8—10 as a single peak. On paper chromatographic analysis after concentration, this fraction gave a single spot. To investigate the sugar composition of this fraction, GLC analysis was performed after methanolysis. Only mannose and glucose were detected in the ratio of 2:1. The molecular weight of the sugar-chain portion was measured by gel filtration (Fig. 4), and the results indicated that the sugar-



chain portion is a trisaccharide. This was further supported by the presence of a cluster ion peak  $(M+Na)^+$  at  $527 m/z$  in the FD-MS. These results indicated that the sugar-chain is composed of two mannose residues and one glucose residue.

Figure 5 shows the results of an experiment to clarify the sugars involved in linking to the protein portion. Figure 5a is a gas chromatogram of the products derived from the glycoprotein by reduction, alkali treatment, methanolysis and acetylation in the order described. Peaks corresponding to mannose and glucose were detected in the ratio of 2:1. Figure 5b illustrates, on the other hand, a chromatogram of the glycoprotein which had been subjected to alkali treatment in the presence of  $NaBH_4$ , methanolysis and acetylation in the order mentioned. Three peaks, each corresponding to mannose, glucose and mannitol, were detected in the ratio of 1:1:1. It was clarified from these results that the sugar was *O*-glycosidically attached to the protein at the OH group linked to  $C_1$  of the mannose molecule.

Then, to identify the non-reducing terminal group of the sugar chain, sugars released by the action of each of the *exo*-enzymes ( $\alpha$ -glucosidase,  $\beta$ -glucosidase and  $\alpha$ -mannosidase) were investigated. Glucose was released only when  $\beta$ -glucosidase was applied. This finding indicates that the non-reducing terminal molecule of the sugar chain is  $\beta$ -glucose. The infrared (IR) spectrum (Nujol) of the sugar chain exhibited an absorbance derived from  $\alpha$ -D-mannopyranose at about  $810 cm^{-1}$ . Thus the  $\alpha$ -type linkage of mannose was indicated. In order to determine the linkage sites of the sugar chain, GLC-MS analysis was carried out on the sugar chain which had undergone methylation, hydrolysis, reduction and acetylation in the order given. The gas chromatogram obtained is illustrated in Fig. 6. The substance derived from each peak gave the mass spectrum as presented in Fig. 7. By comparing the spectra with those of authentic methylated derivatives and also by referring to the data of Björndal *et al.*,<sup>4)</sup> the substance in peak b was identified as 2,3,4-Me<sub>3</sub> mannitol. As for peak a, whether it was derived from non-reducing terminal glucose or mannose could not be determined from the

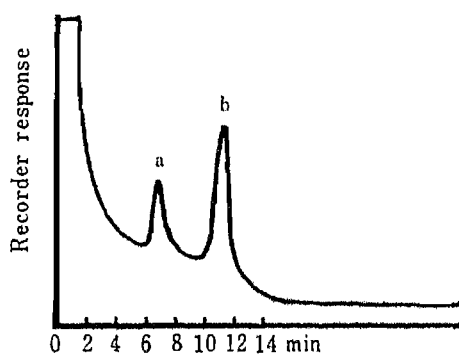


Fig. 6. Gas Chromatogram of Methylated Sugars Derived from Permethylated Oligosaccharide

Conditions: column length, 3 mm  $\times$  1.0 m; column temp., 180°C; packing, 1.5% NGS on Chromosorb W;  $N_2$  flow rate, 25 ml/min; detector, FID; detector temp., 230°C; injection temp., 230°C;  $H_2$  flow rate, 35 ml/min. Peaks: a, 2,3,4,6-Me<sub>4</sub> sorbitol; b, 2,3,4-Me<sub>3</sub> mannitol. Retention times (min): a, 7.2; b, 11.5. The following sugars were methylated by the same procedure to obtain authentic compounds: glucose, mannose, gentiobiose, kojibiose, cellobiose, laminarin, glycogen, mannan from *S. cerevisiae*.

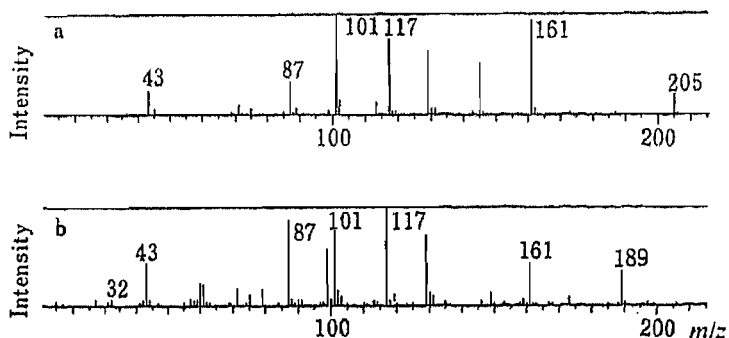


Fig. 7. GLC-MS of Methylated Sugars Derived from Permethylated Oligosaccharide

a, MS of 2,3,4,6-Me<sub>4</sub> sorbitol; b, MS of 2,3,4-Me<sub>3</sub> mannitol.

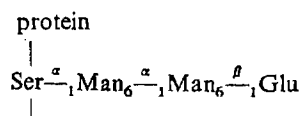


Fig. 8. Probable Structure of Glycoprotein in *Mycosphaerella pinodes*

TABLE II. Amino Acid Composition of the Glycoprotein

Amino acid	Molar ratio (untreated)	Treated with alkali/untreated
Aspartate	4.2	1.1
Threonine	4.0	0.8
Serine	5.2	0.4
Glutamate	1.0	1.0
Proline	9.0	1.0
Glycine	5.4	1.1
Alanine	4.9	1.0
Valine	4.7	1.0
Isoleucine	3.9	0.9
Leucine	6.1	1.0
Phenylalanine	0.6	1.0
NH <sub>3</sub>	23.0	1.2
Arginine	0.4	1.1
Tyrosine	Trace	
Lysine	Trace	
Histidine	Trace	

mass spectral data (Fig. 7). However, from the findings that an enzymic reaction yielded glucose as a non-reducing terminal molecule, and that the sugar chain is composed of glucose and mannose in the ratio of 1 : 2, peak a was assigned to 2,3,4,6-Me<sub>4</sub> sorbitol.

Table II presents the amino acid composition of the glycoprotein (alkali-untreated), and the composition ratios of amino acids before and after alkali treatment. Among the amino acids composing the glycoprotein, proline is contained in the largest quantity, followed by leucine, glycine, serine and alanine in the order given. The content of the amino acids involved in the linkage to sugars, after alkali treatment, is expected to decrease significantly, because those amino acids would be converted to the corresponding keto-acids. This is found to be the case for serine in Table II, which shows a marked alteration in the ratio. Based on the results described above, a probable structure of this glycoprotein is as illustrated in Fig. 8.

It is generally accepted that, in most of the *O*-glycosidic type glycoproteins occurring in nature, the sugar directly linked to the protein portion is *N*-acetylgalactosamine. In this case, however, no *N*-acetylgalactosamine was detected in the sugar-chain hydrolysate, and alkaline hydrolysis in the presence of NaBH<sub>4</sub> gave mannitol as the only sugar alcohol. It has been reported that mannosyl-serine linkages can be found in yeast cell wall mannan and yeast invertase, whereas a mannosyl-threonine linkage is present in a mycotoxin peptide.<sup>5)</sup> Pazur *et al.*<sup>6)</sup> and Lineback,<sup>7)</sup> too, have reported the presence of mannose-serine or mannose-threonine linkages in a fungal glycoamylase.

Albersheim *et al.*<sup>8)</sup> have recently isolated a hexa( $\beta$ -D-glucopyranosyl)-D-glucitol from the cell wall of *Phytophthora megasperma* var. *sojae* and found that it possesses a high elicitor activity. This heptaglucoside is composed of five  $\beta$ -1,6-glucosidically linked glucosyl residues as a main chain and two  $\beta$ -1,3-glucosidically linked side chains branching from the second and fourth glucosyl residues of the main chain. They proposed that a signal for initiation of phytoalexin synthesis arises from the reaction of this glucan with receptors on the surface layer of the soybean leaf cells, and they claimed that heptaglucosides which have side chains at

positions other than the second and fourth glucosyl residues cannot react with the receptors.

If such a mechanism can also be applied to the induction of pisatin synthesis in peas, then the reaction of receptors scattered on the surface of cells with the side chains branching at appropriate intervals from the main chain of the interconidial polysaccharide,<sup>1)</sup> or the glycoprotein, may be a signal for pisatin synthesis. In order to confirm this assumption, it seems necessary to perform further comparative investigations on the elicitor activities of various compounds having side sugar chains branching from the main polysaccharide or the protein at different intervals.

#### References and Notes

- 1) M. Matsubara and H. Kuroda, *Chem. Pharm. Bull.*, **34**, 3306 (1986).
- 2) T. Shiraishi, H. Oku, M. Yamashita and S. Ouchi, *Ann. Phytopath. Soc. Japan*, **44**, 659 (1978).
- 3) Z. Ogita and S. Nakamura, "Denkieido Jikkenho," Bunkodo, Tokyo, 1969, pp. 262—274.
- 4) H. Björndal, B. Lindberg and S. Svensson, *Carbohydr. Res.*, **5**, 433 (1967).
- 5) N. Sharon (translated into Japanese by T. Osawa), "Fukugo Toshitsu," Gakkai Shupansenta, Tokyo, 1977, pp. 39—49.
- 6) J. H. Pazur, H. R. Knull and D. L. Simpson, *Biochem. Biophys. Res. Commun.*, **40**, 110 (1970).
- 7) D. R. Lineback, *Carbohydr. Res.*, **7**, 106 (1968).
- 8) J. K. Sharp, B. Valent and P. Albersheim, *J. Biol. Chem.*, **259**, 11312 (1984); J. K. Sharp, M. McNeil and P. Albersheim, *ibid.*, **259**, 11321 (1984).

[Chem. Pharm. Bull.  
35(1) 256-261 (1987)]

## Photoaffinity Labeling of a $\delta$ -Receptor Component of NG 108-15 Cells with a New Enkephalin Analog<sup>1)</sup>

KUNIO OKUMURA, YASUMARU HATANAKA, HITOSHI NAKAYAMA  
and YUICHI KANAOKA\*

Faculty of Pharmaceutical Sciences, Hokkaido University,  
Sapporo 060, Japan

(Received May 19, 1986)

A new leucine-enkephalin analog containing *p*-azidophenylalanine was synthesized. It binds to the  $\delta$ -opioid receptors of NG 108-15 cells with high affinity. Iodination of the compound decreased the affinity by 5 times, but the iodinated derivative still retains significant binding activity to the cells. Photochemical reactions revealed that the derivative predominantly labeled a 58 kilodaltons (kDa) polypeptide in the cells (possibly a  $\delta$ -receptor component).

**Keywords**—photoaffinity labeling;  $\delta$ -opioid receptor; NG 108-15 cell; enkephalin analog; polypeptide

It has been well established, by pharmacological and by receptor-radioligand binding approaches, that the endogenous opioid peptides interact with at least three types of putative receptors ( $\mu$ ,  $\delta$ , and  $\kappa$ ).<sup>2)</sup> Relatively little is known, however, about the molecular constituents of such receptors, although several pioneering studies were made by solubilization and affinity purification<sup>3-6)</sup> and by affinity labeling.<sup>7)</sup> The photoaffinity labeling technique has been widely used in studies of a variety of biomolecules<sup>8)</sup> and has been quite useful in the case of

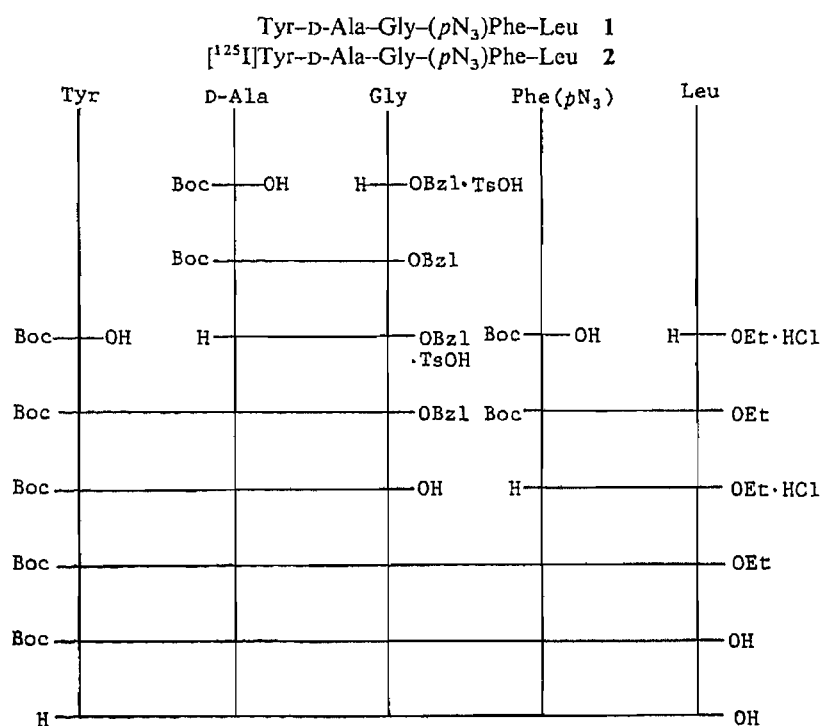


Chart 1. A Synthetic Route for Tyr-D-Ala-Gly-(*p*N<sub>3</sub>)Phe-Leu

transmembrane receptor systems.<sup>9)</sup> As an example of its application to the opioid receptor, we previously reported<sup>10)</sup> an enkephalin analog photoaffinity reagent, [D-Ala<sup>2</sup>, Leu<sup>5</sup>]enkephalin *N*-[(2-nitro-4-phenyl)-amino]ethylamide, which labels opioid receptors of  $\mu$ -type as well as  $\delta$ -type, in accord with the findings<sup>11,12)</sup> that carboxyl-terminal modification of leucine-enkephalin destroys the  $\delta$ -selectivity to elicit rather a  $\mu$ - and  $\delta$ -preference. As a logical extension of that work, we describe here the synthesis of new photoactivable leucine-enkephalin analogs of carboxyl terminal-free ([D-Ala<sup>2</sup>, (*p*N<sub>3</sub>)Phe<sup>4</sup>, Leu<sup>5</sup>]enkephalin **1** and its iodinated derivative **2**) as well as their binding properties, and a successful covalent labeling of  $\delta$ -receptor protein in a neuronal hybrid cell line (NG 108-15) with **2**.

### Experimental

[D-Ala<sup>2</sup>, (*p*N<sub>3</sub>)Phe<sup>4</sup>, Leu<sup>5</sup>] **1** was synthesized by conventional solution methods employing (3+2) fragment condensation (Chart 1).

**Boc-(*p*N<sub>3</sub>)Phe-Leu-OEt (3)**—Boc-(*p*N<sub>3</sub>)Phe-OH<sup>(13,14)</sup> (3.06 g, 10 mmol) was dissolved in THF (10 ml) containing *N*-methylmorpholine (1.01 g, 10 mmol), and then BCC (1.37 g, 10 mmol) was added to the solution under cooling at  $-15^{\circ}\text{C}$ . After 10 min, the mixture was added to a chilled THF solution of Leu-OEt·HCl (1.96 g, 10 mmol) and *N*-methylmorpholine (1.01 g, 10 mmol) under stirring. The reaction mixture was stirred at  $-15^{\circ}\text{C}$  for 1 h and then at room temperature for 2 h. The mixture was concentrated *in vacuo* and the residue was dissolved in AcOEt; the AcOEt layer was washed successively with 10% citric acid, 4% NaHCO<sub>3</sub>, and H<sub>2</sub>O-NaCl, dried over Na<sub>2</sub>SO<sub>4</sub> and then concentrated *in vacuo*. The residue was crystallized from Et<sub>2</sub>O-pet. ether; yield 4.14 g (93%), yellowish prisms, mp 106–108°C,  $[\alpha]_{\text{D}}^{20} -6.2$  ( $c=1$ , MeOH). *Anal.* Calcd for C<sub>22</sub>H<sub>15</sub>N<sub>3</sub>O<sub>5</sub>: C, 59.04; H, 7.43; N, 15.65. Found: C, 59.18; H, 7.43; N, 15.57. IR (Nujol): 3300, 2100, 1720 cm<sup>-1</sup>.

**Boc-Tyr-D-Ala-Gly-(*p*N<sub>3</sub>)Phe-Leu-OEt (4)**—Boc-(*p*N<sub>3</sub>)Phe-Leu-OEt (3) (1.79 g, 4 mmol) was treated with 5N HCl-AcOEt (4 ml, 20 mmol) for 4 h at room temperature. After the mixture was concentrated *in vacuo*, the residue was dried *in vacuo* over KOH pellets and dissolved in THF (15 ml) containing *N*-methylmorpholine (404 mg, 4 mmol) at  $-15^{\circ}\text{C}$ . By addition of Boc-Tyr-D-Ala-Gly-OH<sup>(15)</sup> (1.64 g, 4 mmol), peptide coupling was performed as in the case of the preparation of **3**, to give **4**, which was recrystallized from AcOEt-Et<sub>2</sub>O; yield 2.66 g (90%), pale yellow powder, mp 112–114°C (dec.),  $[\alpha]_{\text{D}}^{20} +15.3$  ( $c=1$ , MeOH). *Anal.* Calcd for C<sub>36</sub>H<sub>50</sub>N<sub>8</sub>O<sub>9</sub>: C, 58.52; H, 6.82; N, 15.17. Found: C, 58.38; H, 6.76; N, 15.09. IR (Nujol): 3300, 2130, 1730 cm<sup>-1</sup>.

**Tyr-D-Ala-Gly-(*p*N<sub>3</sub>)Phe-Leu ([D-Ala<sup>2</sup>, (*p*N<sub>3</sub>)Phe<sup>4</sup>, Leu<sup>5</sup>]enkephalin (1))**—The protected peptide **4** (738 mg, 1 mmol) was hydrolyzed with 1N NaOH (2.1 ml) in MeOH for 1.5 h at room temperature. After the solution was concentrated *in vacuo*, 5 ml of water was added, followed by acidification with 10% citric acid. The product was extracted with AcOEt; the AcOEt layer was washed with H<sub>2</sub>O-NaCl, dried over Na<sub>2</sub>SO<sub>4</sub> and then concentrated *in vacuo*. The residue was treated with 2N HCl-AcOEt (5 ml, 10 mmol) for 1 h at room temperature. After concentration *in vacuo*, the residual material was washed thoroughly with Et<sub>2</sub>O, followed by column chromatography on silica using CHCl<sub>3</sub>-MeOH (2:1) as an eluent; yield 520 mg (75%, recrystallized from 50% aqueous MeOH), pale-yellow fine needles, mp 172–175°C (dec.),  $[\alpha]_{\text{D}}^{20} +81.5$  ( $c=1$ , H<sub>2</sub>O). *Anal.* Calcd for C<sub>29</sub>H<sub>38</sub>N<sub>8</sub>O<sub>7</sub>·1/2H<sub>2</sub>O: C, 53.12; H, 6.61; N, 17.09. Found: C, 53.33; H, 6.31; N, 17.25. IR (Nujol): 3240, 3000, 2130 cm<sup>-1</sup>.

**Iodination of 1**—Lactoperoxidase (1  $\mu\text{g}$ , Boehringer #107174), Na<sup>[125I]</sup> (1.6 mCi, 0.8 nmol; Amersham), and NaI (1.2  $\mu\text{g}$ , 8 nmol) were added to a 100  $\mu\text{l}$  solution of the enkephalin (**1**) (10  $\mu\text{g}$ , 15 nmol), to make 134  $\mu\text{l}$  of 0.1 M sodium acetate buffer (pH 5.6) in a polypropylene tube. Then 3  $\mu\text{l}$  of H<sub>2</sub>O<sub>2</sub> (0.02% solution) was added twice at 10 min intervals, and the mixture was allowed to stand for 10 min at room temperature. Monoiodinated derivative (**2**) was purified on a Biogel P-2 column (0.8 × 14 cm); it was eluted just after the non-iodinated **1** with 1 mM AcOH. The specific radioactivity was 115  $\mu\text{Ci/nmol}$ . Two other derivatives of **2** with lower radioactivity (14  $\mu\text{Ci/nmol}$ ) and no radioactivity, were similarly prepared for use in binding experiments.

**Cells**—NG 108-15 neuroblastoma-glioma hybrid cells, a generous gift from Dr. T. Amano of Mitsubishi-Kasei Institute for Life Science, were grown as described.<sup>16,17)</sup> The confluent cells were harvested in Dulbecco's phosphate-buffered saline [137 mM NaCl, 5.4 mM KCl, 7.76 mM Na<sub>2</sub>HPO<sub>4</sub>, 1.47 mM KH<sub>2</sub>PO<sub>4</sub>], followed by centrifugation at 100 × *g* for 5 min. The pellet was resuspended in a 25 mM Tris-HCl (pH 7.5) buffer containing 0.3 M sucrose (1–3 × 10<sup>6</sup> cells/ml), and used for experiments.

**Binding Experiment in the Dark**—(i) Competition Assay: One milliliter of cell suspension (3 × 10<sup>6</sup> cells) was incubated with 10  $\mu\text{l}$  of [<sup>3</sup>H]DADLE (40 Ci/mmol; NEN) at the fixed concentration of 2 nM in the presence of various concentrations of **1**. Bacitracin (0.1 mg/ml) was added to the incubation mixture and the whole was incubated at 25°C for 30 min in the dark. Then 0.4 ml aliquots were removed (in duplicate) and filtered through Whatman GF/C filter paper under vacuum. The filter paper was quickly washed three times with 2 ml of ice-cold buffer (25 mM Tris-HCl, pH 7.5 containing 0.3 M sucrose), then transferred to a scintillation vial where the radioactivity was measured after mixing with 10 ml of scintillation cocktail (ACS-II; Amersham) and 1 ml of 10% Triton X-100. Nonspecific binding

was determined in the presence of a large excess ( $1 \mu\text{M}$ ) of DALE.

ii) Direct Binding Assay of 2: Various concentrations of 2 ( $14 \mu\text{Ci/nmol}$ ) were added to 1 ml of cell suspension ( $1.5 \times 10^6$  cells) with or without  $1 \mu\text{M}$  of DALE. Bacitracin was included ( $0.1 \text{ mg/ml}$ ) and the sample was incubated at  $25^\circ\text{C}$  for 30 min in the dark. Filtration ( $0.4 \text{ ml}$  aliquots in duplicate) was performed as in (i) and the filter paper was counted in a Packard 5230  $\gamma$ -counter. The specific binding of 2 to the cells was calculated from the difference between total binding and nonspecific binding in the absence and presence of DALE, respectively.

**Photolabeling of Cells**—After preincubation of cell suspension ( $9 \times 10^5$  cells/ml) with  $28 \text{ nM}$  2 ( $115 \mu\text{Ci/nmol}$ ) in the presence of bacitracin ( $0.1 \text{ mg/ml}$ ) at  $25^\circ\text{C}$  for 15 min, the mixture was placed on ice and irradiated with a 100 W low-pressure Hg lamp at a 15 cm distance for 2 min. The irradiated sample was then transferred into a 1.5 ml polypropylene tube and centrifuged at  $150 \times g$  for 5 min. After three cycles of washing and centrifuging, the pellet was solubilized with  $250 \mu\text{l}$  of solubilizing solution [3% SDS, 62.5 mM Tris-HCl (pH 6.8), 10% glycerol, 0.75% DTT] at  $100^\circ\text{C}$  for 5 min and subjected to gel electrophoresis. As a control, nonspecific photolabeling was carried out similarly except for the addition of DALE ( $10 \mu\text{M}$ ) to the preincubation mixture.

**Gel Electrophoresis**—SDS-polyacrylamide gel electrophoresis was performed by a modification of the reported method.<sup>18)</sup> Disc gels ( $0.7 \times 13 \text{ cm}$ ) were prepared as 10% polyacrylamide and the solubilized samples ( $250 \mu\text{l}$ ) described above were applied to upper gels of 3% polyacrylamide. After electrophoresis at  $1.5 \text{ mA/tube}$ , the gels were stained in 0.25% Coomassie blue R-250, 50% MeOH and 10% AcOH for 1 h, then destained in 25% 2-propanol and 10% AcOH. The gels were sliced at 1 mm thickness and each slice was counted in a Packard  $\gamma$ -counter. Protein molecular weight on the gel was estimated by the use of standard proteins (BioRad) simultaneously electrophoresed.

**Protein Concentration**—Protein concentration was determined by Peterson's modification<sup>19)</sup> of the Lowry method, with bovine serum albumin as standard.

## Results and Discussion

### Photolysis of 1

The photoactivable enkephalin analog 1 has an absorption maximum at  $252 \text{ nm}$  ( $\epsilon = 15500$ ). When 1 ( $23 \mu\text{M}$ ) was photolyzed with a 100 W low-pressure Hg lamp (which has its main output near  $254 \text{ nm}$ ), the absorption peak at  $252 \text{ nm}$  disappeared after 1 min at  $0^\circ\text{C}$  (Fig. 1). Under the irradiation conditions, more than 95% of the [ $^3\text{H}$ ]DADLE binding activity of NG 108-15 cells was retained in the absence of 1, and we concluded that this irradiation essentially did not affect the enkephalin binding activity of the cells.

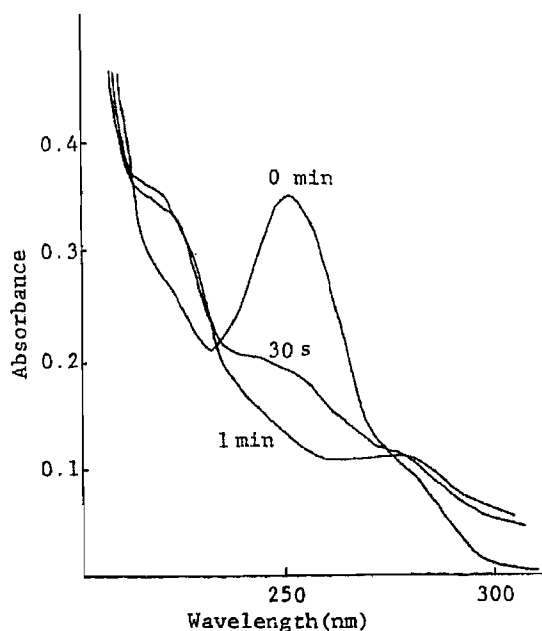


Fig. 1. Absorption Spectra of 1 before and after Photolysis

Compound 1 ( $23 \mu\text{M}$ ) in water was photolyzed with a 100 W low-pressure Hg lamp.

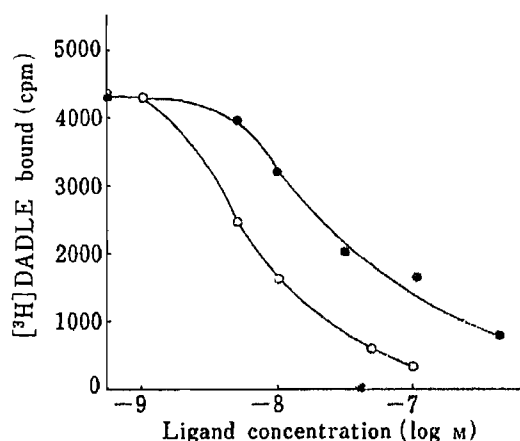


Fig. 2. Displacement Curves of 1 (O) and Its Non-radioactively Iodinated Derivative (●), Using  $2 \text{ nM}$  [ $^3\text{H}$ ]DADLE as a Radioligand

### Binding of **1** and Its Iodinated Derivatives to Cultured NG 108-15 Cells in the Dark

Binding of **1** to the opioid receptors of NG 108-15 cells is of high affinity ( $IC_{50} = 5.4$  nM) and is competitive with respect to [ $^3$ H]-DADLE (Fig. 2). The  $K_d$  value was calculated as 3.0 nM from the following equation<sup>20)</sup>:

$$IC_{50} = K_d (1 + [L]/K_L)$$

where  $IC_{50} = 5.4$  nM,  $[L]$  represents the concentration of [ $^3$ H]DADLE used (2 nM) and  $K_L$  is the dissociation constant of [ $^3$ H]DADLE (2.5 nM, obtained from a separate experiment; this agrees well with the value reported by Gerber *et al.*<sup>16)</sup>). The  $K_d$  obtained was very close to that of DALE,<sup>21)</sup> which indicates that the introduction of an azido group into the Phe<sup>4</sup> of DALE does not much change its binding affinity to the cells. Although iodination of **1** decreases the affinity by 5 times ( $IC_{50} = 29$  nM, therefore  $K_d = 16$  nM by calculation), the iodinated **1** still retains binding activity (Fig. 2). This was confirmed by using **2**, a radioiodinated derivative of **1**, in a direct binding assay. Figure 3 shows that **2** binds to the cells in a saturable manner. A Scatchard plot of the specific binding (Fig. 4) is linear, suggesting homogeneous binding of compound **2** to the cells, and values of  $K_d = 12$  nM and  $B_{max} = 316$  fmol/mg of protein were obtained. The former value is close to the affinity estimated above in the competitive binding assay, and the latter agrees well with the reported value for the cell line.<sup>16,17)</sup> Taken together, these properties suggest that **1** and **2** are promising reagents for photolabeling the opioid receptors in NG 108-15 cells.

### $\delta$ -Receptor Component(s) Photolabeled with **2**

After irradiation of the cultures NG 108-15 cells with 28 nM **2**, a sample was analyzed by disc SDS-polyacrylamide gel electrophoresis. As shown in Fig. 5a, a 58 kilodaltons (kDa) polypeptide was predominantly labeled in a covalent manner. The labeling was markedly suppressed in the presence of DALE (10  $\mu$ M) during the irradiation (Fig. 5b). These results suggest that the labeled polypeptide is a receptor component in NG 108-15 cells. Broad bands between 35—20 kDa which are labeled in the absence of DALE might be candidates for the receptors claimed to be present in rat brain, based on the results of affinity chromatography.<sup>4,5)</sup> Occasionally, however, labeling of these bands was not observed. We cannot yet conclude that these smaller polypeptides are also receptor components. NG 108-15 cells are

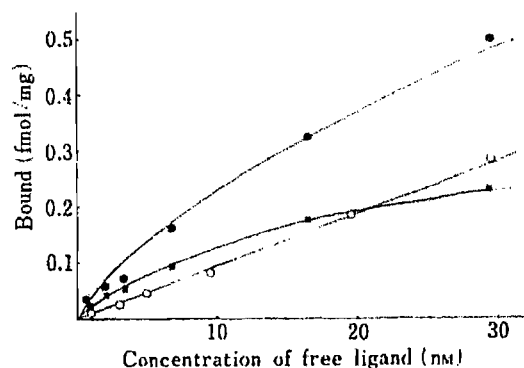


Fig. 3. Saturation Assay for the Binding of **2** to NG 108-15 Cells

Specific binding (■) was obtained by subtracting nonspecific (○) from total (●) binding.

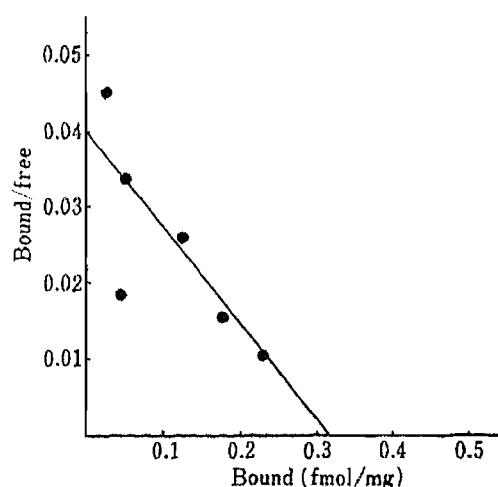


Fig. 4. Scatchard Analysis of the Specific Binding

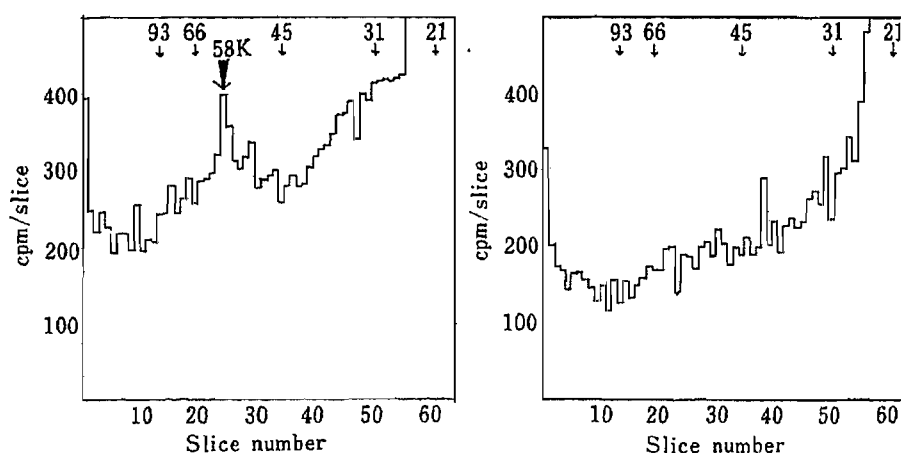


Fig. 5. Distribution of Radioactivity Following SDS Gel Electrophoresis of NG 108-15 Cells Photolyzed with **2** in the Absence (a) and Presence (b) of 10  $\mu$ M DALE

known to carry only a single type of opioid receptor, with  $\delta$ -subtype characteristics.<sup>22)</sup> The nonradioactive counterpart of **2** binds to the cell line in a competitive manner with respect to the typical  $\delta$ -ligand, DADLE, as shown in Fig. 3, and the photolabeling with **2** was effectively prevented by DALE. Therefore, the labeled polypeptide (58 kDa) here is a strong candidate for the ligand-binding component of  $\delta$ -receptor in the cells. Although Klee and his colleagues reported that an opiate (fentanyl) analog labeled a similar 58 kDa protein in the same cell line,<sup>23)</sup> our observation is the first identification of the opioid receptor component(s) of the cells by using an enkephalin analog which is structurally similar to the endogenous ligand, leucine-enkephalin.

It was reported that a 58 kDa protein from rat brain was also affinity-labeled by an enkephalin analog with  $\mu$ - and  $\delta$ -preference.<sup>12)</sup> The authors claimed the labeled 58 kDa protein is a component of  $\mu$ -receptor. It is an intriguing question whether the 58 kDa protein carries functional sites of both  $\mu$ - and  $\delta$ -receptors in rat brain. It should be possible to assess what size of protein(s) is labeled as a  $\delta$ -receptor component(s) of rat brain by using the  $\delta$ -directed reagent described here.

**Acknowledgement** This work was supported in part by Grants-in-Aid for Scientific Research (58105003, 58470116) from the Ministry of Education, Science and Culture, Japan, and grants from Sankyo Foundation of Life Science and from Suzuken Memorial Foundation.

#### References and Notes

- 1) Photoaffinity Labeling. V. Part IV: H. Nakayama, E. Yoshida and Y. Kanaoka, *Chem. Pharm. Bull.*, **34**, 2486 (1986).
- 2) a) R. S. Zukin and S. R. Zukin, *Trends NeuroSci.*, **7**, 160 (1984); b) M. Nozaki, M. Niwa, J. Hasegawa, E. Imai, M. Hori and H. Fujimura, *Life Sci.*, **31**, 1399 (1982).
- 3) W. F. Simons, G. Koski, R. A. Streaty, L. M. Hjelmeland and W. A. Klee, *Proc. Natl. Acad. Sci. U.S.A.*, **77**, 4623 (1980).
- 4) J. M. Bidlack, L. G. Abood, P. Osei-Gylmah and S. Archer, *Proc. Natl. Acad. Sci. U.S.A.*, **78**, 636 (1981).
- 5) R. Maneckjee, R. S. Zukin, S. Archer, J. Michael and P. Osei-Gylmah, *Proc. Natl. Acad. Sci. U.S.A.*, **82**, 594 (1985).
- 6) T. Fujioka, F. Inoue and M. Kuriyama, *Biochem. Biophys. Res. Commun.*, **131**, 640 (1985).
- 7) For a review: A. E. Takemori and P. S. Portoghese, *Ann. Rev. Pharmacol. Toxicol.*, **25**, 193 (1985).
- 8) a) H. Nakayama and Y. Kanaoka, *J. Syn. Org. Chem.* (in Japanese), **40**, 912 (1982); b) H. Bayley, "Photogenerated Reagents in Biochemistry and Molecular Biology," Elsevier, Amsterdam, 1983.
- 9) a) H. Nakayama, E. Yoshida and Y. Kanaoka, *Chem. Pharm. Bull.*, **34**, 2486 (1986); b) A. E. Ruoho, A.



- Rashidbaigi and P. E. Roehder, "Receptors: Biochemistry and Methodology," Vol. 1, ed. by J. C. Venter and L. C. Harrison, Alan R. Liss, New York, 1984, p. 119.
- 10) T. Fujioka, T. Matsunaga, H. Nakayama, Y. Kanaoka, Y. Hayashi, K. Kangawa and H. Matsuo, *J. Med. Chem.*, **27**, 836 (1984).
  - 11) H. W. Kosterlitz and S. J. Peterson, *Proc. R. Soc. Lond. B*, **210**, 113 (1980).
  - 12) E. L. Newman and E. Barnard, *Biochemistry*, **23**, 5385 (1984).
  - 13) The following abbreviations are used: Boc = *tert*-butyloxycarbonyl, *p*N<sub>3</sub>Phe = *p*-azidophenyl alanyl, THF = tetrahydrofuran, BCC = isobutylchloroformate, DALE = [D-Ala<sup>2</sup>, Leu<sup>5</sup>]enkephalin, DADLE = [D-Ala<sup>2</sup>, D-Leu<sup>5</sup>]enkephalin, SDS = sodium dodecylsulfate. All the amino acids used in this paper are of L-configuration except where otherwise noted.
  - 14) R. Schwyer and M. Caviezel, *Helv. Chim. Acta*, **54**, 395 (1971).
  - 15) J. Pless, W. Bauer, F. Cardinax, A. Closse, D. Hauser and R. Huguenin, *Helv. Chim. Acta*, **62**, 398 (1979).
  - 16) L. P. Gerber, S. Stein, M. Rubinstein, J. Wideman and S. Udenfriend, *Brain Res.*, **151**, 117 (1978).
  - 17) W. A. Klee and M. Nirenberg, *Proc. Natl. Acad. Sci. U.S.A.*, **71**, 3474 (1974).
  - 18) U. K. Laemmli, *Nature (London)*, **227**, 680 (1970).
  - 19) G. L. Peterson, *Anal. Biochem.*, **83**, 346 (1977).
  - 20) Y.-C. Cheng and W. H. Prusoff, *Biochem. Pharmacol.*, **22**, 3099 (1973).
  - 21) K.-J. Chang, R. J. Miller and P. Cuatrecasas, *Mol. Pharmacol.*, **14**, 961 (1978).
  - 22) K.-J. Chang and P. Cuatrecasas, *J. Biol. Chem.*, **254**, 2610 (1979).
  - 23) a) W. A. Klee, W. F. Simonds, F. W. Sweat, T. R. Burke, Jr., A. E. Jacobson and K. C. Rice, *FEBS Lett.*, **150**, 125 (1982); b) W. F. Simonds, T. R. Burke, Jr., K. C. Rice, A. E. Jacobson and W. A. Klee, *Proc. Natl. Acad. Sci. U.S.A.*, **82**, 4974 (1985).

[Chem. Pharm. Bull.]  
35(1) 262-270 (1987)

## Potential of Host-Mediated Antitumor Activity in Mice by $\beta$ -Glucan Obtained from *Grifola frondosa* (Maitake)

KYOKO ADACHI, HIROAKI NANBA\* and HISATORA KURODA

Department of Microbiology, Kobe Women's College of Pharmacy,  
Motoyama, Higashinada, Kobe 658, Japan

(Received May 19, 1986)

A polysaccharide (3-branched  $\beta$ -1,6-glucan MT-2) extracted from fruit bodies of *Grifola frondosa* (maitake) showed an antitumor effect against mouse syngeneic tumors (MM-46 carcinoma and IMC-carcinoma). It is not only directly activates various effector cells (macrophages, natural killer cells, killer T cells, etc.) to attack tumor cells, but also potentiates the activities of various mediators including lymphokines and interleukin-1. Thus, it acts to potentiate cellular functions and at the same time to prevent a decrease of immune functions of the tumor-bearing host.

**Keywords**—*Grifola frondosa*; antitumor polysaccharide; macrophage; natural killer cell; killer T cell;  $\beta$ -1,6 glucan

In the previous paper<sup>1)</sup> it was reported that a polysaccharide fraction ( $\beta$ -1,6 glucan with  $\beta$ -1,3 branches at a high frequency, hereinafter abbreviated as MT-2) containing about 0.6% protein, obtained from the fruit body of Maitake (*Grifola frondosa*), acts as an immunostimulant in the immunization of mice to an allogeneic tumor. Recently, Yadomae *et al.* found that the 6-branched  $\beta$ -1,3 glucan extracted from *G. frondosa* increased the weight or cell number of the spleen and enhanced carbon clearance activity.<sup>2)</sup> It is well known that activated macrophages (M $\phi$ ), killer T cells (Tc), natural killer cells (NK cell) and killer cells (K cell) play important roles in immunoresistance to tumors. Antitumor polysaccharides known at present are reported to activate single or multiple effectors.<sup>3)</sup> However, in the experiment using an allogeneic tumor reported in the previous paper,<sup>1)</sup> possible involvement of allograft rejection owing to a difference of major histocompatibility antigen (MHA) could not be ruled out. In this paper, the antitumor action of MT-2 on syngeneic tumors, and the effects of MT-2 on M $\phi$ , Tc and NK cells were examined.

### Materials and Methods

(1) **Preparation of Polysaccharide (MT-2)**—The fruit body of Maitake, supplied by the Mushroom Research Institute of Japan (Kiryu, Gunma), was treated as described in the previous paper.<sup>1)</sup> That is, a substance insoluble in 50% AcOH and soluble in 6% NaOH was obtained from the residue after processing the matter soluble in hot water containing 25% cetyltrimethylammonium hydroxide. After deproteinization, it was purified by ion-exchange column chromatography, and a polysaccharide which was not adsorbed on a Con A-Sepharose affinity column was obtained (MT-2).

(2) **Animals**—Male mice of ICR (4 weeks), C3H (6 weeks), CDF<sub>1</sub> (6 weeks) and BALB/C (5 weeks) strains, purchased from Japan Charles River Co., Ltd., were raised for one week before being used for tests.

(3) **Tumor Growth-Inhibiting Effect**—MM-46 tumor cells ( $2 \times 10^6$ ) were implanted in male C3H mice (7 weeks), IMC-carcinoma cells ( $2 \times 10^6$ ) in male CDF<sub>1</sub> mice (7 weeks), and Meth-A fibrosarcoma cells ( $1 \times 10^6$ ) in male BALB/C mice (6 weeks) in the right axillary region. After 24 h 1 mg/kg/d of MT-2 was administered intraperitoneally for 10 d. On the 25th day after tumor transplantation, the solid tumor was extirpated and weighed to obtain the tumor growth inhibition ratio (TIR).

(4) **Collection of M $\phi$  in Peritoneal Cavity**—Peritoneal cells were obtained by washing the peritoneal cavity of mice killed by vertebral dislocation with Hanks' solution. After centrifugation at 1200 rpm for 10 min, the

precipitated cells were collected and adjusted with RPMI-1640 medium to  $1 \times 10^6$  cells/ml. Aliquots of 1.5 ml each were cultured in an incubator at  $37^\circ\text{C}$  for 2 h in a humidified atmosphere of 5%  $\text{CO}_2$  in air to that  $\text{M}\phi$  were adsorbed selectively on the plate. The non-adherent cells were eliminated by washing 3 times with Hanks' solution.

(5) **Measurement of Superoxide Anion (SOA)**—Male mice of ICR (5 weeks), C3H (7 weeks) and BALB/C (6 weeks) strains were given 50  $\mu\text{g}$  of MT-2 intraperitoneally for 5 consecutive days. On the 5th day after completion of injection,  $\text{M}\phi$  were collected, and SOA was measured by the method of Ito *et al.*<sup>4)</sup> Then 1.5 ml of phosphate buffered saline (PBS) containing 10 mM glucose, 80 mM ferricytochrome C and 0.2 mg/ml of opsonized zymosan was added to  $\text{M}\phi$  adhering to the plate, and the plate was incubated for 90 min at  $37^\circ\text{C}$ . After incubation, the culture was centrifuged at 3000 rpm for 5 min, the supernatant was transferred into an ice-chilled test tube, and the absorbance was measured at 550 nm. On the other hand, 1 ml of 0.5% sodium dodecyl sulfate was added to the precipitated cells, then after standing for 5 min, the cells were well dispersed, and the amount of protein was measured by the Lowry-Folin method. The amount of ferricytochrome C was obtained from the absorbance at 550 nm, according to the formula:  $\Delta E_{550} = 2.1 \times 10^4 \text{ M}^{-1}$  and free SOA per unit protein was calculated.

(6) **Opsonization of Zymosan**<sup>5)</sup>—Zymosan A was adjusted with PBS to 10 mg/ml, boiled for 1 h, washed 3 times, and resuspended to PBS at 50 mg/ml. A mixture of 1 volume of zymosan (50 mg/ml) and 4 volumes of human serum was incubated at  $37^\circ\text{C}$  for 30 min. Then, after centrifugation, PBS was added to precipitate zymosan. A 10 mg/ml solution of opsonized zymosan was prepared.

(7) **Preparation of Spleen Cell Suspension**<sup>6)</sup>—A male C3H mouse (7–8 weeks) was killed by vertebral dislocation. The mouse was bled by cutting the femoral vein and the spleen was extirpated. After being washed with Eagle's minimum essential medium (MEM), the spleen was teased with scissors and passed through an 80 mesh stainless steel sieve. Cells were collected by centrifugation at 1200 rpm for 10 min, then 2 ml of 10-fold dilution of Eagle's MEM was added to lyse contaminating erythrocytes hypotonically for 10 s, and 2 ml of Eagle's MEM (2-fold concentration) was added promptly and mixed. The whole was centrifuged at 1200 rpm for 10 min, and the cells thus obtained were adjusted to  $1 \times 10^7$  cells/ml with RPMI-1640 medium. This was used as the whole spleen cell suspension. This suspension was placed in a Petri dish 5 cm in diameter and incubated for 60 min. Non-adherent cells were collected and adjusted to  $1 \times 10^7$  cells/ml with RPMI-1640 medium, and used as non-adherent spleen cells.

(8) **Elimination of T Cells**<sup>7)</sup>—A mixture of 1 ml of non-adherent spleen cell suspension obtained from male C3H mice (9 weeks) and 20  $\mu\text{l}$  of 5% Thy-1.2 F7D5 monoclonal immunoglobulin M cytotoxic antibody (Serotec Ltd., England) was incubated for 30 min, then washed once with RPMI-1640 medium. After that, 1 ml of RPMI-1640 medium with fetal bovine serum containing 5% guinea-pig complement was added and the whole was further incubated for 30 min. The cells that reacted with antibody were selectively destroyed. The remaining cells were centrifuged at 1200 rpm for 10 min and adjusted to  $1 \times 10^7$  cells/ml.

(9) **Labeling of Target Cells**<sup>8)</sup>—After being washed with RPMI-1640 medium, P-815 tumor cells were adjusted to  $1 \times 10^6$  cells/ml. Then 25  $\mu\text{l}$  of 45  $\mu\text{Ci/ml}$   $^3\text{H}$ -uridine solution was added to 1 ml of the cell suspension and after a 45 min incubation, cells were collected by centrifugation at 1200 rpm for 10 min, and washed with RPMI-1640 medium. A suspension of  $2 \times 10^5$  cells/ml ( $1.0 \times 10^5$ – $2.1 \times 10^5$  dpm/ $1 \times 10^6$  cell) was prepared.

(10) **Cytotoxicity**<sup>9)</sup>—One milliliter of the labeled target cell suspension ( $2 \times 10^5$  cells/ml) was mixed with 1 ml of the lymphocyte suspension ( $1 \times 10^7$  cells/ml) and 0.5 ml aliquots were incubated for 4 h. Then, 0.4 ml of reaction mixture was suction-filtered through a Millipore filter (0.45  $\mu\text{m}$  pore size). After being washed with 15 ml of cold 5% trichloroacetic acid solution, the filter was dried and mixed with 10 ml of lipophilic scintillator (5 g of 2,5-diphenyloxazole (PPO), 0.3 g of 1,4-bis[2-(4-methyl-5-phenyloxazolyl)]benzene (DMPOPOP) and 1000 ml of toluene). Radioisotope (RI) activity was measured with an Aloka LSC-700 scintillation counter. The cytotoxicity ( $P\%$ ) was calculated according to the following formula:

$$P(\%) = \left( 1 - \frac{\text{dpm with immunolymphocytes} - \text{background dpm}}{\text{dpm when target cells only were incubated} - \text{background dpm}} \right) \times 100$$

(11) **Preparation of Solution Containing Interleukin-1 (IL-1)**<sup>9)</sup>—MT-2 (50  $\mu\text{g}$ ) was given to male C3H mice (7 weeks) for 5 successive days intraperitoneally. On the 5th day,  $\text{M}\phi$  were collected, adjusted  $1 \times 10^6$  cells/ml, placed on 24-well plates (0.4 ml each), and incubated for 60 min. The plates were washed with RPMI-1640 medium, 0.4 ml of RPMI-1640 medium without fetal bovine serum was added to each well, and the plates were incubated for a further 72 h. The supernatant was passed through a 0.45  $\mu\text{m}$  Millipore filter for sterilization, and stored at  $-80^\circ\text{C}$ .

(12) **Measurement of Lymphocyte Growth Reaction**<sup>9)</sup>—The thymus was extirpated from male C3H mice (7 weeks) which had been killed by bleeding from the femoral vein and carotid artery. Cells were teased out in Eagle's MEM and, after being passed through an 80 mesh stainless steel sieve, were used as the cell suspension. The suspension was adjusted to  $1.5 \times 10^7$  cells/ml with RPMI-1640 medium containing 25  $\mu\text{M}$  of 2-mercaptoethanol, then divided to 0.1 ml aliquots on 96-well plates (Corning Glass Works). The supernatant (0.05 ml) obtained as described (11) and 0.05 ml of RPMI-1640 medium or 0.05 ml of 10  $\mu\text{g/ml}$  phytohemagglutinin-P (PHA-P) were added, and the total volume of 0.2 ml was incubated for 72 h. At 6 h before the end of incubation, 0.5  $\mu\text{Ci}$  of [methyl- $^3\text{H}$ ]thymidine was added. The reaction mixture was filtered through a glass-fiber filter, and dried after being washed with 5% TCA

solution. The ratio activity was measured by using a liquid scintillation counter.

(13) **Preparation of Lymphokines**<sup>10)</sup>—Cells from mouse spleen were suspended in 10 ml of RPMI-1640 medium, 0.5 ml of 100  $\mu\text{g/ml}$  concanavalin A (Con A) was added and the mixture was incubated at 37°C for 48 h. After centrifugation, the supernatant containing lymphokines was stored at -80°C.

(14) **Statistical Processing of the Experimental Data**—The experimental data obtained were checked by Student's *t*-test to evaluate the significance of differences between the control and MT-2 administration groups.

### Results and Discussion

A purified polysaccharide fraction obtained from *G. frondosa* by the method of Chihara was charged onto a Con-A Shepharose column (1.2  $\times$  15 cm) to eliminate  $\beta$ -glucan, and the fraction not adsorbed was collected and used as MT-2 (yield, about 250 mg from 500 g of dried fruit body). It was homogeneous on centrifugation ( $s_{20w} = 6.09\text{S}$ ). This MT-2 gave about 70–80% growth inhibition of an allogeneic tumor (ICR mouse–Sarcoma-180 system), as stated in the previous paper.<sup>11)</sup> However, the possibility remained that allograft rejection due to a difference of major histocompatibility antigens (MHA) between tumor cells and host cells might have been involved. Thus, C3H mouse–MM-46 carcinoma, CDF<sub>1</sub> mouse–IMC carcinoma and BALB/C mouse–Meth-A fibrosarcoma systems were used as the syngeneic tumor systems with the same MHA, and a study was carried out according to the MT-2 administration schedule (1 mg/kg/d for 10 d) which resulted in most effective inhibition. The results are summarized in Table I.

MT-2 significantly inhibited the growth of the syngeneic tumors tested (about 50% for MM-46 and IMC carcinoma, about 25% for Meth-A fibrosarcoma). Thus MT-2 (C-3-branched  $\beta$ -1,6-glucan) enhanced the antitumor immune response independently of allograft

TABLE I. Antitumor Activities of MT-2 against Syngeneic Tumors in Mice

Tumor in mice	Agent	Tumor wt. (g) (mean value $\pm$ S.D.)	TIR (%)
MM-46 in C3H	Saline	8.3 $\pm$ 2.7	---
	MT-2	4.2 $\pm$ 1.2 <sup>a)</sup>	49.0
IMC-carcinoma in CDF <sub>1</sub>	Saline	5.9 $\pm$ 1.6	-
	MT-2	3.1 $\pm$ 1.6 <sup>a)</sup>	47.7
Meth-A fibrosarcoma in BALB/C	Saline	9.0 $\pm$ 0.8	-
	MT-2	6.7 $\pm$ 0.5 <sup>b)</sup>	25.6

MT-2: 1 mg/kg/d  $\times$  10 d. *t*-test: a)  $p < 0.05$ , b)  $p < 0.001$ .

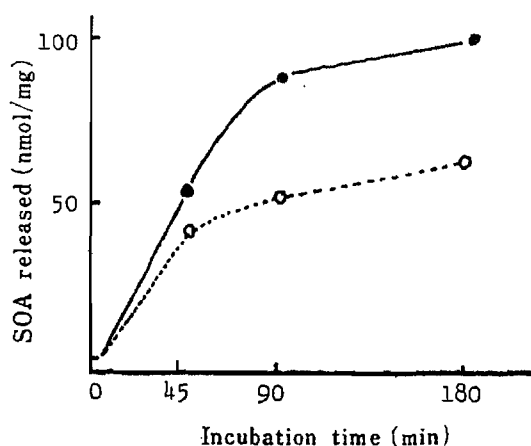


Fig. 1. SOA Release versus Time after Stimulation with Opsonized Zymosan  
●—●, MT-2; ○---○, control.

rejection. Similar results were obtained when 6-branched  $\beta$ -1,3-glucan extracted from *G. frondosa* was injected into syngeneic tumor-bearing mice by Miyazaki *et al.*<sup>2)</sup> Thus, to clarify the mechanism of tumor growth inhibition by MT-2, its influence on activation of M $\phi$ , NK cell and Tc that are the carriers of host-mediated tumor growth inhibition effect, was studied. The MT-2 dose was set at 50  $\mu$ g/d *in vivo* and 5  $\mu$ g/ml *in vitro* based on the previous results.<sup>1)</sup> Since it had already been clarified that spreading rate and latex phagocytosis of M $\phi$  were potentiated by MT-2,<sup>1)</sup> the study was centered on the amount of SOA released by M $\phi$  in phagocytosis, as one of the criteria of cytotoxicity of activated M $\phi$ . Figure 1 shows the results for M $\phi$  obtained from BALB/C mice injected with MT-2 (50  $\mu$ g/d) 5 times intraperitoneally after Meth-A fibrosarcoma transplantation.

Up to 90 min after the start of phagocytosis, both MT-2 and the control group showed a rapid increase, but after that there was relatively little change. Thus, a 90 min incubation time was employed. Table II shows the results for M $\phi$  obtained from normal mouse.

ICR and C3H mice showed increases of about 1.4 times, and BALB/C mice about 1.2 times at the dose of 50  $\mu$ g of MT-2. It can be concluded that cytotoxicity of M $\phi$  is potentiated by MT-2. Simultaneous addition of SOD to the experimental systems greatly decreased the yield of reduced cytochrome C, confirming the involvement of SOA. Generally the immune status of the tumor-bearing host is lowered. Thus, after the syngeneic tumors were grafted into ICR, C3H and BALB/C mice, 50  $\mu$ g/d of MT-2 was injected for 5 d and the amount of SOA released from M $\phi$  obtained 5 d later was examined. As shown in Table III, there was a decrease of released SOA in the case of the tumor-bearing mouse (control), while M $\phi$  of the MT-2-injected mouse showed SOA release equivalent to that of normal mouse. Next, the time

TABLE II. Release of SOA by MT-2-Induced Peritoneal Macrophages from Normal Mice

Mice	Agent	SOA release (nmol/mg protein)	Ratio
ICR	Saline	81.2 $\pm$ 2.5	1.00
	MT-2	112.1 $\pm$ 10.5 <sup>a)</sup>	1.38
C3H	Saline	90.6 $\pm$ 0.5	1.00
	MT-2	128.9 $\pm$ 4.9 <sup>b)</sup>	1.42
BALB/C	Saline	94.9 $\pm$ 10.5	1.00
	MT-2	116.8 $\pm$ 4.2 <sup>a)</sup>	1.23
	MT-2 + SOD	5.4 $\pm$ 1.2	-

MT-2: 50  $\mu$ g/d  $\times$  5 d. *t*-test: a)  $p < 0.01$ , b)  $p < 0.001$ .

TABLE III. Release of SOA by Induced Peritoneal Macrophages from Tumor-Bearing Mice

Mice (tumor)	Agent	SOA released <sup>a)</sup> (nmol/mg protein)	Ratio (a/b)
ICR (Sarcoma 180)	Saline	65.8 $\pm$ 3.1	1.00
	MT-2	82.2 $\pm$ 0.8 <sup>b)</sup>	1.01
C3H (MM-46)	Saline	55.7 $\pm$ 4.1	0.61
	MT-2	118.4 $\pm$ 7.8 <sup>c)</sup>	1.31
BALB/C (Meth-A)	Saline	88.9 $\pm$ 4.1	0.94
	MT-2	100.9 $\pm$ 1.8 <sup>c)</sup>	1.06

a) Released SOA by macrophages from normal mice (ICR; 81.2  $\pm$  2.5 C3H; 90.6  $\pm$  0.5 BALB/C; 94.9  $\pm$  10.5). MT-2: 50  $\mu$ g/d  $\times$  5 d. *t*-test: b)  $p < 0.05$ , c)  $p < 0.001$ .

TABLE IV. Time Course of SOA Release by MT-2-Induced Macrophages from Tumor-Bearing Mice

Days after tumor inoculation	Agent	SOA released <sup>a)</sup> (nmol/mg protein)	Ratio (a/b)
10	Saline	88.9 ± 4.1	0.94
	MT-2	100.9 ± 1.8 <sup>c)</sup>	1.06
19	Saline	57.9 ± 1.1	0.61
	MT-2	75.4 ± 2.6 <sup>b)</sup>	0.79
21	Saline	51.7 ± 0.7	0.54
	MT-2	73.1 ± 3.2 <sup>b)</sup>	0.77
28	Saline	54.1 ± 0.3	0.57
	MT-2	92.3 ± 0.9 <sup>c)</sup>	0.97

a) SOA release by M $\phi$  from normal mice (BALB/C; 94.9 ± 10.5). MT-2: 50  $\mu$ g/d × 5 d. t-test: b)  $p < 0.01$ , c)  $p < 0.001$ .

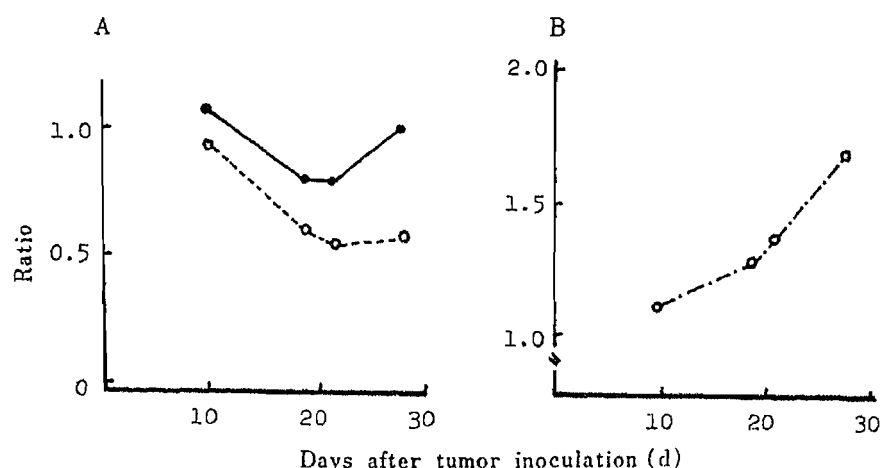


Fig. 2. Time Course of SOA Release by MT-2-Induced M $\phi$  from Tumor-Bearing Mice

A: ○---○, ratio of SOA released by M $\phi$  obtained from tumor-bearing mice to that from normal mice. ●—●, ratio of SOA released by M $\phi$  obtained from MT-2-treated tumor-bearing to that from normal mice.

B: ○---○, ratio of SOA released by M $\phi$  obtained from MT-2-treated tumor-bearing to that from tumor-bearing mice.

course of SOA production from M $\phi$  of the tumor-bearing mouse was examined (Table IV).

MT-2 (50  $\mu$ g) was injected for 5 d after grafting Meth-A fibrosarcoma into BALB/C mice, and the amounts of SOA from M $\phi$  collected on the 19th, 21st and 28th days after tumor implantation were measured. SOA volume is rapidly decreased in the control group, but the decrease was less in the MT-2 group and tended to approach the level of normal mouse (Fig. 2-A). SOA in tumor-bearing mice injected with MT-2 increased rapidly as compared with that in saline-injected tumor-bearing mice (Fig. 2-B)

It can be presumed from these results that MT-2 prevents the deterioration of immune functions caused by the tumor-bearing state or increases the cytotoxicity of M $\phi$ . Next, to study whether this activation of M $\phi$  is due to the direct action of MT-2 or secondary action (activation of other immunologically competent cell), SOA release upon application of MT-2 *in vivo* was measured. Figure 3 shows the SOA release when RPMI-1640 medium containing 5  $\mu$ g/ml of MT-2 was added to M $\phi$  induced by methyl cellulose (MC) and kept in contact for 6—48 h. That is, the test was carried out using M $\phi$  collected on the 4th day after 3.0 ml of

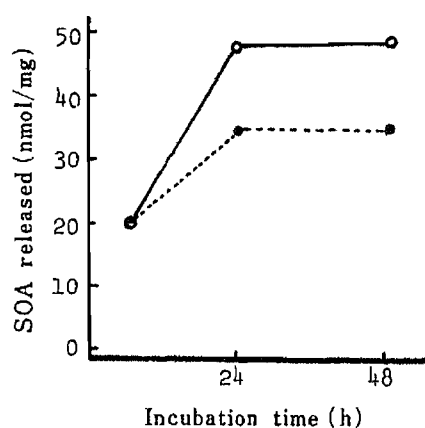


Fig. 3. SOA Release *versus* Time after Addition of MT-2

○—○, MT-2; ●---●, control.

TABLE V. SOA Release by Methylcellulose-Induced Peritoneal Macrophages Pre-cultured with MT-2 *in Vitro*

Agent	SOA released (nmol/mg protein)	
	(-)	Lymphokine (+)
Saline	34.2 ± 0.6 (1.00)	57.1 ± 0.4 (1.00)
MT-2	46.8 ± 1.0 <sup>a)</sup> (1.37)	76.2 ± 1.9 <sup>b)</sup> (1.33)

MT-2: 5 µg/ml. *t*-test: a)  $p < 0.01$ , b)  $p < 0.001$ .

1.5% MC was dosed to BALB/C mice intraperitoneally. SOA release was increased about 1.4 times at 24 and 48 h as compared with the control.

Furthermore, as shown in Table V, activation of Mφ by MT-2, even *in vitro*, was also noted in the presence of lymphokines. Namely, MC-induced Mφ was incubated for 24 h after adding RPMI-1640 medium containing 5 µ/ml of MT-2 or the same medium with a supernatant containing lymphokines which were obtained by lectin stimulation of mouse spleen. SOA released in the reaction mixture was measured after washing 3 times with Hank's solution. When only lymphokines were contacted with MC-induced Mφ, SOA was increased 1.73 times, but if MT-2 was added, it was increased 1.33 times. The SOA release was increased by addition of MT-2, regardless of the presence of lymphokines.

These results suggest that MT-2 directly potentiates the cytotoxicity of Mφ independently of complement or lymphocytes, and also potentiates the activity of lymphokines secreted from T lymphocytes. Next, the effects of MT-2 on NK cells (nonspecifically injuring tumor cells), and Tc (specifically injuring only the antigen-presenting cells) were studied. First of all, NK cells, which are induced from pre-NK cells by IFN,<sup>11)</sup> were studied. Suzuki *et al.* report that the administration of glucan extracted from *G. frondosa* to mice increased the weight and nucleated cell number of the spleen.<sup>2)</sup> Therefore, we attempted to clarify the effect of MT-2 on spleen cells *in vivo* and *in vitro*. Spleen cells were used as a cell group containing NK cells, and P-815 tumor cells were labeled with <sup>3</sup>H-uridine as target cells. Table VI shows the effect of MT-2 examined *in vivo*. C3H mice were given 50 µg/d of MT-2 for 5 d, and whole spleen cells and non-adherent spleen cell suspension were prepared from the extirpated spleen. The cytotoxicity of these cell fractions against P-815 tumor cells was measured. As both fractions were potentiated 2 to 3 times on the 5th day of MT-2 administration, it was assumed

TABLE VI. Effect of MT-2 on NK Activity of Whole Spleen Cells and Non-adherent Spleen Lymphocytes in Relation to the Timing of Administration

Days after MT-2 administration	NK activity (%) (relative cytotoxicity)	
	Whole spleen cells	Non-adherent spleen lymphocytes
Control	12.0 ± 0.3 (1.00)	6.7 ± 1.9 (1.00)
3	15.3 ± 0.1 <sup>b)</sup> (1.27)	11.6 ± 1.3 (1.73)
5	22.8 ± 2.7 <sup>b)</sup> (1.90)	19.9 ± 4.6 <sup>a)</sup> (2.97)
7	17.8 ± 2.8 <sup>a)</sup> (1.49)	11.7 ± 1.1 <sup>a)</sup> (1.74)

MT-2: 50 µg/d × 5 d. *t*-test: a)  $p < 0.05$ , b)  $p < 0.001$ .

TABLE VII. Effect of Pre-incubation of Spleen Cells from Normal Mice with MT-2 on Their NK Activities

Agent	NK activity (%) (relative cytotoxicity)	
	Whole spleen cells	Non-adherent spleen lymphocytes
Control	11.8 ± 1.1 (1.00)	7.7 ± 1.0 (1.00)
MT-2	24.0 ± 1.3 <sup>b)</sup> (1.09)	14.3 ± 1.7 <sup>a)</sup> (1.86)

MT-2: 5 µg/ml. *t*-test: a)  $p < 0.05$ , b)  $p < 0.01$ .

that MT-2 acts to induce NK precursor cells to NK cells, or to potentiate the NK cell activity directly. Next, the effect *in vitro* was examined (Table VII).

When the cytotoxicity of NK cells to P-815 tumor cells was measured by adding 5 µg/ml of MT-2 for 48 h, the activities of whole spleen cells and non-adherent spleen cells were both potentiated about 2-fold. Furthermore, 5 µg/ml of MT-2 and tumor cells were mixed with spleen cells without preincubation, and the cytotoxicity was measured after 4 h, as shown in Table VIII the same level of potentiation was observed as in the case of preincubation.

These results suggested that MT-2 directly potentiates the cytotoxicity of NK cells, or accelerates the differentiation of inactive pre-NK cells to active NK cells. Saijo *et al.*<sup>6)</sup> have reported that a muramic acid derivative (N-CWS) obtained from cell wall of *Actinomyces* potentiates NK cell activity, while Herberman *et al.*<sup>12)</sup> have reported a similar finding with lentinan obtained from Shiitake (*Lentinus edodes*). Furthermore, Salata *et al.*<sup>11)</sup> reported that NK cells are activated in different ways by interferon and lipopolysaccharide in *E. coli*. In this study, too, whole spleen cell suspension always gave higher NK cell activity than non-adherent spleen cell suspension (Tables VI, VII and VIII). Thus, MT-2 (3-branched  $\beta$ -1,6-glucan) may directly potentiate NK cell activity, like lentinan (6-branched  $\beta$ -1,3-glucan) and N-CWS, while it may also activate the cytotoxicity of M $\phi$  in the cell suspension and increase the activity of NK cells indirectly through interferon produced by M $\phi$ . Generally, Tc shows



TABLE VIII. Effect of Incubation of Spleen Cells from Normal Mice with MT-2 on Their NK Activities (No Pre-incubation)

Agent	NK activity (%) (relative cytotoxicity)	
	Whole spleen cells	Non-adherent spleen lymphocytes
Control	13.1 (1.00)	5.7 (1.00)
MT-2	22.8 <sup>a)</sup> (1.75)	16.2 <sup>b)</sup> (2.83)

MT-2: 5 µg/ml. *t*-test: a)  $p < 0.01$ , b)  $p < 0.001$ .

TABLE IX. Effect of MT-2 on the Development of Allogeneic Cytotoxic T-lymphocytes

Agent	Treatment ( <i>in vitro</i> )	Cytolysis (%)	Ratio
Control	—	14.7 ± 1.5	1.00
	Anti-Thy 1.2 + C'	4.9 ± 0.8	0.31
MT-2	—	20.5 ± 1.1 <sup>a)</sup>	1.00
	Anti-Thy 1.2 + C'	8.00 ± 1.9	0.38

MT-2: 50 µg/d × 5 d. C': guinea pig complement. *t*-test: a)  $p < 0.05$ .

specific cytotoxicity against allogeneic cells used for immunization. Hamuro *et al.*<sup>13,14)</sup> have reported that  $\beta$ -1,3-glucans including lentinan potentiate mouse Tc induction *in vitro* and *in vivo*. MT-2, a  $\beta$ -1,6-glucan may show a similar effect. After sensitization by grafting P-815 tumor cells as antigen cells intraperitoneally into C3H mice, 50 µg/d of MT-2 was injected for 5 d, and cells were collected on the 14th day. The cytotoxicity of whole spleen cell suspension was increased by MT-2 (Table IX), but the fractions lacking T cells showed a marked decrease. The result suggest that the cytotoxicity potentiated by MT-2 administration is derived from T cells.

That is, MT-2 accelerated the induction of Tc. For such induction of Tc in addition to antigen cells and Tc precursor cells, IL-1 produced by activated M $\phi$  and IL-2 produced from helper T cells by IL-1 stimulation are required. Yamazaki *et al.*<sup>15)</sup> succeeded in cloning of Tc specifically injured mouse malignant 203-glioma, in the presence of IL-2. Furthermore, Rosenberg *et al.*<sup>16)</sup> also successfully induced Tc injuring NK-resistant tumor cells by processing mouse spleen cells with IL-2. As stated, MT-2 activated M $\phi$  *in vivo* and *in vitro*. Therefore, it is likely that MT-2 also activates production of IL-1 by M $\phi$  followed by IL-2 production from helper T cells, so that Tc induction is accelerated. Next, the effect of MT-2 on production of IL-1, as the first step of these reactions, was studied. On the 5th day of intraperitoneal administration of 50 µg/d of MT-2 for 5 d to C3H mice, M $\phi$  were collected and a solution containing IL-1 was prepared in the same manner as mentioned above. This solution, together with thymus cells obtained from a normal C3H mouse, was incubated for 72 h in the presence of PHA-P in an amount insufficient to be mitogenic alone, or in its absence. At 6 h before the end of incubation, <sup>3</sup>H-thymidine was added and the mixture was further incubated. Incorporation of radioactivity into intracellular deoxyribonucleic acid (DNA) was measured (Table X). Upon administration of MT-2, incorporation of <sup>3</sup>H-thymidine into DNA was increased about 2 to 2.5 times whether PHA-P was present or

TABLE X. Interleukin-1 Activity Produced Macrophages from Mice

	<sup>3</sup> H-TdR uptake (dpm)	
	(+)	(-)
Control	1415.1 ± 121.2 (1.00)	635.4 ± 20.3 (1.00)
MT-2	2589.5 ± 286.5 <sup>a)</sup> (1.83)	1576.9 ± 201.3 <sup>a)</sup> (2.48)

MT-2: 50 µg/d × 5 d. t-test: a)  $p < 0.001$ .

absent. This suggests that MT-2 enhances not only the cytotoxic activity of  $M\phi$  but also the production of IL-1, the first mediator in the activation of T cell lines. In summary, MT-2 extracted and purified from the fruit body of Maitake (*Grifola frondosa*) showed antitumor action against several mouse syngeneic tumors tested. It acts not only by direct activation of various effector cells ( $M\phi$ , NK cells, Tc, etc.) to attack tumor cells, but also by potentiating the activities of various mediators including lymphokines and IL-1. Thus, MT-2 glucan acts to potentiate cellular functions and to prevent a decrease of immune functions of the tumor-bearing host. The action mechanism of MT-2 (3-branched  $\beta$ -1,6-glucan) seems to be similar to that of lentinan (6-branched  $\beta$ -1,3-glucan), isolated from Shiitake. However, their chemical structures are different, and a future study of the structure-activity relationship should be helpful to obtain more specific immunostimulants.

**Acknowledgement** The authors wish to thank Dr. Kanichi Mori and Mr. Tetsuro Toyomatsu, Mushroom Research Institute of Japan, for kindly supplying the Maitake.

#### References

- 1) H. Nanba, A. Hamaguchi and H. Kuroda, *Chem. Pharm. Bull.*, in press.
- 2) I. Suzuki, T. Hani, N. Ohno, S. Oikawa, K. Sato, T. Miyazaki and T. Yadomae, *J. Pharmacobio-Dyn.*, **8**, 217 (1985).
- 3) Y. Akiyama and J. Hamuro, *Protein, Nucleic Acid and Enzyme (Japan)*, **26**, 208 (1981).
- 4) M. Ito, H. Suzuki, N. Nakano, N. Yamashita, E. Sugiyama, M. Maruyama, K. Hoshino and S. Yano, *Gann*, **74**, 128 (1983).
- 5) R. B. Johnston, B. B. Keele, H. P. Misra, J. E. Lehmyer, L. S. Webb, R. L. Baehner and K. V. Ralagopalan, *J. Clin. Invest.*, **55**, 1357 (1975).
- 6) N. Saijo, A. Ozaki, Y. Beppu, N. Irimajiri, M. Shimizu, T. Takigawa, T. Taniguchi and A. Hoshi, *Gann*, **74**, 137 (1983).
- 7) H. Nakajima, S. Abe, Y. Masuko, J. Tsubouchi, M. Yamazaki and D. Mizuno, *Gann*, **72**, 723 (1981).
- 8) K. Hashimoto and T. Kitagawa, *Cell Antigen IV*, 352 (1972).
- 9) H. Nakajima, Y. Kita, T. Takashi, M. Akasaki, F. Yamaguchi, S. Ozawa, M. Tsukada, S. Abe and D. Mizuno, *Gann*, **75**, 260 (1984).
- 10) M. S. Meltzer and J. J. Oppenheim, *J. Immunol.*, **8**, 77 (1977).
- 11) R. A. Salata, M. E. Kleinherz, B. Z. Schacter and J. J. Ellener, *Cancer Res.*, **44**, 1044 (1984).
- 12) R. B. Herberman, J. Y. Djeu, H. D. Kay, J. R. Ortaldo, C. R. Iccardi, G. D. Bonnard, H. T. Holden, R. Fargnani, A. Santoni and P. Pucetti, *Immunol. Rev.*, **44**, 43 (1979).
- 13) J. Hamuro, H. Wagner and M. Rollinghoff, *Cell Immunol.*, **38**, 328 (1978).
- 14) J. Hamuro, M. Rollinghoff and H. Wagner, *Cancer Res.*, **38**, 3080 (1978).
- 15) T. Yamazaki, H. Handa, T. Yamashita, Y. Namba and M. Hanaoka, *Cancer Res.*, **44**, 1776 (1984).
- 16) M. Rosenstein, I. Yron, Y. Kaufmann and S. A. Rosenberg, *Cancer Res.*, **44**, 1964 (1984).

[Chem. Pharm. Bull.]  
35(1) 271-276 (1987)

## Chemical Characterization of Rabbit $\alpha_2$ -Macroglobulin

ATSUKO HINATA, MICHIKO IJIMA, YASUKO NAKANO,  
TERUFUMI SAKAMOTO, and MOTOWO TOMITA\*

*School of Pharmaceutical Sciences, Showa University,  
1-5-8 Hatanodai, Shinagawa-ku, Tokyo 142, Japan*

(Received June 10, 1986)

Rabbit  $\alpha_2$ -macroglobulin was isolated from rabbit plasma by polyethylene glycol precipitation, diethyl aminoethyl-Sephacel chromatography and gel chromatography. The protein subunit migrated as a single band with a molecular weight of 190000 on sodium dodecyl sulfate-gel electrophoresis under reducing conditions. Its amino-terminal amino acid sequence was determined for the first 13 residues. The amino terminus corresponded to the third residue of human  $\alpha_2$ -macroglobulin, and eleven of the 13 residues determined were identical with those of human  $\alpha_2$ -macroglobulin. These results, together with the amino acid compositions, indicate that rabbit and human  $\alpha_2$ -macroglobulins have a very similar structure. However, rabbit  $\alpha_2$ -macroglobulin was much more sensitive to methylamine inactivation than human  $\alpha_2$ -macroglobulin, and rat antisera against rabbit  $\alpha_2$ -macroglobulin did not react with human  $\alpha_2$ -macroglobulin.

**Keywords**— $\alpha_2$ -macroglobulin; rabbit plasma; amino acid sequence; amino acid composition; amino terminus; methylamine

### Introduction

$\alpha_2$ -Macroglobulin is a unique plasma proteinase inhibitor that inhibits all types of endopeptidases.<sup>1)</sup> The inhibitor contains a "bait region", which is highly susceptible to proteolytic cleavage. When this region is cleaved by a proteinase, a conformational change occurs in the inhibitor, resulting in covalent bond formation between the proteinase and the inhibitor. The internal thioester bond between glutamyl and cysteinyl residues in the inhibitor molecule is responsible for the covalent bond formation.<sup>2)</sup> Recently the complete amino acid sequence of human  $\alpha_2$ -macroglobulin has been determined (1451 amino acid residues).<sup>3)</sup>

Since abnormal plasma levels of  $\alpha_2$ -macroglobulin are found in patients with a number of diseases,<sup>4)</sup> the analysis of its plasma level is important in diagnosis of these diseases. The rabbit is an experimental animal that is suitable for studying the molecular pathology of those diseases. Several groups have reported the purification of rabbit  $\alpha_2$ -macroglobulin.<sup>5-8)</sup> However, those reports are mainly concerned with physiological and immunological studies, and little is known about the chemical properties of rabbit  $\alpha_2$ -macroglobulin. The rabbit, as well as the rat and mouse, contains two  $\alpha$ -macroglobulins,  $\alpha_1$  and  $\alpha_2$ , at comparable levels, although the human contains only  $\alpha_2$ -macroglobulin.<sup>1)</sup> Some physiological studies suggest that rabbit  $\alpha_1$ -macroglobulin, but not  $\alpha_2$ -macroglobulin, is the homologue to human  $\alpha_2$ -macroglobulin,<sup>5)</sup> though rabbit  $\alpha_2$ -macroglobulin is similar in electrophoretic mobility to human  $\alpha_2$ -macroglobulin.

In the present study we report that the chemical properties of rabbit  $\alpha_2$ -macroglobulin are homologous to those of human  $\alpha_2$ -macroglobulin, though the physiological and immunological properties of the  $\alpha_2$ -macroglobulins of the two species are significantly different.

## Materials and Methods

**Materials**—Trypsin (TPCK-treated) was purchased from Worthington Biochemicals, soybean trypsin inhibitor and high-molecular weight standard mixture (SDS-6H) from Sigma chemical Co., and *N* $\alpha$ -benzoyl-arginine-*p*-nitroanilide hydrochloride from Aldrich Chemicals. All other reagents were of reagent grade. Human  $\alpha_2$ -macroglobulin was purified by the method of Swenson and Howard.<sup>9)</sup>

**Purification of Rabbit  $\alpha_2$ -Macroglobulin**—Rabbit  $\alpha_2$ -macroglobulin was purified by a modification of the method of Swenson and Howard,<sup>9)</sup> which was initially developed for the isolation of human  $\alpha_2$ -macroglobulin. Pooled rabbit plasma (600 ml), stored at  $-70^\circ\text{C}$ , was adjusted to pH 7.4 with 1 N HCl at  $4^\circ\text{C}$ . The solution was then adjusted to 5% (w/v) polyethylene glycol (PEG 4000) by slow addition of 15% (w/v) polyethylene glycol in 100 mM phosphate buffer, pH 7.4, containing 150 mM ethylenediamine tetraacetic acid (EDTA), 50 mM  $\epsilon$ -aminocaproic acid (EACA) and 150 mM NaCl. After 30 min of mixing, the suspension was centrifuged at  $8000 \times g$  for 20 min, and the polyethylene glycol concentration of the supernatant was raised to 12% (w/v) by the addition of 26% (w/v) polyethylene glycol in the same buffer. After standing of the mixture for 30 min, the precipitate was collected by centrifugation at  $8000 \times g$  for 20 min, and dissolved in 300 ml of 3.2 mM phosphate buffer, pH 7.4, containing 10 mM EDTA and 50 mM EACA. The solution was applied to a diethyl aminoethyl (DEAE)-Sephacel column (4.5  $\times$  38 cm) equilibrated with the same buffer, and eluted with a linear gradient of 0–300 mM NaCl (total 4l) in the same buffer. Fractions (20 ml) were collected, and assayed by measuring the trypsin-binding activity of  $\alpha_2$ -macroglobulin. Fractions 31–45 (Fig. 1) containing  $\alpha_2$ -macroglobulin were combined. The protein in the pool was precipitated by the addition of solid ammonium sulfate to 50% saturation with continuous stirring. The precipitate was collected by centrifugation at  $18000 \times g$  for 10 min and dissolved in a minimum volume (5 ml) of phosphate-buffered saline. The solution was applied to a Bio-gel A-0.5 m column (2.5  $\times$  90 cm) equilibrated with the same buffer. Fractions (4 ml) were collected. Fractions 43–50 (Fig. 2) containing  $\alpha_2$ -macroglobulin were combined.

**Measurement of Trypsin-Binding Activity of  $\alpha_2$ -Macroglobulin**—The activity was measured by a modification of the method developed by Ganrot.<sup>10)</sup> The assay is based upon the ability of  $\alpha_2$ -macroglobulin-bound trypsin to hydrolyze small synthetic substrates while being unaffected by soybean trypsin inhibitor. Samples containing up to 100 pmol of  $\alpha_2$ -macroglobulin were dissolved in 800  $\mu\text{l}$  of 0.1 M Tris buffer, pH 8.1, and 25  $\mu\text{l}$  of trypsin solution (1 mg/ml) in 1 mM HCl was added to each sample solution. After 1 min of standing at room temperature, 25  $\mu\text{l}$  of soybean trypsin inhibitor solution (1 mg/ml) in water was then added to inhibit unbound trypsin. One milliliter of 3 mM *N* $\alpha$ -benzoyl-DL-arginine-*p*-nitroanilide HCl was added to the reaction mixture and the whole was incubated for 30 min at  $37^\circ\text{C}$ . The  $\alpha_2$ -macroglobulin-bound trypsin, but not soybean trypsin inhibitor-bound trypsin, can hydrolyze the synthetic small substrate. The reaction was terminated by adding 100  $\mu\text{l}$  of 30% acetic acid, and the absorbance at 410 nm was measured.

**Analytical Methods**—Slab gel electrophoresis in the presence of sodium dodecyl sulfate (SDS) was done using the gel (7.5% acrylamide) and buffer system described by Laemmli.<sup>11)</sup> After electrophoresis, gels were stained with Coomassie brilliant blue. Cellulose acetate electrophoresis was done with veronal buffer, pH 8.6, as described.<sup>12)</sup> Proteins were stained with Coomassie brilliant blue. For amino acid analysis, dry samples containing 100  $\mu\text{g}$  of protein were hydrolyzed with 100  $\mu\text{l}$  of 6N HCl at  $110^\circ\text{C}$  for 22 h. The amino acid analysis was performed on a Hitachi 835 amino acid analyzer. For amino-terminal amino acid sequence analysis, 90  $\mu\text{g}$  of protein in 200  $\mu\text{l}$  was dialyzed against 0.02% SDS. The sample solution was applied to an Applied Biosystems 470A gas-phase protein sequencer. phenylthiohydantoin (PTH)-amino acids were identified by high-performance liquid chromatography on a Senshupak SEQ-4 column (4.6  $\times$  300 mm) using a gradient system of acetonitrile-40 mM acetate buffer (pH 5.2)-distilled water.

**Preparation of Antibodies to Rabbit and Human  $\alpha_2$ -Macroglobulins**—Human or rabbit  $\alpha_2$ -macroglobulin (100  $\mu\text{g}$ ) in phosphate-buffered saline was emulsified in an equal volume of complete Freund's adjuvant. A rat was given the antigen by intraperitoneal injection. After two weeks, a booster injection was given with the same dose of antigen. The rat was exsanguinated two weeks later. The prepared antisera were assayed by double diffusion gel precipitation (Ouchterlony method).<sup>13)</sup>

## Results

### Purification

Figure 1 shows the elution profile of the 5–12% polyethylene glycol precipitate on DEAE-Sephacel chromatography. The pool containing  $\alpha_2$ -macroglobulin was further fractionated by gel chromatography on a Bio-gel A-0.5 m column after ammonium sulfate precipitation (Fig. 2). The isolated material showed  $\alpha_2$ -globulin mobility on cellulose acetate electrophoresis. The mobility was almost identical to that of human  $\alpha_2$ -macroglobulin. Therefore, we used this material as rabbit  $\alpha_2$ -macroglobulin. Rabbit  $\alpha_2$ -macroglobulin showed

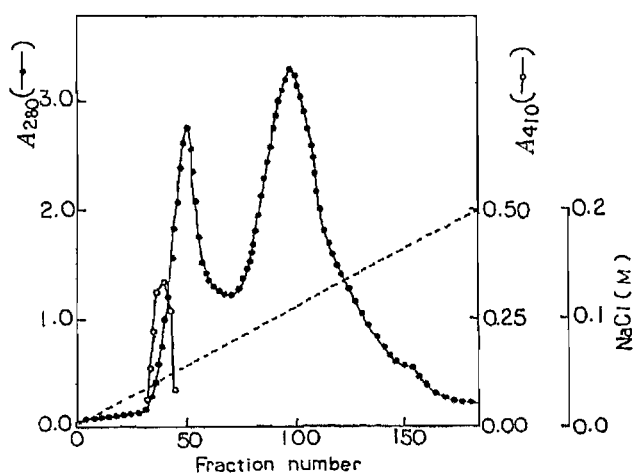


Fig. 1. Ion-Exchange Chromatography of the 5--12% Polyethylene Glycol Precipitate of Rabbit Serum on DEAE-Sephacel

The column (4.5 × 38 cm) was equilibrated with 3.2 mM phosphate buffer (pH 7.4) containing 10 mM EDTA and 50 mM EACA, and the 5--12% polyethylene glycol precipitate was applied as described in Materials and Methods. Proteins were eluted with a linear gradient of 0--300 mM (4 l in total). Column effluent was monitored by measurement of the absorbance at 280 nm (—●—) and the trypsin-binding activity, which was determined by measurement of the absorbance at 410 nm (—○—).

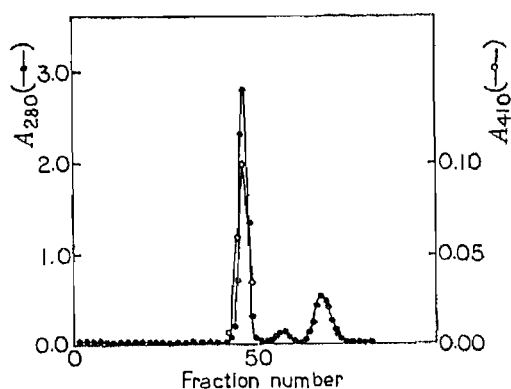


Fig. 2. Purification of Rabbit  $\alpha_2$ -Macroglobulin by Gel Chromatography on Bio-Gel A-0.5 m

The sample prepared as described in Materials and Methods was applied to a Bio-gel A-0.5 m column (2.5 × 90 cm) equilibrated with phosphate-buffered saline. Column effluent was monitored as described in Fig. 1.

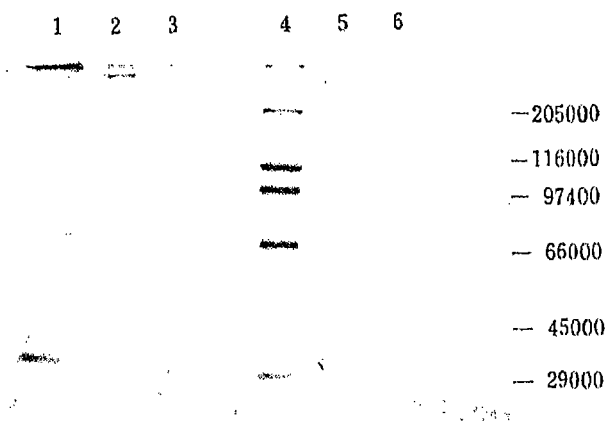


Fig. 3. Gel Electrophoresis of Rabbit  $\alpha_2$ -Macroglobulin in the Presence of SDS

Standard proteins, 1 and 4; human  $\alpha_2$ -macroglobulin, 2 and 5; rabbit  $\alpha_2$ -macroglobulin, 3 and 6. Non-reduced samples were run on lanes 1, 2 and 3 and reduced samples were run on lanes 4, 5 and 6. Standard protein markers were myosin (205 K),  $\beta$ -galactosidase (116 K), phosphorylase B (97.4 K), bovine serum albumin (66 K), egg albumin (45 K), and carbonic anhydrase (29 K).

a single band (molecular weight 190000) on SDS-gel electrophoresis under reduced conditions (Fig. 3). Mammalian  $\alpha_2$ -macroglobulins are known to have tetrameric structures composed of four identical subunits. Rabbit  $\alpha_2$ -macroglobulin had virtually the same molecular weight as human  $\alpha_2$ -macroglobulin. The amount of the purified preparation obtained from 600 ml of plasma was 55 mg. Since the plasma level of rabbit  $\alpha_2$ -macroglobulin was reported to be about 1.5 mg/ml,<sup>5)</sup> the yield was estimated to be about 6%.

#### Chemical Characterization

The amino acid composition of rabbit  $\alpha_2$ -macroglobulin was very similar to that of human  $\alpha_2$ -macroglobulin (Table I). Its amino-terminal sequence was determined for the first 13 amino acid residues (Fig. 4). The amino-terminus corresponded to the third residue of human  $\alpha_2$ -macroglobulin. Eleven of the 13 residues were identical between the two macroglobulins, indicating a fairly high homology. Therefore, it can be concluded that rabbit  $\alpha_2$ -macroglobulin is the homologue of human  $\alpha_2$ -macroglobulin.

TABLE I. Amino Acid Composition of  $\alpha_2$ -Macroglobulin

Amino acid	mol%		Amino acid	mol%	
	Rabbit	Human		Rabbit	Human
Asp	8.7	8.0	Met	1.6	1.2
Thr	6.9	6.8	Ile	5.5	3.9
Ser	7.9	8.9	Leu	10.2	9.6
Glu	12.3	12.1	Tyr	3.5	3.6
Pro	5.7	6.2	Phe	4.4	3.8
Gly	6.5	8.5	Lys	6.6	5.9
Ala	6.8	6.5	His	2.5	2.5
Val	7.3	7.7	Arg	3.2	3.2
Cys	0.5	0.7			

Values are not corrected for losses during hydrolysis (24h).

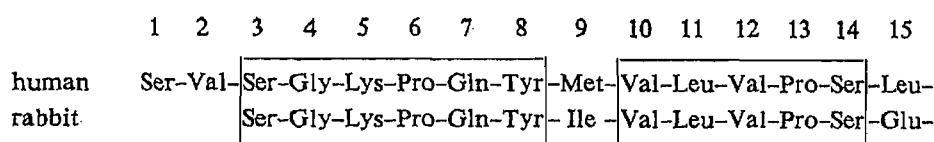


Fig. 4. Amino-Terminal Amino Acid Sequence of Rabbit  $\alpha_2$ -Macroglobulin

The sequence is compared with the sequence of human  $\alpha_2$ -macroglobulin reported by Jensen *et al.*<sup>3)</sup>

### Inactivation

The bait region of human  $\alpha_2$ -macroglobulin is readily cleaved by trypsin to produce a fragment with a molecular weight of 85000.<sup>9)</sup> Rabbit  $\alpha_2$ -macroglobulin was also cleaved by trypsin to produce a fragment of similar size (Fig. 5). However, the fragment was somewhat heterogenous, indicating that there might be several trypsin-sensitive sites in the bait region of rabbit  $\alpha_2$ -macroglobulin. Rabbit  $\alpha_2$ -macroglobulin was more susceptible to trypsin than human  $\alpha_2$ -macroglobulin, and the bait region was completely cleaved at an enzyme/substrate molar ratio of 0.25 : 1. Further cleavage was not observed after the cleavage of the bait region. The trypsin-binding capacity of our preparation was determined to be about 1.2 mol of trypsin/mol of  $\alpha_2$ -macroglobulin by titration with trypsin; a theoretical value for fully active protein is considered to be 2.0.<sup>2)</sup> Therefore, thioester bonds might be partially hydrolyzed in our preparation.

Faint bands observed with human  $\alpha_2$ -macroglobulin (molecular weights of 125000 and 62000) are autolytic cleavage products at a thioester bond formed in the presence of SDS.<sup>2)</sup>

$\alpha_2$ -Macroglobulin has one internal thioester bond per subunit, which reacts with methylamine.<sup>2)</sup> The methylamine-bound protein does not exhibit any proteinase-inhibitory activity. Figure 6 shows the sensitivity of rabbit  $\alpha_2$ -macroglobulin to methylamine. Surprisingly, rabbit  $\alpha_2$ -macroglobulin was marked more sensitive than human  $\alpha_2$ -macroglobulin.

### Immunological Properties

The antibody against rabbit  $\alpha_2$ -macroglobulin was prepared in a rat. The antibody showed one precipitin band with rabbit  $\alpha_2$ -macroglobulin on Ouchterlony double diffusion, but did not give a band with human  $\alpha_2$ -macroglobulin. This indicates that the antigenic structures exposed on the surfaces of those protein molecules are significantly different from each other.

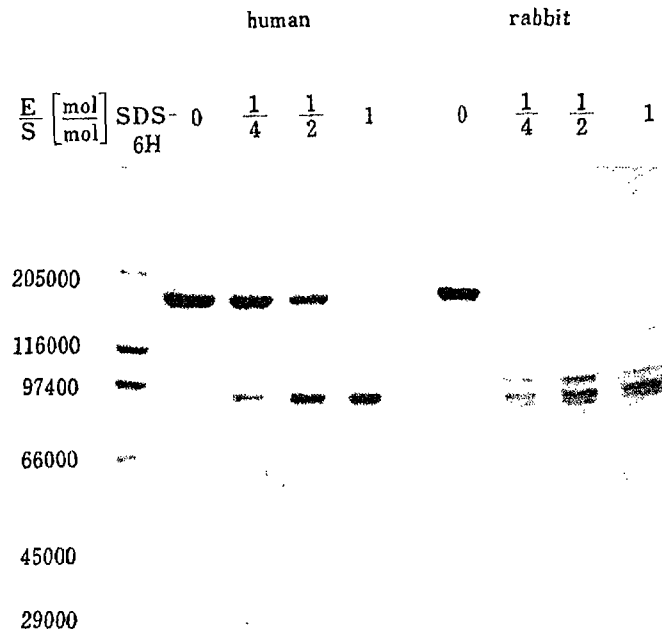


Fig. 5. Cleavage of Rabbit  $\alpha_2$ -Macroglobulin with Trypsin

The reaction mixture (75  $\mu$ l) containing 15  $\mu$ g of  $\alpha_2$ -macroglobulin (human or rabbit) in 50 mM Tris-HCl, 0.85% NaCl, 0.16% sodium citrate, pH 8.0, was incubated at 37 °C for 1 h with 0.05 mg/ml of trypsin at an enzyme/substrate molar ratio of 0.25:1---1:1. The cleavage products were electrophoresed under reduced conditions on a 7.5% slab gel with Laemmli's buffer system. E/S (mol/mol) is the molar ratio of trypsin to  $\alpha_2$ -macroglobulin.

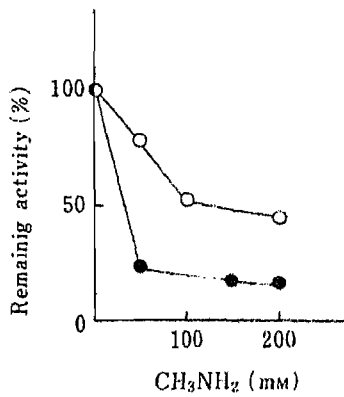


Fig. 6. Inactivation of  $\alpha_2$ -Macroglobulin by Methylamine Treatment

An aliquot of methylamine solution was added at a final concentration of 0-200 mM to 300  $\mu$ l of  $\alpha_2$ -macroglobulin (1 mg/ml) in phosphate-buffered saline, and the mixture was incubated at 25 °C for 1 h, then extensively dialyzed against phosphate-buffered saline at 4 °C overnight. The remaining activity of  $\alpha_2$ -macroglobulin was determined by measuring trypsin-binding activity. Human  $\alpha_2$ -macroglobulin, (—○—); rabbit  $\alpha_2$ -macroglobulin, (—●—).

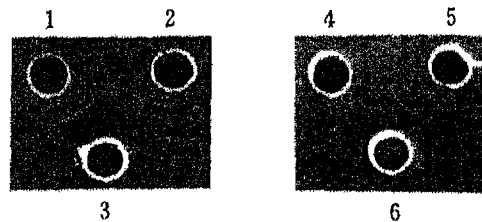


Fig. 7. Ouchterlony Immunodiffusion of  $\alpha_2$ -Macroglobulin with Rat Antisera

Rabbit  $\alpha_2$ -macroglobulin, 1 and 4; human  $\alpha_2$ -macroglobulin, 2 and 5; rat anti-rabbit  $\alpha_2$ -macroglobulin, 3; rat anti-human  $\alpha_2$ -macroglobulin, 6.

### Discussion

Our method for the isolation of rabbit  $\alpha_2$ macroglobulin gives a rather low yield compared with those cited in other reports.<sup>5)</sup> However, the major advantage of our method

over the others is that many other plasma proteins could also be purified simultaneously from the same serum.

The high homology of the amino-terminal sequence between rabbit and human  $\alpha_2$ -macroglobulins indicates that rabbit  $\alpha_2$ -macroglobulin is the homologue of human  $\alpha_2$ -macroglobulin, although the physiological properties of rabbit  $\alpha_2$ -macroglobulin have been reported to show low homology with those of human  $\alpha_2$ -macroglobulin.<sup>51</sup> Further studies are in progress in order to elucidate the chemical properties of rabbit  $\alpha_1$ -macroglobulin, which might also be a homologue of human  $\alpha_2$ -macroglobulin.

#### References

- 1) P. C. Harpel and M. S. Brower, *Ann. N. Y. Acad. Sci.*, **421**, 1 (1983).
- 2) S. R. Feldman, S. L. Gonias, and S. V. Pizzo, *Proc. Natl. Acad. Sci. U.S.A.*, **82**, 5700 (1985).
- 3) L. S. Jensen, T. M. Stepanik, T. Kristensen, D. M. Wierzbicki, C. M. Jones, P. B. Lonblad, S. Magnusson, and T. E. Petersen, *J. Biol. Chem.*, **259**, 8318 (1984).
- 4) M. A. Bridges and D. A. Applegarth, *Ann. N. Y. Acad. Sci.*, **421**, 360 (1983).
- 5) C. Versavel, A. Feve, F. Esnard, T. L. De Vonne, and H. Mouray, *Comp. Biochem. Physiol.*, **75B**, 701 (1983).
- 6) R. Got, H. Mouray, J. Morretti, *Biochem. Biophys. Acta*, **107**, 278 (1965).
- 7) K. L. Knight and S. Dray, *Biochemistry*, **7**, 3830 (1968).
- 8) D. Ganea, A. Teodorescu, and M. Teodorescu, *Immunology*, **45**, 227 (1982).
- 9) R. P. Swenson and J. B. Howard, *J. Biol. Chem.*, **254**, 4452 (1979).
- 10) P. O. Ganrot, *Acta Chem. Scand.*, **21**, 602 (1967).
- 11) U. K. Laemmli, *Nature (London)*, **227**, 680 (1970).
- 12) J. Kohn, *Nature (London)*, **181**, 839 (1958).
- 13) O. Ouchterlony, *Prog. Allergy*, **VI**, 30 (1962).



[Chem. Pharm. Bull.]  
35(1) 277-281 (1987)

## Effects of Isoniazid and Its Metabolites on Phenytoin Biotransformation in Isolated Rat Hepatocytes

HIROSHI NODA,\*<sup>a</sup> SEIJI ETO,<sup>a</sup> MASAO MINEMOTO,<sup>a</sup>  
ATSUKO NODA,<sup>b</sup> and KOHJI OHNO<sup>b</sup>

*Department of Hospital Pharmacy, School of Medicine, University of Occupational  
and Environmental Health, Japan (Sangyo Ika-daigaku),<sup>a</sup> 1-1 Iseigaoka,  
Yahatanishi-ku, Kitakyushu, 807, Japan, Faculty of Pharmaceutical  
Sciences, Kyushu University,<sup>b</sup> 3-1-1 Maidashi,  
Higashi-ku, Fukuoka 812, Japan*

(Received June 25, 1986)

The inhibitory effects of isoniazid, its metabolites and related compounds on phenytoin biotransformation were studied in an isolated rat hepatocyte system. Oxidation of phenytoin was inhibited strongly by isoniazid, acetylhydrazine, benzoylhydrazine and phenylhydrazine, and weakly (but significantly) by acetylisoniazid and hydrazine. Isonicotinic acid and diacetylhydrazine showed no effect. These observations may indicate that active hydrazine compounds are ones which can give a relatively significant rise to reactive intermediates such as radicals, diazene compounds or their relatives during the oxidation metabolism. On the other hand, glucuronidation of the oxidized metabolite, 5-phenyl-5-(*p*-hydroxyphenyl)hydantoin, was not affected by isoniazid.

**Keywords**—phenytoin monooxygenation; inhibition; isoniazid; acetylhydrazine; hydrazine; isolated rat hepatocyte; microsomal cytochrome P-450; difference spectrum; spin trapping; glucuronidation

Isoniazid (INH) can inhibit the microsomal mixed function oxidase activity, leading to a reduction of the clearance and an elevation of the plasma level of a co-administered drug.<sup>1)</sup> In such cases, drug intoxication may develop in patients. The interactions between INH and phenytoin (PHT) have been well studied. The first clinical cases were reported by Murray in 1962; he found that PHT intoxication symptoms developed in approximately 10% of 630 epileptic patients when they were given INH for the prophylaxis of tuberculosis.<sup>2)</sup> Later, Kutt *et al.*<sup>3)</sup> and Buttar *et al.*<sup>4)</sup> found that the formation of the pharmacologically inactive oxidation metabolite, 5-phenyl-5-(*p*-hydroxyphenyl)hydantoin (5-HPPH), was inhibited dose-dependently by co-administration of INH. However, the exact mode of inhibition has still not been fully elucidated, although a spectral investigation of the inhibition on cytochrome P-450 by INH was conducted using rat hepatic microsomes by Muakkassah *et al.*<sup>5)</sup> We examined the effect of INH and some of its metabolic intermediates on the biotransformation of PHT<sup>6)</sup> by using isolated rat hepatocytes, which retain the fundamental metabolic functions of the whole liver.

### Experimental

**Materials**—INH, isonicotinic acid (INA), acetyl hydrazine (AcHz), hydrazine (Hz) sulfate, benzoylhydrazine (BzHz), phenylhydrazine (PhHz) hydrochloride, PHT, 5-HPPH and  $\alpha$ -phenyl-*tert*-butylnitron (PBN) were obtained commercially. Acetylisoniazid (AcINH) and diacetylhydrazine (DAcHz) were prepared by the acetylation of INH and AcHz with acetic anhydride. Collagenase (*Clostridium histolyticum*) was purchased from Boehringer Mannheim GmbH. Reduced nicotinamide adenine dinucleotide phosphate (NADPH) was obtained from Oriental Yeast Co., Ltd. All chemicals were of reagent grade.

**Preparation and Incubation of Isolated Rat Hepatocytes**—Isolated hepatocytes were prepared from male Wistar rats (180–220 g) according to the collagenase perfusion method as described by Moldéus *et al.*<sup>7)</sup> The viability judged by the lactic dehydrogenase (LDH) latency test<sup>8)</sup> was 98–99% for all preparations. Incubation of the hepatocytes was performed at 37 °C in rotating round-bottomed flasks under a 95%O<sub>2</sub>–5%CO<sub>2</sub> atmosphere at a cell concentration of 3 × 10<sup>6</sup> cells/ml in a Krebs–Henseleit buffer, pH 7.4, supplemented with 13 mM HEPES (*N*-2-hydroxyethylpiperazine-*N*-2-ethanesulfonic acid) and 10 mM glucose. To obtain the time-courses of PHT elimination and 5-HPPH formation in the presence of INH, each substrate was used at 80 μM. For the examination of the effect on glucuronidation of 37 μM 5-HPPH, 36.5 and 73.0 μM INH were employed.

**Sample Preparations and Assay**—After incubation for an appropriate period, 0.1 ml aliquots of the mixture were added to 0.3 ml of acetonitrile solution containing 2 μg of phenacetin as an internal standard. 5-HPPH glucuronide was determined as 5-HPPH after heating of the incubation mixture with 3 N HCl at 100 °C for 1 h. PHT and 5-HPPH were assayed by using a Shimadzu LC3-A high-performance liquid chromatograph equipped with a Chemcosorb 3-ODS-H column (75 × 4.6 mm; Chemco Scientific Co.) and a ultraviolet detector (SPD-2A). The mobile phase was a 33:67 (v/v) mixture of acetonitrile–0.05 M phosphate buffer (pH 6.5). The flow rate was 1.0 ml/min and the eluate was monitored at 210 nm.

**Microsomal Cytochrome P-450 Determination**—Microsomes were isolated from livers of male Wistar rats (200–250 g) according to Ernster *et al.*<sup>9)</sup> The rats were either untreated or received phenobarbital (three daily i.p. injections of 80 mg/kg) prior to sacrifice. Protein content was determined according to the method of Lowry *et al.*<sup>10)</sup> and cytochrome P-450 content in rat liver microsomes according to Matsubara *et al.*<sup>11)</sup> The effect of INH, AcHz or Hz on cytochrome P-450 was estimated under the conditions described in the legend to Table II.

**Spectral Investigation of AcHz with Rat Liver Microsomal Cytochrome P-450**—The difference spectrum of AcHz with cytochrome P-450 was recorded at room temperature (20 ± 2 °C) on a Shimadzu MPS-2000 spectrometer. The experiment was performed in the reaction mixture described in the legend to Fig. 2.

**Spin Trapping of Acetyl Radical by PBN during Microsomal Metabolism of AcHz**—The reaction mixture, containing 5.6 ml of microsomal suspension (4.4 mg/ml), 2.0 ml of PBN solution (25 mM), 0.2 ml of AcHz solution (10 mM) and 0.2 ml of NADPH solution (1 mM), was incubated at 37 °C for 20 min, and extracted with benzene. Electron spin resonance (ESR) and mass spectral measurements of the extract were performed by the same method as used for the assignment of hydrazine radical.<sup>14)</sup>

## Results and Discussion

The effect of INH on PHT elimination through metabolic oxidation was investigated by using an isolated rat hepatocyte system. The effects of the following compounds were also examined: AcINH, INA, Hz, AcHz and DAcHz (metabolites of INH), and BzHz and PhHz (structurally similar to INH). As shown in Fig. 1-A, INH, AcHz, BzHz and PhHz inhibited PHT elimination strongly, whereas AcINH and Hz showed a relatively weak (but significant) inhibition. On the other hand INA and DAcHz did not have any effect on the elimination rate of PHT (Fig. 1-B). The results are consistent with the simultaneous formation of 5-HPPH, during the first 20 min period of incubation (Table I), in that the formation of 5-HPPH was retarded markedly by INH and AcHz, almost completely by BzHz and PhHz, and slightly but significantly by AcINH and Hz. The rate of 5-HPPH formation was not affected by INA or DAcHz, as expected.

The main course of PHT metabolism is known to be oxidation followed by glucuronidation.<sup>12)</sup> Muakkassah *et al.* investigated the mechanism of the inhibitory action of INH on microsomal drug metabolism.<sup>5)</sup> They found that the addition of INH to rat liver microsomes

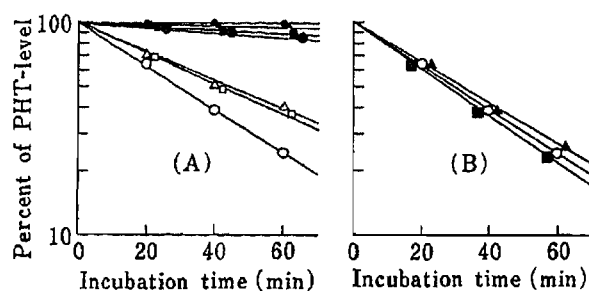


Fig. 1. Effects of INH-Related Compounds on PHT Elimination in Isolated Rat Hepatocytes (80 μM/3 × 10<sup>6</sup> cells/ml)

(A): ○, control; ■, INH; ●, PhHz; ▲, BzHz; ●, AcHz; △, Hz; □, AcINH. (B): ○, control; ▲, DAcHz; ■, INA.

TABLE I. Effects of INH and Related Compounds on 5-HPPH Formation

INH and related compounds	5-HPPH formation <sup>a)</sup>	Inhibition (%)	Statistical significance
Control	31.7 ± 0.4	0.0	—
INH	4.7 ± 0.3	85.1	<i>p</i> < 0.001
PhHz	0.8 ± 0.1	97.5	<i>p</i> < 0.001
BzHz	2.2 ± 0.4	93.2	<i>p</i> < 0.001
AcHz	6.7 ± 0.7	79.0	<i>p</i> < 0.001
Hz	26.6 ± 1.1	16.3	<i>p</i> < 0.02
AcINH	28.6 ± 1.7	10.0	<i>p</i> < 0.05
INA	31.3 ± 1.1	1.2	NS
DAcHz	30.1 ± 1.6	5.2	NS

Each initial substrate concentration was 80 μM. Each value represents the mean ± S.D. of three experiments. Results were compared by means of Student's *t*-test. a) μM/3 × 10<sup>6</sup> cells/ml/20 min. NS: Not significant.

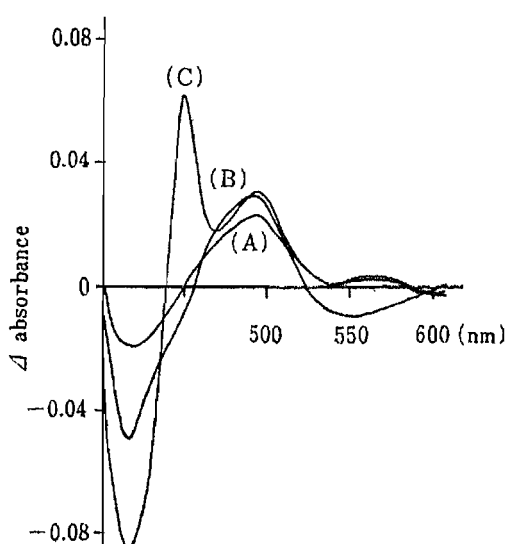


Fig. 2. Difference Spectra Produced by Interaction of AcHz with Cytochrome P-450

Rat liver microsomes were suspended in potassium phosphate buffer solution (pH 7.4), and 5.6 ml of the suspension (4.4 mg/ml) was divided into two cuvettes. After recording a flat base-line, 0.1 ml of AcHz solution was added at a concentration of 0.1 mM to the sample cuvette and an equal volume of buffer was added to the reference cuvette. The tracings A, B and C represent the difference spectra recorded 2, 4 and 6 min after the addition of NADPH solution (1.0 mM) to both cuvettes.

(A), 2 min; (B), 4 min; (C), 6 min.

produced an immediate decrease in the binding of carbon monoxide to reduced cytochrome P-450, which could contribute to the inhibition of the mixed function oxidase system by INH. Nicotinic acid hydrazide and BzHz had the same effect, whereas AcHz was inactive. From these findings, they suggested that the hydrazine moiety (-NHNH<sub>2</sub>) bearing an aroyl group is a dominant functional group in the inhibition of cytochrome P-450. Our results also indicate that the free hydrazine terminal is an essential functional group for the inhibition of PHT monooxygenation. However, the presence of an aroyl group is not essential. The oxidation of PHT was inhibited almost completely by PhHz, strongly by AcHz and weakly (but significantly) by Hz itself, and these are not aroyl compounds (Fig. 1-A, Table I). It was reported that the oxidation of PhHz with microsomal cytochrome P-450 gave phenyl diazene through the formation of a radical intermediate.<sup>13)</sup> Our group has also found that Hz is oxidized via the successive formation of hydrazine radical (H<sub>2</sub>NNH) and diimide (NH=NH) during incubation in rat liver microsomal suspensions, as well as in isolated rat hepatocytes.<sup>14)</sup> In addition, it was found that Hz produces an NADPH-dependent difference spectrum characterized by a maximum at 448 nm, which can be inhibited by metyrapone. This suggested the formation of a complex of diimide and rat liver cytochrome P-450.

As for the interaction of AcHz with rat liver cytochrome P-450, Muakkassah *et al.*

TABLE II. Effects of INH, AcHz and Hz on Cytochrome P-450 Contents in Rat Liver Microsomes

Substrate concentration (mM)	Cytochrome P-450 content (%)		
	INH	AcHz	Hz
0	100	100	100
0.5	87.9 ± 1.7 <sup>a)</sup>	92.3 ± 1.2 <sup>b)</sup>	86.4 ± 0.8 <sup>a)</sup>
1.0	85.6 ± 1.7 <sup>a)</sup>	89.0 ± 2.9 <sup>b)</sup>	85.6 ± 1.6 <sup>a)</sup>

The reaction mixture, containing 2.8 ml of microsomal suspension (3.5 mg/ml), 0.2 ml of the substrate solution and 1.0 ml of NADPH solution (1.0 mM), was incubated at 37 °C for 10 min, and the cytochrome P-450 contents were measured according to Matsubara *et al.*<sup>11)</sup> The control value of 1.67 ± 0.03 nmol/mg protein is expressed as 100%. Each value represents the mean ± S.E. of 3–5 experiments. a)  $p < 0.01$ , b)  $p < 0.05$ .

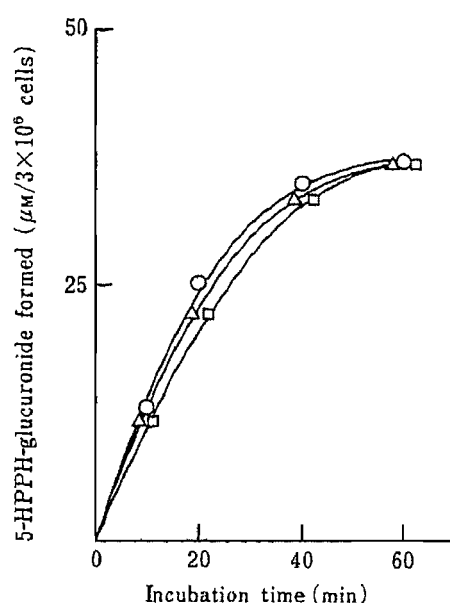


Fig. 3. Effect of INH on 5-HPPH Glucuronidation in Isolated Rat Hepatocytes

Initial concentration of 5-HPPH: 37 µM. ○, control; △, 36.5 µM INH; □, 73.0 µM INH.

reported that AcHz was inactive towards cytochrome P-450.<sup>5)</sup> However, AcHz gave a fairly stable NADPH-dependent difference spectrum characterized by maxima at 451 nm (sharp) and 495 nm (broad), as shown in Fig. 2. Pretreatment of the microsomes with metyrapone (0.02 M) decreased  $\Delta A_{451-540}$  to 36.9% and  $\Delta A_{495-540}$  to 89.0% of each control value. Pretreatment with PBN (5.0 mM) instead of metyrapone lowered  $\Delta A_{451-540}$  to 86.3% and  $\Delta A_{495-540}$  to 58.9% of the control values, respectively. It may be concluded that the peak at 451 nm arises from the cytochrome P-450 complex with a diazene-type metabolite (RN=NH), and the absorption at 495 nm is due to acetyl radical (CH<sub>3</sub>ĊO). Acetyl radical formation is also supported by the fact that the mass spectrum of the benzene extract of the microsomal oxidation mixture of AcHz in the presence of a spin trapping agent, PBN, clearly showed the formation of the corresponding PBN-adduct ( $m/z$  220). Furthermore, as shown in Table II, cytochrome P-450 contents in the microsomal suspensions were significantly decreased by the addition of AcHz, Hz or INH. These results argue against the conclusion of Muakkassah *et al.* concerning the inactivity of AcHz towards cytochrome P-450.<sup>5)</sup>

These observations may imply that active hydrazine compounds are the ones which can give a relatively significant rise to reactive intermediates such as radicals, diazene derivatives, or their relatives, which probably participate in the inhibitory effect on the mixed function oxidase systems responsible for PHT oxidation. AcINH can be hydrolyzed metabolically to

afford active AcHz and inert INA,<sup>6)</sup> which could explain the relatively weak inhibitory effect of AcINH.

Buttar investigated the biliary excretion of PHT and its metabolites in rats, and suggested that administration of INH inhibited the glucuronidation of 5-HPPH as well as the *p*-hydroxylation of PHT.<sup>4a)</sup> Isolated hepatocytes, which retain a variety of fundamental metabolic functions including glucuronidation, were used to elucidate whether PHT intoxication is related to the inhibition of 5-HPPH glucuronidation by INH, which may result in the induction of a negative feedback on the formation of 5-HPPH.<sup>15)</sup> INH, however, had no effect on the conjugation (Fig. 3).

The results mentioned above probably indicate that the delay in PHT elimination was predominantly due to the inhibition of the monooxygenation of PHT by INH and its active metabolites possessing a free hydrazine terminal or their biotransformed active ones. Further investigations are in progress.

**Acknowledgement** The authors are grateful to Dr. M. Hirata, Shionogi Research Laboratories, Shionogi and Company, Ltd., for his helpful comments on the experiments.

#### References

- 1) V. C. Valsalan and G. L. Cooper, *Brit. Med. J.*, **285**, 261 (1982); G. Sutton and H. J. Kupferberg, *Neurology*, **25**, 1179 (1975); A. R. Rosenthal, T. H. Self, O. E. Baker and R. A. Linden, *J. Am. Med. Assoc.*, **238**, 2177 (1977); H. R. Ochs, D. J. Greenblatt, G. M. Roberts and H. J. Dengler, *Clin. Pharmacol. Ther.*, **29**, 671 (1981); R. R. Millar, J. Porter and D. J. Greenblatt, *Chest*, **75**, 356 (1979); D. R. Witmer and W. A. Ritschel, *Drug Intell. Clin. Pharm.*, **18**, 483 (1984).
- 2) F. J. Murray, *Am. Rev. Resp. Dis.*, **86**, 729 (1962).
- 3) H. Kutt, K. Verebely and F. McCowell, *Neurology*, **18**, 706 (1968); H. Kutt, R. Brennan, H. Dehejia and K. Verebely, *Am. Rev. Resp. Dis.*, **101**, 377 (1970).
- 4) a) H. S. Buttar, *Res. Commun. Chem. Pathol. Pharmacol.*, **18**, 35 (1977); b) H. S. Buttar, L. T. Wong and J. H. Moffatt, *Arch. Int. Pharmacodyn. Ther.*, **235**, 9 (1978).
- 5) S. F. Muakkassah, W. R. Bidlack and C. T. Yang, *Biochem. Pharmacol.*, **30**, 1651 (1981).
- 6) W. W. Weber and D. W. Hein, *Clin. Pharmacokin.*, **4**, 401 (1979) and references cited therein.
- 7) P. Moldéus, J. Horberg and S. Orrenius, *Methods in Enzymol.*, **52**, 60 (1978).
- 8) J. Högborg and A. Kristoferson, *Eur. J. Biochem.*, **71**, 77 (1977); D. Köster-Albrecht, H. Kappus and H. Remmer, *Toxicol. Appl. Pharmacol.*, **46**, 499 (1978).
- 9) L. Ernster, P. Siebivity and G. Palade, *J. Cell Biol.*, **15**, 541 (1962).
- 10) O. H. Lowry, N. J. Rosebrough, A. L. Farr and R. J. Randall, *J. Biol. Chem.*, **193**, 265 (1951).
- 11) T. Matsubara, M. Kōike, A. Touchi, Y. Tochino and K. Sugeno, *Anal. Biochem.*, **75**, 596 (1976).
- 12) N. Gerber, W. L. Weller, R. Lynn, R. E. Rangno, B. J. Sweetman and M. T. Bush, *J. Pharmacol. Exp. Ther.*, **178**, 567 (1971); T. Inaba and T. Umeda, *Drug. Metab. Dispos.*, **3**, 69 (1975).
- 13) H. G. Jonen, J. Werringloer, R. A. Prough and R. W. Estabrook, *J. Biol. Chem.*, **257**, 4404 (1982).
- 14) A. Noda, H. Noda, K. Ohno, T. Sendo, A. Misaka, Y. Kanazawa, R. Isobe and M. Hirata, *Biochem. Biophys. Res. Commun.*, **133**, 1086 (1986).
- 15) P. Borondy, T. Chang and A. J. Glazko, *Pharmacologist*, **31**, 582 (1972).

[Chem. Pharm. Bull.]  
35(1) 282-288 (1987)

## Complexation of Several Drugs with Water-Soluble Cyclodextrin Polymer

JULIANNA SZEMAN,<sup>a,b</sup> HARUHISA UEDA,<sup>a</sup> JOZSEF SZEJTLI,<sup>b</sup>  
EVA FENYVESI,<sup>b</sup> YOSHIHARU MACHIDA,<sup>a</sup>  
and TSUNEJI NAGAI<sup>\*a</sup>

*Faculty of Pharmaceutical Sciences, Hoshi University,<sup>a</sup> Ebara 2-4-41, Shinagawa-ku,  
Tokyo 142, Japan and Chiroin Pharmaceutical and Chemical Works Ltd.,<sup>b</sup>  
Endrodi S.u. 38-40, Budapest, Hungary*

(Received May 26, 1986)

The complex-forming abilities of a water-soluble  $\beta$ -cyclodextrin-epichlorohydrin polymer (CDPS) and two different molecular weight fractions of CDPS were studied and compared with those of  $\beta$ -cyclodextrin ( $\beta$ -CyD) and dimethyl- $\beta$ -cyclodextrin (DM- $\beta$ -CyD).

CDPS was separated into two main fractions by gel chromatography. CDPS and its fractions formed inclusion compounds with several drugs and these complexes were readily soluble. The low-molecular-weight fraction formed rather stable complexes with small guest molecules. The high-molecular-weight fraction was found to be more efficient in binding larger substrates.

**Keywords**—cyclodextrin polymer; complexation; solubility method; stability constant

Cyclodextrins (CyD) are known to form noncovalent inclusion compounds with various kinds of molecules. The formation of CyD complexes is a method used to improve the solubility and dissolution rate of drugs.<sup>1)</sup> Although  $\beta$ -CyD is the most practical compound to use, its complexes are only slightly soluble. Alkylation of the hydroxyl function of CyDs results in enhanced water solubility, and such derivatives have been found to be very effective in binding guest molecules.<sup>1-5)</sup> However, the methylated CyD derivatives (2,6-di-*O*-methyl- $\beta$ -CyD and 2,3,6-tri-*O*-methyl- $\beta$ -CyD) show surface activity, and in consequence, high hemolytic values. Other CyD derivatives, for example hydroxypropyl- $\beta$ -CyD, hydroxypropylmethyl- $\beta$ -CyD or CyD-epichlorohydrin polymer, show reduced hemolytic activity.<sup>6,7)</sup>

An alternative approach to CyD modification is to prepare water-soluble CyD polymers.<sup>8-10)</sup> These polymers simultaneously offer the advantages of the amorphous state and CyD-type complexation. Several kinds of condensation products effectively solubilized steroids in water. Enhanced dissolution rates were also observed, and sublingual/buccal administration of some of these complexes led to effective absorption and entry of the hormones into the systemic circulation. These CyD derivatives had no untoward or toxic effects, and they neither entered nor damaged oral tissue.<sup>11,12)</sup>

A convenient way to prepare the polymers is the crosslinking of CyD molecules with epichlorohydrin. The degree of polymerization depends on the preparation procedure, so it is possible to influence the properties of the polymer products.<sup>10)</sup> The CyD-epichlorohydrin polymers were found to be useful for improving the solubility, dissolution rate and oral bioavailability of phenytoin.<sup>13)</sup>

The stability constants of the different molecular weight fractions of water-soluble  $\beta$ -CyD-epichlorohydrin polymer were studied with congo red, which is a large model molecule. The high-molecular-weight fraction of polymer formed a more stable complex with this guest molecule.<sup>10)</sup> When methyl orange was used as a guest for spectroscopic investigation of different

molecular weight fractions of  $\alpha$ -CyD-epichlorohydrin polymer, the complexes showed the same spectral splitting patterns.<sup>14)</sup>

In this work we have studied the complex-forming ability of a water-soluble  $\beta$ -CyD-epichlorohydrin polymer (CDPS) and two different molecular weight fractions of CDPS with several drugs, and compared the results with those for  $\beta$ -CyD and dimethyl- $\beta$ -CyD (DM- $\beta$ -CyD).

### Experimental

**Materials**—Water-soluble cyclodextrin polymer used was a pilot product of Chinoin Pharm. Chem. Works Ltd. (Hungary),<sup>10)</sup> and was supplied as a white powder with the following characteristics;  $\beta$ -CyD content 52.6%, average molecular weight about 4200. The following materials were also used:  $\beta$ -CyD (Nihon Shokuhin Kako Co., Ltd.), DM- $\beta$ -CyD (Toshin Chemical Co., Ltd.), butylparaben (Tokyo Kasei T. C. I.), hydrocortisone (Nakarai Chemicals Ltd.), cinnarizine (Eisai Co., Ltd.), tolnaftate (Yamanouchi Pharmaceutical Co., Ltd.), furosemide (Hoechst Japan Co., Ltd.), acetoexamide (Shionogi Pharmaceutical Co., Ltd.).

**Chromatographic Separation**—The molecular weight distribution of CDPS was characterized by gel chromatography on Ultrogel AcA 54 and 34, and Sephadex G 50 Fine gels. The eluent was purified water containing 0.02% (w/v)  $\text{NaN}_3$ , and the separation was followed by using a SEPA-200 high-sensitivity polarimeter (Horiba). The chromatogram was calibrated on the basis of the relationship between the relative elution volumes and molecular weight.<sup>10)</sup> Two main fractions were collected, dialyzed (using 1-7/8 DM 50 FT cellulose tubing, Union Carbide Corporation) and freeze-dried.

The CyD contents of samples were determined by the acidic-hydrolysis method,<sup>8)</sup> which is accurate to about  $\pm 10\%$ .

**Solubility Studies**—Solubility measurements were carried out according to Higuchi and Connors.<sup>15)</sup> An excess amount of a drug was added to aqueous solutions containing various concentrations of CyD or CyD derivatives and shaken at  $25 \pm 0.5^\circ\text{C}$ . After equilibrium was attained (3–5 d), an aliquot was filtered through a  $0.45 \mu\text{m}$  membrane filter (EKICRODISC 13, Nishio). A portion of each sample was diluted and analyzed spectrophotometrically (Hitachi model 200-20 spectrophotometer). The 1:1 stability constants ( $k'$ ) were calculated from the initial straight line portion of the phase solubility diagrams.<sup>15)</sup> In the cases of  $A_p$  and  $A_n$  type phase diagrams, the 1–3 mM CyD concentration range was employed for the calculation of stability constants ( $k'$ ).

### Results

#### Chromatographic Separation

As shown in Fig. 1, CDPS could be separated into two main fractions; the use of Ultrogel AcA 54 polyacrylamide gel gave the best separation. The lower-molecular-weight fraction, CDPS-L, is a mixture of different isomers of CyD glyceryl ether, its average molecular weight being about 1600, and its  $\beta$ -CyD content 51.7%. The other peak represents polymeric CDPS, *i.e.*, molecules composed of 4, 5 or more CyD rings connected with longer or shorter glyceryl ether chains. The chains can also form loops. The average molecular weight of this high-

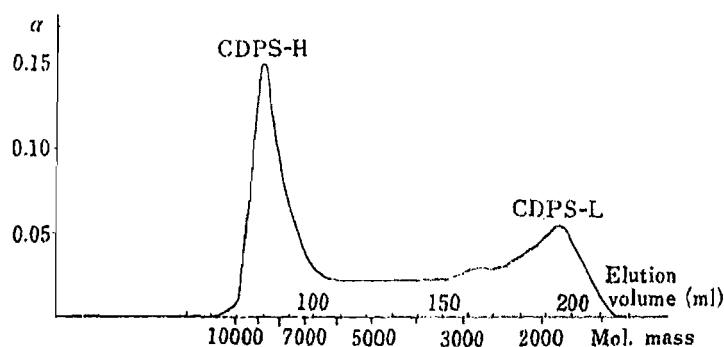


Fig. 1. Elution Profile of the Water-Soluble  $\beta$ -Cyclodextrin-Epichlorohydrin Polymer (CDPS) on Ultrogel AcA 54

Elution volume ranges of CDPS fractions: CDPS-H, 60–110 ml; CDPS-L, 170–220 ml.

molecular-weight fraction, CDPS-H, is more than 9000, and its  $\beta$ -CyD content is 51.4%. The weight ratio of the separated fractions was found to be about 1:1, but there was presumably some loss of the low-molecular-weight part of CDPS in the dialysis step, since cyclodextrins can permeate dialysis membranes, though slowly.<sup>11)</sup>

### Complexing Efficacy Observed by the Solubility Method

The complex-forming ability of CDPS and its fractions was studied with smaller and larger drug molecules. The drugs were selected according to their molecular size, structure, and their observed stability constants with  $\beta$ -CyD published or determined by ourselves. For example, a small guest molecule may have only one guest part which can fit well into the CyD cavity. On the other hand, a large guest molecule may have two or more guest parts.

Butylparaben (BPB), a small guest molecule, can fit well into the  $\beta$ -CyD ring. The  $\beta$ -CyD derivatives, DM- $\beta$ -CyD, CDPS and its fractions, formed more stable complexes with BPB than the parent  $\beta$ -CyD. With CDPS and DM- $\beta$ -CyD negatively bent solubility curves of  $A_N$  type were obtained,<sup>15)</sup> as shown in Fig. 2. The results are summarized in Table I.

$\beta$ -CyD and DM- $\beta$ -CyD effectively solubilized a large guest molecule, hydrocortisone (HC). The stability constants of CDPS and of its fraction with HC were not large, probably

TABLE I. Observed Stability Constants ( $k'$ ), Type of Solubility Curves and Increase of Solubility of Butylparaben with  $\beta$ -CyD and Some CyD Derivatives in Water at 25 °C

CyD	Stability constant $k'$ ( $M^{-1}$ )	Type of sol. curve	Increase of sol. <sup>a)</sup> $c_x/c_0$
$\beta$ -CyD	2130	$B_S$	3.6
CDPS	7260	$A_N$	90
CDPS-H	8160	$A_L$	95
CDPS-L	8160	$A_L$	95
DM- $\beta$ -CyD	7260	$A_N$	70

a)  $c_0$ , water solubility of butylparaben;  $c_x$ , solubility in 100 mM solution of the respective CyD; in the case of  $\beta$ -CyD, maximal solubility (ca. 15 mM).

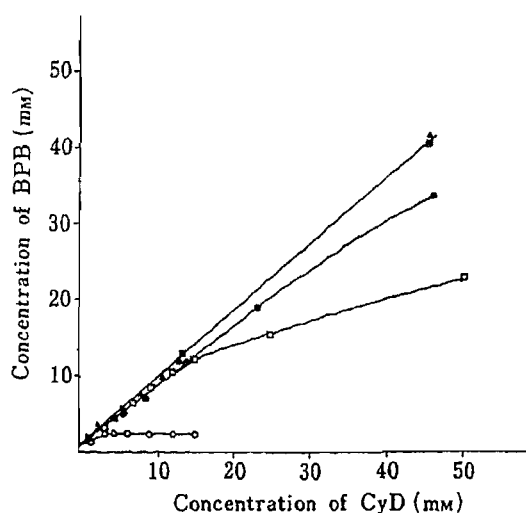


Fig. 2. Phase-Solubility Diagram of Butylparaben- $\beta$ -CyD and Butylparaben- $\beta$ -CyD Derivative Systems in Water at 25 °C

○,  $\beta$ -CyD; ●, CDPS; ▲, CDPS-H; ■, CDPS-L; □, DM- $\beta$ -CyD.

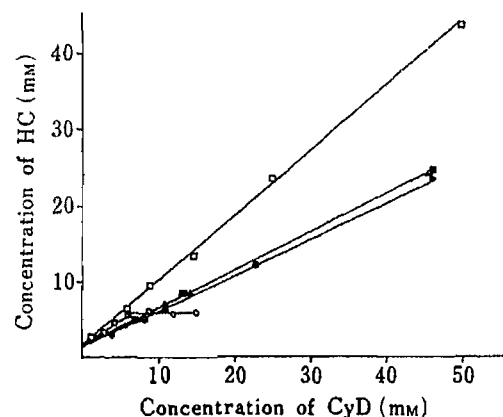


Fig. 3. Phase-Solubility Diagram of Hydrocortisone- $\beta$ -CyD and Hydrocortisone- $\beta$ -CyD Derivative Systems in Water at 25 °C

○,  $\beta$ -CyD; ●, CDPS; ▲, CDPS-H; ■, CDPS-L; □, DM- $\beta$ -CyD.



TABLE II. Observed Stability Constants ( $k'$ ), Type of Solubility Curves and Increase of Solubility of Hydrocortisone with  $\beta$ -CyD and Some CyD Derivatives in Water at 25°C

CyD	Stability constant $k'$ ( $M^{-1}$ )	Type of sol. curve	Increase of sol. <sup>a)</sup> $c_x/c_0$
$\beta$ -CyD	4170	B <sub>S</sub>	5.5
CDPS	990	A <sub>L</sub>	45
CDPS-H	1250	A <sub>L</sub>	50
CDPS-L	1250	A <sub>L</sub>	50
DM- $\beta$ -CyD	5910	A <sub>L</sub>	70

a)  $c_0$ , water solubility of hydrocortisone;  $c_x$ , solubility in 100 mM solution of the respective CyD; in the case of  $\beta$ -CyD, maximal solubility (ca. 15 mM).

TABLE III. Observed Stability Constants ( $k'$ ), Type of Solubility Curves and Increase of Solubility of Cinnarizine with  $\beta$ -CyD and Some CyD Derivatives in Water at 25°C

CyD	Stability constant $k'$ ( $M^{-1}$ )	Type of sol. curve	Increase of sol. <sup>a)</sup> $c_x/c_0$
$\beta$ -CyD	4510	B <sub>S</sub>	7.5
CDPS	2490	A <sub>P</sub>	300
CDPS-H	5200	A <sub>L</sub>	330
CDPS-L	2190	A <sub>P</sub>	500
DM- $\beta$ -CyD	8640	A <sub>P</sub>	2500

a)  $c_0$ , water solubility of cinnarizine;  $c_x$ , solubility in 100 mM solution of the respective CyD; in the case of  $\beta$ -CyD, maximal solubility (ca. 15 mM).

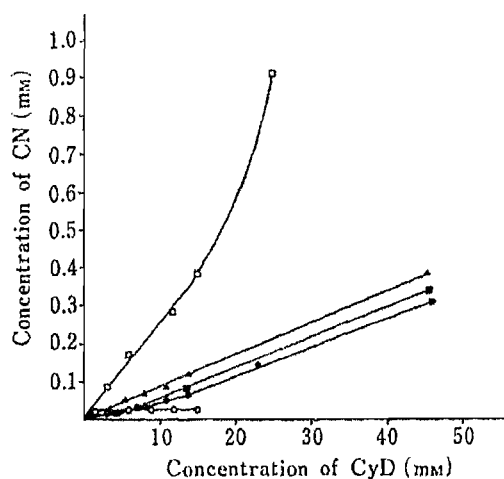


Fig. 4. Phase-Solubility Diagram of Cinnarizine- $\beta$ -CyD and Cinnarizine- $\beta$ -CyD Derivative Systems in Water at 25°C

○,  $\beta$ -CyD; ●, CDPS; ▲, CDPS-H; ■, CDPS-L; □, DM- $\beta$ -CyD.

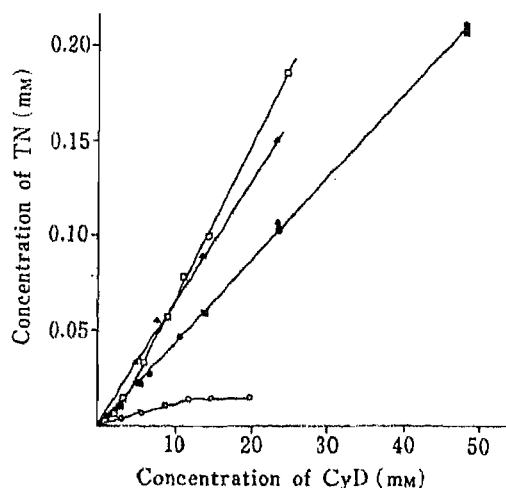


Fig. 5. Phase-Solubility Diagram of Tolnafate- $\beta$ -CyD and Tolnafate- $\beta$ -CyD Derivative Systems in Water at 25°C

○,  $\beta$ -CyD; ●, CDPS; ▲, CDPS-H; ■, CDPS-L; □, DM- $\beta$ -CyD.

because of the steric hindrance by the hydrophilic substituents on the  $\beta$ -CyD rings. In spite of this, the increase of solubility is about 10-fold compared to  $\beta$ -CyD, because CDPS and its complexes are readily soluble, as shown in Table II. Figure 3 shows that the solubility curves

TABLE IV. Observed Stability Constants ( $k'$ ), Type of Solubility Curves and Increase of Solubility of Tolnaftate with  $\beta$ -CyD and Some CyD Derivatives in Water at 25 °C

CyD	Stability constant $k'$ ( $M^{-1}$ )	Type of sol. curve	Increase of sol. <sup>a)</sup> $c_x/c_0$
$\beta$ -CyD	7140	B <sub>S</sub>	70
CDPS	17000	A <sub>L</sub>	3000
CDPS-H	42000	A <sub>L</sub>	4000
CDPS-L	17000	A <sub>L</sub>	3000
DM- $\beta$ -CyD	17000	A <sub>P</sub>	45000

a)  $c_0$ , water solubility of tolnaftate;  $c_x$ , solubility in 100 mM solution of the respective CyD; in the case of  $\beta$ -CyD, maximal solubility (ca. 15 mM).

TABLE V. Observed Stability Constants ( $k'$ ), Type of Solubility Curves and Increase of Solubility of Acetohexamide with  $\beta$ -CyD and Some CyD Derivatives in Water at 25 °C

CyD	Stability constant $k'$ ( $M^{-1}$ )	Type of sol. curve	Increase of sol. <sup>a)</sup> $c_x/c_0$
$\beta$ -CyD	890	B <sub>S</sub>	4.1
CDPS	1900	A <sub>L</sub>	190
CDPS-H	890	A <sub>L</sub>	90
CDPS-L	890	A <sub>L</sub>	90
DM- $\beta$ -CyD	810	A <sub>P</sub>	125

a)  $c_0$ , water solubility of acetohexamide;  $c_x$ , solubility in 100 mM solution of the respective CyD; in the case of  $\beta$ -CyD, maximal solubility (ca. 15 mM).

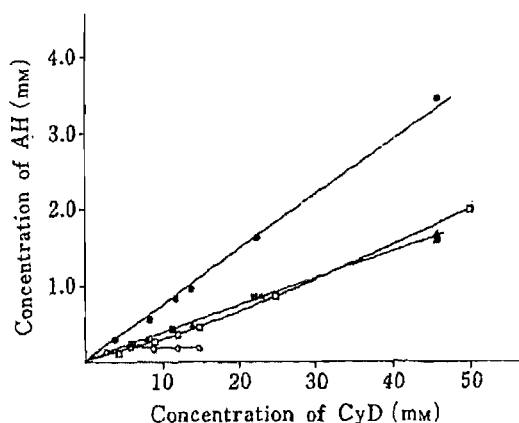


Fig. 6. Phase-Solubility Diagram of Acetohexamide- $\beta$ -CyD and Acetohexamide- $\beta$ -CyD Derivative Systems in Water at 25 °C

○,  $\beta$ -CyD; ●, CDPS; ▲, CDPS-H; ■, CDPS-L; □, DM- $\beta$ -CyD.

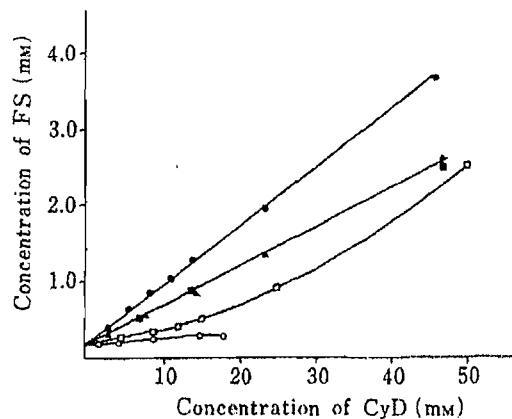


Fig. 7. Phase-Solubility Diagram of Furosemide- $\beta$ -CyD and Furosemide- $\beta$ -CyD Derivative Systems in Water at 25 °C

○,  $\beta$ -CyD; ●, CDPS; ▲, CDPS-H; ■, CDPS-L; □, DM- $\beta$ -CyD.

are of A<sub>L</sub> type<sup>15)</sup> except for that of  $\beta$ -CyD, where the complex usually begins to precipitate at lower CyD concentrations.

Cinnarizine (CN) is also a large molecule, but CDPS and CDPS-L were less effective than the  $\beta$ -CyD or DM- $\beta$ -CyD. The results are summarized in Table III. The observed stability constant ( $k'$ ) of CDPS-H with CN is between the  $k'$  values of  $\beta$ -CyD and DM- $\beta$ -CyD. As

TABLE VI. Observed Stability Constants ( $k'$ ), Type of Solubility Curves and Increase of Solubility of Furosemide with  $\beta$ -CyD and Some CyD Derivatives in Water at 25°C

CyD	Stability constant $k'$ ( $M^{-1}$ )	Type of sol. curve	Increase of sol. <sup>a)</sup> $c_x/c_0$
$\beta$ -CyD	62	B <sub>s</sub>	8.8
CDPS	590	A <sub>L</sub>	45
CDPS-H	330	A <sub>L</sub>	32
CDPS-L	330	A <sub>L</sub>	32
DM- $\beta$ -CyD	160	A <sub>p</sub>	70

a)  $c_0$ , water solubility of furosemide;  $c_x$ , solubility in 100 mM solution of the respective CyD; in the case of  $\beta$ -CyD, maximal solubility (ca. 15 mM).

shown in Fig. 4, solubility curves of A<sub>p</sub> type<sup>15)</sup> were obtained with DM- $\beta$ -CyD, CDPS and CDPS-L.

The tolnaftate (TN)-CyD systems have large stability constants because of the extremely low water solubility of TN, as shown in Table IV. The high-molecular-weight fraction showed the largest complexing ability, but DM- $\beta$ -CyD was the most effective in increasing the solubility of TN, because of its A<sub>p</sub> type<sup>15)</sup> solubility curve, as shown in Fig. 5.

Acetohexamide (AH) formed stable inclusion complexes of similar stability with  $\beta$ -CyD and its derivatives used except the non-separated CDPS, which had a superior solubilizing effect on AH. An A<sub>p</sub> type solubility curve was obtained with DM- $\beta$ -CyD. The results are summarized in Table V and Fig. 6.

Figure 7 shows that similar results were obtained with another guest molecule, furosemide (FS). The complex-forming ability of the non-separated CDPS was the best, and the different molecular weight fractions of CDPS have larger stability constants than  $\beta$ -CyD or DM- $\beta$ -CyD with FS, as summarized in Table VI.

### Discussion

CDPS and its two different molecular weight fractions form more or less stable inclusion complexes with several drug molecules. The water solubilities of these complexes are much greater than those of the complexes of the parent  $\beta$ -CyD with the same guest molecules. The composition of CDPS is heterogeneous: its  $\beta$ -CyD rings are substituted with glyceryl groups, and some rings are connected with glyceryl chains. The complex-forming ability of CDPS and its fractions depends on the structure of the guest molecules; the hydrophilic substituents on the  $\beta$ -CyD rings may either prevent or enhance the inclusion of guest molecule.

According to our results, the solubilizing properties of CDPS and its fractions were found to be equivalent to that of DM- $\beta$ -CyD with a small drug molecule (BPB). The CDPS without separation formed less stable complexes with large molecules (HC, CN) and equally stable or more stable complexes with smaller molecules (TN, AH, FS) as compared with  $\beta$ -CyD or DM- $\beta$ -CyD. Some components of CDPS could have been lost in the steps of separation and dialysis. This fact and possible cooperation between the constituents of CDPS may account for the larger stability constants of non-separated CDPS with FS and AH than those of its fractions.

The complexing efficacy of the low-molecular-weight fraction, CDPS-L, was usually found to be equivalent to or slightly smaller than that of the non-separated CDPS. The solubilizing effect of the high-molecular-weight fraction, CDPS-H, was better with larger guest molecules (CN, TN). This could be due to cooperation of the adjacent CyD units on a

polymer chain in the binding.<sup>9)</sup> Though CDPS is a mixture of CDPS-H and CDPS-L, individual stability constants and phase diagram curves were found to exhibit many differences in this experiment. Considering the elution profile of CDPS, it can be assumed that residual components of CDPS not included in CDPS-H and CDPS-L may be responsible for these differences. In any case, detailed investigation of the binding of more drugs seems to be desirable.

The complex stability is a limiting factor affecting both the bioavailability and the stabilizing effect. Excessive large or small stability constants of complexes usually give unsatisfactory results. Our findings suggest that the use of different molecular weight CyD polymers may make it possible, within limits, to manipulate the stability constants of drug complexes.

**Acknowledgement** This study was supported by the Otani Research Grant, Hoshi University.

#### References

- 1) J. Szejtli, "Cyclodextrins and Their Inclusion Complexes," Akademia Kiado, Budapest, 1982.
- 2) J. Szejtli, E. Bolla, and A. Stadler, Hungarian Patent 181.703 (9th May, 1980).
- 3) J. Pitha, *Life Sci.*, **29**, 307 (1981).
- 4) J. Pitha and L. Szente, *Life Sci.*, **32**, 719 (1983).
- 5) Y. Nakai, K. Yamamoto, K. Terada, and H. Horibe, *Chem. Pharm. Bull.*, **30**, 1796 (1982).
- 6) B. W. Müller and U. Brauns, *Int. J. Pharm.*, **26**, 77 (1985).
- 7) I. Jodal, Personal communication, Budapest, 1985.
- 8) N. Wiedenhof, J. N. J. J. Lammers, and C. L. van Panthaleon van Eck, *Starke*, **21**, 119 (1969).
- 9) A. Harada, M. Furue, and S. Nozakura, *Polymer J.*, **13**, 777 (1981).
- 10) E. Fenyvesi, M. Szilasi, B. Zsardon, J. Szejtli, and F. Tudos, "Proceedings of the 1st International Symposium on Cyclodextrins," ed. by J. Szejtli, D. Reidel Publishing, Dordrecht, 1981, pp. 345—356.
- 11) Jozef Pitha and Jan Pitha, *J. Pharm. Sci.*, **74**, 987 (1985).
- 12) J. Pitha, S. M. Harman, and M. E. Michel, *J. Pharm. Sci.*, **75**, 165 (1986).
- 13) K. Uekama, M. Otagiri, T. Irie, H. Seo, and M. Tsuruoka, *Int. J. Pharm.*, **23**, 35 (1985).
- 14) M. Suzuki, E. Fenyvesi, M. Szilasi, J. Szejtli, M. Kajtar, B. Zsardon, and Y. Sasaki, *J. Inclusion Phenom.*, **2**, 715 (1984).
- 15) T. Higuchi and K. A. Connors, *Adv. Anal. Chem. Instr.*, **4**, 117 (1965).

[Chem. Pharm. Bull.]  
35(1) 289—293 (1987)

## Development of a Tablet Excipient from Bagasse<sup>1)</sup>

YUDI PADMADISASTRA,<sup>a</sup> YOICHI SAWAYANAGI,<sup>a, b, 2)</sup> TSUNEJI NAGAI,<sup>b</sup>  
and IGOR GONDA<sup>\*. a, b</sup>

*Department of Pharmacy, University of Sydney,<sup>a</sup> Sydney, NSW 2006, Australia,*

*and Faculty of Pharmaceutical Sciences, Hoshi University,<sup>b</sup>*

*Ebara-2-4-41, Shinagawa-ku, Tokyo 142, Japan*

(Received May 27, 1986)

This paper describes our attempts to prepare a direct compression excipient from bagasse (DICEB) and its properties, particularly as they pertain to tablet making. After a process somewhat similar to the manufacture of microcrystalline cellulose (MCC), a white powder was obtained which was used in compression studies. Variation of the compression pressure, particle size distribution and moisture content did not yield caffeine-containing DICEB tablets which would be of the same satisfactory quality in terms of mechanical stability and disintegration time as those prepared from commercial MCC. These findings were interpreted to be the result of poor water uptake by DICEB. Removal of residual wax from bagasse yielded a powder with promising properties as an excipient for direct compression of tablets.

**Keywords**—bagasse; tablet excipient; direct compression excipient; crystallinity; tablet compression

Bagasse is an abundant waste product in the manufacture of sugar from cane. It is the woody fibrous residue containing the remnants of the cane juice and moisture.<sup>3)</sup> Millions of tonnes of bagasse are produced each year and a large proportion of this potentially valuable resource is wasted.<sup>4,5)</sup> The average composition is given in Table I.<sup>6)</sup> It is the high percentage of  $\alpha$ -cellulose which makes bagasse an interesting starting material for the production of pharmaceutical excipients. In particular, we were attracted<sup>1)</sup> to the possibility of preparing a tablet excipient similar to the very successful microcrystalline cellulose (MCC) made typically by acid hydrolysis of wood pulp followed by spray drying.<sup>7)</sup>  $\alpha$ -Cellulose is the major constituent of MCC and also of a recently described direct compression aid.<sup>8)</sup> Utilization of bagasse for the manufacture of fine chemicals for the pharmaceutical industry could be particularly advantageous in the sugar cane producing developing countries.<sup>9)</sup>

We wish to report here our attempts to prepare a direct compression excipient from bagasse (DICEB) and the results of preliminary tests of its properties pertinent to tablet manufacture.

### Experimental

**Materials**—Sugar cane bagasse was obtained from the Kadipaten factory in West Java, Indonesia. The following materials were also used: from Ajax Chemicals Pty. Ltd. (Australia): AR grade sodium hydroxide and hydrochloric acid, 30% technical grade aqueous ammonia solution; from BDH Biochemicals (Australia): caffeine; from FMC Corporation, American Viscose Division (U.S.A.): Avicel PH102; from Chlorine Discounters Australia: Dis Chlor (calcium hypochlorite, 125 g chlorine/liter of aqueous solution).

**Preparation of DICEB**—Bagasse was dried in room air for about 1 month and reduced in size to approximately 1—3 cm long fibres in a hammermill (Christie & Norris, England). The small pith was largely removed by sieving through 1 mm orifice screen. The material was washed with water and dried in room air. 150 g aliquots were treated with 1250 ml 1.4% NaOH by autoclaving (Atherton, model DSEC 1636, Australia) for 40 min at 130°C.

TABLE I. Average Composition of Bagasse<sup>3,6)</sup>

Component	% dry basis
$\alpha$ -Cellulose	30—40
Hemicellulose	ca. 30
Lignin	ca. 20
Ash	2—3
Wax and resin	Unknown

TABLE II. Sieve Fractions of Avicel PH102

Sieve fraction ( $\mu\text{m}$ )	Percent weight retained (mean $\pm$ S.D.)
<90	42.2 $\pm$ 1.3
90—125	8.6 $\pm$ 1.3
125—180	19.9 $\pm$ 1.3
180—250	23.5 $\pm$ 0.9
250—355	5.3 $\pm$ 0.3
355—500	0.2 $\pm$ 0.2

The slurry was filtered through a dusting stockinet placed in a Buchner filter funnel and washed with water until the filtrate became clear. The stockinet was squeezed to remove water and the remaining solid was suspended in 1000 ml of fresh water containing 100 ml of the hypochlorite solution. The mixture was placed in a flask covered with a plastic sheet and left standing overnight at room temperature for the first stage bleaching. Using the filtration system as above, the solid was washed with water until the chlorine odour disappeared. A suspension of the resulting material in 1000 ml 0.45% NaOH was autoclaved overnight at 90 °C. It was then filtered and washed until the filtrate turned colourless and it was subjected to the second bleaching in 1000 ml water plus 50 ml of the hypochlorite solution. The suspension was left standing with occasional mixing at room temperature for 1 d, and washed and filtered as after the previous bleaching. The damp bleached material was hydrolyzed with 1000 ml 2.5 N HCl in an autoclave for 15 min at 105 °C. After filtration and washing with distilled water until a clear filtrate resulted, the product was neutralized with dilute ammonia and washed with distilled water until the smell of ammonia was removed. This was followed by another sequence of bleaching and washing as explained previously. Eight aliquots of the material prepared as described above were mixed and large clumps were separated manually into small bundles which were spread on a tray and dried at room temperature for one week. 100 g portions of the dry product were cut in a blender (Waring Commercial Blender, model HGB 200, U.S.A.). 150 g quantities of this powder were then processed in a ball mill (Erweka, Type KUI, W. Germany) for about 20 h at speed level 3, until the product appeared sufficiently fine by visual examination. 100 g portions of the powder (DICEB), or Avicel PH102, were placed in a sieving machine (Endecott test sieve shaker EFL1, Mk II, England) for 20 min. After weighing the sieve fractions of Avicel PH 102, the DICEB powder was reconstituted by thorough randomized manual mixing of the sieve fractions in the same proportions as Avicel (Table II).

**X-Ray Powder Diffraction**—Samples were tested in an X-ray powder diffractometer (Rigaku, Miniflex 2005, Japan) scanning from 3—30° using Cu-K $\alpha$  radiation, scale range 2000 cps, fast chart speed, time constant 2 s.

**Moisture Content**—Appropriate quantities of the powder were placed on the pan of a moisture balance (CENCO, Cat. no. 26680-8, Central Scientific Company, U.S.A.) and dried until constant reading. The results were expressed as 100  $\times$  loss/initial weight.

**Manipulation of Water Content in DICEB**—About 300 g of the powder was placed in a fluidized bed drier (Glatt, model TR2, W. Germany) for various lengths of time. The moisture content was determined subsequently as described above.

**Preparation of Tablets**—Flat-faced tablets (diameter 13 mm) were prepared by compression of a 550 mg powder (50 mg caffeine plus 500 mg DICEB, or Avicel PH102, thoroughly mixed) at various pressures for 30 s in a hydraulic press used to prepare KBr discs for infrared spectroscopy (30 ton press H30-1, Mk 2, Research & Industrial Company, England).

**Hardness of Tablets**—For each test, 10 tablets were crushed in a tablet hardness tester (Schleuniger, model 2E, Switzerland).

**Disintegration Time of Tablets**—Six tablets were placed in distilled water at (37  $\pm$  1) °C in an apparatus similar to the USP XX specifications with discs. The result recorded was the time when the last tablet disintegrated.

**Friability of Tablets**—In each test 20 tablets were placed in the Erweka apparatus (model TAP, W. Germany) for 4 min at 25 cycles/min. The results were calculated as 100  $\times$  loss/initial weight.

## Results

### X-Ray-Powder Diffraction Patterns of DICEB

The DICEB powder prepared by the methods described above had a white colour and, qualitatively, it appeared to be free-flowing by visual inspection. The X-ray powder diffraction patterns of the commercial MCC Avicel PH102 and DICEB are compared in Fig.

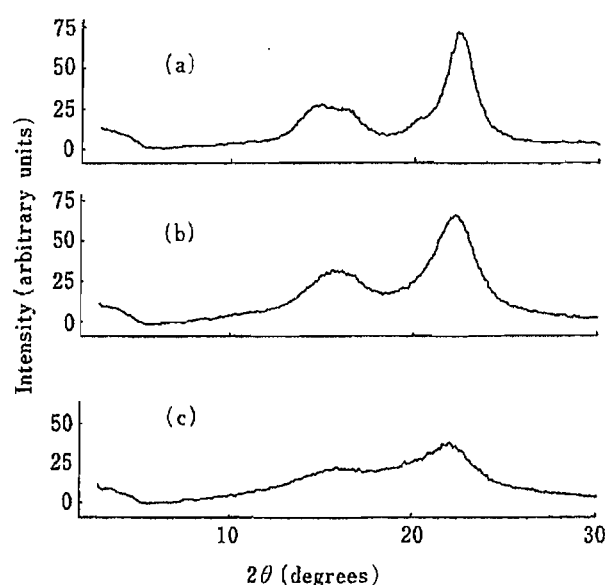


Fig. 1. X-Ray Powder Diffraction Patterns of Avicel PH102 (a), DICEB Ground for 6 h (b), and DICEB Ground for 55 h (c)

TABLE III. Effect of Compression Pressure on Hardness, Disintegration Time and Friability of Tablets

Compression pressure (psi)	Hardness (kPa) (mean $\pm$ S.D.)	Disintegration time (min)	Friability (%)
Caffeine and DICEB <sup>a)</sup>			
130	7.3 $\pm$ 0.3	> 15	0.7
120	7.6 $\pm$ 0.5	3.8	1.0
110	6.7 $\pm$ 0.4	3.5	> 1
100	5.6 $\pm$ 0.3	2.5	> 1
95	4.8 $\pm$ 0.2	2.5	> 1
80	4.8 $\pm$ 0.2	2.0	> 1
Caffeine and Avicel PH102			
171	14.8 $\pm$ 0.4	1.4	0.3

a) DICEB had particle size similar to Avicel PH102 (Table II).

1. Grinding of DICEB for prolonged periods of time resulted in reduced crystallinity (Fig. 1c) as observed by previous authors in similar experiments with MCC.<sup>10)</sup> It is thought that the degree of crystallinity for MCC depends mainly on particle size, and this is probably true for DICEB, too. The reconstituted DICEB (particle size similar to Avicel PH102) had a diffraction pattern almost indistinguishable from that of DICEB after 6 h of grinding (Fig. 1b).

#### Effect of Compression Pressure on Hardness, Disintegration Time and Friability of Tablets Made from Caffeine and DICEB

Results of compression of tablets at different pressures using mixtures of caffeine and reconstituted DICEB are given in Table III with a result of control tablet made from caffeine and Avicel PH102. In comparison, hard Avicel PH102 tablets with friability 0.3% had disintegration time 1.4 min. Thus, the behaviour of the DICEB-based tablets was comparatively poor. Satisfactory friability (<1%) corresponding to hardness in excess of 7 kPa was accompanied by unacceptably slow disintegration.

TABLE IV. Effect of Particle Size of DICEB on Hardness and Disintegration Time of Tablets Made from Caffeine and DICEB

Sieve fraction ( $\mu\text{m}$ )	Compression pressure (psi)	Hardness (kPa) (mean $\pm$ S.D.)	Disintegration time (min)
125—180	90	$3.3 \pm 0.5$	4
90—125	90	$5.2 \pm 0.2$	13
<90	90	$4.4 \pm 0.3$	8
125—180	120	$14.5 \pm 0.5$	9
90—125	120	$16.4 \pm 0.3$	> 20
<90	120	> 20	> 30

TABLE V. Effect of Moisture Content in DICEB on Hardness and Disintegration Time of Tablets Made from Caffeine and DICEB<sup>a)</sup> at Compression Pressure 100 psi

Moisture content (%)	Hardness (kPa) (mean $\pm$ S.D.)	Disintegration time (min)
2.3	— <sup>b)</sup>	6.5
3.0	$6.7 \pm 0.2$	10.5
3.9	$9.6 \pm 0.4$	> 15
5.4	$11.2 \pm 0.3$	> 15

a) DICEB had particle size similar to Avicel PH102 (Table II). b) Insufficient material for test.

### Effect of Particle Size of DICEB on Hardness and Disintegration Time of Tablets made from Caffeine and DICEB

In order to test whether a different choice of particle size might yield better tablets, three sieve fractions of DICEB were separately compressed at compression pressure 90 and 120 psi. As shown in Table IV, all disintegration times were at least 4 min even for tablets with very low hardness. Small particles tended to give longer disintegration times, probably because of the reduced porosity<sup>10)</sup> and the disappearance of the capillary structure important for water uptake.<sup>11,12)</sup>

### Effect of Moisture Content in DICEB on Hardness and Disintegration Time of Tablets Made from Caffeine and DICEB

The possibility that a critical moisture content of DICEB may be required for optimum tablet behaviour<sup>13)</sup> was investigated. The reconstituted DICEB, with particle size distribution similar to Avicel PH102, plus caffeine was compressed at 100 psi—a pressure which previously just gave tablets with disintegration time less than 3 min but unacceptably high friability (Table III). As the moisture content increased, both hardness and disintegration time went up (Table V). At low moisture content, the tablets were soft, yet the disintegration time was greater than 6 min.

### Discussion

At this stage, we considered a number of reasons potentially responsible for the poor behaviour of DICEB compared to the commercial MCC. There could be difference in: 1, chemical composition; 2, structure of the cellulose; 3, properties and distribution of crystalline and amorphous regions; 4, degree of porosity and capillary structure. The X-ray powder



diffraction patterns (Fig. 1) suggested that 2, and 3, were unlikely to be the major causes of the poor performance of DICEB tablets compared to those made from Avicel PH102. Furthermore, Parvez and Bolton reported<sup>8)</sup> that purified  $\alpha$ -cellulose (which is in the modern nomenclature just the pure cellulose<sup>14)</sup>) need not be highly crystalline to give satisfactory tablet properties. The effects of particle size on porosity and capillary structure (point 4 above) were at least partly eliminated by reconstitution of DICEB from similar sieve fractions as Avicel PH102.

The X-ray powder diffraction pattern also excluded the presence of significant quantities of crystalline substances other than natural cellulose in a form similar to that found in MCC.<sup>15)</sup> We noticed, however, that the tablets had a shiny appearance typical of formulations containing high proportions of extragranular hydrophobic lubricants. It occurred to us that, despite all the chemical treatment, there might be still sufficiently high levels of wax<sup>16)</sup> left in DICEB which would result in poor water uptake properties of this material, and therefore long disintegration time.<sup>12)</sup> Reconstituted DICEB was therefore refluxed with petroleum ether for 3 h and filtered. Evaporation of the solvent from the filtrate yielded a waxy substance. The treated DICEB was dried in oven at 50 °C and compressed. Preliminary experiments indicated that the tablets thus prepared had excellent disintegration properties because they took up water and swelled up very rapidly, even though they were hard and had an acceptable level of friability. Insufficient material prevented us from further experiments at this stage. Preparation of a large batch of this new material for detailed studies is under way.

**Acknowledgement** The authors would like to thank Lee Bailey for typing the manuscript. This project is supported by the Australian Development Assistance Bureau.

#### References and Notes

- 1) A part of this work was presented at the 106th Annual Meeting of the Pharmaceutical Society of Japan, Chiba, 1986.
- 2) Present address: *Fujinaga Pharmaceutical Co., Ltd., Shoan-1-13-5, Suginami-ku, Tokyo 167, Japan.*
- 3) G. M. Meade and J. C. P. Chen, "Cane Sugar Handbook," 10th Edition, J. Wiley and Sons, New York, pp. 95--108.
- 4) R. C. Trickett and F. G. Neytzell-de Wilde, *CHEMSA*, **8**, 11 (1982).
- 5) W. H. M. Rawlins, "Research Review 1979," CSIRO Division of Chemical Technology, South Melbourne, 1979, p. 65.
- 6) J. M. Paturau, "By-products of the Cane Sugar Industry," 2nd Edition, Sugar Series 3, Elsevier, Amsterdam, 1982, p.33 (Chapter 3).
- 7) O. A. Battista, U. S. Patent 3146168 (1964) [Problem Solver and Reference Manual, FMC Corporation (1984)].
- 8) R. Parvez and S. Bolton, *Drug. Dev. Ind. Pharm.*, **11**, 565 (1983).
- 9) J. H. M. Bueno, *Rev. Cienc. Farm.*, **5**, 191 (1983).
- 10) Y. Nakai, E. Fukuoka, S. Nakajima, and J. Hasegawa, *Chem. Pharm. Bull.*, **25**, 96 (1977).
- 11) Y. Sawayanagi, N. Nambu, and T. Nagai, *Chem. Pharm. Bull.*, **31**, 2064 (1983).
- 12) H. Nogami, T. Nagai, E. Fukuoka, and T. Sonobe, *Chem. Pharm. Bull.*, **17**, 1450 (1969).
- 13) T. M. Jones, *Pharm. J.*, **231**, 301 (1983).
- 14) T. P. Nevell and S. H. Zeronian, "Cellulose Chemistry and Its Applications," ed. by T. P. Nevell and S. H. Zeronian, Ellis Horwood Ltd., Chichester, 1985, pp. 16--17 (Chapter 1).
- 15) J. Soltys, Z. Lisowski, and J. Knapezky, *Acta Pharm. Tech.*, **30**, 174 (1984).
- 16) A. H. Warth, "The Chemistry and Technology of Waxes," Second Edition, Reinhold Publishing Co., New York, 1956, p. 218.

[Chem. Pharm. Bull.]  
35(1) 294-301 (1987)

## Effects of Albumin and $\alpha_1$ -Acid Glycoprotein on the Transport of Imipramine and Desipramine through the Blood-Brain Barrier in Rats<sup>1)</sup>

TSU-HAN LIN, YASUFUMI SAWADA, YUICHI SUGIYAMA,  
TATSUJI IGA\* and MANABU HANANO

*Faculty of Pharmaceutical Sciences, University of Tokyo, Hongo,  
Bunkyo-ku, Tokyo 113, Japan*

(Received June 9, 1986)

The permeability of the blood-brain barrier (BBB) of rats to <sup>3</sup>H-imipramine (IMP) and <sup>3</sup>H-desipramine (DMI) was measured by a tissue-sampling single-injection technique to examine the protein mediated transport. Increased concentrations of serum proteins added to the carotid injection solution resulted in decreases in the brain extraction and  $PS_{app}$  of <sup>3</sup>H-IMP and <sup>3</sup>H-DMI. The extraction ratio of <sup>3</sup>H-IMP (0.92) was higher than that of <sup>3</sup>H-DMI (0.24) in the case of the buffer injection solution. The values of *in vitro* binding activity ( $n/K_d$ ) of <sup>3</sup>H-IMP to bovine serum albumin (BSA), human serum albumin (HSA) and  $\alpha_1$ -acid glycoprotein ( $\alpha_1$ -AGP) were 4.52, 1.48 and 57.89  $\text{mM}^{-1}$ , respectively, and that of <sup>3</sup>H-DMI to  $\alpha_1$ -AGP was 38.92  $\text{mM}^{-1}$ . On the other hand, the *in vivo*  $n/K_d$  values of the binding of <sup>3</sup>H-IMP to BSA, HSA and  $\alpha_1$ -AGP estimated from the single-injection experiment were 0.597, 0.754 and 14.73  $\text{mM}^{-1}$ , respectively, and that of <sup>3</sup>H-DMI to  $\alpha_1$ -AGP was 5.90  $\text{mM}^{-1}$ . The *in vitro*  $n/K_d$  values of the binding of <sup>3</sup>H-IMP and <sup>3</sup>H-DMI to various serum proteins were thus larger than the corresponding *in vivo*  $n/K_d$  values. A marked difference was found between the observed extraction ratios and what would be predicted if only the unbound <sup>3</sup>H-IMP or <sup>3</sup>H-DMI is transported, although the difference was not large in the case of HSA. These results suggest that protein mediated transport, previously found for propranolol and lidocaine with  $\alpha_1$ -AGP by Pardridge *et al.* (*J. Clin. Invest.*, **71**, 900 (1983)), also operates for <sup>3</sup>H-IMP and <sup>3</sup>H-DMI, and this phenomenon seems to be independent of both the species and the source of serum protein, at least for <sup>3</sup>H-IMP. Further, the brain extraction ratio of <sup>3</sup>H-DMI was much lower than that of the parent drug <sup>3</sup>H-IMP, probably due to their different degrees of lipophilicity.

**Keywords**—blood-brain barrier; brain uptake; imipramine; desipramine; albumin effect; BSA; HSA;  $\alpha_1$ -acid glycoprotein

Basic lipophilic drugs such as imipramine, desipramine, propranolol and lidocaine are widely used in clinical practice. The pharmacological effect of these drugs is related to the total drug concentration in plasma.<sup>2-4)</sup> It has been shown that many basic drugs bind not only to albumin,<sup>5,6)</sup> but also to  $\alpha_1$ -acid glycoprotein,<sup>7-9)</sup> and lipoprotein.<sup>7,10)</sup> The concentrations of these proteins, particularly  $\alpha_1$ -acid glycoprotein, are affected in various diseases and by surgery, and this variation would affect plasma drug levels *via* drug protein binding. Although it has generally been believed that only the drug unbound to protein is available for entry into tissues,<sup>11,12)</sup> recent reports have indicated that serum protein-bound ligands are also available for transport into tissues such as the liver<sup>13-16)</sup> and brain.<sup>17-20)</sup> Moreover, there is a paucity of data in regard to the permeability properties of the blood-brain barrier (BBB) to drugs that act on the central nervous system (CNS). In the present studies, an antidepressant drug, imipramine, and its pharmacologically active metabolite, desipramine, both of which bind extensively to serum proteins with high affinity and act on the CNS, were selected as model drugs to examine the possibility of the protein-mediated transport into the rat brain, and the permeability properties of these drugs were compared.

### Experimental

**Materials**—All isotopes were purchased from New England Nuclear Co., Boston, MA. The specific activities given by the manufacturer were: [2,4,6,8-<sup>3</sup>H]imipramine hydrochloride (IMP) 44.2 Ci/mmol, [2,4,6,8-<sup>3</sup>H]desipramine hydrochloride (DMI) 68.0 Ci/mmol, and *n*-[1-<sup>14</sup>C]butanol 1.0 mCi/mmol. These radioactive compounds were at least 98% pure, except the <sup>3</sup>H-desipramine which was 95% pure by thin layer chromatography (TLC). The <sup>51</sup>Cr-labelled microspheres (16 ± 0.3 μ; 40 mCi/g) were suspended in 10% dextran solution with 0.01 v/v% Tween 80. Human serum albumin (HSA, fraction V), human α<sub>1</sub>-acid glycoprotein (α<sub>1</sub>-AGP) and bovine serum albumin (BSA, fraction V) were purchased from Sigma Chemical Co., St. Louis, MO. All other chemicals were commercial products of analytical grade.

**Preparation of Injection Solution**—HEPES-buffered Ringer's solution (5 mM HEPES) was titrated with 2 N NaOH to pH 7.55 and was equilibrated with 95% O<sub>2</sub>-5% CO<sub>2</sub> gas to maintain a pH of 7.4. The injection solution contained 5–10 μCi/ml <sup>3</sup>H-test compound (<sup>3</sup>H-IMP or <sup>3</sup>H-DMI) and 1–2 μCi/ml <sup>14</sup>C-butanol and either buffer alone or various concentrations of serum protein.

**Animal Study**—The permeability of the BBB to labelled IMP and DMI was measured by the tissue-sampling single-injection technique developed by Oldendorf.<sup>21</sup> Male Wistar rats (200–250 g) were used. They had free access to tap water and standard laboratory chow (CE-2, Clea Japan Inc., Tokyo) except before experiments, when they were fasted for 24 h.

1) **Hemodynamic Study**: The radioactive microsphere method<sup>22,23</sup> was utilized to measure the brain blood flow. The animal was anesthetized with intraperitoneal pentobarbital (Somnopentyl; 65 mg/kg) (Pitman-Moone, Inc., Washington Crossing, U.S.A.). The right carotid artery was cannulated with polyethylene tubing. The right and left femoral arteries and left femoral vein were also cannulated with polyethylene tubing. The microspheres labelled with <sup>51</sup>Cr were injected into the left ventricle over 20 s through a cannula passed down the right carotid artery, in a total volume of 0.2 ml. Simultaneously, arterial blood from the femoral artery was withdrawn at 0.83 ml/min for 90 s with a syringe pump (Harvard Apparatus, Millis, MA). Subsequently, the animals were killed with pentobarbital (250 mg/kg) by bolus injection into the femoral vein, and the brain was weighed and counted in a gamma counter (Aloka ARC-300, Aloka Co., Tokyo, Japan). Brain blood flow was determined by using the following equation.

$$\text{brain blood flow (ml/min/g brain)} = \frac{\text{reference sample withdrawal rate (ml/min)}}{\text{radioactivity in brain (dpm/g brain)}} \times \frac{\text{radioactivity in reference blood sample (dpm)}}{\text{radioactivity in reference blood sample (dpm)}}$$

The mean arterial blood pressure and heart rate were monitored from the right femoral arterial catheter by using a transducer coupled with a chart recorder (Nihon Koden, Tokyo).

2) **Brain Uptake Study**: The animal was anesthetized with intraperitoneal pentobarbital (65 mg/kg) and placed in a supine position, and the left common carotid artery was isolated. The <sup>3</sup>H-test compound (<sup>3</sup>H-IMP or <sup>3</sup>H-DMI) and <sup>14</sup>C-butanol, a freely diffusible internal reference, were rapidly injected (<0.5 s) into the common carotid artery as an approximately 200 μl bolus (the exact volume is immaterial) of injection solution through a sharp 27 gauge needle. Because the rate of injection (<0.5 s) exceeds the rate of carotid blood flow, the injection solution traverses the brain microcirculation as a bolus without significant mixing with the circulating blood.<sup>20,24,25</sup> The animal was decapitated 15 s after injection, except in the experiment to measure the extraction time course of IMP to determine its efflux rate. This period is sufficient for a single pass of the bolus through the brain, but short enough to minimize the efflux of labelled compound from the brain or the recirculation of labelled compound.<sup>26</sup> The cerebral hemisphere ipsilateral to the injection was removed from the cranium, solubilized in triplicate in 1.5 ml of Protosol (New England Nuclear, Boston, MA) at 50 °C overnight in an incubator, and decolorized with 33% H<sub>2</sub>O<sub>2</sub>, then 10 ml of Biofluor (New England Nuclear, Boston, MA) was added before double-isotope liquid scintillation counting. An aliquot of the injection solution added to the control brain tissue was similarly treated. The radioactivities of <sup>3</sup>H-IMP, <sup>3</sup>H-DMI and <sup>14</sup>C-butanol were determined in a liquid scintillation spectrometer (model 3255, Packard Instrument, Downers Grove, IL).

**Equilibrium Dialysis Method**—The unbound fraction (*f<sub>u</sub>*) of the labelled drug in the injection solution containing various concentrations of serum protein was measured by equilibrium dialysis at 37 °C using HEPES-buffered Ringer's solution (pH 7.4) in semimicrocells (Kokugo-Gomu Co., Tokyo) with a semipermeable membrane (Spectrum Medical Industries Inc., Los Angeles, CA). After equilibration was attained (at 6 h), the drug concentration on the protein side and the buffer side were measured in a liquid scintillation spectrometer.

**Data Analysis**—The brain uptake index (BUI) was calculated as follows<sup>27</sup>:

$$\text{BUI} = \frac{{}^3\text{H}/{}^{14}\text{C dpm (in brain)}}{{}^3\text{H}/{}^{14}\text{C dpm (in injection solution)}} = \frac{E_T}{E_R} \quad (1)$$

where *E<sub>T</sub>* and *E<sub>R</sub>* are the extraction ratios of the test compound and the reference compound, respectively, 15 s after injection. The *E<sub>T</sub>* or *E<sub>R</sub>* represents the maximal extraction of unidirectional influx into the brain minus the efflux of the

test or reference compound during the period between bolus flow through the brain (2–5 s after injection) and decapitation (15 s after injection). With regard to the reference compound,  $^{14}\text{C}$ -butanol, the maximal extraction ( $E_{R,\max}$ ) was reported to be 100%.<sup>26,27</sup> The relationship between  $E_{R,\max}$  and the extraction at 15 s  $E_{R(15s)}$  is defined as<sup>28</sup>

$$E_{R(15s)} = E_{R,\max} \cdot e^{-k_{\text{efflux}} \cdot t'} \quad (2)$$

where  $k_{\text{efflux}}$  is the efflux rate constant for  $^{14}\text{C}$ -butanol ( $0.67 \text{ min}^{-1}$ ).<sup>29</sup> Substitution of the values for  $E_{R,\max}$  and  $k_{\text{efflux}}$ , with  $t' = 10 \text{ s}$  (the time between bolus entry into the brain and decapitation), into Eq. 2 gives  $E_{R(15s)} = 90\%$  for  $^{14}\text{C}$ -butanol. The test drugs are retained by the brain and return to the blood very slowly ( $t_{1/2} \approx 4 \text{ min}$ ), as shown later, probably due to extensive binding to the cellular components. Therefore, the drug extraction ratio measured in the present studies represents the maximal extraction of the unidirectional influx into the brain.

The value of  $(n/K_d)_{\text{in vitro}}$  was calculated by

$$f_{u,\text{in vitro}} = \frac{C_u}{C_t} = \frac{C_u}{C_u + (n \cdot (P) \cdot C_u) / (K_d + C_u)} \quad (3)$$

where  $C_t$  is the total concentration of drug,  $C_u$  is the unbound concentration of drug,  $n$  is the number of binding sites per protein molecule,  $(P)$  is the molar concentration of protein and  $K_d$  is the dissociation constant of the drug.

At the tracer dose, where  $K_d \gg C_u$ , Eq. 3 can be expressed as

$$f_{u,\text{in vitro}} = \frac{1}{1 + (n/K_d)_{\text{in vitro}} \cdot (P)} \quad (4)$$

Thus, rearrangement of Eq. 4 gives

$$1/f_{u,\text{in vitro}} = 1 + (n/K_d)_{\text{in vitro}} \cdot (P) \quad (5)$$

The value of  $(n/K_d)_{\text{in vitro}}$  was calculated as follows. If we assume that only unbound drug could be transported across the BBB, the following Kety–Renkin–Crone equation<sup>30</sup> is obtained.

$$E_T = 1 - \text{Exp} \left( - \frac{f_{u,\text{in vitro}} \cdot PS_u}{Q} \right) \quad (6)$$

where  $Q$  is the brain blood flow (the value measured by the  $^{51}\text{Cr}$ -microsphere method was  $0.50 \text{ ml/min/g}$  brain) and  $PS_u$  is the BBB permeability–surface area product for the unbound drug in the brain capillaries.

Furthermore, if Eq. 7 (similar to Eq. 4) holds *in vivo*,

$$f_{u,\text{in vivo}} = \frac{1}{1 + (n/K_d)_{\text{in vivo}} \cdot (P)} \quad (7)$$

Equation 6 becomes

$$PS_{\text{app}} = -Q \cdot \ln(1 - E_T) = \frac{PS_u}{1 + (n/K_d)_{\text{in vivo}} \cdot (P)} \quad (8)$$

Rearrangement of Eq. 8 gives

$$\frac{PS_u}{PS_{\text{app}}} = 1 + (n/K_d)_{\text{in vivo}} \cdot (P) \quad (9)$$

**Statistical Analysis**—Student's *t*-test was utilized to estimate the significance of differences between the buffer-injected groups and protein-containing solution injected groups with  $p = 0.05$  as the minimal criterion of significance. The comparison between IMP and DMI was carried out only for the case of buffer-injected groups.

## Results

The  $E_T$  values for  $^3\text{H}$ -IMP at various times after carotid injection with nonprotein buffer solution are shown in Fig. 1. The efflux rate constant ( $k_{\text{efflux}}$ ) calculated from the slope was  $0.0696 \text{ min}^{-1}$ , which is equivalent to a  $t_{1/2}$  of 4.32 min. The drug was thus retained by the brain and returned to the blood very slowly. Increased concentrations of serum proteins added to the carotid injection solution resulted in decreases in the brain extraction and  $PS_{\text{app}}$  of  $^3\text{H}$ -IMP and  $^3\text{H}$ -DMI, as summarized in Table I. However,  $PS_{u,\text{app}}$  corrected for the *in vitro* binding increased as the protein concentration increased, suggesting protein-mediated brain uptake. The extraction ratio (*ca.* 0.92) of  $^3\text{H}$ -IMP was higher than that of  $^3\text{H}$ -DMI (*ca.* 0.24)

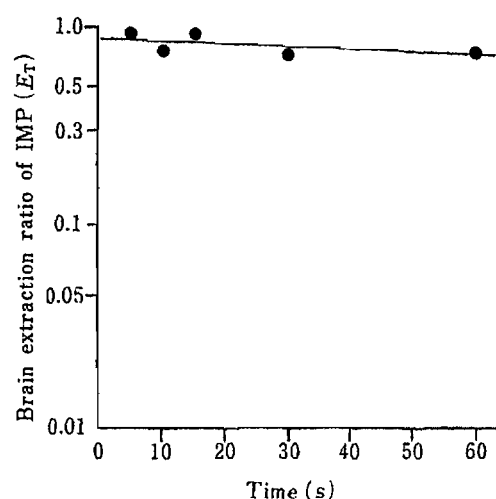


Fig. 1. Time Course of Rat Brain Extraction Ratio of Imipramine (IMP) after Carotid Injection

The line represents the best fit to these data by a least-squares regression.

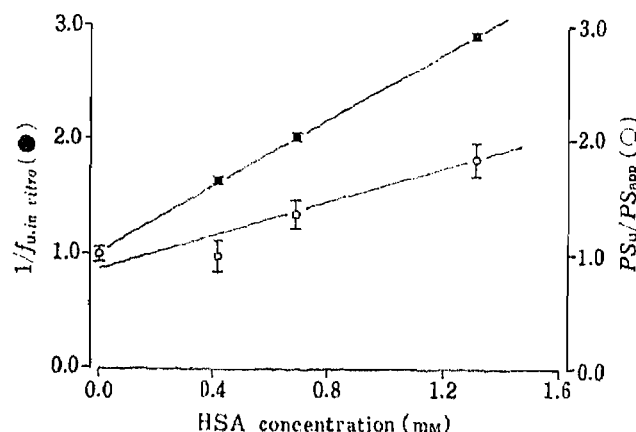


Fig. 2. Reciprocal of *in Vitro* Unbound Fraction ( $1/f_{u, \text{in vitro}}$ ) and  $PS_u/PS_{\text{app}}$  for Imipramine as a Function of HSA Concentration In Carotid Injection Solution

The slopes of these lines yield the  $(n/K_d)_{\text{in vitro}}$  (●) of Eq. 5 and  $(n_i/K_d)_{\text{in vitro}}$  (○) of Eq. 9.

TABLE I. Parameters of the Brain Uptake of Imipramine (IMP) and Desipramine (DMI) with Various Concentrations of Human Serum Albumin (HSA), Bovine Serum Albumin (BSA) and Human  $\alpha_1$ -Acid Glycoprotein ( $\alpha_1$ -AGP) in the Carotid Injection Solution

Compound	Exp. No.	Protein concentration in injection solution % (w/v)	BUI (%)	$E_T$	$f_{u, \text{in vitro}}$	$PS_{\text{app}}$ (ml/min/g)	$PS_{u, \text{app}}$ (ml/min/g)
IMP	1	Buffer (0%)	99.09 ± 0.99	0.892 ± 0.009	1	1.100 ± 0.040	1.100 ± 0.040
		HSA 3%	98.43 ± 4.22	0.886 ± 0.038	0.610	1.146 ± 0.093	1.880 ± 0.153 <sup>a)</sup>
		HSA 5%	88.83 ± 2.06 <sup>a)</sup>	0.800 ± 0.018 <sup>a)</sup>	0.494	0.800 ± 0.048 <sup>a)</sup>	1.621 ± 0.098 <sup>a)</sup>
		HSA 10%	77.38 ± 3.30 <sup>b)</sup>	0.696 ± 0.030 <sup>b)</sup>	0.341	0.597 ± 0.055 <sup>b)</sup>	1.748 ± 0.160 <sup>a)</sup>
	2	Buffer (0%)	101.7 ± 3.24	0.916 ± 0.026	1	1.254 ± 0.137	1.254 ± 0.137
		BSA 3%	97.96 ± 2.28	0.822 ± 0.020	0.402	1.070 ± 0.086	2.664 ± 0.215 <sup>b)</sup>
		BSA 5%	89.82 ± 3.28	0.809 ± 0.030	0.223	0.825 ± 0.083	3.696 ± 0.373 <sup>b)</sup>
		BSA 10%	82.29 ± 4.96 <sup>c)</sup>	0.742 ± 0.044 <sup>c)</sup>	0.142	0.681 ± 0.090 <sup>c)</sup>	4.706 ± 0.571 <sup>b)</sup>
		$\alpha_1$ -AGP 0.1%	104.9 ± 2.42	0.945 ± 0.036	0.499	1.554 ± 0.137	3.114 ± 0.301 <sup>b)</sup>
		$\alpha_1$ -AGP 0.2%	79.02 ± 3.05 <sup>a)</sup>	0.711 ± 0.028 <sup>a)</sup>	0.338	0.616 ± 0.045 <sup>a)</sup>	1.825 ± 0.135 <sup>c)</sup>
DMI	3	Buffer (0%)	26.29 ± 1.66 <sup>c)</sup>	0.237 ± 0.015 <sup>c)</sup>	1	0.133 ± 0.010 <sup>c)</sup>	0.133 ± 0.010 <sup>c)</sup>
		$\alpha_1$ -AGP 0.1%	29.21 ± 3.39	0.263 ± 0.030	0.543	0.151 ± 0.022	0.278 ± 0.038 <sup>d)</sup>
		$\alpha_1$ -AGP 0.2%	22.50 ± 3.04	0.203 ± 0.027	0.364	0.112 ± 0.017	0.308 ± 0.046 <sup>a)</sup>
		$\alpha_1$ -AGP 0.3%	22.56 ± 3.29	0.203 ± 0.030	0.269	0.112 ± 0.018	0.417 ± 0.067 <sup>a)</sup>

The abbreviations are as follows. BUI (%), brain uptake index based on an internal reference substance ( $^{14}\text{C}$ -butanol) calculated according to Eq. 1;  $E_T$ , maximal unidirectional extraction ratio;  $f_{u, \text{in vitro}}$ , unbound fraction determined by equilibrium dialysis;  $PS_{\text{app}}$ , BBB permeability-surface area product for IMP and DMI calculated according to Eq. 8 [ $PS_{\text{app}} = -Q \cdot \ln(1 - E_T)$ , where brain blood flow ( $Q$ ) =  $0.50 \pm 0.05$  ml/min/g brain (determined by the  $^{51}\text{Cr}$  microsphere method)];  $PS_{u, \text{app}}$ ,  $PS_{\text{app}}$  corrected for the *in vitro* binding calculated according to  $PS_{u, \text{app}} = PS_{\text{app}}/f_{u, \text{in vitro}}$ . Data are expressed as mean  $\pm$  S.E. ( $n=4-8$ ). a) Significantly different ( $p < 0.01$ ) from the buffer injected group in the same Exp. No.; b) Significantly different ( $p < 0.001$ ) from the buffer-injected group in the same Exp. No.; c) Significantly different ( $p < 0.05$ ) from the buffer-injected group in the same Exp. No.; d) Significantly different ( $p < 0.02$ ) from the buffer-injected group in the same Exp. No. e) Significantly different ( $p < 0.001$ ) from the case of IMP.

TABLE II. *In Vitro* and *In Vivo*  $n/K_d$  Values of Imipramine (IMP) and Desipramine (DMI) for Various Serum Proteins<sup>a)</sup>

Protein	<i>In vitro</i> $n/K_d$ ( $\text{mM}^{-1}$ )		<i>In vivo</i> $n/K_d$ ( $\text{mM}^{-1}$ )	
	IMP	DMI	IMP	DMI
BSA	$4.52 \pm 0.43$	ND <sup>b)</sup>	$0.597 \pm 0.214$	ND <sup>b)</sup>
HSA	$1.48 \pm 0.20$	ND <sup>b)</sup>	$0.754 \pm 0.244$	ND <sup>b)</sup>
$\alpha_1$ -AGP	$57.79 \pm 5.92$	$38.92 \pm 4.48$	$14.73 \pm 4.07$	$5.90 \pm 3.46$

a) The *in vitro*  $n/K_d$  value were calculated by means of Eq. 4 based on the data determined by equilibrium dialysis. The *in vivo*  $n/K_d$  values were calculated by means of Eq. 8 based on the data obtained by the carotid injection technique. The parameters were expressed as mean  $\pm$  computer calculated S.D. b) Not determined.

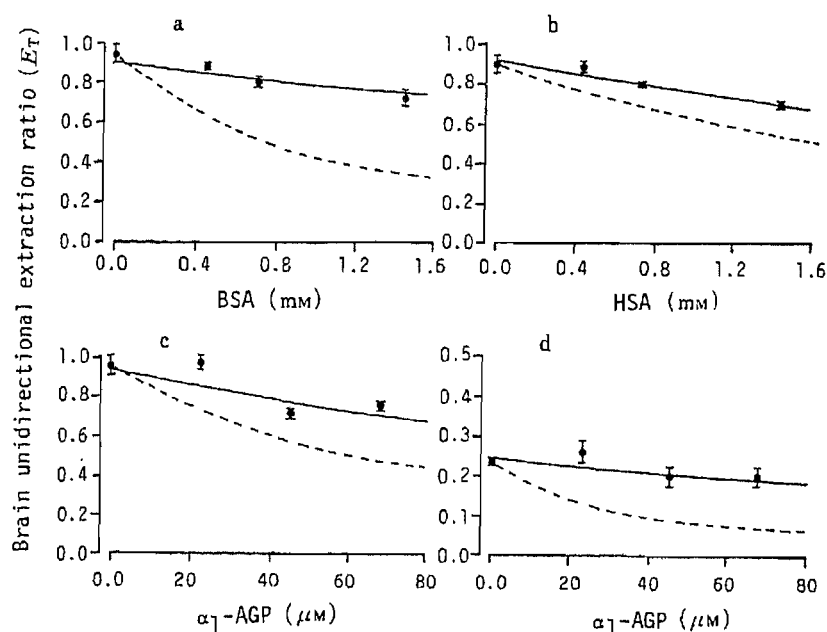


Fig. 3. Predicted and Observed Brain Unidirectional Extraction Ratios ( $E_T$ ) for Various Concentrations of Proteins in Carotid Injection Solution

Panels a, b, and c: imipramine (IMP). Panel d: desipramine (DMI). The solid circles represent the observed values (mean  $\pm$  S.E.,  $n=4-8$  rats, per point), and the dotted line was simulated according to Eq. 8 using the  $n/K_d$  values determined *in vitro* by equilibrium dialysis instead of  $(n/K_d)_{in vivo}$ .

—, observed; ----, predicted.

in the buffer injection solution (Table I). Linearized plots according to Eqs. 5 and 9 comparing the *in vitro* and *in vivo*  $n/K_d$  values of  $^3\text{H}$ -IMP to HSA, are shown in Fig. 2. The *in vitro*  $n/K_d$  value obtained from the slope is approximately twice as large as that *in vivo*. We further calculated the *in vitro* and *in vivo*  $n/K_d$  values using a computer-aided nonlinear least-squares method according to Eqs. 4 and 8, respectively, and the results are listed in Table II. The *in vitro*  $n/K_d$  values of  $^3\text{H}$ -IMP to BSA, HSA and  $\alpha_1$ -AGP were approximately 8, 2 and 4 times the corresponding *in vivo*  $n/K_d$  values, and that of  $^3\text{H}$ -DMI to  $\alpha_1$ -AGP was approximately 7 times of the corresponding *in vivo*  $n/K_d$  value.

The observed extraction ratios and those predicted by Eq. 8 using the *in vitro*  $n/K_d$  values are shown in Fig. 3. A marked difference was found between the observed values and what would be predicted if only the unbound IMP is transported, although the difference was not large in the case of HSA. A similar difference between the observed and predicted values was

found for the transport of DMI. These studies suggested that serum protein-bound IMP and DMI are available for transport into the brain.

### Discussion

Figure 1 validates the assumption that the efflux of lipophilic basic drugs such as IMP can be neglected within 15 s. Therefore, it may be reasonable to assume that the extraction ratio of the drug at 15 s is essentially identical to the maximal extraction ratio of unidirectional influx. The carotid artery injection technique was used to quantitate the extraction of the drug in the present studies. Crucial to this technique is the assumption that there is minimal mixing of the injection solution bolus with the circulating plasma following rapid artery injection. Recently, Pardridge *et al.*<sup>24)</sup> reported that mixing does not occur to any significant extent in this technique.

Data obtained in the present studies show that serum protein-bound drugs such as IMP and DMI are readily available for transport into the brain. The transport of drugs into the brain was inhibited by serum protein, but the extent of inhibition was less than that predicted based on the "free drug hypothesis," which assumes that only the unbound drug *in vitro* is available for transport into tissues *in vivo* (Fig. 3). This result may be related to the previous report<sup>2)</sup> that a linear correlation was observed between the clinical effect and the total plasma concentration of IMP or DMI and that there seems to be no need to take into account only the unbound drug concentration.

There have been several reports suggesting the serum protein-mediated transport of metabolic substances<sup>13,15,19)</sup> hormone<sup>17)</sup> and drugs<sup>14,18,31)</sup> into the liver and brain. For instance, Weisiger *et al.*<sup>13,16)</sup> presented the albumin receptor-mediated transport concept to account for the transport of fatty acid, sulfobromophthalein and bilirubin into the liver, and Forker and Luxon<sup>14,15)</sup> suggested the presence of albumin-mediated transport in the liver for rose bengal and taurocholate. Subsequently, we also found an albumin-mediated hepatic uptake of warfarin using the multiple indicator dilution method.<sup>31)</sup> Pardridge *et al.*<sup>18,19)</sup> suggested a "free intermediate model" to explain the transport of many substances such as steroid hormone and *l*-propranolol (PL) into the brain. Recent *in vivo* studies showed that the transit time of albumin through the liver and brain is not delayed compared with that of an extracellular marker such as sucrose.<sup>32,33)</sup> In addition, *in vitro* studies using liver plasma membranes<sup>34)</sup> and brain microvessels<sup>33)</sup> could not detect any specific binding to albumin and failed to support the albumin receptor-mediated transport concept in either liver or brain. However, as suggested by Pardridge *et al.*,<sup>33)</sup> this fact does not preclude the possibility of rapid nonspecific interactions of circulating serum proteins with the glycocalyx of capillary endothelial cell surface. In fact, it has been suggested that charged moieties on the plasma proteins interact electrostatically with the negatively charged moieties of the endothelial glycocalyx.<sup>35,36)</sup>

The relation of the *in vitro* and *in vivo*  $n/K_d$  values for IMP and DMI is shown in Fig. 4, together with those for other substances reported by Pardridge *et al.*<sup>18,37,38)</sup> It was shown that the *in vivo*  $n/K_d$  values were markedly lower than those measured *in vitro* except for two cases (PL-BSA, IMP-HSA). Our data showed that the decrease in the *in vivo*  $n/K_d$  value compared to the *in vitro* value seems to be independent of the species and the source of serum proteins, although no marked difference was observed for IMP-HSA. As discussed above, no specific binding of albumin to brain capillaries was detected either *in vivo* or *in vitro*. However, Mizuma *et al.*<sup>39)</sup> recently succeeded in detecting the interaction between albumin and liver cells using electron spin resonance (ESR) and fluorescence spectroscopy, although this binding also appeared to be nonspecific. Therefore, the nonspecific interaction between the protein and the cell surface might be possible mechanism to explain the discrepancy between

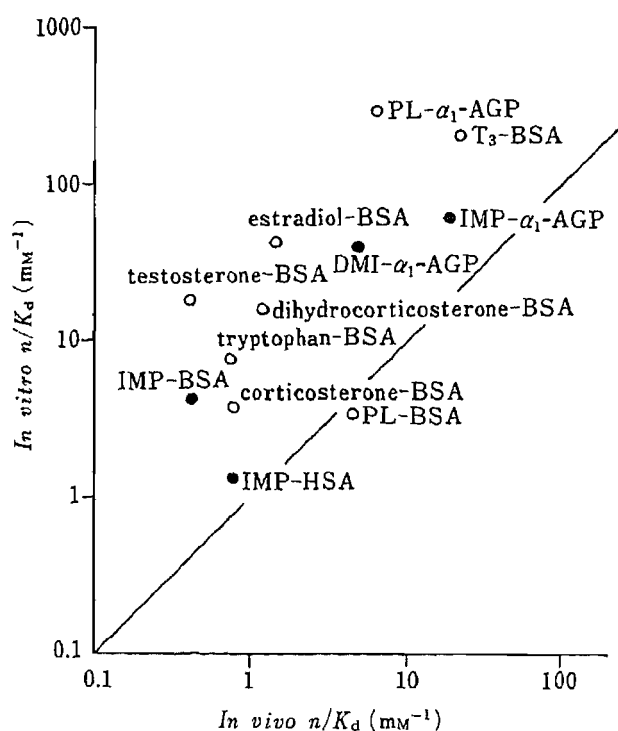


Fig. 4. Relationship of the *in Vitro* and *in Vivo*  $n/K_d$  Values

The solid circles represent the values obtained by the carotid injection technique in the present studies, while the open circles represent the values obtained from the reports by Pardridge *et al.*<sup>18,37,38)</sup> The solid line represents a positive 1:1 relationship. Abbreviations are as follows. PL, propranolol; T<sub>3</sub>, liothyronine.

*in vitro* and *in vivo*  $n/K_d$  values (Fig. 2, Table II), *i.e.*, the protein-mediated brain uptake of drugs.

It seemed interesting to estimate the contributions of albumin and  $\alpha_1$ -AGP to the protein-mediated brain uptake of IMP. The serum concentrations of albumin and  $\alpha_1$ -AGP in normal humans are approximately 5% (0.075 mM) and 0.07% (0.016 mM), respectively. Therefore, the contribution of each protein to the binding of IMP to the circulating serum may be calculated as follows based on the *in vitro*  $n/K_d$  values (Table II) under the condition of linear binding.

$$(\text{binding to albumin}) : (\text{binding to } \alpha_1\text{-AGP}) = 1.48 \times 0.075 : 57.8 \times 0.016 = 1.3 : 1$$

On the other hand, in order to estimate the contribution of each protein to the brain uptake of IMP, it may be reasonable to use the *in vivo*  $n/K_d$  value (Table II), since the *in vivo* values may represent the drug binding in the brain capillaries from which the drug is taken up into the brain. A similar calculation yields:

$$(\text{binding to albumin}) : (\text{binding to } \alpha_1\text{-AGP}) = 0.75 \times 0.075 : 14.7 \times 0.016 = 2.6 : 1$$

Thus, in the *in vivo* brain capillaries, the binding of IMP to albumin may be a few times greater than that to  $\alpha_1$ -AGP.

As shown in Table I, no increase in the  $PS_{u,app}$  value for IMP was observed with increase in the HSA concentration in the injection solution, although an increase in the  $PS_{u,app}$  value was observed for other proteins. The reason for this finding is not known, but the lower binding affinity of IMP to HSA may be related to this phenomenon. That is, the range of  $f_u$  values of IMP associated with the change in the HSA concentrations (3–10%) was relatively small due to the lower affinity of IMP to HSA. This may explain why we could not detect any increase in the  $PS_{u,app}$  value with increase in the HSA concentration.

The value of  $E_T$  for DMI was much lower than that of IMP in the case of the buffer solution injection (Table I). The smaller extraction for DMI may be attributed to its lower lipophilicity as compared with IMP, because the lipophilicity is one of the major factors which



could affect the transport of substances through the BBB. In fact, Glasser and Krieglstein reported that the partition coefficient of DMI was approximately one-tenth of that for IMP in octanol/pH 7.4 phosphate buffer.<sup>40)</sup>

**Acknowledgement** This study was supported in part by a grant-in-aid for scientific research provided by the Ministry of Education, Science and Culture of Japan.

#### References and Notes

- 1) Abstracted in part from a dissertation submitted by T.-H. Lin to the Graduate School, Division of Pharmaceutical Sciences, University of Tokyo, Tokyo, Japan, in partial fulfillment of the requirements for the degree of Doctor of Philosophy.
- 2) N. Reisby, J. F. Gram, P. Bech, A. Nagy, G. O. Petersen, J. Ortmann, I. Ibsen, S. J. Dencker, O. Jacobsen, O. Krautwald, I. Sondergaard and J. Christiansen, *Psychopharmacol.*, **54**, 263 (1977).
- 3) G. Johnsson and C.-G. Regardh, *Clin. Pharmacokinet.*, **1**, 233 (1976).
- 4) K. A. Collinsworth, S. M. Kalman and D. C. Harrison, *Circulation*, **50**, 1217 (1974).
- 5) P. R. Jackson, G. T. Tuckert and H. F. Woods, *Clin. Pharmacol. Ther.*, **32**, 295 (1982).
- 6) F. M. Belpaire and M. Rosseneu, *Eur. J. Clin. Pharmacol.*, **22**, 253 (1982).
- 7) E. Pike, B. Skuterud, P. Kierulf, D. Fremstad, S. M. Abdel Sayed and P. K. M. Lunde, *Clin. Pharmacokinet.*, **6**, 367 (1981).
- 8) E. Pike, B. Skuterud, P. Kierulf, J. E. Bredesen and P. K. M. Lunde, *Clin. Pharmacokinet.*, **9** (Suppl.), 84 (1984).
- 9) Y. Suzuki, Y. Sugiyama, Y. Sawada, T. Iga and M. Hanano, *J. Pharm. Pharmacol.*, **37**, 712 (1985).
- 10) J. J. Vallner and L. Chen, *J. Pharm. Sci.*, **66**, 420 (1977).
- 11) J. Koch-Weser and E. M. Sellers, *N. Eng. J. Med.*, **294**, 311 (1976).
- 12) C. J. Hull, *Br. J. Anaesth.*, **51**, 579 (1979).
- 13) R. K. Ockner, R. A. Weisiger and J. L. Gollan, *Am. J. Physiol.*, **245**, G13 (1983).
- 14) E. L. Forker and B. A. Luxon, *J. Clin. Invest.*, **72**, 1764 (1983).
- 15) E. L. Forker and B. A. Luxon, *J. Clin. Invest.*, **67**, 1517 (1981).
- 16) R. Weisiger, J. Gollan and R. Ockner, *Science*, **211**, 1048 (1981).
- 17) W. M. Pardridge, *Endocr. Rev.*, **2**, 103 (1981).
- 18) W. M. Pardridge, R. Sakiyama and G. Fierer, *J. Clin. Invest.*, **71**, 900 (1983).
- 19) W. M. Pardridge and W. H. Oldendorf, *J. Neurochem.*, **28**, 5 (1977).
- 20) W. M. Pardridge and L. J. Mietus, *J. Clin. Invest.*, **64**, 145 (1979).
- 21) W. H. Oldendorf, *Brain Res.*, **24**, 372 (1970).
- 22) D. G. Mcdevitt and A. S. Nies, *Cardiovasc. Res.*, **10**, 494 (1976).
- 23) S. Ishise, B. L. Pegram, J. Yamamoto, Y. Kitamura and D. Frohlich, *Am. J. Physiol.*, **239**, H443 (1980).
- 24) W. M. Pardridge, E. M. Landaw, L. P. Miller, L. D. Braun and W. H. Oldendorf, *J. Cerebr. Blood Flow Metab.*, **5**, 576 (1985).
- 25) W. M. Pardridge and L. J. Mietus, *J. Clin. Invest.*, **66**, 367 (1980).
- 26) W. M. Pardridge and W. H. Oldendorf, *Biochim. Biophys. Acta*, **382**, 377 (1975).
- 27) W. H. Oldendorf and L. D. Braun, *Brain Res.*, **113**, 219 (1976).
- 28) W. H. Oldendorf, W. M. Pardridge, L. D. Braun and P. D. Crane, *J. Neurochem.*, **38**, 1413 (1982).
- 29) W. M. Pardridge, T. L. Moeller, L. J. Mietus and W. H. Oldendorf, *Am. J. Physiol.*, **239**, E96 (1980).
- 30) C. Crone, *Acta Physiol. Scand.*, **58**, 292 (1963).
- 31) S. C. Tsao, Y. Sugiyama, Y. Sawada, S. Nagase, T. Iga and M. Hanano, *J. Pharmacokinet. Biopharm.*, **14**, 51 (1986).
- 32) Y. R. Stollman, U. Gartner, L. Theilmann, N. Ohmi and A. W. Wolkoff, *J. Clin. Invest.*, **72**, 718 (1983).
- 33) W. M. Pardridge, J. Eisenberg and W. T. Cefalu, *Am. J. Physiol.*, **249**, E264 (1985).
- 34) W. Stermmel, B. Potter and P. D. Berk, *Biochim. Biophys. Acta*, **756**, 20 (1983).
- 35) C. C. Michel, M. E. Phillips and M. R. Turner, *J. Physiol. (London)*, **332**, 111 (1982).
- 36) E. E. Schneeberger and M. Hamelin, *Am. J. Physiol.*, **247**, H206 (1984).
- 37) W. M. Pardridge, *Endocrinol.*, **105**, 605 (1979).
- 38) W. M. Pardridge, *Life Sci.*, **25**, 1519 (1979).
- 39) T. Mizuma, T. Horie, M. Hayashi and S. Awazu, *J. Pharmacobio-Dyn.*, **9**, 244 (1986).
- 40) H. Glasser and E. Krieglstein, *J. Nuuyv-Sch. Arch. Pharmacol.*, **265**, 321 (1970).

[Chem. Pharm. Bull.]  
35(1) 302-307 (1987)

## Glycation<sup>1)</sup> of Erythrocyte Superoxide Dismutase Reduces Its Activity

TAMIKO SAKURAI,\* MOTOTAKA MATSUYAMA and SEISHI TSUCHIYA

*Tokyo College of Pharmacy, 1432-1 Horinouchi, Hachioji,  
Tokyo 192-03, Japan*

(Received June 12, 1986)

Commercially available Cu, Zn superoxide dismutase (SOD) from bovine erythrocytes was purified. Purified SOD was incubated with 1 M glucose at 37°C for 14 d under sterile conditions. Nonenzymatic addition of glucose to SOD molecules increased linearly until 7 d, and then increased only slightly. The enzyme activity decreased to 88% after 7 d and 60% after 14 d. The glycated amino acid residue is not the N-terminal  $\alpha$ -amino group but the  $\epsilon$ -amino group of lysine. It seems that lysine at the active center, which assists the interaction of O<sub>2</sub><sup>-</sup> and the SOD molecule, is affected during 14 d.

**Keywords**—glycation; nonenzymatic glycosylation; superoxide dismutase; lysine residue; diabetes

Interest in radical scavenger-enzymes, especially superoxide dismutase, has increased markedly in recent years in relation to aging and pathogenesis.<sup>2)</sup> Cu, Zn superoxide dismutase (SOD) in erythrocytes, cooperating with catalase and glutathione peroxidase, protects the plasma membrane from oxygen toxicity due to active oxygen species such as O<sub>2</sub><sup>-</sup>, H<sub>2</sub>O<sub>2</sub> and ·OH. Increase in SOD activity in erythrocytes is observed in sickle cell anemia<sup>3)</sup> and muscular dystrophy<sup>4)</sup> and decrease is observed in diabetic children<sup>5)</sup> and diabetic rats.<sup>6,7)</sup>

On the other hand, it has been reported that, in diabetic patients<sup>8-11)</sup> or in experimental diabetes,<sup>12,13)</sup> the amount of glucose adducts of various proteins increases as well as hemoglobin A<sub>1c</sub>.<sup>14)</sup> Glycation of proteins causes changes in their functions; a decrease in ligand binding capacity of human serum albumin,<sup>15)</sup> an increase in oxygen affinity of hemoglobin,<sup>14)</sup> and a reduction of the susceptibility of plasmin.<sup>16)</sup> In enzyme proteins, glycation resulted in a decrease in the activities of pancreatic ribonuclease<sup>17)</sup> and kidney  $\beta$ -N-acetyl-glucosaminidase.<sup>18)</sup> Glycation has been extensively studied in relation to the pathogenesis of diabetic complications.<sup>19)</sup> In this paper, in order to study the possible cause of the lowering of erythrocyte SOD activity in diabetes, we investigated the *in vitro* glycation of SOD.

### Materials and Methods

**Materials**—SOD (92F-9340, 2800 U/mg) from bovine blood, cytochrome c (Type III) from horse heart, polylysine hydrobromide (55000 dalton) were obtained from Sigma Chemical Co. The content of reduced form of cytochrome c was estimated by the addition of sodium dithionite.<sup>20)</sup> Xanthine and xanthine oxidase (20 U/ml) from cow's milk were purchased from Wako Pure Chem. Ind., Ltd., and Boehringer Mannheim, respectively. Matrex gel (PBA-10) was obtained from Amicon Corp.

**Purification and Assay of Superoxide Dismutase**—SOD (50 mg) was applied to a diethyl aminoethyl (DEAE)-cellulose column (Whatman DE-52, 1.2 × 32 cm) equilibrated with 2.5 mM potassium phosphate buffer (pH 7.8) and was eluted with a linear gradient of buffer (200 ml) from 2.5 to 200 mM.<sup>21)</sup> Three separate peaks observed at 280 nm, with area ratios of 0.33 (peak I), 0.31 (peak II) and 0.36 (peak III), corresponded to the buffer concentrations of 21.8, 27.8 and 36.7 mM, respectively. Peak III was dialyzed against distilled water followed by lyophilization and was used

as purified SOD. The purified SOD showed a broad single band on disc polyacrylamide gel electrophoresis.<sup>22)</sup> The SOD activity after glycation was assayed by the cytochrome c method using 50 mM sodium carbonate buffer (pH 10.2) containing  $1 \times 10^{-4}$  M ethylenediaminetetraacetic acid (EDTA).<sup>23)</sup>

**Copper Content**—About 10  $\mu$ g of enzyme protein was added to a standard solution of copper and the copper content was analyzed by flameless atomic absorption spectroscopy (Shimadzu AA-646 atomic absorption spectrophotometer).

**Glycation *in Vitro***—Purified SOD was dissolved to 0.5% (w/v) in 67 mM sodium phosphate buffer (pH 7.4) containing 1 M glucose. This solution was filtered through a Millipore filter (Millex-GS, 0.22  $\mu$ m) and poured into dry-heat sterilized tubes followed by incubation for 14 d at 37 °C. After adequate dialysis, aliquots were frozen at  $-20$  °C until assayed. The same procedure without glucose was carried out as a control. The amount of glucose added to SOD was estimated by the thiobarbituric acid method<sup>24)</sup> by using ampules for acid hydrolysis. Protein concentration was assayed by the Lowry method.

Poly-lysine (0.1% w/v) dissolved in 67 mM phosphate buffer (pH 7.4) containing 150 mM glucose was incubated at 37 °C for 5 d, followed by dialysis and lyophilization. The resulting powder was referred to glucose adduct of poly-lysine.

**Amino Acid Analysis**—The SOD solution incubated for 7 d with 1 M glucose was dialyzed and loaded on a phenylboronate affinity column (Matrex gel, PBA-10).<sup>15)</sup> Glycated SOD eluted by 25 mM sodium phosphate buffer (pH 8.5) containing 100 mM sorbitol was dialyzed and lyophilized. The lyophilized protein (8 mg) was dissolved in 5 ml of 35 mM sodium phosphate buffer (pH 7.8) and reduced for 4 h at room temperature by the addition of 9 mg of sodium borohydride. The reaction was terminated by the addition of 1 M HCl, followed by dialysis and lyophilization. The reduced protein (2 mg) was hydrolyzed in 2 ml of distilled 6 M HCl containing phenol (0.1%) at 110 °C for 24 h. Reduction and acid hydrolysis of commercial SOD, purified SOD and poly-lysine for amino acid analysis were carried out by the same procedure. Amino acid analysis was carried out with a Hitachi 835 high-performance amino acid analyzer.

**Preparation of Apoenzyme**—Apoprotein fraction which had lost 95% of the theoretical copper content of SOD was obtained by overnight dialysis of purified SOD solution against 80 mM acetic acid/20 mM sodium acetate (pH 3.8) buffer.<sup>22)</sup> The sample was adequately dialyzed against distilled water and was used for measurement of circular dichroism (CD) spectra.

**CD Spectra**—Molar CD  $\Delta\epsilon$  is defined as  $\Delta\epsilon = [\theta]/3300$  where  $[\theta]$  is the molar ellipticity. Spectra were measured in the wavelength range from 200 to 350 nm using a JASCO 500C spectropolarimeter. Protein concentrations ranged from 7 to 0.5 mg/ml. Cuvettes of 1 and 0.1 cm light path length were used to obtain the maximum sensitivity at any wavelength.

## Results

Peak III, which was eluted from the ion exchange column at the buffer concentration of 36.7 mM (see Materials and Methods), showed an absorption spectrum having fine structure from 250 to 270 nm, which is characteristic of SOD of bovine erythrocytes,<sup>21)</sup> and only this fraction showed the absorption of copper at 680 nm. In peak III, the excitation maximum of fluorescence spectrum was at 275 nm (305 nm emission), and the emission maximum was at 305 nm (275 nm excitation). Only peak III showed SOD activity by the cytochrome c method. The result of amino acid analysis of this purified SOD is given in Table I with the theoretical values.<sup>25)</sup> Though purified SOD showed lower contents of valine, isoleucine and histidine residues than the theoretical values, the contents of other amino acid residues agreed fairly well with the theoretical values.

The CD spectrum of purified SOD is shown in Fig. 1. The ellipticity band of purified SOD coincided in position with that given for the holoenzyme in the literature<sup>26)</sup> but the molar CD  $\Delta\epsilon$  of purified SOD at 260 nm was about 55% of that of the holoenzyme. A striking difference of CD spectrum in the ultraviolet (UV) region between apo- and holoenzyme has been reported,<sup>26)</sup> that is, the positive ellipticity at 255–265 nm is destroyed in the apoenzyme. As the presence of apoenzyme without copper was suggested, the copper content of purified SOD was assayed. It was estimated to be  $61.9 \pm 9.1\%$  ( $n=9$ ) of the theoretical value. These results indicate the presence of 38.1% of apoenzyme in the purified SOD.

Figure 2 summarizes the result obtained after incubation of purified SOD with 1 M glucose for 14 d. The amount of glucose added to SOD molecules during incubation, which

TABLE I. Amino Acid Composition of Superoxide Dismutase

Amino acid residue	Theoretical value <sup>a)</sup>	Commercial SOD	Purified SOD	Glycated SOD <sup>c)</sup>
Asp, Asn <sup>b)</sup>	22, 12	26.45	33.10	32.52
Thr	24	16.02	23.00	22.35
Ser	16	11.36	15.59	15.55
Glu, Gln <sup>b)</sup>	16, 6	19.82	22.65	23.09
Gly	50	31.55	48.06	46.32
Ala	18	14.88	18.36	19.26
Cys	6	— <sup>b)</sup>	—	—
Val	30	19.67	23.32	21.71
Met	2	1.96	1.64	1.79
Ile	18	10.21	13.19	12.69
Lue	16	16.00	16.00	16.00
Tyr	2	0.54	1.75	2.07
Phe	8	7.96	7.90	10.90
Lys	20	15.44	18.75	15.26
His	16	9.97	13.50	13.20
Arg	8	7.07	7.74	7.84
Pro	12	9.46	10.86	10.49

a) The data of Steinman *et al.*<sup>25)</sup> b) Present but not quantitated. c) This was obtained from the adsorbed fraction on the phenylboronate affinity column.

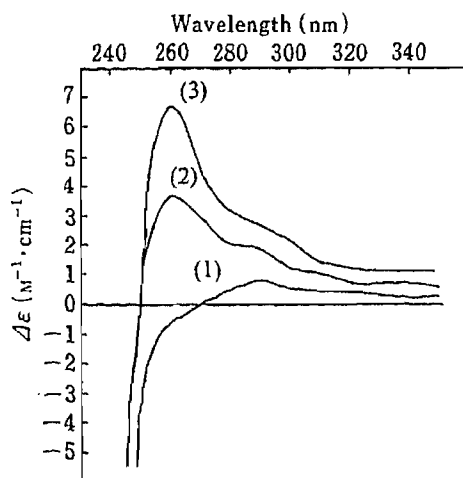


Fig. 1. Circular Dichroism Spectra of (1) Apo-enzyme, (2) Purified SOD and (3) Holoenzyme

Solutions of apoenzyme (7.03 mg/ml) and purified SOD (1.87 mg/ml) were measured in a cuvette of 1 cm light path length. The spectrum of the holoenzyme is taken from the literature.<sup>26)</sup>

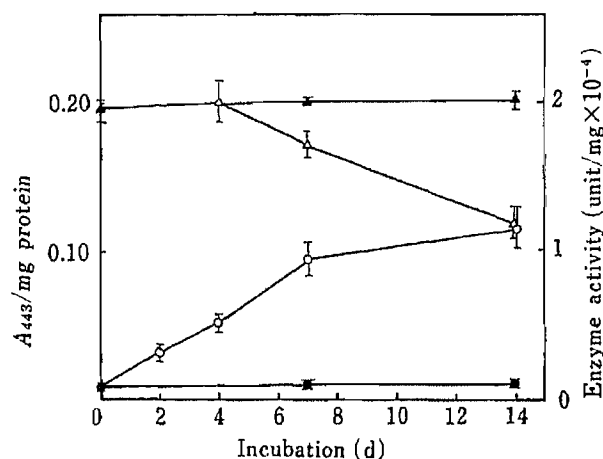


Fig. 2. Addition of Glucose to Purified SOD and Its Activity

Addition of glucose to SOD incubated with (—○—) and without (—●—) 1 M glucose was estimated by measuring the absorbance at 443 nm after reaction with thiobarbituric acid (0.2—1.0 mg protein was used). SOD activity during incubation with (—△—) and without (—▲—) 1 M glucose was estimated by the cytochrome c method at pH 10.2.

was estimated by measuring absorbance at 443 nm in the thiobarbituric acid method, increased linearly until 7 d, and after that increased only slightly. The enzyme activity decreased to about 88% after 7 d and 60% after 14 d. On the other hand, incubation without glucose caused no alteration in the enzyme activity.

To separate glycated SOD from nonglycated SOD, purified SOD incubated for 7 d with 1 M glucose was applied to a phenylboronate affinity column. The amino acid analysis of

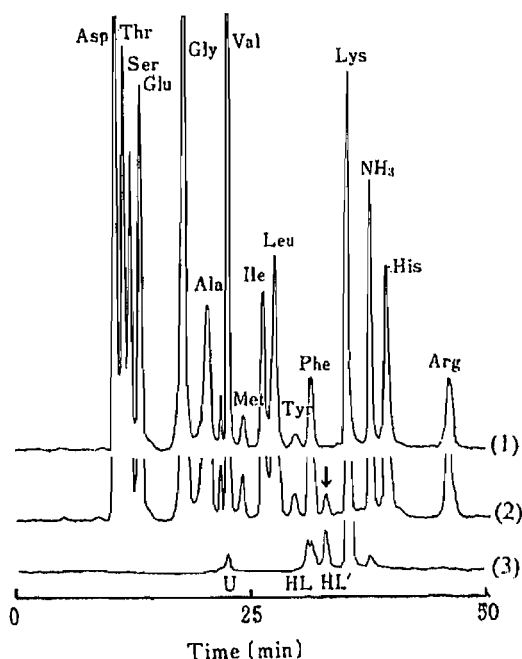


Fig. 3. Elution Patterns of (1) Purified SOD, (2) Glycated SOD and (3) Glucose Adduct of Poly-lysine from the Amino Acid Analysis Column

HL and HL' are hexitol-lysine and its acid rearrangement product, respectively, and U is an unknown product. An arrow indicates a new peak in glycated SOD.

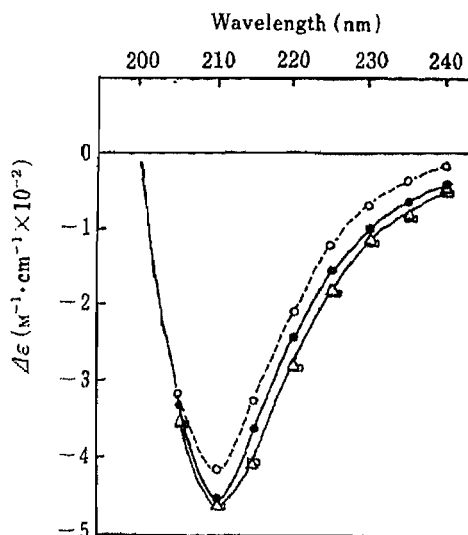


Fig. 4. Circular Dichroism Spectra of Purified SOD Incubated with and without 1 M Glucose

Solutions of SOD (0.5 mg/ml) were measured in a cuvette with 0.1 cm light path length.  $-\square-$ , control (not incubated, without glucose);  $-\triangle-$ , incubated with glucose for 7 d;  $-\circ-$ , incubated with glucose for 14 d;  $\bullet$ , incubated without glucose for 14 d.

glycated SOD is also listed in Table I. Comparison of purified SOD with glycated SOD clarified the glycated amino acid residues. The numbers of glycine, valine and lysine decreased (1.7, 1.6, and 3.5 respectively), but on the other hand, the number of phenylalanine increased (3.0). The other amino acid residues remained unchanged.

The elution profiles of the amino acid analysis column are shown in Fig. 3. In glycated SOD a new peak appeared between phenylalanine and lysine. Elbe *et al.*<sup>17)</sup> reported that the new peak can be used for quantitating of glycated lysine residues, that is, the content of fructose lysine. To confirm the correspondence of this new peak to the acid rearrangement product of  $\epsilon$ -(1-deoxyhexitolyl)-lysine observed by Elbe *et al.*, the acid hydrolysate after reduction of the glucose adduct of poly-lysine was applied to the amino acid analysis column. One peak (HL) appeared at the same position as that of phenylalanine and the other (HL') was eluted between phenylalanine and lysine. The area of HL' was 36% of the sum of HL and HL', agreeing with Elbe's result. This indicates that the yield of HL' is reproducible. So, the number of fructose lysine in glycated SOD estimated to be 3.6, by using the area of the new peak between phenylalanine and lysine, and the color factor of alanine. This value agreed well with the decrease in the number of lysine residues, 3.5 (Table I). The increased number (3.0) of phenylalanine in glycated SOD (Table I) clearly reflects the elution of HL at the same position.

Figure 4 shows the CD spectra from 200 to 240 nm of incubated SOD with or without 1 M glucose and control (no incubated) SOD. The control SOD has negative ellipticity with the maximum at 210 nm, indicating typical  $\beta$ -sheet structure.<sup>27)</sup> The molar ellipticity at 210 nm of the SOD incubated with glucose for 7 d gave almost the same value as that of the control SOD. On the other hand, in the case of the SOD incubated with glucose for 14 d, a slight

decrease of negative ellipticity at 210 nm was observed, though SOD incubated without glucose showed no significant change.

### Discussion

The purity of SOD was confirmed by observations of a characteristic absorption spectrum, tyrosine fluorescence and amino acid analysis. Bovine erythrocytes SOD contains two tyrosine residues, but no tryptophan residue.<sup>25)</sup> When even a trace of tryptophan coexists with tyrosine, a characteristic fluorescence of tyrosine at 305 nm is hidden by a strong fluorescence at 340 nm of tryptophan. Though the contents of the amino acid residues partially disagreed with the theoretical values (Table I), we considered that there was almost no contamination of other proteins, especially carbonic anhydrase B, which is a usual contaminant and contains 8 tryptophan residues. The SOD molecule consists of two identical subunits and each unit contains one copper atom at the catalytic site. As this purified SOD contained 38.1% apoprotein (Fig. 1), copper and zinc were added to the purified SOD. However, the enzyme activity was not increased. Thus, we used this purified SOD for our *in vitro* glycation experiments.

The glycation of a protein proceeds by bimolecular condensation of glucose with amino groups such as N-terminal and  $\epsilon$ -amino of lysine residues in the protein. This reaction is apparent first order with respect to the concentration of glucose,<sup>28)</sup> since the Schiff-base formation is fast and the subsequent Amadori rearrangement is slow. The extent of glycation either *in vivo* or *in vitro* is dependent upon the number of potentially reactive amino groups on the protein, the concentration of glucose in the medium and the life time of the protein. It seems that SOD in erythrocytes can not escape continuous modification by glucose during the lifespan of red cells (120 d). In this experiment, a high concentration of glucose (1 M, which is 40 times higher than that of about 25 mM in diabetic blood plasma) was chosen to shorten the incubation period to about one-tenth of the lifespan.

SOD has net negative charge at physiological pH, since the pI value is 4.95.<sup>29)</sup> The interaction of  $O_2^-$  with this anionic enzyme was shown to be assisted by the positive charge on lysine residues which provides a long-range electrostatic guidance for  $O_2^-$ .<sup>30)</sup> Lysine 134 has an important role in directing  $O_2^-$  to the highly positive catalytic binding site at the bottom of the  $\beta$ -barrel.<sup>31)</sup> To clarify the glycated amino acid residues, amino acid analysis was carried out after separation of glycated SOD by phenylboronate affinity column. In glycated SOD, 3.5 lysine residues were lost and 3.6 fructose lysine were formed (confirmed by a new peak on the amino acid analysis column). The fact that there was no decrease in alanine residues in glycated SOD indicates the absence of glycation at the  $\alpha$ -amino group of N-terminal alanine. The main glycated amino acid residue is lysine. The reason for the decrease in glycine (1.7) and valine (1.6) is not clear.

The fact that incubation for 14 d caused a decrease to 60% in SOD activity, though only a little more glucose was added to SOD incubated for 7 d, suggests that it resulted from secondary changes induced by glycation of some lysine residues. In general, the CD signals at 200–240 nm originate from conformations sensitive to secondary structures of proteins.<sup>32)</sup> The decrease of negative ellipticity at 210 nm after 14 d incubation with glucose (Fig. 4) suggests a decrease in  $\beta$ -structure. Wood *et al.*<sup>26)</sup> showed that the addition of 8 M urea to the holoenzyme caused only a small decrease in negative ellipticity at 210 nm, though in the case of the apoenzyme it caused a larger decrease, showing a CD spectrum similar to that of random coil structure. This means that copper and zinc contributed to stabilizing the final structure and even the  $\beta$ -barrel through the complex network of hydrogen bonds. This network may be perturbed by the glycation of lysine residues. We found nondisulfide cross-linking of human serum albumin in *in vitro* glycation.<sup>33)</sup> The secondary structural change

caused by glycation of lysine residues during 14d incubation may involve intra- or intermolecular cross-linking. We propose the post-translational modification of SOD by glucose as one possible cause of the lowering in erythrocytes SOD activity observed in diabetes.<sup>5-7)</sup>

According to the topological model of SOD proposed by Richardson *et al.*,<sup>34)</sup> five lysine residues, 3, 9, 23, 89, and 151 are oriented to the outside of the barrel. It seems that these residues may be protonated, since they are in contact with the bulk solution. As it is considered that a protonated lysine residue is difficult to be glycated, the other five lysine residues, 67, 68, 73, 120, and 134, located in the two large loops, may be more easily glycated. As lysines 120 and 134 are only 12 Å and 13 Å from the copper at the active center,<sup>30)</sup> the easily glycated lysine residues may be those at positions 67, 68, and 73.

**Acknowledgement** The authors thank Professor K. Kasai (Teikyo University) for making available the amino acid analyzer.

#### References

- 1) Glycation is used to designate nonenzymatic glycosylation, to differentiate it from enzymatic glycosylation.
- 2) B. Boutouyrie, P. M. Sinet and H. Jerome, "Oxy Radicals and Their Scavenger Systems. Vol. II, Cellular and Medical Aspects," ed. by R. A. Greenwald and G. Cohn, Elsevier Science Publishing Co., Inc., New York, 1983, pp. 396—399.
- 3) K. Salil and Das Rajagopalan C. Nair, *Brit. J. Haematol.*, **44**, 87 (1980).
- 4) B. Matkovich, K. Gyurkovits, A. Laszlo and L. Szabo, "Oxy Radicals and Their Scavenger Systems. Vol. II. Cellular and Medical Aspects," eds. by R. A. Greenwald and G. Cohn, Elsevier Science Publishing Co., Inc., New York, 1983, pp. 411—415.
- 5) B. Hagglof, S. L. Marklund and G. Hormgren, *Acta Endocrinologica*, **102**, 235 (1983).
- 6) B. Matkovich, "Superoxide, Superoxide Dismutase," ed. by A. M. Michelson, Proc. EMBO Workshop, Banyuls, Fr., 1977, pp. 501—515.
- 7) R. Crouch, G. Kimsey, D. G. Priest, A. Sarda and M. G. Buse, *Diabetologia*, **15**, 53 (1978).
- 8) R. L. Garlick, J. S. Mazer, L. T. Chylack, Jr., W. H. Tung and H. F. Bunn, *J. Clin. Invest.*, **74**, 1742 (1984).
- 9) R. L. Garlick and J. S. Mazer, *J. Biol. Chem.*, **258**, 6142 (1983).
- 10) S. T. Schneider and R. R. Cohn, *J. Clin. Invest.*, **67**, 1630 (1981).
- 11) E. Schleicher, T. Deufel and O. H. Wieland, *FEBS Lett.*, **129**, 1 (1981).
- 12) A. Y. Chang and E. Nobel, *Life Science*, **26**, 1329 (1980).
- 13) H. Vlassara, M. Brownlee and A. Cerami, *Diabetes*, **32**, 670 (1983).
- 14) H. F. Bunn, K. H. Gabby and P. M. Gallop, *Science*, **200**, 21 (1978).
- 15) S. Tsuchiya, T. Sakurai and S. Sekiguchi, *Biochem. Pharmacol.*, **33**, 2967 (1984).
- 16) M. Brownlee, H. Vlassara and A. Cerami, *Diabetes*, **32**, 68 (1983).
- 17) A. S. Elbe, S. R. Thorpe and J. W. Baynes, *J. Biol. Chem.*, **258**, 9406 (1983).
- 18) R. Dolhofer, E. A. Siess and O. H. Wieland, *Hoppe-Seyler's Z. Physiol. Chem.*, **363**, 1427 (1982).
- 19) J. J. Harding, "Advances in Protein Chemistry," Vol. 37, Academic Press Inc., New York, 1985, pp. 249—265.
- 20) J. D. Crapo, J. E. McCord and I. Fridovich, *Methods Enzymol.*, **53**, 382 (1978).
- 21) J. M. McCord and I. Fridovich, *J. Biol. Chem.*, **244**, 6049 (1969).
- 22) C. Beauchamp and I. Fridovich, *Anal. Biochem.*, **44**, 276 (1971).
- 23) H. A. Forman and I. Fridovich, *J. Biol. Chem.*, **248**, 2645 (1973).
- 24) N. Manda, H. Nakayama, S. Aoki, M. Satoh, S. Kadota, S. Nakagawa and M. Kudo, *Tonyobyo*, **25**, 691 (1982).
- 25) H. M. Steinman, V. R. Naik, J. Abernethy and R. L. Hill, *J. Biol. Chem.*, **249**, 7326 (1974).
- 26) E. Wood, D. Dalglish and W. Bannister, *Eur. J. Biochem.*, **18**, 187 (1971).
- 27) N. Grienfield and G. D. Fasman, *Biochemistry*, **8**, 4108 (1969).
- 28) C. W. Waykamp and T. J. Penders, *Clin. Chim. Acta*, **125**, 341 (1982).
- 29) J. Bannister, W. Bannister and E. Wood, *Eur. J. Biochem.*, **18**, 178 (1971).
- 30) A. Cudd and I. Fridovich, *J. Biol. Chem.*, **257**, 11443 (1982).
- 31) E. D. Getzoff, J. A. Tainer, P. K. Weiner, P. A. Kollmann, J. S. Richardson and D. C. Richardson, *Nature (London)*, **306**, 287 (1983).
- 32) P. Manavalan and W. C. Johnson, Jr., *Nature (London)*, **305**, 831 (1983).
- 33) T. Sakurai, H. Takahashi and S. Tsuchiya, *FEBS Lett.*, **176**, 27 (1984).
- 34) J. S. Richardson, K. A. Thomas, B. H. Rubin, and D. C. Richardson, *Proc. Nat. Acad. Sci. U.S.A.*, **72**, 1349 (1975).

[Chem. Pharm. Bull.]  
35(1) 308—314 (1987)

## Binding of Drugs to Sera of Patients with Renal Disease and Liver Disease

YASUO MATSUSHITA,<sup>\*a</sup> JUNKO EKI,<sup>a</sup> MARIKO TSUKIORI,<sup>b</sup>  
TATSUO SUZUKI,<sup>b</sup> and IKUO MORIGUCHI<sup>a</sup>

*School of Pharmaceutical Sciences, Kitasato University,<sup>a</sup>  
and Kitasato Institute Hospital,<sup>b</sup> Shirokane,  
Minato-ku, Tokyo 108, Japan*

(Received June 16, 1986)

The drug binding characteristics of pooled sera from patients with acute or chronic hepatitis and with chronic renal failure were investigated by means of equilibrium dialysis and ultracentrifugation, and were compared with those of healthy adult serum and human serum albumin. The drugs used were diazepam, naproxen, warfarin, and phenylbutazone. Serum from patients with renal disease showed markedly impaired binding with diazepam and naproxen at the primary binding site. However, almost no decrease of the binding was observed with warfarin and phenylbutazone. The impaired bindings of diazepam and naproxen were restored after active-charcoal treatment of the serum. This result suggested that, in the serum from patients with renal disease, the apparent decrease of the binding is probably due to the presence of some substance(s) which inhibit the binding of these drugs to the primary sites. On the other hand, no abnormal binding behavior was recognized in the serum from patients with liver disease. Thus, care is necessary when drugs binding to the diazepam site (such as diazepam and naproxen) are administered to patients with renal diseases, because a marked elevation of unbound drug concentration in the serum may occur.

**Keywords**—protein binding; human serum; binding site; renal disease; liver disease; equilibrium dialysis; ultracentrifugation; diazepam site; warfarin site

It has been pointed out that the binding of drugs to serum protein is influenced by some diseases.<sup>1)</sup> For several drugs, decreased protein binding has been reported in patients with uremia<sup>2,3a,b,4,5)</sup> and with certain liver diseases.<sup>3c,5-7)</sup> The decrease of the protein binding is considered to be caused possibly by a decrease of serum albumin concentration,<sup>3c,7,8)</sup> an increase of some endogenous substances,<sup>2,9,10)</sup> changes of albumin structure,<sup>11,12)</sup> the existence of some protein binding inhibitors,<sup>3a,13,14)</sup> *etc.* Previously, we reported<sup>15)</sup> marked differences in the fluorescence spectrum of pyrene-1-butyrate (PYB) in serum from patients with renal disease (RPS), or with liver disease (LPS), or serum from healthy adults (HS), or in the presence of human serum albumin (HSA), and we suggested the existence of some inhibitors which hindered the protein binding in RPS. Albumin is the principal binding protein for many drugs in serum, and at least two different specific drug binding sites are proposed to exist on the HSA molecule.<sup>16,17)</sup>

In this study, we evaluated the binding parameters of diazepam, naproxen, warfarin, and phenylbutazone (the former two drugs are known to bind at the diazepam site and the latter two at the warfarin site) with RPS, LPS, HS, and HSA in order to elucidate the abnormal binding behavior of RPS, as observed in terms of the PYB fluorescence spectrum.<sup>15)</sup>

### Experimental

**Materials**—For HSA, fraction V (Miles Laboratories Co., Elkhart, IN) was used. The molecular weight was



assumed to be  $67000^{18)}$  and the concentration was determined by measuring the absorbance at 280 nm using  $E_{1\%}^{1\text{cm}} = 5.30^{19)}$  Four pools of sera each from healthy adults (HS I–IV), patients with liver disease (LPS I–IV), and patients with renal disease (RPS I–IV) were obtained from Kitasato Institute Hospital. All pooled serum samples except RPS I were obtained from several persons. RPS I was obtained by the plasma exchange of a patient with purpura nephritis. The serum samples were collected and stored frozen at  $-20^{\circ}\text{C}$ . The liver disease included acute and chronic hepatitis and the renal disease included chronic renal failure. Clinical data for the pooled sera are presented in Table I. Warfarin was generously provided by Eisai Co. (Tokyo), phenylbutazone by Nihon Ciba-Geigy Co. (Tokyo), diazepam by Yamanouchi Seiyaku Co. (Tokyo), and naproxen by Tanabe Seiyaku Co. (Tokyo). All other reagents used were commercial products of special grade. All final solutions were made with 0.15 M Tris-HCl buffer, pH 7.4.

**Charcoal Treatment of Pooled Serum**—RPS I was treated with activated charcoal (Norit A, Wako Pure Chemical Industries, Ltd., Osaka) by the method of Chen.<sup>20)</sup> Fifty milligrams of charcoal was added per milliliter of serum, the pH was lowered to 3.0 with 1 N HCl, and the solution was mechanically mixed for 1 h in an ice bath. The charcoal was then removed by centrifugation, and the serum was adjusted back to pH 7.4 with 1 N NaOH.

**Equilibrium Dialysis (ED) Method**—By using a 3.0 ml dialysis cell devised by Goto *et al.*,<sup>21)</sup> sample solutions (2.0 ml) were shaken for 16 h at  $25 \pm 1^{\circ}\text{C}$  in a thermostated environment. Spectrapor 1 dialysis membrane (Spectrum Medical Inc., Los Angeles, CA) was used after being boiled four times in distilled water. The decrease in the unbound drug content was measured, and the binding parameters were calculated. Adsorption of drugs on the membrane was negligible. The concentrations of drugs in the experiments and the wavelengths used for spectrophotometry are listed in Table II. The concentration of albumin was  $5.0 \times 10^{-5}$  M. Each point in the Scatchard plots (Figs. 1a, 2a, 3, and 4) represents the mean value of two experiments.

**Ultracentrifugation (UC) Method**—The general procedure and treatment of data were the same as described previously.<sup>22)</sup> The concentration of albumin was  $2.0 \times 10^{-5}$  M. The concentrations of drugs are listed in Table II. All the experiments were performed at  $25 \pm 2^{\circ}\text{C}$ . Each point in the Scatchard plots (Figs. 1b and 2b) represents the mean value of two experiments.

TABLE I. Clinical Data for Human Pooled Sera

Pooled serum	Vol. (ml)	GOT <sup>a)</sup>	GPT <sup>b)</sup>	LAP <sup>c)</sup>	$\gamma$ -GTP <sup>d)</sup>	TP <sup>e)</sup>	ALB <sup>f)</sup>	A/G <sup>g)</sup>	UA <sup>h)</sup>	BUN <sup>i)</sup>	Crtn(s) <sup>j)</sup>
HS <sup>k)</sup> I	30	11	9	NT <sup>l)</sup>	NT	7.09	4.45	1.68	NT	15	0.80
HS II	25	17	12	116	24	6.92	4.47	1.82	4.1	19	0.76
HS III	9	14	7	116	19	6.80	4.37	1.79	5.0	17	0.89
HS IV	8	14	8	122	20	6.94	4.51	1.85	4.7	16	0.94
LPS <sup>m)</sup> I	30	79	62	NT	NT	7.28	4.15	1.68	NT	15	0.91
LPS II	18	114	115	249	101	7.44	4.23	1.31	5.5	16	0.97
LPS III	8	70	52	246	99	7.17	4.05	1.29	4.8	17	1.12
LPS IV	8	42	30	200	58	7.26	3.68	1.02	5.6	23	1.09
RPS <sup>n)</sup> I	60	8	3	145	25	4.43	3.30	2.92	5.2	14	1.02
RPS II	22	20	9	132	27	6.97	4.10	1.42	6.0	25	1.60
RPS III	8	19	8	246	102	6.19	3.78	1.56	6.5	52	4.74
RPS IV	8	18	9	186	34	6.85	3.92	1.33	7.1	56	5.01

a) Glutamic oxaloacetic transaminase. b) Glutamic pyruvic transaminase. c) Leucine aminopeptidase. d)  $\gamma$ -Glutamyltranspeptidase. e) Total protein. f) Albumin. g) Albumin/globulin ratio. h) Uric acid. i) Blood urea nitrogen. j) Serum creatinine. k) Healthy adult serum. l) Not tested. m) Serum from patients with liver disease. n) Serum from patients with renal disease.

TABLE II. Drug Concentrations Used in the Experiments and Wavelengths for Spectrophotometry

Drug	Concn. in ED method ( $10^{-5}$ M)	Concn. in UC method ( $10^{-5}$ M)	Wavelength (nm) for spectrophotometry
Diazepam	3.0—60.0	2.0—50.0	230
Naproxen	3.0—100.0		230
Warfarin	3.0—100.0	2.0—40.0	308
Phenylbutazone	3.0—100.0		264

**Calculation**—The binding data obtained by the ED and UC methods were analyzed by means of Scatchard plots.<sup>23)</sup> The binding parameters were calculated by linear regression when the Scatchard plot was linear. When the plot was curved; the binding parameters were obtained by using Karush's equation:

$$r = n_1 K_1 C / (1 + K_1 C) + n_2 K_2 C / (1 + K_2 C)$$

where  $r$  is the number of moles of drug bound per mole of protein;  $n_1$  and  $n_2$ , the number of binding sites in each class;  $K_1$  and  $K_2$ , the binding constants for these sites; and  $C$ , the concentration of free drug. The curve fitting calculation was performed by means of a JEOL digital computer, model JEC-7E.

## Results and Discussion

First, the bindings of diazepam and warfarin in RPS and LPS were determined by the ED and UC methods and compared to those in HS and HSA. The binding data in each serum were analyzed by means of a Scatchard plot. Figures 1 and 2 show the plots for binding of diazepam and warfarin, respectively, to HS I, LPS I, RPS I, and HSA. These drugs are known to be almost exclusively bound to albumin in the serum. Diazepam and warfarin have more than two classes of binding sites with HSA, HS, and LPS. As shown in Fig. 1, however, a marked decrease of binding at lower drug concentrations was observed for diazepam with RPS I by using the ED and UC methods, compared to the binding with HS I and HSA. This abnormal binding behavior of diazepam observed with RPS I was also recognized with other RPS samples tested. On the other hand, the binding of warfarin to RPS I gave a similar plot to those obtained with HS I and HSA (Fig. 2). There was close agreement between the results obtained by the two different methods, ED and UC. Accordingly, the ED method was exclusively used in the binding experiments hereafter.

Figure 3 shows Scatchard plots for the binding of naproxen and phenylbutazone, which are analogous to those for diazepam and warfarin, respectively. The characteristic behavior of the binding of naproxen with RPS I was also observed with other RPS samples tested.

The calculated binding parameters are listed in Tables III and IV. It is indicated that the rather high binding affinity of diazepam at the primary binding site shown in HS, HSA, and LPS ( $\log n_1 K_1$  values of 4.71—5.73) was entirely absent in all the RPS samples tested. In the case of naproxen, the disappearance of the affinity to the primary site in RPS was also

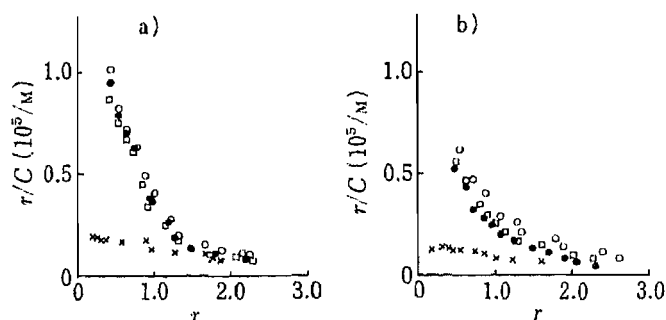


Fig. 1. Scatchard Plots for the Binding of Diazepam Determined by Using the ED Method (a) and UC Method (b)

●, HSA (fraction V); ○, HS I; □, LPS I; ×, RPS I.

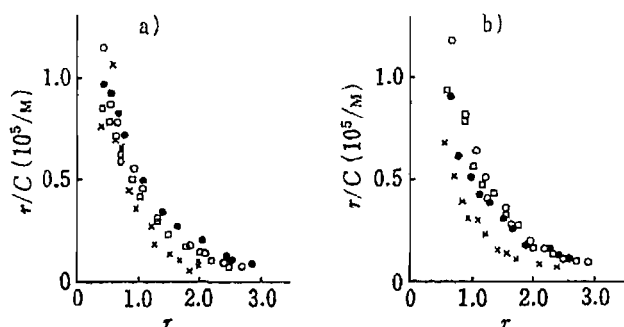


Fig. 2. Scatchard Plots for the Binding of Warfarin Determined by Using the ED Method (a) and UC Method (b)

●, HSA (fraction V); ○, HS I; □, LPS I; ×, RPS I.

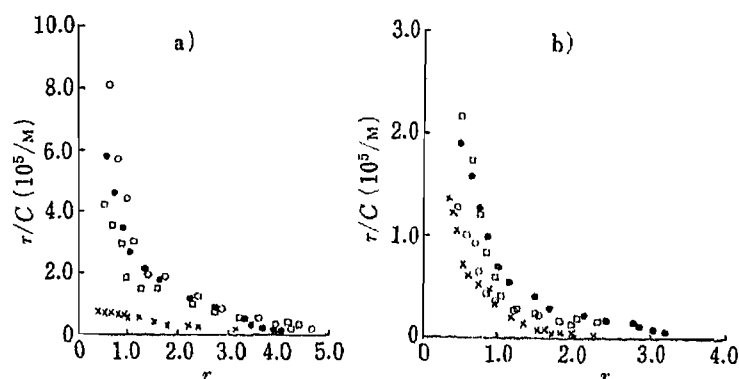


Fig. 3. Scatchard Plots for the Binding of Naproxen (a) and Phenylbutazone (b) Determined by Using the ED Method

(a) ●, HSA (fraction V); ○, HS II; □, LPS III; ×, RPS I. (b) ●, HSA (fraction V); ○, HS III; □, LPS III; ×, RPS I.

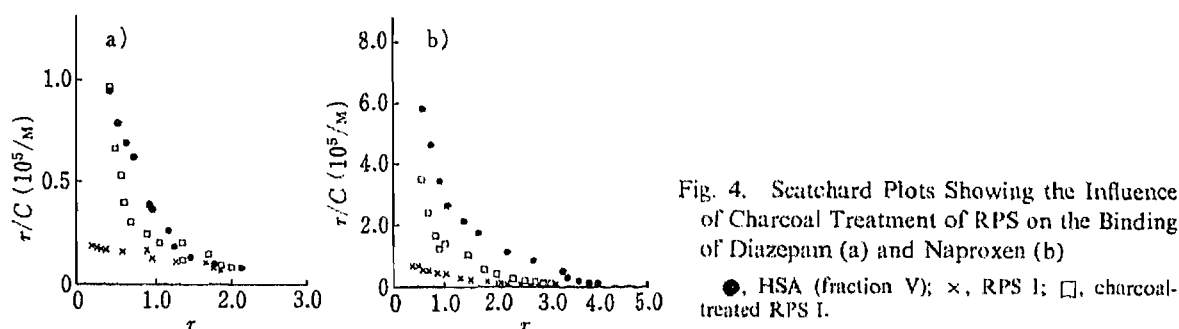


Fig. 4. Scatchard Plots Showing the Influence of Charcoal Treatment of RPS on the Binding of Diazepam (a) and Naproxen (b)

●, HSA (fraction V); ×, RPS I; □, charcoal-treated RPS I.

recognized, whereas  $\log n_1 K_1$  values for LPS and HS were similar. On the other hand, the binding of warfarin and phenylbutazone to RPS showed no exceptional behavior in comparison with those to HS and HSA. In LPS, the binding of the four drugs at the primary binding site showed no difference from those in HS and HSA.

It has been reported that the binding of several drugs in serum is affected by diseases. For example, Sjöholm *et al.*<sup>3a)</sup> reported that the binding of diazepam was impaired in both uremic serum and serum from liver cirrhosis patients,<sup>3a,c)</sup> and that the binding of warfarin was decreased in uremic serum. Their results, which were analyzed by using an equation for one class of sites, do not agree with our detailed observations. The disagreement may be in part due to the pathological difference of the serum samples studied.

It has been proposed that at least two different specific binding sites exist in the HSA molecule<sup>16,17)</sup>; diazepam and naproxen bind to the diazepam site, while warfarin and phenylbutazone bind to the warfarin site. Therefore, it was considered that some changes of molecular environment might occur around the diazepam site of albumin in RPS. It seems very likely that some substances inhibiting the binding of drugs at the diazepam site exist in RPS. Thus, for the purpose of confirming this, RPS I was treated with active charcoal at pH 3.0 according to Chen's method<sup>21)</sup> to remove such substances. Figure 4 shows the Scatchard plots for binding of diazepam and naproxen with the charcoal-treated RPS I, along with those in the cases of non-treated RPS I and HSA. For both drugs, binding at the primary site is clearly recovered after the charcoal treatment of RPS, as seen in the lower  $r$  region of the plots. Binding of warfarin and phenylbutazone in RPS was unaffected by the charcoal-treatment. The binding parameters ( $\log n_1 K_1$ ) with the charcoal-treated RPS were shown to be 5.65 and 6.14 for diazepam and naproxen, respectively, which were almost the same as those

TABLE III. Parameters for Binding of Diazepam and Naproxen

Pooled serum	Diazepam						Naproxen					
	$n_1$	$K_1$ ( $10^5/M$ )	$\log n_1 K_1$	$n_2$	$K_2$ ( $10^3/M$ )	$\log n_2 K_2$	$n_1$	$K_1$ ( $10^5/M$ )	$\log n_1 K_1$	$n_2$	$K_2$ ( $10^3/M$ )	$\log n_2 K_2$
HSA (Fr. V)	0.92	1.52	5.17	6.05	1.12	3.83	0.51	44.29	6.35	3.49	51.91	5.26
HS I	0.87	2.11	5.26	5.48	1.77	3.99	NT					
HS II	0.60	8.89	5.73	18.81	0.81	4.18	0.80	25.20	6.30	3.93	32.36	5.10
HS III	0.80	0.64	4.71	4.46	3.12	4.14	NT					
HS IV	NT <sup>a)</sup>						0.59	17.97	6.18	4.77	25.08	5.08
LPS I	0.97	1.47	5.15	5.71	1.17	3.81	NT					
LPS II	0.61	4.07	5.39	4.17	3.49	4.16	0.41	51.32	6.32	3.19	63.30	5.31
LPS III	NT						0.58	17.97	6.18	4.77	25.08	5.08
LPS IV	0.42	12.76	5.73	3.20	6.49	4.32	NT					
RPS I	—	—	—	3.00	6.85	4.31	—	—	—	3.19	17.09	4.74
RPS I (charcoal- treated)	0.35	12.85	5.65	2.35	9.19	4.33	0.54	25.47	6.14	2.65	25.13	4.82
RPS II	—	—	—	3.49	11.59	4.61	NT					
RPS III	NT						—	—	—	4.30	49.89	5.33
RPS IV	—	—	—	2.94	10.59	4.49	NT					

a) Not tested.

TABLE IV. Parameters for Binding of Warfarin and Phenylbutazone

Pooled serum	Warfarin						Phenylbutazone					
	$n_1$	$K_1$ ( $10^5/M$ )	$\log n_1 K_1$	$n_2$	$K_2$ ( $10^3/M$ )	$\log n_2 K_2$	$n_1$	$K_1$ ( $10^5/M$ )	$\log n_1 K_1$	$n_2$	$K_2$ ( $10^3/M$ )	$\log n_2 K_2$
HSA (Fr. V)	0.99	1.51	5.17	3.01	4.95	4.17	0.75	5.89	5.65	3.20	8.27	4.42
HS I	1.15	1.45	5.22	3.45	3.75	4.11	NT					
HS II	1.00	1.54	5.19	2.66	5.19	4.14	0.99	4.74	5.67	1.31	6.89	3.96
HS III	NT <sup>a)</sup>						0.86	2.54	5.34	3.69	3.03	4.05
HS IV	1.06	1.79	5.28	4.20	3.29	4.14	NT					
LPS I	1.01	1.24	5.10	3.55	3.17	4.05	NT					
LPS II	1.01	1.19	5.08	3.55	3.15	4.05	NT					
LPS III	NT						0.64	16.35	6.02	3.50	5.86	4.31
LPS IV	1.18	1.14	5.23	5.84	1.33	3.89	NT					
RPS I	0.65	3.07	5.30	1.69	11.03	4.27	1.08	1.32	5.15	3.73	1.10	3.61
RPS I (charcoal- treated)	0.74	3.22	5.38	1.89	6.14	4.06	0.68	4.62	5.50	4.59	2.50	4.06
RPS II	0.68	2.88	5.29	4.14	3.40	4.18	0.54	6.10	5.52	4.85	4.28	4.32
RPS III	NT						0.50	1.44	4.86	2.15	2.63	3.75
RPS IV	0.80	2.42	5.29	4.19	3.00	4.10	NT					

a) Not tested.

with HSA (Table III). Therefore, the disappearance of the binding of these drugs at the diazepam site in RPS was considered to be due to binding inhibitors present in the serum. The chemical nature of the inhibitors in RPS is not yet known. Depner and Gulyassy<sup>13)</sup> reported the presence of a phenytoin-binding inhibitor in uremic plasma, and Kinniburgh and Boyd<sup>14)</sup> described the isolation of a peptide present in uremic serum and responsible for the altered HSA binding. It remains to be established whether or not these substances are identical with the diazepam-site inhibitor(s) described above. Further work is in progress.

In conclusion, the binding of drugs to the diazepam site was remarkably impaired in serum from patients with renal disease, probably owing to the presence of some binding inhibitor(s). The drug binding in serum from patients with liver disease did not show any abnormal behavior in terms of the Scatchard plots and binding parameters. Clearly, care is necessary when the drugs, especially those with a high affinity to the diazepam site, are administered to patients with renal disease.

**Acknowledgment** The authors wish to thank Miss S. Tanaka for her technical assistance in a part of this work. The authors are also indebted to the cited manufactures for gifts of the drugs.

#### References

- 1) J. P. Tillement, F. Lhodte, and J. F. Giudicelli, *Clin. Pharmacokinetics*, **3**, 144 (1979).
- 2) M. M. Reidenberg, *Clin. Pharmacokinetics*, **1**, 121 (1976).
- 3) a) I. Sjöholm, A. Kober, I. Odar-Cederlöf, and O. Borgå, *Biochem. Pharmacol.*, **25**, 1205 (1976); b) A. Kober, I. Sjöholm, O. Borgå, and I. Odar-Cederlöf, *ibid.*, **28**, 1037 (1979); c) A. Kober, A. Jenner, I. Sjöholm, O. Borgå, and I. Odar-Cederlöf, *ibid.*, **28**, 2729 (1979).
- 4) K. Bachmann, R. Shapiro, and J. Mackiewicz, *Clin. Pharmacol.*, **16**, 468 (1976).
- 5) S. Goto, H. Yoshitomi, A. Miyamoto, K. Inoue, and M. Nakano, *J. Pharmacobio-Dyn.*, **3**, 667 (1980).
- 6) R. Gugler, J. W. Kurten, C. J. Jensen, U. Klehr, and J. Hartlapp, *Eur. J. Clin. Pharmacol.*, **15**, 341 (1979).
- 7) G. W. Wilkinson and D. G. Shand, *Clin. Pharmacol. Ther.*, **18**, 377 (1975).
- 8) R. Carlos, R. Aclvo, and S. Erill, *Clin. Pharmacokinetics*, **4**, 144 (1979).
- 9) K. O'Malley, M. Velasco, A. Pruitt, and J. L. McNay, *Clin. Pharmacol. Ther.*, **18**, 53 (1975).
- 10) C. J. Bowmer and W. E. Lindup, *Biochem. Pharmacol.*, **31**, 319 (1982).
- 11) D. W. Shoeman and D. L. Azarnoff, *Pharmacology*, **7**, 169 (1972).
- 12) S. W. Boobis, *Clin. Pharmacol. Ther.*, **22**, 147 (1977).
- 13) T. A. Depner and P. F. Gulyassy, *Kidney Int.*, **18**, 86 (1980).
- 14) D. W. Kinniburgh and N. D. Boyd, *Clin. Pharmacol. Ther.*, **30**, 276 (1981).
- 15) Y. Matsushita, M. Tsukiori, T. Suzuki, and I. Moriguchi, *J. Pharm. Sci.*, **75**, 193 (1986).
- 16) G. Sudlow, D. J. Birkett, and D. N. Wade, *Mol. Pharmacol.*, **12**, 1052 (1976).
- 17) I. Sjöholm, B. Ekman, A. Kober, I. Liungstedt-Pählman, B. Seiving, and T. Sjödin, *Mol. Pharmacol.*, **16**, 767 (1979).
- 18) C. J. Halfman and T. Nishida, *Biochemistry*, **11**, 3493 (1972).
- 19) C. F. Chignell, *Mol. Pharmacol.*, **5**, 244 (1969).
- 20) C. F. Chen, *J. Biol. Chem.*, **242**, 173 (1967).
- 21) S. Goto, H. Yoshitomi, and M. Kishi, *Yakugaku Zasshi*, **97**, 1219 (1977).
- 22) Y. Matsushita and I. Moriguchi, *Chem. Pharm. Bull.*, **33**, 2948 (1985).
- 23) G. Scatchard, *Ann. N. Y. Acad. Sci.*, **51**, 660 (1949).

[Chem. Pharm. Bull.]  
[35(1) 315-319 (1987)]

## Improvement of Chemical Instability of Carmoful in $\beta$ -Cyclodextrin Solid Complex by Utilizing Some Organic Acids

MASAHIKO KIKUCHI, FUMITOSHI HIRAYAMA, and KANETO UEKAMA\*

*Faculty of Pharmaceutical Sciences, Kumamoto University,  
5-1 Oe-honmachi, Kumamoto 862, Japan*

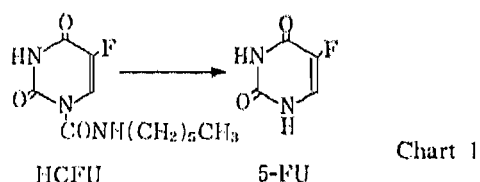
(Received June 21, 1986)

Degradation of carmoful (HCFU) in the solid state was significantly accelerated by  $\beta$ -cyclodextrin ( $\beta$ -CyD) complexation owing to the hygroscopic nature of  $\beta$ -CyD. The instability of HCFU in the solid complex was found to be markedly improved by the addition of some organic acids such as citric, L-(+)-tartaric and DL-malic acids, whereas DL-aspartic acid and neutral additives such as talc, lactose, cellulose and methyl cellulose had insignificant stabilizing effects. The results indicated that organic acids having lower  $pK_a$  value and higher aqueous solubility are particularly useful to prevent the hydrolysis of HCFU by providing an acidic environment around the complex after moisture sorption.

**Keywords**—carmoful;  $\beta$ -cyclodextrin; inclusion complex; solid-state degradation; organic acid; stabilization

### Introduction

Carmoful (1-hexylcarbamoyl-5-fluorouracil, HCFU) is one of the masked forms of 5-fluorouracil (5-FU) and has been widely used to treat carcinomas of breast and gastrointestinal tract.<sup>1,2)</sup> We have previously reported<sup>3)</sup> that cyclodextrin (CyD) complexation is of great value in improving some pharmaceutical properties of HCFU in aqueous solution, such as the low solubility, the chemical instability, and the oral bioavailability. In the course of the study, however, the degradation of HCFU in the solid state was found to be rather accelerated by



CyD complexation (Chart 1). In this study, therefore, we have attempted to improve the solid-state instability of HCFU within the  $\beta$ -CyD complex, by utilizing some pharmaceutical additives.

### Experimental

**Materials**—HCFU was donated by Mitsui Pharmaceutical Co., Ltd.  $\beta$ -CyD was supplied by Nihon Shokuhin Kako Co., Ltd., and used after recrystallization from water. All other materials and solvents were of analytical reagent grade, and deionized double-distilled water was used throughout the study.

**Preparation of Solid Complex**—HCFU- $\beta$ -CyD complex (1:1 molar ratio) containing pharmaceutical additives (HCFU:additive=1:1 weight ratio) was prepared by the kneading method.<sup>4)</sup> For example, 1.00 g of HCFU, 4.41 g of  $\beta$ -CyD and 1.00 g of additives were added to a small portion of phosphate buffer (pH 3.0), under which conditions the hydrolysis of HCFU was negligible.<sup>3,5)</sup> The mixture was further kneaded for about 40 min, and then dried under reduced pressure at room temperature for 24 h.

**Stability Studies**—Stability tests of HCFU- $\beta$ -CyD complex (50 mg, 100 mesh) in the presence and absence of the additives were conducted under conditions of constant temperature and relative humidity (R.H.), using a Tabai Platinous Rainbow PR-1G incubator. At appropriate intervals, the test sample was dissolved in 50% (v/v) methanol-phosphate buffer (pH 3.0), and subjected to high-performance liquid chromatography (HPLC) for simultaneous determination of intact HCFU and its degradation product, 5-FU, in the complex. The HPLC conditions were as follows: pump and detector, Hitachi 635A machine and 638-41 ultraviolet (UV) monitor, respectively; column, LiChrosorb RP-18 (10  $\mu$ m, 4 $\phi$   $\times$  250 mm, Merck); mobile phase, methanol-water (4:1 v/v); flow rate, 0.8 ml/min; detection, 261 nm. Components were quantitated by measuring peak heights and comparing them with those of known amounts of an internal standard, *p*-hydroxybenzoic acid hexyl ester.

**Moisture Sorption Studies**—The test samples (500 mg, 100 mesh) in weighing bottle were placed in the incubator at various R. H. values and constant temperature, and at appropriate intervals the weight of the sample was measured on a Shimadzu Libror AEL-160 electric reading balance. The water content of the complex was estimated from the increase in weight after moisture sorption equilibrium was attained (2 d).

**Solubility of Organic Acid**—Excess amounts of organic acid were added to water, and were shaken at  $25 \pm 0.5$  °C. After equilibration (approximately 1 week), an aliquot was centrifuged. A portion of the sample was removed with a pipette and placed in a test tube. The sample was evaporated at 50 °C under vacuum, and the weight of the residue was measured.

**Dissolution and *in Vivo* Absorption Studies**—These studies were carried out under the same conditions as reported previously.<sup>3)</sup>

## Results and Discussion

### Degradation Rate of HCFU in $\beta$ -CyD Solid Complex

Figure 1 shows the time courses of the degradation of HCFU in the free state and in the  $\beta$ -CyD solid complex at 75% R.H. and 70 °C. It is apparent that the degradation rate of HCFU in the solid complex was extremely fast, whereas the guest molecule in the free state was practically stable. The degradation product of HCFU under these experimental conditions was found to be 5-FU, and no appreciable side reactions such as ring opening of the uracil moiety were observed. Solid-phase reactions are known not to be simply describable in terms of gas- or liquid-phase kinetics, because they are significantly influenced by various topochemical and physicochemical factors such as particle shape and size, and adsorbed solvents.<sup>6)</sup> In the present system, however, the degradation rate of HCFU was tentatively expressed in terms of first-order kinetics because the reaction, after a short lag time (about 10 min), closely followed first-order kinetics. Therefore, first-order treatments were used hereinafter to evaluate the solid-state stability of HCFU.

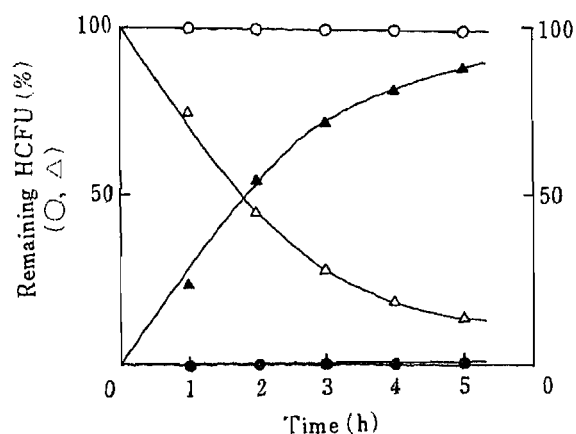


Fig. 1. Time Courses of Decomposition of HCFU and HCFU- $\beta$ -CyD Complex at 70 °C and 75% R.H.

O, HCFU;  $\Delta$ , HCFU- $\beta$ -CyD complex. Closed symbols indicate the appearance of 5-FU from the respective HCFU.

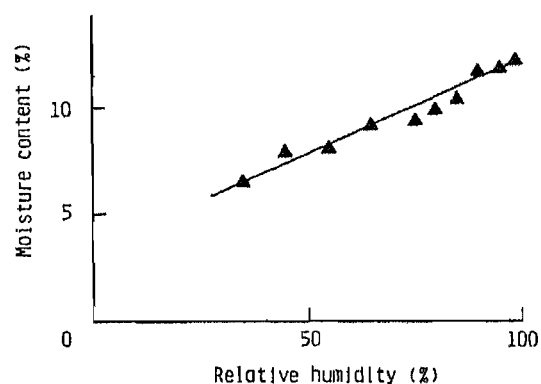


Fig. 2. Moisture Sorption Curve of HCFU- $\beta$ -CyD Complexes at 25 °C under Various R.H. Conditions



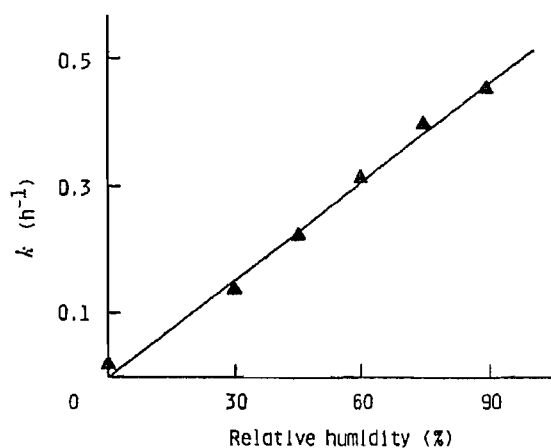


Fig. 3. Relationship between Apparent First-Order Rate Constant ( $k$ ) and Relative Humidity for the Decomposition of HCFU in  $\beta$ -CyD Complex at 70 °C

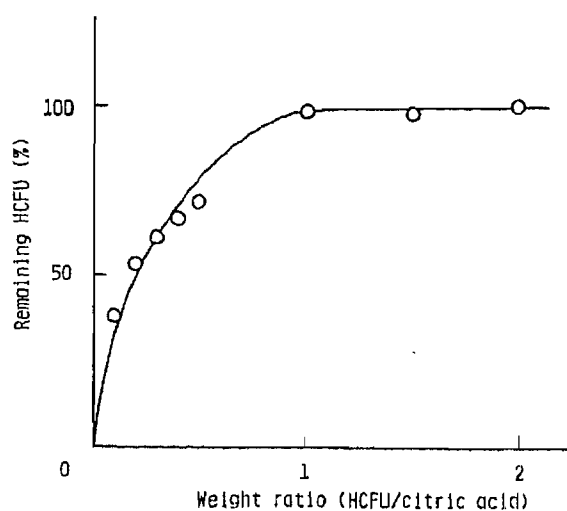


Fig. 4. Stability of HCFU in  $\beta$ -CyD Complex Containing Various Amounts of Citric Acid after Incubation for 48 h at 60 °C and 75% R.H.

TABLE I. Effects of Additives on the Decomposition of HCFU in  $\beta$ -CyD Complex after Incubation for 48 h at 60 °C and 75% R.H.

Additive	Remaining <sup>a)</sup> HCFU (%)	Yield of 5-FU (%)
Without additive	3.8	96.1
Citric acid	97.2	2.9
L-(+)-Tartaric acid	99.2	0.7
DL-Malic acid	98.5	1.6
Maleic acid	96.6	3.1
Malonic acid	95.3	4.7
Fumaric acid	43.3	56.3
DL-Aspartic acid	2.7	98.1
Methyl cellulose	10.5	91.2
Microcrystalline cellulose	2.4	96.9
Talc	1.2	99.0
Lactose	2.5	97.4
D-Mannitol	5.5	93.8

a) Remaining HCFU without  $\beta$ -CyD was 94.2%.

It is expected that the highly hygroscopic character of natural CyDs<sup>7)</sup> may significantly influence the degradation rate of HCFU in the solid complex, because HCFU is extremely susceptible to base- and water-catalyzed hydrolysis, as reported previously.<sup>4)</sup> Therefore, the moisture sorption behavior and the chemical stability of HCFU- $\beta$ -CyD solid complex were investigated under various R.H. conditions. Figure 2 shows the moisture sorption curve of HCFU- $\beta$ -CyD complex; the water content of HCFU- $\beta$ -CyD complex increased with increasing R.H. value. Figure 3 shows the apparent first-order degradation rate constants ( $k$ ) of HCFU in the complex as a function of R.H., indicating that the degradation rate increases with increase of R.H. value. These results suggest that adsorbed water molecules on the solid particle play an important role in the degradation of HCFU.

TABLE II. Effects of Organic Acids on the Decomposition of HCFU in  $\beta$ -CyD Complex at 70 °C and 75% R.H.

Organic acid	Apparent first-order rate constant ( $\times 10^4 \text{ h}^{-1}$ )
HCFU alone	25.6
Without organic acid	4000.0
Citric acid	7.3
L-(+)-Tartaric acid	7.8
DL-Malic acid	22.5
Maleic acid	38.1
Malonic acid	55.0
Fumaric acid	140.0

TABLE III. Relation between Inhibitory Effects of Organic Acids on the Decomposition of HCFU- $\beta$ -CyD Complex and Physicochemical Properties of Organic Acids

Organic acid	$\text{p}K_a^a$	Solubility in water (g/dl, 25 °C)	Inhibition <sup>b)</sup> ratio
Citric acid	3.06	78.7	550
	4.76		
	5.40		
L-(+)-Tartaric acid	3.02	74.5	510
	4.54		
DL-Malic acid	3.40	71.1	180
	5.05		
Maleic acid	2.00	52.7	100
	6.26		
Malonic acid	2.85	75.8	70
	6.10		
Fumaric acid	3.03	0.6	30
	4.47		
DL-Aspartic acid	1.99	0.8	0.24
	3.90		
	10.00		

a) N. A. Lange, "Handbook of Chemistry," McGraw-Hill Book Company, Inc. New York, 1961.

b) Calculated from the apparent first-order rate constants in Table II.

### Effects of Pharmaceutical Additives on the Degradation of HCFU in $\beta$ -CyD Complex

Stabilization of HCFU- $\beta$ -CyD complex in the solid state was attempted by utilizing some pharmaceutical additives. Table I shows the effects of various additives on the degradation of HCFU in the  $\beta$ -CyD complex. It is apparent that some organic acids were very effective to stabilize HCFU in the  $\beta$ -CyD complex, whereas DL-aspartic acid and neutral additives such as talc, lactose, cellulose and methyl cellulose had little stabilizing effect. Furthermore, the HCFU- $\beta$ -CyD complex containing organic acids, prepared by the kneading method, was found to be more stable than the physical mixture of the complex and organic acids.

Figure 4 shows the remaining HCFU (percent) after 48 h as a function of citric acid concentration in the solid complex under the conditions of 75% R.H. and 60 °C. The stabilizing effect of citric acid increased with increasing concentration, and in the presence of the acid at over 1 : 1 (organic acid : HCFU) weight ratio, no degradation was observed within the time employed. Since similar trends were observed for the other organic acid systems, the

amount of the organic acids to be added to the complex was fixed at 1:1 in a weight ratio throughout the study. The apparent first-order degradation rate constants of HCFU in the presence and absence of the organic acids are summarized in Table II. Citric and L-(+)-tartaric acids retarded by over 500 times the degradation rate of HCFU in the complex, and retarded it by 3 times even when compared with HCFU in the free state. Furthermore, the degradation of HCFU in the  $\beta$ -CyD complex containing citric, L-(+)-tartaric or DL-malic acid was found to be completely inhibited even for periods exceeding 6 months under the conditions of the standard stability test, 75% R.H. and 40 °C, suggesting that quality could be maintained sufficiently to allow an expiration date of 3 years.<sup>8-10)</sup>

Table III lists the inhibition ratios calculated from the rate constants in Table II, and the aqueous solubilities and  $pK_a$  values of the organic acids. As is apparent from Table III, there seems to be a tendency for the inhibition ratio to increase with decreasing  $pK_a$  value or with increasing solubility of organic acids. When L-(+)-tartaric acid is compared with fumaric acid, for example, the former (having a large solubility) showed a greater stabilizing effect than the latter, in spite of having the same acidity, as expected from  $pK_a$  value.

These results suggest that the organic acids may provide an acidic environment around the CyD complex after moisture sorption, since HCFU is chemically stable under acidic conditions, as demonstrated previously from the hydrolysis rate-pH profiles.<sup>3)</sup> In addition, other factors such as ternary complex formation between the host, guest and organic acid molecules and/or change in the molecular behavior of the complex in the presence of adsorbed water and organic acids at various R.H. conditions should be considered in order to elucidate in detail the stabilization mechanism in the solid state.<sup>6,11)</sup>

It is also important to compare the dissolution and *in vivo* absorption behaviors of HCFU- $\beta$ -CyD complex containing organic acid with those of the complex without the acid.<sup>3)</sup> However, no differences in these characteristics were observed between the complexes with and without the acid. These results suggest that HCFU- $\beta$ -CyD complex containing organic acids may be superior to the parent CyD complex, particularly from the viewpoint of quality assurance of solid  $\beta$ -CyD complex preparations, and the present approach may be applicable to other CyD complexes having undesirable physicochemical properties.

**Acknowledgement** The authors are grateful to Professor M. Otagiri for helpful discussions throughout this work.

#### References

- 1) A. Hoshi, M. Iigo, A. Nakamura, M. Yoshida, and K. Kuretani, *Gann*, **67**, 725 (1967).
- 2) Y. Koyama and Y. Koyama, *Cancer Treatment Reports*, **64**, 861 (1980).
- 3) M. Kikuchi, Y. Uemura, F. Hirayama, M. Otagiri, and K. Uekama, *J. Incl. Phenom.*, **2**, 623 (1984).
- 4) W. Saenger, *Angew. Chem. Int. Ed. Engl.*, **19**, 344 (1980).
- 5) T. Miura, T. Uchiyama, M. Takahishi, K. Yamamoto, S. Koizumi, K. Fukamatsu, and J. Saito, *Iyakuhin Kenkyu*, **11**, 73 (1980).
- 6) J. T. Carstensen, "Solid Pharmaceutics: Mechanical Properties and Rate Phenomena," Academic Press, New York, 1980.
- 7) T. Imai, T. Irie, M. Otagiri, and K. Uekama, *J. Incl. Phenom.*, **2**, 597 (1984).
- 8) T. Nagai, N. Nambu, H. Ueda, A. Ejima, T. Shibazaki, H. Ogata, S. Yoshida, N. Ogusa, G. Katsui, S. Bessho, S. Abe, T. Kitaura, and E. Yumioka, *Yakuzaigaku*, **42**, 118 (1982).
- 9) K. Hirayama, *Nippon Yakuzaishi Zasshi*, **36**, 137 (1984).
- 10) Y. Takagishi and H. Okuda, *Nippon Yakuzaishi Zasshi*, **36**, 143 (1984).
- 11) Y. Nakai, *Yakugaku Zasshi*, **105**, 801 (1985).

[Chem. Pharm. Bull.]  
35(1) 320-325 (1987)

## Interaction of 3',4'-Dideoxykanamycin B and Submaxillary Mucin

YUKIHIKO ARAMAKI,<sup>a</sup> JUN-JI NIIBUCHI,<sup>a</sup> SEISHI TSUCHIYA<sup>\*,a</sup>  
and JUN-ICHI HOSODA<sup>b</sup>

*Tokyo College of Pharmacy,<sup>a</sup> 1432-1 Horinouchi, Hachioji,  
Tokyo 192-03, Japan and Tokyo Medical College,<sup>b</sup> 7-1  
Nishishinjuku-6, Shinjuku-ku, Tokyo 160, Japan*

(Received July 11, 1986)

The interactions of an aminoglycoside antibiotic, 3',4'-dideoxykanamycin B (DKB), with submaxillary mucin were investigated by equilibrium dialysis and affinity chromatography.

DKB binds to mucin and forms a complex of low solubility. This binding was dependent on the pH and ionic strength. Scatchard plot analysis showed that mucin had one class of binding sites for DKB. The binding coefficient was  $1.30 \times 10^{-5} \text{ M}$  and the concentration of binding sites was 0.243  $\mu\text{mol}$  per mg of mucin at 25°C. The binding of DKB to mucin was inhibited in the presence of  $\text{Ca}^{2+}$  or amines, such as ethylenediamine, spermidine and glucosamine. The N-pentaacetyl derivative of DKB did not bind to mucin. The binding of DKB to asialomucin was decreased. After binding to a DKB-conjugated Sepharose 4B column, a small amount of mucin was eluted with NaCl solution and a large amount of mucin was eluted with *N*-acetylneuraminic acid solution.

These results suggest that the binding of DKB to mucin involves an ionic interaction between the amino groups of DKB and the carboxyl groups of the sialic acid residues of submaxillary mucin.

**Keywords**—binding; mucin; 3',4'-dideoxykanamycin B; aminoglycoside; absorption

### Introduction

The mucosal surface of the digestive tract is covered with mucin. The physiological function of mucin is obscure, but it has been suggested that gastric mucin serves to protect the mucosal cells from the damaging effects of digestive fluids and enzymes.<sup>1)</sup> The high viscosity of mucin suggests that it may act as a diffusion barrier to absorption.<sup>2)</sup> When polyoxyethylene cetyl ether, a less irritating surface active agent, was added to suppositories, the rectal absorption of 3',4'-dideoxykanamycin B (DKB) significantly increased because the mucus of the rectum was washed off.<sup>3)</sup> On the other hand, some drugs such as streptomycin, gentian violet,<sup>4)</sup> and quaternary ammonium compounds,<sup>5,6)</sup> form nonabsorbable complexes with intestinal mucin. We recently reported that some  $\beta$ -lactams and aminoglycosides bind to rat intestinal mucin, and removal of the mucin by the use of detergent significantly increases the absorption of these drugs from the rat intestine.<sup>7)</sup> It is suggested that these interactions may be partially responsible for the poor absorption of these drugs from the gastrointestinal tract, but it remains unclear whether the mucus acts as a barrier against DKB absorption or whether it forms an unabsorbable complex with the drug.

In this report, the characteristics of the interaction of DKB and mucin were investigated. The mucin from porcine stomach is not sufficiently soluble, and so soluble submaxillary mucin was selected as a model of the mucopolysaccharide. The binding studies were performed by the equilibrium dialysis and affinity chromatographic methods.

### Materials and Methods

**Materials**—DKB was kindly given by Meiji Seika Kaisha Co., Ltd. (Tokyo). Bovine submaxillary mucin (type

I, bound sialic acids approx. 5%), bovine serum albumin (fraction V), neuraminidase (type VI, from *Clostridium perfringens*), and *N*-acetylneuraminic acid were purchased from Sigma (U.S.A.). Visking tubing from Union Carbide Corp. (Tokyo) was used. Other reagents were of special grade and were obtained from Wako Pure Chemical Industries, Ltd. (Tokyo).

**Equilibrium Dialysis**—A solution of 1.0 mg/ml submaxillary mucin or asialomucin (2.0 ml) and various concentrations of DKB was dialyzed against 2.0 ml of 10 mM phosphate buffer (pH 6.5) at 4 and 25 °C for 24 h. The non-specific binding of DKB to the dialysis membrane or vessels was negligible. The amount of DKB bound to the submaxillary mucin was determined from the concentration of DKB in the outside compartment.

During the experiment, a white precipitate was observed in the inside compartment of the dialysis cell when 0.5 to 1 mg of DKB was added to the solution of mucin. Because both DKB and mucin have sufficient solubility at these concentrations, the precipitate might be the complex of DKB and mucin, produced to a level beyond its solubility. The precipitate was filtered off with a Millipore filter (0.22  $\mu$ m). Ethylenediamine solution (10<sup>-2</sup> M) dissociated DKB from the precipitate and solubilized it (see Table III). Because this concentration of ethylenediamine did not affect the bioassay of DKB, the DKB concentrations in the precipitate and dialysate were both determined. For Scatchard plot analysis, the DKB amount in the precipitate was subtracted from the added DKB and the concentration was plotted on the abscissa.

**3',4'-Dideoxykanamycin B-Conjugated Sepharose 4B Affinity Chromatography**—The binding of DKB to submaxillary mucin was investigated by using an affinity column of DKB-conjugated Sepharose 4B. The DKB-conjugated Sepharose 4B was prepared as described in the previous report.<sup>9)</sup> The amount of DKB bound to 1 mg of the gel was 2.4  $\mu$ mol. The column (1.5  $\times$  11 cm) was equilibrated with 10 mM Tris-HCl (pH 7.0), and then the submaxillary mucin (2.0 mg) dissolved in the buffer was applied. The bound mucin was eluted with the buffer containing 50 mM NaCl or *N*-acetylneuraminic acid.

**Determination of Concentration of 3',4'-Dideoxykanamycin B, Sialic Acids, and Protein**—The concentration of DKB was determined by the bioassay method using *Bacillus subtilis* ATCC 6633 as the indicator organism.<sup>9)</sup> The quantitation of sialic acids was carried out by the method of Helen and Edward.<sup>10)</sup> The protein concentration was determined by the method of Lowry *et al.*<sup>11)</sup>

**Preparation of *N*-Pentaacetyl-3',4'-dideoxykanamycin B and Asialomucin**—Acetylation of DKB was carried out by the method reported by Jennings *et al.*<sup>12)</sup> *N*-Pentaacetyl-DKB was purified on an ion exchange column (Dowex 50, H<sup>+</sup> form, 50—100 mesh). It was characterized by thin layer chromatography<sup>13)</sup> using Merck cellulose (Merck Art. 5577) and silica gel (Merck Art. 5715) plates with the developing solution of *n*-BuOH:EtOH:CHCl<sub>3</sub>:NH<sub>4</sub>OH(17%)=4:5:2:5. *N*-Pentaacetyl-DKB was detected as a single spot with a 10% H<sub>2</sub>SO<sub>4</sub> spray, and no free amino group could be detected by using ninhydrin spray. Thus, all of the amino groups of DKB were acetylated by this method. The yield of *N*-pentaacetyl-DKB was about 75%. Under these conditions, acetylation of the hydroxyl group of DKB could not occur, since the reaction was carried out in an alkaline solution of saturated NaHCO<sub>3</sub>.<sup>12)</sup>

Asialomucin was prepared according to the method of Forstner and Forstner.<sup>1)</sup> In brief, bovine submaxillary mucin and neuraminidase (Sigma, type VI) in 0.05 M acetate buffer (pH 5.0) were incubated at 37 °C for 4 h. After incubation, free sialic acids were removed by dialysis, and the asialomucin was separated from neuraminidase by Sepharose 4B chromatography. Seventy-five percent of the sialic acid was removed from the mucin.

## Results and Discussion

### Binding of 3',4'-Dideoxykanamycin B and Mucin

The DKB binding to submaxillary mucin was studied by the equilibrium dialysis method and analyzed by means of the Scatchard plot.<sup>14)</sup> As shown in Fig. 1, about 8.2% of the DKB was bound to the mucin when 940  $\mu$ g of DKB interacted with 1 mg of mucin at 25 °C. DKB did not bind to dextran or bovine serum albumin, used as the control (inset). The Scatchard plots were linear at both 4 and 25 °C. The linear plot indicates that submaxillary mucin has one class of binding sites to which DKB binds. A binding coefficient of 1.30  $\times$  10<sup>-5</sup> M, and a binding site concentration of 0.243  $\mu$ mol per mg of mucin were obtained from the Scatchard plot at 25 °C. At 4 °C, the binding coefficient was 1.56  $\times$  10<sup>-5</sup> M, and the binding site concentration was 0.125  $\mu$ mol per mg of mucin. The binding of DKB to mucin at 4 °C was decreased by about 62% as compared with that at 25 °C. The lower binding of DKB at lower temperature is due to the decrease in the number of binding sites, because the binding coefficients were almost the same at both temperatures.

The effects of the pH and ionic strength on the binding of DKB and submaxillary mucin were examined. The sum of the complex in solution and in the precipitate in the inside

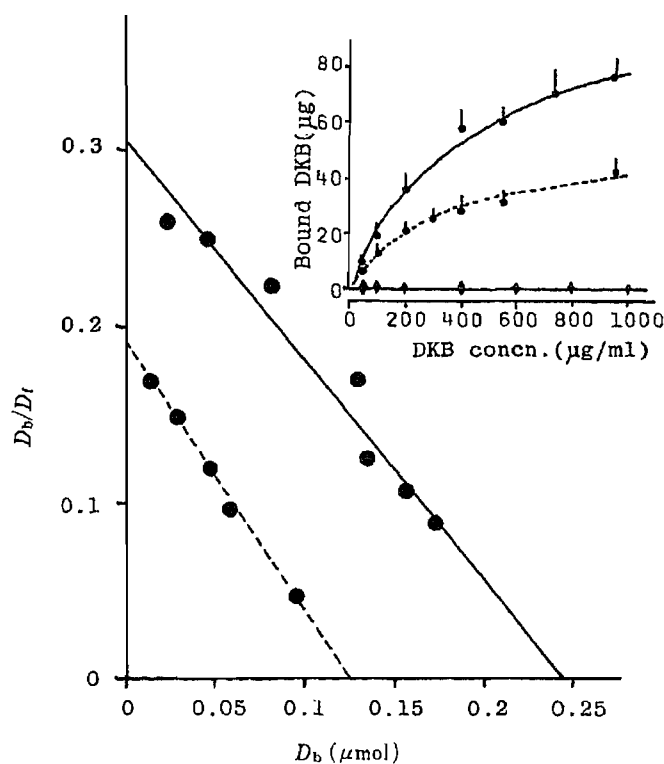


Fig. 1. Scatchard Plot of DKB Binding to Submaxillary Mucin

Equilibrium dialysis was performed at 25°C (—●—) and 4°C (---●---) for 24 h. Regression lines were obtained by the least squares method.  $D_b$  and  $D_f$  indicate the concentration of bound and free drugs, respectively. The inset shows a direct plot of the data. The interaction of DKB with bovine serum albumin (—△—) or dextran (—▲—) was run as a control. Each value is the mean  $\pm$  S.D. ( $n=3$ ). Experimental details are described in Materials and Methods.

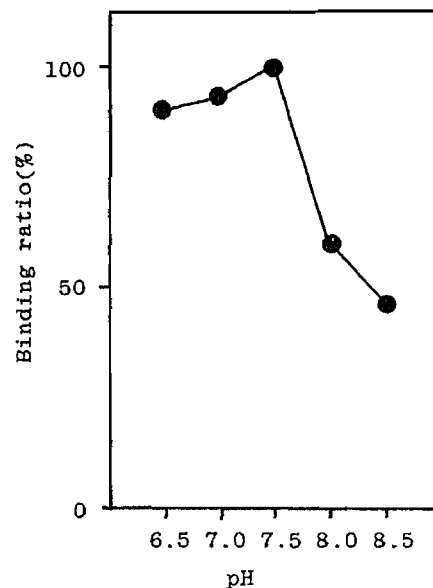


Fig. 2. Effect of pH on the Binding of DKB to Submaxillary Mucin

TABLE I. Effect of Ionic Strength on the Binding of DKB to Submaxillary Mucin

NaCl concn. (M)	Ionic strength	Bound DKB ( $\mu\text{g}/\text{mg}$ mucin)	%
$1.0 \times 10^{-3}$	0.121	114.6	100.0
$5.0 \times 10^{-3}$	0.125	103.7	90.5
$1.0 \times 10^{-2}$	0.130	93.3	81.4
$5.0 \times 10^{-2}$	0.170	74.6	65.1
$1.0 \times 10^{-1}$	0.220	59.6	52.4
$5.0 \times 10^{-5}$	0.620	45.2	39.4
1.0	1.120	23.6	20.6

compartment was estimated from the free DKB concentration in the outside compartment of the dialysis cell. Figure 2 shows the ratio of the complex generated at various pH values to that at pH 7.5, because the highest binding was observed at pH 7.5. The binding of DKB to mucin occurred in the acidic pH range, but decreased remarkably in the alkaline range. DKB contains five amino groups in its molecule, all of which take ionized form in the acidic pH range.

The binding of DKB to submaxillary mucin was investigated at various concentrations of NaCl. As the ionic strength of the incubation medium was increased, the complex formation between DKB and mucin decreased, as shown in Table I.

These findings suggest that the DKB cation is important in the binding of DKB to mucin. These results are consistent with the observations that the bindings of aminoglycoside antibiotics to acidic mucopolysaccharides, such as chondroitin sulfate, heparin, and hyaluronic acid, are also affected markedly by the pH or ionic strength of the incubation medium.<sup>15)</sup> There is a possibility that mucin undergoes a conformational change when the pH or ionic strength of the incubation medium increases; this change may affect the binding of DKB. However, the DKB binding sites on mucin were found to be of one class according to the Scatchard plot analysis (Fig. 1) and may be considered to be sialic acid residues. Tulkens and Trouet<sup>9)</sup> reported that protein (calf serum) binding of DKB does not occur, and in this study, DKB did not bind to bovine serum albumin (Fig. 1). Thus, it is reasonable to consider that even if conformational change of mucin does occur at high ionic strengths or pH, it does not cause the decrease in the binding of DKB with mucin.

#### Binding Site of 3',4'-Dideoxykanamycin B to Mucin

To determine the binding site of DKB to submaxillary mucin, the effects of  $\text{Ca}^{2+}$  and certain kinds of amines on the binding were investigated. Both DKB and mucin were chemically modified for this purpose.

As is evident from Table II, the generation of the complex of DKB and mucin was decreased in the presence of  $\text{Ca}^{2+}$ , and about 70% inhibition occurred when  $10^{-3}\text{ M Ca}^{2+}$  was added to the medium. There are two possible reasons for this; first  $\text{Ca}^{2+}$  may bind to the carboxyl groups of the sialic acid residues of mucin, and secondly  $\text{Ca}^{2+}$  may bind to the carboxyl groups of the core protein of mucin. Forstner and Forstner<sup>1)</sup> reported that  $\text{Ca}^{2+}$  binds to rat intestinal goblet cell mucin through its interaction with the carboxyl groups of sialic acid residues. Thus, the inhibition observed in this study may occur as a result of the binding of  $\text{Ca}^{2+}$  with the carboxyl groups of submaxillary mucin—particularly those of the sialic acid residues.

The effects of amines, such as glucosamine, ethylenediamine, and spermidine, on the complex formation of DKB and submaxillary mucin were also investigated. Since DKB is an amino sugar and contains five amino groups in its molecule, amines would affect the complexation. As shown in Table III, the binding of DKB was inhibited in the presence of each amine. Particularly in the case of  $10^{-2}\text{ M}$  ethylenediamine, the binding was completely inhibited, while the addition of glucose had almost no effect on this binding. Thus, it is assumed that the amino groups of DKB participate in the binding of DKB to mucin. The competition of the amino groups of DKB and the co-existing amines may cause a decrease in the binding of DKB to mucin, because low concentrations of the polyamines, ethylenediamine and spermidine affected the binding of DKB to mucin.

TABLE II. Effect of  $\text{Ca}^{2+}$  on the Binding of DKB to Submaxillary Mucin

$\text{Ca}^{2+}$ concn. (M)	Bound DKB ( $\mu\text{g}/\text{mg}$ mucin)	%
Control (0)	105.6	100.0
$10^{-6}$	99.6	94.3
$10^{-5}$	87.6	83.0
$10^{-4}$	75.0	71.0
$10^{-3}$	32.7	31.0

TABLE III. Effect of Amines on the Binding of DKB to Mucin

Conc. (M)	Glucose		Glucosamine		Ethylenediamine		Spermidine	
	Bound DKB ( $\mu\text{g}/\text{mg}$ mucin)	%	Bound DKB ( $\mu\text{g}/\text{mg}$ mucin)	%	Bound DKB ( $\mu\text{g}/\text{mg}$ mucin)	%	Bound DKB ( $\mu\text{g}/\text{mg}$ mucin)	%
Control (0)	118.4	100.0	118.4	100.0	118.4	100.0	118.4	100.0
$10^{-5}$	107.7	91.0	84.1	71.0	29.6	25.0	62.8	53.0
$10^{-4}$	107.7	91.0	74.6	63.0	29.6	25.0	55.6	47.0
$10^{-3}$	103.0	87.0	65.1	55.0	10.7	9.0	45.0	38.0
$10^{-2}$	103.0	87.0	53.3	45.0	0	0	17.8	15.0

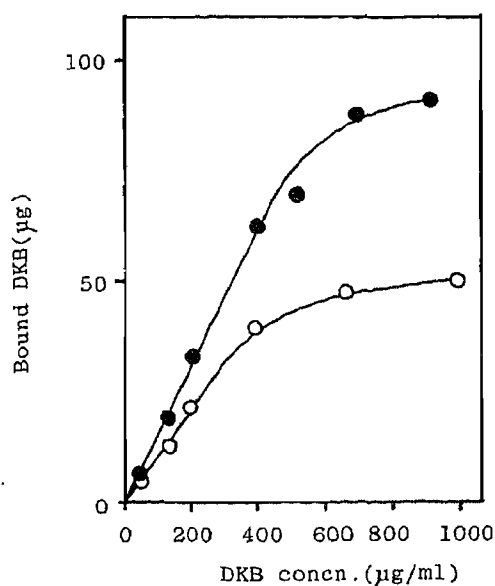


Fig. 3. Binding of DKB to Asialomucin

The equilibrium dialysis of asialomucin (1 mg) and the indicated concentrations of DKB was carried out using 10 mM phosphate buffer (pH 6.5) at 25 °C for 24 h.

—●—, mucin; —○—, asialomucin.

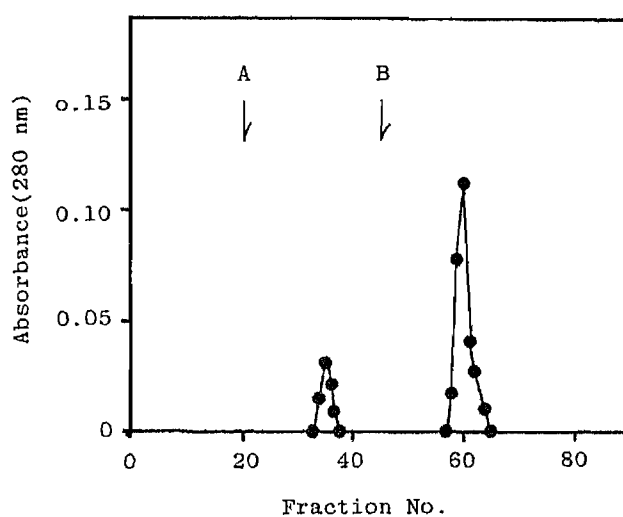


Fig. 4. Affinity Chromatography of Submaxillary Mucin on a DKB-Conjugated Sepharose 4B Column

A. The elution buffer was changed from 10 mM Tris-HCl buffer (pH 7.0) to the same buffer containing 50 mM NaCl.

B. The elution buffer was changed from 10 mM Tris-HCl buffer (pH 7.0) containing 50 mM NaCl to the same buffer containing 50 mM *N*-acetylneuraminic acid.

*N*-Pentaacetyl-DKB was not able to bind to mucin. As described in Materials and Methods, the *N*-acetylation of the five amino groups of DKB was complete and thus no free amino group remained in this molecule. These results indicate that the amino groups of DKB play a very significant role in the binding of DKB to mucin.

Next, the binding of DKB to asialomucin was studied, and the result is shown in Fig. 3. The binding of DKB to asialomucin was inhibited by about 50% as compared with that to the submaxillary mucin. This decrease corresponded fairly well to the residual sialic acid concentration in asialomucin obtained in this experiment, since 75% of the sialic acid was removed from mucin by neuraminidase treatment. This suggests that the binding sites of submaxillary mucin are the sialic acid residues.

Using a DKB-conjugated Sepharose 4B column, the binding sites of mucin were further investigated. To determine whether the binding of mucin to DKB was specific for sialic acids or



not, 50 mM NaCl or 50 mM *N*-acetylneuraminic acid was used as the eluente. Submaxillary mucin was retained by the affinity column (yield 84%). In the preliminary experiment, no non-specific binding of mucin to the Sepharose 4B column was observed. As shown in Fig. 4, about 20% of mucin was eluted with Tris-HCl buffer containing 50 mM NaCl solution (arrow A), and when the elution buffer was changed to the buffer containing 50 mM *N*-acetylneuraminic acid, 80% of mucin was eluted (arrow B). Since the binding of DKB to mucin was inhibited by NaCl solution (Table I), the mucin should be eluted by NaCl solution. These results show that mucin binds to DKB of the affinity column specifically through the sialic acid residues of the mucin molecule.

Many kinds of mucin in the gastrointestinal tract are secreted into the lumen and act as a barrier against absorption. In general, the water solubility of aminoglycoside antibiotics is so high that they can not be absorbed from the gastrointestinal tract. The results of the present experiment on the model system of submaxillary mucin and DKB, suggest that the aminoglycoside antibiotics interact with mucin and form insoluble complexes.

It may be concluded that the binding of DKB to submaxillary mucin occurs through the ionic interaction of the amino groups of DKB with the carboxyl groups of the sialic acid residues of mucin.

**Acknowledgements** The authors would like to thank Meiji Seika Kaisha Co., Ltd., (Tokyo) for the generous gift of DKB.

#### References

- 1) J. F. Forstner and G. G. Forstner, *Biochim. Biophys. Acta*, **386**, 283 (1975).
- 2) R. H. Reuning and G. Levy, *J. Pharm. Sci.*, **56**, 843 (1967).
- 3) S. Tsuchiya, Y. Aramaki, S. Ozawa and H. Matsumaru, *Int. J. Pharm.*, **14**, 279 (1983).
- 4) M. Gibaldi, "Introduction to Biopharmaceutics," Lea and Febiger, Philadelphia, 1971, p. 16.
- 5) R. R. Levine, M. R. Blair and B. B. Clark, *J. Pharmacol. Exp. Ther.*, **114**, 78 (1955).
- 6) R. R. Levine and E. W. Pelikan, *J. Pharmacol. Exp. Ther.*, **131**, 319 (1961).
- 7) J. Niibuchi, Y. Aramaki and S. Tsuchiya, *Int. J. Pharm.*, **30**, 181 (1986).
- 8) Y. Aramaki, A. Inaba, J. Niibuchi and S. Tsuchiya, *Chem. Pharm. Bull.*, **31**, 321 (1983).
- 9) P. Tulkens and A. Trouet, *Biochem. Pharmacol.*, **27**, 415 (1976).
- 10) H. H. Helen and R. Edward, *J. Biol. Chem.*, **239**, 3215 (1964).
- 11) O. H. Lowry, N. J. Rosebrough, A. L. Farr and R. J. Randall, *J. Biol. Chem.*, **193**, 265 (1951).
- 12) H. J. Jennings, C. Lugowski and N. M. Toung, *Biochemistry*, **19**, 4712 (1980).
- 13) I. Komiya, Y. Ayasaka, S. Murata, T. Komai and K. Umemura, *Jpn. J. Antibiot.*, **26**, 49 (1973).
- 14) N. Kardos, A. Eichholz and P. Schallner, *J. Antibiot.*, **34**, 103 (1981).
- 15) T. Deguchi, A. Ishii and M. Tanaka, *J. Antibiot.*, **31**, 150 (1978).

[Chem. Pharm. Bull.]  
35(1) 326-334 (1987)

## Effect of Adriamycin on Cultured Mouse Embryo Myocardial Cells

KYOKO TAKAHASHI,\*<sup>1)</sup> YASUKO FUJITA, TADANORI MAYUMI,  
TAKAO HAMA and TAKEO KISHI

*Faculty of Pharmaceutical Sciences, Kobe-Gakuin University,  
Nishi-ku, Kobe 673, Japan*

(Received May 27, 1986)

Adriamycin (ADM) inhibited the beating of cultured mouse embryo myocardial cells dose- and time-dependently and subsequently lysed the cells. Fifty percent inhibition of beating cell number was observed when cultures were exposed to 430–520  $\mu\text{M}$  ADM for 0.5 h, 70–100  $\mu\text{M}$  ADM for 4 h and 3.5  $\mu\text{M}$  for 36 h. When cultures were exposed to 3.5  $\mu\text{M}$   $^3\text{H}$ -ADM, the radioactivity in the cells reached almost the maximum within 8 h, and about 90% was recovered as ADM itself even after 72 h. However, the beating cell number and the beating rate did not appreciably decrease within 8 h, then decreased to 78.5 and 67.1% at 24 h, and 5.6 and 5.2% at 72 h, respectively. Lysis of the cells was conspicuous at 48 h or later. It was also supported with the decrease in cellular proteins and the release of lactate dehydrogenase. These results indicate that ADM stimulates lysis of the cytoplasmic membrane following inhibition of beating. When cultures were exposed to 70  $\mu\text{M}$  ADM for 4 h and then incubated in ADM-free medium, about 50% of ADM in cells was released within 24 h. However, inhibition of beating and lysis of such cells still advanced at about the same rate as in continuously exposed cells. ADM also decreased the cellular adenosine triphosphate (ATP) content in the same fashion as antimycin A, which inhibited beating in advance of ATP reduction. These results suggested that the beating state of myocardial cells is a sensitive and reliable parameter in this system for studies on the cardiotoxicity of ADM. The system may be useful for studies not only on ADM but also on agents having effects on the heart.

**Keywords**—adriamycin; antimycin A; ATP; rotenone; beating; mouse embryo; lactate dehydrogenase; cardiac cell culture

Adriamycin (doxorubicin, ADM) is known to produce various adverse effects on the heart, as well as such side-effects as myelosuppression and anorexia, that are commonly observed with antineoplastic agents. In particular, the cumulative dose-dependent cardiomyopathy due to ADM is a serious problem that limits the dose and application of ADM in cancer therapy.<sup>2)</sup>

ADM has been reported to induce a number of biochemical changes, most of which relate to (a) mitochondrial dysfunction,<sup>3,4)</sup> (b) accumulation of oxygen radicals or lipid peroxides,<sup>5,6)</sup> (c) inhibition of nucleic acid synthesis,<sup>7,8)</sup> (d) membrane perturbation,<sup>9,10)</sup> or (e) disturbance of electrolyte balance.<sup>11,12)</sup> However, the interrelations between such biochemical changes and the cardiotoxicity of ADM have not been clarified. If some of these biochemical abnormalities cause the cardiotoxicity, they must develop before or in parallel to the structural and functional alterations of myocardial tissue by ADM. In order to follow the biochemical changes and the functional alterations caused by ADM in the heart simultaneously, cultured heart cells appear to be a simple and convenient material, because they retain the structural integrity of the heart cell and its ability to beat autorhythmically.

In this study, the inhibitory effect of ADM on beating of cultured mouse cardiac cells was investigated in order to establish a basic system to elucidate the biochemical mechanisms resulting in the ADM cardiotoxicity.

### Experimental

**Materials**— $^3\text{H}(\text{G})$ -Labelled ADM ( $198.2 \mu\text{Ci}/\text{mg}$ ) and unlabeled ADM were kindly donated by Kyowa Hakko Co., Chiyoda-ku, Tokyo, Japan. Other materials were purchased from the following sources: Nunc dishes from Japan Inter-Med Co., Minato-ku, Tokyo, Japan; trypsin (1:250) from Difco Laboratories, Detroit, Mich., U.S.A.; collagenase (type I) and firefly lantern extract (FEL-50) from Sigma Chemical Co., St. Louis, Mo., U.S.A.; Eagle's MEM, Ham's F-12 medium and Dulbecco's phosphate buffered saline (PBS) from Nissui Seiyaku, Tokyo, Japan; calf serum from Commonwealth Serum Laboratories, Victoria, Australia; ACS-II from Amersham Co., Arlington Heights, Ill., U.S.A.. The other agents were of analytical reagent grade.

**Mouse Embryo Cardiac Cell Culture**—The cardiac cell culture was prepared by a modification of Goshima's method<sup>13)</sup> as described below. The basal medium in Goshima's method, *i.e.*, Eagle's MEM containing 10% calf serum and 20 mM *N,N'*-bis(2-hydroxyethyl)-2-aminoethanesulfonic acid (BES), was replaced by Ham's F-12 medium which was supplemented with 10% calf serum and buffered at pH 7.3 with sodium bicarbonate. Such a modification allowed the cultures to keep beating so longer. BES somewhat depressed the beating of cells when the incubation period was extended over 6 h.

Hearts from 14- to 16-d-old mouse embryos (ICR strain) were minced and digested with 5 ml of 0.125% trypsin-0.025% collagenase solution at 37°C for 20 min. The dispersed myocardial cells were collected by centrifugation at about  $200 \times g$  for 10 min, and then resuspended in Ham's F-12 medium. The cell suspension was adjusted to a density of  $2-4 \times 10^6$  cells/ml. Viable cells counted by a trypan blue exclusion method<sup>14)</sup> always amounted to 80% or more of the total cells in the suspension. Nunc dishes (35 mm i.d., Cat. No. 153066) containing 1 ml of Ham's F-12 medium were seeded with 0.1 ml of the cell suspension, and incubated at 37°C in a humidified environment of 5%  $\text{CO}_2$ -95% air. The medium was renewed every 48 h thereafter. The treatment of cultures with the test agents was begun 1-2 d after the cells were seeded, at which time they were beating rhythmically, and was ended before the cells formed into a monolayer sheet.

**Measurement of Beating**—The beating status of cultured cardiac cells was monitored with an inverted phase-contrast microscope at magnification of 150 to 400 in a chamber controlled at 37°C. In each culture dish, about twenty cells or clusters, which were beating regularly in the range of 33-171 beats/min, were selected for each experiment, and their beating rates, shapes and locations in the dish were recorded before application of the test agents. Beating of each cell or cluster was usually counted for 60 s at the time indicated. Each experiment was repeated at least three times by using separately prepared cell cultures, and the results were averaged.

**Determination of Uptake and Metabolites of ADM**— $^3\text{H}(\text{G})$ -ADM instead of unlabeled ADM was dissolved in Ham's F-12 medium and added to the culture. At the time indicated, the cultured cells were rinsed 3 times with 0.5 ml of PBS, and then dissolved in 0.5 ml of 0.1 M sodium hydroxide solution for 30 min. Two thirds of the solution was transferred to a scintillation vial and mixed with 12 ml of ACS-II. The radioactivity was measured with a Packard Tri-Carb 460 liquid scintillation counter. The remaining part of the solution was used for the measurement of protein content by the method of Lowry *et al.*<sup>15)</sup> For analysis of ADM metabolites, labelled compounds were extracted with methanol from the cells burst by freezing, and divided to fractions of ADM, adriamycinone and the remaining eluate by a high-performance liquid chromatography (HPLC) as described by Haneke *et al.*<sup>16)</sup> The radioactivities were determined with a scintillation counter. The HPLC column was Finepak  $\text{C}_{18}$ -5 ( $5 \mu\text{m}$  particles,  $250 \times 4.6$  mm i.d.) and the flow rate was 0.8 ml/min.

**Measurement of ATP**—The ATP content of cultured cells was determined by a modified luciferase method.<sup>17)</sup> ATP in adherent cells was extracted with chilled 0.6 M perchloric acid for 30 min. The extract was neutralized with 3 M potassium hydroxide and then centrifuged at  $350 \times g$  for 5 min at 4°C. The supernatant was used as a sample solution for the ATP assay. One milliliter of the reaction mixture in a quartz cell contained 0.5 ml of 0.1 M sodium arsenate-40 mM magnesium sulfate at pH 7.4, 0.2 ml of the supernatant, and 0.25 ml of water. Diluted firefly lantern extract (0.05 ml) was then added to the reaction mixture, and bioluminescence intensity was measured with a CHEM-GLOW photometer. Counts accumulated during 60 s were compared to those from the standard solution of ATP.

**Measurement of Lactate Dehydrogenase (LDH)**—LDH activity released into the culture medium was determined spectrophotometrically by a modified Wroblewski-LaDue method.<sup>18)</sup> The reaction mixture (1.17 ml total) in a quartz microcell contained 0.9 ml of 50 mM potassium phosphate buffer at pH 7.5, 0.1 ml of 23 mM sodium pyruvate, 0.05 ml of a sample (the culture medium) and 0.12 ml of water. The reaction mixture was brought to 25°C before the assay. An aliquot of 0.03 ml of 6.12 mM reduced nicotinamide adenine dinucleotide (NADH) containing 59.5 mM sodium bicarbonate was added to the reaction mixture and mixed immediately. The change in extinction at 340 nm during 4-5 min was measured with a Parkin-Elmer Model 551 UV-VIS double-beam spectrophotometer. The LDH activity was expressed as the rate of oxidation of NADH by the sample medium, in nmol/min/ml.

**Determination of Protein Content**—Cellular proteins were solubilized with 0.1 M sodium hydroxide solution from the cells attaching on the growing surface of the dish and determined by the method of Lowry *et al.*<sup>15)</sup>

## Results

### Inhibitory Effect of ADM on Beating Cells

On cultivation for one day, trypsin-dispersed heart cells became attached and spread out on the surface of culture dishes. Two different cell types, myocardial cells and fibroblast-like cells, could be relatively easily distinguished under a phase contrast microscope, as previously noted by Goshima and Tonomura<sup>19)</sup>: the fibroblast-like cells were very thin, well-spread cells. Because they were so thin, they were transparent and poorly refractile under phase optics. The myocardial cells were thick, highly refractile cells. The percentage of myocardial cells in our culture prepared from fetal mouse heart was about 80% and most of them exhibited spontaneous beating (Table I).

Table II shows the average beating status of mouse myocardial cells, which served for this series of ADM experiments. In the basal medium, almost all the cells selected at initial stage continued beating rhythmically during incubation for up to 72 h, and their mean beating rate increased gradually up to 147.1% of the initial rate during the period of 72 h. In the presence of 3.5  $\mu\text{M}$  ADM, the number of beating cells and their beating rates started decreasing concomitantly with a time lag of about 24 h, and decreased to about 5% of the initial values of 72 h. Most cells acquired irregular beating and/or structural alterations within this period.

Figure 1 shows morphological changes of cardiac cells under the same conditions as in Table II. Most cells in the presence of 3.5  $\mu\text{M}$  ADM did not show marked morphological changes up to 24 h (Fig. 1A, B). After 48 h of incubation, however, they tended to lyse and to become detached from the surface (Fig. 1C). Many of the cells disappeared from the surface

TABLE I. Percentage of Myocardial Cells

Cultivation time (h)	Myocardial cells among attached cells (%)	Beating cells among myocardial cells (%)
48	80 $\pm$ 4	96 $\pm$ 3
72	73 $\pm$ 7	88 $\pm$ 9
96	81 $\pm$ 6	—

The values are means  $\pm$  SE of 6 experiments. A total of 780—1230 cells was counted for each value.

TABLE II. Inhibitory Effects of Adriamycin on the Beating Cell Number and the Beating Rate of Cultured Mouse Myocardial Cells

Incubation time (h)	Beating cell number (%)		Beating rate (%)	
	None	3.5 $\mu\text{M}$ ADM	None	3.5 $\mu\text{M}$ ADM
0	88/88 (100)	107/107 (100)	100 <sup>a)</sup>	100 <sup>b)</sup>
4	60/60 (100)	—	111 $\pm$ 8	—
8	55/60 (92)	—	106 $\pm$ 9	—
24	74/88 (84)	84/107 (79)	134 $\pm$ 16	67 $\pm$ 5 <sup>d)</sup>
48	81/85 (95)	13/107 (29) <sup>c)</sup>	150 $\pm$ 11	28 $\pm$ 5 <sup>d)</sup>
72	46/48 (96)	6/107 (6) <sup>c)</sup>	147 $\pm$ 15	5 $\pm$ 2 <sup>d)</sup>

Beating cell number and beating rate are given as the ratio of beating cells at the indicated time to that at 0 h. Figures in parentheses show the percentage of beating cell number. Beating rates are expressed as averaged beating rates (mean  $\pm$  SE) of individual cells. a) 99  $\pm$  5 beats/min at 37°C, mean  $\pm$  SE ( $n=88$ ). b) 104  $\pm$  6 beats/min at 37°C, mean  $\pm$  SE ( $n=107$ ). Values with superscripts c) and d) are significantly different from the corresponding control (values at 0h) with  $p < 0.001$  by the  $X^2$ -test and unpaired  $t$ -test, respectively.

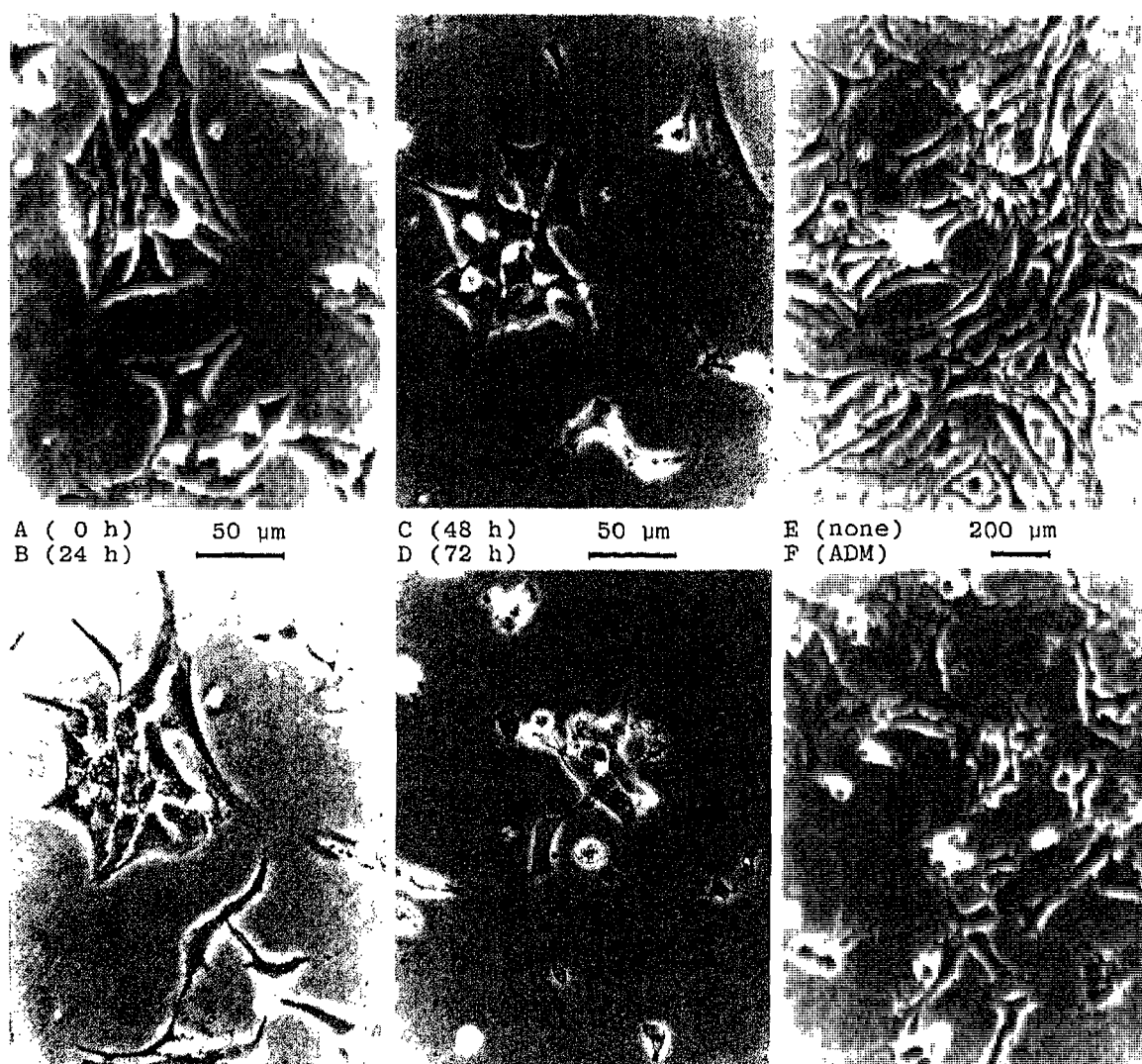


Fig. 1. Morphological Changes of Cardiac Cells Incubated with  $3.5 \mu\text{M}$  Adriamycin

A, B, C and D are phase contrast micrographs of cells observed at a magnification of 400 at 0 h, 24, 48, and 72 h after the addition of  $3.5 \mu\text{M}$  ADM, respectively. The scale shows  $50 \mu\text{m}$ . E and F show phase contrast micrographs, which were observed at a magnification of 100, of the cultures incubated without and with  $3.5 \mu\text{M}$  ADM for 48 h, respectively. The scale shows  $200 \mu\text{m}$ .

after 72 h (Fig. 1D). Such morphological changes could be seen more clearly at a lower magnification as shown in the micrographs of two groups of cells grown with and without  $3.5 \mu\text{M}$  ADM at 48 h in Fig. 1E and F.

Lysis of cells during incubation with ADM was also supported by the decrease in the total cellular protein content and the increase in the release of LDH, a cytosolic enzyme. Table III shows the total protein content of the cells attached to the growing surface. The protein content of cells in the presence of  $3.5 \mu\text{M}$  ADM decreased gradually to about half the initial content during cultivation for 72 h, while that of parallel control cells increased to twice the initial content at 72 h.

Table IV shows the amounts of LDH released from cells during cultivation for 72 h. ADM increased the release of LDH to about twice that of the parallel control. These results indicate that ADM stimulates lysis of the cytoplasmic membrane following inhibition of beating. Figure 2 shows the effects of various doses of ADM on beating cells. The decrease in

TABLE III. Effect of Adriamycin on Protein Content of Cardiac Cells

Incubation time (h)	Protein content (%)	
	None	3.5 $\mu\text{M}$ ADM
24	114 $\pm$ 9 (13)	83 $\pm$ 12 (9)
48	170 $\pm$ 12 (13)	77 $\pm$ 17 (9)
72	190 $\pm$ 18 (13)	54 $\pm$ 6 (13)

Protein contents are expressed as mean percentage  $\pm$  SE of the initial content. Figures in parentheses are the number of experiments. The initial protein content of cardiac cells was  $22.0 \pm 2.2 \mu\text{g}$  per dish.

TABLE IV. The Release of Lactate Dehydrogenase from Cardiac Cells by Adriamycin

Incubation time (h)	LDH activity in culture medium (nmol/min/ml)	
	None	ADM 3.5 $\mu\text{M}$
24	16.9 $\pm$ 6.2	36.0 $\pm$ 9.9
48	38.8 $\pm$ 7.7	68.2 $\pm$ 14.5 <sup>a)</sup>
72	83.2 $\pm$ 8.5	195.5 $\pm$ 17.0 <sup>b)</sup>

The data on the LDH activity are expressed as mean  $\pm$  SE of 11 experiments. Values with superscripts *a)* and *b)* are significantly higher than the corresponding controls with  $p < 0.05$  and  $p < 0.001$ , respectively.

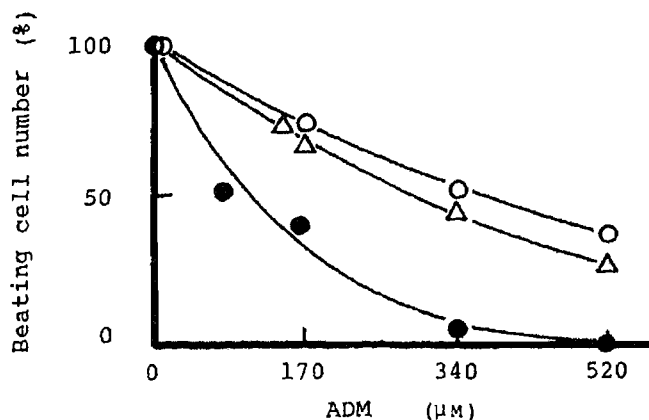


Fig. 2. Dose and Time Dependencies of the Inhibitory Effect of Adriamycin on Beating of Cultured Myocardial Cells

Beating cell numbers were counted at the indicated times after the addition of various concentrations of ADM. Open circles, open triangles and closed circles show incubation periods of 0.5, 1.0 and 4.0 h, respectively.

the beating cell number by ADM was dose- and exposure time-dependent. Fifty percent cessation of beating of cells was observed on incubation with 430–520  $\mu\text{M}$  ADM for 0.5 h, 280  $\mu\text{M}$  ADM for 1 h, 70–100  $\mu\text{M}$  for 4 h or 3.5  $\mu\text{M}$  ADM for 36 h.

#### Incorporation of $^3\text{H}(\text{G})\text{-ADM}$

Table V shows the amounts of  $^3\text{H}(\text{G})\text{-ADM}$  incorporated into the cells under the same conditions as in Table II. The radioactivity in cells reached almost the maximum within 8 h, and more than 90% was from ADM itself even 72 h after the addition, as confirmed by HPLC analysis.

Table VI shows the relationship between the amount of ADM incorporated into cells and the inhibitory effect on beating. When cultures were incubated with 70  $\mu\text{M}$   $^3\text{H}(\text{G})\text{-ADM}$ , uptake of the isotope by the cells was 13.4 pmol/ $\mu\text{g}$  protein at 4 h and reached the maximum level at 24 h, while the beating cell number was 53.5% of the control at 4 h and decreased as the incubation time was prolonged. When cultures were incubated with 70  $\mu\text{M}$  ADM for 4 h

TABLE V. Uptake and Metabolism of Adriamycin by Cardiac Cells  
(in the presence of 3.5  $\mu\text{M}$  adriamycin)

Incubation time (h)	Total uptake of $^3\text{H}$ -ADM (pmol ADM eq/ $\mu\text{g}$ protein)	ADM found (% of total uptake)
0.5	1.42 $\pm$ 0.05 (6)	—
1	1.52 $\pm$ 0.04 (6)	—
2	2.03 $\pm$ 0.10 (6)	—
4	2.30 $\pm$ 0.12 (6)	—
8	2.80 $\pm$ 0.15 (6)	—
24	2.72 $\pm$ 0.21 (28)	95.9 $\pm$ 8.64 (7)
48	3.43 $\pm$ 0.17 (28)	90.2 $\pm$ 4.72 (7)
72	2.97 $\pm$ 0.17 (28)	96.2 $\pm$ 4.46 (7)

Radioactivity of  $^3\text{H}$ (G)-ADM used in the experiments was 198.2  $\mu\text{Ci}/\text{mg}$ . The data are expressed as mean  $\pm$  SE and figures in parentheses are the number of experiments. The total uptake of  $^3\text{H}$ -ADM was estimated by measuring radioactivity of the isotope incorporated in cells. ADM found in cells was determined by HPLC as described in the text.

TABLE VI. Uptake of Adriamycin by Cardiac Cells (in the presence of 70 and 140  $\mu\text{M}$  adriamycin)

ADM ( $\mu\text{M}$ )	Incubation time (h)	Cellular radioactivity <sup>a)</sup> (pmol ADM eq/ $\mu\text{g}$ protein)	Beating cell number (% <sup>b)</sup> )
70	4	13.4 $\pm$ 0.61 (45)	61/114 (53.5)
	24	24.1 $\pm$ 1.96 (12)	—
	28	—	19/114 (16.7)
	48	18.7 $\pm$ 2.25 (12)	—
	52	—	1/114 (0.9)
	72	14.7 $\pm$ 1.10 (6)	—
	76	—	0/114 (0)
70	4 (24) <sup>c)</sup>	6.37 $\pm$ 0.35 (40)	23/114 (20.2)
	(48)	4.94 $\pm$ 2.25 (12)	6/114 (5.3)
	(72)	7.23 $\pm$ 0.68 (6)	3/114 (2.6)
140	1	11.0 $\pm$ 1.92 (17)	38/ 54 (70.4)
	4	19.3 $\pm$ 3.08 (17)	23/ 54 (42.3)

a) The total cellular radioactivity from  $^3\text{H}$ (G)-ADM was calculated in ADM eq and is expressed as the mean  $\pm$  SE, figures in parentheses are the number of experiments. b) Ratio of beating cell number at the indicated incubation time to that before ADM treatment; figures in parentheses show the percentage of the beating cell number. c) The cells were incubated with  $^3\text{H}$ (G)-ADM for 4 h and then incubated in the basal medium (ADM-free) after being washed three times with the basal medium. Figures in parentheses show the incubation time after the removal of ADM.

and then with ADM-free medium for 24 to 72 h, the ADM content of the cells decreased to less than half that of the cells exposed continuously to ADM. However, inhibition of beating of such rinsed cells still progressed at about the same rate as that of the cells exposed continuously to 70  $\mu\text{M}$  ADM, resulting in lysis of cells. When cultures were incubated with 140  $\mu\text{M}$   $^3\text{H}$ (G)-ADM, the amount of the isotope incorporated in the cells within 1 h was almost the same as that within 4 h at 70  $\mu\text{M}$  ADM. The uptake of ADM at 4 h increased further and reached twice that at 1 h. At the same time, the beating cell number decreased rapidly from 70.4% of the initial beating cells at 1 h to 42.3% at 4 h. These results suggest that not the metabolites of ADM but ADM itself produces the inhibitory effect on the beating of myocardial cells and that this effect may result from some biochemical changes induced by ADM, since the time lag was prolonged as the dose of ADM was lowered.

TABLE VII. Inhibitory Effect of Adriamycin on ATP Content of Cardiac Cells

Incubation time (h)	ATP content (pmol/ $\mu$ g protein)	
	None	3.5 $\mu$ M ADM
24	37.5 $\pm$ 0.90	36.6 $\pm$ 1.67
48	37.7 $\pm$ 0.82	25.4 $\pm$ 0.92 <sup>a)</sup>
72	39.7 $\pm$ 1.23	17.5 $\pm$ 0.49 <sup>a)</sup>

Values show the mean  $\pm$  SE in 8 experiments. The values with superscript *a)* are significantly lower than those from the parallel control (none) with  $p < 0.001$  by the unpaired *t*-test.

TABLE VIII. Inhibitory Effects of Antimycin A and Rotenone on ATP Content and Beating of Myocardial Cells

Inhibitor ( $\mu$ M)	ATP content (pmol/ $\mu$ g protein)	Beating cell number (%)
None	26.7 $\pm$ 0.47	100
Antimycin A	18	27.5 $\pm$ 0.76
	55	25.7 $\pm$ 1.14
	91	16.9 $\pm$ 1.07 <sup>b)</sup>
	128	9.83 $\pm$ 0.63 <sup>b)</sup>
Rotenone	13	29.6 $\pm$ 1.98
	25	23.8 $\pm$ 0.78 <sup>a)</sup>
	51	23.4 $\pm$ 0.80 <sup>a)</sup>
	127	21.1 $\pm$ 1.38 <sup>a)</sup>

ATP content was determined after the cells were incubated in the medium with the inhibitors for 0.5 h. Values of ATP content are the mean  $\pm$  SE of 9 experiments. Beating cell numbers are shown as percentages of 30–52 beating cells at the start of the incubation. Values with superscripts *a)* and *b)* are significantly lower than the control (none) with  $p < 0.01$  and  $p < 0.001$  by the unpaired *t*-test, respectively.

### Effect of ADM on the ATP Content of Cells

Table VII shows the relationship between the inhibitory effect of ADM on beating and the ATP level of cardiac cells under the same conditions as in Table II. ADM depressed ATP level in the cells at incubation periods of longer than 48 h. This reduction in ATP content by ADM, however, developed more slowly than the decreases in the number of beating cells and the beating cell rate, that is, about 24 h later.

Table VIII shows the inhibitory effects of antimycin A and rotenone, potent inhibitors of mitochondrial electron transport, on beating and ATP content. The concentrations of 55  $\mu$ M antimycin A and 25  $\mu$ M rotenone caused about 50% reduction in the number of beating cells. Reduction of ATP content by antimycin A, however, was caused only by higher concentrations than 91  $\mu$ M. In addition, rotenone at concentrations up to 127  $\mu$ M did not much reduce the ATP content.

### Discussion

The incidence of ADM-induced cardiomyopathy in patients increases dramatically at cumulative ADM doses of above 550 to 600 mg/sq m.<sup>20)</sup> A variety of morphological changes, including loss of myofibrils, mitochondrial swelling, vacuolization, and z-band disruption, have been noted upon autopsy in the hearts of patients who had succumbed to ADM-induced congestive heart failure.<sup>21)</sup> Similar morphological changes have been observed in various animal species.<sup>22)</sup>



Some attempts to use heart cell cultures to evaluate ADM-induced toxicity have been reported,<sup>23-25)</sup> though most of them did not systematically investigate the relationships between dose levels, exposure time, cellular uptake of ADM and biochemical and physiological functions of myocardial cells. Lampidis *et al.*<sup>26)</sup> in one such study showed that structural and functional alterations induced by ADM in cultured rat heart cells are similar to those seen *in vivo*, and can be related to ADM dose and exposure time. The present results on the inhibitory effect of ADM on mouse embryo myocardial cells are similar to their results. The doses of 3.5 and 140  $\mu\text{M}$  ADM in our work seem to correspond to their low or intermediate doses and high doses, *i.e.*, the levels for so-called chronic and acute toxicities, respectively. They also suggested that the beating rate is not a reliable parameter for study since the beats/min of individual ADM-treated cultures overlapped those of untreated cultures, but the present results have proved that the beating rate and the beating cell number are sensitive and reliable parameters of ADM toxicity. This discrepancy may be due to the use of cardiac cell cultures at different stages. While we used a primary culture rich in myocardial cells after cultivation for 1 to 2 d (Table I), they used a confluent cell culture after 7 d which contained many fibroblast-like cells as well as myocardial cells. At a low dose of 3.5  $\mu\text{M}$  ADM (Table II), the amount of ADM incorporated into the cells reached nearly the maximum level in 8 h, and remained unchanged till 72 h. Nevertheless, cessation of beating developed gradually after a lag time of almost one day, and lysis of cells followed, as shown by release of cellular proteins and lactate dehydrogenase (Tables III and IV). Such a time lag for inhibition of beating by ADM, though it was shortened as the ADM dose was increased, suggested that the beat inhibition may be a secondary effect of some biochemical changes induced in the cells by the addition of ADM and that the true form inducing such changes is not an ADM metabolite such as adriamycinone, but ADM itself (Table V). Exposure of myocardial cells to 70  $\mu\text{M}$  ADM was lethal even if ADM was completely removed from the culture medium after 4 h (Table VI). Furthermore, beating of such cells was inhibited almost as effectively as that of cells continuously exposed to 70  $\mu\text{M}$  ADM. Consequently, it appears that about 3 pmol or more of ADM per  $\mu\text{g}$  protein in cardiac cells results in irreversible inhibition of beating.

The myocardium is a most-energy consuming tissue, and the energy for the myocardial function is generated and supplied mainly through the mitochondrial respiratory chain, which is abundant in the heart tissue. ADM is known to produce structural and functional alterations in heart mitochondria *in vivo*.<sup>27)</sup> Thus, the effect of ADM on mitochondria in heart has been studied intensively. In 1974 Gosalvez *et al.*<sup>28)</sup> showed that ADM inhibited mitochondrial respiration. Iwamoto *et al.*<sup>29)</sup> revealed that ADM inhibited mitochondrial succinoxidase and NADH-oxidase activities from beef heart. We have also shown previously that CoQ<sub>10</sub> reduced the inhibitory effect of ADM on such CoQ-enzymes.<sup>30)</sup> Bertazzoli *et al.*<sup>31)</sup> also reported upon the protective effect of CoQ<sub>10</sub> against cardiotoxicity of ADM in an isolated rabbit heart system. Further, the relation between mitochondrial injury and cardiomyopathy was emphasized by the observations that ADM produced a reduction in the cardiac store of ATP in the isolated perfused rat heart<sup>32)</sup> and that ADM associated strongly with cardiolipin, a phospholipid specific to the mitochondrial inner membrane.<sup>33)</sup> The present results also showed that ADM depresses ATP content in cultured cardiac cells (Table V). At a dose of 3.5  $\mu\text{M}$  ADM, however, the decrease in ATP content was observed after the beat inhibition. Accordingly, the reduction in ATP content does not seem to explain the time lag. Antimycin A, a strong inhibitor of cytochrome b-c<sub>1</sub>, however, also inhibited beating in advance of ATP reduction. Therefore, it is necessary to accumulate more evidence before the relationship between ADM cardiotoxicity and cellular respiration can be understood.

#### References and Notes

- 1) Present address: Third Department of Internal Medicine, Osaka University Medical School, Fukushima-ku, Osaka

553, Japan.

- 2) M. R. Bristow, M. E. Billingham, J. W. Mason and J. R. Daniels, *Cancer Treat. Rep.*, **62**, 873 (1978).
- 3) E. Goormaghtigh, R. Brasseur and J. Guysschaert, *Biochem. Biophys. Res. Commun.*, **104**, 314 (1982).
- 4) H. Muhammed and C. K. R. Kurup, *C. Biochem. J.*, **217**, 493 (1984).
- 5) P. J. Thornalley and N. J. F. Dodd, *Biochem. Pharmacol.*, **34**, 669 (1985).
- 6) C. E. Myers, W. P. McGuire, R. H. Liss, I. Ifrim, K. Grotzinger and R. C. Young, *Science*, **197**, 165 (1977).
- 7) F. Zunino, R. Gambetta and A. Di Marco, *Biochem. Pharmacol.*, **24**, 309 (1975).
- 8) J. Merski, Y. Daskal and H. Busch, *Cancer Treat. Rep.*, **62**, 771 (1978).
- 9) J. A. Siegfried, K. A. Kennedy, A. C. Sartorrelli and T. R. Tritton, *J. Biol. Chem.*, **258**, 339 (1983).
- 10) L. B. Wingard, T. R. Tritton and K. A. Egler, *Cancer Res.*, **45**, 3529 (1985).
- 11) A. B. Combs, D. Acosta and K. Ramos, *Biochem. Pharmacol.*, **34**, 1115 (1985).
- 12) M. Gosalvez, G. D. V. van Rossum and M. F. Blanco, *Cancer Res.*, **39**, 257 (1979).
- 13) K. Goshima, *J. Mol. Cell. Cardiol.*, **8**, 217 (1976).
- 14) B. B. Mishell, S. M. Shiigi, C. Henry, E. L. Chan, J. North, R. Galliliy, M. Slomich, K. Miller, J. Marbrook, D. Parks and A. H. Good, "Selected Methods in Cellular Immunology," W. H. Freeman and Company, San Francisco, 1980, pp. 15—16.
- 15) O. H. Lowry, N. J. Rosebrough, A. L. Farr and R. J. Randall, *J. Biol. Chem.*, **193**, 265 (1951).
- 16) A. C. Haneke, J. Crawford and A. Aszalos, *J. Pharm. Sci.*, **70**, 1112 (1981).
- 17) M. S. P. Manandhar and K. van Dyke, *Anal. Biochem.*, **58**, 368 (1974).
- 18) F. Wroblewski and J. S. LaDue, *Proc. Soc. Exp. Biol. Med.*, **90**, 210 (1955).
- 19) K. Goshima and Y. Tonomura, *Exp. Cell Res.*, **56**, 387 (1969).
- 20) R. A. Minow, R. S. Benjamin, E. T. Lee and J. A. Gottlieb, *Cancer*, **39**, 1397 (1977).
- 21) I. C. Henderson and E. Frei, III, *Am. Heart J.*, **99**, 671 (1980).
- 22) C. M. Czarnecki, *Comp. Biochem. Biophys.*, **79C**, 9 (1984).
- 23) A. Necco, T. Dasdia, S. Cozzi and M. Ferraduti, *Tumori*, **62**, 537 (1976).
- 24) D. Petrovic, S. M. Brown and M. B. Yatvin, *Int. J. Rad. Oncol. Biol. Phys.*, **2**, 505 (1977).
- 25) M. W. Seraydarian and L. Artaza, *Cancer Res.*, **39**, 2940 (1979).
- 26) T. J. Lampidis, I. C. Henderson, M. Israel and G. P. Canellos, *Cancer Res.*, **40**, 3901 (1980).
- 27) M. E. Ferrero, E. Ferrero, G. Gaja and A. Bernelli-Zazzera, *Biochem. Pharmacol.*, **25**, 125 (1975).
- 28) M. Gosalvez, M. Blanco, J. Hunter, M. Miko and B. Chance, *Eur. J. Cancer*, **10**, 567 (1974).
- 29) Y. Iwamoto, I. L. Hansen, T. H. Porter and K. Folkers, *Biochem. Biophys. Res. Commun.*, **58**, 633 (1974).
- 30) T. Kishi, T. Watanabe and K. Folkers, *Proc. Natl. Acad. Sci. U.S.A.*, **73**, 4653 (1976).
- 31) C. Bertazzoli, L. Sala and M. G. Tosana, *Int. Res. Commun. Sys. Med. Sci.*, **3**, 367 (1975).
- 32) H. Ohhara, H. Kanaide and M. Nakamura, *J. Mol. Cell. Cardiol.*, **13**, 741 (1981).
- 33) E. Goormaghtigh, G. Pollakis and J. M. Ruyschaert, *Biochem. Pharmacol.*, **32**, 889 (1983).

[Chem. Pharm. Bull.]  
[35(1) 335-343 (1987)]

## Effects of Recombinant Human Interferon-Gamma (Met-Gln Form) on Expression of Fc Receptor and Ia-like Antigen on Human Peripheral Monocytes and Lymphocytes: A Comparative Study with Natural Human Interferon-Alpha and -Beta

SHUU MATSUMOTO,\* MASAMI MORIYAMA and HIDEYO IMANISHI

*Basic Research Laboratories, Toray Industries Inc.,  
Tebiro 1111, Kamakura 248, Japan*

(Received July 5, 1986)

The effects of recombinant human interferon (IFN)-gamma (Met-Gln form), having the same amino acid sequence as that of natural human IFN-gamma except for the N-terminal Met residue, on the expression of Fc receptor (FcR) and Ia-like antigen in human monocytes and lymphocytes were comparatively investigated with those of natural human IFN-alpha and -beta. IFN-gamma (Met-Gln form) increased dose-dependently the number of FcRs binding to anti-chicken red blood cell (CRBC) immunoglobulin G on monocytes and the number of monocytes bearing the FcR, whereas the two natural IFNs did not. IFN-gamma (Met-Gln form) also enhanced the expression of Ia-like antigen on monocytes but the natural IFNs did not. On the other hand, IFN-gamma (Met-Gln form) had no effect on the expression of the FcR and Ia-like antigen on lymphocytes or on antibody-dependent cell-mediated cytotoxic activity against CRBCs, as was also the case with the natural IFNs. These results indicate that IFN-gamma (Met-Gln form) has a potent ability to induce or enhance the expression of FcR and Ia-like antigen on human monocytes though IFN-alpha and -beta do not, whereas IFN-gamma (Met-Gln form) has no effect on the expression on human lymphocytes, like the natural IFNs.

**Keywords**—interferon; monocyte; lymphocyte; Fc receptor; HLA antigen; ADCC activity

### Introduction

It is well known that various interferons (IFNs) possess many biological activities including antiviral, antiproliferative and immunomodulating activities in man and animals.<sup>1)</sup> Natural human IFN-gamma, which is called "immune interferon," has been expected to have many potent immunomodulating activities, but the limited supply of highly purified IFN has prevented extensive study of this interesting lymphokine. A large amount of highly purified human IFN-gamma has recently become available by gene cloning into a strain of *Escherichia coli*.<sup>2)</sup> Recombinant human IFN-gamma (Met-Gln form) used in our study is a natural type having the same amino acid sequence as that of natural human IFN-gamma elucidated by Rinderknecht *et al.*,<sup>3)</sup> except for the N-terminal methionine residue. In our previous studies,<sup>4)</sup> we found that IFN-gamma (Met-Gln form) augmented human natural killer, antibody-dependent cell-mediated cytotoxic (ADCC) and antibody-dependent monocyte-mediated cytotoxic (ADMC) activities like other IFNs, and that the augmentation of ADMC activity against anti-chicken red blood cell (CRBC) immunoglobulin G (IgG)-coated CRBC by IFN-gamma (Met-Gln form) was more potent than that by natural human IFN-alpha and -beta when compared on the basis of antiviral activity. Since it is well known that, in the ADCC reaction, the effector cells are Fc receptor (FcR)-bearing cells and an increase of effector cell/target cell ratio enhances ADCC activity, it is supposed that the greater increase in the number of monocytes bearing FcR induced by IFN-gamma (Met-Gln form) as compared

with natural human IFN- $\alpha$  and - $\beta$  might result in more effective augmentation of the ADMC activity. We, therefore, tried to confirm this hypothesis by measurement of the number of FcR-bearing monocytes after IFN treatment using flow cytometry and fluorescein isothiocyanate-labelled (FITC-) anti-CRBC IgG in this study. In addition to the analysis of FcR on human monocytes, we further studied the effects of these IFNs on the expression of FcRs on human lymphocytes and on the antibody-dependent lymphocyte-mediated cytotoxic (ADLC) activity against anti-CRBC IgG-coated CRBC.

Since there are many studies demonstrating the augmenting ability of IFN- $\gamma$  on the expression of Ia-like antigen on various cells, including monocytes and macrophages,<sup>5)</sup> we were very interested to examine whether IFN- $\gamma$  (Met-Gln form) enhances the expression of the antigen on monocytes and lymphocytes. Therefore, we compared the effects of IFN- $\gamma$  (Met-Gln form) on the expression with those of natural human IFN- $\alpha$  and - $\beta$ .

### Experimental

**Interferons**—Recombinant human IFN- $\gamma$  (specific activity:  $2.72 \times 10^7$  units/mg protein, % purity (sodium dodecyl sulfate-polyacrylamide gel electrophoresis): 99.9%, lymulus amoebocyte lysate: 0.03 ng/mg protein) was supplied by Genentech, Inc. (South San Francisco, U.S.A.). Natural human IFN- $\beta$  ( $1.0 \times 10^7$  unit/mg protein) was prepared in our laboratories by the superinduction method using human diploid foreskin fibroblasts as previously described.<sup>6)</sup> Natural human IFN- $\alpha$  ( $3.72 \times 10^6$  unit/mg protein) was kindly provided by Dr. K. Cantell (Central Public Health Laboratory, Helsinki, Finland). The titer of each IFN was calculated in terms of the antiviral activity determined by the 50% cytopathic effect reduction method using FL cells and vesicular stomatitis virus or Sindbis virus.

**Preparation of Human Monocytes and Lymphocytes**—Blood from healthy volunteers was collected by venipuncture using a heparinized syringe. The blood was diluted with an equal volume of Dulbecco's phosphate-buffered saline not containing  $Mg^{2+}$  or  $Ca^{2+}$  (Dulbecco PBS(-)). Mononuclear cells were separated from the diluted blood solution by centrifugation for 30 min at  $400 \times g$  on Lymphoprep (Nyegaard, Oslo, Norway). The interface cells, namely mononuclear cells, were harvested with a pipette, washed three times with Dulbecco PBS (-), and then suspended in RPMI 1640 medium (Nissui Seiyaku, Tokyo, Japan) containing heat-inactivated 10% fetal calf serum (FCS; Commonwealth Serum Laboratories, Melbourne, Australia). Lymphocytes were separated from the mononuclear cell suspensions by the binding of adherent cells, *i.e.*, monocytes, to macrophage separating plates (MSP-P; Japan Immunoresearch Laboratories, Takasaki, Japan), and then monocytes were removed from these plates by using MSP-E (exfoliating solution containing ethylenediaminetetraacetic acid). The lymphocytes and monocytes were washed three times with Dulbecco PBS (-) and suspended in RPMI 1640 medium containing 10% FCS. Monocyte purity in the monocyte suspension was >90% as determined by esterase and Giemsa staining and lymphocyte purity in the lymphocyte suspension was >98% as determined by flow cytometry.

**Treatment of Monocytes and Lymphocytes with IFN**—For flow cytometry,  $1-5 \times 10^6$  monocytes in 1 ml of RPMI 1640 medium containing 10% FCS were treated with 1 ml of IFN solution or control solution (RPMI 1640 medium containing 10% FCS) in Falcon 60  $\times$  15 mm plastic dishes (Becton Dickinson, Oxnard, U.S.A.). These dishes were incubated for 20 h at 37 °C in a humidified atmosphere of 95% air-5% CO<sub>2</sub>. At the end of this incubation period, monocytes were gently exfoliated with a rubber policeman, and then washed with and suspended in RPMI 1640 medium containing 10% FCS. On the other hand,  $1 \times 10^7$  lymphocytes in 1 ml of RPMI 1640 medium containing 10% FCS were added to 1 ml of IFN solution or control solution in Falcon 15 ml plastic tubes. These tubes were incubated under the same conditions as described above. After the incubation, lymphocytes were washed three times and suspended in RPMI 1640 medium containing 10% FCS. For ADLC assay,  $3 \times 10^5$  lymphocytes in 100  $\mu$ l of RPMI 1640 medium containing 10% FCS and 100  $\mu$ l of IFN solution or control solution were mixed in each well of Nunc plastic tissue culture plates (U-bottomed, 96 wells; Inter Med, Denmark) prior to incubation under the same conditions as described above. Thereafter, lymphocytes in each well were washed three times by the aspiration technique and 100  $\mu$ l of RPMI 1640 medium containing 10% FCS was added to each well.

**FcR and Ia-like Antigen Analysis by Flow Cytometry**—Half a million monocytes or lymphocytes, which were treated with IFN or control solution, were labelled by incubation with 100  $\mu$ l of a diluted solution (1/1000) of rabbit FITC-anti-CRBC IgG (Cappel Laboratories, Cochranville, U.S.A.) or FITC-OKIa1 (Ortho Diagnostic Systems, Raritan, U.S.A.) at 4 °C for 30 min and washed three times with Dulbecco PBS (-). These labelled monocytes or lymphocytes were analyzed with a Cytofluorograf system 50H (Ortho Diagnostic Systems, Raritan, U.S.A.). In addition to the histograms obtained from the distribution analyzer, regional analysis was performed as follows. One thousand and twenty-four channels of the fluorescence detectors on the Cytofluorograf were divided into six regions,

*i.e.* region I, channel 1—100; region II, 101—200; region III, 201—400; region IV, 401—600; region V, 601—800; region VI, 801—1024. Monocytes or lymphocytes in each region were counted. We checked that there was no peak in the higher fluorescence intensity side in the analysis of FITC-antibody-untreated monocytes or lymphocytes and FITC-mouse IgG1 (monoclonal antibody; Becton Dickinson, Oxnard, U.S.A.) or -mouse IgG2a+b (monoclonal antibody; Becton Dickinson, Oxnard, U.S.A.)-treated monocytes or lymphocytes. To determine the percentages of monocytes or lymphocytes bearing FcR or Ia-like antigen in the monocytes or lymphocytes preparation, we used a Spectrum III (Ortho Diagnostic Systems, Raritan, U.S.A.) because it is easier to fix the boundary line between FITC-positive and -negative cells in a flow cytometer than in the Cytofluorograf system 50H. Namely, after the histograms of the monocytes or lymphocytes existing in the predetermined monocyte or lymphocyte field in 0°/90° light scattergrams were obtained on the Spectrum III, the percentages were calculated from the number of FITC-positive cells in the histograms. The percentage of the monocytes or lymphocytes labelled by FITC-mouse IgG1 or -mouse IgG2a+b was <1.3%. The percentage of the monocytes or lymphocytes labelled by FITC-anti-Leu7, monoclonal antibody specific for large granular lymphocytes (Becton Dickinson, Oxnard, U.S.A.), was <6% or <25%, respectively. By fluorescence microscopy, we confirmed that F(ab')<sub>2</sub> of FITC-anti-CRBC IgG prepared according to Nisonoff *et al.*<sup>7)</sup> did not bind to monocytes.

**Measurement of ADLC Activity**—ADLC activity was measured by <sup>51</sup>Cr-release assay using CRBC as target cells. CRBCs were separated from heparinized fresh whole blood of White Leghorn chicken (female). After washing, 5 × 10<sup>7</sup> CRBCs were incubated in 600 μl of RPMI 1640 medium containing 300 μCi of Na<sub>2</sub><sup>51</sup>CrO<sub>4</sub> (New England Nuclear, Boston, U.S.A.) and 5% FCS for 3 h at 37 °C in a humidified atmosphere of 95% air-5% CO<sub>2</sub>. These <sup>51</sup>Cr-labelled CRBCs were subsequently washed three times and adjusted to the desired density with RPMI 1640 medium containing 10% FCS. ADLC assay was performed using Nunc plastic tissue culture plates (U-bottomed, 96 wells). Namely, 100 μl of lymphocyte suspension (3 × 10<sup>5</sup> cells), 50 μl of <sup>51</sup>Cr-labelled CRBC suspension (1 × 10<sup>4</sup> cells) and 50 μl of antibody solution of 1/2500 diluted rabbit anti-CRBC IgG (Fujizoki Pharmaceutical, Tokyo, Japan) were added to each well. These plates were incubated at 37 °C for 6 h in a humidified atmosphere of 95% air-5% CO<sub>2</sub> prior to separation of the supernatants by automated equipment (Titertek Supernatant Collection System; Flow Laboratories, Virginia, U.S.A.). Their radioactivities were measured with a well-type gamma counter (Aloka LDC-751; Aloka, Tokyo, Japan). The following formula was used to calculate percent specific lysis:

$$\% \text{ specific lysis} = \frac{\text{experimental cpm} - \text{SR cpm}}{\text{MR cpm} - \text{SR cpm}} \times 100$$

In this formula, MR cpm was determined as cpm in the supernatant obtained after the lysis of <sup>51</sup>Cr-labelled CRBCs with distilled water. SR cpm was determined as cpm released from <sup>51</sup>Cr-labelled CRBCs incubated with RPMI 1640 medium containing 10% FCS alone in the absence of lymphocytes.

## Results

### Analysis of FcR on Monocytes

Table I shows the effects of recombinant human IFN-gamma (Met-Gln form) and natural human IFN-alpha and -beta on the numbers of monocytes treated with FITC-anti-CRBC IgG in the six regions obtained by flow cytometry. As seen in Table I, IFN-gamma (Met-Gln form) greatly decreased the number of monocytes in region I but increased those in region II, III and IV. Further, another experiment revealed that this increasing effect was dose-dependent (Fig. 1). However, the two natural IFNs did not show any apparent effect on the numbers in the six regions (Table I).

The change of the percentage of monocytes bearing FcR binding to anti-CRBC IgG after treatment with each IFN or control solution is shown in Fig. 2A. Even on overnight incubation of fresh monocytes in control solution, the percentage was markedly decreased to 25% of the fresh control value. IFN-gamma (Met-Gln form) greatly increased the percentage when compared with the overnight control value (Fig. 2A) and this increase was dose-dependent (Fig. 3). On the other hand, the natural IFNs showed no effect at 1000 unit/ml (Fig. 2A).

### Analysis of FcR on Lymphocytes

The effects of the three IFNs on the number of lymphocytes treated with FITC-anti-CRBC IgG in the six regions obtained by flow cytometry are shown in Table II. These results indicate no significant change of the numbers in all regions when compared with the fresh

TABLE I. Effects of IFNs on the Population of Human Monocytes in Six Fluorescence Intensity Regions Determined Flow Cytometrically Using FITC-anti-CRBC IgG

Treatment	Cell numbers in region					
	I	II	III	IV	V	VI
Fresh control	7419 ± 71	2492 ± 64 <sup>c)</sup>	63 ± 8	18 ± 4	6 ± 2 <sup>a)</sup>	95 ± 5 <sup>c)</sup>
Overnight control	8239 ± 242	1289 ± 208	69 ± 8	29 ± 3	14 ± 1	360 ± 51
IFN-alpha	8117 ± 380	1500 ± 351	69 ± 2	15 ± 3	9 ± 2	290 ± 46
IFN-beta	7888 ± 301	1704 ± 276	87 ± 9	21 ± 4	12 ± 6	287 ± 72
IFN-gamma	4766 ± 520 <sup>c)</sup>	3138 ± 430 <sup>b)</sup>	1642 ± 369 <sup>b)</sup>	123 ± 31 <sup>a)</sup>	16 ± 2	351 ± 50

Each value represents the mean ± S.E. of three donors. The IFN concentration used in the treatment of monocytes was 1000 unit/ml. Significant difference from overnight control, a)  $p < 0.05$ ; b)  $p < 0.02$ ; c)  $p < 0.01$ .

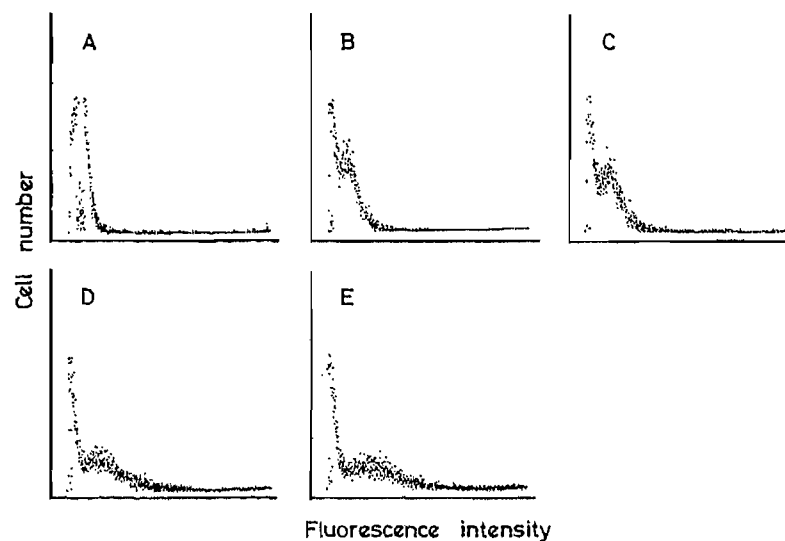


Fig. 1. Dose-Dependent Effect of IFN-Gamma on Expression of FcR Binding to Anti-CRBC IgG on Human Monocytes

A, fresh control; B, overnight control; C, 10 unit/ml; D, 100 unit/ml; E, 1000 unit/ml.

These data were obtained from one donor. Similar results were also obtained from two other donors (data not shown), but we did not calculate mean values because there were some individual differences between the patterns of the three histograms.

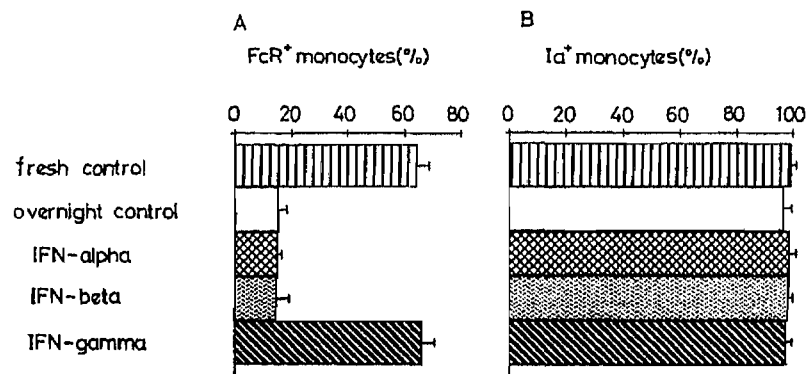


Fig. 2. Effects of IFNs on FcR and Ia-like Antigen Expression in Human Monocytes

A, percentage of monocytes bearing FcR binding to anti-CRBC IgG in monocyte preparation; B, percentage of Ia-positive monocytes in monocyte preparation.

Each value is the mean ± S.E. of three donors.

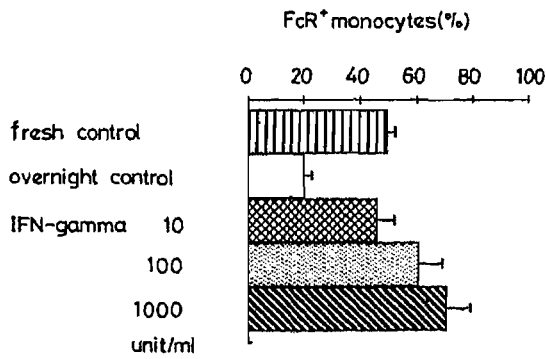


Fig. 3. Dose-Dependent Effect of IFN-Gamma on FcR Expression in Human Monocytes  
Each value is the mean  $\pm$  S.E. of three donors.

TABLE II. Effects of IFNs on the Population of Human Lymphocytes in Six Fluorescence Intensity Regions Determined Flow Cytometrically Using FITC-anti-CRBC IgG

Treatment	Cell numbers in region					
	I	II	III	IV	V	VI
Fresh control	9552 $\pm$ 153	393 $\pm$ 149	37 $\pm$ 17	8 $\pm$ 3	7 $\pm$ 6	12 $\pm$ 8
Overnight control	9712 $\pm$ 102	259 $\pm$ 95	25 $\pm$ 8	2 $\pm$ 1	1 $\pm$ 1	9 $\pm$ 3
IFN-alpha	9697 $\pm$ 113	290 $\pm$ 114	17 $\pm$ 6	1 $\pm$ 1	0 $\pm$ 0	6 $\pm$ 3
IFN-beta	9709 $\pm$ 93	274 $\pm$ 90	16 $\pm$ 6	2 $\pm$ 1	1 $\pm$ 1	7 $\pm$ 3
IFN-gamma	9675 $\pm$ 111	299 $\pm$ 113	23 $\pm$ 6	2 $\pm$ 2	0 $\pm$ 0	8 $\pm$ 7

Each value represents the mean  $\pm$  S.E. of three donors. The IFN concentration used in the treatment of lymphocytes was 1000 unit/ml.

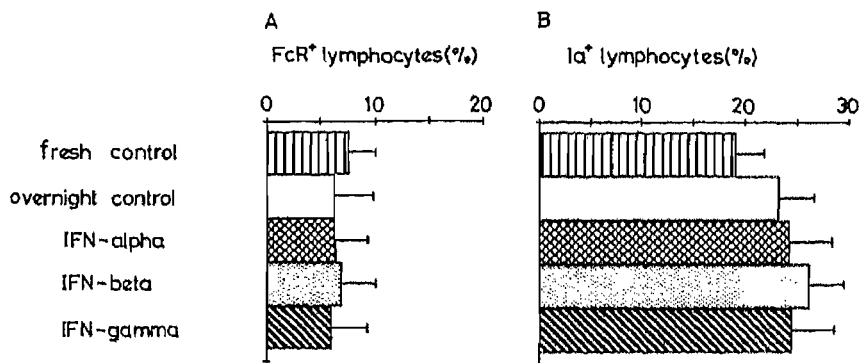


Fig. 4. Effects of IFNs on FcR and Ia-Like Antigen Expression in Human Lymphocytes

A, percentage of lymphocytes bearing FcR binding to anti-CRBC IgG in lymphocyte preparation; B, percentage of Ia-positive lymphocytes in lymphocyte preparation. Each value is the mean  $\pm$  S.E. of three donors.

control.

Figure 4A shows the effects of the three IFNs on the percentage of lymphocytes bearing FcR binding to anti-CRBC IgG in the lymphocyte preparation. The percentage was unchanged by the treatment with each IFN or control solution in comparison with that of fresh lymphocytes.

**Effects of IFNs on ADLC Activity**

Figure 5 shows the effects of the three IFNs on ADLC activity. The ADLC activity was not augmented even by treatment with 1000 unit/ml IFNs.

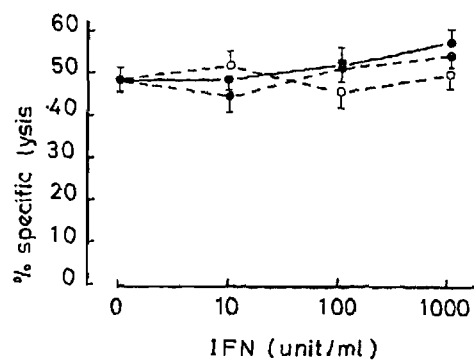


Fig. 5. Effects of IFNs on Human ADLC Activity

○---○, IFN-alpha; ●---●, IFN-beta; ●---●, IFN-gamma. Each value is the mean  $\pm$  S.E. of three donors.

TABLE III. Effects of IFNs on the Population of Human Monocytes in Six Fluorescence Intensity Regions Determined Flow Cytometrically Using FITC-OKIa1

Treatment	Cell numbers in region					
	I	II	III	IV	V	VI
Fresh control	769 $\pm$ 107 <sup>a)</sup>	332 $\pm$ 80	1797 $\pm$ 466	2643 $\pm$ 166 <sup>a)</sup>	1525 $\pm$ 151	2966 $\pm$ 450
Overnight control	2212 $\pm$ 321	652 $\pm$ 95	1142 $\pm$ 424	1238 $\pm$ 341	1032 $\pm$ 178	3724 $\pm$ 902
IFN-alpha	3025 $\pm$ 869	478 $\pm$ 28	652 $\pm$ 100	804 $\pm$ 193	809 $\pm$ 182	4233 $\pm$ 826
IFN-beta	2732 $\pm$ 431	484 $\pm$ 42	656 $\pm$ 130	739 $\pm$ 188	735 $\pm$ 167	4177 $\pm$ 1026
IFN-gamma	3001 $\pm$ 533	547 $\pm$ 65	288 $\pm$ 53 <sup>a)</sup>	184 $\pm$ 47 <sup>a)</sup>	205 $\pm$ 68 <sup>b)</sup>	5775 $\pm$ 676 <sup>a)</sup>

Each value represents the mean  $\pm$  S.E. of three donors. The IFN concentration used in the treatment of monocytes was 1000 unit/ml. Significant difference from overnight control, a)  $p < 0.05$ ; b)  $p < 0.01$ .

TABLE IV. Effects of IFNs on the Population of Human Lymphocytes in Six Fluorescence Intensity Regions Determined Flow Cytometrically Using FITC-OKIa1

Treatment	Cell numbers in region					
	I	II	III	IV	V	VI
Fresh control	7863 $\pm$ 323	539 $\pm$ 102	356 $\pm$ 114	241 $\pm$ 108	208 $\pm$ 35	815 $\pm$ 106
Overnight control	7584 $\pm$ 257	792 $\pm$ 148	442 $\pm$ 110	160 $\pm$ 30	99 $\pm$ 34	945 $\pm$ 109
IFN-alpha	7598 $\pm$ 233	798 $\pm$ 141	450 $\pm$ 92	142 $\pm$ 32	84 $\pm$ 27	952 $\pm$ 54
IFN-beta	7608 $\pm$ 206	789 $\pm$ 140	415 $\pm$ 88	141 $\pm$ 17	81 $\pm$ 30	991 $\pm$ 102
IFN-gamma	7767 $\pm$ 177	786 $\pm$ 181	398 $\pm$ 90	124 $\pm$ 6	73 $\pm$ 17	874 $\pm$ 181

Each value represents the mean  $\pm$  S.E. of three donors. The IFN concentration used in the treatment of lymphocytes was 1000 unit/ml.

#### Analysis of Ia-like Antigen on Monocytes

The change of the numbers of monocytes binding to FITC-OKIa1 in the six regions after treatment with each IFN or control solution is shown in Table III. IFN-gamma (Met-Gln form) greatly decreased the number in region III, IV and V and increased that in region VI, but the natural IFNs caused no significant change as compared with the overnight control value.

The effects of the three IFNs on the percentage of Ia-positive monocytes in the monocyte preparation are shown in Fig. 2B. Almost all of the monocytes were Ia-positive after overnight incubation in the control solution, and the three IFNs did not change the percentage.



### Analysis of Ia-like Antigen on Lymphocytes

Table IV shows the numbers of lymphocytes binding FITC-OKIa1 in the six regions after treatment with each IFN or control solution. The three IFNs did not change the numbers. The three IFNs also did not affect the percentage of Ia-positive lymphocytes in the lymphocyte preparation, as shown in Fig. 4B.

### Discussion

We analyzed the FcR binding to anti-CRBC IgG on human monocytes using flow cytometry, demonstrating a dose-dependent increase of the number of FcRs on monocytes and monocytes bearing the FcR after treatment with recombinant human IFN-gamma (Met-Gln form) (Figs. 1 and 3). The increasing effects on the number of monocytes bearing FcR induced by the IFN-gamma (Met-Gln form) were not observed with natural human IFN-alpha and -beta (Figs. 2 and 3). These results may directly explain why IFN-gamma (Met-Gln form) augmented ADMC activity against anti-CRBC IgG-coated CRBC more effectively than the natural IFNs when compared on the basis of antiviral activity, as shown in our previous report.<sup>4)</sup> Namely, IFN-gamma (Met-Gln form) seems to augment ADMC activity by increasing the number of monocytes bearing FcRs binding to anti-CRBC IgG more effectively than the natural IFNs. In relation to these results, Guyre *et al.* demonstrated that recombinant human IFN-gamma (Cys-Tyr-Cys-Gln form) having Cys-Tyr-Cys-Gln at the N-terminal increased the number of FcR on human monocytes and cell line HL-60 and U-937 more markedly than recombinant human IFN-alpha and -beta.<sup>8)</sup> In the same report, they stated that their IFN-gamma enhanced ADCC activity without presenting any experimental data.<sup>8)</sup> Their results and ours indicate that human monocyte activation induced by recombinant human IFN-gamma may not require the N-terminal residue, Cys-Tyr-Cys, as described elsewhere.<sup>4)</sup> Since the present study showed no significant effect of the natural IFNs on the number of FcR-bearing monocytes, the weak or moderate augmentation of ADMC activity by the natural IFNs as shown in our previous report<sup>4)</sup> cannot be explained by an increase in the number of FcR-bearing monocytes. Therefore, other mechanisms of ADMC-augmentation by IFNs, for example, the enhancement of lytic ability of monocytes after binding to target cells or recruitment of monocytes participating in the ADMC reaction, cannot be excluded.

Although the expression of FcR on cell membrane of monocytes was induced by IFN-gamma (Met-Gln form), such induction was not observed in lymphocytes (Fig. 2 and Table II). The finding is consistent with the lack of ADLC-augmentation by IFN-gamma (Met-Gln form) (Fig. 4). The natural IFNs also had no effect on the expression of FcR or ADLC activity in lymphocytes (Figs. 2 and 4 and Table II). These results conflict with many previous studies demonstrating the IFN-induced augmentation of ADLC activity.<sup>9)</sup> However, in contrast with those studies, several other studies have observed no augmentation of ADLC activity.<sup>10)</sup> It is considered that this discrepancy is possibly caused by a difference of target cells used, *i.e.* tumor cells were used in the studies demonstrating IFN-induced augmentation of ADLC activity, whereas erythrocytes were mostly used in the studies showing negative results. For example, Rumpold *et al.* reported that natural human IFN-alpha and -beta did not augment ADLC activity against autologous human RBC coated with antibody.<sup>10a)</sup> Platsoucas *et al.* also found no augmentation of the ADCC activity of human peripheral blood non-T lymphocytes by natural human IFN-alpha.<sup>10b)</sup> Platsoucas further demonstrated that recombinant human IFN-gamma (Cys-Tyr-Cys-Gln form) or -alpha did not augment ADLC activity against IgG-coated CRBC in two-thirds of the donors examined.<sup>10c)</sup> Taking into consideration their results and ours, it is postulated that IFNs cannot augment ADLC activity against anti-CRBC IgG-coated CRBC. The reason why IFNs can augment ADLC

activity against tumor cells but not that against CRBCs is still unclear, but the possibility that CRBCs may be resistant to the enhanced lytic ability of lymphocytes induced by IFNs or that IFNs may not augment the recruitment of lymphocytes binding to anti-CRBC IgG-coated CRBCs cannot be excluded.

It is well known that MHC class II antigens are involved in the presentation of antigens to helper T cells by antigen-presenting cells including macrophages and monocytes.<sup>11)</sup> The present study demonstrated that IFN-gamma (Met-Gln form) enhanced the expression of Ia-like antigen on monocytes, but the two natural IFNs did not. Several investigators reported similar results for recombinant human IFN-gamma (Cys-Tyr-Cys-Gln form).<sup>12)</sup> Further, Zlotnik *et al.* reported that recombinant human IFN-gamma (Cys-Tyr-Cys-Gln form) induced the antigen-presenting ability of human macrophage line P388D1 to T cell hybridoma, whereas natural human IFN-alpha and -beta did not.<sup>13)</sup> Therefore, it is expected that IFN-gamma (Met-Gln form) may enhance the antigen-presenting ability of human monocytes whereas natural IFNs may not.

The lack of enhancing effect of recombinant human IFN-gamma on the expression of Ia-like antigens in human lymphocytes demonstrated in this study (Fig. 5 and Table IV) is consistent with the data reported by Rosa *et al.*<sup>14)</sup> However, Lisowska-Grospierre *et al.* observed enhancement of the expression of HLA-DR antigens on normal human peripheral lymphocytes by recombinant glycosylated human IFN-gamma derived from transformed Chinese hamster ovary cells.<sup>15)</sup> Although it is still unclear whether the discrepancy was caused by glycosylation of IFN-gamma or not, it seems that human IFN-gamma may enhance the expression of MHC class II antigens on lymphocytes less effectively than that on macrophages and monocytes in humans.

We are very interested in the pharmacological significance and clinical potential of IFN-gamma (Met-Gln form) in humans. Although Momburg *et al.* have recently demonstrated that recombinant murine IFN-gamma induced or enhanced the expression of Ia antigens in various mouse tissues after *in vivo* treatment,<sup>16)</sup> the pharmacological significance of this is still unclear. In relation to the clinical potential of IFN-gamma (Met-Gln form), Nathan *et al.* have recently reported that the administration of IFN-gamma (Met-Gln form) to cancer patients enhanced the monocyte secretion of hydrogen peroxide.<sup>17)</sup> However, they did not monitor the expression of FcR and Ia-like antigen on the monocytes. To elucidate the pharmacological significance and clinical potential of IFN-gamma (Met-Gln form), further investigations using recombinant murine IFN-gamma and animal models and further clinical trials monitoring FcR and Ia-like (or HLA-DR) antigen expression in monocytes will be required.

**Acknowledgment** The authors thank Miss M. Kondoh and Mrs. K. Yamanaka for their skillful technical assistance. We are grateful to Dr. A. Kitai and Mr. N. Naruse for their encouragement and support of this study.

#### References

- 1) M. Ho, *Pharmacol. Rev.*, **34**, 119 (1982).
- 2) P. W. Gray, D. W. Leung, D. Pennica, E. Yelverton, R. Najarian, C. C. Simonsen, R. Derynck, P. J. Sherwood, D. M. Wallace, S. L. Berger, A. D. Levinson and D. V. Goeddel, *Nature* (London), **295**, 503 (1982).
- 3) E. Rinderknecht, B. H. O'Connor and H. Rodriguez, *J. Biol. Chem.*, **259**, 6790 (1984).
- 4) S. Matsumoto and H. Imanishi, *Chem. Pharm. Bull.*, **34**, 4767 (1986).
- 5) F. Rosa and M. Fellous, *Immunology Today*, **5**, 261 (1984).
- 6) S. Kobayashi, M. Iizuka, M. Hara, H. Ozawa, T. Nagashima and J. Suzuki, "The Clinical Potential of Interferons," ed. by R. Kono and J. Vilček, University of Tokyo Press, Tokyo, 1982, pp. 57-68.
- 7) A. Nisonoff, F. C. Wissler, L. N. Lipman, D. L. Woerley, *Arch. Biochem. Biophys.*, **89**, 230 (1960).
- 8) P. M. Guyre, P. M. Morganelli and R. Miller, *J. Clin. Invest.*, **72**, 393 (1983).
- 9) M. Moore, "Interferons: From Molecular Biology to Clinical Application," eds. by D. C. Burke and A. G.

- Morris, Cambridge University Press, Cambridge, 1983, pp. 181—209.
- 10) a) H. Rumpold, D. Kraft, O. Scheiner, P. Meindl and G. Bodo, *Int. Archs. Allergy Appl. Immun.*, **62**, 152 (1980);  
b) C. D. Platsoucas, G. Fernandes, S. L. Gupta, S. Kempin, B. Clarkson, R. A. Good and S. Gupta, *J. Immunol.*, **125**, 1216 (1980); c) C. D. Platsoucas, "The Biology of the Interferon System 1983," eds. by E. DeMaeyer and H. Schellekens, Elsevier Science Publishers B. V. Amsterdam, 1983, pp. 305—310.
  - 11) E. Thorsby, *Human Immunology*, **9**, 1 (1984).
  - 12) a) T. Y. Basham and T. C. Merigan, *J. Immunol.*, **130**, 1492 (1983); b) T. Basham, W. Smith, L. Lanier, V. Morhenn and T. Merigan, *Human Immunology*, **10**, 83 (1984); c) H. P. Koeffler, J. Ranyard, L. Yelton, R. Billing and R. Bohman, *Proc. Natl. Acad. Sci. U.S.A.*, **81**, 4080 (1984).
  - 13) A. Zlotnik, R. P. Shimonkevitz, M. L. Gefter, J. Kappler and P. Murrack, *J. Immunol.*, **131**, 2814 (1983).
  - 14) F. Rosa, D. Hatat, A. Abadie and M. Fellous, *Ann. Inst. Pasteur/Immunol.*, **136C**, 103 (1985).
  - 15) B. Lisowska-Grospierre, D. J. Charron, C. de Prèval, A. Durandy, C. Griscelli and B. Mach, *J. Clin. Invest.*, **76**, 381 (1985).
  - 16) F. Momburg, N. Koch, P. Möller, G. Moldenhauer, G. W. Butcher and G. J. Hämmerling, *J. Immunol.*, **136**, 940 (1986).
  - 17) C. F. Nathan, C. R. Horowitz, J. De La Harpe, S. Vadhan-Raj, S. A. Sherwin, H. F. Oettgen and S. E. Krown, *Proc. Natl. Acad. Sci. U.S.A.*, **82**, 8686 (1985).

[Chem. Pharm. Bull.]  
[35(1) 344-349 (1987)]

## Oxidation Products of Linoleate and Linolenate Exposed to Nitrogen Dioxide

KIYOMI KIKUGAWA\*<sup>a</sup> and KUNITAROU KOGI<sup>b</sup>

*Tokyo College of Pharmacy,<sup>a</sup> 1432-1 Horinouchi, Hachioji, Tokyo 192-03, Japan  
and Kanagawa Prefectural Public Health Laboratories,<sup>b</sup> 52-2  
Nakao-cho, Asahi-ku, Yokohama 241, Japan*

(Received July 21, 1986)

Nitrogen dioxide at 100 ppm in air greatly accelerated the oxidation of methyl esters of linoleic and linolenic acid in both non-aqueous and aqueous systems. Nitrogen dioxide stimulated oxygen uptake, conjugated diene formation and increase in the peroxide value of methyl linoleate and methyl linolenate. The products formed from methyl linoleate were identified as four isomeric hydroperoxides; the ratio of the amounts of the isomers was similar to that of the hydroperoxides formed by autoxidation. No nitrogen-containing products were formed. The products formed from methyl linolenate were identified as eight isomeric hydroperoxides that were also formed by autoxidation.

**Keywords**—nitrogen dioxide; methyl linoleate; methyl linolenate; conjugated diene; peroxide value; hydroperoxide; chain initiation

Nitrogen dioxide is a toxic pollutant of urban air. It is a free radical and is reactive enough to initiate free radical chain reactions.<sup>1,2)</sup> Evidence for lipid oxidation resulting from nitrogen dioxide inhalation is mostly indirect. Inhalation of nitrogen dioxide by rats induced lipid oxidation of lung lipids as measured in terms of conjugated diene formation,<sup>3)</sup> or production of ethane and pentane.<sup>4)</sup> Exposure of unsaturated fatty acid esters to nitrogen dioxide resulted in lipid oxidation as measured in terms of the formation of conjugated diene and thiobarbituric acid reactive-substances.<sup>4,5)</sup>

It has been tentatively shown that nitrogen dioxide adds to the double bond of unsaturated fatty acids to produce a nitroalkyl radical, or it abstracts a hydrogen radical from unsaturated fatty acids to produce nitrous acid and an allylic radical species.<sup>6-9)</sup> Formation of a nitro-peroxyl radical in the reaction of oleic acid with nitrogen dioxide in the presence of oxygen was demonstrated by Kobayashi.<sup>10)</sup> It is not known, however, what products were formed on exposure of unsaturated fatty acids to nitrogen dioxide at low concentrations such as that present in the atmosphere. This study was conducted in order to identify the products formed from unsaturated fatty acids exposed to nitrogen dioxide at a low concentration.

### Experimental

**Materials**—Standard nitrogen dioxide in air (93 or 103 ppm) (NO<sub>2</sub>/Air), standard nitrogen dioxide in nitrogen (99 ppm) (NO<sub>2</sub>/N<sub>2</sub>), and dried air (Air) were obtained from Nippon Sanso Ltd., Tokyo, Japan. Methyl oleate, methyl linoleate and methyl linolenate were of reagent grade from Sigma Chemical Company, St. Louis, MO., U.S.A.

Coating of silica gel with unsaturated fatty acid methyl esters was performed according to the method of Wu *et al.*<sup>11)</sup> Thus, about 40 g of silica gel (Wakogel C-200, Wako Pure Chemical Industries, Ltd., Osaka, Japan), dried at 120 °C, was suspended in a solution of 9.0 g of a methyl ester in 800 ml of *n*-hexane, and the mixture was stirred for 1 h and allowed to stand for 10 min. The silica gel was collected by filtration with a Teflon membrane filter and dried *in vacuo*. The amount of the ester coated on silica gel was estimated to be 0.130 g/g for methyl linoleate, 0.138 g/g for methyl oleate and 0.151 g/g for methyl linolenate.

**Analysis**—Absorption spectra were measured with a Hitachi 323 recording spectrophotometer. Thin-layer chromatography (TLC) was done with Silica gel 60 F<sub>254</sub> (Merck 5715) plates developed with *n*-hexane-ethyl acetate (17:5). Spots were visualized by irradiation at 254 nm, by exposure to iodine vapor and by spraying saturated potassium iodide in 50% acetic acid. High-performance liquid chromatography (HPLC) was carried out by the use of a Shimadzu LC-4A liquid chromatograph equipped with a stainless steel column. The peaks due to conjugated diene were detected at 235 nm by means of a Shimadzu SPD-2AS spectrophotometric detector. The hydroperoxides from methyl linoleate were separated on a column of Unisil-ODS (6.0 i.d. × 150 mm) by elution with ethanol-water (6:4) at 30 °C and 1.0 ml/min, and the hydroxides were separated on a column of Partisil-5 (4.0 i.d. × 500 mm) by elution with ethanol-*n*-hexane (0.25:99.75) at 30 °C and 1.0 ml/min, according to the method of Chan and Levett.<sup>12)</sup> The hydroxides from methyl linolenate was separated on a column of Partisil-5 (8.0 i.d. × 250 mm) by elution with ethanol-*n*-hexane (0.3:99.7) according to the method of Peers *et al.*<sup>13)</sup> Reduction of the hydroperoxides to the hydroxides was performed as described elsewhere.<sup>14)</sup>

Peroxide value (POV) was determined according to the method of Wheeler.<sup>15)</sup> The sample was freed from nitrogen dioxide by extraction with Saltzman reagent<sup>16)</sup> before POV analysis. Thus, 100 mg of the sample was dissolved in chloroform and the solution was washed with 25 ml of a mixture of 5 g of sulfanilic acid, 0.05 g of *N*-(1-naphthyl)-ethylenediamine 2-acetate and 50 ml of glacial acetic acid in 1 l of water. This washing was repeated until the washing solution became colorless. The chloroform layer was subjected to POV determination.

Nitrogen of nitrite and nitrate ions in aqueous solutions was determined by use of the Bratton-Marshall reagent<sup>17)</sup> and sodium salicylate,<sup>18)</sup> respectively.

**Exposure of Unsaturated Fatty Acid Methyl Esters to Nitrogen Dioxide**—Exposure of Methyl Linoleate to Nitrogen Dioxide: A slim tube was attached to a gas-introducing tube linked to a gas outlet. The temperature of the tube, containing 1.0 g of methyl linoleate, was thermostatically controlled. NO<sub>2</sub>/Air, NO<sub>2</sub>/N<sub>2</sub> or Air was passed over the methyl linoleate at a constant flow rate by the use of an accurate flow meter for up to 48 h.

Exposure of Unsaturated Fatty Acid Methyl Esters on Silica Gel to Nitrogen Dioxide in Aqueous System: A suspension of 2.5 g of the silica gel coated with the fatty acid methyl ester and 20 ml of 0.1 M phosphate buffer (pH 7.4) was placed in a 50-ml flask, and NO<sub>2</sub>/Air or Air was introduced into the suspension at a constant rate of 20 ml/min at 37 °C with stirring. The mixture was extracted with 20 ml of chloroform and centrifuged at 3000 rpm for 10 min. This extraction was repeated twice more. The chloroform extracts were combined, washed with 20 ml of water, and filtered through a Teflon membrane filter. The solvent was removed *in vacuo* and the residue was dried for subsequent analysis.

## Results

Nitrogen dioxide at about 100 ppm in air (NO<sub>2</sub>/Air) or in nitrogen (NO<sub>2</sub>/N<sub>2</sub>) was passed over methyl linoleate at 37 °C. The weight of methyl linoleate gradually increased (16% increase after 48 h) during NO<sub>2</sub>/Air exposure, whereas no weight increase was observed during NO<sub>2</sub>/N<sub>2</sub> exposure (Fig. 1A). Most of the increase may be due to oxygen, since the total amount of nitrogen dioxide introduced was only 1.1% of methyl linoleate. Methyl linoleate exposed to NO<sub>2</sub>/Air showed an absorption spectrum with a maximum at 235 nm, characteristic of conjugated diene and similar to that of the standard methyl linoleate hydroperoxides.<sup>12)</sup>

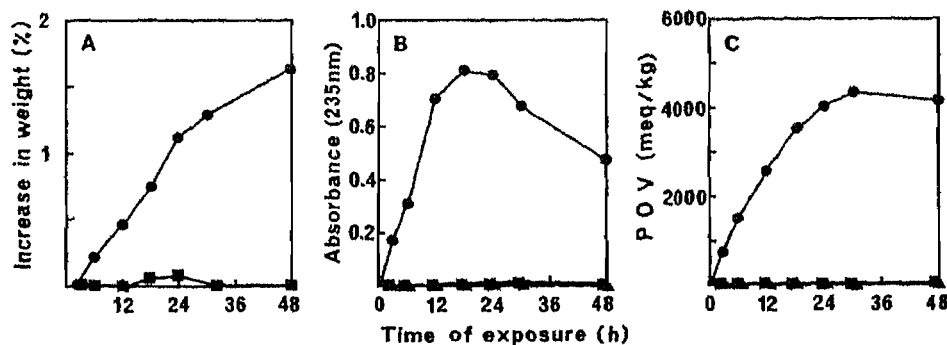


Fig. 1. Time Course of the Increase in Weight (A), Absorbance (B) and POV (C) of Methyl Linoleate Exposed to Nitrogen Dioxide at 37 °C

Methyl linoleate (1.00 g) was exposed to NO<sub>2</sub>/Air (●), NO<sub>2</sub>/N<sub>2</sub> (■) or Air (▲) at 20 ml/min. During the period of 48 h, the total amount of nitrogen dioxide passed was about 11 mg. The absorbance is presented on the basis of the concentration of 30 μg/ml ethanol.

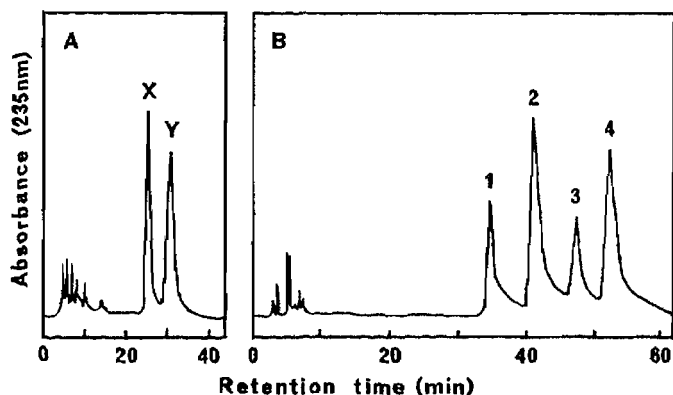


Fig. 2. HPLC of Methyl Linoleate Exposed to Nitrogen Dioxide and Its Reduction Products

A: HPLC of methyl linoleate exposed to  $\text{NO}_2/\text{Air}$  at  $37^\circ\text{C}$  for 48 h (POV: 4100 meq/kg) on a column of Unisil-ODS. The methyl linoleate exposed to Air at  $98^\circ\text{C}$  and 80 ml/min for 3 h (POV: 2500 meq/kg) revealed peaks with the same retention times. X=a mixture of *cis, trans*-9- and 13-hydroperoxides and Y=a mixture of *trans, trans*-9- and 13-hydroperoxides.<sup>12)</sup> B: HPLC of the reduction products of methyl linoleate exposed to  $\text{NO}_2/\text{Air}$  at  $60^\circ\text{C}$  for 3 h on a column of Partisil-5. The ester was reduced with sodium borohydride.<sup>14)</sup> The reduction products of methyl linoleate exposed to Air at  $60^\circ\text{C}$  for 10 h revealed four peaks with the same retention times. 1 = *cis, trans*-13-; 2 = *trans, trans*-13-; 3 = *cis, trans*-9-; and 4 = *trans, trans*-9-hydroxy compounds.<sup>12)</sup>

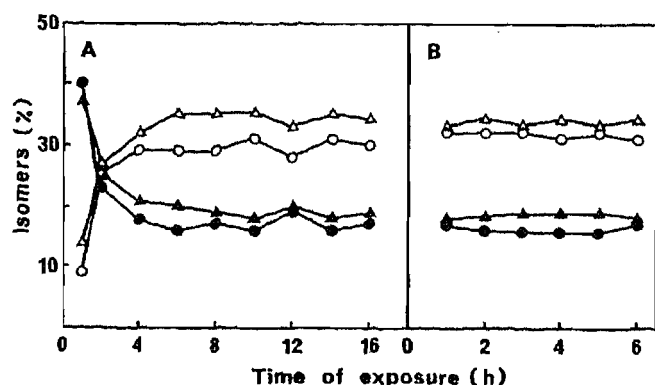


Fig. 3. Time Course of the Composition Ratio of the Isomeric Products Formed from Methyl Linoleate Exposed to Air (A) and Nitrogen Dioxide (B)

The reduction products of the methyl linoleate exposed to Air at  $60^\circ\text{C}$  (A) and those of the methyl linoleate exposed to  $\text{NO}_2/\text{Air}$  at  $60^\circ\text{C}$  (B) were analyzed by HPLC on a column of Partisil-5 as described in the legend to Fig. 2. The percentages of the isomers were obtained from the height of each peak. ●, *cis, trans*-13-; ○, *trans, trans*-13-; ▲, *cis, trans*-9-; △, *trans, trans*-9-hydroxy compounds.

The time course of the absorbance at 235 nm in  $\text{NO}_2/\text{Air}$  exposure showed that it reached a maximum level after 18 h and then gradually decreased (Fig. 1B). At the maximum level, the absorbance was 30% of that of methyl linoleate hydroperoxides ( $\epsilon$ : 25900—28600).<sup>12)</sup> No increase in the absorbance was observed during exposure to  $\text{NO}_2/\text{N}_2$  or air alone (Air). The time course of POV of the  $\text{NO}_2/\text{Air}$  exposure showed that it reached a maximum level of 4340 meq/kg (70% POV of methyl linoleate hydroperoxides) after 30 h (Fig. 1C). No POV increases were observed during the exposures to  $\text{NO}_2/\text{N}_2$  and Air. The increases of the absorbance and POV of methyl linoleate exposed to  $\text{NO}_2/\text{Air}$  at  $60^\circ\text{C}$  were much faster than those of methyl linoleate exposed to Air at  $60^\circ\text{C}$ ; the periods required to reach an absorbance of 0.3 or POV of 1000 meq/kg were 1.5 h in the  $\text{NO}_2/\text{Air}$ -exposure and 9 h in the Air exposure. These results indicated that the exposure of methyl linoleate to  $\text{NO}_2/\text{Air}$  resulted in accelerated oxygen uptake and oxidation of the ester.

TLC of methyl linoleate exposed to  $\text{NO}_2/\text{Air}$  revealed a major spot ( $R_f$  0.31), which absorbed ultraviolet light and liberated iodine from iodide. Elemental analysis of methyl linoleate exposed to  $\text{NO}_2/\text{Air}$  (POV: 4400 meq/kg) revealed 0.21% nitrogen and a 13% increase in oxygen content. HPLC of the methyl linoleate revealed two ultraviolet-absorbing peaks X and Y (Fig. 2A). Peak X corresponded to a mixture of *cis, trans*-9- and 13-hydroperoxides and peak Y to a mixture of *trans, trans*-9- and 13-hydroperoxides, which are produced in autoxidation.<sup>12)</sup> HPLC of the sample that had been reduced with sodium borohydride revealed four peaks 1—4 (Fig. 2B). The peaks have been identified as four hydroxy isomers; the *cis, trans*-13- (1), *trans, trans*-13- (2), *cis, trans*-9- (3) and *trans, trans*-9- (4) hydroxy compounds.<sup>12)</sup> No nitrogen-containing products were detected. Quantitative estimation of the four hydroxy isomers obtained from methyl linoleate exposed to Air at  $60^\circ\text{C}$  for more than 4 h showed constant ratios of 1:2:3:4 = 17:30:19:34 and *cis, trans*:*trans, trans* = 36:64 (Fig. 3A). Methyl linoleate exposed to  $\text{NO}_2/\text{Air}$  at  $60^\circ\text{C}$  showed similar

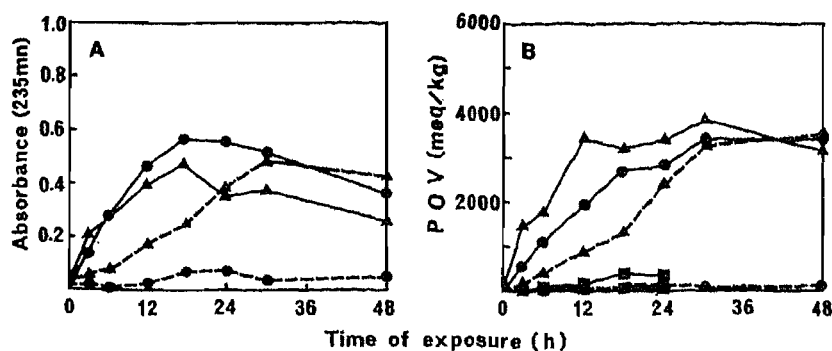


Fig. 4. Time Course of Absorbance (A) and POV (B) of Unsaturated Fatty Acid Methyl Esters on Silica Gel Exposed to Nitrogen Dioxide at 37°C in Phosphate Buffer

Methyl linoleate (●), methyl linolenate (▲) and methyl oleate (■) coated on silica gel (2.5 g) were exposed to  $\text{NO}_2/\text{Air}$  (---) or Air (—) in 20 ml of 0.1 M phosphate buffer (pH 7.4) at 20 ml/min. The esters were recovered by chloroform extraction. The absorbance is presented on the basis of the concentration of 30  $\mu\text{g}/\text{ml}$ .

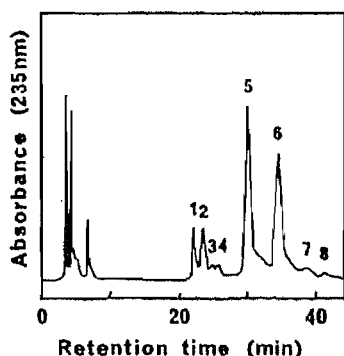


Fig. 5. HPLC of the Reduction Products of Methyl Linolenate on Silica Gel Exposed to Nitrogen Dioxide in Phosphate Buffer

Methyl linolenate on the silica gel was exposed to  $\text{NO}_2/\text{Air}$  for 3 h (POV: 1500 meq/kg) [see the legend to Fig. 4]. The ester was reduced and analyzed by HPLC on a column of Pertisil-5. The methyl linolenate on silica gel exposed to Air for 18 h (POV: 1300 meq/kg) showed the same eight peaks. The peaks were assigned as 1 = *cis, trans, cis*-13-; 2 = *cis, trans, cis*-12-; 3 = *cis, trans, trans*-12-; 4 = *trans, trans, cis*-13-; 5 = *cis, cis, trans*-16-; 6 = *trans, cis, cis*-9-; 7 = *cis, trans, trans*-16-; and 8 = *trans, trans, cis*-9-hydroxy compounds<sup>13)</sup> from their retention times.

ratios of the isomers during the periods tested; 1 : 2 : 3 : 4 = 16 : 32 : 19 : 33 and *cis, trans* : *trans, trans* = 35 : 65 (Fig. 3B). Thus, the exposure of methyl linoleate to  $\text{NO}_2/\text{Air}$  resulted in the production of the same isomers of the hydroperoxides as those produced in autoxidation in a similar ratio.

Suspensions of methyl linoleate, methyl linolenate and methyl oleate coated on silica gel surfaces were exposed to  $\text{NO}_2/\text{Air}$  in phosphate buffer (pH 7.4) at 37°C. The conjugated diene formation and the increase in POV of methyl linoleate and methyl linolenate exposed to  $\text{NO}_2/\text{Air}$  were much more marked than those of the compounds exposed to Air (Fig. 4). The increase in POV of methyl oleate was not significant on exposure to  $\text{NO}_2/\text{Air}$  or Air. Since nitrogen dioxide can be converted into nitrite and nitrate ions in an aqueous system,<sup>14)</sup> the conversion of the gas under the conditions used was estimated. Total nitrogen introduced into the buffer was calculated to be 790  $\mu\text{g}$  (12 h) and 3170  $\mu\text{g}$  (48 h), when  $\text{NO}_2/\text{Air}$  was introduced at 20 ml/min at 37°C. Nitrogen of nitrite and nitrate ions produced was found to amount to 67  $\mu\text{g}$  (12 h) and 263  $\mu\text{g}$  (48 h), and 150  $\mu\text{g}$  (12 h) and 664  $\mu\text{g}$  (48 h), respectively. Thus, 25–30% of nitrogen dioxide was converted into nitrite and nitrate ions. When methyl linolenate was exposed to Air in buffer containing 1000  $\mu\text{g}$  nitrogen of nitrite or nitrate at 37°C and 20 ml/min for 24 h, no significant increase in POV was observed. Thus, the ions did not accelerate the oxidation of methyl linoleate under the conditions used. Increase in the absorbance and POV of methyl linoleate and methyl linolenate may be due to the unconverted nitrogen dioxide.

TLC and HPLC of methyl linoleate exposed to  $\text{NO}_2/\text{Air}$  in the buffer revealed a major

spot of *Rf* 0.31 and two peaks *X* and *Y*, respectively. The methyl linolenate exposed to  $\text{NO}_2/\text{Air}$  in the buffer showed two major spots with *Rf* values of 0.29 and 0.20, each absorbing ultraviolet light and liberating iodine from iodide. Autoxidized methyl linolenate revealed the same two spots. The reduction products from methyl linolenate exposed to  $\text{NO}_2/\text{Air}$  revealed eight components, which can be assigned as eight hydroxy isomers produced in autoxidation (Fig. 5).<sup>13)</sup> Thus, exposure of linoleic and linolenic acid methyl esters to  $\text{NO}_2/\text{Air}$  in the buffer resulted in the production of the same hydroperoxides as those formed in autoxidation of the esters.

### Discussion

Nitrogen dioxide reacts with alkenes by addition to the double bond to form a nitro-alkyl radical at ambient temperatures and high concentrations (1–40%), and in the presence of air this reaction produces a nitro-peroxyl radical.<sup>6–9,20,21)</sup> The nitroperoxyl radical can then abstract a hydrogen radical from another olefin molecule to produce a stable nitro- $\beta$ -hydroperoxide and an alkyl radical. Pryor *et al.*<sup>6–9)</sup> suggested the formation of the nitroperoxyl radical in the reaction of polyunsaturated fatty acids with nitrogen dioxide at high concentrations in air. Kobayashi<sup>10)</sup> demonstrated that the nitro-peroxyl radical was produced in reaction of oleic acid with nitrogen dioxide at 5000 ppm.

Pryor *et al.*<sup>7–9)</sup> suggested that at concentrations below 100 ppm, nitrogen dioxide reacts with alkenes almost exclusively by abstraction of an allylic hydrogen, leading to the formation of an allylic radical and nitrous acid. While none of the products has been identified, it has been assumed that the allylic radical can combine with nitrogen dioxide to give an unsaturated nitro or nitrite compound or with oxygen to give an allylic hydroperoxide or nitrate esters.<sup>8)</sup>

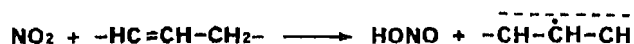


Chart 1

Our data demonstrated that nitrogen dioxide at 100 ppm in air greatly accelerated the oxidation of unsaturated fatty acid methyl esters, and the products were the same as those produced in autoxidation of the esters. Nitrogen dioxide stimulated oxygen uptake, conjugated diene formation, and increase in POV of methyl linoleate, methyl linoleate in an aqueous system and methyl linolenate in an aqueous system. The products formed from methyl linoleate were identified as four isomeric hydroperoxides. The ratio of the four isomers was similar to that of the hydroperoxides produced in autoxidation. The products formed from methyl linolenate in an aqueous system were identified as the eight isomeric hydroperoxides. In these reactions, no nitrogen-containing products were formed. Although nitrogen dioxide was partially converted into nitrite and nitrate ions in an aqueous system, these ions were unable to accelerate oxidation of the esters.

The reaction of nitrogen dioxide at a low concentration may initially produce an allylic radical by abstraction of a hydrogen radical from the unsaturated fatty acid esters, which may in turn combine with oxygen in air to produce a peroxyl radical. The peroxyl radical abstracts a hydrogen radical from another molecule of the ester to produce a stable hydroperoxide, as in the autoxidation of the ester. Thus, nitrogen dioxide at the low concentration may initially abstract a hydrogen radical from the unsaturated fatty acids to produce an allylic radical, which initiates free radical chain reactions in the presence of oxygen. Nitrogen dioxide at this concentration must be involved in the chain initiation reactions but not in the chain propagation reactions.



## References

- 1) W. A. Pryor, "Free Radicals in Biology," Vol. I, ed. by W. A. Pryor, Academic Press, Inc., New York, 1976, p. 1.
- 2) D. B. Menzel, "Free Radicals in Biology," Vol. II, ed. by W. A. Pryor, Academic Press, Inc., New York, 1976, p. 181.
- 3) H. V. Thomas, P. K. Mueller and R. L. Lyman, *Science*, **159**, 532 (1968).
- 4) M. Sagai, T. Ichinose, H. Oda and K. Kubota, *Lipids*, **16**, 64 (1981).
- 5) J. N. Roehm, J. G. Hadley and D. B. Menzel, *Arch. Environ. Health*, **23**, 142 (1971).
- 6) R. S. Collard and W. A. Pryor, *Lipids*, **14**, 748 (1979).
- 7) W. A. Pryor and J. W. Lightsey, *Science*, **214**, 435 (1981).
- 8) W. A. Pryor, J. W. Lightsey and D. F. Church, *J. Am. Chem. Soc.*, **104**, 6685 (1982).
- 9) W. A. Pryor, *Ann. N. Y. Acad. Sci.*, **393**, 1 (1982).
- 10) T. Kobayashi, *Chemosphere*, **12**, 1317 (1983).
- 11) G. S. Wu, R. A. Stein and J. F. Mead, *Lipids*, **12**, 971 (1977).
- 12) H. W.-S. Chan and G. Levett, *Lipids*, **12**, 99 (1977).
- 13) K. E. Peers, D. T. Coxon and H. W.-S. Chan, *J. Sci. Food Agric.*, **32**, 898 (1981).
- 14) M. Hamberg and B. Samuelsson, *J. Biol. Chem.*, **242**, 5329 (1967).
- 15) D. H. Wheeler, *Oil and Soap*, **9**, 89 (1932).
- 16) B. E. Saltzman, *Anal. Chem.*, **32**, 135 (1960).
- 17) R. J. Elliott and A. G. Ponter, *Analyst*, **96**, 522 (1971).
- 18) G. Loof, *Pharm. Zentralhalle*, **31**, 700 (1890).
- 19) H. Komiyama and H. Inoue, *Chem. Eng. Sci.*, **35**, 154 (1980).
- 20) H. Baldock, N. Levy and C. W. Scaife, *J. Chem. Soc.*, **1949**, 2627.
- 21) J. C. D. Brand and I. D. R. Stevens, *J. Chem. Soc.*, **1958**, 629.

[Chem. Pharm. Bull.]  
[35(1) 350—356 (1987)]

## Studies on Syntheses and Reactions of Methoxypyridazines. II. Methoxylation of 3,4,6-Trichloropyridazine<sup>1,2)</sup>

HIROMU NAGASHIMA,\* KIYOSHI UKAI, HIROHISA ODA,  
YUKIO MASAKI, and KENJI KAJI

Gifu Pharmaceutical University, 5-6-1, Mitahora-higashi,  
Gifu 502, Japan

(Received June 9, 1986)

Methoxylation of 3,4,6-trichloropyridazine (**1**) with sodium methoxide was investigated in detail. Dimethoxylation of **1** afforded 6-chloro-3,4-dimethoxypyridazine (**5**) and a molecular complex (*M*) which is composed of **5** and 3-chloro-4,6-dimethoxypyridazine (**6**) in a ratio of 1:1. The nature of the complex (*M*) was examined by thermal and X-ray analyses. The molecular complex (*M*) was also obtained by monomethoxylation of 3,6-dichloro-4-methoxypyridazine (**3**) with sodium methoxide.

**Keywords**—3,4,6-trichloropyridazine; methoxylation; pyridazinone; dimethoxymonochloropyridazine; trimethoxypyridazine; molecular complex; thermal analysis; X-ray analysis

Our previous article described the result of methoxylation of 3,4,5-trichloropyridazine.<sup>2)</sup> In this paper, we report some observations concerning the methoxylation of isomeric 3,4,6-trichloropyridazine (**1**), involving the formation of several types of methoxypyridazines and especially a unique molecular complex which is composed of 6-chloro-3,4-dimethoxypyridazine (**5**) and 3-chloro-4,6-dimethoxypyridazine (**6**).

Eichenberger *et al.*<sup>3)</sup> obtained 3,6-dichloro-4-methoxypyridazine (**3**) in 70% yield<sup>4)</sup> by monomethoxylation of **1** with NaOMe. On the other hand, Schönbeck and Kloimstein<sup>5)</sup> reported that dimethoxylation of **1** with 2 eq of NaOMe afforded 6-chloro-3,4-dimethoxypyridazine (**5**) in 40% yield and a compound which was assigned as 3-chloro-4,6-dimethoxypyridazine (**6**) (mp 95—96 °C) in 52% yield.

From these reports it can be presumed that the monomethoxylated pyridazine **3** may be an intermediate in the formation of the dimethoxypyridazines **5** and **6**. Therefore, monomethoxylation of **3** with 1 eq of NaOMe was investigated in detail. The methoxylation resulted in the formation of two products, **5** and a molecular complex *M* in 44% and 47% yields, respectively.<sup>6)</sup> The melting point of the complex *M* was identical with that of the compound **6** which was obtained by Schönbeck and Kloimstein<sup>5)</sup> as described above. Some doubts concerning the structure of Schönbeck's compound **6**, however, arose from an examination of its proton nuclear magnetic resonance (<sup>1</sup>H-NMR) spectral data. The <sup>1</sup>H-NMR spectrum of the complex *M* showed two sets of signals which are composed of those of **5** [ $\delta$  6.81 (1H, s, C<sub>5</sub>-H), 3.98 (3H, s, OMe) and 4.17 (3H, s, OMe)] and **6** [ $\delta$  6.38 (1H, s, C<sub>5</sub>-H), 4.10 (3H, s, OMe) and 3.96 (3H, s, OMe)] (Fig. 1 and Table I). The ratio of **5** and **6** in the complex *M* was determined to be 1:1 on the basis of the integral ratio of C<sub>5</sub>-H in the <sup>1</sup>H-NMR spectrum. Reinvestigation of the dimethoxylation of **1** also gave **5** and *M* in the same yields as in the case of monomethoxylation of **3**. These results indicate that the complex *M* (Schönbeck's compound **6**) is a complex composed of **5** and **6** in a ratio of 1:1. Attempts to separate **5** from **6** in the complex *M* by fractional recrystallization from many kinds of solvents or by chromatography were unsuccessful.

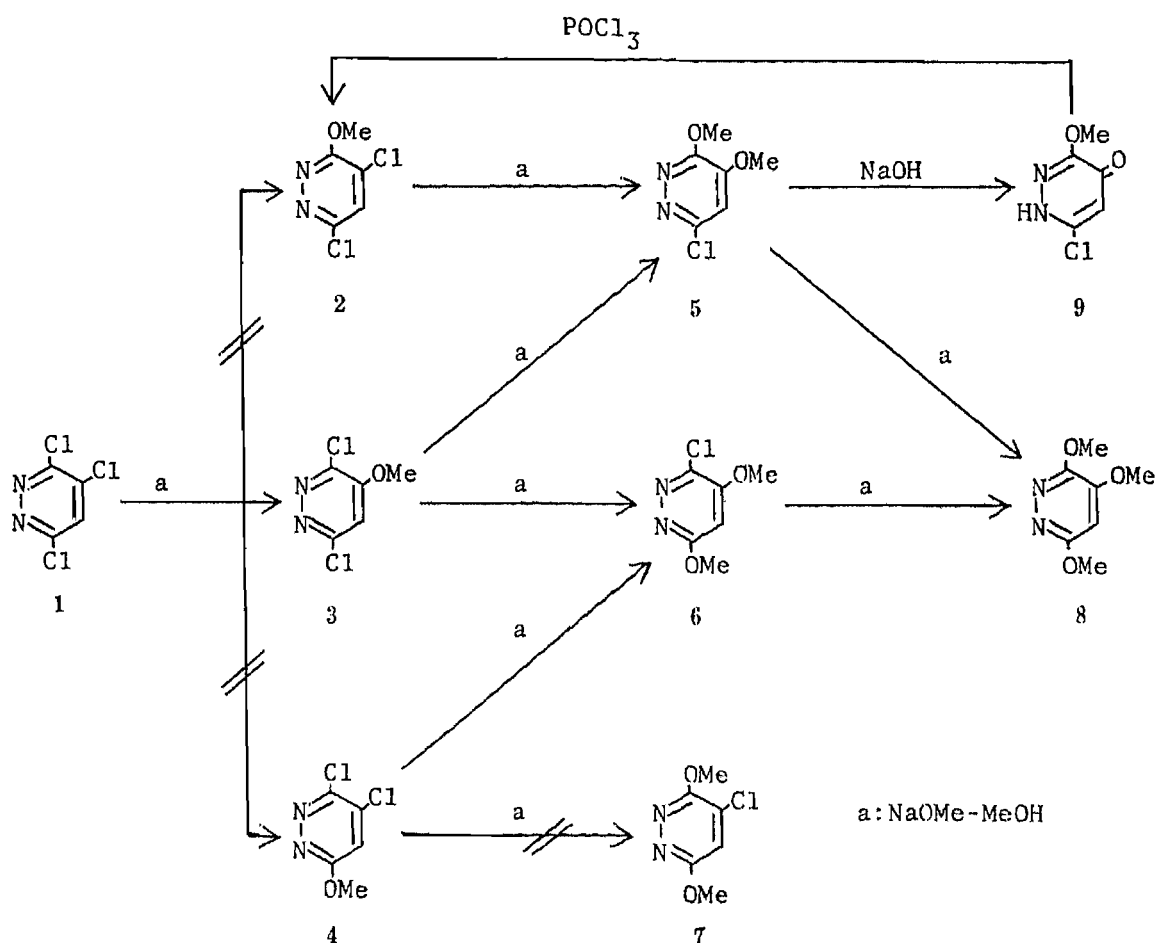
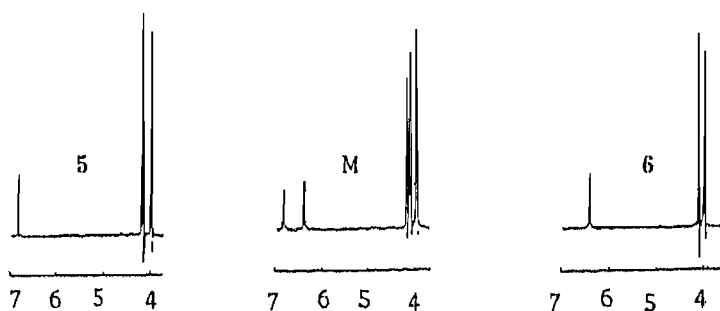


Chart 1

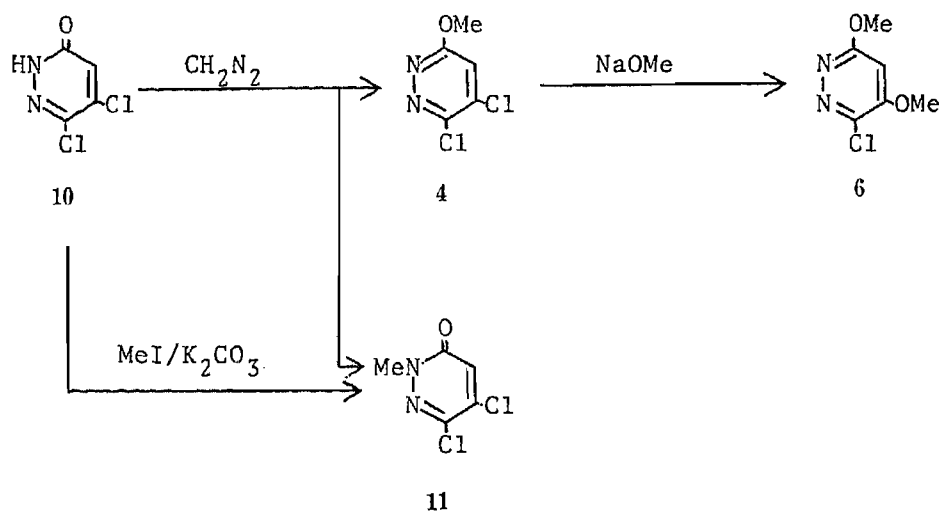
Fig. 1. <sup>1</sup>H-NMR Spectra of Compounds 5, 6 and Complex M

Alkaline degradation of the complex M allowed isolation of 6. After hydrolysis of the complex M with 5% NaOH at 100 °C for 20 min, the unresolved materials, which was proved to contain 5 and 6 in a ratio of 1 : 3 by <sup>1</sup>H-NMR spectral analysis, was collected and submitted to fractional recrystallization from MeOH to afford 6 as pure crystals together with the complex M. The melting point of 6 thus obtained was identical with that of 6 described by Landquist and Meek.<sup>7)</sup> From 17.5 g of the complex M, 1.6 g of 6 was isolated. The above separation method is based on the fact that the methoxyl group at position 4 of 5 is hydrolyzed faster than that of 6.

As described above, the methoxylation *via* 3 is unsatisfactory for the preparation of 6. An

TABLE I.  $^1\text{H-NMR}$  Spectral Data for Methoxypyridazines 2-8 ( $\text{CDCl}_3$ ;  $\delta$  ppm)

Product No.	$\text{C}_5\text{-H}$ (each 1H, s)	$\text{OCH}_3$ (each 3H, s)
2	7.50	4.18
3	6.98	4.06
4	7.16	4.17
5	6.81	3.98
		4.17
6	6.38	3.96
		4.10
8	6.29	3.89
		4.02
		4.10



alternative synthetic route *via* 3,4-dichloro-6-methoxypyridazine (4) leading to 6 was examined. The methoxypyridazine 4 has been prepared by Schönbeck and Kloimstein<sup>5)</sup> by the treatment of 5,6-dichloro-3(2*H*)-pyridazinone (10) with diazomethane (Chart 2). However, the above reaction under Schönbeck's conditions gave another compound, 5,6-dichloro-2-methyl-3(2*H*)-pyridazinone (11),<sup>7)</sup> in 52% yield in addition to 4 (16%). The structure of 11 was determined by comparison of the melting point and spectral data with those of the previously reported 11.<sup>8)</sup> The pyridazinone 11 was independently synthesized in 67% yield by methylation of 10 with methyl iodide in the presence of potassium carbonate as shown in Chart 2. It is noteworthy that the pyridazine 6 was synthesized by monomethoxylation of 4. By chlorination of 6-chloro-3-methoxy-4(1*H*)-pyridazinone (9)<sup>5)</sup> with phosphorus oxychloride, 4,6-dichloro-3-methoxypyridazine (2) was synthesized in 90% yield, and monomethoxylation of 2 afforded 5 in 91% yield.

The trimethoxylation of 1 with excess NaOMe was investigated. A solution of 1 and excess NaOMe in MeOH was refluxed and the reaction was monitored by  $^1\text{H-NMR}$  spectroscopy. After 30 h, the ratio of 5, 6 and trimethoxylated compound 8 was 5.4:1.5:1. These results indicate the very slow conversion of the dimethoxylated compounds 5 and 6 into 8. After refluxing for 1 h, however, MeOH was evaporated off until the temperature of the

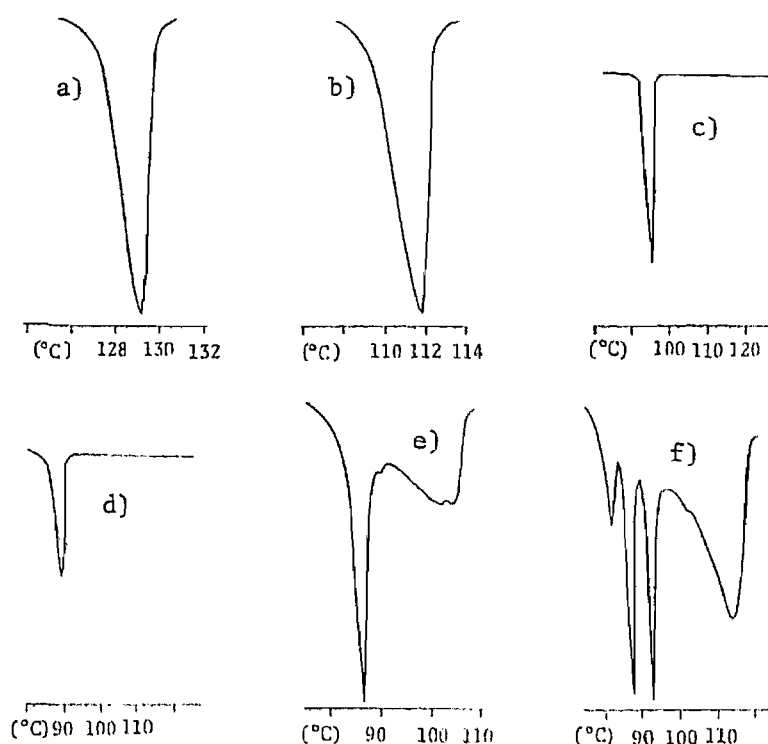


Fig. 2. DSC Curves of Compounds 5, 6 and M, M' and Their Molten Mixture  
a) 5; b) 6; c) M; d) M'; e) 6=83%; f) 6=24%.

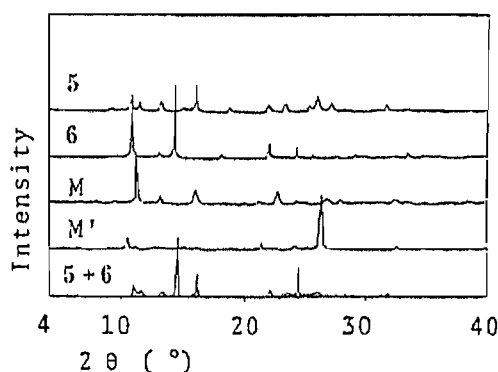


Fig. 3. X-Ray Diffraction Patterns of Compounds 5, 6 and M, M' and Physical Mixture of 5 and 6

reaction mixture reached 80°C, and then the mixture was further heated for 10 h to afford **8** and **9** in 55% and 9% yields, respectively.

The structure of the interesting complex M was examined by the thermal and X-ray analyses.

**Thermal Analysis:** The differential scanning calorimetry (DSC) curves of **5**, **6**, M, M' (the molten mixture of **5** and **6** in a weight ratio of 1:1) and molten mixtures of **5** and **6** in various weight ratios were recorded using a DSC apparatus (TA 3000, Mettler) in the range of 40–140°C at a rate of 5°C/min.

The measurement of each sample was repeated to obtain the DSC curves of physical mixture and molten mixture. Examples of the DSC curves are shown in Fig. 2. Sharp endothermic peaks owing to melting of **5**, **6**, M and M' appeared at 129, 110, 94 and 90°C, respectively (Fig. 2a, 2b, 2c and 2d). The molten mixture containing 66–98% of **5** in **6** showed the melting of **5** and a eutectic peaks at around 110 and 80–88°C, respectively (Fig. 2e), while

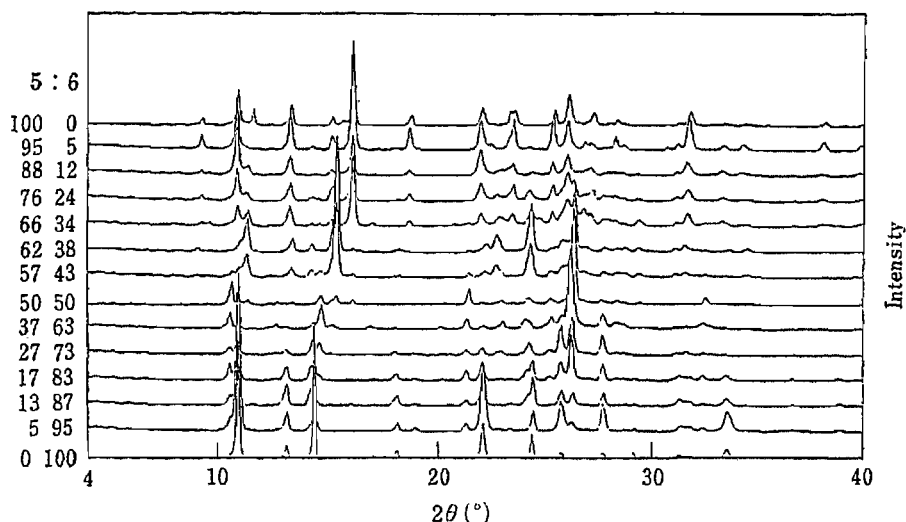


Fig. 4. X-Ray Diffraction Patterns of Compounds 5 and 6 and Their Eutectic Mixtures

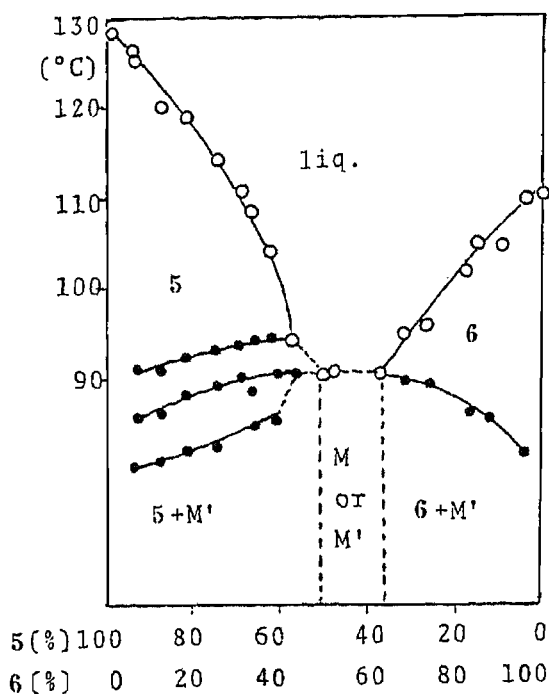


Fig. 5. Phase Diagram

○, temperature of melting peaks; ●, temperature of pre-melting peaks.

the mixtures of 10–40% of 6 in 5 showed four peaks (Fig. 2f). This suggests the existence of complex phases at lower concentration ratios of 5. The molten mixture containing 62.5% of 6 in 5 showed one sharp peak similar to that in Fig. 2d.

**Powder X-Ray Analysis:** Powder X-ray diffraction patterns of compounds 5, 6, M, M', physical mixture of 5 and 6, and the molten sample after thermal analyses were measured by using an X-ray diffractometer (RAD-rVB, Rigaku Denki; Cu- $K_{\alpha}$ ; 50 kV; 120 mA) with a non reflex sample holder (Fig. 3 and Fig. 4).

The diffraction patterns of 5, 6, M, M' were different, M and M' being polymorphs with 5°C difference in their melting points. No changes due to melting were found for 5 and 6. It was clear that M was not a simple mixture of 5 and 6, since the physical mixture of 5 and 6 differed from M and M' in terms of the diffraction patterns. The patterns of the melts

containing 5—43%, 50—60% and 79—95% **6** were identical with those of the physical mixture of **5** and **M**, **M'** and the physical mixture of **6** and **M'**, respectively. When the weight percentage of **6** was 0—43, irregular shifts of diffraction peaks were found compared with the case of weight percentage > 73.

The phase diagram of the mixture of **5** and **6** was drawn on the basis of DSC measurement (Fig. 5). The reasonable correspondence between the phase diagram in Fig. 5 and the changes of X-ray diffraction patterns in Fig. 3 suggested that **M** was not a simple crystalline mixture of **5** and **6** but a solid solution or a molecular compound formed when the equimolar mixture crystallized.

### Experimental

Melting points were determined by the capillary method, and are uncorrected. <sup>1</sup>H-NMR spectra were taken on a Hitachi R-20B spectrometer (60 MHz), and chemical shifts are given in the (ppm) scale with tetramethylsilane as an internal standard.

**Monomethoxylation of 3,6-Dichloro-4-methoxypyridazine (3)**—A solution of 1 M NaOMe in MeOH (100 ml) was added to a stirred suspension of **3** (17.9 g) in MeOH (100 ml), and the mixture was heated under reflux for 1 h. The MeOH was evaporated off and water (50 ml) was added to the residue. The mixture was extracted with CHCl<sub>3</sub> and dried over K<sub>2</sub>CO<sub>3</sub>. The solvent was evaporated off and the residue was recrystallized from MeOH to give two products, 6-chloro-3,4-dimethoxypyridazine (**5**) and complex **M**. Compound **5**: 7.69 g (44%), mp 128—129 °C (lit.<sup>3</sup>) mp 130—131 °C). Complex **M**: 8.20 g (47%), mp 95—96 °C. *Anal.* Calcd for C<sub>6</sub>H<sub>7</sub>ClN<sub>2</sub>O<sub>2</sub>: C, 41.28; H, 4.04; N, 16.05. Found: C, 41.17; H, 3.97; N, 16.12.

**Separation of 3-Chloro-4,6-dimethoxypyridazine (6) from Complex M**—A mixture of complex **M** (17.5 g) and 5% NaOH solution (200 g) was heated with stirring at 100 °C for 20 min. The reaction mixture was extracted with CHCl<sub>3</sub>. The organic layer was dried over K<sub>2</sub>CO<sub>3</sub> and concentrated to dryness. The residue was recrystallized from MeOH to give 1.6 g (18%) of **6** as colorless crystals, mp 110—111 °C (lit.<sup>7</sup>) mp 110 °C). *Anal.* Calcd for C<sub>6</sub>H<sub>7</sub>ClN<sub>2</sub>O<sub>2</sub>: C, 41.28; H, 4.04; N, 16.05. Found: C, 41.41; H, 4.04; N, 16.04.

**Reaction of 10 with Diazomethane**—An ethereal solution of diazomethane [prepared from methylnitrosourea (5.15 g) and 5% KOH solution (15 ml)] in ether (50 ml) was added dropwise to a stirred suspension of **10** (4.95 g) in acetone (45 ml) at room temperature. After the evolution of N<sub>2</sub> gas had stopped, the solvent was evaporated off and the residue was recrystallized from *n*-hexane to give 1.80 g of 5,6-dichloro-2-methyl-3(2*H*)-pyridazinone (**11**), mp 97—98 °C (lit.<sup>8</sup>) mp 97—98 °C). The mother liquor was submitted to column chromatography on alumina using CHCl<sub>3</sub> as the eluent to afford an additional 1.0 g of **11** (total: 2.8 g, 52%) and 0.88 g (16%) of 3,4-dichloro-6-methoxypyridazine (**4**) as colorless crystals, mp 68—69 °C (*n*-hexane) (lit.<sup>5</sup>) mp 49—52 °C). **4**: *Anal.* Calcd for C<sub>5</sub>H<sub>4</sub>Cl<sub>2</sub>N<sub>2</sub>O: C, 33.55; H, 2.25; N, 15.65. Found: C, 33.20; H, 2.11; N, 15.40. **11**: *Anal.* Calcd for C<sub>5</sub>H<sub>4</sub>Cl<sub>2</sub>N<sub>2</sub>O: C, 33.55; H, 2.25; N, 15.65. Found: C, 33.41; H, 2.22; N, 15.54.

**5,6-Dichloro-2-methyl-3(2*H*)-pyridazinone (11)**—A mixture of **10** (1.65 g), K<sub>2</sub>CO<sub>3</sub> (1.52 g) and iodomethane (1.56 g) in *N,N*-dimethylformamide (DMF) (20 ml) was stirred for 3 h at room temperature. The DMF was evaporated off under reduced pressure, then the residue was dissolved in a small amount of water and extracted with CHCl<sub>3</sub>. The extract was dried over K<sub>2</sub>CO<sub>3</sub> and concentrated to dryness. The residual solid was recrystallized from *n*-hexane to give 1.2 g (67%) of **11**, mp 97—98 °C, which was identical with a sample obtained above by the mixed melting point test.

**3-Chloro-4,6-dimethoxypyridazine (6)**—A solution of **4** (89.5 mg) in MeOH (2 ml) was added to a solution of 0.1 M NaOMe in MeOH (5 ml), and the mixture was refluxed for 1 h. The MeOH was evaporated off and water was added to the residue. The whole was extracted with CHCl<sub>3</sub> and the extract was dried over K<sub>2</sub>CO<sub>3</sub>. Removal of the solvent gave a solid, which were recrystallized from *n*-hexane to afford 62.8 mg (72%) of **6** as colorless crystals, mp 110—111 °C. This product was identical with a sample obtained from complex **M** by direct comparison of the <sup>1</sup>H-NMR spectra and by the mixed melting point test.

**4,6-Dichloro-3-methoxypyridazine (2)**—A mixture of **9** (16.1 g) and phosphorus oxychloride (153 g) was stirred at 80 °C until the crystals dissolved (a few min). The reaction mixture was poured into ice-water and slightly alkalinized by adding dil. NaOH solution. The mixture was extracted with CHCl<sub>3</sub>, and the extract was dried over K<sub>2</sub>CO<sub>3</sub> and evaporated to dryness. The residue was recrystallized from cyclohexane to give 16.1 g (90%) of **2** as colorless crystals, mp 80—81 °C. *Anal.* Calcd for C<sub>5</sub>H<sub>4</sub>Cl<sub>2</sub>N<sub>2</sub>O: C, 33.55; H, 2.25; N, 15.65. Found: C, 33.45; H, 2.22; N, 15.62.

**6-Chloro-3,4-dimethoxypyridazine (5)**—A 1 M NaOMe solution in MeOH (10 ml) was added to a solution of **2** (1.79 g) in MeOH (10 ml) and the mixture was refluxed for 1 h. The MeOH was removed *in vacuo* and water was added to the residue. The whole was extracted with CHCl<sub>3</sub>. Evaporation of the solvent left crystals which were recrystallized from MeOH to give 1.60 g (91%) of **5**, mp 128—129 °C. This product was identical with a sample obtained from **3** by the mixed melting point test.

**Trimethoxylation of 3,4,6-Trichloropyridazine (1)**—A 1 M NaOMe solution in MeOH (200 ml) was added dropwise to an ice-cooled solution of **1** (9.15 g) in MeOH (50 ml) and then the mixture was heated for 1 h. The MeOH was evaporated off until the temperature of the reaction mixture reached 80 °C, and then the mixture was heated for 10 h and worked up as usual to afford 4.70 g (55%) of 3,4,6-trimethoxypyridazine (**8**) as colorless crystals, mp 121 °C (MeOH) (lit.<sup>9</sup>) mp 121 °C). *Anal.* Calcd for C<sub>7</sub>H<sub>10</sub>N<sub>2</sub>O<sub>3</sub>: C, 49.41; H, 5.92; N, 16.46. Found: C, 49.31; H, 5.84; N, 16.27. The mother liquor was acidified (Congo red) with dil. HCl and the precipitate was collected and recrystallized from water to give 0.74 g (9%) of **9**, mp 225–228 °C. This product was identical with an authentic sample<sup>5</sup>) by the mixed melting point test.

**Acknowledgement** We are grateful to Dr. Hideo Nakamachi, Central Research Division, Takeda Chemical Industry, Ltd., for advice concerning thermal and X-ray analyses.

#### References and Notes

- 1) A part of this work was presented at the Meeting of Tokai Branch, Pharmaceutical Society of Japan, Nagoya, Nov. 1984 and also at the 105th Annual Meeting of the Pharmaceutical Society of Japan, Kanazawa, Apr. 1985.
- 2) H. Nagashima, H. Oda, J. Hida, and K. Kaji, *Chem. Pharm. Bull.*, **35**, 421 (1987).
- 3) K. Eichenberger, R. Rometsch, and J. Druey, *Helv. Chem. Acta*, **39**, 1755 (1956).
- 4) We reexamined the same reaction and obtained **3** in 94% yield.
- 5) R. Schönbeck and H. Kloimstein, *Monatsh. Chem.*, **99**, 15 (1968).
- 6) Itai and Natsume isolated only **5** from the same reaction [T. Itai and S. Natsume, *Chem. Pharm. Bull.*, **10**, 643 (1962)].
- 7) J. K. Landquist and S. E. Meek, *J. Chem. Soc., Perkin Trans. 1*, **1972**, 2735.
- 8) Y. Maki, M. Takaya, and M. Suzuki, *Yakugaku Zasshi*, **86**, 487 (1966).
- 9) T. Itai and H. Igeta, *Yakugaku Zasshi*, **75**, 966 (1955).



[Chem. Pharm. Bull.]  
35(1) 357-363 (1987)

## Ruthenium Tetroxide Oxidation of *N*-Alkylactams

SHIGEYUKI YOSHIFUJI,\* YUKIMI ARAKAWA,  
and YOSHIHIRO NITTA

*School of Pharmacy, Hokuriku University, Kanagawa-machi,  
Kanazawa 920-11, Japan*

(Received July 31, 1986)

Ruthenium tetroxide ( $\text{RuO}_4$ ) oxidation of *N*-alkylactams proceeded regioselectively depending on the size of lactam ring, except for the seven-membered ring. Four- and eight-membered *N*-methyl- and *N*-ethylactams were oxidized at the exocyclic  $\alpha$ -carbon adjacent to nitrogen to produce the *N*-acyllactams and NH-lactams, while five- and six-membered lactams underwent endocyclic oxidation to yield the cyclic imides. Oxidation of seven-membered lactams yielded a mixture of products arising from both exocyclic and endocyclic oxidations. These regioselectivities were confirmed in the oxidation of substrates having a tertiary carbon at the oxidation position.

**Keywords**—oxidation; ruthenium tetroxide oxidation; regioselective oxidation; hydroxylation; imide synthesis; *N*-alkylactam; *N*-acyllactam; imide; ruthenium tetroxide; two-phase method

Ruthenium tetroxide ( $\text{RuO}_4$ ) is a good reagent for the conversion of *N*-acylated cyclic amines to the corresponding lactams,<sup>1)</sup> by oxidation of one of two carbons adjacent to nitrogen. As a common feature of the  $\text{RuO}_4$  oxidation in this conversion (**1a** to **2** in Chart 1) and in the transformation of cyclic ethers into the corresponding lactones,<sup>2)</sup> it has been considered that  $\text{RuO}_4$  predominantly oxidizes a secondary carbon rather than a tertiary one. However, as reported previously,<sup>3)</sup> we obtained an opposite result in the  $\text{RuO}_4$  oxidation of some 1-azabicycloalkan-2-ones, such as quinolizidin-4-one (**1b**), which gave the hydroxylated products, such as **3**, resulting from the oxidation of the tertiary carbon. At that time, we predicted that the 1-azabicycloalkan-2-ones might belong not to the category of *N*-acyl cyclic amines but to that of *N*-alkylactams, in terms of  $\text{RuO}_4$  oxidation. However, to date, there has been no report on the latter category. Here we wish to describe a systematic study on the  $\text{RuO}_4$  oxidation of *N*-alkylactams.

As model compounds, simple *N*-methyl- and *N*-ethylactams ranging in size from four- to eight-membered rings were selected for the present work. The  $\text{RuO}_4$  oxidation of these substrates was carried out at room temperature under catalytic conditions using a catalytic amount of ruthenium dioxide ( $\text{RuO}_2$ ) in combination with an excess of 10% aqueous sodium metaperiodate ( $\text{NaIO}_4$ ). In the catalytic procedure of  $\text{RuO}_4$  oxidation, a two-phase system of organic solvent-water is usually employed as a reaction medium and the organic phase is a chlorinated methane such as carbon tetrachloride ( $\text{CCl}_4$ )<sup>4)</sup> or the combination of  $\text{CCl}_4$  and

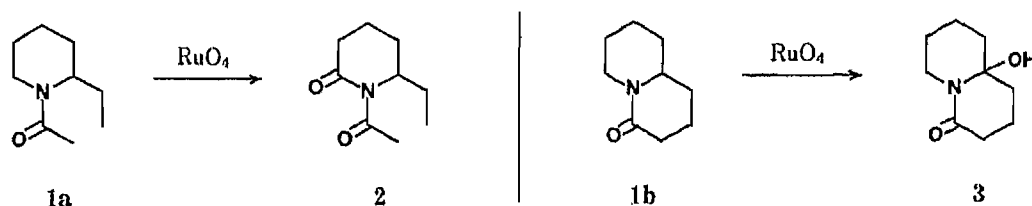


Chart 1

TABLE I. RuO<sub>4</sub> Oxidation of *N*-Alkylactams

Ring size	I	R	Reaction time (h)	Product (%)		
				II	III	IV
4 ( <i>n</i> =1)		4a: H	72	4c: 36	4d: 86	
		4b: CH <sub>3</sub>	42			
5 ( <i>n</i> =2)		5a: H	28			5c: 87
		5b: CH <sub>3</sub>	15			5d: 93
6 ( <i>n</i> =3)		6a: H	30			6c: 92
		6b: CH <sub>3</sub>	9			6d: 88
7 ( <i>n</i> =4)		7a: H	71	7c: 24	7d: 35	7e: 38
		7b: CH <sub>3</sub>	73		7f: 40	7g: 53
8 ( <i>n</i> =5)		8a: H	186	8c: 71	8d: 7	
		8b: CH <sub>3</sub>	95	8e: 6	8e: 77	

acetonitrile developed by Sharpless *et al.*<sup>5)</sup> Recently we developed a new solvent system of ethyl acetate (AcOEt)–water which gave short reaction times and high yields of the products in the transformation of *N*-acylated L-proline esters into the corresponding L-pyrroglutamic acid derivatives.<sup>1c)</sup> Therefore, our new system was applied to the present work. However, in the oxidation of the four-membered lactams, the organic phase (AcOEt) was omitted due to the ready solubility of these compounds in water. The oxidation reaction was monitored by observing the disappearance of the starting lactams on thin layer chromatographic (TLC) plates; it proceeded slowly, with a yellow color which indicated the existence of active RuO<sub>4</sub> generated *in situ* from RuO<sub>2</sub> under the above conditions. The results are summarized in Table I.

A highly regioselective oxidation depending on the ring size of the lactams, except for seven-membered lactams, was observed. Four- and eight-membered lactams were oxidized at the exocyclic  $\alpha$ -carbon to nitrogen. *N*-Methyl- $\beta$ -lactam afforded a low yield of the demethylated NH-lactam. Eight-membered *N*-methylactam also gave predominantly the NH-lactam together with a small amount of the *N*-formyllactam. *N*-Ethylactams were transformed into the *N*-acyllactams (and the NH-lactam in the case of the eight-membered lactam). Formation of the NH-lactams must be based on the elimination of aldehyde (formaldehyde or acetaldehyde) from the intermediates leading to the *N*-formyl or *N*-acetyl lactams and/or on the hydrolytic deacylation of the *N*-acyllactams.

Five- and six-membered lactams were oxidized at the endocyclic  $\alpha$ -carbon to provide the corresponding cyclic imides in high yields. The precursors of these imides are the corresponding  $\alpha$ -hydroxylactams which could be detectable in the early stage of the oxidation on TLC analysis. In an incomplete run with 1-methylpyrrolidin-2-one (5a) using a traditional two-phase system of CCl<sub>4</sub>–H<sub>2</sub>O, 2-hydroxy-1-methylpyrrolidine-5-one was isolated from the aqueous phase in 16% yield. When the hydroxy compound was oxidized with RuO<sub>4</sub> according to our standard procedure, *N*-methylsuccinimide (5c) was obtained in 97% yield.

Alternatively, treatment of seven-membered lactams with RuO<sub>4</sub> provided a mixture of products arising from endocyclic and exocyclic oxidations.

Next, in order to confirm the above mentioned regioselectivity depending on the size of the lactam ring, further RuO<sub>4</sub> oxidation was done under the same conditions with some *N*-

alkylactams bearing a tertiary carbon at the oxidation position. These compounds were chosen because a tertiary carbon is less susceptible to  $\text{RuO}_4$  than a primary or secondary carbon.<sup>1,2,4)</sup> The results are shown in Chart 2. *N*-Isopropyl- $\beta$ -lactam (**9**) was oxidized with

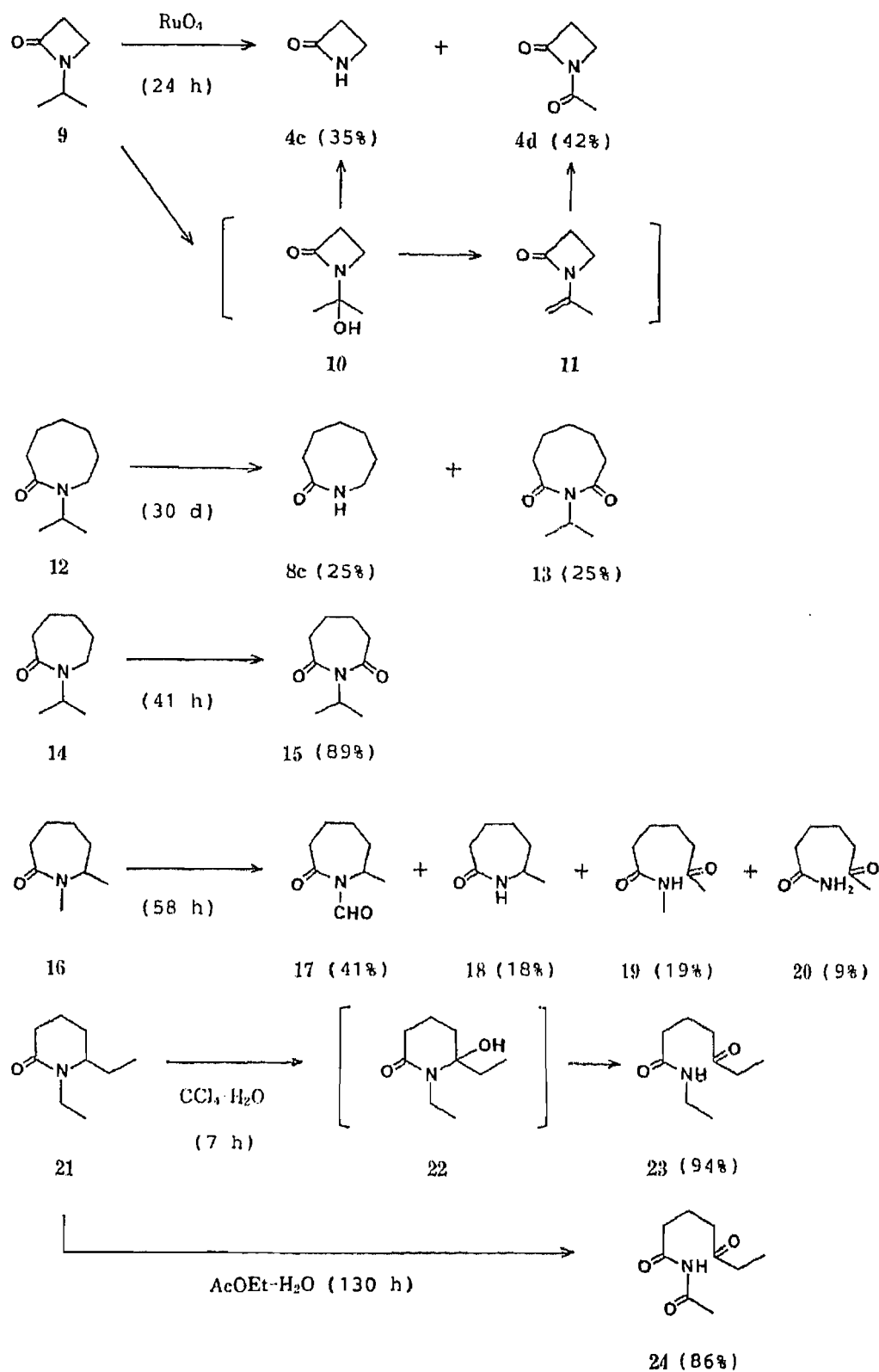


Chart 2

long reaction times to afford two products, an NH-lactam (**4c**) and a *N*-acetyllactam (**4d**), in 35% and 42% yields, respectively. Apparently, this oxidation occurred at the exocyclic tertiary carbon and these products (**4c, d**) were formed from a common intermediate, the hydroxylactam (**10**), which could not be isolated. Presumably **10** was decomposed directly to **4c** by the loss of acetone and indirectly to the acetyl derivative (**4d**) via dehydration to the *N*-isopropenyllactam (**11**) and oxidative cleavage of the double bond of **11**. RuO<sub>4</sub> oxidation of the eight-membered *N*-isopropylactam (**12**) proceeded very sluggishly and was not completed within 30 d; a little of the starting lactam (7%) was recovered. This must be due to the difficulty of access of RuO<sub>4</sub> to the exocyclic  $\alpha$ -position. Only a low yield of the exocyclic oxidized product (**8c**, 25%) was obtained together with the cyclic imide (**13**, 25%) generated in the kinetically controlled reaction. In this regard, the analogous oxidation of the seven-membered lactams gave reasonable results. *N*-Isopropylcaprolactam (**14**) was oxidized exclusively at the endocyclic  $\alpha$ -position to produce the cyclic imide (**15**) in 89% yield. On the other hand, the reaction of 1,2-dimethylcaprolactam (**16**) with RuO<sub>4</sub> provided a mixture of products resulting from the exocyclic and endocyclic oxidations: four compounds, **17** (41%), **18** (18%), **19** (19%), and **20** (9%), were obtained on chromatographic separation of the mixture.

Although regioselective endocyclic oxidation in the five- and six-membered lactams having a tertiary carbon at the oxidation position has already been observed with 1-azabicycloalkan-2-ones such as **1b** (Chart 1),<sup>3)</sup> 1,2-diethylpiperidin-6-one (**21**) was examined as a model compound. Thus, treatment of **21** with RuO<sub>4</sub> as described above using the CCl<sub>4</sub>-H<sub>2</sub>O system gave a 94% yield of the ring-opened product (**23**), which is equivalent to the hydroxylactam (**22**). When the AcOEt-H<sub>2</sub>O system was used in the above oxidation of **21**, the major product was the ring-opened imide (**24**) as a result of further oxidation of the initially formed amide (**23**).<sup>6)</sup>

On the basis of the results described above, it is possible to conclude that the RuO<sub>4</sub> oxidation of *N*-alkyllactams proceeds regioselectively depending on the size of the lactam ring, except for the seven-membered ring, even when a saturated tertiary carbon (which has not previously been reported to be oxidized by RuO<sub>4</sub>) occupies the oxidation position in the four-, five-, and six-membered *N*-alkyllactams. Recently, a similar type of reaction has been reported in the direct or indirect anodic oxidation of *N*-alkyllactams.<sup>7)</sup> Our RuO<sub>4</sub> oxidation can be regarded as superior to these oxidations in respect of the high regioselectivity of the reaction and the high yield of the products.

### Experimental

Melting points were taken on a Yanagimoto melting point apparatus. All melting points and boiling points are uncorrected. Infrared (IR) spectra were recorded on a JASCO IRA-2 or a Hitachi 270-30 spectrophotometer. Mass spectra (MS) were measured on a JEOL JMS D-100 or a JEOL JMS D-300 spectrometer. Nuclear magnetic resonance (<sup>1</sup>H-NMR) spectra were obtained at 23 °C on a JEOL JNM-MH-100 or a JEOL FX-100 spectrometer with tetramethylsilane as an internal standard.

**Starting Materials**—All starting materials were obtained from commercial suppliers (**5a**, **5b**, **6a**) or prepared according to the established methods.<sup>8)</sup>

New compounds were characterized as described below.

**1-Isopropylazetid-2-one (9)**—A colorless oil, bp 83–85 °C (17 mmHg). MS *m/z*: 113 (M<sup>+</sup>). IR  $\nu_{\max}^{\text{film}} \text{ cm}^{-1}$ : 1737 (C=O). <sup>1</sup>H-NMR (CDCl<sub>3</sub>)  $\delta$ : 1.18 (6H, d, *J* = 7 Hz, 2 × CH<sub>3</sub>), 2.81 (2H, t, *J* = 4 Hz, C<sub>3</sub>-H<sub>2</sub>), 3.16 (2H, t, *J* = 4 Hz, C<sub>4</sub>-H<sub>2</sub>), 3.75–4.05 (1H, m, CH).

**1-Isopropylcaprolactam (12)**—A colorless oil, bp 76 °C (2 mmHg). MS *m/z*: 169 (M<sup>+</sup>). IR  $\nu_{\max}^{\text{film}} \text{ cm}^{-1}$ : 1610 (C=O). <sup>1</sup>H-NMR (CDCl<sub>3</sub>)  $\delta$ : 1.14 (6H, d, *J* = 7 Hz, 2 × CH<sub>3</sub>), 1.35–1.93 (8H, m, C<sub>4</sub>-H<sub>2</sub>, C<sub>5</sub>-H<sub>2</sub>, H<sub>6</sub>-H<sub>2</sub>, and C<sub>7</sub>-H<sub>2</sub>), 2.4–2.61 (2H, m, C<sub>3</sub>-H<sub>2</sub>), 3.32–3.47 (2H, m, C<sub>8</sub>-H<sub>2</sub>), 4.44–4.92 (1H, m, CH).

**Standard Procedure for RuO<sub>4</sub> Oxidation of *N*-Alkylactams**—A solution of a substrate (12 mmol) to be oxidized in an organic solvent (AcOEt, 40 ml) was added to a mixture of RuO<sub>2</sub> hydrate [Aldrich Chemical Co.] (120 mg) and 10% aqueous NaIO<sub>4</sub> (120 ml). The mixture was vigorously stirred using a mechanical stirrer with a

glass blade at room temperature. The reaction was monitored by TLC. In the case of the four-membered lactams, the organic solvent (AcOEt) was omitted.

**Work-up (A)** [Isolation of the Product from the Organic Phase]: After the starting material had disappeared as determined by TLC, the layers were separated. The aqueous layer was extracted with AcOEt (3 × 40 ml). The combined organic solution was treated with isopropyl alcohol (2 ml) for 3 h to decompose RuO<sub>4</sub>, and then filtered. The filtrate was washed with 10% aqueous Na<sub>2</sub>S<sub>2</sub>O<sub>3</sub> (10 ml) and dried over anhydrous Na<sub>2</sub>SO<sub>4</sub>. The solution was evaporated *in vacuo* to leave a residue, which was purified by column chromatography on silica-gel or alumina using a solvent system of AcOEt-hexane as the eluent, and/or by recrystallization for solid products or by vacuum distillation for oily substances.

**Work-up (B)** [Isolation of the Product from the Aqueous Phase]: The aqueous layer, which had been extracted with AcOEt as described above, was concentrated under reduced pressure to dryness and the resulting white solid was extracted with hot AcOEt (3 × 40 ml). The combined extracts were dried over anhydrous Na<sub>2</sub>SO<sub>4</sub> and evaporated *in vacuo* to leave a residue, which was purified.

**Work-up (C)** [For the Four-Membered Lactams]: The reaction solution was washed with CCl<sub>4</sub> (3 × 40 ml) and concentrated under reduced pressure to dryness, leaving a white solid, which was extracted with hot AcOEt (3 × 40 ml). The combined AcOEt extract was dried over anhydrous Na<sub>2</sub>SO<sub>4</sub> and evaporated *in vacuo* to afford the crude product.

The results (reaction time and yield) of all oxidations are summarized in Table I and Chart 2. The identification of the oxidation products was done by comparison of their physical and spectral data with those of authentic samples, whenever they were known (4c,<sup>9)</sup> 5c,<sup>10)</sup> 5d,<sup>11)</sup> 6c,<sup>10)</sup> 6d,<sup>12)</sup> 7c,<sup>13)</sup> 7e,<sup>10)</sup> 7f,<sup>14)</sup> 8c,<sup>13)</sup> 18,<sup>15)</sup>. New compounds were characterized as described below.

**1-Acetylazetidin-2-one (4d)**—A colorless oil, bp 102–105°C (17 mmHg, bath temp.). MS *m/z*: 113 (M<sup>+</sup>). IR  $\nu_{\max}^{\text{film}}$  cm<sup>-1</sup>: 1784, 1696 (C=O). <sup>1</sup>H-NMR (CDCl<sub>3</sub>)  $\delta$ : 2.35 (3H, s, COCH<sub>3</sub>), 3.05 (2H, t, *J* = 5 Hz, C<sub>3</sub>-H<sub>2</sub>), 3.58 (2H, t, *J* = 5 Hz, C<sub>4</sub>-H<sub>2</sub>).

**Isolation of 2-Hydroxy-1-methylpyrrolidin-5-one in the Oxidation of 1-Methylpyrrolidin-2-one (5a)**—Oxidation of 5a was carried out under the standard conditions, but CCl<sub>4</sub> was used instead of AcOEt. After 10 d, the reaction mixture was treated as follows: work-up (A) gave 1-methylsuccinimide (5c, 78%) and work-up (B) gave 2-hydroxy-1-methylpyrrolidin-5-one (16%), which was identical with an authentic sample<sup>16)</sup> prepared from 1-methylsuccinimide on NaBH<sub>4</sub> reduction.

2-Hydroxy-1-methylpyrrolidin-5-one was oxidized with RuO<sub>4</sub> under the standard conditions (AcOEt-H<sub>2</sub>O system, 28 h) to afford 5c in 97% yield.

**Oxidation of Hexahydro-1-methyl-2*H*-azepin-2-one (7a)**—A mixture of two products, 1-formylhexahydro-2*H*-azepin-2-one (7d) and hexahydro-1-methyl-2*H*-azepin-2,7-dione (7e), was obtained on work-up (A) and separated by column chromatography. Hexahydro-2*H*-azepin-2-one (7c) was obtained on work-up (B).

**7d**: A colorless oil, bp 148°C (16 mmHg, bath temp.). IR  $\nu_{\max}^{\text{film}}$  cm<sup>-1</sup>: 1720, 1682 (C=O). <sup>1</sup>H-NMR (CDCl<sub>3</sub>)  $\delta$ : 1.50–2.0 (6H, m, C<sub>4</sub>-H<sub>2</sub>, C<sub>5</sub>-H<sub>2</sub>, and C<sub>6</sub>-H<sub>2</sub>), 2.6–2.8 (2H, m, C<sub>3</sub>-H<sub>2</sub>), 3.8–3.9 (2H, m, C<sub>7</sub>-H<sub>2</sub>), 9.34 (1H, s, CHO).

**Oxidation of 1-Ethylhexahydro-2*H*-azepin-2-one (7b)**—A mixture of two products, 1-acetylhexahydro-2*H*-azepin-2-one (7f) and 1-ethylhexahydro-2*H*-azepin-2,7-dione (7g), was obtained on work-up (A) and separated by column chromatography.

**7g**: A colorless oil, bp 103°C (3 mmHg, bath temp.). IR  $\nu_{\max}^{\text{film}}$  cm<sup>-1</sup>: 1710, 1660 (C=O). <sup>1</sup>H-NMR (CDCl<sub>3</sub>)  $\delta$ : 1.11 (3H, t, *J* = 7 Hz, CH<sub>3</sub>), 1.8–2.0 (4H, m, C<sub>3</sub>-H<sub>2</sub> and C<sub>6</sub>-H<sub>2</sub>), 2.7–2.9 (4H, m, C<sub>4</sub>-H<sub>2</sub> and C<sub>5</sub>-H<sub>2</sub>), 3.77 (2H, q, *J* = 7 Hz, CH<sub>2</sub>-CH<sub>3</sub>).

**Oxidation of 1-Methyloctahydroazocin-2-one (8a)**—Work-up (A) gave 1-formyloctahydroazocin-2-one (8d) and work-up (B) gave octahydroazocin-2-one (8c).

**8d**: A colorless oil. IR  $\nu_{\max}^{\text{film}}$  cm<sup>-1</sup>: 1710, 1690 (C=O). <sup>1</sup>H-NMR (CDCl<sub>3</sub>)  $\delta$ : 1.3–2.0 (8H, m, C<sub>4</sub>-H<sub>2</sub>, C<sub>5</sub>-H<sub>2</sub>, C<sub>6</sub>-H<sub>2</sub>, and C<sub>7</sub>-H<sub>2</sub>), 2.5–2.7 (2H, m, C<sub>3</sub>-H<sub>2</sub>), 3.7–3.9 (2H, m, C<sub>8</sub>-H<sub>2</sub>), 9.32 (1H, s, CHO).

**Oxidation of 1-Ethylloctahydroazocin-2-one (8b)**—Work-up (A) gave 1-acetyloctahydroazocin-2-one (8e) and work-up (B) gave octahydroazocin-2-one (8c).

**8e**: A colorless oil, bp 105°C (4 mmHg). MS *m/z*: 169 (M<sup>+</sup>). IR  $\nu_{\max}^{\text{film}}$  cm<sup>-1</sup>: 1688 (b, C=O). <sup>1</sup>H-NMR (CDCl<sub>3</sub>)  $\delta$ : 1.27–2.0 (8H, m, C<sub>4</sub>-H<sub>2</sub>, C<sub>5</sub>-H<sub>2</sub>, C<sub>6</sub>-H<sub>2</sub>, and C<sub>7</sub>-H<sub>2</sub>), 2.49 (3H, s, COCH<sub>3</sub>), 2.54–2.74 (2H, m, C<sub>3</sub>-H<sub>2</sub>), 3.74–4.0 (2H, m, C<sub>8</sub>-H<sub>2</sub>).

**Oxidation of 1-Isopropyloctahydroazocin-2-one (12)**—On work-up (A), a mixture of two products, octahydroazocin-2-one (8c) and 1-isopropyloctahydroazocin-2,8-dione (13) was obtained together with the starting lactam (12). NH-Lactam (8c) was also obtained on work-up (B).

**13**: A colorless oil, bp 90°C (1 mmHg, bath temp.). MS *m/z*: 183 (M<sup>+</sup>). IR  $\nu_{\max}^{\text{film}}$  cm<sup>-1</sup>: 1698, 1655 (C=O). <sup>1</sup>H-NMR (CDCl<sub>3</sub>)  $\delta$ : 1.30 (6H, d, *J* = 7 Hz, 2 × CH<sub>3</sub>), 1.47–2.0 (6H, m, C<sub>4</sub>-H<sub>2</sub>, C<sub>5</sub>-H<sub>2</sub>, and C<sub>6</sub>-H<sub>2</sub>), 2.7–2.9 (4H, m, C<sub>3</sub>-H<sub>2</sub> and C<sub>7</sub>-H<sub>2</sub>), 4.6–5.0 (1H, m, N-CH).

**Oxidation of 1-Isopropylhexahydro-2*H*-azepin-2-one (14)**—1-Isopropylhexahydro-2*H*-azepin-2,7-dione (15) was obtained on work-up (A).

**15**: A colorless oil, bp 84°C (2 mmHg, bath temp.). MS *m/z*: 169 (M<sup>+</sup>). IR  $\nu_{\max}^{\text{film}}$  cm<sup>-1</sup>: 1710, 1660 (C=O). <sup>1</sup>H-

NMR (CDCl<sub>3</sub>)  $\delta$ : 1.31 (6H, d,  $J=7$  Hz,  $2 \times \text{CH}_3$ ), 1.8—2.0 (4H, m, C<sub>4</sub>-H<sub>2</sub> and C<sub>5</sub>-H<sub>2</sub>), 2.6—2.8 (4H, m, C<sub>3</sub>-H<sub>2</sub> and C<sub>6</sub>-H<sub>2</sub>), 4.5—5.0 (1H, m, N-CH).

**Oxidation of 1,2-Dimethylhexahydro-2H-azepin-7-one (16)**—After the oxidation under the standard conditions was completed, the two layers were separated and the aqueous layer (aq-1) was extracted with AcOEt ( $2 \times 30$  ml). The extracts were combined with the original AcOEt solution and treated with isopropyl alcohol (3 ml). The solution was filtered and the filtrate was concentrated under reduced pressure to leave a residue, which was dissolved in a mixture of H<sub>2</sub>O (20 ml) and hexane (40 ml). After vigorous shaking, the two layers were separated and the aqueous layer was extracted with hexane ( $2 \times 40$  ml). This aqueous layer was combined with the above aqueous layer (aq-1) and subjected to work-up (B) to give a mixture of products. Chromatography on alumina using CHCl<sub>3</sub>-hexane (1 : 1, v/v) as the eluent gave three products (18, 19, and 20). The hexane solution was dried over anhydrous Na<sub>2</sub>SO<sub>4</sub> and evaporated *in vacuo* to give 1-formyl-hexahydro-2-methyl-2H-azepin-7-one (17).

17: A colorless oil, bp 135 °C (13 mmHg, bath temp.). IR  $\nu_{\text{max}}^{\text{film}}$  cm<sup>-1</sup>: 1712, 1686 (C=O), <sup>1</sup>H-NMR (CDCl<sub>3</sub>)  $\delta$ : 1.34 (3H, d,  $J=7$  Hz, CH<sub>3</sub>), 1.49—2.1 (6H, m, C<sub>3</sub>-H<sub>2</sub>, C<sub>4</sub>-H<sub>2</sub>, and C<sub>5</sub>-H<sub>2</sub>), 2.63—2.87 (2H, m, C<sub>6</sub>-H<sub>2</sub>), 4.75—5.2 (1H, m, C<sub>2</sub>-H), 9.36 (1H, s, CHO).

Hexahydro-2-methyl-2H-azepin-7-one (18): Colorless needles, mp 91—92 °C. MS  $m/z$ : 127 (M<sup>+</sup>). IR  $\nu_{\text{max}}^{\text{KBr}}$  cm<sup>-1</sup>: 3200, 3100 (NH), 1663 (C=O). <sup>1</sup>H-NMR (CDCl<sub>3</sub>)  $\delta$ : 1.23 (3H, d,  $J=7$  Hz, N-CH<sub>3</sub>), 1.3—2.10 (6H, m, C<sub>3</sub>-H<sub>2</sub>, C<sub>4</sub>-H<sub>2</sub> and C<sub>5</sub>-H<sub>2</sub>), 2.36—2.55 (2H, m, C<sub>6</sub>-H<sub>2</sub>), 3.36—3.68 (1H, m, C<sub>2</sub>-H), 5.8—6.3 (1H, b, NH).

*N*-Methyl-6-oxoheptanamide (19): Colorless scales, mp 60—61 °C. MS  $m/z$ : 157 (M<sup>+</sup>). IR  $\nu_{\text{max}}^{\text{KBr}}$  cm<sup>-1</sup>: 3300 (NH), 1710, 1703, 1642 (C=O). <sup>1</sup>H-NMR (CDCl<sub>3</sub>)  $\delta$ : 1.52—1.72 (4H, m, C<sub>3</sub>-H<sub>2</sub> and C<sub>4</sub>-H<sub>2</sub>), 2.15 (3H, s, COCH<sub>3</sub>), 2.1—2.3 (2H, m, C<sub>5</sub>-H<sub>2</sub>), 2.38—2.60 (2H, m, C<sub>2</sub>-H<sub>2</sub>), 2.78 (3H, d,  $J=5$  Hz, N-CH<sub>3</sub>), 5.64—6.12 (1H, b, NH). *Anal.* Calcd for C<sub>8</sub>H<sub>15</sub>NO<sub>2</sub>: C, 61.12; H, 9.62; N, 8.91. Found: C, 61.22; H, 9.58; N, 8.89.

6-Oxoheptanamide (20): Colorless needles, mp 80 °C. MS  $m/z$ : 143 (M<sup>+</sup>). IR  $\nu_{\text{max}}^{\text{KBr}}$  cm<sup>-1</sup>: 3400, 3210 (NH<sub>2</sub>), 1700, 1663, 1614 (C=O). <sup>1</sup>H-NMR (CDCl<sub>3</sub>)  $\delta$ : 1.55—1.76 (4H, m, C<sub>3</sub>-H<sub>2</sub> and C<sub>4</sub>-H<sub>2</sub>), 2.13 (3H, s, COCH<sub>3</sub>), 2.1—2.4 (2H, m, C<sub>5</sub>-H<sub>2</sub>), 2.4—2.6 (2H, m, C<sub>2</sub>-H<sub>2</sub>), 6.00 (2H, brs, NH<sub>2</sub>).

**Oxidation of 1,2-Diethylpiperidin-6-one (21)**—Oxidation of 21 was carried out under the standard conditions, but with CCl<sub>4</sub> as the organic phase, giving *N*-ethyl-5-oxoheptanamide (23) on work-up (A). When AcOEt was used as the organic phase, the further oxidized product, *N*-acetyl-5-oxoheptanamide (24), was obtained after 130 h.

23: Colorless scales, mp 63—64 °C. MS  $m/z$ : 171 (M<sup>+</sup>). IR  $\nu_{\text{max}}^{\text{KBr}}$  cm<sup>-1</sup>: 3310 (NH), 1715, 1635 (C=O). <sup>1</sup>H-NMR (CDCl<sub>3</sub>)  $\delta$ : 1.05 (3H, t,  $J=7$  Hz, C<sub>7</sub>-H<sub>3</sub>), 1.13 (3H, t,  $J=7$  Hz, NCH<sub>2</sub>CH<sub>3</sub>), 1.78—2.06 (2H, m, C<sub>3</sub>-H<sub>2</sub>), 2.1—2.3 (2H, m, C<sub>4</sub>-H<sub>2</sub>), 2.39 (2H, q,  $J=7$  Hz, C<sub>6</sub>-H<sub>2</sub>), 2.49 (2H, t,  $J=6.5$  Hz, C<sub>2</sub>-H<sub>2</sub>), 3.1—3.44 (2H, m, N-CH<sub>2</sub>CH<sub>3</sub>, added D<sub>2</sub>O, q,  $J=7$  Hz), 5.76 (1H, brs, NH, added D<sub>2</sub>O, disappeared).

24: Colorless needles, mp 90—92 °C. MS  $m/z$ : 185 (M<sup>+</sup>). IR  $\nu_{\text{max}}^{\text{KBr}}$  cm<sup>-1</sup>: 3268, 3180 (NH), 1730, 1704, 1654 (C=O). <sup>1</sup>NMR (CDCl<sub>3</sub>)  $\delta$ : 1.05 (3H, t,  $J=7$  Hz, C<sub>7</sub>-H<sub>3</sub>), 1.73—2.08 (2H, m, C<sub>3</sub>-H<sub>2</sub>), 2.32 (3H, s, NCOCH<sub>3</sub>), 2.3—2.65 (6H, m, C<sub>2</sub>-H<sub>2</sub>, C<sub>4</sub>-H<sub>2</sub>, and C<sub>6</sub>-H<sub>2</sub>), 9.18 (1H, s, NH).

**Acknowledgement** The authors are greatly indebted to Professor Tozo Fujii of Kanazawa University and ex-Professor Yoshio Arata of Hokuriku University for their kind encouragement.

#### References and Notes

- 1) a) J. C. Sheehan and R. W. Tulis, *J. Org. Chem.*, **39**, 2264 (1974); b) N. Tangari and V. Tortorella, *J. Chem. Soc., Chem. Commun.*, **1975**, 71; c) S. Yoshifuji, K. Tanaka, T. Kawai, and N. Nitta, *Chem. Pharm. Bull.*, **33**, 5515 (1985).
- 2) A. B. Smith, III and R. M. Scarborough, Jr., *Synth. Commun.*, **10**, 205 (1980).
- 3) S. Yoshifuji, Y. Arakawa, and Y. Nitta, *Chem. Pharm. Bull.*, **33**, 5042 (1985).
- 4) D. G. Lee and M. van den Engh, "Oxidation in Organic Chemistry," Part B, ed. by W. S. Trahanovsky, Academic Press, New York, 1973, Chapter 4.
- 5) P. H. J. Carlsen, Y. Katsuki, V. S. Martin, and K. B. Sharpless, *J. Org. Chem.*, **46**, 3936 (1981).
- 6) RuO<sub>4</sub> oxidation of *N*-acylated alkylamines to the corresponding imides is a new method for the general synthesis of imides. K. Tanaka, S. Yoshifuji, and Y. Nitta, *Chem. Pharm. Bull.*, **35**, 364 (1987).
- 7) a) M. Okita, T. Wakamatsu, and Y. Ban, *J. Chem. Soc., Chem. Commun.*, **1979**, 749; b) M. Okita, T. Wakamatsu, M. Mori, and Y. Ban, *Heterocycles*, **14**, 1089 (1980); c) M. Masui, S. Hara, and S. Ozaki, *Chem. Pharm. Bull.*, **34**, 975 (1986).
- 8) a) H. Takahata, T. Hashizume, and T. Yamazaki, *Heterocycles*, **12**, 1449 (1979); b) H. Takahata, Y. Ohnishi, and T. Yamazaki, *ibid.*, **14**, 467 (1980).
- 9) R. W. Holley and A. D. Holley, *J. Am. Chem. Soc.*, **71**, 2129 (1949).
- 10) W. Flitsch, *Chem. Ber.*, **97**, 1542 (1964).
- 11) W. Kantlehner, T. Maier, W. Löffler, and J. J. Kapassaklidis, *Justus Liebigs Ann. Chem.*, **1982**, 507.

- 
- 12) H. K. Hall, Jr. and A. K. Schneider, *J. Am. Chem. Soc.*, **80**, 6409 (1958).
  - 13) This sample was obtained from a commercial supplier.
  - 14) L. G. Donaruma, R. P. Scelia, and S. E. Schonfeld, *J. Heterocycl. Chem.*, **1**, 48 (1964).
  - 15) H. E. Ungnade and A. D. McLaren, *J. Org. Chem.*, **10**, 29 (1945).
  - 16) J. C. Hubert, J. P. A. Wignberg, and W. N. Speckamp, *Tetrahedron*, **31**, 1437 (1975).

[Chem. Pharm. Bull.]  
35(1) 364-369 (1987)

## Ruthenium Tetroxide Oxidation of *N*-Acylated Alkylamines: A New General Synthesis of Imides<sup>1)</sup>

KEN-ICHI TANAKA,\* SHIGEYUKI YOSHIFUJI,  
and YOSHIHIRO NITTA

School of Pharmacy, Hokuriku University, Kanagawa-machi,  
Kanazawa 920-11, Japan

(Received September 1, 1986)

Oxidation of various *N*-acylalkylamines with ruthenium tetroxide (RuO<sub>4</sub>) was systematically investigated. *N*-Acylalkylamines having an electron-donating group at the α- or β-position with respect to amide nitrogen or an electron-donating alkyl function in the acyl group were smoothly oxidized to the corresponding imides in excellent yields. On the other hand, *N*-acylalkylamines having an electron-withdrawing group were not oxidized at all, and most of the starting material was recovered. It appears that the reactivity of *N*-acylalkylamines is closely correlated with the acidity of the carboxylic acid from which the *N*-acyl group is derived, and also with the electron density at the methylene moiety adjacent to the amide nitrogen atom.

**Keywords**—oxidation; ruthenium tetroxide oxidation; imide synthesis; acyclic imide; amide; ruthenium tetroxide; substituent effect

Ruthenium tetroxide (RuO<sub>4</sub>) is well known as an effective multipurpose oxidant<sup>2)</sup> and has recently been used for the oxidation of some *N*-acylated cyclic amines to lactams and imides.<sup>3)</sup> In contrast, only one example of RuO<sub>4</sub> oxidation of an *N*-acylated acyclic amine, *i.e.*, the conversion of *N*-hexylheptanamide into *N*-hexanoylheptanamide, has been reported.<sup>4)</sup> The oxidation was carried out in a one-phase system of carbon tetrachloride (CCl<sub>4</sub>) solution containing a stoichiometric amount of RuO<sub>4</sub> oxidant to afford the imide in a low yield. To date, no detailed and systematic study on RuO<sub>4</sub> oxidation of *N*-acylated alkylamines has been done, and the above procedure seems not to represent a generally applicable synthetic method for acyclic imides in terms of yield.

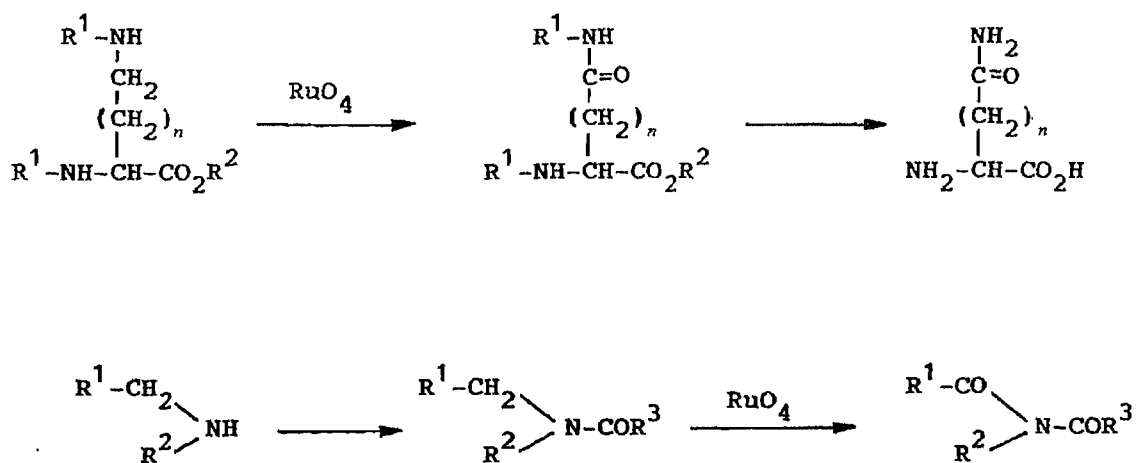


Chart 1





In connection with our program aimed at developing a strategy for the oxidative transformation<sup>5)</sup> of *L*- $\alpha,\omega$ -diamino acids into the corresponding *L*- $\omega$ -carbamoyl- $\alpha$ -amino acids by employing RuO<sub>4</sub> oxidation, we decided to investigate the oxidation of *N*-acylated alkylamines, as outlined in Chart 1. We report in the present paper the RuO<sub>4</sub> oxidation of *N*-acylated alkylamines in detail.

As the first model of alkylamines for the present study, we selected a propylamine, which was acylated with various acyl chlorides under the Schotten-Baumann reaction conditions. Initially, we investigated the relationship between the *N*-acyl group and reactivity. In our recent studies on RuO<sub>4</sub> oxidation, we developed an improved oxidation method<sup>3c)</sup> employing ethyl acetate (AcOEt) as an organic solvent in a two-phase system instead of the traditional halogenated solvents (CCl<sub>4</sub> and CHCl<sub>3</sub>). In our system, the oxidation time was significantly shortened and products were obtained in high yields in comparison with those by employing the traditional solvent systems. This was also confirmed by the present results (Table I, entries 7–9) obtained in the oxidation of *N*-acetylpropylamine **1g** under various conditions. Thus, the RuO<sub>4</sub> oxidation of a variety of *N*-acylated propylamines was carried out using a small amount of RuO<sub>2</sub> hydrate and excess 10% aqueous sodium metaperiodate in a two-phase system of AcOEt–water at room temperature according to our procedure<sup>3c)</sup> reported previously. The consumption of the starting materials was checked by thin layer chromatography (TLC). The corresponding *N*-acylated amides (imides) were obtained and their structures were assigned on the basis of the spectral data (proton nuclear magnetic resonance (<sup>1</sup>H-NMR) spectra, infrared (IR) spectra, and mass spectra (MS)). The individual results are summarized in Table I.

As shown in Table I, the *N*-acylamines (**1a–g**) were oxidized to give the corresponding imides (**2a–g**) in 67–96% yields. However, in the case of *N*-trichloroacetylpropylamine **1h**, the reaction did not occur at all even after 120 h and most of the starting material was recovered unchanged. Among the results obtained above, the shortest reaction time was observed with the pivaloyl group, as shown in entry 1. It was found that the reaction rate of the *N*-acylamines is dependent on the *N*-acyl group. Thus, the relative oxidation rates of these compounds are approximately parallel to the acidity of the carboxylic acids from which the *N*-

TABLE I. Oxidation of *N*-Acylpropylamines

Entry	CH <sub>3</sub> CH <sub>2</sub> CH <sub>2</sub> NH-COR		RuO <sub>4</sub> → CH <sub>3</sub> CH <sub>2</sub> CONH-COR		
	1	2	Reaction time (h)	Product yield (%)	p <i>K</i> <sub>a</sub> of RCO <sub>2</sub> H <sup>(a)</sup> (25°C, H <sub>2</sub> O)
1	a	(CH <sub>3</sub> ) <sub>3</sub> C	4	89	5.05
2	b		5	96	
3	c		5	67	4.20
4	d	CH <sub>3</sub> (CH <sub>2</sub> ) <sub>10</sub>	72	92	–
5	e	(CH <sub>3</sub> ) <sub>2</sub> CH	10	92	4.86
6	f	CH <sub>3</sub> (CH <sub>2</sub> ) <sub>2</sub>	10	90	4.82
7	g	CH <sub>3</sub>	24	81	
8			120 <sup>(a)</sup>	25 (65) <sup>(b)</sup>	4.76
9			120 <sup>(c)</sup>	45	
10	h	Cl <sub>3</sub> C	120	– <sup>(d)</sup>	0.63

a) In a two-phase method using CCl<sub>4</sub> as an organic solvent. b) Recovery (%) of the substrate. c) In a one-phase method using aq. NaIO<sub>4</sub>–RuO<sub>2</sub>·*x*H<sub>2</sub>O. d) Recovery of the substrate.

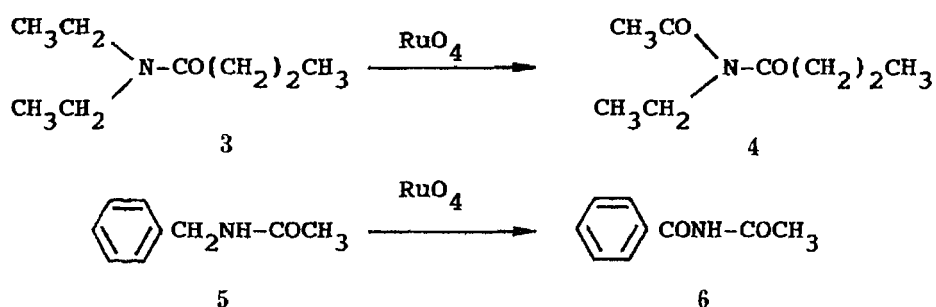
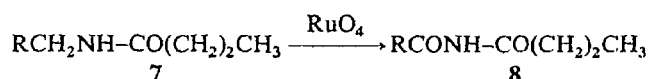


TABLE II.



7	R	Reaction time (h)	Yield (%) of 8
a	(CH <sub>3</sub> ) <sub>2</sub> CH	6	92
b	ClCH <sub>2</sub>	20	82
c	H <sub>5</sub> C <sub>2</sub> O <sub>2</sub> CCH <sub>2</sub>	120	— <sup>a)</sup>
d	NC	120	— <sup>a)</sup>
e	H <sub>5</sub> C <sub>2</sub> O <sub>2</sub> C	120	— <sup>a)</sup>

a) Recovery of the substrate.

acyl groups were derived. Namely, the reactivity of RuO<sub>4</sub> oxidation is dependent on the electron density at the nitrogen atom. This is consistent with an earlier suggestion<sup>3a)</sup> by Sheehan and Tulis, who investigated the oxidation of *N*-acylated cyclic amines with RuO<sub>4</sub>. It has been shown that the product yields are little affected by the bulkiness or acidity of the *N*-acyl group.

Next, we examined the oxidation of various amines having an acyl group (Chart 2 and Table II). An *N*-acylated secondary amine **3** was smoothly oxidized to the corresponding imide **4** in 96% yield. This observation can be explained in terms of the increase of electron density at the nitrogen atom. An arylalkylamide **5** of benzylamine type was oxidized to *N*-benzoylalkylamide **6** in moderate yield, as in the case of *N*-benzoylpropylamine **1c** (Table I), due to oxidative degradation of the aromatic ring.<sup>7)</sup> When the reaction was carried out at 0 °C, the yield of **6** was found to increase to 84%. This suggests that the oxidative degradation of the aromatic ring is prevented at the lower reaction temperature. *N*-Butyrylamines (**7a** and **7b**) having an alkyl or halogen group at the β-position with respect to the nitrogen atom were smoothly oxidized to the corresponding imides (**8a** and **8b**) in 92% and 82% yields, respectively. However, with the *N*-butyrylamines (**7c**—**e**) bearing an electron-withdrawing group at the α- or β-position from the nitrogen atom, the reaction did not progress even after 120 h. These results show that the electron density at the methylene moiety adjacent to the nitrogen atom significantly affects the reactivity.

In conclusion, RuO<sub>4</sub> oxidation should be a useful method for the synthesis of simple symmetrical and unsymmetrical acyclic imides, which have generally been prepared under drastic reaction conditions which have resulted in low yields.<sup>8)</sup>

#### Experimental

All melting points were measured on a Yanagimoto micro melting point apparatus and are uncorrected. IR

spectra were recorded on a JASCO IRA-2 or Hitachi 270-30 spectrometer. MS were measured on a JEOL JMS D-300 spectrometer. NMR spectra were obtained at 23°C using tetramethylsilane as an internal standard with a JEOL JNM-MH-100 spectrometer. Column chromatography was performed on Merck silica gel (70–230 mesh).

**Starting Materials for the RuO<sub>4</sub> Oxidation**—All the starting *N*-acylamines (**1a–h**, **3**, **5**, and **7a–e**) were prepared from commercially available amines and amino acid esters by acylation with the corresponding acid chlorides under the Shotten-Baumann reaction conditions (benzene- or EtOH-aqueous Na<sub>2</sub>CO<sub>3</sub>, 0–5°C) and purified by distillation or recrystallization.

The samples for the RuO<sub>4</sub> oxidation were characterized as described below.

*N*-Propylpivalamide (**1a**): bp 75–76°C (1 mmHg), colorless solid. *Anal.* Calcd for C<sub>8</sub>H<sub>17</sub>NO: C, 67.09; H, 11.96; N, 9.78. Found: C, 67.14; H, 11.82; N, 9.66.

*N*-Propylcyclohexanecarboxamide (**1b**): mp 65–67°C, colorless solid. *Anal.* Calcd for C<sub>10</sub>H<sub>19</sub>NO: C, 70.96; H, 11.32; N, 8.28. Found: C, 70.88; H, 11.21; N, 8.10.

*N*-Propylbenzamide (**1c**): mp 81–82°C (lit.<sup>9</sup> mp 84.5°C), colorless plates (from hexane).

*N*-Propyl-dodecanamide (**1d**): mp 57–58°C, colorless scales. *Anal.* Calcd for C<sub>15</sub>H<sub>31</sub>NO: C, 74.63; H, 12.94; N, 5.80. Found: C, 74.54; H, 12.87; N, 5.82.

*N*-Propyl-isobutyramide (**1e**): bp 90–91°C (1 mmHg), colorless solid. *Anal.* Calcd for C<sub>7</sub>H<sub>15</sub>NO: C, 65.07; H, 11.70; N, 10.84. Found: C, 65.21; H, 11.73; N, 10.79.

*N*-Propylbutyramide (**1f**): bp 83–84°C (1 mmHg) (lit.<sup>10</sup> bp 93°C (0.3 mmHg)), colorless solid.

*N*-Propylacetamide (**1g**): bp 91–93°C (8 mmHg) (lit.<sup>10</sup> bp 110–112°C (10 mmHg)), colorless oil.

*N*-Propyltrichloroacetamide (**1h**): bp 88–89°C (1 mmHg), colorless solid. *Anal.* Calcd for C<sub>5</sub>H<sub>8</sub>Cl<sub>3</sub>NO: C, 29.37; H, 3.94; N, 6.85. Found: C, 29.20; H, 3.88; N, 6.84.

*N,N*-Diethylbutyramide (**3**): bp 71–72°C (4 mmHg) (lit.<sup>11</sup> bp 89°C (12 mmHg)), colorless oil.

*N*-Benzylacetamide (**5**): mp 56.5–57°C (lit.<sup>12</sup> mp 60–61°C), colorless needles (from hexane).

*N*-Isobutylbutyramide (**7a**): bp 110°C (5 mmHg) (lit.<sup>13</sup> bp 137°C (17 mmHg)), colorless oil.

*N*-2-Chloroethylbutyramide (**7b**): bp 111°C (5 mmHg), colorless solid. *Anal.* Calcd for C<sub>6</sub>H<sub>12</sub>ClNO: C, 48.17; H, 8.09; N, 9.36. Found: C, 48.10; H, 8.21; N, 9.43.

TABLE III. MS and IR Spectral Data and Elemental Analyses for the Imides

Compounds	MS <i>m/z</i> (M <sup>+</sup> )	IR $\nu_{\text{max}}^{\text{KB}} \text{ cm}^{-1}$	Analysis (%) Calcd (Found)		
			C	H	N
<b>2a</b>	157	3330, 1742	61.12	9.62	8.91
		1520, 1510	(61.02)	9.54	8.89)
<b>2b</b>	183	3280, 1738	65.54	9.35	7.64
		1522	(65.46)	9.32	7.54)
<b>2c</b>	177	3296, 1716			
		1682, 1506			
<b>2d</b>	255	3389, 3272	70.54	11.45	5.48
		1742, 1546	(70.46)	11.61	5.56)
<b>2e</b>	143	3290, 1740	58.72	9.15	9.78
		1530	(58.65)	9.20	9.73)
<b>2f</b>	143	3276, 1740	58.72	9.15	9.78
		1550, 1525	(58.70)	9.18	9.69)
<b>2g</b>	115	3270, 1735			
		1538, 1510			
<b>4</b>	157	1700 <sup>a)</sup>	61.12	9.62	8.91
			(61.15)	9.62	8.87)
<b>6</b>	163	3280, 1742			
		1516			
<b>8a</b>	157	3280, 1734	61.12	9.62	8.91
		1528	(61.02)	9.49	8.84)
<b>8b</b>	163	3270, 1748	44.05	6.16	8.56
		1544, 1504	(44.17)	6.04	8.47)

a) Measured neat.

TABLE IV. <sup>1</sup>H-NMR Spectral Data for the Imides

Compounds	<sup>1</sup> H-NMR (CDCl <sub>3</sub> ) δ
2a	1.51 and 2.94 (3H, t, and 2H, q, <i>J</i> =7 Hz, COEt), 8.66 (1H, br s, NH)
2b	1.07 and 2.56 (3H, t, and 2H, q, <i>J</i> =7 Hz, COEt), 1.09—1.92 and 2.20—2.48 (total 11H, m, C <sub>6</sub> H <sub>11</sub> ), 7.88 (1H, br s, NH)
2c	1.16 and 2.89 (3H, t, and 2H, q, <i>J</i> =7 Hz, COEt), 7.10—7.34 and 7.56—7.70 (3H, m, and 2H, m, aromatic H), 9.00 (1H, br s, NH)
2d	0.92 (3H, t, <i>J</i> =7 Hz, CH <sub>3</sub> ), 1.20 (3H, t, <i>J</i> =7 Hz, COCH <sub>2</sub> CH <sub>3</sub> ), 1.13—1.89 (18H, m, COCH <sub>2</sub> (CH <sub>2</sub> ) <sub>9</sub> CH <sub>3</sub> ), 2.74 (2H, t, <i>J</i> =7 Hz, COCH <sub>2</sub> C <sub>10</sub> H <sub>23</sub> ), 2.76 (2H, q, <i>J</i> =7 Hz, COCH <sub>2</sub> CH <sub>3</sub> ), 9.62 (1H, br s, NH)
2e	1.15 and 2.94 (3H, t, and 2H, q, <i>J</i> =7 Hz, COEt), 1.28 (9H, s, CMe <sub>3</sub> ), 8.66 (1H, br s, NH)
2f	0.98 (3H, t, <i>J</i> =7 Hz, CO(CH <sub>2</sub> ) <sub>2</sub> CH <sub>3</sub> ), 1.16 (3H, t, <i>J</i> =7 Hz, COCH <sub>2</sub> CH <sub>3</sub> ), 1.49—1.89 (2H, m, COCH <sub>2</sub> CH <sub>2</sub> ), 2.65 (2H, q, <i>J</i> =7 Hz, COCH <sub>2</sub> CH <sub>2</sub> ), 2.68 (2H, q, <i>J</i> =7 Hz, COCH <sub>2</sub> CH <sub>3</sub> ), 9.60 (1H, br s, NH)
2g	1.18 and 2.64 (3H, t, and 2H, q, <i>J</i> =7 Hz, COEt), 2.42 (3H, s, COMe), 9.68 (1H, br s, NH)
4	1.02 (3H, t, <i>J</i> =7 Hz, CO(CH <sub>2</sub> ) <sub>2</sub> CH <sub>3</sub> ), 1.25 (3H, t, <i>J</i> =7 Hz, NCH <sub>2</sub> CH <sub>3</sub> ), 1.64—1.98 (2H, m, COCH <sub>2</sub> CH <sub>2</sub> ), 2.53 (3H, s, COMe), 2.80 (2H, t, <i>J</i> =7 Hz, COCH <sub>2</sub> ), 3.94 (2H, q, <i>J</i> =7 Hz, NCH <sub>2</sub> )
6	2.55 (3H, s, COMe), 7.34—7.62 and 7.80—7.98 (3H, m, and 2H, m, aromatic H), 9.32 (1H, br s, NH)
8a	0.97 (3H, t, <i>J</i> =7 Hz, CH <sub>2</sub> CH <sub>3</sub> ), 1.16 and 1.23 (total 6H, each s, Me <sub>2</sub> ), 1.53—1.86 (2H, m, COCH <sub>2</sub> ), 2.58—2.98 (3H, m, COCH and COCH <sub>2</sub> ), 8.88 (1H, br s, NH)
8b	0.99 (3H, t, <i>J</i> =7 Hz, Me), 1.56—1.82 (2H, m, CH <sub>2</sub> Me), 2.62 (2H, t, <i>J</i> =7 Hz, COCH <sub>2</sub> Et), 4.38 (2H, s, COCH <sub>2</sub> Cl), 8.99 (1H, br s, NH)

Ethyl *N*-Butyryl-β-alaninate (7c): bp 138—140 °C (7 mmHg), colorless oil. *Anal.* Calcd for C<sub>9</sub>H<sub>17</sub>NO<sub>3</sub>: C, 57.73; H, 9.15; N, 7.48. Found: C, 57.65; H, 9.00; N, 7.55.

*N*-Cyanomethylbutyramide (7d): bp 154 °C (5 mmHg) (lit.<sup>14</sup>) bp 146—148 °C (3 mmHg), colorless oil.

Ethyl *N*-Butyryl-glycinate (7e): bp 128—130 °C (8 mmHg) (lit.<sup>15</sup>) bp 124 °C (3 mmHg), colorless oil.

**General Procedure for the RuO<sub>4</sub> Oxidation of *N*-Acylamines (1a—h, 3, 5, and 7a—e) in a Two-Phase System Using AcOEt**—A solution of substrates (6 mmol) to be oxidized in AcOEt (20 ml) was added to a mixture of RuO<sub>2</sub>·xH<sub>2</sub>O (100 mg) and 10% aqueous NaIO<sub>4</sub> (30 ml). The mixture was vigorously stirred in a sealed flask at room temperature. After the starting material had disappeared as determined by TLC, the layers were separated. The aqueous layer was extracted with three 20-ml portions of AcOEt. The combined AcOEt solution was treated with isopropyl alcohol (2 ml) for 2—3 h to destroy the RuO<sub>4</sub> oxidant. Black-colored RuO<sub>2</sub> which precipitated from the solution was filtered off and the filtrate was washed with saturated NaCl solution, then dried over anhydrous Na<sub>2</sub>SO<sub>4</sub>. The solution was concentrated *in vacuo* to leave a residue, which was purified by recrystallization for the solid products or by vacuum distillation for the oily products. The results are summarized in Tables I and II, and Chart 2. Analytical and spectral (MS, IR, and <sup>1</sup>H-NMR) data for the oxidation products (2a—g, 4, 6, 8a, and 8b) are listed in Tables III and IV.

*N*-Propionylpivalamide (2a): mp 60—61 °C, colorless prisms (from H<sub>2</sub>O).

*N*-Propionylcyclohexanecarboxamide (2b): mp 124.5—125 °C, colorless prisms (from 70% EtOH).

*N*-Propionylbenzamide (2c): mp 96—98 °C (lit.<sup>16</sup>) mp 98 °C, colorless prisms (from hexane).

*N*-Propionyl-isobutyramide (2e): mp 124—126 °C, colorless needles (from hexane).

*N*-Propionylbutyramide (2f): mp 112.5—113 °C, colorless needles (from hexane).

*N*-Acetylpropionamide (2g): mp 89—90 °C (lit.<sup>17</sup>) mp 86—87 °C, colorless needles (from hexane).

*N*-Acetyl-*N*-ethylbutyramide (4): The oxidation of 3 was carried out under the general conditions for 3 h to give 4 (96%) as a colorless oil, bp 110—115 °C (bath temp.)/6 mmHg.

*N*-Acetylbenzamide (6): 1) The oxidation of 5 was carried out under the general conditions for 2 h to give 6 as a colorless solid (64%), which was recrystallized from 70% EtOH as colorless needles, mp 116.5—117 °C (lit.<sup>18</sup>) mp 117—118 °C.

2) A similar oxidation of 5 was carried out at 0 °C for 7 h to give 6 (84%).

*N*-Isobutyrylbutyramide (8a): mp 113—114 °C, colorless needles (from hexane).

*N*-Chloroacetylbutyramide (8b): mp 115—116 °C, colorless prisms (from hexane).

**RuO<sub>4</sub> Oxidation of 1g in a One-Phase System**—The substrate (1g) (607 mg, 6 mmol) was added to a mixture of

$\text{RuO}_2 \cdot x\text{H}_2\text{O}$  (100 mg) and 10% aqueous  $\text{NaIO}_4$  solution (30 ml), and the mixture was vigorously stirred at room temperature in a sealed flask. After disappearance of the substrate, the reaction mixture was extracted with three 20-ml portions of AcOEt. The aqueous layer was concentrated *in vacuo* to leave a white solid, which was triturated with two 20-ml portions of AcOEt. The AcOEt extracts were combined, dried over anhydrous  $\text{Na}_2\text{SO}_4$  and concentrated *in vacuo* to give crude **2g**, which was purified by column chromatography on  $\text{SiO}_2$  with AcOEt-hexane (1:2, v/v) as an eluent to give **2g** (310 mg, 45%).

**RuO<sub>4</sub> Oxidation of 1g in a Two-Phase System Using CCl<sub>4</sub>**—Oxidation of **1g** was carried out under the general conditions in  $\text{CCl}_4$  as an organic solvent for 120 h, then the reaction mixture was worked up in a manner similar to that described above. The crude oxidation products were purified by column chromatography on  $\text{SiO}_2$  with AcOEt-hexane (1:2, v/v) as an eluent. From the earlier part of the eluate, **2g** (25%) was obtained. From the later part, **1g** (65%) was recovered.

**Oxidation of 1h, Ethyl N-Butyl- $\beta$ -alaninate (7c), N-Cyanomethylbutyramide (7d), and Ethyl N-Butylglycinate (7e)**—The oxidation of these compounds (**1h**, **7c**, **7d**, and **7e**) did not progress under the general conditions for 120 h. The recovery of each starting material was 86–92%.

#### References

- 1) A part of this work was presented at the 11th Symposium on Progress in Organic Reactions and Syntheses, Nagasaki, Japan, Nov. 1984, p. 81.
- 2) D. G. Lee and M. van den Engl, "Oxidation in Organic Chemistry," Part B, ed. by W. S. Trahanovsky, Academic Press, New York, 1973, Chapter 4.
- 3) a) J. C. Sheehan and R. W. Tulis, *J. Org. Chem.*, **39**, 2264 (1974); b) N. Tangari and V. Tortorella, *J. Chem. Soc., Chem. Commun.*, **1975**, 71; c) R. Perrone, G. Bettoni, and V. Tortorella, *Synthesis*, **1976**, 598; d) G. Bettoni, G. Carbonara, C. Franchini, and V. Tortorella, *Tetrahedron*, **37**, 4159 (1981); e) S. Yoshifuji, K. Tanaka, T. Kawai, and Y. Nitta, *Chem. Pharm. Bull.*, **33**, 5515 (1985).
- 4) L. M. Berkowitz and P. N. Rylander, *J. Am. Chem. Soc.*, **80**, 6682 (1958).
- 5) S. Yoshifuji, K. Tanaka, and Y. Nitta, *Chem. Pharm. Bull.*, **33**, 1749 (1985).
- 6) Z. Rappoport, "Handbook of Tables for Organic Compound Identification," 3rd ed., CRC Press, Inc., Cleveland, 1967, p. 428.
- 7) D. C. Ayres, *J. Chem. Soc., Chem. Commun.*, **1975**, 440.
- 8) R. B. Bates, F. A. Fletcher, K. D. Janda, and W. A. Miller, *J. Org. Chem.*, **49**, 3038 (1984) and references cited therein.
- 9) A. W. Titherly, *J. Chem. Soc.*, **79**, 405 (1901).
- 10) G. M. Burnett and K. M. Riches, *J. Chem. Soc. (B)*, **1966**, 1229.
- 11) C. R. Hauser and H. G. Walker, Jr., *J. Am. Chem. Soc.*, **69**, 295 (1947).
- 12) H. Amsel and A. W. Hofmann, *Ber.*, **19**, 1286 (1886).
- 13) S. I. Gertler and A. P. Yerington, U. S. Dep. Ag. Research Service, Entomol. Research Branch ARS-33-31, 1956, p. 10 [*Chem. Abstr.*, **50**, 17297h (1956)].
- 14) A. Kotelko, *Acta Polon. Pharm.*, **19**, 109 (1962) [*Chem. Abstr.*, **59**, 1482f (1963)].
- 15) G. Ya. Kondrateva and C.-H. Hung, *Zh. Obshch. Khim.*, **32**, 2348 (1962) [*Chem. Abstr.*, **58**, 7919h (1963)].
- 16) J. B. Polya and T. M. Spotwood, *Recl. Trav. Chim. Pays-Bas*, **67**, 927 (1948) [*Chem. Abstr.*, **43**, 4221b (1949)].
- 17) Q. E. Thompson, *J. Am. Chem. Soc.*, **73**, 5841 (1951).
- 18) A. W. Titherly and T. H. Holden, *J. Chem. Soc.*, **101**, 1871 (1912).

[Chem. Pharm. Bull.  
35(1) 370-376 (1987)]

## Interactions between Furosemide and Spironolactone in Normal Subjects

KATSUYOSHI UCHINO,\*<sup>a</sup> SADA0 ISOZAKI,<sup>a,1a)</sup> NAOMI TANAKA,<sup>b,1b)</sup>  
YUKIYA SAITOH<sup>a</sup> and FUJIO NAKAGAWA<sup>a</sup>

*Hospital Pharmacy<sup>a</sup> and The First Department of Medicine,<sup>b</sup>  
Faculty of Medicine, University of Tokyo, 3-1, Hongo  
7-chome, Bunkyo-ku, Tokyo 113, Japan*

(Received July 23, 1986)

Furosemide (FD) and spironolactone (SP) were co-administrated to human volunteers, and the pharmacokinetics and time course of diuresis were examined. The time courses of FD plasma concentration and diuresis after a single co-administration of FD plain tablet and SP were similar to those in the case of FD plain tablet. However, the plasma concentration of SP metabolites (determined as canrenone) during the 2-6 h period after a single co-administration of FD plain tablet and SP was about 0.05-0.15  $\mu\text{g/ml}$  higher than that after administration of SP. The steady-state distribution volume of SP metabolites after co-administration of FD plain tablet and SP was about 30% less than that after administration of SP, while the elimination rate constant of SP metabolites was about 1.5-fold greater. The diuresis during 24 h after a single administration of SP was 0.1-0.3 l.

After multiple administration of SP, the plasma concentration of SP metabolites during the 2-6 h period after co-administration of FD plain tablet and SP was also about 0.1-0.3  $\mu\text{g/ml}$  higher than expected from the time course of SP metabolites simulated by using the data obtained after a single administration of SP. The elevation of SP metabolites concentration in plasma was prevented without any change of diuresis over 24 h by using FD retard capsule instead of FD plain tablet.

We concluded that the phenomenon of elevation of SP metabolites concentration in plasma was caused by FD plain tablet, which induced strong diuresis and considerable loss of body fluids within a short time.

**Keywords**—furosemide; spironolactone; fluorogenic spironolactone metabolite; drug interaction; plasma concentration; diuresis; normal subject

Furosemide (FD) has been widely used for the treatment of cirrhotic patients with ascites. When FD is administered to such patients, side effects such as hypokalemia, disturbance of other electrolytes and hepatic encephalopathy have been reported.<sup>2)</sup> Therefore, the concomitant administration of FD with spironolactone (SP) is recommended for the prophylaxis of hypokalemia and hepatic encephalopathy or the treatment of hyperaldosteronism.<sup>3)</sup> While side effects, mainly gynecomastia, have also been reported during chronic therapy with SP,<sup>4)</sup> their appearance depends on the dose and duration of the drug administration.<sup>4d, e)</sup> Therefore, care is necessary when both drugs are concomitantly administered to cirrhotic patients with ascites. There are few reports concerning the pharmacokinetic interactions between FD and SP after concomitant administration of the drugs in man. Homeidia *et al.*<sup>5)</sup> have reported that the pharmacokinetics of FD was not influenced by SP. Nevertheless, the report did not examine the influence of FD on the pharmacokinetics of SP, or on the diuresis.

The present paper describes the pharmacokinetics and time course of diuresis after concomitant administration of FD and SP to human volunteers.

## Experimental

**Drugs and Reagents**—Authentic FD and canrenone used for all experiments were supplied by Hoechst Japan Ltd., Tokyo, Japan and Dainippon Pharmaceutical Co., Ltd., Osaka, Japan, respectively. Plain tablets (Lasix®) and retard capsules (Eutensine®) containing 40 mg of FD used in this study were obtained from Hoechst Japan Ltd. Tablets (Aldactone® A) containing 25 mg of SP used in this study were obtained from Dainippon Pharmaceutical Co., Ltd. All the other solvents and reagents used were of reagent grade and were obtained from Wako Pure Chemical Industries Ltd., Tokyo.

**Subjects**—The subjects in this study were 3 males, 24–35 years old, weighing 56–68 kg. They were healthy as judged by ordinary clinical examinations and laboratory tests, and participated in this study after being informed of its purpose, procedure and potential hazards. The normal subjects were fed identical meals as reported previously<sup>61</sup> and drank 2000 ml of water a day dispensed in 500 ml aliquots for each time period, *i.e.* 9:00–13:00, 13:00–17:00, 17:00–21:00 and 21:00–9:00 on the next day. The control urine was collected at 9:00–21:00 and 21:00–9:00 on the next day for 5 d without drug in the same manner as described above. The urine volumes measured in each time-interval for 5 d were averaged to obtain control values. The diuresis after administration of each drug was evaluated by subtracting the mean control value from the urine volume observed after administration of the drug.

**Single Dose Study**—FD Plain Tablet: The plasma and urine data after oral administration of FD plain tablet (40 mg) are described in our preliminary report.<sup>61</sup>

SP: Each subject was given orally 50 mg of SP as two 25 mg tablets at 9:00 and blood samples were collected at 0.5, 1, 1.5, 2, 3, 4, 6, 8, 10 and 24 h thereafter, while urine samples were collected at 0–6, 6–12 and 12–24 h.

**Concomitant Administration**—FD Plain Tablet and SP (FD Plain Tablet + SP): Forty milligrams of FD plain tablet and 50 mg of SP were concomitantly administered to three normal subjects at 9:00. Blood samples were collected at 0.5, 0.75, 1, 1.5, 2, 2.5, 3, 4, 5, 6, 8, 10, 12 and 24 h, and urine samples were collected at 1–2, 2–3, 3–4, 4–5, 5–6, 6–8, 8–10, 10–12 and 12–24 h after the administration of the two drugs.

FD Retard Capsule and SP (FD Retard Capsule + SP): Forty milligrams of FD retard capsule and 50 mg of SP were concomitantly administered to one (K.U.) of three normal subjects at 9:00. The samples of blood and urine were collected in the same manner as described for the single dose study of FD plain tablet + SP.

**Multiple Dose Study**—SP (50 mg) was administered to three normal subjects once a day at 9:00 for 8 d. On the 6th day, 50 mg of SP plus 40 mg of FD plain tablet were concomitantly administered. The blood samples on the 1st day after the drug administration were collected at 1, 2, 3, 4 and 24 h, and urine samples were collected at 0–6, 6–12 and 12–24 h. On the 2nd, 3rd, 4th, 5th and 7th days, blood samples were collected at 2 and 24 h, and urine samples were collected in the same manner as described for the 1st day. The samples of plasma and urine on the 6th day were collected in the same manner as described for the single dose study of FD plain tablet + SP, and those on the 8th day were collected in the same manner as described for the single dose study of SP.

**Collection and Treatment of Samples**—Blood was drawn through an indwelling cannula (Hakko® 9G, Hakko Co., Ltd., Tokyo) at the stated time in each study. Plasma was immediately separated from whole blood by centrifugation, and stored at –20°C until the drug analysis. Urine was excreted just before drug administration and collected at the stated time-intervals thereafter in each study. Urine volume was measured and an aliquot was stored at –20°C until analysis.

**Determinations of FD and SP Metabolites in Plasma**—The concentration of FD in plasma was analyzed by high-performance liquid chromatography (HPLC) according to the method of Uchino *et al.*<sup>71</sup>

When SP is administered to man, it is metabolized to canrenone, canrenoate, 7 $\alpha$ -thiomethylspiro lactone, 6 $\beta$ -hydroxy-7 $\alpha$ -thiomethylspiro lactone and others.<sup>61</sup> Since many SP metabolites show fluorescence, total fluorogenic fraction of SP metabolites was used as a measure of effective concentration in this study. These metabolites in plasma were determined as equivalent concentration of canrenone by the modified method of Sadée *et al.*<sup>61</sup> Accordingly, 2 ml of 2 M hydrochloric acid was added to 1 ml of plasma. After standing for 15 min at room temperature, the mixture was extracted with 5 ml of methylene chloride by shaking for 5 min on a mechanical shaker, followed by centrifugation on a KN-70 centrifuge (Kubota Seisakusho, Tokyo) at 1680 g for 5 min. Then 4 ml of the upper organic phase was transferred to another test tube, and 2 ml of 0.1 M sodium hydroxide was added. The mixture was rapidly stirred for 1 min with a Thermo-Mixer TM-105 (Thermonics Co., Ltd., Tokyo). After centrifugation, 3 ml of the upper organic phase was transferred to another test tube, to which 4 ml of 62% sulfuric acid (62 volumes of 96% sulfuric acid and 38 volumes of distilled water) was added. The mixture was shaken for 10 min and centrifuged for 5 min. The upper organic phase was removed by aspiration, and the aqueous phase was allowed to stand for 1 h at room temperature. This solution was used to determine the concentration of SP metabolites in plasma. The apparatus used was a Hitachi 204 fluorescence spectrophotometer (Hitachi Seisakusho, Hitachi, Japan) and the excitation and emission wavelengths for fluorimetric detection of canrenone were set at 465 and 525 nm, respectively. The calibration curve for canrenone concentration in plasma was linear over the concentration range of 0.025 to 0.4  $\mu$ g/ml and passed through the origin.

**Calculation of Pharmacokinetic Parameters from Time Course of Plasma Concentration of FD and SP Metabolites**—The disposition of FD was approximated by a one-compartment open model with apparent first

order absorption and elimination processes, and that of SP metabolites was approximated by two-compartment open model with apparent first order appearance, distribution and elimination processes. The pharmacokinetic parameters of FD or SP metabolites were calculated by using a nonlinear least-squares microcomputer program (MULTI).<sup>10</sup> The disposition of SP metabolites was also calculated by using model-independent analysis.<sup>11</sup>

## Results

The time courses of plasma concentration of FD and diuresis after a single administration of FD plain tablet, or of FD plain tablet+SP in three normal subjects are shown in Fig. 1. The data on FD plain tablet in the upper and lower figures were taken from the previous report.<sup>6</sup> The time course of FD plasma concentration after administration of FD plain tablet+SP was similar to that in the case of FD plain tablet. The diuresis in both cases reached a maximum value of 1.5 l within 3 h, and decreased gradually to about 1.2 l during 24 h.

The plasma concentration of SP metabolites after a single administration of SP reached a maximum value of 0.3–0.45  $\mu\text{g/ml}$  within 3 h. However, the plasma concentration of SP metabolites during the 2–6 h period after a single administration of FD plain tablet+SP was 0.05 to 0.15  $\mu\text{g/ml}$  higher than that after SP administration (Fig. 2). In all subjects, the rate constants of appearance ( $k_{ap}$ ) of SP metabolites in the blood were comparable after administrations of SP and FD plain tablet+SP. The steady-state distribution volume ( $Vd_{ss}$ ) of SP metabolites after administration of FD plain tablet+SP decreased by about 30% compared to that after SP administration. The elimination rate constant ( $k_{el}$ ) of SP metabolites after administration of FD plain tablet+SP was about 1.5-fold higher than that after SP administration. However, total body clearance ( $Cl$ ) of SP metabolites in each subject varied after administration of FD plain tablet+SP. In one subject (Y. Y.),  $Cl$  after SP

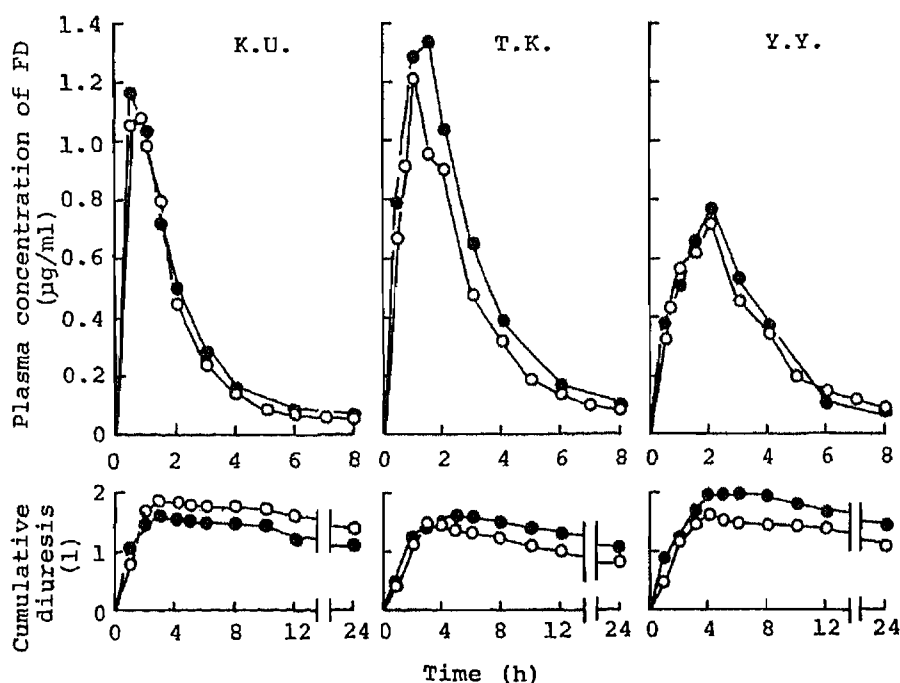


Fig. 1. Time Courses of Plasma Concentration of FD (Upper) and Cumulative Diuresis (Lower) in Three Normal Subjects after Administration of 40 mg of FD Plain Tablet and Concomitant Administration of 40 mg of FD Plain Tablet with 50 mg of SP (FD Plain Tablet+SP)

Observed points for FD plain tablet in the upper and lower figures are taken from the previous study (ref. 6). ○, FD plain tablet; ●, FD plain tablet+SP.



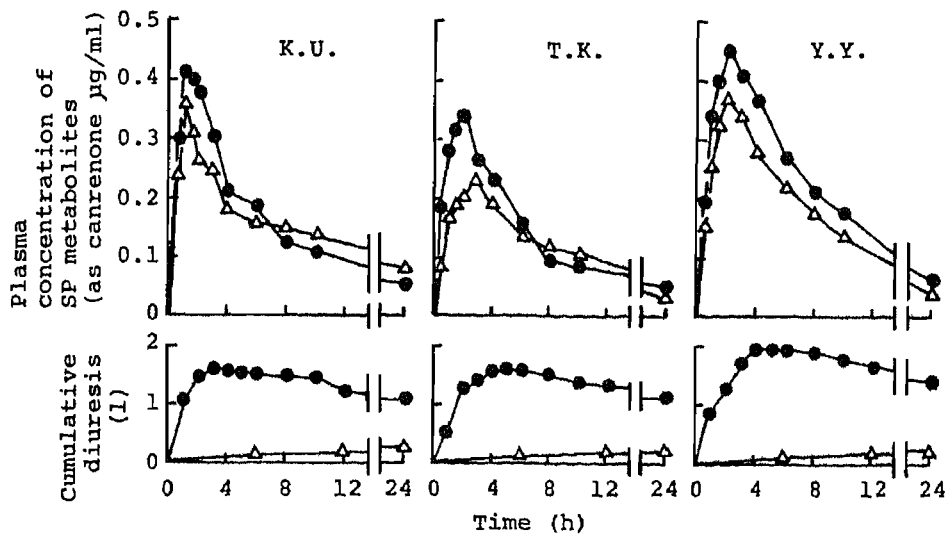


Fig. 2. Time Courses of Plasma Concentration of SP Metabolites (Upper) and Cumulative Diuresis (Lower) in Three Normal Subjects after Administration of 50 mg of SP and Concomitant Administration of 40 mg of FD Plain Tablet with 50 mg of SP (FD Plain Tablet + SP)

Observed points for diuresis after FD plain tablet + SP are the same data as plotted in Fig. 1.  $\Delta$ , SP;  $\bullet$ , FD plain tablet + SP.

TABLE I. Pharmacokinetic Parameters of SP Metabolites Obtained after Single Administration of SP or Concomitant Administration of FD Plain Tablet with SP (FD Plain Tablet + SP)

Drug	Dose (mg)	Subjects	Parameters							
			$\alpha$ ( $h^{-1}$ )	$\beta$ ( $h^{-1}$ )	$k_{ap}^{a)}$ ( $h^{-1}$ )	$k_{el}$ ( $h^{-1}$ )	$AUC$ ( $\mu g/ml \cdot h$ )	$MRT$ (h)	$Vd_{ss}^{b)}$ (l)	$Cl^{c)}$ (l/h)
SP	50	K.U.	1.076	0.031	1.306	0.108	6.327	31.08	245.6	7.90
		T.K.	0.324	0.032	0.566	0.109	3.616	24.05	338.8	14.09
		Y.Y.	0.393	0.058	0.668	0.142	4.466	15.01	160.7	10.71
		Mean $\pm$	0.598	0.040	0.847	0.120	4.803	23.38	248.4	10.90
		S.D.	0.416	0.015	0.401	0.019	1.387	8.06	89.1	3.10
FD Plain tablet + SP	40 + 50	K.U.	0.798	0.064	1.223	0.201	3.878	13.73	177.0	12.89
		T.K.	0.057	0.056	0.742	0.208	3.189	14.34	224.8	15.67
		Y.Y.	0.362	0.079	0.728	0.154	4.675	11.30	120.9	10.71
		Mean $\pm$	0.406	0.066	0.898	0.188	3.914	13.12	174.2	13.06
		S.D.	0.372	0.012	0.282	0.029	0.744	1.61	52.0	2.49

a) Rate constant of appearance of SP metabolites. b) Calculated as  $Vd_{ss} = \text{dose} \cdot f \cdot MRT / AUC, f = 1$ . c) Calculated as  $Cl = Vd_{ss} / MRT$ .

administration was in fair agreement with that after administration of FD plain tablet + SP, whereas  $Cl$  after SP administration in the other subjects was larger than that after administration of FD plain tablet + SP. The mean residence time ( $MRT$ ) of SP metabolites

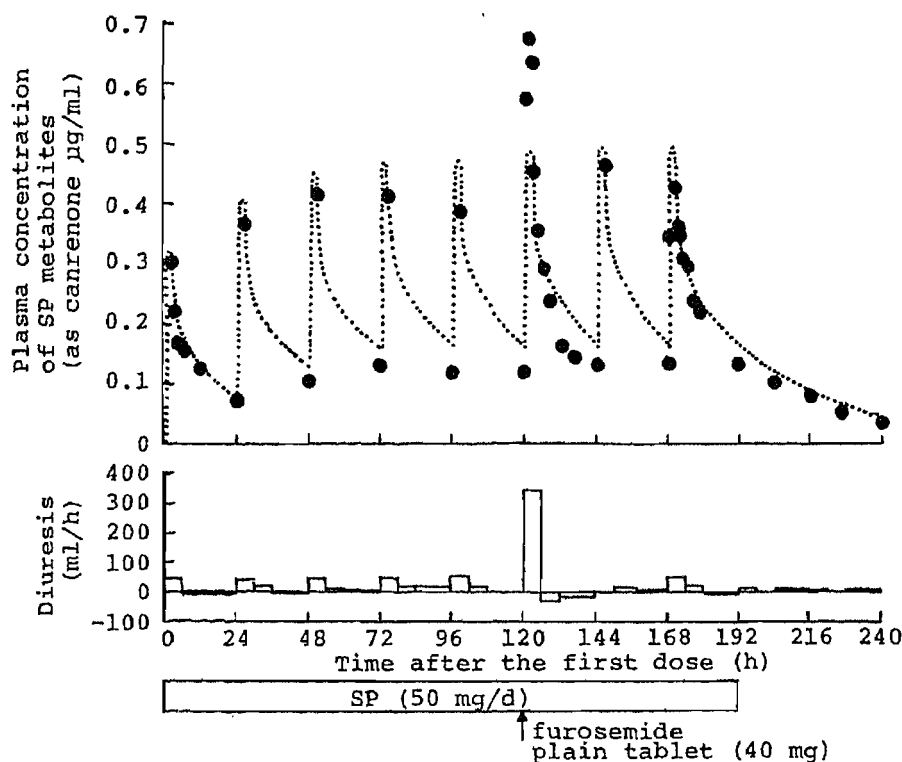


Fig. 3. Time Courses of Plasma Concentration of SP Metabolites (Upper) and Diuresis (Lower) in a Normal Subject (K.U.) during and after an Oral Multiple Administration of 50 mg of SP Once a Day

The dotted line in the upper figure represents the simulation based on pharmacokinetic parameters obtained from the single-dose study of SP.

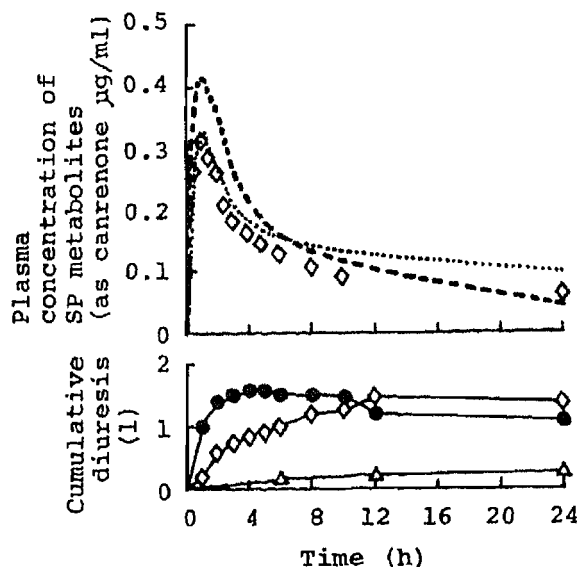


Fig. 4. Time Courses of Plasma Concentration of SP Metabolites (Upper) and Cumulative Diuresis (Lower) in a Normal Subject (K.U.) after Oral Concomitant Administration of 50 mg of SP with 40 mg of FD Retard Capsule

In the upper figure, dotted and broken lines represent the simulations based on pharmacokinetic parameters obtained from single-dose studies of SP and SP+FD plain tablet as shown in Figs. 1 and 2, respectively. In the lower figure, data points (●, △) for diuresis are taken from Figs. 1 and 2, respectively.

decreased by administration of FD plain tablet+SP (Table I).  $Vd_{ss}$  and  $Cl$  of SP metabolites calculated by compartment analysis were approximately consistent with those obtained by model-independent analysis. The diuresis over 24 h after a single administration of SP was very weak, 0.1–0.3 l.

A typical time course after multiple administration of 50 mg of SP once a day in a normal

subject (K. U.) is shown in Fig. 3. The plasma concentrations of SP metabolites observed every day fitted the time course after multiple administration of SP which was simulated by using the pharmacokinetic parameters of SP metabolites after a single administration of SP, with the exception of the 6th day. After a single administration of FD plain tablet+SP, the plasma concentration of SP metabolites during the 2–6 h period on the 6th day was about 0.1 to 0.3  $\mu\text{g/ml}$  higher than that on the 5th day. On the 7th day, the plasma concentration of SP metabolites reverted to the simulated curve.

The diuresis after multiple administration of SP was about 0.3 l a day except on the 6th and 7th days. The diuresis profiles on these days were similar to that after a single administration of SP. On the 6th day, the diuresis was 1.2 l a day and the profile was similar to that after a single administration of FD plain tablet+SP. The diuresis on the 7th day was  $-0.6$  l a day (less than the control value) (Fig. 3).

To control the elevation of plasma concentration of SP metabolites produced by the concomitant administration of FD plain tablet+SP, 50 mg of SP and 40 mg of FD retard capsule were concomitantly administered to a subject (K.U.). The time course of plasma concentration of SP metabolites during the 2–6 h period was similar to that after SP administration (Fig. 4).  $Vd_{ss}$  of SP metabolites after administration of FD retard capsule+SP was 249.6 l, which was similar to that after SP administration, 245.6 l. The  $k_{el}$  and  $Cl$  of SP metabolites after administration of FD retard capsule+SP were  $0.174\text{ h}^{-1}$  and 13.2 l/h, respectively, while the corresponding values after SP administration were  $0.108\text{ h}^{-1}$  and 7.9 l/h. However, the value for  $MRT$  after administration of FD retard capsule+SP, 20.1 h, was smaller than that after SP administration, 31.08 h. The diuresis measured during a 24 h period after administrations of FD retard capsule+SP and FD plain tablet+SP amounted to 1.45 and 1.50 l, respectively. However, quite different diuresis profiles were observed between the two dosage forms.

### Discussion

The disposition of FD and time course of diuresis were not influenced by concomitant administration of SP. A similar finding with respect to intravenous administration of FD was reported by Homeidia *et al.*<sup>5)</sup>

It has been reported that SP after oral administration is metabolized into many metabolites.<sup>8)</sup> Canrenone, one of these metabolites, was measured by fluorimetric assay in previous studies.<sup>9)</sup> However, the method lacks specificity, as other fluorogenic metabolites were measured concomitantly.<sup>13)</sup> Recently, SP and its metabolites in plasma after oral administration of the drug were determined by HPLC separation by Overdiek *et al.*<sup>8d)</sup> However, the fluorimetric method seems to be the appropriate one for a study concerning SP therapy, since the assay value obtained by this method most probably provides a good measure of effective concentration.<sup>12)</sup> The fraction of SP metabolites in plasma was determined as concentration of canrenone by the fluorimetric method in this study.

The time course of SP metabolites after multiple administration of 50 mg of SP was linear in the present study. The pharmacokinetics of canrenone measured by HPLC after a single or multiple administration of SP has been reported to be non-linear.<sup>12a, 13)</sup> This discrepancy may be explained by the fact that the dose of SP giving in non-linear pharmacokinetics of canrenone in the other reports was 2- to 10- fold higher than that used in the present study, and furthermore the inter-dose interval in the other reports was shorter.

The elevation of plasma concentration of SP metabolites by administration of FD plain tablet+SP observed in the single- and multiple-dose studies may arise as follows. Since FD plain tablet induced strong diuresis, and considerable amount of body fluids were lost in normal subjects within a short time,  $Vd_{ss}$  of SP metabolites might become smaller. Such a

decrease of  $Vd_{ss}$  would result in the elevation of SP metabolites concentration in plasma.

It was concluded that the alteration of  $Cl$  of SP metabolites by administration of FD plain tablet + SP arise from individual variations in the extents of decrease of  $Vd_{ss}$  and  $k_{el}$ .

To prevent the elevation of plasma concentration of SP metabolites, FD should be supplied at a rate such that gentle diuresis is maintained for a long time. We reported that the diuresis after administration of retard capsule as a sustained-release dosage form of FD was moderately prolonged compared to that after administration of FD plain tablet, and furthermore the diuresis during a 24 h period was the same for the two dosage forms.<sup>6)</sup> When FD retard capsule and SP were concomitantly administered to a normal subject, the plasma concentration during the 2—6 h period and  $Vd_{ss}$  of SP metabolites after a single administration of FD retard capsule + SP were similar to those after SP administration, and the diuresis over 24 h in the case of FD retard capsule + SP was also similar to that after administration of FD plain tablet + SP (Fig. 4). It is suggested that the elevation of SP metabolites concentration in plasma observed after concomitant administration of SP and FD plain tablet is caused by the strong diuresis induced by FD plain tablet. Thus, we succeeded in preventing the elevation of SP metabolites concentration in plasma without affecting diuresis over 24 h by using FD retard capsule instead of FD plain tablet.

When the concomitant administration of FD with SP is required for the treatment of cirrhotic patients with ascites, the plasma concentration of SP metabolites will probably be elevated by the administration of FD plain tablet. Thus, the use of FD retard capsule should reduce the incidence of side effects following SP administration.

**Acknowledgement** This work was supported in part by a Grant-in-Aid for Co-operative Research (60304083) from The Ministry of Education, Science and Culture of Japan. The authors are grateful to Mrs. Michele McNeil for assistance in the preparation of this manuscript.

#### References and Notes

- 1) a) Present address: Hospital Pharmacy, Tokyo Teishin Hospital, 14-23, Fujimi 2-chome, Chiyoda-ku, Tokyo 102, Japan; b) Present address: The Department of Medicine, Institute of Clinical Medicine, University of Tsukuba, Sakura-mura, Nihari-gun, Ibaraki 305, Japan.
- 2) S. Sherlock, B. Senewiratne, A. Scott and J. G. Walker, *Lancet*, **1**, 1049 (1966); C. A. Naranjo, U. Busto and L. Cassis, *Am. J. Hosp. Pharm.*, **35**, 794 (1978); C. A. Naranjo, E. Pontigo, C. Valdengro, G. Gonzalez, I. Ruiz and U. Busto, *Clin. Pharmacol. Ther.*, **25**, 154 (1979).
- 3) AMA Division of Drug, "AMA Drug Evaluations," 5th ed., American Medical Association, Philadelphia, 1983, pp. 759—760; A. G. Gilman, L. S. Goodman, T. W. Rall and F. Murad, "The Pharmacological Basis of Therapeutics," 7th ed., MacMillan Publishing Co., New York, 1985, p. 901.
- 4) a) N. M. Mann, *J. Am. Med. Assoc.*, **184**, 778 (1963); b) R. M. Sussman, *Lancet*, **1**, 58 (1963); c) E. Clark, *J. Am. Med. Assoc.*, **193**, 163 (1965); d) R. Caminos-Torres, L. Ma and P. J. Snyder, *J. Clin. Endocrinol. Metab.*, **45**, 255 (1977); e) G. Schrijver and M. H. Weinberger, *Clin. Pharmacol. Ther.*, **25**, 33 (1979).
- 5) M. Homeidia, C. Roberts and R. Branch, *Clin. Pharmacol. Ther.*, **21**, 402 (1977).
- 6) K. Uchino, S. Isozaki, J. Amano, N. Tanaka, Y. Saitoh, F. Nakagawa, Z. Tamura and H. Oka, *J. Pharmacobio-Dyn.*, **6**, 684 (1983).
- 7) K. Uchino, S. Isozaki, Y. Saitoh, F. Nakagawa, Z. Tamura and N. Tanaka, *J. Chromatogr.*, **308**, 241 (1984).
- 8) a) A. Karim, *Drug Metab. Rev.*, **8**, 151 (1978); b) A. Karim, J. Hribar and M. Doherty, *Xenobiotica*, **7**, 585 (1977); c) U. Abshagen, H. Rennkamp and G. Luszpinski, *Naunyn-Schmiedberg Arch. Pharmacol.*, **296**, 37 (1976); d) H. W. P. M. Overdiek, W. A. J. J. Hermens and F. W. H. M. Merkus, *Clin. Pharm. Ther.*, **38**, 469 (1985).
- 9) a) W. Sadée, M. Dagioglu and S. Riegelman, *J. Pharm. Sci.*, **61**, 1126 (1972); b) C. Gochman and C. L. Gant, *J. Pharmacol. Exp. Ther.*, **135**, 1312 (1962).
- 10) K. Yamaoka, Y. Tanigawara, T. Nakagawa and T. Uno, *J. Pharmacobio-Dyn.*, **4**, 879 (1981).
- 11) K. Yamaoka, T. Nakagawa and T. Uno, *J. Pharmacokinet. Biopharm.*, **6**, 547 (1978); L. Z. Benet and R. L. Galeazzi, *J. Pharm. Sci.*, **68**, 1071 (1979).
- 12) U. Abshager, E. Besenfelder, R. Endeke, K. Kooch and B. Neubert, *Eur. J. Clin. Pharmacol.*, **16**, 255 (1979); W. Sadée and G. C. M. Beelen, "Drug Level Monitoring Analytical Technique, Metabolism, and Pharmaceuticals," John Wiley & Sons, Inc., New York, 1980, pp. 423—426.
- 13) P. C. Ho, D. W. A. Bourne, E. J. Triggs and V. Healewood, *Eur. J. Clin. Pharmacol.*, **27**, 441 (1984).

[Chem. Pharm. Bull.]  
35(1) 377-388 (1987)

## Determination of Partition Coefficient and Acid Dissociation Constant by High-Performance Liquid Chromatography on Porous Polymer Gel as a Stationary Phase

KEISHIRO MIYAKE,\*<sup>a</sup> FUKIKO KITaura,<sup>a</sup> NOBUYASU MIZUNO<sup>a</sup>  
and HIROSHI TERADA<sup>b</sup>

*Faculty of Pharmaceutical Sciences, Mukogawa Women's University,<sup>a</sup> Edagawa-cho,  
Nishinomiya 663, Japan and Faculty of Pharmaceutical Sciences,  
University of Tokushima,<sup>b</sup> Shomachi-1,  
Tokushima 770, Japan*

(Received August 4, 1986)

The availability of porous polymer gel as a stationary phase in high-performance liquid chromatography (HPLC) for determination of the partition coefficient between octanol and water ( $P_{\text{oct}}$ ), and the acid dissociation constant ( $\text{p}K_{\text{A}}$ ) was examined for a wide variety of compounds.

The log of capacity factor  $k'$  increased linearly with increase in  $\log P_{\text{oct}}$ , when the hydrogen bonding ability of compounds was taken into account. However, aromatic compounds that possess an amino group such as procaine, anilines and sulfonamides showed anomalous chromatographic behavior from the viewpoint of the hydrogen-bonding ability. Furthermore, quinolines and pyridines also were anomalous. With these chromatographic characteristics in mind,  $\log P_{\text{oct}}$  can be determined very accurately for various compounds by HPLC over a wide range of pH.

Since this stationary phase is stable over a wide range of pH, HPLC could be run in the alkaline region, in contrast to the octadecyl silica (ODS) column, which is unstable above pH 7. From the capacity factor  $k'$  at various pH,  $\text{p}K_{\text{A}}$  values of various acids, bases and amphoteric compounds were determined very accurately.

In conclusion, the porous polymer gel can be used as a stationary phase in HPLC in a range between acidic and alkaline regions. This stationary phase is effective for determining  $P_{\text{oct}}$  and  $\text{p}K_{\text{A}}$  values simultaneously or separately.

**Keywords** — porous polymer gel; mobile phase; capacity factor; HPLC; partition coefficient; octanol-water; acid dissociation constant; amphoteric compound

### Introduction

Studies of quantitative structure-activity relations (QSAR) showed that the partition coefficient between octanol and water  $P_{\text{oct}}$  is one of the most effective physical parameters of bioactive compounds for predicting their biological activities.<sup>1)</sup> However, determination of  $P_{\text{oct}}$  by the conventional shaking-flask method is tedious and not simple. Furthermore, it is very difficult to determine  $P_{\text{oct}}$  of very hydrophobic compounds.<sup>2)</sup> Recently, high-performance liquid chromatography (HPLC) has been widely used for determination of  $P_{\text{oct}}$ , since this method is very simple, rapid and accurate.<sup>3,4)</sup>

In many cases, a linear relation between  $\log P_{\text{oct}}$  and the logarithm of the capacity factor  $k'$  in HPLC is observed.<sup>3-5)</sup> By using this relation,  $\log P_{\text{oct}}$  values have been determined.<sup>3-5)</sup> However, the value of  $k'$  is dependent largely on the nature of the stationary phase and the composition of the mobile phase. We recently reported that glyceryl-coated controlled pore glass beads (Gly-CPG) represent a very efficient stationary phase to determine  $\log P_{\text{oct}}$ , because they provide a single correlation curve for a wide variety of compounds. With this stationary phase,  $\log P_{\text{oct}}$  up to 6 can be determined accurately.<sup>6)</sup>

Octadecyl silica (ODS) is the most widely used stationary phase in reversed-phase high-performance liquid chromatography (RP-HPLC). Determination of  $\log P_{\text{oct}}$  with this column has also been studied extensively.<sup>7)</sup>  $\log P_{\text{oct}}$  up to about 8 or more was reported to be determined.<sup>8)</sup> However, the value of  $k'$  is dependent on the hydrogen-bonding ability of test compounds,<sup>9)</sup> unlike the case with the Gly-CPG column.

Though the HPLC method with these columns is very useful for determination of  $\log P_{\text{oct}}$ , chromatography cannot be carried out in the alkaline region, because the chemically bonded stationary phase becomes unstable and the supporting silica becomes soluble in the aqueous mobile phase, though they are stable in acidic and neutral regions.<sup>10)</sup> Thus, determination of  $\log P_{\text{oct}}$  has been carried out mostly with unionizable compounds or the neutral form of acids. However, the  $\log P_{\text{oct}}$  value of the neutral form of a basic compound whose acid dissociation constant,  $\text{p}K_{\text{A}}$ , is more than about 6 cannot be determined by chromatography on these columns.

The porous polymer resin styrene-divinylbenzene copolymer (Hitachi gel 3011-O) has been used as a packing material in the analysis of peptides<sup>11)</sup> and miscellaneous drugs.<sup>12)</sup> Since this does not contain any silanol group, it is stable in the alkaline region as well as in the acidic region.<sup>13)</sup> Thus, we studied the chromatographic behavior of basic and acidic compounds with this stationary phase, and examined the applicability of this stationary phase for determination of  $\log P_{\text{oct}}$  and  $\text{p}K_{\text{A}}$  by HPLC over a wide range of pH of the mobile phase.

### Experimental

Chemicals used were commercial products, and they were used without further purification. They were dissolved in methanol (MeOH) to a concentration of about 0.5 mg/ml, and 0.2–4  $\mu\text{l}$  of the solution was injected onto the column.

RP-HPLC was carried out with a TRIOTAR-II (JASCO, Tokyo) equipped with a ultraviolet-detector, UVIDEC-III (JASCO). Hitachi gel 3011-O was packed in stainless steel tubing (i.d. 4.6 mm  $\times$  50 mm), and used as the stationary phase. The acidic mobile phase was a mixture of phosphoric acid, pH 2.0, and an organic solvent, and the alkaline mobile phase was a mixture of NaOH solution, pH 11.0, and an organic solvent. Either MeOH or acetonitrile ( $\text{CH}_3\text{CN}$ ) was used as an organic modifier, and its concentration was expressed in terms of % (v/v).

When the  $k'$  values were determined at various pH's (section 3), a mixture of citric acid, phosphoric acid, boric acid, NaOH and  $\text{HCl}$ <sup>14)</sup> between pH 2–8, and that of sodium bicarbonate and NaOH between pH 8–12 were used as the mobile phase. In both cases, MeOH was added to make 30%.

Chromatography was performed at 30 °C, and the flow-rate of the mobile phase was 0.5–2 ml/min. The retention time  $t_{\text{R}}$  was determined from those in 3 to 5 runs with various sample injection volumes. The  $t_{\text{R}}$  was confirmed to take a constant value.

The value of  $k'$  was determined from the retention times of the sample compound and of the unretained reference compound  $t_0$  by means of Eq. 1. Potassium iodide was used as a non-retained reference compound.<sup>6,9)</sup>

$$k' = (t_{\text{R}} - t_0) / t_0 \quad (1)$$

Values of  $\log P_{\text{oct}}$  for some benzyl alcohols were determined by the shaking-flask method. The water-saturated octanol (5 ml) was equilibrated with the octanol-saturated aqueous sample solution (20 ml), and  $\log P_{\text{oct}}$  was calculated from the sample concentrations, before and after equilibration, in the aqueous phase determined spectrophotometrically at the maximum absorption wavelength.

## Results and Discussion

### 1. Dependence of $k'$ on the Concentration of Organic Modifier in the Mobile Phase

Figure 1A shows the dependence of  $\log k'$  of the neutral compounds benzene and cyanobenzene, and the acidic compound 4-methylphenol on the concentration of  $\text{CH}_3\text{CN}$ , in the range of 10 to 60% in the acidic mobile phase at pH 2.0. The changes are not linear, unlike the cases with ODS<sup>9)</sup> and Gly-CPG.<sup>6)</sup> A similar dependence of  $\log k'$  on the  $\text{CH}_3\text{CN}$  concentration was observed with the basic compounds 3-chloropyridine, 2-methoxyaniline and quinoline at pH 11.0, as shown in Fig. 1B. It is apparent that the data points fall well on

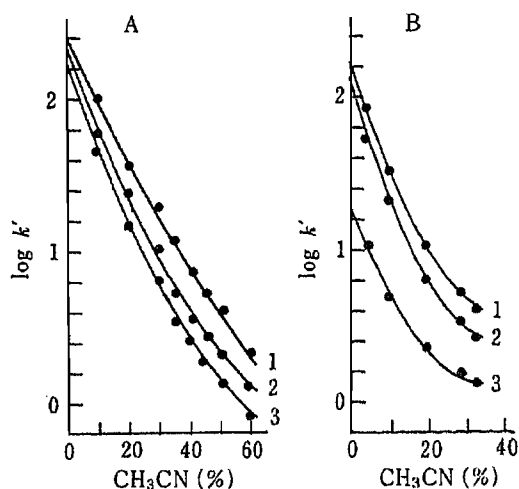


Fig. 1. Effect of  $\text{CH}_3\text{CN}$  Concentration in the Mobile Phase on  $\log k'$

A) Performed at pH 2.0. 1, benzene; 2, cyanobenzene; 3, 4-methylphenol.

B) Performed at pH 11.0. 1, 3-chloropyridine; 2, 2-methoxyaniline; 3, quinoline.

The continuous lines in the figure represent change of  $k'$  obtained by least squares calculation based on the quadratic relation between  $\log k'$  and the  $\text{CH}_3\text{CN}$  concentration.

TABLE I. Effect of Acetonitrile Concentration on the Correlation for Phenols at pH 2.0 in Eq. 2,  $\log P_{\text{oct}} = a_1 + b_1 \log k'$

$\text{CH}_3\text{CN}$ (%)	$a_1^{a)}$	$b_1^{a)}$	$n^{b)}$	$r^{c)}$	$s^{d)}$
10	0.14 (0.49)	1.09 (0.32)	5	0.987	0.076
20	0.33 (0.13)	1.33 (0.10)	6	0.998	0.031
30	0.58 (0.11)	1.61 (0.13)	6	0.998	0.032
35	0.91 (0.28)	2.00 (0.52)	6	0.983	0.104
40	1.17 (0.21)	1.92 (0.48)	6	0.984	0.100
45	1.39 (0.22)	2.06 (0.67)	6	0.973	0.129
50	1.62 (0.21)	2.04 (0.84)	6	0.958	0.161
60	2.17 (0.19)	2.93 (1.06)	6	0.967	0.143

a) Values in parentheses are 95% confidence limits. b) Number of compounds. c) Correlation coefficient. d) Standard deviation.

the quadratic curves shown as continuous lines in Fig. 1, and thus, the value of  $k'_0$  ( $k'$  without organic modifier) cannot be determined by linear extrapolation to 0%  $\text{CH}_3\text{CN}$ . Similarly, the dependence of  $\log k'$  on the concentration of MeOH was quadratic for these compounds in both the acidic and the alkaline region (data not shown).

## 2. Relation between $\log k'$ and $\log P_{\text{oct}}$

It has been reported that  $\log k'$  determined with a mobile phase containing a certain amount of organic modifier increases linearly with  $\log P_{\text{oct}}$ .<sup>6,7a,b,9,15</sup> Such a linear relation is expressed by Eq. 2.

$$\log P_{\text{oct}} = a_1 + b_1 \log k' \quad (2)$$

With a Hitachi gel column, Eq. 2 was found to be available for various compounds. However, as described in section 2, this relation was dependent on the hydrogen-bonding ability of compounds. Values of  $a_1$  and  $b_1$  for phenols at various  $\text{CH}_3\text{CN}$  concentrations in the acidic

TABLE II. Values of  $\log P_{\text{oct}}$  and  $\log k'$ 

Compound class	Chemicals	$\log P_{\text{oct}}^{a)}$	$\log k'$			
			Methanol		Acetonitrile	
			pH 11.0	pH 2.0	pH 11.0	pH 2.0
I	Benzene	2.13	0.90	0.91	1.21	1.08
	Toluene	2.69	1.17	1.17	1.48	1.29
	Chlorobenzene	2.84	1.23	1.25	1.58	1.38
	Bromobenzene	2.99	1.37	1.32	1.69	1.53
	Ethylbenzene	3.15	1.35	1.33	1.74	1.54
	Iodobenzene	3.25	1.45	1.50	1.86	1.65
II	Cyanobenzene	1.56	0.60	0.97	0.93	0.74
	Nitrobenzene	1.85	0.95	1.01	1.16	0.98
	Methoxybenzene	2.10	1.02	1.06	1.20	1.05
	Methylbenzoate	2.23	0.94	1.04	1.11	1.13
	Ethylbenzoate	2.64	1.23	1.26	1.41	1.34
	Diphenyl ketone	3.18	1.56	1.79	1.76	1.66
	Diphenyl ether	4.21	1.88	2.08	2.28	2.07
III	Benzyl alcohol (BAL)	1.10	0.05	0.10	0.17	0.11
	4-Methyl-BAL	1.59	0.25	0.36	0.37	0.38
	2-Chloro-BAL	1.77 <sup>b)</sup>	0.41	0.35	0.57	0.49
	4-Chloro-BAL	1.96	0.42	0.48	0.57	0.51
	2,6-Dichloro-BAL	2.02 <sup>b)</sup>	0.50	0.52	0.69	0.69
	3-Iodo-BAL	2.55	0.72	0.80	0.88	0.91
	3,5-Dichloro-BAL	2.90 <sup>b)</sup>	0.81	1.05	1.06	0.91
	4-Phenyl-BAL	3.16	1.14	1.27	1.17	1.08
IV	Phenol	1.48	—	0.22	—	0.29
	4-Methoxyphenol	1.37	—	0.28	—	0.24
	4-Cyanophenol	1.60	—	0.28	—	0.31
	4-Methylphenol	1.94	—	0.46	—	0.55
	4-Chlorophenol	2.39	—	0.70	—	0.79
	4-Bromophenol	2.59	—	0.84	—	0.77
	Benzoic acid (BA)	1.87	—	0.37	—	0.44
	4-Cyano-BA	1.56	—	0.35	—	0.30
	4-Chloro-BA	2.65	—	0.81	—	0.75
	4-Bromo-BA	2.86	—	0.99	—	0.88
V	Aniline	0.90	0.26	—	0.56	—
	4-Methoxyaniline	0.78	0.20	—	0.39	—
	3-Methoxyaniline	0.93	0.33	—	0.49	—
	3-Nitroaniline	1.37	0.60	—	0.83	—
	4-Nitroaniline	1.39	0.51	—	0.82	—
	4-Chloroaniline	1.83	0.66	—	1.01	—
	<i>N</i> -Ethylaniline	2.16	0.95	—	1.25	—
	2-EtOOC-Aniline	2.57	1.11	—	1.33	—
VI	Pyridine	0.65	−0.12	—	0.10	—
	3-Aminopyridine	0.20	−0.46	—	−0.19	—
	2-Aminopyridine	0.58	−0.22	—	0.01	—
	3-Chloropyridine	1.43	0.37	—	0.56	—
	2-Chloropyridine	1.45	0.33	—	0.61	—
	3-Bromopyridine	1.58	0.51	—	0.69	—
	Quinoline	2.03	0.63	—	0.80	—
	Isoquinoline	2.08	0.68	—	0.88	—

a) Cited from ref. 16, except b) which was determined by the shaking-flask method.



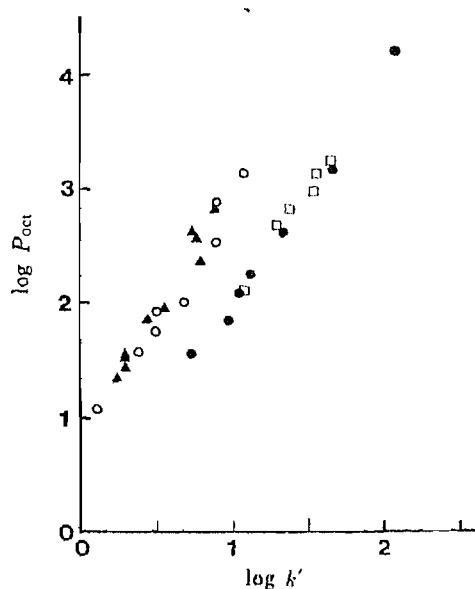


Fig. 2. Relationships between  $\log P_{\text{oct}}$  and  $\log k'$  with 35%  $\text{CH}_3\text{CN}$ -Containing Mobile Phase at pH 2.0

□, class I compounds; ●, class II compounds; ○, class III compounds; ▲, class IV compounds.

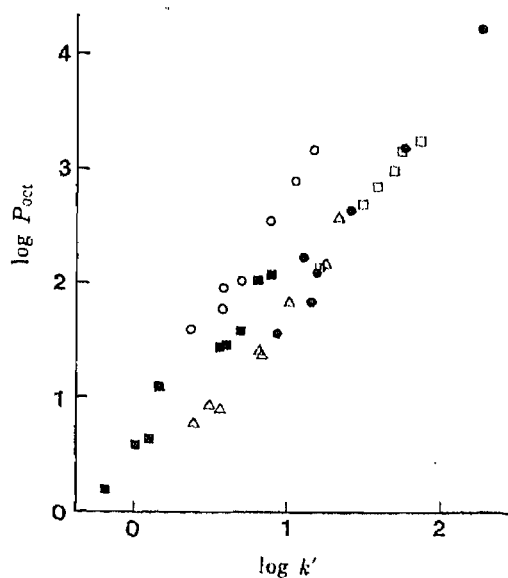


Fig. 3. Relationships between  $\log P_{\text{oct}}$  and  $\log k'$  with 35%  $\text{CH}_3\text{CN}$ -Containing Mobile Phase at pH 11.0

□, class I compounds; ●, class II compounds; ○, class III compounds; △, class V compounds; ■, class VI compounds.

TABLE III. Regression Coefficients for  $\log P_{\text{oct}} = a_1 + b_1 \log k'$  with the Mobile Phase Containing 35% Acetonitrile

pH	Class of compounds	$a_1$	$b_1$	$n$	$r$	$s$	Eq. No.
2.0	I (Non-H-bonders)	0.11 (0.69)	1.94 (0.49)	6	0.983	0.080	3
	II (H-acceptors)	-0.02 (0.28)	2.00 (0.21)	7	0.996	0.090	4
	III (Benzyl alcohols)	0.80 (0.31)	2.10 (0.44)	8	0.979	0.152	5
	IV (Phenols and benz. acids)	0.87 (0.20)	2.18 (0.34)	10	0.982	0.108	6
	All compounds	1.18 (0.25)	1.28 (0.25)	31	0.891	0.326	7
11.0	I (Non-H-bonders)	0.04 (0.44)	1.76 (0.28)	6	0.994	0.051	8
	II (H-acceptors)	-0.16 (0.53)	1.92 (0.36)	7	0.987	0.160	9
	III (Benzyl alcohols)	0.75 (0.18)	2.02 (0.24)	8	0.993	0.088	10
	V (Anilines)	-0.04 (0.27)	1.84 (0.31)	8	0.987	0.114	11
	VI (Pyridines and quinolines)	0.50 (0.13)	1.72 (0.22)	8	0.987	0.160	12
	All compounds	0.63 (0.18)	1.47 (0.16)	37	0.921	0.351	13

Values in parentheses are 95% confidence limits. For  $n$ ,  $r$  and  $s$ , see Table I.

mobile phase were determined as summarized in Table I. The phenols used are summarized in Table II.

In Table I, the values of coefficients,  $a_1$  and  $b_1$  in Eq. 2 increase with increase in the  $\text{CH}_3\text{CN}$  concentration, indicating that  $t_R$  becomes smaller with increase in the concentration of the organic modifier, as observed with ODS.<sup>9)</sup> The correlation between  $\log P_{\text{oct}}$  and  $\log k'$  generally becomes more significant at lower  $\text{CH}_3\text{CN}$  concentration. A similar dependence of  $k'$  on the  $\text{CH}_3\text{CN}$  concentration was observed with basic compounds (chemical classes V and VI in Table II) at pH 11.0 (data not shown).

At less than 20%  $\text{CH}_3\text{CN}$  and 60% MeOH, determination of  $k'$  for hydrophobic compounds became very difficult due to the long  $t_R$ . Thus, hereafter, we determined  $k'$  at 35%  $\text{CH}_3\text{CN}$  and at 70% MeOH to study the chromatographic behavior on the Hitachi gel column. Values of  $k'$  determined at these organic modifier concentrations are listed in Table II, together with the  $\log P_{\text{oct}}$  values.<sup>16)</sup>

Figure 2 shows the relation between  $\log P_{\text{oct}}$  and  $\log k'$  of the non-H-bonders halogeno- and alkyl-benzenes (class I), the H-acceptors such as cyanobenzene (class II), and the amphiprotics benzyl alcohols (class III), phenols and benzoic acids (class IV compounds in Table II) with eluent containing 35%  $\text{CH}_3\text{CN}$  at pH 2.0. Apparently,  $\log P_{\text{oct}}$  tends to increase linearly with increase in  $\log k'$ . However, the linear relation seems to be dependent on hydrogen-bonding ability, suggesting that hydrogen bond formation plays a role in the chromatographic behavior. Thus, we analyzed the experimental data according to Eq. 2, taking into account the hydrogen-bonding ability of compounds. A similar tendency was also found in HPLC performed at pH 11.0 with 35%  $\text{CH}_3\text{CN}$  as shown in Fig. 3 for anilines (class V), pyridines and quinolines (class VI), benzyl alcohols (class III), and various non-H-bonders

TABLE IV. Regression Coefficients for  $\log P_{\text{oct}} = a_1 + b_1 \log k'$  with the Mobile Phase Containing 70% Methanol

pH	Class of compounds	$a_1$	$b_1$	$n$	$r$	$s$	Eq. No.
2.0	I (Non-H-bonders)	0.35 (0.68)	2.01 (0.54)	6	0.982	0.086	14
	II (H-acceptors)	0.23 (0.60)	1.81 (0.44)	7	0.978	0.207	15
	III (Benzyl alcohols)	1.06 (0.17)	1.74 (0.24)	8	0.990	0.104	16
	IV (Phenols and benz. acids)	1.01 (0.17)	1.93 (0.29)	10	0.983	0.107	17
	All compounds	1.19 (0.33)	1.33 (0.32)	31	0.916	0.287	18
11.0	I (Non-H-bonders)	0.33 (0.58)	2.02 (0.46)	6	0.987	0.072	19
	II (H-acceptors)	0.12 (0.60)	2.07 (0.49)	7	0.980	0.199	20
	III (Benzyl alcohols)	1.06 (0.23)	1.99 (0.36)	8	0.984	0.134	21
	V (Anilines)	0.36 (0.20)	1.96 (0.31)	8	0.987	0.111	22
	VI (Pyridines and quinolines)	0.90 (0.09)	1.63 (0.20)	8	0.993	0.091	23
	All compounds	0.85 (0.17)	1.62 (0.20)	37	0.941	0.305	24

Values in parentheses are 95% confidence limits. For  $n$ ,  $r$  and  $s$ , see Table I.

(class I) and H-acceptors (class II). Furthermore, HPLC with a mobile phase contained 70% MeOH were performed with the compounds listed in Table II at both pH values. The values of coefficients  $a_1$  and  $b_1$  in Eq. 2 are summarized in Table III (35% CH<sub>3</sub>CN), and in Table IV (70% MeOH).

In Tables III and IV, it is apparent that the correlation with each chemical series is very high and the values of the slope  $b_1$  in Eq. 2 are similar irrespective of the hydrogen-bonding ability of compounds and the sort of organic modifier. However, the values of the intercept  $a_1$  are dependent on the chemical series, and the sort of organic modifier.

It has been shown that chromatographic characteristics of all the amphiprotics (classes III and IV) are almost the same at pH 2.0. The HPLC with basic compounds (classes V and VI) was not carried out, because they take protonated form at this pH. On the other hand, the correlations of the amphiprotics benzyl alcohols (class III) and anilines (class V) are different at pH 11.0. Though anilines are regarded as amphiprotic,<sup>16)</sup> the relation with anilines is very similar to that of H-acceptors, such as cyanobenzene, nitrobenzene and methoxybenzene (class II). Thus, anilines may act as H-acceptors in the chromatography. Furthermore, though pyridines and quinolines (class VI) are H-acceptors, their chromatographic behavior was similar to that of amphiprotics benzyl alcohols. This could be because the interaction of the stationary phase with pyridines and quinolines, in which electron-donating nitrogen is directly involved in the ring structure, is different from the interaction of H-acceptors, in which an H-acceptor group is introduced into a benzene ring. Probably their chromatographic behavior is coincidentally similar to that of benzyl alcohols. These anomalous chromatographic properties of anilines, pyridines and quinolines, should be observed at any pH with both organic modifiers, because those with benzyl alcohols are the same at pH 2.0 and 11.0 with CH<sub>3</sub>CN and MeOH (Tables III and IV).

In view of the above results, we performed regression analysis according to Eq. 25 by introducing the indicator variable HB

$$\log P_{\text{oct}} = a_2 + b_2 \log k' + c_2 \text{HB} \quad (25)$$

into Eq. 2: HB = 1 with compounds in classes III, IV and VI, and HB = 0 with compounds in classes I, II and V. The results of the analyses are summarized in Table V. By comparing Eq. 7 with Eq. 28, Eq. 13 with Eq. 29, Eq. 18 with Eq. 26, Eq. 24 with Eq. 27, respectively, it is apparent that introduction of the HB term results in an improvement of the correlations, and that relation between  $\log P_{\text{oct}}$  and  $\log k'$  with all compounds can be expressed by a single equation. The values of  $\log P_{\text{oct}}$  predicted from  $\log k'$  according to Eqs. 26–29 agreed very well with  $\log P_{\text{oct}}$  values obtained by the shaking-flask methods, mostly within a deviation of

TABLE V. Regression Coefficients for All Compounds for Eq. 25,  
 $\log P_{\text{oct}} = a_2 + b_2 \log k' + c_2 \text{HB}^a)$

Modifier	pH	$a_2$	$b_2$	$c_2$	$n$	$r$	$s$	Eq. No.
MeOH	2.0	0.40 (0.26)	1.81 (0.19)	0.65 (0.18)	31	0.972	0.173	26
	11.0	0.34 (0.11)	1.95 (0.15)	0.61 (0.15)	37	0.982	0.172	27
CH <sub>3</sub> CN	2.0	-0.06 (0.20)	2.05 (0.14)	0.96 (0.14)	31	0.987	0.116	28
	11.0	-0.13 (0.18)	1.90 (0.14)	0.77 (0.15)	37	0.982	0.174	29

a) HB = 1 with compounds of classes III and IV at pH 2.0 and HB = 1 with compound of classes III and VI at pH 11.0. Values in parentheses are 95% confidence limits. For  $n$ ,  $r$  and  $s$  see Table I.

$\log P_{\text{oct}}$  of 0.1.

It should be noted that the compounds that take  $\text{HB} = 1$  are amphiprotics except anilines (class V) and quinolines and pyridines (class VI), and the compounds of  $\text{HB} = 0$  belong to non-H-bonders (class I) and H-acceptors (class II). As described above, all the basic compounds, such as anilines, pyridines and quinolines, showed anomalous chromatographic behavior from the viewpoint of hydrogen-bonding ability. Further study is necessary to clarify the mechanism(s) operating in chromatography of these basic compounds.

### 3. Change of $k'$ with pH of the Mobile Phase

Since Hitachi gel is stable in the alkaline region, unlike other stationary phases composed of silica gel such as ODS and Gly-CPG, it should be possible to determine  $k'$  over a wide range of pH. Thus, we measured  $k'$  of various compounds between pH 2.0 and 12.0 with mobile phases containing 30% MeOH.

Figure 4 shows the pH-dependences of  $k'$  of 3-methylbenzoic acid, 2-chlorophenol and procaine. In the case of 3-methylbenzoic acid,  $k'$  was about 200 at pH 2.0. With increase in pH of the mobile phase;  $k'$  became smaller. The steep decrease in  $k'$  took place at about pH 4.0. This change became smaller at about pH 5.5, reaching a constant value of 3. A similar curve was obtained with 2-chlorophenol, but the curve was shifted to about 5 pH unit higher than that with 3-methylbenzoic acid.

In the case of procaine, an opposite pH-profile of  $k'$  to that of 3-methylbenzoic acid was observed:  $k'$  was small at acidic pH, but it began to increase at about pH 7.5, attaining a constant value at about pH 10.0. From these pH-profiles of  $k'$ , the acid dissociation constant

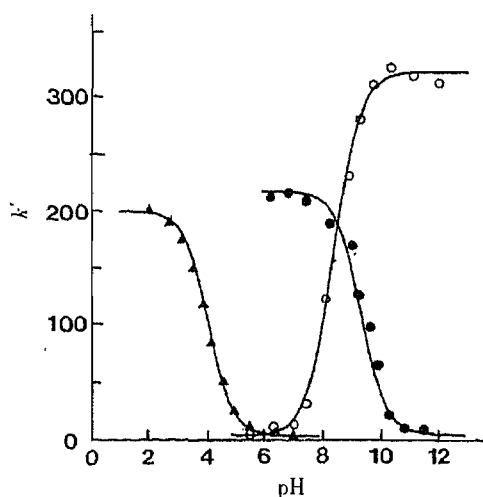


Fig. 4. Change of  $k'$  with pH in the Mobile Phase Containing 30% MeOH

Continuous lines were obtained by calculation according to Eq. 28 for 3-methylbenzoic acid ( $\blacktriangle$ ) and 2-chlorophenol ( $\bullet$ ), and according to Eq. 29 for procaine ( $\circ$ ).

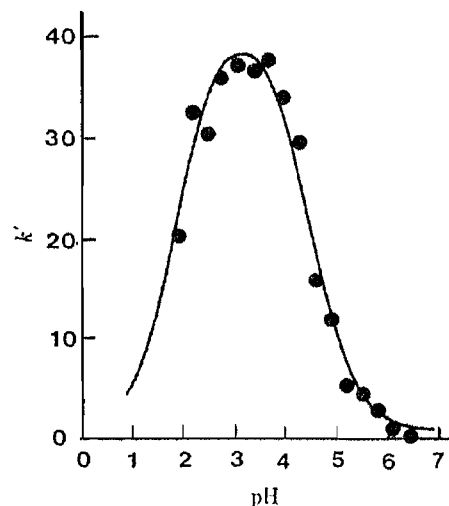


Fig. 5. Change of  $k'$  for 2-Aminobenzoic Acid with pH in the Mobile Phase Containing 30% MeOH

The continuous line was obtained by calculation according to Eq. 30 with the following values obtained by non-linear least-squares calculation.

$$k'_{(0)} = 41.69, k'_{(+)} = 1.10, k'_{(-)} = 0.51, \text{p}K_{A(+)} = 2.02, \text{p}K_{A(-)} = 4.60.$$

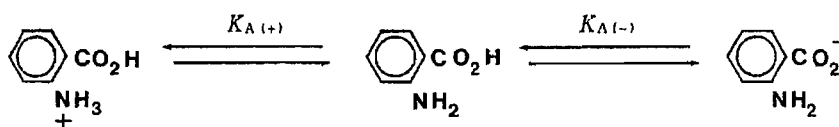


Chart 1

$K_A$  can be determined by means of Eq. 28 with acids ( $K_A$  is denoted as  $K_{A(-)}$ ) and by Eq. 29 with bases ( $K_A$  is denoted as  $K_{A(+)}$ ).<sup>17)</sup>

$$k = \frac{k'_{(0)} + k'_{(-)}K_{A(-)}/[H^+]}{1 + K_{A(-)}/[H^+]} \quad (28)$$

$$k' = \frac{k'_{(0)} + k'_{(+)}[H^+]/K_{A(+)}}{1 + [H^+]/K_{A(+)}} \quad (29)$$

Here,  $k'_{(0)}$ ,  $k'_{(-)}$  and  $k'_{(+)}$  are capacity factors with regard to the neutral, anionic and cationic forms, respectively.

Figure 5 shows the pH-profile of  $k'$  of the amphoteric compound 2-aminobenzoic acid. The change of  $k'$  was quite different from those of mono-ionizable acids and bases, such as 3-methylbenzoic acid and procaine. The small  $k'$  at acidic pH increased with increase in pH, being maximum at about pH 3.0, and then  $k'$  decreased, attaining a constant level at above pH 6.5.

Such a biphasic change of  $k'$  with pH can be interpreted as being due to dissociation of protons first from the protonated amino moiety (acid dissociation constant:  $K_{A(+)}$ ), and then from the carboxylic acid moiety ( $K_{A(-)}$ ) as shown in Chart 1. By putting  $k'_{(0)}$ ,  $k'_{(+)}$  and  $k'_{(-)}$  as the capacity factors of the neutral, cationic and anionic forms of amphoteric compounds, respectively, the acid dissociation constants  $K_{A(+)}$  and  $K_{A(-)}$  can be determined by using Eq. 30 (ref. 17a).

$$k' = \frac{k'_{(0)} + k'_{(-)}K_{A(-)}/[H^+] + k'_{(+)}[H^+]/K_{A(+)}}{1 + K_{A(-)}/[H^+] + [H^+]/K_{A(+)}} \quad (30)$$

It would be interesting to see how the pH-profile of  $k'$  changes with the values of acid dissociation constants and capacity factors of these molecular species. Figure 6 shows the dependence of the pH-profile of  $k'$  on  $pK_{A(-)}$  of model amphoteric compounds with given values of  $k'_{(0)} = 50$ ,  $k'_{(+)} = 5$ ,  $k'_{(-)} = 2$  and  $pK_{A(+)} = 2.0$ . In Fig. 6, curves for compounds whose  $pK_{A(-)}$  values are 7 and over show plateaus. The value of  $k'$  at this plateau corresponds to

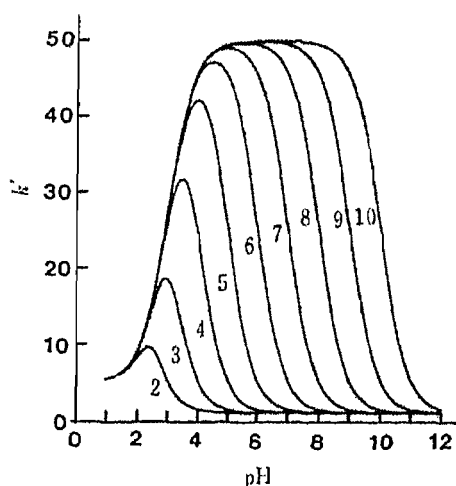


Fig. 6. Change of the pH-Profile of  $k'$  Determined by Calculation According to Eq. 30 with Given Values of  $k'_{(0)} = 50$ ,  $k'_{(-)} = 2$ ,  $k'_{(+)} = 5$  and  $pK_{A(+)} = 2$

Numbers beside the traces are values of  $pK_{A(-)}$ .

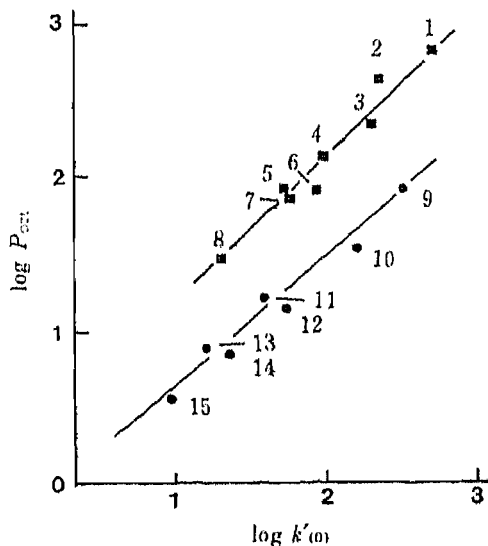


Fig. 7. Relationship between  $\log P_{0.01}$  and  $\log k'_{(0)}$  Determined with the Mobile Phase Containing 30% MeOH

Numbers beside data points represent compounds in Table VI.

TABLE VI. Acid Dissociation Constants<sup>a)</sup> and Partition Coefficients<sup>b)</sup> Determined by HPLC with 30% Methanol Containing Mobile Phase

No.	Chemicals	$pK_{A(+)}$	$pK_{A(-)}$	$\log P_{\text{HPLC}}$	$\log k'_{(0)}$	$\log k'_{(-)}$	$\log k'_{(+)}$
1	2-Naphthol		9.67 (9.63)	2.75 (2.84)	2.69	1.00	
2	4-Bromophenol		9.41 (9.36)	2.44 (2.59)	2.34	0.69	
3	3-Methylbenzoic acid		4.16 (4.27)	2.41 (2.37)	2.30	0.50	
4	2-Chlorophenol		9.30 (8.48)	2.13 (2.15)	1.98	0.24	
5	4-Methylphenol		10.27 (10.14)	1.91 (1.94)	1.73	0.24	
6	4-Nitrophenol		7.15 (7.15)	2.10 (1.91)	1.95	0.33	
7	Benzoic acid		4.14 (4.18)	1.93 (1.87)	1.76	0.14	
8	Phenol		10.93 (9.98)	1.54 (1.48)	1.31	-0.21	
9	Procaine	8.46 (8.80)		1.92 (1.92)	2.51		
10	Sulfadimethoxine	2.00 (2.07)	5.87 (6.70)	1.64 (1.50)	2.20	-0.21	0.22
11	2-Aminobenzoic acid	2.02 (2.05)	4.60 (4.37)	1.13 (1.21)	1.62	-0.29	0.04
12	Sulfisoxazole	1.77 (-)	4.76 (4.62)	1.24 (1.15)	1.74	-0.52	0.01
13	Aniline	3.96 (4.58)		0.78 (0.90)	1.22		0.01
14	4-Aminosalicylic acid	1.50 (1.70)	3.48 (3.90)	0.92 (0.87)	1.38	-0.65	-0.02
15	4-Aminobenzoic acid	2.28 (2.30)	4.61 (4.64)	0.60 (0.68)	1.02	-1.01	-0.30

a) Values in parentheses with  $pK_{A(+)}$  and  $pK_{A(-)}$  are from ref. 18. b) Values in parentheses with  $\log P_{\text{HPLC}}$  is  $\log P_{\text{oct}}$  cited from ref. 16.  $\log P_{\text{HPLC}}$  is obtained by Eq. 33.

that of  $k'_{(0)}$ . In these cases we can determine the value of  $k'_{(0)}$  directly from the curves. However, with compounds whose  $pK_{A(-)}$  values are 6 and under, we cannot determine  $k'_{(0)}$  from the pH-profile of  $k'$ , because there is no plateau in these curves.

It is apparent in Fig. 6 that there is no plateau for amphoteric compounds whose  $pK_A$  difference ( $=pK_{A(-)} - pK_{A(+)}$ ) is less than 4. In the case of 2-aminobenzoic acid, the  $pK_A$  difference is 2.6, and thus the maximum  $k'$  ( $=38$ , Fig. 5) is not  $k'_{(0)}$  ( $=42$ , see Table VI).

Apparently values of  $k'_{(0)}$ ,  $k'_{(+)}$  and  $k'_{(-)}$  cannot be determined from Fig. 5 directly. Thus, these values should be determined by non-linear least squares calculation based on Eq. 30. We used the Gauss-Newton method for this purpose. Values of  $pK_A$  of various amphoteric compounds, including 2-aminobenzoic acid, thus determined as well as those of mono-acids and bases are summarized in Table VI. Values of  $pK_A$  for mono-acids and bases were also determined by non-linear least-squares calculations. Values of  $\log k'_{(0)}$ ,  $\log k'_{(-)}$  and  $\log k'_{(+)}$  are also included in Table VI. In these experiments the mobile phase containing 30% MeOH was used. The reason for the use of such a low proportion of MeOH is to measure the capacity factors of ionized molecular species accurately. Accordingly, with this mobile phase, the pH-profile of  $k'$  for hydrophobic compounds could not be determined. Thus, the compounds listed in Table VI are different from those used in section 2. It should be noted that the values

of pH in the mobile phase are expressed as the pH of the original buffer solution, before adding the organic modifier. This pH was slightly different from that after addition of the organic modifier. However, as reported previously,<sup>17b)</sup> the  $pK_A$  values based on the former pH values agreed with those determined potentiometrically better than those based on the latter pH. The reason is not clear at present, but this may be related to the fact that absorption of  $H^+$  and  $OH^-$  takes place at the surface of the stationary phase.<sup>19)</sup> It is shown in Table VI that the values of acid dissociation constants obtained by HPLC are generally in good agreement with those from the literature. Thus, with a Hitachi Gel column we can accurately determine the acid dissociation constants of various acids and bases, and amphoteric compounds.

Figure 7 shows the relation between  $\log k'_{(0)}$ , determined from  $k'$  with 30% MeOH and reported values of  $\log P_{\text{oct}}$ <sup>16)</sup> for the compounds listed in Table VI. Since the physical quantity of  $k'_{(0)}$  is the same as that of  $k'$  determined in section 2, the results in Fig. 7 should show a similar tendency to those in Figs. 2 and 3. As expected,  $\log P_{\text{oct}}$  values tended to increase with increase in  $\log k'_{(0)}$ . This tendency became clearer when these data points were divided into two groups: one consisting of phenols and benzoic acids (compounds 1—8), and the other consisting of amino-substituted benzenes such as procaine, anilines and sulfonamides (compounds 9—15). In Fig. 7,  $\log P_{\text{oct}}$  in each series increases linearly with increase in  $\log k'_{(0)}$ , and the slopes of these straight lines are almost the same, suggesting that all the  $\log P_{\text{oct}}$  values can be expressed by a single function of  $\log k'_{(0)}$  by the introduction of the indicator variable HB as in Eq. 25. These relations are described by Eq. 31—33 with high statistical significance.

With compounds No. 1—8;

$$\log P_{\text{oct}} = 0.11 + 1.02 \log k'_{(0)} \quad (31)$$

(0.49) (0.24)  $n=8, r=0.973, s=0.111$

with compounds No. 9—15;

$$\log P_{\text{oct}} = -0.13 + 0.78 \log k'_{(0)} \quad (32)$$

(0.31) (0.18)  $n=7, r=0.981, s=0.089$

with compounds No. 1—15;

$$\log P_{\text{oct}} = 0.38 + 0.88 \log k'_{(0)} - 0.68 \text{HB} \quad (33)$$

(0.30) (0.14) (0.14)  $n=15, r=0.987, s=0.113$

HB = 1 for bases and amphoteric compounds.

It is interesting that in the regression analyses of the relation between  $\log P_{\text{oct}}$  and  $\log k'$  shown in Table V, the HB term was required for anilines as well as non-H-bonders and H-acceptors. Here again, amino-substituted benzenes including anilines required the HB term. (Non-H-bonders and H-acceptors were not examined here.) Thus, all the amino-substituted benzenes act as H-acceptors, though sulfonamides and aminobenzoic acids have an amphiprotic group besides the amphiprotic amino group. It is interesting that the amino group plays a decisive role in the retention behavior on HPLC.

Like  $k'_{(0)}$ ,  $k'_{(+)}$  and  $k'_{(-)}$  also showed linear dependence on  $\log P_{\text{oct}}$  (Fig. 7). However, in this case,  $k'_{(-)}$  and  $k'_{(+)}$  for all compounds showed a simple linear relationship with  $\log P_{\text{oct}}$ , probably because these values are not great enough to distinguish differences in the hydrogen-bonding ability of the compounds. Note that  $k'_{(+)}$  is always greater than  $k'_{(-)}$ , in agreement with the case of amino acids in HPLC with porous polymer.<sup>20)</sup>

### Conclusion

In conclusion, Hitachi gel is a very useful column for determination of  $\log P_{\text{oct}}$  and  $pK_A$ , because it allows HPLC to be done in the alkaline region as well as the acidic region. The

relation between  $\log k'_{(0)}$  and  $\log P_{\text{oct}}$  is dependent on the hydrogen-bonding ability of compounds, as in the case of HPLC on an ODS-column. However, the chromatographic behavior of some compounds such as sulfonamides, procaine and aniline is anomalous from the viewpoint of the hydrogen-bonding ability. This should be further examined.

It is of interest that  $\log k'$  with ionized molecular species as well as with neutral forms increased linearly with increase in  $\log P_{\text{oct}}$ . The value of  $k'$  with ionized molecular species is smaller by about two log units than that of the neutral molecular species (*cf.* Table IV). If these values reflect the differences of hydrophobicity of these molecular species, they are very small compared with the corresponding values based on partition between octanol and water, where the difference was reported to be of the order of three log units.<sup>21,22)</sup> This may be because in the chromatography, the difference in the affinity of both species for the surface of the stationary phase is measured, while in the partition system that of the amount transferred into the octanol phase was measured.

In some drug actions, it is possible that both molecular species interact with the surface of biopolymers such as proteins and membranes and induce the pharmacological activity.<sup>23)</sup> In these cases, chromatographic indices, such as  $\log k'$ , of these molecular species could be better parameters for predicting biological activity than  $\log P_{\text{oct}}$ . This problem is also interesting in connection with studies of drug action from the viewpoint of QSAR.

#### References

- 1) R. Franke, "Theoretical Drug Design Methods," Elsevier, Amsterdam, 1984, Chapters 4 and 8.
- 2) H. Koenemann, R. Zelle, F. Busse and W. E. Hammers, *J. Chromatogr.*, **178**, 559 (1979).
- 3) R. Kaliszan, *J. Chromatogr.*, **220**, 71 (1981).
- 4) H. Terada, *Quant. Struct.-Act. Relat.*, **5**, 81 (1986).
- 5) T. Hanai, "Kuromatogurahui Bunri Sisutemu," ed. by S. Hara, S. Mori and T. Hanai, Maruzen, Tokyo, 1981, Chapter 5.
- 6) K. Miyake and H. Terada, *J. Chromatogr.*, **240**, 9 (1982).
- 7) a) J. Haky and A. M. Young, *J. Liq. Chromatogr.*, **7**, 675 (1984); b) R. E. Koopmans and R. F. Rekker, *J. Chromatogr.*, **285**, 267 (1984); c) T. Braumann and L. H. Grimme, *ibid.*, **206**, 7 (1981); d) W. Butte, C. Fooker, R. Klusmann and D. Schuller, *ibid.*, **214**, 59 (1981); e) S. H. Unger and G. H. Chiang, *J. Med. Chem.*, **24**, 262 (1981); f) J. K. Baker, D. O. Rauls and R. F. Born, *ibid.*, **22**, 1301 (1979); g) T. Yamagami, H. Takami, K. Yamamoto, K. Miyoshi and N. Takao, *Chem. Pharm. Bull.*, **32**, 4994 (1984).
- 8) J. L. G. Thus and J. C. Kraak, *J. Chromatogr.*, **320**, 271 (1985).
- 9) K. Miyake, N. Mizuno and H. Terada, *Chem. Pharm. Bull.*, **34**, 4787 (1986).
- 10) a) L. R. Snyder and J. J. Kirkland, "Introduction to Modern Liquid Chromatography," 2nd ed., John Wiley & Sons, Inc., New York, 1979, pp. 500—501; b) K. K. Unger, N. Becker and P. Roumeliotis, *J. Chromatogr.*, **125**, 115 (1976).
- 11) Y. Kimura, H. Kitamura, T. Araki, K. Noguchi and M. Baba, *J. Chromatogr.*, **206**, 563 (1981).
- 12) R. Matsuda, T. Yamamiya, M. Tatsuzawa, A. Ejima and N. Takai, *J. Chromatogr.*, **173**, 75 (1979).
- 13) M. Ito, M. Tukada and S. Ganno, 2nd Meeting "Ekitaikuromatogurahui Touronkai," Tokyo, 1981, p. 5.
- 14) K. Diem and C. Lentner (ed.), "Scientific Tables," 7th ed., Ciba-Geigy, Basel, 1970, p. 280.
- 15) J. E. Garst and W. C. Wilson, *J. Pharm. Sci.*, **73**, 1616 (1984).
- 16) C. Hansch and A. J. Leo, "Substituent Constants for Correlation Analysis in Chemistry and Biology," John Wiley & Sons, Inc., New York, 1979, pp. 48—319.
- 17) a) C. Horvath, W. Melander and I. Molnar, *Anal. Chem.*, **49**, 142 (1987); b) K. Miyake, K. Okumura and H. Terada, *Chem. Pharm. Bull.*, **33**, 769 (1985).
- 18) a) G. Kortuem, W. Vogel and K. Andrussow, "Dissociation Constants of Organic Acids in Aqueous Solution," Butterworths, London, 1961, pp. 240—536; b) A. Albert and E. P. Serjeant (Tr. by S. Matsuura), "Ionteisuu," Maruzen, Tokyo, 1963, pp. 121—140; c) D. W. Newton and R. B. Kluza, *Drug Intell. Clin. Pharm.*, **12**, 546 (1978).
- 19) E. P. Kroff and D. J. Pietrzyk, *Anal. Chem.*, **50**, 502 (1978).
- 20) Su Puon and F. F. Cantwell, *Anal. Chem.*, **49**, 1256 (1977).
- 21) H. Terada, K. Kitagawa, Y. Yoshikawa and F. Kametani, *Chem. Pharm. Bull.*, **29**, 7 (1981).
- 22) T. Inagi, T. Muramatu, H. Nagai and H. Terada, *Chem. Pharm. Bull.*, **29**, 2330 (1981).
- 23) H. Terada, "Yakubutu no Kouzoukaseisoukan," ed. by Kouzoukatuseisoukan Konwakai, Nankodo, 1979, Chapter 3.



## Notes

[Chem. Pharm. Bull.]  
35(1) 389-393 (1987)]

## Interaction of Short-Chain Alkylammonium Salts with Cyclodextrins in Aqueous Solutions

KOICHIRO MIYAJIMA,\* MASATOSHI IKUTO and MASAYUKI NAKAGAKI

*Faculty of Pharmaceutical Sciences, Kyoto University, Yoshida  
Shimoadachi-cho, Sakyo-ku, Kyoto 606, Japan*

(Received July 2, 1986)

The formation constants of short chain alkylammonium salt-cyclodextrin complexes in aqueous solutions were investigated by conductometry for various values of alkyl chain length and the number of alkyl groups attached to the nitrogen atom.  $\alpha$ -Cyclodextrin ( $\alpha$ -CD),  $\beta$ -CD and  $\gamma$ -CD form complexes with alkylammonium salts having alkyl groups longer than *n*-butyl, *n*-hexyl and *n*-decyl, respectively. The formation constants of *n*-alkylammonium salts with  $\alpha$ -CD increase with the number of alkyl groups attached to the nitrogen atom. The entropy change of complex formation was negative. The effect of the terminal group on the complex formation is discussed in relation to the formation constants of alkanol-CD complexes.

**Keywords**— $\alpha$ -,  $\beta$ -,  $\gamma$ -cyclodextrin; *n*-alkylammonium salt; inclusion complex; formation constant; free energy; entropy; ionic hydration; hydrophobic hydration; cavity size

Cyclodextrins (CDs) interact with various types of hydrophobic compounds to form inclusion complexes. The formation constant of the complex depends on both the size of the CD cavity and the size and the hydrophobicity of the guest molecule. The contributions of various interactions to the complex formation have been calculated semi-empirically, and van der Waals and hydrophobic interaction have been assigned as the main interactions involved in the complex formations.<sup>1)</sup>

In contrast to the large amounts of equilibrium data for the interaction of CDs with aromatic and alicyclic compounds, few studies have been done on the interaction of CDs with aliphatic chain molecules. On complex formation between different kinds of CD and aliphatic compounds with definite chain length, the van der Waals interaction between CD and the guest molecule may be the most important factor governing the formation constant, because the cavity size is considerably different among three kinds of CDs and the diameter of methylene chains in *trans* zig-zag form is constant.

On the other hand, the formation constant of an aliphatic chain molecule with an ionic group would be decreased as compared with the case of a non-ionic group, such as a hydroxyl group, because an ionic group is usually strongly hydrophilic and reduces the hydrophobicity of the molecule by virtue of the ionic hydration. The signs of the free energy and enthalpy changes for the complex formation are generally negative, but the sign of the entropy change may be negative or positive, depending on the particular combination of the guest molecule and CD molecule.<sup>2)</sup>

We have determined the formation constants of CD-*n*-alkylammonium salt complexes with various alkyl chain lengths and the numbers of alkyl groups attached to the nitrogen atom, and compared the formation constants and the entropy changes with those of alkanol.<sup>3,4)</sup>

### Experimental

**Materials**—Primary and secondary ammonium chlorides prepared by the reaction of the corresponding amines with hydrochloric acid gas in dry ether were recrystallized from a mixed solvent of ethanol and dry ether twice or more. The purities of amines were confirmed by gas chromatography. Reagent-grade tetrapentylammonium bromide purchased from Nakarai Chemical Co., Ltd., was used after drying *in vacuo* at 40°C. Reagent-grade CDs were obtained from Wako Chemical Co., Ltd., and were recrystallized twice from water. Solutes were dissolved in water purified by distillation and deionization.

**Determination of Formation Constant**—The formation constant was determined by conductance measurement using a universal bridge (model 4255A) manufactured by Yokogawa-Hewlett-Packard Co., Ltd., in a thermostated bath controlled to  $\pm 0.01$  °C. To remove the contribution of dissolved carbon dioxide to the conductance, the conductance of water was subtracted from the experimental conductance of solutions.

**Viscosity Correction**—Viscosity correction was made to the equivalent conductance of alkylammonium salt (AA) in CD solutions.<sup>5)</sup>

$$A_{\text{corr}} = (1 + B_{\eta}C_{\text{cd}} + D_{\eta}C_{\text{cd}}^2)A_{\text{cd}} \quad (1)$$

where  $A_{\text{corr}}$  and  $A_{\text{cd}}$  are the corrected equivalent conductance and the equivalent conductance of AA in CD solution, respectively, and  $B_{\eta}$  and  $D_{\eta}$  are the viscosity  $B$  and  $D$  coefficients of CD in aqueous solution, respectively.  $C_{\text{cd}}$  is the molar concentration of CD. The values of  $B$  and  $D$  are shown in Table I.<sup>6)</sup> As reported previously,<sup>5)</sup> the value of  $A_{\text{cd}}$  is always smaller than the equivalent conductance in water. The value for  $A_{\text{corr}}$  of AA, which does not form a complex with CD, coincides with the equivalent conductance in water, while the value of  $A_{\text{corr}}$  of AA forming a CD complex is smaller than the equivalent conductance in water.

**Calculation of Formation Constant ( $K$ ) and the Thermodynamic Quantities**—The formation constant was calculated on the assumption that CD forms a 1-1 complex with AA as expressed by Eq. 2.



Then  $K$  is expressed as

$$K = \frac{x}{(C_{\text{cd}} - x)(C_{\text{mx}} - x)} \quad (3)$$

where  $C_{\text{mx}}$  and  $x$  are the concentrations of AA and CDAA.

When  $C_{\text{cd}} \gg x$ , Eq. 3 is reduced to

$$K = \frac{x}{C_{\text{cd}}(C_{\text{mx}} - x)} \quad (4)$$

On the other hand,  $A_{\text{corr}}$  is expressed by Eq. 5 with  $A_{\text{mx}}$  and  $A_{\text{inc}}$ , which are the equivalent conductances of free and included AA, respectively.

$$C_{\text{mx}}A_{\text{corr}} = (C_{\text{mx}} - x)A_{\text{mx}} + xA_{\text{inc}} \quad (5)$$

Here we introduce  $\Delta A$  and  $a$ , which are defined by Eqs. 6 and 7.

$$\Delta A = A_{\text{mx}} - A_{\text{corr}} \quad (6)$$

$$a = A_{\text{mx}} - A_{\text{inc}} \quad (7)$$

Then Eq. 4 can be rewritten as

$$\frac{1}{\Delta A} = \frac{1}{KaC_{\text{cd}}} + \frac{1}{a} \quad (8)$$

TABLE I. Viscosity  $B$  and  $D$  Coefficients of CDs at Various Temperatures

	Temp. (°C)	$\alpha$ -CD	$\beta$ -CD	$\gamma$ -CD
$B_{\eta}$ ( $\text{M}^{-1}$ )	15	2.50	—	3.90
	25	2.39	2.80	3.74
	35	2.24	—	3.62
$D_{\eta}$ ( $\text{M}^{-2}$ )	15	8.6	—	17
	25	7.8	—	16
	35	7.8	—	15

The value of  $K$  is determined graphically from the slope and the intercept of the  $1/\Delta A$  vs.  $1/C_{cd}$  curve.

The thermodynamic quantities for the complex formation are given by Eqs. 9, 10 and 11.

$$\Delta G^\circ = -RT \ln K \quad (9)$$

$$\Delta S^\circ = (-\delta \Delta G^\circ / \delta T)_p \quad (10)$$

and

$$\Delta H^\circ = \Delta G^\circ + T\Delta S^\circ \quad (11)$$

where  $R$  and  $T$  have the usual meanings.

## Results and Discussion

Figure 1 depicts the  $1/\Delta A$  vs.  $1/C_{cd}$  curves for various AA- $\alpha$ -CD systems. Good linearity is observed in every system, supporting indirectly the 1-1 complex formation in each system. From these curves, we determined the  $K$  values and  $\Delta G^\circ$  (free energy change for complex formation), and these values are shown in Table II. The experimental determination of  $K$

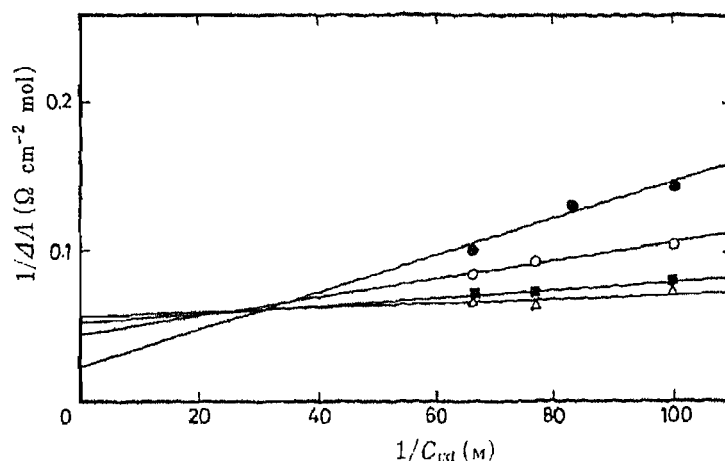


Fig. 1.  $1/\Delta A$  vs.  $1/C_{cd}$  Curves for Various AA at 25°C

●, hexylamine·HCl; ○, heptylamine·HCl; ■, octylamine·HCl; △, decylamine·HCl. At 25°C,  $C_{max} = 1 \times 10^{-3}$  M.

TABLE II. Formation Constant and Free Energy Change of Complex Formation for CD-AA Systems

Alkylammonium halide	$\alpha$ -CD		$\beta$ -CD		$\gamma$ -CD	
	$K$ ( $M^{-1}$ )	$\Delta G^\circ$ ( $kcal\ mol^{-1}$ )	$K$ ( $M^{-1}$ )	$\Delta G^\circ$ ( $kcal\ mol^{-1}$ )	$K$ ( $M^{-1}$ )	$\Delta G^\circ$ ( $kcal\ mol^{-1}$ )
<i>n</i> -Propylamine·HCl	ni.					
<i>n</i> -Butylamine·HCl	3	-0.6	ni.			
<i>n</i> -Dibutylamine·HCl	10	-1.4	ni.			
Isoamylamine·HCl	10	-1.4	ni.		ni.	
<i>n</i> -Amylamine·HCl	110	-2.8	ni.		ni.	
<i>n</i> -Diamylamine·HCl	200	-3.1	nd.		nd.	
TPAB	450	-3.6	ni.		nd.	
<i>n</i> -Hexylamine·HCl	130	-2.9	10	-1.4	ni.	
<i>n</i> -Heptylamine·HCl	220	-3.2	70	-2.5	ni.	
<i>n</i> -Octylamine·HCl	280	-3.3	150	-3.0	ni.	
<i>n</i> -Decylamine·HCl	600	-3.8	230	-3.2	100	-2.7

TPAB, tetra-*n*-pentylammonium bromide; ni, not included; nd, not determined.

values is precise to  $\pm 5 M^{-1}$ . As can be seen in Table II,  $\alpha$ -,  $\beta$ - and  $\gamma$ -CDs form inclusion complexes with AA having *n*-alkyl groups longer than *n*-butyl, *n*-hexyl and *n*-decyl, respectively. Kano *et al.* reported that *n*-propylamine and *n*-butylamine form inclusion complexes with  $\beta$ -CD, as determined by the fluorescence method.<sup>7)</sup> However, we cannot detect the complex formation with  $\beta$ -CD by this method. The formation constant increases with alkyl chain length in each system. The *K* values of decylammonium chloride decrease in the order  $\alpha > \beta > \gamma$ -CD, that is, the larger the size of the cavity, the smaller the formation constant. This is because the van der Waals interaction depends on the reciprocal of the sixth power of interatomic distance. The diameter of methylene chains in *trans* zig-zag form is approximately 5.1 Å.<sup>8)</sup> Since the diameters of the cavities of  $\alpha$ -,  $\beta$ - and  $\gamma$ -CDs are 5.7, 7.8, and 9.5 Å,<sup>9)</sup> respectively, the cavities of  $\beta$ - and  $\gamma$ -CDs are too large to accommodate the methylene chain tightly, resulting in small formation constants as compared with that of  $\alpha$ -CD.

As can be seen in Table II, the formation constants of amylammonium salts increase with the number of amyl groups attached to the nitrogen atom. Judging from the size of the cavity of  $\alpha$ -CD, it is impossible to include the whole molecule of di- or tetrapentylammonium ion in the cavity, and it is also impossible to include two methylene chains. It may be possible that two molecules of  $\alpha$ -CD can include the two methylene chains of AA separately. However, the linearities observed in the  $1/\Delta A$  vs.  $1/C_{cd}$  curves are incompatible with this possibility.

On the other hand, the ionic character of AA decreases with increase of alkyl chain length and the number of alkyl groups attached to the nitrogen atom, because the ionic atmosphere around the nitrogen atom is shielded by the polymethylene chain. This effect facilitates inclusion complex formation. In fact,  $\alpha$ - and  $\beta$ -CDs include the lower homologues of *n*-alkanol, *i.e.* methanol, ethanol and *n*-propanol, as well as higher homologues.<sup>3)</sup> The *K* values of the  $\alpha$ -CD complexes of 1-pentanol, 1-hexanol and 1-heptanol are 324, 891 and 2291  $M^{-1}$ , respectively. These values are considerably larger than the *K* values of the corresponding *n*-alkylammonium salts. This is because the strong hydrophilic nature of the terminal group reduces the hydrophobicity of the alkyl group and weakens the complex formation.

As can be seen in Table III, the *K* values of  $\alpha$ -CD-AA complexes decrease with increasing temperature, resulting in negative entropy change of complex formation. The thermodynamic quantities for the complex formation of *n*-alkanols with  $\alpha$ -CD obtained from spectroscopic<sup>3)</sup> and calorimetric<sup>4)</sup> studies are in conflict. Negative enthalpy and entropy changes were obtained from spectroscopy and negative enthalpy and positive entropy changes from calorimetry. Table III shows the enthalpy and entropy changes of complex formation for  $\alpha$ -CD-*n*-decylammonium chloride and  $\alpha$ -CD-*n*-diamylammoniumchloride at 25°C. Both the enthalpy and entropy changes were negative, as in the  $\alpha$ -CD-*n*-alkanol system determined by spectroscopy, suggesting that the van der Waals interaction is predominant in these systems. The entropy change of complex formation in the 1-tetra-decyltrimethylammonium salt- $\alpha$ -CD system is slightly positive.<sup>10)</sup> This may be due to the long-chain alkyl group and

TABLE III. Temperature Dependence of the Formation Constants of *n*-Diamylamine·HCl- and *n*-Decylamine·HCl- $\alpha$ -CD

	<i>K</i> ( $M^{-1}$ )		$\Delta H$ (kcal mol <sup>-1</sup> )	$\Delta S$ (cal mol <sup>-1</sup> deg <sup>-1</sup> )
	15°C	25°C	35°C	
<i>n</i> -Diamylamine·HCl	250	200	160	-4.0
<i>n</i> -Decylamine·HCl	800	600	450	-5.1

the terminal trimethylammonium group, because the ionic nature of the trimethylammonium group is weaker than that of the ammonium group owing to the shielding effect of methyl groups, and the *n*-tetradecyl group is more hydrophobic than the *n*-decyl group. Long-chain alkyl compounds without net charge, such as *n*-alkanoic acids<sup>11)</sup> and lysolecithins<sup>12)</sup> form water-insoluble complexes of torus type. An  $\alpha$ -CD molecule covers 5–6 methylene units in torus-type complexes. Judging from the facts that the alkylammonium salts with groups shorter than propyl do not form inclusion complexes with  $\alpha$ -CD and that 5–6 units of methylene group per  $\alpha$ -CD are required for torus-type complexes, the possibility of torus-type complex formation is small.

In conclusion, CDs form inclusion complexes with *n*-alkylammonium salts. The formation of a complex and the formation constant depend on the size of cavity and the alkyl chain length. The formation constant is in the order  $\alpha$ - >  $\beta$ - >  $\gamma$ -CD. The terminal ionic group reduces complex formation. The entropy of complex formation for  $\alpha$ -CD was negative, indicating that van der Waals interaction is predominant, as in the *n*-alkanol- $\alpha$ -CD system.

#### References

- 1) I. Tabushi, Y. Kiyosuke, T. Sugimoto and K. Yamamura, *J. Am. Chem. Soc.*, **100**, 918 (1978).
- 2) J. Szejtli, "Cyclodextrins and Inclusion Complexes," Akademiai Kiado, Budapest, 1982, p. 103.
- 3) Y. Matsui and K. Mochida, *Bull. Chem. Soc. Jpn.*, **52**, 2808 (1979).
- 4) S. Takagi and Y. Kimura, *J. Inc. Phenomena*, **2**, 775 (1984).
- 5) K. Miyajima, M. Sawada, T. Ueda and M. Nakagaki, *Nippon Kagaku Kaishi*, **1984**, 527.
- 6) K. Miyajima, M. Sawada and M. Nakagaki, *Bull. Chem. Soc. Jpn.*, **56**, 827 (1983).
- 7) K. Kano, I. Takenoshita and T. Ogawa, *J. Phys. Chem.*, **86**, 1833 (1982).
- 8) M. Nakagaki, "Koroido to Hyomenjyotai," Tokyo Kagaku-Dojin, Tokyo, 1979, p. 69.
- 9) J. Szejtli, "Cyclodextrins and Inclusion Complexes," Akademiai Kiado, Budapest, 1982, p. 25.
- 10) T. Ohkubo, H. Kitano and N. Ise, *J. Phys. Chem.*, **80**, 24 (1976).
- 11) W. Schlenko and D. M. Sand, *J. Am. Chem. Soc.*, **83**, 2312 (1961).
- 12) K. Miyajima, K. Tomita and M. Nakagaki, *Chem. Pharm. Bull.*, **33**, 2587 (1985).

[Chem. Pharm. Bull.]  
35(1) 394—397 (1987)

## A Simplified Synthesis of 32-Oxygenated Lanosterol Derivatives

YOSHIKO SONODA, YOSHIE TANOUE, MAKIKO YAMAGUCHI,  
and YOSHIHIRO SATO\*

*Kyoritsu College of Pharmacy, Shibakoen 1-chome, Minato-ku,  
Tokyo 105, Japan*

(Received June 16, 1986)

A simplified synthesis of lanost-8-ene-3 $\beta$ ,32-diol, lanost-7-ene-3 $\beta$ ,32-diol, 3 $\beta$ -hydroxylanost-8-en-32-al, and 3 $\beta$ -hydroxylanost-7-en-32-al, in which 3 $\beta$ -acetoxy lanostan-7 $\alpha$ -ol prepared by the hydrogenation of 3 $\beta$ -acetoxy lanost-8-en-7-one is the key compound, is described.

**Keywords**—32-oxygenated sterol; 3 $\beta$ -acetoxy lanostan-7 $\alpha$ -ol; lanosterol 14-demethylation; cholesterol biosynthesis

The biosynthesis of cholesterol from lanosterol requires the removal of the three methyl groups at carbons 4 and 14. The initial step in the removal of these methyl groups has been considered to be the 14-demethylation,<sup>1)</sup> which is a complex process, and many aspects of the overall mechanisms remain unclear. A probable intermediate is the lanosterol derivative with a 14-hydroxymethyl, 14-aldehyde or 15-hydroxy group.

Recently, it has been shown that 24(*S*),25-epoxycholesterol<sup>2)</sup> is produced in the liver by way of a branch in the sterol biosynthetic pathway, beginning with the formation of squalene 2,3(*S*); 22(*S*),23-dioxide, and the dioxide is known to accumulate in cultured cells that have been treated with oxidosqualene cyclase blocking agents. The squalene dioxide is converted first to 24(*S*),25-oxidolanosterol and finally to 24(*S*), 25-epoxycholesterol, which has been shown to be present in the liver. We have reported<sup>3)</sup> that 24(*S*),25-oxidolanosterol and 24(*S*),25-epoxycholesterol inhibited cholesterol biosynthesis from 24,25-dihydrolanosterol *in vitro*. Further, we recently reported<sup>4)</sup> that 15-oxygenated lanosterol derivatives inhibit cholesterol biosynthesis from 24,25-dihydrolanosterol *in vitro*. On the other hand, the 32-hydroxylated lanosterol derivatives<sup>5)</sup> have been shown to inhibit sterol biosynthesis in animal cells in culture. Such naturally occurring oxygenated steroids may be important in regulating sterol biosynthesis.

With the intention of investigating the effects of the natural precursors on cholesterol biosynthesis from 24,25-dihydrolanosterol, we studied the synthesis of the 32-oxygenated derivatives of 24,25-dihydrolanosterol. This report describes a simplified synthesis of lanost-8-ene-3 $\beta$ ,32-diol (**6**), lanost-7-ene-3 $\beta$ ,32-diol (**7**), 3 $\beta$ -hydroxylanost-8-en-32-al (**9**), and 3 $\beta$ -hydroxylanost-7-en-32-al (**10**).

For the synthesis of 32-oxygenated compounds, 3 $\beta$ -acetoxy lanostan-7 $\alpha$ -ol (**2**) was used as the key compound. Barton and Thomas<sup>6)</sup> obtained **2** by the reduction of 3 $\beta$ -acetoxy lanost-8-en-7-one with lithium in liquid ammonia, followed by catalytic reduction, though in unspecified yield. On the other hand, Parish *et al.*<sup>7)</sup> obtained **2** by the reduction of a mixture of 7 $\alpha$ , 8 $\alpha$ - and 8 $\alpha$ , 9 $\alpha$ -epoxy lanostan-3 $\beta$ -ols, followed by selective acetylation, but the yield was low and the procedure troublesome. In this study, catalytic hydrogenation of 3 $\beta$ -acetoxy lanost-8-en-7-one (**1**) in the presence of platinum dioxide in acetic acid afforded **2**, which was identical with an authentic sample synthesized by the method of Parish *et al.*,<sup>7)</sup> in 26% yield. The other products were separated by column chromatography, affording 3 $\beta$ -

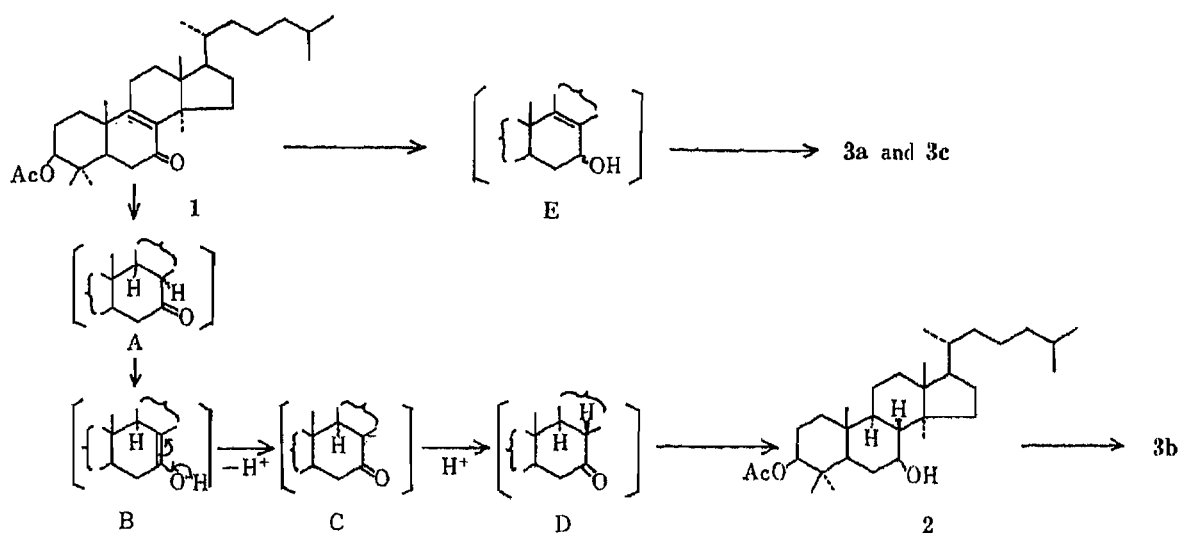


Chart 1

TABLE I. Isotopic Analysis of Deuterated Products

Deuterium content (%)	Deuterated compound			
	2	3a	3b	3c
$^2\text{H}_0$	3.8	1.5	1.2	7.1
$^2\text{H}_1$	15.1	13.8	7.0	29.3
$^2\text{H}_2$	21.4	46.9	27.6	33.2
$^2\text{H}_3$	42.8	28.4	43.3	10.6
$^2\text{H}_4$	14.8	9.4	18.6	10.1
$^2\text{H}_5$	2.2	0	2.3	9.7

acetoxylanost-8-ene (**3a**),  $3\beta$ -acetoxylanost-7-ene (**3b**), and  $3\beta$ -acetoxylanosta-7,9 (11)-diene (**3c**). The reaction probably proceeds as shown in Chart 1. The *cis* addition of  $\text{H}_2$  from the  $\alpha$ -side forms A, which is transformed to **2** via the enol compound (B), through deprotonation and protonation of intermediates (C and D, respectively), followed by hydrogenation of the latter. Here, **2** would be transformed to **3b** by dehydration. Compounds **3a** and **3c** would be formed via the  $7\alpha$ -hydroxy compound (E). In an attempt to clarify the mechanism of this reaction, **1** was catalytically hydrogenated in the presence of platinum dioxide in acetic acid- $^2\text{H}_1$  ( $\text{CH}_3\text{COO}^2\text{H}_1$ ). The products contained unanticipated species ( $^2\text{H}_0$ - to  $^2\text{H}_5$ -compounds) as determined by mass spectrometric analysis (Table I). It is thought that this result is due to exchange between gas-phase hydrogen and the deuterium atom in acetic acid- $^2\text{H}_1$ .<sup>8)</sup> Although the distribution of deuteriums was not fully established, one deuterium at C-7 in **2**, **3a**, **3b** and **3c** and also one deuterium at C-8 in **2** were confirmed by comparison of the proton and/or carbon-13 nuclear magnetic resonance ( $^1\text{H}$ - and/or  $^{13}\text{C}$ -NMR) spectra with those of undeuterated samples; these findings are consistent with the steps (A—E) in Chart 1. Now, **2** was reacted with lead tetraacetate according to the procedure of Parish *et al.*<sup>7)</sup> to yield the 7,32-oxide (**4**) and  $3\beta$ -acetoxy-7-oxolanostane (**5a**). Upon hydrolysis, **5a** gave 7-oxolanostan- $3\beta$ -ol (**5b**). The circular dichroism spectrum of **5b** showed the same negative Cotton effect as that of 18-acetoxylanostan- $3\beta$ -ol-7-one.<sup>9)</sup> This result clearly indicated that the stereochemistry of the B/C ring in **2** and **5a** must be *trans* as in the natural product. Treatment of **4** with pyridinium hydrogen chloride-acetic anhydride followed by alkaline hydrolysis gave

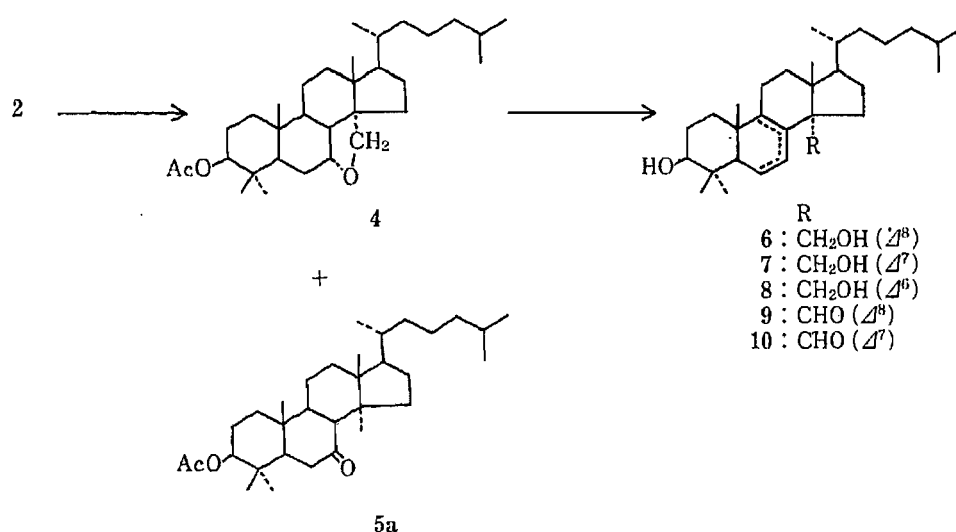


Chart 2

a mixture of 3,32-diols (**6**, **7**, and **8**). These compounds were separated by high-performance liquid chromatography (HPLC) on a  $\mu$ Bondapak-NH<sub>2</sub> column using CHCl<sub>3</sub>-*n*-hexane as the eluent. The  $\Delta^6$ -3,32-diol (**8**) was eluted first, followed by  $\Delta^7$ -3,32-diol (**7**) and finally the  $\Delta^8$ -3,32-diol (**6**). Compound **6** was oxidized with Jones reagent followed by reduction with KBH<sub>4</sub> to give the  $\Delta^8$ -32-al (**9**), and **7** was also converted to **10** in a similar manner.

#### Materials and Methods

<sup>1</sup>H- and <sup>13</sup>C-NMR spectra were obtained on JEOL FX-200 NMR machines. Mass spectra (MS) were recorded on a JEOL D-100 spectrometer at 75 eV ionizing potential. HPLC was done on a  $\mu$ Bondapak-NH<sub>2</sub> column (7.8 mm × 30 cm), using a Waters pump (model 510) and a Waters detector (model 480 spectrophotometer, set at 247 nm). Chloroform-*n*-hexane (1 : 1, v/v) was used as an eluent (flow rate 2.0 ml/min, pressure 100 kg/cm<sup>2</sup>). Optical rotations were measured on a JASCO DIP-SL automatic polarimeter with a cell of 1 cm light path length, and circular dichroism (CD) spectrum was taken in 0.5 mm cell at room temperature (24–25 °C) in chloroform on a JASCO J-20 recording spectropolarimeter.

**3β-Acetoxylanost-7α-ol (2)**—A solution of 3β-acetoxylanost-8-en-7-one<sup>10</sup> (**1**, 2 g) in AcOH (100 ml) was shaken under a stream of hydrogen in the presence of PtO<sub>2</sub> (0.5 g) at room temperature, absorbing 340 ml of hydrogen. After removal of the catalyst by filtration, the filtrate was poured into water and extracted with methylene chloride. The organic layer was washed with water, sat. NaHCO<sub>3</sub>, and water, then dried (Na<sub>2</sub>SO<sub>4</sub>), and concentrated *in vacuo*. The residue was chromatographed on silica gel (50 g). Elution with benzene gave a solid (1.2 g), which was a mixture of 3β-acetoxylanost-8-ene (**3a**), 3β-acetoxylanost-7-ene (**3b**), and 3β-acetoxylanosta-7,9(11)-diene (**3c**). **3a**, **3b** and **3c** were separated by HPLC (yield; 40%, 8%, and 8%, respectively). Further elution with methylene chloride gave a solid (0.65 g), which was recrystallized from MeOH to give colorless needles of **2** (yield, 26%), mp 208–209 °C, undepressed on admixture with an authentic specimen.<sup>7)</sup> <sup>1</sup>H-NMR  $\delta$  (ppm): 0.74 (3H, s, 18-CH<sub>3</sub>), 0.86 (3H, d, 26 or 27-CH<sub>3</sub>,  $J=6.6$  Hz), 0.87 (3H, d, 26 or 27-CH<sub>3</sub>,  $J=6.6$  Hz), 0.95 (3H, s, 19-CH<sub>3</sub>), 1.08 (3H, s, 14-CH<sub>3</sub>), 2.04 (3H, s, 3β-OCOCH<sub>3</sub>), 4.06 (1H, m, 7β-H,  $W_{1/2}=8$  Hz), 4.53 (1H, m, 3α-H). MS  $m/z$ : 488 (M<sup>+</sup>), 470 (M<sup>+</sup> - H<sub>2</sub>O), 455 (M<sup>+</sup> - CH<sub>3</sub>, H<sub>2</sub>O), 395 (M<sup>+</sup> - CH<sub>3</sub>, H<sub>2</sub>O, base peak).  $[\alpha]_D^{25}$ : +13.3 ( $c=1.0$ , CHCl<sub>3</sub>) (lit.,<sup>7)</sup> +13.9).

**Hydrogenation of 1 in Acetic Acid-<sup>2</sup>H<sub>1</sub>**—The reaction was carried out by the same procedures as described above except for the use of acetic acid-<sup>2</sup>H<sub>1</sub> (CH<sub>3</sub>COO<sup>2</sup>H<sub>1</sub>).

**Lanost-8-ene-3β,32-diol (6), Lanost-7-ene-3β,32-diol (7), and Lanost-6-ene-3β,32-diol (8)**—Treatment of 3β-acetoxylanostan-7α-ol (**2**, 0.5 g) with lead tetraacetate (2.5 g) followed by alumina chromatography of the crude reaction product gave 3β-acetoxylanostan-7α,32-oxide (**4**, mp 201–202 °C, yield, 72%) and 3β-acetoxylanostan-7-one (**5a**, mp 170–172 °C, yield, 7%). Treatment of **4** (0.25 g) with pyridinium hydrogen chloride (0.5 g) and acetic anhydride (50 ml) followed by hydrolysis gave a mixture of **6**, **7**, and **8**, which were separated by HPLC. The first eluted product was lanost-6-ene-3β,32-diol (**8**) (15% yield), mp 191–192 °C (lit.,<sup>7)</sup> 191.5–192.5 °C). The next eluted product was lanost-7-ene-3β,32-diol (**7**) (42% yield), mp 206–207 °C (lit.,<sup>7)</sup> 207–208.5 °C). The last eluted product was lanost-8-ene-3β,32-diol (**6**) (20% yield), mp 173–174 °C (lit., 161–163 °C<sup>7)</sup> and 174–175 °C<sup>5)</sup>). The melting



points of **6**, **7**, and **8** were undepressed on admixture with the corresponding authentic specimens.

**7-Oxolanostan-3 $\beta$ -ol (5b)**—**5a** was hydrolyzed with 5% methanolic KOH under reflux for 1 h. After usual work-up, the residue was recrystallized from MeOH to give colorless needles of **5b**, mp 169–170 °C (lit.,<sup>6)</sup> 171–173 °C). <sup>1</sup>H-NMR  $\delta$  (ppm): 0.75 (3H, s, 18-CH<sub>3</sub>), 0.83 (3H, s, 4 $\beta$ -CH<sub>3</sub>), 0.85 (3H, d, 26 or 27-CH<sub>3</sub>,  $J=6.6$  Hz), 0.86 (3H, d, 26 or 27-CH<sub>3</sub>,  $J=6.6$  Hz), 0.90 (3H, s, 19-CH<sub>3</sub>), 0.95 (3H, s, 4 $\alpha$ -CH<sub>3</sub>), 1.08 (3H, s, 19-CH<sub>3</sub>), 2.27–2.41 (3H, m, 6-H<sub>2</sub> and 8-H), 3.26 (1H, m, 3 $\alpha$ -H). MS  $m/z$ : 444 ( $M^+$ ), 429 ( $M^+ - CH_3$ ), 411 ( $M^+ - CH_3, H_2O$ ), 393 ( $M^+ - CH_3, 2H_2O$ ), 304, 222 (base peak). CD ( $c=2.55$ , methanol)  $[\theta]^{24}$  (nm): –1915 (294) (negative maximum).

**3 $\beta$ -Hydroxylanost-8-en-32-al (9)**—Jones oxidation of lanost-8-ene-3 $\beta$ ,32-diol (**6**, 15 mg) gave the 3,32-dioxo compound (9 mg), which was partially reduced with KBH<sub>4</sub> (3 mg) to give **9** (4 mg), mp 159–160 °C, (lit.,<sup>11)</sup> 160–161 °C). <sup>1</sup>H-NMR  $\delta$  (ppm): 0.75 (3H, s, 18-CH<sub>3</sub>), 0.82 (3H, s, 4 $\beta$ -CH<sub>3</sub>), 0.85 (3H, d, 26 or 27-CH<sub>3</sub>,  $J=6.6$  Hz), 0.86 (3H, d, 26 or 27-CH<sub>3</sub>,  $J=6.6$  Hz), 0.97 (3H, s, 4 $\alpha$ -CH<sub>3</sub>); 1.05 (3H, s, 19-CH<sub>3</sub>), 3.23 (1H, m, 3 $\alpha$ -H), 9.44 (1H, s, 32-CHO). MS  $m/z$ : 413 ( $M^+ - CHO$ , base peak), 395 ( $M^+ - CHO, H_2O$ ).

**3 $\beta$ -Hydroxylanost-7-en-32-al (10)**—Jones oxidation of 3 $\beta$ -hydroxylanost-7-ene-3 $\beta$ ,32-diol (**7**, 30 mg) gave the 3,32-dioxo compound (20 mg), which was partially reduced with KBH<sub>4</sub> (6 mg) to give **10** (7 mg), mp 119–120 °C (lit.,<sup>5)</sup> 121–122 °C). <sup>1</sup>H-NMR  $\delta$  (ppm): 0.73 (3H, s, 18-CH<sub>3</sub>), 0.85 (3H, d, 26 or 27-CH<sub>3</sub>,  $J=6.6$  Hz), 0.86 (3H, d, 26 or 27-CH<sub>3</sub>,  $J=6.6$  Hz), 0.89 (6H, s, 4 $\beta$  and 19-CH<sub>3</sub>), 0.98 (3H, s, 4 $\alpha$ -CH<sub>3</sub>), 3.24 (1H, m, 3 $\alpha$ -H), 5.44 (1H, m, 7-H), 9.62 (1H, s, 32-CHO). MS  $m/z$ : 413 ( $M^+ - CHO$ , base peak), 395 ( $M^+ - CHO, H_2O$ ).

**Acknowledgement** Part of this work was supported by The Science Research Promotion Fund of Japan Private School Promotion Foundation (1985).

#### References

- 1) N. B. Myant, "The Biology of Cholesterol and Related Steroids," Willium Heinemann Medical Books Ltd., London, 1981, pp. 163–213.
- 2) S. E. Saucier, A. A. Kandutsch, F. R. Taylor, T. A. Spencer, S. Phirwa, and A. K. Gayen, *J. Biol. Chem.*, **260**, 14571 (1985).
- 3) Y. Sato, Y. Sonoda, M. Morisaki, and N. Ikekawa, *Chem. Pharm. Bull.*, **32**, 3305 (1984).
- 4) M. Morisaki, Y. Sonoda, T. Makino, N. Ogihara, N. Ikekawa, and Y. Sato, *J. Biochem. (Tokyo)*, **99**, 597 (1986).
- 5) G. F. Gibbons, C. R. Pullinger, H. W. Chen, W. K. Cavence, and A. A. Kandutsch, *J. Biol. Chem.*, **255**, 395 (1980).
- 6) D. H. R. Barton and B. R. Thomas, *J. Chem. Soc.*, **1953**, 1842.
- 7) E. J. Parish and G. J. Schroepfer, Jr., *J. Lipid Res.*, **22**, 859 (1981).
- 8) M. L. Eidinoff, J. E. Knoll, D. K. Fukushima, and T. F. Gallagher, *J. Am. Chem. Soc.*, **74**, 5280 (1952).
- 9) G. G. Habermehl, J. H. Kirsch, and K. J. Reibstein, *Heterocycles*, **17**, 183 (1982).
- 10) J. T. Pinky, B. J. Ralph, J. J. H. Simes, and M. Wootton, *Aust. J. Chem.*, **23**, 2141 (1970).
- 11) G. F. Gibbons, K. A. Mitropoulos, and C. R. Pullinger, *Biochem. Biophys. Res. Commun.*, **69**, 781 (1976).

[Chem. Pharm. Bull.  
35(1) 398-401 (1987)]

## Utilization of Organoselenium Compounds. II.<sup>1)</sup> Reaction of Fused Isoselenazoles with Alkylamines

TAISEI UEDA, SATOKO KAWAI and JINSAKU SAKAKIBARA\*

*Faculty of Pharmaceutical Sciences, Nagoya City University,  
Tanabe-dori, Mizuho-ku, Nagoya 467, Japan*

(Received July 8, 1986)

A facile conversion of the methyl group of 5-amino-6-methyl-3-phenyl-4(3*H*)-pyrimidinone (1) or 4-aminoantipyrine (5) to an alkyliminomethyl group by isoselenazole ring formation followed by reaction with alkylamines was carried out. 7-Oxo-6-phenyl-6*H*-isoselenazolo[4,3-*d*]pyrimidine (2), which was obtained from 1 and selenium dioxide, was reacted with alkylamines, such as *n*-propylamine, isopropylamine and 3-methoxypropylamine, to give 6-alkyliminomethyl-5-amino-3-phenyl-4(3*H*)-pyrimidinones (3*a*—*d*) in 47—58% yields. Treatment of 3*a*—*d* with silica gel gave 5-amino-6-formyl-3-phenyl-4(3*H*)-pyrimidinone (4) in 91% yield. Similarly the reaction of 5,6-dihydro-4-methyl-6-oxo-5-phenyl-4*H*-pyrazolo[4,3-*c*]isoselenazole (6) with alkylamines gave 3-alkyliminomethyl-4-amino-1-phenyl-3-pyrazolin-5-ones (7*a*—*f*) in 50—97% yields.

**Keywords**—isoselenazole; isoselenazolo[4,3-*d*]pyrimidine; pyrazolo[4,3-*c*]isoselenazole; alkylamine; 4-aminoantipyrine; pyrimidine; selenium dioxide

Recently, chemical and biological applications of organoselenium compounds have developed considerably.<sup>2)</sup> Studies on the syntheses of selenium containing heterocycles have also been carried out in our laboratory, and some biologically interesting compounds and reactions have been reported.<sup>1,3)</sup> As a continuation of our work, this paper deals with a facile conversion of the methyl group of 5-amino-6-methyl-3-phenyl-4(3*H*)-pyrimidinone<sup>4)</sup> (1) or 4-aminoantipyrine<sup>5)</sup> (5) to an alkyliminomethyl group by isoselenazole ring formation followed by reaction with alkylamines.

Synthesis of 7-oxo-6-phenyl-6*H*-isoselenazolo[4,3-*d*]pyrimidine (2) by the reaction of 1 with selenium dioxide in dioxane was reported by us previously.<sup>3*a*)</sup> It is said that organoselenium compounds are susceptible to nucleophilic attack on the selenium atom, usually resulting in cleavage of the weak C—Se bond.<sup>2*a*)</sup> Thus, it appeared to be interesting to examine the reaction of 2 with alkylamines. Treatment of 2 with primary alkylamines, such as *n*-propylamine, isopropylamine, *n*-butylamine, and 3-methoxypropylamine in ethanol under reflux for 7—24 h gave 6-alkyliminomethyl-5-amino-3-phenyl-4(3*H*)-pyrimidinones (3*a*—*d*) in 47—58% yields. These products were purified by recrystallization from ethanol. An attempt to purify 3 by column chromatography on silica gel gave 5-amino-6-formyl-3-phenyl-4(3*H*)-pyrimidinone (4) in 91% yield. Similarly, the reaction of 5,6-dihydro-4-methyl-6-oxo-5-phenyl-4*H*-pyrazolo[4,3-*c*]isoselenazole<sup>6)</sup> (6) with alkylamines gave 3-alkyliminomethyl-4-amino-1-phenyl-3-pyrazolin-5-ones (7*a*—*f*) in 50—97% yields. The infrared (IR) spectra of all these compounds (3*a*—*d*, 4, 7*a*—*f*) showed NH<sub>2</sub> absorptions, and elemental analyses and mass spectra were consistent with the assigned structures (Tables I and II). Recrystallization of 7*a*—*f* from ethanol gave analytically pure samples. However, treatment of 7*a*—*f* with silica gel gave reddish intractable glutinous substances, from which only a trace amount of a compound of mp 137—139 °C [*m/z* = 217 (M<sup>+</sup>)], possibly 4-amino-3-formyl-2-methyl-1-phenyl-3-pyrazolin-5-one (8), was obtained.

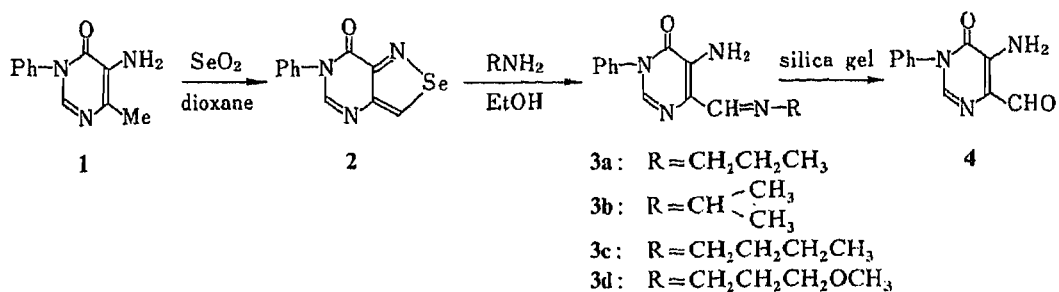


Chart 1

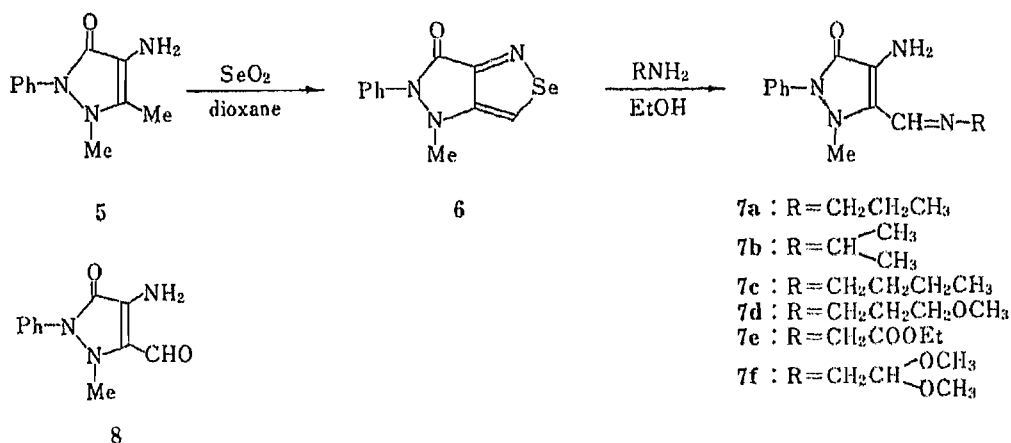


Chart 2

The reaction mechanism in the formation of **3** or **7** from **2** or **6** seems to be as follows. The canonical forms of the fused isoselenazoles can be depicted as in Chart 3. The nucleophilic substitution reaction takes place initially at the carbon atom adjacent to selenium which has exceptionally low electron density. Rupture of the isoselenazole ring followed by deselenation gives **3** or **7**.

Consequently our new method to convert the methyl group of **1** or **5** to an alkylimino-methyl group or formyl group should be convenient and useful for the synthesis of further annelated compounds which might show important pharmacological activities.

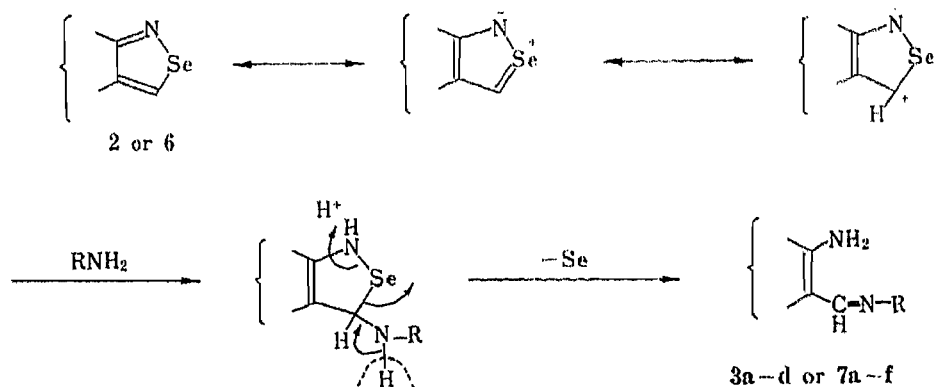


Chart 3

TABLE I. 6-Alkyliminomethyl-5-amino-3-phenyl-4(3*H*)-pyrimidinones

Compd. No.	mp (°C)	Yield (%)	Reaction time (h)	Formula	Analysis (%)			MS <i>m/z</i> (M <sup>+</sup> )
					Calcd (Found)			
					C	H	N	
3a	151—153	53	7	C <sub>14</sub> H <sub>16</sub> N <sub>4</sub> O	65.61 (65.47)	6.29 (6.06)	21.86 (21.82)	256
3b	138—140	58	24	C <sub>14</sub> H <sub>16</sub> N <sub>4</sub> O	65.61 (65.80)	6.29 (5.98)	21.86 (21.74)	256
3c	135—137	47	7	C <sub>15</sub> H <sub>18</sub> N <sub>4</sub> O	66.65 (66.69)	6.71 (6.41)	20.72 (20.53)	270
3d	124—125	55	7	C <sub>15</sub> H <sub>18</sub> N <sub>4</sub> O <sub>2</sub>	62.92 (62.75)	6.34 (6.21)	19.57 (19.81)	286

TABLE II. 3-Alkyliminomethyl-4-amino-2-methyl-1-phenyl-3-pyrazolin-5-ones

Compd. No.	mp (°C)	Yield (%)	Reaction time (h)	Formula	Analysis (%)			MS <i>m/z</i> (M <sup>+</sup> )
					Calcd (Found)			
					C	H	N	
7a	90—92	92	5	C <sub>14</sub> H <sub>18</sub> N <sub>4</sub> O	65.09 (65.08)	7.02 (6.95)	21.69 (21.67)	258
7b	140—142	95	5	C <sub>14</sub> H <sub>18</sub> N <sub>4</sub> O	65.09 (65.35)	7.02 (7.15)	21.69 (21.54)	258
7c	92—94	97	5	C <sub>15</sub> H <sub>20</sub> N <sub>4</sub> O	66.15 (66.20)	7.40 (7.59)	20.57 (20.76)	272
7d	120—121	90	5	C <sub>15</sub> H <sub>20</sub> N <sub>4</sub> O <sub>2</sub>	62.48 (62.32)	6.99 (6.94)	19.43 (19.57)	288
7e	96—97	50	10	C <sub>15</sub> H <sub>18</sub> N <sub>4</sub> O <sub>3</sub>	59.59 (59.43)	6.00 (5.81)	18.53 (18.29)	302
7f	82—83	86	5	C <sub>15</sub> H <sub>20</sub> N <sub>4</sub> O <sub>3</sub>	59.19 (58.91)	6.62 (6.41)	18.41 (18.55)	304

### Experimental

All melting points were determined on a Yanagimoto micro melting point apparatus and are uncorrected. The IR spectra were measured with an IR-810 machine from Nihon Bunko Spectroscopic Co., Ltd. Mass spectra (MS) were measured with a Japan Electron Optics Laboratory Co. JMS-DX 300 mass spectrometer. The proton nuclear magnetic resonance (<sup>1</sup>H-NMR) spectra were recorded with a Japan Electron Optics Laboratory Co. JNM-MH 100 spectrometer using tetramethylsilane as an internal standard. Abbreviations are as follows: s, singlet; m, multiplet; br, broad.

**6-Alkyliminomethyl-3-phenyl-4(3*H*)-pyrimidinones (3a—d)**—A mixture of 7-oxo-6-phenyl-6*H*-isoseleazol[4,3-*d*]pyrimidine<sup>3a)</sup> (2) (1 mmol) and an alkylamine (10 mmol) in 20 ml ethanol was refluxed for 7 or 24 h. The resulting black substance (Se) was removed by filtration. Solvent and excess alkylamine were distilled off from the filtrate, and the residue was recrystallized from ethanol to give the pure product. Melting points and elemental analytical data are listed in Table I.

**5-Amino-6-formyl-3-phenyl-4(3*H*)-pyrimidinone (4)**—A solution of 5-amino-3-phenyl-6-propyliminomethyl-4(3*H*)-pyrimidinone (3a) 256 mg (1 mmol) in chloroform-methanol (30:1) was passed through a silica gel column. The eluate was collected and the solvent was distilled off. The residue was recrystallized from ethanol to give colorless needles of mp 192—194°C. Yield 196 mg (91%). IR  $\nu_{\max}^{\text{KBr}}$  cm<sup>-1</sup>: 3400, 3290 (NH<sub>2</sub>), 1680, 1660 (C=O). MS *m/z*: 215 (M<sup>+</sup>). Anal. Calcd for C<sub>11</sub>H<sub>9</sub>N<sub>3</sub>O<sub>2</sub>: C, 61.39; H, 4.21; N, 19.53. Found: C, 61.24; H, 4.20; N, 19.40. <sup>1</sup>H-NMR (CDCl<sub>3</sub>)  $\delta$ : 9.95 (1H, s, CHO), 7.60 (1H, s, -N-CH=N-), 7.00 (2H, br, NH<sub>2</sub>), 7.20—7.55 (5H, m, Ph).

**3-Alkyliminomethyl-4-amino-2-methyl-1-phenyl-3-pyrazolin-5-ones (7a—f)**—A mixture of 5,6-dihydro-4-

methyl-6-oxo-5-phenyl-4*H*-pyrazolo[4,3-*c*]isoseleazole<sup>61</sup> (**6**) (1 mmol) and an alkylamine (10 mmol) was treated as described for **3a**—**d**. Melting points and elemental analytical data are listed in Table II.

**4-Amino-3-formyl-2-methyl-1-phenyl-3-pyrazolin-5-one (8)**—A solution of 4-amino-2-methyl-1-phenyl-3-propyliminomethyl-3-pyrazolin-5-one (**7a**) (258 mg, 1 mmol) in chloroform–methanol (30:1) was passed through a silica gel column. The eluate was collected and the solvent was distilled off. The residue was extracted with ether. The extract was column chromatographed on silica gel and eluted with ether. The eluate was collected and concentrated. On standing, needles were formed with a red tarry substance. The needles were collected by filtration and washed with a small amount of a mixture of ether–ethanol (1:1) to give reddish needles of mp 137–139°C. Yield 3 mg (1.4%). IR  $\nu_{\text{max}}^{\text{KBr}}$  cm<sup>-1</sup>: 3420, 3250 (NH<sub>2</sub>), 1680, 1640 (C=O). MS *m/z*: 217 (M<sup>+</sup>).

**Acknowledgment** This work was supported in part by a Grant-in-Aid by the Ishida Foundation. The authors are indebted to Miss T. Naito and Miss S. Kato of this Faculty for elemental analyses and NMR measurements.

#### References and Notes

- 1) Part I: T. Ueda, Y. Shibata and J. Sakakibara, *Chem. Pharm. Bull.*, **33**, 3065 (1985).
- 2) a) H. J. Reich, *Acc. Chem. Res.*, **12**, 22 (1979); b) D. Liotta, *ibid.*, **17**, 28 (1984); c) P. C. Srivastava and R. K. Robins, *J. Med. Chem.*, **26**, 445 (1983); d) W. C. Groutas, M. C. Theodorakis, W. A. F. Tomkins, G. Herro and T. Gaynor, *ibid.*, **27**, 548 (1984); e) T. A. Ventslavskayaa, L. L. Stazhadze and V. V. Korzhova, *Farmakol. Toksikol.*, **47**, 38 (1984) [*Chem. Abstr.*, **100**, 167960h (1984)]; f) T. Arunachalam and E. Caspi, *J. Org. Chem.*, **46**, 3415 (1981).
- 3) a) T. Ueda, Y. Shibata, J. Sakakibara, M. Inoue and T. Ishida, *Chem. Pharm. Bull.*, **30**, 3424 (1982); b) T. Ueda, H. Yoshida and J. Sakakibara, *Synthesis*, **1985**, 695; c) H. Ito, J. Sakakibara and T. Ueda, *Cancer Lett.*, **28**, 61 (1985).
- 4) T. Ueda, N. Oda and I. Ito, *Heterocycles*, **8**, 263 (1977).
- 5) This material was purchased from Wako Pure Chemical Industries Ltd.
- 6) H. Hidaka and J. Sakakibara, Jpn. Kokai Tokkyo Koho, 1984, JP 5920274 [*Chem. Abstr.*, **101**, 7192b (1984)].

[Chem. Pharm. Bull.]  
35(1) 402-408 (1987)

**Furo[3,2-*b*]indole Derivatives. V.<sup>1)</sup> Synthesis and Structure-Activity Studies of 4-Substituted 2-(4-Methylpiperazinylcarbonyl)-6-trifluoromethylfuro[3,2-*b*]indole Derivatives with Analgesic and Antiinflammatory Activities<sup>2)</sup>**

YUTAKA KAWASHIMA,\*<sup>a</sup> SHIGERU OKUYAMA,<sup>a</sup> MASAKAZU SATO,<sup>a</sup> YUICHI HATADA,<sup>a</sup>  
FUSAO AMANUMA,<sup>a</sup> YOSHIMOTO NAKASHIMA,<sup>a</sup> KAORU SOTA,<sup>a</sup>  
and IKUO MORIGUCHI<sup>b</sup>

Research Center, Taisho Pharmaceutical Co., Ltd.,<sup>a</sup> Yoshino-cho, Ohmiya, Saitama 330, Japan  
and School of Pharmaceutical Sciences, Kitasato University,<sup>b</sup> Shirokane  
5-chome, Minato-ku, Tokyo 108, Japan

(Received June 3, 1986)

Based on the quantitative structure-activity relationships (QSAR) of 4,6-disubstituted 2-morpholinocarbonylfuro[3,2-*b*]indole derivatives (53 compounds) previously reported, 4-substituted 2-(4-methylpiperazinylcarbonyl)-6-trifluoromethylfuro[3,2-*b*]indole derivatives (12 compounds) were synthesized. Their analgesic and antiinflammatory activities were examined by using the acetic acid writhing test in mice and the carrageenin edema test in rats, respectively. Most of these compounds showed potent analgesic and antiinflammatory activities as compared with tiaramide. The QSAR of the furo[3,2-*b*]indole derivatives (65 compounds) including the newly synthesized compounds was analyzed by using the adaptive least-squares method. The results confirmed that the QSARs for 2-morpholinocarbonyl derivatives and 2-(4-methylpiperazinylcarbonyl) derivatives can be expressed in one model where the steric nature of the 4- and 6-substituents mainly affects both the analgesic and antiinflammatory potencies.

**Keywords**—furo[3,2-*b*]indole-2-carboxamide; quantitative structure-activity relationship; adaptive least-squares method; analgesic activity; antiinflammatory activity; 4-substituted 2-(4-methylpiperazinylcarbonyl)-6-trifluoromethylfuro[3,2-*b*]indole

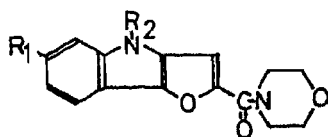
In the previous papers,<sup>1,3)</sup> we reported the synthesis, analgesic and antiinflammatory activities, as well as quantitative structure-activity relationship (QSAR) studies, of 4,6-disubstituted 2-morpholinocarbonylfuro[3,2-*b*]indole derivatives (I). Equations 1 and 2 were formulated for the QSAR of analgesic and antiinflammatory activities, respectively.

$$Y = -0.68E_s(1) + 0.11L(2) + 1.19Nc\beta_a + 1.91D_{acyl} + 1.27D_{alkyl} - 3.10 \quad (1)$$

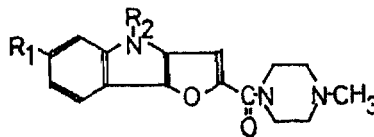
$n = 53 \quad n_{mis} = 6(0) \quad R_S = 0.91 \quad R_S(pred) = 0.87$

$$Y = 2.84B_1(1) - 1.70F(1) + 0.63Nc\beta_a + 0.71D_{acyl} + 1.18D_{alkyl} - 4.47 \quad (2)$$

$n = 53 \quad n_{mis} = 9(1) \quad R_S = 0.87 \quad R_S(pred) = 0.84$

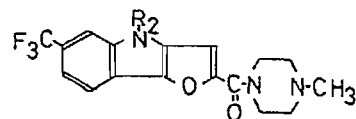


I



II

Chart 1

TABLE I. 2-(4-Methylpiperazinylcarbonyl)-6-trifluoromethylfuro[3,2-*b*]indole Derivatives (II)


No.	R <sub>2</sub>	mp (°C)	Recrystn. solvent <sup>a)</sup>	Formula	Analysis (%)			Analgesic activity <sup>b)</sup>	Anti-inflammatory activity <sup>c)</sup>
					Calcd (Found)				
					C	H	N		
II-1	COOiso-Pr	178—179	E-T	C <sub>21</sub> H <sub>22</sub> F <sub>3</sub> N <sub>3</sub> O <sub>4</sub> · Mal <sup>d)</sup>	54.25 (54.10)	4.74 (4.73)	7.59 (7.66)	85.5 <sup>h)</sup>	64.3 <sup>h)</sup>
II-2	COOBu	141—142	E	C <sub>22</sub> H <sub>24</sub> F <sub>3</sub> N <sub>3</sub> O <sub>4</sub>	58.53 (58.68)	5.36 (5.54)	9.31 (9.28)	69.4 <sup>h)</sup>	—0.6
II-3	COOiso-Bu	194.5—195.5	M	C <sub>22</sub> H <sub>24</sub> F <sub>3</sub> N <sub>3</sub> O <sub>4</sub> · Mal	55.02 (55.18)	4.97 (4.98)	7.40 (7.50)	91.7 <sup>h)</sup>	50.0 <sup>g)</sup>
II-4	COiso-Bu	174.5—175.5	T-H	C <sub>22</sub> H <sub>24</sub> F <sub>3</sub> N <sub>3</sub> O <sub>3</sub> · Mal	56.62 (56.54)	5.12 (5.12)	7.62 (7.60)	81.6 <sup>h)</sup>	64.1 <sup>h)</sup>
II-5	Bu	174—176	T	C <sub>21</sub> H <sub>24</sub> F <sub>3</sub> N <sub>3</sub> O <sub>2</sub> · Mal	57.36 (57.45)	5.39 (5.39)	8.02 (8.06)	75.5 <sup>h)</sup>	55.0 <sup>h)</sup>
II-6	iso-Bu	170—173.5	E-M	C <sub>21</sub> H <sub>24</sub> F <sub>3</sub> N <sub>3</sub> O <sub>2</sub> · Mal	57.36 (57.09)	5.39 (5.32)	8.02 (7.86)	55.6 <sup>h)</sup>	20.1 <sup>f)</sup>
II-7	Pentyl	224—226	E-H	C <sub>22</sub> H <sub>26</sub> F <sub>3</sub> N <sub>3</sub> O <sub>2</sub> · HCl <sup>e)</sup>	57.71 (57.47)	5.94 (6.22)	9.17 (8.96)	62.5 <sup>h)</sup>	58.4 <sup>h)</sup>
II-8	Isopentyl	159—160	T	C <sub>22</sub> H <sub>26</sub> F <sub>3</sub> N <sub>3</sub> O <sub>2</sub> · Mal	58.10 (58.03)	5.63 (5.60)	7.82 (7.71)	93.5 <sup>h)</sup>	75.8 <sup>h)</sup>
II-9	Hexyl	199—200	T-H	C <sub>23</sub> H <sub>28</sub> F <sub>3</sub> N <sub>3</sub> O <sub>2</sub> · HCl	58.53 (58.30)	6.19 (6.18)	8.90 (9.03)	77.6 <sup>h)</sup>	67.2 <sup>h)</sup>
II-10	Isohexyl	144—145	E-M	C <sub>23</sub> H <sub>28</sub> F <sub>3</sub> N <sub>3</sub> O <sub>2</sub> · Mal	58.79 (58.52)	5.85 (5.77)	7.62 (7.49)	95.9 <sup>h)</sup>	54.7 <sup>h)</sup>
II-11	Heptyl	161—168	T	C <sub>24</sub> H <sub>30</sub> F <sub>3</sub> N <sub>3</sub> O <sub>2</sub> · HCl	59.34 (59.00)	6.43 (6.35)	8.65 (8.80)	85.4 <sup>h)</sup>	63.1 <sup>h)</sup>
II-12	Octyl	167.5—168.5	E-M	C <sub>25</sub> H <sub>32</sub> F <sub>3</sub> N <sub>3</sub> O <sub>2</sub> · Mal	60.09 (59.86)	6.26 (6.35)	7.25 (7.16)	45.3 <sup>h)</sup>	50.3 <sup>g)</sup>
Tiaramide								74.8 <sup>h)</sup>	52.4 <sup>h)</sup>

a) E=ether, H=hexane, M=MeOH, T=EtOH. b) % inhibition of acetic acid writhing in mice (100 mg/kg, *p.o.*). c) % inhibition of carrageenin edema in rats (100 mg/kg, *p.o.*). d) Mal=maleate. e) HCl=hydrochloride. Statistically significant at f)  $p < 0.05$ , g)  $p < 0.01$ , h)  $p < 0.001$ .

In these expressions,  $Y$  is the discriminant score for the classification of activity ratings,  $E_s$  is the Taft steric substituent parameter,<sup>4)</sup>  $B_1$  and  $L$  are the STERIMOL parameters,<sup>5)</sup>  $F$  is the new Swain–Lupton field constant,<sup>6)</sup> and  $Nc\beta_a$  is the number of  $\beta$ -carbon atoms of the alkoxy moiety as  $R_2$ . The figure in parentheses after the descriptor indicates the position of the substituent ( $R_1$  or  $R_2$  in Chart 1). The indicator variables  $D_{acyl}$  and  $D_{alkyl}$  are assigned a value of 1 for the presence of an acyl moiety and an alkyl (or alkenyl) moiety as  $R_2$ , respectively. Further,  $n$  represents the number of compounds,  $n_{mis}$  is the number misclassified, and the figure in parentheses after the value of  $n_{mis}$  is the number misclassified by two grades,  $R_s$  is the Spearman rank correlation coefficient for the recognition, and  $R_s(\text{pred})$  is that for the prediction by the use of the leave-one-out technique. These equations indicate that, as regards the substituents of the indole moiety, bulky and branched substituents are favorable for the analgesic activity, and that steric and electron withdrawing effects are required for high antiinflammatory potency. We thought that the relationship would be valid for 2-(4-methylpiperazinylcarbonyl)furo[3,2-*b*]indole derivatives (II), and this prompted us to undertake the present study.

This paper describes the synthesis and activity of the derivatives (II) and an analysis of the QSAR of the overall compounds (I and II) for analgesic and antiinflammatory activities using the adaptive least-squares (ALS) method.<sup>7,8)</sup>

### Results and Discussion

Based on the results of our previous structure–activity study<sup>1)</sup> of 2-morpholino-carbonylfuro[3,2-*b*]indole derivatives (53 compounds), various 4-substituted 2-(4-methylpiperazinylcarbonyl)-6-trifluoromethylfuro[3,2-*b*]indole derivatives (12 compounds) were designed. The  $R_1$  substituent was fixed as  $\text{CF}_3$ , which was expected to be most favorable for the activities from its  $E_s$ ,  $B_1$ , and  $F$  values. The  $R_2$  substituents were chosen from alkoxycarbonyl, acyl, and alkyl groups. These compounds (II-1—12) were synthesized by the method described in the previous paper,<sup>3)</sup> and were examined for analgesic activity by using

TABLE II. Structural Features and Analgesic and Antiinflammatory Activities of 2-(4-Methylpiperazinylcarbonyl)-6-trifluoromethylfuro[3,2-*b*]indole Derivatives (II)

No.	$R_2$	Analgesic activity			Antiinflammatory activity			Descriptor		
		Obsd. <sup>a)</sup>	Recog. <sup>b)</sup>	Pred. <sup>c)</sup>	Obsd. <sup>d)</sup>	Recog. <sup>e)</sup>	Pred. <sup>e)</sup>	$E_s(1)^f)$	$L(2)^g)$	$Nc\beta^h)$
II-1	COOiso-Pr	3	3	3	3	3	3	-2.4	5.97	2
II-2	COOBu	2	3	3	1	3	3	-2.4	8.00	1
II-3	COOiso-Bu	3	3	3	3	3	3	-2.4	6.77	1
II-4	COiso-Bu	3	3	3	3	3	3	-2.4	6.12	1
II-5	Bu	3	3	3	3	3	3	-2.4	6.17	0
II-6	Iso-Bu	2	2	2	2	3	3	-2.4	5.05	0
II-7	Pentyl	2	3	3	3	3	3	-2.4	7.11	0
II-8	Isopentyl	3	3	3	3	3	3	-2.4	6.17	0
II-9	Hexyl	3	3	3	3	3	3	-2.4	8.22	0
II-10	Isohexyl	3	3	3	3	3	3	-2.4	6.97	0
II-11	Heptyl	3	3	3	3	3	3	-2.4	9.03	0
II-12	Octyl	2	3	3	3	3	3	-2.4	10.27	0

a) Activity ratings based on the percent inhibition of acetic acid writhing at 100 mg/kg, *p.o.* in mice: class 1, 0–39; class 2, 40–69; class 3, 70–100. b) From Eq. 4. c) Using the leave-one-out technique. d) Activity ratings based on the percent inhibition of carrageenin edema at 100 mg/kg, *p.o.* in rats: class 1, less than 15; class 2, 15–49; class 3, 50–100. e) From Eq. 6. f) See ref. 4). g) See ref. 5). h)  $Nc\beta$  is the number of  $\beta$  carbon atoms of the alkoxy or acyl moiety  $R_2$ .



TABLE III. ALS Discriminant Functions for 65 Furo[3,2-*b*]indole Derivatives

Eq. No.	$n^{a)}$	Recognition		Prediction <sup>b)</sup>	
		$n_{\text{mis}}^{c)}$	$R_S^{d)}$	$n_{\text{mis}}^{c)}$	$R_S^{d)}$
Analgesic activity					
3	$Y = -0.97E_s(1) + 0.56Nc\beta - 1.99$ ( $CI=0.90$ ) <sup>f)</sup> (0.41) <sup>f)</sup>	65	15 (1) <sup>c)</sup> 0.75	16 (1)	0.75
4	$Y = -1.02E_s(1) + 0.04L(2) + 0.63Nc\beta - 2.32$ ( $CI=0.95$ ) (0.05) (0.46)	65	13 (0) 0.82	14 (0)	0.80
Antiinflammatory activity					
5	$Y = -0.87E_s(1) - 1.33$ ( $CI=0.80$ )	65	14 (3) 0.78	14 (3)	0.78
6	$Y = -0.69E_s(1) + 0.04L(2) - 1.41$ ( $CI=0.64$ ) (0.05)	65	15 (1) 0.82	15 (1)	0.83

a) Number of points used for calculations. b) Using the leave-one-out technique. c) Number of misclassified compounds. d) Spearman rank correlation coefficient with a correction of many ties; the values are all significant at  $p < 0.01$ . e) Number of compounds misclassified by two grades. f) Contribution index (CI).

the acetic acid writhing test<sup>9)</sup> in mice and for antiinflammatory activity by using carrageenin edema test in rats.<sup>10)</sup> The biological and physical data are summarized in Table I. Most of the obtained compounds showed potent analgesic and antiinflammatory activities. The analgesic activities of II-1, -3, -4, -8, -10, and -11 were higher than that of tiaramide. The antiinflammatory activities of II-1, -4, -8, -9, and -11 were also more potent than that of tiaramide.

Then, the QSAR of 65 furo[3,2-*b*]indole derivatives [53 2-morpholinocarbonyl compounds and 12 2-(4-methylpiperazinylcarbonyl) compounds] was analyzed by using the ALS method. The descriptors and activity ratings for the newly synthesized compounds analyzed in this study are listed in Table II. Good discriminant functions for the two kinds of activity are expressed by Eqs. 3–6 (Table III), which were derived within 20 iterations.

In these equations  $Nc\beta$  is the number of  $\beta$  carbon atoms of the alkoxy or acyl moiety for  $R_2$ . The figure in parentheses under the coefficient for each descriptor is the contribution index ( $= |\text{coef.}| \times \text{S.D. of descriptor}$ ), which is a measure of the contribution of the descriptor to the discriminant score. The cross-correlation matrix of the descriptors used in Eqs. 3–6 is shown in Table IV, indicating that there is little likelihood of chance correlations.

TABLE IV. Cross-Correlation Matrix of Descriptors Used in Eqs. 3–6

	$E_s(1)$	$L(2)$	$Nc\beta$
$E_s(1)$	1.00		
$L(2)$	-0.24	1.00	
$Nc\beta$	0.21	-0.10	1.00

On the basis of Eq. 4 for the analgesic activity, a bulky substituent  $R_1$  (in terms of  $-E_s$ ) is favorable to the potency. For the  $R_2$  substituent, long and more branched groups (in terms of  $L$  and  $Nc\beta$ ) are favorable to the analgesic activity. Equation 6 for the antiinflammatory activity resembles Eq. 4, with a negative coefficient for  $E_s(1)$  and a positive coefficient for  $L(2)$ , indicating that a bulky substituent  $R_1$  and a long substituent  $R_2$  enhance both potencies.

The use of an indicator variable for the distinction between the 2-morpholinocarbonyl

TABLE V. Spectral Data for 2-(4-Methylpiperazinylcarbonyl)-6-trifluoromethylfuro[3,2-*b*]indole Derivatives (II)

No.	Yield (%)	IR $\nu_{\max}^{\text{KBr}} \text{cm}^{-1}$	MS $m/e$ ( $M^+$ )	$^1\text{H-NMR}$ Chemical shifts ( $\delta$ ) (in $\text{DMSO-}d_6$ )
II-1	40.2	1720 1640	553	1.50 (6H, d, $J=7$ Hz), 2.86 (3H, s), 3.31 (4H, m), 4.04 (4H, m), 5.25 (1H, m), 6.15 (2H, s), 7.40 (1H, s), 7.72 (1H, dd, $J=8, 2$ Hz), 8.02 (1H, d, $J=8$ Hz), 8.52 (1H, d, $J=2$ Hz)
II-2	38.9	1750 1645	451	1.00 (3H, t, $J=7$ Hz), 1.50 (2H, m), 1.80 (2H, m), 2.25 (3H, s), 2.42 (4H, m), 3.78 (4H, m), 4.47 (3H, t, $J=7$ Hz), 7.26 (1H, s), 7.68 (1H, dd, $J=8, 2$ Hz), 7.97 (1H, d, $J=8$ Hz), 8.46 (1H, d, $J=2$ Hz)
II-3	38.9	1750 1645	567	1.06 (6H, d, $J=7$ Hz), 2.20 (1H, m), 2.83 (3H, s), 3.30 (4H, m), 4.04 (4H, m), 4.30 (2H, d, $J=7$ Hz), 6.10 (2H, s), 7.40 (1H, s), 7.73 (1H, dd, $J=8, 2$ Hz), 8.04 (1H, d, $J=8$ Hz), 8.50 (1H, d, $J=2$ Hz)
II-4	59.0	1725 1630	551	1.10 (6H, d, $J=7$ Hz), 2.18 (1H, m), 2.86 (3H, s), 3.05 (2H, d, $J=7$ Hz), 3.32 (4H, m), 4.07 (4H, m), 6.12 (2H, s), 7.70 (1H, s), 7.75 (1H, dd, $J=8, 2$ Hz), 8.04 (1H, d, $J=8$ Hz), 8.87 (1H, d, $J=2$ Hz)
II-5	98.0	1705 1615	523	0.90 (3H, t, $J=7$ Hz), 1.28 (2H, m), 1.82 (2H, m), 2.83 (3H, s), 3.29 (4H, br s), 4.44 (2H, t, $J=7$ Hz), 6.10 (2H, s), 7.48 (1H, dd, $J=8, 2$ Hz), 7.69 (1H, s), 8.00 (1H, d, $J=8$ Hz), 8.11 (1H, d, $J=2$ Hz)
II-6	30.0	1615	523	0.90 (6H, d, $J=7$ Hz), 2.25 (1H, m), 3.30 (4H, m), 4.04 (4H, m), 4.26 (2H, d, $J=7$ Hz), 6.10 (2H, s), 7.47 (1H, dd, $J=8, 2$ Hz), 7.69 (1H, s), 7.99 (1H, d, $J=8$ Hz), 8.11 (1H, d, $J=2$ Hz), 2.84 (3H, s)
II-7	66.0	1615	457	0.82 (3H, t, $J=7$ Hz), 1.27 (4H, m), 1.92 (2H, m), 2.82 (3H, s), 3.20 (2H, br s), 3.50 (4H, br s), 4.42 (2H, t, $J=7$ Hz), 4.66 (2H, d, $J=8$ Hz), 7.47 (1H, dd, $J=8, 2$ Hz), 7.69 (1H, s), 8.00 (1H, d, $J=8$ Hz), 8.09 (1H, d, $J=2$ Hz), 11.63 (1H, br s)
II-9	53.0	1620	471	0.82 (3H, t, $J=7$ Hz), 1.14 (6H, m), 1.88 (2H, br s), 2.82 (3H, s), 3.20 (2H, br s), 3.58 (4H, br s), 4.43 (2H, t, $J=7$ Hz), 4.68 (2H, br s), 7.47 (1H, dd, $J=8, 2$ Hz), 7.70 (1H, s), 8.00 (1H, d, $J=8$ Hz), 8.10 (1H, d, $J=2$ Hz), 11.66 (1H, br s)
II-10	15.0	1620	551	0.86 (6H, d, $J=7$ Hz), 1.20 (2H, m), 1.56 (1H, br s), 1.85 (2H, m), 2.84 (3H, s), 3.30 (4H, m), 4.06 (4H, m), 4.42 (2H, t, $J=7$ Hz), 6.11 (2H, s), 7.47 (1H, dd, $J=8, 2$ Hz), 7.68 (1H, s), 7.98 (1H, d, $J=8$ Hz), 8.08 (1H, d, $J=2$ Hz)
II-11	40.0	1620	485	0.81 (3H, t, $J=7$ Hz), 1.22 (8H, m), 1.82 (2H, br s), 2.82 (3H, s), 3.26 (2H, br s), 3.48 (4H, br s), 4.42 (2H, t, $J=7$ Hz), 4.66 (2H, d, $J=8$ Hz), 7.47 (1H, dd, $J=8, 2$ Hz), 7.70 (1H, s), 8.00 (1H, d, $J=8$ Hz), 8.10 (1H, d, $J=2$ Hz), 11.76 (1H, br s)
II-12	67.0	1613	579	0.83 (3H, t, $J=7$ Hz), 1.26 (10H, br s), 1.80 (2H, m), 2.83 (3H, s), 3.33 (4H, m), 4.07 (4H, m), 4.40 (2H, t, $J=7$ Hz), 6.10 (2H, s), 7.40 (1H, dd, $J=8, 2$ Hz), 7.60 (1H, s), 7.93 (1H, d, $J=8$ Hz), 8.00 (1H, d, $J=2$ Hz)

series (I) and the 2-(4-methylpiperazinyl)carbonyl series (II) was not effective in the QSAR for the two activities. The importance of the electron-withdrawing effect of the substituent  $R_1$  for antiinflammatory activity of 2-morpholinocarbonyl compounds<sup>1)</sup> was not significant in the present study, probably owing to a higher intercorrelation between steric and electron withdrawing properties caused by the increase in the number of compounds having a  $\text{CF}_3$  group as  $R_1$  in the data set. The contribution of hydrophobic character was insignificant, perhaps on account of the small difference of hydrophobicity from molecule to molecule within the set of compounds studied.

The resulting recognition and leave-one-out prediction in both activities were a little inferior to those<sup>1)</sup> for the 2-morpholinocarbonyl compounds in terms of  $R_s$  values (Table III). However, the results of prediction, which were almost equivalent to those of recognition in this study, were fairly good, and all the  $R_s$  values for Eqs. 3—6 showed a significance level of  $p < 1\%$ .

Thus, it was confirmed for furo[3,2-*b*]indole derivatives that the QSAR for series I and II can be expressed in one model where the steric nature of the substituents  $R_1$  and  $R_2$  mainly affects both the analgesic and antiinflammatory potencies.

### Experimental

Melting points were determined on a Mitamura Riken micro melting point apparatus and are uncorrected. Infrared (IR) spectra were taken on a JASCO DS-301 spectrometer. Proton nuclear magnetic resonance ( $^1\text{H-NMR}$ ) spectra were recorded on a Hitachi-Perkin-Elmer R-20 spectrometer. Chemical shifts are given in ppm with tetramethylsilane as an internal standard, and the following abbreviations are used: singlet (s), broad singlet (brs), doublet (d), double doublet (dd), double triplet (dt), triplet (t), quartet (q) and multiplet (m). Mass spectra (MS) were taken on a Shimadzu LKB 9000 spectrometer.

#### Chemistry

**4-Isopentyl-2-(4-methylpiperazinylcarbonyl)-6-trifluoromethylfuro[3,2-*b*]indole Maleate (II-8)**—A solution of 2-(4-methylpiperazinylcarbonyl)-6-trifluoromethyl-4*H*-furo[3,2-*b*]indole (3.5 g) in dimethylformamide (DMF) (20 ml) was added dropwise with stirring to a suspension of sodium hydride (NaH) (60% in oil, 0.16 g) in DMF (10 ml), then the mixture was stirred for 0.5 h. Isopentyl bromide (1.8 g) was added thereto, and the whole was stirred for 1 h at room temperature, then poured into ice-water. The resulting product was collected by filtration (2.6 g, 63%).

On the treatment with maleic acid in ethanol, the product was converted to the corresponding maleate salt and the salt was recrystallized from ethanol to give an amorphous solid, mp 159–160 °C. IR  $\nu_{\text{max}}^{\text{KBr}}$   $\text{cm}^{-1}$ : 1620. MS *m/e*: 537 ( $M^+$ ).  $^1\text{H-NMR}$  (DMSO- $d_6$ )  $\delta$ : 0.94 (6H, d,  $J=7$  Hz,  $(\text{CH}_3)_2\text{CH}$ -), 1.52 (1H, m,  $(\text{CH}_3)_2\text{CH}$ -), 1.74 (2H, q,  $J=7$  Hz,  $\text{N-CH}_2\text{CH}_2$ -), 2.82 (3H, s,  $\text{N-CH}_3$ ), 3.27 (4H, m, piperazinyl-H), 4.04 (4H, m, piperazinyl-H), 4.44 (2H, t,  $J=7$  Hz,  $\text{N-CH}_2\text{CH}_2$ -), 6.08 (2H, s, maleate-H), 7.47 (1H, dd,  $J=8, 2$  Hz,  $\text{C}_7$ -H), 7.65 (1H, s,  $\text{C}_3$ -H), 7.98 (1H, d,  $J=8$  Hz,  $\text{C}_8$ -H), 8.06 (1H, d,  $J=2$  Hz,  $\text{C}_5$ -H), *Anal.* Calcd for  $\text{C}_{26}\text{H}_{30}\text{F}_3\text{N}_3\text{O}_6$ : C, 58.10; H, 5.63; N, 7.82. Found: C, 58.03; H, 5.60; N, 7.71.

**Other Compounds of This Series (II-1–7 and II-9–12)**—These compounds were prepared in the same manner as II-8.

#### Biological Methods

**Acetic Acid Writhing Method**—Groups of 10 male ddY mice weighing 19–23 g were used. The test compounds and tiaramide were administered orally (100 mg/kg) 30 min before the intraperitoneal injection (10 ml/kg) of 0.7% acetic acid solution. The number of writhes of each mouse was counted during a period of 10 to 20 min after the acetic acid injection. The inhibition (percent) was calculated by comparing the number of writhes with that in the untreated control group.

**Carrageenin Edema Method**—Groups of 6 male Wistar rats weighing 140–170 g were used. The test compounds and tiaramide were administered orally (100 mg/kg) 30 min before the subplantar injection (0.1 ml/rat) of 1% carrageenin suspension into the left hind paw. The paw volume compared with the pre-drug volume was determined and the inhibition (percent) was calculated on the basis of the swelling percent in the control group.

**Data Analysis**—Student's *t*-test was used for statistical evaluation.

#### ALS Method

**Activity Classes**—Twelve furo[3,2-*b*]indole derivatives (II-1–12) were classified into three groups based on the acetic acid writhing test and the carrageenin edema test at a dose of 100 mg/kg *p.o.*, as shown in Table II, according to the same criteria as used for the 53 2-morpholinocarbonyl derivatives previously reported.<sup>11</sup>

**ALS Method**—The ALS system,<sup>7,8)</sup> which is a nonparametric pattern classifier, categorizes multidimensional structural patterns into multiple ordered classes by means of a single equation. The equation (discriminant function) is formulated by a feedback adaptation procedure in a linear form, as in Eq. 7.

$$Y = w_0 + w_1x_1 + w_2x_2 + \dots + w_px_p \quad (7)$$

where  $Y$  is the discriminant score for the classification,  $x_k$  ( $k=1, 2, \dots, p$ ) is the  $k$ th descriptor for the structure, and  $w_k$  ( $k=0, 1, \dots, p$ ) is the weight coefficient. The value of  $w_k$  is determined by the least-squares adaptation using the starting score,  $a_j$  ( $j=1, 2, \dots, m$  in the  $m$ -group case) and the correction term,  $C_i(t)$ . In this study, the version of 1981 (ALS 81)<sup>11)</sup> was used. The correction term  $C_i(t)$  for misclassified compound  $i$  at the  $t$ -th iteration is given by Eq. 8.

$$C_i(t) = 0.1/[\delta_i(t) + 0.45]^2 + 0.1 \quad (8)$$

where

$$\delta_i(t) = Y_i(t) - b_k$$

In this equation,  $Y_i(t)$  is the discriminant score, and  $b_k$  is the cutting point (nearer to  $Y_i(t)$ ) of the observed class for compound  $i$ . ALS iteration was performed a maximum of 20 times. The best discriminant function was selected

according to the reported criteria.<sup>8)</sup>

**Structural Descriptors**—In the parametrization of structural features for the ALS study, we used the same parameters as in the previous study<sup>1)</sup> except for a few indicator variables as described in the text.

#### References

- 1) Part IV: Y. Kawashima, F. Amanuma, M. Sato, S. Okuyama, Y. Nakashima, K. Sota, and I. Moriguchi, *J. Med. Chem.*, **29**, 2284 (1986).
- 2) A part of this work was presented at the 106th Annual Meeting of the Pharmaceutical Society of Japan, April, 1986.
- 3) Y. Nakashima, Y. Kawashima, M. Sato, S. Okuyama, F. Amanuma, K. Sota, and T. Kameyama, *Chem. Pharm. Bull.*, **33**, 5250 (1985).
- 4) R. W. Taft, Jr., "Steric Effects in Organic Chemistry," Wiley, New York, 1979.
- 5) A. Verloop, W. Hoogenstraaten, and J. Tipker, *Drug Design*, **7**, 165 (1976).
- 6) C. G. Swain, S. H. Unger, N. R. Rosenquist, and M. S. Swain, *J. Am. Chem. Soc.*, **105**, 492 (1983).
- 7) I. Moriguchi and K. Komatsu, *Chem. Pharm. Bull.*, **25**, 2800 (1977).
- 8) I. Moriguchi, K. Komatsu, and Y. Matsushita, *J. Med. Chem.*, **23**, 20 (1980).
- 9) R. Koster, M. Anderson, and J. Dobber, *Fed. Proc. Fed. Amer. Soc. Exp. Biol.*, **18**, 412 (1958).
- 10) C. A. Winter, E. A. Risley, and G. W. Nuss, *Proc. Soc. Exp. Biol. Med.*, **111**, 544 (1962).
- 11) I. Moriguchi and K. Komatsu, Abstracts of Papers, 8th Symposium on Structure-Activity Relationships, Tokyo, Oct. 1981, p. 55.

[Chem. Pharm. Bull.]  
35(1) 409-412 (1987)

## Stereospecific Inhibition of Cholinesterases by Mefloquine Enantiomers

TONG LAN NGIAM and MEI LIN GO\*

Department of Pharmacy, National University of Singapore,  
10 Kent Ridge Crescent, Singapore, 0511,  
Republic of Singapore

(Received July 24, 1986)

Mefloquine enantiomers (+)-**1**, (-)-**1** were found to be stereospecific in their inhibition of acetylcholinesterase and butyrylcholinesterase, (-)-**1** being the more potent inhibitor in both cases. Similar observations were also made with respect to (-)-quinine and (+)-quinidine, which are configurational analogues of (+)-**1** and (-)-**1**, respectively. A positive synclinal conformation for the "N-C-C-O" segment of mefloquine appeared to be necessary for good activity.

**Keywords**— mefloquine; enantiomers; stereospecific; anticholinesterase; quinine; quinidine

### Introduction

Structure-activity relationship studies of inhibitors of acetylcholinesterase (AChE) have shown that these agents generally possess a positively charged nitrogen which is separated from an electro-negative oxygen by two or three carbon atoms, as in the N-C-C-O segment of acetylcholine. The positively charged nitrogen interacts with the anionic site of the enzyme, while the electro-negative oxygen interacts with an acid group *via* hydrogen bonding. It should be noted that as a chemical class, aminoethanols have the necessary N-C-C-O segment for anti-AChE activity. The nitrogen atom of aminoethanols ( $pK_a$  9.5) is protonated at pH 7.4, carrying a positive charge, while the hydroxyl oxygen is inherently electronegative.

Mefloquine [(±)-**1**] is one of the best known and most widely used aminoalcohol antimalarials discovered during the mid-1960s under an extensive research program sponsored by the US Army Medical Research and Development Command.<sup>11</sup> Synthetic mefloquine is a racemate, the *erythro* isomers of  $\alpha$ -(2-piperidinyl)-2,8-bis-(trifluoromethyl)-4-quinolinemethanol. Thus, mefloquine is structurally an aminoethanol, with chiral C9 and C10 (see Fig. 1). Since it has a pharmacophoric N-C-C-O segment (*i.e.* N11-C10-C9-O16, Fig. 2), mefloquine is expected to be an inhibitor of AChE, and the comparative inhibitory activities of its enantiomers, whose N-C-C-O segments are mirror images of one another,

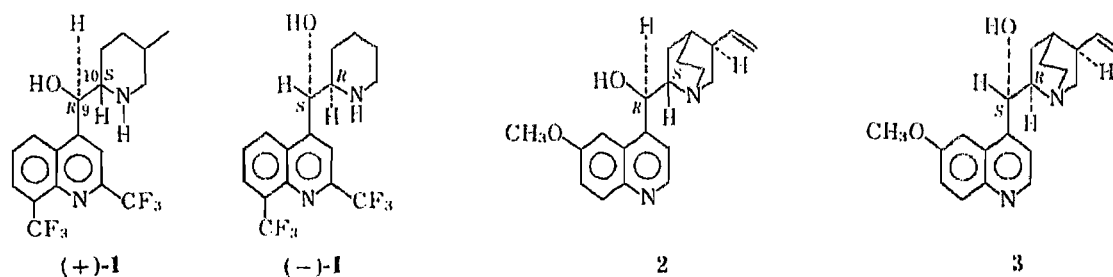


Fig. 1. Structural Formulac of (+)-**1**, (-)-**1**, **2** and **3**

would shed some light on the structural and conformational requirements of the enzyme receptor.

In the present study, the anti-AChE and anti-butrylcholinesterase (anti-BChE) activities of (+)-1 and (-)-1, as well as that of the racemate, were determined at pH 7.4 using a pH-stat method. The activities of (-)quinine (2) and (+)-quinidine (3) were similarly studied.

### Experimental

(-)-Quinine sulfate [(8*S*,9*R*)-6'-methoxy-cinchonan-9-ol sulfate] and (+)-quinidine [(8*R*,9*S*)-6'-methoxy-cinchonan-9-ol sulfate] were obtained from British Drug House and the racemic mefloquine hydrochloride [(±)-(*R*\*,*S*\*)-2,8-bis(trifluoromethyl)-α-(2-piperidinyl)-4-quinolinemethanol] was supplied by Roche Pharmaceuticals. The racemic mefloquine was resolved with (+)-3-bromo-8-camphorsulphonic acid in methanol according to the method of Carroll and Blackwell.<sup>2)</sup> (+)-1 and (-)-1 were obtained in 26% and 11% yields, respectively. The melting points and specific rotation of the resolved enantiomers were in agreement with reported values.<sup>2)</sup>

A modification of the constant pH titration method of Stanely *et al.* was followed for the enzyme inhibition studies.<sup>3)</sup> At least two concentrations of each inhibitor were employed for the determination of inhibitory activity. All glassware used for the preparation and storage of solutions containing inhibitors was initially coated with dimethyldichlorosilane. (+)-1 and (-)-1, isolated as the free bases, were each dissolved in a minimum volume of 10% (v/v) 0.1 M HCl and made up to volume with double-distilled water, while solutions of the other inhibitors were prepared in double-distilled water. Enzyme activity was determined at pH 7.4 and 23°C, using a Radiometer TTT2 autotitrator assembly. For the determination of AChE activity, a solution of electric eel AChE (EC 3.1.1.7, Sigma Type VI-S), containing 4 units/ml, was prepared in 0.002 M phosphate buffer (pH 7.4) containing 0.15 M NaCl and 0.01% (w/v) gelatin. The hydrolysis of the substrate acetylcholine iodide (Sigma Chemical Co.), over the concentration range of 0.8–1.5 mM, was determined in 20 ml of 0.1 M MgCl<sub>2</sub> solution. The hydrolysis was initiated by addition of 0.4 units of the enzyme and the acetic acid liberated was titrated with 0.005 M NaOH over a period of 4 min. The reaction velocity (moles of alkali consumed per minute per unit of enzyme) was determined from the slope of the curve (ml of alkali *versus* time) between 2 and 4 min. The Michaelis constant of AChE was found to be constant at  $2.38 \times 10^{-4}$  M (S.E.M.  $0.15 \times 10^{-4}$  M for 12 determinations). For the determination of BChE activity, horse serum BChE (EC 3.1.1.8, Sigma Type XI) containing 17.2 units/ml was similarly prepared in phosphate buffer. Hydrolysis of ACh iodide over the concentration range of 1.6–0.2 mM, by 1.72 units of the enzyme, was determined in 20 ml of 0.1 M MgCl<sub>2</sub>. The reaction velocity of each hydrolysis was determined by titration with 0.01 M NaOH over 4 min as in the case of AChE. The Michaelis constant for BChE was found to be  $1.05 \times 10^{-3}$  M (S.E.M.  $0.52 \times 10^{-3}$  M for 12 determinations). The reaction velocities were determined in the presence and absence of inhibitor for each enzyme. The results were analyzed by means of ROSFIT,<sup>4)</sup> a computer program written for the discrimination between rival inhibitory models and for estimation of kinetic parameters. The inhibitory constants of the compounds are listed in Table I.

### Results and Discussion

Mefloquine [(±)-1] and its enantiomers, (+)-1 and (-)-1, were found to be non-competitive inhibitors of AChE and BChE in the present study. Neostigmine, an established anti-AChE agent, exhibited competitive kinetics under similar experimental conditions. Table

TABLE I.  $K_i$  Values for Inhibition of AChE and BChE

Compound	$K_i \times 10^4$ (M <sup>-1</sup> )	
	AChE	BChE
(±)-1	0.445 (±0.0049)	1.22 (±0.027)
(+)-1	1.03 (±0.025)	1.76 (±0.033)
(-)-1	0.288 (±0.0045)	0.957 (±0.017)
2	8.40 (±0.14)	0.328 (±0.0062)
3	5.72 (±0.072)	0.0815 (±0.0019)

a) Values in parentheses indicate standard error of the mean (S.E.M.) for 20 observations.

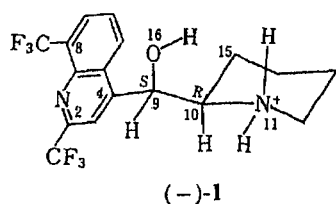


Fig. 2. Conformation of (-)-1

$\tau$  N11-C10-C9-O16 =  $+60^\circ$ ; C4-C9-C10-N11 =  $180^\circ$ ;  $\tau$  C3-C4-C9-C10 =  $+90^\circ$ . The structure has been numbered so as to facilitate discussion of the conformation.

I gives the  $K_i$  values of mefloquine and its enantiomers against AChE and BChE, computed from the ROSFIT model for classical non-competitive inhibition.<sup>4)</sup> As expected, one of the enantiomers, (-)-1, was found to be much more active than its optical antipode, (+)-1, as an inhibitor of AChE. The same was also true with respect to inhibition of BChE. The activity of racemic mefloquine was intermediate between those of the enantiomers.

Carroll and Blackwell had previously assigned the absolute configurations of (+)-1 and (-)-1 as C9 (*R*) C10 (*S*) and C9 (*S*) C10 (*R*) respectively.<sup>2)</sup> This was done by comparing the circular dichroism spectra of (+)-1 and (-)-1 with those of (-)-quinine (2) and (+)-quinidine (3), the absolute configurations of which have been reported.<sup>5)</sup> It is clear from their study that (+)-1 and (-)-1 are configurational analogues of 2 and 3, respectively. It would be interesting to find out whether 2 and 3 show similar stereospecificity in their inhibitions of cholinesterases. This was indeed found to be the case in the present study. (+)-Quinidine was more active than (-)-quinine against both AChE and BChE (Table I). Thus, there is in this case a correlation between the absolute configurations and anti-cholinesterase activities among the stereoisomers.

It appears from Table I that the difference in anti-ChE activities between 2 and 3 is more pronounced with respect to BChE than AChE. This may be due to the fact that the steric requirement of the AChE anionic site is more stringent than that of BChE.<sup>6)</sup> The nitrogen of the N-C-C-O segment of quinine and quinidine is located at the bridge head of the bulky quinuclidine ring. Attachment of the N-C-C-O segment to the enzyme receptor would not be easy, and the situation would be more difficult with AChE. Thus, the  $K_i$  values of 2 and 3 against AChE are comparatively high, but nevertheless 3 is still a better inhibitor.

Conformational study using Dreiding models of the mefloquine enantiomers has shown that when C9 is equatorial to the piperidine ring, the conformer with the least steric interaction is the one in which the quinoline ring and the piperidinyll nitrogen are *anti* to each other, *i.e.*  $\tau$ C4-C9-C10-N11 =  $180^\circ$  (Fig. 2). The stability of this conformer may also be enhanced by a possible, though weak, internal hydrogen bonding between the protonated piperidinyll nitrogen (at pH 7.4) and the hydroxyl group. It is reasonable to expect this stable conformer to play a major role in the interaction of mefloquine with the cholinesterase receptors. One should mention that in a parallel conformational study of an analogous group of aminoalcohols—the  $\alpha$ -piperidinyll-3,6-bis-(trifluoromethyl)-9-phenanthrenemethanols—Loew and Sahakian have similarly concluded that the most stable conformers are those in which the bulky phenanthrene ring and the piperidinyll nitrogen are *anti* to each other.<sup>7)</sup> There is no reason to suspect that (+)-1 and (-)-1 would behave otherwise.

Thus, with  $\tau$ C4-C9-C10-N11 of the mefloquine enantiomers at  $180^\circ$ , the corresponding N11-C10-C9-O16 torsion angle is either  $+60^\circ$  or  $-60^\circ$ , depending on the absolute configuration of the enantiomers. Taking into consideration the absolute configurations of (+)-1 and (-)-1 as assigned by Carroll and Blackwell,<sup>2)</sup> the N11-C10-C9-O16 torsion angle of (+)-1 is  $-60^\circ$  and that of (-)-1 is  $+60^\circ$ . As the N-C-C-O segment of mefloquine has been identified as the pharmacophoric moiety for anti-ChE activity, one may conclude that a positive synclinal conformation, as found in (-)-1, is essential for good anti-ChE activity.

---

**References**

- 1) C. J. Ohnmacht, A. R. Patel and R. E. Lutz, *J. Med. Chem.*, **14**, 926 (1971).
- 2) F. I. Carroll and J. T. Blackwell, *J. Med. Chem.*, **17**, 210 (1974).
- 3) J. W. Stanley, I. W. Mathison and J. G. Beasley, *J. Med. Chem.*, **17**, 8 (1974).
- 4) W. R. Greco, R. L. Priore, M. Sharma and W. Korytnyk, *Comp. Biomed. Res.*, **15**, 39 (1982).
- 5) G. G. Lyle and L. K. Keefer, *Tetrahedron*, **23**, 3253 (1967).
- 6) M. I. Kabachnik, A. P. Brestkin, N. N. Godovikov, M. J. Michelson, E. V. Rozengart and V. I. Rozengart, *Pharmacol. Rev.*, **22**, 355 (1970).
- 7) G. H. Loew and R. Sahakian, *J. Med. Chem.*, **20**, 103 (1977).



[Chem. Pharm. Bull.]  
35(1) 413-415 (1987)

### 3,4-Secolupane-Type Triterpene Glycosyl Esters from Leaves of *Acanthopanax divaricatus* SEEM

KAZUHIRO MATSUMOTO, RYOJI KASAI, FUJIKO KANAMARU,  
HIROSHI KOHDA and OSAMU TANAKA\*

*Institute of Pharmaceutical Sciences, Hiroshima University School of Medicine,  
Kasumi, Minami-ku, Hiroshima 734, Japan*

(Received July 4, 1986)

From leaves of *Acanthopanax divaricatus* (Araliaceae), two 3,4-secolupane type triterpene glycosyl esters, chiisanoside and isochiisanoside, were isolated, both of which have already been isolated from leaves and stem-bark of *A. chiisanensis*. Besides these compounds, a new glycoside named divaroside and hyperin (quercetin-3-*O*- $\beta$ -D-galactopyranoside) were also isolated from the leaves. Divaroside was established to be the  $\beta$ -D-glucopyranosyl(1 $\rightarrow$ 6)- $\beta$ -D-glucopyranosyl ester of chiisanogenin.

**Keywords**—*Acanthopanax divaricatus*; Araliaceae; divaroside; chiisanoside; isochiisanoside; hyperin; 3,4-secolupane-type triterpene; oligo-glycosyl ester

Recently, we reported the isolation and structural determination of three novel 3,4-secolupane-type triterpene glycosyl esters, chiisanoside (**1**) and its two homologues, isochiisanoside (**2**) and the methyl ester of **2**(**3**), from the leaves and stem-bark of *Acanthopanax chiisanensis* NAKAI (Araliaceae),<sup>1,2)</sup> which is a Korean folk medicine used as a tonic, an anti-rheumatic and an anti-inflammatory. This is the first example of the isolation of 3,4-seco-triterpene glycosides from a natural source.

As a continuation of our work on glycoside constituents of *Acanthopanax* species, the chemical constituents of leaves of *A. divaricatus* SEEM (Japanese plant name: Keyama-ukogi), which grows widely in Japan, have been studied.

A methanolic extract of the leaves of *Acanthopanax divaricatus* (collected in Hiroshima) was defatted with ether and repeatedly chromatographed to give a new glycoside named divaroside (**4**) (yield: 0.03%) together with the known glycosides, chiisanoside (**1**) (yield: 3.0%), isochiisanoside (**2**) (yield: 0.09%) and hyperin (quercetin-3-*O*- $\beta$ -D-galactopyranoside) (**5**) (0.37%). The known glycosides **1** and **2** were identified by comparison of their proton and carbon-13 nuclear magnetic resonance (<sup>1</sup>H- and <sup>13</sup>C-NMR) spectra, electron impact mass spectra (EI-MS) of the trimethylsilyl ether and optical rotation ( $[\alpha]_D$ ) with those of authentic samples, and the identification of **5** was established by comparison of the melting point (mp) and <sup>13</sup>C-NMR spectrum with reference data.<sup>3,4)</sup>

Acid hydrolysis of **4** gave D-glucose.<sup>5)</sup> The <sup>13</sup>C-NMR signals due to the aglycone moiety of **4** (Table I) were observed at almost the same positions as those of **1**, indicating that **4** is a glycosyl ester of chiisanogenin (**6**).<sup>2)</sup> The <sup>1</sup>H- and <sup>13</sup>C-NMR spectra showed the presence of two glucosyl units. The EI-MS of the trimethylsilyl ether of **4** exhibited fragment ions at *m/z* 829 [(Glc-Glc)TMS<sub>7</sub>], 451[(Glc)TMS<sub>4</sub>] and 583[Glc(TMS)<sub>4</sub>-OCH<sub>2</sub>-CH=O<sup>+</sup>-TMS, a characteristic fragment ion due to aldohexosyl(1 $\rightarrow$ 6)aldohexose].<sup>6)</sup> Inspection of the <sup>13</sup>C-NMR signals due to the sugar moiety revealed the presence of a  $\beta$ -gentiobiosyl ester moiety in **4** (Table I). Based on these results, **4** is formulated as the  $\beta$ -D-glucopyranosyl(1 $\rightarrow$ 6)- $\beta$ -D-glucopyranoside of (1*R*)-1,11 $\alpha$ -dihydroxy-3,4-seco-lupa-4(23),20(29)-diene-3,28-dioic acid

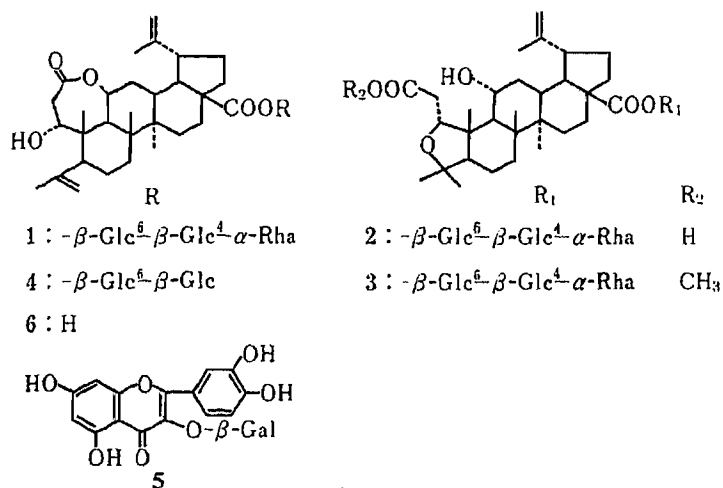


Chart 1

TABLE I.  $^{13}\text{C}$  Chemical Shifts ( $\delta$ ) in  $\text{C}_5\text{D}_5\text{N}$ 

		1	4			1	4
Aglycone moiety	1	75.0	75.1	Sugar moiety	Glc-1	95.2	95.4
	2	38.6	38.8		-2	73.8	74.1
	3	173.1	173.0		-3	78.4	78.1 <sup>b)</sup>
	4	147.6	147.7		-4	70.5	70.9
	5	49.5	49.6		-5	76.3	78.4 <sup>b)</sup>
	6	25.1	25.1		-6	69.2	69.5
	7	33.4	33.5		Glc-1'	104.7	105.3
	8	41.6	41.7		-2'	75.2	75.2
	9	44.0	44.1		-3'	76.9	78.4 <sup>b)</sup>
	10	44.0	44.1		-4'	78.4	71.5
	11	70.2	70.5		-5'	77.8	78.7
	12	32.2	32.2		-6'	61.3	62.6
	13	35.2	35.2		Rha-1	102.5	
	14	42.1	42.2		-2	72.5 <sup>b)</sup>	
	15	30.7	30.8		-3	72.3 <sup>b)</sup>	
	16	32.5	32.2		-4	73.8	
	17	56.7	56.8		-5	70.2	
	18	47.5	47.6		-6	18.3	
	19	49.5	49.6				
	20	150.7	150.1				
21	29.5	29.5					
22	36.8	36.8					
23	113.9	113.9					
24	23.5	23.5					
25	18.9 <sup>a)</sup>	18.9 <sup>a)</sup>					
26	17.9 <sup>a)</sup>	18.0 <sup>a)</sup>					
27	13.8	13.8					
28	175.0	175.1					
29	18.9 <sup>a)</sup>	19.1 <sup>a)</sup>					
30	110.6	110.7					

*a, b)* These assignments may be interchanged in each column. Glc,  $\beta\text{-D}$ -glucopyranosyl; Rha,  $\alpha\text{-L}$ -rhamnopyranosyl.

3,11-lactone (=desrhamno-chiisanoside) (Chart 1).

The preliminary investigation of methanolic extracts of leaves of five other Japanese *Acanthopanax* spp. (*A. hypoleucus* MAKINO, *A. japonicus* FR. et SAV., *A. sciadophylloides* FR.

et SAV., *A. senticosus* HARMS and *A. spinosus* MIGUEL) by thin layer chromatography (TLC) indicated the absence of these 3,4-secolupane type triterpene glycosides, suggesting a unique taxonomical position of *A. divaricatus* and *A. chiisanensis* in this genus.

### Experimental

**General Procedure**—Melting points were determined on a Yanaco micro hot stage and are uncorrected. Optical rotations were measured with a Union PM-101 automatic digital polarimeter. Infrared (IR) spectra were taken on a Shimadzu IR-408 spectrometer. NMR spectra were recorded on a JEOL FX-100 instrument using tetramethylsilane (TMS) as an internal standard. For gas liquid chromatography (GLC), a Shimadzu GC-6A apparatus was used. MS were taken on a JEOL JMS-01-SG-2 spectrometer by the direct inlet method; ionization voltage 75 eV. For column chromatography, Kieselgel 60 (70–230 mesh, Merck), LiChroprep RP-8 (40–63  $\mu$ m, Merck), Diaion HP-20 (Mitsubishi Chem. Ind. Co., Ltd.) and Sephadex LH-20 (Pharmacia) were used. All solvent systems for chromatography were homogeneous.

**Extraction and Separation of Glycosides**—Dried leaves of *Acanthopanax divaricatus* (148 g) collected in Hiroshima prefecture were extracted with MeOH, and the MeOH extract was concentrated to dryness. The residue (37.8 g) was suspended in H<sub>2</sub>O and then washed with Et<sub>2</sub>O. The aqueous layer was chromatographed on a column of highly porous polymer (Diaion HP-20) and eluted with H<sub>2</sub>O, 60% MeOH, 80% MeOH, MeOH and Me<sub>2</sub>CO, successively. The 60% MeOH eluate was chromatographed on a reversed-phase column (LiChroprep RP-8, 65% MeOH) to give crude 5 and 2. The crude 5 and 2 were purified by column chromatography on Sephadex LH-20 (MeOH) and silica gel (CHCl<sub>3</sub>–MeOH–H<sub>2</sub>O (6:4:1)) to give 5 (78 mg) and 2 (a white powder, 19 mg), respectively. The 80% MeOH eluate was subjected to chromatography on a LiChroprep RP-8 column (68% MeOH) and then a silica gel column (CHCl<sub>3</sub>–MeOH–H<sub>2</sub>O) (10:5:1) to give two fractions (fr. 1 and fr. 2). Fraction 1 was purified by high performance liquid chromatography (column, TSK-GEL ODS-120T 21 mm  $\times$  30 cm; solvent, 60% MeOH; flow rate, 7 ml/min; detection, RI) to give 4 (16 mg). Fraction 2 was chromatographed on LiChroprep RP-8 to give 1 (1.4 g).

The identification of 1 and 2 was established by direct comparison (TLC,  $[\alpha]_D$ , <sup>1</sup>H- and <sup>13</sup>C-NMR) with authentic samples. The identification of 5 was established by comparison of the melting point and <sup>13</sup>C-NMR data with reference data.<sup>3,4)</sup>

Compound 4: a white powder,  $[\alpha]_D^{20} + 30.0^\circ$  ( $c=0.59$ , MeOH). *Anal.* Calcd for C<sub>42</sub>H<sub>64</sub>O<sub>15</sub>·4H<sub>2</sub>O: C, 57.26; H, 8.24. Found: C, 57.11; H, 8.24. IR (Nujol) cm<sup>-1</sup>: 3450 (OH), 1750, 1710 (COOR), 1640, 890 (C=CH<sub>2</sub>). <sup>1</sup>H-NMR (C<sub>5</sub>D<sub>5</sub>N, 100 MHz)  $\delta$ : 6.22 (1H, d,  $J=8$  Hz, anomeric H of Glc'), 5.01 (1H, d,  $J=8$  Hz, anomeric H of Glc). <sup>13</sup>C-NMR data are given in Table I.

**Acid Hydrolysis of 4 and Identification of the Resulting Monosaccharide**<sup>5)</sup>—A sample (10 mg) was heated with 3.5% HCl in H<sub>2</sub>O–dioxane (1:1, 1 ml) in a sealed micro-tube at 80°C for 3 h. The reaction mixture was diluted with H<sub>2</sub>O and then washed with CHCl<sub>3</sub>. The aqueous layer was neutralized with Amberlite MB-3 ion exchange resin and then concentrated to give a sugar fraction. A solution of the sugar fraction (1 mg) in 50  $\mu$ l of H<sub>2</sub>O was treated with a solution of 1-(–)- $\alpha$ -methylbenzylamine (9 mg) and NaBH<sub>3</sub>CN (0.6 mg) in 50  $\mu$ l of EtOH, and the mixture was kept at 40°C for 4 h. Then several drops of acetic acid were added, and the whole was concentrated to dryness. The residue was trimethylsilylated with *N*-trimethylsilylimidazole and subjected to GLC analysis (dual flame ionization detector; carrier gas, He 2.5 ml/min; WCOT glass capillary column (0.25 mm i.d.  $\times$  25 m) coated with Carbowax 20M; isothermal, 150°C; injection temperature, 190°C; retention time, 46.29 min). D-Glucose was identified by comparison of the retention time with that of an authentic sample.

### References

- 1) D.-R. Hahn, R. Kasai, J.-H. Kim, S. Taniyasu and O. Tanaka, *Chem. Pharm. Bull.*, **32**, 1244 (1984).
- 2) R. Kasai, K. Matsumoto, S. Taniyasu, O. Tanaka, J.-H. Kim and D.-R. Hahn, *Chem. Pharm. Bull.*, **34**, 3284 (1986).
- 3) S. Matsuura and M. Inuma, *Yakugaku Zasshi*, **97**, 452 (1977).
- 4) K. R. Markham, B. Ternai, R. Stanley, H. Geiger and T. J. Mabry, *Tetrahedron*, **34**, 1389 (1978).
- 5) R. Oshima, J. Kumamoto and C. Watanabe, *J. Chromatogr.*, **259**, 159 (1983).
- 6) N. K. Kochetkov, O. S. Chizhov and N. V. Molodtsov, *Tetrahedron*, **24**, 5587 (1968).

[Chem. Pharm. Bull.]  
[35(1) 416—420 (1987)]

## Depression of Salicylamide Glucuronidation by Bacterial Lipopolysaccharide

MAMI KUSHIYA, RYUICHI HASEGAWA,\* TETSUO KOMURO  
and HIROSHI ISAKA

*National Institute of Hygienic Sciences, Osaka Branch 1-1-43,  
Hohenzaka, Higashi-ku, Osaka 540, Japan*

(Received May 12, 1986)

The effect of lipopolysaccharide (LPS) on the urinary excretion of salicylamide (SAM) (10 mg/head) given orally to rats was examined 24 h after intraperitoneal administration of LPS (0.5 mg/kg) by the direct analysis of urine samples by high-performance liquid chromatography. The cumulative amount of SAM glucuronide excreted in urine in 4 h was decreased by 40—70% in the LPS-administered rats, while that of SAM sulfate was increased by 7—15% compared with the control in the same rats. The amounts of the conjugates of gentisamide (the hydroxylated metabolite of SAM) excreted in urine were decreased by approx. 70% compared with the control. LPS administration provoked a decrease in the activities of aniline hydroxylase of liver and uridine diphosphate (UDP)-glucuronyltransferase of liver, lung and kidney, but did not change the activities of sulfotransferase of liver or UDP-glucuronyltransferase obtained from the small intestine. The mechanism of the decreased urinary excretion of SAM glucuronide in LPS-administered rats is discussed.

**Keywords**—lipopolysaccharide; salicylamide; salicylamide glucuronide; salicylamide sulfate; urinary excretion; aniline hydroxylase; UDP-glucuronyltransferase; sulfotransferase

### Introduction

Lipopolysaccharide (LPS), an endotoxin and an essential component of the gram-negative bacteria, possesses many biological activities.<sup>1)</sup> LPS-treated animals show metabolic abnormalities related to the depression of hepatic microsomal drug-metabolizing enzymes such as aniline hydroxylase, aminopyrine N-demethylase and pentobarbital oxidase.<sup>2—5)</sup> Prolongation of pentoarbital-induced sleeping time<sup>4)</sup> and the retardation of aminopyrine<sup>6)</sup> and phenytoin metabolism<sup>3)</sup> by LPS have been reported. As regards the effect of LPS on hepatic drug conjugation, administration of LPS was reported to depress the activity of uridine diphosphate (UDP)-glucuronyltransferase, but not that of the sulfotransferase.<sup>5)</sup>

Salicylamide (SAM) is a mild analgesic and antipyretic agent which is relatively widely used. This drug is a valuable tool to elucidate the influence of LPS on the drug-conjugating capacity of metabolizing enzymes in experimental animals because it is eliminated almost entirely by biotransformation and shows rapid absorption from the intestine and rapid elimination into urine.<sup>7,8)</sup> In rats, SAM is reported to be mostly metabolized to the glucuronide and sulfate, and a small part to gentisamide, which is a hydroxylated derivative of SAM.<sup>8)</sup> Recently, Morris and Levy<sup>9)</sup> reported a rapid, precise and direct assay method for SAM metabolites in biological fluids by using high-performance liquid chromatography (HPLC). In the present study, we investigated the influence of LPS on the urinary excretion of SAM in rats by using the above HPLC method.

### Materials and Methods

**Materials**—Chemicals were purchased from the following sources: SAM and *p*-nitrophenol from Nakarai

Chemicals, Ltd. (Tokyo, Japan); UDP-glucuronate (3Na) from Seikagaku Kogyo Co., Ltd. (Tokyo, Japan); *p*-fluorophenol and tetrabutylammonium bromide from Tokyo Kasei Kogyo Co., Ltd. (Tokyo, Japan); potassium *p*-nitrophenyl sulfate from Aldrich Chemical Co. (Milwaukee, Wis., USA);  $\beta$ -glucuronidase (550000 unit/mg) type B-1 and  $\beta$ -glucuronidase (500000 unit/mg, containing aryl sulfatase 22300 unit/mg) from Abalone Entrals, from Sigma Chemical Co. (St. Louis, MO., USA); tetrabutylammonium hydroxide solution from Wako Pure Chemical Industries, Ltd. (Osaka, Japan). All other chemicals and reagents used in the present experiment were of analytical grade or better. LPS was extracted from *E. coli* UKT-B strain according to Westphal *et al.*<sup>10)</sup> and purified by ultracentrifugation in the usual way.

**Animals**—Male albino rats of Wistar strain weighing 200 to 250 g (purchased from Kearsy Co., Ltd., Kyoto, Japan) were used throughout the present experiments.

**Analysis of the Metabolites of Salicylamide in Rat Urine**—Rats ( $220 \pm 5$  g) were administered 10 mg of SAM (dissolved in 1 ml of 50% (v/v) propylene glycol) orally after fasting for 24 h, and the urine was collected every 30 min up to 4 h after the administration. Periodical urination was stimulated by making the rats sniff at a cotton pad wetted with ether. At the 5th d after the first trial, the same rats were each administered LPS (0.5 mg/kg) intraperitoneally and fasted for 24 h. After that, 10 mg of SAM was administered and urine samples were collected in the same manner as described above. The metabolites of SAM in urine were determined by the following methods.

**Chromatographic Analysis of SAM Metabolites**—Amounts of SAM metabolites were determined by the method of Morris and Levy<sup>9)</sup> with some modifications. A high-performance liquid chromatograph (model 440, Waters Ltd., Tokyo, Japan) equipped with a ultraviolet (UV) detector set at 254 nm was used in this experiment. Urine samples were suitably diluted with distilled water containing *p*-nitrophenyl- $\beta$ -D-glucuronide as an internal standard, and an aliquot of the sample was injected into the chromatograph. The chromatographic mobile phase was 3 mM tetrabutylammonium hydroxide in 15% (v/v) methanol and 7% (v/v) acetic acid, which was passed at a flow rate of 0.9 ml/min through an octadecyltrichlorosilane-bonded column (TSK LS-410AK, Toyo Soda, Tokyo, Japan) 20 cm in length. Column temperature was ambient.

**Determination of Drug-Metabolizing Enzyme Activity**—Rats ( $240 \pm 10$  g) were injected LPS (0.5 mg/kg) intraperitoneally and fasted for 24 h. In the control experiments, saline was injected into the rats instead of LPS. After decapitation, the liver, kidneys, lungs and small intestine were removed and immediately homogenized with 4 volumes of 0.154 M KCl in Teflon-glass or all-glass homogenizers as necessary. The 9000  $\times g$  supernatants were prepared in the usual way to be used for the enzyme activity measurements.

Aniline hydroxylase activity of the hepatic 9000  $\times g$  supernatant was measured according to the method of Hart and Fouts.<sup>11)</sup>

UDP-glucuronyltransferase activity was assayed by the method of Gorski and Kasper,<sup>12)</sup> using a reaction mixture containing 150  $\mu$ l of the 9000  $\times g$  supernatant, 1.5  $\mu$ mol of UDP-glucuronate (3Na), 208 nmol of *p*-nitrophenol and 5  $\mu$ mol of MgCl<sub>2</sub> in a total volume of 250  $\mu$ l of 83 mM Tris-acetate buffer (pH 7.5). After incubation at 37°C for 30 min, the reaction was terminated by the addition of 1 ml of ethanol. The precipitate was removed, and the supernatant was diluted with 0.1 M ethylenediaminetetraacetic acid (EDTA) (pH 9.6). The absorbance was measured at 400 nm. A blank was similarly prepared but without addition of UDP-glucuronate (3Na) to the reaction mixture.

Sulfotransferase activity was assayed by the following method. A 200  $\mu$ l aliquot of the 9000  $\times g$  supernatant of liver was incubated at 37°C for 30 min with 0.3  $\mu$ mol of *p*-nitrophenol, 400  $\mu$ l of phosphoadenosine phosphosulfate solution prepared by the method of van Kempen and Jansen,<sup>13)</sup> and 40  $\mu$ mol of EDTA in a total volume of 600  $\mu$ l of 0.4 M Tris-HCl buffer (pH 7.4). The incubation was terminated by the addition of 800  $\mu$ l of 10% perchloric acid containing *p*-fluorophenol as an internal standard. After centrifugation, the supernatant obtained was injected into a HPLC apparatus equipped with a UV detector set at 300 nm<sup>14)</sup> and a TSK-LS 410AK-packed column, 20 cm in length. The mobile phase was 30 mg/l tetrabutylammonium bromide and 0.5 g/l KNO<sub>3</sub> in 30% (v/v) methanol and 15% (v/v) acetic acid. The flow rate was 1.5 ml/min and column temperature was ambient.

**Statistics** Group means, variances and standard deviations were calculated and compared by using Student's *t*-test. The level of significance was set at  $p < 0.05$ .

## Results

### Determination of Salicylamide Metabolites in Rat Urine

Salicylamide metabolites in the urine were analyzed by the direct injection of the urine samples into the high-performance liquid chromatograph. Two major peaks and two minor peaks were found in the chromatographic patterns by comparison of urine samples collected before and after oral administration of 10 mg of SAM. Under the conditions used in the present experiment, free SAM was not detected in any urine sample collected after SAM administration.

These peaks were fractionated chromatographically for identification of metabolites.

Fractions containing major metabolites were hydrolyzed with  $\beta$ -glucuronidase at 37 °C for 4 h and/or sulfatase containing  $\beta$ -glucuronidase at 37 °C overnight. Here, the enzyme mixture was used for hydrolysis of the sulfate conjugate because of the lower capacity of sulfatase.<sup>9)</sup> The hydrolysates were re-chromatographed, and identified by comparison with authentic standards. The peaks were concluded to be due to SAM glucuronide and SAM sulfate.

Fractions containing minor peaks were hydrolyzed with  $\beta$ -glucuronidase containing arylsulfatase at 37 °C overnight. Each hydrolysate was purified by HPLC by using the same mobile phase without tetrabutylammonium hydroxide, and identified mass-spectrophotometrically. These peaks were concluded to be due to the glucuronide and sulfate conjugates of gentisamide.

#### Effect of Lipopolysaccharide on Salicylamide Metabolites in Rat Urine

Urinary excretion rates of SAM conjugates were determined in each 30-min urine sample after single administration of SAM (10 mg/head). Three rats were used in control experiment first, and then the same rats were used in the LPS experiment 5 d later. On the semilogarithmic plots, the excretion rates of SAM glucuronide and sulfate declined linearly from 30 min to 4 h after SAM administration. This linearity was not affected by pretreatment with 0.5 mg/kg of LPS, which was injected intraperitoneally 24 h before SAM administration. The excretion rate of SAM glucuronide in the LPS-administered rats was lower than that of the control. On the other hand, the excretion of SAM sulfate in the LPS-administered rats was observed to be rather increased in comparison with the control.

A comparison of the cumulative amounts of SAM conjugates excreted in urine over 4 h showed that the amount of SAM glucuronide excreted in urine was decreased from 40% to 70% by the LPS administration, whereas SAM sulfate was slightly increased from 7% to 15%. The cumulative amounts of the two gentisamide conjugates excreted in urine were decreased in the LPS-administered rats to approx. 70% (as peak height), but they were not determined precisely because the amounts were so small.

#### Activities of Drug-Metabolizing Enzymes in Various Tissues Obtained from Lipopolysaccharide-Administered Rats

To investigate the effect of LPS on body weight and some organs macroscopically, rats were given 0.5 mg/kg of LPS intraperitoneally. As presented in Table I, there was a marked decrease in the body weight of LPS-administered rats (24 g) as compared with the control (14 g). At the same time, LPS caused a significant increase in the liver-to-body weight ratio but no effect was seen on the lung or kidney.

On histological observation of LPS-administered rats, widespread hemorrhage and edema in the lung and a fatty liver with congestion were observed in all cases. Homogenates of

TABLE I. Effect of Lipopolysaccharide on the Body Weight and Several Organ Weights of Rats<sup>a)</sup>

	Control	LPS-treated
Body weight (change)	-14.0 ± 0.9 g	-24.3 ± 1.7 g <sup>b)</sup>
Organ weight (% in BW)		
Liver	3.06 ± 0.17	3.94 ± 0.05 <sup>b)</sup>
Lung	0.50 ± 0.07	0.52 ± 0.04
Kidney	0.76 ± 0.07	0.79 ± 0.02

a) Lipopolysaccharide (0.5 mg/kg, i.p.) was given to rats ( $n=5$ ) and after a 24-h fast, the rats were killed. The weights of the given tissues were determined. For the control experiments, saline was given to rats instead of lipopolysaccharide. Results are given as means ± S.D. ( $n=5$ ) b) Significantly different from control value ( $p < 0.05$ ).

TABLE II. Effect of Lipopolysaccharide on the Activities of Drug-Metabolizing Enzymes in Various Tissues<sup>a)</sup>

Enzymes	Tissues	Enzyme activities ( $\mu\text{mol/h/g}$ wet weight)	
		Control	LPS-treated
Aniline hydroxylase	Liver	$0.874 \pm 0.110$	$0.406 \pm 0.210^b$
Sulfotransferase	Liver	$2.00 \pm 0.08$	$1.81 \pm 0.22$
UDP-glucuronyltransferase	Liver	$3.52 \pm 0.60$	$2.30 \pm 0.02^b$
	Lung	$2.52 \pm 0.36$	$1.96 \pm 0.26^b$
	Kidney	$1.86 \pm 0.37$	$1.33 \pm 0.23^b$
	Intestine	$1.25 \pm 0.18$	$1.30 \pm 0.33$

a) Five rats were intraperitoneally injected with lipopolysaccharide (0.5 mg/kg) or saline as a control. After a 24-h fast, the rats were killed. The isolated tissues were homogenized to prepare the  $9000 \times g$  supernatants for the assay of the enzyme activities. Results are given as means  $\pm$  S.D. ( $n=5$ ) b) Significantly different from control value ( $p < 0.05$ ).

the kidney isolated from LPS-administered rats appeared to be more blood-red in color than the control. LPS also caused a diarrhea.

Table II shows the effect of LPS on the activities of drug-metabolizing enzymes in the liver, lung, kidney and small intestine. Activity of hepatic aniline hydroxylase was decreased approx. 50% by the administration of LPS. This may contribute to the reduction of the gentisamide conjugates excreted in urine of LPS-administered rats as compared with the control. Activities of UDP-glucuronyltransferase in the liver, lung and kidney isolated from LPS-administered rats were observed to be markedly decreased, as predicted from the significant decrease of SAM glucuronide excreted in the urine. Activities of UDP-glucuronyltransferase in the small intestine and sulfotransferase in the liver were not affected by the administration of LPS.

### Discussion

The present results indicate that the urinary excretion rate of SAM glucuronide and its cumulative amount excreted in urine for 4 h were significantly decreased in LPS-administered rats compared with the control experiment in the same rats. These findings suggested that hepatic drug-metabolizing enzyme activity might be decreased by the administration of LPS, as the liver is usually considered to be the major organ for drug biotransformation. This expectation is supported by the results presented in Table II; UDP-glucuronyltransferase activity of the liver isolated from the LPS-administered rats was decreased significantly compared with the control. However, the enzyme activities of extrahepatic organs such as lung and kidney were also significantly affected. It is not clear to what degree SAM glucuronide formation was reduced in these organs. Further investigation will be necessary to establish this.

Altered metabolism of SAM observed in the LPS-administered rats may be due to multiple factors, *i.e.*, not only enzyme activities but also changes in the concentrations of substrates or cofactors in the hepatocytes, which might be adversely affected by the administration of LPS. As a result, the LPS-induced state may bring about a delay in the total metabolism of SAM in the liver and also in the extrahepatic organs. At present, it is unclear how much hemodynamic factors contribute to the total metabolism of SAM. The above speculation, therefore, requires further investigation. Few data are available in the literature regarding the relationship between drug metabolism and hemodynamic disorder induced by

the administration of LPS in rats.

We cannot account for the difference between the unchanged sulfonation and the depressed glucuronidation of SAM in the LPS-administered rats. However, free SAM was not detected in urine under the present experimental conditions, which indicates that SAM was completely metabolized before excretion. We also observed that the cumulative amounts of total SAM metabolites were not significantly different between LPS-administered rats and the control. Furthermore, the amounts of SAM sulfate excreted in urine was observed to be rather increased in the LPS-administered rats as compared with the control. It appears that there some compensatory effects might occur in the metabolism of the LPS-administered rats.

In recent studies, some investigators have established the role of extrahepatic glucuronidation for phenolic substances.<sup>14-17)</sup> A similar observation was made in our study with SAM. As indicated in Table II, UDP-glucuronyltransferase activities in liver, lung and kidney were significantly decreased by the intraperitoneal administration of LPS, which would account in part for the decreased amounts of SAM glucuronide excreted in urine. LPS-induced alterations in the metabolisms of lipid and sugar<sup>18)</sup> should be also investigated in more detail to improve our understanding of the overall LPS-induced changes in drug metabolism.

#### References

- 1) C. Galanos, M. A. Freudenberg, O. Lüderitz, E. T. Rietschel and O. Westphal, "Biomedical Application of the Horseshoe Crab," Alan R. Liss, Inc., New York, 1979, p. 321.
- 2) R. Gorodischer, J. Krasner, J. J. McDevitt, J. P. Nolan and S. J. Yaffe, *Biochem. Pharmacol.*, **25**, 351 (1976).
- 3) K. Sasaki, M. Saitoh and G. Takayanagi, *Oyo Yakuri*, **24**, 717 (1982).
- 4) K. Sasaki, M. Ishikawa-Saitoh and G. Takayanagi, *Jpn. J. Pharmacol.*, **34**, 241 (1984).
- 5) M. Falzon, A. S. Milton and M. D. Burke, *Biochem. Pharmacol.*, **33**, 1285 (1984).
- 6) K. Sasaki, M. Saitoh and G. Takayanagi, *Yakugaku Zasshi*, **101**, 932 (1981).
- 7) V. P. Seeberg, D. Hansen and B. Whitney, *J. Pharmacol. Exp. Ther.*, **101**, 275 (1951).
- 8) G. Levy and T. Matsuzawa, *J. Pharmacol. Exp. Ther.*, **156**, 285 (1967).
- 9) M. E. Morris and G. Levy, *J. Pharm. Sci.*, **72**, 612 (1983).
- 10) O. Westphal, O. Lüderitz and F. Bister, *Z. Naturforsch. Band 7b*, **3**, 148 (1952).
- 11) L. G. Hart and J. R. Fouts, *Proc. Soc. Exp. Biol. Med.*, **114**, 388 (1963).
- 12) J. P. Gorski and C. B. Kasper, *J. Biol. Chem.*, **252**, 1336 (1977).
- 13) G. M. H. van Kempen and G. S. I. M. Jansen, *Anal. Biochem.*, **46**, 438 (1972).
- 14) M. Machida, Y. Morita, M. Hayashi and S. Awazu, *Biochem. Pharmacol.*, **31**, 787 (1982).
- 15) G. J. Dutton and B. Burchell, *Pro. Drug. Metab.*, **2**, 1 (1978).
- 16) M. K. Cassidy and J. B. Houston, *J. Pharm. Pharmacol.*, **32**, 57 (1980).
- 17) M. K. Cassidy and J. B. Houston, *Biochem. Pharmacol.*, **29**, 471 (1980).
- 18) L. J. Berry (ed.), "Handbook of Endotoxin," Vol. 3, Cellular Biology of Endotoxin, Elsevier, Amsterdam, 1985.



[Chem. Pharm. Bull.]  
35(1) 421-424 (1987)

## Studies on Syntheses and Reactions of Methoxypyridazines. I. Methoxylation of 3,4,5-Trichloropyridazine<sup>1)</sup>

HIROMU NAGASHIMA,\* HIROHISA ODA, JUN-ICHI HIDA,  
and KENJI KAJI

*Gifu Pharmaceutical University, 5-6-1, Mitahora-higashi,  
Gifu 502, Japan*

(Received June 9, 1986)

The reaction of 3,4,5-trichloropyridazine (**1**) with 1 eq amount of NaOMe resulted in the formation of three dichloromonomethoxypyridazines (**2**, 3-OMe; **3**, 4-OMe; **4**, 5-OMe) in the ratio of 1:3:6. The 4-OMe compound **3** was isolated from the reaction mixture and the 3-OMe compound **2** was synthesized independently. Further methoxylation of **2**, **3** and **4** was also investigated in order to prepare various substituted pyridazines.

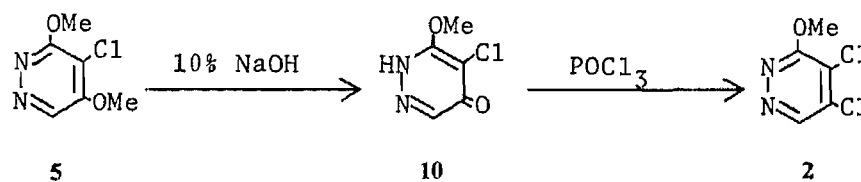
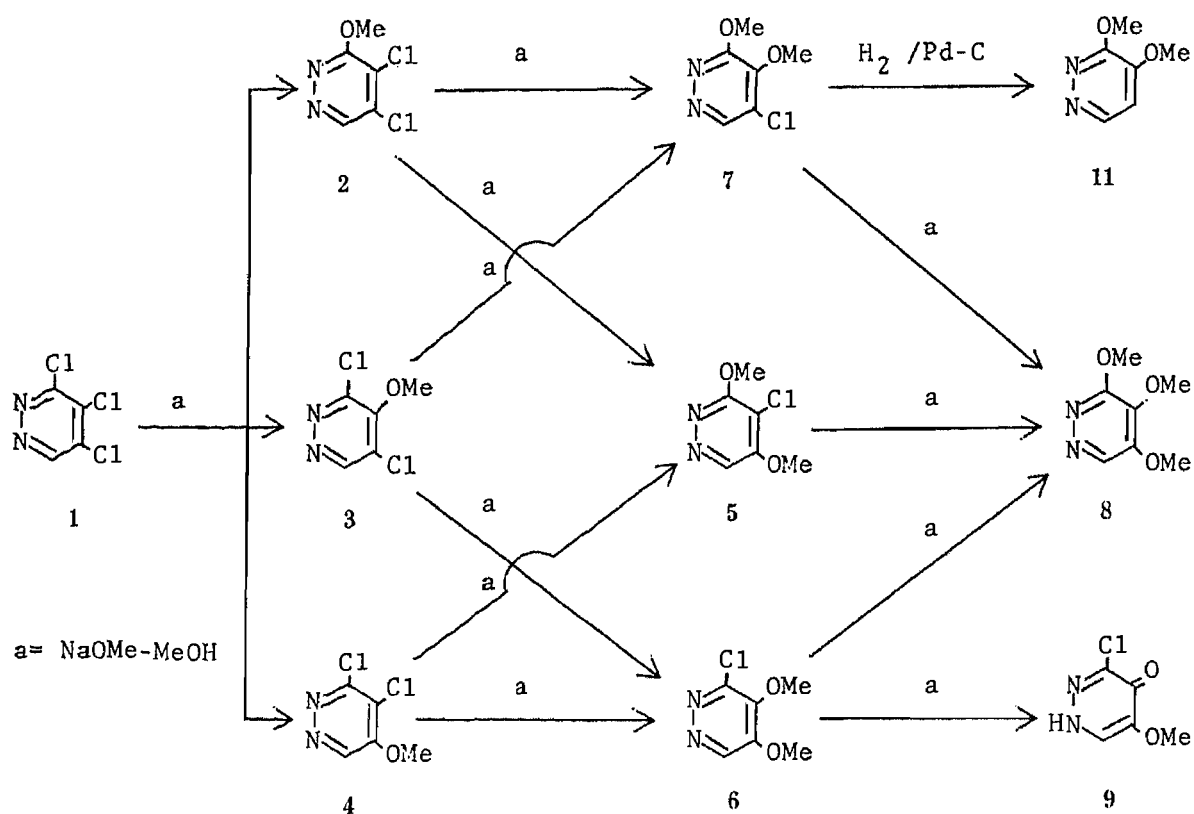
**Keywords**—3,4,5-trichloropyridazine; methoxylation; dichloromonomethoxypyridazine; monochlorodimethoxypyridazine; pyridazinone; 3,4,5-trimethoxypyridazine

Nucleophilic substitution reaction of halogens in heterocyclic compounds with alkoxide anions is important as one of the conventional methods for the chemical manipulation of heterocycles. Some research groups have reported methoxylation of 3,4,5-trichloropyridazine (**1**).<sup>2-4)</sup> The reaction, however, has not been thoroughly examined. We investigated in detail the methoxylation of **1** in order to examine the reactivity of trichloropyridazine toward nucleophiles and its further synthetic application.

In 1965 Itai and Kamiya reported that the reaction of **1** with 1 equimolar amount of NaOMe afforded 3,4-dichloro-5-methoxypyridazine (**4**) without isolation of other products.<sup>2a)</sup> Under analogous conditions, the reaction of **1** with NaOMe was reinvestigated. The proton nuclear magnetic resonance (<sup>1</sup>H-NMR) spectrum of the crude reaction mixture showed three signals ascribed to a ring proton (C<sub>6</sub>-H) at  $\delta$  8.81, 9.03 and 8.92 in the integral ratio of 1:3:6. This result indicates the existence of three compounds in the reaction mixture. An attempt to isolate **3** and **4** from the reaction mixture by fractional recrystallization was unsuccessful. Employment of column chromatography (alumina; ether), however, allowed efficient isolation of 3,5-dichloro-4-methoxypyridazine (**3**) (mp 61 °C) and **4** (mp 101–102 °C) in 24% and 55% yields, respectively.

The monomethoxylation of **3** with NaOMe gave 3-chloro-4,5-dimethoxypyridazine (**6**) and a new dimethoxy derivative (**7**) in 58% and 15% yields, respectively. The structure of the new dimethoxy compound (**7**) was proved to be 5-chloro-3,4-dimethoxypyridazine by its hydrogenation over Pd-C leading to the known 3,4-dimethoxypyridazine (**11**).<sup>5)</sup> On the basis of this result, the structure of **3** was confirmed to be 3,4-dichloro-4-methoxypyridazine. Reaction of **4** with 1 equimolar amount of NaOMe afforded two known products, 4-chloro-3,5-dimethoxypyridazine (**5**) (52%) and **6** (26%), in agreement with the previously reported data.<sup>2a)</sup>

Attempts to isolate the remaining 4,5-dichloro-3-methoxypyridazine (**2**) by chromatography were unsuccessful. The residue obtained by elution with ether-methanol after the isolation of **3** (26%) and **4** (52%) was a complex mixture which showed many spots on thin layer chromatography (TLC) (alumina; ether). Thus, the independent synthesis of **2** starting

TABLE I.  $^1\text{H-NMR}$  Chemical Shifts ( $\delta$  in  $\text{CDCl}_3$ ) of Methoxypyridazines (2–8)

Compd. No.	$\text{C}_6\text{-H}$	$\text{OMe}$
2	8.81 (1H, s)	4.23 (3H, s)
3	9.03 (1H, s)	4.15 (3H, s)
4	8.92 (1H, s)	4.15 (3H, s)
5	8.73 (1H, s)	4.23 (3H, s)      4.09 (3H, s)
6	8.92 (1H, s)	4.10 (3H, s)      4.08 (3H, s)
7	8.73 (1H, s)	4.26 (3H, s)      4.12 (3H, s)
8	8.67 (1H, s)	4.18 (3H, s)      4.03 (6H, s)

from **5** was carried out (see Chart 2). Treatment of **5** with 10% NaOH led to the formation of 5-chloro-6-methoxy-4(1*H*)-pyridazinone (**10**). The reaction of **10** with  $\text{POCl}_3$  afforded **2**, which is different from **3** and **4** in all respects. In conclusion, the unisolable product in the reaction of **1** with NaOMe was proved to be **2** by comparison of the  $^1\text{H-NMR}$  spectrum with that of **2** independently prepared above. The reaction of **2** with 1 equimolar amount of NaOMe afforded **7** (29%) and **5** (55%).

The product distribution of **2**, **3** and **4** in the reaction of **1** with NaOMe is concluded to be

1 : 3 : 6 on the basis of the  $^1\text{H-NMR}$  spectra, indicating that the reactivity of the three chlorine atoms of **1** is in the order of  $\text{Cl-5} > \text{Cl-4} > \text{Cl-3}$ :

Monomethoxydichloropyridazines (**5**, **6** and **7**) were treated with excess NaOMe in refluxing MeOH to give 3,4,5-trimethoxypyridazine (**8**),<sup>6)</sup> although the reaction times reflect the reactivity of chlorine in **5**, **6** and **7** (16 h for **7**, 46%; 18 h for **5**, 13%; 10 h for **6**, 55%). The reaction of **6** with NaOMe gave 3-chloro-5-methoxy-4(1*H*)-pyridazinone (**9**) (10%) as a by-product, whose structure was proved by its conversion to the 3,4-dichloroderivative **4**. The  $^1\text{H-NMR}$  spectral data ( $\text{CDCl}_3$ ) of the methoxypyridazines (**2**—**8**) discussed above are summarized in Table I.

### Experimental

Melting points were determined by the capillary method in a silicone-bath and are uncorrected.  $^1\text{H-NMR}$  spectra were recorded with a Hitachi R-20B spectrometer (60 MHz) in  $\text{CDCl}_3$  with tetramethylsilane as an internal standard.

**Monomethoxylation of 3,4,5-Trichloropyridazine (1)**—NaOMe (0.5 M solution in MeOH) (100 ml) was added to a solution of **1** (9.17 g) in MeOH (100 ml) with stirring below 0°C. Stirring was continued for 1 h at room temperature, then the solvent was evaporated off under reduced pressure. Water (500 ml) was added to the residue and the insoluble product **4** was collected by filtration. The aqueous filtrate was extracted three times with  $\text{CHCl}_3$  (50 ml), dried ( $\text{K}_2\text{CO}_3$ ) and evaporated. The residue was chromatographed on alumina (ether) to give **3** from the less polar fraction and **4** from the polar fraction. Recrystallization of **3** from ether gave colorless crystals (2.15 g, 24%), mp 61°C. *Anal.* Calcd for  $\text{C}_5\text{H}_4\text{Cl}_2\text{N}_2\text{O}$ : C, 33.55; H, 2.25; N, 15.65. Found: C, 33.42; H, 2.21; N, 15.43. The products obtained by filtration and by chromatography were combined and recrystallized from MeOH to give colorless crystals of **4** (4.90 g, 55%), mp 101—102°C.

**5-Chloro-6-methoxy-4(1H)-pyridazinone (10)**—A suspension of **5** (17.5 g) in 10% NaOH was refluxed with stirring for 4.5 h. After cooling, the solution was acidified (Congo red) with concentrated HCl. The precipitate was collected by filtration and recrystallized from water to give **10** as colorless crystals (13.9 g, 87%), mp 188°C (dec.). *Anal.* Calcd for  $\text{C}_5\text{H}_5\text{ClN}_2\text{O}_2$ : C, 37.40; H, 3.14; N, 17.45. Found: C, 37.59; H, 3.42; N, 17.28.

**4,5-Dichloro-3-methoxypyridazine (2)**—A mixture of **10** (11.2 g) and  $\text{POCl}_3$  (107 g) was stirred at 50°C for several minutes and poured into ice-water. The solution was made alkaline with NaOH solution and extracted with  $\text{CHCl}_3$ . The organic layer was dried ( $\text{K}_2\text{CO}_3$ ) and evaporated. The residue was recrystallized from cyclohexane to give colorless crystals of **2** (6.16 g, 49%), mp 96—97°C. *Anal.* Calcd for  $\text{C}_5\text{H}_4\text{Cl}_2\text{N}_2\text{O}$ : C, 33.55; H, 2.25; N, 15.65. Found: C, 33.21; H, 2.13; N, 15.38.

**Monomethoxylation of 2**—NaOMe (0.5 M solution in MeOH) (40 ml) was added to a solution of **2** (3.58 g) in MeOH (40 ml) and the mixture was refluxed for 1 h, then evaporated to dryness. Water (200 ml) was added to the residue. A precipitate was filtered off and recrystallized from MeOH to give colorless crystals of **5** (1.73 g, 55%), mp 161—162°C. *Anal.* Calcd for  $\text{C}_6\text{H}_7\text{ClN}_2\text{O}_2$ : C, 41.28; H, 4.04; N, 16.05. Found: C, 41.12; H, 4.07; N, 15.83. Compound **5** was identical with an authentic sample<sup>20)</sup> by the mixed melting point test. The aqueous layer was extracted with  $\text{CHCl}_3$ . The  $\text{CHCl}_3$  solution was dried ( $\text{K}_2\text{CO}_3$ ) and evaporated. The residue was recrystallized from ether to give **7** as colorless crystals (1.02 g, 29%), mp 59—60°C. *Anal.* Calcd for  $\text{C}_6\text{H}_7\text{ClN}_2\text{O}_2$ : C, 41.28; H, 4.04; N, 16.05. Found: C, 40.95; H, 3.88; N, 15.78.

**Monomethoxylation of 3**—Compound **3** (3.93 g) in MeOH (44 ml) was treated with NaOMe (0.5 M solution in MeOH) (44 ml) as described for compound **2**. The products were separated by fractional recrystallization from ether to give **6** as colorless crystals (2.25 g, 58%) and **7**, mp 59—60°C, as colorless crystals (0.59 g, 15%). **6**: mp 95—97°C. *Anal.* Calcd for  $\text{C}_6\text{H}_7\text{ClN}_2\text{O}_2$ : C, 41.28; H, 4.04; N, 16.05. Found: C, 41.32; H, 4.15; N, 16.11. The former compound (**6**) was identical with an authentic sample<sup>20)</sup> by the mixed melting point test, and the latter (**7**) was identical with a sample obtained from **2** by the mixed melting point test.

**Monomethoxylation of 4**<sup>20)</sup>—Products **5** (1.81 g, 52%, mp 161—162°C) and **6** (0.91 g, 26%, mp 92—95°C) were obtained from **4** (3.58 g) by the same procedure as noted above.

**3,4-Dimethoxypyridazine (11)**—A mixture of **7** (0.349 g), 5% Pd-C (0.3 g) and KOH (0.135 g) in dry MeOH (50 ml) was hydrogenated under atmospheric pressure at room temperature. After evaporation of the solvent, the residue was recrystallized from ether to give colorless crystals of **11** (0.109 g, 39%), mp 55—57°C. This product was identical with an authentic sample<sup>5)</sup> by the mixed melting point test.  $^1\text{H-NMR}$   $\delta$ : 8.76, 6.84 (each 1H, d,  $J=6$  Hz, arom H), 4.14, 4.22 (3H  $\times$  2, each s, OMe  $\times$  2).

**Synthesis of 3,4,5-Trimethoxypyridazine (8)**—General Procedure: A mixture of monochlorodimethoxypyridazine and NaOMe (0.5 M solution in MeOH) (2 eq) was refluxed with stirring. After the spot of starting material had disappeared on TLC (alumina;  $\text{CHCl}_3$  as developing solvent), the solvent was evaporated off and water was added to the residue. The mixture was extracted ( $\text{CHCl}_3$ ), and the extract was dried ( $\text{K}_2\text{CO}_3$ ) and evaporated. The crude

product was recrystallized from cyclohexane to give **8** as colorless crystals (mp 77—78 °C). a) From **7** (0.20 g), **8** (86 mg, 46%) was obtained (reflux, 16.5 h). *Anal.* Calcd for C<sub>7</sub>H<sub>10</sub>N<sub>2</sub>O<sub>3</sub>: C, 49.40; H, 5.92; N, 16.46. Found: C, 49.49; H, 5.98; N, 16.42. b) From **5** (1.08 g), **8** (0.135 g, 13%) was obtained (reflux, 18 h). c) From **6** (0.679 g), **8** (0.365 g, 55%) was obtained (reflux, 10 h).

#### References

- 1) A part of this work was presented at The 96th Annual Meeting of the Pharmaceutical Society of Japan, Nagoya, Apr. 1976.
- 2) a) T. Itai and S. Kamiya, *Chem. Pharm. Bull.*, **11**, 1059 (1963); b) G. Okusa and S. Kamiya, *ibid.*, **16**, 143 (1968).
- 3) F. Miyazawa, T. Hashimoto, S. Iwahara, T. Itai, I. Suzuki, S. Sako, S. Kamiya, S. Natsume, T. Nakashima, and G. Okusa, *Eisei Shikensho Houkoku*, **81**, 98 (1963).
- 4) K. Eichenberger, R. Rometsch, and J. Druey, *Helv. Chim. Acta*, **39**, 1755 (1956).
- 5) T. Itai and S. Natsume, *Chem. Pharm. Bull.*, **10**, 643 (1962).
- 6) G. B. Barlin and P. Lakshminarayana, *J. Chem. Soc., Perkin Trans. 1*, **1977**, 1038.

## Communications to the Editor

[Chem. Pharm. Bull.]  
[35(1) 425-428 (1987)]

EFFICIENT SYNTHESIS OF 6H-PYRIDO [3,2-b] CARBAZOLE DERIVATIVES FROM  
3-AMINO-1,4-DIMETHYL CARBAZOLE

Jean-Charles Lancelot,<sup>a</sup> Sylvain Rault,<sup>a</sup> Max Robba,<sup>a</sup> and Nguyen Huy Dung,<sup>b</sup>

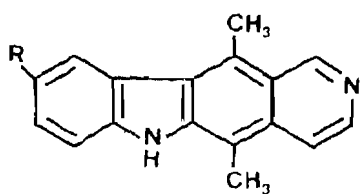
Laboratoire de Chimie Thérapeutique, U.E.R. des Sciences Pharmaceutiques,<sup>a</sup>  
1, rue Vaubénard, 14032 Caen Cédex, France, Laboratoire de Chimie Minérale  
et Structurale,<sup>b</sup> 1, rue Vaubénard, 14032 Caen Cédex, France.

The synthesis of 3-amino-1,4-dimethylcarbazole is described and its reaction with  $\beta$ -ketoesters gives new 6H-pyrido [3,2-b] carbazole derivatives.

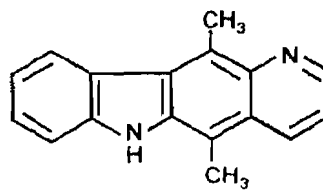
KEYWORDS — 3-Amino-1,4-dimethylcarbazole ; 6H-pyrido [3,2-b] carbazole ; Conrad-Limpach reaction ; lactam-lactim tautomerism

Since the isolation of ellipticine 1 and methoxyellipticine 1a and the discovery of their potent anticancer activity,<sup>1)</sup> numerous syntheses of pyridocarbazoles have been reported. However in contrast with the intense activity directed toward the synthesis of pyrido [4,3-b]<sup>2)</sup>, [3,4-b]<sup>3)</sup>, [3,2-c], [4,3-c], [3,4-c], and [2,3-c]<sup>4)</sup> carbazoles, very little attention has been focused on the isomeric pyrido [3,2-b] carbazoles 2. Surveying the literature, we have only found papers about 2,4-disubstituted derivatives.<sup>5)</sup>

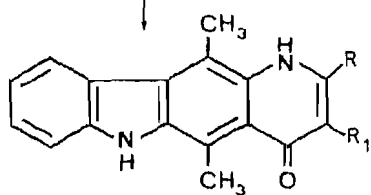
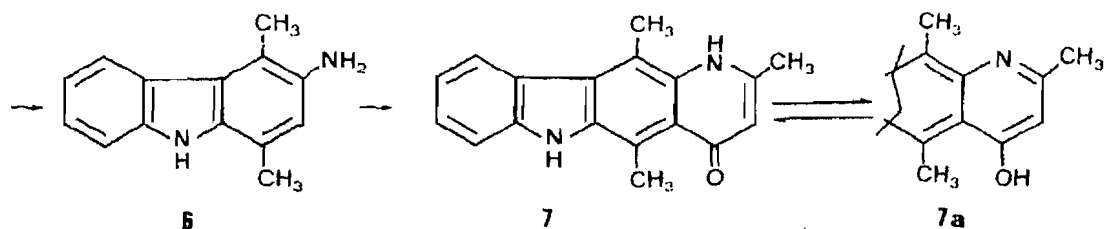
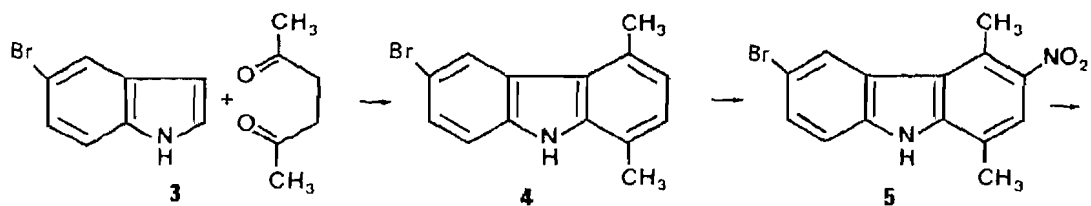
We describe now a convenient approach for the construction of 5,11-dimethyl-6H pyrido [3,2-b] carbazole derivatives making use of 3-amino-1,4-dimethylcarbazole 6. We have adjusted the conditions for the synthesis of this latter, yet unknown key intermediate 6 during the course of our work in the preparation of nitrocarbazoles.<sup>6)</sup> This compound 6 was obtained in three steps starting from 5-bromoindole 3 via 6-bromo-1,4 dimethylcarbazole.<sup>7)</sup> 4 first by nitration in acetic anhydride, followed by reduction with hydrogen under pressure over palladium charcoal. This latter reaction resulted in the reduction of the nitro group and the debromination at the 6 position (the presence of the bromine atom is necessary for the reaction to permit a selective mononitration at the 3 position). Condensation of ethyl acetoacetate with the amine 6 led to a non-isolable intermediate which was then cyclized by heating at 230°C in diphenylether to give the pyridocarbazolone 7 in 65% yield. This compound exhibits the lactam-lactim tautomerism. In the solid state CO and NH absorption in the IR spectrum, and an X-ray crystallographic study<sup>8)</sup> clearly established the existence of the lactam form 7. However in solution, the OH absorption in the IR spectrum (CH<sub>3</sub>CN) and the formation of acetoxy compound 8 during the reaction of 7 with acetic anhydride indicate the



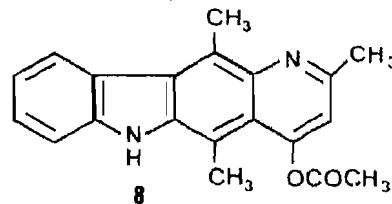
**1** R=H  
**1a** R=OCH<sub>3</sub>



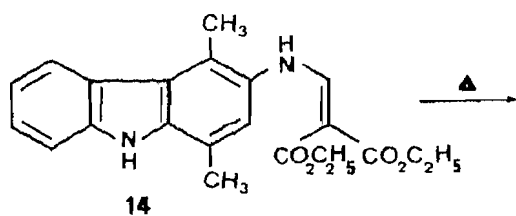
**2**



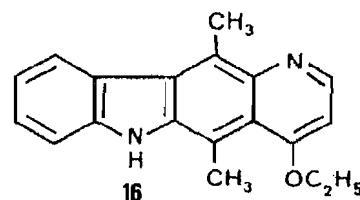
**9** R=CF<sub>3</sub> - R<sub>1</sub>=H      **12** R=R<sub>1</sub>=CH<sub>3</sub>  
**10** R=(CH<sub>2</sub>)<sub>2</sub>CH<sub>3</sub> - R<sub>1</sub>=H    **13** R=CH<sub>3</sub> - R<sub>1</sub>=CH<sub>2</sub>C<sub>6</sub>H<sub>5</sub>  
**11** R=CH(CH<sub>3</sub>)<sub>2</sub> - R<sub>1</sub>=H    **15** R=H - R<sub>1</sub>=CO<sub>2</sub>C<sub>2</sub>H<sub>5</sub>



**8**



**14**



**16**

TABLE 1 : M.P., IR <sup>1</sup>HNMR SPECTROSCOPIC DATA OF CARBAZOLES

Compd No	m.p.(°C)	IR(KBr) (ν C=O and NH cm <sup>-1</sup> )	HNMR(DMSO-d <sub>6</sub> /δppm)					
			H2	H5	H6	H7	H8	Others
5	228	3310 (NH) 1310 (NO <sub>2</sub> )	7.66	8.03	-	7.77	7.33	NH : 11.69 CH <sub>3</sub> (1) : 2.43 CH <sub>3</sub> (4) : 2.71
6	198	3140 (NH) 3380,3320,1600 (NH <sub>2</sub> )	6.66	8.13	7.06	7.36	7.36	NH : 10.63 NH <sub>2</sub> : 4.45 CH <sub>3</sub> (1) : 2.43 CH <sub>3</sub> (4) : 2.50
14	230	3280 (NH) 1675,1650 (C=O)	7.13	8.13	7.13	7.40	7.40	NH : 11.22, 11.09 CH <sub>3</sub> (1) : 2.51 CH <sub>3</sub> (4) : 2.71 CH : 8.38 CH <sub>2</sub> CH <sub>3</sub> : 4.13, 1.23

TABLE 2 : M.P., IR <sup>1</sup>HNMR SPECTROSCOPIC DATA OF PYRIDO[3,2-b] CARBAZOLES

Compd No	m.p.(°C)	IR(KBr) (ν C=O and NH cm <sup>-1</sup> )	HNMR(DMSO-d <sub>6</sub> /δppm)						
			H2	H3	H7	H8	H9	H10	Others
7*	265	3420,3240 (NH) 1620 (C=O)	-	5.73	7.41	7.41	7.06	8.25	NH : 9.95, 11.01 CH <sub>3</sub> : 3.11, 2.98, 2.38
8	170	3240 (NH) 1720 (C=O)	-	7.03	7.43	7.43	7.19	8.23	NH : 11.03 CH <sub>3</sub> : 2.86, 2.66, 2.46 CHOCH <sub>3</sub> : 2.46
9	250 (sublim)	3400,3300 (NH) 1625 (C=O)	-	7.16	7.33	7.33	7.06	8.03	NH : 7.83, 10.93 CH <sub>3</sub> : 2.76, 2.59
10	251	3420,3260 (NH) 1610 (C=O)	-	5.76	7.43	7.43	7.10	8.26	NH : 9.83, 10.99 CH <sub>3</sub> : 3.10, 2.96 (CH <sub>2</sub> ) <sub>2</sub> CH <sub>3</sub> : 2.60, 1.70, 0.96
11	240	3420,3200 (NH) 1610 (C=O)	-	5.80	7.43	7.43	7.06	8.26	NH : 9.70, 11.00 CH <sub>3</sub> : 3.10, 3.00 CH(CH <sub>3</sub> ) <sub>2</sub> : 3.29, 1.30
12	265 (sublim)	3425,3160 (NH) 1610 (C=O)	-	-	7.43	7.43	7.06	8.26	NH : 9.66, 10.89 CH <sub>3</sub> : 3.10, 2.96, 2.43, 1.96
13	280	3420,3200 (NH) 1610 (C=O)	-	-	7.40	7.40	7.06	8.20	NH : 9.70, 10.90 CH <sub>3</sub> : 3.06, 2.93, 2.33 CH <sub>2</sub> : 3.86 C <sub>6</sub> H <sub>5</sub> : 7.09
15	275	3340,3250 (NH) 1685,1620 (C=O)	8.26	-	7.43	7.43	7.10	8.26	NH : 11.19 CH <sub>3</sub> : 3.03, 2.90 CH <sub>2</sub> CH <sub>3</sub> : 4.16, 1.25
16	264	3200 (NH)	8.50	6.75	7.43	7.43	7.13	8.23	NH : 10.93 CH <sub>3</sub> : 3.20, 3.00 CH <sub>2</sub> CH <sub>3</sub> : 4.16, 1.48

\* IR (CH<sub>3</sub>CN) νOH = 3650 and 3550 cm<sup>-1</sup>

existence of the lactim form 7a. Structure 8 is confirmed by a single CO absorption on the IR spectrum ( $1720\text{ cm}^{-1}$ ) and by the deshielding of H-3 in the  $^1\text{H}$  NMR spectrum. In a similar manner in 50-70% yield condensation of various  $\beta$ -ketoesters with the amine 6 led to the corresponding pyridones 9-13.

On the other hand, when diethyl ethoxymethylidenemalonate was used, the reaction yielded the isolable intermediate 14 which gave either the 3-carbethoxypyridone 15 in 60% yield by heating in diphenylether or the 4-ethoxy pyridine 16 in 33% yield by sublimation in vacuo at  $260^\circ\text{C}$ . In the light of the in vitro antimitotic activity (Leukemia L 1210 culture cells) of compounds 7, 8 and 16 <sup>9)</sup> further studies concerning the chemistry and biological activity of title and related compounds are in progress.

#### REFERENCES

- 1) (a) S. Goodwin, A.F. Smith and E.C. Horning, *J. Am. Chem. Soc.*, 81, 1903 (1959)  
 (b) R.B. Woodward, G.A. Iacobucci and F.A. Hochstein, *ibid*, 81, 4434 (1959)  
 (c) G.H. Svoboda, G.A. Poore and M.L. Montfort, *J. Pharm. Sci.*, 57, 1720 (1968)
- 2) For reviews, see :  
 (a) M. Sainsbury, *Synthesis*, 1977, 437.  
 (b) R. Barone and M. Chanon, *Heterocycles*, 16, 1357 (1981).
- 3) G. Saulnier and W. Gribble, *J. Org. Chem.*, 48, 2690 (1983)
- 4) S. Pelaprat, R. Oberlin, I. Le Guen and B.P. Roques, *J. Med. Chem.*, 23, 1330 (1980)
- 5) (a) J.C. Perche, G. Saint-Ruf and N.P. Buu-Hoi, *J. Chem. Soc.*, 1972, 260  
 (b) N.S. Kozlov, V.V. Misenzhnikov, T.P. Shulyateva and L.D. Dryabkina, *Katalit. Syntez. Organ. Soedin.*, 1976, 40, 4 (1976).  
 (c) N.S. Kozlov, V.V. Misenzhnikov, T.P. Shulyateva, V.M. Adanin and V.G. Sakharovskü, *Khim. Geterotsikl. Soedin.*, 1983, (4), 498.
- 6) J.C. Lancelot, J.M. Gazengel, S. Rault, Nguyen Huy Dung and M. Robba, *Chem. Pharm. Bull.*, 32, 4447 (1984) (and reference cited therein).
- 7) (a) P.A. Cranwell and J.E. Saxton, *J. Chem. Soc.*, 1962, 3482  
 (b) L.K. Dalton, S. Demerac, B.C. Elmes, J.W. Loder, J.M. Swan and T. Teitei, *Austr. J. Chem.*, 20, 2715 (1967).  
 (c) L.K. Dalton and T. Teitei, *ibid*, 21, 2053 (1968).
- 8) Nguyen Huy Dung, B. Viossat, J.C. Lancelot and M. Robba, *Chem. Pharm. Bull.*, 1987 (to be published).
- 9) J.C. Lancelot, S. Rault, M. Robba, T. Tabka, P. Gauduchon and J.Y. Le Talaer, 22e Rencontres Internationales de Chimie Thérapeutique. Clermont-Ferrand, 3-5 Septembre 1986.

(Received October 13, 1986)



## Communications to the Editor

[Chem. Pharm. Bull.]  
35(1) 429--432 (1987)

MICROBIOLOGICALLY MODIFIED 4,9-DIMETHYL- $\Delta^{4(10)}$ -OCTAL-3,7-DIONES AS THE CHIRAL SYNTHON FOR FORMAL TOTAL SYNTHESSES OF C(8) OXYGENATED SESQUITERPENOIDS

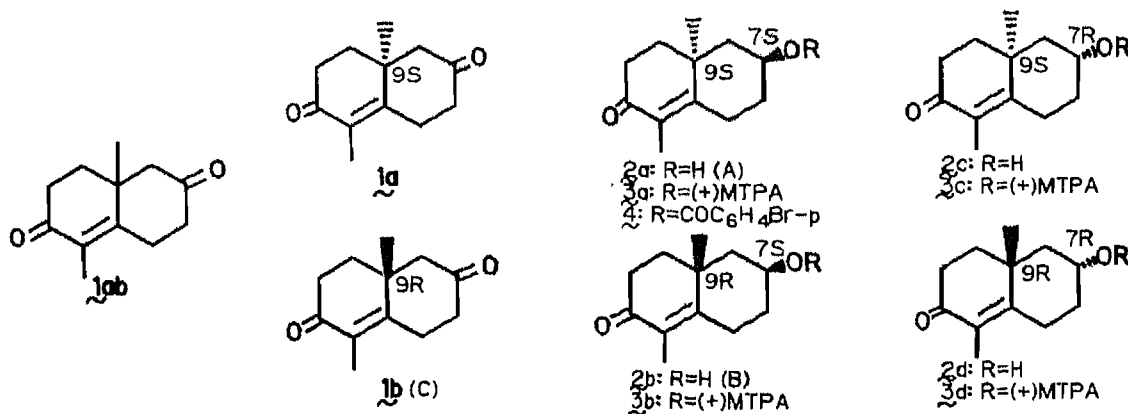
Seiichi Inayama,<sup>\*a</sup> Nobuko Shimizu,<sup>a</sup> Tamiko Ohkura,<sup>a</sup> Hiroyuki Akita,<sup>b</sup>  
Takeshi Oishi,<sup>b</sup> and Yoichi Iitaka<sup>c</sup>

Pharmaceutical Institute, School of Medicine, Keio University,<sup>a</sup>  
Shinanomachi, Shinjuku-ku, Tokyo 160, Japan,  
Institute of Physical and Chemical Research,<sup>b</sup>  
Hirosawa, Wako-shi, Saitama 351-01, Japan, and  
Faculty of Pharmaceutical Sciences, University of Tokyo,<sup>c</sup>  
Hongo, Bunkyo-ku, Tokyo 113, Japan

4,(9S)- (2a) and 4,(9R)-dimethyl-(7S)-hydroxy- $\Delta^{4(10)}$ -octal-3-one (2b) were prepared in high optical purity (>99% ee) and in moderate yield by asymmetric reduction of the corresponding racemic diketone (1ab) using yeasts. These compounds were used for the formal total synthesis of C(8) oxygenated sesquiterpenoids such as (-)-artemisin, (-)-yomogin, (-)-3-oxodiplophyllin,  $\beta$ -elemenone, (+)-isotelekin and (+)-cuaudemone.

KEYWORDS — asymmetric induction; microbiological reduction; 3,7-octaldione; (7S)-hydroxyoctal-3-one; yeast; *Rhodotorula rubra*; chiral synthon; sesquiterpenoids; (-)-artemisin; (+)-isotelekin

Earlier we reported<sup>1)</sup> the enantioselective reduction of 4-carbomethoxy-3,8-dioxo-9-methyl- $\Delta^{4(10)}$ -octalin with certain specialized yeasts, such as *Hansenula anomala*, to yield the optically pure ketol (>99% ee) along with the highly optically pure diketone (>99% ee) corresponding to the starting racemate. This indicates that a kinetical resolution of the diketoester was effected by the



microorganisms. On the other hand, the attempted preparation of C(8) oxygenated sesquiterpenoids by microbiological oxidation of the corresponding desoxy congener has not always been successful. Nor has the many-step chemical modification had practical results, as in the transformation from  $\beta$ - $\alpha$ -santonin to artemisin.<sup>2)</sup> The chiral octalin derivatives with an oxygen functional group at C(7) (equivalent to C(8) in sesquiterpenoids) are some of the most important optically active synthons to be used in the syntheses of naturally occurring sesquiterpenoids. Some examples are (-)-artemisin,<sup>3a)</sup> (-)-yomogin,<sup>3b)</sup> (-)-3-oxodiplophyllin,<sup>3c)</sup>  $\beta$ -elemenone,<sup>3d)</sup> (+)-isotelekin,<sup>3e)</sup> and (+)-cuauhtemone.<sup>3f)</sup> Nevertheless, the chiral diketones have not been synthesized by conventional asymmetric cyclization.<sup>4)</sup>

Here we describe the enantioselective reduction of ( $\pm$ )-4,9-dimethyl- $\Delta^4(10)$ -octal-3,7-dione (1ab)<sup>5)</sup> using yeasts. As before,<sup>1)</sup> the microbial transformation of ( $\pm$ )-1ab with some selected yeasts, among various microorganisms, especially *Rhodotorula rubra* CCY 20-7-1,<sup>6,7)</sup> produced the two ketols A,<sup>8)</sup>  $[\alpha]_D^{19} -147.9^\circ$  (c = 1.0; CHCl<sub>3</sub>) (mp 69-75°C), and B,<sup>7)</sup>  $[\alpha]_D^{21} +157.2^\circ$  (c = 1.0; CHCl<sub>3</sub>) (mp 98-101°C), along with recovered diketone,  $[\alpha]_D^{20} +9.4^\circ$  (c = 1.0; CHCl<sub>3</sub>) (mp 86-89°C), in 34%, 25% and 24% yield, respectively. As shown in Fig. 1, the absolute configuration of the main product A was determined by X-ray analysis of its p-bromobenzoate (4) to be 7S, 9S (hence A = 2a).<sup>9)</sup> The other ketol B was oxidized with Jones reagent to provide the diketone C,  $[\alpha]_D^{21} +7.8^\circ$  (c = 1.0; CHCl<sub>3</sub>), which was identical except for the sign of the optical rotation with (9S)-diketone (1a)  $[\alpha]_D^{21} -11.5^\circ$  (c = 1.0; CHCl<sub>3</sub>) obtained by Jones oxidation of the foregoing ketol (7S,9S)-A (2a). Since the sign of  $[\alpha]_D$  in C was opposite to that in 1a, the absolute configuration of C and the recovered diketone was found to be 9R (hence C = 1b). There was a downward chemical shift of the angular methyl signal of B in <sup>1</sup>H-NMR ( $\Delta +0.198$  ppm) in comparison with A (2a) and an upward shift of the corresponding methyl signal of the acetate of B ( $\Delta -0.090$  ppm) in comparison with B. This accords with the earlier report<sup>10)</sup> of the 1,3 diaxial relationship between the hydroxyl group and the methyl group, showing that the stereochemistry of C(7)-OH in B is axially oriented. This is also supported by the C(7) equatorial OH of 2a found in the X-ray analysis of 4. Therefore the absolute configuration of B was determined to be 7S, 9R (hence B = 2b).

In order to determine the optical purity of the reduction products, four possible stereoisomers (2a-d) were synthesized from the ( $\pm$ )-diketone (1ab) as follows. Reduction of the diketone (1ab) with diisobutylaluminum hydride followed by manganese dioxide oxidation afforded a racemic *cis* ketol (2bc) and a racemic *trans* ketol (2ad) in 35% and 26% over-all yields. These two racemic ketols were treated directly with (+)- $\alpha$ -methoxy- $\alpha$ -trifluoromethyl-phenylacetic acid chloride [(+)-MTPACL]<sup>11)</sup> to give the corresponding (+)-MTPA esters, 3ad and 3bc. Two NMR signals due to each angular methyl group appeared in distinctly different fields at  $\delta$  1.318 and  $\delta$  1.326 for 3ad and at  $\delta$  0.978 and  $\delta$  1.128 for 3bc. Then, the first product (7S,9S)-2a obtained by the microbial reduction was converted to the corresponding (+)-MTPA ester 3a ( $\delta$  1.318); its optical purity was found to be more than 99% ee. Therefore, the remaining NMR signal ( $\delta$  1.326) of 3ad should be ascribed to (7R,9R)-3d. The second reduction product (7S,9R)-2b was also converted to the corresponding (+)-MTPA ester 3b ( $\delta$  0.978). This was found to be 67% ee by taking account of a small signal ( $\delta$  1.128) due to its enantiomer (7R,9S)-

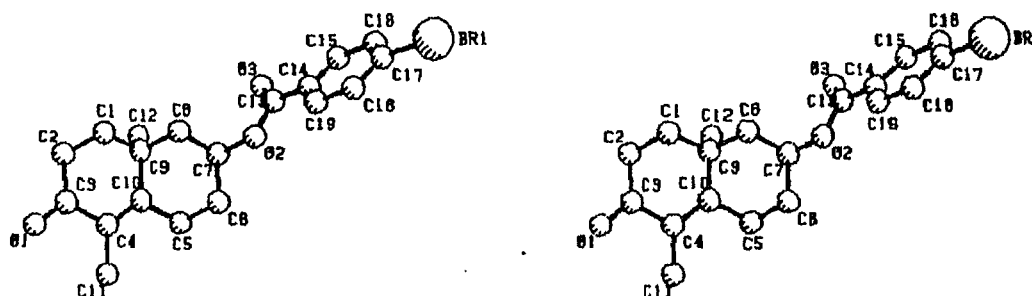


Fig. 1 Stereoview of p-Bromobenzoate (4) of 4, (9S)-Dimethyl-(7S)-hydroxy- $\Delta^{4(10)}$ -octal-3-one (2a)

3c. The optical purity of the recovered diketone (1b) was, as above determined, to be 60-61% ee.

Since the relationship between the absolute structure and the chemical shift of the four possible (+)-MTPA esters (3a-d) was thus established, we have begun the following microbial screening experiments. To find more effective reducing microorganisms to produce (7S,9R)-2b selectively, a series of reductions with a variety of yeasts was undertaken.

Reduction of ( $\pm$ )-1ab with *Trichosporon fermentans* IFO-1199<sup>7)</sup> provided the *cis*-ketol (7S,9R)-2b,  $[\alpha]_D^{19} +198.8^\circ$  ( $c = 1.0$ ;  $\text{CHCl}_3$ ), corresponding to >99% ee in 34% yield and a small amount of the *trans*-ketol (7S,9S)-2a (>99% ee, 6%), along with the recovered diketone (9S)-1a,  $[\alpha]_D^{19} -4.5^\circ$  ( $c = 1.0$ ;  $\text{CHCl}_3$ ), corresponding to 39% ee, by direct comparison of  $[\alpha]_D^{21} -11.5^\circ$  ( $c = 1.0$ ;  $\text{CHCl}_3$ ), in 44% yield. Another asymmetric reduction with *Torulopsis famata*<sup>7)</sup> gave a complex mixture in which the optical purity of product 2b (14% yield) was very high (>99% ee).

In conclusion, with properly selected microorganisms, microbial asymmetric reduction of 4,9-dimethyl- $\Delta^{4(10)}$ -octal-3,7-dione (1ab) afforded 4, (9S)- (2a) and/or 4, (9R)-dimethyl-(7S)-hydroxy- $\Delta^{4(10)}$ -octal-3-one (2b) with high optical purity (>99% ee) in moderate yield.

Since the six racemic sesquiterpenoids corresponding to the respective natural products mentioned above have been synthesized,<sup>12)</sup> the aforementioned preparation of the optically active key intermediates, i.e. (-)-4, (9S)- (1a) and (+)-4, (9R)-dimethyl- $\Delta^{4(10)}$ -octal-3,7-dione (1b) constitutes the formal total synthesis of the sesquiterpenoids, i.e. artemisin,<sup>12a)</sup> yomogin,<sup>5)</sup> 3-oxodiplophyllin,<sup>5)</sup>  $\beta$ -elemenone,<sup>12b)</sup> isotelekin<sup>12c)</sup> and cuauhtemone<sup>12d)</sup> starting from these leading chiral synthons.

#### REFERENCES AND NOTES

- 1) S. Inayama, N. Shimizu, T. Ohkura, H. Akita, T. Oishi and Y. Iitaka, *Chem. Pharm. Bull.*, **34**, 2660 (1986).
- 2) K. Yamakawa, K. Nishitani, M. Iida and A. Mikami, *Chem. Pharm. Bull.*, **34**, 1319 (1986).

- 3) a) Merck's Jahresber, 1894, p. 3 in J. Shimonsen and D.H.R. Barton, "The Terpenes," Vol. III, Cambridge University Press, Cambridge, 1951, p. 312; b) T.A. Geissman, *J. Org. Chem.*, 31, 2523 (1966); c) Y. Asakawa, M. Toyota, T. Takemoto and C. Suire, *Phytochemistry*, 18, 1007 (1979); d) I. Ognjanov, V. Herout, M. Horak and F. Šorm, *Collect. Czech. Chem. Commun.*, 24, 2371 (1959); e) V. Benešová, V. Herout and F. Šorm, *ibid.*, 26, 1350 (1961); f) K. Nakanishi, C. Crouchi, I. Miura, X. Dominguez, A. Zamidio and R. Villarreal, *J. Am. Chem. Soc.*, 96, 609 (1974).
- 4) U. Eder, G. Sauer and R. Wiechert, *Angew. Chem. Int. Ed. Engl.*, 10, 496 (1971).
- 5) D. Caine and G. Hasenhuettle, *J. Org. Chem.*, 45, 3278 (1980).
- 6) K. Horikoshi, A. Furuichi, H. Koshiji, H. Akita and T. Oishi, *Agric. Biol. Chem.*, 47, 435 (1983).
- 7) The reduction period and the substrate concentration were 72 h and 0.5%, respectively.
- 8) A: Anal. high-resolution MS ( $M^+$ , m/z) Calcd for  $C_{12}H_{18}O_2$ , 194.130; Found, 194.128. IR  $\nu_{\max}^{CHCl_3}$  ( $cm^{-1}$ ) 3600, 3445, 1658, 1610.  $^1H$ -NMR ( $CDCl_3$ , 400 MHz)  $\delta$ : 1.245 (3H, s, 9- $CH_3$ ), 1.782 (3H, s, 4- $CH_3$ ), 4.030-4.107 (1H, m, 7-H).  
B: Anal. high-resolution MS ( $M^+$ , m/z) Calcd for  $C_{12}H_{18}O_2$ , 194.130; Found, 194.132. IR  $\nu_{\max}^{CHCl_3}$  ( $cm^{-1}$ ) 3600, 3450, 1650, 1610.  $^1H$ -NMR ( $CDCl_3$ , 400 MHz)  $\delta$ : 1.439 (3H, s, 9- $CH_3$ ), 1.792 (3H, s, 4- $CH_3$ ), 4.220-4.224 (1H, m, 7-H).
- 9) Crystal data of 4:  $C_{19}H_{21}O_3Br$ , MW = 377.3, triclinic, space group P1, Z = 2,  $D_{\text{calc}} = 1.407 \text{ g cm}^{-3}$ , a = 11.230(6), b = 10.788(7), c = 8.470(5) Å,  $\alpha = 105.79(6)$ ,  $\beta = 74.63(4)$ ,  $\gamma = 113.61(6)^\circ$ , U = 890.5 Å<sup>3</sup>, R = 0.063.
- 10) Y. Kawazoe, Y. Sato, M. Natsume, H. Hasegawa, T. Okamoto and K. Tsuda, *Chem. Pharm. Bull.*, 10, 338 (1962). Cf. R.F. Zurcher, *Helv. Chim. Acta.*, 44, 1380 (1961).
- 11) a) J.A. Dole, D.L. Dule and H.S. Mosher, *J. Org. Chem.*, 43, 2542 (1969); b) J.A. Dole and H.S. Mosher., *J. Am. Chem. Soc.*, 95, 512 (1973).
- 12) a) M. Nakazaki and K. Naemura, *Tetrahedron Lett.*, 1966, 2615; b) G. Najetich, P.A. Grieco and M. Nishizawa, *J. Org. Chem.*, 43, 2327 (1977); c) R.B. Miller and E.S. Behare, *J. Am. Chem. Soc.*, 96, 8102 (1974); d) D.J. Goldsmith and I. Sakano, *J. Org. Chem.*, 41, 2095 (1976).

(Received October 23, 1986)

## Communications to the Editor

[Chem. Pharm. Bull.]  
35(1) 433-435 (1987)

SUCCESSFUL ASYMMETRIC DIELS-ALDER APPROACH TO  
OPTICALLY ACTIVE  $\underline{C}$ -NUCLEOSIDES. ENANTIOSELECTIVE TOTAL  
SYNTHESIS OF  $\underline{D}$ -SHOWDOMYCIN AND  $\underline{D}$ -2,5-ANHYDROALLOSE DERIVATIVES

Hiroimitsu Takayama, Akira Iyobe, and Toru Koizumi\*  
Faculty of Pharmaceutical Sciences, Toyama Medical and  
Pharmaceutical University, Sugitani 2630, Toyama 930-01, Japan

Using an asymmetric Diels-Alder reaction of ( $\underline{S}$ ) $\underline{S}$ -3-(2-pyridylsulfanyl)acrylate with furan, a highly enantioselective synthesis of a common key intermediate (+)-(1) was achieved, and this was successfully converted to  $\underline{C}$ -nucleosides,  $\underline{D}$ -showdomycin (2) and  $\underline{D}$ -3,4- $\underline{Q}$ -isopropylidene-2,5-anhydroallose (3).

KEYWORDS— $\underline{C}$ -nucleoside;  $\underline{D}$ -showdomycin; 3-(arylsulfanyl)acrylate; 3-(heteroarylsulfanyl)acrylate; asymmetric Diels-Alder reaction; chiral sulfoxide;  $\underline{D}$ -anhydroallose

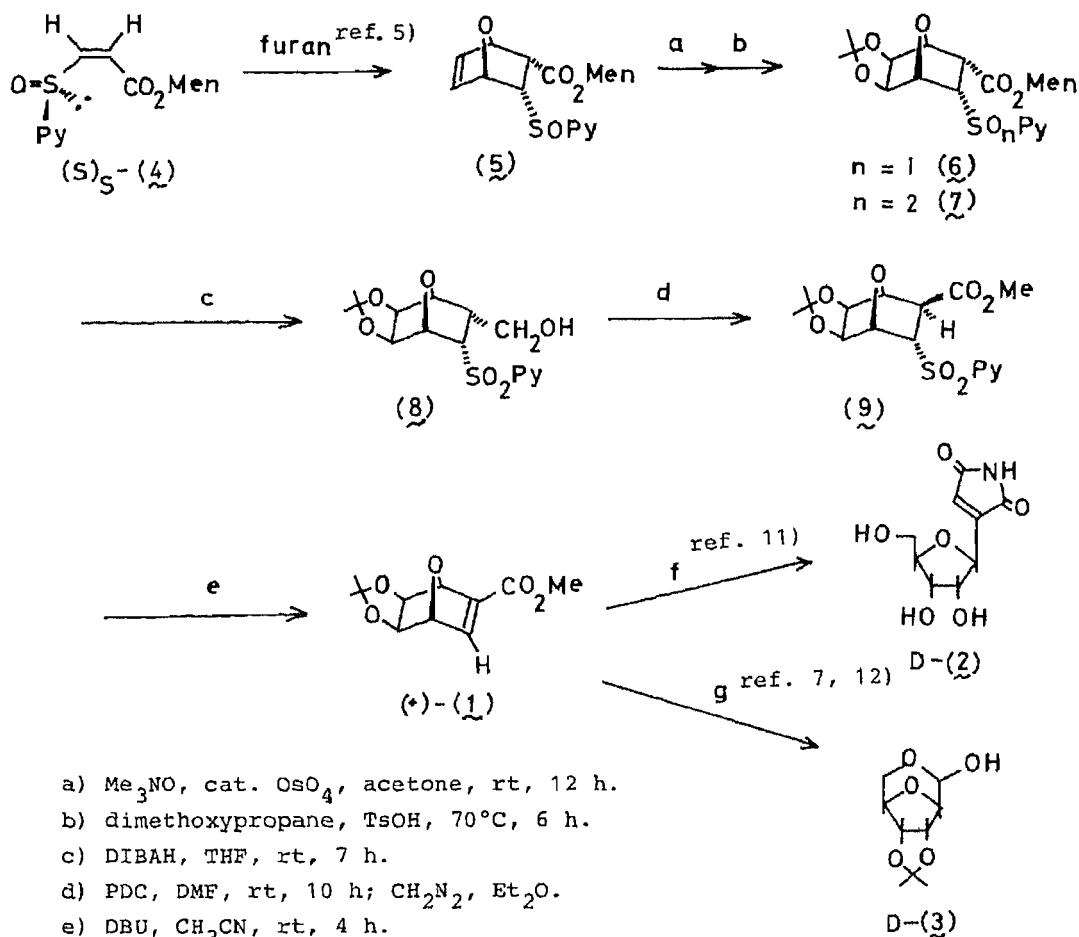
Much attention has been focused on synthetic approaches to naturally occurring  $\underline{C}$ -nucleosides because of their interesting biological activities.<sup>1)</sup> Methods hitherto developed for the synthesis of optically active  $\underline{C}$ -nucleosides fall into the following three categories: 1) chemical transformation of natural carbohydrate precursors,<sup>2)</sup> 2) conventional optical resolution of synthetic intermediates,<sup>3)</sup> and 3) production of chiral intermediates by a chemicoenzymatic strategy.<sup>4)</sup> There has been no report on the total synthesis of  $\underline{C}$ -nucleosides using asymmetric organic reactions. The recent progress in the asymmetric reactions, especially the asymmetric Diels-Alder reaction, presents a new method for the preparation of chiral synthetic intermediates of  $\underline{C}$ -nucleosides.

Recently we have introduced novel chiral dienophiles, menthyl 3-(2-pyridylsulfanyl)acrylates ( $\underline{S}$ ) $\underline{S}$ - and ( $\underline{R}$ ) $\underline{S}$ -(4),<sup>5)</sup> which react smoothly with furan in a highly diastereoselective manner, and suggested that the asymmetric D-A reaction may be a new way to synthesize chiral  $\underline{C}$ -nucleosides.

Here we report our recent results along this line, presenting the highly enantioselective synthesis of a common key intermediate (+)-1<sup>6)</sup> using the asymmetric Diels-Alder reaction of ( $\underline{S}$ ) $\underline{S}$ -4 and its transformation to  $\underline{D}$ -showdomycin(2)<sup>6)</sup> and  $\underline{D}$ -3,4- $\underline{Q}$ -isopropylideneallose(3).<sup>7)</sup>

The major cycloadduct (5) (mp 94-96°C,  $[\alpha]_{\underline{D}}$  -23.8°) derived from ( $\underline{S}$ ) $\underline{S}$ -(4), having the desired absolute configuration for the synthesis of naturally occurring  $\underline{C}$ -nucleosides, was oxidized with OsO<sub>4</sub>(OsO<sub>4</sub> and Me<sub>3</sub>NO) then acetonized (2,2-dimethoxypropane and *p*-toluenesulfonic acid) to give sulfoxide (6) (mp 145°C,  $[\alpha]_{\underline{D}}$  -84.8°) and sulfone (7) (mp 132-133°C,  $[\alpha]_{\underline{D}}$  +10.4°) in 33% and 56% yields, respectively.<sup>8)</sup> The sulfoxide (6) was converted to the corresponding sulfone (7) by

m-chloroperbenzoic acid (mCPBA) oxidation, in a quantitative yield. The menthyl ester was converted to methyl ester in sulfone (7) as follows.<sup>9)</sup> The reduction of (7) with diisobutylaluminum hydride(DIBAH) gave the primary alcohol (8) (mp 174-175° C,  $[\alpha]_D -30.7^\circ$ ) in 73% yield, which was then oxidized with pyridinium dichromate (PDC) and the resultant carboxylic acid was treated with diazomethane to afford the methyl ester (9) (mp 107-110°C,  $[\alpha]_D -46.8^\circ$ ) in 83% yield. Treatment of (9) with DBU produced (+)-(1) (mp 133°C,  $[\alpha]_D +54.6^\circ$ ) in 80% yield. The enantiomeric excess of (+)-(1) proved to be no less than 98% as checked by the 270 MHz NMR spectrum using chiral shift reagent.<sup>10)</sup>



- a)  $\text{Me}_3\text{NO}$ , cat.  $\text{OsO}_4$ , acetone, rt, 12 h.  
 b) dimethoxypropane,  $\text{TsOH}$ , 70°C, 6 h.  
 c) DIBAH, THF, rt, 7 h.  
 d) PDC, DMF, rt, 10 h;  $\text{CH}_2\text{N}_2$ ,  $\text{Et}_2\text{O}$ .  
 e) DBU,  $\text{CH}_3\text{CN}$ , rt, 4 h.  
 f)  $\text{O}_3$ ;  $\text{LiAlH}(\text{O}t\text{Bu})_3$ ;  $t\text{-BuMe}_2\text{SiCl}$ ; DMSO-DCC;  
 $\text{Ph}_3\text{P}=\text{CHCONH}_2$ ;  $\text{CF}_3\text{COOH}$ . g)  $\text{O}_3$ ;  $\text{NaBH}_4$ ;  $\text{NaIO}_4$ .

The methyl ester (+)-(1) was successfully transformed in 9% overall yield to the optically pure D-showdomycin(2), mp 152-154°C,  $[\alpha]_D +49.9^\circ$  ( $c=0.51$ ,  $\text{H}_2\text{O}$ ), lit.<sup>6)</sup> mp 153-154°C,  $[\alpha]_D +49.9^\circ$  ( $c=1$ ,  $\text{H}_2\text{O}$ ), according to the procedure reported by Just et al.<sup>11)</sup> in their synthesis of racemic showdomycin.

The intermediate (+)-(1) was also converted by three steps ( $\text{O}_3$ ,  $\text{NaBH}_4$ ,  $\text{NaIO}_4$ )<sup>12)</sup> to D-(3), mp 165°C,  $[\alpha]_D +6.3^\circ$  ( $c=0.29$ ), in about 40% overall yield. The racemate (3)

had been used previously by Just *et al.*<sup>12)</sup> as a key intermediate for the synthesis of  $\underline{C}$ -nucleoside analogues.

The method developed in this work provides a new entry for the total synthesis of optically active  $\underline{C}$ -nucleosides. We are currently studying the chiral synthesis of both enantiomers of natural and modified  $\underline{C}$ -nucleosides using the present method starting from the chiral dienophiles, ( $\underline{S}$ )<sub>S</sub>- and ( $\underline{R}$ )<sub>S</sub>-4.

**Acknowledgement** We are grateful to Dr. T. Komeno and Dr. M. Yoshioka of Shionogi Research Laboratory for a generous gift of showdomycin, and to Prof. G. Just of McGill University for the IR spectrum of ( $\pm$ )-3 for the identification. This work was supported by a grant from the Japan Research Foundation for Optically Active Compounds.

#### References and Notes

- 1) R. J. Suhadolnik, "Nucleoside Antibiotics"; Wiley-Interscience: New York, 1970, 354. G. D. Danes, Jr., C. C. Cheng, *Progr. Med. Chem.*, **13**, 303(1976).
- 2) A. O. Stewart and R. M. Williams, *J. Am. Chem. Soc.*, **107**, 4289(1985), and references cited therein.
- 3) T. Sato, Y. Hayakawa, and R. Noyori, *Bull. Chem. Soc. Jpn.*, **57**, 2515(1984), and references cited therein.
- 4) M. Ohno, Y. Itoh, M. Arita, T. Shibata, K. Adachi, and H. Sawai, *Tetrahedron*, **40**, 145(1984).
- 5) H. Takayama, A. Iyobe, and T. Koizumi, *J. Chem. Soc. Chem. Commun.*, **1986**, 771.
- 6) a) H. Nishimura, M. Mayama, Y. Komatsu, H. Kato, N. Shimaoka, and Y. Tanaka, *J. Antibiot.* **17A**, 148(1964); b) Y. Nakagawa, H. Kano, H. Tsukuda, and H. Koyama, *Tetrahedron Lett.*, **1967**, 4105.
- 7) a) G. Just and M. Ramjeesingh, *Tetrahedron Lett.*, **1975**, 985; b) G. Just, M. Ramjeesingh, and T. J. Liak, *Can. J. Chem.*, **54**, 2940(1976).
- 8) All new compounds reported here gave satisfactory spectroscopic and analytical data. Optical rotations were taken in CHCl<sub>3</sub> ( $\alpha$  0.95-1.01) unless otherwise noted. Some of the spectral data are listed below.
  - (6). IR(KBr) cm<sup>-1</sup>: 1740. NMR(CDCl<sub>3</sub>)  $\delta$ : 2.19(3H, s), 2.33(3H, s), 3.35(1H, dd, J=11.8, 5.6, C<sub>2</sub>-H), 3.75(1H, dd, J=11.8, 5.6, C<sub>3</sub>-H), 4.25(1H, d, J=5.6, C<sub>4</sub>-H), 4.59(2H, d, J=5.6, C<sub>1</sub>-&C<sub>5</sub>), 5.20(1H, d, J=5.6, C<sub>6</sub>-H).
  - (7). IR(KBr) cm<sup>-1</sup>: 1740, 1325. NMR(CDCl<sub>3</sub>)  $\delta$ : 3.30(1H, dd, J=11.6, 5.6, C<sub>2</sub>-H), 4.62(1H, dd, J=5.6, 1.0, C<sub>4</sub>-H), 4.83(1H, dd, J=5.6, 1.0, C<sub>1</sub>-H), 5.00(1H, d, J=5.6, C<sub>6</sub>-H), 5.01(1H, dd, J=11.6, 5.6, C<sub>3</sub>-H), 5.30(1H, d, J=5.6, C<sub>5</sub>-H).
  - (8). IR(KBr) cm<sup>-1</sup>: 3420, 3370. NMR(CDCl<sub>3</sub>)  $\delta$ : 2.90(1H, m, C<sub>2</sub>-H), 3.88(1H, m, C<sub>2</sub>-CHOH), 4.08(1H, dd, J=11.1, 5.6, C<sub>3</sub>-H), 4.33(1H, m, C<sub>2</sub>-CHOH), 4.58(1H, dd, J=5.4, 1.0, C<sub>1</sub>-H), 4.62(1H, broad-d, J=5.6, C<sub>4</sub>-H), 4.64(1H, d, J=5.4, C<sub>6</sub>-H), 5.31(1H, d, J=5.4, C<sub>5</sub>-H).
  - (9). IR(KBr) cm<sup>-1</sup>: 1735. NMR(CDCl<sub>3</sub>)  $\delta$ : 3.18(1H, d, J=5.5, C<sub>2</sub>-H), 3.63(3H, s, C<sub>2</sub>-COOMe), 4.36(1H, t, J=5.5, C<sub>3</sub>-H), 4.53(1H, d, J=5.4, C<sub>5</sub> or 6-H), 4.74(1H, s, C<sub>1</sub>-H), 4.88(1H, broad-d, J=5.4, C<sub>4</sub>-H), 5.25(1H, J, J=5.4, C<sub>5</sub> or 6-H).
  - (1). IR(KBr) cm<sup>-1</sup>: 1710, 1605. NMR(CDCl<sub>3</sub>)  $\delta$ : 1.34(3H, s), 1.52(3H, s), 3.78(3H, s), 4.41(1H, d, J=5.2, C<sub>5</sub>-H), 4.47(1H, d, J=5.2, C<sub>6</sub>-H), 4.93(1H, broad-s, C<sub>4</sub>-H), 5.03(1H, d, J=1.2, C<sub>1</sub>-H), 7.07(1H, d, J=2, C<sub>3</sub>-H).
- 9) The menthyl derivative of (1) was prepared by the DBU treatment of the sulfone (7). The O<sub>3</sub> oxidation of this compound followed by the metal hydride reduction [LiAlH(OtBu)<sub>3</sub>] did not yield the corresponding diol-ester. Furthermore, the conversion of the menthyl ester into the simple alkyl ester in cycloadduct (5), the sulfone (7), or the menthyl ester derivative of (1) did not give satisfactory results, under conditions in which the 7-oxabicyclo[2.2.1]heptane system was untouched. Therefore, the menthyl ester derivatives could not be used to prepare D-showdomycin.
- 10) In the nmr spectrum, ( $\pm$ )-(1) was resolved to a pair of doublets due to the olefinic proton at 7.46 and 7.40 ppm using a chiral shift reagent Eu(hfc)<sub>3</sub>. The spectrum of (+)-(1) showed the olefinic proton at 7.46 ppm and the corresponding enantiomer was not observed within the limit of detection (< 1 %).
- 11) G. Just, T. J. Liak, M. Lim, P. Potvin, and Y. S. Tsantrizos, *Can. J. Chem.*, **58**, 2024(1980).
- 12) G. Just, A. Martel, K. Grozinger, and M. Ramjeesingh, *Can. J. Chem.*, **53**, 131(1975).

(Received October 29, 1986)

## Communications to the Editor

[Chem. Pharm. Bull.]  
[35(1) 436-439 (1987)]

ENHANCEMENT OF IA-LIKE ANTIGEN EXPRESSION BY INTERFERON-GAMMA  
IN POLYMORPHONUCLEAR LEUKOCYTES

Shuu Matsumoto\*, Makiko Takei, Masami Moriyama and Hideyo Imanishi

Basic Research Laboratories, Toray Industries Inc.,  
Tebiro 1111, Kamakura 248, Japan

The effects of interferons (IFNs) on Ia-like antigen expression in human peripheral blood polymorphonuclear leukocytes (PMNs) were examined in vitro using flow cytometry and FITC-labelled monoclonal antibody specific for the Ia-like antigen OKIa1. Recombinant human IFN-gamma markedly enhanced the expression of Ia-like antigen on PMNs and increased the number of Ia-positive PMNs. In contrast, natural human IFN-alpha and -beta had no effect on the expression when compared on the basis of anti-viral activity.

KEYWORD       interferon; polymorphonuclear leukocytes; Ia-like antigen;  
flow cytometry

After Gray and coworkers first succeeded in cloning human interferon (IFN) genes in 1982,<sup>1)</sup> numerous studies using highly purified recombinant human IFN-gamma have shown the various immunomodulating activities of IFN-gamma.<sup>2)</sup> We have also demonstrated the several immunomodulating activities of recombinant human IFN-gamma (Met-Gln form), which has the same amino acid sequence as natural human IFN-gamma except that the N-terminal residue is Met. These activities include the enhancement of Ia-like antigen expression in human monocytes and the antibody-dependent cellular cytotoxic activity of human polymorphonuclear leukocytes (PMNs).<sup>3)</sup> Although there are many studies of IFN-gamma demonstrating its ability to augment the expression of HLA-DR or Ia-like antigen on various cells,<sup>4)</sup> there are no reports concerning the effect of IFN-gamma on the expression of the antigen on PMNs. Therefore, we examined the effect of IFN-gamma (Met-Gln form) on the expression of Ia-like antigen on the PMN surfaces in comparison with natural human IFN-alpha and -beta.

Human PMNs were prepared from peripheral blood of healthy volunteers by 1 x g gradient sedimentation and by one-step gradient centrifugation as described in our previous report.<sup>3b)</sup> The Ia-like antigen was analyzed by a method described previous-



ly.<sup>3a)</sup> In brief,  $1 \times 10^6$  PMNs, which were treated with IFN (1000 unit/ml) or control solution at 37°C for 20 h in a humidified atmosphere of 95% air-5% CO<sub>2</sub>, were labelled with FITC-OKIa1 (Ortho Diagnostic Systems). These labelled PMNs were analyzed by Cytofluorograf system 50H (Ortho Diagnostic Systems) or Spectrum III (Ortho Diagnostic Systems).

The histograms of PMNs treated with IFN and control solution and fresh PMNs obtained by flow cytometry using FITC-OKIa1 are shown in Fig. 1. IFN-gamma significantly enhanced the expression of Ia-like antigen on the PMN surfaces (Fig. 1E). IFN-gamma also significantly increased the number of Ia-positive PMNs compared with overnight control (Fig. 2). But IFN-alpha and -beta had no effect on either the expression (Fig. 1C & 1D) or the number (Fig. 2).

There are many reports of the expression of MHC class II (HLA-DR and Ia-like) antigen being enhanced by recombinant human IFN-gamma. Many kinds of cells are reported: monocytes,<sup>3a)5)</sup> melanoma cells,<sup>6)</sup> keratinocytes,<sup>7)8)</sup> melanocytes,<sup>6)8)</sup> dermal fibroblasts,<sup>9)</sup> vascular endothelial cells,<sup>9)10)</sup> epidermal langerhans cells,<sup>11)</sup> myeloid leukemic cells<sup>12)</sup> and brain cells.<sup>13)</sup> But there are no previous reports demonstrating IFN-gamma-induced enhancement of the antigen on PMNs. Our study has shown that IFN-gamma greatly increases the number of Ia-positive PMNs and enhances the expression of the antigen on PMNs (Fig. 1E and 2). We also found that IFN-alpha and -beta does not augment the expression when compared on the basis of antiviral

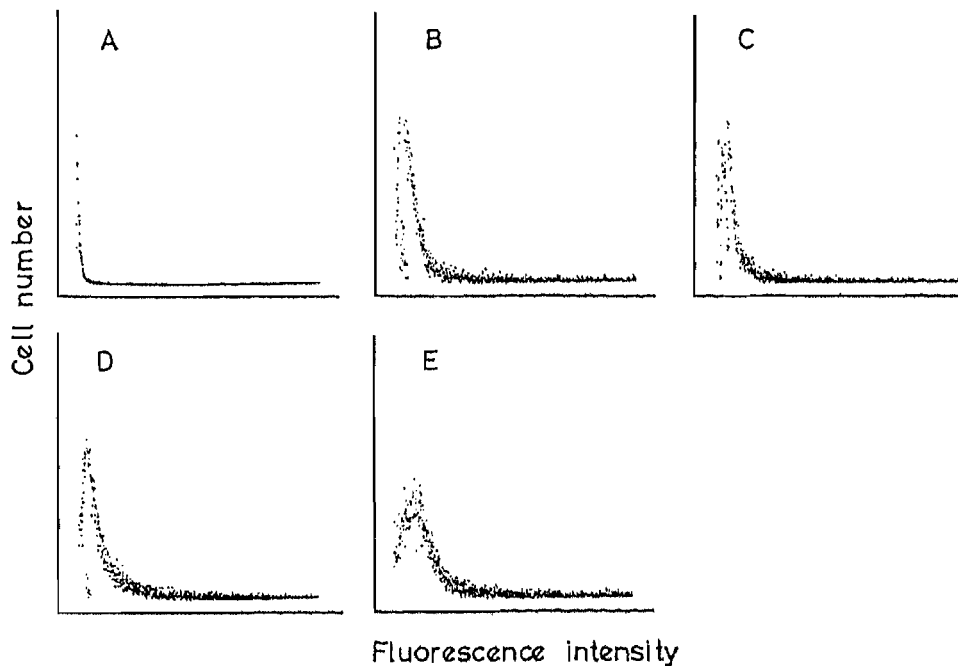


Fig. 1. Effects of IFNs on Ia-Like Antigen Expression in PMNs

A, fresh control; B, overnight control; C, IFN-alpha;  
D, IFN-beta; E, IFN-gamma.

These data were obtained from a single donor. Similar results were also obtained from two other donors (data not shown).

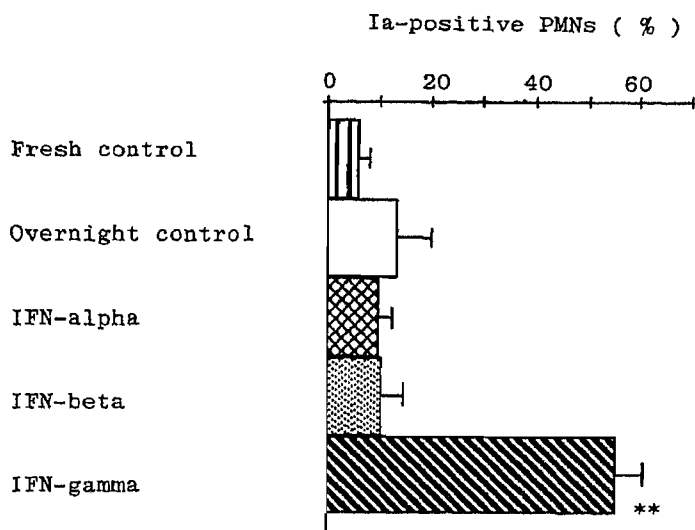


Fig. 2. Effects of IFNs on Percentage of Ia-positive PMNs in PMN Preparation

The results represent the mean  $\pm$  S.E. of three donors.  
 \*\* significant difference from control,  $p < 0.01$ .

activity (Fig. 1C, 1D and 2). This accords with our previous results indicating that IFN-alpha and -beta do not enhance the expression of Ia-like antigen on human monocytes.<sup>3a)</sup> Since it is well known that MHC class II antigens are involved in the presentation of antigens to helper T cells by antigen-presenting cells<sup>14)</sup> and it was shown that Ia-positive PMNs had antigen-presenting ability in mice,<sup>15)</sup> it appears that IFN-gamma may enhance the antigen presenting ability of human PMNs whereas IFN-alpha and -beta may not. However, the role of Ia-positive PMNs induced by IFN-gamma in the immune system is still unclear. To discern pharmacological significance of the PMN-modulating activity of IFN-gamma, further investigations are needed using animal IFN-gamma in animals.

**Acknowledgment** The authors thank Miss M. Kondoh and Mrs. K. Yamanaka for their skillful technical assistance. We are grateful to Dr. A. Kitai and Mr. N. Naruse for their encouragement and support of this study.

## REFERENCES

- 1) P.W. Gray, D.W. Leung, D. Pennica, E. Yelverton, R. Najarian, C.C. Simonsen, R. Derynck, P.J. Sherwood, D.M. Wallace, S.L. Berger, A.D. Levinson and D.V. Goeddel, *Nature(London)*, 295, 503 (1982).
- 2) G. Trinchieri and B. Perussia, *Immunology Today*, 6, 131 (1985).
- 3) a) S. Matsumoto, M. Moriyama and H. Imanishi, *Chem. Pharm. Bull.*, in press (1987).  
b) S. Matsumoto, M. Takei, M. Moriyama and H. Imanishi, *Chem. Pharm. Bull.*, in press (1987).
- 4) F. Rosa and M. Fellous, *Immunology Today*, 5, 261 (1984).
- 5) a) T.Y. Basham and T.C. Merigan, *J. Immunol.*, 130, 1492 (1983); b) T. Basham, W. Smith, L. Lanier, V. Morhenn and T. Merigan, *Human Immunology*, 10, 83 (1984); c) S. Becker, *J. Immunol.*, 132, 1249 (1984).
- 6) A.N. Houghton, T.M. Thomson, D. Gross, H.F. Oettgen and L.J. Old, *J. Exp. Med.*, 160, 255 (1984).
- 7) T.Y. Basham, B.J. Nickoloff, T.C. Merigan and V.B. Morhenn, *J. Invest. Dermatol.*, 83, 88 (1984).
- 8) J. Aubock, D. Niederwieser, N. Romani, P. Fritsch and C. Huber, *Arch. Dermatol. Res.*, 277, 270 (1985).
- 9) J.S. Pober, T. Collins, M.A. Gimbrone, R.S. Cotran, J.D. Gitlin, W. Fiers, C. Clayberger, A.M. Krensky, S.J. Burakoff and C.S. Reiss, *Nature(London)*, 305, 726 (1983).
- 10) J.S. Pober, M.A. Gimbrone, R.S. Cotran, C.S. Reiss, S.J. Burakoff, W. Fiers and K.A. Ault, *J. Exp. Med.*, 157, 1339 (1983).
- 11) B. Berman, M.R. Duncan, B. Smith, V.A. Ziboh and M. Palladino, *J. Invest. Dermatol.*, 84, 54 (1985).
- 12) V.E. Kelley, W. Fiers and T.B. Strom, *J. Immunol.*, 132, 240 (1984).
- 13) G.H.W. Wong, P.F. Bartlett, I. Clark-Lewis, J.L. McKimm-Breschkin and J.W. Scharader, *J. Neuroimmunol.*, 7, 255 (1985).
- 14) E. Thorsby, *Human Immunology*, 9, 1 (1983).
- 15) K. Okuda, B.C. Neely and C.S. David, *Transplantation*, 28, 354 (1979).

(Received November 11, 1986)

## Communications to the Editor

[Chem. Pharm. Bull.]  
35(1) 440-442 (1987)

STRUCTURE OF SAFRAMYCIN D, A NEW DIMERIC ISOQUINOLINEQUINONE  
ANTIBIOTIC

Akinori Kubo,<sup>\*,a</sup> Naoki Saito,<sup>a</sup> Yoshiyasu Kitahara,<sup>a</sup> Katsuhiro Takahashi,<sup>b</sup>  
Katsukiyo Yazawa,<sup>b</sup> and Tadashi Arai<sup>b</sup>

Meiji College of Pharmacy,<sup>a</sup> 1-35-23 Nozawa, Setagaya-ku, Tokyo 154, Japan  
and Department of Antibiotics, Research Institute for Chemobiodynamics,  
Chiba University,<sup>b</sup> 1-8-1 Inohana, Chiba 280, Japan

The structure of saframycin D (4), a new dimeric isoquinolinequinone antibiotic, is described.

**KEYWORDS** ——— dimeric isoquinolinequinone; *Streptomyces lavendulae*; <sup>1</sup>H-<sup>1</sup>H shift-correlated NMR; <sup>1</sup>H-<sup>13</sup>C shift-correlated NMR; homoallylic coupling

Saframycins<sup>1)</sup> are antitumor antibiotics produced by *Streptomyces lavendulae*. They constitute a class of the dimeric isoquinolinequinone antibiotic group, which includes safracins<sup>2)</sup> and renieramycins.<sup>3)</sup>

So far, we have isolated and characterized ten saframycins: A-H, R and S. Of these, saframycin A (1) has the highest antitumor activity against various experimental tumors.<sup>4)</sup> The structures of saframycins A (1) and B (2) were elucidated by comparing their spectroscopic data with those of saframycin C (3) whose structure has been determined by X-ray crystallography.<sup>5)</sup>

In this paper we describe the structure of saframycin D (4) determined by 400MHz NMR spectroscopy, which precluded our efforts to get suitable crystals for X-ray analysis.

Saframycin D (4), yellow prisms, mp 150-154°C (AcOEt),  $[\alpha]_D^{20} +141.1^\circ$  (c=1.0, MeOH), C<sub>28</sub>H<sub>31</sub>N<sub>3</sub>O<sub>9</sub>, gave the following spectral data: MS *m/z*: 553 (M<sup>+</sup>), 453, 236, 220; IR (CHCl<sub>3</sub>): 3560, 3400, 1720, 1685, 1660, 1630 cm<sup>-1</sup>; UV λ<sub>max</sub><sup>MeOH</sup> nm (log ε): 243 (4.14), 274 (4.24), 369 (3.75). The UV spectrum indicated that 4 has a chromophore different from the other saframycins [e.g., 2 λ<sub>max</sub><sup>MeOH</sup> nm (log ε): 269 (4.35), 368 (3.13)].

To establish the chromophore of 4, we first studied additivity. The UV spectrum of 4 agreed well with the additive curve for 5-ethyl-2-methoxy-3,6-dimethyl-1,4-benzoquinone and 2,5-dihydroxy-4-methoxy-3-methylbenzaldehyde.<sup>6)</sup>

Next, we reexamined the <sup>1</sup>H- and <sup>13</sup>C-NMR spectra of 2 by 2D NMR; the assignment of the <sup>1</sup>H- and <sup>13</sup>C-signals were made on the basis of the <sup>1</sup>H-<sup>1</sup>H and <sup>1</sup>H-<sup>13</sup>C

shift-correlated spectra (Tables I and II).

The  $^1\text{H}$ -NMR spectrum ( $\text{CDCl}_3$ ) of **4** (Table II) indicated the presence of six methyl groups: two aromatic methyls ( $\delta$  1.89 and 2.15), a carbonyl methyl ( $\delta$  2.26), an N-methyl ( $\delta$  2.43), and two aromatic methoxys ( $\delta$  3.93 and 4.02).

Also, the existence of three exchangeable protons due to an amide proton ( $\delta$  6.28) and two phenolic protons ( $\delta$  5.51 and 11.89) was confirmed.

The  $^{13}\text{C}$ -NMR spectrum ( $\text{CDCl}_3$ ) (Table I) indicated the presence of an amide carbonyl ( $\delta$  160.3), two quinone carbonyls ( $\delta$  181.2 and 186.1), and two carbonyls ( $\delta$  195.8 and 203.7), but the other two quinone carbonyls present in **2** ( $\delta$  181.5 and 185.8) were not observed. These data and the foregoing results indicated that **4** has the same carbon skeleton as **2** and contains paraquinone and hydroquinone moieties. Moreover, the absence of a  $^{13}\text{C}$ -signal corresponding to the C-14 methylene carbon ( $\delta$  22.8 in **2**) and the presence of a carbonyl carbon ( $\delta$  203.7) localized the carbonyl at the C-14 position in **2**. This conclusion was supported by the fact that the  $^{13}\text{C}$ -signal for C-13 ( $\delta$  65.5) in **4** is shifted -13 ppm downfield from the corresponding carbon ( $\delta$  52.3) in **2**.

The connectivity of each proton was assigned on the basis of double irradiation and selective proton decoupling experiments, and by the  $^1\text{H}$ - $^1\text{H}$  shift-correlated 2D NMR (Table II, Fig. 1).

We were especially interested in determining whether ring A is a paraquinone or a hydroquinone. In the  $^1\text{H}$ -NMR spectra of **2** and **4**, the diagnostic homoallylic coupling<sup>7)</sup> between 1-H and 4-Hb over five bonds was observed. But this homoallylic coupling is negligible in the spectra of several model compounds having a benzene moiety as the ring A.<sup>8)</sup> These observations unequivocally indicate that ring A of **4** is a paraquinone. The high-resolution MS spectrum also confirmed this conclusion.<sup>2,5)</sup> Thus, on the basis of these results, saframycin D can be represented by the formula **4**.

#### REFERENCES AND NOTES

- 1) T. Arai and A. Kubo, "The Alkaloids," Vol. 21, ed. by A. Brossi, Academic Press, Inc., New York, 1983, pp. 55-100; T. Arai, K. Yazawa, K. Takahashi, A. Maeda, and Y. Mikami, *Antimicrob. Agents Chemother.*, **28**, 5 (1985) and references therein.
- 2) Y. Ikeda, H. Matsuki, T. Ogawa, and T. Munakata, *J. Antibiot.*, **36**, 1284 (1983); R. Cooper and S. Unger, *J. Antibiot.*, **38**, 24 (1985).
- 3) J. M. Frincke and D. J. Faulkner, *J. Am. Chem. Soc.*, **104**, 265 (1982).
- 4) T. Arai, K. Takahashi, K. Ishiguro, and Y. Mikami, *Gann*, **71**, 790 (1980).
- 5) T. Arai, K. Takahashi, A. Kubo, S. Nakahara, S. Sato, K. Aiba, and C. Tamura, *Tetrahedron Lett.*, **1979**, 2355; T. Arai, K. Takahashi, S. Nakahara, and A. Kubo, *Experientia*, **36**, 1025 (1980).
- 6) A. Kubo and Y. Kitahara, unpublished results.
- 7) L. M. Jackmann and S. Sternhell, "Application of Nuclear Magnetic Resonance Spectroscopy in Organic Chemistry," 2nd ed., Pergamon Press, Inc., New York, 1969, pp. 316-328.
- 8) A. Kubo and N. Saito, unpublished results.

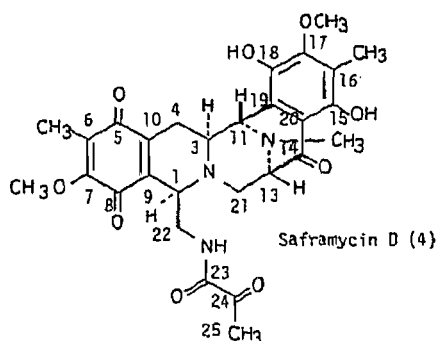
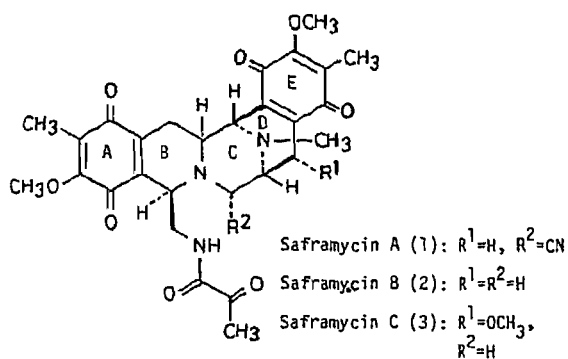


Table I.  $^{13}C$ -NMR Chemical Shifts and Assignments for Saframycin D (4) and Saframycin B (2)

Carbon No.	Saframycin D (4)	Saframycin B (2)	Assignment
5, 15	186.1	153.3	187.2 or 185.8
6, 16	127.5	118.7	129.4 or 128.4
7, 17	156.3	154.9	156.2 or 155.7
8, 18	181.2	139.4	183.0 or 181.5
9, 19	136.6	112.2	136.7 or 136.4
10, 20	141.8	118.2	142.9 or 141.8
C-CH <sub>3</sub>	8.9	8.6	8.9 8.6
O-CH <sub>3</sub>	61.2	61.0	61.1 61.0
N-CH <sub>3</sub>	42.4		41.3
1	57.6(d)		57.6(d)
3	57.0(d)		54.9(d)
4	24.5(t)		25.8(t)
11	57.4(d)		57.1(d)
13	65.5(d)		52.3(d)
14	203.7(s)		22.8(t)
21	54.8(t)		58.8(t)
22	40.8(t)		40.6(t)
23	160.3(s)		160.2(s)
24	195.8(s)		196.6(s)
25	24.3(q)		24.4(q)

Chemical shifts in ppm downfield from TMS.  
 Solvent:  $CDCl_3$ .

Table II. Proton Chemical Shifts<sup>a)</sup> and Coupling Constants<sup>b)</sup> for Saframycin D (4) and Saframycin B (2) in  $CDCl_3$

Proton	Saframycin D (4)	Saframycin B (2)
1-H	3.68 (4.0, 3.0, 1.5)	3.66 (4.2, 2.9, 1.3)
3-H	2.93 (11.0, 3.0, 3.0)	2.74 (10.7, 3.5, 2.4)
4-H <sub>a</sub>	2.96 (18.0, 3.0)	2.76 (16.7, 3.5)
4-H <sub>b</sub>	1.58 (18.0, 11.0, 3.0)	1.28 (16.7, 10.7, 2.9)
11-H	4.31 (3.0, 0.5)	4.03 (2.4, 0.5)
13-H	3.28 (3.0, 2.0, 0.5)	3.17 (7.3, 2.4, 2.0, 0.5)
14-H <sub>a</sub>	—	2.78 (18.1, 7.3)
14-H <sub>b</sub>	—	2.24 (18.1)
21-H <sub>a</sub>	2.93 (10.5, 2.0)	2.82 (10.7, 2.0)
21-H <sub>b</sub>	3.28 (10.5, 3.0)	2.98 (10.7, 2.4)
22-H <sub>a</sub>	3.71 (14.0, 9.0, 1.5)	3.70 (14.1, 9.8, 1.3)
22-H <sub>b</sub>	3.06 (14.0, 4.0, 3.0)	3.20 (14.1, 4.2, 3.5)
N-H	6.28 (9.0, 4.0)	6.90 (9.8, 3.5)
O-CH <sub>3</sub>	4.02, 3.93	4.01, 4.00
C-CH <sub>3</sub>	2.15, 1.89	2.00, 1.90
N-CH <sub>3</sub>	2.43	2.28
COCH <sub>3</sub>	2.26	2.24
O-H	11.89, 5.51	—

a) Chemical shifts are given relative to internal TMS as a reference.

b) Coupling constants (Hz) in parentheses.

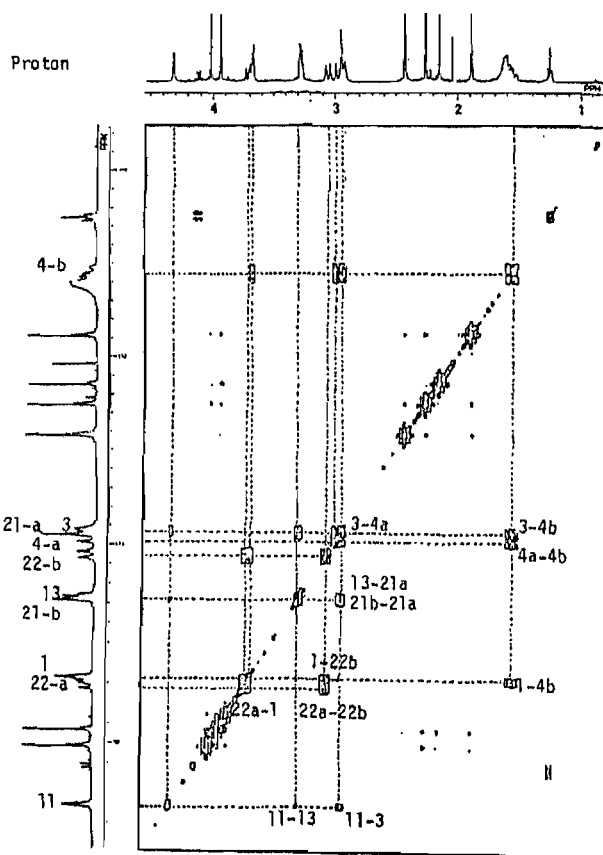
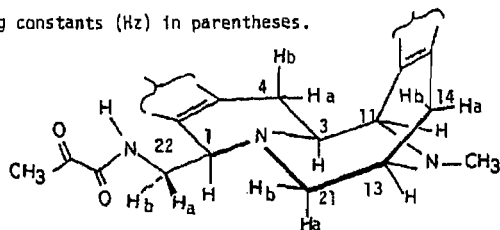


Fig.1 Contour Map of the  $^1H$ - $^1H$  Shift-Correlated Spectrum of Saframycin D (4)

(Received November 13, 1986)

## Communications to the Editor

[Chem. Pharm. Bull.]  
35(1) 443-446 (1987)

GUAVINS A, C AND D, COMPLEX TANNINS FROM PSIDIUM GUAJAVA

Takuo Okuda,<sup>\*,a</sup> Takashi Yoshida,<sup>a</sup> Tsutomu Hatano,<sup>a</sup> Kazufumi Yazaki,<sup>a</sup>  
Yukihiko Ikegami<sup>a</sup> and Tetsuro Shingu<sup>b</sup>

Faculty of Pharmaceutical Sciences, Okayama University,<sup>a</sup> Tsushima, Okayama 700,  
Japan and Faculty of Pharmaceutical Sciences, Kobe Gakuin University,<sup>b</sup>  
Ikawadani, Nishi-ku, Kobe 673, Japan

Three new tannins named guavins A (1), C (2) and D (3), were isolated from the leaves of Psidium guajava and their structures, each consisting of a hydrolyzable tannin part and a flavan unit, were established.

KEYWORDS — guavin A; guavin C; guavin D; complex tannin; hydrolyzable tannin; C-glucosidic tannin; ellagitannin; condensed tannin; Psidium guajava; Myrtaceae

In addition to the hydrolyzable tannins and the proanthocyanidins obtained from the leaves of Psidium guajava L. (Myrtaceae),<sup>1,2)</sup> we have isolated three tannins with novel structures, guavins A (1), C (2) and D (3). Each is composed of interlinked hydrolyzable tannin and a condensed tannin unit.

The new tannins were isolated from the ethyl acetate-soluble portion of the crude extract by centrifugal partition chromatography<sup>3)</sup> (n-butanol-n-propanol-water, 2:1:3, normal-phase development) and droplet countercurrent chromatography, followed by column chromatography over Sephadex LH-20 and Toyopearl HW-40.

Guavin A (1),  $C_{56}H_{40}O_{32} \cdot 9H_2O$ ,  $[\alpha]_D -36^\circ$  ( $c=0.5$ , MeOH), was obtained as a light brown amorphous powder. The  $^1H$ -NMR spectrum<sup>4)</sup> (400 MHz, in acetone- $d_6$ ) of 1 indicates the presence of a galloyl group ( $\delta 7.03$ , 2H, s) and a hexahydroxydiphenoyl (HHDP) group ( $\delta 6.65$ , 6.60, 1H each, s) in its molecule. As in stachyurin (4), a C-glucosidic tannin,<sup>5)</sup> an open-chain form of the glucose core appears in 1 ( $\delta 5.68$ , dd,  $J=4.5$ , 8.5 Hz, H-4; 5.57, broad d,  $J=8.5$  Hz, H-5; 5.44, s, H-2; 5.13, d,  $J=4.5$  Hz, H-3; 4.65, broad d,  $J=12.5$  Hz, H-6; 4.10, d,  $J=12.5$  Hz, H-6; 4.09, s, H-1) although the H-1 signal of 1 shifts higher than that of 4 ( $\delta 4.93$ ). The presence of a dehydrohexahydroxydiphenoyl (DHHDP) group is also shown by an aromatic proton at  $\delta 7.02$  (s) and a methine proton at  $\delta 4.37$  (s). These structural characteristics, together with the lack of a vinyl proton in the DHHDP group, are analogous to those of gemin E (5).<sup>6)</sup> There are also three aromatic protons forming an ABX system ( $\delta 6.94$ , d,  $J=2$  Hz, H-2'; 6.88, d,  $J=8$  Hz, H-5'; 6.74, dd,  $J=2$ , 8 Hz, H-6'), an aromatic proton ( $\delta 6.09$ , s, A-ring H), and four aliphatic protons attributable to a methine-methine-methylene system ( $\delta 5.09$ , d,  $J=6$  Hz, H-2; 4.45, dt,  $J=5.5$ , 6 Hz, H-3; 2.82, dd,  $J=5.5$ , 16 Hz, H-4; 2.72, dd,  $J=6$ , 16 Hz, H-4). These signals are characteristic of the 8-substituted (+)-catechin moiety, as in procyanidin B-1<sup>7)</sup> and procyanidin B-3 (6).<sup>7)</sup> The upfield shift of the H-1 signal of the glucose core in 1 can be explained by the absence of the hydroxyl group at C-1 of the glucose core and the presence of a C-C bond between C-1 of the glucose core and C-8 (or C-6) of the catechin moiety. The substitution at C-8<sup>7)</sup> is indicated by a significant

downfield shift of the H-2 signal of the catechin moiety in 1 from the corresponding signal of (+)-catechin ( $\delta 4.59 \rightarrow 5.09$ ). This may be due to the anisotropic effect of the conjugated carbonyl group in the DHHDP group. These structural features are also consistent with the  $^{13}\text{C-NMR}$  spectrum of 1.<sup>8,9)</sup> The equilibration between the five- and six-membered hemiacetal structures of the DHHDP group, as found in geraniin<sup>10)</sup> and other tannins having DHHDP groups,<sup>6,11)</sup> does not occur in the  $^{13}\text{C-NMR}$  spectrum of 1. The five-membered ring structure (C-1 - C-6 - O - C-6' - C-1') of the DHHDP group is indicated for 1, based on the comparison with the chemical shifts of the DHHDP carbons of geraniin.<sup>10)</sup>

The methylation of 1 with dimethyl sulfate and potassium carbonate afforded the hexadecamethyl derivative (7),  $\text{C}_{72}\text{H}_{72}\text{O}_{32}$ ,  $[\alpha]_{\text{D}} -59^\circ$  ( $c=0.5$ ,  $\text{CHCl}_3$ ), which was acetylated in the usual way to give a monoacetate (8),  $\text{C}_{74}\text{H}_{74}\text{O}_{33} \cdot \text{H}_2\text{O}$ ,  $[\alpha]_{\text{D}} -43^\circ$  ( $c=0.5$ ,  $\text{CHCl}_3$ ),  $^1\text{H-NMR}$  (in  $\text{CDCl}_3$ )  $\delta 1.88$  ( $\text{CH}_3\text{CO-}$ ). Upon methanolysis with sodium methoxide in methanol, 7 afforded (*S*)-dimethyl hexamethoxydiphenate (9),  $[\alpha]_{\text{D}} -32^\circ$  ( $c=0.5$ ,  $\text{EtOH}$ ), and methyl tri-*O*-methylgallate (10). Although glucose was not liberated by the methanolysis, it was detected upon hydrolysis of 1 with 1 N  $\text{H}_2\text{SO}_4$  in a boiling water-bath for 6.5 h, and identified by GLC after trimethylsilylation.

Hydrolysis of 1 with tannase afforded a partial hydrolysate (11).<sup>12)</sup> The  $^1\text{H-NMR}$  spectrum of 11 shows an absence of the HHDP protons and upfield shifts of the H-4 and H-6 signals of the glucose core characteristic of 1. This proves that the HHDP group of guavin A is at O-4 and O-6 of the glucose core. Thus, the locations of the other acyl groups in guavin A are assigned as in structure 1, considering the conformation of the glucose core of 1, which is almost the same as that of stachyurin (4) and gemin E (5).

The positive Cotton effect at 340 nm in the CD spectrum of 11<sup>12)</sup> indicates that the chirality at C-1' of the DHHDP group is *S*, although the expected Cotton effect around 200 nm, due to the chirality of the DHHDP group,<sup>13)</sup> is obscured by the presence of the catechin moiety in 11. The strong couplets at 200-220 nm in the CD spectra of procyanidins were reported to originate from the interaction between the two aryl chromophores of the two monomer units, and to be related to the chirality at C-4 on the interflavan linkage.<sup>14)</sup>

Since the configuration at C-1 of the glucose residue in 11 is the same as that of 4, as revealed by the coupling pattern ( $J_{1,2} \neq 0$ ) of H-1 of the residue in the  $^1\text{H-NMR}$  spectrum, the strong couplet around 205 nm in the CD spectrum of 11<sup>12)</sup> is attributable to an interaction between the conjugated ketone chromophore of the DHHDP group and the A-ring chromophore of the catechin moiety, occurring in a way analogous to the interaction observed for procyanidin B-3 (6) (Fig. 1). These data indicate structure 1 for guavin A, which is presumed to be produced biogenetically from gemin E (5) and (+)-catechin.

Guavin C (2),  $\text{C}_{56}\text{H}_{40}\text{O}_{33} \cdot 5\text{H}_2\text{O}$ ,  $[\alpha]_{\text{D}} -52^\circ$  ( $c=0.5$ ,  $\text{MeOH}$ ), was obtained as a light brown amorphous powder. The  $^1\text{H-NMR}$  spectrum of 2<sup>15)</sup> is similar to that of guavin A (1) except for the replacement of the ABX signals, due to the B-ring of the catechin moiety in 1, by a 2H singlet at  $\delta 6.42$ . Thus, structure 2 was assigned for guavin C, in which the catechol ring of the catechin moiety in 1 is substituted by a pyrogallol ring.

Guavin D (3),  $\text{C}_{51}\text{H}_{38}\text{O}_{29} \cdot 6\text{H}_2\text{O}$ ,  $[\alpha]_{\text{D}} -97^\circ$  ( $c=0.5$ ,  $\text{MeOH}$ ), was obtained as a light brown amorphous powder. The  $^1\text{H-NMR}$  spectrum (300 MHz, in acetone- $d_6+D_2O$ ) of 3 indicates the presence of a 8-substituted (-)-epicatechin moiety ( $\delta 6.65$ , d,  $J=2$  Hz, H-2'; 6.62, d,  $J=8$  Hz, H-5'; 6.49, dd,  $J=2, 8$  Hz, H-6'; 6.10, s, A-ring H; 5.36, broad s, H-2; 4.57, m, H-3; 2.81, d,  $J=17$  Hz, H-4; 2.43, dd,  $J=4, 17$  Hz, H-4), an acetyl group ( $\delta 2.08$ , 3H, s), an HHDP group ( $\delta 6.59, 6.53$ , each s), a 3'-substituted DHHDP group ( $\delta 7.07$ , s, H-3; 4.32, s, H-1') and a glucose core of the open-chain form

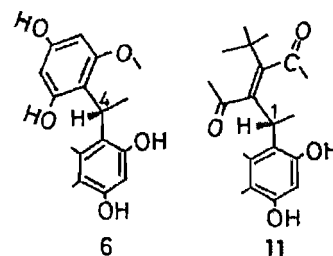
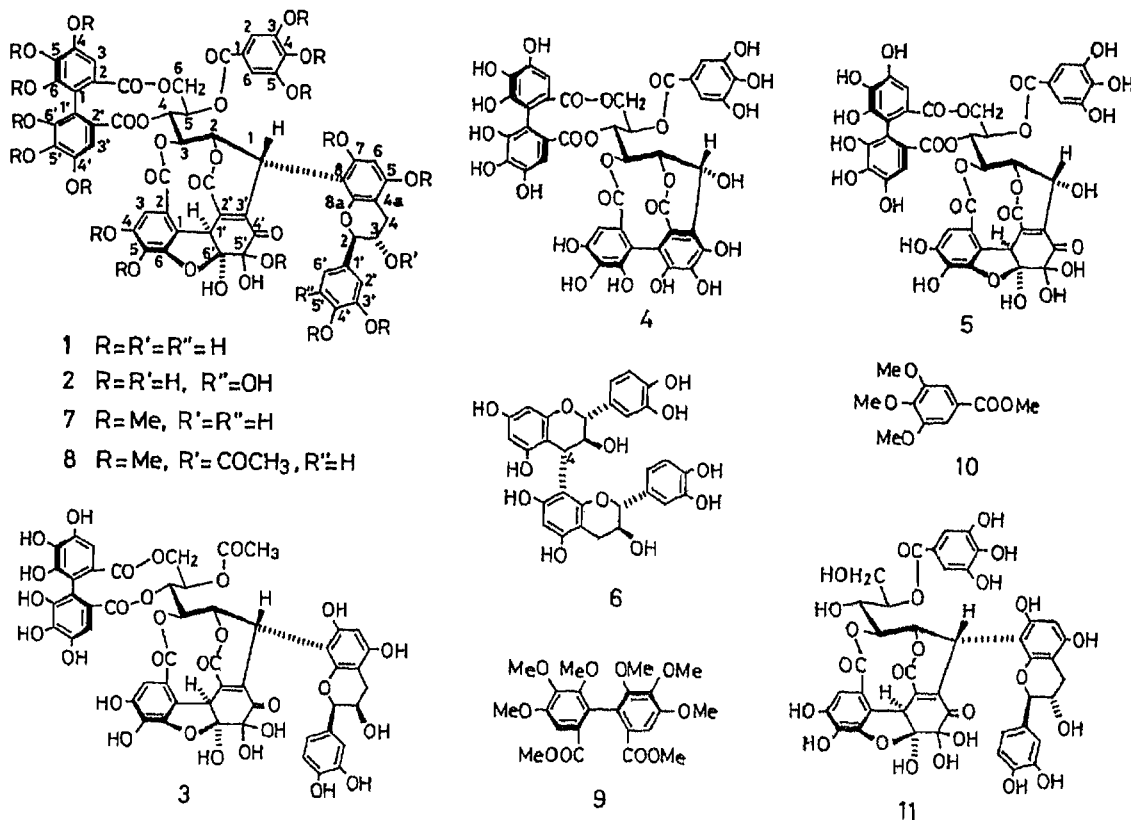


Fig. 1. Partial Structures of 6 and 11





( $\delta$ 5.77, s, H-2; 5.59, t,  $J=8$  Hz, H-4; 5.50, broad d,  $J=8$  Hz, H-5; 5.22, d,  $J=8$  Hz, H-3; 4.49, broad d,  $J=13$  Hz, H-6; 4.22, s, H-1; 4.00, d,  $J=13$  Hz, H-6). The substitution at C-8 of the epicatechin moiety is shown by the downfield shift of H-2 from the corresponding signal of (-)-epicatechin ( $\delta$ 4.84 $\rightarrow$ 5.36). The  $^{13}\text{C}$ -NMR spectrum of 3<sup>16)</sup> is also in accord with these construction units. This shows that the DHHDP group forms a five-membered hemiacetal ring.<sup>10)</sup> The  $\underline{S}$ -configuration of the HHDP group in 3 was evidenced by the production of ( $\underline{S}$ )-dimethyl hexamethoxydiphenate (9) upon the methanolysis of methylated 3. The CD spectrum (in MeOH) of 3 ( $[\theta]_{340} +14000$ ) shows that the configuration at C-1' of the DHHDP group is also  $\underline{S}$ . Therefore, structure 3 was assigned for guavin D.

The tannins such as guavins A, C and D, each consisting of a monomer of condensed tannin and a hydrolyzable tannin, can be classified as "complex tannins" as we proposed previously for guavin A.<sup>17)</sup>

**ACKNOWLEDGEMENTS** We thank Dr. Y. Takeda and Mr. K. Kida, Faculty of Pharmaceutical Sciences, Tokushima University, and Dr. K. Inoue, Faculty of Pharmaceutical Sciences, Kyoto University, for the 200 MHz  $^1\text{H}$ -NMR spectra.

#### REFERENCES AND NOTES

- 1) T. Okuda, T. Yoshida, T. Hatano, K. Yazaki and M. Ashida, *Phytochemistry*, **21**, 2871 (1982).
- 2) T. Okuda, T. Hatano and K. Yazaki, *Chem. Pharm. Bull.*, **32**, 3787 (1984).
- 3) T. Okuda, T. Yoshida, T. Hatano, K. Yazaki, R. Kira and Y. Ikeda, *J. Chromatogr.*, **362**, 375 (1986).
- 4) The assignments were based on the  $^1\text{H}$ - $^1\text{H}$  shift correlation spectrum.
- 5) T. Okuda, T. Yoshida, M. Ashida and K. Yazaki, *J. Chem. Soc., Perkin Trans. 1*, **1983**, 1765.

- 6) T. Yoshida, Y. Maruyama, M. U. Memon, T. Shingu and T. Okuda, *Phytochemistry*, **24**, 1041 (1985).
- 7) R. S. Thompson, D. Jacques, E. Haslam and R. J. N. Tanner, *J. Chem. Soc., Perkin Trans. 1*, **1972**, 1387.
- 8)  $^{13}\text{C}$ -NMR spectrum of 1 (in acetone- $d_6$ , 100 MHz):  $\delta$ 46.5 (Glu C-1), 49.5 (DHHDP C-1'), 64.4 (Glu C-6), 67.3 (Cat C-3), 71.2 (Glu C-4), 71.7 (Glu C-5), 75.8 (Glu C-3), 81.2 (Glu C-2), 81.6 (Cat C-2), 90.5 (DHHDP C-5'), 90.8 (Cat C-6), 102.2 (Cat C-4a), 104.9 (Cat C-8, DHHDP C-6'), 107.3, 109.0 (HHDP C-3,3'), 108.6 (DHHDP C-3), 110.3 (Gal C-2,6), 111.6 (DHHDP C-1), 114.4 (Cat C-2'), 115.3, 116.0 (HHDP C-1,1'), 116.4 (Cat C-5'), 120.6 (Cat C-6'), 121.0 (Gal C-1), 123.8 (DHHDP C-2), 125.4, 127.0 (HHDP C-2,2'), 131.1 (Cat C-1'), 135.9, 136.7, 137.3, 137.6 (HHDP C-5,5', DHHDP C-3',5), 139.3 (Gal C-4), 144.5, 144.6, 145.2, 145.3, 145.4, 145.6 (HHDP C-4,4',6,6', Cat C-3',4'), 145.7 (Gal C-3',5'), 146.2, 149.6 (DHHDP C-4,6), 151.9 (DHHDP C-2'), 158.3, 160.0 (Cat C-5,7,8a), 165.7, 165.8, 167.3, 168.1, 169.0 ( $-\text{COO}-$ ), 195.7 (DHHDP C-4') [Glu=glucose, Cat=catechin, Gal=galloyl].
- 9) The assignments were based on the  $^1\text{H}$ - $^{13}\text{C}$  shift correlation spectrum and the DEPT measurement, and on the comparison with the spectra of stachyurin (4),<sup>5)</sup> (+)-catechin and geraniin.<sup>10)</sup>
- 10) T. Okuda, T. Yoshida and T. Hatano, *J. Chem. Soc., Perkin Trans. 1*, **1982**, 9.
- 11) a) T. Okuda, T. Hatano, H. Nitta and R. Fujii, *Tetrahedron Lett.*, **21**, 4361 (1980). b) T. Okuda and K. Seno, *Nippon Kagaku Kaishi*, **1981**, 671. c) T. Okuda, T. Hatano and K. Yazaki, *Chem. Pharm. Bull.*, **30**, 1113 (1982).
- 12) CD spectrum of 11 (in MeOH):  $[\theta]_{200} +133000$ ,  $[\theta]_{212} -98000$ ,  $[\theta]_{238} -128000$ ,  $[\theta]_{290} -38000$ ,  $[\theta]_{340} +11500$ .  $^1\text{H}$ -NMR spectrum (400 MHz, in acetone- $d_6$ ):  $\delta$ 7.09 (2H, s, Gal H-2,6), 6.90 (d, J=2 Hz, Cat H-2'), 6.70 (s, DHHDP H-3), 6.67 (d, J=8 Hz, Cat H-5'), 6.64 (dd, J=2,8 Hz, Cat H-6'), 6.11 (s, Cat H-6), 5.56 (s, Glu H-2), 5.01 (d, J=9 Hz, Cat H-2), 4.74 (d, J=8 Hz, Glu H-3), 4.63 (broad t, J=5.5 Hz, Glu H-5), 4.31 (s, DHHDP H-1'), 4.10 (broad d, J=8 Hz, Glu H-4), 4.01 (dt, J=5.5, 9 Hz, Cat H-3), 3.98 (s, Glu H-1), 3.70 (dd, J=6, 12 Hz, Glu H-6), 3.49 (dd, J=5, 12 Hz, Glu H-6), 3.02 (dd, J=5.5, 16 Hz, Cat H-4), 2.60 (dd, J=9, 16 Hz, Cat H-4).
- 13) T. Okuda, T. Yoshida, T. Hatano, T. Koga, N. Toh and K. Kuriyama, *Tetrahedron Lett.*, **23**, 3941 (1982).
- 14) M. W. Barrett, W. Klyne, P. M. Scopes, A. C. Fletcher, L. J. Porter and E. Haslam, *J. Chem. Soc., Perkin Trans. 1*, **1979**, 2375.
- 15)  $^1\text{H}$ -NMR spectrum of 2 (200 MHz, in acetone- $d_6$ ):  $\delta$ 7.04 (2H, s, Gal), 7.03 (s, DHHDP H-3'), 6.58, 6.51 (each s, HHDP H-3,3'), 6.42 (2H, s, Gct H-2',6'), 6.07 (s, Gct H-6), 5.82 (dd, J=5.5, 8 Hz, Glu H-4), 5.68 (broad d, J=8 Hz, Glu H-5), 5.38 (s, Glu H-2), 5.24 (d, J=4.5 Hz, Gct H-2), 5.17 (d, J=5.5 Hz, Glu H-3), 4.54 (broad d, J=13 Hz, Glu H-6), 4.41 (m, Gct H-3), 4.34 (s, DHHDP H-1'), 4.12 (d, J=13 Hz, Glu H-6), 4.08 (s, Glu H-1), 2.76 (dd, J=4, 16 Hz, Gct H-4), 2.71 (dd, J=4.5, 16 Hz, Gct H-4) [Gct=gallocatechin].
- 16)  $^{13}\text{C}$ -NMR spectrum of 3 (75 MHz, in acetone- $d_6$ ):  $\delta$ 22.8 ( $\text{CH}_3\text{CO}-$ ), 46.3 (Glu C-1), 49.1 (DHHDP C-1'), 63.6 (Glu C-6), 65.8 (EC C-3), 67.2, 69.8, 71.2 (Glu C-3,4,5), 76.4 (Glu C-2), 78.5 (EC C-2), 88.1, 89.2 (EC C-6, DHHDP C-5'), 99.4 (EC C-4a), 102.5 (EC C-8), 105.3, 106.2, 106.5 (HHDP C-3,3', DHHDP C-3,6'), 111.6 (DHHDP C-1), 113.4, 114.6, 116.0 (EC C-2',5', HHDP C-1,1'), 122.9, 123.4, 125.6, 125.7 (EC C-6', HHDP C-2,2', DHHDP C-2), 129.3 (EC C-1'), 134.1, 134.3, 135.5, 138.5 (HHDP C-5,5', DHHDP C-3',5), 142.3, 143.0, 143.3, 143.4, 143.7, 143.8 (EC C-3',4, HHDP C-4,4',6,6'), 144.3, 147.5 (DHHDP C-4,6), 150.2 (DHHDP C-2'), 157.2, 158.8 (EC C-5,7,8a), 162.0, 165.2, 165.4, 166.2, 167.7 ( $-\text{COO}-$ ), 195.2 (DHHDP C-4') [EC=epicatechin].
- 17) T. Okuda, T. Hatano and K. Yazaki, The 103rd Annual Meeting of Pharmaceutical Society of Japan, Tokyo, April 1983.

(Received November 17, 1986)

---

**Communications to the Editor**

---

[Chem. Pharm. Bull.]  
35(1) 447-449 (1987)

**A FACILE ONE-STEP SYNTHESIS OF PHOSPHATIDYLHOMOSERINES  
BY PHOSPHOLIPASE D-CATALYZED TRANSPHOSPHATIDYLATION**

Satoshi Shuto<sup>\*</sup>, Sigeyuki Imamura, Kiyofumi Fukukawa,  
Hideo Sakakibara, and Jun-ichi Murase

Research Laboratories, Toyo Jozo Co., Ltd, 632-1, Mifuku,  
Ohito-cho, Tagata-gun, Shizuoka 410-23, Japan

Phospholipase D from *Streptomyces* effectively catalyzed the transfer reaction of the phosphatidyl residue from phosphatidylcholines to the primary hydroxyl group of homoserine in a two-phase system. Various phosphatidylhomoserines were easily prepared in good yields by this reaction.

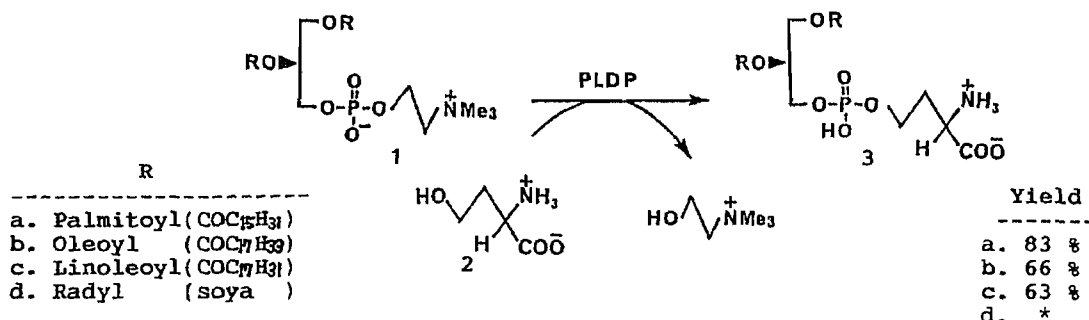
**KEYWORDS** — transphosphatidylation; phospholipase D; phosphatidylserine; phosphatidylhomoserine; phosphatidylcholine; two-phase reaction; enzymatic synthesis

It has been recognized that phosphatidylserines have various biological activities,<sup>1</sup> and have important roles in studies of model membrane systems.<sup>2</sup> We have been engaged in the synthesis of phosphatidylhomoserines, homologues of phosphatidylserines, because of their biological interest. This paper describes the first synthesis of phosphatidylhomoserines.

The procedure for synthesizing phosphatidylserine may be applied to the synthesis of phosphatidylhomoserines in general. Although phosphatidylserines have been prepared by a variety of methods,<sup>3</sup> an efficient general procedure for the chemical synthesis of saturated and unsaturated phosphatidylserines has not been reported. In particular, the preparation of unsaturated phosphatidylserines is difficult because of their lability.

On the other hand, Confurius and co-workers reported an enzymatic method<sup>4</sup> of preparing saturated and unsaturated phosphatidylserines in 40-50% yields. This method involves cabbage phospholipase D-catalyzed transphosphatidylation,<sup>5</sup> the transfer reaction of the phosphatidyl residue from phosphatidylcholine to primary alkanols. More recently we found that phospholipase D from *Streptomyces* sp. AA 586 (phospholipase D-P, PLDP) also effectively catalyzes the transphosphatidylation, and we have used PLDP to prepare a variety of 5'-phosphatidylnucleosides.<sup>6</sup> In the cabbage phospholipase D-catalyzed transphosphatidylation, acceptors of the phosphatidyl residue are limited to primary lower alkanols.<sup>5</sup> But PLDP catalyzes the transfer reaction of the phosphatidyl residue to a variety of alkanols as acceptors.<sup>7</sup> In addition, PLDP is very stable under the conditions of transphosphatidy-

lation. So it affords phosphatidyl derivatives in higher yields than phospholipase D from cabbage leaves. Therefore we tried to utilize PLDP as a catalyst of transphosphatidylation to prepare phosphatidylhomoserines.



\* From 500 mg of soya-phosphatidylcholine, 305 mg of corresponding phosphatidylhomoserine was obtained.

In the presence of an excess L-homoserine (2), 1,2-dipalmitoyl-*sn*-glycero-3-phosphocholine (DPPC, 1a)<sup>8</sup> was treated with PLDP in a two-phase system of chloroform and acetate buffer (pH 5.6) at 45°C for 2 h. This gave desired 3-*sn*-phosphatidylhomoserine (3a) in 83% yield.<sup>9</sup> In the same reaction condition, cabbage phospholipase D gave only a trace of 3a and mostly the hydrolysis product. In the same way, various 3-*sn*-phosphatidylhomoserines were easily obtained in high yields by the PLDP-catalyzed transphosphatidylation with corresponding 3-*sn*-phosphatidylcholines as phosphatidyl donors. Structures of the compounds were confirmed by instrumental analysis.

In this enzymatic reaction system, phosphatidylcholine and L-homoserine are dissolved in the organic layer and the aqueous layer, respectively, PLDP probably catalyzes the transfer reaction at the interface. The presence of the chloroform layer and an excess of L-homoserine as an acceptor of the phosphatidyl residue is required to allow the transphosphatidylation to proceed and to prevent the hydrolysis of the phosphatidylcholines. This is because phospholipase D catalyzes the hydrolysis better than the transfer reaction. Unreacting L-homoserine can be easily recovered if necessary. Chloroform is a good solvent for phosphatidylcholines and may also protect the phosphatidyl-enzyme, the reaction intermediate, from hydrolysis. When the chloroform layer is absent, the rate of the transfer reaction decreases and the hydrolysis rate increases.

The general usefulness of transphosphatidylation to synthesize phospholipid derivatives depends upon the range of alkanols accepted; PLDP catalyzes transphosphatidylation with a large variety of alkanols as phosphatidyl acceptors.<sup>7</sup> Furthermore, PLDP is reliably stable in reaction systems containing various organic solvents such as chloroform, benzene, diethylether, acetonitrile, etc. So, this method can be widely used to synthesize various types of phospholipid derivatives containing a complicated structural polar-head group.

**A typical procedure:** L-homoserine (15 mmol) and PLDP (5 mg, 910 units) are dissolved in 100 mM CaCl<sub>2</sub>-containing 100 mM acetate buffer (pH 5.6, 5 ml). A CHCl<sub>3</sub> solution (12 ml) of phosphatidylcholine (0.5 mmol) is then added and the mixture is stirred at 45°C. After 2 h, 2 N HCl (5 ml), CHCl<sub>3</sub> (28 ml), and MeOH

(20 ml) are added. Unreacting L-homoserine is recovered from the aqueous layer. The organic layer is evaporated and the residue is chromatographed on silica gel ( $\text{CHCl}_3$  : MeOH = 15 : 1  $\rightarrow$  1 : 1). This is followed by partition ( $\text{CHCl}_3$  : MeOH : 0.5N HCl = 20 ml : 10 ml : 6 ml) to afford the pure product from the organic layer.

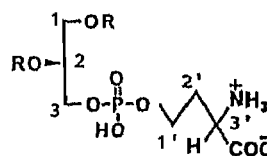
**Acknowledgements** The authors wish to thank Professors T. Ueda (Hokkaido University) and T. Takano (Teikyo University) for their helpful advice and encouragement throughout this work.

#### References and Notes

1. For example see; a) D.L.Turner, M.J.Silver, E.Baczynski, R.R.Holburn, S.F.Herb, and F.E.Luddy, *Lipids*, 5, 650 (1970). b) T.W.Martin, and D.Lagunoff, *Biochemistry*, 19, 3106 (1980). c) R.Takeuchi, T.Imanaka, S.Ohkuma, and T.Takano, *J.Biochem.*, 98, 933 (1985).
2. For example see; P.A.Cuyppers, J.W.Corsel, M.P.Janssen, J.M.M.Kop, W.T.Hermens, and H.C.Hemker, *J.Biol.Chem.*, 258, 2426 (1983).
3. A.Hermetter, F.Paltauf, and H.Hauser, *Chem.Phys.Lipids*, 30, 35 (1982) and references cited therein.
4. P.Confurius and R.F.A.Zwaal, *Biochim.Biophys.Acta*, 488, 36 (1977).
5. S.Kovatchev and H.Eibl, *Adv.Exp.Med.Bio.*, 101, 221 (1978) and references cited therein.
6. S.Shuto, S.Ueda, S.Imamura, K.Fukukawa, A.Matsuda, and T.Ueda, *Tetrahedron Lett.*, in press.
7. In preliminary experiments, the following alkanols were acted as acceptors of the phosphatidyl residue; methanol, 1-butanol, 1-hexanol, 2-chloroethanol, hydroxyacetic acid, 2-hydroxypropionic acid, D-glucose, D-galactose, D-ribose, L-serine, adenosine, uridine, 2'-deoxycytidine, thymidine, and others.
8. H.Van Den Bosh, L.M.G.Van Golde, H.Eibl and L.L.M.Van Deenen, *Biochim.Biophys. Acta*, 144, 613 (1967).
9. The physical constants of 3a: mp 170-172° C.  
*Anal.* Calcd for  $\text{C}_{39}\text{H}_{76}\text{N}_1\text{O}_{10}\text{P}_1 \cdot 2/3\text{H}_2\text{O}$ : C; 61.47, H; 10.23, N; 1.84.  
 Found: C; 61.50, H; 10.23, N; 1.82.  $^1\text{H-NMR}^*$  (400 MHz,  $\text{CDCl}_3$ : $\text{CD}_3\text{OD}$ =3:1);  $\delta$  ppm, 5.23(m, 1H, H-2), 4.40(dd, 1H, H-1a,  $J=3.3\text{Hz}$ ,  $J=12.1\text{Hz}$ ), 4.19(dd, 1H, H-1b,  $J=6.6\text{Hz}$ ,  $J=12.1\text{Hz}$ ), 4.06-3.99(m, 5H, H-3ab, H-1'ab, and H-3'), 2.40(m, 1H, H-2'a), 2.32(q, 4H,  $2 \times \text{CH}_2\text{COO}^-$ ), 2.08(m, 1H, H-2'b), 1.60(broad, 4H,  $2 \times \text{CH}_2\text{CH}_2\text{COO}^-$ ), 1.27(s, 48H,  $24 \times \text{CH}_2$ ), 0.89(t, 6H,  $2 \times \text{CH}_3$ ).

IR (KBr,  $\text{cm}^{-1}$ ): 1730 ( $\nu_{\text{C=O}}$ ), 1615 ( $\delta_{\text{NH}}$ ), 1215 ( $\nu_{\text{P=O}}$ ), 1050 ( $\nu_{\text{P-O-C}}$ ).

\* Phosphatidylhomoserines were numbered as follows:



(Received November 20, 1986)

## Communications to the Editor

[Chem. Pharm. Bull.]  
35(1) 450-452 (1987)

THREE NEW CARBAZOLE ALKALOIDS FROM MURRAYA EUCHRESTIFOLIA

Chihiro Ito,<sup>a</sup> Tian-Shung Wu,<sup>b</sup> and Hiroshi Furukawa<sup>\*,a</sup>  
Faculty of Pharmacy, Meijo University,<sup>a</sup> Tempaku, Nagoya 468, Japan;  
Department of Applied Chemistry, Providence College of Arts and  
Science,<sup>b</sup> Taichung 400, Taiwan, R. O. C.

The structures of a monomeric carbazole, isomurrayafoline-B (1), and two new dimeric carbazoles, bismurrayafolinol (3) and oxydimurrayafoline (9), from Murraya euchrestifolia Hayata (Rutaceae) have been studied in spectral and chemical experiments.

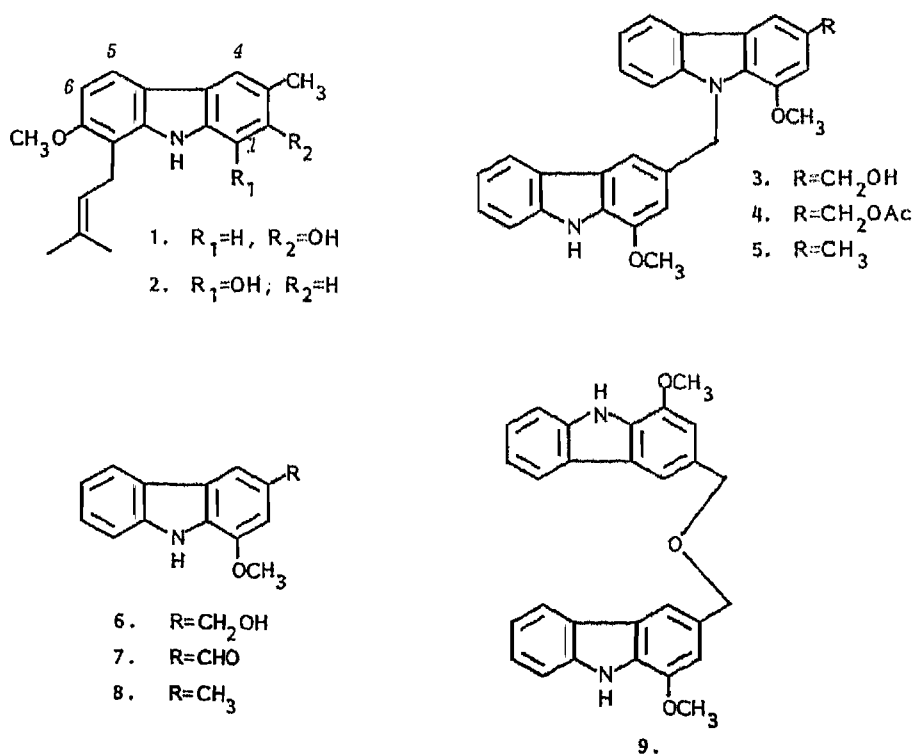
KEYWORDS—isomurrayafoline-B; bismurrayafolinol; oxydimurrayafoline; carbazole alkaloid; dimeric carbazole; Murraya euchrestifolia; Rutaceae

We reported earlier that the root bark of Murraya euchrestifolia Hayata (Rutaceae), collected in Taiwan, contained many kinds of monomeric and dimeric carbazole alkaloids.<sup>1-5</sup> Here, we describe the isolation and structure determination of three more new carbazole alkaloids from the stem bark of that plant.

Isomurrayafoline (1) was obtained as colorless prisms from ether, mp 158-161°C. The high resolution mass spectrum gave the molecular formula C<sub>19</sub>H<sub>21</sub>NO<sub>2</sub> [m/z 295.1567 (M<sup>+</sup> found); 295.1571, calcd]. The UV spectrum was typical of a carbazole nucleus<sup>6,7</sup> [ $\lambda_{\max}$  nm (MeOH): 213, 237, 264, 310, and 330 (sh.)]. The <sup>1</sup>H-NMR spectrum (400 MHz, CDCl<sub>3</sub>) showed the presence of a prenyl [ $\delta$  1.74 (3H, s), 1.88 (3H, s), 3.60 (2H, d, J = 7 Hz), and 5.30 (1H, t, J = 7 Hz)], a methoxy [ $\delta$  3.90 (3H, s)], an aryl methyl group [ $\delta$  2.38 (3H, s)], and two D<sub>2</sub>O exchangeable protons [ $\delta$  4.74 (1H, br s, OH) and 7.70 (1H, br s, NH)]. In aromatic proton signals [ $\delta$  7.70 and 6.82 (each 1H, a pair of doublets, J = 8 Hz), 7.67 (1H, s), and 6.82 (1H, s)], lower-field signals at  $\delta$  7.70 and 7.67 are well known as being characteristic of H-5 and H-4 of a carbazole nucleus,<sup>8</sup> respectively, thus suggesting the location of substituents at C-1 (or 2), 3, 7, and C-8. In nuclear Overhauser effect (NOE) experiments, irradiation of the aryl methyl proton ( $\delta$  2.38) gave a 12.6% enhancement only of the signal at  $\delta$  7.67 (H-4). Further, a 26.6% enhancement of the signal at  $\delta$  6.82 (H-6) appeared on irradiation of the methoxy signal ( $\delta$  3.90), but there was no NOE enhancement at any proton signal on irradiation of the benzylic methylene proton of a prenyl moiety ( $\delta$  3.60). According to these observations, isomurrayafoline-B can be represented by structure 1. The structural isomer, murrayafoline-B (2),<sup>1</sup> has been isolated from the root bark of the same plant.

Bismurrayafolinol (3), colorless oil, was found to have the molecular formula  $C_{28}H_{24}N_2O_3$  [ $m/z$  436.1784 ( $M^+$  found); 436.1785, calcd]. The presence of a carbazole skeleton in the molecule was also clearly indicated by the UV spectrum<sup>6,7)</sup> [ $\lambda_{max}$  nm (MeOH): 225, 244, 252, 281, 292, 329, and 340]. The mass spectrum exhibited a base peak at  $m/z$  210 due to about a half of the molecule, strongly suggesting a dimeric carbazole structure of bismurrayafolinol. The  $^1H$ -NMR spectrum (270 MHz,  $CDCl_3$ ) showed the presence of two methoxy groups ( $\delta$  3.83 and 3.97), and in the aromatic proton region, there were two 1H-singlets at  $\delta$  6.78 and 7.00 assignable to H-2 and H-2', lower-field signals at  $\delta$  7.92 and 8.07 (each 1H, d,  $J = 8$  Hz), and 7.74 (1H, s), characteristic of H-5, 5', and H-4 in the carbazole nucleus,<sup>8)</sup> along with overlapped 7H-signals from  $\delta$  7.10 to 7.50. Additionally, an appearance of two 2H-singlets at  $\delta$  6.01 and 4.86, which appeared at  $\delta$  6.01 and 5.27 in the acetate (4)<sup>9)</sup> indicated the presence of two benzylic methylenes directly bonded to a nitrogen and oxygen atom, respectively. These signal patterns in the  $^1H$ -NMR spectrum of bismurrayafolinol were in close agreement with those of bismurrayafoline-A (5),<sup>3)</sup> a dimeric carbazole alkaloid previously isolated by us, except for an oxybenzylic methylene signal appearing at  $\delta$  4.86 instead of an aryl methyl signal at  $\delta$  2.46 in the spectrum<sup>3)</sup> of 5. On the basis of these spectral results, the structure of bismurrayafolinol was proposed for 3.

In order to confirm the structure of this alkaloid, dimerization of 1-methoxy-3-oxymethylcarbazole (6) was carried out. Treatment of murrayanine (7),<sup>10,11)</sup> an already known alkaloid in the same plant,<sup>1)</sup> with  $NaBH_4$  in MeOH, followed by HCl in  $CHCl_3$  for 5 min.,<sup>12)</sup> and then, without purification, by  $Ac_2O$  in pyridine gave 4, which was identical ( $^1H$ -NMR, IR, UV, MS, and co-TLC) with the acetate of natural bismurrayafolinol (3). Consequently, the structure of bismurrayafolinol was established as formula 3.



Oxydimurrayafoline (9), colorless oil,  $C_{28}H_{24}N_2O_3$  [ $m/z$  436.1809 ( $M^+$  found); 436.1785, calcd], UV  $\lambda_{max}$  nm (MeOH): 226, 242, 253, 260, 280, 291, 324, and 337;  $^1H$ -NMR (270 MHz,  $CDCl_3$ )  $\delta$ : 8.27 (2H, br s, NH), 8.03 (2H, dd,  $J = 7$  & 1 Hz), 7.68 (2H, d,  $J = 1$  Hz), 7.46 (2H, d,  $J = 7$  Hz), 7.40 (2H, dt,  $J = 7$  & 1 Hz), 7.22 (2H, dt,  $J = 7$  & 1 Hz), 6.98 (2H, d,  $J = 1$  Hz), 4.76 (4H, s), and 4.01 (6H, s). The simplicity of the  $^1H$ -NMR spectrum and the presence of the base peak at  $m/z$  211, about a half of the molecule ion in the mass spectrum together with the UV bands suggested that two equivalent monomeric carbazole units were disposed in symmetrical manner in this alkaloid. Furthermore, the signal patterns of the  $^1H$ -NMR spectrum were similar to those of murrayafoline-A (8),<sup>1)</sup> except for the singlet at  $\delta$  4.76 and 2.42 in the spectra of oxydimurrayafoline and 8, respectively. An appearance of a singlet at  $\delta$  4.76, instead of an aryl methyl signal at  $\delta$  2.42 in the spectrum of 8 showed the presence of benzylic oxymethylene moiety. In NOE experiments, an 18.9% enhancement of the singlet at  $\delta$  6.98 (H-2) appeared on irradiation of the methoxy signal at  $\delta$  4.01. As expected, irradiation of the benzylic methylene signal at  $\delta$  4.76 caused a 19.4% and 11.8% enhancements of the aromatic proton signals at  $\delta$  7.68 (H-4) and 6.98 (H-2), respectively. Based on these results, we assigned structure 9 to oxydimurrayafoline. Since our first isolation of binary carbazole alkaloids from the plant of the genus Murraya,<sup>2)</sup> seven kinds of binary carbazole alkaloids have been identified to date.<sup>2,3,5,13)</sup> However, isolation of oxydimurrayafoline (9) is the first example of a binary carbazole alkaloid having ether linkage.

**ACKNOWLEDGEMENT** We thank Dr. H. Tanino and Mr. K. Masuda of Meijo University for NOE experiments and measurements of high resolution mass spectra, respectively.

#### REFERENCES AND NOTES

- 1) H. Furukawa, T.-S. Wu, T. Ohta, and C.-S. Kuoh, Chem. Pharm. Bull., **33**, 4132 (1985).
- 2) A. T. McPhail, T.-S. Wu, T. Ohta, and H. Furukawa, Tetrahedron Letts., **24**, 5377 (1983).
- 3) H. Furukawa, T.-S. Wu, and T. Ohta, Chem. Pharm. Bull., **31**, 4202 (1983).
- 4) H. Furukawa, M. Yogo, C. Ito, T.-S. Wu, and C.-S. Kuoh, Chem. Pharm. Bull., **33**, 320 (1985).
- 5) H. Furukawa, T.-S. Wu, and C.-S. Kuoh, Chem. Pharm. Bull., **33**, 2611 (1985).
- 6) W. Otting and G. Staiger, Chem. Ber., **88**, 828 (1955).
- 7) H. J. Tuber and G. Staiger, Chem. Ber., **89**, 489 (1956).
- 8) D. P. Chakraborty, "Fortschritte d. Chem. Org. Naturst.," Vol. 34, ed. by W. Herz, H. Grisebach, and G. W. Kirby, Springer-Verlag, New York, 1977, p. 299.
- 9)  $^1H$ -NMR (270 MHz,  $CDCl_3$ ):  $\delta$  2.13 (3H, s), 3.84 (3H, s), 3.96 (3H, s), 5.27 (2H, s), 6.01 (2H, s), 6.78 (1H, s), 6.96 (1H, s), 7.10-7.50 (7H, overlapped), 7.76 (1H, s), 7.92 (1H, d,  $J = 8$  Hz), 8.07 (1H, d,  $J = 8$  Hz), and 8.16 (1H, br. s, exchangable with  $D_2O$ ); IR  $\nu_{max}$  ( $CHCl_3$ ): 1740  $cm^{-1}$ ; MS  $m/z$ : 478 ( $M^+$ ), 269, 226, 211, 210 (base peak), 195, and 167; UV  $\lambda_{max}$  nm (MeOH): 226, 243, 252, 261(sh.), 281, 292, 330, and 342.
- 10) D. P. Chakraborty and B. K. Chowdhury, J. Org. Chem., **33**, 1265 (1968).
- 11) D. P. Chakraborty, B. K. Barman, and P. K. Bose, Tetrahedron, **21**, 681 (1965).
- 12) In longer reaction time, further polymerisation products (trimer, tetramer and so on) could be detected.
- 13) Y.-C. Kong, K.-F. Cheng, R. C. Cambie, and P. G. Waterman, J. C. S., Chem. Comm., **47**, (1985).

(Received November 27, 1986)



## Communications to the Editor

[Chem. Pharm. Bull.]  
[35(1) 453--455 (1987)]

GARDNERIA ALKALOIDS PART 14.<sup>1)</sup> THE STRUCTURE OF GARDFLORAMINE  
AND 18-DEMETHOXYGARDFLORAMINE

Shin-ichiro Sakai,<sup>\*,a,b</sup> Norio Aimi,<sup>a</sup> Keiichi Yamaguchi,<sup>a</sup>  
Koreharu Ogata<sup>b</sup> and Joju Haginiwa<sup>a</sup>

Faculty of Pharmaceutical Sciences,<sup>a</sup> and Chemical Analysis Center,<sup>b</sup>  
Chiba University, 1-33 Yayoi-cho, Chiba 260, Japan

The structure of gardfloramine (1), which has been isolated as one of the minor bases from *Gardneria multiflora*, was determined by X-ray analysis. Its oxygenation pattern on the aromatic ring was revealed to be 9-methoxy-10,11-methylenedioxy and is different from that of gardneramine. The structure of another minor alkaloid, 18-demethoxygardfloramine (2) was also determined by comparing the <sup>13</sup>C-NMR spectra of 1 and 2.

KEYWORDS — gardneria alkaloid; gardfloramine; 18-demethoxygardfloramine; *Gardneria multiflora*; Loganiaceae; X-ray analysis; <sup>13</sup>C-NMR

Gardfloramine(1) is one of the minor alkaloids of *G. multiflora* (Japanese name: Chitose-kazura). Its structure has been proposed as shown in Fig. 1 from the spectroscopic evidence.<sup>2)</sup> In this structure the exact positions of the oxygen functions on the aromatic ring and the configuration of the side chain double bond remain undetermined. In regard to the oxygen problem we thought the benzene part, having the methoxy group on C<sub>12</sub> and the methylene oxide between C<sub>9</sub> and C<sub>10</sub> would be the most likely structure from the biogenetic stand point,<sup>3)</sup> but this was not the case (*vide infra*).

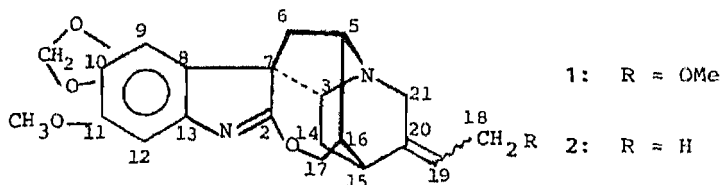


Fig. 1

X-ray analysis was used to elucidate the ambiguous parts of the structure. Gardfloramine(1) crystals, grown from acetone, belong to monoclinic space group P2<sub>1</sub> with  $a = 10.252(2)$ ,  $b = 20.162(4)$ ,  $c = 9.628(3)\text{\AA}$ ,  $\beta = 90.79(2)^\circ$ ,  $z = 2$ , two molecules per Z : four molecules per unit cell. A total of 3462 unique and

significant reflections ( $F_o \geq 3\sigma(F_o)$ ) within the range  $3^\circ \leq 2\theta \leq 155^\circ$  were measured on a four-circle diffractometer using Cu K $\alpha$  radiation ( $\lambda = 1.5\text{\AA}$ ).

The structure was analyzed by the direct method MULTAN 80 (UNICS III system<sup>4</sup>) and refined by the block-diagonal least squares method to  $R = 0.078$ . The ORTEP drawing of the structure of gardfloramine (1) is shown in Fig. 2.

So the aromatic ring was found to have the methoxyl group on C<sub>9</sub> and the methylenedioxy group between C<sub>10</sub> and C<sub>11</sub>. On the other hand, the configuration of the C<sub>19</sub> side chain was confirmed to be Z-form as in gardneramine(3),<sup>4,5</sup> the main alkaloid of *G. multiflora*.

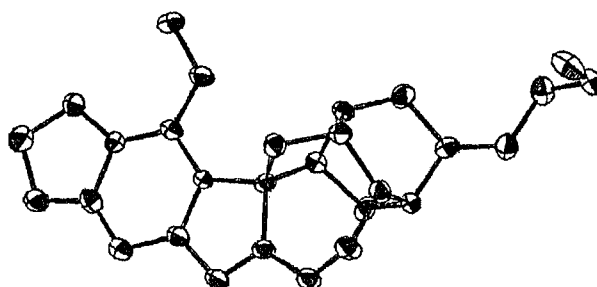


Fig. 2. ORTEP drawing of gardfloramine (1)

Each signal of the <sup>13</sup>C-NMR spectrum of gardfloramine was assigned by comparing with the gardneramine spectrum<sup>7</sup>) (TABLE I). The substituted benzene ring carbon signals were assigned by referring to the <sup>13</sup>C-NMR spectra of indole alkaloids.<sup>8</sup>)

As the structure of 1 was confirmed unambiguously, the structure of another minor base, 18-demethoxygardfloramine (2),<sup>2</sup>) which has been isolated along with gardfloramine (1), was also determined.

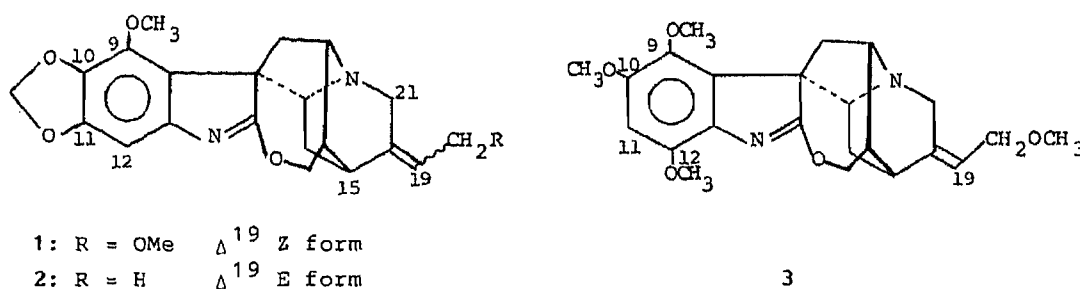


Fig. 3

As is evident from the <sup>13</sup>C-NMR data, 2 and 1 have the same aromatic moiety structure. By comparing the <sup>13</sup>C-NMR chemical shift values of C<sub>15</sub> and C<sub>21</sub> of 18-demethoxygardfloramine (2) with those of gardfloramine (1), it was revealed that the configuration of the C<sub>19</sub> side chain of 2 is E form.<sup>7</sup>)

Thus, as shown in Table I, 18-demethoxygardfloramine (2) exhibits a high field shift of 7.1 ppm for C<sub>15</sub> and a downfield shift of 3.0 ppm for C<sub>21</sub> compared to the corresponding signals of gardfloramine (1). This demonstrates the opposite orientation of the substituents on C<sub>19</sub>.

It is interesting to note that the oxygenation pattern on the aromatic ring of gardfloramine (1) and 18-demethoxygardflormine (2) are at the 9, 10 and 11 positions, whereas that of gardneramine (3) and all of the hitherto isolated trimethoxylated gardneria alkaloids are at the 9, 10 and 12 positions.

TABLE I.  $^{13}\text{C}$  Chemical Shifts of 1 and 2 (in  $\text{CDCl}_3$ )

Carbon	1	2
2	181.3	181.5
3	61.2	61.8
5	60.2	60.0
6	31.2	30.5
7	62.9	62.8
8	122.0	122.1
9	139.6	139.5
10	133.2	133.2
11	146.8	146.8
12	95.8	95.8
13	149.3	149.2
14	31.4	31.5
15	36.9	29.8
16	41.9	41.7
17	71.9	72.2
18	68.0	12.6
19	115.0	112.0
20	147.4	142.0
21	46.2	49.2
18-OCH <sub>3</sub>	58.1	
arom.-OCH <sub>3</sub>	59.7	59.8
-OCH <sub>2</sub> O-	100.7	100.7

a) The values are in ppm downfield from TMS.

b) Assignments bearing the same superscript on the vertical column may be interchangeable.

#### REFERENCES AND NOTES

- 1) Part 13: S. Sakai, N. Aimi, K. Yamaguchi, E. Yamanaka and J. Haginiwa, *J. Chem. Soc., Perkin Trans. 1* **1982**, 1257.
- 2) S. Sakai, N. Aimi, K. Yamaguchi, H. Ohhira, K. Hori and J. Haginiwa, *Tetrahedron Lett.*, **1975**, 715.
- 3) S. Sakai, *Heterocycles* **4**, 134 (1976).
- 4) T. Sakurai and K. Kobayashi, *Rep. Inst. Phys. & Chem. Res.*, **55**, 69 (1979).
- 5) N. Aimi, S. Sakai, Y. Iitaka and A. Itai, *Tetrahedron Lett.*, **1971**, 2061.
- 6) S. Sakai, N. Aimi, A. Kubo, M. Kitagawa, M. Hanasawa, K. Katano, K. Yamaguchi, and J. Haginiwa, *Chem. Pharm. Bull.*, **23**, 2805 (1975).
- 7) N. Aimi, K. Yamaguchi, S. Sakai, J. Haginiwa and A. Kubo, *Chem. Pharm. Bull.*, **26**, 3444 (1978).
- 8) G. A. Webb ed. "Annual Reports on NMR Spectroscopy" vol. 8, Academic Press, 1978.

(Received December 4, 1986)